EMECS'11 SeaCoasts XXVI

Joint conference

Proceedings of International Conference

"Managing risks to coastal regions and communities in a changing world"

August 22-27, 2016 St Petersburg, Russia

Proceedings of International Conference

"MANAGING RISKS TO COASTAL REGIONS AND COMMUNITIES IN A CHANGING WORLD" EMECS'11 - SEACOASTS XXVI

August 22-27, 2016 Russia, St. Petersburg

Executive Committee

Motoyuki Suzuki, International EMECS Center, Japan
Toshizo Ido, International EMECS Center, Governor of Hyogo Prefecture, Japan
Leonid Zhindarev, Working Group "Sea Coasts" RAS, Russia
Valery Mikheev, Russian State Hydrometeorological University, Russia
Masataka Watanabe, International EMECS Center, Japan
Robert Nigmatullin, P.P. Shirshov Institute of Oceanology RAS, Russia
Oleg Petrov, A.P. Karpinsky Russian Geological Research Institute, Russia

Scientific Programme Committee

Ruben Kosyan, Southern Branch of the P.P. Shirshov Institute of Oceanology RAS, Russia – **Chair**
Masataka Watanabe, Chuo University, International EMECS Center, Japan – **Co-Chair**
Petr Brovko, Far Eastern Federal University, Russia
Zhongyuan Chen, East China Normal University, China
Jean-Paul Ducrotoy, Institute of Estuarine and Coastal Studies, University of Hull, France
George Gogoberidze, Russian State Hydrometeorological University, Russia
Sergey Dobrolyubov, Academic Council of the Russian Geographical Society, M.V. Lomonosov Moscow State University, Russia
Evgeny Ignatov, M.V. Lomonosov Moscow State University, Russia
Nikolay Kasimov, Russian Geographical Society, Technological platform "Technologies for Sustainable Ecological Development"
Igor Leontyev, P.P. Shirshov Institute of Oceanology RAS, Russia
Svetlana Lukyanova, M.V. Lomonosov Moscow State University, Russia
Menasveta Piamsak, Royal Institute, Thailand
Erdal Ozhan, MEDCOAST Foundation, Turkey
Daria Ryabchuk, A.P. Karpinsky Russian Geological Research Institute, Russia
Mikhail Spiridonov, A.P. Karpinsky Russian Geological Research Institute, Russia
Ivica Trumbic, UNESCO-IHP, Croatia
Eric Wolanski, James Cook University, Australia
Tetsuo Yanagi, Kyushu University, International EMECS Center, Japan

CONTENTS

INNOVATIVE TECHNOLOGIES FOR DECISION SUPPORT IN SOCIO-ECONOMIC DEVELOPMENT WITHIN COASTAL SYSTEMS OF RUSSIAN NORTHERN SEAS TAKING INTO ACCOUNT NATURAL RISKS AND ADAPTATION TO CLIMATE CHANGE

Valery Abramov, Russian State Hydrometeoropogical University, Russia
George Gogoberidze, Russian State Hydrometeoropogical University, Russia
Christiane Schmullius, Friedrich-Schiller University, c.schmullius@uni-jena.de, Germany
Marcel Urban, Friedrich-Schiller University, marcel.urban@uni-jena.de, Germany
Mathieu Belbeoch, Joint Commission on Oceanography and Marine Meteorology Operations, France
Eugene Istomin, Russian State Hydrometeoropogical University, Russia
Nikolay Popov, Russian State Hydrometeoropogical University, Russia
Ruslan Bachiev, Russian State Hydrometeoropogical University, Russia
Alice Popova, Russian State Hydrometeoropogical University, Russia
Julia Malakhova, Russian State Hydrometeoropogical University, Russia
Stanislav Berboushi, Russian State Hydrometeoropogical University, Russia

val.abramov@mail.ru

Socio-economic development within coastal systems of the Russian Northern seas is an important component of the Strategy for development of the Arctic zone of the Russian Federation (AZRF) till 2020 (here and after AS-2020). When implementing AS-2020 important aspect is the management of natural risks. The planning horizon of AS-2020 requires the development of measures to adapt to climate change. Management of natural risks and adaptation to climate change require the development of innovative technologies for decision support based on the principles of geo-information management for spatial areas including marine planning. We present the results of research on the development of such technologies over the last years in the Arctic and Subarctic Institute at the Russian State Hydrometeorological University (ASI RSHU). During research we widely use the instruments of international cooperation.

Platform https://www.researchgate.net/profile/Valery_Abramov2/?ev=hdr_xprf gave excellent opportunities to preliminary discussion and data exchange in the frame of this research. The Ministry of education and science of Russia provides financial support for this research with the state order 2525.2014/166.

Key words: geo-information management, decision support, marine planning, northern seas, natural risks, climate change

I. INTRODUCTION

Socio-economic development within coastal systems of the Russian Northern seas is an important component of the Strategy of development for the Arctic zone of the Russian Federation (AZRF) till 2020 (AS-2020) [1-3]. When implementing AS-2020 important aspect is the

management of natural risks [4]. The planning horizon of AS-2020 requires the development of measures to adapt to climate change. We proposed that management of natural risks and planning of adaptation to climate change must be conducted with using innovative technologies for decision support, based on the principles of geo-information management [5-7], including principles of integrated water recourses management (IWRM) [8] and air quality management (AQM). Partly these technologies include ship expeditions [9], remote sensing [10] and Argo buoy array [11-13].

In natural risk management within AZRF we have to take into consideration some tens dangerous nature phenomena in four geo-spheres [4] among which the iceberg hazard is the least studied [14]. Additional complexity is in the fact that the last regular monitoring of icebergs in Russian Arctic stopped in 1992.

Climatologists know that in the Arctic the rate of climate change is approximately two times higher than the similar process on the planet as a whole. Some of them think that a possible cause is the arrival of black carbon in the Arctic due to the General circulation of the atmosphere, including from Russia. To manage climate risks due to black carbon we proposed strategy for the development of clean technologies in the framework of the national system for control black carbon [15-18].

II. METHODS AND DATA

We used in research: Foresight technologies, risk management approach, theory of decision making under uncertainties, methods of data bases (DB) constructing, statistical methods of information processing, mathematical modeling method including statistical modeling, bootstrapping strategy [4]. From the point of view of geographic information management we structured geo-space to allocate the interconnected components of the solution space [5, 7]. In research of iceberg hazard we used iceberg observations DB [14].

Web-source http://www.argo.net contains essentials about Argo project including technical details on Argo buoy measuring cycle. We propose using of Argo buoys for assessing water change of Atlantic and Pacific with Arctic Ocean as a climate change factors. We use the methods for the present Argo buoys data study that are similar for iceberg hazard research [14] when small groups of point drifters move offshore. We used in the research the developed sub databases “DB ARGO Bering” [12] and “DB ARGO ATL” [13]. The databases contain data of around hundred Argo buoys. This array covers about fifteen-year period from 2001 till now.

In study of black carbon we used experimental methods of determination of mass and quantitative content of aerosols in the atmosphere and statistics in the research area; statistical methods of information processing and risk management approach. In research for St.-Petersburg area we used official web-sources with aerosol measurements http://gov.spb.ru/gov/otrasl/ecology/ and http://gov.spb.ru/gov/otrasl/ecology/infosupply [17]. For Moscow area we used similar web-sources http://www.mosecom.ru and http://ecomos.ru [18].

III. RESULTS AND DISCUSSION

Development Strategy of the Russian Arctic till 2020 (hereinafter referred to Arctic Strategy or AS-2020) is essential document that determines the prospects for socio-economic development of the Russian Arctic [1-3]. The management of natural risks is important aspect when implemented AS-2020 [4]. Planning horizons of AS-2020 necessitate considering the so-called climate risks, and

determining the potential climate changes [4]. It should be noted that natural risk management has to be a part of the whole program for socio-economic development of the coastal regions in the Russian Arctic. On a fig.1 we present block diagram of the utility model "Information analytical system for support of decision-making in the field of sustainable development for marine planning in the Arctic zone of the Russian Federation taking into account different scales of climate change" that was patented accordingly Russian legislation (Patent Ref. No: RU 135162 U1, 2013). This utility model combines the investment objectives of the socio-economic project with the need for adequate consideration of natural risks, including climate risks.

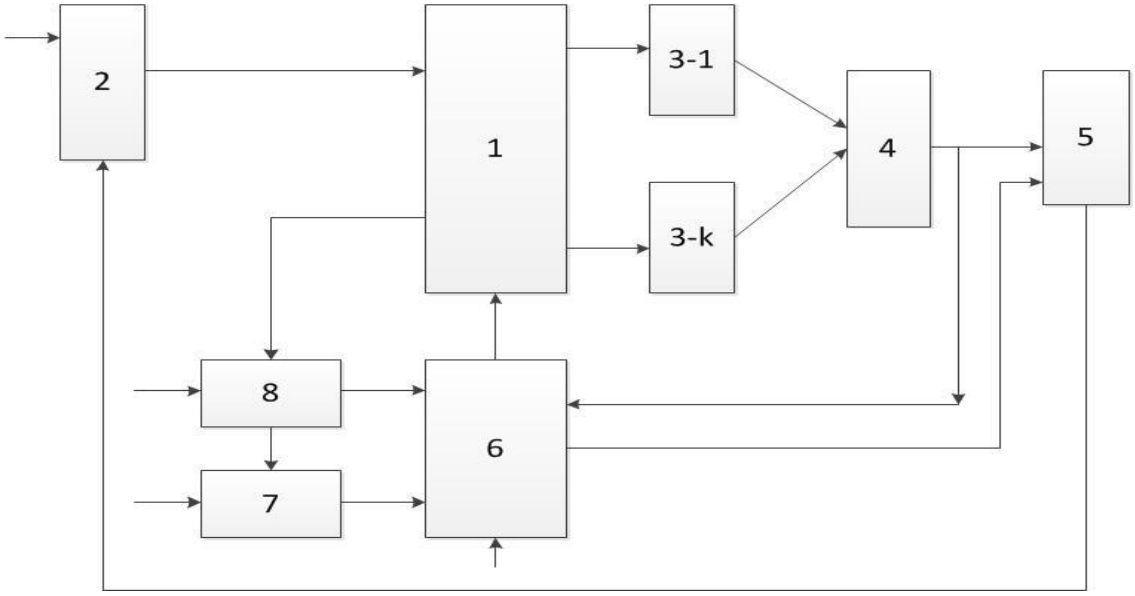

Fig. 1. Block diagram of the utility model "Information analytical system for support of decision-making in the field of sustainable development for marine planning in the Arctic zone of the Russian Federation taking into account different scales of climate change" (explanations in text below)

Fig. 1 shows the following blocks: 1 – block distribution of resources; 2 – forming unit resources; 3 - forming unit of private income; 4 - forming unit of total income; 5 - forming unit of share investment of resources; 6 - forming unit of comparison with an acceptable level of risk; 7 – forming unit of a time-varying set of natural risk (including climate risks) characteristic for the Arctic zone of the Russian Federation; 8 – forming unit of environmental monitoring, which is characteristic for sustainable development in marine planning in the Arctic zone of the Russian Federation taking into account different scales of climate change.

AS-2020 indicates the importance of Maritime activities within the coastal regions of the Russian Arctic especially in the area of North Sea Rout (NSR) which are the part of Russian Arctic transport system (RATS). We present on fig. 2 the map with our estimations of Marine Economic Potential (MEP) for Russian Arctic Zone by using indicator method and GIS-technologies [1]. According to our estimates, now Russian Arctic coastal regions can be divided into 2 groups:

- regions with a stable economic situation (Yamalo-Nenets Autonomous Okrug, Krasnoyarsk Krai, Republic of Sakha (Yakutia) and Chukotka Autonomous Okrug, the values of the MEP are in the range from 0 to 0.5);
- regions with unstable economic situation (Murmansk oblast, Republic of Karelia and Arkhangelsk region, values of MEP are within the -0.5 to 0).

Fig. 2. Map of the Maritime economic potential of the Arctic coastal regions of Russia, as of 2011

For the Russian Arctic the main types of Maritime activities in the framework of AS-2020 will be the offshore extraction of hydrocarbon resources and transportation of goods using the NSR as a transport corridor. For such activities iceberg hazard is a source of catastrophic environmental risk of the first kind [4]. The importance of this factor is confirmed by the tragic incident with the ship "Hans Hedtoft" in 1959 during its first trip within the opening of regular Maritime traffic between Denmark and Greenland. The ship had collision with an iceberg in the conditions of the icy storm. All the passengers and crew members of ice class vessel with a displacement of about 3,000 tons died. This incident effectively put an end for the strategic plans of regular Maritime traffic to Greenland instead of the existing expensive air service. Iceberg risk management has to basing on the adequate models for the physical mechanism of the formation of iceberg risk [13-15] and advantageously carrying out with the use of tools to support decision-making for example as it on fig. 1.

We propose using geo-information management when managing iceberg risk in the Russian Arctic seas management [5-7], based on the wide use of geographic information systems (GIS) as tools to support decision-making. The use of GIS allows greatly enhance the visualization display

capabilities for spatially-distributed objects of different nature on a common cartographic basis. For example, on the fig.3 displayed using GIS episode of attack of a group of five icebergs to the area of the Stockman gas condensate field (SGCF), the inner safety zone for SGCF. The episode that occurred in April 1987 was discovered by V. M. Abramov in the course of cluster analysis. The green points show the position of the icebergs from the group's invasion on April 8th 1987, and blue triangles indicate their position in the next episode of observations on April 10th. Black and red signs in the form of squares and polygons displayed icebergs that are not in the group of invasion. Evident continuity between episodes 8 and 10 April 1987 allows talking about the kinematic connection between icebergs recorded in these episodes. The front of the invasion coincides with the bandwidth of the Novaya Zemlya's shelf bounded by the 200-meter isobaths as shown on the fig.3. During the invasion the icebergs are moving in sync, keeping the positional relationship. The figure also contains the provisions of the promising oil and gas fields, description of which are not included in this article.

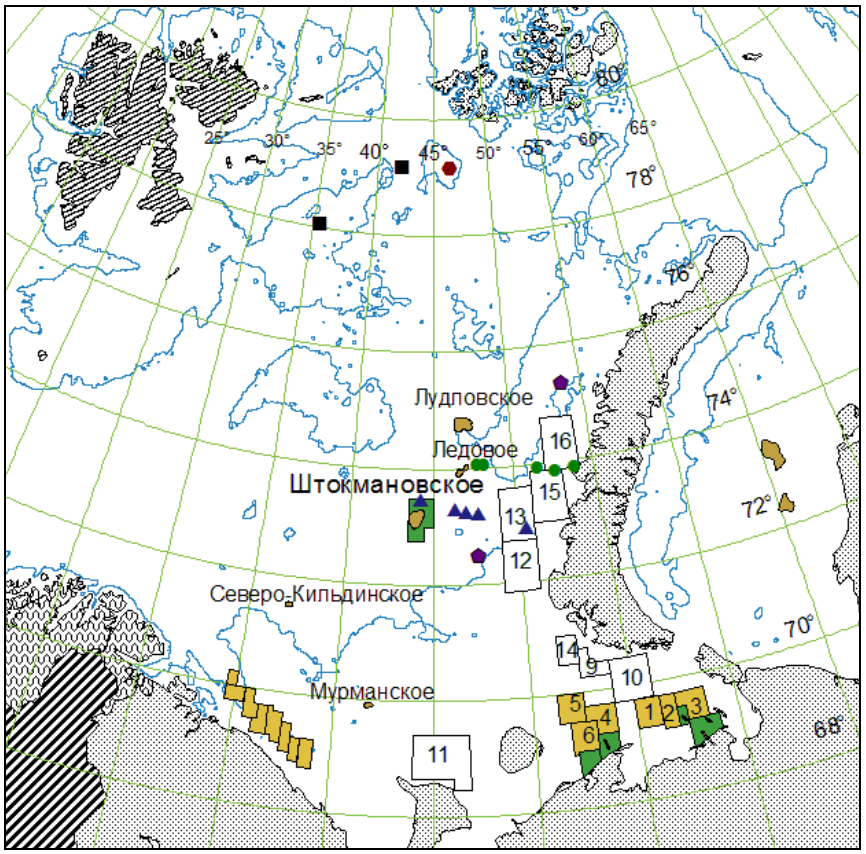

Fig. 3. Iceberg the attack on SGCF in April 1987 (designations in text above)

Water changes of Atlantic and Pacific with Arctic Ocean are the very important factors for climate change in Arctic. We propose using of Argo buoys for those goals. The typical cycle of an Argo buoy is presented on fig.4 [11]. Note that now volume of Argo data overwhelms traditional sources and the quality of the data is high. Argo target called for temperature and salinity accuracies of 0.005 °C and 0.01 salinity units, with a pressure accuracy of 2.5 dbars (equivalent to a depth error

of about2.5 m). About 80% of the raw profile data meet these standards, with little or no correction required [11]. The rest of the data are corrected using delayed-mode quality control procedures and eventually meeting the accuracy goals [11]. At present, about 90% of Argo profiles are distributed electronically within 24 hours of acquisition. [11].

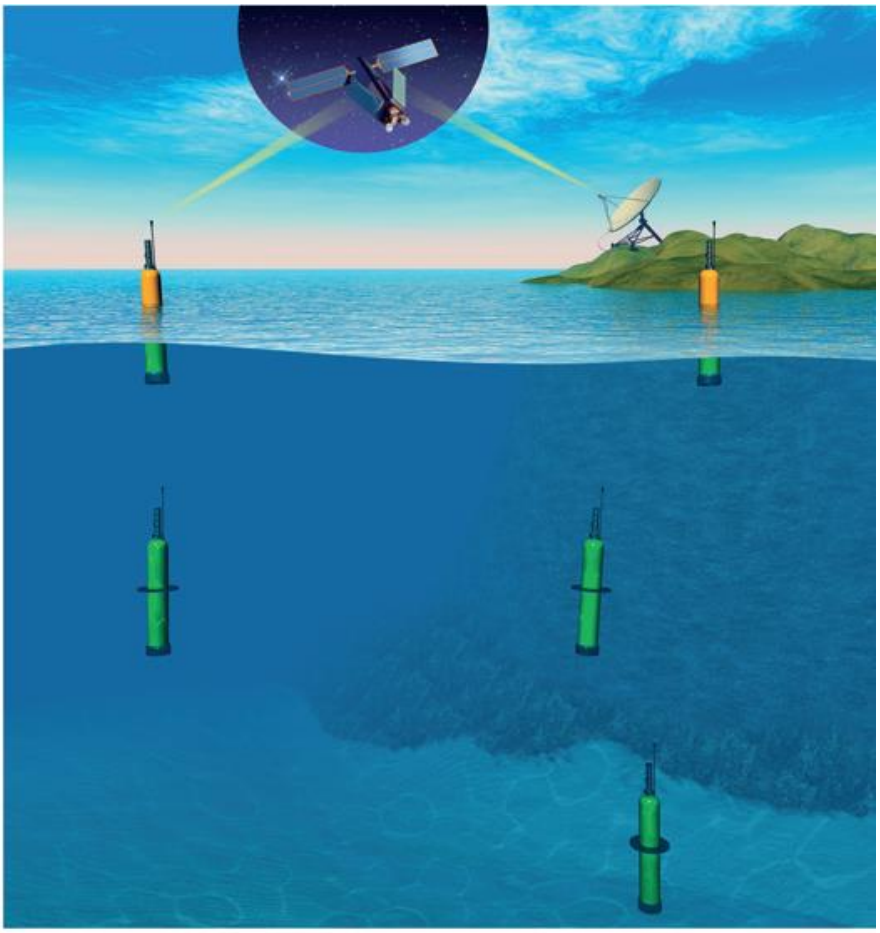

Fig.4 The typical cycle of an Argo buoy [11]

In the research we used developed sub databases “DB ARGO Bering” [12] and “DB ARGO ATL” [13]. Those sub DB contain data of around hundred Argo buoys. This array covers about fifteen-year period from 2001 till now. On recent stage essential goal is to study trajectory of Argo buoys from above mentioned sub DB for visualization of water masses movements. We found that one of Argo buoys from “DB ARGO ATL” with id #4901101 had unique long journey from warm waters near southern coast of Nova Scotia to high latitude arctic area near most northern cap of Novaya Zemlya. This trip began 2008 summer and lasted near five years. Over 180 vertical profiles of temperature and salinity provided with 10 days interval and transferred to ARGO Data Centers. Over year this buoy moved inside depth of Barents Sea dragged by Atlantic Waters. It crossed area of SGCF in 2012 and then came to northern cap of Novaya Zemlya where ended functioning at 2013 early spring. Till now it is the only Argo buoy appearance in the Barents Sea [13].

On fig. 4 we present all trajectories of Argo buoys from “DB ARGO Bering” within deep part of Bering Sea and near Pacific. Essential attention we contribute to Argo buoys that come and go by

straits in Aleutian Islands to investigate patterns and scenarios of water exchange between the Pacific and deep water part of the subarctic Bering Sea [12]. Note that very first Argo buoy station within the Bering Sea was14 August 2001. As result of research we described the basic schema of Alaskan Stream waters influence on climate change in Arctic and Subarctic [12]. Also we illustrated the main ways of Alaskan Stream waters penetration into deep water part of the Bering Sea using Argo buoys trajectories. We found some cases with untypical buoy trajectories regarding known circulation system in the Bering Sea [12].

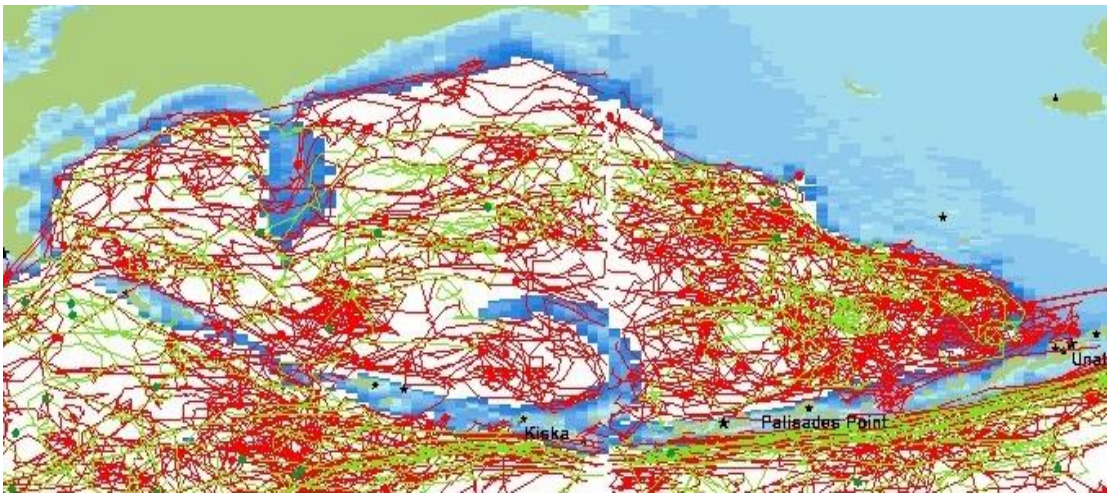

Fig.5. Trajectories of Argo buoys from "DB ARGO Bering" within deep part of Bering Sea and near Pacific

As Argo buoys have to reach the sea surface to transmit their data, they could not originally target ice-covered parts of the oceans [11]. But there is plan to expand Argo into Arctic Ocean some later when sea ice there will have seasonal character. Now there are new algorithms to help survive Argo buoys in icy waters [11]. On fig. 6 we present the map with scheme for future Argo zone in the Arctic Ocean where rose trapezoids use for calculating the extra Argo buoys resources. Green points on map are active buoys and ice stations.

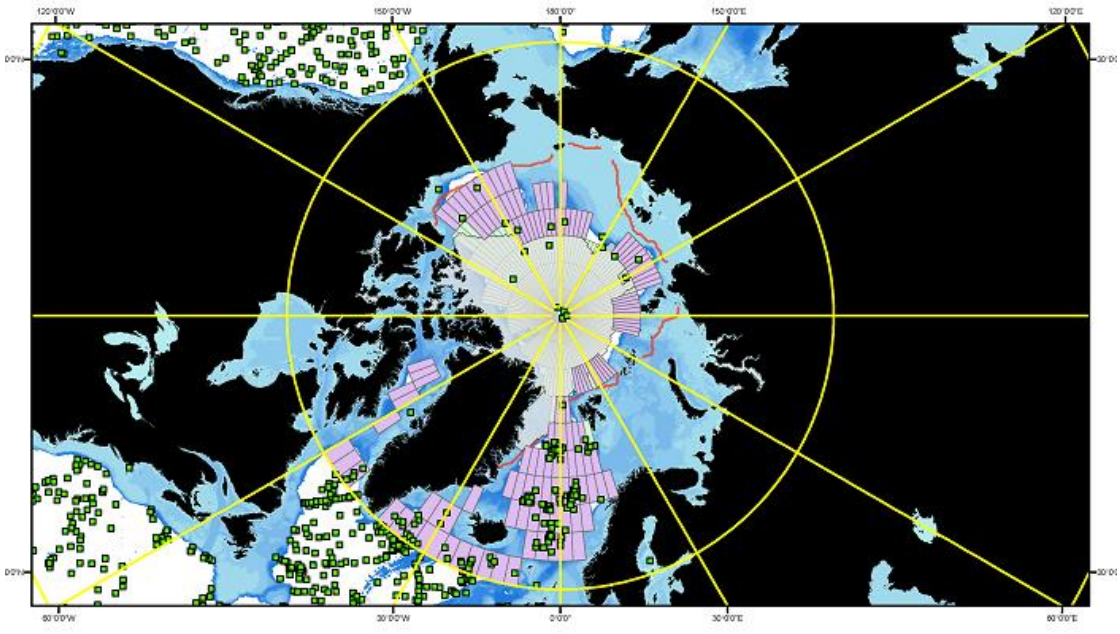

Fig.6. Scheme of future Argo zone in the Arctic Ocean

While discussion about future Argo zone in the Arctic Ocean we note it will be great move forward in Arctic Ocean study and recommend most important places for implementing: Barents Sea Opening between Norway and Svalbard, west and north of Svalbard, Fram Strait, Danish Strait and continental slope at Russian bank.

Let's go to black carbon (BC) as climate change factor. Some specialists suppose that BC is one of the most important parts of aerosol or particulate matter (*PM*) that have influence on climate change and health [19]. Cities and especially megacities are the important sources of BC [15]. Currently measuring black carbon in Russia is not made. It is quite a significant portion of PM_{10} and a large part of $PM_{2.5}$. The study of long series of measurements of PM_{10} and PM_{10} in large cities of Russia is important, including for the development of the national system of monitoring the income of black carbon in the Arctic [15]. In [15] we presented the strategy for development of basic clean technologies that have to be used within national BC controlling system (NBCCS) in the Russian Arctic as part of geo-information management, a most modern approach to the management of spatially-distributed systems and territories [5-7]. This NBCCS have to be compliant with other management systems as Air Quality Management and Integrated Water Resources Management for Russian arctic and subarctic rivers [8]. Also NBCCS developing strategy have to take into account common concept of environmental monitoring in the Russian Arctic [20], principles of different arctic and subarctic measuring methods and systems including remote sensing [10] and traditional ship expedition [9] that have to be used for support decision.

Cities and especially megacities are the important sources of BC [15]. On this stage of research we estimate content and variability of BC in the air of two Russian megacities Moscow [18] and St.-Petersburg [17] within decadal and climate scales. Till now there was no direct measurement of BC in Russia including Moscow and St.-Petersburg [17, 18]. We tried to assess the BC contents the air of Moscow [18] and St.-Petersburg [17] within decadal scales for the first time on the base of PM data with using method of analogues [16]:

$$PM^{BC}_{x,\text{est}} = K^{BC}_{x,\text{est}} \cdot PM_{x,\text{est}}, \quad (1)$$

where set of values subscript x = {10, 2.5,}, $PM_{x,\text{est}}$, $PM^{BC}_{x,\text{est}}$ refer to the studied region and $K^{BC}_{x,\text{est}}$ refer to region-analogue. While using method for this case we searched region-analogues for $K^{BC}_{x,\text{est}}$ borrowing. During the searching we reviewed scientific literature containing the results of targeted experiments to determine $K^{BC}_{x,\text{est}}$ for different regions in the world including Europe. We considered a few dozen such sources. According to a search result we choose as an analogue the city of Thessaloniki (Greece), where the variability of particulate matter and black carbon is formed under influence as the busy car traffic with numerous corks [21]. From the chosen region-analogue we borrowed the following values $K^{BC}_{10,\text{est}}$ = 0.14 and $K^{BC}_{2.5,\text{est}}$ = 0.16 [21]. The results of calculations are in Tab.1 We can see that mean values of the random variability for average annual $PM^{BC}_{10,\text{est}}$ in the air of both Russian megacities are practically the same but the range of variability between maximal and minimal annual values in St.-Petersburg is much bigger then one in Moscow. We compared our assessments with the similar results of studies in the world (see fig.7 from [22]) and found considerable overlap.

Table 1. Mean annual $PM^{BC}_{10,\text{est}}$ и $PM^{BC}_{2.5,\text{est}}$ in Moscow and St. Petersburg for 2003 – 2011

Year	$PM^{BC}_{10,\text{est}}$, μg/m		$PM^{BC}_{2.5,\text{est}}$, μg/m^3	
	Moscow	St.-Petersburg	Moscow	St.-Petersburg
		$PM^{BC}_{10,\text{est}}$, μg/m^3	$PM^{BC}_{2.5,\text{est}}$, μg/m^3	-
2003	4.62	7,98	-	-
2004	5.18	9,38	-	-
2005	4.76	4,06	-	-
2006	4.62	4,62	-	-
2007	4.90	5,88	-	-
2008	5.18	3,92	-	-
2009	4.62	2,66	-	-
2010	6.16	3,50	-	-
2011	4.06	2,80	1.92	2,72
Mean	4.90	4.98	-	-
Max	6.16	9.38	-	-
Min	4.06	2.66	-	-

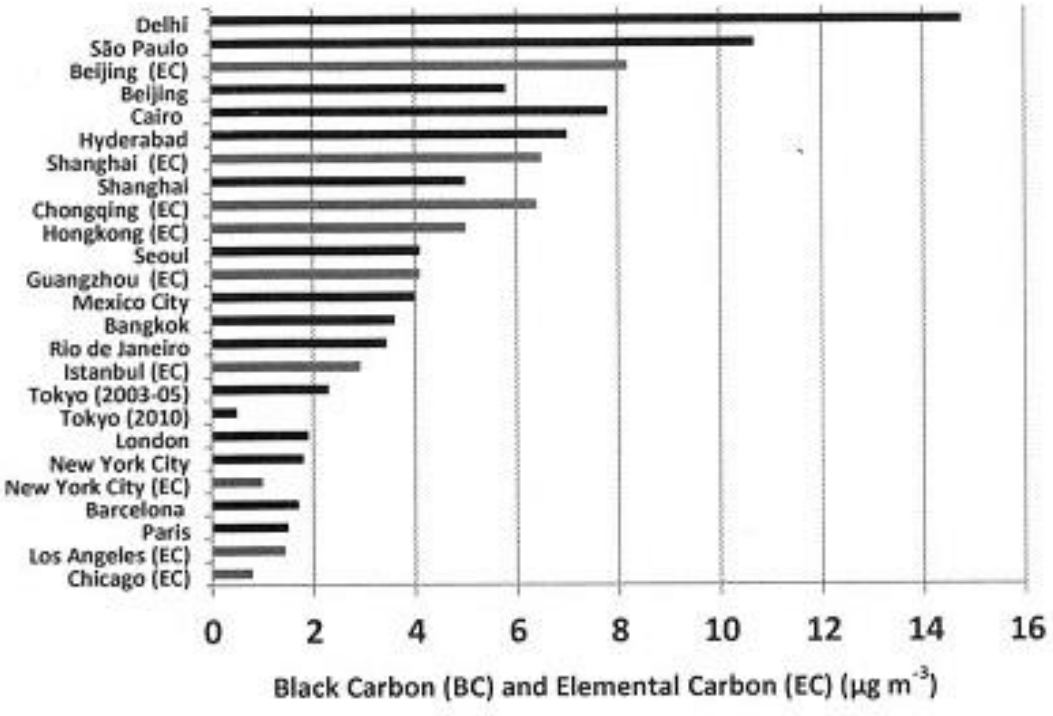

Fig. 7 Concentrations of black carbon (black) and elemental carbon (grey) observed in megacities across the world [22].

It was turned out that the average annual content of $PM_{10,\mathrm{est}}^{BC}$ in Moscow and St. Petersburg are between the indices of Istanbul and Hong Kong that are modern post-industrial megacities.

Let us discuss the recent picture of climate change in Arctic and possibilities of remote sensing in climate Arctic research. It is known that Arctic ecosystems have been afflicted by vast changes in recent decades [10]. Specialists know that changes in temperature, as well as precipitation, have an impact on snow cover, vegetation productivity and coverage, vegetation seasonality, surface albedo, and permafrost dynamics. The coupled climate-vegetation change in the arctic is thought to be a positive feedback in the Earth system, which can potentially further accelerate global warming [10]. Our research with different decadal data including remote sensing products shows that now climate change in Arctic has spot character [10, 23, 24] when some territories demonstrate positive trends in chosen climatic indicators but near them there are territories with negative trends or with mix ones.

The consistent and operational monitoring of different essential climate and ecosystem parameters is of high importance for future climate Arctic research. Earth observation data from various sources and techniques are available to retrieve spatial information and compensate the lack of ground measurements for remote areas. As the coverage of available meteorological stations in the Arctic is sparse, the interpolation between the climate stations is introducing uncertainties of unknown magnitude, which needs to be taken into account. Hence, the continuity of satellite observation services for the integration of long-term time series information into climate monitoring and modeling approaches is essential [10].

IV. Summary and conclusion

Socio-economic development within coastal systems of the Russian Northern seas is an important component of AS-2020. Important aspect while implementing AS-2020 is the management of natural risks and the development of measures to adapt to climate change. As we show in the article, the natural risks management and adaptation to climate change have be conducted with using innovative technologies for decision support, based on the principles of geo-information management with wide usage of GIS-technologies. In article we present the results of successful research over the last years in the Arctic and Subarctic Institute at the Russian State Hydrometeorological University (ASI RSHU). While research we use the instruments of international cooperation including personal contacts between leading researchers from different countries.

V. Acknowledgment

Platform https://www.researchgate.net/profile/Valery_Abramov2/?ev=hdr_xprf gave excellent opportunities to preliminary discussion and data exchange in the frame of this research. The Ministry of education and science of Russia provides financial support for this research with the state order 2525.2014/166.

VI. References

[1] Gogoberidze G.G., Karlin L.N., Abramov V.M., Lednova J.A., Malakhova J.A. Marine economic potential assessment for environmental management in the Russian Arctic and subarctic coastal regions, International Multidisciplinary Scientific GeoConference Surveying Geology and Mining Ecology Management, SGEM, Bulgaria, 2014.

[2] Gogoberidze, G., Karlin, L., Abramov, V., Lednova, J. Indicator method of estimation of human impact assessment for coastal local municipalities, Measuring and Modeling of Multi-Scale Interactions in the Marine Environment - IEEE/OES Baltic International Symposium, BALTIC 2014, Estonia, 2014.

[3] Lednova J., Gogoberidze G., Abramov V.M., Karlin L.N., Berboushi, S. Concept of environmental monitoring in the Russian arctic coastal regions, International Multidisciplinary Scientific GeoConference Surveying Geology and Mining Ecology Management, SGEM, Bulgaria, vol. 1, issue 5, pp 161-168, 2014

[4] Karlin L.N., Abramov V.M. Environmental and ecological risks management, St.-Petersburg, RSHU, 2013 – 332 c.- DOI: 10.13140/2.1.1978.8482

[5] Istomin E. P., Sokolov A. G, Abramov V. M., Gogoberidze G.G., Popov N.N. Geoinformation management as a modern approach to the management of spatially-distributed systems and territories, International Multidisciplinary Scientific GeoConference Surveying Geology and Mining Ecology Management, SGEM, Bulgaria, vol. 1, issue 2, pp 607-614, 2015.

[6] Istomin E. P., Sokolov A. G, Abramov V. M., Gogoberidze G.G., Fokicheva A.A. Methods for external factors assessing within geoinformation management of territories,

International Multidisciplinary Scientific GeoConference Surveying Geology and Mining Ecology Management, SGEM, Bulgaria, vol. 1, issue 2, pp 729-736, 2015

[7] Istomin E. P., Sokolov A. G, Abramov V. M., Fokicheva A.A., Popov N.N. CLUSTERS WITHIN GEOSPATIAL INFORMATION MANAGEMENT FOR DEVELOPMENT OF THE TERRITORY, International Multidisciplinary Scientific GeoConference Surveying Geology and Mining Ecology Management, SGEM, Bulgaria, vol. 1, book 2, pp 601-608, 2016.

[8] Abramov V.M., Karlin L.N., Gogoberidze G.G., Golosovskaya V.A. On route to Integrated Water Resources Management for Russian arctic and subarctic rivers, International Multidisciplinary Scientific GeoConference Surveying Geology and Mining Ecology Management, SGEM, Bulgaria, vol. 1, issue 3, pp 495-501, 2014.

[9] Gogoberidze G., Abramov V.M., Lednova J., Karlin L.N., Isaev A., Khaimina, O. Main results of summer oceanographic surveys in the eastern gulf of Finland in the framework of the Topcons project, International Multidisciplinary Scientific GeoConference Surveying Geology and Mining Ecology Management, SGEM, Bulgaria, vol. 3, issue 5, pp 253-260, 2014.

[10] Urban M., Forkel M., Hüttich C., Schmullius C., Herold M. Pan-Arctic Climate and Land Cover Trends Derived from Multi-Variate and Multi-Scale Analyses (1981–2012), *Remote Sens.* 2014, *6*, 2296-2316; doi:10.3390/rs6032296

[11] Riser S.C., Freeland H., Belbeoch M. et all. Fifteen years of ocean observations with the global Argo array, Nature Climate Change, February 2016. - DOI: 10.1038/nclimate2872

[12] Abramov V.M., Karlin L.N., Gogoberidze G.G., Alexandrova L.V., Popov N.N. Water exchange between the Pacific and the Bering sea with impact on climate change in the Arctic and Subarctic, International Multidisciplinary Scientific GeoConference Surveying Geology and Mining Ecology Management, SGEM, Bulgaria, vol. 2, issue 3, pp. 701-708, 2014

[13] Abramov V.M., Karlin L.N., Gogoberidze G.G., Alexandrova L.V., Bournashov, A.V. On Atlantic water inflow to Arctic ocean: Unique Argo buoy trip across Atlantic and Barents sea, International Multidisciplinary Scientific GeoConference Surveying Geology and Mining Ecology Management, SGEM, Bulgaria, vol. 2, issue 3, pp. 661-668, 2014.

[14] Karlin L.N., Abramov V.M., Ovsyannikov A.A. THE TEMPORAL STRUCTURE OF THE ICEBERG HAZARD IN THE CENTRAL PART OF THE BARENTS SEA, Oceanology, 2009, vol. 49, No 3.

[15] Abramov V.M., Karlin L.N., Lednova J.A., Gogoberidze G.G., Popov N.N. Clean technologies development strategy for the national black carbon controlling system in the Russian Arctic, International Multidisciplinary Scientific GeoConference Surveying Geology and Mining Ecology Management, SGEM, Bulgaria, vol. 2, issue 4, pp 313-320, 2014.

[16] Abramov V.M., Gogoberidze G.G., Popov N.N., Isaev A.V., Berboushi S.V. Method of assessment for black carbon random fields within Russia for climate management in the Arctic, International Multidisciplinary Scientific GeoConference Surveying Geology and Mining Ecology Management, SGEM, Bulgaria, vol. 1, issue 4, pp 953-960, 2015.

[17] Abramov V.M., Karlin L.N., Lednova J.A., Malakhova J.A., Gogoberidze G.G., Berboushi S.V. Variability of particulate matter in Saint-petersburg megacity air within climatic time scale, International Multidisciplinary Scientific GeoConference Surveying Geology and Mining Ecology Management, SGEM, Bulgaria, vol. 2, issue 4, pp 599-606, 2014.

[18] Abramov V. M., Popov N.N., Bachiev R.I. DECADAL VARIABILITY OF PARTICULATE MATTER IN MOSCOW MEGACITY AIR, International Multidisciplinary Scientific GeoConference Surveying Geology and Mining Ecology Management, SGEM, Bulgaria, vol. 2, book 4, pp 323-330, 2016.

[18] Abramov V. M., Gogoberidze G.G., Popov N.N., Berboushi S.V., Bachiev R.I. SCIENTIFIC BASIS FOR THE ICEBERG RISKS MANAGEMENT WITHIN THE RUSSIAN ARCTIC SEAS IN THE FRAME OF RATIONAL NATURE USAGE IN A CHANGING CLIMATE, Proceeding of Russian Hydrometeorological University: theoretical research journal, 2015, issue 39, pp 132-141.

[19] Bond T. C. et all. Bounding the role of black carbon in the climate system: A scientific assessment, J. Geophys. Res. Atmos., 118, 5380–5552, 2013. - DOI: 10.1002/jgrd.50171

[20] Lednova J., Gogoberidze G., Abramov V.M., Karlin L.N., Berboushi, S. Concept of environmental monitoring in the Russian arctic coastal regions, International Multidisciplinary Scientific GeoConference Surveying Geology and Mining Ecology Management, SGEM, Bulgaria, vol. 1, issue 5, pp 161-168, 2014.

[21] Samara C., Voutsa D., Kouras A., Eleftheriadis K., Maggos T., Saraga D., Petrakakis M. Organic and elemental carbon associated to PM10 and PM2.5 at urban sites of northern Greece, Environmental Science and Pollution Research, USA, 21(3), 2014. - DOI:10.1007/s11356-013-2052-8

[22] Beekmann M. et all. In situ, satellite measurement and model evidence on the dominant regional contribution to fine particulate matter levels in the Paris megacity, Atmos. Chem. Phys., 15, 9577-9591, 2015. - DOI: 10.5194/acp-15-9577-2015

[23] Abramov N.V. Climate warming and contemporary changes in the regime of the rivers within the water basin of Northern Dvina, Proc. of Final Session of RSHU Scientific Council, 2005, pp 3-5.

[24] Abramov V.M. ICEBERG HAZARD FOR MARITIME ACTIVITIES WITHIN THE RUSSIAN ARCTIC IN THE CLIMATE CHANGE CONDITIONS, Proc. of 9th Int. Conference “GEORISK-2015”, Moscow, 2015, v.2, pp 443-448.

CLIMATE CHANGE: HOW DOES THIS INFLUENCE ON ECOSYSTEM HEALTH IN THE LAGOON OF THE BALTIC SEA?

Sergey Aleksandrov, Atlantic Research Institute of Marine Fisheries and Oceanography, Russia
Julia Gorbunova, Atlantic Branch of P.P. Shirshov's Institute of Oceanology of Russian Academy of Sciences, Russia

hydrobio@mail.ru

Lagoons are one of the most vulnerable ecosystems to impacts of natural environmental and anthropogenic factors. The Curonian and Vistula Lagoons are one of the largest lagoons of Europe. The Curonian Lagoon is choke mostly freshwater, while the Vistula Lagoon is restricted brackish water. Hydrological, chemical and biological researches were carried out monthly since 1991 to 2014. Reductions of nutrients loading in 1990s did not result in improvement of the ecological situation. Hydrological and chemical parameters are the main factors that influence on the algal blooms and ecosystem health in these lagoons. The Curonian Lagoon may be characterized as hypertrophic water body with "poor" water quality. Climate change in 1990s-2010s combined with other factors (freshwater, slow-flow exchange, high nutrients concentrations) creates conditions for Cyanobacteria "hyperblooms". Harmful algal blooms result in deterioration of the water chemical parameters and death of fish. "Hyperblooms" is the most dangerous for coastal towns and tourist resorts (UNESCO National Park "Curonian Spit"). Climate change in 1990s-2000s have been also observed in Vistula Lagoons (mean annual temperature increased by 1.4°C for 40 years), but brackish water prevent harmful algal hyperblooms. After the invasion of the filter-feeding mollusk Rangia water quality was significantly improved in 2011-2014, but ecosystem productivity remained at a stable long-term level.

Key words: climate change, Curonian and Vistula Lagoons, primary production, phytoplankton, eutrophication

I. INTRODUCTION

Till 40th of XX century Baltic Sea was oligotrophic with relatively low biological productivity. During the XX century there has been intense human impact, especially in the coastal zone. In XX century the eutrophication of waters increased due to increase nutrients loading, and simultaneously climatic changes were observed in the Baltic Sea and its coastal bays and lagoons. The annual warming trend for the Baltic Sea basin has been shown to be 0.08°C/decade. This is somewhat larger than the trend for the entire globe (1861–2000), which is about 0.05°C/decade. The increase in water temperature can affect nutrient recycling and influence on phytoplankton species composition and primary production. For example, water warming may stimulate summer bloom warm-water Cyanobacteria [1, 2].

The Curonian Lagoon and Vistula Lagoon are the largest coastal lagoons of the Baltic Sea separated from the sea by narrow sand spits. These Lagoons are similar in ground types, mean depths, wind and temperature regimes, however quite different in continental runoff and water salinity. The Curonian and Vistula Lagoons are playing an important part in many fields of economy of Russia (Kaliningrad region), Lithuania and Poland. The watershed areas are located in density populated district with highly developed industry and agriculture. During recent decades, significant anthropogenic changes occurred in the Lagoons and their watershed areas. The Curonian Lagoon receives water from the River Nemunas, the third-largest contributor (after the Vistula and Oder) of total nitrogen and phosphorus to the Baltic Sea. The Vistula Lagoon receives water from the River Pregolya. Until the late 1980s nutrients loading exceeded by many times the permissible nutrients loading leading to eutrophication of water body with such mean depths. Multiple reductions of nutrients loading from the watershed area in 1990s owing to the economic crisis in the industry and agriculture did not result in considerable improvement of the ecological situation. Ongoing eutrophication and harmful algal blooms are the most important problems in the lagoons. Harmful algal blooms result in deterioration of the water chemical parameters, accumulation of algal toxins, oxygen deficiency and death of fish in the coastal zone.

Coastal lagoons are most vulnerable to direct impacts of natural environmental and anthropogenic factors including the processes observable at climate change and anthropogenic eutrophication. Due to this sensitivity, the analysis of long-term changes of hydrological, chemical and biological parameters in lagoons could help to demonstrate the actual relationship between global and local changes, discrimination what is “natural” from what is due to the human action. The purpose of this article is to analyze temporal changes of phytoplankton production, chlorophyll and nutrients concentrations in the water and to evaluate the impact of abiotic factors on eutrophication and primary production of the Curonian and Vistula Lagoons.

II. Materials and methods

The researches was carried out at 12 stations in the Russian parts of the Curonian Lagoon and 9 stations in the Russian parts of the Vistula Lagoon monthly from March (April) to November (October) since 1991 to 2014 (Fig. 1). Monitoring includes a lot of biological (chlorophyll, primary production, phytoplankton), chemical (nutrients, BOD_5, etc.), physical (transparency, temperature, salinity) parameters.

Fig. 1. Sampling sites in the Russian part of the Curonian Lagoon and Vistula Lagoon

The hydrological and hydrochemical parameters (water temperature, transparency and salinity, concentration of nutrients, including phosphate, nitrate, ammonia nitrogen, total phosphorus and nitrogen) were assessed in water samples from the surface layer with standard methods [3]. Concentration of chlorophyll *a* (Chl) was estimated at the surface, at the lower boundary of the photic zone and near the bottom. The concentration Chl *a* was determined by spectrophotometric method. Water samples were filtered through 0.3 μm membrane filters. The filters containing the phytoplankton were extracted using a 90% acetone solution and the optical density was measured at 5 wavelengths, i.e., 750, 664, 647, and 630 nm [4]. The photosynthesis intensity was measured applying the oxygen modification of the bottle method with short-period (3-5 hours) exposition of samples. In calculations of the primary production per unit area (m^2) the rates of photosynthesis and mineralization of organic matter were measured at 4 depth levels of the photic zone (100, 46, 10, 1 % of subsurface light intensity), and in the near-bottom layer. The sampling depths of subsurface light intensity are determined with underwater photometer or with use of dependence between subsurface light intensity and transparency of water on Secchi disk. The lower boundary of the photic zone was assumed at the depths of 1% of subsurface light intensity [5].

Long-term data on the water temperature were estimated on the basis of daily observations at standard hydrometeorological stations in the Curonian Lagoon (v. Otkrytoye) and Vistula Lagoon (v. Krasnoflotskoye), which were submitted by the Kaliningrad Center for Hydrometeorology.

The assessment of water eutrophication of the Curonian Lagoons was carried out according to trophic classification [6, 7]. According to these classifications (on the basis of Chl *a*, nutrients and primary production) 4 types of trophic state are allocated: oligotrophic, mesotrophic, eutrophic and hypertrophic.

III. Results and Discussion

Trophic status and effect of the climate change in the Curonian Lagoon

The Curonian Lagoon may be characterized as a hypertrophic water body on the basis of long-term chemical and biological data according to trophic classification [6, 7]. Hypertrophic status is observed on all water area of the Curonian Lagoon. In July-October intensive development of Cyanobacteria leading to the water "blooming" was observed in the Curonian Lagoon [8, 9]. The initial reason of hypertrophic state the Curonian Lagoon and blooms of Cyanobacteria was intensive external nutrients loading in XX century as the watershed area is located in density populated district with highly developed industry and agriculture. During 1989-1990, in the period of maximum fertilizers usage in agriculture and industrial development, the annual input of phosphorus were 3.7-8.5 g/m^2 and that of nitrogen – 60.8-109.6 g/m^2. Reduction of industrial production and fertilizers usage in 1990s resulted in a decrease of the external nutrients loading by 3-4 times to 0.75-2.3 g/m^2 of phosphorus and to 20.8-40.4 g/m^2 of nitrogen per year [10]. However, the research showed that neither a decrease of the trophic status nor an improvement of the ecological situation occurred in the Curonian Lagoon in 1990s-2010s. In the Russian part of the lagoon in 2001-2014 increased the number of stations where the average for the growing season Chl *a* concentration greater than 100 mg/m^3, and at these stations there is an extremely high level of eutrophication of waters. The concentration of Chl *a* and primary production in this lagoon are one of greatest in water bodies of basin of the Baltic Sea. The eutrophication processes and water "blooming" were most pronounced in the southern and central parts (the Russian zone) of the Curonian Lagoon (75% of the area), where the environmental conditions (high concentrations of nutrients in silt, continuously resuspension into the water column due to shallow depths, absence of the sea water intrusion, slow water exchange, fresh water) were favored for Cyanobacterial development. In northern, Lithuanian part the Curonian Lagoon the level of eutrophication and phytoplankton production are usually lower. This area adjoins to sea strait and is under influence of river flow Neman and Baltic Sea. Hydrodynamic activity (high flowing velocity) and brackish water prevent the "hyperblooming" of Cyanobacteria.

Eutrophication of the Curonian Lagoon affects at all trophic levels and primarily the intensity of phytoplankton development. The species typically abundant in eutrophicated waters prevailed in the phytoplankton (*Aphanizomenon flos-aquae, Microcystis aeruginosa, Aulacosira islandica*, *Actinocyclus normanii, Stephanodiscus hantzchii, S. minutulis,* etc) [9]. In summer, the ratio of mineral forms nitrogen and phosphorus (N:P <7) and phosphate concentration (30-40 mgP/m^3) create conditions for regular hyperblooms of Cyanobacteria (concentration Chl *a* > 100 mg/m^3). The annual cycle of primary production is characterized by summer maximum, which corresponds to maximal temperature of water and beginning bloom of Cyanobacteria (Fig. 2). During hyperblooms in the Curonian Lagoon Chl *a* reaches to 208-904 mg/m^3 and primary production - 9-16 g C /(m^3 day). This phenomenon is typical of eutrophic water bodies. A similar model of seasonal dynamics was already recorded in 1974-1976. A specific feature of 2000s was a high rate of primary production within a considerable part of growing period. In particular, in 2002 values of primary production, chlorophyll concentration and phytoplankton biomass close to maximum were recorded for three months (from July to September), which can be attributed to the hydrometeorological features of this year, e.g., high temperature (20°C and more) persisted until mid-September. Only after

cooling and a temperature drop down to 7-8°C, which was recorded in November or October, blooming of Cyanobacteria in the Curonian Lagoon ceased and organic matter production by phytoplankton abruptly decreased.

On the average for the period 2001-2014 phytoplankton primary production exceeded mineralization of organic matter on 30%. Such ratio testifies to accumulation of organic matter in water and sediments and further eutrophication of the Curonian Lagoon where on greater part of area slow water exchange is observed (Fig. 2a).

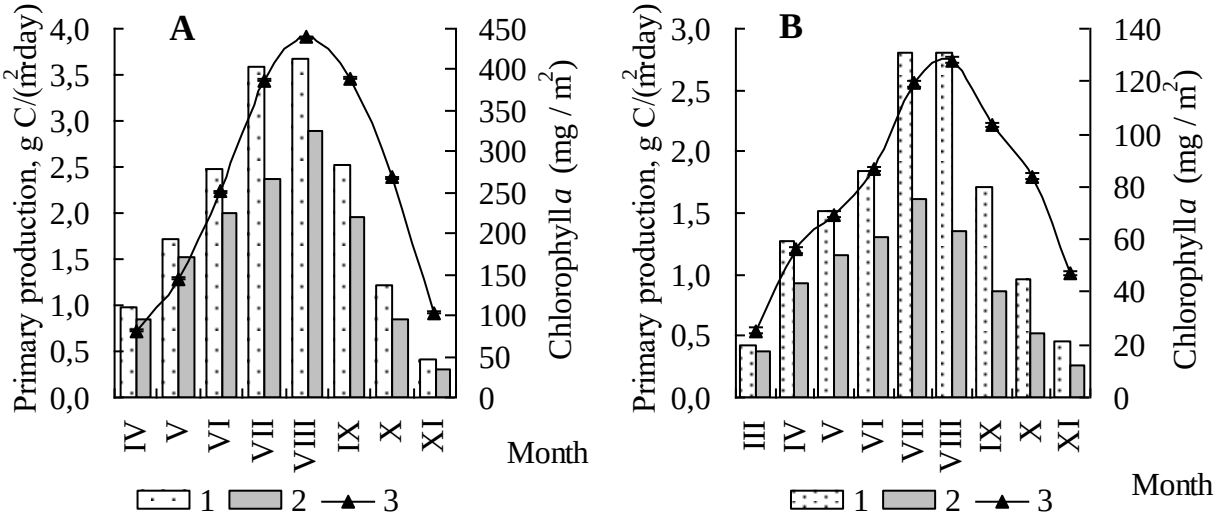

Fig. 2. Primary production (1), mineralization of organic matter (2) and Chl a (3) in the water column (mean for period 2001-2014) of the Curonian Lagoon (A) and Vistula Lagoon (B)

The Curonian Lagoon is characterized with high variability of Chl *a*, primary production and others trophic status indices in different years. The mean concentration of Chl *a* for the growing season (April - October) in varied between 36.2 and 210.0 (mean 99.7) mg/m^3. The primary production varies between 360 and 668 (mean 553) gC/(m^2·year) (Fig. 3).

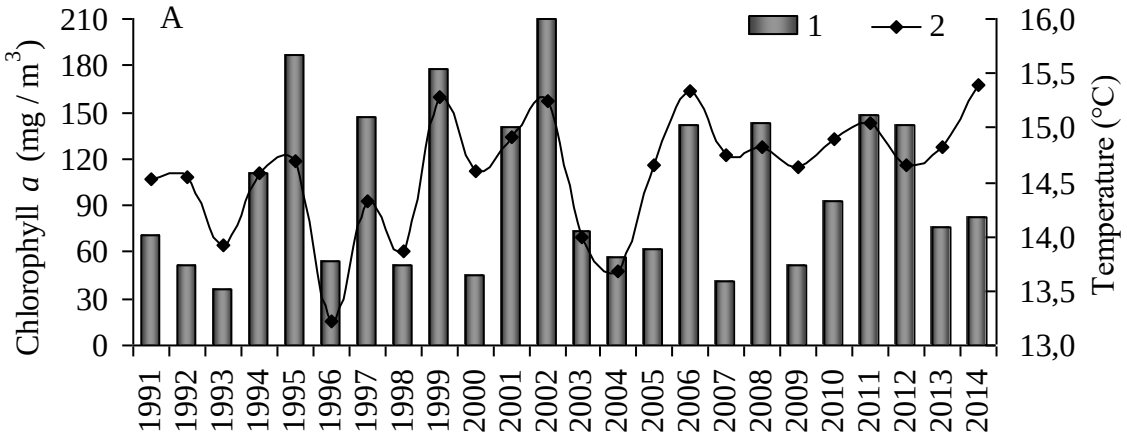

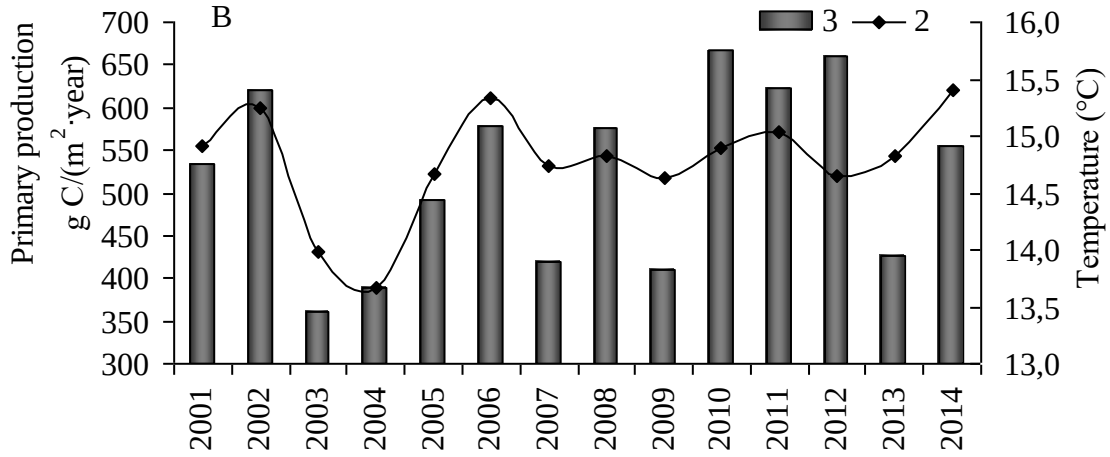

Fig. 3. The mean for the growing season (April - October) chlorophyll concentration (1) and temperature of water (2) and primary production (3) in the Curonian Lagoon

The years of maximum values of Chl *a* and primary production coincide with the years of maximum water warming-up and the hyperbloom of Cyanobacteria. For the period 1991–2014 Pearson correlations between average for the growing season (April–October) water temperature (t) and Chl *a* was 0.65. Of the hydrological and hydrochemical conditions existing in the most parts of the Lagoon, water temperature is the key factor determining the seasonal and long-tern variability of the primary production and abundance of phytoplankton. The optimal temperature for reproduction "outburst" and nitrogen fixing for *Aphanizomenon flos-aquae* which produces water hyperblooming is above 20°C [11, 12]. "Hyperblooming" of Cyanobacteria was observed at the mean water temperature above 20°C for summer and above 14.5 °C for the growing season (April-October) in the Curonian Lagoon. Small fluctuations of the mean summer water warming-up (in 2-3ºC) resulted in 2-4-fold variations of the trophic status indices (Fig. 3).

In XX and XXI centuries in the Baltic Sea and its watershed area warming trend were observed due to climatic changes. The trend to increase the mean water warming-up was recorded in the Curonian Lagoon (from 14.10°C in 1970s to 14.96°C in 2010s, i.e. equaled to 0.86°C for the latest 45 years). During the latest decades the trend towards increase number of "warm" years has been observed. The mean for the growing season water temperature above 14.5°C, typical to "hyperblooming", was observed 3 times in 1970s, 4 times in 1980s, 6 times in 1990s, and 13 times in 2000s (Fig. 4). In these "warm" years Cyanobacteria formed high biomass in summer and autumn owing to "outburst" reproduction pattern in combination with consumption of ammonia nitrogen and nitrogen fixation and high concentration of phosphorus in the water, which results in hyperblooms in the Curonian Lagoon.

The research of phytoplankton in 1980s-2010s showed that biomass of Cyanobacteria and Chl *a* in summer was always at the level of intensive bloom (10-100 g/m^3 in summer or 100 mg Chl *a*/m^3 average for the growing season) and during 13 seasons it reached the hyperbloom state (above 100 g/m^3 and 100 mg Chl *a*/m^3). "Hyperblooming" of Cyanobacteria was observed during 3 years in 1980s in the period of the most intensive nutrients loading and the remaining 10 years "hyperblooming" of Cyanobacteria were observed in 1990s-2010s when the input of nutrients from lagoon's watershed area multiple decreased [8, 9, 13].

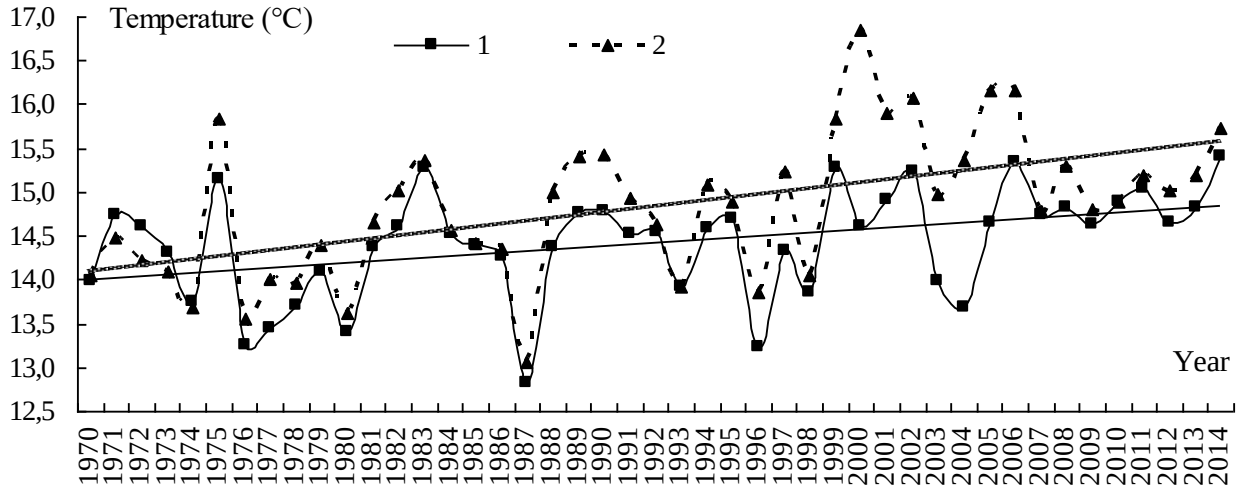

Fig. 4. The mean for the growing season (April – October) temperature of water in the Curonian Lagoon (1) and Vistula Lagoon (2)

The trend to increase the primary production of phytoplankton was recorded in the Curonian Lagoon in 2000s and 2010s (Fig. 5). Mean annual primary production in 2000s and 2010s (490 and 570 gC/(m^2·year)) is 2 times higher, than in the middle of 1970s (300 gC/(m^2·year)). That can testify about significant eutrophication in this lagoon for last thirty years where hyperbloom of Cyanobacteria are observed.

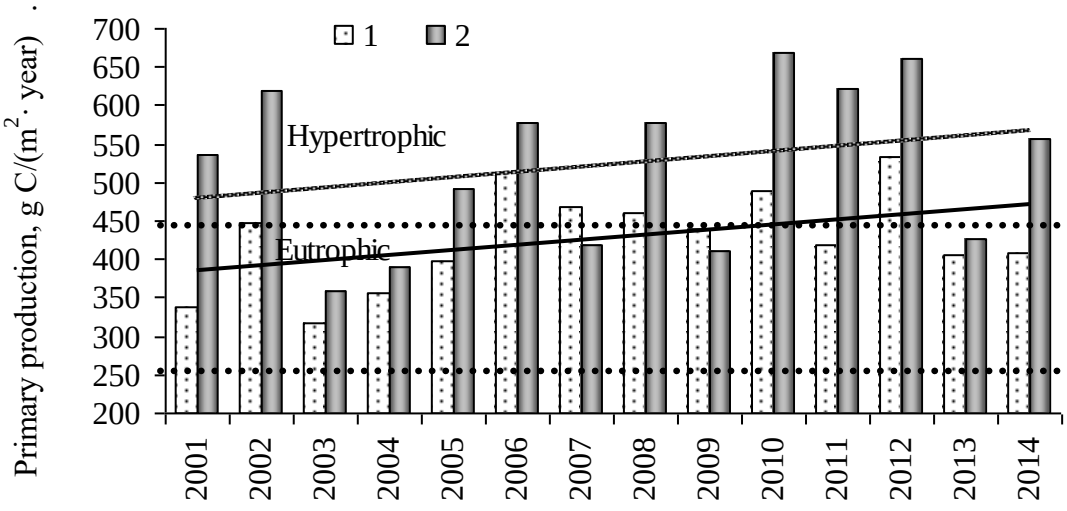

Fig. 5. Long-term trend of the primary production of phytoplankton in the Vistula Lagoon (1) and Curonian Lagoon (2)

In the years of hyperbloom of the Curonian Lagoon, Cyanobacteria biomass during the months July-October exceeded the level at which the eutrophication and pollution of the water body is observed. During the hyperbloom the biomass of Cyanobacteria may attain 1200-2500 mg/l, and concentration of Chl *a* - 700-3400 μg/l. Concentration and decomposition of Cyanobacteria leads to the oxygen deficit till to absolute absence (16% – 0% saturation) and death fish in the coastal zone [9]. These phenomena are of local nature and determined by direction of the wind during the bloom period. The years with persistent east winds in July-August resulted in the wind-driven aggregation

of Cyanobacteria near the western coast, which is the most inhabited and recreationally developed area (the resort city Zelenogradsk and the National Park of Curonian Spit) are most unfavorable.

Cyanobacteria blooming have become a serious problem in recent decades, because many bloom-forming species are reported to be able to produce secondary metabolites toxic to many organisms, including fish, mammals and humans. The toxic Cyanobacteria species found in the Curonian Lagoon and can produce microcystins, neosaxytoxins, anatoxin. During the period of Cyanobacteria blooming concentration microcystins varied between 0.1 and 134 μg/l in water of the Curonian Lagoon Curonian Lagoon whereas safe level of 1.0 μg/l for drinking water Algae toxins also detected in sediments, mussels and fish. Fishes are most vulnerable to Cyanobacteria effect [13, 14]. Fish intoxication by toxins of Cyanobacteria results in pathological damages. In the period of Cyanobacteria hyperblooming in the Curonian Lagoon the morphopathological and histopathological changes were found in 70-80% of mature bream (*Abramis brama*). The detected pathological changes in fish were similar to the symptoms of affected by toxins of Cyanobacteria which dominated in summer and autumn [15]. This indicates the possible toxic impact of Cyanobacteria on fish and pollution effect on the ecosystem.

So, the more intensive water warming and the increase in the number of “warm” years in 1990s-2010s created favorable conditions for hyperblooming Cyanobacteria and increase of primary production. The local climate warming in the Baltic region is a probable reason of the ongoing eutrophication and harmful algal blooms of the Curonian Lagoon despite of significant reduction of external nutrients loading in 1990-2000s. Climate changes represents a risk for coastal water bodies, as this stimulates hyperblooms of Cyanobacteria.

Trophic status and effect of the climate change in the Vistula Lagoon

Vistula Lagoon is located in the densely populated area with developed industry and agriculture. Lagoon is subject to the strong impact of the anthropogenic factors (nutrients and pollutants input with river flow and waste water). Vistula Lagoon receives the intensity of external nutrient load to the river runoff and waste water from cities (especially from Kaliningrad). Eutrophication is most strongly expressed in east freshened part Vistula Lagoon, where salinity of water is less than 4.5 ‰. In this area according to the values of Chl *a*, phytoplankton abundance and primary production the hypertrophic levels are observed. The combination of environmental factors (high concentrations of nutrients in water and silt, continuously resuspension due to shallow depths. strong summer warming-up of water) creates optimal conditions for the "blooms" of phytoplankton. In the central part of the lagoon where the mean annual salinity of 4.5 PSU and more, a sharp decrease primary production and chlorophyll (to 2 times) to eutrophic level is observed, which are further stabilized in the whole area to the sea strait. In summer, the ratio of mineral forms nitrogen and phosphorus (N:P < 7) and phosphate concentration (30-40 mgP/m^3) create conditions for algae blooms (Chl *a* concentration usually exceed 30-40 μg/l and sometimes reaching 100 μg/l).

The annual cycle of primary production is characterized by summer maximum, which corresponds to maximal temperature of water and algae bloom (Fig. 2b). On the average for the period 2001-2014 phytoplankton primary production exceeded mineralization of organic matter on 60%. Such ratio testifies to accumulation of organic matter in water and sediments and further pollution of the Vistula Lagoon and in the adjacent water area of the Baltic Sea.

The Vistula Lagoon is characterized by a rather low variability of Chl *a*, primary production and others trophic status indices in comparison with the Curonian Lagoon (Fig. 6). The mean Chl *a* for the growing season (April - October) in 1991-2010 varied between 29.0 and 51.2 (mean 40.8) mg/m^3. After the invasion of the North American filter-feeding bivalve *Rangia cuneata* Chl *a* decreased by 2 times (from 39 mg/m^3 in 2001-2010 to 20 mg/m^3 in 2011-2014). The primary production in 1991-2014 varies between 316 and 533 (mean 428) gC/(m^2·year).

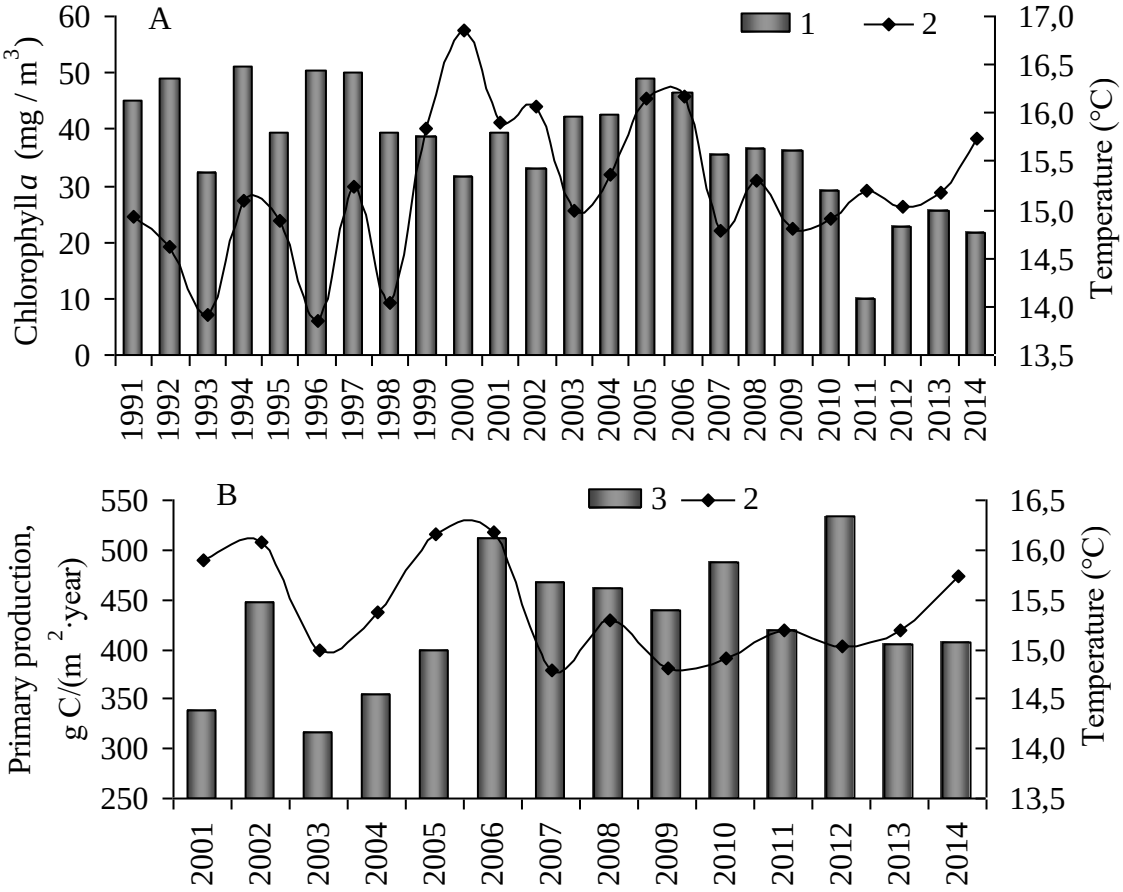

Fig. 6. The mean for the growing season (April - October) chlorophyll concentration (1) and temperature of water (2) and primary production (3) in the Vistula Lagoon

The climate change in 1990s-2010s also affected the water temperature in the Vistula Lagoon. During the latest decades the trend towards increase number of "warm" years has been observed. The mean for the growing season water temperature above 15.0°C was observed only once in 1970s, 4 times in 1980s and 1990s, and 12 times in 2000s (Fig. 4). Mean annual temperature water increased by 1.2°C for 40 years (from 14.2 °C in 1970s to 15.4 °C in 2000-2010s), and warming and the increase in the number of "warm" years combined with other factors created conditions for phytoplankton "blooms" in 1995-2014. In "warm" years the tendency of a growth abundance and biomass phytoplankton and increase in the share of Cyanobacteria in total biomass. In "cold" years the phytoplankton abundance decreases and the share of Bacillariophyta and Chlorophyta in the total biomass increases [16].

The trend to increase the primary production of phytoplankton was recorded in the Vistula Lagoon in 2000s and 2010s (Fig. 5). Mean annual primary production in 2000s and 2010s (415 and 450 gC/(m^2·year)) is considerable higher, than in the middle of 1970s (300 gC/(m^2·year)).

Great changes have taken place in the Vistula Lagoon in the 2010s after the invasion of the North American brackish water filter-feeding bivalve *Rangia cuneata* [17]. The benthic biomass increased by 20 times (from 29 g/m^2 in 2000s to 650 g/m^2 in 2012) and Chl *a* decreased by 2 times (from 40 g/m^3 in 2000s to 20 g/m^3 in 2010s). Before the invasion the regular algae "hyperbloomings" were observed in the lagoon. In 2011 and 2012, the summer algae bloom was not observed and the Chl *a* was at minimal level (Fig. 6). In the last 2 years the seasonal dynamics of phytoplankton recovered, but the abundance of phytoplankton and Chl *a* have stabilized at a lower level compared with the previous decade. Invasion mollusk has impact on the primary production. The phytoplankton assimilation numbers as an indicator of the rate of photosynthesis increased by 2-3 times (to 300-400 mgC/(mgChl·day). Transparency also increased by 2 times and now the photic zone reaches the bottom. As a result, primary production under m^2 in 2011 remained at long-term level, despite Chl decreased by 4 times. In 2012, primary production increased due to the spring bloom, and it reached a maximum.

So, invasion filter-feeding mollusks significantly improved water quality but primary production in the ecosystem of the Vistula Lagoon remained on long-term eutrophic-hypertrophic level, which creates favorable conditions for the other trophic groups (zooplankton, benthos, fish). If global warming continues, can be expect to remain long-term trend of increasing primary production and eutrophication in the Vistula Lagoon. In the Vistula Lagoon intensive filter-feeding mollusks and "critical salinity" will prevent harmful algal blooms and promote the conservation water quality at possible levels.

IV. Conclusions

Curonian and Vistula Lagoons are the largest coastal lagoons of the Baltic Sea, relating to the most highly productive water bodies of Europe. Reductions of nutrients loading in 1990s did not result in improvement of the ecological situation. In these Lagoons, unlike many inland and coastal marine waters, eutrophication of water continues. Hydrological and chemical parameters are the main factors that influence on the algal blooms and ecosystem health in these lagoons. The Curonian Lagoon may be characterized as a hypertrophic water body. In recent decades "hyperblooms" of Cyanobacteria are observed more frequently in the Curonian Lagoon. The Vistula Lagoon may be characterized as eutrophic or hypertrophic for different parts. The more intensive water warming and the increase in the number of “warm” years in 1990s-2000s created favorable conditions for algae blooming and high rates of primary production in the lagoons. The local climate warming in the Baltic region is a probable reason of the ongoing eutrophication of the Curonian and Vistula Lagoon despite of significant reduction of external nutrients loading in 1990-2000s. If global warming continues, can be expect to remain long-term trend of increasing primary production and eutrophication in the Curonian Lagoon and the Vistula Lagoon. In the Curonian Lagoon climate changes represents a risk for ecosystem, as this stimulates hyperblooms of Cyanobacteria. Harmful algal blooms result in deterioration of the water chemical parameters and death of fish in the Curonian Lagoon. "Hyperblooms" is the most dangerous for coastal towns and tourist resorts

(UNESCO National Park "Curonian Spit"). In the Vistula Lagoon intensive development of filter-feeding mollusks will prevent harmful algal blooms and promote the conservation ecological state at possible levels.

V. References

[1] "Environment of the Baltic Sea Area 1994-1998", *Baltic Sea Environment Proceedings*, vol. 82. HELCOM, 2002.

[2] "Climate Change in the Baltic Sea Area", *Baltic Sea Environment Proceedings*, vol. 111. HELCOM, 2007.

[3] "Chemical measurements in the Baltic Sea: Guidelines on Quality assurance", *ICES techniques in marine environmental sciences*, vol. 35. Copenhagen, 2004.

[4] L. Edler, "Recommendations on methods for marine biological studies in the Baltic Sea. Phytoplankton and chlorophyll", Baltic Marine Biologist, vol. 38, 1979.

[5] R.A. Vollenweider, J. F. Talling, D.F. Westlake, *A manual on methods for measuring primary production in aquatic environments*. Backwell Scientific Publications, 1974.

[6] L. Hakanson, V.V. Boulion, *The like foodweb- modeling predation and abiotic/biotic interactions*. Leiden: Backhuys Published, 2002.

[7] N. Wasmund et al., "Trophic status of the south-eastern Baltic sea: a comparison of coastal and open areas", *Estuarine, Coastal and Shelf Science*, vol. 53, pp. 849-864, 2001.

[8] I. Olenina, "Long-term changes in the Kursiu Marios lagoon: Eutrophication and phytoplankton response", *Ecologija*, vol. 1, pp. 56-65, 1998.

[9] S.V. Aleksandrov and O.A.Dmitrieva, "Primary Production and Phytoplankton Characteristics as Eutrophication Criteria of Kursiu Marios Lagoon, the Baltic Sea", *Water Resources*, vol. 33 (1), pp. 97-103, 2006.

[10] A. Cetkauskaite, D. Zarkov, L. Stoskus, "Water-quality control, monitoring and wastewater treatment in Lithuania 1950 to 1999", *Ambio*, vol. 30 (4-5), pp. 297-305, 2000.

[11] G.J. Waughman, "The effect of temperature on nitrogenase activity", *Journal of Experimental Botany*, vol. 28 (105), pp. 949-960, 1977.

[12] B.A. Whitton, "Freshwater plankton", *The biology of blue-green algae*, vol. 9, pp. 353-367, 1973.

[13] O.I. Belykh et al., "Identification of toxigenic Cyanophyta of the genus Microcystis in the Curonian Lagoon (Baltic Sea)", *Oceanology*, vol. 53 (1), pp. 71-79, 2013.

[14] A. Paldaviciene, H. Mazur-Marzec, A. Razinkovas, "Toxic cyanobacteria blooms in the Lithuanian part of the Curonian Lagoon", *Oceanologia*, vol. 51 (2), pp. 203-216, 2009.

[15] N. Chukalova and O. Dmitrieva, "Main results of fish disease monitoring in the Curonian Lagoon (the South East Baltic Sea)", *Health and Diseases of Aquatic Organisms: Bilateral Perspectives. International Standard Book. Living Ocean Foundation*. Michigan State University, 2010. pp. 24-31.

[16] S.N. Semenova and V.A. Smyslov, “Peculiarities of the State of Phytoplankton in the Baltic Sea's Vistula Lagoon at the Turn of 21st Century”, *Inland Water Biology*, vol. 2 (4), pp. 305-311, 2009.

[17] S. Aleksandrov, J.Gorbunova, L. Rudinskaya, “Effect of climate change and mollusc invasion on eutrophication and algae blooms in the lagoon ecosystems of the Baltic Sea”, *Geophysical Research Abstracts*, vol. 17. EGU General Assembly, 2015. EGU 2015-5846.

ICE AGE AND COASTAL ADAPTATIONS

Aleksey Amantov, VSEGEI, Russia
Willy Fjeldskaar, Tectonor, Norway

4448470@mail.wplus.net

Eustatic changes have interrelations with other long-term processes, connected with the glacial activity and related isostatic adjustment. Topographic changes in glacial and periglacial areas, linked with sediment- and hydro-isostasy, influence the redistribution of amount of water globally before and after glaciations. Glacial erosion is a significant, but variable factor. Many enclosed basins of different order- including the Baltic -were created or strongly modified by this process. In relation to the ice age onset they can hold additional amount of water, even if related isostasy reduces its volume. Accumulation replaces ocean water by low-compacted sediments, with additional subsidence, but part of deposition remains in coastal areas. Negative topographic elements, previously occupied by central parts of ice sheets (Bothnian, Hudson Bay) would likely remain stable water storage with gradual shallowing up to future system of giant lakes. Hydro-isostasy impacted non-uniform relocation of coastal zone in local and regional scale.

Key words: glaciation, erosion, accumulation, isostasy, modeling, hydro-isostasy, mantle, rheology

I. INTRODUCTION

The Ice Age is known to influence ocean level and shorelines globally in different way (e.g. [1, 2]). The obvious major impact is usually assigned to the processes of growing and melting of ice sheets, linked with eustatic changes. Such changes of a shape and thickness of former ice sheets and water volumes influenced the load of Earth's crust, generating isostatic adjustment movements in response to the loading – unloading cycles. However, glacial and periglacial areas experienced variable, but often strong, geomorphological changes caused by erosion and accumulation. Glaciers could commonly modify, deepen pre-glacial lowlands and overdeepen their fragments, creating small or huge, isolated or complex basins. It would not be exaggeration that the Baltic Sea lowland was in high degree created and sculptured by glaciations. Here we focus on gradual topographic changes mostly in glacial and periglacial areas under the rare point of view: changing the redistribution of amount of water globally before and after glaciations under the influence of erosion, accumulation and isostasy.

II. METHODS

In estimations we performed modeling of topographic changes in time for ice sheets of Atlantic region, mostly in North Europe and adjacent areas, and – in less degree – North America segments. It included reconstructions of possible ice expansion and decay with thickness

approximation, water and sediment redistribution, and isostatic adjustments caused by mentioned processes.

Our automated modeling was made with 10 km grid spacing and less. It used different reconstructions of ice sheets in time [3, 4, 5, 6], with variable interval of time slices up to 1000 ka for the last deglaciation. Reconstructions of an ice sheet thickness were independent from the isostatic adjustment reconstructions, in comparison with some other models [5]. In spite of numerous variants due to climatic and glaciological uncertainties, our modeling accounts for the flow law and general pattern of ice sheets, including determination of fast-flow ice stream erosion and areas of stagnation, changes of the pattern in time due to topographic, geological and climatic factors, which could result in different ice-bed conditions. Different models were tested.

Climatic, geological, geomorphological and tectonic features could influence the history of glacial grows and decays of prominent regions. The first-order pre-glacial landscape elements were among the major factors that could partly control centers of ice nucleation and its basal velocities in favorable circumstances. In time, many landforms were in various degree modified by glacial and periglacial processes, in particular by erosion. Estimation of Plio-Pleistocene erosion and deposition was performed by combining regional geological-geomorphological analysis and rate-based time-scale reconstructions, with mass-balance control [7].

The model has been calibrated on Russian platform, where it was possible to examine preserved elements of pre-glacial Neogene topography in bordering non-glaciated areas, and distinguish their gradual erosion modifications in neighboring regions that underwent assorted duration of glacial activity. Such time-scale reconstructions are based on software tools to infer reasonable glacial erosion and sedimentation rates, and with geological and physical constraints. As in the case of ice sheet thickness reconstructions, we use the same information about an ice sheet position over time, accounting for the speed of growing and decay in calculated interval. Ice boundaries give a hint of likely concentric changes of the erosion rates, increasing to the margins. Even details of outlines may indicate the differentiation of ice flow, when fast-flowing ice streams have largest erosion capacity. Further determination of such differentiation was performed using detailed bedrock grid analysis (or other surfaces, indicating interglacial stages if they could be compiled), and special filtering.

Attention was also focused on bedrock lithological properties and different rock resistance. Soft rock types could be eroded faster in zones of erosion, but also content of fresh resistant abrasive is likely of importance. To account for this special grids were involved, with rock complexes coded in values of relative erodability. Additional complications of the pattern by fluvioglacial activity were accounted for in simplified form, without consideration on exact position of particular generated landscape elements, like tunnel valleys.

Upper regional unconformity separates bedrock from the Pleistocene and Holocene sediments with thickness up to 300-400 m onshore, but much larger accumulation is known on the continental slope. Overall simplified isopach map was compiled from numerous published sources to compare with modeling results (Fig. 1). Glacial sedimentation was balanced with erosion, being computed in simple agreement with general basic tendencies of redistribution and migration, but without accounting for bottom currents and some other factors. Subglacial accumulation was placed

in reconstructions randomly in relevant zones with higher degree of its expectation due to sub-glacial topography.

Forecast of permafrost was also required, as a candidate to change basal conditions with ice stagnation or low velocity. Permafrost also increases erosion resistance for many types of sediment. The depth of permafrost distribution and time changes could be approximated, solving Stefan's problem. However, scenarios of glaciations, their shape and climate changes are disputable, increasing uncertainties of the modeling process and resulting options. Several known climate reconstructions were involved to estimate mean annual temperatures and quantify possible permafrost depth, accounting for possible ice-sheet related temperature depressions. In time-slices they were reinterpolated in agreement with changing the outlines of the ice sheets.

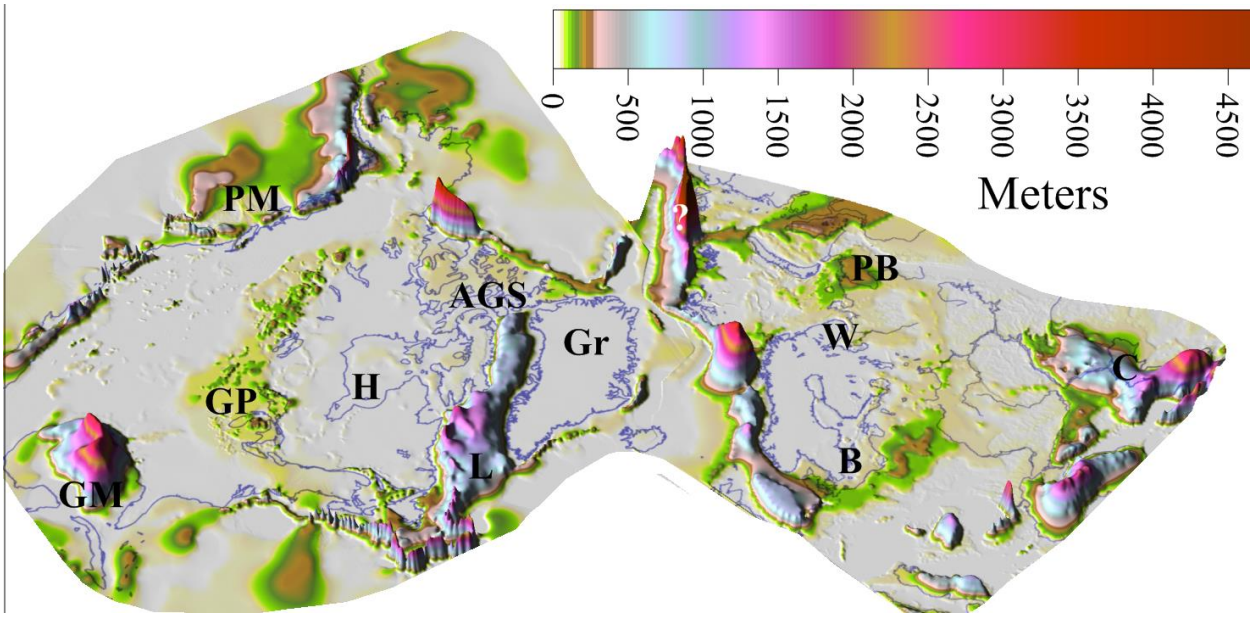

Fig. 1. Dominantly Pleistocene-Holocene accumulation.
Compiled by A. Amantov (1989, VSEGEI Report) from numerous published sources. PM-Pacific Margin, GP-Great Plains, GM-Gulf of Mexico, H-Hudson Bay, AGS-Arctic Gulfs and Sounds, Gr-Greenland, B-Baltic Sea, W-White Sea, PB-Petschora Basin, C-Caspian Sea.

Models of the basal sub-ice temperature based on relevant models for Greenland and Antarctic ice sheets were used to estimate possible zonation and variability of warming effects of ice sheets [4]. Special additional grids, with relevant information (like showing geologically proved frozen-bed conditions) were used as additional input.

Moving back in time, eroded volumes were put back, with restoration of topography and drainage pattern over time. Special analysis was addressed to overdeepenings of different order, which are widespread in glaciated areas. They were estimated using landscape grid filtering with changing rectangular sub-array of nodes. However, correct topography restoration is impossible without determination of isostatic changes caused by redistribution of sediments, ice and water.

The isostatic response to deglaciation was modeled using an Earth model with a layered mantle viscosity overlain by an elastic lithosphere. Different values of flexural rigidity and asthenosphere viscosity were checked to get a best fit between theoretical and observed present rate

of uplift and tilting of paleoshorelines. The best fit was achieved with a low-viscosity asthenosphere of thickness less than 150 km and viscosity less than 7.0x10^19 Pa s above a uniform mantle of viscosity 10^21 Pa s, and an effective elastic lithosphere thickness (te) of 30-40 km (flexural rigidity less than 10^24 Nm).

III. RESULTS AND DISCUSSION

Glaciations in time

The continental part of the North Atlantic segment with adjacent shelf regions was repeatedly covered with a continental ice sheet, at least since Gelasian. However the patterns and extents of the early glaciations are very disputable. In contrary to common opinion on the relatively local ice sheets, we believe that extensive Gelasian glaciations are likely. The first 2.4 Ma recorded advance of the Laurentide Ice Sheet reached 39°N near the extreme southern limit of North American glaciation [8]. Far-reaching glaciation of comparable age, covering the Barents Sea and Fennoscandia, was expected in paleogeographical reconstructions of possible pro-glacial lakes close to Caspian depression with rare possible indications of such ice sheet [9]. We assume such option in the modeling. However, specific features are reasonable at the beginning of the ice age. Specific ice base conditions are expected, because of broad distribution of saprolites or weathering crusts. They could cause relatively thin fast-moving ice, with short-term exception in areas of extensive discontinuous permafrost.

More distinct radial glacial erosion pattern and larger basal ice velocities seem likely at the beginning of the early ice-age stage, with partial widening of pre-glacial drainage elements. Intensive cryo-hydration weathering, solifluction or gelifluction at slopes, and intensive (coastal retreat rates up to 1 m/year and more) thermal abrasion are expected in areas without direct glacial influence because of general climatic changes. Wide - originated from Cenozoic stages -lowlands with meandering rivers (often in permafrost conditions) could provoke early stage onset of ice-streams, but only in favorable conditions. Over time, further complication of the pattern from radial to "spider web" is expected due to gradual developing of topographic ice-streams. It is also worth mentioning progressive exhumation of resistant formations, additional complications of the pattern by fluvioglacial activity and glacial sedimentation, "pendulum" principle, with increasing amount of glacial and interglacial sedimentation in eroded material [7].

Approximated variable permafrost distribution seems to be an additional weighty aspect, changing erosion rates during some time intervals. This contributed to differentiation of erosion with heights, because thick continuous permafrost could be developed on relative highlands without protection of large water bodies that did not freeze to the bottom, keeping “warming effect”. Such effect was dependent on eustatic changes and outlines of continental shelf and inner basins, in spite of known possibility of thin permafrost occurrence in cold Arctic seas in restricted height intervals. During onset of glaciation, permafrost-free areas could be subject to faster ice flow and increased erosion. Vice versa, lowlands bearing major topographic ice streams were likely represented by taliks not affected by continuous permafrost or - depending on scenarios and parameters - were shortly affected by reduced permafrost with thick active layer. So, zones were likely stable in space. Also, linear taliks of discontinuous permafrost zone on terrigenous sediments could contribute tunnel valley formation.

Accumulation

In areas that underwent strong ice sheet activity, the upper regional unconformity represents bedrock surface, sculptured by different erosion agents. Their role is often debated [7], but volumes of deposits unquestionably show huge sediment redistribution during ice age. The bedrock is usually covered by the Pleistocene and Holocene sediments, with non-uniform thickness ranging from 0 to 400 m and even more in continental part, but the offshore sedimentation on the continental slope and ocean bottom is known to be an order larger [10, 11]. Such zones of accumulation bound zones of variable erosion and weak deposition, exhibiting general concentric arrangement of glacial activity. However, it usually shows concentric pattern either from the last glacial dome, or from the most active and stable one. It could also differ from the pattern of older or weaker ice sheets, not indicating fluctuations of the position. In parts, resulting zone of accumulation (Fig. 1) covers zone of deep erosion, which was formed mainly by early and/or largest ice sheets. Zone of accumulation in platform domains of Europe extends from Poland and Buelorussia to Petschora basin of the Arctic region (Fig. 1). The average thickness here is more than 50 m, often exceeding 100 –150 m, while the section commonly belongs to several glaciations [12, 13]. Similarly, on the opposite side of Atlantic, sedimentary record of the great western plains of Canada shows that the Laurentide glaciers advanced across the plains at least five times [14, 15]. From southern New York and Ontario westward over the Mississippi valley, west and northwest of the Appalachian Escarpment on the great western plains of Canada, thickness exceeds an average of 25 - 35 m over wide areas, up to 150 – 200 m and more in numerous places [16, 17, 18]. Large areas in the southern peninsula of Michigan, western and southwestern Minnesota, eastern Dakota, western Iowa, and the Great Bear Plain are underlain by more than 70 m of glacial sediment. The pattern of distribution of accumulated material and thickness changes looks very similar to the European one, but some differences could be mentioned. Mostly they are connected with the development of active Cordillera mountain belt, providing its own distinct ice sources of montane glacier, local ice caps, sometime joining into Cordilleran Ice Sheet. It affected onshore accumulating belt from western directions. Everywhere on a soft sedimentary cover deeply incised valleys are common as newly created forms or as modifications of preglacial and interglacial valleys by glacial and fluvio-glacial erosion. They are partly filled with stratified glacial (often representing several glaciations) and Holocene sediments, commonly more than 60 - 100 m thick.

The above-mentioned zones of platform accumulation are only a small part, indicating glacial erosion because of transportation of suspension material into the main peripheral sedimentary basins and on adjacent ocean slope. Large sedimentary fans with definite glacier derived input are well known around Barents Sea continental margins and Norwegian shelf [19, 20]. In Europe main arteries of such transfer of sediments are: Baltic and Kama - Volga marginal (in relation to the glacial boundaries) paths, Dnieper and Don radial conduits [21].

In North America several equivalents exist. The eastern branch of sediment delivery from the central areas of major ice sheets was along the Hudson Bay path - through Hudson Strait with Ungava Bay into the Labrador Sea. Sediment supply results in thick Plio-Pleistocene sedimentary section of the Labrador Sea totaling hundreds of meters [22, 23]. The Arctic Junction Arteries include system of Arctic gulfs and sounds. Radial troughs of Gulf of Boothia with Prince Regent Inlet as well as Mc-Clintoc Channel and Peel Sound combined with crossing marginal system

McClure Strait –Viscount Melville Sound to Lancaster Sound. This system of glacial avenues with imprint of deep glacial scour rather than fluvial erosion [24] redistributed ice-rafted debris sourced from northern part of the Hudson Bay Lowland and adjacent part of Canadian Shield in opposite directions from approximate divide at longitude of Boothia peninsula. Lancaster Sound was a path of sediment delivery to the east into trough-mouse fan of Baffin Bay [25]. Alternate destination was Arctic Ocean via McClure Strait.

The Mackenzie Path followed marginal bedrock lowland between the Canadian Shield and sedimentary cover in Lake Athabasca, Great Slave Lake, Great Bear Lake sector with approximate length of around 4 000 km. It transported eroded material from the western part of the Canadian Shield and Rocky Mountains into the Beaufort Sea. As a result oceanward prograding sequences of large delta complex have been deposited, thickening from zero edge on the landward side to over 4000 m in the north Beaufort Sea [26].

The Mississippi Path transferred and redistributed material from the sector between Appalachian Mountains and Rocky Mountains into the Gulf of Mexico as an excellent example of glacial reorganization [11]. It also captured part of material from the Mississippi Path around Great Lakes (especially Lakes Huron – Erie – Ontario segment).

Pacific margin is known to be complicated, with intensive linked tectonic and denudation processes producing large amount of sediments. It also shows large-distance transportation of debris using sophisticated sediment-transport conduits to distal fans and abyssal plains. Such redistribution seems to be controlled by ocean bottom topography, which is strongly generated by structural influence of ocean ridges, rift valleys and transverse fracture zones [27, 28].

In Greenland glacigenic debris was deposited in the Amundsen Basin of the Arctic Ocean, on the East Greenland continental margin, Baffin and Labrador Seas, with partial redistribution in the Atlantic Ocean by bottom currents [29, 30]. The North Pole fan also developed from a source area at the North Greenland and Canadian Arctic continental margin [31, 32].

As a result voluminous amount of debris has been added into the ocean during ice age, for the Arctic – North Atlantic glaciated segment. It is less consolidated material in comparison with eroded bedrock. The accumulation also caused subsequent isostatic compensation, mostly subsidence of large depocenters (Fig. 2). However, it is important that smaller, but still voluminous amount of Pleistocene – Holocene sediments rests on-shore. For example, its volume in areas around the southern Baltic is comparable with large part of supposed erosion of this entire lowland. Onshore accumulation belts, changing the topography and drainage pattern, could also contribute to creation of «water storages».

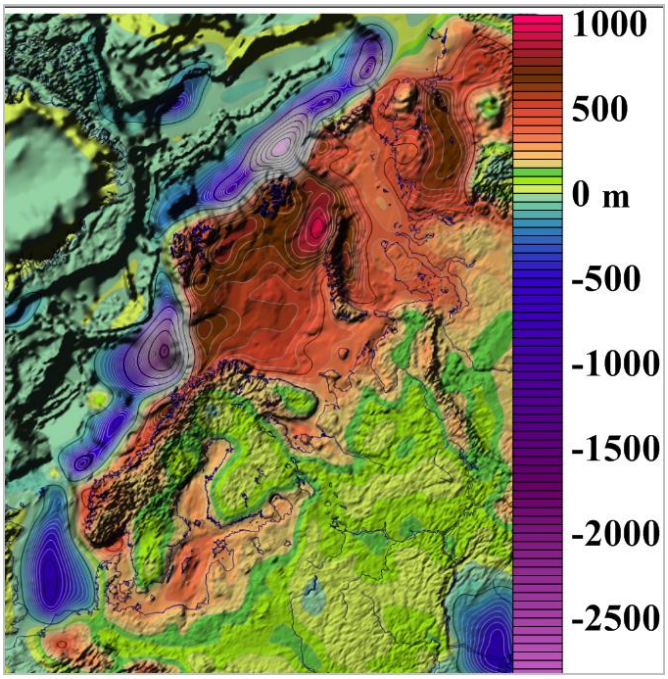

Fig. 2. Calculated isostatic response of Pleistocene-Holocene accumulation and erosion in Fennoscandia and adjacent regions.

Erosion

Glacial erosion is a significant, but variable factor. In particular – as one of the well-known and most recognizable features - it creates numerous overdeepenings of different scale in favorable conditions (Fig. 3), especially in zones of ice streams with reduction of the angle of the base. It is common to different landform types of variable scale, like glacial corries (cirques), lowlands in fjords [33], or just isolated basins of different size. In many cases glacial erosion deepened such areas hundreds meters below the drainage thresholds and "normal" non-excavated thalweg heights. Many huge enclosed basins - including the Baltic Sea - were created or strongly modified by this process. In counting the water-balance we are mostly interested in possible changing of water storage in continental parts. In relation to the ice age onset they hold additional amount of water in inner lakes and seas. In case of huge first-order overdeepenings, the related isostatic uplift often reduces its volume. Only extensive erosion zones - like the Baltic – White Sea lowland - have distinct relevant isostatic rebound component, in opposite to local overdeepenings.

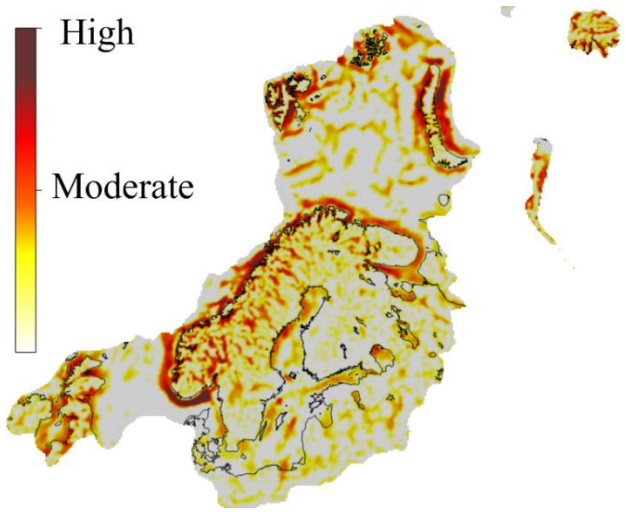

Fig. 3. Largest zones of glacial overdeepenings from automatic landscape analysis.

Water redistribution

Climate factors, with growing and decay of ice sheets and glaciers, contributing to erosion and accumulation are linked with water redistribution on the Earth surface. All processes are tied with isostatic adjustment and overall landscape changes in a sophisticated closed circle. The role of isostasy of water change is larger than many expect. To simplify, we would mention global (ocean) and local (inner seas and prominent lakes) components. Eustatic changes caused isostastic adjustment not only of the ocean bottom, but of the continents, normally with the reversed direction. Since the surface land area is only 29-30%, its "reversed response" could be much larger than the ocean adjustment (e.g. [1]).

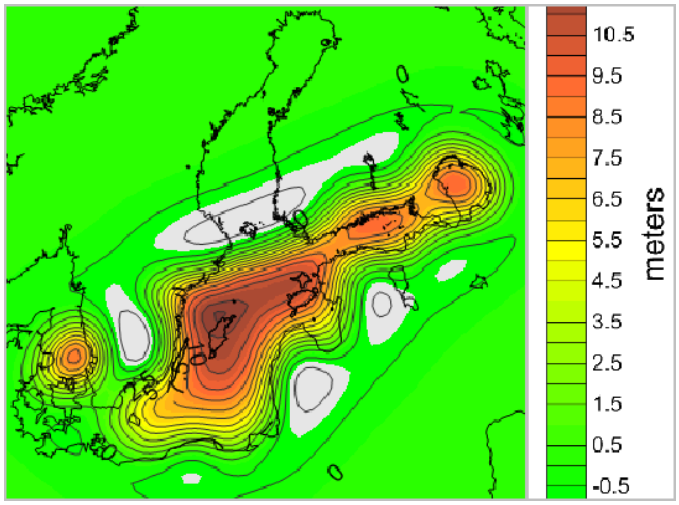

Fig. 4. Modelled hydro-isostatic reaction on the largest final Baltic Ice Lake drop.

Local component is also important to calculate deviations from the "pure" glacial isostatic adjustment. Here we show example of a model of the hydro-isostatic reaction on the final Baltic Ice Lake drop (Fig. 4).

Central zones

It is normally accepted that central zones of the expanded ice sheets were strongly depressed, depending on the ice thickness in areas of ice divide. After the melting they exhibited huge water

storage with additional weight. Water volumes have different estimations because of uncertainties of ice models and rheological parameters used by different researchers. In the same way remaining uplift is estimated differently. Our model and the resulting landscape are shown Figure 5.

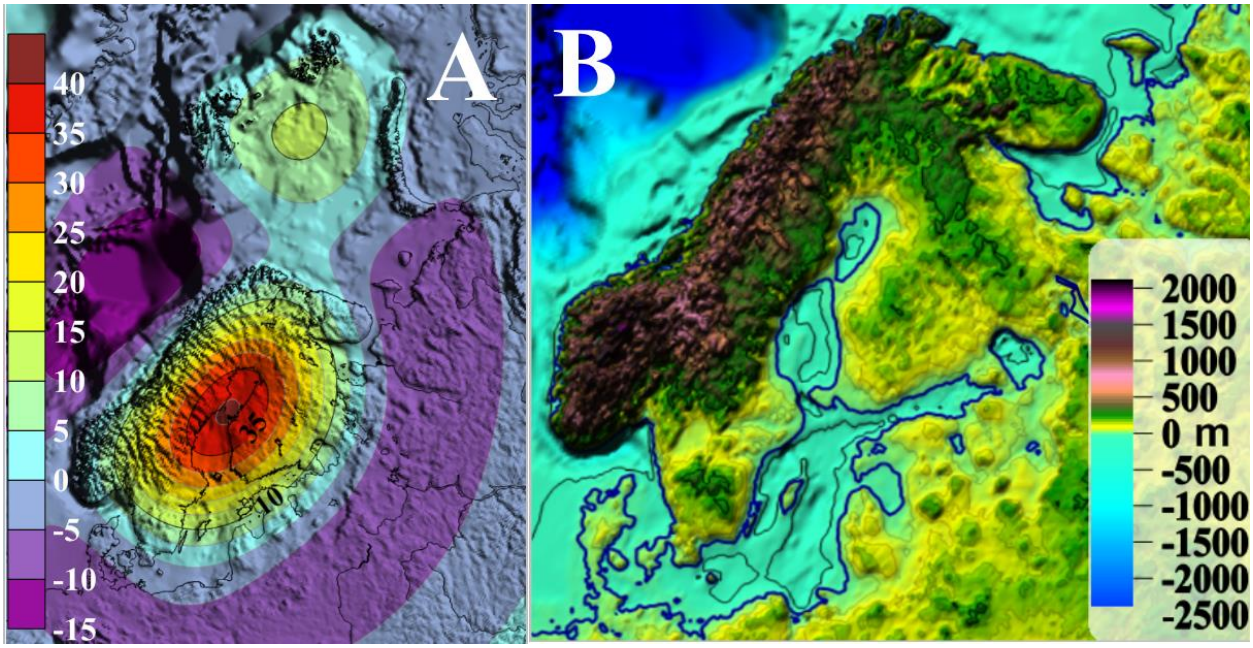

Fig. 5. Remaining isostatic uplift (m) of Fennoscandia from best-fit parameters and one of the ice sheet models (A), and possible landscape changes model, accounting for future uplift, eustatic changes and sediment redistribution (B).

In spite of different history of glacial isostasy, negative topographic elements on pliable sedimentary rocks, previously occupied by central parts of ice sheets (Bothnian Sea, Bothnian Bay, Hudson Bay) would likely remain stable water storage with gradual shallowing up to future system of giant lakes.

IV. CONCLUSIONS

Eustatic changes have interrelations with other long-term processes. These processes are connected with the glacial activity and related isostatic adjustment. Here we focus on gradual topographic changes mostly in glacial and periglacial areas, changing the redistribution of amount of water globally before and after glaciations. In coastal areas they are linked with sediment- and hydro-isostasy.

Glacial erosion is a significant, but variable factor. It creates overdeepenings of different scale in favorable conditions. Many huge enclosed basins - including the Baltic -were created or strongly modified by this process. In relation to the ice age onset they can hold additional amount of water, even if related isostasy often reduces its volume.

Negative topographic elements, previously occupied by central parts of ice sheets (Bothnian, Hudson Bay) would likely remain stable water storage with gradual shallowing up to future system of giant lakes.

Vice versa, accumulation replaces water by low-compacted sediments, with additional subsidence. Large part of deposition was concentrated on positive topographic features.

Hydro-isostasy impacted non-uniform relocation of coastal zone in local and regional scale. The local one is connected with water load changes of the enclosed basins. The regional influence could be subsidence of the ocean floor and subsequent uplift of continents caused by global eustatic changes.

V. REFERENCES

[1] W. Fjeldskaar, "Rapid eustatic changes - never globally uniform," *Correlations in Hydrocarbon Exploration*. Norwegian Petroleum Society, 1989, pp. 13-19.

[2] W. Fjeldskaar, "Geoidal-eustatic changes induced by the deglaciation of Fennoscandia," *Quaternary International*, vol. 9, 1991, pp. 1-6.

[3] J. I. Svendsen, H. Alexanderson, V.I. Astakhov, I. Demidov, J.A Dowdeswell, S. Funder, V. Gataullin, M. Henriksen, C. Hjort, M. Houmark-Nielsen, H.W. Hubberten, O. Ingolfsson, M. Jakobsson, K.H. Kjaer, E. Larsen, H. Lokrantz, J.P. Lunkka, A. Lysa, J. Mangerud, A. Matiouchkov, A. Murray, P. Moller, F. Niessen, O. Nikolskaya, L. Polyak, M. Saarnisto, C. Siegert, M.J. Siegert, R.F. Spielhagen and R. Stein, "Late Quaternary ice sheet history of northern Eurasia," *Quaternary Science Review,* vol. 23, 2004. 1229–1271.

[4] A. Amantov and W. Fjeldskaar, "Geological-geomorphological features of the Baltic region and adjacent areas: imprint on glacial-postglacial stages of development," *Regional Geology and Metallogeny,* vol. 53, 2013. 90–104.

[5] W.R. Peltier, D.F. Argus and R. Drummond, "Space geodesy constrains ice-age terminal deglaciation: The global ICE-6G\C (VM5a) model," *J. Geophys. Res. Solid Earth* , vol. 120, 2015, pp. 450-487.

[6] A.L.C Hughes, R. Gyllencreutz, Ø.S. Lohne, J. Mangerud and J.I. Svendsen, "The last Eurasian ice sheets – a chronological database and time-slice reconstruction DATED-1," *Boreas,* vol. 45, 2016, pp. 1–45.

[7] A. Amantov, W. Fjeldskaar and L.M. Cathles, "Glacial erosion of the Baltic Sea region, and the effect on the post-glacial uplift," In *The Baltic Sea Basin*. J. Harff, S. Bjorck, and P. Hoth, Eds, Springer, Heidelberg, Chapter 3, 2011, pp. 53–75.

[8] G. Balco and C.W. Rovey, "Absolute chronology for major Pleistocene advances of the Laurentide Ice Sheet," *Geology,* vol. 38, no. 9, 2010, pp. 795-798.

[9] V. Zybakov, "Barents Sea Aktchagyl Hyperglaciation," *Problems of Correlation of Pleistocene Events of the Russian North*. Abstracts Vol. SPB, p. 111, December 4-6, 2006.

[10] F. Riis and W. Fjeldskaar, "On the magnitude of the Late Tertiary and Quaternary erosion and its significance for the uplift of Scandinavia and the Barents Sea," In: Larsen, R.M., Brekke, H., Larsen, B.T. and Talleraas, E., Eds: *Structural and tectonic modelling and its application to petroleum geology*. Norwegian Petroleum Society. Elsevier, 1992, pp. 163-185.

[11] W.W. Hay, "Pleistocene-Holocene fluxes are not the earth's norm". In *Material Fluxes on the Surface of the Earth,* W.W. Hay and T. Usselmann, Eds., Studies in Geophysics, National Academy Press, 1994, pp. 15-27.

[12] J.E. Mojski, "Geology of Poland (Stratigraphy, Quaternary)," Wydawnictwa Geologiczne, Warsaw, 1985, pp. 1-244.

[13] A. Gaigalas, “Glacial history of Lithuania,” In *Glacial Deposits in North-East Europe,* J. Ehlers, S. Kozarski and Ph. Gibbard, Eds., Balkema. Rotterdam, 1995, pp. 127–135.

[14] R.W. Klassen, “Quaternary geology of the southern Canadian Interior Plains,” In *Quaternary Geology of Canada and Greenland*, R.J. Fulton, Ed., Geological Survey of Canada, *Geology of Canada*, Chapter 2-1, 1989, pp. 138-174.

[15] M.M. Fenton, “Quaternary stratigraphy of the Canadian prairies”, In *Quaternary Stratigraphy of Canada* - A Canadian Contribution to IGCP Project 24. R.J. Fulton (ed.). Geological Survey of Canada, Paper 84-10, 1984, pp. 57-68.

[16] D.R. Soller, "Map showing the thickness and character of Quaternary sediments in the glaciated United States east of the Rocky Mountains," *U.S.G.S. Bulletin*, 1992, 54 p.

[17] G. Mossop and I. Shetsen, “Geological Atlas of the Western Canada Sedimentary Basin,” *Canadian Society of Petroleum Geologists*, Calgary, Alberta, 1994.

[18] J.G. Pawlowicz and M.M. Fenton, “Drift thickness of Alberta,” *Alberta Geological Survey Map* (1:2 000 000 scale), 1995.

[19] T.O. Vorren, J.S. Laberg, F. Blaume, J.A. Dowdeswell, N.H. Kenyon, J. Mienert, J. Rumohr and F. Werner, “The Norwegian-Greenland Sea continental margins: morphology and Late Quaternary sedimentary processes and environment,” *Quat. Sci. Rev.,* vol. 17, 1998, pp. 273-302.

[20] J.A., Dowdeswell and A. Elverhøi, “The timing of initiation of fast-flowing ice streams during a glacial cycle inferred from glacimarine sedimentation”. *Marine Geology*, vol. 188, 2002, pp. 3-14.

[21] A. Amantov, “Plio-Pleistocene erosion of Fennoscandia and its implication for the Baltic Area,” *PPIG CXLIX, Proceedings of the 3rd Marine Geological Conference “The Baltic”*, Warszawa, 1995, pp 47–56.

[22] D.J.W. Piper and R.A. Myers, “Deep water sediments I, Labrador sea, Acoustic interpretation, Mid - Pliocene to Basal Pleistocene,” In *Labrador sea/Mer du Labrador. East Coast Basin Atlas Series. Geological Survey Of Canada,* J.S. Bell, R.D. Howie, N. J. McMillan, C.M. Hawkins, and J.L. Bates, Eds., 1989, pp. 18-19.

[23] H.W. Josenhans and J. Zevenhuizen, “Quaternary Geology IV, Labrador sea, Isopach and surface texture,” In *Labrador sea/Mer du Labrador. East Coast Basin Atlas Series. Geological Survey Of Canada*, J.S. Bell, R.D. Howie, N. J. McMillan, C.M. Hawkins, and J.L. Bates, Eds., 1989, pp. 14-15.

[24] W.A. White, “More on deep glacial erosion by continental ice sheets and their tongues of distributary ice,” *Quaternary Research*, vol. 30, 1988, pp. 137-150.

[25] A. E. Aksu and D.J.W Piper, “Late Quaternary sedimentation in Baffin Bay,” *Can. J. Earth Sci*., vol. 24, 1987, pp. 1833-1846.

[26] J. Dixon, J.R. Dietrich and D.H. McNeil, “Upper Cretaceous to Pleistocene sequence stratigraphy of the Beaufort-Mackenzie and Banks Island areas, northwest Canada,” *Geol. Surv. Can., Bull*., vol. 407, 90 p.

[27] G.G. Zuffa, W.R. Normark, F. Serra and C.A., Brunner, “Turbidite megabeds in an oceanic rift valley recording jökulhaups of late Pleistocene glacial lakes of the western United States,” *J. Geol.*, vol. 108, 2000, pp. 253-274.

[28] W.R. Normark and J.A. Reid, “Extensive deposits on the Pacific Plate from late Pleistocene North American glacial lake outbursts,” *J. Geol*., vol. 111, 2003, pp. 617-637.

[29] J.A. Dowdeswell, N.H. Kenyon and J.S. Laberg, “The glacier-influenced Scoresby Sund Fan, East Greenland continental margin: evidence from GLORIA and 3.5kHz records,” *Marine Geology*, vol. 143(1-4), 1997, pp. 207-221.

[30] C. O´ Cofaigh, J. Taylor, J.A. Dowdeswell and C.J Pudsey, “Palaeo-ice streams, trough mouth fans and high-latitude continental slope sedimentation,” *Boreas*, Vol. 32, 2003, pp. 37–55.

[31] W. Jokat, E. Weigelt, Y. Kristoffersen, T. Rasmussen, T. Schone, “New insights into the evolution of the Lomonosov Ridge and the Eurasia Basin,” *Geophys. J.* Int. 122, 1995, pp. 378-392.

[32] Y. Kristoffersen, M. Sorokin, W. Jokat, O. Svendsen, “A submarine fan in the Amundsen Basin, Arctic Ocean,” *Mar. Geol*., vol. 204, 2004, pp. 317-324.

[33] A. Nesje, “Fjords of Norway: Complex Origin of a Scenic Landscape,” *Geomorphological Landscapes of the World*, 2010, pp. 223-234.

SITE-SPECIFIC EQUATIONS OF STATE FOR COASTAL SEA AREAS AND INLAND WATER BODIES

Natalia Andrulionis, Shirshov Oceanology Institute, Russia
Ivan Zavialov, Shirshov Oceanology Institute, Russia
Elena Kovaleva, Shirshov Oceanology Institute, Russia
Peter Zavialov, Shirshov Oceanology Institute, Russia
Alexander Osadchiev, Shirshov Oceanology Institute, Russia
Alevtina Alukaeva, Shirshov Oceanology Institute, Russia
Alexander Izhitskiy, Shirshov Oceanology Institute, Russia

natalya@ocean.ru

This article presents a new method of laboratory density determination and construction equations of state for marine waters with various ionic compositions and salinities was developed. The validation of the method was performed using the Ocean Standard Seawater and the UNESCO thermodynamic equation of state (EOS-80). Density measurements of water samples from the Aral Sea, the Black Sea and the Issyk-Kul Lake were performed using a high-precision laboratory density meter. The obtained results were compared with the density values calculated for the considered water samples by the EOS-80 equation. It was shown that difference in ionic composition between Standard Seawater and the considered water bodies results in significant inaccuracies in determination of water density using the EOS-80 equation. Basing on the laboratory measurements of density under various salinity and temperature values we constructed a new equation of state for the Aral Sea and the Black Sea water samples and estimated errors for their coefficients.

Key words: density of sea water, equation of state, ionic composition, density meter, Standard Seawater, Aral Sea, Black Sea, Issyk-Kul Lake

I. INTRODUCTION

The Law of Constant proportions, which states that proportion among quantities of the major ions in the open ocean waters is almost constant and does not significantly depend on their concentration, i.e., salinity, was assumed to be true till the middle of the 20th century. However, research studies in the second part of the 20th century detected significant variability of ionic compositions even in the open ocean waters.

Differences with standard seawater ionic composition (Table 1) are especially large at semi-enclosed seas and water bodies, coastal areas and areas adjacent to continental discharge sources. Moreover, saline lakes, e.g., the Aral Sea and the Caspian Sea, are generally characterized by ionic composition which is totally different from the standard seawater one. As a result application of certain practically important dependences among the main physical parameters (which are true for open ocean water) to many inland seas, coastal areas and saline lakes causes significant errors. In particular, it refers to equations of state, e.g., the dependences of water density on its temperature,

salinity and pressure. Usage of seawater equations of state for hyperhaline lakes is limited not only by differences in ionic composition, but also by salinity, because ocean equations of state are applicable only for waters, which salinity and temperature lie within the ranges 0-40‰ and -2-40 °C respectively.

Table 1. Concentrations of the major ions in standard ocean water taken from [1].

Ion	Average concentration	Range	Units (per kg)
Lithium	174	average	ug
Boron	4,5	average	mg
Carbon	27,6	24 - 30	mg
Nitrogen	420	>1 - 630	ug
Fluorine	1,3	average	mg
Sodium	10,77	average	g
Magnesium	1,29	average	g
Aluminium	540	<10 - 1200	ng
Silicon	2,8	<0,02 - 5	mg
Phosphorus	70	<0,1 - 110	ug
Sulphur	0,904	average	g
Chloride	19,354	average	g
Potassium	0,399	average	g
Calcium	0,412	average	g
Manganese	14	5-200	ng
Iron	55	5 - 140	ng
Nickel	0,5	0,1 - 0,7	ug
Copper	0,25	0,03 - 0,4	ug
Zinc	0,4	<0,01 - 0,6	ug
Arsenic	1,7	1,1 - 1,9	ug
Bromine	67	average	mg
Rubidium	120	average	ug
Strontium	7,9	average	mg
Cadmium	80	0,1 - 120	ng
Iodine	50	25 - 65	ug
Caesium	0,29	average	ug
Barium	14	4 - 20,0	ug
Mercury	1	0,4 - 2	ng
Lead	2	1 - 35	ng
Uranium	3,3	average	ug

The most widely used equation of state (EOS-80, [2]) was established in 1980 by the UNESCO Joint Panel on Oceanographic Tables and Standards. Density and several other related seawater properties are calculated using this equation for more than 30 years. A new thermodynamic

equation of state of seawater (TEOS-10, [3]) was established by the Scientific Committee on Oceanic Research (SCOR) and the Working Group 127 (WG127) of the International Association for the Physical Sciences of the Oceans (IAPSO) in 2009. The main advantage of TEOS-10 comparing to EOS-80 consists in fact that TEOS-10 does not use practical salinity, which is measured by water conductivity, but operates with absolute salinity, i.e., mass fraction of salt in seawater.

Thus, individual equations of state, which depend on ionic compositions of the considered water bodies, designed for calculation water density basing on its temperature and salinity are required for many sea areas and saline lakes. This article describes a methodology for constructing such equations on the basis of laboratory measurements as well as the first resultsof its application to waters of the modern Aral Sea, north-eastern shelf of the Black Sea adjacent to the Sochi River mouth and the Issyk-Kul Lake.

II. METHOD

High accuracy and precision density measurements of sea and lake water samples were performed using laboratory density meter *Anton Paar DMA 5000M*. This device is applicable to any liquid within a wide range of density and viscosity values; method of measurement does not depend on water ionic composition. The method is based on measurement of vibrations of a *U*-tube which contains the analyzed water. Resonant frequency of the oscillation tube, measured by optical sensors, depends only on fluid density. Density of a water sample is reconstructed from accurately determined resonant frequency using specific mathematical operations. Errors related to viscosity are automatically corrected for the whole range of viscosities by measuring damping effect of a viscous sample, followed by mathematical correction of density value. Nominal accuracy of density measurements is equal to 10^{-6} g/cm³. Temperature control of a sample with 0.01 °C accuracy is provided by two embedded platinum thermometers and Peltier elements. The instrument can automatically vary temperature of sample from 0 to 90°C.

The ionic composition of sea and lake water samples were determined by a ion chromatograp *Metrohm 930 Compact IC Flex* equipped with column thermostat, sequential chemical suppression system, and two built-in degassers: for eluent and for sample. Results obtained by the chromatograph for water samples from the Aral Sea, the Black Sea and the Issyk-Kul Lake showed significant differences with ionic composition of open ocean water (Table 2).

Table 2. Ionic composition of Ocean Standard Seawater taken from [1] and ionic composition of water samples from the Aral Sea, the Black Sea and the Issyk-Kul Lake measured by the chromatograph.

Ion	Cl^-	$SO4^{2-}$	Br^-	$HCO3^-$	$NO3^-$	Na^+	K^+	Ca^+	Mg^+	$Cl^-/SO4^{2-}$
Ocean water										
Concentration, g/kg	19,4	2,7	0,1	0,1	–	10,8	0,4	0,4	1,3	0,14
Concentration, %	55,1	7,7	0,2	0,4	–	30,6	1,1	1,2	3,7	
Black Sea (bottom layer), 12 m, 2014										
Concentration, g/kg	12,0	1,2	0,03	–	–	4,3	0,2	0,3	0,5	0,10
Concentration, %	64,7	6,4	0,1	–	–	23,4	0,8	1,4	2,8	
Black Sea (bottom layer), 17 m, 2014										
Concentration, g/kg	10,9	1,1	0,02	–	–	4,2	0,2	0,2	0,6	0,10
Concentration, %	63,7	6,3	0,1	–	–	24,3	0,9	1,4	3,3	
Aral Sea (surface layer), 2014										
Concentration, %	61	15,5	–	0,4	–	16,4	0,5	0,8	5,4	0,25
Aral Sea (bottom layer), 34 m, 2014										
Concentration, %	48	19,3	–	0,6	–	23,7	0,6	0,5		0,40
Issik-Kull Lake (surface layer), 2015										
Concentration, g/kg	2,1	3,9	–	–	0,1	1,1	0,1	0,1	0,2	1,84
Concentration, %	27,5	50,7	–	–	6,5	14,9	0,7	1,7	3	
Issik-Kull Lake (bottom layer), 640 m, 2015										
Concentration, g/kg	2,1	2,6	–	–	–	1,2	0,1	0,1	0,2	1,29
Concentration, %	32,5	41,8	–	–	–	19	0,9	1,9	3,7	

Water samples were initially filtered using 0.7 and 0.1 micron membrane filters in order to remove suspended and organic matter. Absolute salinity of samples was determined as concentration of total dissolved solids obtained by gravimetric analysis which included water evaporation and burning of organic matter. The initial samples were diluted with the distilled deionized water in different proportions in order to obtain series of water samples with the same ionic composition and different salinities. Every analyzed water sample was measured three times at the density meter. The obtained results of density measurements were compared with the density values calculated by EOS-80 for the corresponding values of the temperature and salinity. The same procedure was performed for the *OSIL* Ocean Standard Seawater sample, which is a "standard" of sea water with salinity equal to 35 ‰. As it was expected, the measured and the calculated values for the Ocean Standard Seawater were almost the same (Fig. 1), while for the Aral Sea, the Black Sea and the Issyk-Kul Lake samples they showed significant differences, which is discussed below.

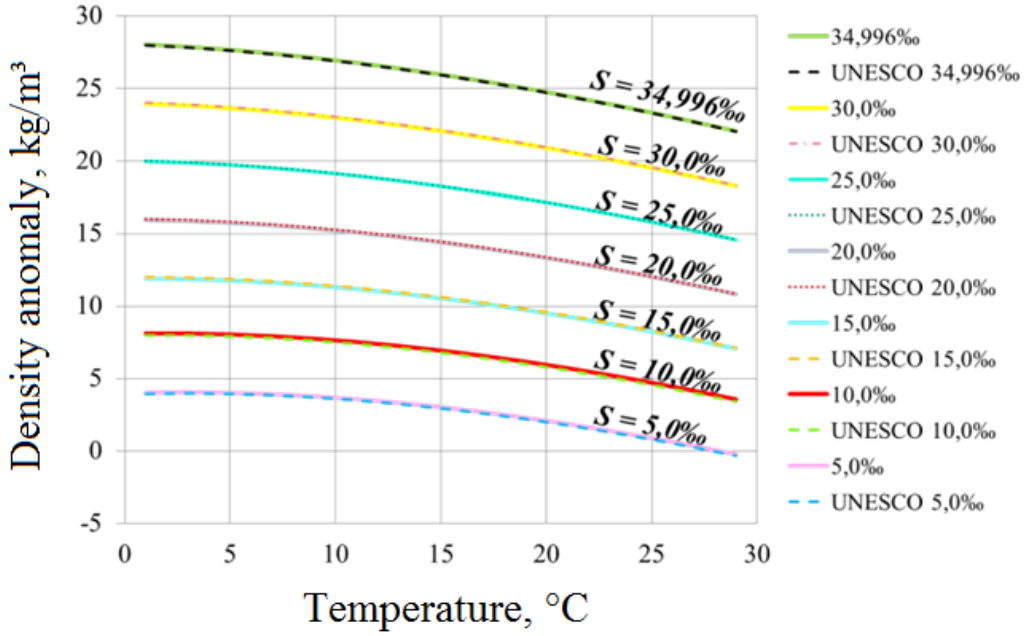

Fig. 1. Dependence of density anomaly on water temperature for Ocean Standard Seawater samples diluted to different salinity concentrations measured experimentally (solid lines) and calculated using EOS-80 (dashed lines).

Then the individual equations of state for the analyzed water bodies were constructed in the following way. We assumed that dependence of density on temperature and salinity is expressed by a bilinear polynomial form:

$$\rho(T, S) = A_0 + A_1T + A_2T^2 + A_3S + A_4S^2 + A_5TS, \quad (1)$$

where ρ is density (in kg/m³), T is temperature (in °C), S is salinity (g/kg), and searched for coefficients $A_0,...,A_5$, which provide minimal mean square deviation of (1) from results of direct measurements of (T, S, ρa).

Further analysis requires estimation of measurement errors and determination of confidence intervals for the coefficients of the equations of state. We assume that error of determination of density is equal to standard deviation calculated for three density measurements performed for each water sample. About 68% of values of a random variable with normal distribution lie within one standard deviation of the mean. Therefore we calculate values of coefficients $A_0,...,A_5$ for the "upper" (mean value plus standard deviation) and "lower" (mean value minus standard deviation) values of confidence limits of density measurements and assume that the obtained sets of coefficients determine confidence limits for values of $A_0,...,A_5$.

III. RESULTS

The equation of state for the western basin of the Aral Sea

The Aral Sea is a body of water which exhibited significant degradation caused by human activity [4]. Water samples from the western basin of the Large Aral Sea were collected during the expedition of Shirshov Oceanology Institute in October 2014 (Fig. 2).

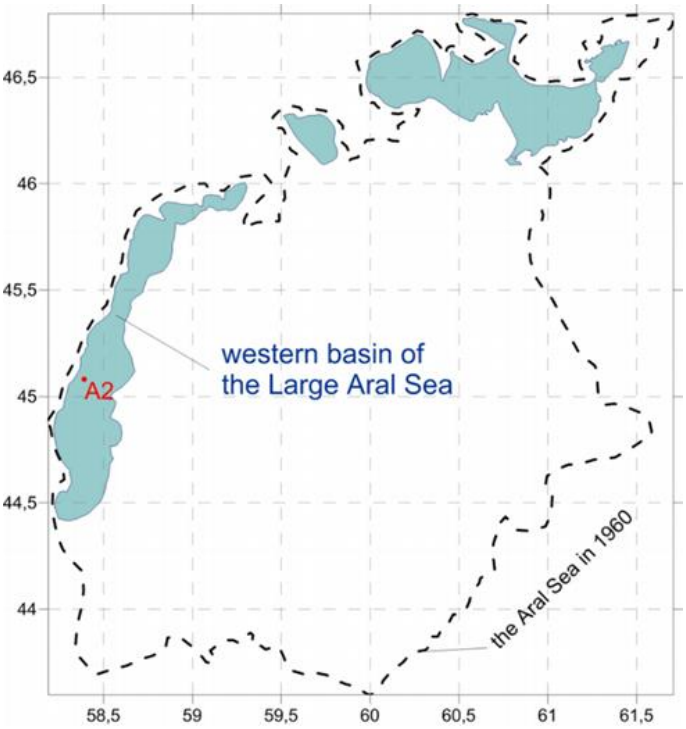

Fig.2. Modern outlines of the Aral Sea, its 1960 border (the dashed line) and the sampling point (station A2)

We analyzed two water samples, he first one was taken from the surface layer and its salinity is equal to 121.6 g/kg, while the second one was taken from the bottom layer (34 m depth) and had salinity of 115.4 g/kg. The first sample was diluted to obtain salinity values equal to 60.8, 30.4 and 15.2 g/kg. Density of each diluted sample was measured three times using a density meter in a temperature range of 1 to 29 °C with a step of 1 °C. The measurement results were compared with density calculated using the formal extrapolation of EOS-80 on hyperhaline salinity ranges (Fig. 3). As it was expected usage of EOS-80 resulted in large errors which exceeded 10 kg/m³.

The coefficients of (1) for surface and bottom layers of the Aral Sea, as well as their standard deviations are presented in Tables 3 and 4. The mean square error for the bottom layer did not exceed 0.21 kg/m^3, and for the surface layer did not exceed 0.14 kg/m³.

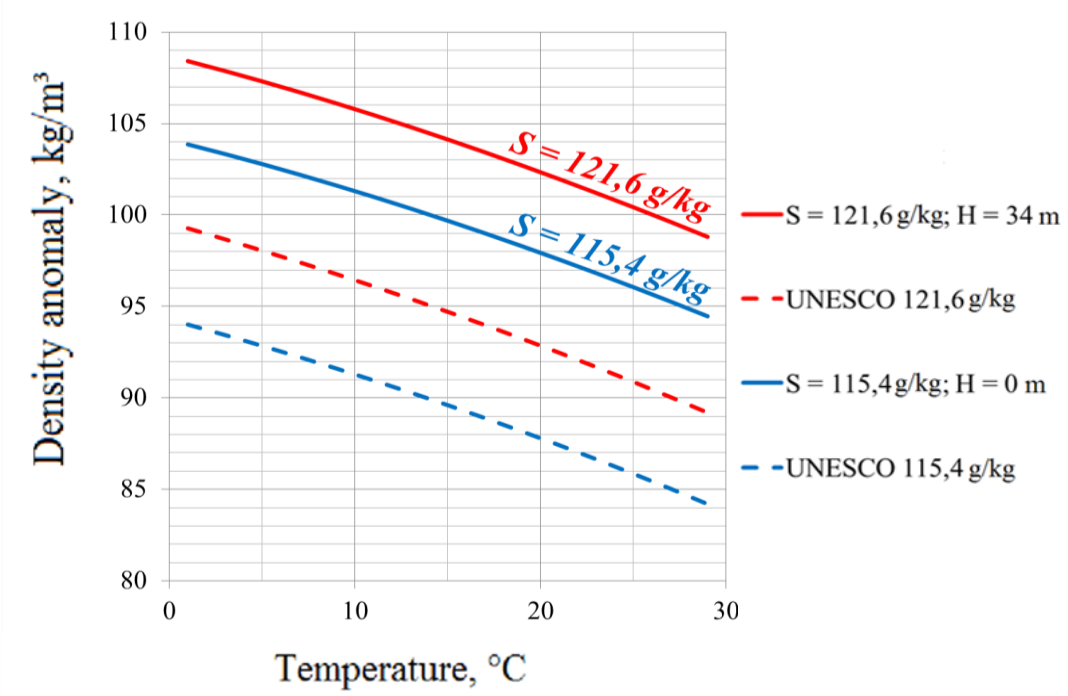

Fig. 3. Dependence of density anomaly on water temperature for the Aral Sea samples taken from the surface (blue) and bottom (red) layers measured experimentally (solid lines) and calculated using EOS-80 (dashed lines).

Table 3. The coefficients of the equation of state for the bottom layer (34 m depth) of the western basin of the Aral Sea.

Coefficient	Value	Standard deviation
A_0	0.809	0.1306
A_1	-0.0354	0.0007
A_2	-0.0042	0.0001
A_3	0.8491	0.0056
A_4	-0.0003	0.00005
A_5	-0.0014	0.0001

Table 4. The coefficients of the equation of state for the surface layer of the western basin of the Aral Sea.

Coefficient	Value	Standard deviation
A_0	1.052	0.0289
A_1	-0.0334	0.0212
A_2	-0.0042	0.0006
A_3	0.8540	0.00165
A_4	-0.0003	0.00001
A_5	-0.0014	0.00001

The equation of state for the north-eastern coastal zone of the Black Sea

Water samples from the north-eastern coastal zone of the Black Sea were collected during the expedition of Shirshov Oceanology Institute in May 2014 near the mouth of the Sochi River. The Black Sea is characterized by moderate salinity which is equal to 17-18‰ at the surface layer and up to 22.5‰ at the bottom layer. However, salinity of coastal areas of the Black Sea is significantly influenced by continental discharge [5]. In this work we analyzed two samples taken from the Black Sea. The first one was collected near the mouth of the Sochi River and its salinity is equal to 15.5‰, the second one was collected about 1 km far from the shore and had salinity of 16.5‰.

The procedure described above was applied to these water samples and the resulting densities were compared with density values calculated by EOS-80. Fig. 4 illustrates that usage of EOS-80resulted in about 1 kg/m³ underestimation of density for both analyzed samples. The coefficients of (1) for bottom layer of the Black Sea, as well as their standard deviations are presented in Tables 5 and 6.

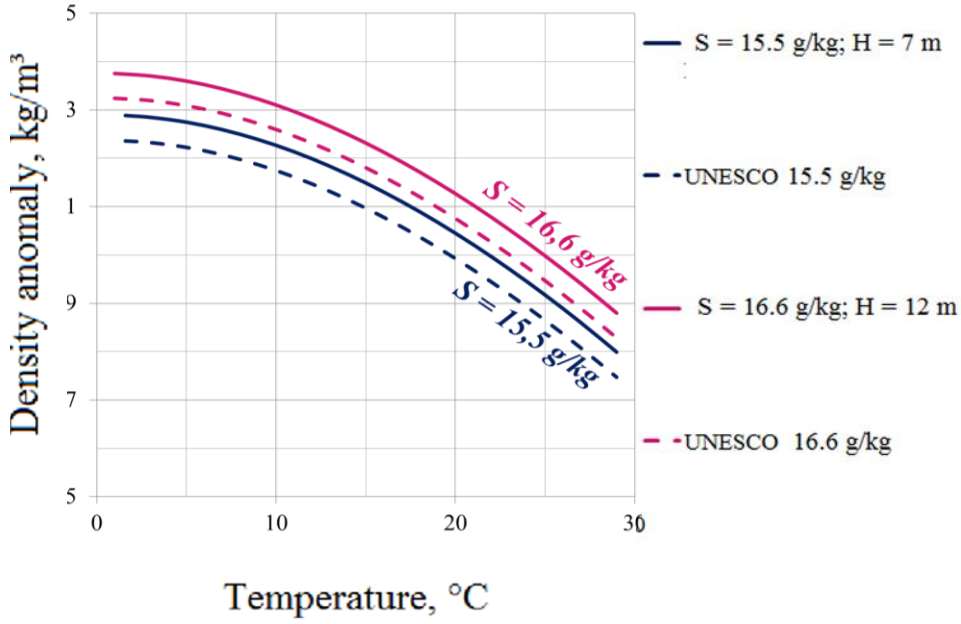

Fig. 4. Dependence of density anomaly on water temperature for the Black Sea samples taken from the bottom layer from the depth of 7 m (blue) and the depth of 12 m (red) measured experimentally (solid lines) and calculated using EOS-80 (dashed lines).

Table 5. The coefficients of the equation of state for the bottom layer (7 m depth) of the north-eastern coastal zone of the Black Sea.

Coefficient	Value	Standard deviation
A_0	-0.2439	0.0234
A_1	0.0237	0.00615
A_2	-0.0056	0.0002517
A_3	0.9947	0.0029
A_4	-0.009	0.0001
A_5	-0.0021	0.0002

Table 6. The coefficients of the equation of state for the bottom layer (12 m depth) of the north-eastern coastal zone of the Black Sea.

Coefficient	Value	Standard deviation
A_0	0.2819	0.02405
A_1	0.0232	0.006
A_2	-0.0056	0.0002517
A_3	0.8119	0.0025
A_4	0.0005	0.0001
A_5	-0.0021	0.00015

Density measurements of water samples from the Issyk-Kul Lake

The Issyk-Kul Lake is an endorheic lake in the northern Tian Shan mountains in eastern Kyrgyzstan which receives discharge from about 120 small-size rivers, the largest are the Djyrgalan and Tyup [6]. This low salinity lake is the 6th deepest lake in the world. Water samples from the Issyk-Kul Lake were collected during the expedition of Shirshov Oceanology Institute in June 2015. Water was taken from the surface layer (salinity of 5.9 g/kg) and the bottom layer at the depth of 640 m (salinity of 5.7 g/kg). Unstable vertical distribution of salinity was compensated by a strong thermocline.

The procedure described above was applied to these water samples and the resulting densities were compared with density values calculated by EOS-80. Fig. 6 illustrates that usage of

EOS-80 resulted in about 1 g/kg underestimation of density for both analyzed samples.

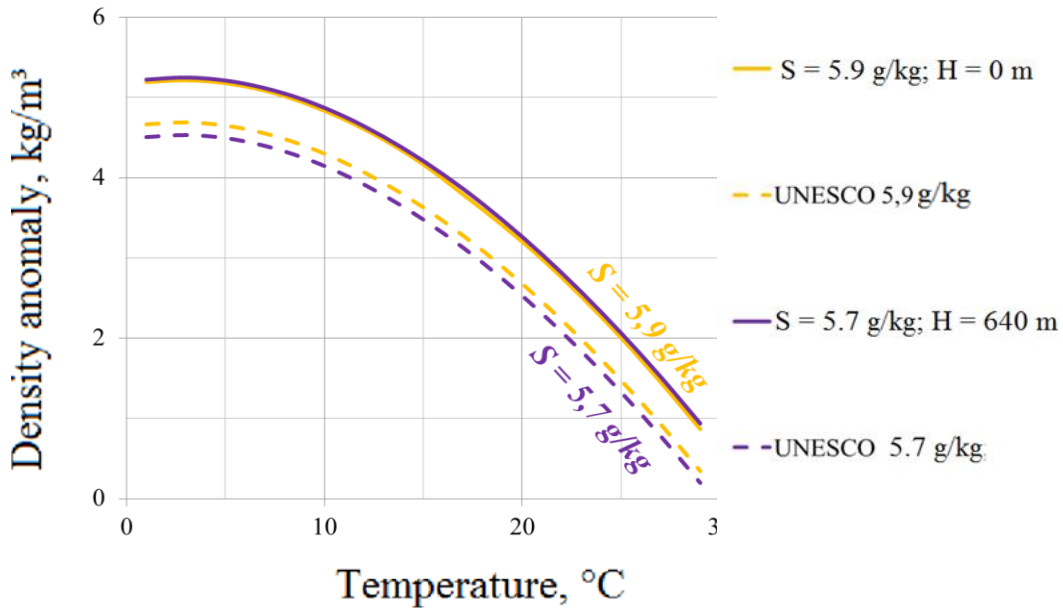

Fig. 6. Dependence of density anomaly on water temperature for the Issyk-Kul Lake samples taken from the surface layer (yellow) and from the bottom layer from the depth of 640 m (blue) diluted to different salinity concentrations measured experimentally (solid lines) and calculated using EOS-80 (dashed lines).

IV. ACKNOWLEDGEMENTS

Funding of this research was provided by the Russian Scientific Foundation, research project 14-50-00095. Authors wish to thank P.N. Makkaveev and members of the Laboratory of Hydrochemistry of Shirshov Oceanology Institute; many colleagues who participated in field works at the Aral Sea, the Black Sea and the Issyk-Kul Lake in 2014-2015; "Avrora-lab" Ltd. and personally S.K. Dedushenko and N.P. Kolbyagin.

V. REFERENCES

[1] C.P. Summerhayes and S.A. Thorpe, “Oceanography: an illustrated guide, “ *Oceanographic Literature Review*, vol. 43, pp. 165-181, 1996.

[2] N.P. Fofonoff, “Physical properties of seawater: A new salinity scale and equation of state for seawater,” *J. Geophys. Res.*, vol. 90, pp. 3332-3342, 1985.

[3] T.J. McDougall, R. Feistel, F.J Millero, D.R. Jackett, D.G. Wright, B.A. King, G.M. Marion, C.T.A. Chen, and P. Spitzer. “Calculation of the Thermophysical Properties of Seawater,” in *Global Ship-based Repeat Hydrography Manual*, IOCCP Report, vol. 14, 2009.

[4] A.S. Izhitskiy, P.O. Zavialov, P.V. Sapozhnikov, G.B. Kirillin, H.P. Grossart, O.Y. Kalinina, A.K. Zalota, I.V. Goncharenko, and A.K. Kurbaniyazov, “Present state of the Aral Sea: diverging physical and biological characteristics of the residual basins,” *Scientific Reports*, vol. 6, 2016.

[5] П.О. Завьялов, П.Н. Маккавеев, Б.В. Коновалов, А.А. Осадчиев, П.В. Хлебопашев, В.В. Пелевин, А.Б. Грабовский, А.С. Ижицкий, И.В. Гончаренко, Д.М. Соловьев, и А.А. Полухин, “Гидрофизические и гидрохимические характеристики морских акваторий у устьев малых рек российского побережья Черного моря,” *Океанология*, т. 54, с. 293-308, 2014

[6] K. Savvaitova and T. Petr, “Lake Issyk-Kul, Kirgizia,” *International Journal of Salt Lake Research*, vol. 1, pp. 21-46, 1992.

THE APPLICATION FEATURES AN INTEGRATED ASSESSMENT METHOD FOR THE ANALYSIS OF TOURIST AND RECREATIONAL CAPACITY ON THE EXAMPLE OF THE MUNICIPALITY OF TUAPSINSKY DISTRICT

Mikael Arakelov, branch of the Russian State Hydrometeorological University in Tuapse town, Russia
Arthur Arakelov, branch of the Russian State Hydrometeorological University in Tuapse town, Russia
George Gogoberidze, Russian State Hydrometeorological University, Russia

kafirnigan@mail.ru

Tourism is one of the most dynamically developing branches of economy in the Russian Federation in general and on the Black Sea coast in particular, in this regard, the assessment of tourism potential is one of the most important tasks of regional management.

Key words: tourist and recreational capacity, the integral model, indicator, analysis, Tuapsinsky district

Analysis of tourist and recreational potential of the territory represents a rather urgent problem. Despite the relatively large number of different evaluation methods in the field, in the scientific literature there is no single approach that would allow a comprehensive analysis of the various components of the tourism potential of the region. Therefore, we have devised a comprehensive analysis and evaluation of recreational resources based on the construction of integral models [1, 2, 3]. Based on this model, we propose to use two types of indicators: indicators of natural environmental and socio-economic component of tourism and recreational potential of the territory, which in the end are reduced to a single integral indicator of tourist and recreational potential [4, 5, 6]. Approbation of this method was carried out on the example of urban and rural settlements included in the municipality Tuapse district, based on the data of official statistics and administrative sources [7, 8, 9, 10, 11, 12, 13, 14].

The objects of analysis we select only those administrative units which is located on the Black sea coast, because the aspect of data creates a distinct advantage in comparison with the mountain areas do not have access to the marine resource.

Therefore, the objects of our analysis will be [15]:

- urban settlement of Dgubga;
- rural settlement of Tenginka;
- urban settlement of Novomikhailovsky;
- rural settlement of Nebug;
- urban settlement of Tuapse;
- rural settlement of Shepsi.

1. The indicator of the length of the cost I_{LC} (1) (table 1):

$$I_{LC} = \frac{L_{BS}/L_S}{L_{BM}/L_M} - 1 \quad (1)$$

L_{BS} – the value of the length of the beaches of settlement with a width of more than 10m, km;
L_{BM} – he value of the length of the beaches of municipality with a width of more than 10m, km;
L_S – the coastline of the settlement, km;
L_M – the coastline of the municipality, km.

Table 1. The indicator of the length of the cost

The name of the settlement	**L_{BS}**	**L_S**	**I_{LC}**
Dgubga	6	12	0.1594
Tenginka	4.5	6	0.7391
Novomikhailovsky	8	16	0.1594
Nebug	15	18	0.9324
Tuapse	3.5	6	0.3527
Shepsi	4	8	0.1594
TOTAL	41	66	-

2. The indicator of the level of solar activity I_S (2) (table 2) [16]:

$$I_S = 2 * \frac{S_S - S_{min}}{S_{max} - S_{min}} - 1 \quad (2)$$

S_S – the number of days with clear Sunny weather in the settlement, days.;

S_{min} – min number of days with clear, Sunny weather at the municipality, days;

S_{max} - max number of days with clear, Sunny weather at the municipality, days.

Table 2. The indicator of the level of solar activity

The name of the settlement	**The indicator of the level of solar activity**	
	The number of days of sunshine in year	**The value of the indicator**
Dgubga	238	-1,00
Tenginka	238	-1,00
Novomikhailovsky	239	0,00
Nebug	240	1,00
Tuapse	240	1,00
Shepsi	240	1,00

3. Indicator of forest area of the territory I_{FA} (3) (table 3):

$$I_{FA} = \frac{S_{F_S}/S_S}{S_{F_M}/S_M} - 1 \quad (3)$$

S_{F_S} – the forest area of the settlement, km^2;

S_{F_M} – the forest area of the municipality, km^2;

S_S – the area of settlement, km^2;

S_M – the area of municipality, km^2.

Table 3. Indicator of forest area of the territory

The name of the settlement	S_{F_S}	S_S	**I_{FA}**
Dgubga	12.5	36.7	-0.6
Tenginka	14.8	18.2	-0.0449
Novomikhailovsky	21	47.4	-0.4797
Nebug	51.4	55.3	0.0917
Tuapse	3.1	17.4	-0.7908
Shepsi	18.6	22.6	-0.0334
TOTAL	121.4	197.6	-

4. The indicator of the magnitude of wastewater discharges I_{WD} (4) (table 4):

$$I_{WD} = 1 - \frac{WD_S/L_S}{WD_M/L_M} \quad (4)$$

WD_S – the inflow of waste dumps in the surrounding area of the settlement, kt.;
WD_M – the inflow of waste dumps in the surrounding area of the municipality, kt.

Table 4. The indicator of the magnitude of wastewater discharges

The name of the settlement	**WD_S**	**L_S**	**I_{WD}**
Dgubga	2324	12	0.1727
Tenginka	375	6	0.7330
Novomikhailovsky	1894	16	0.4943
Nebug	1149	18	0.7273
Tuapse	9392	6	-1
Shepsi	316	8	0.8313
TOTAL	15450	66	-

5. The indicator of the magnitude of the emissions I_{EM} (5) (Table 5):

$$I_{EM} = 1 - \frac{QE_S/S_S}{QE_M/S_M} \quad (5)$$

QE_S – the quantity of emissions released to the atmosphere for settlement, kt.;
QE_M – the quantity of emissions released to the atmosphere for municipality, kt.

Table 5. The indicator of the magnitude of the emissions

The name of the settlement	**QE_S**	**S_S**	**I_{EM}**
Dgubga	4.805	36.7	-0.5234
Tenginka	0.553	18.2	0.6464
Novomikhailovsky	3.324	47.4	0.1840
Nebug	1.895	55.3	0.6013
Tuapse	6.419	17.4	-1
Shepsi	2.886	22.6	-0.4859
TOTAL	19.882	197.6	-

6. The indicator of receipt of solid waste I_{SW} (6) (table 6):

$$I_{SW} = 1 - \frac{SW_S/S_S}{SW_M/S_M} \quad (6)$$

SW_S – the income amount of solid waste in the surrounding area of the settlement, kt.;
SW_M – the income amount of solid waste in the surrounding area of the municipality, kt. [17].

Table 6. The indicator of receipt of solid waste

The name of the settlement	SW_S	**S_S**	I_{SW}
Dgubga	108982	36.7	-0.1351
Tenginka	21786	18.2	0.5424
Novomikhailovsky	97563	47.4	0.2132
Nebug	37567	55.3	0.7403
Tuapse	231250	17.4	-1
Shepsi	19792	22.6	0.6652
TOTAL	516940	197.6	-

7. The indicator of volume of production per capita I_{VP} (7) (table 7):

$$I_{VP} = 2 * \frac{VP_S - VP_{min}}{VP_{max} - VP_{min}} - 1 \quad (7)$$

VP_S – the volume of production per capita in settlement, RUB;

VP_{min} - the minimum volume of production per capita in municipality, RUB.;

VP_{max} - the maximum volume of production per capita in municipality, RUB.

Table 7. The indicator of volume of production per capita

The name of the settlement	**The indicator of volume of production per capita**	
	The volume of production per capita, RUB.	**The value of the indicator**
Dgubga	41130,29	-0,803
Tenginka	14753,26	-1,000
Novomikhailovsky	69742,67	-0,589
Nebug	54542,34	-0,703
Tuapse	282547,22	1,0
Shepsi	31741,86	-0,873

8. The indicator of the average income level of the population I_{AIL} (8) (table 8):

$$I_{AIL} = 2 * \frac{AIL_S - AIL_{min}}{AIL_{max} - AIL_{min}} - 1 \quad (8)$$

AIL_S – the average income level of the population in the settlement, RUB;

AIL_{min} - the minimum average income level of the population of municipality, RUB.;

AIL_{max} - the maximum average income level of the population of municipality, RUB.

Table 8. The indicator of the average income level of the population

The name of the settlement	**The indicator of the average income level of the population**	
	The average monthly salary, RUB.	**The value of the indicator**
Dgubga	28567,4	0,104
Tenginka	26984,3	-1,0
Novomikhailovsky	28754,6	0,235
Nebug	29745,8	0,926
Tuapse	29851,2	1,000
Shepsi	27671,2	-0,521

9. The indicator of employment I_{EMP} (9) (table 9):

$$I_{EMP} = 2 * \frac{Emp_S - Emp_{min}}{Emp_{max} - Emp_{min}} - 1 \quad (9)$$

Emp_S – the average level of employment in the settlement, %;

Emp_{min} - the minimum level of employment of municipality, %;

Emp_{max} - the maximum level of employment of municipality, %. [18].

Table 9. The indicator of employment

The name of the settlement	The indicator of employment	
	The share of employment in economy, %	The value of the indicator
Dgubga	45,46	-0,057
Tenginka	44,55	-1,0
Novomikhailovsky	45,65	0,140
Nebug	45,1	-0,430
Tuapse	46,48	1,0
Shepsi	44,82	-0,720

10. The indicator of level of development of transport infrastructureI_{TI} (10-14) (table 10):

$$I_{TI} = \frac{I_{LR} + I_{LRW}}{2} - 1 \quad (10)$$

$$I_{LR} = 1 - \frac{LR_S / S_S}{LR_M / S_M} \quad (11)$$

$$I_{LRW} = 1 - \frac{LRW_S / S_S}{LRW_M / S_M} \quad (12)$$

$$LR_S = LRF_S + 0{,}8 * LRR_S + 0{,}6 * LRL_S \quad (13)$$

$$LR_M = LRF_M + 0{,}8 * LRR_M + 0{,}6 * LRL_M \quad (14)$$

I_{LR} – indicator of length of roads, ed.;
I_{LRW} – indicator of length of railways, ed.;
LRF_S – the length of paved roads of Federal importance in the settlement, km;
LRR_S – the length of paved roads of regional significance in the settlement, km;
LRL_S – the length of roads localities in the settlement, km;
LRF_M – the length of paved roads of Federal importance in the whole municipality, km;
LRR_M – the length of paved roads of regional significance in the whole municipality, km;
LRL_M – the length of roads localities in the whole municipality, km;
LRW_S – the length of railways in the settlement, km;
LRW_M – the length of railways in General at the municipality, km;
0.8, 0.6 – weighting factors that take into account different importance of roads and railways [19].

Table 10. The indicator of level of development of transport infrastructure

The name of the settlement	LRF, km	LRR, km	LRL, km	LRW, km	S, km^2	I_{LR}	I_{LRW}	I_{TI}
Dgubga	40	10	225	0	36.7	-1.0	1.0	0.0
Tenginka	10	5	28	0	18.2	0.2982	1.0	0.6491
Novomikhailovsky	24.5	20	57	0	47.4	0.3465	1.0	0.6732
Nebug	18	6	35	0	55.3	0.6715	1.0	0.8358
Tuapse	9	0	134	6	17.4	-1.0	-1.0	-1.0
Shepsi	15	7	37	11	22.6	0.2147	-1.0	-0.3927
TOTAL	116.5	48	516	17	197.6	–		

11. The indicator of collective accommodation I_{CA} (15) (table 11):

$$I_{CA} = \frac{N_{CA_S}/S_S}{N_{CA_M}/S_M} - 1 \quad (15)$$

N_{CA_S} – the total number of collective accommodation facilities on the territory of the settlement, ed.;

N_{CA_M} – the number of collective accommodation facilities in the territory of municipality, ed.

Table 11. The indicator of collective accommodation

The name of the settlement	N_{CA_S}	S_S	I_{CA}
Dgubga	28	36,70	-0,17
Tenginka	11	18,20	-0,34
Novomikhailovsky	62	47,40	0,43
Nebug	44	55,3	-0,131
Tuapse	14	17,40	-0,122
Shepsi	22	22,60	0,063
TOTAL	**181**	**197,6**	-

12. The indicator of download of collective accommodation $I_{T_{CA}}$ (16) (table 12):

$$I_{T_{CA}} = \frac{N_{T_{CA_S}}/Nbp_{CA_S}}{N_{T_{CA_M}}/Nbp_{CA_M}} - 1 \quad (16)$$

$N_{T_{CA_S}}$ - the number of tourists rested in the settlement of collective means of accommodation, people.

$N_{T_{CA_M}}$ - the number of tourists rested on the territory of the municipality in collective accommodation facilities, people.

Nbp_{CA_S} – the total number of bed-places in collective accommodation facilities on the territory of the settlement, ed.;

Nbp_{CA_M} – the total number of bed-places in collective accommodation facilities on the territory of the municipality, ed.;

Table 12. The indicator of download of collective accommodation

The name of the settlement	$N_{T_{CA_S}}$	Nbp_{CA_S}	$I_{T_{CA}}$
Dgubga	37294,00	5038	-0,227
Tenginka	18762,00	2159	-0,092
Novomikhailovsky	122193,00	11156	0,144
Nebug	81264,00	7917	0,072
Tuapse	21186,00	2519	-0,121
Shepsi	32746,00	3959	-0,136
TOTAL	**313445**	**32748**	-

13. The indicator of returns from the performance of collective accommodation facilities I_{Ica} (17) (table 13):

$$I_{Ica} = \frac{I_{CA_S}/N_{CA_S}}{I_{CA_M}/N_{CA_M}} - 1 \quad (17)$$

где,

I_{CA_S} – income derived from the activities of collective means of accommodation on the territory of the settlement district, RUB mln.

I_{CA_M} - income derived from the activities of collective means of accommodation on the territory of the municipality, RUB mln. [20].

Table 13. The indicator of returns from the performance of collective accommodation facilities

The name of the settlement	I_{CA_S}	N_{CA_S}	I_{Ica}
Dgubga	731,00	28	0,056
Tenginka	294,00	12	-0,009
Novomikhailovsky	1769,00	62	0,154
Nebug	1134,00	44	0,042
Tuapse	234,00	14	-0,324
Shepsi	338,00	22	-0,379
TOTAL	**4500**	**182**	-

14. The indicator of room fund I_{RF} (18) (table 14):

$$I_{RF} = \frac{N_{RF_S}/S_M}{N_{RF_M}/S_P} - 1 \quad (18)$$

N_{RF_S} – the number of room fund in the settlement, ed.;

N_{RF_M} – the number of room fund in the municipality, ed.;

Table 14. The indicator of room fund

The name of the settlement	N_{RF_S}	S_S	I_{RF}
Dgubga	1858	36,70	-0,172
Tenginka	796	18,20	-0,284
Novomikhailovsky	4115	47,40	0,420
Nebug	2920	55,3	-0,136
Tuapse	929	17,40	-0,126
Shepsi	1460	22,60	0,057
TOTAL	**12080**	**197,6**	-

15. The indicator of number of specialized accommodation facilities I_{SAF} (19) (table 15):

$$I_{SAF} = \frac{N_{SAF_S}/S_S}{N_{SAF_M}/S_M} - 1 \quad (19)$$

N_{SAF_S} – the total number of specialized accommodation facilities on the territory of the settlement,

ed.;

N_{SAF_M} – the total number of specialized accommodation facilities on the territory of the municipality, ed.;

Table 15. The indicator of number of specialized accommodation facilities

The name of the settlement	N_{SAF_S}	S_S	I_{SAF}
Dgubga	29	36,70	-0,024
Tenginka	11	18,20	-0,254
Novomikhailovsky	46	47,40	0,199
Nebug	58	55,3	0,295
Tuapse	1	17,40	-0,929
Shepsi	15	22,60	-0,180
TOTAL	160	**197,6**	-

16. The indicator of download specialized accommodation facilities I_{Tsaf} (20) (table 16):

$$I_{Tsaf} = \frac{N_{T_{SAF_S}}/Nbp_{SAF_S}}{N_{T_{SAF_M}}/Nbp_{SAF_M}} - 1 \quad (20)$$

$N_{T_{SAF_S}}$ - the number of tourists rested in the settlement in a specialized accommodation facilities, thousand people

$N_{T_{SAF_M}}$ - ко the number of tourists rested in the municipality in a specialized accommodation facilities, thousand people.

Nbp_{SAF_S} – the total number of bed-places in specialized accommodation facilities on the territory of the settlement, ed.;

Nbp_{SAF_M} – the total number of bed-places in specialized accommodation facilities on the territory of the municipality, ed.

Table 16. The indicator of download specialized accommodation facilities

The name of the settlement	$N_{T_{SAF_S}}$	Nbp_{SAF_S}	I_{Tsaf}
Dgubga	32,45	4,59	-0,276
Tenginka	12,74	1,74	-0,251
Novomikhailovsky	75,47	7,27	0,061
Nebug	111,25	9,17	0,240
Tuapse	0,84	0,16	-0,457
Shepsi	14,65	2,37	-0,368
TOTAL	**247,4**	**25,3**	-

17. The indicator of hotels and similar accommodation facilities I_H (21) (table 17):

$$I_H = 1 - \frac{N_{H_S}/S_S}{N_{H_M}/S_M} \quad (21)$$

N_{H_S} – the total number of hotels and similar accommodation facilities on the territory of the settlement, ed.;

N_{H_M} – the total number of hotels and similar accommodation facilities on the territory of the municipality, ed.;

Table 17. The indicator of hotels and similar accommodation facilities

The name of the settlement	N_{H_S}	S_S	I_H
Dgubga	3	36,70	-0,266
Tenginka	3	18,20	0,481
Novomikhailovsky	6	47,40	0,137
Nebug	5	55,3	-0,188
Tuapse	4	17,40	1
Shepsi	1	22,60	-0,603
TOTAL	**22**	**197,6**	-

18. The indicator of the level of download of hotels and similar accommodation facilities I_{Th}s (22) (table 18):

$$I_{Th} = 1 - \frac{N\tau_{H_S}/Nbp_{H_S}}{N\tau_{H_M}/Nbp_{H_M}} \quad (22)$$

$N\tau_{H_S}$ - the number of tourists accommodated in hotels, on the territory of the settlement, thousand people

$N\tau_{H_M}$ - the number of tourists accommodated in hotels, on the territory of the, thousand people

Nbp_{H_S} – the total number of bed-places in hotels on the territory of the settlement, ed.;

Nbp_{H_M} – the total number of bed-places in hotels on the territory of the municipality, ed.;

Table 18. The indicator of the level of download of hotels and similar accommodation

The name of the settlement	$N\tau_{H_S}$	Nbp_{H_S}	I_{Th}
Dgubga	9,84	1014,55	-0,132
Tenginka	10,28	1014,55	-0,093
Novomikhailovsky	24,87	2029,09	0,097
Nebug	20,06	1690,91	0,062
Tuapse	17,2	1352,73	0,139
Shepsi	0,84	338,182	-0,778
TOTAL	**9,84**	**7440**	-

19. The indicator of tax revenues from tourist and recreational industry I_F (23) (table 19):

$$I_F = 1 - \frac{F_{T_S}/F_S}{F_{T_M}/F_M} \quad (23)$$

F_{T_S} – tax deductions to the municipal budget from the tourism industry in settlement, bln. RUB;

F_{T_M} - tax deductions to the municipal budget from the tourism industry, bln. RUB;

F_S – the total amount of tax payments to the municipal budget from the settlement, bln. RUB;

F_M – the total amount of tax payments to the municipal budget, bln. RUB.

Table 19. The indicator of tax revenues from tourist and recreational industry

The name of the settlement	F_{TS}	F_S	I_F
Dgubga	77,72	725	0,396
Tenginka	35,28	402	0,143
Novomikhailovsky	202,28	915	1,0
Nebug	126,08	843	0,947
Tuapse	28,08	3406	-0,893
Shepsi	40,56	349	0,513
TOTAL	**510**	**6640**	-

In the process of analysing the main indicators of tourism and recreational potential of the territory, we obtained various indicators of development of the region. Previously, we divided all indicators in two groups. We reduce the resulting indicators in two generalized index of natural environmental (I_{NE}) and socio-economic (I_{SE}) components of the tourist-recreational potential (24, 25) [20] (tables 20, 21).

$$I_{NE} = \frac{I_{LC} + I_S + I_{FA} + I_{WD} + I_{EM} + I_{SW}}{6} \quad (24)$$

$$I_{SE} = \frac{I_{VP} + I_{AIL} + I_{EMP} + I_{TI} + I_{CA} + I_{TCA} + I_{Ica} + I_{RF} + I_{SAF} + I_{Tsaf} + I_H + I_{Th} + I_F}{13} \quad (25)$$

Table 20. The index of natural environmental component of tourism and recreation potential of urban and rural settlements of Tuapse area

The name of the settlement	I_{LC}	I_S	I_{FA}	I_{WD}	I_{EM}	I_{SW}	I_{NE}
Dgubga	0.1594	-1,0	-0.6	0.173	-0.523	-0.135	-0,321
Tenginka	0.7391	-1,0	-0.0449	0.733	0.646	0.542	0,269
Novomikhailovsky	0.1594	0,0	-0.4797	0.494	0.184	0.213	0,095
Nebug	0.9324	1,0	0.0917	0.727	0.601	0.74	0,682
Tuapse	0.3527	1,0	-0.7908	-1.0	-1,0	-1.0	-0,406
Shepsi	0.1594	1,0	-0.0334	0.831	-0.486	0.665	0,356

Table 21. The index of socio-economic component of tourist-recreational potential of urban and rural settlements of Tuapse area

Indicator	Dgubga	Tenginka	Novomikhailovsky	Nebug	Tuapse	Shepsi
I_{VP}	-0,803	-1	-0,589	-0,703	1	-0,873
I_{AIL}	0,104	-1	0,235	0,926	1	-0,521
I_{EMP}	-0,057	-1	0,14	-0,43	1	-0,72
I_{TI}	0.0	0.649	0.673	0.836	-1.0	-0.393
I_{CA}	-0,17	-0,34	0,43	-0,131	-0,122	0,063
$I_{T_{CA}}$	-0,227	-0,092	0,144	0,072	-0,121	-0,136
I_{Ica}	0,056	-0,009	0,154	0,042	-0,324	-0,379
I_{RF}	-0,172	-0,284	0,420	-0,136	-0,126	0,057
I_{SAF}	-0,024	-0,254	0,199	0,295	-0,929	-0,18
$I_{\mathrm{T}saf}$	-0,276	-0,251	0,061	0,24	-0,457	-0,368
I_{H}	-0,266	0,481	0,137	-0,188	1	-0,603
I_{Th}	-0,132	-0,093	0,097	0,062	0,139	-0,778
I_{F}	0,396	0,143	1	0,947	-0,893	0,513
I_{SE}	-0,121	-0,235	0,306	0,141	0,013	-0,332

From the received indices to derive the single integral index of tourist-recreational potential (I_{TRP}) (26) (table 22).

$$I_{TRP} = \frac{I_{NE}+I_{SE}}{2} \quad (24)$$

Table 22. The integral index of tourist-recreational potential of urban and rural settlements of Tuapse area

The name of the settlement	I_{NE}	I_{SE}	I_{TRP}
Dgubga	-0,321	-0,121	-0,221
Tenginka	0,269	-0,235	0,017
Novomikhailovsky	0,095	0,306	0,201
Nebug	0,682	0,141	0,411
Tuapse	-0,406	0,013	-0,197
Shepsi	0,356	-0,332	0,012

On the basis of the analysis and the extracted index of tourist and recreational potential, it is possible to draw the following conclusions.

The highest index value in rural settlement of Nebug. This area has the most balanced development of the tourism industry, and there are all prospects for further development and growth in this direction. Nebug's settlement has the highest indicator on the ecological status and the protection of the environment that suggests significant potential in the field of Spa treatment, the development of tourism throughout the year.

With small lag there is urban settlement of Novomikhailovsky. This district also has considerable recreational potential, well-developed services sector. However, the presence of such large enterprises, as, for example state farm «Novomikhailovsky» Ltd. had a negative impact on the environmental status of the district, that hinders the further development of tourism, attracting large investors.

Rural settlements of Shepsi and Tenginka have almost the same indicator values, which is understandable. Both areas have good prospects for the development of tourism and recreation. In areas of developing agriculture, particularly small farms.

In the urban settlement of Tuapse, few prospects for development of sanatorium-resort in connection with the presence of large industrial enterprises, however well-developed economic and social sectors can contribute to the development of business tourism.

Urban settlement of Dgubga has received the lowest value of the indicator. A significant part of the region territory is located in mountainous, unsuitable for recreation area. Existing recreation facilities for the most part, are small businesses. A large part of the basic production assets are obsolete and require significant investment to upgrade. It is necessary to improve the quality of service and provision of tourist services, increase competitiveness and attract more holidaymakers with a high level of income.

Thus, we can conclude that the proposed model of integrated assessment allows us to provide a comprehensive assessment of tourist-recreational potential of territories most effectively to analyze trends in the development of the tourism industry. This method can be successfully applicable for the purposes of strategic planning of development of the whole region and separate entity.

ACKNOWLEDGMENT

The work is done in the framework of the Russian Foundation for Basic Research Grant № 16-05-00724\16.

REFERENCES

1. Bobylev S.N., Makeenko P.A. Indikatory ustoichivogo razvitiya dlya Rossii (ekologo-ekonomicheskie aspekty) [Indicators of sustainable development of Russia (ekologo-economic aspects)], 2002, 124 p.

2. Gogoberidze, G.G. Kompleksnoe regionirovanie primorskikh territorii Mirovogo okeana: Monografiya [Comprehensive raionirovanie coastal areas of the World ocean: a Monograph], 2007, 396 p.

3. Temirov D.S., Yaili E.A., Simonov V.S. Organizatsiya i planirovanie rekreatsionnoi deyatel'nosti [Organization and planning of recreational activities], 2004, 267 p.

4. Amirkhanov, M. M., Arakelov A. S. Teoreticheskie i metodicheskie aspekty otsenki turistsko-rekreatsionnogo potentsiala regionov s rekreatsionnoi spetsializatsiei [Theoretical and methodological aspects of the evaluation of the tourism capacity of the regions with recreation specialization]. Sovremennaya nauchnaya mysl' = Modern scientific thought. 2013. No. 2. P. 147-154.

5. Polynev A.O. Mezhregional'naya ekonomicheskaya differentsiatsiya: metodologiya analiza i gosudarstvennogo regulirovaniya [Inter-regional economic differentiation: methodology of analysis and state regulation], 2003, 208 p.

6. Reteyum A.Yu. Monitoring razvitiya [Monitoring of development], 2004, 160 p.

7. URL: http://www.admjubga.ru//

8. URL: http://www.tenginskoesp.ru//

9. URL: http://www.tenginskoesp.ru//

10. URL: http://www.nebug.tuapse.ru//

11. http://www.tuapseregion.ru/

12. URL: http://www.adm.tuapse.ru//

13. URL: http://www.shepsi.tuapse.ru//

14. URL: http://www.krsdstat.ru/

15. Zenina V.D., Georgievskaya G.V., Kholodova N.M. i dr. «Skhema territorial'nogo planirovaniya munitsipal'nogo obrazovaniya Tuapsinskii raion» [Scheme of territorial planning of the municipality Tuapse region], 2005, 218 p.

16. Sergin S.Ya., Yaili E.A., Tsai S.N., Potekhina I.A. Klimat i prirodopol'zovanie Krasnodarskogo Prichernomor'ya [The climate and nature of the Krasnodar black sea region], 2001, 187 p.

17. Yaili E.A., Muzalevskii A.A. Risk: analiz, otsenka, upravlenie [Risk: analysis, assessment, management], 2005, 232 p.

18. Gogoberidze G. G., M. S. Arakelov, Mavrodi K. P., A. S. Arakelov Methodology of socio-economic zoning, territorial objects of the Krasnodar Black Sea region [Metodika sotsial'no-ekonomicheskogo raionirovaniya territorial'nykh ob''ektov Krasnodarskogo Prichernomor'ya]. Regional'naya ekonomika: teoriya i praktika = Regional Economics: theory and practice, 2013. No. 15. P. 2-8.

19. Temirov, D. S., K. H. Ibragimov, M. S. Arakelov Management of territorial recreational systems. Monograph [Temirov D.S., Ibragimov K.Kh., Arakelov M.S. Upravlenie territorial'nymi rekreatsionnymi sistemami. Monografiya], 2012, 236 p.

20. Arakelov, A. S., M. S. Arakelov, Simonyan G. A., D. S. Temirov Topical issues for analysis and evaluation of the tourism capacity of the territory [Aktual'nye voprosy analiza i otsenki turistsko-rekreatsionnogo potentsiala territorii]. Molodaya nauka – 2013 = Young science – 2013, 2014. P. 98-102.

RUNOFF CALCULATIONS FOR UNGAUGED RIVER BASINS OF THE RUSSIAN ARCTIC REGION

Georgy Ayzel, Institute of Water Problems of Russian Academy of Sciences, Russia

hydrogo@yandex.ru

Arctic coastal systems are very sensitive to the freshwater budget mainly formed by river runoff. Great biases in estimation of total river runoff load to the Arctic Ocean proposed by the number of various scientific groups and insufficiency of physically-based, short-term, spatially diverse runoff predictions lead to strong necessity of state-of-art hydrological techniques implementation. At the moment the most powerful tools for the land hydrological cycle modeling are physically-based, conceptual or data-driven models. Better model – wider sources of hydrometeorological and landscape-related information we need to use to perform robust calculations. Severe climatic conditions of Arctic coastal region have led to weak river runoff monitoring net and a high level of uncertainties related to difficulties of direct measurements. There is the reason we need to develop modern techniques that allow providing effective runoff predictions by state-of-art models in the case of strong research data scarcity (for ungauged basins). Early stage of research aimed to coupling of conceptual hydrological model, cutting edge machine learning techniques and various sources of geographical data will be proposed with the call for intensification of cross-disciplinary research activities for the Arctic region sustainable development and safety.

Key words: arctic, runoff, modeling, ungauged basins, machine learning, SWAP

I. INTRODUCTION

A large part of the world rivers are ungauged in terms of ability to make accurate runoff calculations and predictions [8]. This problem is especially relevant for the Arctic region because of inability to estimate modern state of highly sensitive Arctic coastal ecosystems without high-resolution and well-proved river runoff calculations provided not only for the main large rivers, but also for small and mid-range rivers which usually have neither hydrological nor meteorological observations in their watersheds. Fig. 1 shows hydrologically ungauged area (there are no direct runoff measurement at all) of the Russian Arctic region. At first sight presented area is relatively small, but at the same time it takes the entire coastal zone of the Russian Arctic region. From this point it follows that the contribution of this coastal part to overall river runoff may be inconsiderable, but this tiny water budget plays important role for coastal zone ecosystems evolution and local communities' life.

At the moment there is no one daily runoff database of Russian Arctic rivers for modern period. All available datasets use the same information of river discharges provided by the Global Runoff Data Center (GRDC, Koblenz, Germany) [14] that have some limitations. Firstly, modern Russian Arctic-related data have only monthly resolution that insufficient for use in state-of-art daily hydrological modeling procedures, and secondly, most of the daily data relates to the period of the

late Soviet Union and in most cases we have no data at all after years of 1991-1993 (Fig. 2). Thereby at the moment we still faced the strong need of valid daily hydrological data.

Fig. 1. Hydrologically ungauged (in space) area of the Russian Arctic region

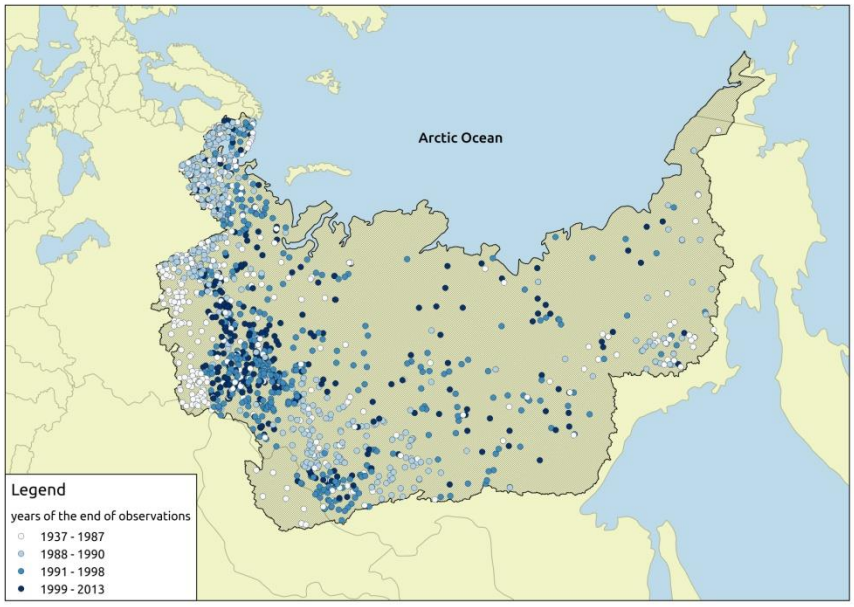

Fig. 2. Years of available river runoff data – hydrologically ungauged (in time) area of the Russian Arctic region (GRDC database)

Hydrological models are powerful, modern research tools for estimation of different features of water cycle processes. Despite of the type of hydrological model you choose (physically-based, conceptual or data-driven), the problem of determining model parameters will be acute [10, 11]. In

the case of the basin under research have suitable direct runoff observations we can set up and solve a task of parameters estimation using calibration – model parameters obtaining procedure as an inverse task of runoff calculations. Implementing of hydrological models for runoff calculations in ungauged basins is a challenging task [13]. The set of methods aimed at finding the model parameters under insufficient hydrological data (fully or partially lack of direct runoff measurements), called regionalization [12]. There are numerous studies related to the problem of hydrological models parameters regionalization for ungauged basins, and typically it can be possible to divide methods presented in them into three main groups: based on physical similarity, based on spatial proximity and regression-based techniques [1, 12]. According to the analysis of more than 30 scientific articles related to the theme of regionalization, there is no universal approach to model parameters estimation for ungauged basins [2]. Thereby, runoff calculations for ungauged basins using highly data-dependent hydrological models require a comprehensive effort to a wide range of scientific issues from the model and its parameterization scheme identification to regionalization technique selection and source of hydrometeorological data we use.

II. DATA AND METHODS

Researched basins

The Nadym River, the Pur River, and the Taz River are one of the major rivers in the northern West Siberia; rivers flow through the territory of the Yamalo-Nenets Autonomous District of Russia and belong to the Kara Sea basin [7] (Fig. 3). All of researched basins are quite similar in geographical and hydrological conditions (Table 1).

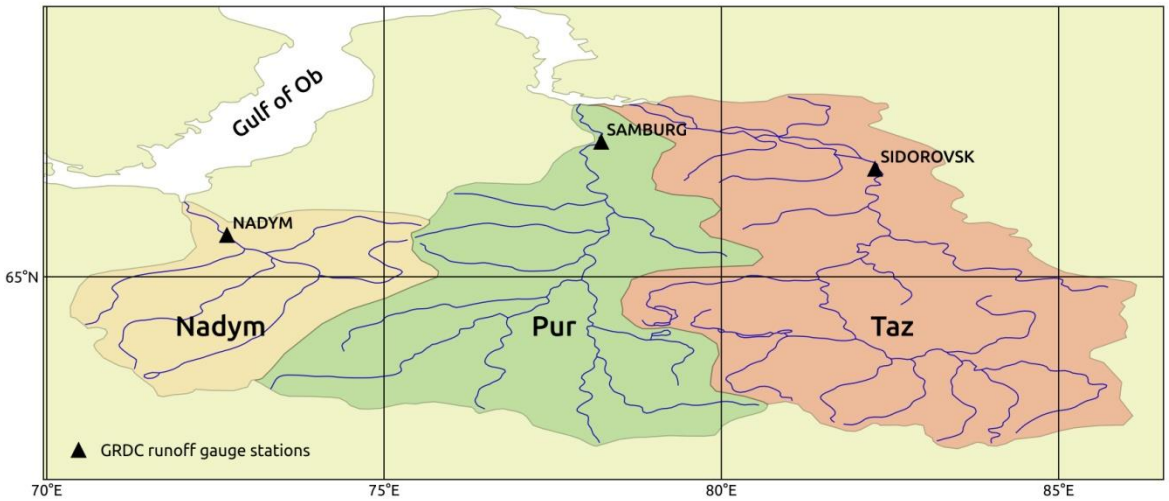

Fig. 3. Researched river basins

Table 1. Comparative characteristics of researched river basins

River	Drainage area, km^2	Length, km	Mean runoff, mm/year
Nadym	64 000	545	290
Pur	112 000	1024	293
Taz	150 000	1401	305

Hydrological data

Observed daily runoff data of researched river basins at closest to the mouths gauges (Fig. 3) were obtained from GRDC database [14] under standard request. Runoff data length was unified for all rivers and contains period from 1979 to 1991 year. Modern data from these gauge stations are not freely available for scientific purpose and are not taken into consideration in this work. Runoff values were converted from m^3/s to mm/day.

Meteorological data

Meteorological forcing data were obtained from WFDEI database [15] that based on ERA-Interim forcing product by the European Centre for Medium-Range Weather Forecasts (ECMWF). WFDEI database have the data of eight meteorological variables with daily time resolution and 0.5º x 0.5º spatial resolution with global land coverage. Temperature and bias-corrected by Climatic Research Unit (CRU) rainfall and snowfall precipitation rates were used as input forcing to conceptual hydrological model. In case of machine learning rainfall-runoff model implementation all available meteorological variables were used. Lumped implementation of developed rainfall-runoff models leads to the need of weighted averaging of all forcing variables across researched basins.

Conceptual hydrological model

In this study simplified conceptual, lumped hydrological model Hydrologiska Byråns Vattenbalansavdelning (HBV) [4] were used. Schematic diagram of processes represented by simplified HBV model is presented on the Fig. 4.

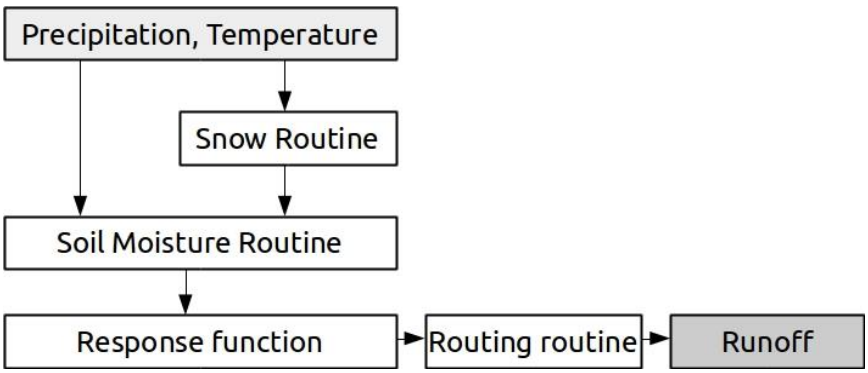

Fig. 4. Schematic structure of HBV model

During the last decades HBV model has been successfully used in numerous scientific studies and engineering tools all over the world. Traditionally HBV model was used to runoff calculations for small and medium sized basins (< 10 000 km^2), but some researchers are attempting to generalize local results to macro (global) scale [3]. In presented study we will investigate the possibility of s-HBV model simulate river from large (> 50 000 km^2) river watersheds.

Machine learning (data-driven) model

The increasing popularity in hydrological modeling methodology refers to modern data-driven (machine learning) techniques. Key concept of these methods – to set up robust relation between meteorological forcing data and runoff observations without any knowledge of specific geographical or hydrological patterns. In this study we implemented the most widely used solution for regression tasks – Decision Tree model. Typical Decision Tree is a "white box" consists of the

range of boolean classifiers which split our samples to tiny "leaf" nodes where all samples constantly refers to the one target value (Fig. 5).

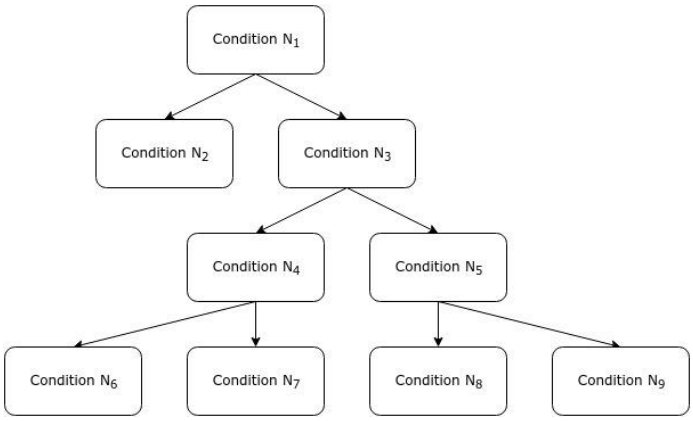

Fig. 5. Scheme of simple ordinary Decision Tree model

Single tree-based implementation of Decision Tree algorithm faced with the case of over-fitting and robustness lack that lead to limited using in real world examples. In our work we used cutting-edge machine learning technique based on ensemble approach to predictions: Random Forest Regression (RFR). RFR is based on ensembles of simple Decision Tree models and provide useful tricks such bagging and bootstrapping which totally reduce over-fitting and make our models suitable to provide robust predictions [5]. There are limited applications of RFR in daily river runoff modeling, but in [6] this technique has been successfully implemented for monthly runoff simulations across the Europe.

Modeling efficiency criterion

In presented study widely used and most-known for runoff modeling efficiency estimation criterion proposed by Nash and Sutcliffe (NS) [9] was used as follows:

$$NS = 1 - \frac{\sum_i (x_i - y_i)^2}{\sum_i (x_i - x_{mean})^2}, \quad (1)$$

where x_i , y_i - observed and simulated runoff in i day, x_{mean} - mean observed runoff.

III. RESULTS AND DISCUSSION

Case study 1: calculations for ungauged (in time) basins

The last year of observational data for all researched basins is the year of 1991 inclusively. It is a reason to refer these basins to “ungauged in time” group – there are no information of their current hydrological state history. To get robust estimates of current river runoff conditions, it is necessary to tune our hydrological model to data we have, i.e. to calibrate model parameters. Model parameters calibration has been carried out on entire observational period (1979-1991) in automatic manner with the use of standard Newton conjugate gradient (Newton-CG) algorithm implementation. Newton-CG is cost-efficient, multivariate function optimization algorithm typically used for local minimum search. In our study it showed comparative performance with algorithm of global optimization – differential evolution – wherein used less computational time. *NS* criterion (Eq. 1) was chosen as an objective function for calibration. Obtained optimal parameters are robust

– up to 10 runs of Newton-CG optimization with different initial conditions showed the same results.

Further calculations of river runoff for entire researched period (1979-2014) were performed (Fig. 6).

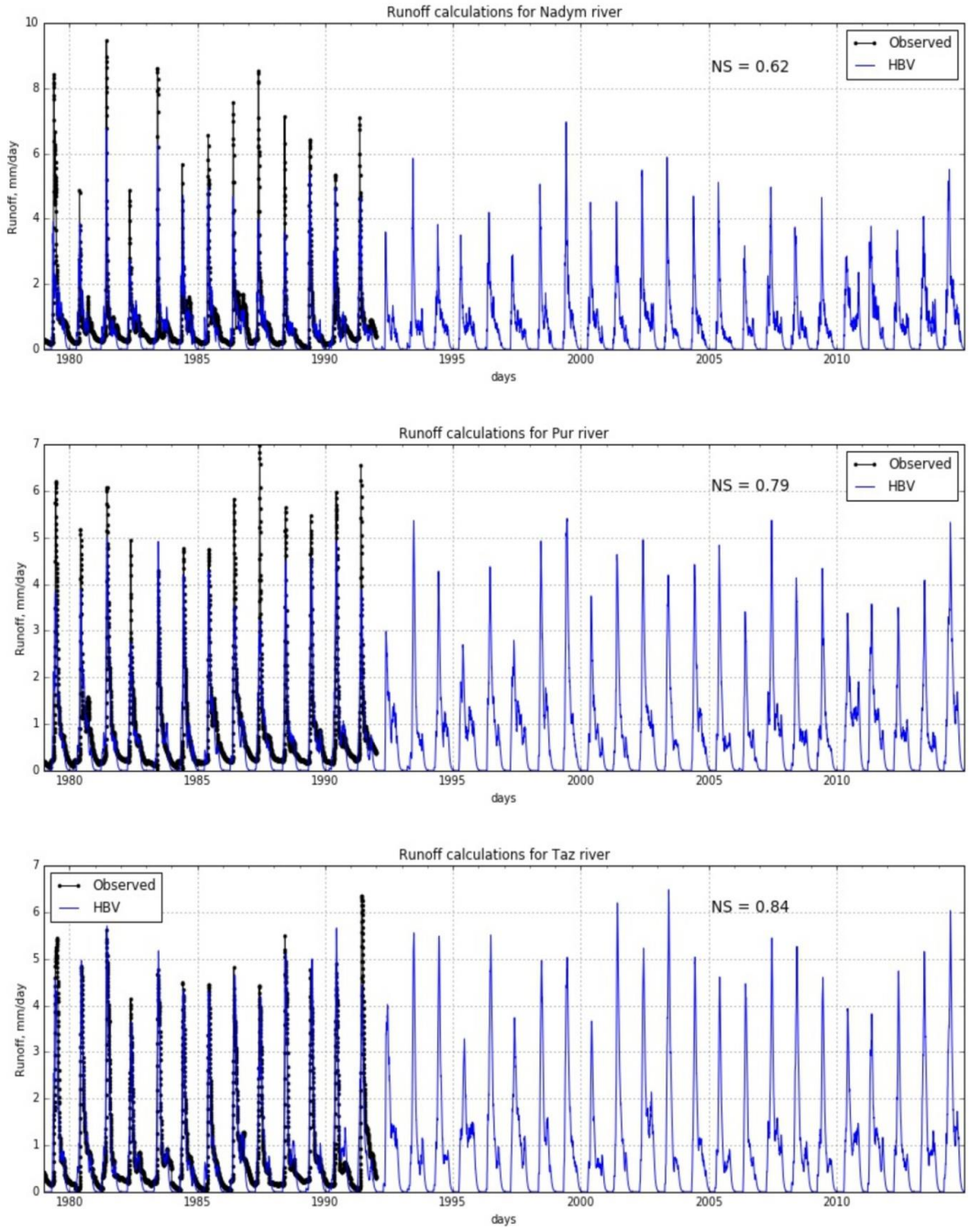

Fig. 6. Runoff modeling results

Obtained results show good performance of HBV model for runoff calculations for large Russian Arctic rivers. The larger river – the better modeling efficiency. We suppose that this fact corresponds with scale effect of runoff formation processes with one hand, and local basin features

with another hand. For all researched basins significant underestimation of autumn-summer period runoff was noted. This effect is caused by HBV hydrological model structure simplification or by using rough estimates of monthly potential evaporation values which can overestimate evaporation potential of observed river basins. Obtained results have much in common with physically-based distributed SWAP model results provided in [7].

Case study 2: calculations for ungauged (in space) basins

In the case of observed runoff lack hydrologists often face with impossibility to provide model parameters calibration procedure. Then different parameters regionalization strategies will be implemented [1, 2, 12, 13]. The most intuitive way to set up model parameters for ungauged basins (and the most used for engineering applications) is regionalization based of spatial similarity which in practice is full transfer of model parameters set (derived by calibration or any other method) from gauged (or donor) to ungauged (or recipient) catchment. In this study we successively implemented all optimal parameters sets (derived for each river through calibration) for all rivers under research and estimated corresponding runoff modeling efficiency (Table 2).

Table 2. Runoff modeling efficiency (NS) with various sets of parameters

River	Optimal set of parameters		
	Nadym	Pur	Taz
Nadym	0.62	0.41	0.37
Pur	0.38	0.79	0.75
Taz	0.57	0.84	0.84

Obtained results show significant modeling efficiency reduction for Nadym River in case of using parameters sets both from Pur and Taz rivers. Further results show that optimal parameters set of HBV model for Nadym River by itself has moderate performance not only for runoff modeling routine, but for regionalization procedure too – efficiency reduction has significant value for both Pur and Taz rivers in case of calculations based on optimal parameters for Nadym River. The best results were obtained for Pur and Taz rivers tandem. For Taz River we have no modeling efficiency reduction using Pur River optimal parameters at all, and for Pur River we have insignificant efficiency reduction.

Finally we suppose that Pur River optimal HBV model parameters are appropriate choice for initial conditions set up or *a priori* parameters set for river basins in similar geographical conditions.

Machine learning technique implementation for runoff post-processing

Simplified HBV model which was implemented in this study provides good daily estimations of river runoff in terms of Nash-Sutcliffe efficiency criterion, but despite this, modeled runoff time-series has similar faults end error in similar water regime phases: in the spring flood HBV model underestimates absolute value of runoff peak, and usually underestimates baseflow in the summer-autumn period. The main idea of machine learning technique implementation in this case consists in hypothesis that all observed HBV model errors have non-random reasons and can be described using complex statistical model such as RFR.

For checking this hypothesis post-processing of modeled runoff time-series based on cutting-edge machine learning algorithm (RFR) was implemented in cross-validation manner: for train period we reserved all available years except one year which related to test period. Input data (feature matrix) for RFR were constructed by meteorological forcing data and HBV modeled runoff output. Residuals between observed and modeled runoff were chosen as output target labels. Thereby for each researched year and river we independently implemented coupled system of conceptual HBV model provided physically-based runoff calculations with machine learning post-processing approach based on RFR model (HBV-ML) and received the results of runoff modeling efficiency for both HBV and HBV-ML models (Fig. 7).

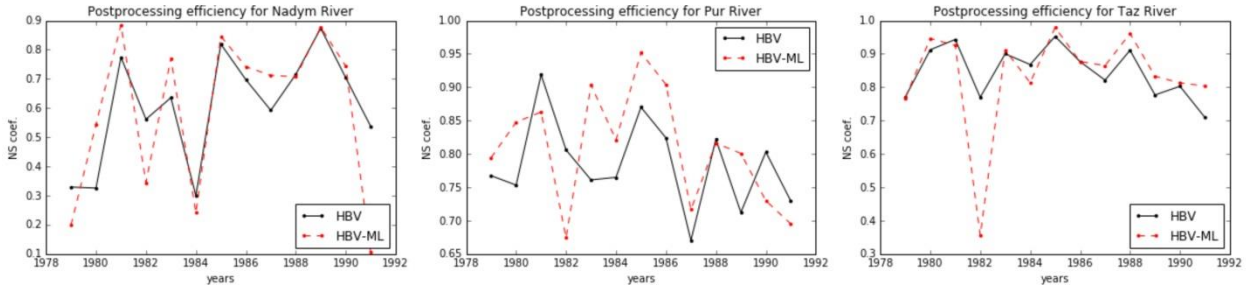

Fig. 7. Cross-validation results for ordinary conceptual model efficiency (HBV) and coupled system of conceptual model and machine learning post-processing technique (HBV-ML)

The results show uncertain efficiency improvements of machine learning based post-processing implementation to modeled runoff. On the average there is no such NS growth for all researched basins, i.e. positive results compensate with negative results of provided post-processing. For the Nadym River provided technique showed better results for 7 of 13 years, for the Pur River – for 8 of 13 years, and for the Taz River – for 9 of 13 years. Further research of provided novel post-processing approach limitations is needed.

Despite of well-proved machine learning models efficiency for decision making in many technological-oriented industries, they face serious limitations and provide significant discrepancies (uncertainties) in actual hydrological case studies. Understanding of runoff formation mechanisms, hydrological processes description and deeper implementation of this knowledge in community mathematical models are still the best way to improve runoff calculations (especially for ungauged basins in permafrost regions) rather than adaption of complex statistical (machine learning) models for modeled river runoff post-processing purposes.

IV. ACKNOWLEDGMENTS

The part of the studies related to mining and analyses of hydrometeorological data, developing data-driven models and runoff calculations for ungauged basins was funded by the Russian Foundation for Basic Research (RFBR) according to the research project № 16-35-00159 mol_a. The part of presented studies related to the developing, adapting and implementing of conceptual hydrological model was financially supported by the Russian Science Foundation (grant № 16-17-10039). The part of the studies related to post-processing efficiency estimation was supported by the Russian Ministry of Education and Science (grant № 14.B25.31.0026).

The present work has been carried out within the framework of the Panta Rhei Research Initiative of the International Association of Hydrological Sciences (IAHS).

V. REFERENCES

[1] G. Ayzel, "Artificial Neural Network Technique Implementation for the Hydrological Model Parameters Search", *Russian Scientific Journal*, 2014, vol. 40, no. 2, pp. 282-287 (In Russian).

[2] G. Ayzel, "River Runoff Calculations for Ungauged Basins: the Potential of Using Hydrological Model and Artificial Neural Network Technique", *Engineering Surveys*, 2014, no. 7, pp. 60-66 (In Russian).

[3] H. Beck et. al., "Global-Scale Regionalization of Hydrologic Model Parameters", *Water Resources Research*, 2016 (in press).

[4] S. Bergström, *Development and Application of a Conceptual Runoff Model for Scandinavian Catchments*. Norrköping: SMHI RHO 7, 1976. 134 p.

[5] L. Breiman, "Random Forests", *Machine learning*, 2001, vol. 45, no. 1, pp. 5-32.

[6] L. Gudmundsson, S. Seneviratne, "Observational Gridded Runoff Estimates for Europe (E-RUN version 1.0)", Earth *Syst. Sci. Data Discuss.*, 2016 (in press).

[7] E. Gusev, O. Nasonova, L. Dzhogan, G. Ayzel, "Simulating the Formation of River Runoff and Snow Cover in the Northern West Siberia", *Water Resources*, 2015, vol. 42, no.4, pp. 460-467.

[8] M. Hrachowitz et al., "A Decade of Predictions in Ungauged Basins (PUB) - a Review", *Hydrological Sciences Journal*, 2013, vol. 58, no. 6, pp. 1198-1255.

[9] J. Nash, J. Sutcliffe, "River Flow Forecasting Through Conceptual Models Part I - A Discussion of Principles", *Journal of hydrology*, 1970, vol. 10, no. 3, pp. 282-290.

[10] O. Nasonova, E. Gusev, G. Ayzel, "Optimizing Land Surface Parameters for Simulating River Runoff from 323 MOPEX-watersheds", *Water Resources*, 2015, vol. 42, no. 2, pp. 186-197.

[11] L. Oudin, A. Kay, V. Andréassian, C. Perrin, "Are Seemingly Physically Similar Catchments Truly Hydrologically Similar?", *Water Resources Research*, 2010, vol. 46, no. 11. 15 p.

[12] T. Razavi, P. Coulibaly, "Streamflow Prediction in Ungauged Basins: Review of Regionalization Methods", *Journal of hydrologic engineering*, 2012, vol. 18, no. 8, pp. 958-975.

[13] M. Sivapalan et al., "IAHS Decade on Predictions in Ungauged Basins (PUB), 2003–2012: Shaping an Exciting Future for the Hydrological Sciences", *Hydrological Sciences Journal*, 2003, vol. 48, no 6, pp. 857-880.

[14] The Global Runoff Data Center, 56068 Koblenz, Germany. www.bafg.de.

[15] G. Weedon et al., "The WFDEI Meteorological Forcing Data set: WATCH Forcing Data Methodology Applied to ERA-Interim Reanalysis Data", *Water Resources Research*, vol. 50, no. 9, pp. 7505-7514.

LARGE BARRIER-LAGOON SYSTEMS ON THE EASTERN AND SOUTH-EASTERN BALTIC SEA COASTS: CONDITIONS OF DEVELOPMENT

Ekaterina Badyukova, Moscow State university, faculty of geography, Russia
Leonid Zhindarev, Moscow State university, faculty of geography, Russia
Svetlana Lukyanova, Moscow State university, faculty of geography, Russia
Galina Solovieva Moscow State university, faculty of geography, Russia

badyukova@yandex.ru

The paper considers the geological structure and evolution of large barrier-lagoon systems in the eastern and southeastern coasts of the Baltic Sea. The data available on some coastal deltaic plains in the Leningrad Region, Latvia and Lithuania are discussed in some details. The considered materials lead the authors to the conclusion about a unified mechanism of the systems' development. A considerable rise of the sea level at the Littorina Sea transgression fostered large transgressive bars developing at the margins of deltaic plains and lagoons formation on the surface of these plains.

Keywords: sea-level oscillation, coast, barrier-lagoon system, paleogeography

INTRODUCTION

The geological and geomorphological context of large barrier-lagoon systems have been recently studied in details in the SE Baltic region including the Curonian and Vistula Spits and the adjacent coasts of the central and eastern Poland [23]. The results strongly suggest the sea level fluctuations to be the leading factor in the barrier system appearance and evolution. The same factor was undoubtedly crucial in the evolution of large constructional landforms on the eastern coasts of the Baltic, including the Gulf of Finland, Latvian and Lithuania coasts. The field studies were confined to several key regions.

I. NEVA LOWLAND

The lowland is confined to the land between the Gulf of Finland and the Ladozhskoye Lake. It is noted for small elevations and flattened surface. Two terrace levels are distinguishable; the upper of them is attributed to the Baltic Ice Lake, which is a freshwater lake formed at the southern margin of the Scandinavian ice sheet. The younger – Littorina Sea terrace – forms a gently sloping plain that occurs as a narrow fringe surrounding the Gulf coasts. Its boundaries marked by ancient beach ridges and scarps modeled by marine erosion [13].

The Neva Lowland includes Sestroretsk and Lakhti depressions, together with the land adjoining the lowermost part of the Neva River . In spite of extensive materials obtained on the geological history of the eastern part of the Gulf of Finland in the Holocene, there are a lot of questions still to be solved.

Sestroretsk basin and Sestroretsk Razliv Lake.

The Sestroretsk Razliv Lake did not come into being until the early 18th century. Instead, there existed two rivers named Sestra and Chernaya; below their confluence the resulting water stream is known under the name of the Gagarka R. The dam construction on the latter in 1723 resulted in flooding of the lowermost parts of the Sestra and Chernaya valleys and a part of the coastal plain. The flooded areas formed the Lake Razliv about 5 km long and 4 km wide; the lake is drained by way of artificial canal (Sestra Zavodskaya) going between two dune ridges.

The Sestroretsk depression enclosing the lake is separated from the Gulf of Finland by a sandy barrier 1–3 km wide and 10 km long. The sandy accumulations are thickest in the western part of the barrier; there they form several ridges of dunes up to 10–12 m high [13] arranged en echelon along the sea coast. The prevalent winds determine the dune movement from west to east, with trunks of earlier buried trees exposed in deflation basins [20]. Similar processes are typical of the Curonian and Vistula spits [23]. There are vast marches at the back of each large sand ridge, such as Kanavnoye and Sestroretsk ones, the latter being the largest of all.

The dune formation on the Gulf of Finland coasts started about 3000–3500 years ago. By that time the region had been already peopled, as follows from archeological finds recovered from under the dunes near the town of Sestroretsk. 11 archeological sites were excavated on the western coast of the Lake Razliv under the dunes; they yielded some Stone Age tools and numerous ceramic fragments attributed to the 3rd – 2nd centuries BC. The Neolithic sites Sosnovaya Gora and Sosnovaya Gora 1 were found on the eastern coast of the Sestroretsk Razliv Lake, within a rather narrow sand ridge. The Sosnovaya Gora 1 site has been studied in details in respect to its stratigraphy, lithology, and geochemistry. The results obtained make possible reconstructing the principal stages in the regional environment evolution and its colonization by the primitive man. The ceramic fragments recovered from that site are dated to ~4th millennium BC – 4890±35 yr. BP (3715–3636 cal. BC) [8].

There are ridges 10–13 m a.s.l. overgrown with pines in the NE of Sestroretsk marsh. Judging from the map and description of them compiled in the 19th century, they may be interpreted as the coastline of the Littorina Sea (one of its stages) and related dune massifs. The former coastline was a barrier bar with a lagoon at its back. (Fig. 1).

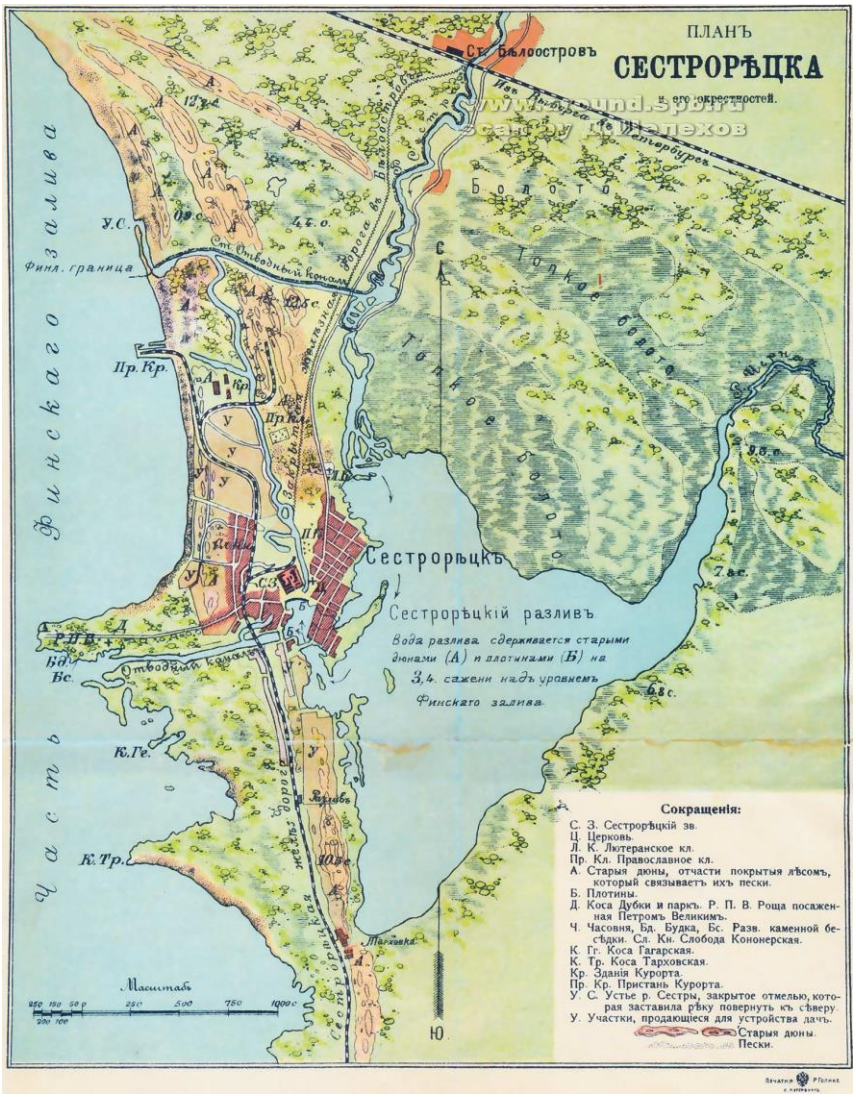

Fig. 1. The Sestroretsk Razliv Lake, mapped at end of the 19th century.

All the boreholes drilled on the Sestroretsk marsh penetrated a peat layer 1.5 to 3 m thick and reac17.hed a diatom gyttja attributable to the Littorina Sea at a depth of 4–5 m. The gyttja is 3–4 m thick, occasionally up to 10 m [3].

Similar deposits are found on the right bank of the Sestra Zavodskaya Canal, 200 m downstream from the railroad bridge; the diatom gyttja of the Littorina age occurs there at a depth of ~3 m under eolian sands. Such a sequence is traceable over a large area [22].

The above facts give grounds to suggest that the infilling of the ancient Sestra R. valley with sediments up to 50 m thick began at the time of Littorina transgression and proceeded along with the coastal plain flooding. The coastal plain was separated from the sea by bar, the first lagoon formed which presents a swamp at present. All the subsequent fluctuations of the sea level and the post-glacial isostatic uplift of the land surface resulted in the shoreline moving gradually seaward and in development of a series of barrier-lagoon systems. The Sestroretsk dunes are the latest large barrier.

Lakhti depression and Lakhtinsky Razliv Lake.

The Lakhtinsky Razliv Lake is in the Lahti depression at a level no more than 3 m a.s.l. The lake receives two rivers – Kamenka and Chernaya and is connected with the Nevskaya Guba bay by a channel. A large barrier bar up to 4 m high separates the lake basin from the sea. The barrier extends towards southeast as a peninsula with alternating ridges and linear hollows oriented from W to E [19].

In the Primorsky district there is a very deep buried valley confined to a deep-seated regional tectonic fault of sublatitudinal trend. The Lakhti depression partly coincides with the buried valley (the side tributaries of the latter are found in the vicinities of Ol'gino village) and partly – with an active submeridional fault [14].

The Lakhti depression occupied for the most part with wetland has been studied since the early 20th century. Of particular interest are detailed works by K.K. Markov [17], the geological sections exposed by boreholes being described in his monograph (fig. 2 A, B). There are two peat horizons with a layer of sandy loam between them. Judging from diatoms assemblages and from pollen diagrams, the layer may be attributed to the Littorina time. Later multidisciplinary studies of the Lakhtinsky Razliv deposits permitted the sequence to be subdivided into series of the Yoldia Sea, the Ancylus Lake and the Littorina Sea sediments (fig. 2 C, D) [18]. A layer of gyttja from a depth of 2.6 to 2.9 m was dated by ^{14}C to 9160±150 yr. BP (10 746–9891 cal. BP).

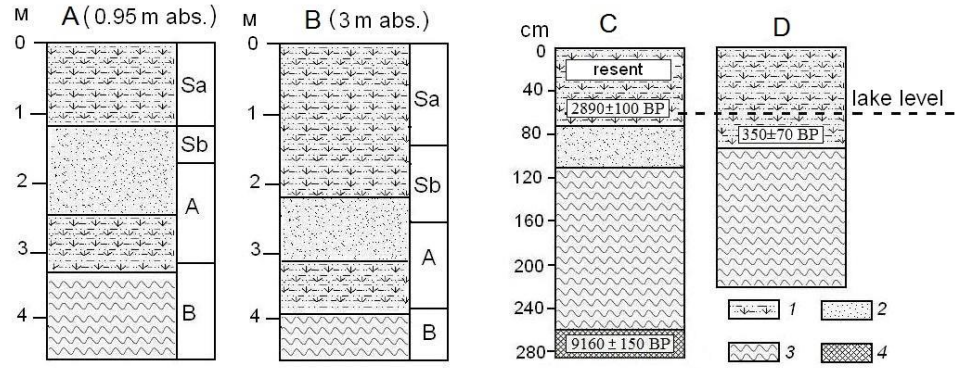

Fig. 2. Boreholes in the Lakhti wetland. A, B – according to [17], C, D – according to [18]. 1 – peat, 2 – sand, 3 – clay, 4 – gyttja

In the borehole C the deposits change upwards first into bluish-gray silty clay with occasional black hydrotroilite interlayers, then into light brown fine sands and clays of the Littorina stage. Still higher they are gradually replaced with dark brown peat. The radiocarbon date obtained for a sample taken at the base of the peat suggests the Littorina Sea regression and the peat accumulation in the region began according to ^{14}C 2890±100 yr. BP (3268–2790 cal. BP [18].

Boreholes drilled near the Ol'gino settlement penetrated marine sands and reached buried peat layer of the Littorina age at a depth of 4–6 m [22]. As follows from the drilling results of the barrier has been gradually migrating landwards. Under conditions of the rising sea level the coastal plain was partly inundated, a lagoon being formed behind the bar. Such a mechanism of the barrier-lagoon system development is universal and has been observed in many coastal regions [1].

Several boreholes drilled within the Lakhtinsky Razliv Lake at different depths reached a poorly decomposed horizon of peat. The age of the latter was estimated at about 300 years old

(314±100 ^{14}C yr BP). Therefore, the Baltic Sea level at that time was below this of the present-day. Geological and geomorphological analysis of the Curonian and Vistula Spits also provided evidence of the Baltic Sea level oscillations at the historical time. In particular, there are traces of a high stand of the sea level (0.5–1.0 m above that of today) datable to ~1700 yr ago and to the Viking epoch (the 9th – 10th centuries) [24].

The Neva Lowland within the limits of St.-Petersburg

Paleoenvironmental reconstructions in the eastern part of the Gulf of Finland are particularly hindered by the man-induced changes in landscapes. That makes studies of archeological objects particularly significant. The first archeological site of the Neolithic – Early Metal age discovered in the Neva River basin – Okhta 1 – is positioned near the St.-Petersburg center, on the Okhtinsky Point [10, 15].

Detailed studies, with recent scientific approach and methods being applied, identified the Littorina Sea coastline within the city limits. The coastline is distinctly seen in the topography as a series of erosion scarps and beach ridges [21] traceable on the Neva Lowland at a distance up to 13 km from the today's coastline. One of the largest constructional landforms on the Neva Lowland within the city boundaries is the sand Ligovka Spit extending from the southern coast of Neva Guba towards NE as far as the Neva channel (fig. 3).

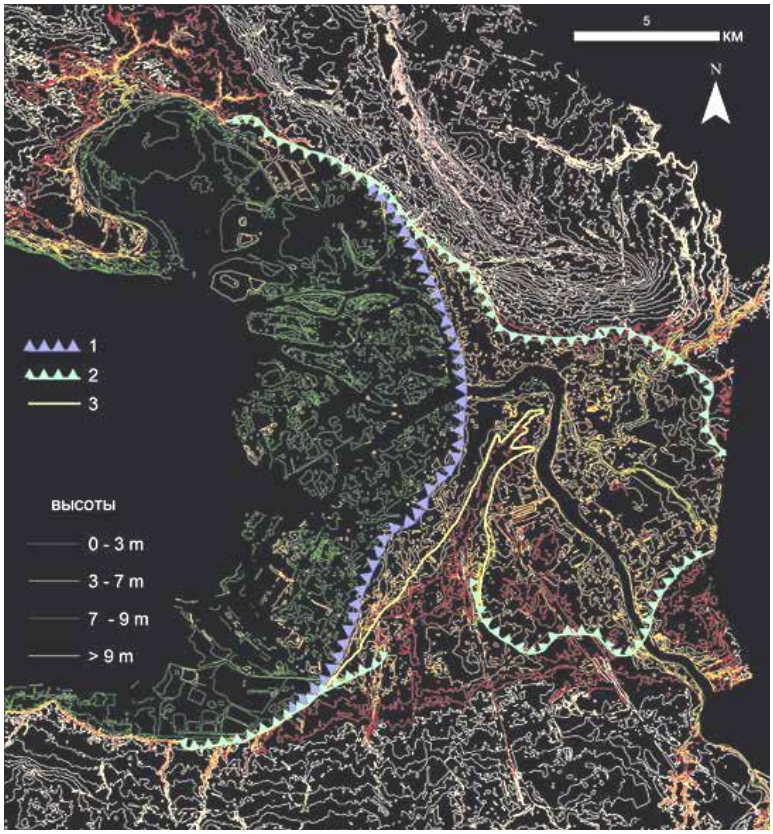

Fig. 3. Areas of the Littorina Sea coastal landforms. 1 – boundary of the "Vasileostrov" terrace 0–3 m a.s.l. attributed to Old Baltic transgression; 2 – "Okhtinskaya" terrace boundary dated to the maximum stage of the Littorina transgression; 3 – Ligovka Spit (outlined by 6 m isohypse), according to [21].

The Ligovka Spit surface under the banked earth is at 7–8 m a.s.l., while the Littorina surface around the spit is 3 to 4 m lower. The spit is about 10 km long and 600 m to 2 km wide. It is composed of cross-bedded (diagonal-bedded) sands of Littorina age replaced upwards with coarse sands with gravel and pebbles. The total thickness of sands varies from 5 to 7 m. The entire spit body does not lie on marine sediments as it is most typical of such constructional landforms; it occurs directly on the continental deposits. The sands superpose peat beds over the entire length of the spit. The deposit of peat (changing occasionally into gyttja) "exceeds in size all the known buried peatlands of the Littorina age" [22]. Within the city boundaries the Littorina deposits up to 13.6 m thick are mostly bluish and gray sands, sandy silts and loams, occasionally they include vivianite particles and peat interlayers traceable along the strike. The gyttja clays, including those known as therapeutic muds in the Sestroretsk Razliv Lake [6] are also assigned to the Littorina Sea deposits.

Judging from the morphological and lithological characteristics of the Ligovka Spit, that landform is not a marine formation emerged gradually to the surface in the course of the marine regression, though such is a viewpoint of a number of investigators [9, 17, 21, 22]. Rather than that, it may be considered to be a large barrier developed at the margin of the coastal plain against the background of rising sea level; in the process a lagoon was formed at the back of the barrier, while the bar itself grew in thickness and moved onto the lagoon. We have studied a similar scenario of the barrier-lagoon systems evolution on the Curonian and Vistula Spits. In fact, such a mechanism of the barrier formation is actually universal and may be observed on all the marine coasts [2, 23].

It may be concluded from the above that the lagoon developed at the initial stages of the Littorina transgression over a sizable part of the present day city area; it was separated from the Gulf of Finland by a large barrier. An undisturbed sedimentation proceeded in the lagoon and resulted in a series of thinly layered sands and silts; they are exposed at present at the confluence of the Neva and Okhta rivers. The environments on the lagoonal coasts were beneficial for human habitation. The earliest archeological sites on the Okhtinsky Point are dated to that time –the first half of the 5^{th} millennium BC [9]. The lagoon was undoubtedly drained at that time (as it received rivers) and was permanently connected with the sea. During the large-scale Littorina transgression and the subsequent regressive stage of the sea, some oscillations of the Baltic Sea level occurred (recorded in particular in the geological context of the Okhta I archeological site). The sea level lowering gave way to its rising which resulted in development of a wide arc of the 'Vasileostrov' terrace modeled by marine erosion [21].

II. THE NARVA–LUGA LOWLAND

The lowland is situated at the mouth of the Narva and Luga rivers and is distinct for a rather complicated topography. Lakes and swamps occupy a considerable proportion of its surface, with constructional coastal landforms of various ages between them. The lowland includes three isolated plateau fragments known as Kurovitsky, Krikovsky and Kurgalsky, the latter forming a peninsula of the same name separating the Narva Bay from the Luga Bay.

The western slope of the peninsula drops towards the Narva Bay as a scarp with a high dune ridge stretching along its edge (Fig. 4 A). The source of the eolian sand was fluvioglacial sediments exposed in a paleo-cliff at the plateau margin.

Fig.4A. An overgrown downwind slope of the dune.

Fig.4B. Fluvioglacial deposits

There are several generations of spits on the lowland varying widely in their size, age, and orientation. The largest of them – Riygiküla, Kudruküla, and Meriküla ones – were first described in details by K.K. Markov [17].

The Riygiküla Spit is the farthest from the sea. It forms an arc encircling the southern periphery of the lowland and is composed mostly of coarse littoral deposits. A radiocarbon date obtained on the archeological site – 5305–5040 yr BC (6212±48, Hela-2742) [7] permits to assign this ancient coastline to an early stage of the Littorina transgression.

A younger constructional landform – that is Kudruküla Spit – extends as an arc 25 km long and 0.2 to 1.5 km wide along the Narva Bay coast. A chain of dunes up to 15 m high marks its axis, though no traces of sands being recently wind-blown have been found on the surface composed mostly of coarse-grained sand and pebbles. In the central part of the arcuate spit there are archeological sites dated at 2215–2020 yr BC (37250±40, Hela-2744). Further on there are dunes up to 20 m high forming a scarp facing east, towards the swamped surface of the ancient lagoon.

To the north of it there is another archeological site dated at 1910 yr BC (3607±31, Hela-2516). The Kudruküla spit borders on the southern slope of the Kurgalsky plateau remnant ~20 m high composed of fluvioglacial deposits (Fig 4 B). There are archeological sites arranged along its edge, their age being estimated at 3970–3940 yr BC (5090±40, Hela-1945) [7].

The Kudruküla spit sites are localized on sandy ridges of a moderate height alternating with swamped hollows. Quite possibly the ridges are former foredunes having developed at the back of the beach under conditions of the slowly receding sea [25]. Similar eolian landforms steadily gaining in elevation landwards are found in other parts of the Narva-Luga Lowland. Both relative elevation and the altitude a.s.l. increase southwards and reach 4–6 m at the distance of 2 km from the sea.

At present the lowland is separated from the sea with a lengthy barrier beach of Meriküla. The presence of sand in large quantities within the littoral zone was instrumental in the development of a series of massive dune ridges up to 20 m high and up to 2 km across on the whole.

As follows from the drilling data given in the monograph by K.K. Markov [17] (Fig. 5), a series of lagoons developed successively on the coastal waterlogged plain during the Littorina. That suggestion is corroborated by the peat occurrence at the base of diatomaceous gyttja of the Littorina

age. An abundance of sand in the coastal zone favored development of large bars and undisturbed deposition of diatom gyttja in lagoons.

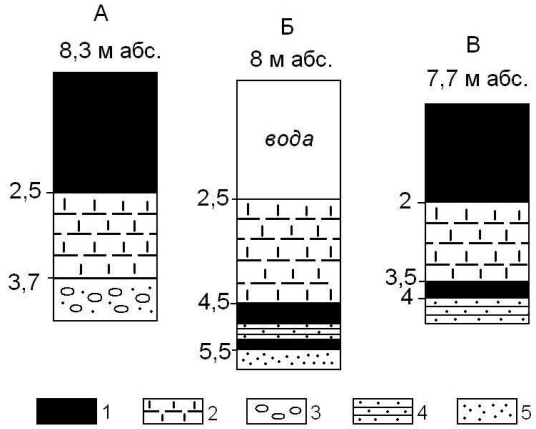

Fig. 5. Boreholes on the Narva-Luga Lowland (according to [17]). 1 – peat, 2 – gyttja, 3 – sand with gravel and pebbles, 4 – sandy loam, 5 – sand

It should be noted in conclusion that facts established by drilling, along with dated archeological artefacts and the results of geomorphological analysis of the Narva-Luga Lowland allow a definite conclusion that the barrier-lagoon systems evolved there throughout the Littorina time which resulted in several generations of lagoons to have been formed on the coastal plain. The lagoons separated from the sea by sand barriers (Riygiküla, Kudruküla, and Meriküla Spits) developed in a successive order on the low deltaic plain advancing slowly seawards. The latter may be ascribed both to isostatic uplift of the Earth's crust and to sediments accumulation in the nearshore zone. Another evidence in favor of the land advancing seawards is given by the age of archeological artefacts (the nearer is the archeological object to the coastline, the younger it is).

III. THE COASTS OF LATVIA

The barrier-lagoon systems are widely spread over the Latvian and Lithuanian coasts. The largest and most thoroughly studied is Ventspils Lagoon 30 km long and up to 15 km wide crossed by the Venta River. The lagoon is separated from the sea by a large barrier bar with several dune massifs on its surface. Both the barrier and the lagoon include a few islands composed of glacial till and fluvioglacial sediments. There are known several sections with lagoonal or beach deposits attributed to the Littorina sea basin occurring above the gyttja or peat beds formed under subaerial conditions on the coastal plain. To take but a few examples, there is a section near Varve settl. 10 km south of Ventspils where a peaty sapropel dated at 7110±170 yr BP occurs under the barrier and lagoon deposits of the Littorina Sea (Fig. 6B) [11]. In the northern part of the lagoon there are sands of lagoonal and fluvial origin 2.5 m thick overlying sapropel dated at 8970±180 yr BP (Fig. 6 C). There is another section on the left bank of the Venta River near Ventspils at 4 m a.s.l. where gyttja is unconformably overlain with marine sands (Fig. 6 A) [12].

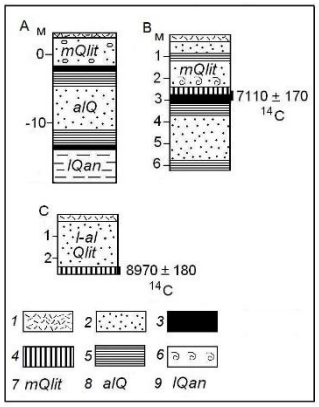

Fig. 6. Boreholes in the Ventspils Lagoon (according to [11, 12]). 1 – soil, 2 – sand, 3 – peat, 4 – gyttja, 5 – clay, 6 – mollusk shells

IV. THE COASTS OF LITHUANIA

An extensive barrier-lagoon system extends for more than 60 km southwards from Liepaja to the Lithuania boundary and further south to Šventoji settl. It abounds in lakes, Liepājas and Tosmares being the largest ones. Formerly the lakes were connected with each other, forming a large gulf the Curonian Gulf same behind the Curonian barrier. At present the lowland surface lies hardly above the sea level and is heavily waterlogged. The peat drilled in one of the largest wetlands is up to 10 m thick [16].

The coastal lowland is separated from the sea with a sandy barrier that includes occasional morainic hills forming minor cusps of the shoreline. The sandy barrier is occasionally up to 2 km wide and bears a series of dune ridges 20–30 m (and more) high. Locally the barrier is partly eroded and reduced in width and elevation.

The considered part of the coast is noted for a presence of a linear uplift in the offshore zone traceable almost from the water edge to a depth of 40 m (Fig. **7**). It is known as Liepaja Swell and marked with boulder fields (eroded till) and outcrops of Pre-Quaternary rocks [5].

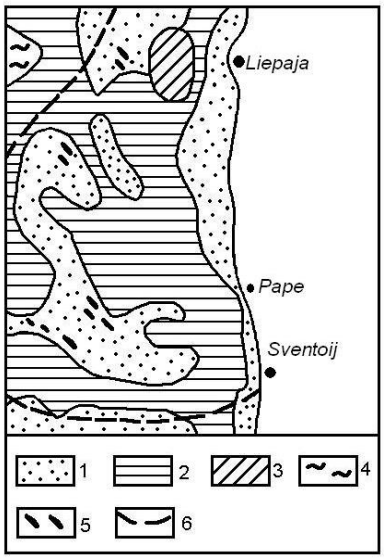

Fig. **7**. Underwater slope (foreshore) between Liepāja and Šventoji (according to [5]). 1 –

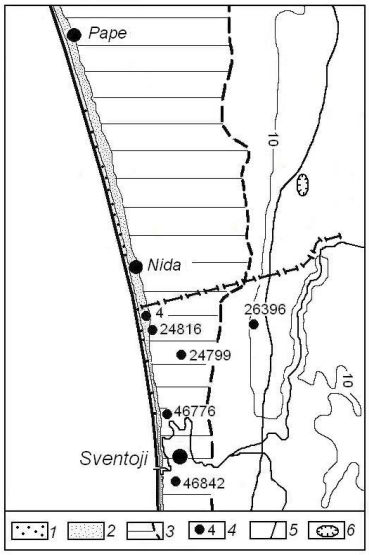

Fig. 8. Boreholes near Šventoji (according to [26]). 1 – beach, 2 – dunes, 3 – paleo-lagoon,

sand, 2 – till (boulder loam), 3 – outcrops of 4 – boreholes, 5 – road, 6 – quarry solid rocks, 4 – clays, 5 – ridges.

There is a load deficiency in the coastal zone which accounts both for the barrier erosion and for its displacement landwards, the coastal wetland being overlain. The process is indicated by some rounded lumps of peat found on the beach and was observed directly. During strong storms (such as in 1967) the lower segments of the barrier are overwashed by waves, the sediments being moved into the lagoon [4]. The most detailed studies of the coastal lowland were performed in the vicinities of the Šventoji town, several boreholes having been drilled there (Fig. 8).

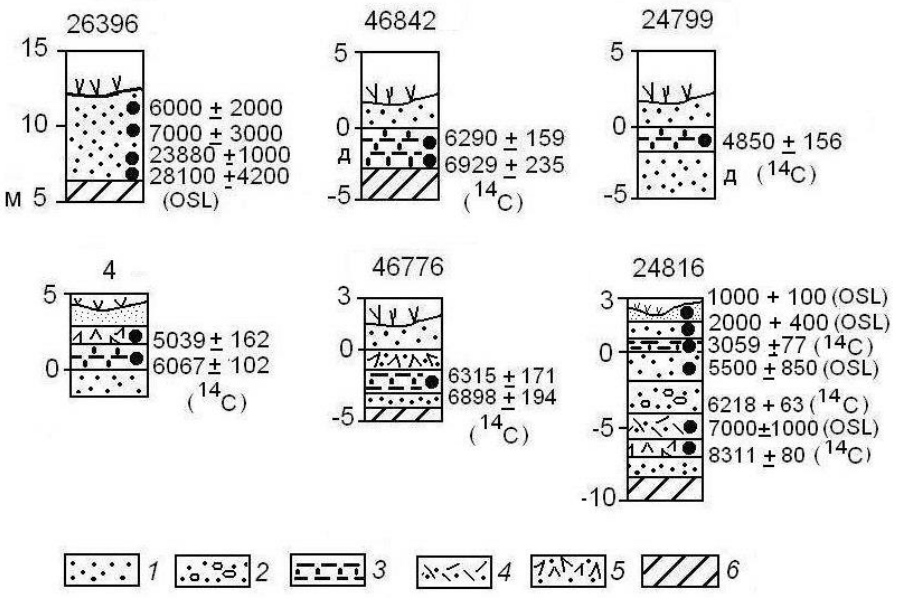

Fig. 9. Cores of sediments drilled in the Šventoji vicinities, according to [26]. 1 – sand, 2 – sand with gravel and pebbles, 3 – gyttja, 4 – sandy peat, 5 – peat, 6 – till

The material thus obtained was further thoroughly studied using palynological analysis and dating by radiocarbon and OSL techniques [26]. As can be seen in given sections, the Littorina transgression deposits are dominated by lagoon facies (Fig. 9).

They occur immediately above the deposits formed earlier on the coastal lowlands, namely fluvial sands, gyttja or peat. Beach facies of the Lttorina age penetrated by borehole 24816 were dated by ^{14}C at 6218±63, which is indicative of the shoreline advance. Similar advancing coastlines have been observed on the Curonian and Vistula Spits [24], as well as on all the above listed segments of the low land.

V. CONCLUSION

Large constructional landforms of barrier type have been studied for the purpose of better understanding of their structure and genesis. The studies were performed on the eastern Baltic coasts including the Gulf of Finland and the coasts of Latvia and Lithuania. The results obtained permitted a definite conclusion on a unified mechanism of their development originally as marine bars formed

in the Holocene off the river mouths. The ice sheet retreat and decay produced a great volume of fluvioglacial sands and gravels that served as a construction material for the barrier formation all over the considered coastal region. Both the formation and further evolution of the barrier were greatly influenced by the sea level transgressive-regressive oscillations. Many of the constructional barriers are essentially syngenetic landforms and include of some earlier formations, such as fragments of deltaic plains, and remnants of till or glacio-lacustrine sediments.

REFERENCES

[1] E.N. Badyukova, A.N. Varushchenko, and G.D. Solovieva, "Impact of the sea level fluctuations of the coastal zone development," *Vestnik MGU*, Ser. 5, No. 6, 1996, pp. 83-89 (In Russian)

[2] E.N. Badyukova and P.A. Kaplin, "Barrier bars," *Geomorfologiya*, No. 3, 1999, pp. 3-13 (In Russian)

[3] V.V. Belikov, *A northern health resort of Russia. Secrets of the Lake Razliv*. St.-Petersburg, 1999, 175 pp. (In Russian)

[4] E.A. Bulgakova, Some specific features of morphology and dynamics of the Baltic Sea present-day coasts," in *The present-day exogenous processes and methods of their investigations*, G.Ya. Eberhards, Ed. Riga: Latvia Univ. Press, 1982, pp. C. 33-56 (In Russian)

[5] A.F. Veinberga, I.G. Veinbergs, Ya.R. Klavins, "Southeastern Baltic Sea bottom topography and specific features of the last ice sheet retreat from that region," in *Relief morphogenesis and paleogeography of Latvia*, O.P. Aboltyns, Ed. Riga: Latvia Univ. Press, 1986, pp. 130-145 (In Russian)

[6] Geological Atlas of St.-Petersburg. St.-Petersburg: Komilfo Publ., 57 pp.

[7] D.V. Gerasimov and M.A. Kholkina, "Archeological studies of ancient lagoon systems: Explorations of the Narva-Luga interfluve in 2012-2014". Electronic library of the Peter the Great Museum of Anthropology and Ethnography (Kunstkammer) RAS // www.kunstkamera.ru/lib/rubrikator/07/978-5-88431-287-6 (In Russian)

[8] E.F. Grinbergs, "Late-glacial and post-glacial history of the Latvian SSR coasts". Riga: Latvian Ac.Sc. Publ., 1957. 122 pp. (In Russian)

[9] T.M. Gusentsova, D.V. Ryabchuk, A.Yu. Sergeyev, M.A. Kul'kova, "Paleogeographic reconstructions of the Neolithic people environment on the eastern coasts of the Gulf of Finland and southern Lake Ladoga basin," in *Geology, geography, evolutionary geography*, vol. XII, E.M. Nesterov and V.A. Snytko, Eds. St.-Petersburg: the Herzen State Pedagogical University of Russia, pp. 157-160 (In Russian)

[10] T.M. Gusentsova, P.E. Sorokin, "Cultural-chronological complexes of the archaeological site Okhta 1 in Saint-Petersburg, Russia // *Geology, Geoecology, Evolutional geography*. 2010. St.-Peterburg. P.164-170 (In Russian).

[11] A.L. Devirts, N.G. Markova, L.R. Serebryanny, "The radiocarbon control over geological estimates of the old coastal formation age on the Baltic Sea," Doklady, the USSR Ac. Sc., vol. 182, No. 6, pp. 1387-1392 (In Russian)

[12] R.N. Djinoridze, G.I. Kleimenova, V.I. Serganov, "New data on the ancient Ventspils lagoon history," in *History of lakes in the North-West*, Materials of the 1st Symposium on the Lake History. Leningrad: Geographic Soc. of the USSR, 1967, pp. 51-56 (In Russian)

[13] O.M. Znamenskaya, "Geomorphological regions and types of relief in the Leningrad vicinities," *Vestnik LGU*, No. 24, 1956, pp. 152-162 (In Russian)

[14] Ya.A. Karpova. Geotechnical support of surface and subterranean construction work under conditions of an active technogenesis of the subterranean volume constituents in the Primorskiy district of St.-Petersburg. Ph. D. Dissertation in Geology. St.-Petersburg, 2014, 271 pp. (In Russian)

[15] M.A. Kulkova, T.V. Sapelko, A.V. Ludikova, D.D. Kuznetsov, D.A. Subetto, E.M. Nesterov, "Paleogeography and archeology of Neolithic – Early Metal age archeological sites at the Okhta R. mouth", *Izvestiya, Russian Geogr. Soc*., vol. 142, 2010, pp. 13-31 (In Russian)

[16] Kurzeme. Riga: Latvian State Publ. House, 1960, 350 pp. (In Russian)

[17] K.K. Markov, "Relief evolution in the NW of the Leningrad Region", Proc. Geol.-Prospect. Dept., the USSR Supreme Council of National Economy (VSNKh), Iss. 117, 1931, 256 pp. (In Russian)

[18] D.A. Morozov, "Reconstruction of paleoenvironmental characteristics based on geochemistry of lake deposits," *Izvestiya, Herzen State Pedagogical University of Russia*, St.-Petersburg, No. 144, 2012, pp. 122-130 (In Russian)

[19] B.B. Polynov, M.M. Yuriev, "The Lakhti depression", *Izvestiya, Research Meliorat. Inst.*, Iss. 8-9, 1924, pp. 76-172 (In Russian)

[20] N.A. Sokolov, "Dunes, their development and inner structure," St.-Petersburg, 1884, 289 pp. (In Russian)

[21] P.E. Sorokin, T.M. Gusentsova, A.Yu. Sergeyev, D.V. Ryabchuk, M.A. Kul'kova, "Paleolandscape of the Litorina Sea coastal zone near the archeological site Okhta 1". Trans. the 2nd Intern. Confer. "Virtual archeology" 2015. St.-Petersburg: State Hermitage Publ., 2015, pp. 112-124 (In Russian)

[22] S.A. Yakovlev, "Deposits and relief in the city of Leningrad and its vicinities", Leningrad, Pt. 1, 1925, 186 pp., Pt. 2, 1926, 264 pp. (In Russian)

[23] E.N. Badyukova, L.A. Zhindarev, S.A. Lukyanova, G.D. Solovieva, "Development of barrier-lagoon systems in the southeastern Baltic Sea," *Oceanology*, vol. 48, No. 4, 2008, pp. 595-601.

[24] E.N. Badyukova, L.A. Zhindarev, S.A. Lukyanova, G.D. Solovieva, "Marine deposits of the Vistula Spit (Baltic Sea)". Proc. of the 2nd Intern. Conf. "Dynamics of coastal zone of non-tidal seas" Baltiysk, 2010, pp.169-172.

[25] E.N. Badyukova, G.D. Solovieva, "Coastal eolian landforms and sea level fluctuations," *Oceanology*, Vol. 55, No. 1, 2015, pp.139-146.

[26] A. Damušytė, "Post-glacial geological history of the Lithuanian coastal area", Summary of doctoral dissertation, Vilnius, 2011, 84 pp.

AN APPROACH TO PARAMETRISATION OF COASTAL SOURCES OF MICROPLASTICS PARTICLES IN NUMERICAL MODELS

Andrei Bagaev, Atlantic branch of Institute of Oceanology, Russia
Irina Chubarenko, Atlantic branch of Institute of Oceanology, Russia

a.bagaev1984@gmail.com

An overview of modern approaches to the problem of parametrisation of sources of marine waters microplastics pollution from the coastline is conducted. The estimates of Europe's plastic production along with mismanaged plastic waste percentage that might be the source of microplastics particles input to marine environment are presented. A semi-empirical formulation for the particles source intensity is suggested. It considers the main factors of local anthropogenic pressure for the coastal spot location for the given coordinates. Both advantages and disadvantages of such an approach along with possible ways for improvement are discussed.

Keywords: microplastics, numerical modelling, the Baltic Sea, anthropogenic pollution

I. INTRODUCTION

Numerical simulation of environmental processes is always a challenging problem: with all our knowledge we are certainly unable to embrace all the forcing, processes and events in both natural environment and human activity. Thus, the necessity of parametrisation of many of them arises, and every parametrisation is supposed to express the influence of some *key factor* but in *the most simple* (i.e. – practically convenient) way. This balance of importance versus model simplicity is always problem-specific and highly dependent on the goal of the simulation, that leads to the development of plenty of model approaches, particular parametrisations, input/output parameters, etc.

In modelling of microplastic pollution of seas and oceans, the most complicated question for today is how to describe coastal sources of microplastic particles. While sources of plastic macro-litter can be associated with cities, popular beaches, or ports, the generation of microplastic particles involves many physically complicated environmental processes like UV-degradation, mechanical destruction in swash zone, settling and re-distribution by currents, re-suspension/re-deposition by storm waves, etc. Which of these processes must be taken into account and how to parametrise them – is a hot question, still practically not discussed in literature.

According to existing naming conventions, the microplastic is the particles of synthetic polymers with different complex shapes and typical size ranges from 1 to 5 mm [1]. Such range is, first of all, determined by the methods of collection and identification of the particles, i.e. neustonic net mesh size, and optical microscopes resolution [2]. Despite emerging interest to that interdisciplinary problem, it is hard to tell that terminology in that area of knowledge is well established and widely accepted.

Very often microplastic appears toxic itself, but what is more dangerous, since it has large effective surface, it adsorbs different ecotoxicants, e.g. poly-chlorinated byphenils [2, 3]. If microplastics gets into a digestive system of marine micro-organisms, it may cause an effect of "false fullness" and propagate up through a food chain, that in turn leads to accumulation of toxic chemicals in the bodies of marine mammals and birds [4]. The researchers found that microplastics might serve as a transport mechanisms for invasive species from different ecosystems [5]. Nowadays microplastics pollution is found even in the Antarctic ice fields [6].

The aim of the present paper is to summarize our knowledge on the sources of microplastics in the marine environment and to propose a new way for parametrisation of the particles input in the model of microplastics transport for the Baltic Sea.

II. NET PLASTICS BALANCE ESTIMATE

Let us concentrate first on the net balance of plastic waste net flow in a semi-enclosed see, like the Baltic Sea, for example. It is widely accepted that 80% of it come from land sources and the rest 20% -- from the sea-based sources. The latter are typically placed along the intense shipping routes and are easily localized in space, but are hard to yield to quantitative assessment. The land-based sources are localized at the river estuaries, major cities, and beaches. All of those places are in contact with two principal natural actors: hydrodynamics and geomorphology which makes distribution of plastic waste at sea very patchy [7]. The human factor makes waste input irregular in time.

For the last decade plastics production and demand in Europe has been showing very slow growth, henceforth the speed of waste dumping into surrounding seas might overcome the growth rate. That might be the reason why plastic pellets became background contamination for the samples taken across the Mediterranean beaches (e.g. Malta, [8]). On the other hand, many Baltic countries implemented "zero dump" laws that prohibit dumping plastic waste to the landfills, which, in turn, might decrease waste input rate. It seems reasonable to assume that plastic waste concentration will remain more or less stable in the Baltic environment for the next decades, despite its much lower abundance.

According to [9], Table 1 shows a volume of "mismanaged plastic waste" (i.e. plastics waste that escaped recycling) for the Baltic countries estimates at 28 000 kg per day.

Table 1. Mismanaged plastic waste input for Baltic countries (from [9])

Country	Coastal population	Inadequately managed plastic waste [kg/day]	Mismanaged plastic waste [kg/person/year]
Denmark	5 376 386	0.0*	0.37
Estonia	878 021	13295.703	6.94
Finland	2 927 674	0.0*	1.83
Germany	8 837 035	0.00014	3.54
Latvia	1 432 078	24650.935	7.19
Lithuania	443 894	8363.564	7.85

Norway	4 131 679	0.0*	2.19
Poland	3 272 933	36715.231	4.75
Russia	10 812 537	197225.826	7.30
Sweden	6 202 234	0.0*	0.37

*According to official data on production and waste management.
Collateral plastic litter input is underestimated.

Fig 1. schematically represents the relation between actual waste input and generation of microplastics pollution with a focus on the unknown links of chain.

Let us now try to estimate a net balance of the microplastics pollution in the Baltic Sea. It is important to take into account the demand of plastics in Europe: which consists of 50% heavy and 50% light [10] plastics. Light particles (with a positive buoyancy) will float away with the surface currents and after a certain time will be removed from the surface waters. Denser particles along with the less dense ones affected by biofouling should sink in a few days and deposit in bottom sediments.

Firstly, the surface currents that mainly outflow to the North Sea seem to be the main factor of the negative balance of microplastics with densities less than brackish water of the Baltic Proper. Actual rate of the removal might be estimated if we improve our knowledge on the mean concentrations of microplastics, but unification of measurement methods [11] is very important.

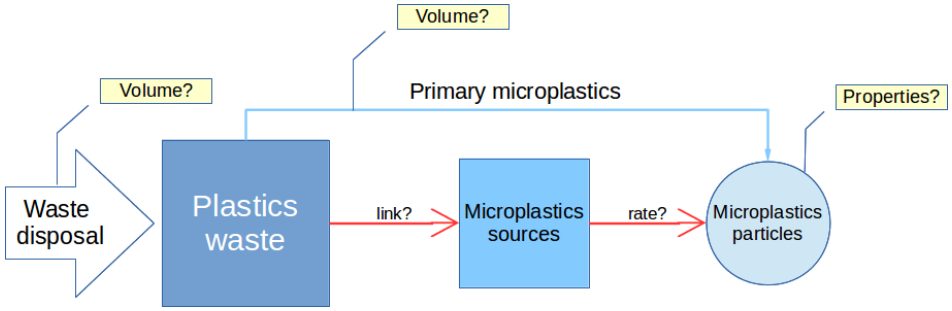

Fig 1. A pathway from unprocessed plastic waste to the microplastics pollution in marine environment.

Secondly, the denser plastics should be accumulated and deposited at the bottom (mainly in the shallow area close to the coast, with a high chance to be re-suspended), but also – in the deep-water area, which might be considered as another way of microplastics removal [5]. To estimate the rate of deposition for different types of plastics, we need to know their settling velocities. Study [12] discovered surprisingly low levels of microplastics at the sea surface when compared to those in the bottom sediments of the deep sea.

These two reasons provide relatively low concentrations of floating microplastics particles in the surface waters of the Baltic Sea [7, 13]. According to different scenarios of numerical modelling in [14] and [15], the Baltic Sea accumulates relatively low levels of plastic waste (much less than Mediterranean or Pacific); possibly, this is due to the currents regime that supports renewal of surface waters. Study [7] reports similar orders (10 particles per litre) of counts of microplastics for

the opposite parts of the Baltic Sea, with a slight increase at the German coast. Authors of [12] give mean microplastics densities in the Mediterranean of 400 particles per litre.

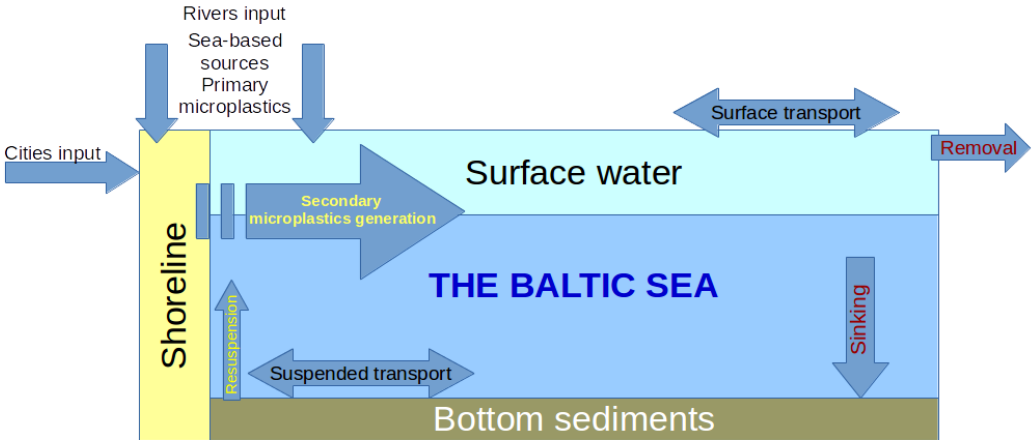

Fig. 2. Conceptual representation of a net plastics balance in the Baltic Sea marine environment.

Common practice is to distinguish "primary" microplastics, e.g. industrial pellets, textile fibres, and microbeads from cosmetics, from the "secondary" microplastics that results from a partitioning of large plastic waste, fishing nets, etc. The latter processes manifest themselves most actively in the coastal zones. Unlike with the macroplastics [16], it is very hard to establish the origins of the microplastics samples, since the macro-waste degradation requires very long exposure to oxygen-rich environment and UV-radiation. The direct input of primary microplastic from the sea-based sources and the land-based sewage facilities might be assumed as much lower than input generated by the breaking pieces of plastic waste and storms removing microplastics from the beaches. Many authors, like [17], support the idea of microplastics particles accumulation at the shoreline, but its rate remains unknown. K-L. Law in [18] hypothesized the processes of microplastics removal from the marine ecosystem, but mentioned that rates remain unknown.

The scheme of the described processes is presented in Fig. 2.

From all that has been said it follows that if we were able to describe the generation of microplastics in the shallow-water bottom sediments, then we would able to parametrise the input of microplastics in the model. In such a case, first thing we need to take into account is the type of the bottom sediments.

When estimating the net input of the microplastics into the marine ecosystem along with surrounding beaches and estuaries, one needs to keep in mind that the only available data on the anthropogenic footprints for now are the statistical information on the average amount of mismanaged plastic waste (see Table 1). Importance of such numbers is contracted by the fact of long exposure of the existing huge plastic deposits to the allocating and equalizing action of the currents and winds. For example, there is no significant distinction in microplastic pollution levels between Slovenian beaches with different extent of human use [19].

III. PRESENT APPROACHES TO THE PROBLEM

Methods of numerical modelling of plastic waste transport are pretty well developed for the Global Ocean [14, 20, 21, 22] and data collected during marine expeditions are summarized in [11, 21]. Meanwhile, there is a huge gap between global and regional scale modelling of microplastics, although there is some progress in [5, 23, 24]. Physical properties of microplastics particles are little-known [25, 26], which interdicts their parameterisation in the numerical models for marine environment.

Table 2. A review of papers on the marine plastic waste transportation

Publication	**Loss of particles**	**Transition from coast to the sea**	**Vertical velocity (loss due to sinking)**	**Sources**
[23]	Sedimentation depends on density and Feret's diameter	Resuspension due to critical erosion velocity	Yes	4 point sources
[27]	Landing, settling, degradation	Resuspension	Yes	5 point sources
[28]	No beaching	N/A	No	Shipping lanes and cities
[14]	A particle is considered 'beached' when it is adjacent to a coastal cell. No removal	is not possible	No	Rivers, shipping lanes and cities. Even releases.
[29]	Removing the particles after 10 days of stagnation at the boundary cell	is not possible	No	Rivers, shipping lanes and cities
[24]	Beaching count, no removal	free	No	Day by day release at each grid cell
[20]	Removing the particles after 5 days of stagnation at the boundary cell	is not possible	No	Instant release at each grid cell
[21]	No beaching	N/A	No	Coastal urban population within 200 km zone; large rivers with urbanised estuaries

Dense plastic transport in suspended state is estimated in [3]. Chances to be re-suspended certainly increase with increase in current velocity and significant wave height. Re-suspension was empirically parametrised in the model [27] as 0.2-0.4 particle per day. Laboratory experiments by [23] showed the critical tension values of 0.14 N per m^2 (which corresponds to velocity of 0.2 cm

per sec) for HD plastics (1055 kg per m^3 with settling velocity of 28 mm per sec and size ~2 mm), while re-deposition started at 0.087 N per m^2.

Submesoscale effects remain unknown, but for the particles with buoyancy close to neutral it is proven that subsurface concentration is influenced by turbulence. Settling velocity is high enough to settle in 1-2 days, but turbulence makes this time high enough for some heavy re-suspended particles of plastics and amber to be washed ashore after severe storms.

III. Results: suggested parameterisations

Coastal related input and stranding processes are crucial for assessing budgets of marine litter. We assume that particles of different sizes enter the sea with equal probability, despite the fact that in-situ measurements do not always confirm such distribution pattern [17, 30]. For spheroids with effective diameter of 1-5 mm, there is a linear dependence between the size and the number of particles generated from a large object of a fixed volume [30]. If a particle fits into one of five size classes from 1 to 5 mm with 1 mm step, then overall final quantity of such particles might be linked to the stock of large plastic waste. Polymer fibres should be treated as a separate class. For now it seems reasonable to introduce two major density classes: “heavy” and “light” particles, which could be modelled separately at the initial stage.Table 3 lists the factors affecting the final parameterisation:

A. Seasonality manifests itself in plastics waste input as much as in the intensity of grinding action of the sea and natural factors in the coastal zone.

B. Distinguishing of the exploited (urbanized, recreational or industrial) coastal zones from those less used reflects the direct anthropogenic pressure. One can assume the cell of a numerical grid as 'exploited' if there is at least one city with a population more than 100 000 people. Presence of objects that increase local level of plastics pollution, such as water treatment plants, ports, industries related to use of polymer pellets, etc. Study [2] demonstrated sufficient increase in the microplastics particle concentration near the water treatment plants at the coasts of the United Kingdom. Putting locations of such objects on the model grid is a very time-consuming task.

C. Population density directly influences the quantity of primary microplastics generated by people, e.g. during visiting the beaches, and the volume of synthetic fibres and microbeads (from cosmetics) dumped into the sewer. Study [7] showed that even waste-water treatment plants could not be a guaranteed barrier to stop microplastics from domestic discharge entering the marine environment. The data on the population density are available according to census bureau [31].

D. The data on the yearly input of the plastics waste (see Table 1) are needed to define the most influenced coastal zones. As it was mentioned before, 'heavy' plastics will be deposited close to the place of macroplastics destruction.

E. Intensity of the wind waves is an additional factor that influences re-suspension and plastics breakdown. It may compensate for low velocities in the near-shore zone for the very tentative approach in the coarse resolved numerical models based on the reanalysis data. Such data are available, for example, via HELCOM [32].

F. Type of bottom sediments, last but not the least, has never been taken before into consideration for the mechanisms of microplastics generation. Different efficiency of mechanical destruction of macroplastics into the microplastics in the coastal zone is determined by the different

types of bottom sediments. The parameter of 'mechanical conversion' for the different types of sediments (sand, granules, stones, pebble) acting to macroplastics samples is now studied experimentally by our team members. We plan to adapt such information for the numerical model along with available maps of sediments content for the Baltic Sea.

Table 3. Parameters list suggested for parameterisation.

#	Parameter	Units	Possible values	Notes	Variable	Reference
1	Season	-	0.5 □□1.0	Waste input is maximal in Summer	S_Y	[5]
2	Anthropogenic pressure	-	0/1	Waste treatment plant, sewer, port or a large river	A_P	[2], [7]
3	Population	persons	-	Alongshore area □ population density	P	[17]
4	Typical plastic waste input for the country	kg/person/year	-	Baltic countries	W	[9]
5	Wind waves	m	-	Climatic value for Significant wave height	S_{WH}	-
6	Shore type	items/kg	clay, sand, pebble, stones	Influences the microplastics generation from macro waste	T_C	-

A combination of the parameters proposed above allows us to parameterise the distribution of intensity of impulse inflow of the microplastics particles for every 'coastal' cell of the numerical grid. Such distribution in turn permits us to include the non-uniform input of the particles in the Lagrangian model of the microplastics transport. The results of the numerical experiments should be then normalized by the direct measurements of the background concentrations of microplastics pollution in the marine waters and in coastal sediments.

The concentration of particles produced in the coastal cell of the grid will depend on the share of the concentration of deposited plastics waste in the yearly input. Upper estimate is $S = \frac{P_i \cdot W_i}{\sum_i P_i \cdot W_i} \in [0..1]$ (here i stands for each of nine Baltic countries). Such concentration is high enough for the calculated nondimensional term S to change insignificantly on account of the waste transport during the period of numerical experiment.

Since the macroplastics decomposition appears non-uniformly, the intensity of the process I should depend on the type of the local bottom sediments T_C, intensity of wind waves action S_{WH}, and the season S_Y; hence, $I \propto S \cdot T_C \cdot S_{WH} \cdot S_Y$. Proportionality coefficients will be defined during our future laboratory experiments.

Specific sources of anthropogenic pressure might also affect the intensity of macroplastics particles input into the coastal grid cell. Such influence may be taken into account with the following parameterisation: $\delta I \propto A_P \cdot S_Y$.

Henceforth, for each grid cell that may act as a generator of microplastics, i.e. where the input of particles in the Lagrangian model must be defined, we will have the value of a scalar non-dimensional function of the source intensity varying from 0 to 1. That allows us to set the impulse input of the particles for the planned calculation of their transport and accumulation in the model proportional to the maximal allowed number of the particles supported by the model and dependent on the reasonable machine time.

IV. Discussion and conclusions

Unlike the existing approaches (see Table 2), we suggested defining and parameterising the input of the primary and secondary microplastics pollution to the marine environment for the subsequent study of its paths of migration and/or deposition. All previous studies transposed the properties of macroplastics to the microparticles and parameterised the source functions from the requirements of the Lagrangian models or from the available data on the plastics waste input. We assume the key factor in that process to be the destruction of plastic objects in the coastal and wave-breaking zones under the influence of photochemical and mechanical agents.

In our study we pointed out the principal agents that define the balance of the microplastics pollution in the Baltic Sea, according to the known in-situ data and circulation patterns of the Baltic Sea. Further on, we listed the parameters that need to be taken into consideration for parameterisation of the microplastics pollution sources. Those factors are relatively easy to define for each grid cell, depending on the available data bases and geological maps. We hope that further laboratory tests will reveal some coefficients of proportionality [33].

As any other semi-empirical approach, our method might be the subject to critics and improvement. Subsequent tests of its efficiency will be done during the numerical experiments.

IV. Acknowledgment

The investigations are supported by Russian Science Foundation via grant number 15-17-10020.

V. References

1. "Sources, fate and effects of microplastics in the marine environment: a global assessment" (Kershaw, P.J., ed.). IMO/FAO/UNESCO-IOC/UNIDO/WMO/IAEA/UN/UNEP/UNDP Joint Group of Experts on the Scientific Aspects of Marine Environmental Protection, 2015. *Rep. Stud. GESAMP* No. 90, 96 p.
2. M. Bergmann, L. Gutow, and M. Klages, *Marine Anthropogenic Litter*. Berlin, Springer, 2015; doi:10.1007/978-3-319-16510-3.
3. M. Cole, P. Lindeque, C. Halsband, T. S. Galloway, "Microplastics as contaminants in the marine environment: A review," *Marine Pollution Bulletin*, Volume 62, Issue 12, Pages 2588-2597, December 2011; http://dx.doi.org/10.1016/j.marpolbul.2011.09.025.
4. P.G. Ryan, C.J. Moore, J.A. van Franeker, and C.L. Moloney, "Monitoring the abundance of plastic debris in the marine environment," *Philosophical Transactions of the Royal Society B: Biological Sciences*, 364(1526), pp 1999-2012, 2009.
5. "Marine litter in the Mediterranean and Black Seas," [F. Briand, ed.]. *CIESM Workshop Monograph* n° 46, 180 p., CIESM Publisher, Monaco, 2014.
6. R.W. Obbard, et al., "Global warming releases microplastic legacy frozen in Arctic Sea ice," *Earth's Future*, 2: 315–320, 2014; doi:10.1002/2014EF000240.
7. J. Talvitie, et al. "Do wastewater treatment plants act as a potential point source of microplastics? Preliminary study in the coastal Gulf of Finland, Baltic Sea," *Water Science and Technology*, 72 (9): 1495-1504, 2015.
8. A. Turner and L. Holmes, "Occurrence, distribution and characteristics of beached plastic production pellets on the island of Malta (central Mediterranean)," *Marine Pollution Bulletin*, Volume 62, Issue 2, Pages 377-381, , February 2011; doi:10.1016/j.marpolbul.2010.09.027.
9. J. R. Jambeck, et al., "Plastic waste inputs from land into the ocean," Science, 347: 768–771, 2015.
10. PlasticsEurope (2015) Plastics – the Facts. Source: 2014/2015. http://www.plasticseurope.org/documents/document/20150227150049-final_plastics_the_facts_2014_2015_260215.pdf (last viewed: 21.01.2016).
11. M. Filella, "Questions of size and numbers in environmental research on microplastics: Methodological and conceptual aspects," Environmental Chemistry, 12, 527–538, 2015; doi:10.1071/EN15012.
12. L.C. Woodall, et al., "The deep sea is a major sink for microplastic debris," Royal Society Open Science, 1(4), 2014; doi:10.1098/rsos.140317.
13. A. Stolte, S. Forster, G. Gerdts, and H. Schubert, "Microplastic concentrations in beach sediments along the German Baltic coast," Marine Pollution Bulletin, Volume 99, Issues 1–2, Pages 216-229, 15 October 2015; doi: 10.1016/j.marpolbul.2015.07.022.
14. L. C.-M Lebreton, S. D. Greer, and J. C. Borrero, "Numerical modelling of floating debris in the world's oceans," Marine Pollution Bulletin, 64, 653–661, 2012.
15. E. van Sebille, M. H. England, and G. Froyland, "Origin, dynamics and evolution of ocean garbage patches from observed surface drifters," Environ. Res. Lett. 7 044040 (6pp), 2012.
16. A. V. Duhec, R. F. Jeanne, N. Maximenko, and J. Hafner, "Composition and potential origin of marine debris stranded in the Western Indian Ocean on remote Alphonse Island, Seychelles,"

Marine Pollution Bulletin, Volume 96, Issues 1–2, Pages 76-86, 15 July 2015; doi:10.1016/j.marpolbul.2015.05.042.
17. Browne, M.A., Crump, P., Niven, S.J., Teuten E.L., Tonkin, A., Galloway T. & Thompson, R.C. (2011). Accumulations of microplastic on shorelines worldwide: sources and sinks. Environmental Science & Technology, 45, 9175-9179.
18. Law KL, Morét-Ferguson SE, Maximenko NA, Proskurowski G, Peacock EE, Hafner J, et al. Plastic accumulation in the North Atlantic Subtropical Gyre. Science 2010;329: 1185–1188. doi: 10.1126/science.1192321
19. Betty J.L. Laglbauer, Rita Melo Franco-Santos, Miguel Andreu-Cazenave, Lisa Brunelli, Maria Papadatou, Andreja Palatinus, Mateja Grego, Tim Deprez, Macrodebris and microplastics from beaches in Slovenia, Marine Pollution Bulletin, Volume 89, Issues 1–2, 15 December 2014, Pages 356-366, ISSN 0025-326X, http://dx.doi.org/10.1016/j.marpolbul.2014.09.036
20. Nikolai Maximenko, Jan Hafner, Peter Niiler, Pathways of marine debris derived from trajectories of Lagrangian drifters, Marine Pollution Bulletin, Volume 65, Issues 1–3, 2012, Pages 51-62, ISSN 0025-326X, http://dx.doi.org/10.1016/j.marpolbul.2011.04.016.
21. van Sebille E et al 2015 A global inventory of small floating plastic debris Environ. Res. Lett. 10 124006 (11pp)
22. Andrady, A.L., (2011). Microplastics in the marine environment. Marine Pollution Bulletin, 62:1596-1605
23. Ballent, A., Pando, S., Purser, A., Juliano, M. F., and Thomsen, L.: Modelled transport of benthic marine microplastic pollution in the Nazaré Canyon, Biogeosciences, 10, 7957-7970, doi:10.5194/bg-10-7957-2013, 2013.
24. J. Mansui, A. Molcard, Y. Ourmières, Modelling the transport and accumulation of floating marine debris in the Mediterranean basin, Marine Pollution Bulletin, Volume 91, Issue 1, 15 February 2015, Pages 249-257, ISSN 0025-326X, http://dx.doi.org/10.1016/j.marpolbul.2014.11.037.
25. Wang J, Tan Z, Peng J, Qiu Q, Li M. The behaviors of microplastics in the marine environment. // Mar Environ Res. 2015 Nov 8; 113:7-17
26. Ballent, A. Purser, P. de Jesus Mendes, S. Pando, and L. Thomsen Physical transport properties of marine microplastic pollution // Biogeosciences Discuss., 9:18755–18798, 2012. doi:10.5194/bgd-9-18755-2012
27. Kay Critchell, Jonathan Lambrechts, Modelling accumulation of marine plastics in the coastal zone; what are the dominant physical processes?, Estuarine, Coastal and Shelf Science, Volume 171, 20 March 2016, Pages 111-122, ISSN 0272-7714, http://dx.doi.org/10.1016/j.ecss.2016.01.036
28. Erikssen, M., Lebreton, L. C. M., Carson, H. S., Thiel, M., Moore, C. J., et al. (2014). Plastic pollution in the world's oceans: More than 5 trillion plastic pieces weighing over 250,000 tons afloat at sea. PLoS ONE, 9, e111913
29. S. Liubartseva, G. Coppini, R. Lecci, S. Creti, Regional approach to modeling the transport of floating plastic debris in the Adriatic Sea, Marine Pollution Bulletin, Volume 103, Issues 1–2, 15 February 2016, Pages 115-127, ISSN 0025-326X, http://dx.doi.org/10.1016/j.marpolbul.2015.12.031

30. Cózar A., Echevarría F., González-Gordillo J. I., Irigoien X., Ubeda B., Hernández-León S., Palma A. T. et al. 2014. Plastic debris in the open ocean. Proceedings of the National Academy of Sciences of the United States of America, 111: 10239–10244
31. Gallego F. (2010) A population density grid of the European Union / Population and Environment , Volume 31, Issue 6, pp 460-473
32. Web-source: http://helcom.fi/baltic-sea-trends/environment-fact-sheets/hydrography/ wave-climate-in-the-baltic-sea. Last revised 20.04.2016
33. I. Chubarenko et al. On some physical and dynamical properties of microplastic particles in marine environment. Marine Pollution Bulletin (Accepted); doi: 10.1016/j.marpolbul.2016.04.048

BALTIC AMBER MIGRATIONS AS A MODEL OF MICROPLASTICS BEHAVIOR IN THE SEA COASTAL ZONE

Irina Chubarenko, P.P.Shirshov Institute of Oceanology, Atlantic branch, Russia
Margarita Bagaeva, P.P.Shirshov Institute of Oceanology, Atlantic branch, Russia

irina_chubarenko@mail.ru

The problem of microplastic pollution is of increasing concern. Behaviour of microplastic particles (0.5 mm < L < 5mm in the largest dimension) in marine environment is difficult to predict, and no field observations are available up to now. Baltic amber (succinite), with its density of about 1.05-1.09 g/cm^3, fits the range of densities of slightly negatively buoyant plastics: polyamide, polystyrene, acrylic, etc. Baltic citizens have observed amber migrations for centuries, and the collected information may shed some light onto general features of microplastic particles behaviour. Events of "amber washing-out" at the sea shore of the Sambian peninsula (Kaliningrad oblast, Russia) typically take place in autumn-winter time. Experience of divers indicates that amber is washed out from the depths as deep as 15 m. Massive presence in amber-containing debris of the red algae *Furcellaria lumbricalis*, dominating in the sea at depths of 6-15 m, proves this fact. From oceanographic viewpoint, important for the "amber washing-out" are: strong and long-lasting storm, phase of wind decrease or direction change, developed long surface waves, shore exposure to wind. Analysis of characteristic wave lengths after long storms, dimensions of their surf zone, and changes in underwater bottom profile is carried out. Conclusion is that slightly negatively buoyant microplastic particles should migrate for a long time between beaches and underwater slopes until they are broken into small enough pieces that can be transported by currents to deeper area and deposited out of reach of stormy waves.

Key words: microplastics, amber washing-out, coastal zone, stormy conditions

I. INTRODUCTION

The Baltic amber has its material density of about 1.05-1.09 g cm^3, which is close to widely used plastics like polyamide (or nylon, 1.02−1.05 g cm^3), polystyrene (1.04−1.1 g cm^3), and acrylic (1.09−1.20 g cm^3) [1]. Textiles, carpets and sportswear, flooring and rubber reinforcement, electrical equipment, films for food packaging and food containers, lids, bottles, trays, clothing, as well as furnishing fabrics, netting and traps, automotive applications, and many other products are made of them (e.g., [2]). Our awareness concerning problems related to plastic pollution of the Baltic Sea [3]), as well as severe lack of information on real migrations of plastics in the sea coastal zone, urges analyzing of any potentially informative cases in this regard. At the same time, Baltic citizens have known the phenomenon of "amber washing-out" and have monitored its behaviour in the coastal

zone for ages. Thus, quite a rich set of natural facts is collected, which allows to shed some light onto the transport and fate of plastic particles as well.

The authors are not aware of any systematic investigation of physical conditions driving the amber migrations in the coastal zone, and have to rely on just descriptions of certain cases in books, newspapers, on web-sites, and on personal communications with amber hunters. (Amber hunting in the sea is considered by law like hobby-fishing or collecting berries or mushrooms in nature.)

The aim of this paper is to collect and analyse information on meteorological and hydrological conditions, surface wave field, locations and other important features corresponding to the cases when amber is washed ashore. Of especial interest are events of “amber washing-out”, when – after the most severe storms – large and heavy pieces of amber are transported to the beach from the depth of about 15-20 m; this phenomenon is termed as “brosy” by local citizens (the term is the derivative from the Russian word meaning "throwing out"). Further physical analysis is driven by the idea to predict some general features of behaviour of plastic litter and microplastic particles in the sea coastal zone.

II. Baltic amber properties and appearance on the beaches

Presence of amber on the swash-line of the Baltic Sea is quite a typical phenomenon for Kaliningrad beaches, and is very attractive for both local citizens and tourists. As a consequence, the conditions when it is observed are well known and very characteristic of this region: any more or less windy weather brings – here or there – an exclusive amber necklace along the beaches. Just windy episodes bring a lot, however, most of it are small amber pieces like crumbs of 1-2mm (Fig. 1), while heavier winds and especially severe winter storms may present amber samples up to 12 kg, like the piece found on the Baltic shore of Prussia in XIX century. Another two giant beached amber samples, reported in historical texts, had about 9700 and 7000 g. Such stones are washed out, however, extremely rare, and all the history knows less than 10 stones heavier than 5 kg [4]. The largest amber piece in the present-day collections is 47cm long and weighs 9.817 kg, it is exhibited in the Berlin Natural Science Museum [5]. Concerning the maximum total volume of the beached amber, local legends mention the event in 1862 when almost 2 tons of amber were beached during one storm [6]. Along with amber, a swash-line after storms contains seaweed, shells, wet wooden pieces, and nowadays they are very often mixed with some plastic garbage and microplastics particles.

Baltic amber is fossil resin produced by pine trees which grew in Northern Europe about 50 million years ago. In the course of time the resin was transformed to amber due to processes of polymerization and oxidation [7]. Until the XIII century seacoast inhabitants collected amber directly from the seashore, and later they learned how to obtain amber by combing the seabed with nets. With the appearance of the diving suit amber became also to be collected directly from the bottom of the sea.

Fig. 1. The Baltic shore after moderate (left, photo by I. Chubarenko) and strong (right, photo from [8]) winds.

The very material of amber is naturally inhomogeneous, and the stones may also have various inclusions. This is why the specific gravity of amber varies from 1.05 to 2 g cm^3 (very rarely). Anyhow, it cannot float in Baltic water (1.006 – 1.014 g cm^3). Interestingly, specific gravity correlates with the colour: transparent amber is about 1.1 g cm^3, while white amber may have the density as small as 0.93-0.96 g cm^3 (as reported on [7], but not confirmed by specialists).

As it is illustrated by Fig. 1, amber pieces are able to move up-slope and appear at the shoreline even at moderate winds, however the major part of observational facts describe the cases after severe storms, when amber "brosy" are impressive indeed. These observations can be summarised as follows.

(I) The events of "brosy" of large amber pieces to the shore take place **only several times per year** and are most often during cold season of a year - spring, autumn and especially winter, however sometimes may happen also in summer (as it was quite recently – on 18 June 2014).

(II) Favourable are the situations when strong northern and western winds rise **especially high waves**.

(III) Duration of a storm is important: at least **two-three stormy days** are necessary.

(IV) **The stage of wind weakening**: amber is washed up from the bottom of the Baltic Sea only *immediately after the storm*, not during or a few days later. It happens several hours after the wind weakening, when winds are ceasing already – but the storm is still vivid, and when waves are still high, but the sea already *begins* to calm down. The cases have also been mentioned when winds change their direction, e.g., from the west to the south, south-east or east, but the waves are still approaching the coast from the west. If this moment is to missed – southerly or easterly winds will lead to water level drop, and the seaweed patches with amber will leave coastal zone together with water.

(V) There are **favourable wind** directions: western, south-western or northern winds.

(VI) The event of "brosy" takes place not along the entire shoreline, but only **at certain separate (quite random) locations** (Fig. 2), where wind is perpendicular to the shoreline. This way, most frequently it happens at some place along the concave 20-km long western fragment of the Kaliningrad shoreline from the Vistula Spit to Yantarny (see the map on Fig. 2): closer to the spit

under northern or north-western winds, closer to Yantarny under western winds and winds with a south-western component. “Brosy” may happen along the northern Kaliningrad shore as well (from cape Taran to Zelenogradsk), when winds are from the north or north-west. The location of amber “brosy” is not permanent also within one stormy event – it changes together with the wind direction.

(VII) **Patchiness:** seaweed with amber comes to the shore in submerged patches, arising quite far from the shore right after the storm. Floating material is distributed within the patch throughout the entire water depth, from the bottom to the surface. The storm lifts the next portion of the seaweed with amber from the bottom, as a rule, in only a separate place. If, by some reason (usually – change of the wind direction), the patch begins drifting off-shore – it never comes back, and the “amber hunters” are then looking for another patch.

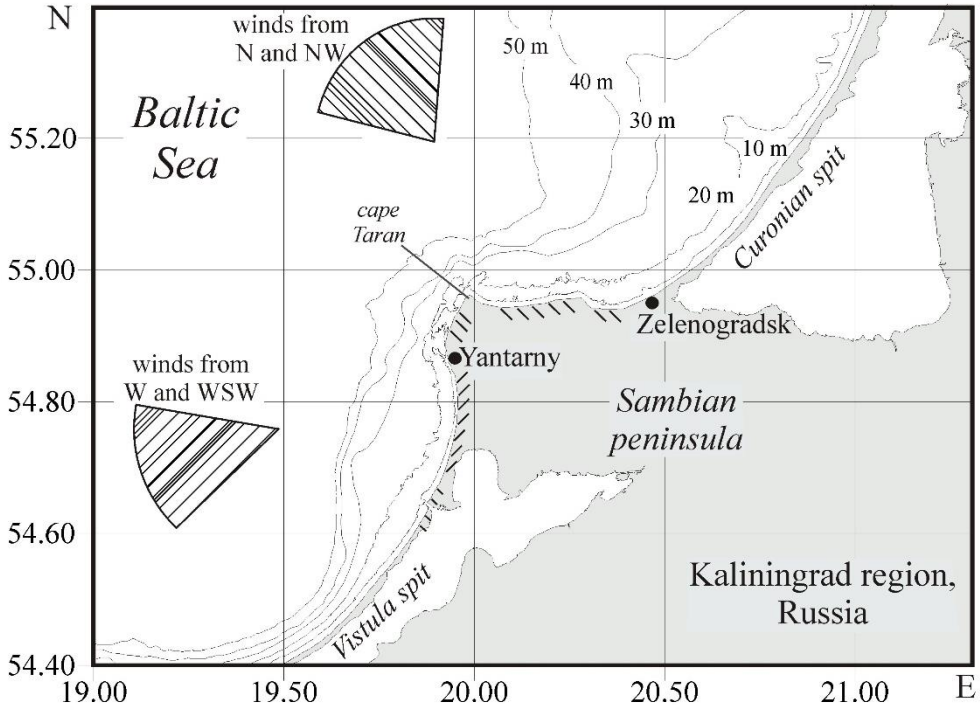

Fig. 2. Map of the region. Correlation of wind directions and locations of amber “brosy” is shown by similar hatching.

III. Where was the beached amber located on the underwater slopes?

The amber is usually found at depths from 3 to 12 m, maximum 15 m. One reason for this is that layers with amber-containing “blue clay” of the ancient Litorina Sea are located at the depths of 4-15 m below the sea level, stretching from Vistula Spit to Curonean Spit and further north [9]. However, amber is never washed ashore without plenty of seaweed, wooden sticks and marine litter. This suggests that the beached amber pieces are not directly washed out the sea bottom, but are just caught by seaweed clouds during their underwater migrations, exactly like other non-buoyant wooden or plastic pieces. An important observation is that amber is typically washed ashore together with red algae *Furcellaria lumbricalis*, which are abundant in the eastern part of the Baltic Proper and compose almost permanent belt along the shore [10], dominating on submerged rocks at the depths of 6-15 m [5]. Interestingly, it can also grow in large floating mats [5], and such mats are also

mentioned quite often as washed ashore together with amber "brosy". One way or another, it is quite obvious that amber pieces, which are heavier than water, are washed out during storms from the depths of about 6-10-15 m.

IV. Discussion: oceanographic viewpoint

The main physically important features of large amber "brosy" can be summarized as follows. In late autumn/winter/early spring, the thickness of the upper mixed layer is large – up to D~50-60 m in the Baltic Proper [11]. Thus, in the regions where the local depth d is smaller than D, vertical wind&convective mixing reaches the bottom, favouring the suspension of bottom material. After several days of storm, surface waves are already well developed, and their length and height can be estimated from their fetch. For the orientation of Kaliningrad shores, winds from the north, the north-west and the west have maximum wind fetch for this area (about 200-250 km [12]), and they rise the highest (H up to 7-8 m) and the longest (L up to 120-140 m) surface waves possible for this region (see the Baltic Sea wave diagram, Fig. 7.11 of [12]).

It is generally assumed that the border between deep and shallow surface waves is associated with the depth $d \sim 0.5\ L$ (i.e., again about 60 m in the considered case), so that over shallower regions the surface waves "feel" the bottom and, hence, bottom sediments "feel" water motion due to surface waves [12]. The surf zone of the highest waves begins at the depth $d \sim 2\ H$ (about 15 m), while other stormy waves are breaking over depths from 2 H to 1-1.5 H (from 15 to 7 m) [12]. This very depth range is pointed out as the source where amber-containing patches arise, and the distance from the shore to the isobaths 15 m and 7 m is only 3-5 km. With quite moderate (for stormy conditions) water currents of the scale of 0.3-0.5 m/s, it should take about 5 km/0.5 m/s=10^4 s ~ 3 h only for the patch to reach the shore.

The observations summarized above (I)-(VII) indicate that both strong wind and developed surface waves are important, however, the very mechanism lifting the patch from the bottom to the surface has not yet been disclosed. We suggest that this can be the Langmuir circulation (LC): the coherent system of large longitudinal rolls, with their axes directed downwind, arising due to instability of wind-induced current in presence of Stokes wave drift. In addition to wind+wave nature of the LC [13], at least two other characteristics of the "brosy" underpin this idea.

First, the most essential feature – the patchiness (in longshore direction) - can be explained by separation of upwelling zones in-between Langmuir rolls. Assuming that the largest Langmuir cells embrace the depth of about 60 m (the thickness of the upper mixed layer) and taking depth-to-width ratio of an individual cell as about D/W~1.3÷3 [14], one can estimate the smallest spacing between upwelling zones as 80-180 m. Since these zones, resulting from instability of wind-induced current in presence of surface wave transport, are inherently different in intensity, the patchiness of the seaweed clouds lifted from the bottom is natural. The resuspension should take place at some distance from the shore – where the cells are not yet modified by the shoaling, which again agrees with field evidence.

The second observation supporting the LC-idea is that the "brosy" arise when the wind speed is already decreasing. It is known [13] that the LC arises at wind speeds of more than 5 m/s and persists at higher and higher winds until stormy mixing destroys its coherent structure (at more than ca. 25 m/s). With the "brosy", we may have an opposite case: stormy wind ceases – and LC

becomes evident. Note that horizontal water transport within the upwelling zones is directed down-wind, so that the patch in the considered case is to be beached at the shore directly exposed to it. This is in full agreement with observations as well.

Is the LC able to lift amber stones or microplastic particles from the bottom? The settling velocity of microplastics (0.5-5 mm long) particles with the amber density of 1.05 g/cm^3 varies between 1 and 5 cm/s [1], while the maximum vertical velocity in LC under (quite moderate) wind speeds of 2–12 m/s ranges from 2 to10 cm/s [15]. Thus, the LC is physically able to suspend the seaweed cloud from the bottom and transport it to the shore line.

IV. Conclusions: application to microplastics

Considering the behaviour of amber pieces as a physically equivalent example for microplastic particles, we may conclude that the latter have a long and complicated path from our beaches to the deep sea. Thrown on the beach, non-buoyant *macro*-plastics are soon captured by developing stormy waves and transported towards the deep sea; but later, when the storm ceases, they are able to come back to the swash zone and the shore line – to be mechanically destroyed and UV-degraded, and washed to the sea again and again – until *micro*-plastic pieces will be small and light enough to leave the coastal zone with stormy water currents.

The main critical factors for microplastics migrations in sea coastal zone are, thus, wind properties, features of surface wave field, and Langmuir circulations. In particular, these phenomena are very difficult to reproduce in numerical models. So, thinking about further numerical modeling of microplastics generation and migration processes, as well as its transport in the Baltic Sea, we suggest that possible solution may be shifting off-shore (to the iso-bath of about 20-25 m) the boundary, which exports the microplastics particles towards the deep sea.

An ecological point is also worth noting here. The red algae *F. lumbricalis*, which seems to be involved in / touched anyhow by the microplastic migration process, is also an important habitat-forming seaweed: its underwater "belts" provide spawning habitat for many fish species, and for this reason some governments even place regulations on the harvesting of this seaweed. This danger of presence of microplastics in marine environment has not been disclosed before the presented analysis.

V. Acknowledgment

Investigation of physical and dynamical features of marine microplastics particles is supported by Russian Science Foundation via grant number 15-17-10020.

VI. References

[1] I. Chubarenko, A. Bagaev, M. Zobkov, E. Esiukova, “On some physical and dynamical properties of microplastic particles in marine environment,” *Marine Pollution Bulletin*, 2016 (in press) DOI: 10.1016/j.marpolbul.2016.04.

[2] V. Hidalgo-Ruz, L. Gutow, R.C. Thompson, and M. Thiel, “Microplastics in the marine environment: A review of the methods used for identification and quantification,” *Environ. Sci. and Technol.,* vol. 46, pp. 3060–3075, 2012.

[3] EU Commission, “Guidance on monitoring of marine litter in European seas,” EU Commission, Joint Research Centre, MSFD Technical Subgroup on Marine Litter, 2013.

[4] http://amberhunters.com/

[5] https://www.wikipedia.org/

[6] http://www.mk.ru/

[7] http://www.amberseaside.com/

[8] http://www.kaliningrad.kp.ru/

[9] O.V. Petrov (Ed), *Atlas of geological and environmental geological maps of the Russian area of the Baltic Sea*. SPb., VSEGEI, 2010. 78 p. ISBN 978-5-93761-165-9

[10] M.S. Kireeva, “Distribution and biomass of seaweed of the Baltic Sea,” *Proceedings of VNIRO,* vol. 42, pp. 195-205, 1960.

[11] M. Leppäranta, K. Myrberg, *Physical Oceanography of the Baltic Sea*. Springer, Praxis Publishing. Chichester, UK. 370 pp. 2008.

[12] R. Feistel, G. Naush, N.J. Wastmund (Eds), *State and Evolution of the Baltic Sea, 1952-2005. A Detailed 50-Year Survey of Meteorology and Climate, Physics, Chemistry, Biology, and Marine Environment.* Wiley & Sons. 712 pp. 2008.

[13] A.D.D. Craik, S. Leibovich, “A rational model for Langmuir circulations,” *Journal of Fluid Mechanics,* vol. 73, pp. 401-426, 1976.

[14] I. Chubarenko, B. Chubarenko, E. Esiukova, H. Baudler, “Mixing by Langmuir circulation in shallow lagoons,” *Baltica,* vol. 23 (1), pp. 13-24, 2010.

[15] S. Leibovich, “The form and dynamics of Langmuir circulations,” *Ann. Rev. Fluid Mech.*, vol. 15, pp. 391-427, 1983.

MONITORING OF THE THERMOABRASIONAL AND ACCUMULATIVE COASTS NEAR THE UNDERWATER GAS PIPELINE ROUTE ACROSS THE BAYDARATSKAYA BAY, KARA SEA

Nataliya Belova, Lomonosov Moscow State University, University of Tyumen, Institute of the Earth Cryosphere, Russia
Alisa Baranskaya, Lomonosov Moscow State University, Russia
Osip Kokin, Lomonosov Moscow State University, State Oceanographic Institute, Russia
Dmitry Kuznetsov, Lomonosov Moscow State University, Russia
Olga Shilova, Lomonosov Moscow State University, Russia
Nataliya Shabanova, Lomonosov Moscow State University, Russia
Aleksey Vergun, Lomonosov Moscow State University, Russia
Stanislav Ogorodov, Lomonosov Moscow State University, Russia

nataliya-belova@ya.ru

The coasts of Baydaratskaya Bay are composed by loose frozen sediments. At Yamal Peninsula accumulative coasts are predominant at the site where pipeline crosses the coast, while thermoabrasional coast are prevail at the Ural coast crossing site. Coastal dynamics monitoring on both sites is conducted using field and remote methods starting from the end of 1980s. As a result of construction in the coastal zone the relief morphology was disturbed, both lithodynamics and thermal regime of the permafrost within the areas of several km around the sites where gas pipeline crosses coastline was changed. At Yamal coast massive removal of deposits from the beach and tideflat took place. The morphology of barrier beach, which previously was a natural wave energy dissipater, was disturbed. This promoted inland penetration of storm surges and permafrost degradation under the barrier beach. At Ural coast the topsoil was disrupted by construction trucks, which affected thermal regime of the upper part of permafrost and lead to active layer deepening. Thermoerosion and thermoabrasion processes have activated on coasts, especially at areas with icy sediments, ice wedges and massive ice beds. Construction of cofferdams resulted in overlapping of sediments transit on both coasts and caused sediment deficit on nearby nearshore zone areas. The result of technogenic disturbances was widespread coastal erosion activation, which catastrophic scale is facilitated by climate warming in the Arctic.

Key words: permafrost coasts, arctic coastal dynamics, monitoring, massive ground ice, technogenic impact, Kara Sea

I. Introduction

Unlithified, ice-bonded sediments characterize 65% of the coast facing directly onto the Arctic Ocean [1]. Long-term (decadal) rates of coastal change are typically in the 1-2 m/year range [2].

Rates of shoreline change significantly vary along the Arctic Ocean coastline due to differences in geological (e.g. ice content, sediment type), geomorphological (e.g. exposure, elevation, slope) structure and hydrometeorological conditions (e.g. wave parameters, sea and air temperature). Most of the literature notes that storm events play a significant role in controlling the short term rate of coastal change [2-5]. The modern climatic changes, especially well expressed in the Arctic, contribute to the growth of the retreat rates of the coasts [1, 2, 4, 6]. The main factors influencing the speed of coastal destruction during warming are the increasing ice-free period and changes in the wave climate determined by this increase [3], while summer air temperatures as such, in most of the cases, show bad correlation with the rates of thermoabrasion [3, 4].

II. Research area

Baydaratskaya Bay is a shallow (up to 30 m depth) gulf in the south-western part of the Kara Sea (Fig.1). The bay is a former delta of the ancient Ob River. By the end of the Late Neopleistocene, sea level was lower than the modern bottom of the inlet; the bay as it is today formed as a result of Holocene transgression, when the eustatic sea level rise exceeded the relatively stable vertical uplift of the Earth's crust in the region [7]. Sea level rise activated the destruction of coasts; periods of sea ice extent decrease correspond to ancient coastlines on the bottom of the bay [8]. Baydaratskaya Bay forms a separate lithodynamic area (Baydaratskiy area), which is one of the four lithoynamic areas in the south-western Kara Sea sector [9]. Along the modern coastline of the bay, abrasional (thermoabrasional, thermodenudational with height up to 40 m) and accumulative coasts alternate. Sediments outcropping in the coastal cliffs are perennially frozen deposits formed in the middle and late Neopleistocene and Holocene. They contain massive ground ice [10] and are often folded into complicated deformations [11].

History of investigations

Systematic investigations of the natural conditions along the gas pipeline "Yamal-Center" projected route started in 1988 with the works of the Arctic marine engineering-geologic expedition (AMIGE), Laboratory of geoecology of the North, Faculty of geography, Lomonosov Moscow State University (MSU) and other organizations. As a result of integrated studies of 1990-1996, conducted by IPO "Eco-system", a monograph [12] characterizing different aspects of the natural conditions of the Baydaratskaya Bay coasts and water area was created. Coastal dynamics monitoring in the area of the coastal transition zone of the pipeline crossing was initiated by the scientists of the Laboratory of geoecology of the North, Faculty of geography, MSU, in 1988 [13].

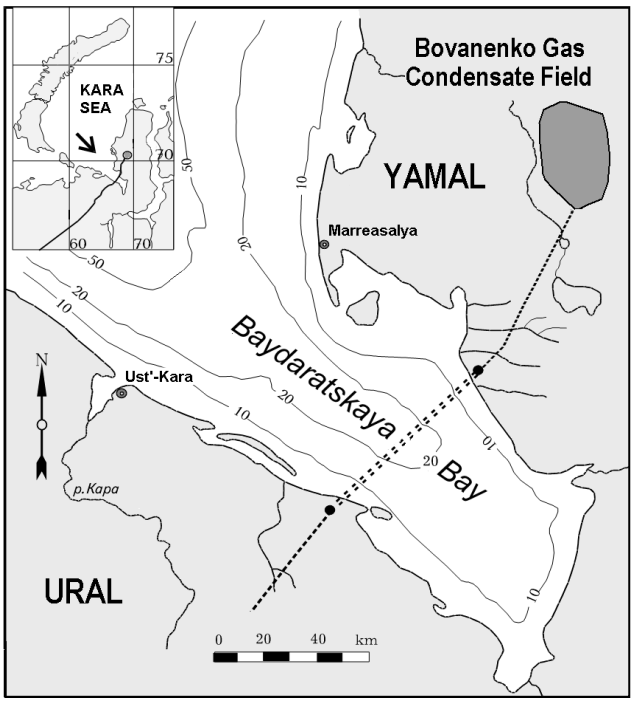

Fig.1. Underwater pipeline route across the Baydaratskaya Bay of the Kara Sea

Methods of coastal monitoring

On both coasts of the bay, in the planned area where the future pipelines would cross the coast, a network of benchmarks was established. In the sections of these benchmarks, repeated trigonometric leveling was conducted; profiles of the coastal zone from the top of the cliff on land to the outer margin of the tidal flat in the sea were drawn. Comparison of multitemporal profiles allowed to quantitatively characterize coastal dynamics for different types of coasts. Direct measurements were conducted in 1990, 1991, 1993, 1997, 2005, 2006, 2007, 2009, 2012 and 2013 within the Ural (29 profiles) and Yamal (17 profiles) coasts; lost monitoring benchmarks were set again, and new ones were established. Besides the direct measurements, coastal retreat rates were determined using the results of multitemporal aerospace imagery. The methods of referencing and processing of the imagery are given in details in [14].

III. YAMAL COAST KEY SITE

Within the Yamal area, coastal dynamics monitoring was conducted at the 16-km long section from Mutniy Cape in the north to the mouth of Liyakha River in the south. The top of the plain come to the coast in the very north and south of the area, forming abrasion-thermodenudational cliffs of 8-12 m height and 4.5 km along the coast to the south of Mutniy Cape, and up to 22-28 m above sea level (a.s.l.) to the mouth of Yara-Yakha River. They are composed by relatively homogenuous strata, represented by sandy sediments with low ice content. In the middle part, where the system of pipelines is laid, the coast represents a Holocene barrier beach, the height of which was 1.6-2.1 m before the beginning of the construction, lowering landwards and followed in this direction by a low laida separating a shallow lagoon (Fig.2).

The coast of the area is protected from northerly and partly north-westerly winds by the Marresalskie Koshki Islands. The longshore sediment flux is directed from the mouth of Yara-Yakha River to the north up to Mutniy Cape, where it decreases, forming a wide tidal flat. In the Yara-Yakha River delta, the sediment flux migration is bilateral; most of the sediments accumulate from the northern side of the delta forming wide tidal flats as well.

During the period from 1988 to 2009, the average retreat rates of high thermoabrasional and thermodenudational coasts within this area were 0.4 m/year for the northern part (high coasts to the south of Mutniy Cape, 4.5 km along the coast), and 0.5 m/year for the southern part (3.5 km along the coast to the south of Yara-Yakha River mouth), respectively. In 2009-2012, after active construction started, the situation slightly changed. Retreat of the northern abrasional segment was enhanced within the 2 km adjacent to the coastal bar, where the rates of coastal destruction increased from 0.1-0.3 m/year in 1988-2009 to 1.3-5 m/year in 2009-2012. Abrasion also increased within 1 km to the south of Yara-Yakha River mouth; probably this was influenced by artificial deepening of the river mouth. Here, the retreat rates grew from 0.3-1.2 m/year in 1988-2009 to 2.3-7.9 m/year in 2009-2012. In 2012-2013, the coast became more stable on both of the areas due to the end of the main stage of construction and artificial sediment input along the barrier beach.

Before the beginning of the construction of the pipeline crossing in 2008, the coast within 3.5 km to the north of Yara-Yakha River mouth used to be accumulative. The cofferdam, erected above the two pipes, formed a re-entrant angle actively filled by sediments, from the southern side. As a result, by 2012, the tidal flat became 40 m wider to the south of the cofferdam and 50 m narrower to the north of it. The shortage of sediment flux which determined the activation of retreat of the abrasional cliffs to the north of the barrier beach is namely connected with the catchment of the longshore sediment flux by the cofferdam along with excavation of sand from the beach and tidal flat at the coastal section from the site of construction till the mouth of Yara-Yakha River (Fig.2, 3a). The barrier beach itself also experienced degradation in 2007-2012, above all, due to excavation of beach sediments and sediments from nearshore zone. In 2012, the maximal height of the coastal bar was 1.2 m (BS-77), while before the start of the construction it was 1.6-2.1 m. As a result of numerous heavy vehicles moving along the barrier beach a coastal cliff started to form in the dense peaty sediments of the barrier beach. In 2011-2012, the coast near the cofferdam was strengthened by concrete mats [15], which slowed up the retreat to some extent; however, already in 2012, these constructions started to be deformed (Fig.3b). No considerable changes in the topography of the barrier beach were seen in 2012-2013. In 2013, within separate areas to the north of the pipeline crossing, an increase of the height of the coastal bar by 0.2-0.6 m compared with 2012 was noticed. It is possible that in the conditions of the

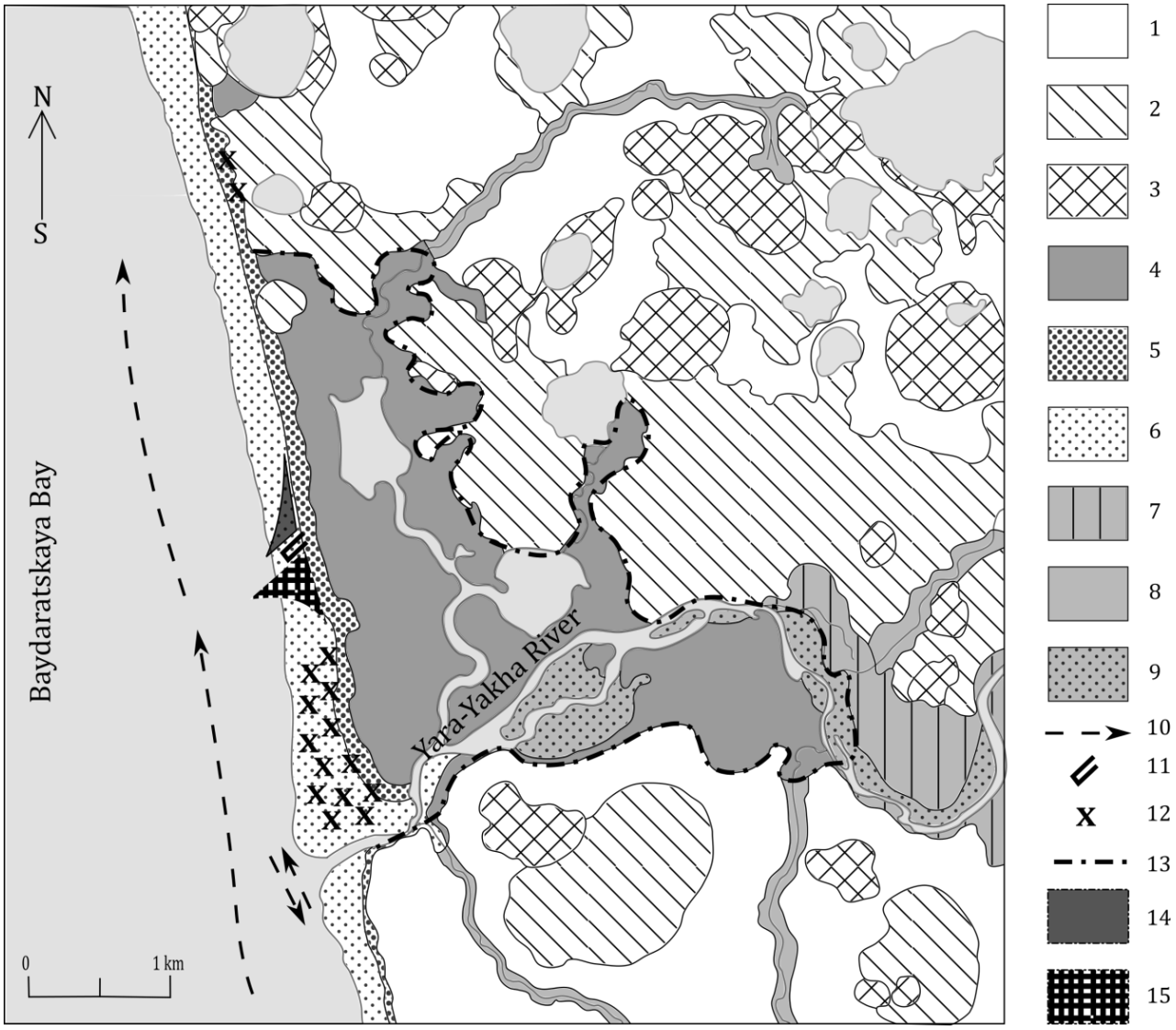

Fig.2. Scheme of Yamal coastal site central part. Geomorphological elements: 1 - surfaces and gradual slopes (< 5°) of 10-20 m a.s.l.; alas floors and gradual slopes: 2 – old, 3 – young; 4 – laida (marshy surface up to 4 m a.s.l.); 5 – beach, incl. barrier beach; 6 – tidal flat; River valleys: 7 – flood basin of large rivers, 8– valleys of small rivers and streams; 9 – river shoals. Coastal dynamics and technogenic impact features (2013 year): 10 – longshore sediment flux; 11 – the approximate location of cofferdam; 12 – sediment extraction sites; 13 – limit of storm waves landward penetration; 14 – zone of sediment deficit; 15 – zone of enhanced accumulation

Fig.3. Technogenic impact on Yamal coastal site: a) site of sediment extraction from the beach and tidal flat to the north of Yara-Yacha River; b) deformation of concrete mats at lagoon coast

lowering technogenic impact and constant artificial sediment input on the beach, the barrier beach started to recover.

IV. URAL COAST KEY SITE

In the area of Oyu-Yakha River mouth, monitoring of coastal dynamics was conducted for a segment between Torasovey and Levdiev islands. Here, surfaces of several types are cut by the coast. They all differ by height, cryolithological composition and coastal retreat rates.

The investigated area is characterized by relatively intense alongshore sediment flux. A unidirectional wave energy flux, beginning at the southern end of Torasovey Island, gradually decreases towards the south-west. The coast is open to wind-wave and ice impact from the Kara Sea.

During the years of field measurements and terrestrial observations, the most representative data without gaps have been received for 11 profiles, situated between the mouths of Oyu-Yakha and Niudiako-Tamyakha rivers (6 km of the coast). From the west to the east, 4 segments are selected.

1) Abrasional-accumulative coastal segment (cliffs 5-8 m a.s.l.), partly protected from the wave impact by a barrier beach, 0.3 km along the coast. Retreat rate before construction (1988-2009) here were 0.3 m/year and increased in 2009-2012 till 1 m/year, probably due to reasons, not connected with construction.

2) High thermoabrasional coasts composed by thick sandy strata with layers of loam and gravel containing thick (up to 3.5 m) massive ice beds [10, 16]; in the eastern part of the area with thick peatlands and ice wedges, with which gully thermoerosion in associated. Here, within 1.8 km along the coast, a surface is complicated by numerous thermokarst depressions and lowered by them to 10-18 m a.s.l., comes out to the shore. Average retreat rate before construction (1988-2009) were 1.4 m/year (up to 2 m/year at profiles with massive ice beds exposures) and haven't changed in 2009-2012.

Within 2 km to the west of Oyu-Yakha mouth, similar sandy strata outcrops in the costal cliff, while the ledge itself is higher (29 m), and the layers of tabular ground ice are thicker (6 m). There were no direct observations after 2007, while during 1988-2007 the coastal retreat rates were similar to those at the segment 2 (up to 2 m/year).

Coastal bluff retreat for the period 1964-2012 were determined for part of segments 2 and 3 based on multitemporal aerospace imagery comparison (Fig.4, [18]).

3) Laida thermoabrasional coast 0.5-2 m high (1.5 km along the coastline) are composed by silty sediments with high ice content due to wedge ice. Low-lying coasts are the most sensitive to changes in parameters affecting coastal dynamics since waves during storm surges penetrate far inland, simultaneously eroding the coast and providing a warming effect to the frozen sediments. The material formed by the erosion of the coast is quickly removed by waves due to its small volume. In 1988-2009 laida retreated with rate about 2.6 m/year, and after the construction beginning – 6 m/year in 2009-2012.

4) At the 1.5 km long fourth segment, separated from the east by Niudiako-Tamyakha River and including the pipeline crossing, a thermoabrasional-thermodenudational cliff is formed in a residual part of a surface of 5-7 m height (up to 8 m near the cofferdams erected above the pipelines, including sandy filling). Here, sandy loams with a system of polygonal ice wedges, along with loamy and silty deposits in the lower part of the cliff, often lying below sea level, are destructed by abrasion [10, 16, 17]. During 2005-2009 retreat rate were about 2.9 m/year, in 2009-2012 it increased till 4.3 m/year. But in exact sites thermoabrasion rates became higher after pipeline crossing construction has started.

Construction of two cofferdams at a distance of 70 m apart lead to lack of sediments between them and high retreat rates of coastal bluff; which were even higher due to linear erosion developing on wedge ice. In 2012 the coast between the cofferdams and 150 m to the east of the eastern cofferdam was protected by artificial boulder filling. Further to the east, the filling was not made, and the coast was affected by active abrasion. However, compared to 2007-2012, changes in the topography of the coastal zone of the Ural area in 2012-2013 were not considerable.

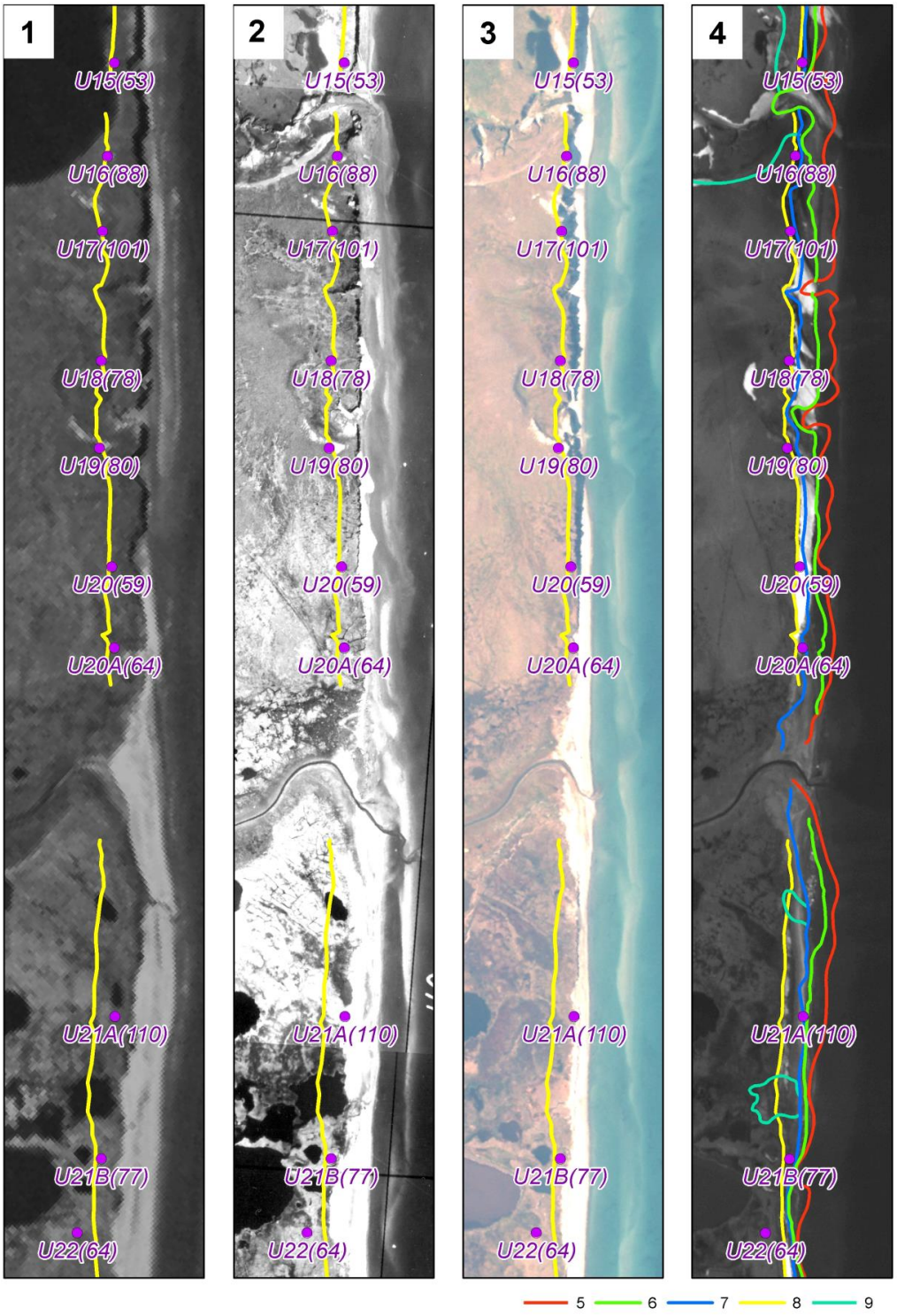

Fig. 4. Dynamcis of thermoabrasinal coastal segment (Ural Coast, Baydaratskaya Bay, Kara Sea [18]): 1 – Corona image (1964), 2 – aerial photo (1988), 3 – QuickBird image (2005), 4 – Formosat2 image (2012) with coastal bluff position in: 5 – 1964, 6 – 1988, 7 – 2005, 8 – 2012; 9 – limits of the modern khasyreys at the place of drained lakes. U21A(110) – number of benchmark of the coastal dynamics monitoring network (value of retreat of the coastal bluff from 1964 to 2012, m, given in brackets)

In 2013 the greatest changes were observed near the eastern cofferdam where heights of the surface near the seaward part of the cofferdam increased by more than 1 m from 2012 to 2013, as a result of which, a tidal flat of about 40 m width formed here. This is connected with high volume of filling made in the period between the monitoring of 2012 and 2013 to prevent the destruction of the cofferdam.

To the east of Niudiako-Tamyakha River, within 3 km up to Levdiev Island, low laida coast with heights up to 2.5 meters is observed. On part of the profiles in this section, observations started in 2005 only; however, the acquired data allow to characterize the dynamics of this area. As on segment 3, the direct measurements confirmed significant variations of coastal retreat rates in time due to low stability of such coasts, and in space due to local technogenic impact (heavy vehicles, see below).

Temporal variability of coastal dynamics

Generally, three typical stages of coastal dynamics can be selected: two periods of abrasion activation (1988-1996 and 2005-2012) and a period of abrasion decrease (1997-2005). These periods have been seen also at Yamal coastal site but were less pronounced there due to lower retreat rates and less diverse sediments types composing coastal bluffs. In 1997-2005, a negative peak is shown for all the profiles at Ural coast. It coincides with a minimum in wind-wave energy due to little occurrence of storm events, in spite of increase in the ice-free period. After 2005 the increase of the ice-free period continued, which resulted in periods of storms and winds falling into the ice-free period. As a result, most of the profiles show a 1.5–2 times increase of retreat rates compared to the average.

In 2009-2012, after the construction of the underwater pipeline crossing, retreat rates became even higher. The biggest retreat values were from 6 to 18 m/year, which is a record for the observations within the Ural coast. Dramatic destruction was observed even within the accumulative laida coast near Levdiev Island. The coast retreated by 55 m in 2009-2013, which corresponds to an average rate of 18 m/year. The reason of such dramatic change lies in the road which came through the beach and laida surface at this segment, with several heavy vehicles a day passing on the beach and littoral. In 2012-2013, this segment didn’t retreat more than 3 m.

V. Conclusions

In general, the Yamal coast of the Baydaratskaya Bay is characterized by lower retreat rates than the Ural coast. The reason lies in the difference in the ice content and composition of permafrost within the two sections. For the Ural coast, high ice content of permafrost is typical. Presence of ice wedges and massive ice beds which results in quicker coastal retreat. Another important feature is that the Ural coast is more influenced by the temperature factor, because of the high ground ice content. On the contrary, the Yamal coast is more dependent on the wave energy amounts. The technogenic impact played a dramatic role for the Ural coast, as well as for Yamal, however, for the Ural coast the consequences were bigger (with retreat rates of up to 18 m/year). This may be also connected with higher ground ice content, especially in the sediments of low laida, which are the most affected by the waves, and which were turned into roads destroying the natural cover of the accumulative forms. Nevertheless, for both coasts there was a trend of decrease in the

coastal destruction in 2013, which testifies that after the period of the highest anthropogenic impact, the destruction is starting to slow down and doesn't turn into a process which cannot be turned back.

In this way, we can conclude that coastal dynamics within the south-western Kara Sea depend on many factors. Quaternary sediments composing the thermoabrasional cliffs, their grain size, mechanical properties, and especially ice content are of great importance. These factors influence considerably lateral distribution of average retreat rates. Changes in temporal distribution of the coasts' retreat velocities are caused in fluctuations of hydrometeorological conditions in the case of undisturbed ecosystems; however, coastal destruction can be dramatically enhanced due to technogenic impact, as it has been shown for the areas of underwater pipeline crossing on both the Ural and Yamal coast of the Baydaratskaya Bay. In this case, low coasts and coasts composed by sediments with high ice content, are also especially vulnerable.

VI. Acknowledgments

The work has been supported by Russian Foundation for Basic Research, projects 16-35-60099 mol_a_dk, 14-05-00408a, 16-45-890076 r_a and 16-35-00453 mol_a.

VII. References

[1] H. Lantuit, P.P. Overduin, N. Couture, F. Aré, D. Atkinson, J. Brown, G. Cherkashov, D. Drozdov, D.L. Forbes, A. Graves-Gaylord, M. Grigoriev, H.-W. Hubberten, J. Jordan, T. Jorgenson, R.S. Ødegård, S. Ogorodov, W. Pollard, V. Rachold, S. Sedenko, S. Solomon, F. Steenhuisen, I. Streletskaya, A. Vasiliev and S. Wetterich,. "The Arctic Coastal Dynamics database: a new classification scheme and statistics on Arctic permafrost coastlines", *Estuaries and Coasts*, 2012, 35:383–400.

[2] D.L. Forbes (editor), *State of the Arctic Coast 2010 – Scientific Review and Outlook*. International Arctic Science Committee, Land-Ocean Interactions in the Coastal Zone, Arctic Monitoring and Assessment Programme, International Permafrost Association. Helmholtz-Zentrum, Geesthacht, Germany, 2011, 178 p. http://arcticcoasts.org

[3] F.E. Are, *Coastal erosion of the arctic lowlands*. Editor-in-chief V.P. Melnikov. Novosibirsk: Academic publishing house "GEO", 2012, 291 p. *(in Russian)*.

[4] S.A. Ogorodov, *The role of sea ice in coastal dynamics*. Moscow: MSU Publishing, 2011, 173 p. *(in Russian)*.

[5] A.A. Vasiliev, I.D. Streletskaya, G.A. Cherkashev and B.G. Vanshtein, "Coastal dynamics of the Kara Sea", *Earth Cryosphere*, vol. X, 2, 2006, pp.56-67 *(in Russian)*.

[6] E.I. Pizhankova, "Modern climate change at high latitudes and their influence on the coastal dynamics of the Dmitry Laptev Strait area", *Earth Cryosphere*, vol. XX, 1, 2016, pp.51-64 *(in Russian)*.

[7] A.V. Baranskaya, I.S. Yozhikov, Yu.I. Kuchanov, H.A. Arslanov, A.Yu. Petrov, F.E. Maksomov, "Quaternary sediments, paleogeography and vertical movements of the earth's crust in the north of Yamal and Gydan peninsula during late Pleistocene-Holocene", *Moscow University Vestnik. Series 5. Geography*, 2016, in press *(in Russian)*.

[8] V.Yu. Biryukov, V.A. Sovershaev, “Bottom relief of the south-western part of the Kara Sea and its Holocene history”, in *Geology and geomorphology of continental shelf and slope*. Moscow: Science, 1985, pp. 89-95 *(in Russian).*

[9] B.A. Popov, V.A. Sovershaev, V.N. Novikov, V.Yu. Biryukov, A.M. Kamalov, E.V. Fedorova, “Coastal zone of the seas of Pechora-Kara region”, in *Investigations of sustainability of northern geosystems*. Moscow: MSU publishing, 1988, pp. 176-190 *(in Russian).*

[10] N.G. Belova, *Massive ice beds of the south-western coast of the Kara Sea*. Moscow: MAKS Press, 2014, 180 p. *(in Russian).*

[11] A.V. Baranskaya, D.Yu. Bolshiyanov, Yu.I. Kuchanov, V.M. Tomashunas, “New data on dislocations in the Quarternary deposits of the Yamal and Gydan peninsula and the latest tectonic movements associated with them by the results of the “Yamal-Arctic-2012” expedition”, *Problemy Arktiki i Antarktiki*, 2013, 4(98), pp. 91-102 *(in Russian).*

[12] *Baydaratskaya Bay environmental conditions. The basic results of studies for the pipeline “Yamal-Center” underwater crossing design*. Moscow: GEOS, 1997, 432 p. *(in Russian).*

[13] A.M. Kamalov, S.A. Ogorodov, V.Yu. Birukov, G.D. Sovershaeva, A.S. Tsvetsinsky, V.V. Arkhipov, N.G. Belova, A.I. Noskov and V.I. Solomatin, “Coastal and seabed morpholithodynamics of the Baydaratskaya Bay at the route of gas pipeline crossing”, *Earth Cryosphere*, vol. X, 3, 2006, pp.3-14 *(in Russian).*

[14] S.A. Ogorodov, N.G. Belova, D.E. Kuznetsov, A.I. Noskov, “Using multi-temporal aerospace imagery for coastal dynamics investigations at Kara Sea”, *Earth from Space – the Most Effective Solutions*, 2011, 10, pp. 66-70 *(in Russian).*

[15] A.A. Ermolov, “Morpholithodynamic research as a part of engineering surveys for construction”, *Engineering Surveys*, 2014, 9-10, pp. 86–89 *(in Russian).*

[16] N.G. Belova, “Buried and Massive Ground Ice on the West Coast of Baidaratskaya Bay in the Kara Sea”, *Ice and Snow*, 2(130), 2015, pp. 93-102 *(in Russian).*

[17] D.M. Aleksyutina, R.G. Motenko, “Thermal properties and phase composition of the water in frozen soils of the Baydaratskaya Bay Ural coast”, *Engineering Geology*, 2013, 3, pp. 36-43 *(in Russian).*

[18] A. Vergun, A. Baranskaya, N. Belova, A. Kamalov, O. Kokin, D. Kuznetsov, N. Shabanova, and S. Ogorodov, “Coastal dynamics monitoring at the Barents and Kara seas”, *Society of Petroleum Engineers – SPE Arctic and Extreme Environments Conference and Exhibition*, AEE 2013, Moscow, vol. 3, 2013, pp. 1972–1990.

MODERN ABRASION PROCESSES OF THE AZOV SEA COAST

Lyudmila Bespalova, Southern Federal University, Russia
Olga Ivlieva, Southern Federal University, Russia
Alla Tsygankova, Southern Federal University, Russia
Alexander Ioshpa, Southern Federal University, Russia
Irina Sknarina, Southern Federal University, Russia
Larisa Kropyanko, Southern Federal University Russia

bespalovaliudmila@yandex.ru

The Azov Sea Coast is subjected to a complex of hazardous exogenous geological processes, landslides and abrasion being the most important ones. Both natural and anthropogenic factors contribute to the development and intensification of these processes. These processes are currently growing due to an increased frequency of storm surges.

Key words: geomorphology of coastline, beach forming material, gullies and ravines network, regulation of river flow, cyclonic activity, shores abrasion, hazardous exogenous geological processes, satellite monitoring.

The Azov Sea Coast is subjected to a complex of hazardous exogenous geological processes, landslides and abrasion being the most significant ones. The development and activity of these processes are intensified by both natural and anthropogenic factors. Climate change that results in increasing cyclonic activity, an increased frequency of western storms and surges, sea-level rise should be referred to natural factors [1]. Adverse environmental conditions (widespread easily-washed clay deposits in the coastal cliffs, low sand power, the shortage of beach forming material), multidirectional nature of neo-tectonic processes in the coastal zone, extensive gullies and ravine network also contribute to the active growth of the processes.

The main man-made effects include the intensive use of the coast by a number of different farmers, who often do not take into account the natural characteristics of the coastal zone (e.g. intensive plowing, deforestation, agriculture irrigation, river flow regulation leading to reduction of beach forming material, an unauthorized removal of sand and shell material from the beaches and spits, the change of sediment balance, deterioration of water quality and the reduction of biological components in the beach construction).

The Azov Sea Coast has been observed for more than 60 years [2-6]. Scientific monitoring is carried out by a reference network within the Russian coasts of the Don, Kuban areas, the Crimea involving 70 major districts. The total length of the studied coastline is over 1,000 km.

A number of observations available have revealed the cycles of intensification and stabilization of abrasion-landslide processes (Fig. 1). Periods of 1980-2002 and 2006-2010 are characterized by the abrasion stabilization, with the average speed at that time not exceeding

1 m/year, while the 2003-2006 and 2010-2014 periods are characterized by an intensification of these processes that is associated with an increased frequency of storm surges from the western part.

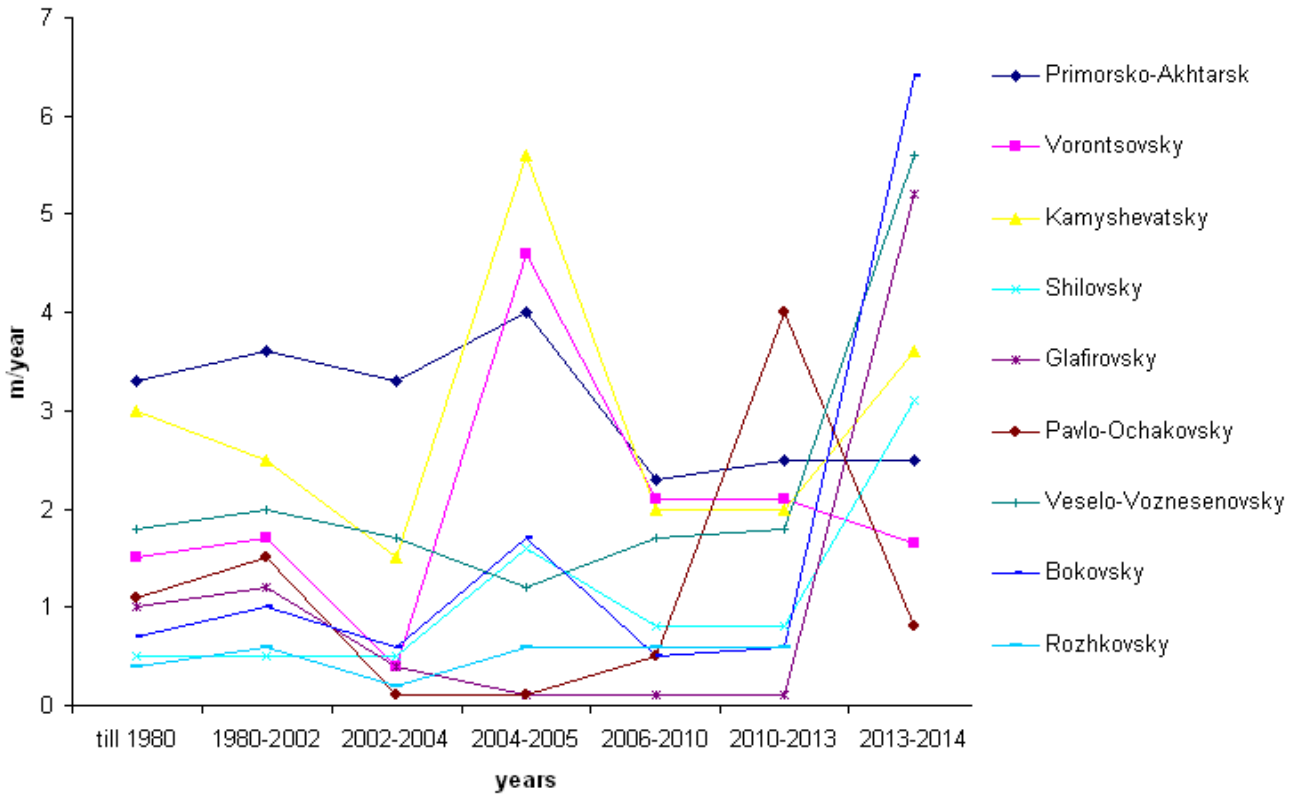

Fig. 1. Abrasion speed dynamics on the Azov Sea Coast

Particularly high rates of the coast destruction were recorded in 2013-2014, that was due to an increased frequency of winds and surges and catastrophic level rise, a notable example of which is the surge that took place on 24, September 2014.

The wind surges caused an increase of water level on the whole eastern coast of the Azov Sea, the Taganrog Bay and at the mouth of the Don River. Most hydrological stations recorded extremely high figures. This surge phenomenon is historically maximum ever recorded from the 1881 – 2014-period- observations.

The storm led to intensive coastal erosion in Primorsko-Akhtarsk, Veselo-Voznesenovsky, Glafirovsky and Shilovsky areas, and to flooding and erosion of the beaches in Dolzhansky, Yeisk, Chumburskaya, Pavlo-Ochakovo spits (Fig. 2). In the period of 2010-2013 abrasion rate reached 1.8 m/year, and in 2013-2014 it was 3.1m/year.

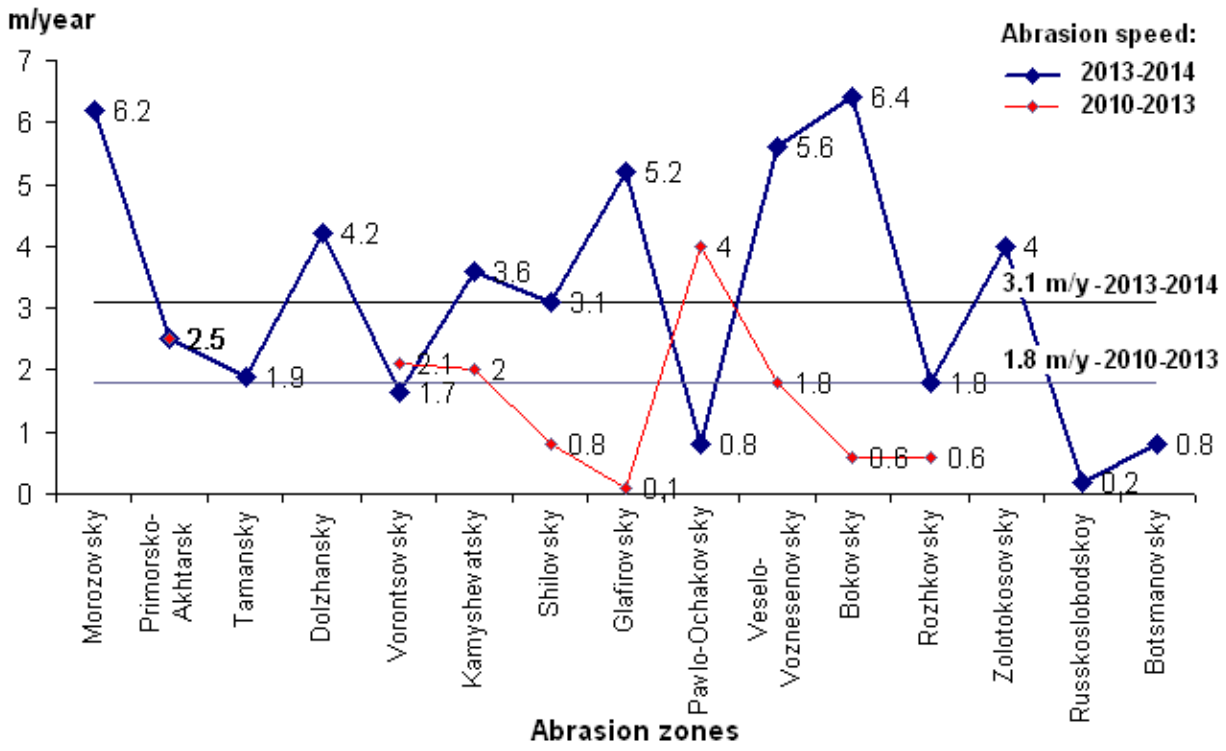

Fig.2. The abrasion rate in the Azov Sea emergency areas in 2013-2014

The coast of the Azov Sea has been zoned into the areas with mild, moderate, severe and very severe abrasion by abrasion processes activity (Fig. 3).

In the modern period (2013-2014) there were 20% of the shores with a weak abrasion (up to 1 m/year). Such abrasion rate was recorded in the areas near Russkaya Sloboda village (0.2 m/year), Pavlo-Ochakovo village (0.8 m/year), Botsmanovo village (0.8 m/year).

The average speed of coastal retreat (1-2 m/year) i.e. 20% of abraded coast has been recorded in such areas as: Vorontsovsky (1.7 m/year), Rozhkovsky (1.8 m/year), Taman (1.9 m/year).

Strongly abraded coast (2-4 m/year) i.e. 27% has been found in the areas of Primorsko-Akhtarsk (2.5 m/year), Shilovsky (3.1 m/year), Kamyshevatsky (3.6 m/year), Zolotokosovsky (4 m/year).

Such settlements as Dolzhansky (4.2 m/year), Glafirovsky (5.2 m/year), Veselo-Voznesenovsky (5.6 m/year), Morozov (6.2 m/year), Bokovsky (6.4 m/year) have been specified as emergency areas (at a rate of 4 m/year) that is 33% if activity of hazardous processes with a very strong abrasion is taken into account (Fig. 3).

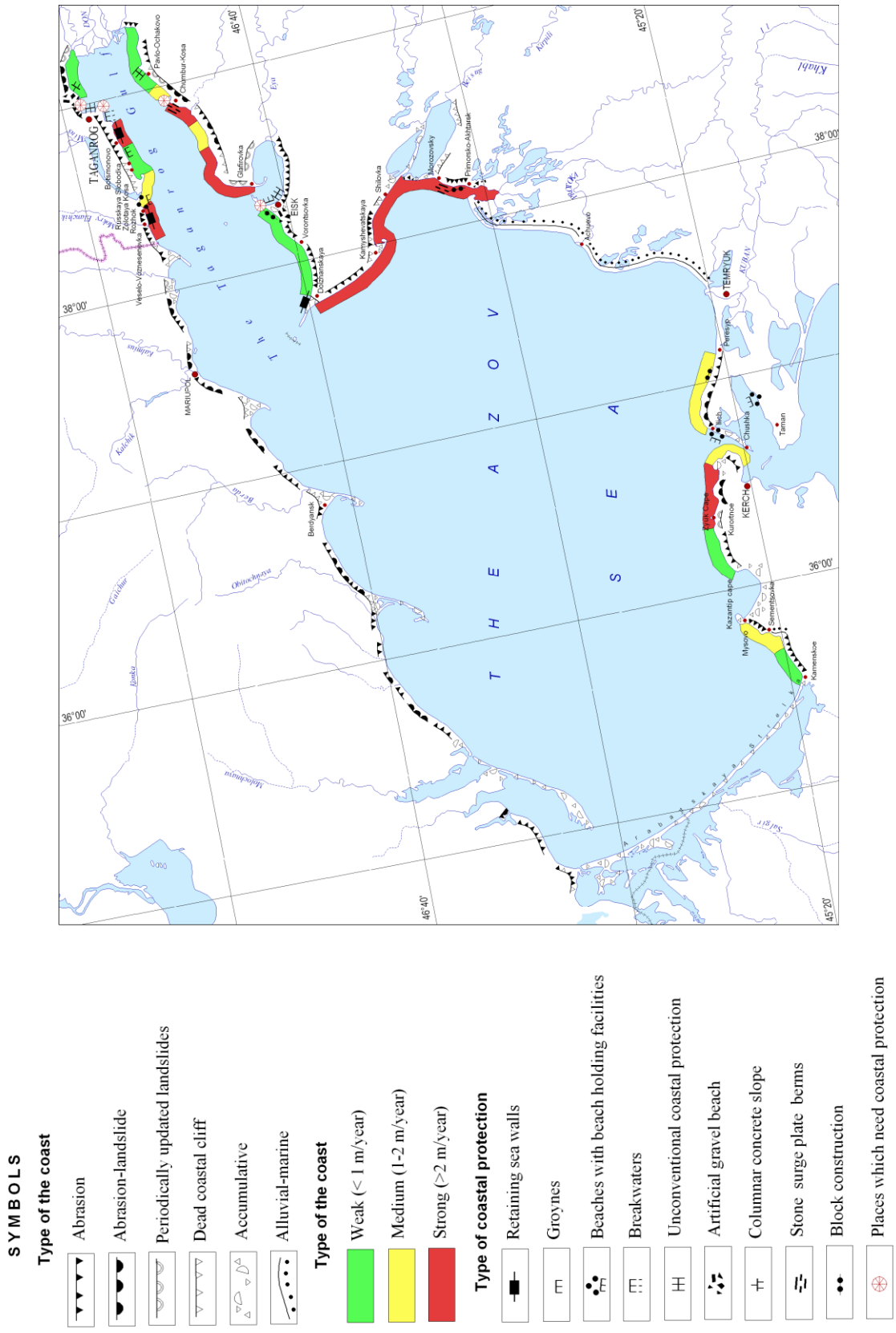

Fig. 3. Zoning of the Azov Sea coast by the abrasion processes degree

It has been found that the percentage of beaches with strong and very strong abrasion increased from 33% in 2010-2012 to 60% in 2013-2014., i.e. almost twice as much.

The Kerch peninsula is dominated by an abrasion and abrasion-accumulative shore, the beach from Cape Zyuk to the Kerch Strait is the most dangerous, which retreats on average 1.6 m/year, and from the eastern side of the Kazantip Gulf to Cape Zyuk - 1.1 m/year.

The shores in such villages as Nasir, Zavodskoe, Kurortnoe, Yakovenkova, Chelyadinov, and settlements as Podmayachny, Geroevskoe can be considered to be the emergency areas of the Kerch peninsula in terms of abrasion-landslide processes.

Nowadays the Kerch Peninsula coastal zone is in extremely poor condition. The coast tends to retreat; it is caused by specific geological and geomorphologic composition and hydrodynamic processes, as well as anthropogenic factors (hydraulic structures in the coastal zone, construction sites on the beaches and coastal dunes, coastal protection made of concrete material, sand and gravel picking from the beaches,).

Evaluation of spatial development of abrasion processes, the amount of material has shown that the variability of these indicators is due mainly to lithological characteristics of rocks (widespread distribution of unconsolidated sedimentary rocks, loess loam and clay) and the occurrence of surges.

Accumulative forms of the Azov Sea are also subjected to considerable deformations. The study is regularly carried out both at reference points, and with remote sensing of the Earth. Comparing the data from the map in 1980 and satellite images for a number of the Azov Sea forelands has shown that the area of the spit during this period did not change. But their displacement is noticeable in the eastern direction.

The western shore is eroded, and the material is redeposited on the eastern coast (Fig. 4). As for Dolzhanskaya Spit (foreland), on the contrary, the eastern shore is eroded, the accumulation of sediment occurs on the western one. The erosion speeds in different parts of the coast vary from 1 to 3 m/year [9-10].

Extreme surges which occurred in March 2013 and in September 2014 seriously affected the accumulative forms of the Azov Sea Spits (forelands): Dolzhanskay, Chumburskya, Pavlo-Ochakovsky, Petrushinskoe. Most of the forelands were flooded, the water level rose to the level of more than 2 m, which led to some catastrophic damage.

Particularly the main buildings, the recreation center, guest houses were badly damaged which are located next to the spit, near the spit base and in close proximity to the original bank.

Constant monitoring of the coastal area, the development and implementation of complex coastal protection and environmental management measures are necessary to preserve the coast infrastructure, cultural and architectural monuments of highways and other facilities.

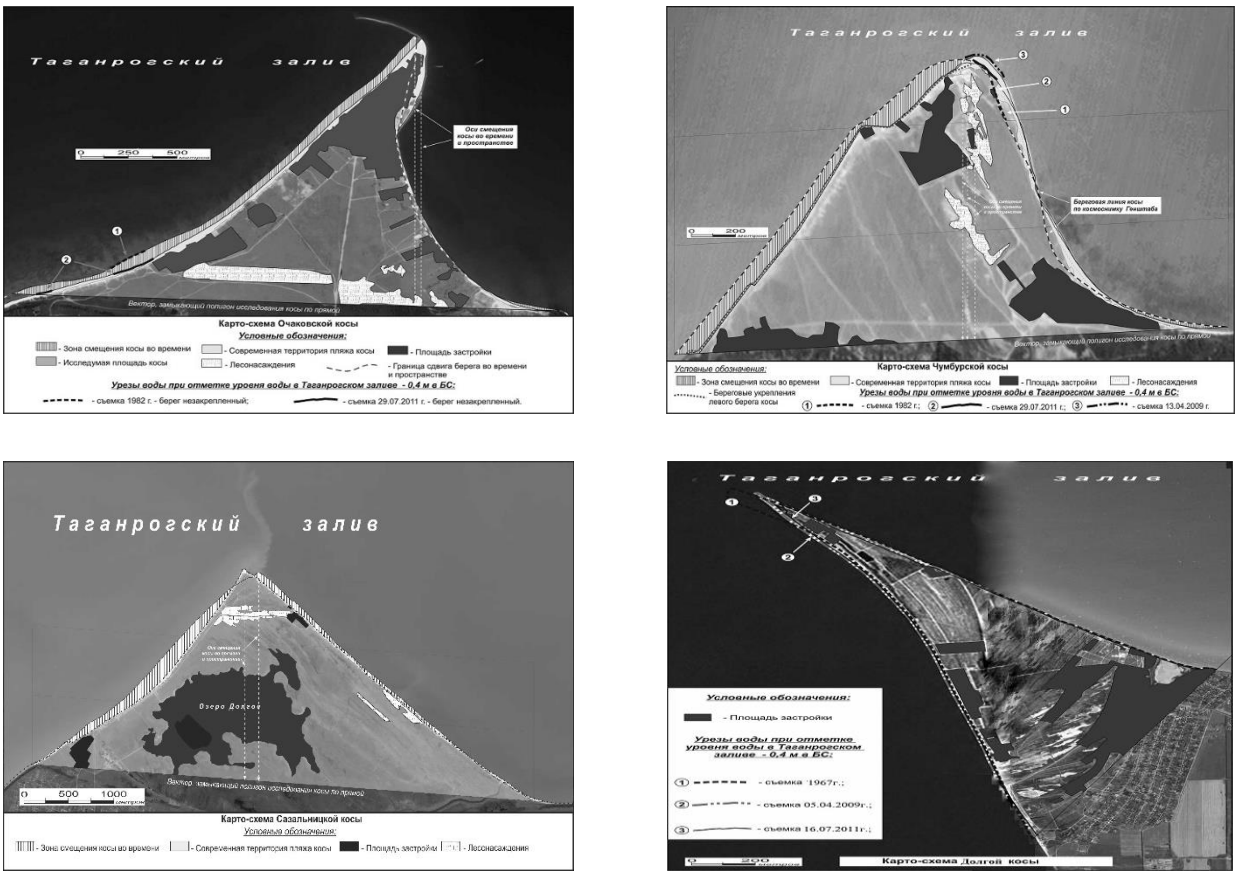

Fig.4. The spit displacement of the Taganrog Bay in 1982-2012

Long-term studies have shown that the Azov Sea coast is badly eroded as a result of dangerous exogenous processes, the most contributing of which are landslides and abrasion. A number of observations available have revealed their activation and stabilization cycles. In the modern period intensification of abrasion-landslide activity is observed, namely, the share of the shores with strong and very strong abrasion increased from 33% in 2010-2012 to 60% in 2013-2014., i.e. being almost twice as much.

An examination of bank protection structures of the Azov Sea coast has revealed that they are in a very poor condition. To date, they have been severely deformed or destroyed, as heavy concrete structures are mainly used on the loamy Azov coast. Rockfill groynes, suppressing surges dams made of natural stone, gravel and pebble beaches have proved to be a positively effecient way of coastal protection.

Research was done within the theme "Development of assessment methods and technology and natural hazards forecasting in Azov region of the Don, Kuban areas, the Crimea" (Southern Federal University grant № 213.01-07-2014/14PCHVG).

REFERENCES

[1] L.A Bespalova., P.M Lurie., A.E Tsygankova., T.A Vetkina., O.Sh Nosikova "Level mode Taganrog Bay in the modern period" //*Modern technology monitoring and development of*

natural resources of the southern seas. International seminar proceedings. (Rostov-on-Don, 15-17 June 2005) –Rostov-on-Don, «TsVVR», 2005. - pp. 27-29.

[2] V.P. Zenkevich "The shores of the Black and Azov Seas". - Moscow: Geographgis, 1958. – p. 373.

[3] V.A. Mamyrkina, Yu.P. Khrustalev "The coast of the Azov Sea" – Rostov-on-Don: RSU Press, 1980. – p. 176.

[4] Yu.V. Artyukhin "Wave destruction of the Azov Sea landsliding coast"// *Geomorphology*. - 1982. – Vol. №4. - pp.51-58.

[5] D.G. Matishov, O.V. Ivlieva, L.A. Bespalova, V.V. Sorokina, P.P. Ivliev "Modern speed abrasion, and the condition of shore facilities of the Russian coast of the Sea of Azov" // *Scientific proceedings of SNC RAS. Vol 1. Geology*. Rostov-on-Don: SNC RAS Press, 2006. - pp. 151-164.

[6] O.V. Ivlieva, L.A. Bespalova, P.P. Ivliev "Modern coastal processes of the Taganrog Gulf" *//University news. North Caucasus Region. Sciences.* – 2010 – Vol №5. - pp. 107-110.

[7] I.A. Labutina "Interpretation of the space images" -Moscow. Aspect Press, 2004 – p. 184 .

[8] O.V. Ivlieva, S.V. Berdnikov. "Contemporary rate of destruction of the Russian coast of the Azov Sea coasts" *//Geomorphology*. – 2005. – Vol № 4. - pp. 74-82.

[9] L.A. Bespalova, O.V. Ivlieva, P.P. Ivliev "Environmental risks of development of the sea coast of Rostov Region". - Moscow: Geos, 2014. - pp. 60-62.

[10] N.S. Yatsun, L.A. Bespalova, O.V. Ivlieva, S.N. Soluyanova "The spits of the Azov Sea: morphodynamics, development issues" //*The 3-d International Conference proceedings « The building of artificial beaches, islands and other structures in the coastal zone of seas, lakes, reservoirs" (Irkutsk, 29 July - 3 August 2013 г.)*. - Irkutsk: Institute of the Earth's crust SO RAS, 2013. – pp. 43-49.

MORPHODYNAMICS OF THE SHORES OF THE VISTULA SPIT (THE BALTIC SEA) IN A PERIOD OF 2002-2015 BY RESULTS OF IN-SITU MEASUREMENTS

Valentina Bobykina, AB IO RAS[1], Russia
Boris Chubarenko, AB IO RAS[1], Russia
Konstantin Karmanov, AB IO RAS[1], Russia

bobyval@mail.ru

For the first time, the quantitative characteristics of the Vistula Spit shore dynamics based on the ground-based monitoring data for 2002-2015 were presented. On the sea shore, 3 sections can be distinguished by the direction of coastal processes, i.e. the stable section to the north of the Strait of Baltiysk, the eroded 4-km section to the south of the Strait of Baltiysk, with maximum erosion rate up to 2 m/year; in the remaining area of the Spit (21 km) to the Polish border there is an alternation of stable, eroded and accumulative areas. Since 2011, a steady erosion (in the stable segments of the third section) and general weakening of the erosion rate (in the second section) have been recorded. 50% of the length of the lagoon shore was the subject to annual active erosion (0.2 - 1.4 m/year). The beaches of the sea and lagoon shores of the Vistula Spit were mainly composed of medium sands. The alongshore variability in particle size distribution on the sea and lagoon shores (according to the 2015 survey data) actually fail to correlate with long-term dynamic processes, with the exception of the steadily eroded 4-kilometer area on the sea coast to the south of the Strait of Baltiysk. Variations in the composition of sediment along the shore on the shoreline are most likely associated with the results of the latest wave processing (or storm processing and eolian transport in the case of an average beach sample).

Key words: Coastal dynamics, monitoring, coastal sediments, Vistula Spit, Baltic Sea.

I. INTRODUCTION

The Vistula Spit with a length of 65 km (the Russian part is 25 km, and it is 35 km taking into account the 10-km section to the north of the Strait of Baltiysk[2]) stretches from the southern end of the Kaliningrad (Sambian) Peninsula and south-west it is adjacent to the bedrock coast of Poland (Fig. 1.). It is a polygenetic depositional feature, a barrier spit that separates the Vistula Lagoon from the Baltic Sea [1].

The Spit was created as a result of the Holocene transgression [2, 3], it took the present shape after the creation of the Strait in 1510, which in the scientific literature, according to [4], is called Strait of Baltiysk. The Spit relief is mainly represented by the generation of uneven-aged forms of

[1] AB IO RAS – Atlantic Branch of P.P.Shirshov Institute of Oceanology of Russian Academy of Sciences, Kaliningrad, Russia
[2] Some studies call it the 'Baltiysk Strait'

wind deposition accruing from the sea [5]. The shores are mainly composed of loose sand, and on the lagoon shore there are the ancient lagoon sediment outputs.

The south-eastern Baltic region is dominated by the west quarter winds, for winds > 5 m/s: SW – 27.4%, W – 37.8%, NW – 22.6% [4].

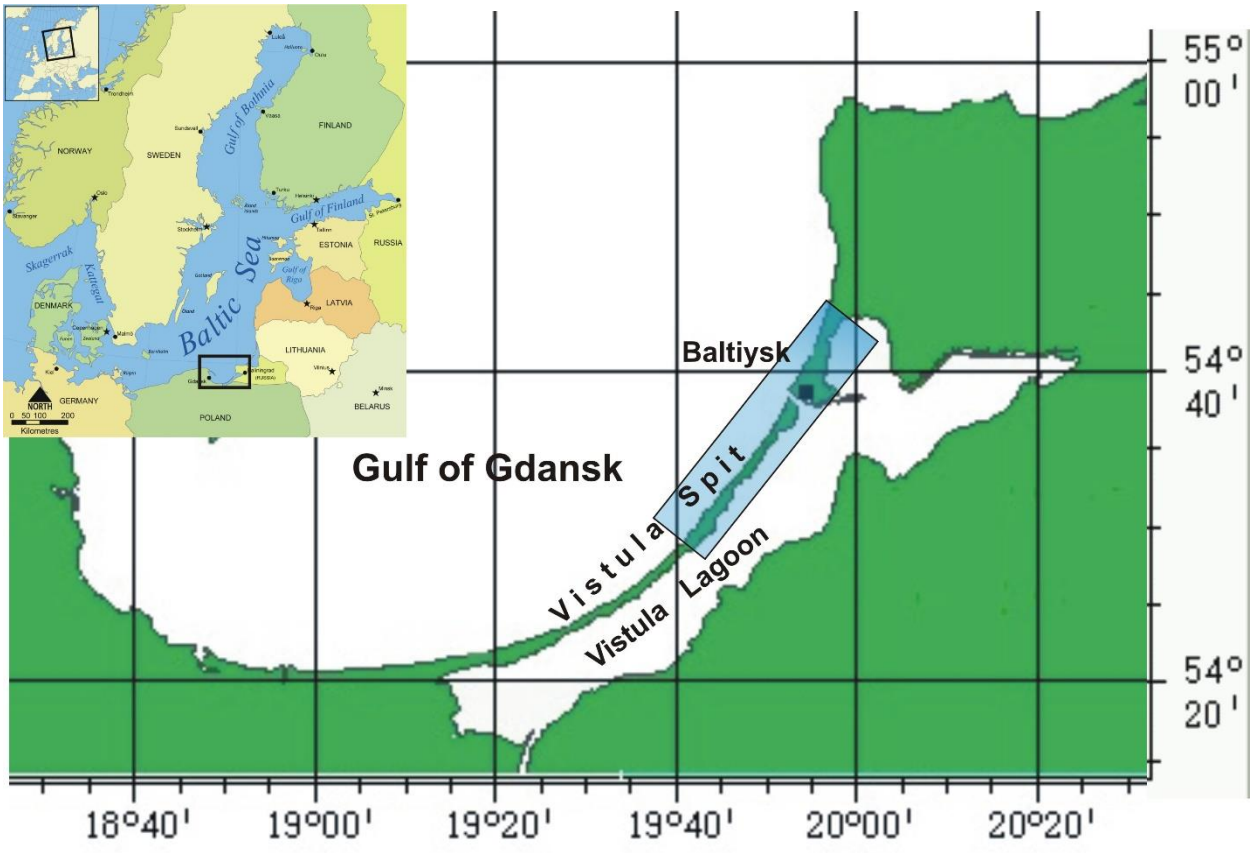

Fig. 1. The Vistula Spit (Russian part of the spit is marked by rectangular).

From 1945 until the end of the 1990s of the last century the Spit shores were unavailable for research. Prior to coastal monitoring conducted by the AB IO RAS, in a similar way to findings for the Curonian Spit, it was believed that the shore of the Vistula Spit was eroded.

The intensified coastal development, active man-induced intervention [6, 7], storm activity strengthening [8], raising the level of the Baltic Sea in the south-eastern Baltic region [9, 10, 11] and an uncontrolled increase in the anthropogenic load [12] created the need to evaluate the current state of the Vistula Spit shores, the direction and intensity of the coastal processes.

The paper summarises the data for a 13-year period (2002-2015) of instrumental observations in comparison with the results of the first 5 years of that period. The data on the dynamics of the lagoon shore of the spit are presented for the first time.

II. MATERIALS AND METHODS

The Russian part of the Vistula Spit shores was studied in the course of monitoring by AB IO RAS in the form of annual surveys by using geodetic profiling, lithological surveys, photographic and visual descriptions of the coast morphology features [13, 14].

Starting from 2002, monitoring has been conducted at 26 profiles (transects) on the sea shore (16 of them at the 5-km consistently erodible section south of the Strait of Baltiysk) and 14 on the lagoon coast on the coastal parts not covered by rooted vegetation (Fig. 1).

During trigonometric levelling along the profile perpendicular to the shore line the following features of the vertical profile were recorded: the edge of the main foredune, its foot; the top or edge of the attached or embryonic foredune; the upper limit of the eolian rig (eolian cushions), the lower limit of eolian rig (terminology according to [15]); beach surface breaks, beach barrier, edge, submerged margin of the beach bench. Altitude profiles were built with Excel.

As an indication of either erosion or coastal accretion (Fig. 2) a change in the distance horizontally from the mark to the dune crest or the edge of the eroded bench (if the shore is retreated) or to the top or line of the slope break of the embryonic foredune (for a stable coast or an accretion coast) [13].

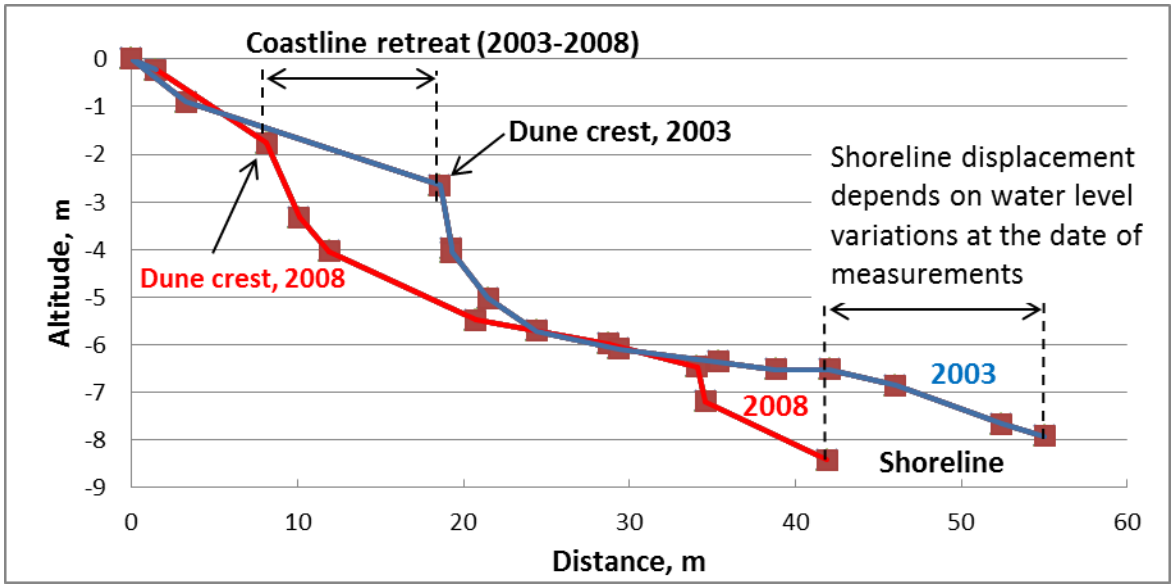

Fig. 2. Altitude profiles of 2003 and 2008 (at profile 7mv) on the eroding sea shore of the Vistula Spit. The beach retreated for 5 years at 11.2 m.

Levelling was performed with the use of high-precision surveying instruments, e.g. 3T5PK theodolite, Trimble GPS receivers (the base station L1 + 5700 mobile complex R3). In recent years, a tacheometer has been used.

Alongside with levelling on each profile to the following nose samples were collected from the sea beach, the beach average sample (starting with the shoreline and to eolian blowing) and the sample separately from the shoreline. Only the beach average sample was taken on the side of the lagoon.

In the cameral conditions, a grain size analysis of samples was carried out on the sieve analyser VP-30T by sieving through a series of sieves with a mesh of <10; 10~7; 7~5; 5~3; 3~2; 2~1; 1~0.5; 0.5~0.25; 0.25~0.1; <0.1 mm.

III. The Vistula Spit sea shore dynamics (2002-2015)

The first generalisation of observations of the morpholitodynamics of the Vistula Spit coast are presented in a number of papers [16, 17, 18, 19, 20, 21]. It has been found that the sea shore of the spit, except for the northern 5-kilometer section adjacent to the Strait, is mainly stable. In the middle of the Russian part of the spit there was a steady accumulation of sediments including the development of an embryonic foredune and extension of its edges of the beach (Fig. 3.)

An analysis of shore process observations for a 13-year period (2002-2015) has shown that a distinction can be made between three sections as far as directionality of shore processes is concerned (Fig. 3, Table 1). Section 1 (10 km, profiles 1ms-4ms) north of the Strait of Baltiysk is stable [18]. Section 2 is represented by a steadily eroded shore at 4 km south of the Strait of Baltiysk (profiles 7mv-1p,). Here, the most heavily eroded is the shore directly adjacent to the south pier, where for 13 years about 23 meters of the remaining fragments of the foredune and coastal platform (profiles 1p, 5p; retreat 2 m/year) have been washed away. On the shore section south the erosion was 10 m (profile 7mv; retreat 0.7 m/year). The maximum erosion per year (10 m) was recorded at the profile 7mv in 2005 after a strong winter storm. In recent years, the erosion has weakened in that area (Table 1).

Section 3 (profiles 1mv-6amv, 21 km) stretches southwest from section 2 to the Polish border and is characterised by alternating eroded, stable and accretion segments (Fig. 3, Table 1). For 13 years the maximum erosion value was recorded in the southern area (profile 1mv) near the Polish-Russian border, and it was 10 m (retreat - 0.8 m/year). Four more erosion segments were identified (profiles 3mv, 4mv, 5mv, 6amv), where the foredune retreated respectively at 7.7 m, 4 m, 3.6 m, 3.7 m (-0.8, -0.6, -0.3, -0.7 m/year). At the same time, especially in the middle part of the third section (profiles 2mv, 4amv, 5amv, 6mv), the accumulation processes were dominating. For example, on the profile 6mv the series of embryonic dunes advanced 15 meters towards the sea. The annual average values of the positive coastal dynamics were +0.08; +0.6; +2.0; +1.2 m/year respectively.

For 13 years of monitoring, a change in evolution of coastal processes at the southern end of the 3rd section of the spit was identified (Fig. 3). At the previously stable segment (profiles 1mv, 3mv, 4mv, 6amv) in recent years, stable erosion has been recorded since 2011. For example, in an extreme storm in 2011-2012 at Rp.1mv 4.5 of the foredune was washed, Rp.3mv – 1.0 м, Rp.6amv – 3.1 m. in the same storm near the southern breakwater, the erosion was maximal for the entire coast: Rp.1p – 6.7 м, Rp.7mv – 6.2 м [22]. At Section 2 a significant weakening of the abrasion rate can be seen for the whole period in comparison with the first 5 years (Table 1).

IV. The Vistula Spit lagoon shore dynamics (2002-2015)

The tortuous indentation of the spit from the bay is created by a number of alternating ridges and lagoon areas. The eroding land, slopes of the ancient dunes and coastal terraces, which make up about 50% of the length of the coastline, are interspersed with some sections of a stable shore confined to aquatic vegetation thickets [23. As few as two months ago, the shore is protected by ice from the wave effects. The rise and fall of the water level in the lagoon is developed with winds

from the south to the north-eastern areas, for winds > 5 m/s: S – 16.2%, SE – 5.5%, E – 5.6%, NE – 2.7% [4].

An analysis of monitoring data showed that the erosion value changes significantly from year to year and has been from 2.7 to 17 m for 13 years (Fig. 3). In most of the profiles the erosion value was 7-9 m. The erosion values vary considerably even for profiles that are close enough, the minimum erosion of 2.7 m was recorded at the 32v profile, and the maximum erosion at the 30v profile. The erosion values vary considerably and within individual local areas 32v-31v (by 4 times) and 30m-27v (nearly by 2 two time).

For most of the lagoon shores the erosion was more intense in 2002-2007 than in the following years, especially in the southern sector. For example, at 32v-31v site the average rates of retreat at the profiles in 2002-2007 (5 years) and 2002-2015 (13 years) were 0.4 and 0.2 m/year and 1.52 and 0.9 m/year respectively. The opposite situation was recorded only in the areas characterised by the profiles 21v, 28v (Table 1).

In terms of the annual average velocities, the rate of erosion of the lagoon shore of the Vistula Spit averages 0.4-0.8 m/year varying in the range of 0.2-1.4 m/year (Table 1). The erosion of the lagoon shore is of the selective nature, in different years, different parts of the shore are eroded with varying intensity (Fig. 4). It is not possible to use the data to register any patterns in the rates of erosion of the lagoon shore in terms of either time, or space.

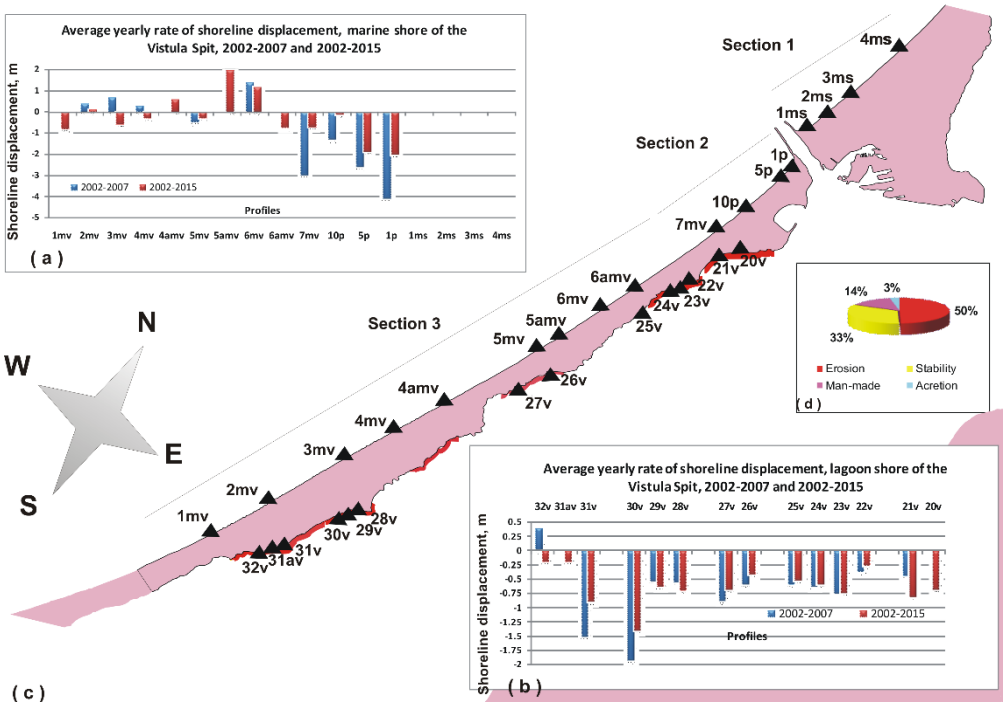

Fig. 3. The dynamics of the sea shore (a) and lagoon shore (b) of the Vistula Spit according to the data of annual monitoring surveys at fixed profiles (c) in 2002 – 2015, and types of shores on the lagoon side of the Vistula Spit (d).

Table 1. The average value (m/year) of the Vistula Spit shore displacement (2002-2015). "-" means coastal retreat

Displacement of the Baltic Sea shore, m						Displacement of the Vistula Lagoon shore, m					
No of profile	2002-2015	2002-2007	No profile	2002-2015	2002-2007	No of profile	2002-2015	2002-2007	No profile	2002-2015	2002-2007
1p	-2.0	-4.1	5mv	-0.3	-0.5	20v	-0.69	-	27v	-0.69	-0.89
5p	-1.9	-2.6	4amv	+0.6	lost	21v	-0.81	-0.44	28v	-0.7	-0.55
10p	-0.14	-1.3	4mv	-0.3	+0.3	22v	-0.26	-0.37	29v	-0.64	-0.54
7mv	-0.7	-3.0	3mv	-0.6	+0.7	23v	-0.75	-0.76	30v	-1.4	-1.93
6amv	-0.74	lost	2mv	+0.1	+0.4	24v	-0.6	-0.64	31v	-0.9	-1.52
6mv	+1.16	+1.4	1mv	-0.8	0	25v	-0.53	-0.6	31av	-0.2	lost
5amv	+2.0	lost				26v	-0.42	-0.6	32v	-0.2	-0.4

V. FRACTIONAL COMPOSITION OF BEACH SEDIMENTS OF THE SEA SHORE OF THE VISTULA SPIT

In 2015, in general, the composition of beach sediments repeated the previously obtained results [20, 21, 24]. In the seashore average beach samples taken in 2015, the fraction over 2 mm could be found only in samples at the 1st section while the 2nd and 3rd sections were dominated by the medium-grained sand (0.25-0.5 mm) accounting for 28 to 70 %, mainly 50-60 % (Fig. 5). At the shoreline the proportion of coarse sand (1-0.5 mm) was a bit bigger (Fig. 6), for example, at the profiles 4amv, 5mv, 6amv, 7mv, 5p, 1p it was more than 50% (52 to 80%). At the profiles at 4 km eroding section the gravel and pebbles, which formed separate clusters in the form of strips in the near-shore swash zone, were found in the sediments.

With the exception of the northern eroded 4-km coastal area, no direct correspondence between the composition of sediment on the beach and shoreline and the coastal dynamics could be determined. Thus, the average beach samples in eroding areas (3mv, 4mv, 5mv) contain a larger proportion of the fine-grained sand than the sediments at the profiles 5amv and 6mv, where there is accumulation. The profiles 1mv and 7mv can be characterised by the same rate of erosion but the coarse sand content varies by 2 times (it is more at 7mv).

At the shoreline, as a part of the samples on profiles 1mv, 3mv, 4amv and 5mv, the proportion of the coarse fraction is consistently increasing, while the reduction in erosion rate is observed for them, even the material accumulation at 4amv.

At section 1 on the profile just outside the northern breakwater (1ms) a significant (over 40%) content of the fine-grained sand was found (Fig. 6) at the shoreline. In the north (2ms – 4ms) impurities contained a large volume of coarse sand (34 – 42%). On the same profiles the maximum content of the coarse fraction for the whole shore (72 to 90 %) was found in the average beach sample (Fig. 5). Although this section of the coast is perfectly stable by its morphometric parameters.

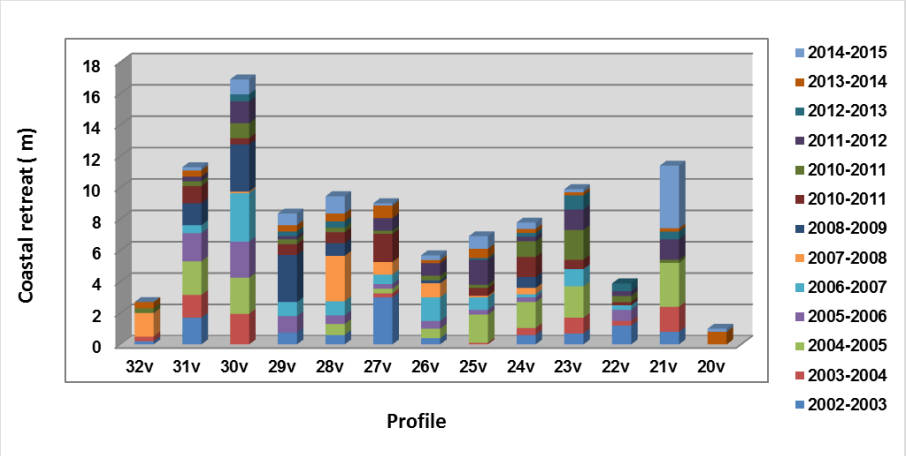

Fig. 4 . Dynamics of the lagoon shore of the Vistula Spit in 2002-2015

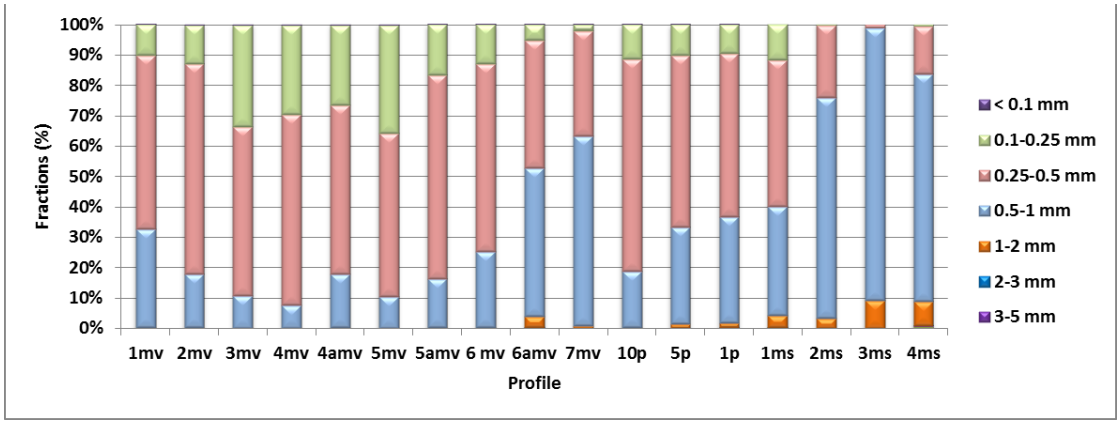

Fig. 5. Grain size distribution of sediments in the average beach samples on the sea shore of the Vistula Spit (2015)

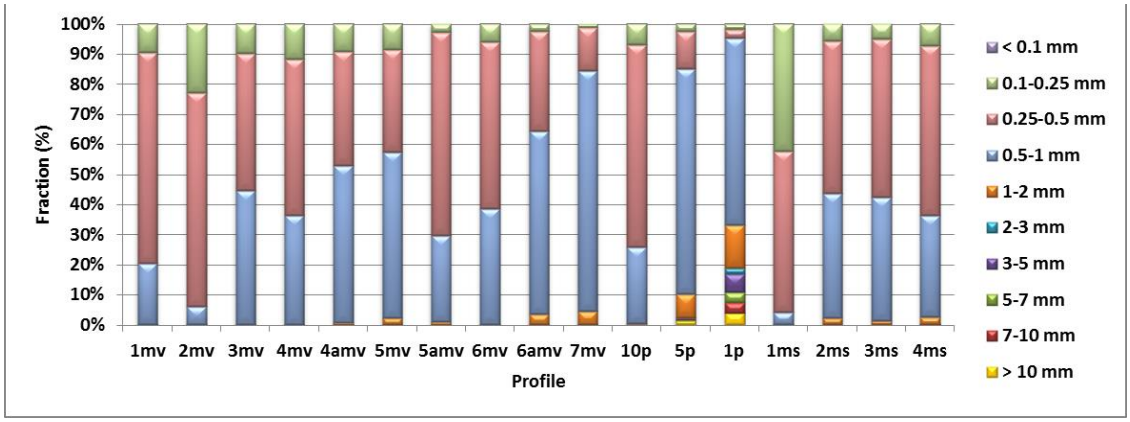

Fig. 6. Grain size distribution of sediments on the shoreline of the sea shore of the Vistula Spit (2015).

Thus, the fractional composition of sediments on the sea beach of the Vistula Spit (the beach average and on the edge) is correlated with the long-term shore dynamics only on the long eroding shore of the 4-kilometer stretch to the south of the Strait of Baltiysk.

Thus, the fractional composition of sediments of one year on the sea coast of the Vistula Spit (neither the beach average, nor on the shoreline) may not be a feature of the long-term shore dynamics. Variations in the sediment composition along the coast on the shoreline are most likely associated with the latest wave processing (or storm processing and the eolian transport in the case of the beach average sample).

VI. The Fractional Composition of Beach Sediments of the Vistula Spit Lagoon Shore

The beaches of the Vistula Spit are sandy from the lagoon side. Their width varies (up to 1-15 m) depending on the height of the standing water level in the lagoon. They are mainly created by the average-grained sand (49-82% of the sample quantity, Fig. 7) as well as on the sea shore but with a significant proportion of the fine-grained sand. Typically, there are no sediments larger than the ones.

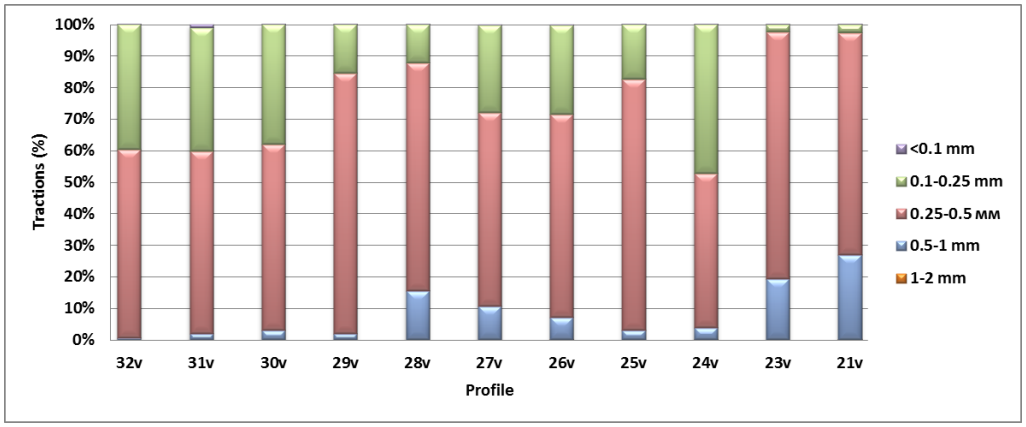

Fig. 7. Grain size composition of beach sediments of the lagoon shore of the Vistula Spit as of 03 July 2015.

On the lagoon shore there is no relation between the composition of sediment on the beach and the coastal dynamics either; e.g. at the section 32v-31v the composition of sediments is the same but the dynamics differ greatly. On the contrary, for profiles 29v, 28v, 27v, 23v, 21v the dynamics are virtually identical but the composition is significantly different.

VII. Conclusions

The developed comprehensive method of land-based shore monitoring made it possible to obtain objective data on the shore dynamics, the direction of the coastal processes at the shore of the Vistula Spit in 2002-2015 (compared to the five-year period 2002-2007). A significant drawback of the method is the point-based character of measurement. In the case of the presently significant spatial variability of morphodynamics the measurements at the profiles represent formally regular sampling but the random ones to represent the processes variability. However, the existing network is quite optimal to determine the evolution of coastal processes.

According to the dynamical conditions, the Vistula Spit seashore can be divided into three parts. Section 1 to the north of the Strait of Baltiysk (10 km) is stable. Section 2 (4 km south of the

Strait of Baltiysk) is steadily eroded, the rates of erosion are maximal and reached 23 meters for 13 years (almost 2 m/year), and for the first 5 years of monitoring 2.5-4 m/year, in other words, the erosion rate slightly weakened. At Section 3 (21 km) there is an alternation of the stable and eroded areas. Since 2011 there has been a drastic change in the coastal processes in the southern part of the Section 3, the annual erosion has started. At the same time, in the middle part of Section 3, the accumulation is stable and has even intensified. Perhaps, the unloading of longshore sediment migration took place here for the indicated period.

On the lagoon side about 50% of the length of the coastline of the Vistula Spit accounts for the eroded coast. Retreat of the lagoon shore of the Spit could be seen annually in 2002-2015. In some years, the edges of the ancient dunes or terraces retreated at 4 m. Moreover, based on the projected future rise in level due to global warming, we should expect further strengthening of the lagoon shore erosion.

In general, the 2015 survey results found no direct correlation between the sediment composition on the beach and shoreline and the long-term coastal dynamics from the sea and lagoon sides of the spit. Variations in the composition of sediment along the coast on the shoreline are most likely associated with the results of the latest wave processing (or storm processing and eolian transport in the case of the beach). The exception is the 4-kilometer consistently eroded section of the sea shore to the south of the Strait of Baltiysk.

The composition of the sediment from the sea and beach sides of the Spit is very similar, it is dominated by medium-grained sands. On the lagoon shore there are no beach sediments larger than the sandy ones.

VIII. Acknowledgement

The monitoring results reported in the paper were summarised in the framework of the Russian Science Foundation Project No 14-17-00547 “A forecast development for evolution of accumulative Russian coasts of tideless seas”.

Full-scale coastal monitoring was conducted by V.P. Bobykina (overall management, sampling, fotomonitoring, description), K.V. Karmanov and V.A. Pilipchuk (levelling). The levelling profile treatment involved V.P. Bobykina, K.V. Karmanov, the particle size analysis was performed by V.P. Bobykina and L. Pankratova. The results analysis was performed by V.P. Bobykina and B.V. Chubarenko. All the monitoring activities were funded by grants, the head of which was B.V. Chubarenko, and conducted during the execution of topic No 0149-2014-0017 of the state assignment of the Institute of Oceanology of the Russian Academy of Sciences.

IX. References

[1] V.P. Zenkovich, *Fundamentals of Seashore Development*, Moscow: Publishing House of the Academy of Sciences of the USSR, 1962, 710 p. In Russian.

[2] V.K. Gudelis, “The Baltic Sea Development History” in *Geology of the Baltic Sea*. Vilnius:, 1975, p.p. 95-116. In Russian.

[3] E.N. Badyukova, A.N. Varuschenko, G.D. Solovieva, “The History of the Vistula Spit in the Holocene”, *Oceanology*, vol. 36, No 5, 1996, p.p. 769-773. In Russian.

[4] Hydrometeorological Conditions of the Vistula Lagoon, N.N. Lazarenko and A. Maevsky, Eds. Leningrad: Hydrometizdat, 1971, 330 p. In Russian.

[5] E.N. Badyukova, L.A. Zhindarev, S.A. Lukyanova, G.D Solovieva, "The Geological-Geomorphological Structure of the Baltic (Vistula) Spit", *Oceanology*, vol. 51, No 4, 2011, pp. 675-682.

[6] V. L. Boldyrev, O.I. Ryabkova, "The Dynamics of Coastal Processes on the Kaliningrad Coast of the Baltic Sea", *Newsletter of the Russian Geographical Society*, vol. 133, Issue 5. SPB: 2001, pp. 41-49. In Russian.

[7] O.V. Bass, L.A. Zhindarev, "Technogenesis in the Coastal Zone of the Sandy Shores of Inland Seas (Art. 1. The Impact of Mining Activities on the Technical Morpholitodynamics of the Coastal Area of the South-Eastern Baltic Region)", *Geomorphology*, No 3, 2007, pp. 17-24. In Russian.

[8] Zh.I. Sont, *Modern Trends in Variability of Hydrometeorological Parameters in the South-Eastern Part of the Baltic Sea and their Effects on Coastal Processes*, synopsis of thesis... PhD in Geography, Kaliningrad, 2014, 22 p. In Russian.

[9] L.A. Zhindarev, V.I. Kulakov, "The Level Mode of the Baltic Sea in the Holocene", *Proceedings of the Russian Academy of Sciences, geography*, No 5, 1996, pp. 55-66. In Russian.

[10] K. Tobolski, "Sous Baltic water level and coastline changes reflected in mires and fossil soils. Case study of the Gardno Leba Plain" in *Relative sea level changes – from subsiding to uplifting coasts.* Abstracts. Gdansk: Polish Geological Institute, 2005. pp. 75-77.

[11] S.E. Navrotskaya, B.V. Chubarenko, "Trends in the Variation of the Sea Level in the Lagoons of the Southeastern Baltic" *Oceanology*, v. 53, No 1, 2013, pp. 13-23.

[12] V.P. Bobykina, K.V. Karmanov, "To Geoecology of the Kaliningrad Region's Coast (according to the monitoring results)", *Transactions of the Kaliningrad State Technical University*, No 35, 2014, p.p.. 44-54. In Russian.

[13] V.P. Bobykina, V.L. Boldyrev, "Methods of Monitoring the Kaliningrad Region's Coast", *Coastal Zone Management and Sustainable Development Problems (files of the XXII International Conference), Gelendzhik, 16-20 May 2007*, p. 52, 2007. In Russian.

[14] E.M. Burnashev, V. L. Boldyrev, V.P. Bobykana, "Photo Monitoring as a Clear Indicator of the Dynamics of the Coastal Zone by the Example of the Kaliningrad Region's Coast", *Dynamics of the Tide-Free Sea Coast: Proceedings of the International Conference (Baltiysk 30 June - 05 July 2008,* Kaliningrad: Terra Baltika Publishers, 2008, pp. 39-41. In Russian.

[15] V.L. Boldyrev, "Problems of Preservation and Improvement of the Curonian Spit Shores", *Problems of Study and Protection of the Natural and Cultural Heritage of the Curonian Spit National Park,* Kaliningrad: Publisher of the I. Kant Russian State University, 2005, pp. 29-38. In Russian.

[16] V.P. Bobykina, V.L. Boldyrev, "The Kaliningrad Region's Shore Development Trend by the Five-Year Monitoring Data", *Scientific Notes of the Russian Geographical Society (Kaliningrad Branch),* V. 7, Part 1, 2008 (CD-ROM version), pp. Q1-Q3. In Russian.

[17] V.A. Chechko, B.V. Chubarenko, V.L. Boldyrev, V.P. Bobykina, V.Yu. Kurchenko, D.A. Domnin, "Dynamics of the Marine Coastal Zone of the Sea Near the Entrance Moles of the Kaliningrad Seaway Channel", *Water Resources*, vol. 35, No 6, 2008, pp. 652 – 661.

[18] V. Boldyrev, V. Bobykina, "The Coasts of the Vistula and Curonian Spits As Transboundary Territory", *Transboundary waters and basins in the South-Eastern Baltic,* B.V. Chubarenko, Ed. Kalininhgrad: Terra Baltica, 2008, pp. 226-238. In Russian.

[19] V.P. Bobykina, K.V. Karmanov, "The Shore Dynamics of the top of the Gulf of Gdansk and the Relation to the Man-Induced Impact", *Creation of Artificial Beaches, Islands and other Structures in the Coastal Zone of the Seas, Lakes and Water Reservoirs: Research of the International Conference 'Creation and Use of the Artificial Land on Shores and Water Body Areas', Novosibirsk, 20-25 July 2009,* F.Sh. Khabidov, Ed. Novosibirsk: Publisher of the Siberian Branch of the Russian Academy of Sciences, 2009, pp. 119-124. In Russian.

[20] J. Kobelyanskay, H. Piekarek-Jankowska, V.L. Boldyrev, V.P. Bobykina, P. Stepnievsk, "The morphodynamics of the Vistyla Spit seaward coast (Southern Baltic, Poland, Russia) ", *Oceanological and Hidrobiological Studies,* V.XXXVIII, 2009, pp. 1-16.

[21] J. Kobelyanskaya, V.P. Bobykina, H. Piekarek-Jankowska, "Morphological and lithodynamic conditions in the marine coastal zone of the Vistula Spit (Gulf of Gdansk, Baltic Sea)", *Oceanologia,* 53 (4), 2011, pp. 1-17.

[22] V.P. Bobykina and Zh. I. Stont, "Winter Storm Activity in 2011–2012 and Its Consequences for the Southeastern Baltic Coast ", *Water Resources, vol. 42, No. 3, 2015, pp. 371–377.*

[23] V.P. Bobykina, "Coastal Reeds of the Vistula Spit and the Lagoon Shore Geoecology", *Environmental Issues of the Kaliningrad Region and the Baltic Region*, Kaliningrad: Kaliningrad State University Publishers, 2002, pp. 151-155. In Russian.

[24] V.P. Bobykina, P.M. Zhurakhovskaya, "The Inter-Annual Variations in the Composition of Beach Sediments of the Vistula Spit", *Scientific Notes of the Russian Geographical Society (Kaliningrad Branch),* Kaliningrad:, CD-ROM version and W-presentation, v. 11, 2010, pp. 4B1-4B8. In Russian.

EVOLUTION OF COASTAL LAGOONS OF THE SAKHALIN ISLAND

Petr Brovko, Far Eastern Federal University, Russia

peter.brofuko@yandex.ru

Lagoons of Sakhalin island is the fifth part of the coast. Two lagoon types predominate in the Sakhalin Island. The first type includes large and medium lagoons located along the edge of seacoast flatlands. This is a "classical" lagoon type. The second type (estuaries) is connected with coast segments in mouths of the rivers. Their development is dominated by alluvial processes. Evolution of lagoons and estuaries the islands of Sakhalin is influenced by increase of global sea level.

Key words: Sakhalin Island, coastal lagoons, barrier-lagoon sedimentary system, marine culture, national park

THE MAIN FEATURES OF LAGOONS

Lagoons are a component of many coastline geomorphologic types: fiords, rias, corals, abrasive accumulative and accumulative flattened coasts. Most lagoons are located along low seacoasts, forming a separate lagoon type of coast [1 – 3]. Lagoon development has been addressed in detail in all major scholarly writings on seacoasts, with main emphasis placed on the formation of sand and pebble barriers separating lagoons from the sea [4-6]. The following specific trend was identified upon a review of relevant literature from the last decades of the past century. Researchers have been showing the greatest interest in relatively small water bodies. Thus, of the 97 explored lagoons, with their area varying from 1 km² to 8,000 km² (average value is 78 km²), the great majority of studies have focused on water bodies with an area of 30–40 km² [7].

The average area of 240 lagoons studied in the Far East of Russia (1–500 km²) is 31.3 km², and the best studied lagoons, Busse on Sakhalin Island and Novgorodskaya in Primorsky Krai, have an area of 43 and 30.7 km2, respectively. One possible explanation for this phenomenon is that medium-size lagoons are the most interesting for analysis of their ecosystems and commercial use. On the other hand, small water bodies do not show individual features of lagoon characteristics due to high impacts of alluvial or eolian input. As for large lagoons, the high wave impact on shores and marine facilities make them less favorable for transportation possibilities and commercial activities.

The lagoons are grouped by size into large (100–500 km²), medium (10–100 km²), small (1–10 km²) and very small (less than 1 km²) ones. The largest of the large lagoons are Baikal and Piltun. In terms of water depth, lagoons are grouped into shallow (less than 1 m deep), medium-depth (1–5 m), deep (5–20 m) and very deep (more than 20 m) ones [8].

Lagoon distribution in terms of their shape is also of interest. The shoreline contour of a water body may be linearly stretched, elongate, rounded, segmental, triangular or rectangular as a result of the evolution of coastal processes. Thus, segmental lagoons are found on the abrasive bay/coast in the northwestern part of the Okhotsk Sea (Ikit Lagoon) and rectangular ones are located

on a fiord-type coast (Severnaya Lagoon, Bering Sea). Spit-blocked estuaries are often triangular (Starka Lagoon, Sea of Japan).

According to the degree of isolation from the sea, and to what degree they are influenced by hydrodynamic conditions, and by biological, chemical and other processes taking place inside lagoons, lagoons can be grouped into open lagoons (Tyk), semi-open (Baikal), semi-closed (Nabil), and closed (Ainskaya). There is also a separate group of dismembered lagoons composing lagoon lakes (Rybachye) that have no connection with the sea.

Two lagoon types predominate in the Sakhalin Island. The first type includes large and medium lagoons located along the edge of seacoast flatlands (Pomr, Piltun, Busse, Saroma, *etc.*). This is a "classical" lagoon type. They have a contour stretched along the coast and are connected with the sea by one of two channels. The second type is associated with seacoast segments of river valleys (Bolshoye, Nabil, Niyvo, Ptichya, *etc.*). These lagoons are often stretched perpendicular or at an angle to the coastline general direction. Their development is dominated by alluvial processes. Small water bodies in straits between islands, typical of low elongate peninsulas, make up a separate lagoon type (Terpeniya).

There is complex differentiation of sediment material taking place in lagoons, governed by the direction and velocities of runoff and tidal currents. Bottom sediment is dominated by silts and fine-grain sands. Gravel, pebble material and shell fragments also occur frequently.

MORPHOLOGY AND EVOLUTION OF LAGOON

Morphology and dynamics of individual topographic forms can have common or local differences. Morphological system of the Sakhalin lagoon shore includes a number of elements, which reflect the morphology and genesis of the landscape, as well as the character of coast-forming processes. It is most obvious in the northeast of the island. They include the following: accumulative underwater coastal slope, bars and bay bars, accumulative plains of lagoon seabed, lagoon and sea terraces, lagoon straits and abrasive ridges between the lagoons.

Accumulative underwater coastal slope is a slightly wavy tilted plain with submerged coastal sand-and-gravel bars. The upper part of the slope has a series of underwater bars, influences by the joint effect of the waves, tidal and wavy alongshore currents. Recurrent surveys show that the bar tend to shift towards the shore. Narrow gravel and pebble deposits lie along the shoreline. Large and average-grain sands cover the slopes and crests of underwater bars.

Bars and bay bars separate lagoons from the Sea of Okhotsk and consist of accumulative formations of various morphological type and size. The surfaces of bars – major formations 20-30 meters long and 6-8 meters wide – have multiple generations of offshore bars cutting each other at different angles. This location of bars shows multiple transformations of the shoreline.

The Piltun Laguna is separated from the Sea of Okhotsk by a very complex bar. Its body includes the original residual hill, which used to be an island in the time of maximal development of the Holocene transgression; later it was connected to the shore by accumulative formations.

Smaller lagoons – Urkt, Ekhabi, Keutu and others are separated by bay bars with one wide bar up to 3 meters high. Lagoon muds in the horizon section also exposed on the underwater coastal slope under the poor layer of modern sand, gravel and pebble sediments, witness about the shifts of bay bars towards the shore and advancing of sea sediments onto the lagoon sediments.

Accumulative plains of the lagoon seabed consist of sub-horizontal and slightly tilted surfaces of three levels. The upper level is occupied by the tidal foreshores almost along the whole coastline. Slightly tilted accumulative plains of the middle level occupy up to 50% of the lagoon seabed area. Central parts of the lagoon seabed (lower level) are taken by the sub-horizontal accumulative plains at the depths of 2-4 meters. They consist of fine aleuritic and clayed silts.

Lagoon and sea terraces of the middle-late Holocene are widely spread on the shores and line up the internal shores of lagoons. The estuaries of major rivers – Paromai, Piltun, Evai and others have well-developed terraces with flat horizontal swampy surface and cryosolic torfhuegels. The majority of terrace coasts are subjected to coastal erosion and rarely gradually transfer into beaches or sand-muddy tide field areas.

Lagoon straits are the most dynamic forms; by the time of existence, they are divided into two types: permanent and seasonal. Permanent straits are the straits of major lagoons with bigger areas of transverse currents – Piltun, Kleye, Anuchin, and Aslanbekov. Their sizes and expected outlines allow judging about the predominant direction of sediment transport. Thus, the Strait of Aslanbekov is actively shifting towards the north; and the Strait of Piltun – to the south.

The evolution of Sakhalin lagoons is associated with the Holocene transgression, during which time they came into existence [9]. As evidenced by well studied coastal-marine depositions, large seawater bodies, separated by sand banks and morphologically close to modern lagoons, started to form at higher sea level in the sub-boreal period. During subsequent sea level fluctuations above the modern level, the inner shoreline contour of lagoons was reshaping. Some water bodies are already at the post-lagoon stage, being partly or fully filled with alluvial, marine, eolian, or biogenic depositions.

HUMAN ACTIVITY

Anthropogenic effect in the Sakhalin lagoon shore involves anthropogenic violation of the natural landscape and disruption of the natural chemical composition of river and lagoon waters, which cause negative changes in the structure of highly efficient biocenosis of closed shallow waters. This effect is mostly related to the development of sand open mines for construction purposes on the bay bars and surf zones. In recent years, over 20 authorized and unauthorized open sand mines have been operating on the Sakhalin shores; half of them on the lagoon bay bars. In some cases, insufficiency of sediments in the coastal area results in a more intensive abrasion.

Anthropogenic impact of the Tunaicha Laguna has increased dramatically over the recent decade. Forests were logged in many water-intake areas; it will undoubtedly result in the decrease of the water transparency and increase in the rate of sediment accumulation due to the increased particles content in the inflowing streams. Additionally, in the mid-1970s, a bridge was constructed across the estuarine part of the Krasnoarmeisk tribute near the settlement of Okhotskoye. Much of the tribute was filled with ground leading to dramatic shallowing of the estuarine zone and complete blockage of seawater entry into the lake. Lake water was a little desalinated. Open sand mines are developed on the bay-bar, which separates the Laguna from the sea.

Biocenosis is very diverse in the Busse Laguna. The Ahnfeltia seaweed is the most valuable; it is in a satisfactory condition. Its resources were seriously depleted in the 1920-60s. Since Ahnfeltia takes a long time to grow, reproduces only in a vegetative way and is vulnerable to

changes in the environmental conditions, an intensive and uncontrolled production of it inevitable results in a dramatic reduction of its amount. Currently, the fields of Ahnfeltia are slowly recovering.

Scientists of the Far East Federal University and Russian Geographic Society have launched a proposal to establish the Tunaichinsky National Park in the Sakhalin southeast, including Tunaicha, Busse, Izmenchivoye and other lagoons. This project could greatly benefit from Japan's experience in establishing their national parks, where beautiful coast, spa resorts and cultured pearl farms can all be found within a relatively small territory of the park [10].

Changes in the chemical composition of waters, regardless of the contamination source, lead to the irreversible structural changes in the structure of seabed biocenosis. Meanwhile, lagoons possess the highest biological productivity and are the most favorable water areas for farming in comparison with straits, open bays and gulfs.

The Sakhalin lagoons have great commercial importance in terms of marine civil and transport construction, development of mineral deposits, production of building materials, fishing and aquaculture, and recreation. Many lagoons are convenient harbors protected against storms. This makes them suitable for the organization of transport facilities and cargo reloading bases, for the construction of sheltered ports for small vessel, and for the erection of wharves and other civil structures, particularly in oil and gas production areas. Usually, these facilities are localized in specific areas and do not involve the whole lagoon; however, the environmental and geomorphological monitoring would have to be conducted in all cases.

ACKNOWLEDGMENT

We thank Dr. Yu. Mikishin, Far Eastern Geological Institute, Vladivostok and Mr. A. Malyugin, Far Eastern Federal University, Vladivostok for facilitating field work and providing strong support for the Sakhalin Lagoons Project.

REFERENCES

1. E. C. F. Bird, *Encyclopedia of the World's Coastal Landforms*, Vol.1. Dordrecht: Springer, 2010. 485 pp.
2. M. L. Schwartz, *Encyclopedia of coastal science*. Springer, 2005. 263 pp.
3. V.P. Zenkovich, *Principles of the Science of the Sea-shore Development*. Moscow: Publishing House of the USSR Academy of Sciences, 1962. 710 pp. (in Russian).
4. S.P. Leatherman, "Barrier beach development. A perspective of the problem", *Shore & Beach* , 1981, No. 49, pp. 3–9.
5. Li Congxian, Chen Gang. "Postglacial transgression and regression and barrier-lagoon sedimentary system", *Acta oceanol. Sin*. 1986, Vol.5. 1, pp. 82-89.
6. G.F. Oertel, "The barrier island system", *J. Marine Geology*. V. 63, 1985, pp. 1-18.
7. S.W. Nixon, Nutrient dynamics, primary production and fisheries fields of lagoons. *Oceanol. Acta*, 1982, No. 4, pp. 357–371.
8. P.F. Brovko, *Coastal lagoons development*, Vladivostok: Far East National University, 1990. 148 pp. (in Russian).

9. P.F. Brovko “The Okhotsk Sea coastal lagoons: Types, evolution and use of resources”, *PICES Scientific Report,* 2008, No. 36 pp. 191-193
10. M. Sutherland, and D. Britton, *National Parks* of *Japan*. Tokyo: Kodanka International Ltd., 1980, 148 pp.

SUSPENDED MATTER CONCENTRATION ALONGSIDE THE NORTHERN COASTLINE OF KALININGRAD REGION (SOUTH-EASTERN PART OF THE BALTIC SEA)

Ekaterina Bubnova, Immanuel Kant Baltic Federal University, Kaliningrad, Russia
Victor Krechik, Immanuel Kant Baltic Federal University, Kaliningrad, Russia
Vadim Sivkov, Immanuel Kant Baltic Federal University, Kaliningrad, Russia

bubnova.kat@gmail.com

South-Eastern part of the Baltic Sea undergoes strong man-caused impact due to high level of shore usage. Suspended matter is an important carrying agent for pollutants. The Kaliningrad region has both the abrasion shore (Sambian peninsula) and the massive accumulative body (Curonian Spit), which is World Heritage site. The interannual and seasonal distribution of suspended matter concentration along the northern shore of Kaliningrad region against the hydrological conditions were studied. The research was made on five-year (2011-2015) monthly (April - October) data-array, consisting of surface and bottom water samplings. Two types of interannual and seasonal distribution of suspended matter concentration (SMC) revealed: Sambian type is defined by vertical gradient of SMC with descending of concentration from surface to bottom, while Curonian type – by horizontal gradient of latter.

Key words: suspended matter, coastal zone, the Baltic Sea

A. INTRODUCTION

In recent times, the coastal zone of the Baltic Sea to the north of the Kaliningrad region of the Russian Federation (fig. 1) experienced increase in usage for commercial purposes (e.g. waterworks building, recreation, fishery, oil exploration, etc.). At the same time, it is directly adjacent to the Curonian Spit which is the object of UNESCO natural and cultural heritage. Thus, there are increasing risks of negative impacts of marine natural management on the environment and growing urgency of research in this sea area.

Suspended in seawater mineral and organic particles (suspended matter) significantly affect the intensity of chemical elements migration, especially in the "coastal barrier zone" [1] where suspended matter concentration (SMC) is significantly higher than in the open sea. Therefore, suspended matter is one of the essential parameters of the marine environmental quality.

Suspended matter in the open part of the Baltic Sea is in a focus of research from 1960s [2], [3], [4]. However, the coastal zone, being so important for humanity, still remains insufficiently explored. Suspended matter data in the Gdansk Basin of the Baltic Sea was obtained during the 5-year period of research characterizes mainly open sea. Coastal erosion by wave action – is the main source of suspended matter in the studied area [5]. The vast majority of river discharge settles in

Curonian and Vistula lagoons; atmosphere aerosols can be neglected. Studies on suspended matter in the coastal zone of the Kaliningrad Region are rare and fragmentary [5], [6], [7].

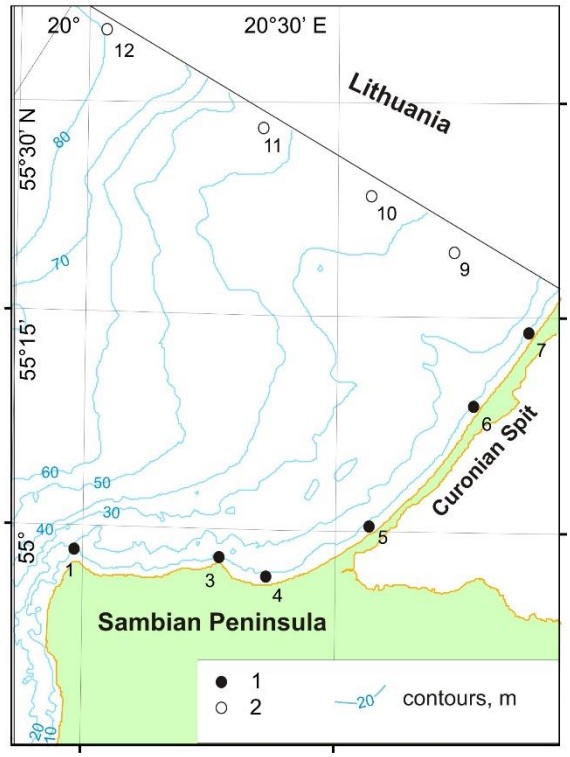

Fig. 1. Study area and location of stationary survey points of LUKOIL-KMN, Ltd. environmental monitoring: 1 – studied alongshore points; 2 – lateral profile points.

The aim of the present work is to summarize data on SMC collected over the last years along the northern coast of the Kaliningrad region as part of operational environmental monitoring of the marine oil production carried out by LUKOIL-KMN, Ltd.

B. MATHERIAL AND METHODS

The research was carried out on 5-year (2011-2015) monthly data-array, collected within spring-summer season (April to October) (fig. 1). The whole route length was about 70 km – from cape Taran to Lithuanian border. The sampling was made coastwise to the north from the Kaliningrad Peninsula and the Curonian Spit. As a result, 6 points (stations) with 2-horizonts (surface and sub-bottom) were made. Suspended matter was then separated from water samples by the mean of pressurized ultrafiltration with a use of previously weighted nuclear filters (0.45 μm membrane diameter) to determine concentration. Interannual and seasonal averaged SMC data were calculated. The simultaneous vertical CTD-profiling (Idronaut 316 probe) was made at all 6 route points, so water temperature and salinity averaged sections can be plotted.

The transition from individual profiling series to the averaged seasonal profiles was performed with the method of layer-by-layer median filtering [9]. The key point of the approach is to calculate the median value for a layer with arbitrary thickness (in this study this parameter was taken as 1m).

C. RESULTS AND DISCUSSION

In general, alongshore distributions of both annual averaged surface and near-bottom SMC demonstrate similarity (fig. 2). However, surface SMC is higher than near-bottom, and annual variations are more contrast. During entire period, increased SMC values with maximum in st. 4 were recorded at the Sambian Peninsula, while decreased values with minimum in st. 7 (close to Lithuanian border) were found at the middle of the Curonian Spit. Anyway, annual variability of SMC is quite high. Highest annual averaged SMC along almost whole investigated coastal zone were recorded in the 2015.

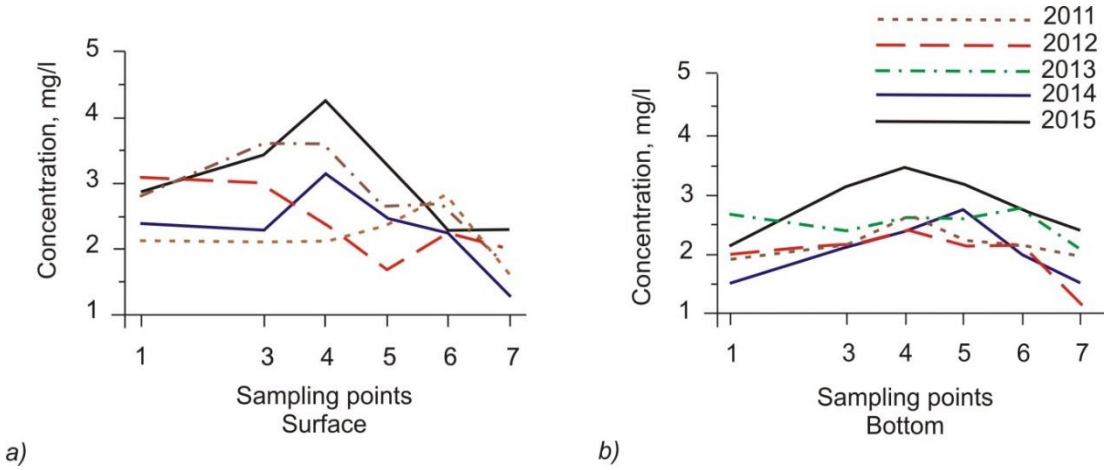

Fig. 2. Annual averaged suspended matter concentration at fixed survey points of monitoring along northern coast of Kaliningrad Region: a) surface layer, b) near-bottom layer.

Data discussed here corresponds with previously obtained results [8]. Maximum values within both near-bottom and surface layers were observed near eastern part of the northern coast of the Sambian Peninsula (fig. 3). However, our data demonstrates that SMC maximum moves to the east – from st. 3 (cape Gvardeysky) to st. 4. Anyway, this evidence do not contradict with an opinion that adjacent coastal area and underwater coastal slope are the main sources of suspended matter for the entire considered coastal area.

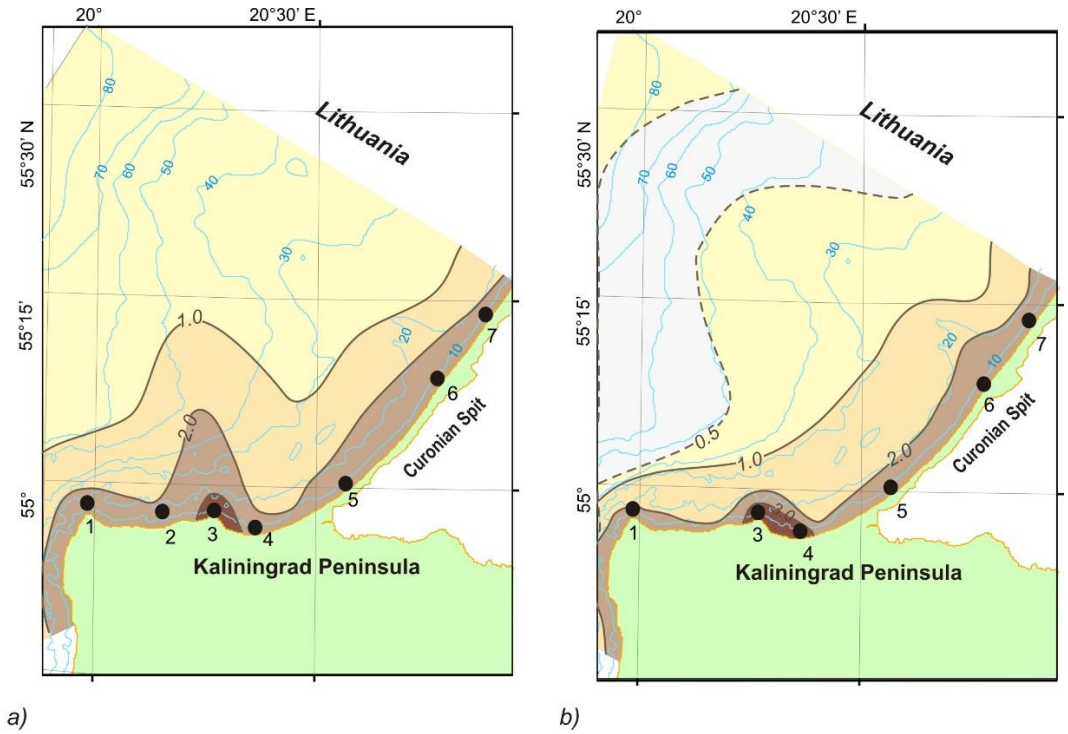

Fig. 3. Interannual averaged (2003-2008) surface suspended matter concentration (mg/l): a) surface layer (0-1 m); b) near-bottom layer (1-2 m from the bottom); black dots – studied alongshore points

The main features of the spatial distribution of suspended matter in the interannual time scale are clearly visible on the lateral profile along the Lithuanian border (fig. 4, after [8]). Seaward, coastal concentration maximum of the suspended matter transforms into subsurface "tongue" with the thickness 10-15 m which is visible at a distance of 50 km from the coastal zone. Near-bottom maximum is located close to center of the Gdansk Basin beginning from a depth 50-60 m.

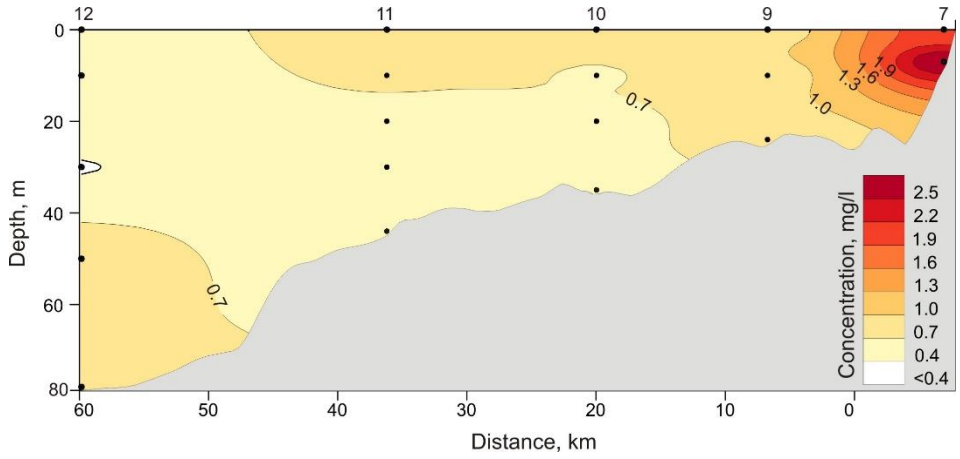

Fig. 4. Distribution of the interannual averaged suspended matter concentrations on the lateral profile from middle part of the Curonian Spit along the Russian-Lithuanian border (see fig. 1, after [8])

Our finding completes previous beliefs about suspended matter distribution in the studied area on the alongshore profiles. Interannual averaged and seasonal SMC data are shown on the hydrological section (fig. 5). For regional hydrological conditions the period from January to March is meant winter, April-June – the spring, July to September – the summer, October-December – autumn [10]. Therefore, there are two full seasons (spring and summer) and October during the time of observation.

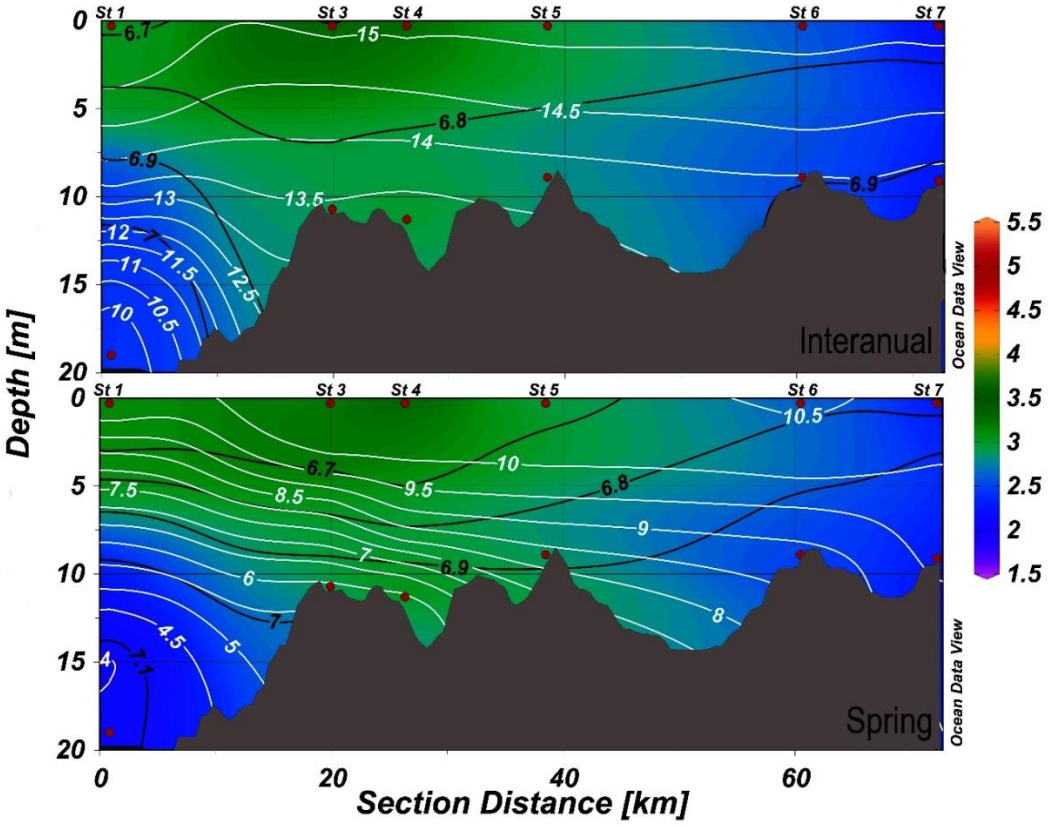

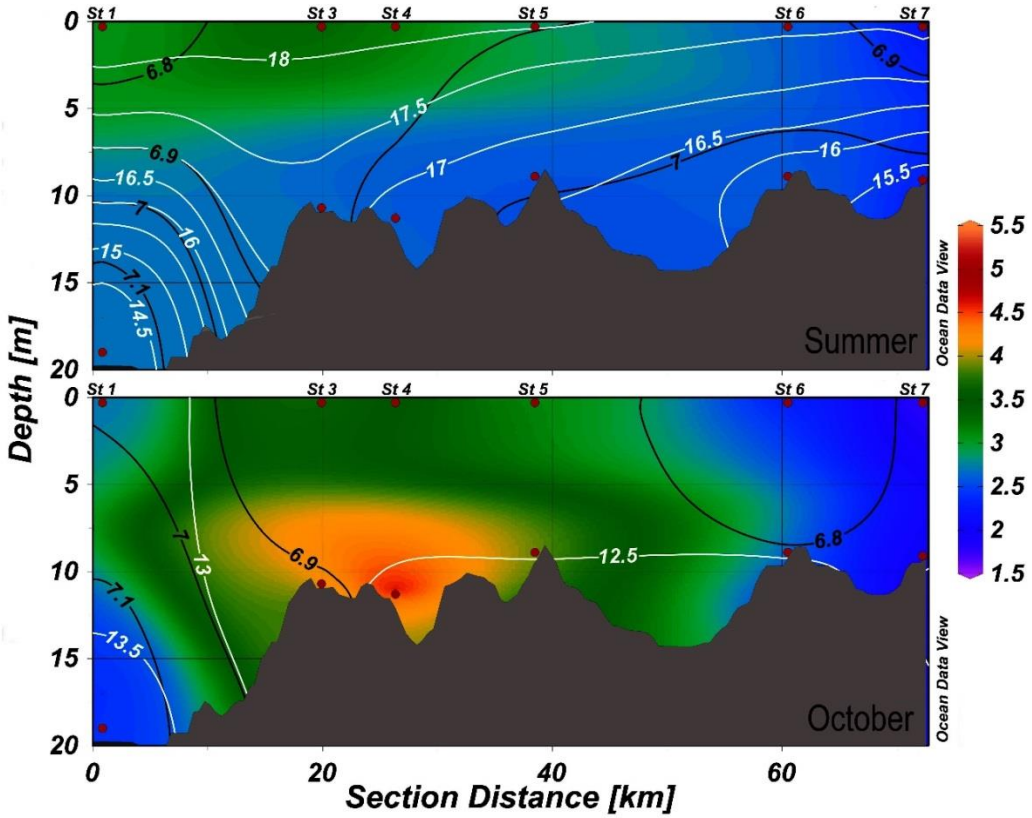

Fig. 5. Averaged SMC (color gradations) and hydrological conditions (white isolines – salinity (psu); black – temperature (°C); red dots – sample points of SMC.

The peak of suspended matter concentration appeared to be located at station 3 and 4, which are nearby the Kaliningrad peninsula. Both the interannual and seasonal pictures show this maximum, besides the highest concentrations occur in October. SMC tend to decrease significantly towards to the Curonian spit, which provides us to the following observation.

Two types of SMC vertical distribution is revealed on interannual section:

Sambian Peninsula coastal zone (stations 1, 3, 4) is characterized by vertical stratification of SMC, while Curonian Spit coastal zone (stations 5-7) – by homogenous distribution of latter. Transition from one stratification type to another takes place near eastern part of Sambian Peninsula (between st. 4 and 5).

Vertical stratification (first type) may maintain when vertical suspended matter movements prevailed, while homogenous distribution (second type) indicate prevailing of the horizontal transport of SMC.

Interannual hydrological structure appears to be less vertically stratified over the entire section; there are no strong gradient zones which can prevent suspended matter transport.

Spring distribution of SMC follows the same pattern as interannual one, along with hydrological structure. Total summer SMC are slightly lower, than in spring. Two types of vertical suspended matter distribution are not clearly visible during summer. In autumn (October) highest SMC values are recorded (influence of beginning of the storm season). Two types of SMC distribution are clearly visible.

It appeared, that summer data shows specific feature – signs of cellular circulation with border at station 3 (cape Gvardeysky). According to [5], circulating cells form inside bays during weak wind conditions. There are strong and storm winds, which destroy those cells and carry sediments towards an open sea. The main run-off of bed load takes place along skirts of bays, infront of capes. During west winds influence, compensating water and sediment outflow focus on eastern bay shores.

According to our data, we can assume that this process is vivid nearby the Gvardeysky cape (st. 3), where the concentration maximum is. The same maximum was observed in [10].

D. CONCLUSIONS

The maximum of SMC is situated alongside the Kaliningrad peninsula, the decrease in concentration takes place towards to the Cronian Spit. Consequently, two types of SMC vertical distribution is recorded on interannual and seasonal alongshore sections: Sambian Peninsula coastal zone is characterized by vertical stratification of SMC, while Curonian Spit coastal zone – by homogenous distribution of latter.

Our findings confirm that the main source of suspended matter for the northern coast area of the Kaliningrad region is located near the middle and eastern part of the northern coast of Sambian Peninsula (cape Gvardeysky).

ACKNOWLEDGEMENTS

The work was financed by the RSF grant 14-37-00047. Authors are grateful to L.D. Bashirova for language editing and help with artwork.

REFERENCES

[1] E.M. Emelyanov. “Sedimentogenesis in basin of the Atlantic Ocean”, Moscow: Nauka, 1982, pp.190 (in Russian).

[2] E.M. Emelyanov. “Geochemistry of suspended matter and bottom sediments of the Gdansk Basin and processes of sedimentation” in *Geology of the Gdansk Basin. Baltic Sea,* Kaliningrad: Yantarny skaz, 2002, pp. 220–302.

[3] E.M. Emelyanov. “Quantitative distribution of suspended matter along Kaliningrad Peninsula and Curonian Spit (Baltic sea)”, *Oceanological research*, no 18, 1968, pp. 203–213.

[4] V.V. Sivkov. “Suspended matter in the water”, in *Neft' i okruzhayushchaya sreda Kaliningradskoj oblasti. Tom II: More (Oil and the Environment of the Kaliningrad Region. Volume II: Sea)*, Kaliningrad: Terra Baltica, 2012, pp. 120-128.

[5] A. N. Babakov. “Dynamics of Sedimentary Substances in the Coastal Zone of the Sea”, in *Oil and the Environment of the Kaliningrad Region. Volume II: Sea,* Kaliningrad: Terra Baltica, 2012, pp. 37-59.

[6] A.B. Kozhakhmetov, V. M. Latschenkov. “Preliminary results of determining of background turbidity on the aggradation area of free sandy beach loads at northern coast of Sambian Peninsula”, in *Problems of geomorphology and Quaternary geology of the shelf seas,* Kaliningrad: 1989, pp. 96-99.

[7] A.I. Blazhchishin, A.N. Babakov, V.A. Tschechko. “Concentration and contamination of suspended loads of the Kaliningrad near-shore zone”, in *Problems of studying and protection of the Curonian Spit*, Kaliningrad: AB IO RAS, 1998, pp. 31-58.

[8] V. Ph. Dubravin, E.V. Dorokhova, V.V. Sivkov, V.A. Smyslov, “Hydrochemical figures and suspended matter”, in *Oil and the Environment of the Kaliningrad Region. Volume II: Sea*, Kaliningrad: Terra Baltica, 2012, pp 276-291.

[9] I. M. Belkin, *Morphological and Statistical Analysis of the Ocean Stratification*, Leningrad: Gidrometeoizdat, 1991, 130 p.

[10] V. Ph. Dubravin, Zh. I. Stont, “Hydrometeorological Mode, Water Structure and Circulation,” in *Oil and the Environment of the Kaliningrad Region. Volume II: Sea*, Kaliningrad: Terra Baltica, 2012, pp. 69-105.

COMPARATIVE ANALYSIS OF THE INFLUENCE OF NATURAL AND ANTHROPOGENIC FACTORS ON THE VISTULA SPIT FOREDUNE EROSION (THE BALTIC SEA)

Burnashov Evgenii, State Organization of the Kaliningrad region "Baltberegozaschita", Russia
Karmanov Konstantin, State Organization of the Kaliningrad region "Baltberegozaschita", Atlantic Branch of P.P.Shirshov Institute of Oceanology of Russian Academy of Sciences, Russia

burnashov_neo@mail.ru

The study gives quantitative estimation of natural landforms sensitivity of accumulative type coasts exposed to human influence. Foredune is an essential element of a morphological structure of thebarrier spits located at the Baltic Sea sand coasts. The study compares contribution of the beach erosion and deflation (soil drifting) to the foredune degradation on the sea shore of the barrier spit with or without the recreational impact. The analysis is performed for three typical polygons located on the Russian part of the Vistula Spit. Chosen polygons present shore segments with various intensity of tourism: visitors from the village, unregulated camp tourism, and nearly natural conditions.

Detailed geodesic survey was carried out on these three polygons (length 515 m, 265 m, and 521 m respectively; total area – 125000 m^2) in July of 2015. It was done with single-frequency geodesic GPS Trimble 5700L1 (base station) and TrimbleR3 (rover). Two DEMs were developed using the results of laser scanning of 2007 and the survey of 2015. Volume deformation for whole polygons and its particular parts (beach and foredune ridge) was made by comparison of the DEMs.

In the case of touristic load the effect of deflation is 5-15 times higher than the marine erosion of foredune edge. If not affected by an anthropogenic factor the foredune erosion is caused mainly by the sea, and its impact is 6 times higher than that of the natural deflation.

Key words: seacoasts, foredune, erosion, deflation, the Vistula Spit, the Baltic Sea.

I. POLYGON SELECTION JUSTIFICATION

In order to determine the characteristics of the temporal dynamics for the Vistula Spit's typical landscape, three typical polygons with varying degrees of exposure to human activities were selected. At the polygons, terrain measurements of the surface part of the Vistula Spit's sea coast were made(Fig. 1) –hereinafter we will call the polygons in the order from north to south as polygons *S (settlement), T (tourist), B (background)*.

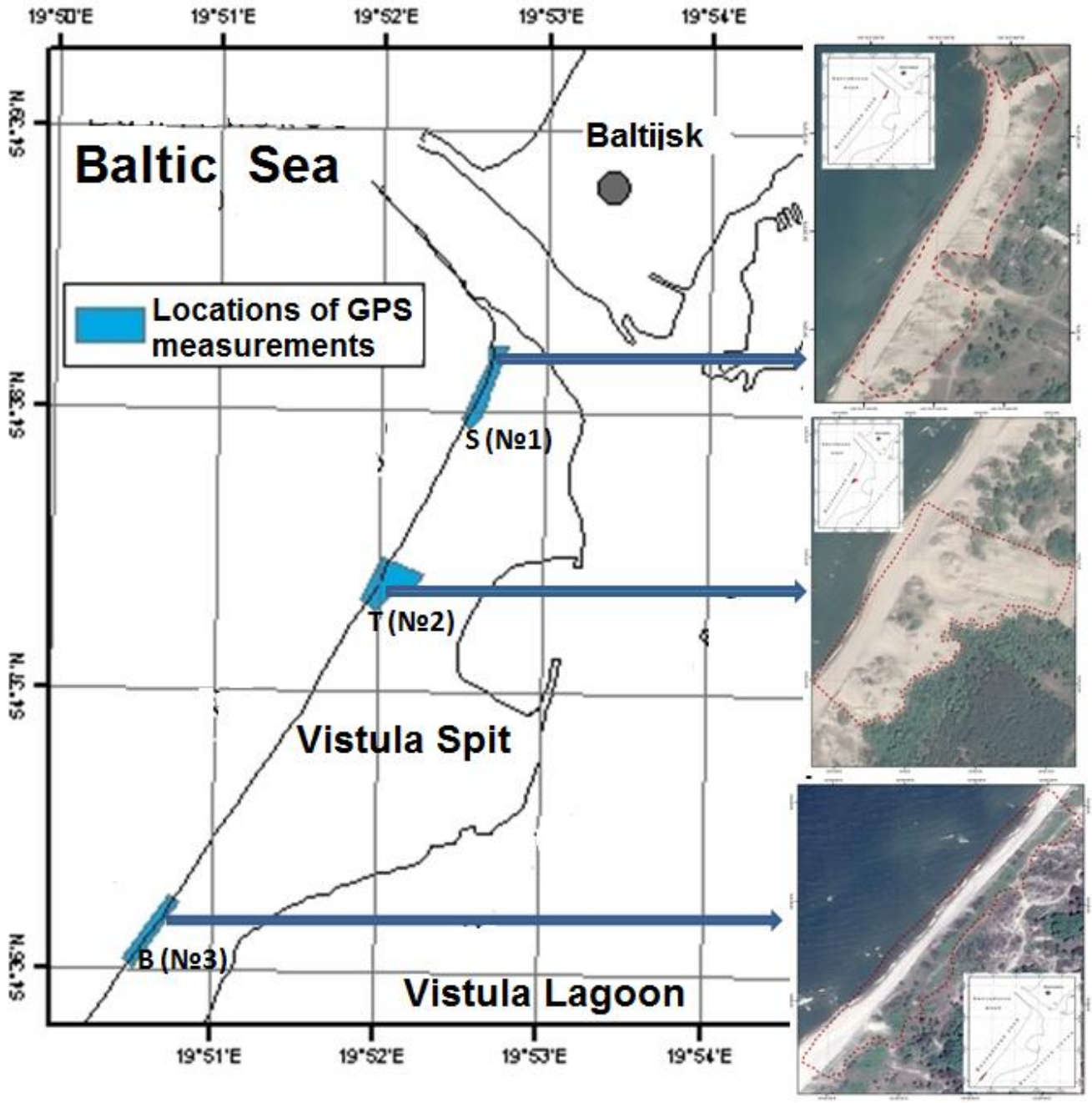

Figure 1. – Polygon location diagram in the northern part of the Vistula Spit.

Polygon (S),length of 524 linear meters,can be characterised by a lower coastal section (from 1.5 to 8 meters in height) adjacent to the residential area of the Kosa village of Baltiysk, which was located in the northernmost part of the Vistula Spit. At the specified polygon an active anthropogenic load was recorded; the load is in the use of this coastal part by the locals and seasonal vacationers for recreational purposes, unauthorised driving down by car to the beach for fishing and collecting amber in the near shore zone.

Polygon (T),length of 272 linear meters, is located at a distance of about two kilometres to the south of the Strait of Baltiysk. Polygon (T) represents a high portion (5 to 14 meters in height) of the coast with intense recreational load caused by the unorganised mass tourism. An active

anthropogenic load is expressed in the use of that part of the coast by plenty of seasonal vacationers and tourists for recreational purposes and for open air events. [1] In contrast to the first polygon, it is not possible to freely access the beach because of the rather high foredune there.

Polygon (B), length of 526 linear meters, can be characterised by the state of the natural coast in height from 8 to 12 meters, which is not subjected to intense anthropogenic pressure and is located at a distance of about five kilometres south of the Strait of Baltiysk. Due to significant remoteness from a populated centre and the lack of access roads near the coast, the said polygon is visited by few tourists mostly when the surroundings are passed by bike. The area is dominated by coastal processes caused mostly by natural processes. That is why the polygon was taken for a comparative analysis as a background.

The total area of the three studied polygons is about 113,000 m^2, where the first polygon is about 40,000 m^2, the second polygon is about 40,000 m^2 and the third polygon is 33,000 m^2respectively.

II. MEASUREMENT AND ANALYSIS TECHNIQUES

To obtain the field data on the polygon terrains on the Vistula Spit sea shore, a GPS survey of three-dimensional coordinates (latitude, longitude, altitude) of the points of the above-water part of the beach and the foredune surface with a system of the single-frequency geodetic GPS Trimble 5700L1 (base station) and TrimbleR3 (mobile receiver) was performed. The minimum mean-square error of the measurement data with the system in an ideal mode is ± 10 mm + 1 ppm in plain view and 20 mm ± 1 ppm + in elevation.

For Polygon (S) from 22,606 measured points selected were 21,059 points, the measurement errors of which lie in a pre-determined limit (<0.5 m), which represents 93.1% of all measurements at this polygon. The average density of points on the polygon was 1 point per 1.9 m^2.

At Polygon (T),in total,21,720 measurements were conducted; of which 19,663 (90.5%) are within the specified measurement error (<0.5 m). The average density of points on the polygon was 1 point per 2.3 m^2.

Within the range of Polygon (B) almost all 16,106 points lie within a pre-determined measurement error (<0.5 m), and only one point was an exception. The average density of points on the polygon was 1 point per 2 m^2.

The key objective of the study was to determine the terrain deformation on the selected polygon for the period from 2007 to 2015. For comparison of the terrain of the sea coast obtained as a result of the GPS survey in 2015, and the terrain obtained by airborne laser scanning in 2007, performed was mutual binding of the data made with GIS tools.

After the planned altitude data correction, the data interpolation was performed to produce three-dimensional terrain models for 2007 and 2015. The interpolation was carried out in GIS by the Inverse Distance Weighted Interpolation method resulting in three-dimensional digital elevation models (DEM) were obtained with a resolution of 0.5 m in plan. For zero surface taken was the ellipsoidal surface used in the WGS-84 coordinate system and reduced to the Baltic height system BK77, the system of normal heights which are counted from the zero level of the Kronstadt tide gauge.

A terrain deformation (change) analysis is conducted relief by deducting from the 2015 model of DEM height values for 2007 which made it possible to identify the areas of positive and negative deformation on polygons and assess their areas and volumes. DEM have been constructed for all the polygons as well as separately for polygon parts, the beach and foredune. This approach allowed us to perform the calculation and analysis of terrain changes differentially between the beach and foredune by separating the beach as a dynamic element of the sea coast.

Two components of the foredune deformation were assessed separately: the one due to direct wave erosion and the second, due to deflation processes strengthened by recreation load (on the first two polygons). This analysis was a basis of assessment of the specific characteristics: the volume of foredune degradation due to wave erosion per one running meter of coastline; the volume of foredune degradation due to deflation (eolian-anthropogenic factor)per one running meter of coastline. These specific characteristics may be used in the future to estimate dune degradation for similar areas of the shore.

III. RESULTS

First polygon(S)

The estimated volume of material on the entire polygon, according to 2007 airborne laser scanning, amounted to 134,202 m^3; and according to the 2015 GPS survey results it is 100,600m3 which indicates a decrease in the volume of material in that section of the sea coast in 2015 compared to 2007 by 33,603 m^3 and is about 25% of the original volume (the volume in 2007). (Figure 2). On a blank part in the middle of the polygon there is a wood tree belt area which was excluded from the calculation in order to reduce the degree of measurement error.

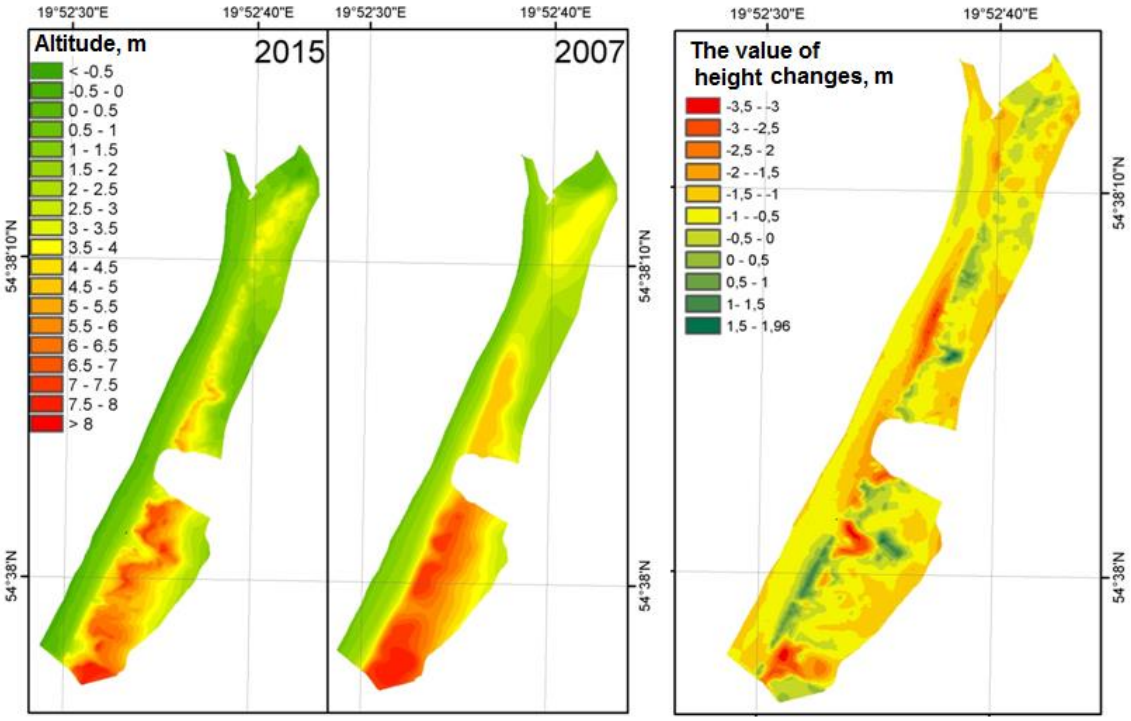

Figure 2. Digital terrain models of the polygon (S) for 2007 and 2015 and the scheme of changing terrain elevations within the polygon (S) in 2007-2015.

The foredune makes the main contribution to the material volume change of Polygon (S) as the results of calculation of the material volume change within the foredune and beach separately indicated:

- the foredune material volume for the period from 2007 to 2015 decreased by 25,126 m^3(21.3%) representing 74.8% of the total material volume changes on the polygon;

- the beach material volume calculated according to 2007 data is greater that the volume of material in 2015 by 8,477 m^3 which corresponds to 25.2% of the total volume of material changes on the polygon.

For the entire polygon, the range of the numerical values of the terrain change is from -3.49 to 1.96 m, i.e. the deformation change amplitude is 5.45 m. The positive deformations hold only 6.2% of the polygon area corresponding to 2 474 m^2, the negative deformations hold the remaining 93.8 % of the polygon equal to 7,231 m^2 .

Most likely, reduction of the foredune dimensions within Polygon (S) is due to the combined effect on the coast of the wave, eolian and anthropogenic factors. Under the influence of the sea waves reaching the foredune during storms, there is erosion of the sea foredune slope with the loss of a large number of sandy material, and as a consequence, a decrease in the size (volume) of the foredune. The eolian transfer on the seashore promotes accretion and retirement of the sand material:

1) under the influence of the wind, the accretion of the sand material at the foredune bottom and on its surface occurs, and;

2) wind redistributes the sandy material along the profile of the coast and beach within the foredune;

3) deflation processes lead to the formation of deflation hollows and the gradual destruction of the integrity of foredune body.

The main impact of the anthropogenic factor is that it aggravates and accelerates the appearance of other destructive processes. Basically, this is manifested at Polygon 1 in that as a result of the residents' and tourists' mass visiting this area in the absence of elemental traffic arrangements (equipped lanes and access roads to the beach) there is widespread trampling of vegetation and surface damage of the foredune thus increasing deflation by several times. [2]

An analysis of the changed material volume of the foredune in terms of the contribution of the above processes was also performed. The calculated difference in volumes of 2007 and 2015 was divided by the part resulting from the action of the sea (retreat of the sea slope of the foredune) and the part resulting from the eolian-human activities. The negative values of changes in the terrain in the rear of the foredune and within deflation hollows on the sea slope and the foredune top were taken as the amount lost due to the eolian-human activities; the rest of the lost material volume was taken as the volume of material lost when exposed to the wave factor. Thus, under the impact of the eolian-anthropogenic factor the foredune lost 21,481 m^3 of material, which is 85.5% of the total volume of the lost material. The lost material volume lost as a result of sea activities account for the remaining 14.5%.

From the above it can be concluded that concerning Polygon (S),the human impact on the foredune leads to the activation of destructive eolian processes, the impact of which is five times greater than the erosion of the sea slope of the foredune ridge caused by the sea.

Second polygon (T)

The estimated volume of material on the entire polygon was 261,748 m^3 in 2007, and in 2015 the material volume of is reduced by 39,457m^3 amounting to 222,291 m^3. As a result, the total amount of the polygon material decreased by 15.1% in 2015 compared to 2007 (Figure 3)

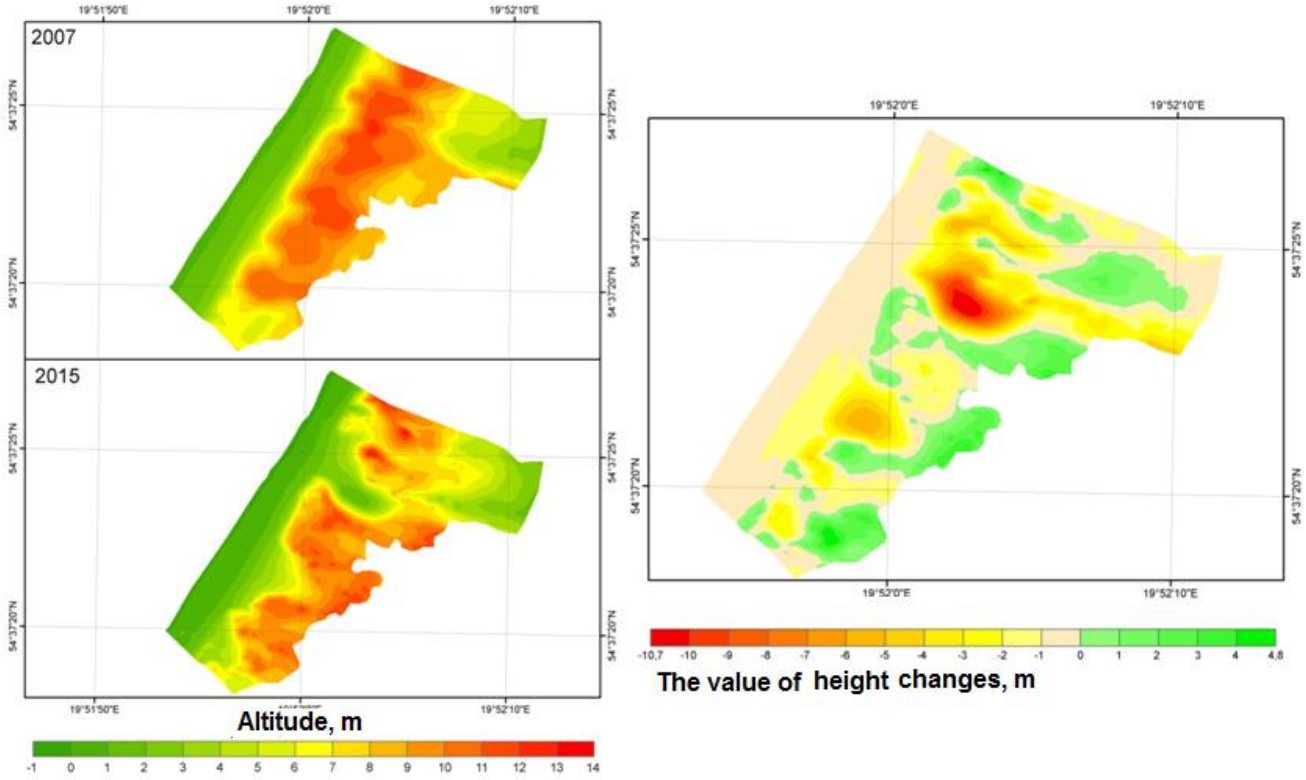

Figure 3. Digital terrain models of Polygon (T) for 2007 and 2015. and the terrain elevation change diagram within the polygon (T) in 2007-2015.

The main changes in the material and terrain volumes recorded within the polygon with foredune ridge. Volume foredune ridge material decreased by 35,301 m^3 accounting for 89.5% of the whole difference between the material volumes. There are no positive deformations within the beach.

For the entire polygon, the whole range of change in the numerical values of the terrain deformations is from -10.7 to 4.8 m, i.e. the amplitude of the deformation change is 15.5 m. The positive deformations occupy 25.3% of the polygon area, which corresponds to 10,063 m^2, the negative deformations occupy the remaining 74.7% of the polygon equal to 29,665 m^2.

For the foredune the area of negative deformations reached 22,919 m^2 which corresponds to 71% of the whole foredune area. In turn, positive deformations occupy 10,063 m^2 or 29% of the total area of the foredune.

According to the performed calculations, the impact of deflation-human factor within the foredune of Polygon (T) is much stronger than that of the wave type. Thus, as a result of exposure to wind and human activities, the foredune material volume within the polygon under research decreased by 33,071 m^3thus accounting for 93.7% of the total change in the foredune material volume. Consequently, the man-induced impact on the foredune leads to the activation of

destructive eolian processes, the impact of which is in many respects exceeds the erosion of the sea slope of the foredune caused by the influence of the sea. An intensive course of destructive eolian processes resulted in the formation within the polygon in the foredune body of a through deflation hollow and a semi-through hollow, via which holiday-makers move to the sea and back. The polygon's accretion sections generally correspond to the foredune surface portions covered with vegetation, forested rear slope and the portions of the base of the rear slope, where deposition of sandy material mainly occurs as a result of the eolian transport. [3]

Third polygon (B)

The estimated volume of material on the entire polygon in 2007 was 221,071m^3 in 2015 the volume of the material decreased by 9,126 m^3 and amounted to 211,945 m^3. As a result, the total amount of the polygon material in 2015 decreased by 4.1% compared to 2007 (Fig. 4)

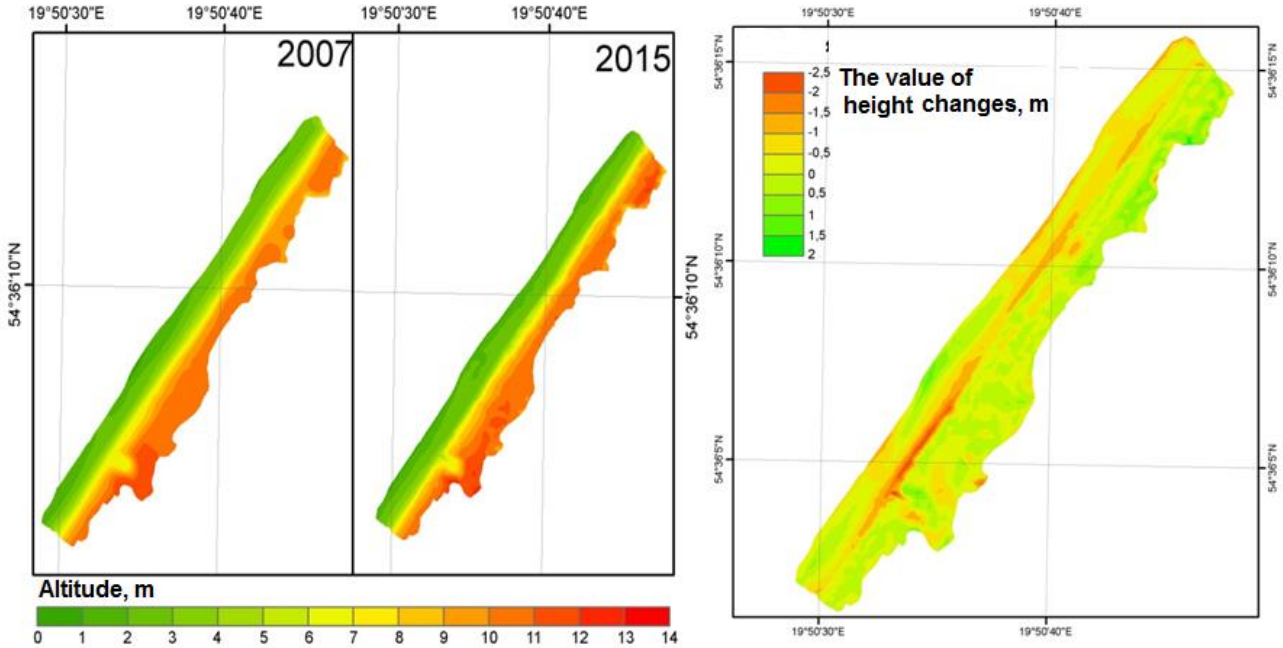

Figure 4 - Digital terrain models of the polygon (B) for 2007 and 2015 and the scheme of changing terrain elevations within the polygon (S) in 2007-2015.

The main changes in the material and terrain volumes occurred with the foredune within the polygon. The foredune material volume decreased by 6,438 m^3 accounting for 70.5% of the difference between the material volume. The amount of the beach material decreased by 2,688 m^3.

For the entire polygon the range of the numerical values of the terrain deformations is from -2.5 to 1.9 m, i.e. the amplitude of the deformation changes is 4.4 m. The positive deformations occupy 35.1% of the polygon area, which corresponds to 10,720m^2,the negative deformations occupy the remaining 67.9% of the polygon area corresponding to 22,722 m^2.

The positive deformations within the beach occupy an area of 2,046 m^2, or 22.8%, the negative deformations were subjected to the remaining 77.2% of the beach area (6,921 m^2).

The range of the change in the deformation values is equal to 4.4 m and is from -2.5 to 1.9 m. For the foredune the of the negative deformations reached 8,669 m^2 which corresponds to 35.5% of the total area of the foredune. Positive deformations, in turn, occupy 15,772 m^2 or 64.5% of the total area of the foredune.

This polygon is different from the other two by the degree of human impact which is relatively low in this part of the Vistula Spit. The calculated amount of the reduced foredune material because of deflation here was 871 m^3 or 13.5% of the total volume of the lost material of the foredune. The remaining 86.5% (5,567 m^3) of the lost material volume of the foredune ridge account for these a storm effects. The action of eolian processes on the territory of the polygon is manifested mainly in a deflationary depression area in the southern part of the polygon, where there is a path and access to the sea. As a result, destructive eolian processes at the part of the sea coast as well as in the rest of the polygons occur mainly with the anthropogenic factor.

All parameters and characteristics of polygon changes and changes of marine shore of Vistula Spit because of influence main natural an anthropogenic factors for the period from 2007 to 2015, are shown in Tabl. 1

IV. CONCLUSIONS

Based on the results of the research within three reference polygons on the coast of the Vistula Spit, you can draw conclusions about the prevalence of the eolian component in the destruction of the sandy foredune body given the simultaneous man-induced impact.

Polygons (S and T) can be characterised by active anthropogenic influence as Polygon (S) is located in the Kosa village, and Polygon (T) is subjected to the intensive load by uncontrolled tourism. Within these polygons there is an intense impact from the deflationary processes leading to the creation of deflation hollows and destruction of the foredune surface. The main-induced factor within these polygons is the main cause of the intensive deflation. The disorganised mass movement on the foredune of a large number of holidaymakers leads to the degradation and destruction of foredune vegetation performing the function of sand binding.

An assessment of the foredune material volume changes according to 2007 and 2015 data shows that for Polygons (S and T) a decrease in the foredune material volume is primarily due to the deflationary process. At Polygon (S) contribution of the deflation to the reduction of the material volume was 85.5% and at Polygon (T) it is 93.7%, indicating that the prevalence of the eolian component over the influence of the sea in the foredune destruction.

At the same time, at Polygon (B), where the degree of the man-induced impact is relatively small compared to the two other polygons, the major role in destroying foredune is by its destruction by the sea. The main share in the decrease in the foredune material volume within the polygon by the sea erosion, the contribution of which amounted to 86.5% in percentage terms.

Table 1. Characteristics of parts of marine shore of the Vistula Spit on polygons and their changes for the period from 2007 to 2015 because of influence of main natural and anthropogenic factors

Polygon parameters	Polygon(S)			Polygon(T)			Polygon(B)		
	Polygon	Beach	Foredune	Polygon	Beach	Foredune	Polygon	Beach	Foredune
L, m	524	524	524	272	272	272	526	526	526
S, m^2	39705	11200	28505	39728	6746	32982	33442	8967	24441
V_{2007}, m^3	134202	16115	118087	261748	9006	252742	221071	19090	200784

$V_{2015,}$ m^3	100600	7638	92962	222291	4852	217441	211945	16402	194346
$\Delta V,$ m^3 (%)	33603 (100)	8477 (25.2)	25126 (74.8)	39457 (100)	4154 (10.5)	35301 (89.5)	9126 (100)	2688 (29.5)	6438 (70.5)
$\Delta V_{defl.,}$ m^3 (%)	-	-	21481 (85.5)	-	-	33071 (93.7)	-	-	871 (13.5)
$\Delta V_{eros,}$ m^3 (%)	-	-	3645 (14.5)	-	-	2230 (6.3)	-	-	5567 (86.5)
S+ ,m^2 (%)	2474 (6.2)	10756 (96.0)	2051 (7.2)	10063 (25,3)	0 (0)	10063 (29)	10720 (35.1)	2046 (22.8)	15772 (64.5)
S-, m^2 (%)	37231 (93.8)	443,5 (4.0)	26455 (92.8)	29665 (74,7)	6746 (100)	22919 (71)	22722 (64.9)	6921 (77.2)	8669 (35.5)
UE, m3/m/year	-	-	0.87	-	-	1.02	-	-	1.32
UD, m3/m/year	-	-	5.12	-	-	15.2	-	-	0.21

Symbols: L–the length of polygon; V- the volume of material, DEM on zero surface;ΔV – difference between the volume of material DEM of 2007 and 2015; $\Delta V_{defl.}$ –difference between the volume material DEM of 2007 and 2015 as results of foredune deflation (eolian-anthropogenic factor); ΔV_{eros}- difference between the volume material DEM of 2007 and 2015 as results of storms (natural factor); S+- the area of positive deformations; S- - the area of negative deformations; UE - the unit volume of foredune erosion due to wave action per running meter per year; UD- the unit volume of foredune deflation (eolian-anthropogenic factor per running meter per year.

For the first time, during the research obtained was a numerical assessment of the impact on the sandy seashore from the Vistula Spit destructive factors such as sea erosion, deflation and the impact of man. The simultaneous effects of anthropogenic factors and eolian foredune on the surface leads to intense leakage deflation that surpasses the marine erosion by more than 5-15 times. However, in the absence of anthropogenic influence the main contribution to the foredune destruction ridge is from the sea erosion exceeding deflation by 6 times.

In conclusion, it should be noted that the Vistula Spit provides another example of what the sea sandy shores of the accretion type are extremely sensitive to the man-induced impact and the implementation of any activities within these shores should be carried out taking into account this fact.

V. Acknowledgement

Technical facilitation of the study, problem identification, data analysis and chose of the polygons were made under support of the theme № 0149-2014-0017 (supervisor – B. Chubarenko) of State Assignment of the P.P.Shirshov Institute of Oceanology of the Russian Academy of Sciences (2015-2017). The polygon survey and preparation of this article was made under the support of the Project No 14-17-00547 “A forecast development for evolution of accumulative Russian coasts of tide less seas”

VI. REFERENCES

[1] V.P. Bobykina, "Morphology and Dynamics of the Sea Coast of the Northern Section of the Vistula Spit," *Environmental Problems of the Kaliningrad Region and the Baltic Sea Region*, Kaliningrad: research set by the publisher of the I. Kant State University, 2007, pp. 20-26.

[2] E.M. Burnashov, "The modern geo-ecological conditions of the Sea Coast in Kaliningrad Region," *Create artificial beaches, islands and other structures in the coastal zone of the seas, lakes and reservoirs,* Novosibirsk: Publishing House of the SB RAS pp. 111-114, August 2011 [*Proceedings of the 2nd International Conf. "Construction of the Artificial Lands in the Coastal and Offshore Areas", Novosibirsk, August 1-6, 2011*].

[3] T.V. Shaplygina and I.I. Volkova, "Modern natural and man-induced pre-conditions of transformation of the eolian coastal marine natural complexes," *Vestnik Immanuel Kant Baltic Federal University*, vol. 1, pp.39-46. 2013.

SEDIMENT BALANCE OF THE VISTULA LAGOON

Vladimir Chechko, Atlantic Branch of P.P.Shirshov Institute of Oceanology of Russian Academy of Sciences, Russia
Boris Chubarenko, Atlantic Branch of P.P.Shirshov Institute of Oceanology of Russian Academy of Sciences, Russia

che-chko@mail.ru

Vistula Lagoon is the second largest lagoon in the Baltic Sea with maximum depth 5.2 m and average depth 2.7 m. Water volume and area are 2.3 km^3 and 838 km^2. Lagoon is connected with the Baltic Sea by single inlet 400 m wide and 10-12 m deep. Sediment budget estimation were made using literature sources, results of field measurements (hydrology, suspended sediment content, upper layer sediment structure, direct measurements of sedimentation in summer and winter conditions). The budget for terrigene and biogenic components of sediments were made, considering their contributions from the rivers, inflow from the Baltic Sea, coastal erosion and aerial flux, biological production within the lagoon, totally - ca. 730 thousands ton per year. Nearly half of total gain is washed out (105 and 244 thousands ton per year of terrigene and biogenic components), another half is dissolved and mineralized (biogenic component), and only 10% is deposited on the bottom, resulting in rather low sedimentation rate - 0.4 mm/year during last 100 years. Paper explain the reason of difference with estimation made in (Chubarenko&Chubarenko, 2002) and concludes that the clarification of estimates of the amounts of sediments transported from the lagoon to the Baltic Sea is a critical element for understanding the evolution of the Vistula Lagoon as a sedimentation system.

I. INTRODUCTION

Lately the modern sediment accumulation processes in the coastal zone of the sea receives close attention of researchers. This is mainly explained by great interest towards the offshore strip due to construction of industrial facilities in this area, construction of ports, navigation channels, creation of new recreation areas, development of coastal navigation and fishing, intensive use of mineral and biological resources.

Multiple economic use facilities also include the Vistula Lagoon – the biggest shallow (maximum depth 5.2 m, average – 2.7 m) lagoon-type basin of the Baltic Sea located in its south-eastern part (Fig. 1). The lagoon is separated from the sea by a narrow sand spit, and water exchange with the sea is achieved through the navigable Strait of Baltiysk (in some studies – the Baltiysk Strait). Kaliningrad Seaway Canal with intensive year-round navigation passes along its northern shore, lagoon water area is actively used for fishing and production of nonmetallic mineral resources. In the recent years the lagoon is becoming more and more significant as a recreation zone. All these factors, without a doubt, increase the anthropogenic load on water body and require

intensification of studies of all components of the aquatic ecosystem, especially the structure and more of anthropogenic flows for development of an effective environment control model.

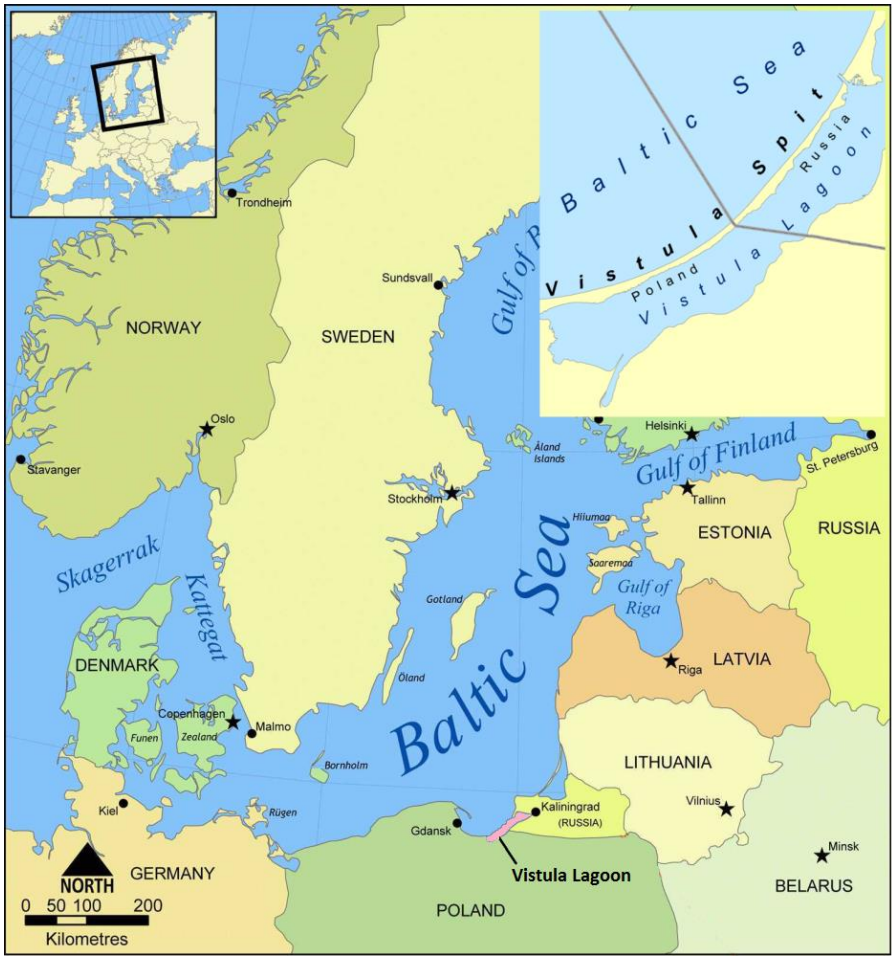

Fig. 1. Location of the Vistula Lagoon in the South-Eastern Baltic.

Because of this there is an important objective of determination of the main sources of sedimentation material in delivery of its individual components, as well as assessment of the absolute weight of the sedimentation material coming in the water body and depositing on its bottom. Extensive factual material accumulated in the course of more than twenty years of studies of the coastal systems by Atlantic Branch of P.P. Shirshov Institute of Oceanology allows for calculation of the sedimentation material balance in the Vistula Lagoon, which is the goal of this paper.

Therefore we should mention that the first attempt of balance calculation of the sedimentation material in the Vistula Lagoon took place earlier [1]. However it did not consider all elements, and some of them require clarification and supplementation.

II. METHODS

Overall, sedimentation balance method developed by the scientific school [2,3,4] was used for achievement of the set objective. Individual elements of the sedimentation material balance were calculated using well known methods currently used in oceanology research.

Water suspension was extracted to determine its concentration and composition using membrane ultra-filtering method with gravimetric estimation of the quantity of suspended matter deposited on the filter [5, 6]. Water samples were filtered in vacuum with -0.6 atmospheres through pre-weighted nuclear filters 47 mm in diameter with pore size 0.45 mcm. After filtration of water filters were flushed in bidistillate, placed in clean Petri dishes, dried down to constant weight in a desiccator. Suspended matter content was determined by weighting with 0.1 mg precision using analytical scales. Weight of the matter on a filter attributed to the filtered water volume gave the total concentration of suspended matter (mg/l). Overall, over 1000 determinations of suspended matter concentration was made in water samples taken during the period from 1992 to 2013 in the lagoon, the Strait of Baltiysk and mouths of rivers.

In order to determine the total organic matter and the suspension (234 determinations between 1992-2013) the water was filtered through fiberglass GF/F filters heat treated under 450–480°C, which were dried, weighted and heat treated again in a muffler at 540°C. After cooling down and achievement of constant weight in a desiccator they were weighted again, and the ratio of mineral and organic components in the sample was determined from the weight difference [7].

To determine the organic carbon (C_{org}) content the water sample was filtered through fiberglass GF/F filters with subsequent determination of C_{org} using express-analyzer AN-7529 with automatic titration by pH value. In total 56 determination were made in the Laboratory of Geology of the Atlantic of AO IO RAS (analytic researcher – N.G. Kudryavtsev).

Eolian material arriving in the lagoon waters in summer was collected using nylon nets entrapping particles due to an electrical charge [8, 9]. A floating trap designed by the author was used as net carrier [10]. Eolian material accumulated in the snow coating of the lagoon was collected and studied using methods accepted in studies of Arctic aerosols [11]. Between 2006 and 2013 a total of 124 samples of eolian material were analyzed.

Sedimentation in the lagoon was studied using method developed by S.N. Antsyferov [12] that is based on entrapment of settling sediments by accumulating traps. To achieve this objective during ice formation the bottom-based sedimentation trap method was used [13]. This method is based in direct catching of the material quantity sedimenting over a certain period inside the trap with known diameters placed on the water body bottom. Total of 164 sedimentation material samples bottom-based sedimentation traps were studied between 1993 and 2011.

Analysis of river run-off and suspended substance from rivers falling in the lagoon was performed in 1999-2000 using methods based on instrumental measurements of stream velocities and determination of water suspension concentration [14]. The collected date was subsequently compared to reference data, and average values calculated.

Calculation of the lagoon balance elements has also used reference data published in a number of well-known papers mentioned below.

III. Results and discussion

In order to identify the main trends of the modern sedimentation process it is important to know ratios of sedimentation material entering the water body from various sources. Based on the field observations and literature data we have calculated the absolute weights of the material entering the

lagoon and leaving it. Calculation results and determined main sedimentation material balance elements are summarized in Table 1.

From the analysis of data presented in this table we can make a conclusion that the vast majority of the terrigene matter enters the lagoon as suspended solids with river runoff (68.8 thousand t/year). Considering the bedload sediments (4 thousand tons), the annual amount of terrigene material arriving the lagoon with river runoff is 72.3 thousand tons (58%).

There is a total of 10 rivers and creeks falling into the Vistula Lagoon with the total annual runoff water volume of 3.67 km^3. According to [15, 16], 44% of the total runoff comes from the Pergola River, and the rest – from small rivers. According to the literature and own data [16, 17, 18, 19], the water turbidity in the rivers falling into the Vistula Lagoon varies between 2.2 and 76.4 mg/l with the average of 27.2 mg/l. In this case the annual runoff of suspended solids in the lagoon water (including the bedload) will be 103.5 thousand tons per year on average.

The principal position in the lagoon's water balance holds water exchange through the Strait of Baltiysk. The total annual inflow from the sea is equal to 16.99 km^3, i.e. four times the runoff from the lagoon catchment. According to [20, 21, 22] and own observation, water suspension concentration in lagoon-adjacent coastal area of the sea varies from 1.2 to 12.8 mg/l (4.4 mg/l on average). Based on this, the annual transfer of suspended and transported deposits from the sea to the lagoon is 76.5 thousand tons. Terrigene material (including bedload) accounts for about 40% (30.1 thousand tons) of this amount, and biogenic material – for 60 % (45.9 thousand tons).

Results of the water suspension studies in the lagoon during offshore currents (water going from the lagoon to the sea) show that its average concentration was 17 mg/l. Therefore the quantity of suspended sedimentary material transferred from the lagoon to the sea in a year is 348.4 thousand tons. And the biggest part (243.9 thousand tons or 70 %) is formed by the biogenic suspended matter.

Eolian deposits, bank and bottom erosion products are estimated by us at 23 thousand tons (17 %) per year. However after more detailed studies this value might go up.

Therefore, the total amount of terrigene material entering the lagoon every year is 125.4 thousand tons.

As far as inflow of the organic matter is concerned, most of it (525 thousand tons or 87.1 %) is composed by autochthonic biogenic products [23, 24]. According to our own observations, river runoff brings 31.2 thousand tons (5.2%) of biogenic material to the lagoon every year, and water exchange with the sea – 45.9 thousand tons (8.0 %). The resulting total amount of the biogenic material produced in the lagoon and being transported to it is 603.1 thousand tons per year.

Outgoing part of the terrigene material balance is composed by bottom sedimentation and transfer to the sea. Calculations show that the majority of terrigene material (104.5 thousand tons or 83.3%) is carried through the strait to the sea. So far we were not able to separately assess the sedimentation balance component describing integral sedimentation of matter in the lagoon due to constant wind and current induced resuspension and re-deposition of the sediments. Therefore, just as in [1], this component was assessed from the assumption of closeness of the entire balance in a year – only 20.9 thousand tons (16.7 %) of the sedimentation material is deposited on the bottom.

243.9 thousand tons of biogenic material is transported to the sea, and only insignificant part is deposited on the bottom. In spite of relatively high biological productivity of the lagoon, the average organic carbon content is 1.3 %. Therefore bottom deposits every year receive 8.3 thousand tons of water suspended biogenic material. Vast majority (350.9 thousand tons or 58 %) of it goes for dissolution and mineralization, as well as consumption by various food chain links.

Earlier the same method was used to prepare the sedimentation material balance of the Couronian Lagoon [25]. It is interesting to compare certain components of balances of the two lagoons located in the same geographic region. Thus, average annual river runoff to the Vistula Lagoon is 3.67 km^3, which is about 6 times less than the river runoff to the Couronian Lagoon (23.1 km^3). The average seawater inflow in the Vistula Lagoon is 17.0 km^3, which is 3.3 times less than the salt water inflow in the Couronian Lagoon (5.1 km^3) (see Fig. 2) I.e., ratio of annual volumes of fresh and salt water entering the lagoons is 1:4.6 for the Vistula Lagoon and 4.5:1 for the Couronian Lagoon, which allows to consider them as coastal waters with mainly marine (Vistula Lagoon) and river (Couronian Lagoon) influence.

Predominance of marine and river influence has a different effect of the sedimentation material quantity entering the lagoon and leaving it. The majority of suspended terrigene material (87%) enters the Couronian Lagoon (river influence dominant) with river runoff, and only 1.6% with seawater. The situation in the Vistula Lagoon (marine influence dominant) is somewhat different. Here 24% of terrigene sedimentation material comes to the water body with seawater, and not more than 58% - with river runoff (Illustration 2). And the majority (84%) of the terrigene sedimentation material entering the Vistula Lagoon is carried out to the sea, and only 16% is deposited on the bottom. At the same time, the majority of the material entering the Couronian Lagoon us deposited on the bottom (74%), and only up to 26% is carried out to the sea. Eventually, this affect the rate of modern deposition of sediments, which on average is 0.4 mm/year[3] [26] for the Vistula Lagoon, i.e. 3.5 times less than for the Couronian Lagoon (1.4 mm/year).

[3] - This rate of deposition of sediments expressed in mm/year means the rate of depth change in the lagoon in average, and bottom of the lagoon is mostly muddy which highly watered. It is not possible to use this data for estimation the term of sediment budget responsible for deposition, because this term expresses the amount of dry sediments, not watered.

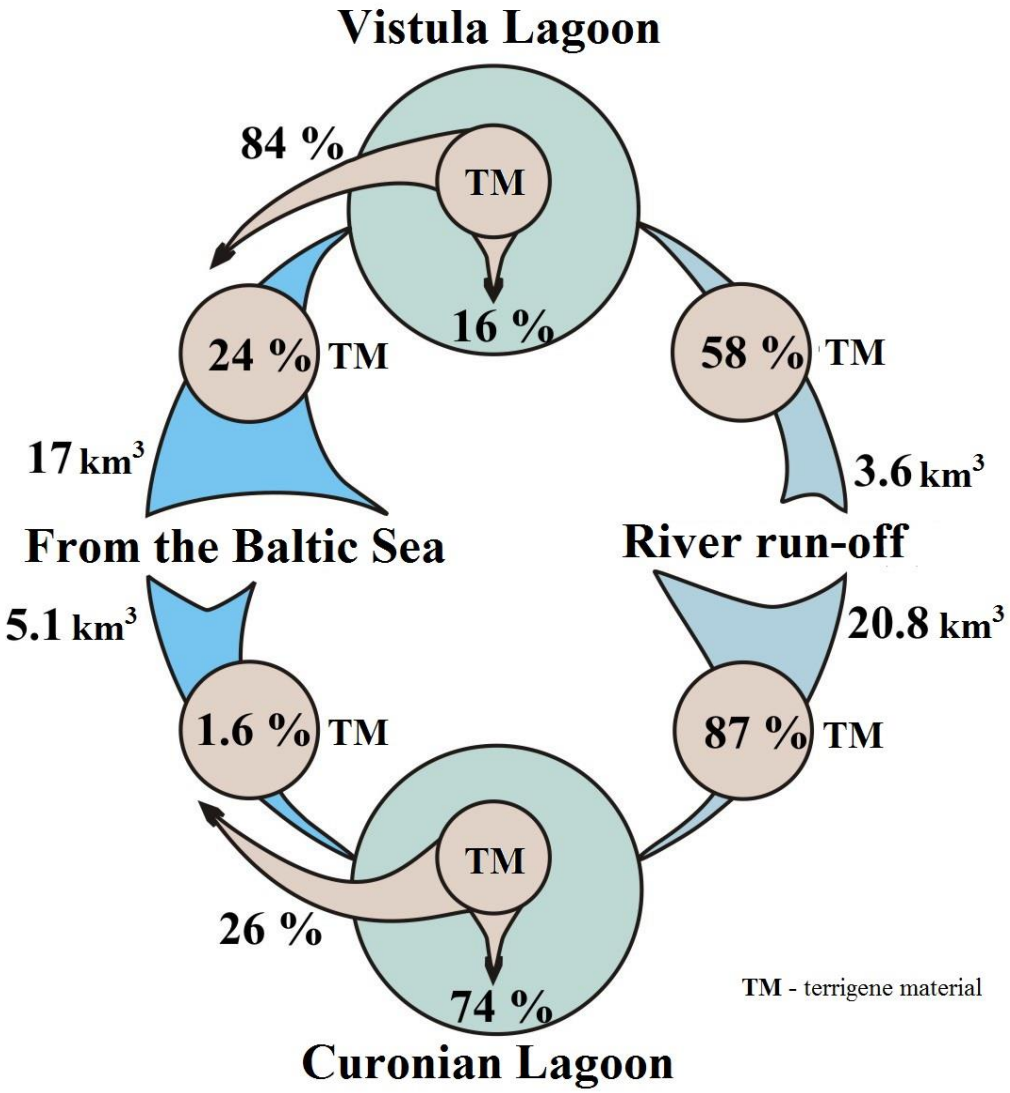

Fig. 2. Water gain and amounts of terrigene material entering the Couronian and Vistula lagoons.

In conclusion we would like to comment on comparison of the results of this study with the balance estimates in [1]. For the water balance our analysis and analysis in [1] rely on the same data [16]. [1] included balance assessment only for the inorganic part of the material, while this article offers significant clarification of the suspension concentration and its separation into the terrigene and biogenic parts, allowing for separate determination of balances for both of these components of the sedimentation material.

In [1] the calculation of terrigene material outflow from the lagoon to the Baltic Sea uses the average suspension concentration value in the lagoon itself (15.7 mg/l, [27]), while this analysis uses the terrigene suspension concentration value in the outflowing water according to the direct measurements in the Strait of Baltiysk – on average 5.1 mg/l. As a result, estimates of the terrigene material transported from the lagoon in a year differ by the factor of 3 (104.5 and 322.164 [1] thousand tons per year), resulting in different conclusions: [1] assumed there is no material

accumulation in the entire lagoon, while our estimates give only low values of deposition of sediments in the lagoon – 29.2 thousand tons per year.

Therefore, the question of estimating the amount of sedimentation material transported from the lagoon through water exchange with the sea remains the key issue, end it will be the subject of further research.

IV. Conclusions.

The calculations show that the absolute weights of the terrigene sedimentation materials in the Vistula Lagoon are formed mainly by river runoff (72.3 thousand tons) and water exchange with the sea (30.1 thousand tons). And 83% of all the incoming terrigene material is transported to the sea, only up to 17% of it is deposited on the bottom.

High productivity of phytoplankton is responsible for inflow of the biogenic material. Its total inflow in the Vistula Lagoon is more than 4 times higher than the terrigene material inflow. However most of the biogenic material is dissolved, mineralized and transported to the sea. Only a small part of it is deposited on the bottom (about 1.5% of the incoming amount).

Annual flow rate of the total sedimentation substance from the lagoon water volume is 728.5 thousand tons, 350.9 thousand tons of which is dissolved, mineralized and consumed by different organisms, 348.4 thousand tons is transported to the sea, and 29.2 thousand tons is deposited on the lagoon bottom. Comparison of the amount of incoming terrigene (125.4 thousand tons) and biogenic (603.1 thousand tons) material demonstrates predominance of biogenic processes and high rates of organic matter production. However only a small part of it is deposited on the bottom of the lagoon. Terrigene process of modern sediments deposition is predominating in the Vistula Lagoon and in the Baltic Sea in general. Contribution of the biogenic material is mainly limited to life support of organisms and the biogeochemical cycle.

In the Vistula Lagoon, unlike the Couronian Lagoon, majority (84%) of incoming terrigene sedimentation material is further transported to the sea, and only 16% is deposited on the bottom; at the same time, majority of the material entering the Couronian Lagoon is deposited on the bottom (74%), and only up to 26% is transported out to the sea.

In a conclusion we can say that the calculated elements of the sedimentation balance of the Vistula Lagoon indicate low rate of sediments deposition currently observed in the lagoon and that in the future it is not threatened by shallowing and siltation. Also we can presume that there is a natural self-cleaning mechanism operating in the lagoon, which transports large volumes on thin sedimentation material from the lagoon to the sea together with various pollutants.

More detailed estimates of the sedimentation balance performed in this article significantly clarify the balance ratios discussed in [1], and show that the clarification of estimates of the amounts of sediments transported from the lagoon to the Baltic Sea is a critical element for understanding the evolution of the Vistula Lagoon as a sedimentation system.

V. Acknowledgement

Data collection was made under support of the theme № 0149-2014-0017 of State Assignment of the P.P.Shirshov Institute of Oceanology of the Russian Academy of Sciences (2015-

2017). Preparation of this article was made under the support of the Project No 14-17-00547 “A forecast development for evolution of accumulative Russian coasts of tideless seas”.

VI. References

1. Chubarenko B.V., Chubarenko I.P. “New way of natural geomorphological evolution of the Vistula Lagoon due to crucial artificial influence,” in *Geology of the Gdansk Basin,* Emelyanov E.M. (ed.), Kaliningrad: Yantarny Skaz, 2002, pp. 371-374. In Russian.

2. Strakhov N.M. “Towards understanding of relationship and mechanisms of marine sedimentation of the Black Sea,” *Transacts of USSR Academy of Sciences, Geological Series*, 1947, No 2, pp. 49090. In Russian.

3. Strakhov N.M. Essays in carbon accumulation in modern water basins. In *For the memory of Academician A.D.Arkhangelsky*, Moscow: Publisher of USSR Academy of Sciences, 1951, pp. 487-567. In Russian.

4. Strakhov N.M., Brodskaya N.G., Knyazeva L.M., Razhivina A.M., Rateev M.A., Sapozhnikov D.G. Sediment formation in nowadays water basins. Moscow: Publisher of USSR Academy of Sciences, 1954, 792 p. In Russian.

5. Lisitsyn A.P. Methods of collection and investigation of water suspended sediments for geological purposes. *Proceedings of the Institute of Oceanology of USSR Academy of Sciences.* 1956, Vol. 19, pp. 204-231. In Russian.

6. Bogdanov Yu.A., Lisitsyn A.P. “Distribution and content of suspended organic matter in the waters of Pacific Ocean,” *Oceanological Studies,* No 18, pp. 75-155, 1968. In Russian.

7. Vitiuk D.M. *Suspended matter and its biogenic components.* Kiev: Naukova dumka, 1983, 212 p. In Russian.

8. Chester R., Johnson L.R. “Atmospheric dusts collected off the West African coast,” *Nature*. Vol. 229, pp 105-107, 1971.

9. Zhivago V.N., Bogdanov Yu. A. *Hydrophysical and hydrooptical studies in the Atlantic and pacific oceans.* Moscow: Nauka, 1974, pp. 259-279. In Russian.

10. Chechko V.A., Kurchenko V.Yu. Study of the fluxes of aerosol by floating trap. *Meteorology and Hydrology*, № 11, pp. 85-90, 2008. In Russian.

11. Shevchenko V.P. *The influence of aerosol on environment and marine sediment accumulation in the Arctic.* Moscow: Nauka, 2006, 226 p. In Russian.

12. Antsyferov S.M. *The method to determine the suspended sediments concentration in the upper part of shelf.* Moscow: Institute of Oceanology, 1987, 64 p. In Russian.

13. Semenovich N.I. *Bottom sediments of the Lake Ladoga*. Moscow: Nauka, 1966, 55 p. In Russian.

14. Shamov G.I. *River sediemnts*. Leningrad: HydrometeoIzdat. 1955, 380 p. In Russian.

15. Mikulski Z. Bilans wodny zalewow przybaltyckich // Wind. Sluzby Hydr. i Met., 59a. - Warszawa, 1964

16. *Hydrometeorological Conditions of the Vistula Lagoon*, N.N. Lazarenko and A. Maevsky, Eds. Leningrad: Hydrometizdat, 1971, 330 p. In Russian.

17. Pustelnikov O.S. *Geological characteristics of the basin and mechanism of sediment formation in the Baltic Sea*. Synopsis of thesis PhD in Geological-mineralogical studies. Vilnius, 1974, 22 p. In Russian.

18. Blazhchishin A.I. *The balance of sediments in the Gdansk basin of the Baltic Sea. Lithology and Mineral Resources*, № 5, pp. 67-76, 1984. In Russian.

19. *The role of sediment flows from the Pregolya River and other rivers in the sediment balance of the Vistula Lagoon: Sci. Report*. Kaliningrad: Atlantic Branch of P.P.Shirshov Institute of Oceanology of Russian Academy of Sciences. 2000. 20 p. In Russian.

20. Emelyanov E.M. "Quantitative distribution of marine suspended sediments near the shore of the Sambian Peninsula – Curonian Spit," *Oceanological Studies,* № 18, pp. 203-212, 1968. In Russian.

21. Pustelnikov O.S. Quantitative distribution of suspended sediments in central and south-eastern parts of the Baltic Sea. *Oceanology*, Vol. 9, Issue 6, pp. 1018-1030, 1969. In Russian.

22. Emelyanov E.M., Pustelnikov O.S., Chemical content of river and marine suspended sediments of the Baltic Sea. Geochemistry, № 6, pp. 918-932, 1975. In Russian.

23. Krylova O.I., Naumenko E.N. Phytoplancton and primary production of the Vistula Lagoon. In *Ecological and fishery studies in the Vistula Lagoon*. Kaliningrad: AtlantNIRO, 1992, pp. 14-33. In Russian.

24. Aleksandrov S.V. *Primary production of phytoplankton in the Vistula and Curonian lagoons.* Synopsis of thesis PhD in biological studies. St.-Petersbrg, 2003, 26 p.

25. *Biogeochemistry of the Curonian Lagoon.* Gudelis V.K., Pustelnikov O.S. Eds. Vilnius. 1983. 159 p.

26. Chechko V.A., Kurchenko V.Yu. "The features of the sediment formation in the shallow semiclosed basin in the ice period (by example of the Vistula Lagoon of the Baltic Sea)," *Proceedings III All-Russia Conference "Ice and thermal process in the water basins of Russia".* Moscow, pp. 352-357, 2011.

27. Chubarenko, B.V., Kuleshov, A.F., Chechko,V.A. Field sudy of spatial-temporal variability of suspended substances and water transparency in Russian part of Vistula lagoon. In *Monographs in System Ecology.* Vol.2, Kalipeda University, 1988, pp. 12-17.

Table 1. Elements of the sedimentation material balance in the Vistula Lagoon

Elements	Inflow						Consumption				
	River runoff	Inflow from the sea	Atmospheric precipitation	Abrasion, erosion and eole.	Produced by organisms	Total	Transported to the sea	Evaporation	Deposition on the bottom	Dissolution and mineralization	total
Water runoff, km^3/year	3,67 *	17,0*	0,50*	-	-	21,17*	20,52*	0,65*	-	-	21,17 *
Suspension concentration, mg/l	27,2	4,4	-	-	-	-	17,0	-	-	-	-
Terrigene material, thousand tons per year	72,3	30,1	-	23,0	-	125,4	104,5	-	20,9		125,4
Biogenic material, thousand tons per year	31,2	45,9	-	1,0	525,0**	603,1	243,9	-	8,3	350,9 **	603,1
Total sedimentation material, thousand tons per year	103,5	76,0	-	24,0	525,0	728,5	348,4	-	29,2	350,9	728,5

* [16]; ** [23, 24]

SEDIMENT TRANSPORT NEAR THE VISTULA SPIT (BALTIC SEA)

Boris Chubarenko, Atlantic Branch of P.P. Shirshov Institute of Oceanology of Russian Academy of Sciences, Immanuel Kant Baltic Federal University (IKBFU), Russia
Alexander Babakov, Atlantic Branch of P.P.Shirshov Institute of Oceanology of Russian Academy of Sciences, Russia

chuboris@mail.ru

The Vistula Spit is a sandy elongated barrier form which borders the Vistula Lagoon from the Baltic Sea. The evolution of the spit as well as nowadays sediment transport along the marine shore of it are still under discussion, especially due to existing of entrance jetties bordered the Strait of Baltiysk, the single inlet to the Vistula Lagoon, and advanced up to 10 m depth seaward. Different hypothesizes about ether uniform transport from north to south or contrary directed fluxes with convergence at various points at the spit shore are discussed. Most of them are based on fact of accumulation of sandy material just to north from the northern entrance jetty as in incoming corner. Basing on statistics of near-surface wind, direct measurements of currents and analysis of direction of the scour hole located between jetties the paper confirms the existence of two opposite fluxes - one brings alluvium from the Vistula River mouth to north as main winds blow from south-west and west, and, in contrast, another one brings material obtained by erosion of the western shore of the Sambian Peninsula to south. Dynamic equilibrium between these fluxes through hundreds of years resulted in formation of present shape of the coastline, and it is expected that the area of the equilibrium in alongshore migrations is in the top of the Yantarny- Baltiysk concave. Appearance of entrance jetties of the Vistula Lagoon inlet, in the area where opposite alongshore migration of material are nearly equalised, leaded to the accretion-erosion pattern, which is pseudo equal to sediment transport from north to south. In fact the accumulation of sand just to north from the northern entrance jetty and erosion to south from southern jetty may be explained by mechanism, when the sand transported in the incoming corner just near the northern mole by southward migrations is excluded from migratory movement and deposited in the zone shadowed by jetties (from northward migrations). Erosion to south of jetties is explained by wind surges in incoming corner for prevailing western winds.

Key words: sediment transport, Vistula Spit, Baltic Sea, current measurements

I. INTRODUCTION.

The study area covers the southern and eastern shores of the Gulf of Gdansk, from the mouth of the Vistula River to the Taran Cape (Fig. 1). Here, most intensive sediment alongshore transport occurs, which has been the subject of research in the last century (all references to studies are given below). The single inlet of the Vistula Lagoon, further called the Strait of

Baltiysk (the ‘Baltiysk Strait” in some studies), is bordered by jetties stretched seaward up to 10 m depth.

The eastern shore of the Gulf of Gdansk has a concave form, the Sambia-Vistula arc, with the shoreline orientation changing from the west-eastern direction (the shore near the mouth of the Vistula River) to the south-north (the shore of the Sambian Peninsula). Thus, the prevailing winds of the western rhumbs [1-4] influence the shore at an acute angle near the mouth of the Vistula River, and on the Sambian Peninsula shore, almost normal to the shore. This creates prerequisites for a change in the sediment transport direction within the Sambia-Vistula arc.

The purpose of this work is to provide an analysis of the prevailing wind direction and the results of the direct measurements of currents in the Strait of Baltiysk area and on that basis conjecture about the direction of sediment transport on the eastern shore of the Gulf of Gdansk distinct from previous hypotheses derived by evaluating the wave energy transport and the accumulative morphodynamic criterion.

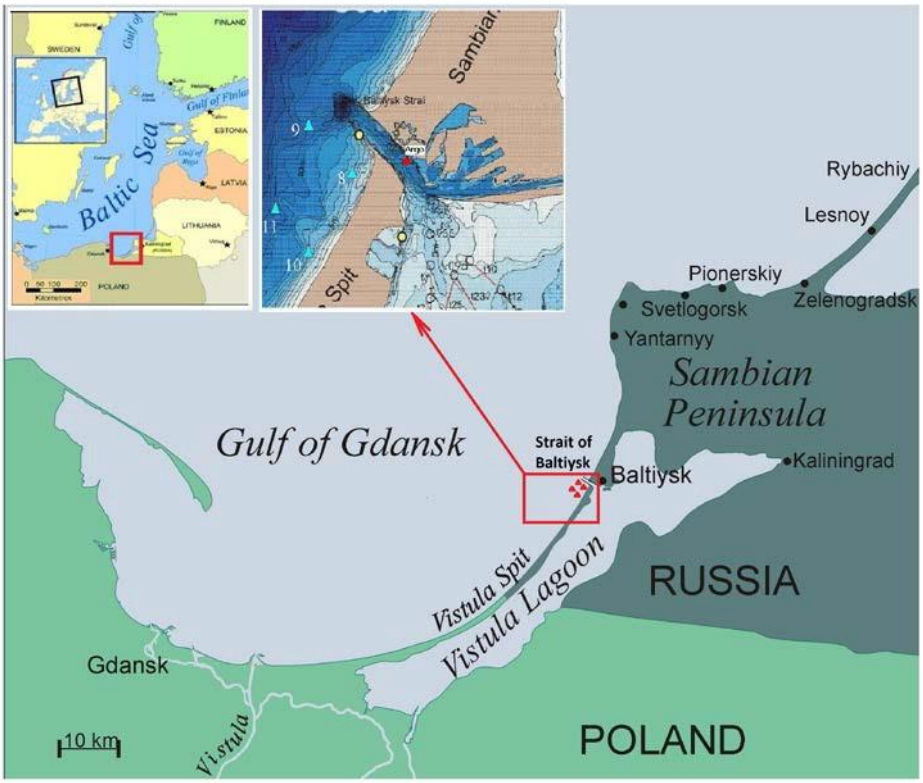

Fig.1. Location of the study area in the South-Eastern Baltic.

The researchers focussing on the phenomenon could not come to a consensus about the outcome of sediment transport along the eastern shore of the Gulf of Gdansk. First Tornquist (1910) [5] and Brükmann (1913) [6] believed that the sediment transport from the south to the north, up to the Taran Cape prevails, while Tidemann (1930) [7] and Pratje (1932) [8] claimed the outcome sediment transport from Yantarny to Baltiysk, but none of them have extended it further to the south.

In Russian literature sources the idea dominant by the end of the last century was that of the unidirectional transfer of sediments to the south of the Taran Cape to the mouth of the Vistula River (Fig. 2a). The idea followers headed by R. Knaps and V.P. Zenkovich were justifying their point of view by changes in the shore morphology [9-14], an increase in the number of underwater bars as soon as sediment flows become saturated [15] and the main argument was the accretion at the northern jetty of the Starit of Baltiysk and the downstream erosion immediately south the southern jetty [13, 14] (Fig. 3b).

As soon as the field and laboratory test data were compiled, the local flows concept was elaborated, which included the idea of the migrations oppositely directed within the limits of a lythodynamic cell [16-19]. The existing schemes of the outcome longshore sediment transport, the availability and location of the transport direction change area can be divided into three groups. According to the current concepts in the literature, the mark (or convergence) change zone of the resulting sediment transport within the Gulf of Gdansk can be at the top of the Baltiysk-Yantarny shore concavity (Fig. 2b, [20]), in the vicinity of the Vistula Lagoon inlet, which is designed with entrance breakwalls that go into the sea to the depths of 10 m (Fig. 2c, [10, 15]), or within the Vistula Spit (Fig. 2d-f, [17, 19, 21, 22]).

I. SCOUR HOLE IN THE VISTULA LAGOON INLET

The scour holes [13] are a typical morphometric manifestation of the excited longshore currents an obstacle in the sea. The existing drainage line at the breakwaters of the Vistula Lagoon inlet stretched out from the southern breakwater to the northern one can show that there are the prevailing currents and intense transit of sediment from SW to NE.

The scour hole has the elliptical shape, and is adjacent to the head of the southern breakwater and crosses the fairway in the NW direction, roughly parallel to the shore. It began to take shape after the construction of the existing jetties (1878) and as early as 1903 it had distinct contours with depths up to 11-14 m (Fig. 3a). At the beginning of the twenty-first century, the maximum depth of the scour hole reached 28.5 m (Fig. 3b), and increased up to 32 m after reconstruction of the breakwater extremities in 2006-2008 and moved closer to the southern breakwater. At that,the depths in the fairway remained 10-12 m.

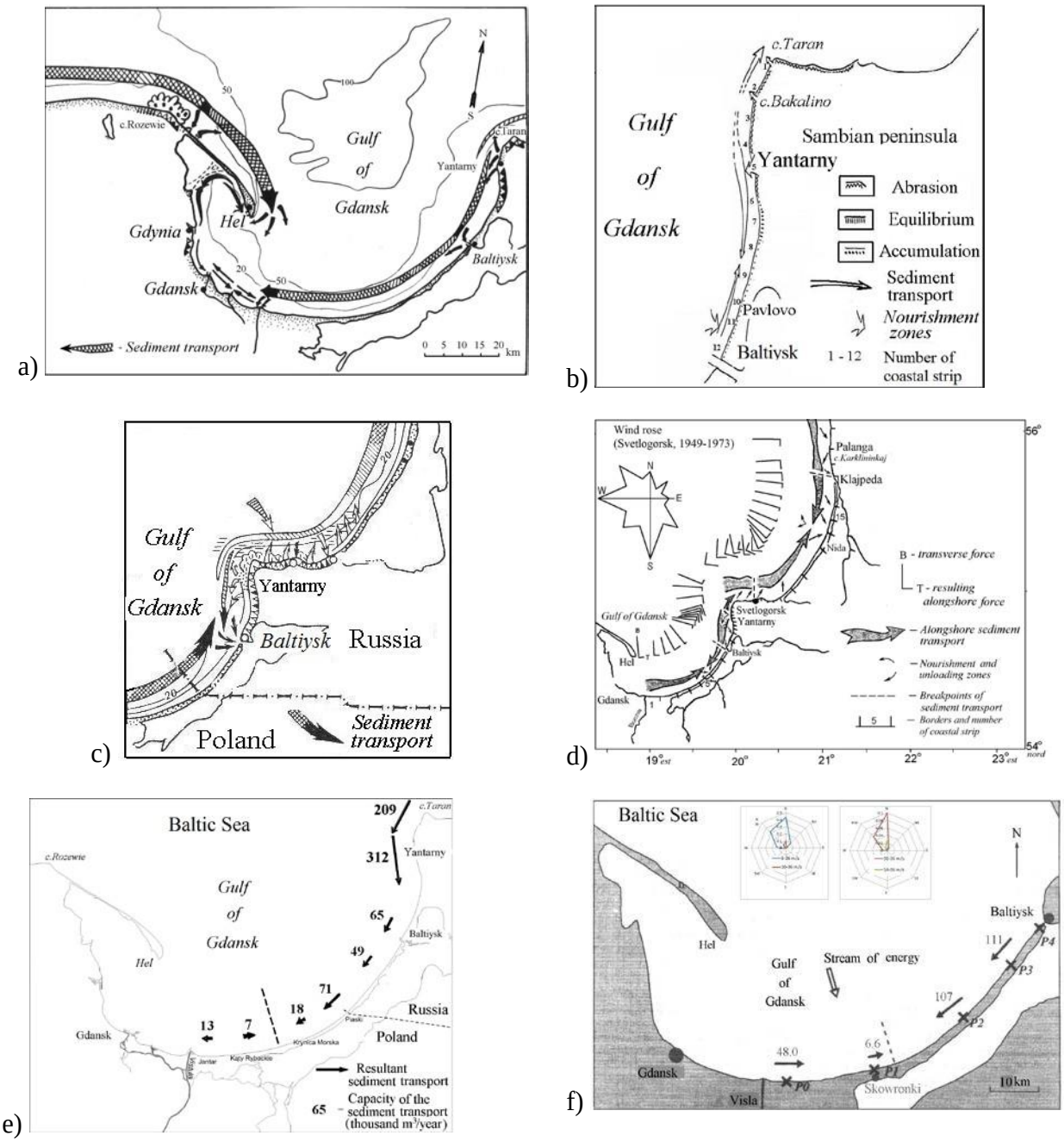

Fig. 2. Different visions on sediment transport structure along the eastern shore of the Gulf of Gdansk: (a) unidirectional flux to south [12] (1958); (b) convergence of fluxes at the Yantarny-Baltiysk concave [20] (1984), or (c) around the Vistula lagoon inlet [10] (1982), or (d) in the central part [17] (2003) or (e,f) at the southern part of the Vistula Spit, [21] (2010) and [22] (2012).

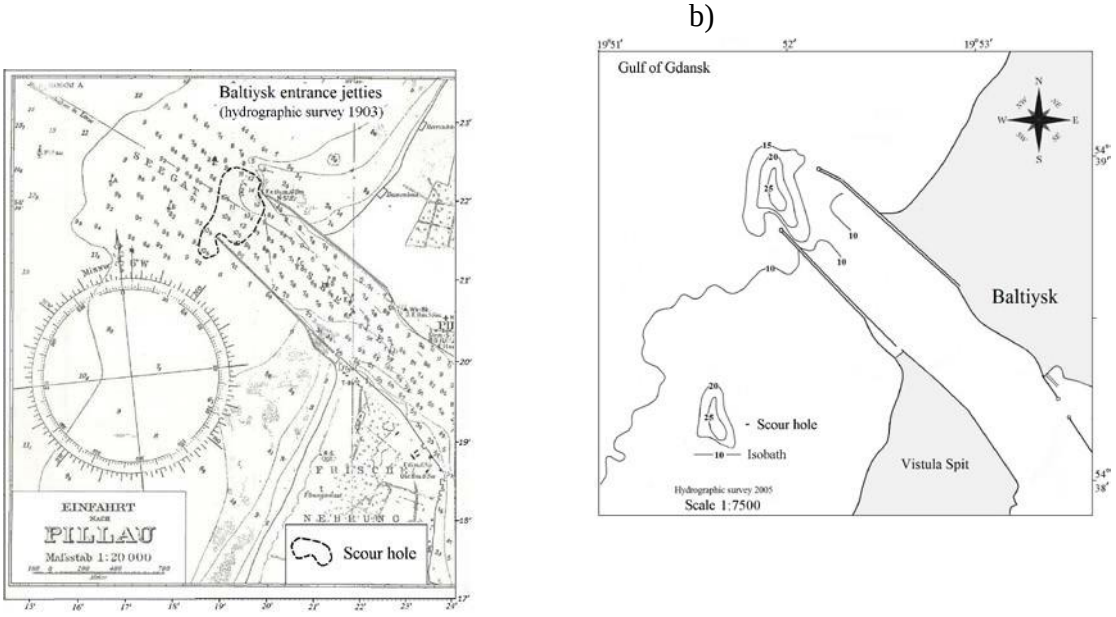

Fig. 3. Scour hole at the seaward end of the jetties of the Vistula lagoon inlet on the map of 1903 (a) and in 2005 (b), the accretion to north and the erosion to south are clear visible (b).

II. WIND AND WAVES IN THE STUDY AREA

According to the weather station in Baltiysk (Fig. 1), the long-term average annual frequency of occurrence of all winds of the SW-W-NW directions is approximately the same (14.68% - 14.95% -14.31%), and only from the N rhumb it is a little less (10.45%). The share of W-SW rhumbs increases for stronger winds; and it significantly decreases from the N side. Such a redistribution of the repeatability of directions for wave-hazardous winds (W>6m/s) is due to seasonal restructuring of the western transfer of air masses, which is manifested in the activation of the winds from the south-western quarter of the horizon in the autumn-winter storm period. For storms (Table 1, W≥14m/s) W wind repeatability (56.4%) exceeds the total repeatability of the other 3 directions (43.6%), respectively, the frequency of the impact of the SW-W storm winds is 72.9%, while the repeatability of the NW-N directions is only 27.1%, and the repeatability of the N wind is very low 3.9%. So, the winds of the W rhumb significantly prevail in the wind direction structure for storm situations.

The resulting azimuth for SW-N winds with the speed more than 6 m/s and more than 14m/s is equal to 276°. The resulting azimuth of SW-N waves with a height of $h \geq 1$ m is 290°, $h \geq 2$ m– 284°, $h \geq 3$ m – 287°.

Due to the orientation of the stretch of the sea shore of the Vistula Spit (azimuth normal to the shore in the Baltiysk area is 300°) the long-term average annual wind pattern in the South-Eastern Baltic (according to data collected in Baltiysk) should favour the predominant sediment transport from SW to NE, i.e. along the spit in the direction of the Baltiysk-Yantarny shore concavity. This tendency is especially obvious for storm winds, during which there are basic motions of sediment. This situation is also typical for the wave repeatability (Table 2),

consequently, it is expected that the longshore component of the wave energy flux is directed in the northern half of the horizon here.

Table 1. Wind frequencies and intensities in wave-hazardous directions (in % of all possible wind directions) for fresh and storm wind speed gradations according to the Baltiysk weather station data for 1949-1988 [1]

Compass point Gradation, m/s	N	NW	W	SW	Σ
6 - 9	2.54	5.55	6.38	7.19	21.66
10-13	0.22	1.06	2.76	1.38	5.42
14-17	0.06	0.30	0.74	0.24	1.34
18-20	0.01	0.11	0.26	0.06	0.44
21-24		0.01	0.01		0.02
25-28			0.01		0.01
Σ (6-28 m/s)	2.83 (9.80)*	7.03 (24.33)	10.16 (35.17)	8.87 (30.70)	28.89 (100)
Σ (14-28 m/s)	0.007 (3.87)	0.42 (23.20)	1.02 (56.35)	0.30 (16.57)	1.81 (100)

* Note. In parentheses the repeatability only for this gradation within the whole wave-hazardous direction sector (N-SW) is indicated.

Table 2 Repeatability (%) of waves in deep water (H=10 m) according to the Baltiysk weather station data for 1975-1984 [23]

Wave height, h m	N	NW	W	SW	∑(N-SW)
h ≥ 0 m	26.61	15.65	28.42	15.17	85.85%
h ≥ 1 m	9.85	9.31	19.53	7.95	46.83%
h ≥ 2 m	1.39	2.26	7.41	1.12	12.19%
h ≥ 3 m	0.27	0.2	1.13	0.11	1.73%

III. CURRENTS NEAR THE EASTERN SHORE OF THE GULF OF GDANSK

The instrumental measurements of near-bottom currents were made by the Atlantic Branch of the Institute of Oceanology of Russian Academy of Sciences at 4 points to the south entrance jetty of the Strait of Baltiysk in the period 12.09-18.11.2005. Mechanical current meters BPV-2 (the sampling frequency is once per hour) were installed at the depth of 12 m (point 9,12.09 - 10.11.2005, and point 11, 12.09 - 18.11.2005) and at the depth 6 m (point 8, 12.09 –18.09; 09.10-18.11.2005, and point 10, 12-16.09.2005).

The measurements period was dominated by the wind from the southern half of the horizon (WSW-S-ESE, 69.7%) and only in 17.8% it acted from the northern half (WNW-N-ENE). The E-W wind direction was recorded in 12.5 % cases. The wind speed did not exceed 8-10 m/s, and in only 4 instances (15.09, 24.10, 27.10 and 15.11) a short increase of wind up to 13,

15, 17 and 14 m/s was recorded [24]. Fig. 4 presents a current rose [18] at the measurement points (indicating the number of samples) constructed for situations with the wind speed of 8 m/s or more (for 6 gradations of wind direction - N, NW, W, SW, S, SE, that were recorded during the measurements for quite a long time). Measurement points were chosen in order to determine the area of influence of jetties [18].

For the oblique onshore winds (N, W directions), bottom currents were oriented in the direction of the longshore component of the wind action with a small deviation in the direction of the sea or shore depending on the water level variations (Fig. 4 a,c). During the period of exposure to the onshore wind normally to the shore (NW) the currents at deeper stations (9 and 11, the depths of 12-15 meters) have a substantial component along the shore to the north, and on the shallower stations (8 and 12), on the contrary, along the shore in a southern direction (Fig. 4b). With the longshore wind from SW the near-bottom velocities are directed along the shore northwards (Fig. 4d). For the winds of coastal rhumbs (SE and SE), the current velocities were mainly directed to the north (Fig. 4e,f).

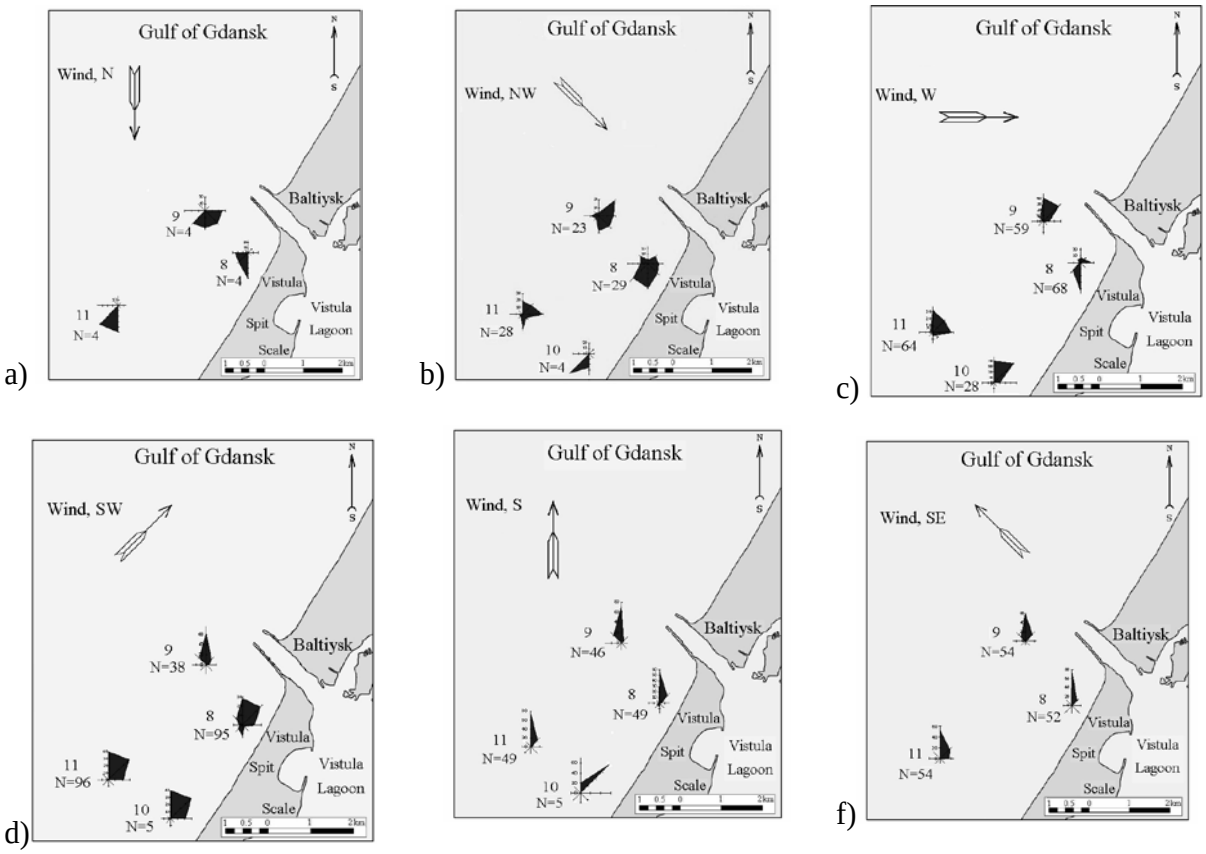

Fig. 4. Roses for coastal currents for the period 12.09.2015-18.11.2005 combined for typical wind directions: (a) N, (b) NW, (c) W, (d) SW, (e) S, (f) SE.

The maximum recorded velocities of the near-bottom currents at stations 8 and 10 reached 45 and 54 cm/s, at deep-water stations 9 and 11, 34 and 44 cm/s respectively.

In general, the measurements fully confirmed the physical pattern, the near-bottom currents are directed towards the longshore component of the wind and wave action starting with the

wind velocities 6-7 m/s [17, 24]. This is manifested in all wind directions (N, NW, W, SW, S), with the longshore wind and oblique onshore winds a one-way flux of near-bottom waters directed along the wind is generated.

IV. DISCUSSION

The foregoing presentation and results indicate a discrepancy between the fact that based on the prevailing direction of strong winds (from west to east), the longshore sediment transport within the Sambian-Vistula lithodynamic system should be directed to the north, and the model estimates of the wave energy direction [21, 22] and geomorphological accretion criteria [13, 14] indicate its southern direction.

The calculations of the wave energy pattern in [21, 22] were based on wind statistics and leaded to the conclusion that the area where longshore transport changes the direction (convergence zone) is located at the root of the Vistula Spit. In [21, 22] the geostrophic wind data were used, while direct measurements lead to other statistics [1, 25] (see sub-section 3). This difference in the statistical distribution of the geostrophic and near-surface winds (the latter acts in the Ekman friction layer) is quite natural. So, the calculations [21, 22] contained the uncertainty in the original data influencing the results.

Models [22] showed that the area where longshore transport changes the direction is in the coastal segment, where the direction of the normal to the shore coincides with the azimuth of the resulting wind action (Fig. 2e,f). Based on this dependence, we can say that taking into account the near-surface wind statistics [1, 25] (see sub-section 3), you should expect the change of alongshore sediment transport within the Baltiysk-Yantarny concavity.

It is essential to note that for any transverse profile two integral opposite longshore flows are shown in [21], i.e. during a long-term period the integrated sediment flow vector is directed north and south depending on the wind situation, and there is a zone to change the mark of the longshore transport, where these flows are equalised. This means, first of all, that there is constantly a significant longshore sediment migration rather than a one-way transfer along the shore of the Vistula Spit. And, secondly, that there are no two converged flows in a one moment in the zone, characterised by the change of alongshore transport direction, this zone may even be called a convergence zone. Thirdly, as the resulted long-term sediment fluxes are directed towards each other from both sides of this zone, the sediment accumulation is expected in this zone. Once, the cross-shore seaward transport of sediments increases along the decrease of alongshore transport, and material deposited on a beach is involved in eolian transport, the flattening of the bottom slope (a), the widening of the beach (b) and the growth of the foredune height (c) are expected in this zone.

Supporters of the idea that the longshore flow is directed from Baltiysk to the south argue their position on the basis of the accumulative morphodynamic criterion: there is the accretion of sediment at the incoming corner (for a sediment flow) before the obstacle set perpendicular to the shore, and abrasion behind the obstacle [13, 14]. As it is traditionally assumed [14] that on the Baltic Sea shore the sediment flow is maintained by alongshore currents, then according to the accretion on the north side of the jetties of the Strait of Baltiysk and abrasion, on the south, the stream of sediments of the subject criterion is directed from north to south. Although, as

shown in Section 3, there are no conditions that determine the prevalence of flows to the south on average per year.

On the shores with predominantly one-way sediment transport such a criterion does point to the direction of the resulting sediment transport. However, it is impossible to make a clear conclusion from the application of the only criterion because according to [26], the current and waves are in different ways involved in the deformation of the shores and bottom near the cross-shore breakwater, a sediment transport caused by the mean water flow (forced by the wind or water level gradient) gives the filling of the incoming corner by sand, and the sediment transport supported by the wind-induced waves lead to surges and erosion in the entrance angle and sediment deposition behind the breakwater.

Fig. 5. Principle scheme of sediment transport on the eastern shore of the Gulf of Gdansk:

1 – alongshore resulted sediment transport; 2 – offload and supply of sediments to alongshore transpo, 3 – area of equilibrium of alongshore sediment migrations

Based on the immutability of the near-surface wind statistics (Section 3) and principle result of [22], that alongshore flux changes the direction at the shore segment having normal windward, we can assume that before the appearance of breakwaters in the XIX century the entire shore from the mouth of the Vistula River to the present location of Yantarny village was the scene of active migration of the sand material with a zone of change of sediment transport direction in the area of the top of the Yantarny-Baltiysk concavity. This view means that the Vistula Spit was built mainly by the Vistula alluvium (by the part of the flow through the Nogat arm from the Vistula Lagoon, and from the sea by the longshore movement of sediment from the

mouth of the Vistula) and only a portion of abrasion material of the western shore of the Sambian Peninsula.

After the appearance of jetties of the Strait of Baltiysk and their extension to a depth of 10 meters, the accretion of material north of jetties and active erosion south of them along with the wind statistics (Section 3) fits into the concept that sediments at the winds in the southern direction fill the incoming corner of the northern jetty and are excluded from migratory movements, as during the winds from west and south this accumulated area is located in a wave shady of the jetties.

The erosion from the upwind side is typical for a long jetty, which have the incoming corner quite extensive and is oriented towards the prevailing storm winds. The resulting surge in the corner justifies an active bottom outflow of water (with sediments) depending on the prevailing wind, either along the shore to the south, or along the southern jetty to its seaward end.

The stability of the location and orientation of the scour hole is another argument in favour of the conclusion about the resulting transport of sediment from the upwind jetty to the downwind jetty, from south to north, towards the Baltiysk-Yantarny concavity.

V. ACKNOWLEDGEMENT

Authors thank colleagues from the Department of Coastal Engineering and Dynamics of the Institute of Hydroengineering of the Polish Academy of Sciences for providing the data for wave measurements for calibration of the model. Research and preparation of this article were supported by the Russian Science Foundation: the study of the dumping sites at the Vistula Spit, Ц by the Project No 14-17-00547, and the modelling of sediments transport near the dumping site on the northern shore of the Sambian Peninsula Ц by the Project No. 14-37-00047.

VI. REFERENCES

1. *Scheme of the Landslide and Shore Protection Actions on the Baltic Shore within the Kaliningrad Region*, Volume 1, Book 1. Natural and Hydrometeorological Conditions of the Kaliningrad Shore of the Baltic Sea. Svetlogorsk, 1999. 130 p.

2. V.A. Chechko, B.V. Chubarenko, V.L. Boldyrev, V.P. Bobykina, V.Yu. Kurchenko, D.A. Domnin, “On the Sea Coastal Zone Dynamics in the Area of Protective Breakwaters of the Kaliningrad Sea Channel”, *Water Resources,* Moscow. vol. 35, no 6, pp. 681-691, 2008.

3. V. Chechko, A. Sokolov, B. Chubarenko, D. Dikii, V. Topchaya, “Dynamics of sediments disposed in the marine coastal zone near the Vistula Lagoon inlet, south-eastern part of the Baltic Sea”, *Baltica*., vol. 28 (2), pp. 189–199, 2015.

4. B.V. Chubarenko, S.E. Navrotskaya, Zn.I. Stont, O.A. Gushin, "Variability of the Hydrometeorological Characteristics near the Shore of the South-Eastern Baltic Observations 1996-2009” in *The Basic Concepts of Modern Coast Use*, vol. IV, L.N. Karlin, M.B. Shilin and P.F. Brovko Eds. Saint-Petersburg: Russian State Hydrometeorological University, 2012, pp. 247 – 269.

5. A. Tornquist, *Geologie von Ostpreussen,* Berlin, 1910.

6. R. Brükmann, “Beodachtungen über Strand verschiebungen an der Küste des Samlands. III. Palmnicken*”, Schrift. Phys. ökonom. Ges. Jahrgang, Leipzig und Berlin*, vol. LIV, pp. 119-144,

1913.
7. B. Tidemann. *Uber Wandern des Sandes Kiistenraum des Samlandes.- Zeitschr*. Bauwesen: 1930, pp. 199-212.
8. O. Pratje *Der Verbleib des Abbruchsmaterials der Samlandkuste*. Schr. d. phys. okon. Ges. Konigsberg: 1932, pp. 5-50.
9. V.R. Boynagryan, "Dynamics and Morphology of the Sambia Peninsula", *Oceanology*, Moscow, vol. VI. Issue 3, pp. 458-465, 1966.
10. V.L. Boldyrev, V.P. Zenkovich, *"The Baltic Sea",* in *The Far East and the Shores of the Seas Surrounding the Territory of the USSR*. Moscow: Science, 1982. pp. 214-218.
11. V.L. Boldyrev, O.I. Ryabkova, "The Dynamics of Coastal Processes on the Kaliningrad Shore of the Baltic Sea", *Proceedings of the All-Union Geographical Society*, Moscow, vol. 133, Issue 5, pp. 41-49, 2001.
12. V.P. Zenkovich, "Some Features of the Polish Shore Dynamics of the Baltic Sea", *Transacts of the USSR Geographical Society,* Moscow, vol. 90, Issue 3, pp. 23-31, 1958.
13. R.Ya. Knaps, "Protecting Structures such as Breakwaters and the Sediment Movement on Sandy Shores", *Newsletter of the Latvian SSR Academy of Sciences, Riga,* No 6 (59). pp. 87-130, 1952.
14. R.Ya. Knaps, "Movement of Sediments near the Eastern Baltic Shore", in *Development under Oscillatory Movements of the Earth's Crust*. Tallinn: Valgurs, 1966. pp. 21-29.
15. V.L. Boldyrev, "Underwater Sand Bars as Indicators of the Longshore Sediment Transport" *Scientific Proceedings of the Institute of Oceanology of the USSR Academy of Sciences*. Moscow, vol. XLVIII. pp.193-201, 1961.
16. A.P. Agapov, L.A. Zhindarev, "Particle Size Distribution of Beach Sediments as an Indicator of the Sediment Movement Mechanism of in the South-Eastern Baltic Coastal Zone", *Lithology and Mineral Resources*, Moscow, No 6. pp. 105-111, 1990.
17. A.N. Babakov, *Spatio-Temporal Structure of Currents and Sediment Transport in the Coastal Zone of the South-Eastern Baltic Region (Sambia Peninsula and Curonian Spit).* Thesis of PhD in Geographical Sciences, Kaliningrad: Faculty of Geography of the Kaliningrad State University, 2003.
18. A.N. Babakov, "Wind-driven currents and their impact on the morfolithology at the eastern shore of the Gulf of Gdansk", *Archives of hydro-engineering and environmental mechanics*, Gdansk: Institute of Hydro-Engineering of Polish Academy of Sciences, vol. 57. no. 2. pp. 85 - 104. June 2010.
19. N.A. Bogdanov, V.A. Sovershaev, L.A. Zhindarev, A.P. Agapov, "The Evolution of Ideas about the Dynamics of the South-Eastern Shores of the Baltic Sea", *Geomorphology*. no 2. pp. 62-69. 1989.
20. A.V. Beloshapkov, .G. Beloshapkova, G.Kh. Brasavs, "Features of the Sediment Dynamics on the Western Coast of the Sambia Peninsula*"*, in *The Structure of the USSR Sea Shelf as a Basis for the Evaluation of Engineering and Geological Conditions. Collection of Research Papers of the All-Soviet Union Research Institute Morgeo*, Riga. 1984, pp. 42-45.
21. R. Ostrowski, Z. Pruszak, M. Skaja & M. Szmytkiewicz, "Variability of hydrodynamic and lithodynamic coastal processes in the east part of the gulf of Gdansk", *Archives of Hydro-*

Engineering & Environmental Mechanics, Gdansk: Institute of Hydro-Engineering of Polish Academy of Sciences, vol. 57 (2), pp. 139-153, 2010.
22. I.O. Leontiev, "Projection of the Shore Development in the Century Scale (by the example of the Vistula Spit)", *Oceanology,* Moscow, vol. 52. no 5. pp. 757-767, 2012.
23. O.I. Ryabkova, *The Dynamics of the Shore of the Sambia Peninsula and the Curonian Spit in the context of the Coastal Protection Problems*. Thesis of PhD in Geographical Sciences, Moscow: Faculty of Geography of the Moscow State University, 1987.
24. A.N. Babakov, "Characteristics of Near-Bottom Currents of the Gulf of Gdansk near the Entrance Breakwaters of the Port of Baltiysk According to Field Measurements', *Scientific Notes of the Russian Geographical Society (Kaliningrad Region),* vol. 7, part 1. Kaliningrad, 2008. pp. G1- G6.4.
25. *Hydrometeorological Conditions of the Vistula Lagoon*, N.N. Lazarenko and A. Maevsky Eds. Leningrad: Gidrometeoizdat, 1971, 330 p.
26. *Guidelines for Research and Calculation Methods and Sediment Movement and Coastal Dynamics in Engineering Surveying.* Moscow: Gidrometeoizdat, 1975. 240 p.

MODERN TECHNOLOGY IN DUNE COMPLEXES MONITORING ON THE VISTULA SPIT

Danchenkov Aleksandr, Atlantic Branch of Shirshov Institute of Oceanology RAS, Immanuel Kant Baltic Federal University, Kaliningrad, Russia

aldanchenkov@mail.ru

Modern technologies, which provide fast and accurate acquisition of high-resolution spatial data, have found widespread application in the monitoring of coastal processes. This paper reports the results of four years' monitoring of a huge deflation/blowout/wind-scour basin *dynamics* at the Vistula Spit (southeast coast of the Baltic Sea). Information about the volume and size dynamics together with deflation/accumulation schemes and 3D elevation maps is presented. Basing on the obtained results, forecast of the deflation basin dynamics for 2016 was proposed. This paper implements the Terrestrial Laserscanning (TLS) method to the coastal processes investigation and demonstrates its high potential in this field.

Key words: terrestrial laserscanning, coastal dunes, annual monitoring, high-resolution monitoring, the Baltic Sea coast

I. INTRODUCTION

Terrestrial laserscanning (TLS) as technology of rapid spatial data acquisition has achieved widespread use in the coastal processes monitoring. Advantages of TLS allow remote and high-precision surveying of complex and/or inaccessible structures. The TLS data received on-site could be easily integrated and analyzed using geographic information systems (GIS) and computer-aided design (CAD) software.

TLS was used for the annual monitoring of fore-dune morphology in 2012-2015. The study site represents an element of a dune complex with rapidly developing deflation basin located in the northwestern part of the Vistula Spit (southeastern coast of the Baltic Sea, Fig.1). The Vistula spit itself represents an accumulative sand body with two-side sand supply formed during sea transgression and located south-west of Sambian Peninsula.

Displacement of marine deposits in the north-south direction is observed along the coast of the Vistula Spit. Until 1958, Sambian peninsula cliff abrasion represented the main sand supply to the Spit, which was later on replaced by the overburden from Kaliningrad Amber Combine tailings. Construction of two piers (North and South) near Baltiysk city has changed the lithodynamics in some parts of the Vistula Spit. Longshore deposits move bypass the piers, thus being displaced in the seaward direction, and then return to the coastline at fifth kilometer of the Vistula Spit length, after which the coast is characterized by relative stability [1, 2]. Annual mean coast erosion at 2.5 kilometers from the South pier is estimated to be 2.2 meters per year [2]. Study site is located 1.98

kilometers from South pier, which corresponds to the area of sand deposits deficiency and coastal erosion.

High-precision TLS monitoring was accomplished in order to evaluate the deflation magnitude in the blowout basing of mixed natural and anthropogenic origin.

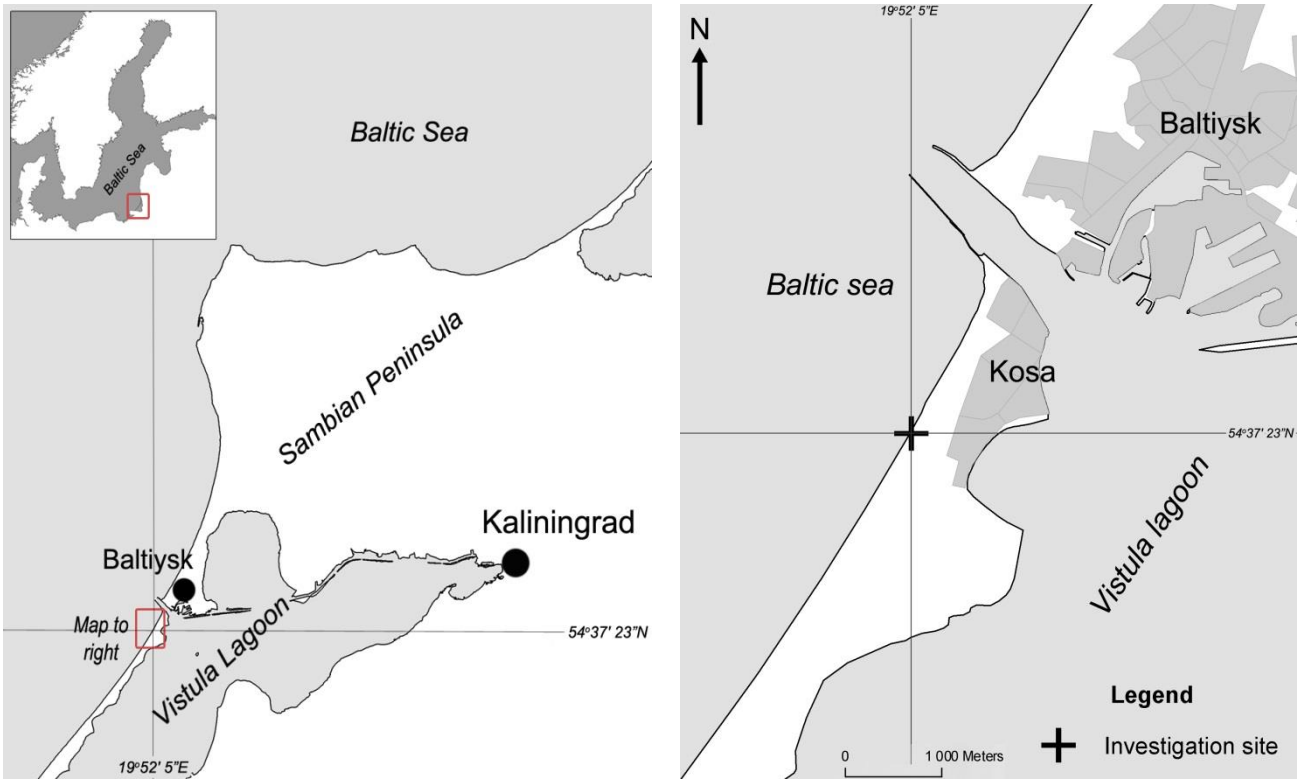

a) Regional scale b) Local scale

Figure 1. Study area. Cross on the right map indicates the location of the study site.

II. MATERIALS AND METHODS

Calculations was performed adapted from TLS data. TLS used early for the coastal processes investigation [3, 4, 5, 6]. Four TLS surveys were performed using two simultaneously operated topographic scanners Topcon GLS-1500 during the monitoring period 2012-2015. Surveys were carried out once in a year in the last week of June. Average point density was 64 points per square meter. Owing to the morphological changes occurred in the study area, the number of stations during each survey varied (24-27). Coordinate referencing was performed using satellite geodesic equipment: two Topcon GR-5 receivers were operated at the Real Time Kinematic (RTK) mode; corrections were received from the reference station in Kaliningrad.

Based on the obtained point clouds, triangular digital terrain models were created with ArcGIS software [reference]. According to these models, borders of the deflation basin were distinguished, and 3D models of dune complex were proposed. Raster digital terrain models with uniform grid (each cell contains information about the surface elevation) were built to estimate the elevation dynamics [7].

Annual volume change (V) in the basin was calculated as follows,

$$V = \sum \left(h_{i,t2} - h_{i,t1} \right) * c^2 , \quad (1)$$

where *h* represents cell elevation; *t1* and *t2* indices denote the elevation in the preceding year and in the year following the measurement; *c* represents length of the cell size.

Magnitude of the elevation change (Δh_i) was calculated (Eq.2) for each cell (*i*) in order to produce maps of relative deflation/accumulation.

$$\Delta h_i = h_{i,t2} - h_{i,t1} \quad (2)$$

III. Results and Discussion

Meteorological situation during the monitoring period was characterized by the following values of annual mean wind speed and direction (Table 1), which were obtained from the automatic hydrometeorological station (AHMS) «Baltiysk».

Table 1. Annual mean wind speed and direction during the monitoring period.

Year	Wind speed (m/s)	Direction
2012	4.2	240 °
2013	3.8	270 °
2014	3.3	195 °
2015	5.1	240 °

According to the high-water marks derived from the digital terrain models, deflation basin borders were defined and used to estimate the area of the basin and its dynamics (Fig.2).

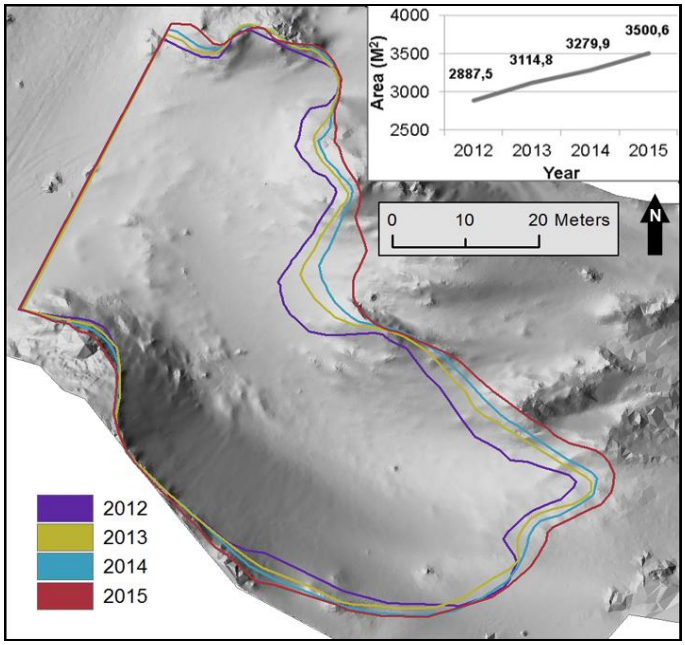

Figure 2. Deflation basin and its dynamics. Borders are depictured on the digital terrain model map of 2014.

Increase of the deflation basin was observed during the monitoring period. This expansion resulted from the reduction of residual foredune structures in the northern part of the basin and from the reduction of the sediment volume in the embryo dune field. Crowding of the borderlines indicates the relative stability of the corresponding sites, which is commonly associated with the presence of vegetation that traps the sand and stabilizes the surface against deflation. Basin axial size and the south border position have not changed much over the monitoring period. Basin area represents linear increasing trend with an average rate of 204 m^2 per year.

The selected spatial dataset was constrained to the maximum deflation basin borderline observed in 2015 and then used to calculate annual elevation change (Eq.2) and produce the corresponding 3D maps (Fig.3).

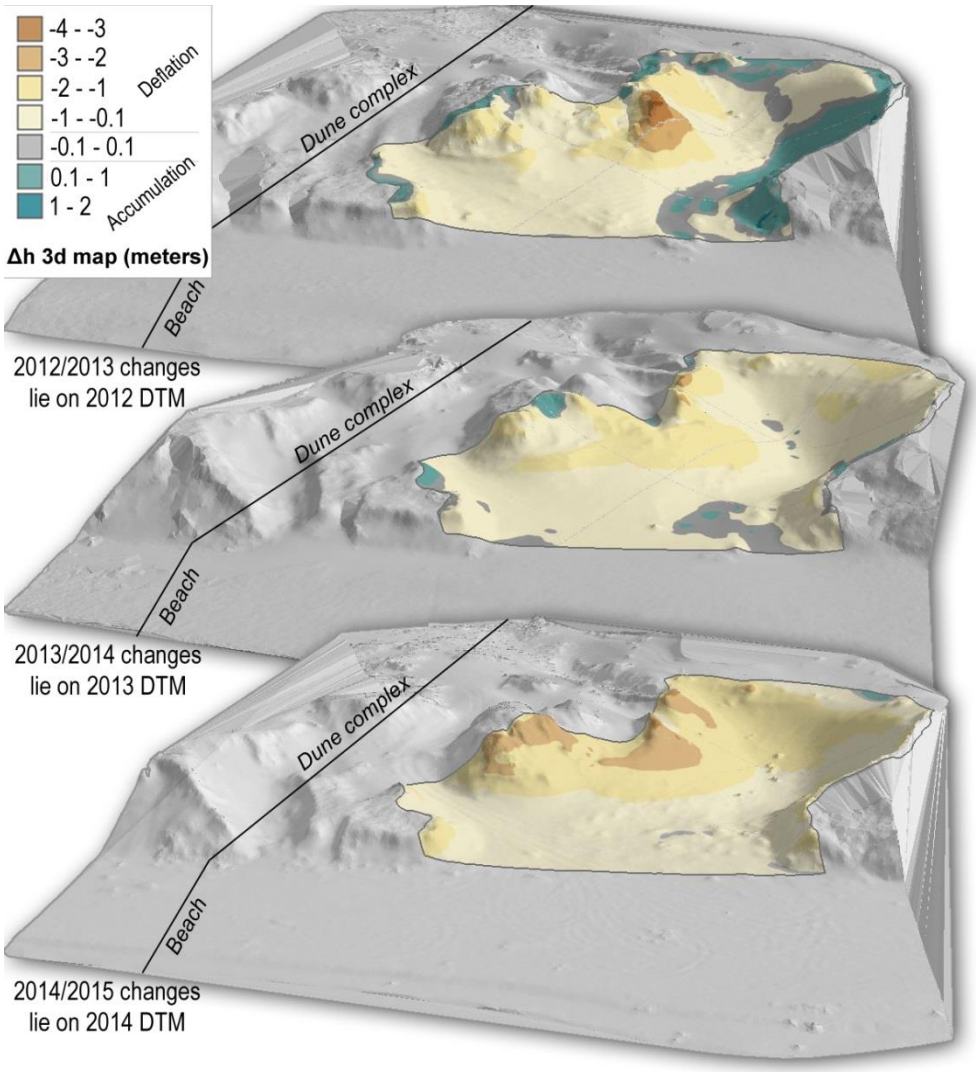

Figure 3. 3D maps of annual elevation change.

The rates of deflation and accumulation and their interannual variability were evaluated. Table 2 represents total volume of the deflation basin and the blowout volume rates.

Table 2. Total volume of the deflation basin and its dynamics

Year	Volume of the basin (m^3)	Blowout volume rate (m^3/year)
2012	7633	992
2013	8625	582
2014	9208	573
2015	9782	

Deflation basin volume increased during the monitoring period with the maximum rate of 992 m^3 per year observed in 2012-2013, which more than twice exceeded the rates in the subsequent years. This significant increase resulted from intense storm activity in autumn 2012. Strong south-west winds (up to 29 m/s) observed at the AHMS "Baltiysk" caused storm activity that affected the morphological structures. The blowout dynamics in the subsequent years was characterized by lower and relatively uniform rates.

According to the 3D maps of annual elevation change (Fig.3), there was a noticeable alternation of the deflation and accumulation processes over the monitoring period. In 2012-2013, the study site yielded noticeable areas of relative accumulation associated with gravitational processes at the south side of the basin, and eolian infill of several depressions and the eastern side of the basin, which caused flattening of the slope. At the same time, areas with intense deflation, which was apparently caused by the storm events, were present. In the following years, the number of accumulation zones decreased and were gradually replaced by the intensified deflation. Quantitative evaluation of these processes is possible through the calculation of deflation/accumulation volume per unit area (Table 4).

Table 3. Quantitative estimation of the processes in the deflation basin

	2012/2013	2013/2014	2014/2015	Average
Deflation, m^3/m^2	0.69	0.65	1.02	0,77
Accumulation, m^3/m^2	0.38	0.09	0.14	0,21
Balance, m^3/m^2	-0.31	-0.56	-0.88	-0.56
Active volume, m^3/m^2	1.08	0.74	1.16	0.99

Obtained results showed heterogeneity of the present-day dynamics of the deflation basin. Overall balance between the processes is negative during the whole period, indicating the prevalence and intensification of deflation processes over the decreasing rates of accumulation. Relatively high accumulation in 2012-2013 has subsequently decreased as a result of migration in the south-west direction.

Considering the dynamics of the basin area and the accumulation/deflation rates, a forecast of the deflation basin state for 2016 was proposed. Figure 4 represents the results of the prediction.

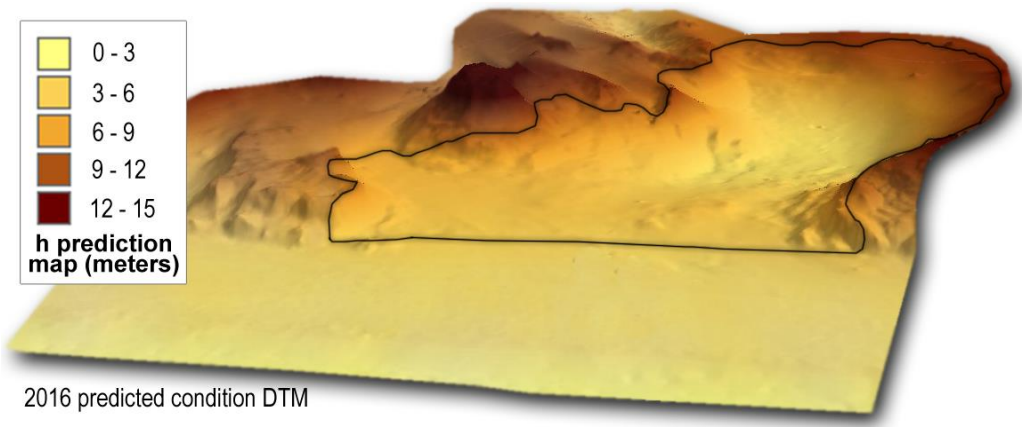

Figure 4. 3D map of the predicted elevation for the 2016.

Natural neighbor method was implemented to model the 3D elevation map. Predicted values of elevation change indicate possible flattening of the basin sides and overall increase of its size with the basin volume expansion of about 730 m^3 per year on the assumption of absence of strong storm events. Continuing deflation of the residual structures at the northern side and sand transport in south-west direction out from the basin is projected. Furthermore, neighboring structures are expected to be gradually drawn in the deflation process.

Overall condition of the basin, significant rate of deflation and its intensifying dynamics demand recovery measures. Consolidation of the residual structures, which are subject to significant destruction at the northern side of the basin, is necessary. It is strongly recommended to eliminate the access of motor transport and limit the walk-in accessibility to the site.

IV. Acknowledgment

The work was partly financed by the Russian Scientific Fund (grant 14-37-00047).

V. References

[1] Jyndarev L.A., 2009. Technogenic accumulative relief forms on a Southeastern baltic coast. *The creation and use of artificial land on the banks of reservoirs and water areas: Proceedings of International Conference*. Novosibirsk, pp. 187-196

[2] Bobykina V.P., Karmanov K.V., 2009 – Coastal dynamics of the Gdansk lagoon and relations with anthropogenic influence. *Proceedings of International Conference*. Novosibirsk, pp. 119-124

[3] Brizi E., Brunetti A., Martino S., Margottini C., Mazzanti P., Mugnozza G. S. 2015. Terrestrial Laser Scanning survey of the Sugano cliff (Orvieto, Italy) for slope stability analyses. *Rend. Online. Soc. Geol. It., Vol 35(2015)*, pp. 38-41.

[4] Montreuil A.-L., Bullard J., Chandler J. H, Millett J. 2003. Decadal and seasonal development of embryo dunes on an accreting macrotidal beach: North Lincolnshire, UK. *Earth Surface Processes and Landforms 38(15).*

[5] Dudzinska-Nowak J, Furmanczyk K. 2009. A laser scanning applications for volumetric changes of the beach and dunes analyses. *2nd International Conference on Climate Change -The environmental and socio-economic response in the southern Baltic region*, Szczecin.

[6] Danchenkov A.R., Belov N.S., 2015. Volumetric estimation of the storm impact on dunes complexes of the Curonian Spit, Baltic Sea. *Geology of seas and oceans: Proceedings of XXI International Conference on Marine Geology. Vol. IV*.: Moscow

[7] Li, Z., Zhu, Q. Gold, C., 2005, *Digital Terrain Modelling: Principles and Methodology*, CRC Press.

TO THE QUESTION OF THE IMPACT OF CLIMATE CHANGE ON THE ECOLOGICAL STATE OF ARTIFICIAL PLANTATIONS OF PITSUNDSKAYA PINE IN THE SEASIDE AREA OF GELENDZHIK

Derevenets Elizaveta, MBOU SOSh №2, Russia

svderevenets@yandex.ru

INTRODUCTION

Everything is interconnected in nature.

Forest areas have a beneficial effect on the composition of the air. In it turn the condition of forests greatly depends on the environment, including atmosphere. The air value can't be overestimated. It is a source of oxygen for our breathing a provider of carbon dioxide for photosynthesis. It is a heat keeper and a climate regulator. It is a habitat for flying beings. And it is chemical raw materials, a source of energy, utilization area and so on.

Different chemical substances are released into environment more and more. There are two main sources of the atmosphere pollution: natural and anthropogenic. Volcanoes, dust storms, wildfires and processes of decomposition of plants and animals are natural sources. Fuel and energy complex enterprises and transport are anthropogenic.

Gelendzhik is a resort town. There are not any industrial companies here. The main anthropogenic factor is transportation. Though Gelendzhik is still related to the cities with a favorable environmental condition, nature damage has already been done. It is due to the rapid increase of vehicles especially in summer. It is becomes evident from the condition of vegetation on Markhotsky ridge.

The relevance of the topic is connected with the fact that indicator species reveal the specific characteristics of the environment due to the anthropogenic load. State of the environment and air pollution sources are of great practical importance. Instrument control provides information about concentrations of pollutants that are presenting in the air at the moment, and plants like monitoring objects can be used to obtain the information about the duration of exposure to pollutants.

(Bioindication 1988)

The object of study: artificial forest plantations of pines along the "Don" federal high-way.

The subject of study: the effect of air pollution on the forest plantations of pines.

Purpose of the study: to study the effect of air pollution on the forest plantations of pines along the "Don" federal high-way.

Objectives of the study:

- to study the composition of the air and ins main pollutants;
- to study the scientific data on the indicative ability of Pitsundskaya Pine;
-to rate the transport effect on the condition of the pines

Technique: bioindication of a condition of the air environment on complex properties of Pitsundskaya pine, standard technique (assessment of the vital state of the forest according to condition of the pine)

Forest ecosystems reaction to adverse environmental conditions is shown in violation of the structure and function both of the entire system and individual components. These violations can be noticed by several sings, which can be seen when you look attentively at the natural object. Common signs of the condition of the forest ecosystemare:

- dryness and weakening of trees
- reducing of the size of the pine's needles compared to previous years
- premature yellowing and defoliation
- slowing of the growth of trees
- the appearance of the chlorosis and necrosis of needles and foliage, reducing of the lifetime of needles
- noticeable increase of trees damage due to diseases, different insects and fungi
- loss of forest communities tubular mushrooms and reducing of the species composition and strength of the plate mushrooms
- reducing of the species composition of epiphytic lichens (living on the trunks) and reducing of the coverage area of trunks with lichens.

These symptoms can be fixed without using of special instruments and scientific equipment. But to observe and evaluate the degree of danger it is necessary to have a starting point that is the normal condition of the ecosystems or some trees in undisturbed forest area.

To determine the life condition of the forest according to condition of the pine we have chosen the following factors:

1. Dechromatsiya (damage of the large coniferous arrays in the area of stable air pollution. These damages are assessed in four main classes. Each class corresponds to a certain percentage of needle loss.

Visual evaluation of forest stands can be carried according to the following scale:

- **0** – Healthy trees – It is allowed to have trees damage no more than 5% of the total tree;
- **1** – Weakened trees –it is allowed to have trees damage no more than 30-40% of needles, this can be a disease and insects branches, drying of individual branches, chlorosis and necrosis no more than 10% of needles or foliage of the tree.
- **2** – Heavily Weakened trees – openwork crown damage and drying of needles up to 60-70%, chlorosis and necrosis more than 10% of needles or foliage of the tree ;
- **3** – Drying trees – severally damage trees – more than 70-80% of needles, lack of the tree growth, chlorosis and necrosis , lifetime of needles no more than 1-2 years.

2. Yellowing is usually assessed in four classes:

0 – no Yellowing

1 – light Yellowing (the loss of coloring 10-25%);

2 – average Yellowing (25-60 %);

3 – strong Yellowing (more than 60 %).

3. Tree growth. Assessment is based on 4-point scale with intervals of 5 cm

- 0 - 15 см,

- 1 – 10 -15 см,
- 2 - 5 – 10 см,
- 3 – less than 5 см.

Each class corresponds to the average estimate of the number of years to complete extinction. 0 class – more than 20 years, 1 class – 10-20 years; 2 class – 3-9 years, 3 class – less then 3 years. To determine the class of damage and needles drying the scheme number 2 is used.

I. 1. Topography, Climate and vegetation features of the study area.

Coniferous forest, which is the object of study, is located on the Black Sea - facing slopes of Markhotsky ridge. According to the research of Kyznetsov and Figurovsky, it belongs to the Crimean-Novorossiysk province. There are a great number of cross narrow valleys, crevices with steep slopes, covered with forests. Description of the soil north-western part of the Black sea coast is shown in works of Zaharov and Gerasimov. Pitsundskaya pine mainly grows on the lower part of Markhotsky ridge along the "Don" federal high-way.

2. Accumulative properties of plants.

Living organisms have a tendency to accumulate pollutants from the environment. These organisms called bioindicators. They may have symptoms that indicate the presence of pollutants in the air.

Bioindication of a condition of the air environment on complex properties of plant is a method of scientific research.

Close to roads trees have the greatest capacity to absorb. Trees along 100-300 meters from road have a high level of accumulation of lead, zinc, nickel, copper and manganese.

II. An estimate of the impact of transport on the pine forest of Markhotsky ridge.

Pitsundskaya Pine (Pinus brutia var. Pityusa) responds to the environment pollution with technogenic products and reflects the overall level of pollution by chemical of different nature.

The assessment of a condition of pines was carried out during 6 years: from 2010 to 2015. For carrying out research we used 6 experimental grounds on the Markhotsky spine and 2 control grounds within the town. We investigated 24 trees on each platform, middle age of the trees were 30 - 40 years.

1. The first site: 70m above the sea level. Distance to the track – 30m.
2. The second site: 100m above the sea level. Distance to the track – 5m.
3. The third site: 90m above the sea level. Distance to the track – 15m.
4. The fourth site: 110m above the sea level. Distance to the track – 250m.
5. The fifth site: 2500m above the sea level. Distance to the track – 200m.
6. The sixth site: 120m above the sea level. Distance to the track – 200m.
7. The seventh site: 10m above the sea level. Distance to the track – 1km.
8. The eighth site: 10m above the sea level. Distance to the track – 1,5km.

III. The results of researchers.

1. An 2010 according to the obtained results from the sites №1,2,3 no more than 3 year left before the complete dying of the trees in the sites. The trees are severely weakened; they have openwork crown, damage and desiccation of needles, dry branches in the middle and upper parts of crown.

2011. The general condition of the pines has not improved. Both the number of necrotic spots and the speed of shrinkage have increased (8-30mm)

2012. This year was unusual because of the shower on the 6th of July in Gelendzhik (3 monthly norms of precipitation fell on this day). The number of tourists and transport was decreased. Thanks to those facts, the environmental situation along the track became more favorable and the condition of the pines became a little better.

2013. There were not any serious deterioration.

2014. Increasing off the number of necrotic spot, drying up of the tree crown, needles drying – 8-20cm; tree growth – no more than 10cm.

2015. The second site: excessive coverage necrotic spot, needles drying – 8-20cm. The fist site: trunks are damaged by insects (10%), strong drying of branches (25%).

2. On the test site №4 and №6 the pines condition was a little better. Assessment of the vital state of the pines – 6-9 years left before the complete dying of the trees of these sites. The needles were clean, almost without necrotic spots, but with some yellowing. There was a partial drying of the crown.

2011. Tree condition has not changed.

2012. Tree condition has not changed. And some tree condition has become better.

2013. The pine condition has remained at the same level.

2014. Compared with 2013 it was possible to observe a slight increase of needles drying (8-10mm), perhaps, because of the high temperature (the summer was very hot and dry, t – 48C)

2015. The pine condition has remained at the same level.

3. The most prosperous sites in 2010 were number 5, 7, 8 – 10-20 years left before the complete dying. №7, №8 – the trees are healthy, the needles were clean, and there was a good trees growth. №5 – there was a slight yellowing and needles drying (no more than 1-2mm). There was a slight necrotic coating and a slight decrease in growth.

2011. The trees condition has remained the same in the 7th and 8th site. But on 5th site the tree condition became worse.

2012. The tree condition was satisfactory. The number of yellow and drying needles decreased. (1-2mm) The tree growth – 15-20cm.

2013. The tree condition has remained at the same.

2014. An increase in the amount of yellowing and drying needles could be seen (1-5mm) and slight decrease of the tree growth (15-18cm).

2015. The tree condition has remained at the same level.

The results of the researches were compiled in the tables.

Conclusion.

The conditions of the trees in the pine forests, which are located close to the “Don” federal high-way, remain unsatisfactory. It is connected with intensive move on the high-way and big

number of tourists transport in summer and also with problem of global warming (summer temperatures has changed).

Gelendzhik is the city with a good ecological shape, but the damage to environment is already caused. If not to take measures, we can lose a unique part of the nature in the future, recreate it will be impossible.

Proposed measures of reduction of negative impact of exhaust gases:

1) to organize car parks outside the town during a holiday season;
2) social advertisement of neutralizer of gases on cars;
3) to organize sparing regimen of the traffic.

The results of the researches were referred to the environmental department of Gelendzhik administration.

Table with results of biomonitoring

Year of research	**2010**								**2011**								**2012**							
№ site	**№1**	**№2**	**№3**	**№4**	**№5**	**№6**	**№7**	**№8**	**№1**	**№2**	**№3**	**№4**	**№5**	**№6**	**№7**	**№8**	**№1**	**№2**	**№3**	**№4**	**№5**	**№6**	**№7**	**№8**
Dehromatsia	2	2	2	1	1	1	0	0	2	3	3	2	2	1	0	0	2	3	3	2	2	1	0	0
Yellowing	2	3	3	1	1	2	0	0	2	3	3	1	1	2	0	0	2	3	3	1	1	2	0	0
Tree growth	1	2	2	0	1	0	0	0	1	2	3	2	2	1	0	0	1	2	3	2	2	1	0	0
Assessment of the vital state	**3**	**3**	**3**	**1**	**1**	**2**	**0**	**0**	**3**	**3**	**3**	**2**	**2**	**2**	**0**	**0**	**3**	**3**	**3**	**2**	**2**	**2**	**0**	**0**

Year of research	**2013**								**2014**								**2015**							
№ site	**№1**	**№2**	**№3**	**№4**	**№5**	**№6**	**№7**	**№8**	**№1**	**№2**	**№3**	**№4**	**№5**	**№6**	**№7**	**№8**	**№1**	**№2**	**№3**	**№4**	**№5**	**№6**	**№7**	**№8**
Dehromatsia	2	3	3	2	2	1	0	0	2	3	3	2	2	1	0	0	2	3	3	2	2	1	0	0
Yellowing	2	3	3	1	1	2	0	0	2	3	3	1	1	2	0	0	2	3	3	1	1	2	0	0
Tree growth	1	2	3	2	2	1	0	0	1	2	3	2	2	1	0	0	1	2	3	2	2	1	0	0
Assessment of the vital state	**3**	**3**	**3**	**2**	**2**	**2**	**0**	**0**	**3**	**3**	**3**	**2**	**2**	**2**	**0**	**0**	**3**	**3**	**3**	**2**	**2**	**2**	**0**	**0**

REFERENCES

1. Alexeev V.A. “Assessment of the vital state of trees”
2. Alexeev V.A. // “Tree research”. 1989. -№ 4. - p. 51-57.
3. Alexeev V.A. “Metals in soil and plants”, 1987.
4. V.V.Batoian, N.S.Kasimov // Research of biochemical laboretory 1990. p. 108-124.
5. Gerasimov I.P., “Soil of Kavkaz”, 1952г.
6. N.I.Kyznetsov “Crimean-Novorossiysk province research”
7. Maleev V.N. “Geobotanic”, 1946г.
8. eugenyshultz.livejournal.com

PROBLEM OF HEAVY METAL SURFACE SEDIMENT CONTAMINATION IN THE EASTERN GULF OF FINLAND

Derugina N.O., A.P.Karpinsky Russian Geological Research Institute (VSEGEI), Saint-Petersburg State University, Russia
Grigoriev A.G., A.P.Karpinsky Russian Geological Research Institute (VSEGEI), Russia
Ryabchuk D.V., A.P.Karpinsky Russian Geological Research Institute (VSEGEI), Saint-Petersburg State University, Russia
Rybalko A.E., State Company «Sevmorgeo», Russia
Zhamoida V.A., A.P.Karpinsky Russian Geological Research Institute (VSEGEI), Saint-Petersburg State University, Russia

natalyderugina@gmail.com

This project defines the pre-industrial quantities of heavy metals in sediment sequences of the Late Holocene from the Eastern Gulf of Finland. A comparative analysis reveals differences and similarities in the current concentrations of heavy metals in bottom sediments and pre-industrial levels. It is found that the maximum concentrations of heavy metals in the bottom sediments of the Gulf of Finland and Neva Bay occurred in the period of 1950-1990. Since the 1990s, the trend has been a slow decline in the contamination levels; however, the concentrations of some heavy metals in bottom sediments remain high.

Key words: sediments, Gulf of Finland, sediment contamination, heavy metals.

I. Introduction

Heavy metals and chemical toxicants are known to accumulate in different components of marine environments, causing vital changes in biological species and damage to the ecosystem. Because they can potentially migrate from sediments to water, sediment contamination is among the most urgent problems requiring ecological and geological research.

The Gulf of Finland is exposed to heavy metal pollution from adjoining urban areas. To preserve the ecosystem of the Baltic Sea, it is necessary to continuously monitor and evaluate the state of the environment. The problem is especially urgent for the easternmost part of the Gulf of Finland, where in the late 1990s, the concentrations of most heavy metals were extremely high [10, 13, 14].

Today, there are no established ecological sediment quality criteria in Russia, despite such indicators having already been developed by many other countries and organizations.

In developing such criteria, the pre-industrial quantities of heavy metals, representing a natural state in sedimentary sequences, and their relation to palaeoenvironmental settings have become the most important topics.

II. Materials and methods

The sediments of the eastern Gulf of Finland have been the subject of many scientific studies and of monitoring over the last two decades. Ecological and geological surveys in the Russian part of the Gulf of Finland were held in the 1990s within the framework of national projects and international expeditions, such as the Baltic Marine Ecological Patrol (MEP). Within the context of the project State Monitoring of geological environment of the Russian part of Baltic Sea, the state company "Sevmorgeo" and the A.P. Karpinsky Russian Geological Research Institute "VSEGEI" conducted annual sediment sampling within the Gulf of Finland (35-38 sites) and Neva Bay (34 sites) from 2005 to 2015. Sediment sampling was conducted using a grab sampler and box-corers, which made it possible to obtain qualitative data and stratified sediment samples. Analytical investigations included the determination of heavy metal concentrations in surface sediments. Consequently, a unique database was collected comprising records of the state of surface sediments in the eastern Gulf of Finland [2, 3, 4, 5, 6, 7]. In addition, undisturbed sedimentary sequences (length 50-60 cm, using the Niemistö gravity corer) from areas of silty clay accumulation, which were recovered during the joint projects of VSEGEI and GTK (Geological Survey of Finland), and their detailed sampling and chemical analyses [14, 15, 16] revealed the vertical distribution of heavy metals in bottom sediments in different sedimentation basins of the eastern Gulf of Finland.

Surface sediments, collected within the framework of the geological monitoring project, were analysed by semiquantitative optical emission spectral analysis (27 elements, including Co, Ni, Cu, Pb, Zn, Cr and V). ICP-MS was used for chemical analyses of Cd and As.

III. Results and discussion

Silty clay sediments are known to intensively absorb and accumulate heavy metals and pollutants; their deposition occurs in local sedimentation basins in the eastern Gulf of Finland. These basins are located in depressions of bottom relief at depths varying from 4-5 m in Neva Bay to 50-60 m near Gogland Island. The depressions are separated by raised bottom areas, characterized by a prevalence of erosion processes, transit, a lack of sedimentation and the formation of coarse-grained sediments, sands and mixed sediments. In the framework of the presented study, six sedimentation basins (including the Neva Bay sedimentation basin) were distinguished by their differences in bathymetry, their source of incoming material and the specifics of their hydrochemical regime (Fig. 1).

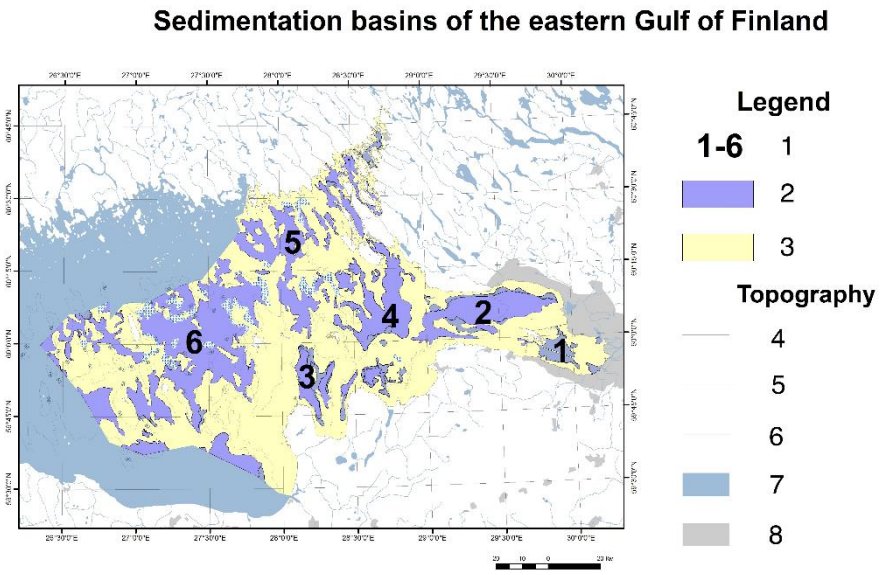

Fig. 1 Sedimentation basins of the Eastern Gulf of Finland: 1- sedimentation basins (1 - Neva Bay, 2 - Kyrortny basin, 3 - Koporsky and Luzhsky basin, 4 – Berezovy basin, 5 – Vyborg basin, 6 – Deepwater basin), 2 – silty clay sediments, 3 – other sediments, 4 – coast line, 5 – isobaths, 6 – rivers, 7 – water areas, 8 – urban areas.

Published data on the vertical distribution of heavy metals in the upper 50-60 cm of soft silty-clay mud [14, 15, 16] allowed us to calculate the pre-industrial values for each sedimentation basin (excluding the "Kurortny" basin), obtained from intervals from 25-30 cm to 40-60 cm depending on the sedimentation rate. The concentration curves show a drastic increase in the concentration of heavy metals in the intervals corresponding to the 1950-1990s. Underlying sediments were interpreted as representing a "natural state" and assumed to be unaffected by human activities. The pre-industrial quantities of heavy metals and their relation to the environmental quality criteria developed by Swedish Environmental Protection Agency [12] are shown in Tab. 1 and Fig. 2.

It is worth noting that some of these values match classes 2 and 3 of the Swedish sediment quality criteria ("low" and "moderate" level of pollution) (Tab. 1). When analysing the technogenic impact, it is necessary to take this aspect into account. Elevated levels of most of the examined elements are specific for the northwestern basins. The highest pre-industrial values of Zn, Ni, As, Co, Cr and V apply to the bottom sediments of Vyborg and that of Cu applies to the Beresovy sedimentation basin (Fig. 2). These features are most likely caused by the geological structure of the eastern Gulf of Finland. Sedimentation basins in the northern part of the Gulf are associated with the crystalline basement of the Baltic Shield. The eroded material from the rocks of the shield appears to be a source of a wide range of chemical elements transported to the basins. Apparently, this case is an example of natural enrichment of the bottom sediments. Reduced levels of heavy metals are noted for the sediments of the Koporsky and Luzhsky basins, where supply results from the rocks of the sedimentary platform, which are significantly less enriched with ore elements [1].

Tab. 1 Pre-industrial concentrations of heavy metals in sediments in comparison with Swedish sediment quality criteria.

	Pb mg/kg	As mg/kg	Zn mg/kg	Cu mg/kg	Ni mg/kg	Co mg/kg	Cr mg/kg
Neva Bay	48,3	1,27	94,3	18,4	16,5	9,41	43,1
Koporsky and Luzhsky basins	17,4	7,58	76,7	17,8	26,7	11,65	47,55
Berezovy basin	30,9	7,2	100,3	45,8	28,9	13,7	67,5
Vyborg basin	30,7	17,1	139	33,9	39,7	17,65	87,7
Deepwater basin	27,2	9,5	121,3	27,9	33,5	14,3	68,2
Class 1	None						
Class 2	Low						
Class 3	Moderate						
Class 4	High						
Class 5	Very high						

Based on the geochemical data acquired during annual monitoring from 2012-2015 by Sevmorgeo and VSEGEI, average heavy metals concentrations were calculated for different sedimentation basins. This interval was proposed due to it having the most complete database (Fig. 3).

Comparative analysis shows that the concentrations of all of the studied elements in surface sediments exceed those in the pre-industrial deposits. The most significant increases occurred in As, Zn and Cu. Generally, for the modern and pre-industrial sediments, enhanced values are inherent for northern basins, pointing toward the essential contribution of natural processes in the geochemical specialization of modern silty clay accumulation.

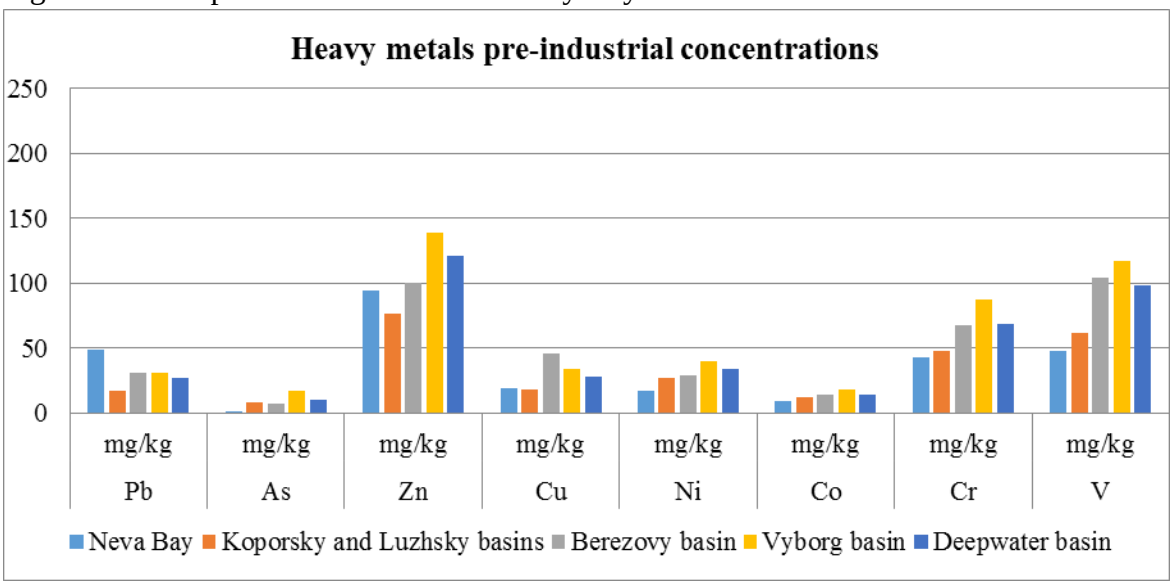

Fig.2 Heavy metals pre-industrial concentrations

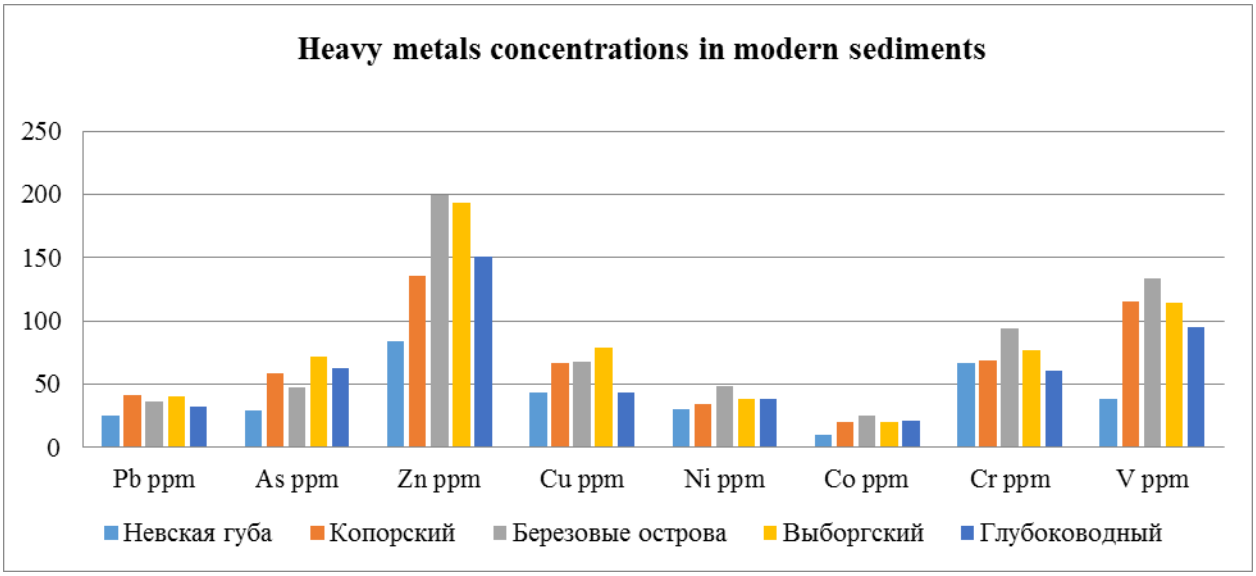

Fig.3 Heavy metals concentrations in modern sediments

In comparison with pre-industrial levels, the concentrations of arsenic increased significantly. Maximum concentrations were found in the Vyborg basin, where values raised from 17 ppm in pre-industrial sediments to 71 ppm in modern deposits.

The concentration of zinc increased in comparison with pre-industrial values in all sedimentation basins. However, the maximum pre-industrial levels existed in the northern and western areas, whereas now peak concentrations are distinctive for the area of the Berezovy basin.

The concentration of lead increased in the Koporsky and Luzhsky basins in modern soft sediments, whereas it decreased in Neva Bay. This result requires additional investigation. The underlying interval of the sequence 05-NG-9 (26-38 cm), representing significantly lower levels of heavy metals than in the "industrial" interval of 1950-1990s, have probably not reached the "natural" state for sediments of this basin. Generally, in the surface sediments of the eastern Gulf of Finland, concentrations of lead for different basins are quite similar, perhaps, due to the enhanced mobility of this element.

The maximum levels of copper in the pre-industrial levels were fixed in the sedimentation basin "Berezovy". In the surface sediments, peak values were noticed in the central part of the bay – i.e., the "Koporsky and Luzhsky basins", the "Vyborg" basin and the "Berezovy" basin.

The changes in the concentrations of Co and Ni were insignificant in comparison with pre-industrial values. Peak levels moved south from the Vyborg area to the "Berezovy" basin. The same trend was observed on the figures for chromium and vanadium; however, these values increased in comparison to pre-industrial intervals.

Summarizing the obtained results, we can conclude that the maximum concentrations of Zn, Ni, Co, Cr and V shifted south from the Vyborg basin to the "Berezovy" area. During the pre-industrial period, the distribution of elements was controlled by geological and physiogeographical settings, whereas today a huge role is assigned to human activities. A huge harbour, a variety of waterways and shipping channels are located in the "Berezovy" area, influencing the content of heavy metals in sediments.

When conducting a comparative analysis, attention was paid to the elevated levels of most elements in the northern basins in the modern and pre-industrial periods, whereas reduced levels were noticed in Neva Bay and the "Koporsky and Luzhsky basins". It is worth noting that the study from the 1990s revealed the opposite result – maximum concentrations were fixed in the eastern part of the bay (Neva Bay and the Kurortny district).

The determined patterns indicate a reduction in the anthropogenic load in the eastern Gulf of Finland over the last decade and the essential contribution of natural components to modern sedimentation processes.

A diagram showing annual geochemical data for sedimentation basins collected during monitoring in 2005-2015 is presented at Fig. 4.

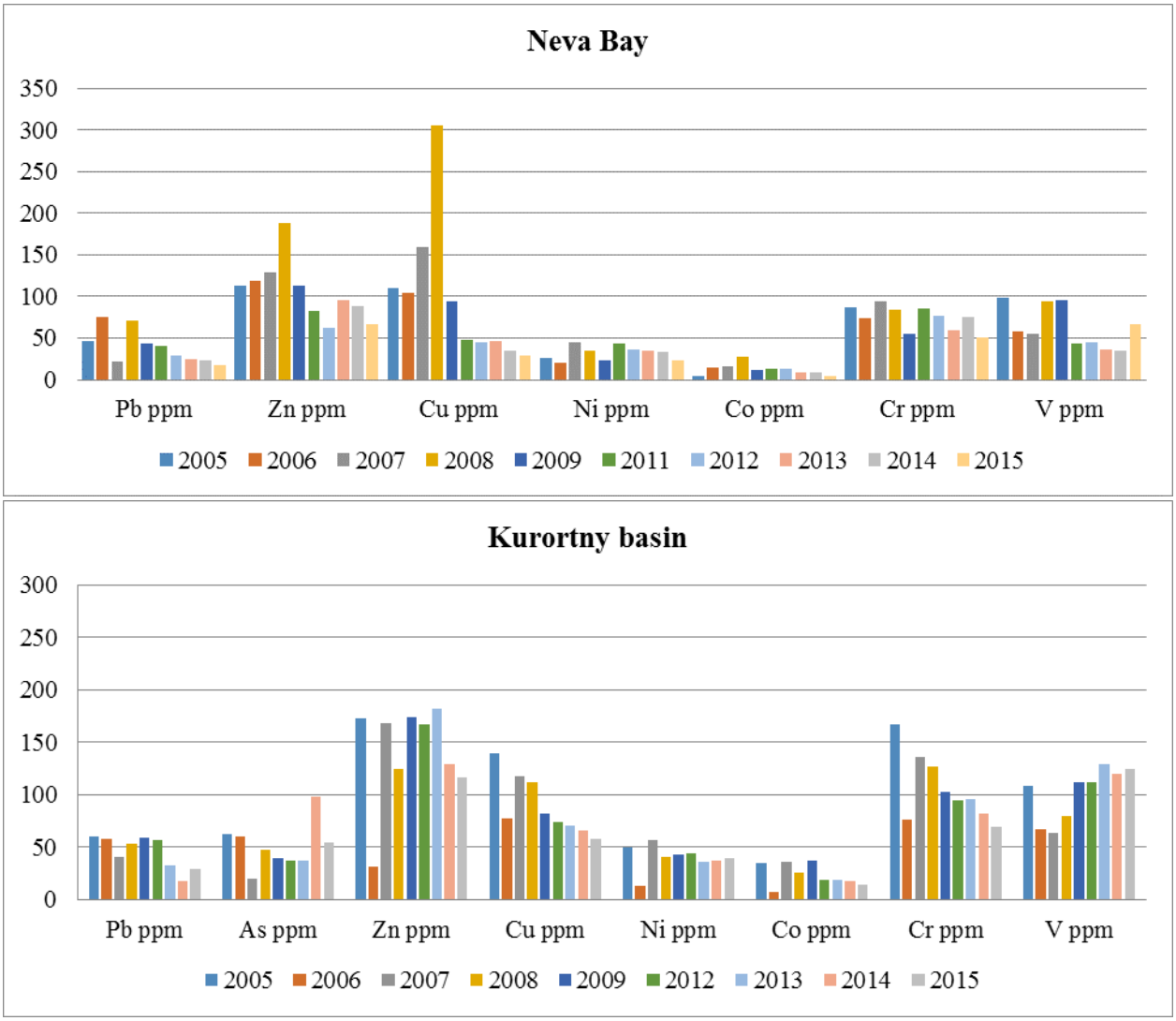

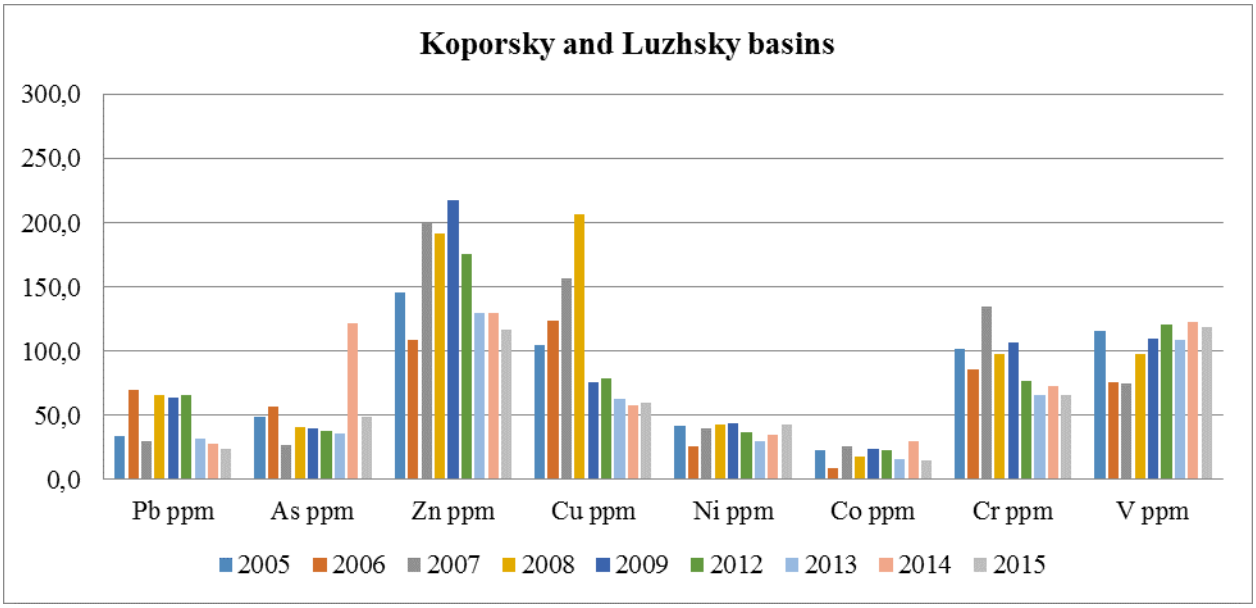
Koporsky and Luzhsky basins
300,0
250,0
200,0
150,0
100,0
50,0
0,0
Pb ppm
As ppm
Zn ppm
Cu ppm
Ni ppm
Co ppm
Cr ppm
V ppm
2005
2006
2007
2008
2009
2012
2013
2014
2015

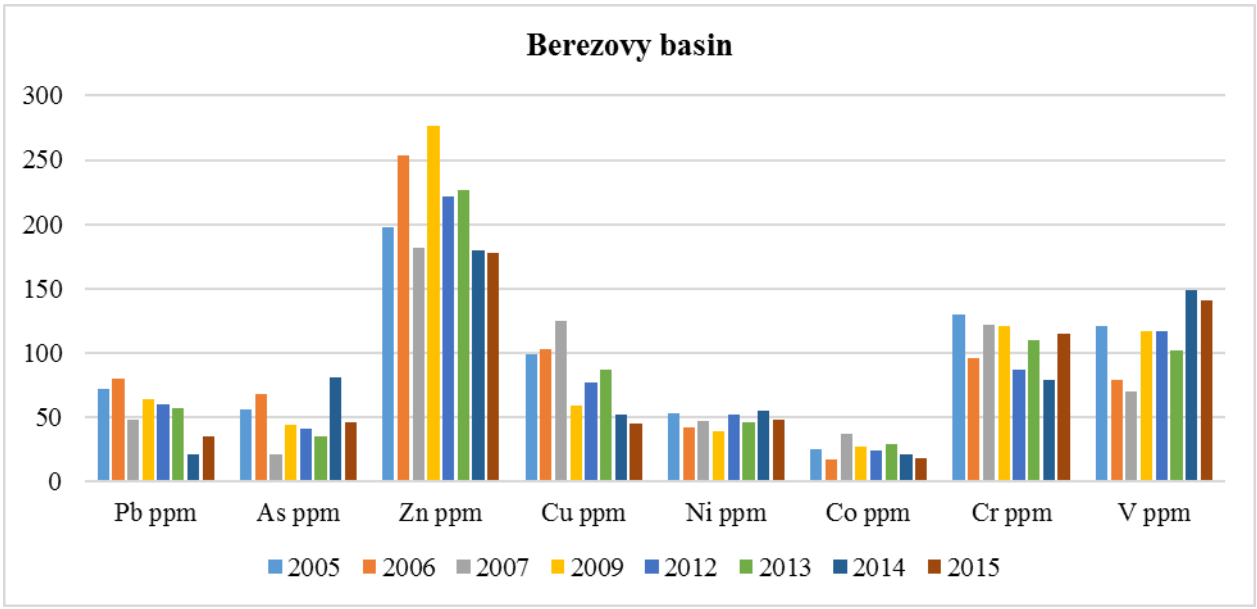
Berezovy basin
300
250
200
150
100
50
0
Pb ppm
As ppm
Zn ppm
Cu ppm
Ni ppm
Co ppm
Cr ppm
V ppm
2005
2006
2007
2009
2012
2013
2014
2015

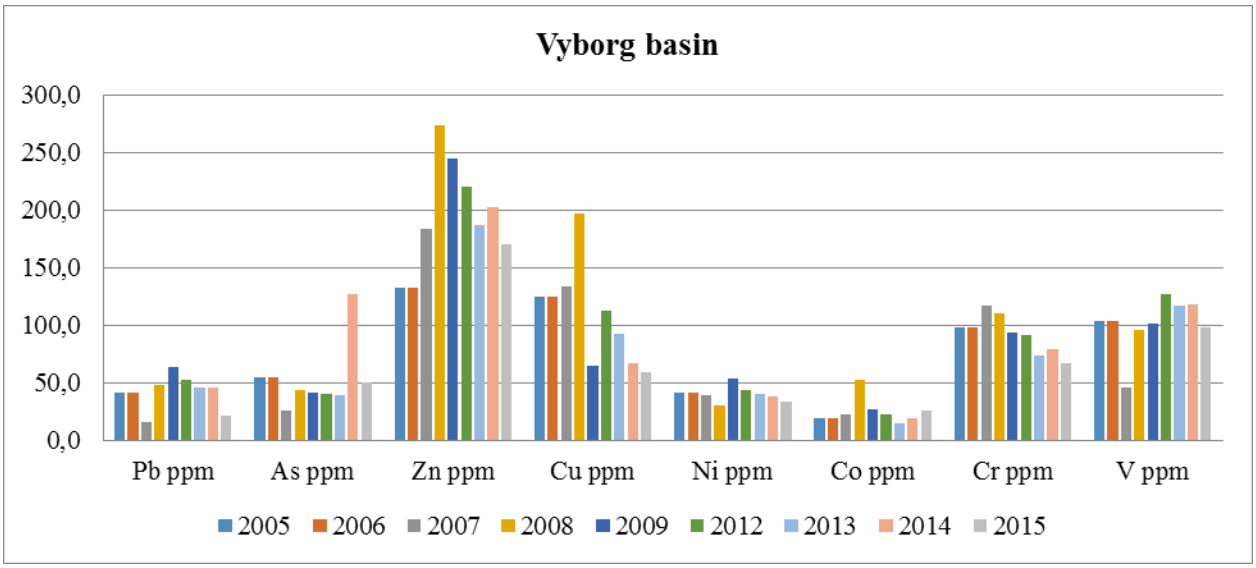
Vyborg basin
300,0
250,0
200,0
150,0
100,0
50,0
0,0
Pb ppm
As ppm
Zn ppm
Cu ppm
Ni ppm
Co ppm
Cr ppm
V ppm
2005
2006
2007
2008
2009
2012
2013
2014
2015

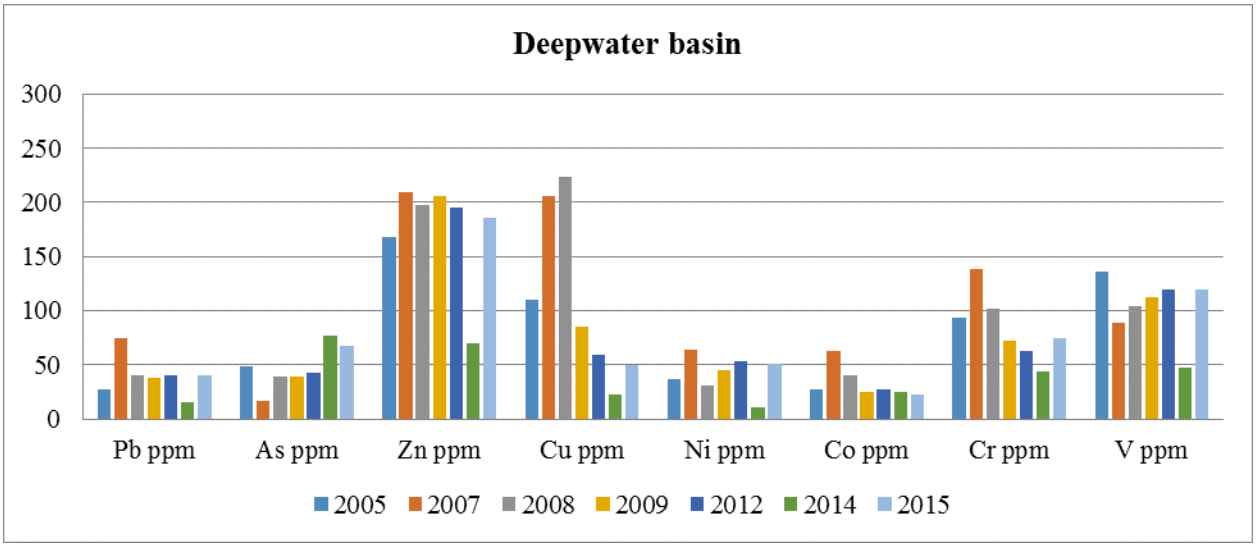

Fig. 4 Average concentrations of heavy metals in sediments during monitoring program

Based on the results of the annual investigations, it is possible to make several conclusions. In almost all basins, a sharp increase in the concentrations of heavy metals occurred in 2007-2009. This elevation was traced most clearly in Neva Bay; nevertheless, high concentrations were noticed in the other basins. Due to hydro technical work held in 2006-2008 (dredging, underwater dumping, new territories creation etc.), the water became oversaturated with suspended matter, which led to the secondary pollution of water and deposits by underlying sediments.

In Neva Bay, the average concentrations of metals, except Cu, decreased during the studied interval. The content of lead has gradually decreased over the past ten years from classes “high” and “moderate” to “none”. Ni reached class 3, “moderate”, in 2007 and 2011, Co did so in 2008. Other elements did not exceed the first two contamination levels [11]. The concentrations of Cu exceeded level 3 pollution during the previous nine years of investigations and decreased in 2015 to class 2, “low”.

In the sedimentation basin “Berezovy”, slight decreases in Pb, Zn, Cu and Co concentrations were noticed. Other elements show stable levels, except V, the concentration of which increased during the monitoring program. According to Swedish quality criteria, all values exceeded the third level of pollution.

Within the project, a decline in the concentrations of Pb, Zn, Cu, Co and Cr occurred in the Kurortny, Koporsky and Luzhsky basins. The vanadium content was slightly elevated, whereas the other elements remained on the same levels.

The Vyborg and Deepwater basins are characterized by enhanced levels of As, Zn and Co. In the Vyborg basin, the values of Pb, Zn, Cu, Ni and Cr have decreased over the last ten years, whereas the patterns of other elements remained constant. The Deepwater basin is distinctive for its permanent concentrations of most of the studied elements; nevertheless, the decline in Cu, Cr and Co values was fixed.

A comparison of average concentrations in different sedimentation basins of the Gulf of Finland with the Swedish sediment quality criteria is shown in Tab. 2.

Table 2. Average concentrations of heavy metals in sediments during the monitoring program in comparison with Swedish sediment quality criteria

Neva Bay

	Pb ppm	Zn ppm	Cu ppm	Ni ppm	Co ppm	Cr ppm
2005	46	113	110	26	5	87
2006	75,5	119	104,5	21	14,5	73,5
2007	21,5	128,5	160	45	16	94,5
2008	71	188	305	35	27	84
2009	43	113,5	94	23,5	11,5	55
2011	40,05	82,05	48,15	43,9	13,45	85,65
2012	29,6	62	44,8	36	13	77
2013	24	95	47	35	8,5	59
2014	23	88	35	34	9,1	75
2015	17	66,5	29,5	23,5	4	50,5

Berezovy basin

	Pb ppm	As ppm	Zn ppm	Cu ppm	Ni ppm	Co ppm	Cr ppm
2005	72	56	198	99	53	25	130
2006	80	68	254	103	42	17	96
2007	48	21	181	125	47	37	122
2009	64	44	276	59	39	27	121
2012	60	41	222	76,5	52	24	87
2013	57	35	226	87	46	29	110
2014	21	81	180	52	55	21	79
2015	35	45,5	177,5	45	48	18	115

Vyborg basin

2005	41	54	133	125	41	19	98
2006	41	54	133	125	41	19	98
2007	16	25	184	134	39	22	117
2008	48	44	274	197	30	52	111
2009	64	41	245	65	53	26	94
2012	53	40	220	113	43	22	92
2013	46	39	187	92	40	14	74
2014	45	127	202	67	38	19	79
2015	21	51	170	59	33	26	67

Deepwater basin

2005	28	49	168	110	37	27	94
2007	74	17	209	206	64	63	139
2008	40	40	197	224	31	41	102
2009	38	40	206	85	45	25	72
2012	40	43	196	60	54	27	63
2014	16	77	70	22	11	25	44
2015	41	67	186	50	51	23	75

Kurortny basin							
2005	60	63	173	140	50	35	168
2006	59	60	32	78	14	7	76
2007	41	20	168	118	57	36	136
2008	53	48	124	112	40	26	126
2009	59	39	174	82	43	37	103
2012	57	38	167	75	45	19	95
2013	33	38	182	71	36	19	96
2014	17	98	130	66	37	18	82
2015	29	55	116	57	39	14	69
Koporsky and Luzhsky basins							
2005	34	49	146	105	42	23	102
2006	70	57	109	124	26	9	85
2007	30	27	201	157	40	26	135
2008	66	40	192	206	43	18	97
2009	64	40	218	76	44	24	107
2012	66	37	175	79	37	22	77
2013	32	36	129	63	30	16	66
2014	28	122	130	58	35	30	73
2015	24	49	116	60	43	15	66
Class 1	None						
Class 2	Low						
Class 3	Moderate						
Class 4	High						
Class 5	Very high						

Concentrations of arsenic reach a “very high” level of pollution in the different time spans over the entire area of the bay. Ferromanganese concretions, widespread in the eastern Gulf of Finland, tend to absorb chemical elements such as arsenic [8]. As stated by ref. [8] the coefficient of concentration of arsenic in ferromanganese nodules can reach 31.2, which exceeds the geochemical background of the territory more than 30 times. This feature explains elevated values of As in sediments. A similar trend is observed for Cu.

In the last years of monitoring, the concentrations of Pb and Cr decreased in all basins (except “Berezovy”), reaching the lowest levels of pollution, according to SEPA.

IV. Conclusions

Based on the investigation of the distribution of heavy metals in the bottom sediments of the eastern Gulf of Finland, the following conclusions can be made:

1. The concentrations of all studied elements in the surface sediments of the sedimentation basins of the eastern Gulf of Finland exceed pre-industrial levels.

2. According to Swedish EPA the most polluted basin is “Berezovy”. Almost all measured values fall in the range from three to five contamination levels.

3. When comparing the general distribution pattern in bottom sediments during the pre-industrial epoch and today, it is worth noting that increased concentrations of most studied elements are specific to the northwestern sedimentation basins, whereas reduced levels are distinctive for Neva Bay and the "Koporsky and Luzhsky basins". This feature is suggested to indicate the difference in the geochemical composition of the sources of incoming material for these sedimentation basins.

4. A study of average concentrations in different sedimentation basins in the pre-industrial and modern periods reveals a curtain variation in the distribution trend. Maximal concentrations of Zn, Ni, Co, Cr and V moved south from Vyborg basin to "Berezovy" basin, which points toward a significant anthropogenic load.

5. Investigations carried out in the 1990s, indicating that the maximal concentrations of heavy metals prevailed in the eastern part of the Gulf of Finland (Neva Bay and the Kurortny basin), lead us to conclude that the sources of pollution in that period of time were industrial and domestic wastewaters of Saint Petersburg.

6. Intense dredging in 2006-2008 caused secondary pollution of waters and deposits with underlying sediments, marked by a drastic increase in the content of heavy metals.

7. A trend of improvement of decreasing levels in the content of heavy metals is observed in all sedimentation basins during the last several years.

Acknowledgements. This research was undertaken in the framework of the project of State monitoring of geological environment of the Russian Baltic, White and Barents Seas. The authors thank the captain and the crew of R/V "Risk" and colleagues from the Department of Marine and Environment Geology, who participated in field work – N.B. Malysheva, I.A. Neevin, O.V. Dron. Part of the analytical work was carried out in the Research Park of St. Petersburg State University (project 103-6002).

V. References

1. Atlas of geological and geoecological maps of the Russian part of the Baltic Sea. 2010. Ed. Petrov, O.V. SPb.: VSEGEI, 78 p. [Атлас геологических и эколого-геологических карт Российского сектора Балтийского моря. Гл. ред. О. В. Петров. СПб.: ВСЕГЕИ, 2010, 78 с.]

2. Information Bulletin N9. State of geological environment of the continental shelf of the Baltic, White and Barents seas. Sevmorgeo, St.Petersburg, 2007. 55 p. [Информационный бюллетень N9 о состоянии геологической среды прибрежно-шельфовых зон Баренцева, Белого и Балтийского морей. Севморгео, Санкт-Петербург, 2007. 55 с.]

3. Information Bulletin N10. State of geological environment of the coastal zone of the Barents, White and Baltic seas. Sevmorgeo, St.Petersburg, 2008. 51 p. [Информационный бюллетень N10 о состоянии геологической среды прибрежно-шельфовых зон Баренцева, Белого и Балтийского морей. Севморгео, Санкт-Петербург, 2008. 51 с.]

4. Information Bulletin N11. State of geological environment of the coastal zone of the Barents, White and Baltic seas. Sevmorgeo, St.Petersburg, 2009. 58 p. [Информационный бюллетень N11 о состоянии геологической среды прибрежно-шельфовых зон Баренцева, Белого и Балтийского морей. Севморгео, Санкт-Петербург, 2009. 58 с.]

5. Information Bulletin. State of geological environment of the coastal zone of the Barents, White and Baltic seas 2011. Ed. Petrov, O.V., Lygin A.M., SPb.: VSEGEI, 2012. 80 p. [Информационный бюллетень о состоянии геологической среды прибрежно-шельфовых зон Баренцева, Белого и Балтийского морей в 2011 г. /Под ред. О.В.Петрова, А.М.Лыгина. СПб.: Картографическая фабрика ВСЕГЕИ, 2012. 80 с.]

6. Information Bulletin. State of geological environment of the coastal zone of the Barents, White and Baltic seas 2012. Ed. Petrov, O.V., Lygin A.M., SPb.: VSEGEI, 2013. 112 p. [Информационный бюллетень о состоянии геологической среды прибрежно-шельфовых зон Баренцева, Белого и Балтийского морей в 2012 г. /Под ред. О.В.Петрова, А.М.Лыгина. СПб.: Картографическая фабрика ВСЕГЕИ, 2013. 112 с.]

7. Information Bulletin. State of geological environment of the coastal zone of the Barents, White and Baltic seas in 2013. Ed. Petrov, O.V., Lygin A.M., SPb.: VSEGEI, 2014. 136 p. [Информационный бюллетень о состоянии геологической среды прибрежно-шельфовых зон Баренцева, Белого и Балтийского морей в 2013 г. /Под ред. О.В.Петрова, А.М.Лыгина. СПб.: Картографическая фабрика ВСЕГЕИ, 2014. 136 с.]

8. Grigoriev A.G., Zhamoida V.A., Comparison of the sorption properties of the shelf (Gulf of Finland) and oceanic ferromanganese concretions// Ocean and marine geology: Materials of XVIII International Conference on Marine Geology V. II 2009, 258-262 pp. [Григорьев А. Г., Жамойда В. А. Сопоставление сорбционных свойств шельфовых (Финский залив) и океанических железомарганцевых конкреций // Геология морей и океанов: Материалы XVIII Международной научной конференции (Школы) по морской геологии, Т. II, 2009, с. 258-262.]

9. Rybalko A.T., Fedorova N.K., Fokin D.P., et al, Change in geochemical structure of bottom sediments in the eastern Gulf of Finland and it's bays under elevated anthropogenic load from 2005 to 2009. // XI International ecological forum "Baltic Sea day", SPb: Maxi-Print, 2010, pp. 186-187. [Рыбалко А.Е., Федорова Н.К. Фокин Д.П. и др. Изменение геохимической структуры донных отложений восточной части Финского залива и его губ под воздействием возросшего антропогенного воздействия за период с 2005 по 2009 г.г. // XI Международный экологический форум «День Балтийского моря». Сборник материалов. СПб ООО «Макси-Принт», 2010. с.186-187]

10. Rybalko A.T., Spiridonov M.A., Opekunov A.Y. et al Lithological and geochemical characteristics of bottom sediments // Gulf of Finland under anthropogenic load, SPb: RAN INOZ, 1999 [Рыбалко А.Е., Спиридонов М.А., Опекунов А.Ю. и др. Литолого-геохимическая характеристика донных осадков //Финский залив в условиях антропогенного воздействия. СПб, РАН ИНОЗ, 1999.]

11. Ryabchuk D., Vallius H.,Malysheva N., Kotilainen A., Zhamoida V., Sukhacheva L. Sedimentation processes and pollution history of the Neva Bay (Eastern Gulf of Finland, the Baltic Sea). // Saint-Petersburg, April 2015, 16 pp. in press

12. SEPA. 2000. Report 5052: Environmental Quality Criteria. Coasts and Seas, Swedish Environmental Protection Agency, Stockholm, Sweden 138 pp.

13. Spiridonov M.A., Rybalko A.T., Moskalenko P.E., Zhamoida V.A., Kotilainen A.T., Winterhalter B. Sedimentation in Eastern Gulf of Finland. Methods of investigations and some

results from the Marine Geological Patrole (MEP) cruises // Proc. of the Final Seminar of the Gulf of Finland Year, Helsinki, 1997 p.p. 106-112

14. Vallius H. Recent sediment of the Gulf of Finland: An environment affected by the accumulation of heavy metals, Abo Akademi University, 1999, ____ p.

15. Vallius H., Ryabchuk D., Kotilainen A., Spiridonov M., Suslov G., Zhamoida V. Pollution history of thr Neva Bay since the foundation of the city of St. Petersburg (1703 AD) // The Baltic Sea geology: The Ninth Marine Geological Conference. Extended abstracts. University of Latvia, Riga, 2006, pp. 115-116.

16. Vallius H., Ryabchuk D., Zhamoida V., Grigoriev A., Alliksaar T., Suuroja S. Changes in heavy metal chemistry of the sediments of the Gulf of Finland during the last two decades // Journal of Marine Systems, in press.

ABNORMAL STATE OF THE NORTHERN SEGMENT OF THE VISTULA SPIT

Anna Dobrovolskaya, Atlantic Branch of the P.P. Shirshov Institute of Oceanology (ABIORAS), Russia
Evgenii Burnashov, State Organization of the Kaliningrad region "Baltberegozaschita", Russia

anny.dobrovolskaya@gmail.com

For a long period of time, the seashore has been eroded and the front dune has been intensely degrading in the area of the Vistula Spit south of the Baltic Strait, connecting the Vistula Lagoon and the Baltic Sea. This leads to the fact that Kosa settlement which is directly behind the front dune gets flooded during the storm events. The settlement was already flooded three times - in December 2011, January 2012 and December 2013. This article aims to provide a substantiation of the critical condition of the northern segment of the Vistula Spit seacoast.

Key words: coastal erosion, monitoring data, coastal protection, Vistula Spit, Baltic Sea

I. SUBSTANTIAL OF THE CRITICAL CONDITION OF THE SEGMENT

The Vistula Spit is located in the south-eastern part of the Baltic Sea and is a narrow strip of land 65 km long, 35 km of which (25 km south of the Baltic Strait and 10 km north of it) are situated on the Russian territory and called "The Baltic Spit". The spit is divided in the north by the Baltic Strait of 400 m wide and 8-12 m deep. [1]. Protective breakwaters of the strait are an obstacle for the natural alongshore movement of sand drifts [2].

Starting from September 1, 1995, the Baltic Spit became available for free visiting for Kaliningrad region residents. At that time, the transportation was performed by a military ferry and it was free of charge. Since 2007, the "Baltic Shipping Company" has launched the private ferry "Baltiysk – the Baltic Spit", which effected carriage 7 times a day at first and then 8 times a day. After the ferry was launched, according to the "Baltic Shipping Company", the flow of visitors to the Baltic Spit increased dramatically.

Currently, the landscape of the major part of the Vistula Spit consists of the front dune, followed by a more ancient coastal dune ridge, usually consisting of two elongated banks. The banks are often split into separate parabolic dunes, approaching the plains located behind them like vast tongues [3]. Almost the entire surface of the spit is covered with woodland.

It should be noted that the northern tip of the Vistula Spit is different in terms of landscape from the rest of the spit, related to the increased anthropogenic influence thereon. Instead of the forests, this area is detected by a low degree of tree and shrub vegetation, and the surface of the front dune is heavily indented by deflationary basins.

This segment of the spit is most strongly exposed to erosion and has been recognized as critical for the past 15 years, both in terms of the front dune degradation, which is considerably above the average retreat rate at the Vistula Spit, and due to the flooding threat for residential

buildings of Kosa settlement, located directly behind the front dune. The critical coastal area is represented by the severely degrading front dune of 500 km long and the adjacent beach. [4]

Fig. 1- Location of the critical segment

Fig. 2 – Location of monitoring points (10 mv – primary monitoring point, 52 - new point)

Shore dynamics monitoring

Shore dynamics in the village of Kosa has been annually specified, from 2003 to 2016 [5, 6]. From 2003 to 2007, the observations were carried out by IO RAS. In 2007, the monitoring point had to be moved inland (Fig. 2), as due to the high rate of the coast erosion, it actually found itself on the beach within 5 years. Further observations were continued at the new monitoring point of the State Organization of the Kaliningrad region "Baltberegozaschita". In 1999, a relatively low coastal dune protecting Kosa settlement from storm waves located on a flat plain was intensely eroded during a storm. [7]

Over the following years, the trend of the coastal abrasion continued, as evidenced by monitoring observation data collected by IO RAS. According to the monitoring data collected from 2003 to 2006, the front dune base moved more than 4.5 m. (Fig. 3a)

On the average, the retreat amounted to -1.1 m / per year, which is higher than the average retreat rate of the front dune retreat at the Vistula Spit, equal to -0.35 m / per year.

Between 2007 and 2015, the base of the sea slope of the front dune retreated nearly by 10 m, the average retreat rate also accounted for -1.1 m / per year. (Fig. 3 b,c). The average beach width remained almost unchanged within the range of 20-30 meters.

The diagram (Fig. 4) shows the way the position of the top and bottom of the sea slope of the front dune, as well as the shoreline from the permanent monitoring point changed between 2007 and 2015.

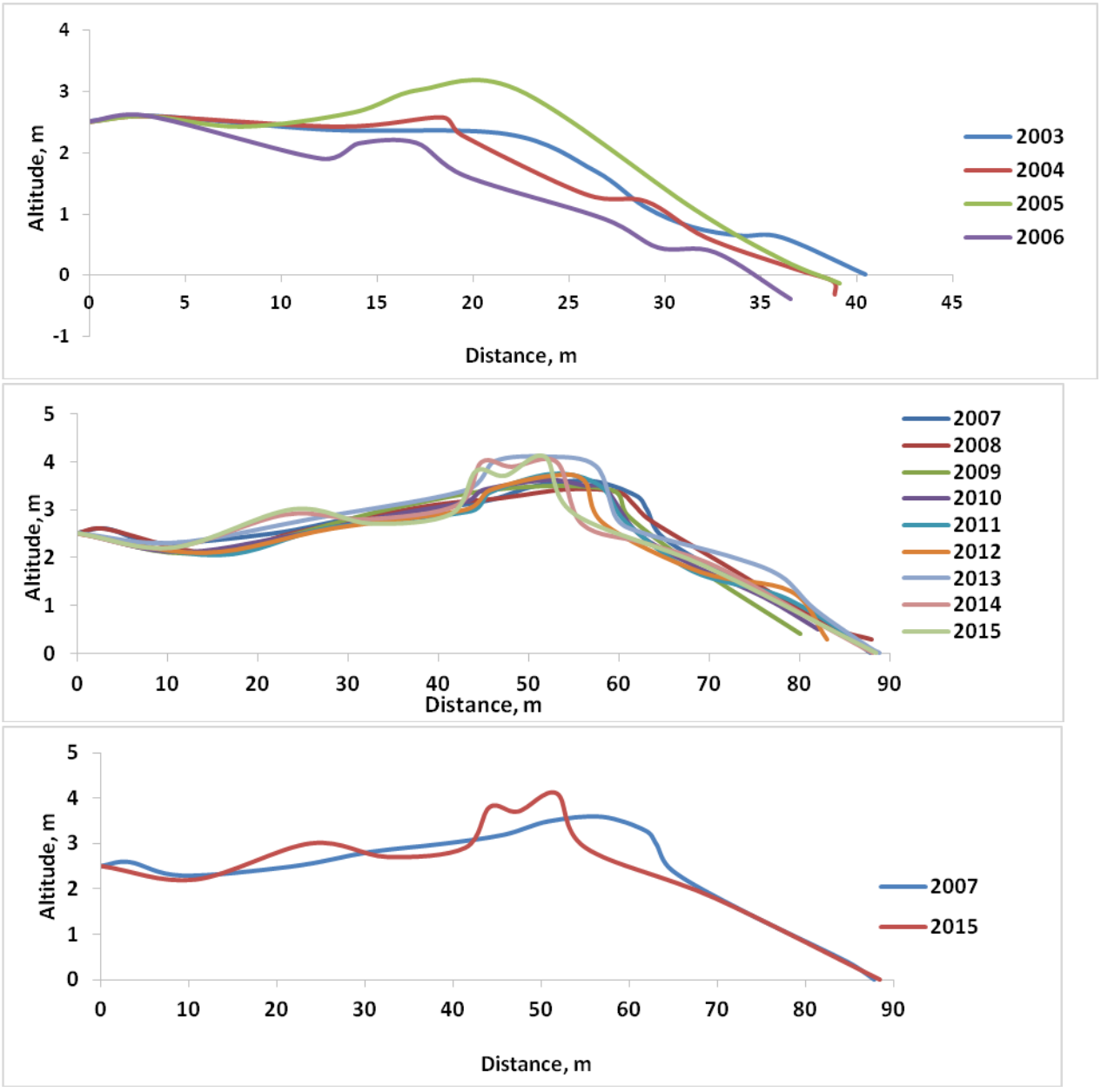

Fig. 3. Seashore dynamics at the village of Kosa: (a) – primary monitoring point, Rp. 10 mv, 2003-2006; (b,c) – new monitoring point, Rp. 52, 2007-2015.

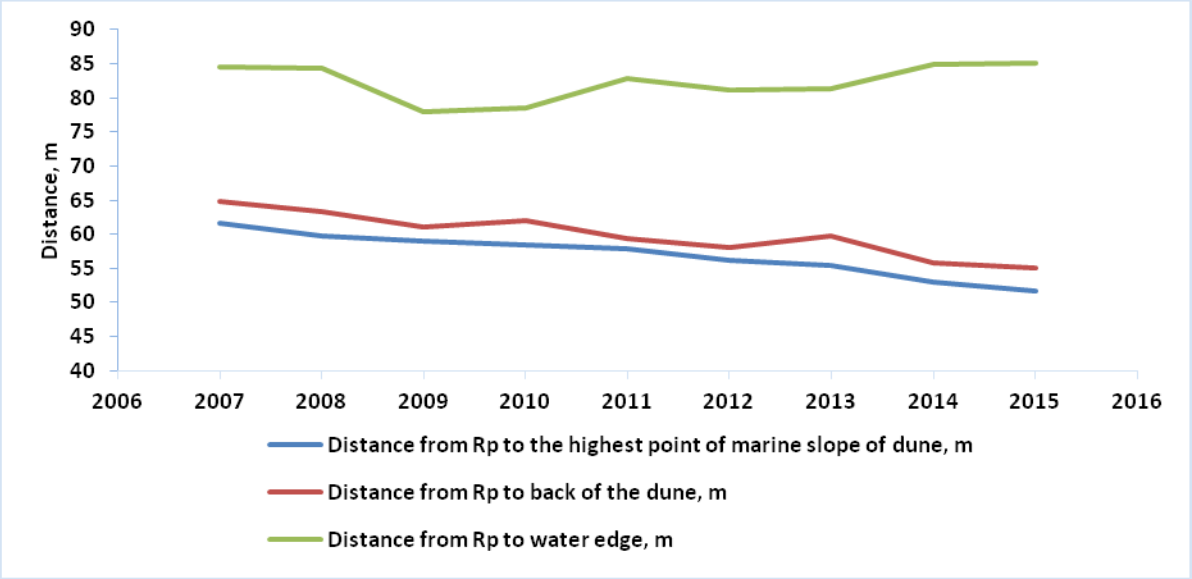

Fig. 4 – Diagram of the change of the seashore position near the village of Kosa between 2007-2015

Assessment of anthropogenic load influence on the segment

Since 2007, the anthropogenic load on the critical segment has increased due to the launch of the private ferry along the route "Baltijsk – the Vistula Spit" instead of the military ferry running between 1995 and 2007. The private ferry began running through the Baltic Strait 7-8 times a day. Passenger traffic of tourists, according to the "Baltic Shipping Company", which was carrying out the transportation, increased between 2008 and 2015 by 17270 persons / per year, the number of imported vehicles increased by 3818 units / per year. (Fig. 5).

Most of the visitors are concentrated on the northern section of the Baltic Spit near the village; tourists use the deflation basins of the front dune as hills and drive down them to the beach by cars, thus increasing degradation of the front dune. (Fig. 6)

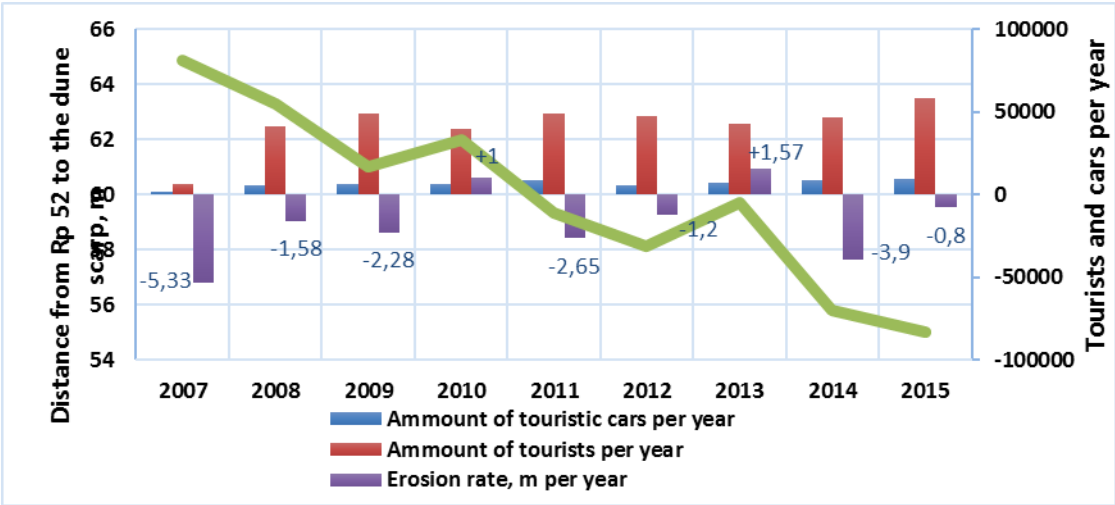

Fig. 5 – Dependence of the coast dynamics on anthropogenic load, 2007-2015

Fig. 6- Cars driving down the degrading front dune

Destruction of the coast continued alongside with increase in the number of tourists visiting the Baltic Spit. However, despite the increase in tourists, the rate of the shore erosion has not increased, which means that the anthropogenic load has almost no effect on erosion of the front dune's sea slope, but it mainly leads to increased deflation and surface degradation of the front dune body located outside of the wave field. The primary reason of the high rate of the front dune erosion is still storm impact and lack of sediment load related to the violation of beach drifting. As a result of degradation of the front dune body due to high anthropogenic load, deflation basins (washout) are formed through which the seawater enters and floods the territory of Kosa village. As a result of high rates of degradation, the volume of the front dune along about 500 m decreased by 25 126 m3 (the front dune in 2015 became 21.3% less than in 2007) between 2007 and 2015. [8].

II. FLOODING OF THE VILLAGE OF KOSA

Increasing rates of the dune's degradation led to the fact that the village of Kosa found itself in the flooding zone. The village was first flooded in November- December 2011, the next flooding happened in January 2012, and finally the village of Kosa was flooded for the third time in December 2013 during Xavier hurricane (Fig. 7).

2011 2012 2013

Fig. 7- Photos of the flooded areas of the village of Kosa

The village of Kosa is located on a flat plain, so there is a threat of flooding of the major part of the village under extreme storm conditions through three main washouts in the front dune body (Fig. 8)

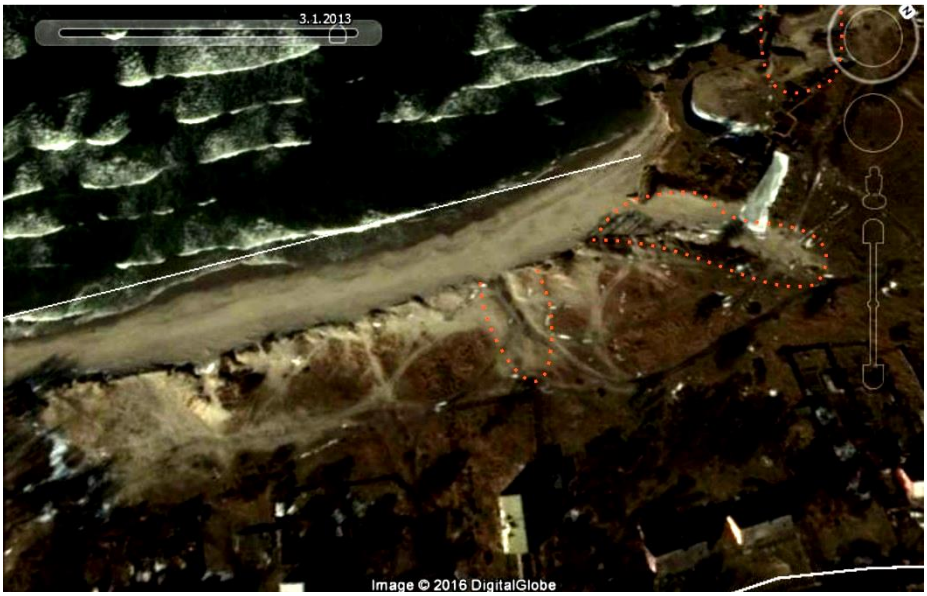

Fig. 8 – Scheme of sea waves' outburst points on the territory of Kosa village

The flooding risk of Kosa village is determined by a combination of such factors as wind speed and direction, storm impact duration, as well as readiness of the shore segment for new hurricane waves (i.e. whether the coast managed to restore its margin of safety after enduring the previous storm).

As a result of the data of after-storm coast survey carried out by the State Unitary Enterprise and State-financed Entity "Baltberegozaschita" in the area of the critical segment between 1981 and 2013, a forecast of the area's flooding was performed according to which one can presumably judge of the future flooding of the territory based on the storm duration and power data.

To assign the definition of "extreme" storm according to criteria of "Baltberegozaschita" to a storm impact on the coast of the Kaliningrad region, the following conditions shall be simultaneously fulfilled:

- wind speed 15 m / s or more;
- storm event duration more than 50 hours;
- dangerous wind direction in relation to the shoreline exposure, i.e. the wind direction when there is a chance of maximum shore erosion;
- sea level rise as a result of surges by 1 m or more.

In case when the wind speed is less than 15 m / s, but there is significant storm duration (80 hours) accompanied by a storm surge and significant coast erosion and abrasion, such a storm shall be also rated as "extreme".

According to the frequency of extreme storms occurrence on the coast of the Kaliningrad region in the twentieth century, their occurrence is determined according to basic parameters (wind strength and storm duration). Table 1 contains the data on major storms that happened over last 33 years.

Table 1- Major storms that happened over last 33 years

Years	Wind speed, m/s	Max. wind speed, m/s (gusts)	Wind direction, rhumb	Wave height, m	Surge height, m	Storm t, accumulative duration hours	Occurrence, %	Was the village of Kosa flooded? Duration?
1983	35	45-50	SW, W, NW	8	2,2	240	1	No
1988	25	35	W, NW	6	2,0	150	2	No
1990	20	25	NW, W	4	1,2	72	4	No
1992	21	29	NW	5	1,8	120	2	No
1993	32	40-45	SW, WSW	6	1,2	70	4	No
1994	18	25	WSW, W, WNW	4	0,8	40	10	No
1999	30	40	NW	6	1,1	130	2	No
2002	30	34	W	6	1,2	60	4	No
2005	25	30	W	3	0,6	20	20	No
2007	25-27	35	W, NW	4	1,2	72	4	No
2011	20	24	SW, W	3,5	0,8	12	20	Yes. Up to 100 m.
2012	13-15	25	W, NW, N	3,5	0,8	80	10	Yes. Up to 150 m
2013	13-18	25-30	SW,W	3,5-4,5	0,6	70	20	Yes. Up to 170 m
Jnr 2015	13-18	25-30	W, NW	4-5	0,5	24	50	No
Nov 2015	12-16	20-22	NW	3	0,3	12	100	No

According to the data presented in Table 1, it is clear that the strength reserve of the front dune in the sea area of Kosa village reached a critical value in 2011. Now, even during a storm of

20% occurrence happening over the coast of the South-Eastern Baltic region and conditioned by the action of west winds, the village of Kosa may be flooded. In case of storms of greater strength, flooding of the village is inevitable.

In order to determine the extent of possible damage, a technique for damage determination was used in relation to the harm that can be caused to life and health of individuals, property of individuals and legal entities as a result of an accident of a hydraulic structure [10], since there are no existing methods to determine the possible damage resulting from flooding due to the front dune erosion under storm conditions.

At the first preliminary phase, a possible scenario of the most severe accident was made, which considered the impact of 1% occurrence storm, which appears 1 time in 100 years. Such a storm with the maximum wind strength of 45 m / s and about 10 days duration eroded and broke through the front dune on the 2nd km of the Curonian Spit in 1983. The maximum length of sea water entering the Curonian Spit was the root of more than 500 m. [11]

The studied area of the Vistula Spit with similar characteristics of 1% storm with the west wind most dangerous for this segment under existing conditions of the degrading front dune (similar to the one at the Curonian Spit) assumes flooding of the village of Kosa from the seaside by more than 500 meters. However, given the water rise in the channel, there could also be observed the splash of water and additional flooding of the village from the channel. The flooding zone includes an object of cultural heritage – the Swedish fort and 35 residential buildings, including a nursery school. The total number of people affected by the flooding of residential houses amounts to about 175 people.

At the second stage, the probable damage is determined in monetary terms. Monetary value of losses calculation as a result of an accident are grouped according to the indicators characterizing the socio-economic effects of hydraulic structures' failures, and then added. According to this method, the damage caused by flooding of the village of Kosa during the impact of 1% occurrence storm shall be 2.1 billion rubles.

III. COASTAL PROTECTION PROPOSALS FOR THE CRITICAL SEGMENT

In order to prevent flooding of the territory of the village pf Kosa at the critical segment, measures to eliminate the threat of an emergency should be urgently taken. The best option is a comprehensive approach that takes into account all the causes of the critical nature of the site and restoration of the natural landscape.

In this area, it is first necessary to restore and strengthen the strength reserve of the front dune. Strengthening of the front dune is possible in case of installation of an artificial nucleus made of either of precast concrete constructions (tetrapods) with stone filling, or geotubes. [12,13] into the front dune body. To secure the surface of the front dune and reduce development of deflation processes, plant turf vegetation planting and installation of wooden stands with brushwood flooring are proposed. Parameters of the front dune shall be calculated based on maximum hydrodynamic conditions of wave disturbance, maximum surge and splash. According to Regulation 32-103-97 [14] and taking into account climatic conditions of the sea coast of the Baltic Spit, the front dune should be at least 8 m high, not less than 500 meters long and 40 m wide. Parameters and facilities design can be adjusted in the process of design and survey works.

The second stage of coastal protection works includes artificial beach aggradation, which is, apart from coast protection functions of aesthetic and recreational value. Therefore, the proposed parameters of the artificial beach were defined taking into account the natural environment and recreational potential of the village of Kosa. The above-water part of the beach should be 60-70 meters wide, with the aggradation beach at least 600 meters long based on calculation of SanPiN 42-128-4690-88 [15], 5 m2 of beach for 1 person.

The next stage of the coast protection works is associated with a need to reduce the loss of natural erosion of the artificial beach. Such works include construction of beach supporting structures - cross dikes and alongshore breakwaters. All parameters of the beach supporting facilities, including their amount, permeability, length, depth and others should be defined by means of mathematical modeling. Conceptual proposals are shown in the diagram of Fig. 9. Estimated cost of construction of the proposed complex of coast protection facilities shall be 300-400 million rubles, well below the damage that may result from flooding of the village of Kosa in case of the extreme storm influence.

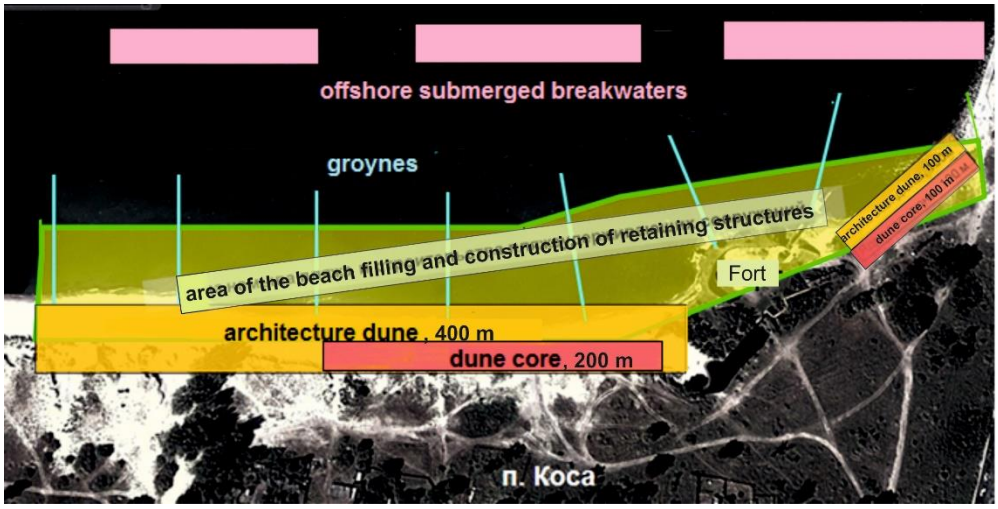

Scheme of the complex of coast protection constructions (view from above)

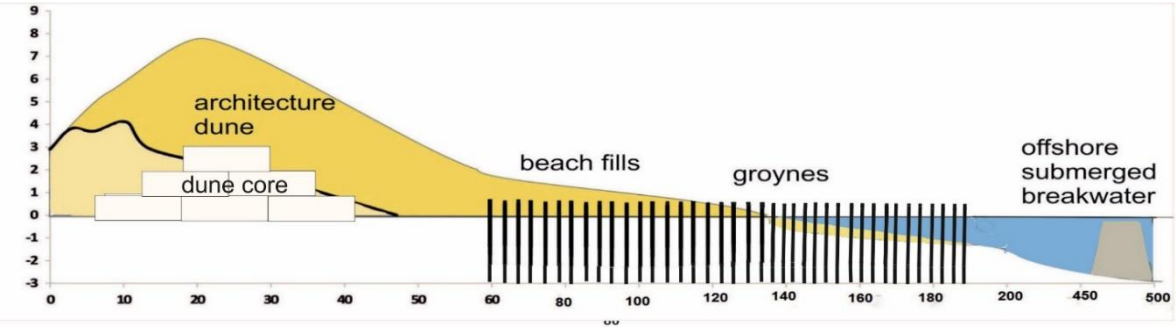

Cross-section scheme of the complex of coast protection constructions

Fig. 9 - Proposed comprehensive approach concept for prevention of emergency situations and elimination of the critical condition of the shore segment.

IV. Conclusions

The study has shown that the segment on the northern tip of the Vistula Spit is critical over a length of 500 m because of two reasons - a high rate of coast destruction and flooding threat of the residential village, located behind the degrading dune. The high rate of the coast destruction is caused by deficiency of shore sand deposits due to violations of alongshore beach drifting after extension of piers. Increased anthropogenic load on the shore segment contributes to degradation of the front dune and formation of deflation basins (washouts), through which the village is flooded.

To avoid the flooding situation in the critical area, measures to eliminate the threat of an emergency should be urgently taken. The best option is a comprehensive approach that takes into account all the causes of the critical nature of the site and restoration of the natural landscape. It is proposed to construct a complex of coast protection facilities with aggradation of the lost coastal areas, as well as marine infrastructure to organize movement of heaps of people across the front dune to the beach. The first step is to prevent emergencies by means of creating a nucleus in the front dune body with restoration of the full strength reserve of the very sand body of the front dune. The next stages of facilities complex construction and beach aggradation shall simultaneously provide a favorable environment for public recreation and maximum reduction of the risks of accidents on the shore caused a significant increase of the anthropogenic load and storm impact.

V. Acknowledgments

Technical facilitation of the study and problem identification was made with support of the theme № 0149-2014-0017 (supervisor – B. Chubarenko) of State Assignment of the P.P.Shirshov Institute of Oceanology of the Russian Academy of Sciences (2015-2017). Preparation of this article was made under the support of the Project No 14-17-00547 “A forecast development for evolution of accumulative Russian coasts of tideless seas”.

VI. References

[1] V.P. Bobykina, V.L. Boldyrev, "On the problem of conservation and sustainable development of sea coasts: Natural and industrial risks of coastal areas”. [*Proceedings of the International Conference, Odessa, September 7-11, 2008*]

[2] V.P. Bobykina, “Seacoast morphology and dynamics of the northern segment of the Baltic Spit // Ecological issues of the Kaliningrad region and the Baltic region”. Kaliningrad: coll. scientific work. Publisher of Immanuel Kant Russian State University, 2007. S.20-26.

[3] E.N. Badyukova, L.A. Zhindarev, S.A. Lukyanova, G.D. Solovieva, “Geological and geomorphological structure of the Baltic (Vistula) Spit. [*The doctrine of the sea coast development: age-old traditions and ideas of modernity: Conference materials. - St. Petersburg: Russian State Hydrometeorological University, 2010. pp. 170-172*]

[4] O.V. Bass, L.A. Zhindarev, “Manmade accumulative landforms in the coastal zone of the South-Eastern Baltic region, Tr. Intern. Conf. “Creation and use of artificial land plots on the shores and water bodies territory” - Novosibirsk: Publisher of SB RAS, 2009. pp. 187-196.

[5] Statistical data of the shore dynamics since 2000-2014. Monitoring of the critical segment in Kosa settlement. Data of State Public Entity of the Kaliningrad region “Baltberegozaschita”

[6] Statistical data of the shore dynamics 2003-2006. Monitoring of the critical section. Data of IO RAS

[7] V.P. Bobykina “On the extreme storm erosion of the coast of the Vistula Spit in December 1999, Scientific notes of the Russian Geographical Society (Kaliningrad branch). Kaliningrad, Publisher of Kazan State University, 2001, pp. 8A-1 - 8A-5

[8] E.M. Burnashov, “Current dynamics and geo-ecological state of the sea coast of the Kaliningrad region: Cand. Sc. Geography: 25.00.06: approved on 15.07.2011.E.M. Burnashov - Barnaul, 2011, p 205.

[9] K.V. Karmanov, E.M. Burnashov, V.Y. Glinka, A.Y. Komogorov, B.V. Chubarenko *Topographic characteristics of dynamically active segments of the front dune of the Russian part of the Baltic.Vistula Spit*, 2015.

[10] RD 03-626-03. Methods of determination of the damage extension that can be caused to life and health of individuals, property of individuals and legal entities as a result of a hydraulic structure accident. - Introduced for the first time; introduced. 2003 10C.

[11] O.I. Ryabkova “The history of coastal protection at the Kaliningrad sea coast”. [*Coastal zone: Morpholithodynamics and geo-ecology: Materials of the conf.Ed. Ed. Prof. V.V. Orlyonok. - Kaliningrad: Publishing House of the Kaliningrad State University, 2004,pp.273-275*].

[12] K.N. Makarov, Fundamentals of bank protection measures Sochi, SGUT and KD, 1999, p. 147

[13] SNIP 33-01-2003. Hydraulic engineering structures. Main provisions. – Instead of SNIP 2.06.01-86; introduced on 30.06.2003. M .: Publisher of Standards, 2004. pp. 8.

[14] SP 32-103-97: Regulation "Designing of marine coast protection facilities” Corporation "Transstroy", Moscow, 1998

[15] SanPiN 42-128-4690-88 “Sanitary rules of maintenance of populated areas”.

MATHEMATICAL MODELING OF NUTRIENT LOADING FROM SMALL CATCHMENTS OF THE VISTULA LAGOON

Dmitry Domnin, Atlantic Branch of P.P. Shirshov's Institute of Oceanology of RAS, Russia
Boris Chubarenko, Atlantic Branch of P.P. Shirshov's Institute of Oceanology of RAS, Russia
Rene Capell, Swedish Meteorological and Hydrological Institute, Sweden

dimanisha@rambler.ru

Vistula Lagoon as a part of the coastal zone translates nutrient load from catchment to the Baltic Sea. Catchments of the Primorskaya River (small settlements, mostly agricultural area, 120 km^2) and Banówka-Mamonovka River (transboundary catchment between Russia and Poland, relatively big settlements, food production enterprises, agricultural activity, 490 km^2) were selected as test ones for the Vistula Lagoon catchment (23 870 km^2).

Assessment of the retention of total nitrogen and phosphorus in the catchment and the transformation of nutrient load from anthropogenic sources while passing the catchment were studied by using open source numerical modeling tools. Initial data comprises the geomorphic characteristics, river net data, information on land use and nutrient point sources, time series of temperature, precipitation. Runoff was simulated by hydrological model HYPE considering the evaporation and infiltration into the soil. Retention and transport of nutrients were accessed using the model FyrisNP.

Source apportionment was made for the nutrient load discharging from both catchments to the Vistula Lagoon. The greatest amount of nutrients in final discharge is coming from the arable land (50-80%), point sources constitute a smaller proportion (5-30%). The results will be used to obtain the first order approximation of the nutrient load from other small rivers of the Vistula Lagoon catchment and from the biggest river in the area, the Pregolya River (15 300 km^2) by analogy.

Key words: mathematical modeling, catchment, nutrient load, Vistula Lagoon.

I. INTRODUCTION

Eutrophication is one among four main problems of the Baltic Sea (State and Evolution of the Baltic Sea, 2008). HELCOM Baltic Sea Action Plan (HELCOM BSAP, 2007) adopted in 2007 recommends the measures on nutrient load reduction. According to national quotas (Copenhagen Ministerial Declaration, 2013) the load from Kaliningrad Oblast has to be reduced by 50% of phosphorus and 25% on nitrogen comparing with nowadays level (HELCOM Summary report…, 2013). Points and diffuse sources are rather dispersed. The first-order approach to distribute quotas within the territory of the Kaliningrad Oblast is to make it in proportion to the area of sub-catchments of all rivers. The next step is to apply numerical modeling tool to simulate the retention of the nutrients within the catchment. The present paper is devoted to application of the numerical

model to pilot catchments of the Banówka-Mamonovka River and the Primorskaya River. The catchments of these rivers cover 3% of the Vistula Lagoon Catchment.

II. MATERIALS AND METHODS

Study area

The Banówka-Mamonovka River catchment is a transboundary catchment between Russia and Poland. The main stream starts on the territory of Poland (here called the Banówka River) and runs into the Vistula Lagoon of the Baltic Sea through the Kaliningrad Oblast of Russia (fig. 1). The stream of the river at the Kaliningrad Oblast is called Mamonovka, referencing the town of Mamonovo. The catchment area is 350 km^2. 140 km^2 of it is located in the south-western part of the Kaliningrad Oblast, and 210 km^2 in the northern part of the Warmia and Masury Voivodeship of Poland. The Mamonovka River has a great number of tributaries. The largest tributaries are the Ignatievka (eastern) and the Vitushka (western). The width of the stream at the outlet is 10-16 meters.

The catchment of the Primorskaya River (120 km^2) is located on the Sambian Peninsula in the western part of the Kaliningrad Oblast. The length of the main stream is about 30 km. The river flows in the Promorsk Bay of the Vistula Lagoon.

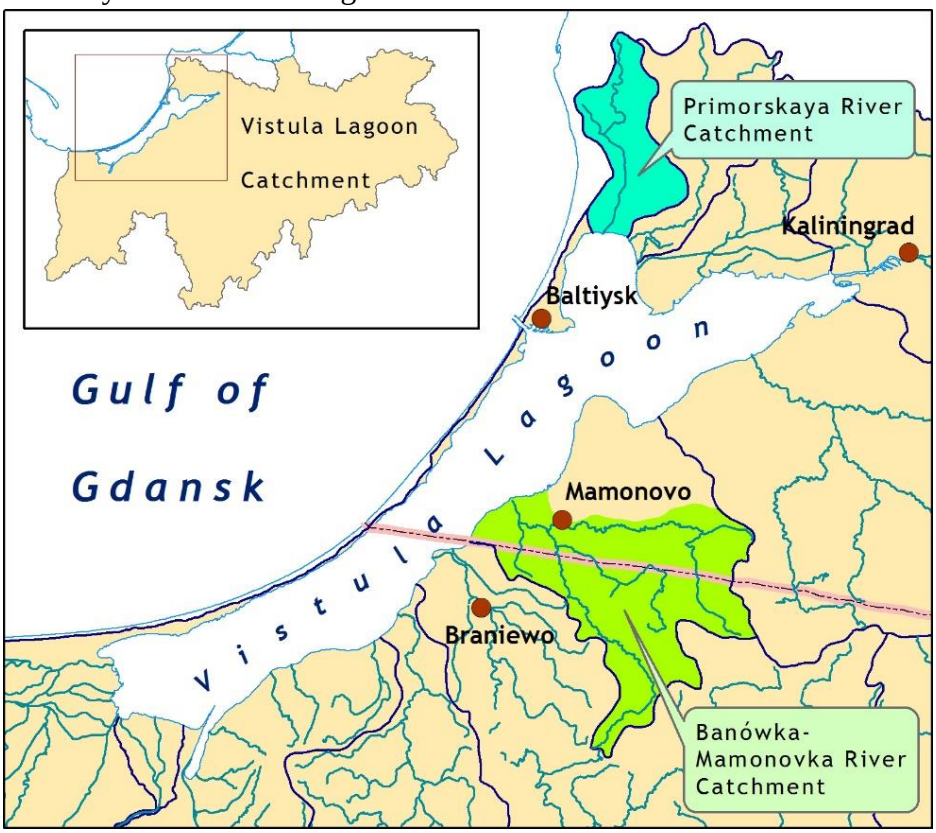

Fig. 1. Locations of Banówka-Mamonovka and Primorskaya Rivers Catchments.

Modeling tools

Two models were used to simulate water quality and determine the proportions between the components of the nutrient loads (from agriculture, point sources, background, etc.): hydrological

model HYPE (developed by Swedish Meteorological and Hydrological Institute) and model for nutrient load assessment FyrisNP (developed by Swedish University of Agricultural Sciences).

The HYPE model estimates time dependence of the daily runoff rate at final cross-sections of the sub-basins system taking into account evaporation and seepage in soils. The input data includes information about the relief, land use structure, soil types, daily time-series of precipitation and air temperature. For the purpose of calibration, runoff time-series are required at monitoring points within the catchment. Model files contain information about boundary conditions according to temperature and the amount of precipitation fallen as well as data on water discharge at a final cross-section and catchment area parameters (Donnelly et. all, 2010).

The dynamic FyrisNP model calculates source apportioned gross and net transport of nitrogen and phosphorus in rivers and lakes. The main scope of the model is to assess the effects of different nutrient reduction measures on the catchment scale. The time step for the model is in the majority of applications one month and the spatial resolution is on the sub-catchment level. Retention, i.e. losses of nutrients in rivers and lakes through sedimentation, up-take by plants and denitrification, is calculated as a function of water temperature, nutrients concentrations, water flow, lake surface area and stream surface area. Data used for calibrating and running the model can be divided into time dependent data, e.g. time series on observed nitrogen and phosphorus concentration, water temperature, runoff and point source discharges, and time independent data, e.g. landuse information, lake area and stream length and width (Hansson at all, 2008).

Input data and calibration

Input data for temperature and precipitation were taken from two meteorological stations among 4 existing in the Kaliningrad Oblast (using open access archive RP5.RU), namely, Mamonovo station for the Banówka-Mamonovka catchment and Kaliningrad station for the Primorskaya catchment. Calibration of the HYPE model (hydrological level) were made by daily measurements, calibration of the FyrisNP model was made by seasonal data on nutrient concentrations. The Mamonovka River sampling point (hydrological and nutrient measurements) is located 7 km upstream the mouth of the on the Banówka-Mamonovka River. The Primorsk sampling point (hydrological and nutrient measurements) is located 1.5 km upstream the mouth of the Primorskaya River. Modeling periods were 2007-2011 and 2010-2014 for the Banówka-Mamonovka and Primorskaya catchments respectively.

Input nutrient load data

Only settlements located in the catchments areas, as well as a fur-farm in the Russian part of the catchment area are regarded as point sources of pollution. Due to difficulties to collect data for all water users, the amount of total nitrogen and phosphorus per person (or per animal) per year was evaluated by means of calculation (Gorbunova, Chubarenko, 2009). Settlements in the rural areas of the Kaliningrad Oblast have no complete treatment systems (Treatment facilities, Velikanov, Proskurin, 2003) and waste water flowing into surface waters were considered as untreated.

Regional statistic data were used to estimate the nutrients load from the population living in sub-catchments. It was assumed that each inhabitant connected to the sewage system produces 5.5 g of nitrogen and 1.2 g of phosphorus per day, and sewage finally brings about 40% of the total

nitrogen and 50% of phosphorus of this gross emissions per person per day (Swedish..., 1995). These relations have been taken into account when calculating the amount of nitrogen and phosphorus produced by local population. It was considered that 20% of the population is not connected to sewage networks. From this population, removal rate is 76% for nitrogen and 88% for phosphorus as an infiltration bed (Swedish..., 1995).

Number of livestock is an important indicator of the agricultural impact on the environment. In recent years the performance of the agricultural sector in the basin has decreased including the areas for crop, livestock population and animal production for both tenant farmer and owner-operated farms. Therefore, agriculture lands on the Russian part of the catchment of the Banówka-Mamonovka River were considered as temporarily underutilized lands ('Open'). For the Primorskaya River catchment potentially agricultural land was partly assigned as "Open" (59%), and partly as 'Arable' (8%) (those we definitely knew that agricultural activity exists). For the Polish part of the basin, land use structure was defined according to the European Programme "Corine Land Cover" (CLC, 2000) for 2005. Information on type specific concentrations of nutrients for different land uses were applied, the values of type specific concentrations were taken as for south-eastern lands of Sweden (SLU data, modeling session, February 2009).

III. RESULTS OF CALIBRATION AND VERIFICATION

Delineation into sub-catchments

For the purpose of modeling the Banówka-Mamonovka catchment was divided into 10 sub-catchments: 5 in the Polish and 5 in the Russian part of the catchments (Figure 2). The area of the smallest sub-catchment is 9 km^2, of the largest one - 78 km^2. They constitute three major sub-catchment "branches", which meet at the sub-catchment ID 501. Two largest sub-basins (IDs 101 and 201) located on the territory of Poland account for 40% of the total catchment area. The final cross-section of the smallest sub-basin (ID 501) located in the Kaliningrad region coincides with this monitoring point. According to the proposed delineation scheme two sub-basins (IDs 104 and 601) are located downstream this monitoring point, and it was taken into account during calibration procedure.

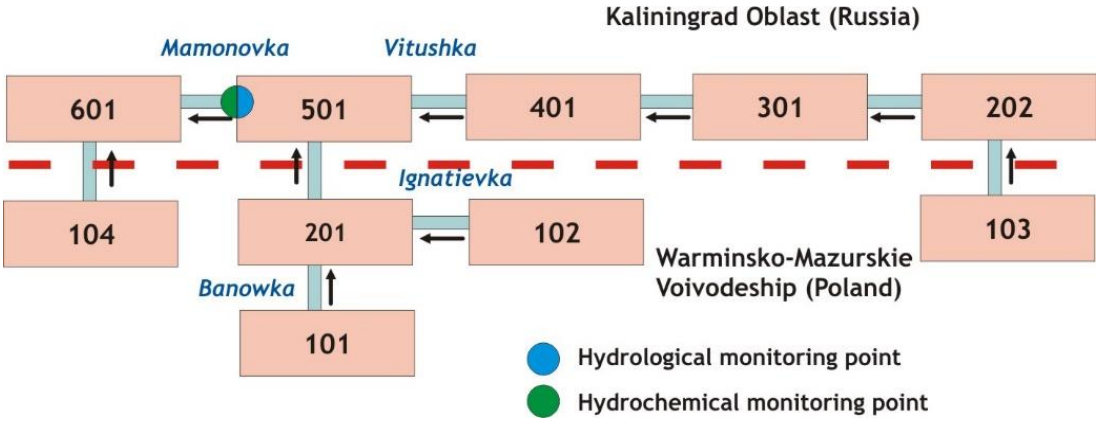

Fig. 2. Sub-catchments delineation scheme for the Banówka-Mamonovka River catchment. Dashed line illustrates the state border between Poland and Russia.

The Primorskaya River catchment (120 km^2) was subdivided into 15 sub-basins. (Figure 3). The areas of these sub-basins were in the range of 1.5 - 19 km^2. Monitoring point located in the sub-basin ID 761 was used. This point was further upstream the area of backwards stream in the mouth. There are 3 sub-basins (ID 717, 718 и 771) are downstream the monitoring point.

Hydrological modeling

The hydrological HYPE model *(HYdrological Predictions for the Environment)* (E-HYPE) was used to obtain data concerning the water discharge rate in the territory of each sub-basin. (Donnelly et. all, 2010). The typical error of the discharge projections is about ±10% calculated on a long term average and compared to the observations. When it comes to individual daily values the number of errors increases, and the same happens when you get down to small areas.

An optimal set of parameters was created with the use of the expert method, by trial and error according to the observation data at the monitoring point. These parameters allowed approximating the curve of the model discharge to the curve of the measured runoff. It turned out that modeling depends mostly on change of parameters influencing evaporation from the catchment area.

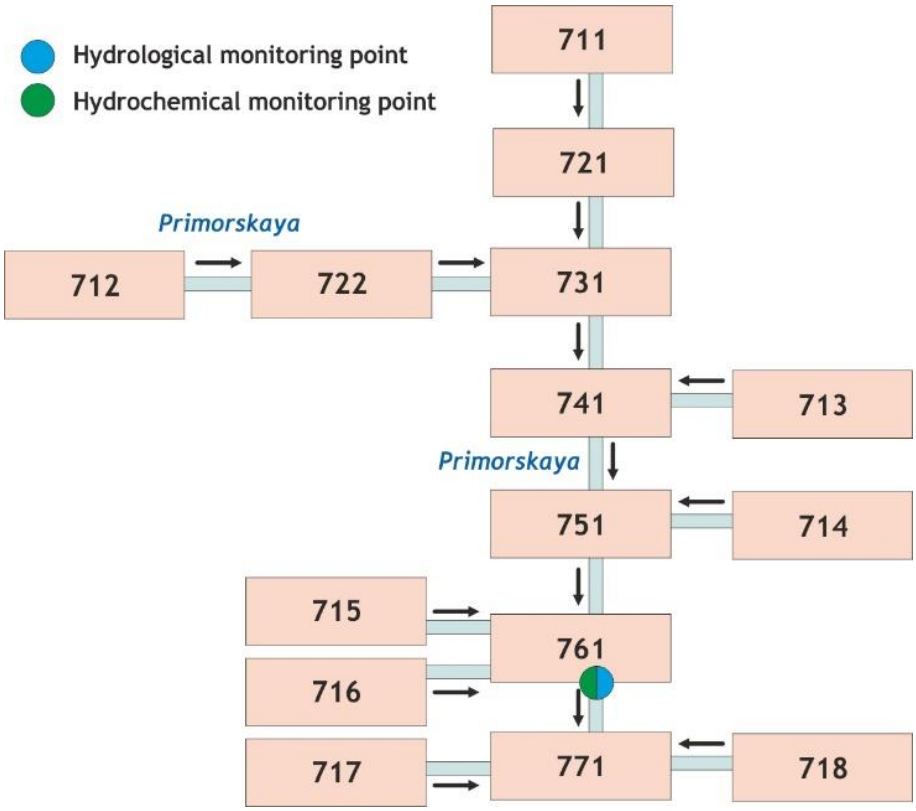

Fig. 3. Sub-catchments delineation scheme for the Primorskaya River catchment.

The period 2008-2010 was chosen as a calibration of water discharge for the Banówka-Mamonovka River catchment. The correlation coefficient (R) between measured and simulated discharges at the final cross section of the sub-basin 501 (Mamonovo demarcated site) was 0.93. Average measured discharge is 4.3 m^3/sec, the simulated one – 4.4 m^3/sec. (Table 1).

Table 1. Mean, maximum and minimum discharge for the Banówka-Mamonovka River, obtained by measurements and calibration simulations by the HYPE model (2008-2010).

Time-series	Mean km^3/year	Mean (m^3/sec)	Maximum (m^3/sec)	Minimum (m^3/sec)
Results of model calibration				
Measured data	0.14	4.3	12.7	1.2
Simulated data, 2008-2010	0.14	4.4	14.0	0.8
Results of model verification				
Measured data	0.14	4.3	6.2	2.3
Simulated data, 2011	0.13	4.0	8.2	1.2

The runoff for 2011 was chosen as a verification set of data for the Banówka-Mamonovka. The result was little worse than for calibration, correlation coefficient was 0.86. Taking into consideration short calibration period, the data for 2011 were also included into calibration data set and new set of calibration parameters for HYPE model was adopted. The resulted time series of simulated and measured discharge for four years (2008-2011) are presented on Figure 4 for expert judgment.

The correlation between measured and simulated discharge for the Primorskaya River for the period of 20101-2013 was 0.88 (final cross-section of the sub-catchment ID 761. Mean water discharge over the whole period was 1.3 m^3/sec obtained by measurements and 1.2 m^3/sec obtained by modeling (see Table 2).

The data for 2014 were taken as verification data set for the Primorskaya River. The result was better than for calibration period, the correlation coefficient was 0.94. Modelled runoff of each of the sub-basin were used for the next step – the modeling the nutrient load from the catchments.

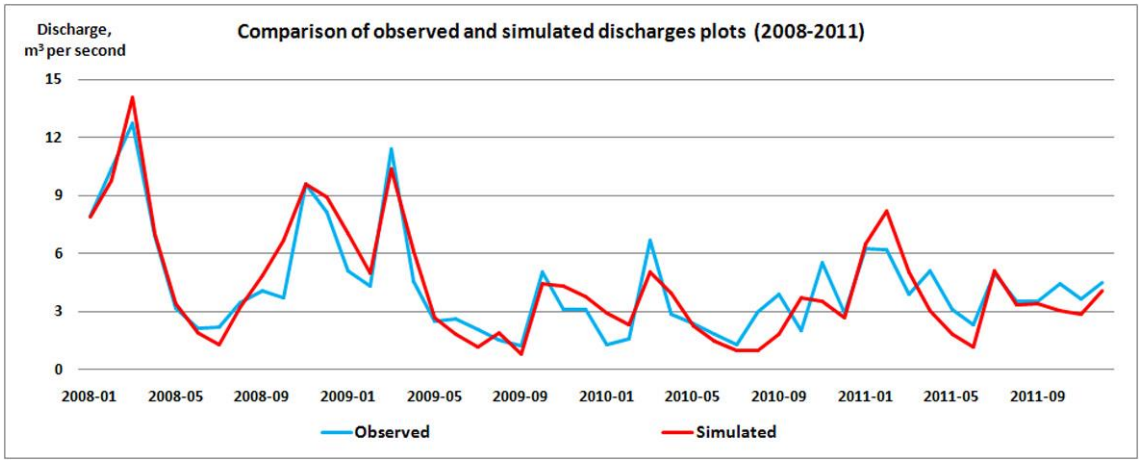

Figure 4. Variations of the Banówka-Mamonovka River discharge at the Mamonovo monitoring station during 2008-2011.

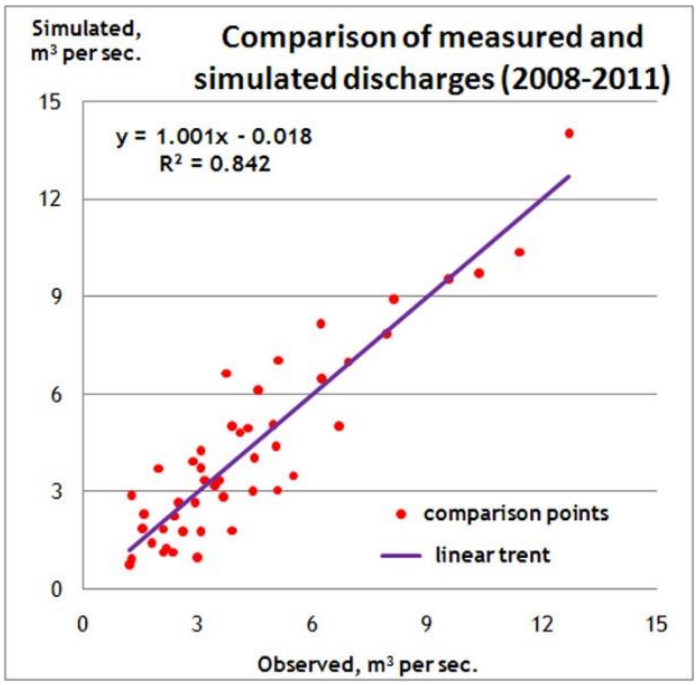

Figure 5. Linear regression between measured and simulated discharges (2008-2011) of the Banówka-Mamonovka River.

Table 2. Mean, maximum and minimum discharge for the Primorskaya River, obtained by measurements and calibration simulations by the HYPE model (2010-2014).

Time-series	Mean km^3/year	Mean (m^3/sec)	Maximum (m^3/sec)	Minimum (m^3/sec)
Results of model calibration				
Measured data	0.04	1.3	4.1	0.1
Simulated data, 2010-2013	0.04	1.2	8.5	0.2
Results of model verification				
Measured data	0.6	0.02	2.1	0.1
Simulated data, 2014	0.6	0.02	4.0	0.1

Modeling of nutrient transport

FyrisNP model has two calibration parameters, namely: *c0[dimensionless]*, an empirical calibration parameter, determines how much the retention is reduced by temperature in a range of 0°-20°C; and *kvs* [LT^{-1}], an empirical calibration parameter for the flow rate adjustment factor.

FyrisNP provides two methods of calibration, the one by using Monte Carlo statistical estimation and the second – by automatic calibration. The first one gave better results for the phosphorus simulations, the second one – for the nitrogen.

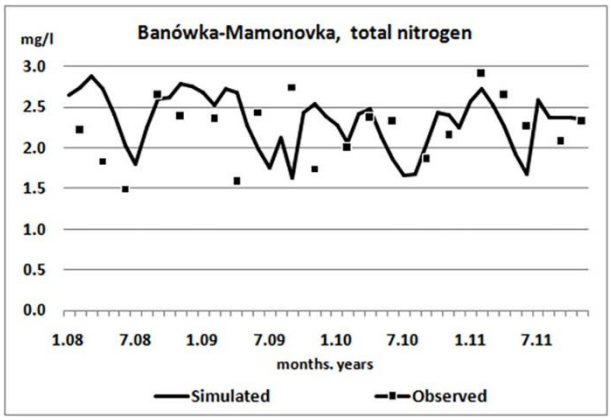

a)

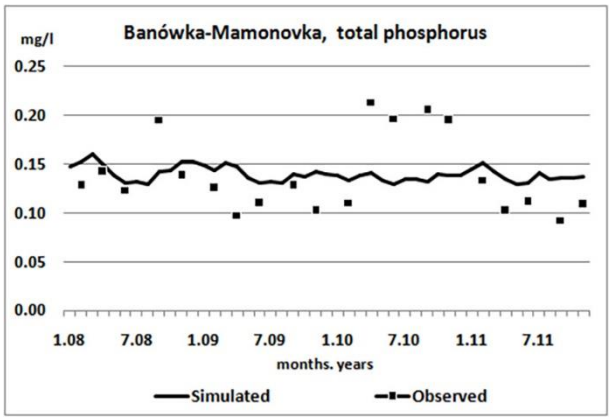

b)

Fig. 6. Time series for concentration of total nitrogen (a) and total phosphorus (b) for the period of 2008-2011 obtained by modeling of Banówka-Mamonovka catchment.

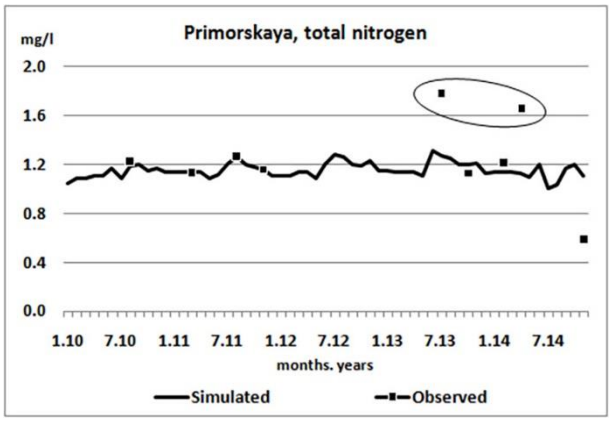

a)

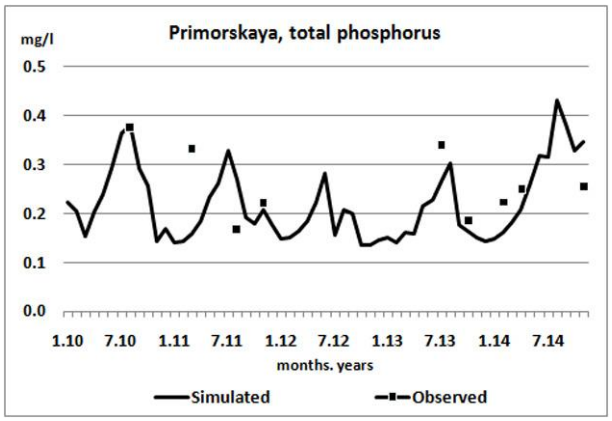

b)

Fig. 7. Time series for concentration of total nitrogen (a) and total phosphorus (b) for the period of 2010-2014 obtained by modeling of Primorskaya catchment.

Table 3. Mean concentration of total nitrogen and phosphorus for the Banówka-Mamonovka and Primorskaya Rivers obtained by measurements and simulations by the FyrisNP model.

River	Total nitrogen		Total phosphorus	
	Observed value (mg/l)	Simulated value (mg/l)	Observed value (mg/l)	Simulated value (mg/l)
Banówka-Mamonovka (2008-2011)	2.22	2.33	0.138	0.140
Primorskaya (2010-2014)	1.24	1.15	0.26	0.22

Results of calibration in terms of modeled time series of nutrients concentrations (mg per liter) against the measured values are presented on the Figure 6 and 7. Temporal variations of nitrogen and phosphorus are presented for the monitoring points: the Banówka-Mamonovka River during 4 years (2008-2011) on the Figure 6, and the Primorskaya River during 5 years (2010-2014) on the Figure 7. Even details of temporal variations are not well described by model, the general

level of concentrations with some seasonal variations are resolved, and mean values for the whole period of calibration are in good agreement (Table 3).

The fact that there is no single set of calibration parameters for both catchments, the Banówka-Mamonovka River and Primorskaya River, despite their similarity, means that uncertainties originated from spatial data, precipitation, and data on nutrient load within the catchment are still high, and the models of nutrient assessment should be tuned for each catchment specifically.

IV. DISCUSSION OF THE SOURCE APPORTIONMENT RESULTS

The average annual removal of total nitrogen from the Banówka-Mamonovka River catchment area to the Vistula Lagoon was of 400 tons per year for the period of 2008-2011. And the removal of total phosphorus from the catchment area was 25 tons per year. The retention in the catchment was estimated as 20% for the total nitrogen and 31% for the total phosphorus.

The nitrogen and phosphorus load source apportionment is presented in Figure 8. The load from an arable lands is the most significant portion (82% for the nitrogen and 61% for the phosphorus).

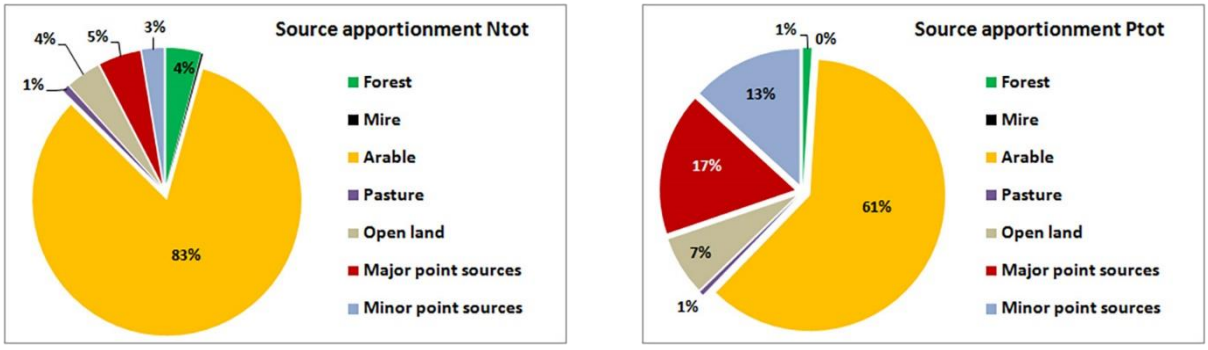

a) b)

Figure 8. Sources apportionment of nitrogen (a) and phosphorus (b) in the Banówka-Mamonovka catchment by results of modeling for the period 2008-2011.

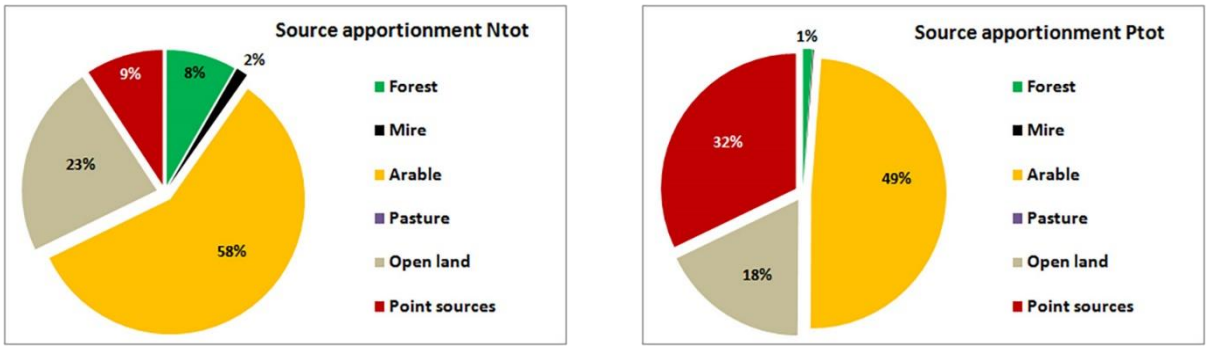

a) b)

Figure 9. Sources apportionment of nitrogen (a) and phosphorus (b) in the Primorskaya catchment by results of modeling for the period 2010-2014.

For the Primorskaya River catchment the average annual removal was estimated as 43 tons of total nitrogen and 6.2 tons of total phosphorus per year for the period of 2010-2014. On average the retention for the catchment was only 8% for the nitrogen and 2% for the phosphorus.

Despite the arable land not occupying the main part of the catchment area, its input in the final release of nutrients from the catchment is rather high - 58% for the nitrogen and 49% for the phosphorus (Figure 9). Open lands occupy about 60% of catchment area, but give 23% of the total nitrogen and 18% of the total phosphorus. The same for the forests and mires, the portion of nutrients they are cause, 8% and 2% of nitrogen and 1% and 0.15 of phosphorus, rather less than the portion of area they occupy. The point sources are one of the most significant nutrient source, they produce 9% of nitrogen and 32% of phosphorus.

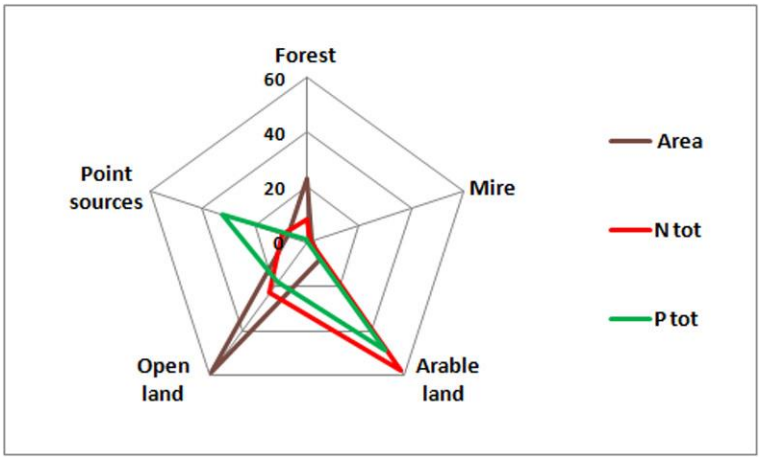

Figure 9. Fractions (in %) of nutrient sources (forest, mire, arable land, open land, point sources) in the area and the nitrogen and phosphorus removal from of the Primorskaya River catchment.

V. CONCLUSIVE REMARKS

The main sources of uncertainty in the model results for catchment of the Kaliningrad Oblast are an area specific data on agricultural practice and fertilization, initial data for calibration (monitoring data), as well as information on time specific concentrations for soils. The temporal frequency of the nutrient monitoring data (today it is once per season) should be increasedto reproduce seasonal variations of the processes. Nowadays state monitoring program doesn't include laboratory analysis on total nitrogen and phosphorus, and only covers ordinary inorganic forms of them (nitrate, nitrite, ammonia, phosphate), while for correct modeling the total nitrogen and phosphorus (inorganic and organic forms) are essential. Time specific concentrations for different types of soils in the Kaliningrad Oblast never were estimated.

Well calibrated hydrological model ensures the correct estimation of total nutrient removal for several years period despite all uncertainties in modeling of nutrient concentrations.

Existed network of meteorological stations in the Kaliningrad Oblast (1 station per 3500 km^2 in average) is very poor to cover spatial variations in atmospheric parameters, especially in rainfall. Re-analysis data (1 point per 1000 km^2) were used for modeling.

The application of numerical model calibrated for 4 years for the Banówka-Mamonovka (2008-2011) and 5 years for the Primorskaya River (2010-2014) gave the estimation that the Banówka-Mamonovka river catchment (350 km^2) and the Primorskaya River catchment (120 km^2) give average annual removal of 400 and 43 ton of total nitrogen and 25 and 6.2 ton of total phosphorus per year. The retention characteristics in these sub-catchments were estimated as 20% and 8% for nitrogen and 31% and 2% for phosphorus respectively.

Obtained results showed that zero-level estimation of load using proportions of different land use in the area of catchment is too much uncertain. There are no alternative to model tool application (even the simplest one) to estimate the nutrient removal from catchment areas as many processes (some of them fully nonlinear) should be taken into consideration.

Acknowledgement

Simulations for the Banówka-Mamonovka basin were made within the Project BaltHazAR Phase II ("Building capacity within environmental monitoring to produce pollution load data from different sources for e.g. HELCOM pollution load compilations"), simulations for the Primorskaya basin were made within grant RFBR-Bonus 14-05-9173015 "Reducing nutrient loadings from agricultural soils to the Baltic Sea via groundwater and streams (Soils2Sea)".

References

1. Corine Land Cover technical guide – Addendum 2000 / Prepared by M.Bossard, J.Feranec, J. Otahel – Published European Environment Agency, 2000, 104 P.
2. Donnelly, C., Dahné. J., Rosberg, J., Strömqvist, J., Yang, W. and Arheimer, B. (2010) High-resolution, large-scale hydrological modelling tools for Europe. Proc. of the Sixth World FRIEND Conference, Fez, Morocco, October 2010). IAHS Publ. 340, 2010.
3. E-HYPE: HYdrological Predictions for the Environment – Europe, URL: http://www.smhi.se/en/Research/Research-departments/Hydrology/hype-in-europe-e-hype-1.7892 (date of last use is 15.05.2016)
4. Gorbunova J., Chubarenko B., Source apportionment modelling of nutrient transport in Instruch River Basin in Kaliningrad Oblast (Russia). Final Report of the Project within the Agreement No HarmoBalt-Kld, Kaliningrad, 2009
5. Hansson K., Wallin M., Djodjic F., Orback C. The FyrisNP model Version 3.1 – A tool for catchment-scale modelling of source apportioned gross and net transport of nitrogen and phosphorus in rivers. A users manual. Uppsala: Dept. of Aquatic Science and Assessment 2008. - 28 p.
6. HELCOM Baltic Sea Action Plan. Krakow, 2007 101 P.
7. HELCOM Copenhagen Ministerial Declaration. Copenhagen, 2013. 19 P.
8. RP5.RU: Archive of weather for Mamonovo. time-table http://rp5.ru/5193/ru (date of last use is 08.06.2012)
9. State and Evolution of the Baltic Sea, 1952-2005: A Detailed 50-Year Survey of Meteorology and Climate, Physics, Chemistry, Biology, and Marine Environment / Ed. R. Feistel, G.Nausch, N. Wasmund. 2008. ISBN: 9780471979685

10. Summary report on the development of revised Maximum Allowable Inputs (MAI) and updated Country Allocated Reduction Targets of the Baltic Sea Action Plan, 2013. 22 P.
11. Swedish Environmental Protection Agency: What does domestic wastewater contain? Swedish EPA Report 4425. 1995
12. Treatment facilities. WEB source: http://www.stroyint.ru/polezinfo/monitoring/ index.php?ELEMENT_ID=574 (in Russian, date of last use is 08.06.2012)
13. Velicanov N. Proskursnin E. Kaliningrad Oblast: Peculiarities of water recourses us-ing. Kaliningrad: Publisher “Yantarny Skaz”, 2003. – 128 p. Original source: Великанов Н.Л., Проскурнин Е.Д. Калининградская область: Особенности использования водных ресурсов. – Калининград: ФГУИПП «Янтарный сказ», 2003. – 128 с.

SEDIMENT MAPPING AND TRANSPORT PATHWAYS IN THE NEARSHORE ZONE OF THE RUSSIAN PART OF THE SOUTH-EASTERN BALTIC SEA

Evgenia Dorokhova, Immanuel Kant Baltic Federal University, Russia
Dmitry Dorokhov, Atlantic Branch of P.P. Shirshov Institute of Oceanology, Russia

zhdorokhova@gmail.com

To achieve a more robust interpretation of sediment conditions and transport, our study combines the two different interpretation techniques. A side-scan sonar survey was used as a basis for detail sedimentological investigation. Grain-size analyses of grab samples provided sediment transport direction and decoding of sonar data. The new detail lithological map of the underwater shore slope of the northern Sambian peninsula and the Russian part of the Curonian spit in 1:50 000 scale is created. For the first time, the stretched zone of very fine sands is outlined at depths of 25-30 m of the Curonian spit underwater slope. These sands are relicts, and their formation is connected with accumulative processes on the ancient shores of the Baltic Sea. Separate morpho-lithodynamic cells are distinguished on the submarine slope of the northern Sambian peninsula coast up to a depth of 20 m. The cape areas of the Sambian peninsula serve as cell boundaries where a divergence of sediment trend and seabed erosion are observed. The convergence of sediment transport directions is confined to the bight's central parts. Fine and very fine-grained sand accumulation prevails here.

Key words: sediments distribution, sediments transport directions, coastal zone, Baltic Sea

I. INTRODUCTION

Surface bottom sediments of the underwater shore slope of the northern coast of the Sambian peninsula and southern half of the Curonian spit have been studied quite extensively and mapped at different scales. However, the mapping has not been sufficient to perform a detailed investigation of such a highly dynamic sedimentation environment. Studies of the sediment dynamics and distributions are contradictory. There has been no consensus on the sediment transport directions and mechanisms of deposit formation until present [1; 2].

To achieve a more robust interpretation of sediment conditions and transport, we combined two different techniques. A side-scan sonar survey was used as a basis for detailed sedimentological investigation and sediment mapping. Grain-size analyses of grab samples provided sediment transport direction and decoding of the sonar data.

Morphologically, the coastline of the study area can be divided into two parts. The first is the abrasion northern Sambian peninsula coast, which has a latitudinal extent and is complicated by the Taran, Kupalnyj and Gvardejskiy capes. The second is the straightened accumulative coast of the Curionian spit, which extends from the southwest to the northeast. The peculiarity of the underwater shore slope is the domination of sediment material from the coastal abrasion and bottom erosion, but not from the river supply [3]. Westerly winds are dominant in the southeast Baltic Sea; coupled with

a general surface water counter-clockwise circulation, these winds induce general sediment transport towards the north/northeast direction.

II. Material and methods

A lithological map (1:50 000) is created up to a depth of 30 m on the base of the bottom sediment type map [4]. The latest map was made by synthesizing bottom surface side-scan sonar surveys and grab sampling conducted by AOIORAN and VSEGEI during different projects in 2006 - 2014. However, this map had significant gaps in sea bottom coverage. New data obtained in 2014 – 2015 during the expeditions of AOIORAN cover these gaps and are used to create a new map. The scheme of the used material is presenting in Fig. 1.

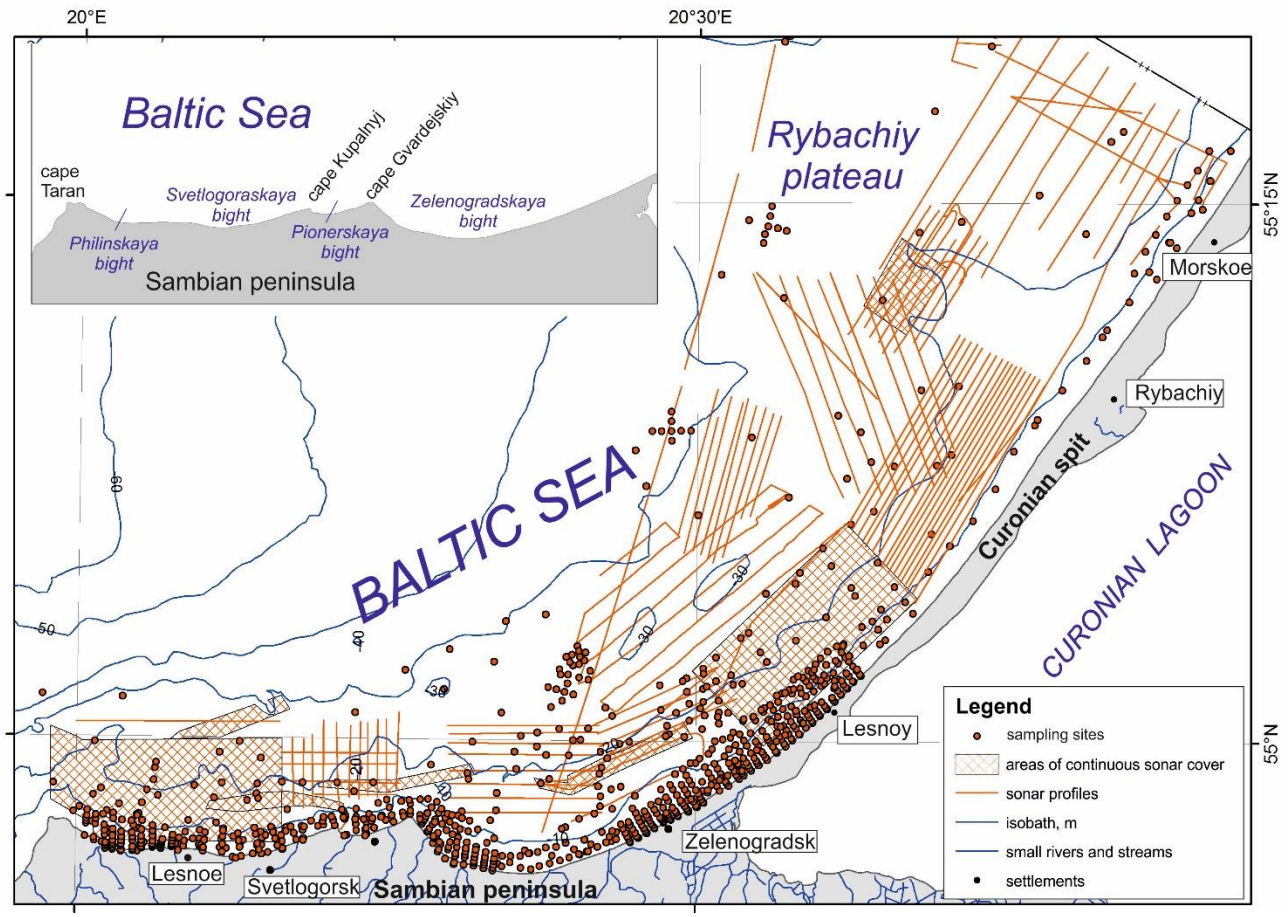

Fig. 1. Map of the study area with the locations of sampling sites and sonar profiles. The northern shore of the Sambian peninsula is shown in the inset.

Towed interferometric side-scan sonar Benthos C3D (200 kHz) was used for side scan sonar and swath bathymetry surveys. Data registration and processing were conducted using the hydrographic software Hypack 2014. Automatic classification of bottom sediments from sonar data was performed using the Hypack Geocoder software.

Surface bottom sediment samples were taken by Van Veen type grab and simple drag samplers. Grain-size distributions were determined by dry sieving analyses, with a set of sieves of 1/2φ intervals. The statistical parameters (mean size, Ma, sorting, So and skewness) of the grain-size

data were calculated according to the graphic method of Folk & Ward [5] in the Gradistat software [6]. The sediment types were determined after the Folk classification [7].

We manually outlined bottom sediment type borders according to the sonar data, grain size analysis and results of the Geocoder automatic sediment classification. The map of bottom sediment types was created using ArcGIS software.

A sediment transport vector net was determined based on the McLaren sediment trend analysis method [8] with modifications of [9] and [10]. McLaren interprets grain size changes between interrelated sampling sites assuming that the sediment in the direction of transport should become either I) coarser, better sorted and more positively skewed (case C) or II) finer, and better sorted and more negatively skewed (case B). In our case of the open sea coastal deposits transported with sediment, coarsening is not suitable. For this reason, transport vectors were only obtained for "case B". To achieve a regular net from irregular sampling data, grid creation in ArcGis was used [10]. It should be noted that the thickness of the transport vector arrows represents the significance of the result at that location, but not the intensity of the process. The areas of high vector strength are characterized by sharp changes of sediment types.

III. Results

The majority of the near-shore bottom surface is covered by sands (60.9 %) ranging from very coarse to very fine (Fig. 2). The sands occupy the flat sea bottom and fill the relief depressions.

Fine-grained sands are the most common sand deposits and cover 39.9 % of the sea bottom. They have a nearly uninterrupted extent along the coast of the Curonian spit up to depths of 5-10 m. The sands are well and moderately well sorted (average sorting is 0.8), with a mean size of 1.9 ϕ (0.25 mm). There is a second extensive zone of fine-grained sands at depths of more than 26-27 m on the underwater slope of the Curonian spit. This area is interrupted by the coarse grain sediments of the Rybachiy plateau.

Very fine-grained sands (12.3 % of the bottom surface) are well sorted (So=0.73), with a mean size of 2.8 ϕ (0.14 mm), reaching depths of 15-20 m in the central parts of the Philinskaya and Svetlogorskaya bights, up to a depth of 15 m in the Zelenogradskaya bight. In contrast, very fine-grained sands are not observed in the shallow zone along the Curonian spit.

Interestingly, the area of very fine-grained sands can be distinguished at depths of 20-30 m on the Curonian spit submarine shore slope to the south of the Rybachiy plateau. The sediments here have a smaller mean size (3.2 ϕ) and worse sorting (So=0.84) than the very fine-grained sands mentioned above.

Medium grained sands, covering 2.4 % of the investigated area, are represented by well sorted deposits (So=0.7), with a mean size of 1.8 ϕ (0.28 mm). They have a limited extent in the narrow zone shallower than 5 m in the Svetlogoraskaya and Pionerskaya bights. Additionally, there are two local fields of medium grained sands on the Sambian peninsula underwater shore slope at depths of 25-27 m.

Coarse and very coarse-grained sands together cover 4.5 % of the bottom surface and form on the periphery of moraine outcrops of the Rybachiy plateau and pre-quaternary deposit outcrops near the Taran cape. The coarse-grained sands have a mean diameter of 0.51 ϕ (0.7 mm) and sorting

of 0.73, and the very coarse-grained sands are moderately well sorted (So=0.52), with a mean size of -0.04 ϕ (1.03 mm).

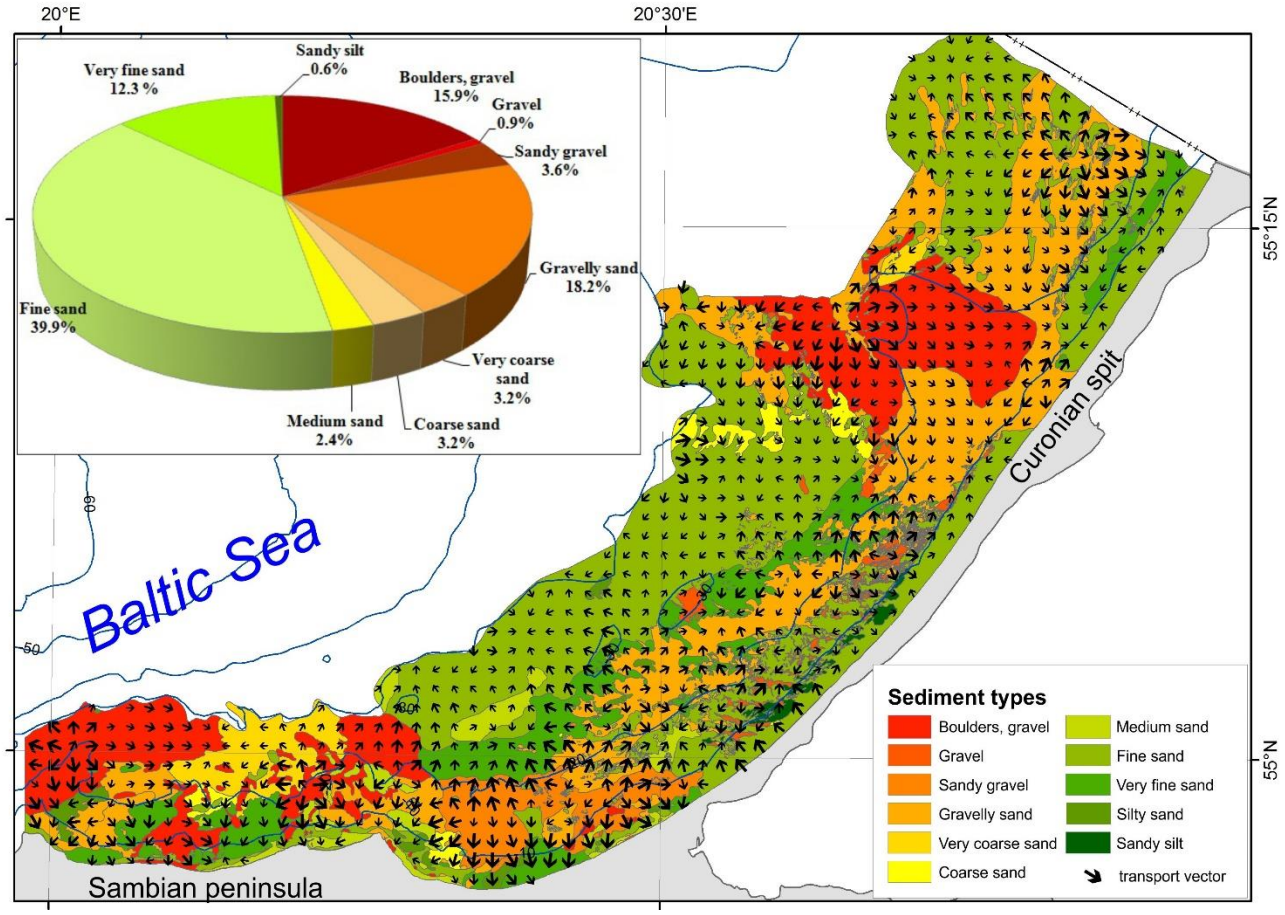

Fig. 2. Sea bottom surface sediment types and sediment transport vectors.
In the inset – percentages of the area covered with different sediment types.

Sandy silts (0.6 % of the sea bottom) are localized at depths of 5-17 m on the underwater shore slope of the southern part of the Curonian spit. They are represented by unique relict lagoon mud deposits, for which the extension, age and formation conditions were described in detail in the works of [11; 12].

Gravelly sands and sandy gravels cover 21.8 % of the study area. These are moderate or poorly sorted sediments (mean sorting is 1.9, with in the range of 0.4 to 3.4), with a mean diameter of 0.36 ϕ (0.8 mm). Gravelly sands and sandy gravel mark the glacial till outcrops near Zelenogradsk and Zelenogradskaya bay at depths of 5-20 m and near the Lesnoy settlement of the Curonian spit at depths of 20-25 m. These sediments are widespread on the Rybachiy plateau and locally adjoin to the shore. They also extend on the central part of the Philinskaya bight up to the 25 m isobath. The seafloor areas covered by gravelly sands and sandy gravels exhibit more complicated relief than the sandy areas.

Boulders, pebbles and pebble-gravely deposits are distributed on the 15.9 % of the bottom surface and mark the bedrock outcrops near the Taran cape and quaternary glacial till outcrops on

the beam of the Kupalnjy and Gvardejskij capes and the Rybachiy plateau. At depths of less than 10 m, the seafloor is often covered by thin layers of fine and very fine-grained sands. The exception is the sea bottom area adjoining to the coast between the Philinskaya and Svetlogorskaya bights, where boulders join to the coastline. The sea bottom relief covered by boulder-pebbles and pebble-gravely deposits is very complicated and rugged.

III. Discussion

Sediment transport appears to be an important factor for the bottom surface sediment distribution. Traditionally, the sediment transport direction in the southeastern Baltic was determined by the concept of continuous Eastern-Baltic littoral drift from the Cape Taran to Cape Kolka near the entry to the Gulf of Riga [13]. However, a new model of relatively separate lithodynamic systems along the eastern Baltic coast was developed [14; 15]. Within the large-scale lithodynamic systems, smaller morpho-lithodymanic cells, separated by capes, were distinguished [16; 1].

Our results confirm the existence of separate morpho-lithodynamic cells on the Sambian peninsula northern underwater shore slope up to a depth of 20 m. Within these cells, divergence and convergence zones of sediment transport are formed. Divergent sediment transport vectors determine the cell boundaries located at beams of the Taran, Kupalnyj, Gverdejskiy and Lesnoe capes and in the vicinity of the Sambian peninsula. This finding is consistent with [14], which showed that according to model simulations and field observations, the zones of sediment transport divergence are formed near the capes areas. The coarse-grained sediments (boulders, pebbles, gravels) prevail in these zones and erosion processes supply an additional material on the submarine slope.

At depths of 20 - 30 m of the northern Sambian peninsula, the coastal transport vectors are directed east and northeast by the prevailing westerly winds.

Convergence sediment transport occurs at the centers of the coastal indentation of the Philinskaya, Svetlogorskaya and Pionerskaya bights, which is in agreement with [17]. Sediment transport of the dominant cross shore direction in these zones and accumulation of fine-grained sandy sediments occur up to depths of 20 m. According to [18], the permanent location of rip currents observed in the centers of the bays causes sediment erosion and seaward removal. However, our data show that transport vectors in the centers of the morpho-lithodymanic cells have an opposite direction toward the shore that contradicts the stable position of the rip currents. Their position is likely unstable and depends on wave parameters. According to [18; 16], the penetration of deposits between cells is limited and occurs only under storm conditions.

A different situation occurs in the Zelenogradskaya bight. Sediment accumulation is observed only in the narrow shallow zone up to depths of 5-10 m, where transport vectors are directed to the shore. There is a glacial till outcrop exposed to intense submarine erosion [2] that extends up to a depth of 20 m.

The particular feature of the sediment distribution on the sea bottom of the Curonian spit underwater slope is a sediment grain size alternation with increasing depth (Fig. 2). Fine-grained sands are distributed on both sides of the Rybachiy plateau at depths of 0-20 m. These sands are formed under recent accumulative processes and can refer to wave accretion deposits [2]. They are

complicated by relict lagoon mud outcrops and coarse-grained sediments. Transport vectors are directed differently here. At depths of 20 m, fine-grained sands transition to gravelly sands, which are also characterized by different transport vectors. Seaward, at approximately 25 m, the zone of very fine-grained sands alternate with gravelly sands. Fine-grained sands with higher mean diameters cover the seafloor deeper than 28–30 m. The transport vectors display a common seaward direction.

The presented sediment alternation on the Curonian spit submarine slope disturbs the "normal" distribution of the bottom deposits with a seaward decreasing grain size [19]. There are different opinions about the very fine-grained sands, which are not typical on the underwater slope. Local zones of coarse silt (aleurite) were outlined on the bottom sediment map of the Gdansk basin by Emelyanov [20] at a depth of approximately 20 m. It should be noted that coarse silts in the classification used by [20] are considered to be very fine sands on the Wentworth scale. Emelyanov connected zones of very fine sands (coarse silts in the original classification) with recent sedimentation processes. However, Blazhchishin [21] interpreted very fine-grained sands at depths greater than 25 m as relict coastal deposits, formed on accumulative terraces associated with the early stages of the Baltic Sea.

The configuration of very fine-grained sands in the straightened form along the coast allows us to suppose that their deposition is connected with accumulative processes near ancient shores. Additionally, 30 m is the off-shore boundary of wave influence on the sea bottom [17]. Therefore, wave-driven sediment movement here is strictly limited. Consequently, very fine-grained sands in this area are relicts. Specification of the genesis and conditions of their formation needs a more detailed study.

Exclusively coarse-grained sediments (boulders, pebbles, gravel and sandy gravel) connected with glacial till outcrops prevail on the Rybachiy plateau. Here, at depths greater than 15 m, transport vectors have a general direction to the shore. These implausible results are likely caused by method particularity and a lack of data. Transport vectors change their direction to alongshore at shallower depths.

IV. Conclusions

A new detailed lithological map of the underwater shore slope of the northern Sambian peninsula and the Russian part of the Curonian spit at a scale of 1:50 000 is created. New features of sediment distribution are obtained. The sediment transport trends are determined according to the grain size parameters. A superposition of the sediment transport vectors on the sediment type map derived from side-scan sonar observations yields some interesting correlations.

Separate morpho-lithodynamic cells are distinguished on the submarine slope of the northern Sambian peninsula coast up to a depth of 20 m. The cape areas of the Sambian peninsula serve as cell boundaries where a divergence of sediment trends and seabed erosion are observed. Coarse-grained sediments are presented with boulders, gravels, sandy gravels and gravelly sands. The convergence of sediment transport directions is confined to the bight's central parts. Fine and very fine-grained sand accumulation prevails here.

For the first time, the stretched zone of very fine sands is outlined at depths of 25-30 m of the Curonian spit underwater slope. These sands are relicts, and their formation is connected with

accumulative processes on the ancient shores of the Baltic Sea during previous stages of its development.

V. Acknowledgment

The work was supported by Russian Science Foundation (grant No. 14-37-00047). Authors are grateful to colleagues from VSEGEI for providing part of grain-size and sonar data, also for A. Krek and E. Bukanova for sediment sampling and grain-size analysis.

VI. References

[1] A.N. Babakov, "Evolution of perspectives about long-shore sediment transport structure in the South-Eastern Baltic," in *Lithodynanic of ocean contact zone. Materials of international conference*. Moscow, GEOS, 2009, pp. 56-58. [in Russian]

[2] O.V. Petrov (Eds.), *Atlas of geological and environmental geological maps of the Russian area of the Baltic Sea*, St.-Petersburg, VSEGEI, 2010, 78 p. [in Russian]

[3] E.M. Emelyanov, "Conclusion. Main features of sedimentogenes processis" in Sedimentation processes in the Gdansk basin (Baltic Sea), Emelyanov E.M., K. Vypyh (Edt.), Moscow: P.P. Shirshov Institute of oceanology AN SSSR, 1987, pp. 248-259 [in Russian]

[4] V. Sivkov, E. Burnashov, V. Chechko, E. Dorokhova, D. Dorokhov, A. Krek, D. Ryabchuk, A. Sergeev, V. Zhamoida, "The bottom surface sediments mapping in the Russian part of the south-eastern Baltic Sea," in *Abstract Volume Baltic 2014 The 12 th Colloquium on Baltic sea Marine Geology September*, Warnemunde: Leibniz Institute for Baltic Sea Research, 2014, pp. 47 - 47.

[5] R.L. Folk, W.C. Ward, "Brazos River bar: a study in the significance of grain size parameters," in *J. Sediment. Petrol.*, 27, 1957, pp. 3–26.

[6] S. Blott, K. Pye, "Gradistat: a grain size distribution and statistics package for the analysis of unconsolidated sediments" in *Landforms*, 2001, V. 26, pp. 1237–1248.

[7] R.L. Folk, "The distinction between grain size and mineral composition in sedimentary-rock nomenclature," *Journal of Geology*, 62, 1954, pp. 344-359.

[8] P. McLaren, D. Bowles, "The effects of sediment transport on grain-size distributions," *J. Sediment. Petrol.*, 55, 1985, pp. 0457–0470.

[9] S. Gao, M. Collins, "Net sediment transport patterns inferred from grain-size trends, based upon definition of "transport vectors," *Sed. Geol.*, 80, 1992, pp. 47–60.

[10] M. Kairyte, R. Stevens, "Composite methodology for interpreting sediment transport pathways from spatial trends in grain size: A case study of the Lithuanian coast," *Sedimentology*, V. 62, 2015, pp. 681–696.

[11] A. Y. Sergeev, V. A. Zhamoida, D. V. Ryabchuk, I. V. Buynevich, V. V. Sivkov, D. V. Dorokhov, A. Bitinas, D. Pupienis, "Genesis, distribution and dynamics of lagoon marl extrusions along the Curonian Spit, southeast Baltic Coast," *Boreas*, 2016.

[12] V.A. Zhamoida, D.V. Ryabchuk, Y.P. Kropatchev, D. Kurennoy, V.L. Boldyrev, V.V. Sivkov, "Recent sedimentation processes in the coastal zone of the Curonian Spit (Kaliningrad region, Baltic Sea)," *Z. dt. Ges. Geowiss.*, 2009, 160, pp. 143–157.

[13] R. J. Knaps, “Sediment transport near the coasts of the Eastern Baltic,” in *Development of sea shores under the conditions of oscillations of the Earth’s crust,* Valgus, Tallinn, 1966, 21–29. [in Russian].

[14] N.A. Bogdanov, “Forming and dynamic of marine placers near accumulative coast of South-Eastern Baltic Sea,” PhD dissertation, Moscow, MGU, 1987, 24 p. [in Russian].

[15] A.N. Babakov, “Spatial – temporal currents structure and sediment dynamic in the coastal zone of the South-Eastern Baltic (Sambian peninsula and Curonian spit),” PhD dissertation, Kaliningrad, Geographical faculty, KGU, 2003, 273 p. [in Russian].

[16] N.A. Aibulatov, L.A. Zhindarev, N.A. Piskareva, “Sediment transport in the coastal zone of South-Eastern Baltic” in Natural basement of environmental conservation, Moscow, 1987, pp. 99-116. [in Russian].

[17] A.N. Babakov, “Sediment dynamic in the coastal zone,” in *Oil and environment of Kaliningrad region*, Kaliningrad: Terra Baltica, V. II. The Sea, 2012, pp. 276-291. [in Russian].

[18] L.A. Zhindarev, A. Sh. Habidov, V.V. Scherbina, “Lithodymanic peculiarities of the tide-less sea and management model of the coastal zone,” in Sea coastal zone: morpho-lithodynamic and geoecology. Materals of XXI International coastal conference, KGU, Kaliningrad, 2004, pp. 34-38. [in Russian]

[19] Uj. S. Dolotov, *Dynamic environments of coastal sedimentation and relief formation*, Moscow, Nauka, 1989, 268 p. [in Russian]

[20] E.M. Emelyanov (Edt.) *Geology of the Gdansk basin. Baltic Sea,* Kaliningrad: Yantarnij skaz, 2002, p. 496.

[21] A.I. Blazhchishin Littoral area in the Baltic Sea off the Sambian peninsula. In: Emelyanov E.M. (ed.). Geology of the Gdansk Basin, Baltic Sea. Yantarny Skaz, Kaliningrad, 2002, p. 375 – 380. [in Russian]

NEWEST TECTONICS OF THE VISTULA SPIT AREA

Nikolay Dunaev, P.P. Shirshov Institute of Oceanology of the Russian Academy of Sciences, Russia
Nadezhda Politova, P.P. Shirshov Institute of Oceanology of the Russian Academy of Sciences, Russia

dunaev@ocean.ru

The interests of forecasting of the area's development simulate to take more attention to the study of its newest tectonics. The most informative tectonic pattern for the studies of coastal zones is neotectonic one, based on the structural principle, which shows the newly formed and inherited dislocations, reflected in the modern landscape and exodynamics of the earth's surface. The question of the manifestations of newest tectonics by way on the example of the Vistula Spit (Baltic Sea) is discussed.

Key words: newest tectonics, coastal zone, sea level, Baltic Sea, Vistula Spit

I. INTRODUCTION

Newest tectonics stress initial and create new irregularities of the earth's surface, thereby controlling the specificity of exogenous morpho- and lithodynamic processes. As a consequence, it influences on the features of development of denudation and accumulative relief, of sediment's transit, of formation of lithologic varieties, of capacity and mechanical properties of the deposits and others. One of the main aspects of the newest tectonics exhibits in the creation of the initial inclination of the earth's surface. The latter, in particular, predetermine the development of the coastal zone according to accumulative or abrasion scenario. The lithological features, as well as the climate, affect mostly on the rate of coastal processes, without being able to radically change their orientation. We can consider the values in the range of 0.001–0.005 as the optimum inclinations of the underwater coastal slope defining relatively calm state of the coastal environment. It should be emphasized that in a coastal zone' conditions a natural situation may appear when the bottom inclination changes only enough 0.001 (tg), so that the accumulative scenario of its development changes for the abrasion or vice versa. And such change can happen tomorrow, because as long as the powerful thermal pot in the entrails of the Earth functions, long geological tectonic quiescence state on its surface will never be. It is believed that the minimum period of restructuring of the underlying processes, initiating the structure-forming movements, is 10 thousand years [1]. Therefore the beginning of the ongoing young tectonic phase can be attributed to the boundary of the Late Pleistocene-Holocene.

Many researchers of the coastal zones often do not attach importance to newest tectonics, because they believe that tectonic movements now are too slow. Indeed, if one projects the amplitudes of vertical movements on the entire period of neotectonic development of the region, we obtain the velocities close to 0.01 or even less. But! Tectonic movements do not occur uniformly,

but as impulses for a geologically short time, they alternate with periods of acceleration, a longer deceleration and even of local short rest. An important feature of the newest tectonic movements, including today, is the fact that, they are characterized by the inheritance of the sign and often of the speed in their temporal manifestation [2]. At the same time the tectonic processes inheritance determines the coastal processes one that are well reflected in the coast's types [3]. The rate of vertical tectonic displacement already considered significant when the value is 1 mm per year and is particularly crucial in the formation of coast's subtypes, the position, size and configuration of coastal accumulative forms, as evidenced by the example of seashores [4]. Some area of the coastal zone is undergoing significant changes even when the area's coastline comes out of the influence of a structural-tectonic element particular expressed at the surface. It also occurs when it passes to another part of the same element, for example, during the transfer from the seaside declining wing of anticline to the opposite wing. Therefore, *the most informative tectonic pattern for the studies of coastal zones is neotectonic one, based on the structural principle*, which shows the newly formed and inherited dislocations, reflected in the modern landscape and exodynamics of the earth's surface. Such patterns allow representing the picture of tectonic organization of geological space (blocks, folds, faults, etc.), focusing and, where possible, the activity of the movement of the selected elements in the tectonic structure more legibly. Criteria for selection of the newest structural and tectonic elements and the evaluation of their dynamics are widely covered in Russian literature and in some foreign publications. In light of above-mentioned it is obvious that the interests of forecasting of the area's development simulate to take more attention to the study of its newest tectonics.

As to the sea shores one can judge the neotectonic manifestations with high confidence on the basis of structural and geomorphological method with study of features in the distribution of various forms and elements of the earth's surface relief, of its morphographic and morphometric properties in the border area land – sea, of the specifics of the spread, occurrence and composition of the adjacent deposits, of the nature of coastal abrasion–accumulation, erosion and denudation, and others processes. The differentiation of the territory according to these criteria regardless of the commitment of the researcher to any geodynamic concepts is the basis for the mapping of neotectonic patterns, including the structural principle, usually with highlighting of raises, depressions and so-called "weak zones" predefined by the disjunctive tectonics.

II. Geomorphological characteristics of the Vistula Spit area

Vistula Spit is located in the south-eastern sector of the Baltic Sea (Fig. 1). In accordance with the indicated methodological approach the southeastern area of the Baltic Sea has the following largest orographic formations (Fig. 2): Sambian elevation, Pregel lowland, Warmia elevation, Paslenk depression, Elblag elevation.

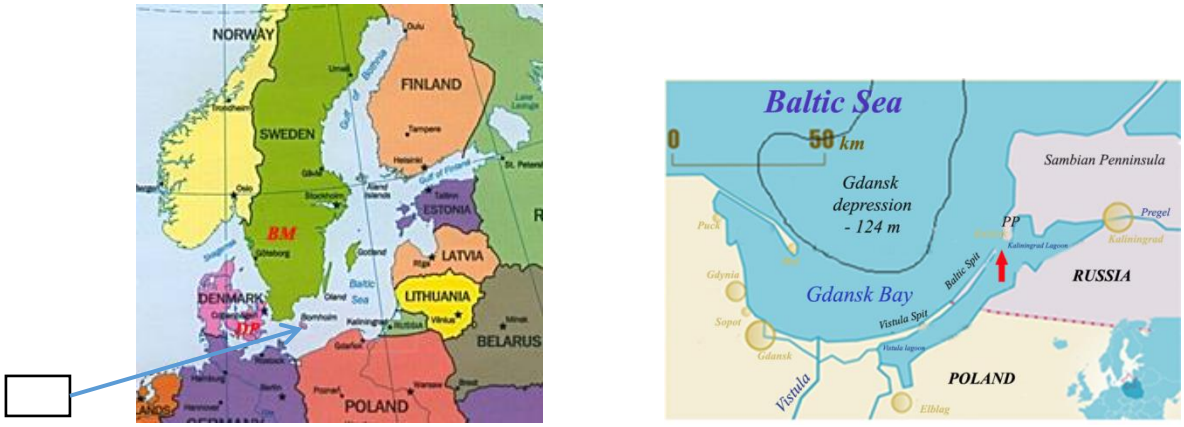

Fig. 1. Position of the Vistula (Baltic) Spit [10 et al.]: PP – Pillau Penninsula; red arrow show the Baltic Channel; BM – Billingen Mountain; DP – area of the Danish passages.

Fig. 2. Main orographic elements of the south-eastern coast of the Baltic Sea: 1 – Sambian elevation; 2 – Pregel lowland; 3 – Warmia elevation; 4 – Paslenk depression; 5 – Elblag elevation; 6 – Vistula lowland

Warmia elevation is in fact the northern slope of Turow hills in Poland. Elblag elevation is relieved by the Vistula lowland to the south, which stretches far inland to the Bydgoszcz city' suburbs.

Within the Vistula Spit one can identify a number of areas on hypsometry scale 1:50 000 in the direction from north to south. 1 – from the Baltic channel to the Chayachy (Taran) Cape. It is characterized by the development of individual low (rarely more than 10 m) and small dunes and a well-defined low near-bay terrace formed on the delta plain and forming the broader land prominences towards the Vistula Lagoon. 2 – from the Chayachy Cape to the Cape Razmytyy. Here the narrowing of the spit occurs and levelled aeolian-marine surface *palve* between the seaward foredune ridge and the ancient high dunes in near-bay area appears (Fig. 3). 3 – from Cape Razmytyy until Cape Vysokiy inclusive. Here the spit expansion approximately twice comes and the signs of a double ridge of dunes occur. Single morphosculptural form with up to 25 m height near Cape Glavnyy is perhaps the rib of delta plain or moraine, as well as a similar, previously noted [5], the rib near the Cape Vysokiy (+24 m). These relief elevations are separated by low-elevation site

with some small (up to 5 m) dunes. 4 – southward to the Cape Vysokiy up to the area of Pyaski (Fig. 4) village the spit again approximately doubled narrows and in almost edgewise the rapid development of dunes up to 30–36 m height is shown. 5 – southward to the Pyaski village up to 54˚32' N the spit's width is slightly increased, accompanied by an extension of the adjacent shallow areas of the bay, and south to latitude 54˚23' the spit again narrows to the size of area 4. Here the double ridge of dunes is clearly traced. The higher (up to 20–27 m) one is shifted to the bay. The ridge with height of 5–15 m is located seaward. 6 – from the southern border of the previous section to the village Borovoye inclusive, this area as compared to the southern part of the previous section, expands about twice and is characterized by a more expressive manifestation of double ridges at similar marks of elevations, sometimes exceeding 40 meters. This area is characterized by the development of the highest dunes of the spit. 7 – southward to the village Borovoye the spit's width is reduced by almost half and high (up to 34 m) dunes along its width occur. This morphosculptural situation continues in the root part of the spit, where from approximately longitude of inner part of the Vistula Lagoon the double expansion of this accumulative form and the division of the dune complex into two ridges such as higher (up to 37 m) coastal and lower (12–15 m) rear separated by a low relief area take place. Thus, the spit largely consists of aeolian sands forming several generations of forms. In its structure there are the ribs of water-glacial plain, preserved from erosion by as sea waves, and the waves of the lagoon [5–7] (Fig. 3, 5).

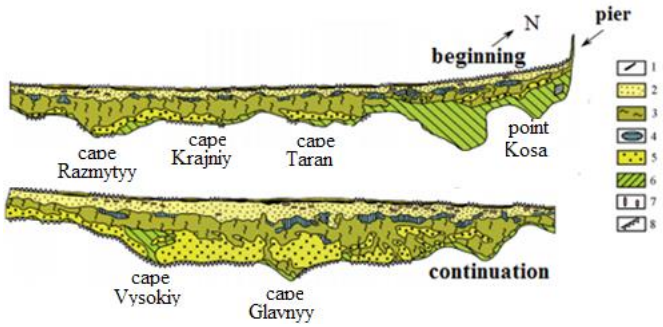

Fig. 3. Geomorphological map of the Vistula Spit [6, with some refinements]: 1 – foredune ridge; 2 – seaside dune swell; 3 – levelled regressive aeolian-marine surface – "palve"; 4 –swampy depressions of the old lagoons; 5 – elevated old dune massifs; 6 –old deltas plaines with low near-bay regressive terrace; 7 – deflation basins in dunes; 8 – ledges of the scouring

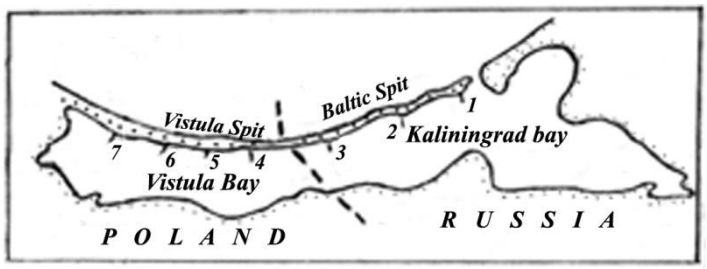

Fig. 4. The shore points. 1 – point Kosa, 2 – cape Razmytyy, 3 – cape Vysokiy, 4 – point Piaski, 5 – point 53˚32' N, 6 – point 53˚23' N, 7 – point Borovoe

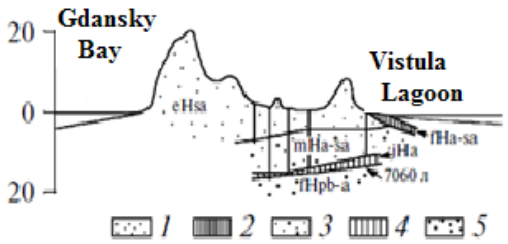

Fig. 5. Fragment of the geological structure of the Vistula Spit [8]: 1 – aeolian sands (eHsa – subatlantic); 2 – alluvial-deltaic sediments (fHa-sa – atlantic-subatlantic); 3 – sea sands (mHa-sa – atlantic-subatlantic); 4 – peat (jHa – atlantic); 5 – fluvial sands (fHpb – preboreal).

III. The cause of geomorphological fragmentation of the Vistula Spit

It should be found the cause of the considered fragmentation of the spit along its strike with its distinct contraction and expansion (in four respectively), as well as bathymetric differentiation of the bay in the history of their origin and development, in the degree of participation of related factors and agents. Late Quaternary deposits are represented here by South Lithuanian moraine complex simulated by fluvial processes. The latter created a low-lying alluvial plain with separate jets of moraine hills, many of which are associated with positive neotectonic structural forms. Under the conditions of the coastal lowland the riverbeds divided into shallow branches. The original nucleuses of concerned accumulative forms were laid during the Holocene transgression as submarine swells, gradually shifting towards the land because of the specificity of coastal hydrodynamics. Under certain conditions the largest ones have been converted into bars. It may be assumed, the latter located primarily in estuarine areas of river valleys with their loose sediments' supply. It is also possible that the bars were formed on the underwater continuation of low watersheds leveled by marine abrasion, when the alluvial moraine material allowed forming a profile of equilibrium quickly, and it is shifted towards the land parallel to itself as far as the advance of marine transgression. In time, in the coastal area along with the transverse movement of sediments their longitudinal movement was formed. The latter has led to damming of branches of subaerial valleys and to joining of the bars into a single spit, which was developed by its own laws, including the active manifestation of aeolian processes. Only the section in the northern part of the bay bar on the continuation of the most developed branch of the Pregel River was the least resistant to sea wind and wave action, and from time to time here the passage into the isolated by spit Vistula Lagoon was formed, so it was turning into the bay.

As a single form the spit was formed in historical times. Even in the XII century there were a few island bars. Since the first half of XVI century the appeared passage was artificially maintained as the Baltic Canal. Southward located fragment of the bay bar became known as the Vistula (Baltic) spit. Sometimes one calls the part of the spit to the south of the Poland-Russia boundary the Vistula, and the northern part – the Baltic spit.

In consideration of the fact that the period of the spit's existence as the bay bar was inevitably accompanied by an opposite longshore flux from the north and south sides, it was to be expected that the broadest part of this form should be in the middle part of spit, in the area of the convergence of the longshore fluxes. It has been observed at present [9, 10] (Fig. 6, 7). However, it

is difficult to explain the location of the spit, the morphological heterogeneity of the spit and the adjacent bay as an effect of the exogenous factors only. It seems that on condition of a practically single geological structure of the substrate of the spit and the bay the prominent role in their formation and in their modern form belongs to differentiated vertical newest tectonic movements of this substrate. It is logical to assume that the latter were intensified due to alternation of glacial loading / unloading. Such activation has occurred the most impressively in the zones of tectonic faults, accompanied by shifts of tectonic blocks on them.

Fig. 6. Lithodynamics of the coastal zone of the Vistula Spit [9]: 1 – predominant fluxes of the sands; 2 – rich sediment flux; 3 – sedimentation from the flux.

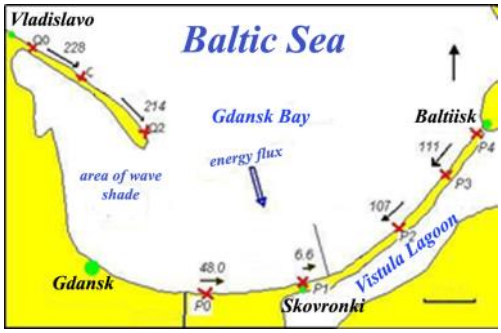

Fig. 7. Scheme of the total flux budget [10]. Arrows show the direction and the value of the alongshore sediment fluxes (thousands m^3 per year), crosses show the position of the estimation points.

IV. Geostructural position and newest tectonics of the area of the Vistula Spit

In geostructural respect the spit is located in the south-east wing of the Gdansk depression [11], complicating the Baltic (the Baltic, the Baltic-Belarusian) gemisyneklise of the Russian plate of the East European platform [12] (Fig. 1, 8). The newest stage of tectonic development of the region began in the late Oligocene, accompanied by subaerial environment and by deformation of the original levelling surface, which is consist of the Rupel layers of early Oligocene. This period is followed by the phases of structural formation and restructuring. Since 6 thousand years BP due to the termination of glacial isostasy [13] the region is subject only to the newest tectonic movements and the seismicity, the energy of which is estimated at 4 magnitude [14] (Fig. 9). Modern geodynamics of the spit according to some researchers is characterized by a weak relative fall movement [14] (Fig. 10).

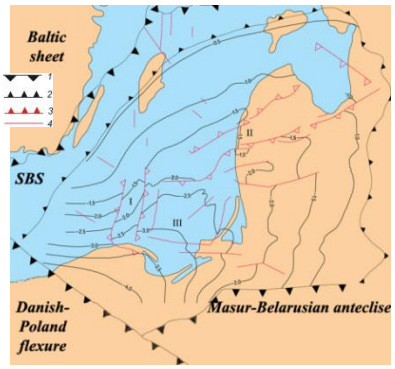

Fig. 8. Baltic hemisyneclise of the Russian plate of the East European platform [12]. I – Leba ledge; II – Liepaja-Pskov anticlinal; III – Gdansk depression; Boundaries: 1 – Baltic sheet; 2 – Baltic syneclise; 3 – major structures of the Baltic syneclise; 4 – faults. SBS – slope of the Baltic Sheet.

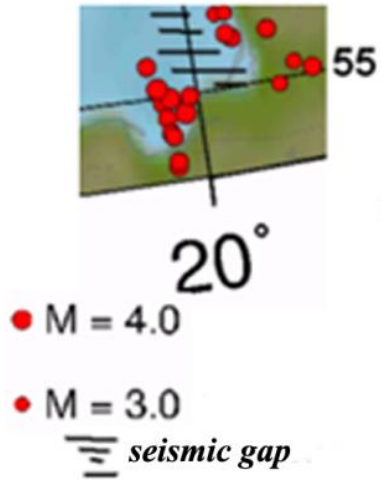

Fig. 9. Seismicity in the Vistula Spit area [14].

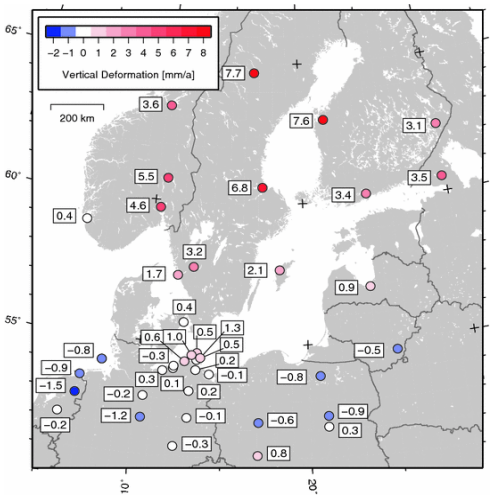

Fig. 10. Recent vertical deformations region of the earth crust in the Baltic (mm / year) nonmetering the newest tectonics [15].

The modelling of cartographic patterns of the newest tectonics of the study area is provided on the basis of its structural and geomorphological analysis accounting the methodological procedures [16, 17]. The most important criteria are the orographic and genetic features of subaerial and subaqueous relief, strike and types of seashores, shape and cross-section isohypses and isobathics, orientation and shape of the river valleys, usually originating in the positive structural forms and developing in negative neotectonic structural forms or in tectonically predetermined lineaments as weakened zones of near-surface horizons of the crust, locking the tectonic faults. As a result of the research the cartographic pattern of newest tectonics of the study area is made (Fig. 11).

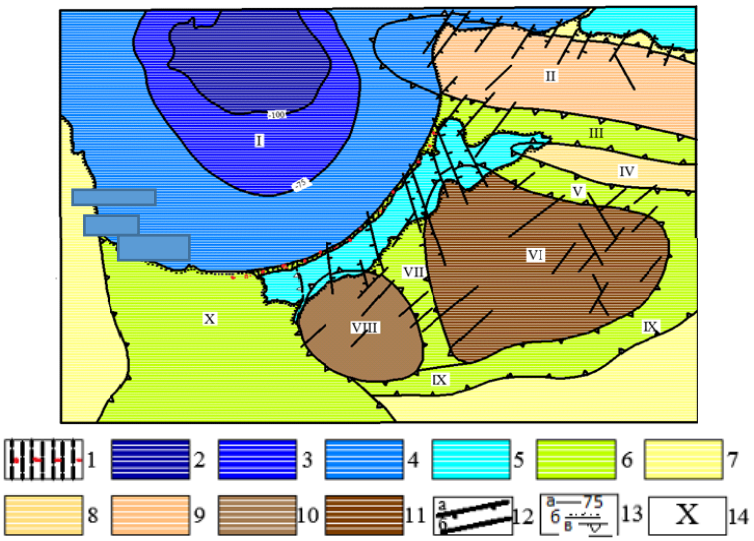

Fig. 11. Cartographic model of the newest tectonics of the Vistula Spit: 1 – Vistula Spit; 2–5 – sea area with depth: 2 – > 100 m; 3 – 100÷75 m; 4 –75÷10 m; 5 –< 10 m; 6–11 – land area with the heights: 6 – 0÷25 m; 7 – 25÷50 m; 8 – 50÷100 m; 9 – 100÷150 m; 10 –150÷200 m; 11 – > 200 m; 12 – explosive deformations: a – with shift; b – others; 13 – boundaries: a – sea depth; b – land; c – structural forms; 14 – structural forms: I – Gdansk depression; Newest elevations: II – Sambian swell; IV – Interfluve swell; VI – Warmia brachymorphic; VIII – Elblag isometric; Newest relative depressions, valley flexures: III – Pregel; V – Prokhladnenskii; VII – Branev; IX – Lava-Lynsk; X – Vistula [by authors].

It shows the dominant development of the plicative newest structural forms in the forms of elevations and depressions in different scale. Disjunctive dislocations generally have a modest value, but are important at the local level. The latter is related directly to the Vistula Spit.

According to the degree of uplift activity determined by their elevations, and the structure and the depths of cuttings of river valleys, they can be ranked in descending order: VI, VIII, II, IV (Fig. 11). The latter apparently is the youngest. As for the faults one can says that their length corresponds to the upper crust origin. Most likely, they are not as newly formed, as present an updated version of the older one, activated by Quaternary glaciers and earthquakes in the adjacent areas. As for the spatial distribution of these disturbances there is the considerable prevalence of north-western strikes in the south of the region, which replaced to the north-eastern strike from Pregel lowland to Sambian swell. This, perhaps, is a sign of the local differentiation of global compressive stresses directed from the Mid-Atlantic Ridge.

According to the presented pattern of newest tectonics, the identified faults with northwest strike complicate the eastern slope of the Gdansk depression, making its weakly differentiated block structure. Within the limits of this structure the formation of the Vistula Spit occurred. The location of the faults in the spit area is in good agreement with those of an earlier study [14], with the only difference that the authors suggest their sublatitudinal strike.

The comparison of geomorphological data from the Vistula Spit with the neotectonic pattern shows that the widest parts of it and the development of high dunes correspond to the raised blocks. Perhaps, these areas were more favorable for the initial slopes, predetermined the earlier formation

of nuclear fragments of spit (original bay bar) and subsequent accumulation of coastal sediments supplied from underwater slope.

In general, the newest geodynamics of the area is characterized by differentiated raising, in which the slope of the Gdansk depression where the Vistula Spit was formed is involved. Among the signs of uplifting the abrupt banks of even small rivers of the sea coast, reducing of the width of valley flexures due to the growth of adjacent elevations, manifestations of faults in the Quaternary sediments, the presence of the Late Holocene overflow coastal terraces and others can be noted. It can be assumed that now the rate of uplift of spit area is approximately comparable (at least, no less) with the uplifting rate of the Baltic Sea level caused by the current, geologically short-lived climatic cycle of the planet. This circumstance can explain the relatively stable state of the spit seashore, since the depth of the underwater coastal slope also remained practically invariable, allowing the wind-wave factor to mobilize available bottom sediments and to carry them to the shore. If the rate of uplift exceeded the transgression one, the sea waves would lose some of the energy away from the shore, and it could lead to the formation of new submarine swell, which do not necessarily have shifted to the modern coastline. When lifting rate is less than the rate of transgression the depth of the underwater slope would increase and sea waves would approach the shore with higher energy, causing its erosion. On near-channel spit area because of the intervention of human factor the coastal hydrodynamics, which determines the erosion of the spit due to the local conditions, plays a major role. The lowering rate of the area in limits 0 ÷ –1 mm / year (Fig. 10) is obtained only by extrapolation, it is relative, and fixes the total transgressive effect of the current climate cycle and neotectonic state of the specific location of its observation.

At the present time the climate is in the cooling phase, which will last about 15 years [18]. As you know, cold weather does not lead to an increase of sea level. So, it follows that eustatic factor will not appreciable influence on the evolution of the Vistula Spit at least in engineering (50–60 years) time scale. The budget and the balance of beach-forming deposits will have main importance in the dynamics of the coastal zone of the spit (Fig. 5, 12, 13, 14). It is not expected the catastrophic changes in the development of the spit on natural scenario for this time, because the coastal morphogenesis adapted to the current situation. In the long term we can expect the disappearance of the Vistula Lagoon because of its filling by sediments and weak tectonic uplift of the area.

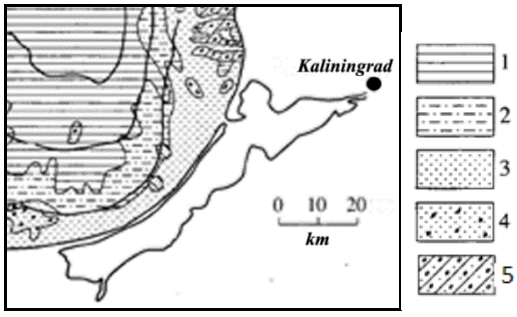

Fig. 12. Bottom sediments in the sea near the Vistula Spit [19]: 1 – muds; 2 – silts; 3 – sands; 4 – coarse-grained sands, gravel, pebble, boulders; 5 – moraine.

Fig. 13 Beach and foredune ridge of the Vistula Spit.

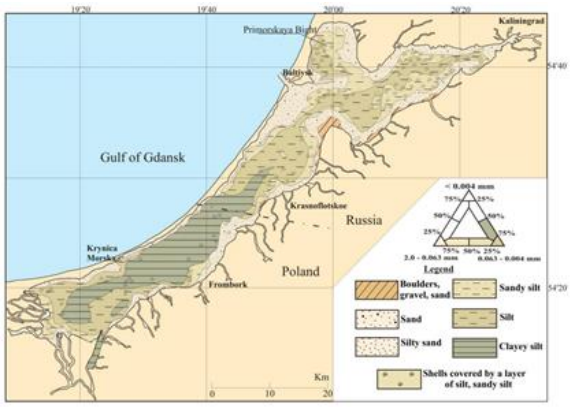

Fig. 14. Distribution of the surface bottom sediments (0–5 sm) in the Vistula (Baltic) Lagoon [20].

V. Acknowledgment

This work was financially supported by the RSF (grant № 14-17-00547, parts: geostructural position and newest tectonics) and by the State programme (theme 0149-2014-0035, parts: geomorphology and lithology).

VI. References

[1] A.F. Grachev, I.V. Kalashnikova, and V.A. Magnitskii "Modern movement of the earth crust and the seismicity", *Izvestiya. Physics of the Solid Earth*, vol.11, pp. 3-11, 1990 (in Russian).

[2] I.V. Kalashnikova and V.A. Magnitskii "On the inherited type of modern movements of the earth crust" *Izvestiya. Physics of the Solid Earth*, vol.10, pp. 13-20, 1978 (in Russian).

[3] V.P. Zenkovich, *Main areas of the investigations of the sea coastal zone in the USSR. Theoretical issues of the sea coast dynamics.* Moscow, Nauka, pp. 3-13, 1964 (in Russian).

[4] L.G. Nikiforov, *Structural geomorphology of the sea coasts.* Moscow: MSU Publ., 175 pp., 1977 (in Russian).

[5] E.N. Badyukova, L.A. Zhindarev, S.A. Luk'yanova and G.D. Solov'eva "Geomorphology and the history of development of the Curonian and the Vistula spits (SE Baltic)" in *Strategiczne pytania swiatowej nauik*, vol. 29. Ecologia, Geografia I geologia. Przemysl (Poland): Nauka i studia, pp. 72-81, 2014 (in Russian).

[6] E.N. Badyukova, L.A. Zhindarev, S.A. Luk'yanova and G.D. Solov'eva "The geologic-geomorphological structure of the Baltic (Vistula) Spit", *Oceanology*, vol. 51 (4), pp. 675-682, 2011.

[7] E.N. Badyukova, L.A. Zhindarev, S.A. Luk'yanova and G.D. Solov'eva "The peculiarities of the geologic-geomorphological structure of the Baltic (Vistula) Spit", Theory of the sea coast development: age-old traditions and ideas of the modernity, pp. 170-172, 2010 [Abstracts Conf., 2010] (in Russian).

[8] A. Tomczak, J.E. Mojski, J. Krzymińska, et al. "New data on geologic structure of the Vistula Bay Bar", *Kwartalnik Geologiczny*, vol. 33 (2), pp. 277-300, 1989.

[9] V.L. Boldyrev and O.I. Ryabkova "Dynamics of the coastal processes on the Kaliningrad coast of the Baltic Sea", *Izvestiya of Russian Geographical Society*, vol. 133 (5), pp. 41-49, 2001 (in Russian).

[10] I. Leont'yev and T. Akivis "Evolution forecast of the gulf of Gdansk sand spits in 21 century", *Sea coasts – evolution, ecology, economy*, vol. 1, pp. 239-243, October 2012 [*Materials XXIV Inter. Coastal Conf.*, 2012] (in Russian).

[11] A.G. Grigoriev, V.A. Zhamojda, M.A. Spiridonov, A.Yu. Sharapova and V.V. Sivkov "New data on the history of the development of the south-eastern part of the Baltic Sea from the Late Ice Age to the present", *Regional geology and metalogeny*, vol. 40, pp. 103-114, 2009 (in Russian).

[12] *Geographical atlas of the Kaliningrad region*, V.V. Orlenok, Ed. Kaliningrad: KSU Publ., 276 pp., 2002 (in Russian).

[13] A.F. Grachev and P.M. Dolukhanov, "Subglacial raising of the earth crust in Canada and Fennoscandia according to the data of radiocarbon dating", *Baltica*, vol. 4, pp. 297-312, 1970 (in Russian).

[14] *Seismotectonics of the old platform plates in the area of the Quaternary glaciation. Part 1. Kaliningrad region and the adjacent area*, R.G. Garetskii and S.A. Nesmeyanov, Eds. Moscow: Book and business, 228 pp., 2009 (in Russian).

[15] M. Lidberg, J.M. Johansson, H.G. Scherneck and·J.L. Davis, "An improved and extended GPS-derived 3D velocity field of the glacial isostatic adjustment (GIA) in Fennoscandia", *Journal of Geodesy*, vol. 81, pp. 213–230, 2007.

[16] N.I. Nikolaev, "On the principles of the drawing up of the newest tectonics maps during the neotectonical zoning", *Izvestiya VUZov, Geology and prospecting*, vol. 4, pp. 3-12, 1982 (in Russian).

[17] *Application of the geomorphological methods in the structural-geomorphological investigations*, Moscow, Nauka, 296 p., 1970 (in Russian).

[18] R.I. Nigamtulin, N.V. Vakulenko and D.M. Sonechkin, "Global warming in reality and in the climatic patterns", *Turbulence, atmosphere dynamics and climate*, pp. 76-79, May 2013 [*Abstracts Inter. Conf.*, 2013] (in Russian).

[19] N.I. Sviridov and E.M. Emelyanov, "Facial-lithological complexes of the Quaternary deposits of the Central and south-eastern parts of the Baltic", *Lithology and Mineral Resources*, vol. 3, pp. 246-267, 2000 (in Russian).

[20] J. Zachowicz and S. Uscinowicz, *Geochemical atlas of the Vistula Lagoon*. Warszawa, 1996.

ACCUMULATIVE COASTS AS RELIABLE INDICATORS OF THE KINEMATICS OF THE SEA LEVEL DURING THE HOLOCENE

Dunaev Nikolay, P.P. Shirshov Institute of Oceanology RAS, Russia
Repkina Tatiana, Lomonosov Moscow State University, Russia

geonik2010@yandex.ru

Currently, there is no single view of the Holocene global sea level kinematics. At the same time, the question of a possibility of it exceeding the current sea level by several meters is being debated. The accumulative coasts of nearly tide-free seas, in areas where the vertical direction of coastal movement remained unchanged are the most convenient objects for studying this major paleogeographic issue. Effects of the sea level fluctuations are revealed in the resulting geomorphological structure and in the nature of sediment areas of the coastal zone developing in an accumulative mode. If the Holocene sea level exceeds its modern marks, then ladders of accumulative terraces would have formed over different parts of the coast. The heights of the terrace ladders would correspond to the amplitudes of these exceedances. The lower sediment levels should reflect the transgressive character of their formation in the structure of geological section, while the higher levels would reflect the regressions. The coast of the Thatcher Peninsula, located in the Bay of Cumberland microcontinent of the South Georgia (Antarctic) was the focus of our research. It was established that the Holocene sea level in the region reached its current state no later than about one thousand years ago and did not exceed it, being subjected to only minor fluctuations of the synoptic scale. The accumulative terraces are located in fragments. The differences in their absolute elevations are related to their correspondence to different tectonic units experiencing differentiated uplift.

Key words: World Ocean, sea level rise, Holocene, sea coasts

I. INTRODUCTION

Information about the state of global sea level is one of the most important in the study process of the Earth's history. To date, in particular, it found that since the Tertiary period, he falls, experiencing fluctuations under the influence of various factors - climatic, tectonic, etc. (Fig 1). The most studied kinematics of the sea level in the Late Quaternary. However, researchers have not come to a complete agreement, even with regard to the latter - the Holocene, stage (Fig. 2). Significant progress in this discussion include recognition of the low position of the sea level at the beginning of the global postglacial transgression (however, estimates of sea level provisions differ), as well as the consent of the researchers in the impossibility of constructing a unified graphical model (curve) of this transgression. Among the major differences are, for example, evaluations of the kinematics of the sea level after the boreal period the Holocene. In this issue clearly delineated *three concepts* (Fig. 2). 1. The sea level increased, asymptotically approaching the modern, and perhaps, felt vibrations of varying duration and low amplitude (within the accuracy of measurement

- a few tens of centimeters). 2. About 6 kilo years ago sea level has become higher than the present for a few meters and then, after some hesitation, occurred noticeable (up to a few meters) undulation between 4.5-2 kilo years ago. Then, the sea level dropped to modern heights and experienced only minor fluctuations. 3. The sea level reached the current situation in the Atlantic period, and subsequently did not significantly changed. There are also other positions of individual researchers, including allowing sea level fluctuations with an amplitude of a few meters the entire second half of the Holocene. Most often controversial question becomes: reflect the forms of coastlines of the Holocene higher position of the sea level or tectonic uplift coast of height close to modern.

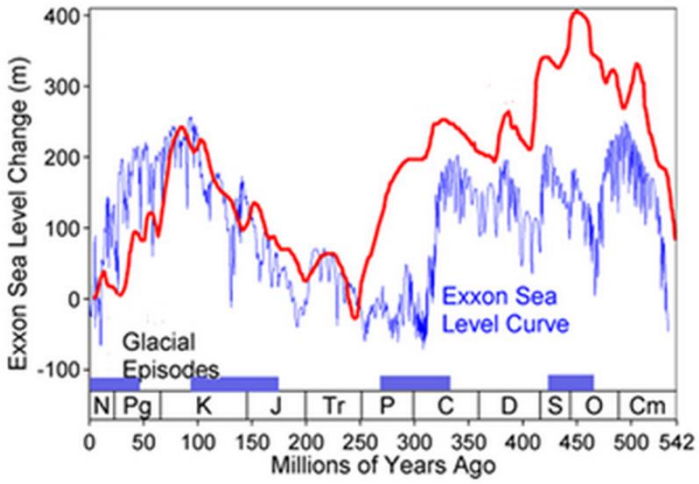

Fig. 1. Panerozoic global sea-level fluctuations [1] with some refinements

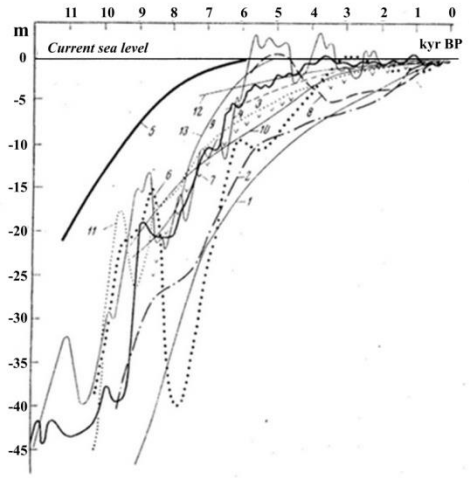

Fig. 2. Representations of the kinematics of Holocene in sea level according to: 1 - Nevessky, 1967 2 - Pavlidis 1961, 3- Bloom, 1965, 4 - Faibridge, 1961 5 - Fisk, 1965 6 - Hopkins, 1967 7 - Jelgersma, 1966 8 - Kelleat, 1975 9 - Mörner, 1969, 10 - Neuman, 1969 11 - Shepard, 1964, 12- Sholl, 1969, 13 - Suggate, 1968 [2]

Allocated problem is not purely scientific. Its decision is due to the forecast of development of the coastal zone and shelf. If the level of the World ocean in the Holocene is constantly grew, slowing down to a relative stabilization, of the modern form of the coastal zone must be regarded as

mature (stable). They have adapted to the dynamic mode of the respective marine areas. If sea levels fluctuate with an amplitude of several meters (or even up to a few tens of meters), it must be supposed that the current relief of the coastal zone is not different relative stability. In this case, the greatest negative consequences are associated with sea level rise.

Thus, the economic development of shore areas depends on understanding the trends of changes land and sea interface zone. A variety of existing kinematics models of sea level in the form of graphs (curves) can be explained by the fact that not always take into account such important factors as the regional and local tectonic setting, often an insufficient number of dating; the subjectivity of the ideas and concepts, and sometimes biased theories and concepts of researchers.

The consequences of sea level fluctuations expressed in the structure of the relief and sediments of the coastal zone. Especially convenient objects for studying this problem are accumulative coasts of nearly tide-free seas, in areas where direction of the vertical movement of the coast were constant and the age of the coastal sediments it can be set. It is now known that the geological deposits of the coastal zone, on accumulative developing scenario, differ mainly in their granulometric compositioin. If the sea level during the Holocene exceeded its current, then the accumulative section of the coastal deposits of this age should be composed of lower - transgressive, and in the upper - regressive sediment units. If this raise was not, then deposits will be presented regressive sediment units.

Thus, a reliable sign of a higher than modern sea-level positions, are accumulative terraces by coastal processes, and located higher the modern coastal zone. The structure of the deposit-units of these terraces must contain *transgressive-regressive* of littoral facies, reflecting the sea level change.

In addition, such fluctuations were to create on different coasts of stairs accumulative terraces with a height corresponding to the amplitudes of the prospective elevation of sea level. At the same time on the coast of elevation the present height of the these terraces should be above their initial position (that is greater, than the expected positive amplitude Holocene transgression) because of the subsequent neotectonic movements.

On the coasts of the positive or negative structural-tectonic deformations can be observed forms of the coastal relief, developing, respectively, abrasion or accumulative scenario. Their formation started at the level of the sea close to the current and possibly only slightly above its. For positive neotectonic structures of the most characteristic elements of the coastal relief, depending on the initial slopes of the coastal land, its lithology and the presence of loose sediments are not active, but well-defined cliffs, abrasion recesses, progradation accumulative terraces, dying lagoons and other forms combined *with regressive structure relevant these forms of littoral sediments*.

Determine whether the sea level was at a particular coast above the present can only be based on an integrated approach involving the results of the study of geology-geomorphological, tectonic and climatic characteristics of a particular region, it paleogeography, the forms and the role of biogenic factors, the specificity of the effect of marine waters on the formation of relief and sediments of the coastal zone.

II. RESUTLTS AND DISCUSSION

The coastal zone of microcontinents Madagascar and South Georgia

Consider the results of the coasts of research that exist in different geological and geographical conditions, but is characterized by stability plan neotectonic structure and consistency in the direction and activities of the Holocene vertical tectonic movements. As an example, first consider the areas of coasts of microcontinents Madagascar and South Georgia. These areas with differences in geological structure, geographical location and the development of history, a tendency to a general raising of the neotectonic stage.

In Madagascar, we explored the coast lowlands fringing the south-east and south-west island for hundreds of kilometers. For example Morondava region (Fig. 3), we see that the accumulative coast is formed regressive sand sediments with the exception of the delta area of the river of the same name. At the mouth of the river alluvial deposits overlap thin transgressive sediments, which is associated with a corresponding neotectonic lowering of fault zone.

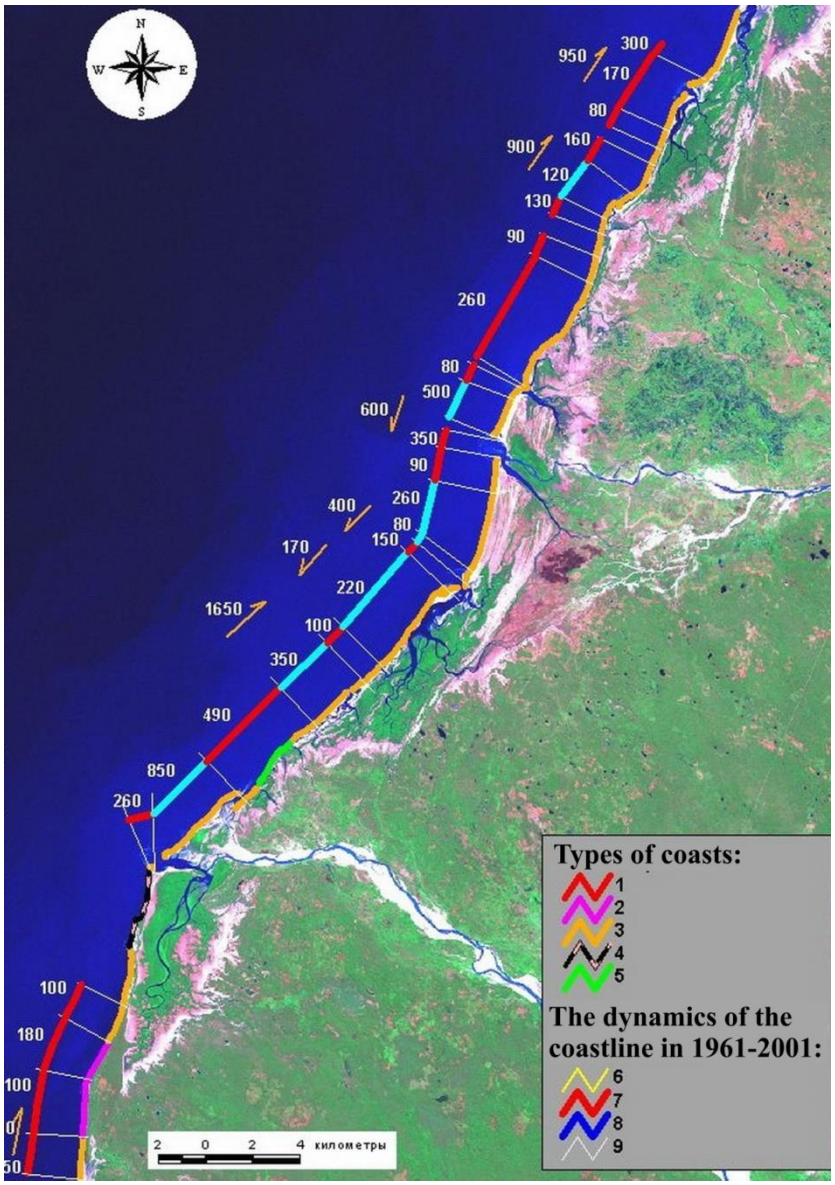

Fig. 3. Types and dynamics of contemporary coastal processes on the accumulative shores of Morondava are

Legend: shores types: 1 - erosion, actively collapsing, developed in the sandy sediments of sea terraces; 2 - accumulative-erosion developed in the sandy sediments of sea terraces. Accumulative: 3 - lagoon, 4 - lagoons, armored of coral platforms, 5 – delta; 6 - border coral platform. The dynamics of the coastline in 1961-2001 yy. (the figures - the maximum displacement of coastline at the site, m): 7 - displacement of remote accumulative forms along the coast, 8 - retreat, 9 - advancing forward; 10 - borders of the sections. The black arrows show the ledge that separates seaside sea and alluvial-sea terraces of alluvial plain. The white arrow shows the site of flooding of the delta r. Morondava

On the coast of microcontinent is widely distributed accumulative sea terrace height of 1.5-4.5 m, created adjoined to each other beach ridges. Age terraces defined in the 3740 ± 90 14C years, and its formation is linked to higher sea level during this period [3]. There are also other terraces of the same origin, including those located at a higher elevation. So, the age of the lower units of the terrace with a height of 12-13 meters in the south-eastern coast of the island is estimated at 2410 and 6455 cal. yr BP [4]. Such a high position terraces logically explain the neotectonic elevation coast. Lush forests of coast of region, which is preserved after a *brief* rise in sea level in the storms and tsunamis, successfully cope with the negative effects, including getting rid of penetrating salts and contained in sea water minerals. On the coast of elevation, with regressive type of formation of sediment, the *upper units* of the geological section of the territory which came out from under the sea level does not contain geochemical evidence of the presence of sea water. With eustatic transgression vegetation flooded coast for a long time, including after the death, it is in subaqueous conditions. Then the fossil fragments of vegetation should be preserved in large numbers in the geological section of the terraces. They should have increased salinity, and contain an abnormal microelements quantity characteristic for the marine environment, particularly strontium. But the geochemical analysis of fossil remains of trees and other coastal vegetation these accumulative terraces, including relations Sr/Ca, does not allow to conclude that the long-term impact on them of the marine environment [4].

North Coast microcontinent South Georgia, characterized by active manifestations neotectonics bloc. Here alternate abrasion and accumulative coast. For the first characteristic inactive cliffs and narrow (from the first meters to 15-20 m) erosion terraces in front of them with the absolute height of 1 ÷ 2 m. Sometimes a terraces covered with a thin (a few tens of centimeters) layer of debris sediments. At a height of 2 ÷ 4 m are also a abrasion recesses with of diameter up to 2 m (Fig. 4). On the second formed accumulative terrace widths of up to a few tens of meters and in height of terrace joint no more than 2.5 m. In the geological section lower units of terraces stacked of rudaceous varying degrees of roundness littoral sediments. The upper unit is represented by peat bogs with poorly decomposed plant residues. Peat power reaches a few tens of centimeters at the terraces joints and is tapers to zero off towards the sea. The surface of the terraces is covered with meadow vegetation, which is towards the sea from a continuous sheet goes into clumps, replaced by separate instances. As an example, the terrace on the south east coast of the peninsula Thatcher, located in Cumberland Bay (Fig.5, 6). The age of lower units of peat is according to radiocarbon dating 860-900 14C years [5]. Higher forms of coastal terraces in the area are not greeted by, although there are all conditions for their formation: gently sloping coastal land, composed of poorly

consolidated subaerial, mainly glacial and slope deposits. Published in the literature [6], the description of the higher accumulative terraces microcontinent in other areas, such as in the area of the Cape of King Edward, also shows a regressive nature their of deposits sections. Current height accumulative terraces microcontinent more logical to link not glacioeustasy (as is done by some researchers), and uplift corresponding to these terraces of tectonic blocks. First, the island's mountain-valley glaciers flowing down the slopes of the mountains directly into the sea, could not have a greater thickness in the range narrow mountain foothills. Secondly, glacio isostatic compensation and alignment of isostasy (if we assume, as it occurs in the literature, subsidence of the crust under the ice load at 1/3 or 2/7 of its thickness), occurs geologically fast - a few hundred - a thousand years. Even in those areas where the glaciers covering hundreds of kilometers in diameter and have a lot of thickness [7, 8]. There is also an extreme point of view, that the phenomenon of post-glacial rebound in general not significant, and this concept needs to be revised [9, 10]. It is known that a decrease in the area of continental glaciation of the world sea level rises. Studies of the dynamics of the Larsen ice shelf on the Antarctic Peninsula have shown that the current size of the glaciers here is minimal during the Holocene epoch [11]. The dynamics of glaciers in Greenland shows other trends [12]. Thus, the question of sea level fluctuations and their causes requires further research.

Fig. 4. Detail of the Holocene terrace with inactive cliff in Bay Fortuna (photo by autors)

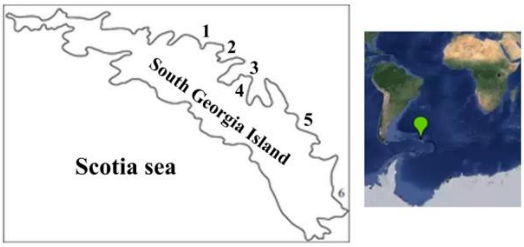

Fig. 5. Toponymy South Georgia Island (Subantarctic): 1 Bay Fortune, Bay Stromness 2-, 3-bay Cumberland 4 - Peninsula Thatcher, 5- Bay Andrew, 6-bay Gold Harbour

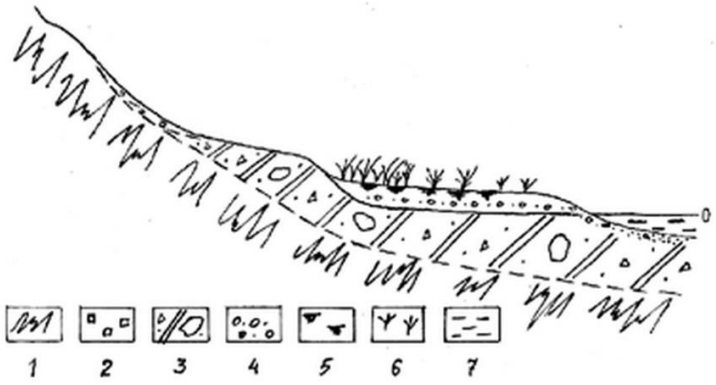

Fig. 6. Diagram of the accumulation terrace on the Peninsula Thatcher
Legend: 1 - bedrock, 2 - slope deposits, 3 - moraine (III_3^4), 4 - Late Holocene terrigenous and littoral sediments, 5 - peat, 6 - vegetation regional oceanic meadows, 7 – waters

The structure of relief and sedimentation of coastal areas of the two microcontinents discussed above indicates a regressive type of formation of coastal lowlands. It can serve as proof that the sea level during the Holocene did not exceed its current height. Differences of heights terraces of two microcontinents, can be considered a consequence of the uneven of uplift of tectonic blocks. Such raising of geostructural major elements of the earth's crust continues to Neogene. Movements Holocene phase of tertiary inherit direction in the respective regions. Thus, the results of the study the accumulation terrace South Georgia microcontinent indicated that raising the rate of the study area for the in recent 900 years is about 2.8 mm/yr.

Accumulative coast of continents (some examples)

Arrangement and development of the accumulative coasts of the structures of continents by the example of the north-eastern of the Black Sea and the south-eastern part of the Baltic Sea. Under the conditions of low-lying coast of the Black Sea in the second half of the Holocene formed a sand spit Anapa (Fig. 7). Genetically she is a regressive formation of a combination of accumulation of bodies in the form of spits and beach ridges, lying on the alluvial deposits. Formation of the spit began seaward of the present position in dzhemetinskoe during the Holocene, about 5 thousands of years ago. During this period, the level of the Black Sea approached during postglacial eustatic transgression to the current height (perhaps about 1 m below). The main stream sediment along the coast sent to south - from Cape Iron Horn to the Cape of Anapa (Fig 7). Counter flow is less important in terms of volume and length. Making of spit close to the modern form was held in nimfetki epoch, that is, in the last 2.5 thousands of years ago. During this period, the sea level was at a height close to the modern and has been relatively stable, undergoing only a slight (within a few tens of centimeters) fluctuations synoptic nature. It is noteworthy that at the moment the seam roof of dzhemetinskih beach deposits exceed the current level of the sea at 1.5-2.5 m and fauna of mollusks in modern sediments spit (Fig. 8) shows that in the second half of the Holocene sea level was not higher than the present [13, 14]. This is confirmed by data on other coasts of the world's oceans (Fig. 9). Shown in Fig. 7 lagoons of artificial origin and is now reduced both the area and depth of water. These as well as other geological and geomorphological materials suggest that the

region of Anapa Spit differential tectonic uplift. Thus, the height of the position of the roof dzhemetinskih unit may indicate of the rise at a rate of 0.5 mm/yr. Faster rise separating the lagoons outlier, then Anapa Cape and Cape Iron Horn (Fig. 7).

Fig. 7. Toponymy north-eastern coast of the Black Sea near Anapa spit

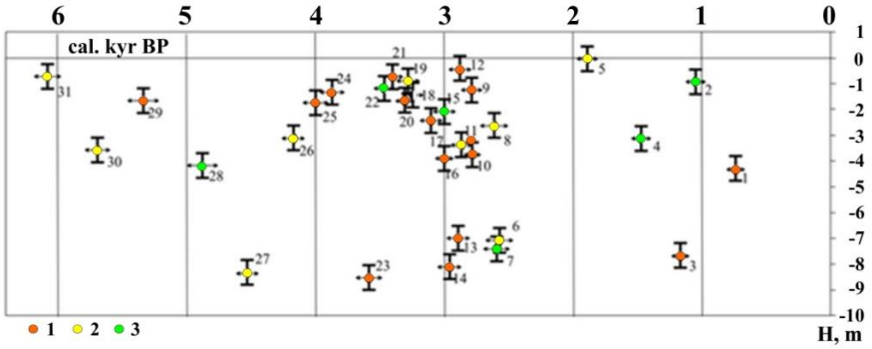

Fig. 8. Hypsometric position of calibrated radiocarbon dating of deposits Anapa spit. The icon in the center indicates the type of fauna of marine mollusks in the range of dating: 1 - dzhemetinsky typical 2 - dzhemetinsky depleted, 3 - calamita [14]

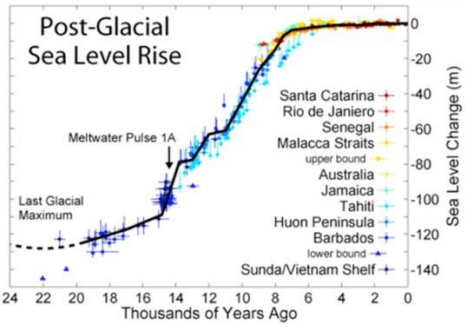

Fig. 9. Post-glacial sea-level [15]

In the south-eastern edge of the Baltic Sea in the historical time of the Holocene formed a sandy Vistula spit. The basis spit developed during the second half of the Holocene transgression as subsea beach ridges, that gradually shifting towards the land by virtue of the specificity of coastal hydrodynamics. Under certain conditions, the largest beach ridges were converted into bars. Even in the XII century there were several island bars. Due to the construction at the beginning of XVI

century in the northern part of the navigable channel spit it became known as the Vistula Spit. After administration, it was divided between Poland and Russia, the Polish part of the Vistula Spit is called, and the Russian - Baltic (Fig.10). Spit largely consists of rebuilt of wind sandy coastal accumulative forms several generations. In its structure there are also outliers glacial and alluvial plains, preserved from erosion as sea waves, and the waves of the lagoon [16, 17, 18] (Fig.11, 12). Investigations revealed that the formation of the Vistula Spit happens in a moderately differentiated block structure of the eastern slope of the Gdansk depression, created by faults directions northwest. Most raised block is located north of the village Borovoye to 54˚23' north. This block corresponds to the widest part of the spit and the highest level of its relief in excess of 40 m. Within blocks, that rising less active, spit narrowed and its height is reduced. In accordance with the above it can be assumed that the structure of the spit reflects the regressive type of its formation. The presence and relief of littoral genesis forms is above the sea level due to tectonic uplift, rather than high-Holocene transgression. It can be assumed that the current rate of uplift in the spit area of roughly comparable (at least, no less) at a rate of slight increase of the level of the Baltic Sea, which caused by the current, a geologically short-lived climatic cycle of the planet [19]. This may explain the relatively stable state coast of the spit, since the depth of the underwater coastal slope also remained largely unchanged, allowing wind-wave factor to mobilize available yet sufficient bottom sediments and move it to the coast.

Fig. 10. Driving south-eastern Baltic.
PP – Pillau Penninsula; red arrow show the Baltic Channel

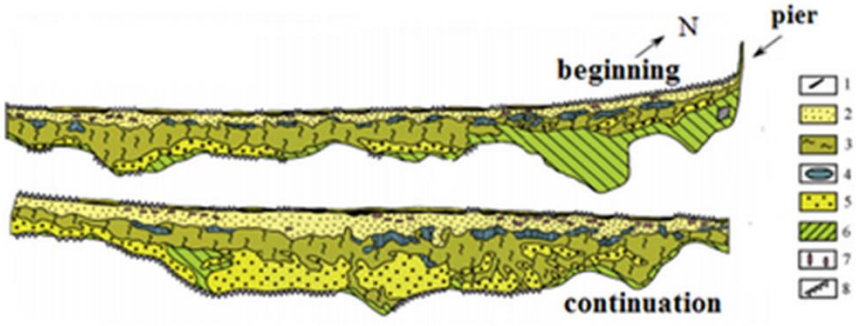

Fig. 11. Geomorphological map of the Vistula Spit [17, with some refinements]: 1 – foredune ridge; 2 – seaside dune swell; 3 – levelled regressive aeolian-marine surface - "palve"; 4 –swampy depressions of the old lagoons; 5 – elevated old dune massifs; 6 –old deltas plaines with low near-bay regressive terrace; 7 – deflation basins in dunes; 8 – ledges of the scouring

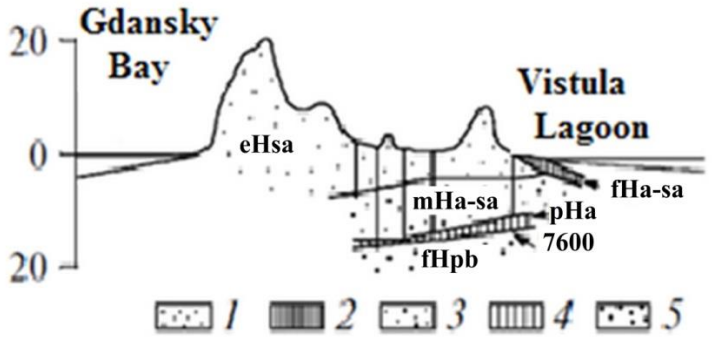

Fig. 12. Fragment of the geological cross-section of the Vistula Spit [18]: 1 – aeolian sands (eHsa – subatlantic); 2 – alluvial-deltaic sediments (fHa-sa – atlantic-subatlantic); 3 – sea sands (mHa-sa – atlantic-subatlantic); 4 – peat (pHa – atlantic); 5 – fluvial sands (fHpb – preboreal)

III. CONCLUSIONS

It was found that the Holocene sea level in the two microcontinents has reached the current state not later than 1 thousand years ago, and not exceed it, subjected to only minor fluctuations in the synoptic scale. Differences of heights terraces of microcontinents, can be considered a consequence of the uneven of uplift of tectonic blocks. A similar situation is often observed as the coasts within the tectonic structures in the continents. The question of sea level fluctuations and their causes requires further research.

IV. ACKNOWLEDGMENT

The work was supported by the State order (0149-2014-0035 theme, the theme of "The Evolution of the natural environment, the dynamics of relief and geomorphological safety of nature", RFBR project № 16-05-00364.

V. REFERENCES

[1] Hallam, A. Phanerozoic sea-level changes. New York, Columbia University Press, 1992. 266 p.

[2] Dunaev N. N. Kolichestvennyj analiz vertikal'nyh tektonicheskih dvizhenij na shel'fe Kuby // Okeanologija, 1977. T. XVII, V. 6. P. 1050-1054.

[3] Battistini R. L'extreme Sud de Madagascar, e'tude geomorphologiue. Paris: Editions Cujas, 1964. 636 pp.

[4] Malika V-S., Katherine J. W., Lindsey G. Threshold response of Madagascar's littoral forest to sea-level rise // *Global Ecology and Biogeography*, 2009, (18). P. 98–110.

[5] Dunaev N. N., Sulerzhickij L. D. Ostrov Juzhnaja Georgija kak blagoprijatnyj poligon dlja izuchenija golocenovyh kolebanij urovnja morja // *Geomorfologicheskie i paleogeograficheskie issledovanija poljarnyh regionov. Sbornik materialov*. SPb, SPbGU, 2012. C. 114-117 (in Russian).

[6] Chalmers M., Clapperton M.A. Geomorphology of the Stromness Bay area, South Georgia // *British Antarctic survey scientific reports*, 1971. № 70. 25 p.

[7] Artjushkov E. V. Chetvertichnye oledenenija i transgressii v Zapadnoj Sibiri // *Izvestija AN SSSR, ser. geol.*, 1967, № 7. S. 98-114 (in Russian).

[8] Artjushkov E. V. Geodinamika. M.: Nauka, 1979. 328 s. (in Russian).
[9] Kuzin I. L. Mify i realii uchenija o materikovyh oledenenijah. SPb.: Izd-vo SZNII «Nasledie», 2013. 178 s. (in Russian).
[10] Chuvardinskij V. G. Bylo li materikovoe oledenenie? Mify i real'nost'. Saarbrjukken, Germanija: Lambert Academic Publishing. 2004. 284 c. (in Russian).
[11] Domack E., Duran D., Leventer A., Ishman S., Doane S., McCallum S. et al. Stability of the Larsen ice shelf on the Antarctic Peninsula during the Holocene epoch // *Nature*. 436, 2005. P. 681-685.
[12] Huybrechts P. Sea-level changes at the LGM fromice-dynamic reconstructions of the Greenland and Antarctic ice sheets during the glacial cycles // *Quaternary Science Reviews*. 21 (2002). P. 203-231.
[13] Izmajlov Ja.A. Jevoljucionnaja geografija poberezhij Azovskogo i Chernogo morej. Kniga 1. Anapskaja peresyp'. Sochi: Lazarevskaja poligrafija 2005. 174 s. (in Russian).
[14] Izmajlov Ja.A., Arslanov H.A., Maksimov F.E. Radiouglerodnaja hronologija formirovanija golocenovyh morskih otlozhenij Anapskoj peresypi (chernomor-skoe poberezh'e). *Fundamental'nye problemy kvartera: Materialy IX Vserossij-sko soveshhanija po izucheniju chetvertichnogo perioda*. g. Irkutsk, 15-20 sentjabrja 2015. Irkutsk: Izdatel'stvo Instituta geografii im. V. B. Sochavy SO RAN, 2015. T. 2. S. 188-190. (in Russian).
[15] Rhode R. A. 2007 postglacial sea-level / http://www.oceans.cat/cursos/files/. 20.03.2016.
[16] Badjukova E.N., Zhindarev L.A., Luk'janova S.A. and Solov'eva G.D. Osobennosti geologo-geomorfologicheskogo stroenija Baltijskoj (Vislinskoj) kosy // *Uchenie o razvitii morskih beregov: vekovye tradicii i idei sovremennosti : mater. konf. SPB.*, 2010. S. 170-172. (in Russian).
[17] Badjukova E.N., Zhindarev L.A., Luk'janova S.A. and Solov'eva G.D. The geologic-geomorphological structure of the Baltic (Vistula) Spit (Geologo-geomorfologicheskoe stroenie Baltijskoj (Vislinskoj) kosy) // *Oceanology*. vol. 51. № 4. P. 675-682, 2011 (in Russian).
[18] Tomczak A., Mojski J.E., Krzymińska J., Michałowska M., Pikies R., Zachowicz J. New data on geologic structure of theVistula Bay Bar // *Kwartalnik Geologiczny*, vol. 33(2), P. 277–300, 1989.
[19] Nigmatulin R.I., Vakulenko N.V., Sonechkin D.M. Global'noe poteplenie v real'nosti i v klimaticheskih modeljah // *Turbulentnost', dinamika atmosfery i klimata : Cb. tez Mezhdunar. konf., posvjashh. pamjati akad. A.M. Obuhova (13-16 maja 2013 g.)*. M.: IFA RAN, 2013. S. 76-79. (in Russian).

LABORATORY STUDIES OF THE OF EDDY FORMATION IN ROTATING AND NON-ROTATING FLUID DUE TO SPATIALLY NON-UNIFORM WIND FORCING

Dmitry Elkin, P.P. Shirshov Institute of Oceanology RAS, Moscow, Russia
Andrey Zatsepin, P.P. Shirshov Institute of Oceanology RAS, Moscow, Russia

dmelkin@mail.ru

Laboratory investigation of eddy formation mechanism due to spatially non-uniform wind impact was fulfilled. Experiment was provided in a cylindrical and a square form tank filled with homogeneous or stratified fluid and displaced on a rotating platform. In the absence of the platform rotation, an impact of the single air jet lead to the formation of a symmetric vortex dipole structure that occupied the whole water area in the tank. In the presence of the platform rotation, a compact anticyclonic eddy was formed in a part of the dipole with anticyclonic vorticity, while in a part with cyclonic vorticity no any compact eddy was observed. The laboratory results were successfully compared with the field observation results fulfilled in the at the Black Sea coastal zone near Gelendzhik.

Key words: Black Sea, spatially non-uniform wind forcing, submesoscale eddies, laboratory study.

I. INTRODUCTION

To a practice of an ecological monitoring of the coastal (shelf) areas in the north-eastern part of the Black Sea, in the recent past has been introduced a new instrumental and methodological approach that provides high spatial and temporal resolution of the measurements. An important result of this approach was a frequent observation of submesoscale (with a diameter of 2-10 km) intense eddies, both cyclonic and anticyclonic. Apparently, these eddies play a significant role in cross shelf water exchange and energy dissipation of the alongshore currents [1, 2].

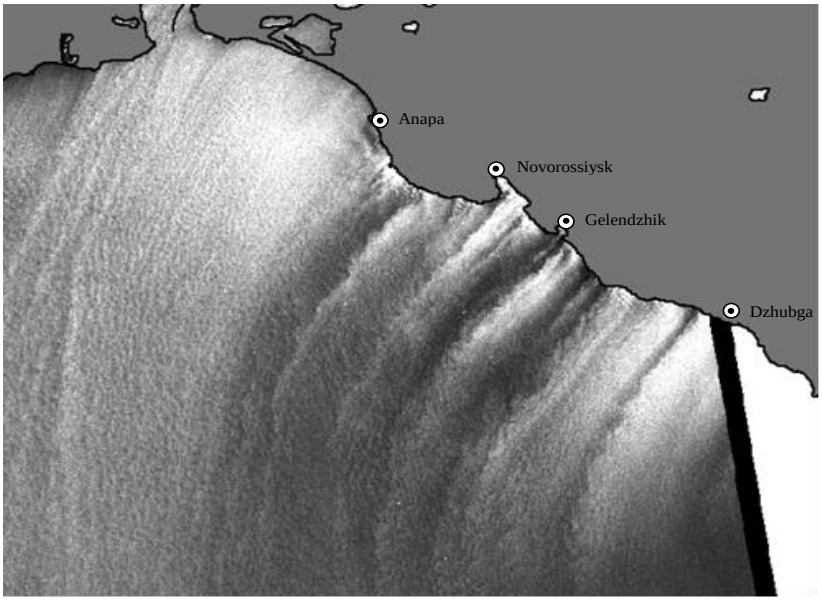

Fig. 1. The satellite SAR image of the north-eastern part of the Black Sea. The bright bands at the sea surface are related with of offshore wind jets, which are separated by dark bands that are related with the areas of weaker offshore wind.

There are at least three possible mechanisms of the submesoscale eddies formation. First mechanism - a periodic formation of eddies behind the capes. It was revealed that in a rotating fluid due to this mechanism only anticyclonic eddies are formed periodically in decelerating cyclonic coastal current [3]. Second mechanism is the shear instability of the coastal current. Due to this mechanism in the rotating fluid the cyclonic eddies are formed predominantly [4]. The third mechanism related to spatially inhomogeneous wind forcing is a subject of a study in this paper.

Coastal zones of many seas (Black Sea, in particular) are surrounded by hills and mountain ranges separated by valleys. Wind directed from the seashore often has a different velocity over the valleys and over the mountains. Due to the complicated orography of the coast the offshore wind over the sea often consists of quasi-parallel wind jets as it is presented at figure 1. The presence of wind jets, separated by the regions with weaker winds, should lead to the formation convergent and divergent Ekman transport and of the furrows-like anomalies of the sea surface level. The instability of such structures could provoke the formation of the mesoscale or submesocale eddy-like structures [5].

The aim of this work is to conduct laboratory experiments to study the possibility of eddy formation in a homogeneous and two-layer non-rotating and rotating fluid due to the impact of one or two offshore air jets parallel to each other.

II. LABORATORY SETUP

Two series of experimental runs in the tanks with different shapes and sizes were conducted.

In the first series the experimental runs were carried out in cylindrical tank with a diameter of 60 cm and a height of 8 cm, filled with distillated water and placed on a rotating platform. Runs were conducted with and without of the platform rotation. The time period of the platform rotation

was as follows: 15 s, 10 s and 5 s (the Coriolis parameter $f = 2\Omega = 0{,}8\ s^{-1}$, 1.25 s^{-1}, 2.5 s^{-1}, respectively). A video camera was placed at the center of the platform above the tank.

Some of the experimental runs were fulfilled in homogeneous fluid, and the others – in two-layer salinity stratified fluid. To create a two-layer salinity stratification a thin (2 cm) layer of the distilled water was accurately flooded over the thicker layer (5 or 25 cm) of the salted water (5, 10 or 20 psu) that was already promoted to the state of solid-body rotation with angular frequency Ω. This method allowed us to minimize the mixing between the layers.

Near the wall of the circular tank four wind blowers with nozzles of 7 cm width were installed. Three of them were directed at an angle of about 70 degrees to the radius of the tank and were used to produce azimuthal wind stress and coastal rim current. The fourth blower was directed radially towards the center of the tank and was used to create the the air stream normal to the shore (Fig. 2a, b).

At the beginning of each experimental run, fine paper pellets were dropped at the water surface for flow visualization. These pellets played a role of passive tracers. In the absence of a azimuthal wind stress and coastal rim current the fourth blower turn on at once with the video camera. In the opposite case the camera was switched on together with the three wind blowers. The fourth wind blower was switch on for a definite time interval (from 5 to 80 s) only when coastal rim current was fully generated.

The velocity V of the wind in different experimental runs varied in the range of from 2 to 8 m/s at a distance of 5 cm from the wind blower nozzles and from 1 to 5 m/s at a distance of 15 cm from them.

The second series of the experimental runs was carried out in a square form tank with a width of 70 cm and height of 10 cm. It was filled by distilled water up to the top. In this series of experimental runs only two wind blowers were used in order to investigate the impact of the parallel neighboring wind jets on the eddy formation in the underlying water layer. Both of them were installed normally to the same side of the tank. One of them was located at a distance 7 cm from the tank corner. The position of the other one was changed from one experimental run to the other and the distance between the blowers L varied from one experimental run to the other as follows: L = 20, 30 and 40 cm. In order to reduce the end wall effect on the results of experiment, approximately one-third part of the water surface near the wall opposite to the blowers was closed by thin organic glass plate. For the comparison with the results of the experiments in circular tank, some experimental runs in a square form tank were conducted with one wind blower installed at the middle of the tank wall (Fig. 2c, d).

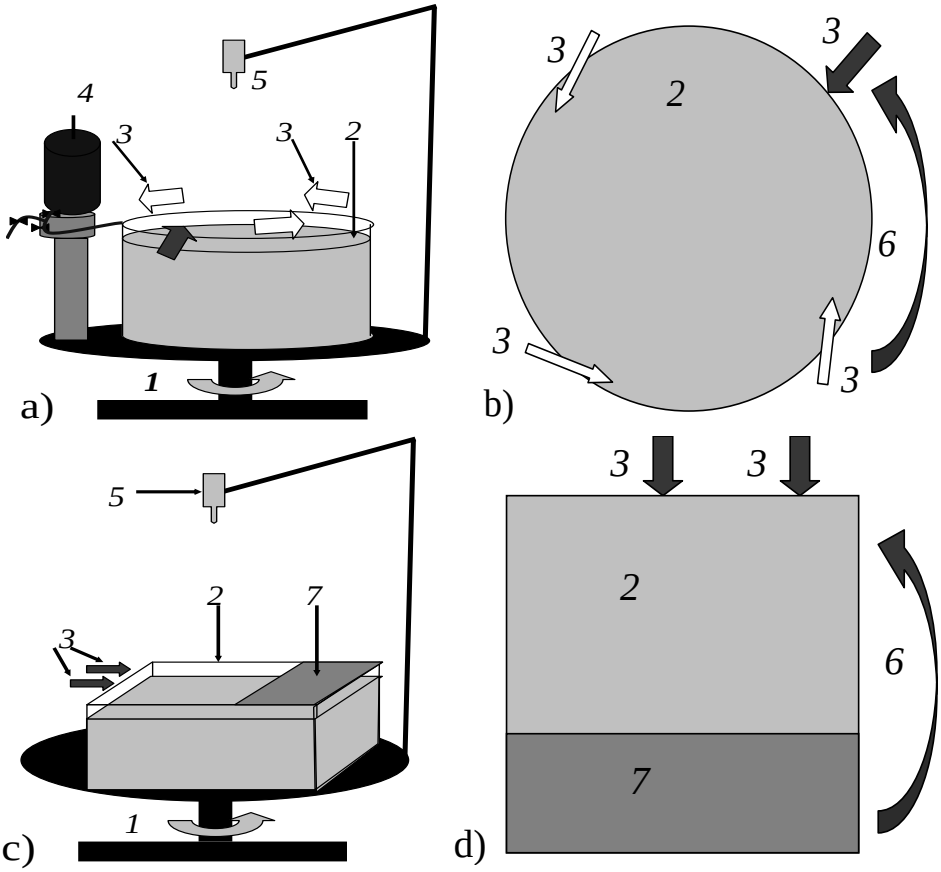

Fig. 2. Scheme of the laboratory set-up: a) - cylindrical tank (side view); b) - cylindrical tank (top view); c) - square tank (side view); d) - square tank (top view).1 - rotating platform; 2 – organic glass tank filled by homogeneous or two-layer fluid; 3 – wind blowers; 4 – constant flux source for the flooding of the upper layer fluid; 5 – video camera; 6 - direction of the platform rotation. 7- organic glass plate covering water surface.

III. ESTIMATE OF WIND STRESS AND SURFACE CURRENT VELOCITY

One of the basic parameters of the experiment is a wind stress at the water surface generated by the wind blower. It could be expressed as follows: $\tau = \rho_a C d U_a^2$. Here U_a is the wind velocity (m/s) at a curtain height z_a above the air-water interface (for the sea z_a = 10 m), Cd – non-dimensional drag coefficient, ρ_a = 1.29 kg/m^3 – density of air. For the natural conditions Cd = (1-2)10^{-3} [6, 7]. But for the certain conditions of the laboratory experiment the value of Cd is unknown. It could be estimated on the base of the theory of turbulent boundary layer and measurements.

Let us divide the air flow above the water layer in the laboratory tank into three zones in vertical direction: 1 - the near surface zone, or the laminar sublayer; 2 – the turbulent zone with constant shear stress, or “logarithmic” sublayer; 3 – the core of the flow, where the air velocity is maximal and nearly constant (Fig.3).

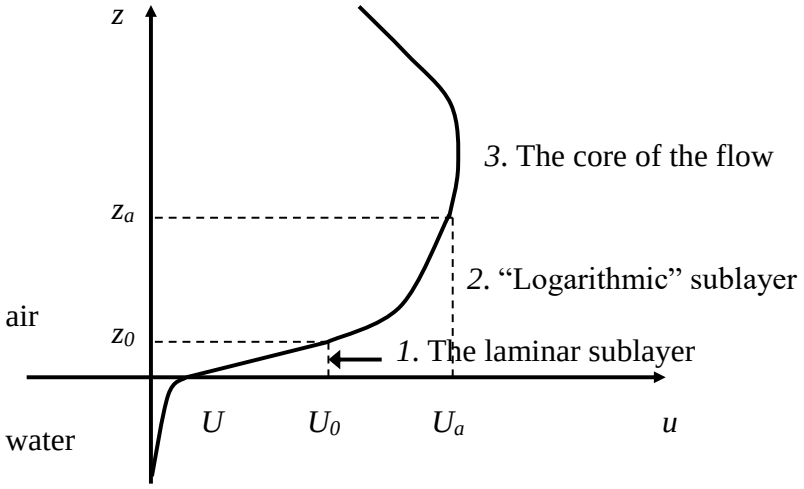

Fig. 3. Dependence of wind velocity on height above air-water interface.

Starting from the condition of continuity of the momentum flux in vertical direction in zones 1 and 2, let us equate the expression for the wind stress on the upper boundary of zone 1 to the expression for this quantity at the lower boundary of zone 2:

$$\tau = \rho_a \nu_a \frac{du}{dz} = \frac{\rho_a \nu_a (U_0 - U)}{z_0} = \rho_a C d U_a^2 \tag{1}$$

Here U is the velocity of air at the water-air interface, U_0 – the velocity at the boundary between zone 1 and zone 2, z_0 – the height of this boundary above the water surface, ν_a (= 0.07 cm^2/s) – kinematic viscosity of the air.

According to the Prandtl – von Karman hypothesis, in the turbulent sublayer (zone 2) momentum exchange coefficient obeys the following law:

$$k(z) = \chi u z \tag{2}$$

Here χ = 0.4 - von Karman constant, u - wind velocity that is a function of the height z.

Using (2) let us equate the expression for the wind stress in the zone 2 to the bulk formula for this quantity:

$$\tau = \frac{\rho_a k(z) du}{dz} = \frac{\rho_a \chi u z du}{dz} = \rho_a C d U_a^2 \tag{3}$$

It follows from the equations (1) and (3) that:

$$u du = \frac{C d U_a^2}{\chi} \frac{dz}{z} \quad \text{and} \quad \frac{1}{2}(U_a^2 - U_0^2) = \frac{C d U_a^2}{\chi} \ln \frac{z_a}{z_0} \tag{4}$$

Let us use the condition of "stitching" of the momentum exchange coefficient at the boundary between zone 1 and zone 2 at the height z_0. This condition is:

$$k(z_0) = \nu_a \qquad \text{or} \qquad \chi u z_0 = \nu_a \tag{5}$$

Now we have a system of three equations:

$$(U_0 - U) = \frac{C d U_a^2 z_0}{\nu_a} \tag{6}$$

$$(U_a^2 - U_0^2) = \frac{2CdU_a^2}{\chi} \ln \frac{z_a}{z_0} \quad (7)$$

$$U_0 z_0 = \frac{\nu_a}{\chi} \quad (8)$$

Taking to the account that the value of U is measured experimentally, there are three unknowns in this equation: Cd, U_0, и z_0

Solving this system we find the following expression for Cd

$$Cd = \frac{\chi U_0 (U_0 - U)}{U_a^2} \quad (9),$$

and for z_0

$$z_0 = \frac{\nu_a}{U_0 \chi} \quad (10),$$

To find U_0 we used an approximate solution method (Newton method) because it is impossible to determine this parameter by pure analytical approach.

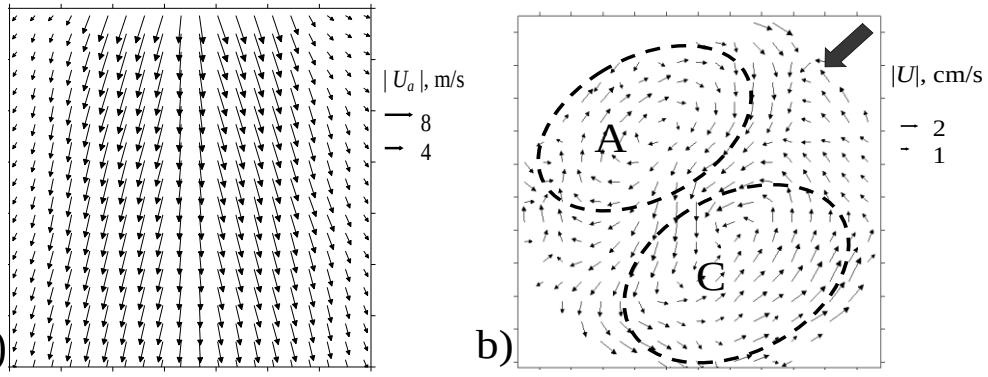

Fig. 4. a) – measured wind velocity field; b) - velocity field at the fluid surface generated by an air jet in initially resting fluid. Eddies in the dipole structure are marked by dotted lines: A – anticyclone, C – cyclone. Thick arrow - the direction of the air jet. Thin arrows – vectors of air velocities.

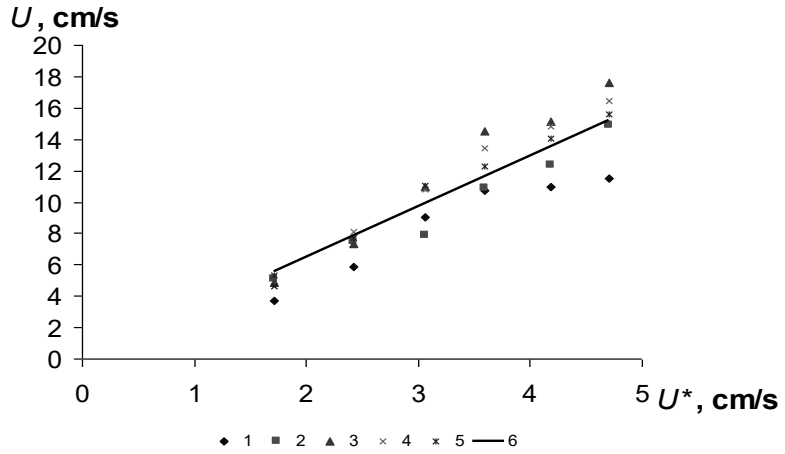

Fig. 5. Dependence of surface fluid velocity on the dynamic friction fluid velocity. 1 - Square tank; 2 - Cylindrical tank, uniform fluid; 3 - Cylindrical tank, two-layer fluid ΔS=20 psu; 4 - Cylindrical tank, two-layer fluid ΔS=10 psu; 5 - Cylindrical tank, two-layer fluid ΔS=5 psu; 6 – trend line.

Using the data of our experiments it was found that in the laboratory conditions $Cd = (2.5\pm0.2)*10^{-2}$. This value is higher by more than an order of magnitude the value of *Cd* for wind flows above the sea surface.

The estimated value of wind stress in laboratory conditions τ changed in the range of 0.3 – 2.2 kg/ms^2 at distance 5 cm from wind blowers nozzle depending on the value of the wind velocity. Respectively the value of the dynamic friction velocity in water, $U^* = (\tau/\rho_w)^{0.5}$, where ρ_w – the density of water, changed in the range 1.7 – 4.7 cm/s. At a distance 15 cm from blowers nozzle that is closer to the area of eddy formation in the laboratory tank, the value of wind stress varied from 0.034 to 0.8 kg/ms^2, and the value of the dynamic friction velocity in water - from 0.6 to 2.8 cm/s. Approximately the same values these parameters have in the natural conditions at the sea surface if the wind velocity at 10 m height is changing in the range of 5-15 m/s.

The wind velocity field produced by the single blower directed radially towards the center of the tank is shown in figure 4a. Dependence of surface current velocity *U* in water just below the axis of wind jet on dynamic friction velocity in water is shown in figure 5. It is close to the linear one: $U=3.2U_1^*$, where U_1^* - dynamic friction velocity in water. The surface current velocity was determined by the short-term pellets displacement measurements at a distance 5 cm from the wind blower nozzile.

Video data of each experiment were processed using a special computer program for calculation of flow velocity vectors from the data on short-term pellets displacement. The results of the calculations were used to analyze the structure and quantitative characteristics of the surface currents produced by wind blowers in a homogeneous or two-layered, non-rotating or rotating fluid in the cylindrical and square form tanks.

IV. Results of the experiment in the cylindrical tank

In the absence of the platform rotation an impact of the single air jet lead to the formation of a symmetric vortex structure dipole that occupies the whole water area in the tank (Fig. 4b). In the presence of the platform rotation single air jet also generates the dipole vortex structure in the underlying fluid. But this structure is asymmetric: in a region with anticyclonic vorticity a compact anticyclonic eddy is formed. It is revealed that if the value of the parameter $U/f < 0.3R$, where R is the radius of the tank, vortex core has a radius $R_e = U/f$, where U is the flow velocity in fluid at the axis of the dipole structure. If the value of $U/f > 0.3R$ than $R_e = 0.3R$. The maximal orbital velocity in the compact eddy, $U_{orb} = 0.7U$. In a region with cyclonic vorticity no compact cyclonic eddy was observed.

In a homogeneous rotating fluid the dynamical structures vanished in a short time due to bottom friction after the end of wind forcing. In a two-layer rotating fluid the compact anticyclonic vortex existed much longer time, as a result of geostrophic adjustment and low friction at the density interface. The surface currents generated by the air jet in the rotating two-layer fluid are shown in figure 6. The dependences of R_e/R , U_{orb}/Rf , U_{orb}/U and eddy Rossby number Ro_e on U/fR are shown on figures 7a-d, respectively.

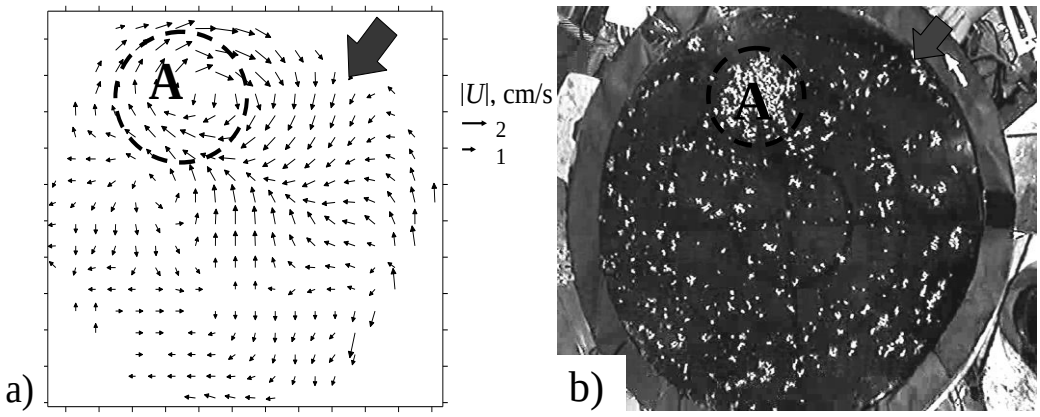

*Fig. 6. a) – structure of surface currents generated by the air jet in the two-layer rotating fluid. The compact anticyclonic eddy **A** is countered by dotted line. Thick arrow - the direction of wind impact. Thin arrows – the velocity vectors at the surface of the fluid layer; b) - the image of the experimental run.*

In the presence of an intense coastal rim current in a rotating fluid, the effect of the normal to the coast air jet was not accompanied by vortex structure formation. However, at the stage of the rim current relaxation the formation of the dipole vortex structure with compact anticyclonic eddy was revealed in case with rather strong wind forcing. Thus, the formation of the vortex dipole structure with compact anticyclonic eddy depends on the ratio between the intensities of coastal rim current and the offshore wind jet (Fig. 8) [8].

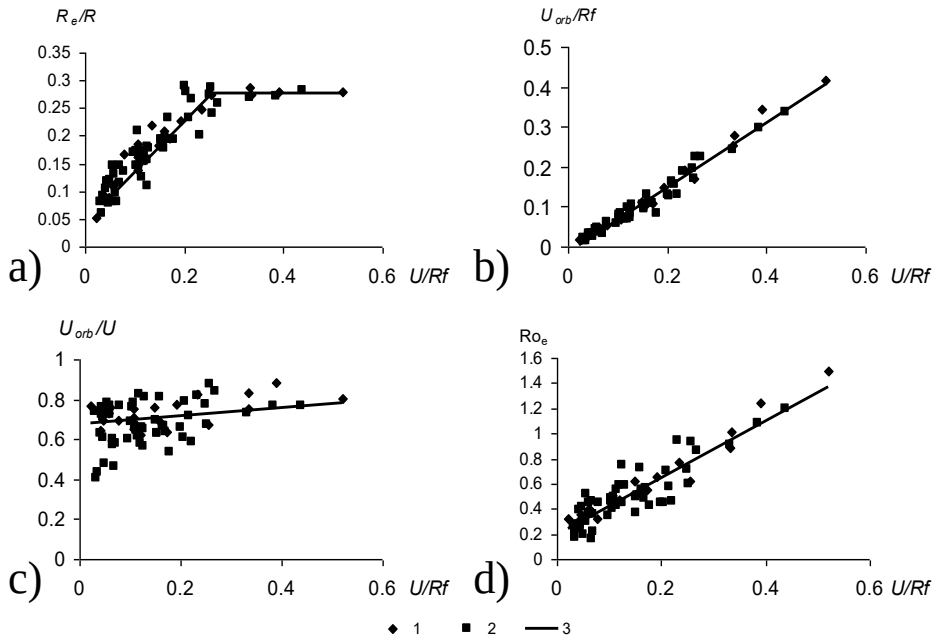

Fig. 7. a) R_e/l vs. U/lf; b) U_{orb}/lf vs. U/lf; c) U_{orb}/U vs. U/lf; d) Ro_e vs. U/lf. 1 - for uniform fluid; 2 – two layer fluid; 3 - trend line.

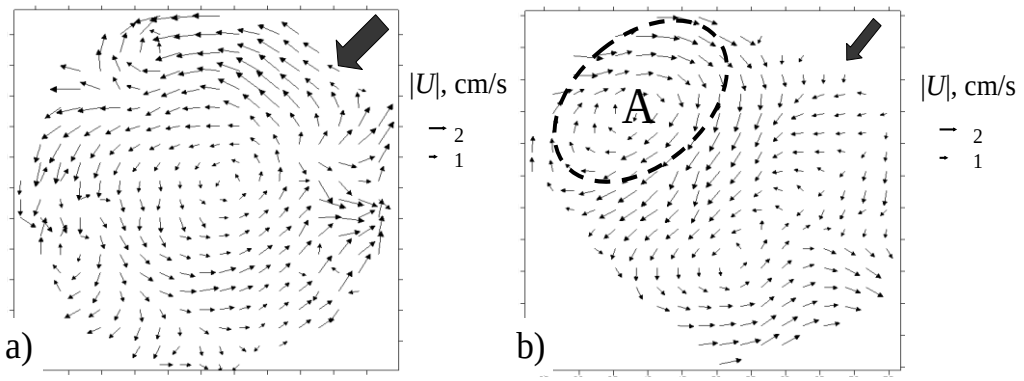

*Fig. 8. Impact of the radial air jet on the surface velocity pattern in a two-layered rotating fluid; a) in the presence of strong cyclonic coastal rim current; b) after the decay of the coastal rim current. The compact anticyclonic eddy **A** is countered by dotted line. Thick arrow - the direction of wind jet. Thin arrows – the surface current velocity vectors.*

V. Results of the experiment in the square tank

In the square tank with one blower locate in the middle, in the absence of the platform rotation, impact of the air jet lead to the formation of a symmetric vortex structure dipole that occupied the whole water area in the tank. In the presence of the platform rotation single air jet also generated in the underlying fluid the dipole vortex structure. But this structure was asymmetric: in a region with anticyclonic vorticity a compact anticyclonic eddy $R_e = U/f$ was formed, where U is the flow velocity in fluid at the axis of the dipole structure. Do the results of experiment were just the same as in the case of cylindrical tank. The flows generated by the air jet at the surface of rotating fluid are shown in figure 9.

The wind velocity field produced by the action of two wind blowers is shown in figures 10a and 10b. In the absence of the platform rotation, if distance between blowers is small, than no eddy formation was observed in the water area between the blowers. If distance *l* between blowers was large (*l* >25 cm), the vortex dipole structures were formed by each of the blowers with no significant interaction between the air jets produced by these blowers.

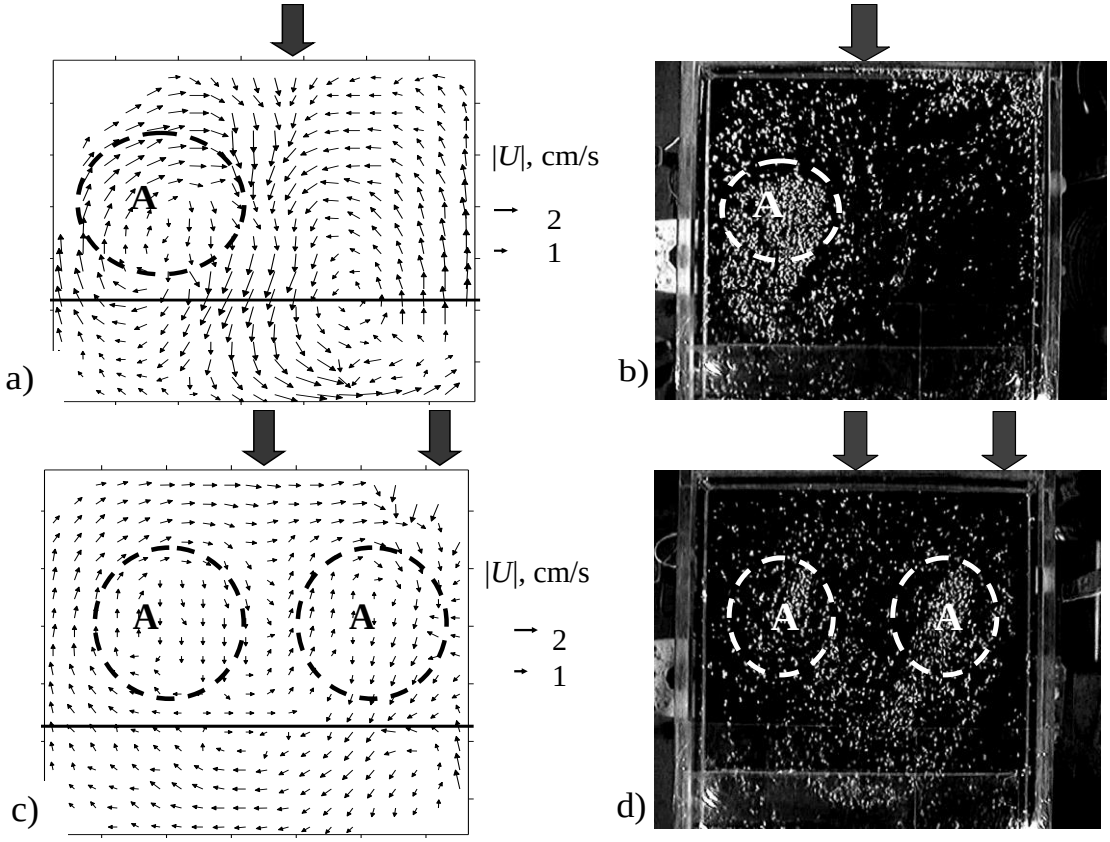

*Fig. 9. a) - currents generated by the air jet at the surface of rotating fluid; b) - the image of this experimental run; c) - currents generated by two air jets at the at the surface of rotating fluid, l=30; d) - the image of this experimental run. The compact anticyclonic eddies **A** are countered by dotted line. Thick arrow - the direction of air jet . Thin arrows – surface current velocity vectors.*

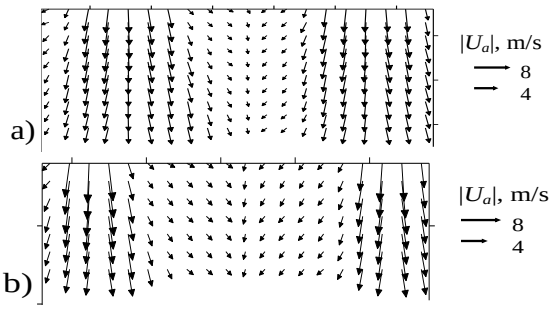

Fig. 10. a) - wind velocity field, in the case of small distance between the two blowers; b) - wind velocity field, in the case of large distance between the two blowers.

In the presence of the platform rotation and in the case of small distance between the blowers no eddy formation was observed in the water area between them. In the case of large distance between blowers a compact anticyclonic eddy was formed at the right side from each blower, while in a region with cyclonic vorticity no compact cyclonic eddy was observed. In that case the compact anticyclone eddy core had a radius $R_e = U/f$ with the maximal orbital velocity $U_{orb} = 0.7U$ – the same as in the experimental runs with one blower.

It is reasonable to introduce and to analyze the non-dimensional parameter which characterizes the influence of the distance between blowers on the eddy formation between them. Such parameter is lf/U. It was revealed, that its critical value is about 5. If $lf/U > 5$, there is a formation of a compact anticyclone between the blowers, if $lf/U < 5$ – there is no compact anticyclonic eddy formation between them.

In the coastal zone of the north-eastern Black Sea the velocity of surface current generated by offshore air jet U could be as much as 10-20 cm/s [5]. It means that the critical length scale $l = 5U/f$ =5-10 км. It follows from figure 1 that typical distance between the offshore air jets is 20-30 km. It's much larger than critical length scale. So it is reasonable to suppose that the observed wind field could generate compact anticyclonic eddies at the water area right to the axes of the air jets. There is evidence that long-term (about a day or more) action north-east wind leads to anticyclonic eddies in the coastal zone of the north-eastern part of the Black Sea [9]. However the problem of generation of compact anticyclonic eddies by offshore wind jets in natural conditions should be treated more systematically.

VI. Conclusions

1. In the absence of fluid rotation the offshore air jet generates the formation of a symmetrical vortex dipole in the underlying fluid layer.
2. In the presence of fluid rotation the offshore air jet generates the formation of an asymmetrical vortex dipole in the underlying fluid layer. This dipole has a compact eddy in its anticyclonic part, while in its cyclonic part the vorticity was distributed rather uniformly.
3. The life time of the vortex dipole is much longer in the rotating two-layered stratified fluid if compared to the case of rotating homogeneous fluid due to geostrophic adjustment and low friction at the density interface.
4. In the presence of strong coastal rim current the offshore air jet usually does not generate the vortex dipole structure in the underlying fluid. In such case the possibility of the vortex dipole structure formation depends on the ratio between the intensities of coastal rim current and the offshore air jet.
5. In the presence of two neighboring offshore wind jets impacting on the underlying rotating fluid layer the formation of compact anticyclonic eddy between them is determined by the non-dimensional parameter lf/U. If $lf/U > 5$, there is a formation of a compact anticyclone between the air jets, if $lf/U < 5$ – there is no compact anticyclonic eddy formation between them.
6. The observed asymmetry in the formation of cyclonic and anticyclonic eddies under the influence of one or more offshore air jets in the described above laboratory experiments was also revealed in the natural conditions [9].

VII. Acknowledgement

The work was performed in the frame of RNF grant №14-50-00095.

VIII. References

1. *Zatsein A.G., Korzh A.O., Kremenetskiy V.V. et al*. Studies of the hydruphysical process ower the shelf and upper part of the continental slope of the Black Sea with the traditional and new observation techniques // Oceanology, 2008. V.48. №4 P.466-475.
2. *Zatsein A.G., Kondrashov A.A., Korzh A.O., et al.* Submesoscale eddies at the Caucasus Black Sea shelf and the mechanisms of their generation // Oceanology, 2011. V. 51. № 4. P. 554-567.
3. *Elkin D.N., Zatsepin A.G.* Laboratory Investigation of the Mechanism of the Periodic Eddy Formation Behind Capes in a Coastal Sea // Oceanology, 2013. V. 53. No.1 .P. 24-35.
4. *Elkin D.N., Zatsepin A.G.* Laboratory study of a shear instability of an Alongshore sea current // Oceanology, 2014. V.55. No.5. P. 576-582.
5. *Zatsein A.G., Piotouh V.B., Korzh A.O., et al.* Variability of currents in coastal zone of the Black sea from long-term measurements by bottom mounted ADCP // Okeanologiya, 2012. V.53. No.5. P. 579-592.
6. *Garratt J.R.* Review of drag coefficients over oceans and continents // Month. Weath. Rev. 1977. V. 105. P. 915-929.
7. *Kondo J.* Air-sea bulk model of the coefficients in diabatic conditions // Boundary-Layer Meteorol 1975. V. 9. № 1. P. 91-112.
8. *Elkin D.N., Zatsein A.G., Kremenetskiy V.V. et al*. Laboratory Study of the Generation Mechanism of Coastal Eddies in the Black Sea due to the Spatially Non-Uniform Wind Impact // Fluxes and structures in fluids. Selected Conference Papers. 2010. P. 117–121.
9. *Ginzburg, A. I., Kostianoy A. G., Soloviev D. M. et al*. Remotely sensed coastal/deep-basin water exchange processes in the Black Sea surface layer // *Satellites, Oceanography and Society*, Ed. D. Halpern, Elsevier Oceanography Series, 63, 273–287, 2000c.

ECOLOGICAL AND GEOMORPHOLOGICAL ASSESSMENT OF THE VULNERABILITY OF THE COASTS OF THE KARA SEA TO THE OIL SPILL

Alexander Ermolov, Moscow State University M. V. Lomonosov, CJSC "Institute of ecological design and research", Russia

alexandr.ermolov@gmail.com

International experience of oil spill response in the sea defines the priority of coastal protection and the need to identify as most valuable in ecological terms and the most vulnerable areas. Methodological approaches to the assessing the vulnerability of Arctic coasts to oil spills based on international systems of Environmental Sensitivity Index (ESI) and geomorphological zoning are considered in the article. The comprehensive environmental and geomorphological approach allowed us to form the morphodynamic basis for the classification of seacoasts and try to adapt the international system of indexes to the shores of the Kara Sea taking into account the specific natural conditions. This work has improved the expert assessments of the vulnerability and resilience of the seacoasts.

Key words: seacoasts; *oil spills; environmental sensitivity; international system of indexes; geomorphological zoning; Kara Sea*

I. INTRODUCTION

The Russian Arctic shelf is very promising in relation to oil. The development of offshore fields is inevitably connected with the development of mining and transport infrastructure (construction of the offshore ice-resistant stationary platforms, pipelines, oil terminals of various types, etc.), including the Northern sea route. This requires the development of measures for environmental protection, including the protection of the coasts, to prevent and eliminate consequences of possible oil spills and oil products. For these goals, developing special environmental sensitivity maps of the coast, reflecting the complex expert evaluation as a tool for operational decision-making.

In this paper, we consider the coast of the Kara Sea, the offshore areas that are evaluated as one of the most promising in respect of oil and gas. The aim of this work is to assess environmental sensitivity to spills of oil and oil products and the mapping of the investigated part of the coasts of the Kara sea on the basis of the international system of indices of ESI (Environmental Sensitivity Index) and morphodynamic typing of the coastal zone.

The index of environmental sensitivity (ESI - Environmental Sensitivity Index) was first proposed in 1978 by American scientists [13] to assess the vulnerability of the coastline to oil pollution and the ranking of banks in the development of measures for oil spill response. Over the years, the method has gained wide recognition, classification of coasts with its use spread along the shores of the seas of many countries. Today, according to the requirements of the International

Maritime Organization (IMO) ecological sensitivity maps of the coast should be prepared for all areas of coastal-marine areas, where there is a risk of oil pollution.

In Russia the assessment of environmental sensitivity to oil pollution in recent years has also received considerable attention [1, 6, 10 et al.]. Active participation in development of methodical approaches to creation of maps of ecologically vulnerable zones and regions of priority protection of water areas and coasts of the Russian Federation from oil spills and oil products adopted the world wildlife Fund (WWF-Russia). Under the auspices of this organization released a number of summarizing publications [2].

II. METHODOLOGICAL APPROACHES

Despite the relevance of this type of research and the presence of well-defined development prospects of oil fields on the continental shelf of Arctic and Far Eastern seas in Russia there is still no single accepted methodology for the assessment of the sensitivity of the coasts. Geological-geomorphological factors underlying international methods are considered very superficially or not addressed at all. This is reflected in the terminology used by the Russian authors in relation to the coastal zone. The geomorphology of the coasts - formed scientific direction, studying the structure, formation conditions and contemporary dynamics of the coastal zone [8].

To emphasize the importance of the geomorphology of the coast in assessing its environmental sensitivity should refer to the original methodology, the basic principles of which remain unchanged for many years [11]. In our opinion, the most important are the following.

- Sensitivity maps are designed to display the necessary environmental information, based on which the decision can be made regarding priorities for oil spill response and appropriate cleaning methods;

- Sensitivity includes three main components: geomorphological, biological, and anthropogenic (social and economic);

- Geomorphological conditions (type of coastline, etc.) involve ranking in order of increasing sensitivity, usually on a scale of 1 to 10. This takes into account the biological component is directly related to geomorphological factors (eg, marshes, swamps, mangroves, etc.);

- Other biological and socio - economic components are shown as out of scale symbols (points , polygons , etc .) without sensitivity values. Their sensitivity may be varied over a wide range depending on the season and other factors.

By following these basic principles of sensitivity, maps do not contain:

- defining the complex sensitivity (for example, geomorphological + biological + socio-economic = final sensitivity). It remains the prerogative of the user with the ability to separately assess the sensitivity of each component and to determine the most appropriate response in a particular case;

- indicate the different sensitivity of similar sites, despite the possibility of increasing the sensitivity when combined with other components, especially biological and socio-economic.

There are 10 main levels/of indices from one (low sensitivity) to ten (high sensitivity) in the international system of the environmental sensitivity index (ESI) [12, 14]. Given the many regional differences, individual levels of ESI include several types of banks, designated by the alphabetic indexes. In total there are 25 types of the coast. Each type is color-coded in accordance with the

increase of the index of environmental sensitivity from cold color to warm, according to the approved color scale. It provides a simple and rapid identification of environmental sensitivity of the shore at the mapping and GIS work in spill response, allows identifying the most vulnerable, and are more resistant to contamination areas. The last is the key point of the planning process to eliminate contaminants in the plans of oil spill, because it determines the choice of priorities when cleaning.

Despite the versatility, the proposed list of the types of banks and their sensitivity towards oil spills require adaptation and detail (if necessary) for each particular region, and especially to the Arctic coast. This is due to specific natural conditions, a variety of morphological and dynamic environments, unequal individual knowledge of the coastal areas, different mapping scale and other factors. The typing of the coasts at any one symptom is not able to reflect all the features of their modern development and environmental sensitivity. Therefore, the basis of the ranking according to the methodology [12] was based on three main factors.

- Characteristics of the shoreline (granulometric composition of the sediments, the profile of the coastal zone) that defines the possibility of penetration and/or burial of oil, oil products on the shore, and move them;

- The impact of waves and tidal energy, which determines the time of natural resilience (safety) of oil on the shore;

- General biological productivity and sensitivity of the coast, socio-economic aspects.

The authors of the original ideas [13] do not recommend the use of integrated assessment - to combine biological, socio-economic and geomorphological component in a single index of sensitivity. When making decisions it is important to have an idea about the relative sensitivity of each of the components of the ecosystem to determine appropriate responses for a specific time and place. Given this, in our work we deliberately do not consider the biological component, of course, the most important from the point of view of nature conservation and socio-economic aspects, with an extremely limited distribution on the coast of the Kara Sea. The evaluation of these factors should be performed by qualified specialists and be accounted for separately from the geological and geomorphological conditions. For these purposes, are encouraged to develop thematic maps, or use proposed by the American specialists of the system of point (regardless of scale) conventional signs covering important ecosystem components. On the shores of the seas to such valuable and sensitive components are rare habitats, breeding sites for birds, the lot of migrating animals, places of feeding and spawning fish, and so on [2].

In this paper, we consider only the basic criteria for zoning shores in their sensitivity according to their sensitivity to pollution by oil and oil products, namely, geological-geomorphological and hydrodynamical conditions of the functioning of coastal systems. We hope that this will allow not only to communicate the sensitivity of the shores of the Kara sea to oil spills with their lithology, morphology and dynamics, but also to link ecological typing with traditional typing for sea coast morphodynamic zoning.

The practical significance of this approach lies in the fact that geomorphological analysis is able partly to offset the lack of information about the banks in remote areas of the Arctic seas. The practical experience gained in similar projects has shown that adopted as the underlying research method and information gathering specialized aerial and videography coastline using a light aircraft is not able to fully satisfy the requirements of completeness and detail of the original information. In

particular, one disadvantage of this approach is a very rough estimate of the granulometric composition of the sediments composing the beach. Another factor complicating predictive assessment of the interaction of oil with the shore, is the low informative value of photographs on the dynamics of sediment transport in the coastal zone, the speed of retreat of the coastal terraces, the power of beach sediments, permafrost conditions, the depth of seasonal thawing, the development of specific coastal processes, underwater slope relief, etc. Without a comprehensive geomorphological assessment of primary data and conducting field studies in key plots it is impossible to assess all factors of sustainability of the coast to the pollution or its capacity to cleanse itself. So, widespread on the coasts of the Arctic seas is the process of thermoabrasion almost did not take into account the international system of indexes. In addition, because it is widely known that due to the destruction of permafrost, the pillars of the Bank, the rate of retreat of coastal scarps can reach up to few meters-tens of meters during a single storm season.

Based on the understanding of the geomorphology of the coastal zone, the proposed morphodynamic approach does not contradict the principles of the international system of indices of sensitivity, as is its broader counterpart, which can and should be the basis for the ecological typification of the seacoast. In our opinion, the assessment of the environmental sensitivity of the coast made taking into account the geomorphological factors is more complete and accurate than the simplified typology for the individual ranking criteria in accordance with the method IMO/IPIECA and OGP [12].

The results of the geomorphologic zonation is most often present in the form of typing morphodynamic of the coast. The type of shore is a generalized morpholithodynamics characteristic of the coastal zone, reflecting the set of shared morphological and dynamic characteristics of a particular segment of coast. It takes into account the manifestations and activities of not only wave propagation but also other factors - hydrodynamic, geological, permafrost, fluvial, which determine the character of the shore is not less than excitement, or push his influence into the background. In addition, the type of Bank reflects the current state of the coastal system and in many ways indicates the trend of further development, accumulation or erosion. This allows taking into account, the features of the movement and sedimentation are necessary to understand the nature of distribution of oil products in the coastal zone, identify areas of possible accumulation of oil and residence time of her on the beach.

III. The shores of the Kara Sea

The most important factor determining the susceptibility of coastal areas to pollution is the geological structure of the banks and the composition of deposits pririsoval (beach) area. On the coasts of the Kara Sea, traditionally there are two main groups of banks composed of solid bedrock and Quaternary sedimentary deposits. Deposits almost everywhere are in a permafrost condition.

Morphodynamic types of the shore of the Kara Sea (scale 1:200 000)

Shores developed in solid bedrock (permafrost):

1. Abrasion and abrasion-denudation, developed in the rocks;
2. Thermodenudation, formed by outlet glaciers;

Shores composed of unconsolidated sediments (permafrost):

3. Abrasion with thermoabrasion-thermodenudation coastal scarps;

4. Abrasion with dead or dying coastal scarps, bordered by accumulative terrace;

5. Abrasion-denudation and thermodenudation (in gulfs, straits and lips);

6. Accumulative aligned, with joined accumulative terrace and tidal flats;

7. Accumulative shallow, lagoons and delta (including marshes, inundated low-lying tundra);

The proposed morphodynamic typology of the coasts can be considered universal for the investigated area, as the use of very capacious names of banks capable of numerous variations of the content of each selected type that are so necessary in the zoning and mapping of such complex objects in a chosen scale. If you change, the scale of mapping classification of banks can be expanded.

Transitions between different types of banks are often elusive and only found differences when comparing sites located at some distance from each other. The sharp boundaries of adjoining shores of various types, as a rule, coincide with tectonic faults, oriented at an angle to the coastline and separating the blocks of the Foundation with different intensity of neotectonic movements. Often, the contact area is accented by elements of hydrographic network and/or different height position of the roof of bedrock. The mouth of the rivers, as well as outstanding in a sea of capes, often share the field with various lithodynamic conditions, respectively, and with different types of banks.

Dissemination of particular types of coasts in the study area is very uneven, which emphasizes the marked differences of the morphological, geological and geomorphological structure of the coasts, the nature of the dismemberment of the coastline. On the Novaya Zemlya archipelago, Vaigach Island, Western part of the Yugor Peninsula and the coast of Taimyr is dominated by abrasion and abrasion-denudation shores developed in solid bedrock. On the coast of the Yugorskiy Peninsula, the Western coast of the Yamal Peninsula is dominated by open coast with thermoabrasion or abrasion-thermodenudation coastal scarp, interspersed with lengthy sections aligned and shallow accumulative shores with joined accumulative forms and lagoon-butovych coasts, the vast space is a sea lady, which are widely spread in the corner of Baidaratskaya lips. On the coast of the Taz Peninsula and Gydan, Yenisei Gulf in the open areas is dominated by thermoabrasion beach, lips and bays protected by the abrasion-denudation and thermoabrasion the shore, as well as extensive space nevanova accumulation. A feature of the shores of New Land and Northern Land is widespread in the coastal zone of outlet glaciers that form the ice thermodenudation scarps. Among the Islands of the Kara sea is composed of many indigenous rock is characteristic of the abrasion and abrasion-denudation type of shore, alluvial island, composed of loose Quaternary sediments are exposed to abrasion and thermoabrasion processes, accumulative plots are of secondary importance.

Analysis of the length of the individual types of banks showed that in the study area is dominated by shore type abrasion (abrasion-denudation, and thermoabrasion-thermodenudation). Accumulative areas together occupy less than 40% of the coastline of the Kara Sea.

IV. ECOLOGICAL AND GEOMORPHOLOGICAL SENSITIVITY OF THE COAST TO OIL SPILLS

Presents ecological and geomorphological approach applied in the creation of a series of maps of environmental sensitivity of the coast of the Kara Sea to oil spills and oil products. Types of

emergencies, distribution models (drift, spreading etc.), possible methods of spill response options and physico-chemical and mechanical interaction of the oil with sediments on the Arctic coasts were adopted in accordance with [7, 9]. In view of the complexity of the object and the scale selected for mapping was not able to exclude some generalizations, but they were all made in accordance with the recommended precautionary principles in favor of the object.

Environmental sensitivity to spills of oil and oil products were determined on the basis of expert assessment of the main ranking criteria using all available data banks (satellite images, aeroformation, literary, stock, field data, etc.) and included analysis of geomorphological, hydrodynamic, geological and geocryological conditions of each segment of the coast, as well as analysis of lithodynamic features of the development of the site. Take into account the peculiarities of interaction of oil with different substrate established experimentally [7, 9], the possibility of a natural burial of oil and displacement of soil, possible ways to eliminate the pollution.

As the basis of typing in the first stage were used morphodynamic zonation, which is in accordance with approaches of the international system ESI additionally took into account the openness of the coast to the excitement and lithology of the rocks composing the coastal zone. A more detailed analysis was conducted under a separate lithodynamic systems or segments of coast with similar characteristics of morphology and lithology. Using a combination of the factors discussed above, each site was assigned an index of sensitivity to oil pollution in accordance with the ESI system.

Just within the surveyed part of the Kara Sea has been allocated 11 types of banks with different indexes of environmental sensitivity:

1A - exposed rocky (ice) shore;

1C - exposed rocky cliffs with boulder talus base;

2A - exposed wave-cut platforms (benches) in bedrock, clay and silt deposits;

3A - fine- to medium-grained sand beaches;

3B - scarps and steep slopes in sand;

5 - mixed sand and gravel beaches;

6A - gravel beaches (gravels and pebbles);

8A - sheltered scarps in bedrock, clay and silt deposits and sheltered rocky shore;

8D - sheltered rocky rubble shores;

9A - sheltered tidal flats;

10A - salt and brackish water marshes (laidy).

Changes the names of types of banks, made to their original names, can be considered minimal. This was achieved due to the "increase capacity" of individual concepts and generalization of the similar nature of the intended interaction with oil and petroleum products types of Bank. Foreign colleagues proposed a gradation of grain size of beach sediments in the name of banks, corresponding to the ESI indices, adopted that position. In the future, it will allow creating a unified typing of the coast of all seas of the Arctic Ocean that meets international standards.

Comparative analysis of morphodynamic and ecological types of banks showed that the same ecological types of banks could be allocated at different dynamic in relation to the land. For example, beaches, sprinkled with various particle size sand and gravel-pebble deposits are found both on accumulative and abrasion areas with dead or dying coastal ledge. This indicates the same

level of environmental sensitivity of such banks. In some cases, the dynamic type of coast can match the coast with different environmental sensitivity index. Otherwise, there is regular correspondence of the individual type's dynamic and environmental banks, which allows the use of a pivot typing is to interpret a poorly known ecological sensitivity of coastal areas.

The length of the individual types of banks in the surveyed part of the coast of the Kara Sea. The most sensitive to oil pollution protected shallow alluvial, lacustrine-deltaic butovye and beach with extensive tidal foreshores and lidumi (indexes 9A and 10A) is more than 2000 km, which is about 20% of the total length of investigated shoreline. They are confined mainly to southern and Southwestern part of the Kara Sea. About the same and is the least sensitive of the abrasion and abrasion-denudation rocky shores of Islands and the northeastern coast (index 1A and 1C) – 2000 km and of the order of 20%. Abrasion and accumulative shores, and the shores with dead or dying cliffs composed of loose sediments of different composition, combine to form a large part of the coastline and are characterized by moderate susceptibility to oil spills. Arctic shores composed of dispersed frozen rocks are from the shores of the ice-free seas a number of specific features. Located in the high latitudes, they develop in short dynamic (ice-free) season, which is 5-10 times shorter than in the seas of temperate latitudes. In the winter months, ice and frozen substrate of the coastal zone block the activity of most relief-forming processes reduced the permeability of sediments for petroleum products. Accordingly, changing the nature of the interaction of the substrate with oil from season to season.

Covered by land fast ice for 6-9 months of the year the coast is almost not sensitive to oil spills in the water area, and are relatively insensitive to spills directly to coastal areas where land fast ice meets (corsets) with the bottom remaining fixed during the freeze-up. Thawing sediments of the upper part of the underwater slope and beach, and therefore the ability to accumulate oil on the shores of the Arctic seas, appears only in the short ice-free period of the year. At the same time possible and distribution of oil in the coastal zone, its direct contact with the shore. This period in the Kara region occurs in June-July and continues until mid-October-November (depending on local conditions). The warming is accompanied by intensive heat exchange of the permafrost with the atmosphere and hydrosphere - thaw of the active layer and activation of exogenous geological processes. It was during this period of time the sea shore are vulnerable from an environmental point of view to the probable oil spills, then the most actively developing morphodynamic coastal processes.

Thus, the presented ecological typification of Arctic coasts will be relevant only for the short ice-free period of the year with maximum depths of seasonal thawing of coastal sediments. This should be considered when developing spill response plans of oil, the probability of which is not restricted to the warm period of the year.

V. Conclusion

Geomorphologic zoning of the coast of the Kara Sea and to assess their environmental sensitivity to oil spills, made in accordance with the system of indices of ESI, along with the decision of assigned tasks demonstrated the capability of this integrated approach in the development of sensitivity maps of the coast. The necessary consideration of the specific natural conditions (permafrost, lithodynamic, ice, etc.) development of the coastal zone and adaptation of

the international system of indexes to the shores of the Arctic seas. But in general, ecological and geomorphological approach does not contradict the principles of the original method (IMO/IPECA/OGP) and allows to take into account how the particle size distribution of coastal sediments and the influence of excitement, and features of the dynamics of substances in the coastal zone, the direction of coastal processes, the morphology of the coastline and so This increases the accuracy of expert estimates of the sensitivity and forecast resilience of banks, but does not replace the recommended conduct field verification studies in the key areas. For the Arctic coasts of the latter circumstance is of particular importance because it allows to define more precisely the areas requiring priority protection from contamination.

Developed geomorphological typing of banks can be considered universal for the investigated area. With slight modifications, it can be used to assess sensitivity to oil pollution in the Arctic and other seas. We emphasize that the proposed ecological typification of current for a relatively short ice-free period of the year with maximum depths of seasonal thawing of coastal sediments (July-October). At this time, you can directly contact the oil spill with the coast, its distribution and accumulation in the coastal zone, blocked by land fast ice for much of the year.

In conclusion, it should be noted that zoning and mapping of the coast in accordance with the index of environmental sensitivity and development of spill response plans are only the first steps towards environmental safety of the Arctic coasts. Not less important are speed alerts, timely response to the spill and the application of the most efficient technologies of liquidation of oil spills in the far north, where carrying out any actions associated with a number of serious limitations.

VI. References

[1] Y. Y. Blinovskaya, Informational provision of ecological safety during development of oil deposits on the shelf. Vladivostok: Mor. GOS. UN-t, 2006. – 232 p.

[2] Y. Y. Blinovskaya, M. V. Gavrilo, N. B. Dmitriev, V.B. Pogrebov., A. Yu. Puzachenko, S. M. Usenko, et al. Methodical approaches to creation of maps of ecologically vulnerable zones and regions of priority protection of water areas and coasts of the Russian Federation from oil spills and oil products. Vladivostok - Moscow - Murmansk - Saint-Petersburg, the world wildlife Fund (WWF Russia), 2012. – 60 p.

[3] A.A. Vasil'ev, I.D. Streleckaja, G.A. Cherkashev, B.G. Vanshtejn Dynamics of the shores of the Kara sea // Cryosphere of the Earth, 2006, vol. X, No. 2, pp. 56-67.

[4] A.A. Vasil'ev, R.S. Shirokov, G.E.Oblogov, I.D. Streleckaja Dynamics of the coasts in Western Yamal // Cryosphere of the Earth, 2011, vol. XV, no. 4, pp. 72-75.

[5] I. A. Nemirovskaya, Oil in the ocean (pollution and natural streams). M.: Scientific world, 2013. – 432 p.

[6] V.B. Pogrebov, A.Ju. Puzachenko, Integral sensitivity of marine ecosystems to oil pollution: Mat. 5 scientific. seminar “Readings in memory of K. M. Deryugin”. SPb.: Ed. St. Petersburg state University. – 2003. – pp. 5–22.

[7] Guide to the elimination of oil spills in seas, lakes and rivers. SPb.: ZAO CNIIMF, – 2002. – 344 p.

[8] G.A. Safyanov, Geomorphology of sea shores. M., 1996. – 400 p.

[9] O.Ya. Sochnev, I.O. Sochneva. Environmental safety of the system of export of oil from fields on the Arctic shelf. M.: Zeitenspiegel, 2003. – 272 p.

[10] A.A. Shavykin, The procedure of mapping the vulnerability of coastal and marine areas from oil. Example maps for Kola Bay // Bulletin of the Kola science centre of RAS, 2015, № 5. – pp. 113-123.

[11] Environmental Sensitivity Index (ESI) Experience [Electronic resource]. Oil-Spill-Info.com (E-Tech International Inc.). 2014. Mode of access: http://www.oil-spill-info.com/sum_esi.html (date accessed 16.05.2016).

[12] IMO/IPIECA/OGP. Sensitivity mapping for oil spill response. – London, 2012. – 39 p.

[13] Gundlach, E.R., Hayes, M.O. Vulnerability of coastal environments to oil spill impacts // Mar. Tech. Soc. Jour. 1978. – № 12. – pp. 18-27.

[14] NOAA Technical Memorandum NOS OR&R 11. Environmental Sensitivity Index Guidelines. Version 3.0. Jill Petersen, Jacqueline Michel, Scott Zengel, Mark White, Chris Lord, Colin Plank. Hazardous Materials Response Division, Office of Response and Restoration, NOAA Ocean Service. - March, 2002. – 192 r. – URL: http://response.restoration.noaa.gov/ sites/default/files/ESI_Guidelines.pdf (date accessed 16.05.2016).

VARIATIONS OF SEA LEVEL AND GLOBAL CLIMATE IN MODERN CONDITIONS

Valeriy N. Malinin, Russian State Hydrometeorological University, Russia
Svetlana M.Gordeeva, Russian State Hydrometeorological University, Russia
Oleg I. Shevchuk, Russian State Hydrometeorological University, Russia
Yuliya V. Mitina, Russian State Hydrometeorological University, Russia
Alexandra A. Ershova, Russian State Hydrometeorological University, Russia

malinin@rshu.ru

Global warming can result in the rise of Sea Level (SL) by 40–100 cm by the end of the XXI century with possible catastrophic consequences for coastal zone. Study and prediction of long-term fluctuations of sea level is among the most important problems of modern hydrometeorology. A series of studies of SL interannual fluctuations have been carried out in RSHU. A reconstruction of SL fluctuations during the observation period of 1861-2010, i.e. 150 years, was performed on the basis of the developed statistical model showing a powerful linear trend describing 94% of the initial row dispersion. During the XX century the trend approached 1.8 mm/year. The comparison of actual and calculated SL trends for two periods (1980–2005 and 1993-2003) has shown that the residual error makes respectively 0.21 and 0.22 mm/year that is three times less, than in the Fourth IPCC report. Also, for the first time the complex of methods of SL longterm forecast was developed: the main advantage of a simple statistical model of SL longterm forecast is a minimum of initial information, but the model accuracy is comparable with complex and expensive ocean and atmosphere circulation models. The two-decade range physical-statistical sea level prediction model was developed for the first time based on the idea that Global Air Temperature (GAT) is a major factor of SL changes. It was experimentally shown that there is a long delay (20 and 30 years) of SL fluctuations with respect to Global Air Temperature.

Key words: global sea level, climate change, interannual fluctuations, statistical model

I. INTRODUCTION

The most important indicator of global climate change is the level of the World Ocean - global sea level (GSL). During the XX century there has been a quite rapid rise of sea level - 1.7-1.8 mm/year [1, 2]. However, in the last two decades the altimetry data showed that rate of the sea level rise has considerably increased and now makes about 3.2 mm/year. By the end of the XXI century, according to different predictions, the sea level can increase by 40–100 cm in comparison with the beginning of the century [2]. If such development of climate change becomes a reality, there is a risk of catastrophic damages to the infrastructure of sea coasts, flooding of coastal territories of many countries and migration of many tens of millions of people. Therefore the problem of study of long-

term fluctuations of global sea level and, in particular, the development of methods of its long-term forecasting is among the most important problems of modern hydrometeorology.

II. MATERIALS AND METHODS

In Russian State Hydrometeorological University a series of research works have been carried out recently on studying of the regularities of global sea level interannual fluctuations on the basis of instrumental observations, with identification of their genesis, assessment of various "sea level forming" factors contribution in the global sea level trend, development of a complex of physical and statistical models of long-term sea level forecast with various ranges and identification of the factors driving the global warming in the last decades. The result was a series of publications in periodicals and two monographs [3,4], with many scientific results received for the first time.

On the basis of the developed statistical model the reconstruction of global sea level fluctuations was carried out for the period of instrumental observations based on data of several long-term observation coastal stations from 1861 to 2010, i.e. for the last 150 years (fig. 1).

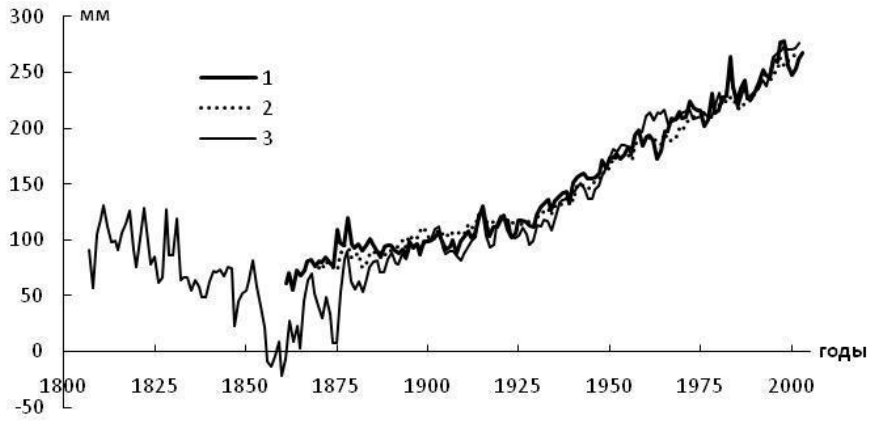

Fig. 1. Comparison of global sea level time series calculated by different authors. 1 – RSHU model [5], 2 – data of Church and White, 2006 [1], 3 – data of Jevrejeva et al. 2006 [6].

Average rate of GSL rise for the considered period is about 1.4 mm/year, and the trend describes 94% of dispersion of the initial row. Thus, the observed powerful linear trend is the main regularity of interannual fluctuations of global sea level. In the GSL main trend there are several distinct periods of various origin of level changes that have different local trends. It is a quite rapid growth of GSL in 1861-1877 (Tr = 2.0 mm/year), followed by the period of 1879-1923 when the level remained almost the same, i.e. there was a phase of nearly-standing level (Tr = 0.4 mm/year); after that up to the present it has been again rising rapidly (Tr = 2.0 mm/year). During the XX century the trend reached nearly 1.8 mm/year.

Note, that GSL calculated on our statistical model is fully compatible with the similar GSL reconstructions of other authors [1,6] based on data including over 1000 stations of global archive of sea level gauges PSMSL. The model certain advantage against the western analogs is that with the same level of accuracy it calculates GSL with a minimum of initial information, namely, data from only several stationary coastal stations.

We found that the trend formation in annual GSL can be considered in the form of a "random walk" statistical model [3]. The essence of the model is in the consecutive summation of intra-annual level increment values (Δh_M), representing the stationary casual process developing in the form of a "red noise" model. The trend of this new row is completely identical to a trend of GSL average annual values, i.e. $Tr(\Sigma\Delta h_M) = Tr(h_M)$. The physical sense of this result is that during the assessment of the contribution of different factors to GSL trend formation it is possible to use the equations of fresh-water budget of the ocean and the changes of water budget of the hydrosphere.

The study of the genesis of GSL interannual fluctuations is possible on the basis of two main approaches. From the equation of the water budget in the hydrosphere representing the system of interacting reservoirs consisting of the ocean, the atmosphere, the cryosphere and fresh waters of land, GSL changes can be presented in the form:

$$\Delta h_M = A_M^{-1}(-\Delta V_C - \Delta V_L + \Delta V_{ster}), \qquad (1)$$

where Δh_M – sea level intra-annual fluctuations; A_M – World Ocean area; ΔV_C – fluctuations of cryosphere water mass; ΔV_L – fluctuations of fresh water mass (land and ground waters), ΔV_{ster} – fluctuations of GSL steric component due to changes of ocean heat content. This is the equation used in foreign studies on assessment of contribution of various factors to GSL changes. Generalization of the obtained results is presented in the Assessment Reports of the Intergovernmental Panel on Climate Change (IPCC), and in the multi-author monograph [7].

Another approach developed in RSHU is the assessment of contribution of various factors performed with the equation of fresh-water budget of the World Ocean as a sum of eustatic and steric factors. Therefore, we have:

$$\Delta h_M = A_M^{-1}(P_{WO} + M + I - E_{WO} + \Delta V_{ster}), \qquad (2)$$

where P_{WO} – precipitation on the surface of the World Ocean (WO); M – land (surface and ground) flow to WO; I – ice flow to WO; E_{WO} – evaporation from the surface of WO.

Foreign researchers use the method of trends, i.e. linear trends of “sea level forming” factors are calculated for various periods and then their sums are compared with the actual trend of GSL. It is clear, that the method of trends is adequate only for monotonous data rows and allows a quite approximate judgement of the contribution of separate factors because of the strong dependence on the trend value and the contribution of the trend coefficient of determination to dispersion of the initial process. It is known that for short rows the trend value depends on the row length, and the row length changes only on one value can cause the significant change of the trend value, up to the sign change.

III. RESULTS AND DISCUSSION

Let’s consider the generalizing results of numerous studies on assessment of contribution of various factors to the GSL trend presented in IPCC reports. In the XX century (1910-1990) the total contribution of the “sea level forming” factors (with mountain glaciers) ranged from -0.8 to 2.2 mm/year with the average value of 0.7 mm/year (Table 1) [8]. If we exclude the thawing of

mountain glaciers from total contribution the total value will decrease to 0.4 mm/year. It is obvious that IPCC experts make a principal mistake here, considering the thawing of mountain glaciers as a contribution to GSL changes. Thawing of mountain glaciers, which is indeed very essential, can give a direct contribution to GSL changes only from the glaciers located on islands in the Arctic Ocean, and perhaps partially from the territory of Alaska, and therefore their contribution to GSL rise does not exceed 0.1 mm/year. Mountain glaciers in Europe, Asia, Africa and South America can influence GSL only through the flow of river water to the ocean. Therefore, it is hardly necessary to consider their direct contribution to the GSL trend.

Because the actual rise of GSL according to observations was Tr = 1.5 mm/year, we have a huge residual error (imbalance) between the calculated and actual trend values in GSL, exceeding the contribution of any of the "sea level forming" factor.

Table 1. Contributions of various factors to GSL trend formation based on the IPCC Reports

GSL driving factors	Trend values, mm/year			
	1910–1990 [8]	1961–2003 [9]	1993–2003 [9]	1993–2010 [2]
Thermal expansion	0,51 ± 0,20	0,42 ± 0,12	1,6 ± 0,5	1,1 (0,8-1,4)
Glaciers and icecaps	0,30 ± 0,09	0,5 ± 0,18	0,77 ± 0,22	0,76 (0,39-1,13)
Greenland Ice Sheet	0,06 ± 0,05	0,05 ± 0,12	0,21 ± 0,07	0,33 (0,25-0,41)
Antarctic Ice Sheet	-0,09 ± 0,10	0,14 ± 0,41	0,21 ± 0,35	0,27 (0,16-0,38)
Land waters	-0,07 ± 0,78	-	-	0,38 (0,26-0,49)
Total	0,70 ± 0,82	1,1 ± 0,5	2,8 ± 0,7	2,8 (2,3-3,4)
Observed sea level	1,5 ± 0,50	1,8 ± 0,5	3,1 ± 0,7	3,2 (2,8-3,6)

The same high residual errors are observed for other periods. For the period 1961-2003 the residual error without mountain glaciers makes 1.0 mm/year, and for 1993-2003 – 0.9 mm/year [9], for 1993-2010 – 1.2 mm/year [2], and on absolute value they exceed the contribution of any factor of GSL formation (Table 1). Highly doubtable is also the assessment of considerable reduction of surface and ground water reserves which contribution to GSL trend for 1993-2010 (based on data from [2]) was 0.38 mm/year exceeding the contribution of ice sheets of Antarctica and Greenland. This must by all means be manifested in the sharp growth of continental flow to the World Ocean. However, Russian scientists do not confirm this fact [10, 11]. Therefore, we can surely claim that the use of the equation of water mass budget in the hydrosphere for the GSL trend assessment by foreign researchers is hardly justified because it requires the knowledge of a large number of the different difficult to determine factors which accuracy in many cases even can not be checked.

In our opinion, to assess the role of different factors in GSL trend formation the equation (2) should be used with easier determined components than the components of the equation (1), and with the accuracy that is possible to check [12]. The study [4] presents the assessment of interannual variability of evaporation and rainfall, and their difference on the basis of CDAS reanalysis (Climate Data Assimilation System) for the period of global warming (1980-2006). The pronounced positive

trend describing more than 50% of dispersion is characteristic of time series of rainfall and evaporation. The trend for rainfall over the World Ocean is *Tr* = 4.2 mm/year, and for evaporation *Tr* = 3.6 mm/year; respectively the trend in effective evaporation is negative. Thereof, during 1980-2005 there was a GSL rise at a rate of 0.6 mm/year corresponding to 217 km^3/year. Correlation of series of evaporation and rainfall with global air temperature makes *r* = 0.82 and *r* = 0.80 respectively.

The RSHU studies of various "sea level forming" factors allowed to perform a comparison of the actual and calculated GSL trends for two periods (1980–2005 and 1993-2003) shown in Table 2. Here the calculated GSL trend was determined as a sum of trends of eustatic and steric components. It is easy to see that the residual error of calculations makes respectively 0.21 and 0.22 mm/year. It is more than three times lower than the IPCC estimates in case of excluding the contribution of mountain glaciers.

Table 2. Estimates of the contribution of various factors to GSL trend formation for 1980–2005 and 1993-2003 using the equation of fresh-water budget of the World Ocean, mm/year, based on data from [3]

Sources of GSL rise	1980–2005	1993–2003
Steric sea level fluctuations	0,30	1,60
Total flow from Greenland	0,14	0,22
Solid flow from Antarctica	0,24	0,44
Input of land waters	0,16	0,19
Vertical water exchange (rainfall minus evaporation)	0,62	0,43
Total contribution of factors	1,56	2,88
GSL rise based on observations	1,79	3,10
Misbalance (residual error)	0,23	0,22

A complex of methods of GSL longterm forecast was developed in RSHU for the first time: long-range forecast (century), short-range forecast (several decades) and for the current period (several years). Such division is explained, on one hand, by physical regularities of the sea level fluctuations and influence of various factors, and on the other hand – by practical needs of consumers. For long-range forecasting (for the end of the XXI century) the simple statistical GSL forecasting model [13] is offered. It is based on the use of the global air temperature (GAT) modelling with a complex of numerical models of ocean and atmosphere circulation (OACM). The comparison of global estimates of GAT anomalies and GSL values during 1960-2008 based on coastal observational data showed a well expressed linear dependence between them. This allowed to calculate a linear statistical model which describes 73% of GSL dispersion.

A probable range of GSL rise for the end of 2090-2099 [9] was calculated on the statistical model for the 6 main scenarios of climate change and with the probable range of temperature rise for the end of 2090-2099 set according to a complex of 16 climatic models. The comparison of predicted GSL data for the end of the XXI century on the statistical model and on the OACM

complex showed almost full agreement (Table 3). The obvious advantage of the model is that it requires a minimum of initial information, providing at the same time the same level of accuracy as in the complex and expensive OACM. This means that in approximate predictive GSL calculations it is quite reasonable to exclude the use of OACM.

Table 3. Estimates of possible changes of global surface temperature and global sea level by the end of XXI century (2090–2099) as compared to the end of XX century (1980 – 1999)

Emission scenario	Ensemble of 16 models of ocean and atmosphere circulation [9]		Statistical model [13]
	Probable range of temperature rise by 2090-2099, °C	Probable range of GSL rise by 2090–2099, m	Probable range of GSL rise by 2090–2099, m
Scenario *B1*	1,1 – 2,9	0,18 – 0,38	0,12 – 0,31
Scenario *A1T*	1,4 – 3,8	0,30 – 0,45	0,15 – 0,41
Scenario *B2*	1,4 – 3,8	0,20 – 0,43	0,15 – 0,41
Scenario *A1B*	1,7 – 4,4	0,21 – 0,48	0,18 – 0,47
Scenario *A2*	2,0 – 5,4	0,23 – 0,51	0,21 – 0,58
Scenario *A1FI*	2,4 – 6,4	0,26 – 0,59	0,26 – 0,68

The physical and statistical model of interannual fluctuations of global sea level is developed and presented in order to predict the long-term changes for two decades [14] which does not have analogs in foreign studies. It is based on the formulated concept that GAT changes are the most important defining factor of GSL variations. It was experimentally shown that there is a long delay (20 and 30 years) of GSL fluctuations in relation to GAT changes. It allows to use the procedure of the shift step-wise multiple regression for determination of optimum models of GSL fluctuations depending on air temperature values set at the nodes of the grid area over the ocean. A complete complex of step-wise models was calculated on the dependent series (1901-1999) for shifts from τ = 0 to τ = 33 years by the method of inclusion of variables up to 15 predictors, so that the total number of models was over 500. Their analysis allowed to set the shift of τ = 21 years when the GAT influence on GSL fluctuations is manifested at the maximum level. As a result it was possible to calculate the prognostic estimates of GSL up until 2028 (Figure 2). The trend value for the specified period is *Tr* = 3.0 mm/year that satisfactorily corresponds to the altimetry GSL trend value (2.9-3.0 mm/year) for the beginning of XXI century. The adequacy of obtained results was confirmed by the similar physical and statistical models constructed for GSL time series taken from studies [1, 6].

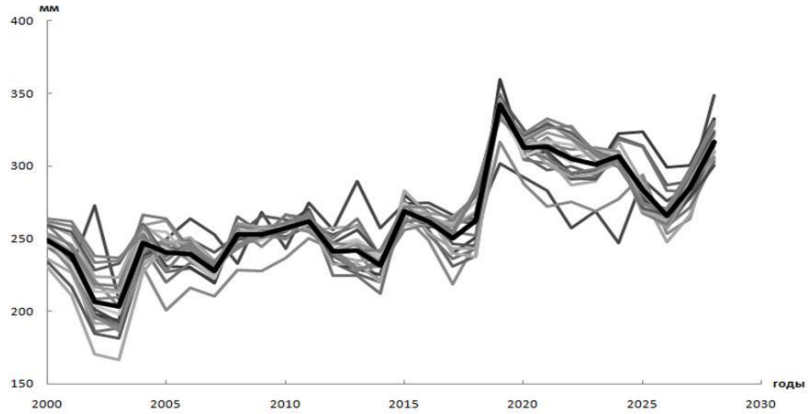

Fig. 2. Predicted GSL for 2000-2028 calculated on the statistical model for different amount of parameters from m=1 to m=19 [14]. Solid line – averaged curve for 19 GSL values for each year.

IV. CONCLUSION

As a conclusion and summing up the results we can say that the Russian leader in the study and forecasting of global sea level fluctuations can be considered Russian State Hydrometeorological University. This direction owing to the huge practical value within many decades will remain the most important problem of modern hydrometeorology.

V. REFERENCES

[1]. Church J.A., White N.J. A 20th century acceleration in global sea-level rise // Geophysical Res. Letters. 2006, V. 33. N 1. L01602.

[2]. IPCC. Climate Change 2013: The Physical Science Basis. Contribution of Working Group to the Fifth Assessment Report of the Intergovernmental Panel on Climate Change / Eds. Stocker T.F. at al. Cambridge (UK); N. Y.: Cambridge University Press, 2013.1535 pp.

[3]. Malinin V.N. Global sea level: present and future. St.Petersburg: RSHU, 2012. 260 p.

[4]. Malinin V.N. Global water budget. - Lambert Academic Publishing, 2011, 158 p.

[5]. Malinin V.N., Gordeeva S.M., Shevchyk O.I. Variability of global sea level in last 140 years. Uchenye zapiski RGGMU. 2007. Vol. 4. p.125-132.

[6]. Jevrejeva S., Grinsted A., Moore J.C., Holgate S. Nonlinear trends and multiyear cycles in sea level records // J. Geophys. Res. 2006, V. 111. N C9. C09012.

[7]. Understanding Sea-level Rise and Variability // Eds. John A. Church, Philip L. Woodworth, Thorkild Aarup, W. Stanley Wilson.– Wiley-Blackwell, 2010. 456 p. ISBN: 978-1-4443-3451-7.

[8]. IPCC. Climate Change 2001: The Scientific Basis. Contribution of Working Group I to the Third Assessment Report of the Intergovernmental Panel on Climate Change / Eds. Houghton, J.T. et al.– Cambridge; New York, Cambridge university press. 2001. 881 p.

[9]. IPCC. Climate Change 2007: The Physical Science Basis. Intergovernmental Panel on Climate Change Fourth Assessment Report Climate Change 2007 / Eds. Bernstein L. et al.– Cambridge; New York, Cambridge University Press. 2007. 940 p.

[10]. Babkin V.I., Klige R.K. River flow to the World Ocean // Uchenie zapiski RGGMU. 2009. Vol. 13, p. 17-20.

[11]. Dobrovolskiy S.G. Global changes of river flow. – Moscow: GEOS, 2011, 660 p.

[12]. Malinin V.N. Water exchange in the system ocean-atmosphere. – Leningrad: Hydrometeoizdat, 1994, 197 p.

[13]. Malinina U.V. To the assessment of possible damage from expected sea level rise in XXI // Uchenye zapiski RGGMY. 2010. №14. p.162-176.

[14]. Malinin V.N., Shevchyk O.I. On possible global sea level changes in future decades // Obshchestvo. Sreda. Razvitie, 2009, №2, p.172-180.

CORRELATION OF THE BLACK, MARMARA AND AEGEAN SEAS DURING THE HOLOCENE

Nikolay Igorevich Esin, Southern Branch of the P.P. Shirshov Institute of Oceanology, Russian Academy of Science, Russia
Vladimir Ocherednik, Southern Branch of the P.P. Shirshov Institute of Oceanology, Russian Academy of Science, Russia

esinnik@rambler.ru

A mathematical model describing the change in the Black Sea level depending on the Aegean Sea level changes is presented in the article. Calculations have shown that the level of the Black Sea has been repeating the course of the Aegean Sea level for the last at least 6,000 years. And the level of the Black Sea above the Aegean Sea level in the tens of centimeters for this period of time.

Key words: mathematical model, water flow in the Bosphorus and Dardanelles straits, seas levels correlation.

I. INTRODUCTION

The dependence of the Black Sea level with the Marmara Sea level is one of the important features of the process of changing the level of the Black Sea during the Holocene. In turn, the course of the Marmara Sea level depends on changes in the Aegean Sea level. This feature is often not taken into account in the study of change of the Black Sea level. For this reason, the curves of change of the one sea level are not compared with the curves of the other seas level change.

References [1; 2; 3; 4] represent a mathematical model of filling of the Black Sea basin by water in the Late Pleistocene and Holocene. There are shown that the level of the Black Sea has to repeat the course of the Mediterranean Sea during the Holocene. It should be borne in mind that the Black Sea has an excess of fresh water in the amount of 240-300 km^3/year. In order for this water amount plus the amount of water compensating of the Bosphorus bottom counterflow could to flow in the Marmara Sea during 1 year, it is necessary that the average difference in seas levels was approximately 0.3 m. In order for the excess volume of water flowed in the Aegean Sea, between the Marmara and the Aegean Sea also the level difference has to be. For this reason, the level of the Black Sea above the Marmara Sea level and the level of the Marmara Sea above the Aegean Sea level.

The aim of this work is to identify the correlation between the levels of the Black and Aegean seas.

II. METHOD OF WORK

The method of mathematical modeling of flows in the straits of Bosphorus and Dardanelles is used to achieve the goal set in the article. This method proved to be effective in the study of water exchange through the Bosphorus Strait at the end of the late Pleistocene and Holocene.

Previously, we offered the single-layer flow model of a viscous incompressible fluid in the Bosphorus Strait in conditions of low World Ocean level [1] and the two-layer flow in conditions of high level of the ocean [5]. In the latter case, the bottom flow of water in the strait is effected by the fact that the density of water in the bottom flow more than the density of water in the upper flow. The difference in water levels or pressure gradient directed towards the Marmara Sea is the driving force of the upper flow. It has been shown that the upper flow plays the leading role in the two-layer stream. If the water discharge in the upper flow is increasing then the water discharge in the bottom flow is reducing. American study [6] has shown that the shear stresses created by the upper flow on the boundary of contact with the lower layer capture some part of water of the bottom flow and return it to the Marmara Sea.

Neglecting the influence of the bottom flow on the water-level in the straits, and using the results obtained in the paper [4], we can write the system of two equations. The first equation describes the dependence of the Black Sea level with the level of the Marmara Sea, and the second – the dependence of the Marmara Sea level with the Aegean Sea level. Using data on the current state of the investigated process [6; 7; 8; 9; 10; 11] and data on eustatic level change in the Mediterranean Sea during the Holocene [2; 12], in the first approximation we performed calculation of the eustatic changes in the Black Sea level during the last 6,000 years.

III. RESULTS AND DISCUSSION

In order to reconstruct the changes of the Black and Marmara seas levels depending on the Aegean Sea level course, a simple mathematical model was obtained based on the solution of the Navier-Stokes equations. The system of equations describing the investigated process is as follows:

$$\begin{cases} \dfrac{dH_1}{dt} S_1 = W_1 - \dfrac{\left(H_1^{\,4} - \left(H_2 + h_*\right)^4\right) g l_1}{12 \nu_1 L_1}; \\ \dfrac{dH_2}{dt} S_2 = W_2 - \dfrac{\left(H_2^{\,4} - H_3^{\,4}\right) g l_2}{12 \nu_2 L_2}; \\ H_3 = f(t). \end{cases} \tag{1}$$

Here H_1 – the depth of the upper flow in the northern end of the Bosphorus Strait, characterizing the level of the Black Sea, S_1 – the area of the Black Sea, W_1 – the average water discharge through the upper flow of the Bosphorus Strait, h_* – the difference between the levels of the interfaces of the upper and lower flows in the straits of Bosphorus and Dardanelles, g – acceleration of gravity, l_1 – the width of the Bosphorus Strait, ν – the kinematic viscosity coefficient, L_1 – the length of the Bosphorus Strait, H_2 – the depth of the upper flow in the northern

part of the Dardanelles Strait, H_3 – the depth of the upper flow in the southern end of the Dardanelles Strait, S_2 – the area of the Marmara Sea, W_2 – the average water discharge through the upper flow of the Dardanelles Strait, l_2 – the width of the Dardanelles Strait, L_2 – the length of the Dardanelles Strait.

Below is a schematic drawing showing the main features of the used approximation to describe the flows in the straits (Fig. 1).

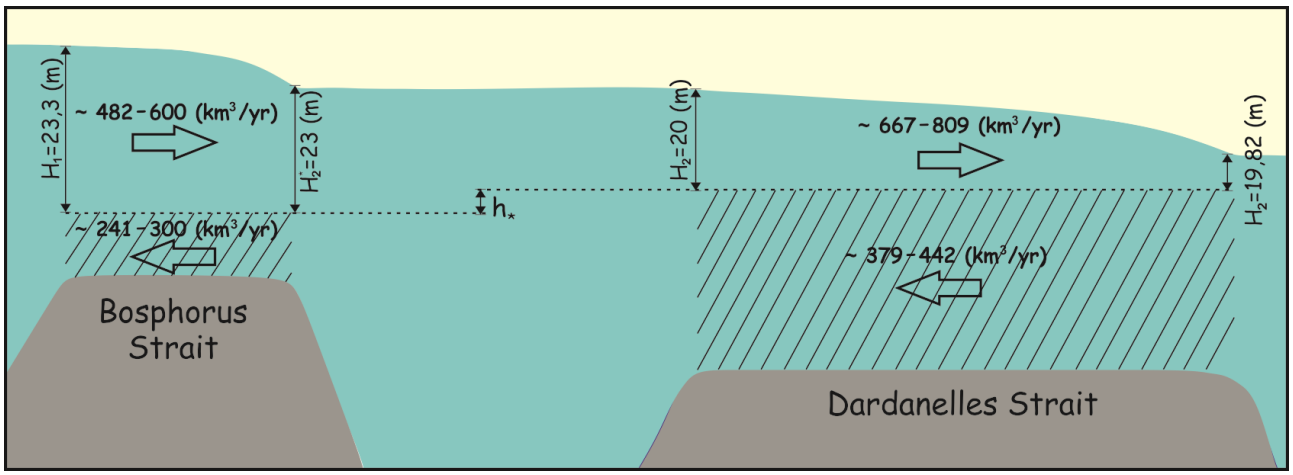

Fig. 1. Scheme of the modeled flows of water in the straits of Bosphorus and Dardanelles.

Current average annual water discharge through the upper flow of the Bosphorus Strait is 482–600 km^3/year [2; 8]. Theoretical calculations Oguz et al. [11] and field observations Jarosz et al. [6] have shown that at present in the area of the shallowest part of the Bosphorus Strait, average for year the surface of the counterflow locates at depth of approximately 23 m, i.e. the depth of the upper flow at this point is 23 m and the depth of the lower flow is 13 m. The difference in the average levels of the Black and Marmara seas is 0.3 m [6; 9]. Width of the narrowest section of the Bosphorus Strait is 700 m. These data allow us to determine the value of the coefficient ν_1, at which 15,284 m^3/s (482 km^3/year) of water would flow in the channel with depth of 23 m, width 700 m and the level difference of 0.3 m, and thus to adapt the model to the concrete conditions.

$$\nu_1 = \frac{\left(H_1^{\,4} - H_2^{*4}\right) g l_1}{12 Q L_1}. \qquad (2)$$

Taking in (2) H_1 = 23.3 m, H_2^* = 23 m, g = 9.81 m/s^2, l_1 = 700 m, Q = 15,284 m^3/s, L_1 = 30,000 m, получим $\nu_1 = 1.8 \cdot 10^{-2}$ m^2/s. The resulting value of the kinematic coefficient of viscosity coincides with its calculated value according to the natural measurements in [6].

The length of the Dardanelles Strait is about 64 km, minimum width is approximately 1.4 km, the minimum fairway depth is about 60 m. According to Jarosz et al. [10] 442 km^3/year (14,020 m^3/s) of water flows from the Mediterranean Sea to the Marmara Sea through the Dardanelles Strait. The upper Dardanelles stream outflows from the Marmara Sea of about 809 km^3/year (25,660 m^3/s)

of water with a lower salinity than in the Mediterranean Sea. According to others data [13] average water discharge in the upper and lower streams are 667 and 379 km^3/year respectively. Separately taken survey [10] (7-9 February 2009) demonstrates that the depth of the upper stream in the northern part of the strait is about 20 m, the depth of lower stream – 40 m (Fig. 2). The difference between the levels of Marmara and Aegean seas is about 18 cm [7]. These data allow us to determine the value of the coefficient ν_2 for flow of water from the Marmara Sea to the Aegean Sea via the Dardanelles Strait. If take H_2 = 20 m, H_3 = 19.82 m, g = 9.81 m/s^2, l_2 = 1,400 m, Q = 25,660 m^3/s, L_2 = 64,000 m, we have ν_2 = 4·10^{-3} m^2/s.

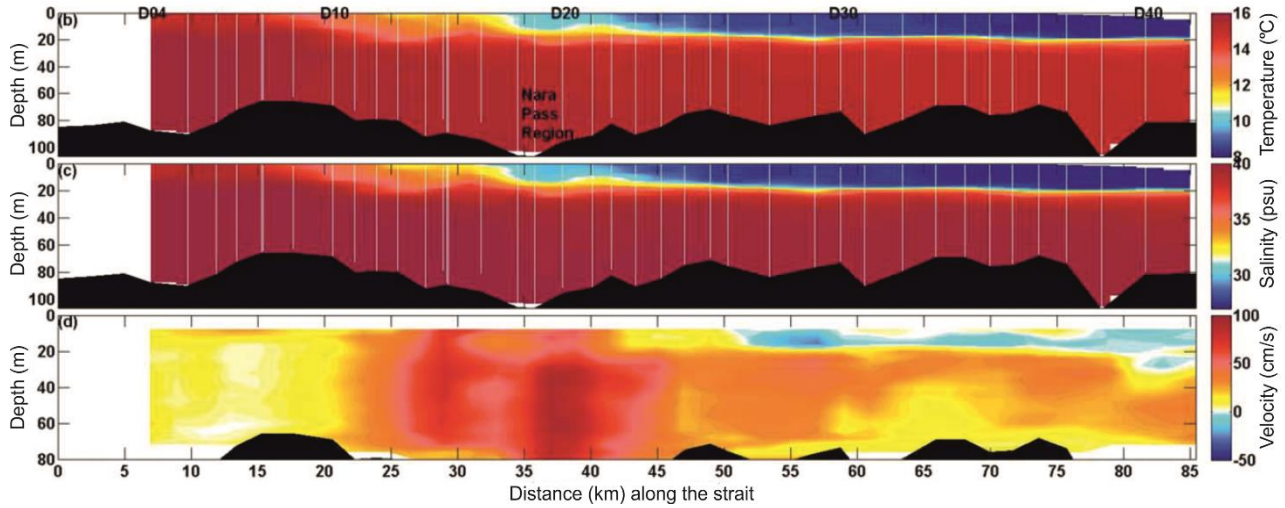

Fig. 2. The results of field observations of the vertical gradient of temperature, salinity and velocity of flows in the Dardanelles Strait [10].

The area of the Black Sea is 422,000 km^2, Marmara Sea – 11,350 km^2. If as an example we take a linear function of the level rise of the Mediterranean Sea at a velocity of, for example, 30 mm/year, then solving the system of equations (1) we get the following charts of levels changes of the three seas (Fig. 3a). From the calculations it follows that the levels of the Black and Marmara seas repeat the trend of the Mediterranean Sea level rise, but the velocity of rise of the Marmara Sea level would be 29.4 mm/year, and the velocity of rise of the Black Sea level would be 28.4 mm/year. If as the change of the Mediterranean Sea level $f(t)$ take the function $19.82 + 30 \cdot 10^{-3} \cdot t + \left(1 - \cos\left(\frac{2\pi t}{20}\right)\right)$, i.e. to assume that the level of the Aegean Sea rises and fluctuates in the scale 2 m, we get graphs of the levels changes of the three seas (Fig. 3b). As can be seen from Fig. 3, the levels of the Black and Marmara seas in general repeat the course of the Aegean Sea level.

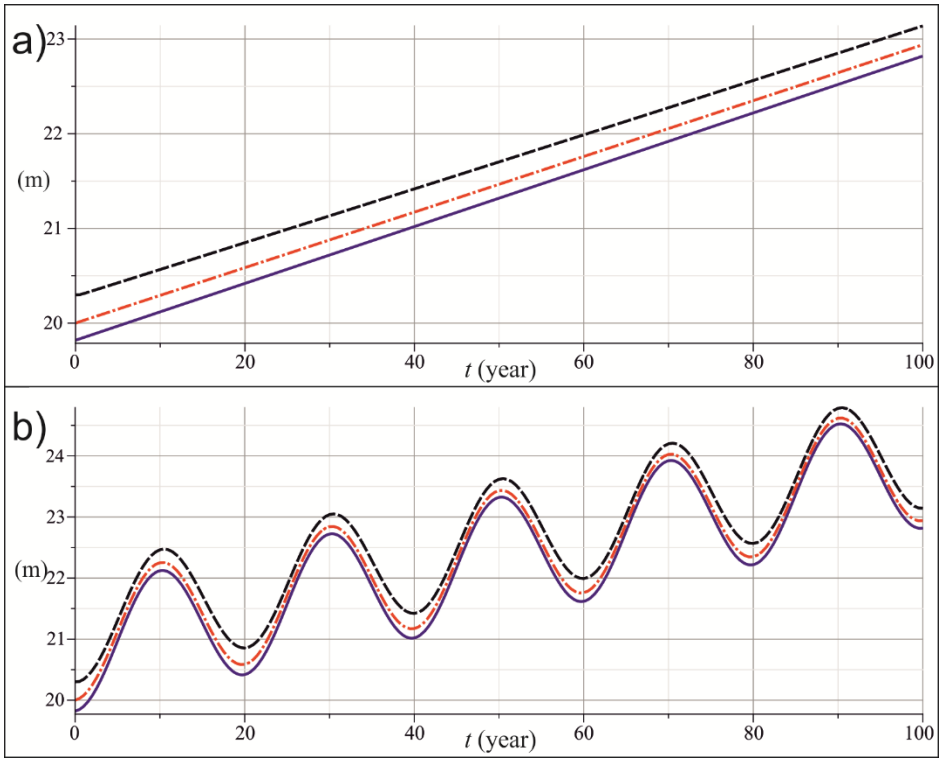

Fig. 3. Changes in average levels of the Mediterranean (blue line), Marmara (red line) and Black (black line) seas for 100 years (in today's climate), if the level of the Mediterranean Sea: a) rises at a velocity of 30 mm/year; b) rises with an average velocity of 30 mm/year and oscillating with an amplitude of 1 m.

The proposed mathematical model and the curve obtained earlier for the eustatic changes of the Mediterranean Sea level [2; 12] give the possibility to calculate the curve of the Black Sea level change in the last 6,000 years (Fig. 4). The calculations are performed under the assumption that the freshwater balance of the Black Sea during this period of time remained close to the present.

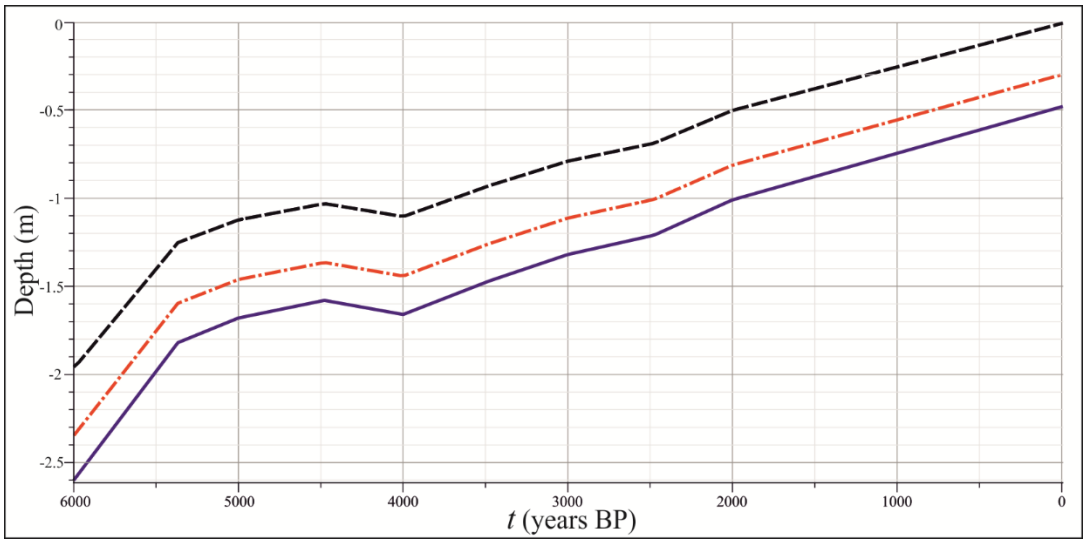

Fig. 4. Changes in average levels of the Mediterranean (blue line), Marmara (red line) and Black (black line) seas during the Holocene.

IV. Conclusion

The mathematical model presented in the paper shows that the levels of the Black and Marmara seas depend on the level of the Aegean Sea. In terms of the existence of straits with two-layer flow and a positive freshwater balance of the Black Sea, the levels of the Marmara and Black seas repeat the course of the Aegean Sea level, constantly staying tens of centimeters above the level of the Aegean Sea.

The calculated curves of the levels changes of the Black and Marmara seas (Fig. 4) depend mainly on the shape of the used eustatic curve of the Mediterranean Sea level change. The curve of the eustatic changes of the Mediterranean Sea level was obtained as a result of mathematical processing of a large number of data geological studies on the local changes in the level of the Mediterranean Sea. However, it should be noted that currently it is not possible to get an accurate curve of a sea level in the past. In the construction a curve of the sea level change using the radiocarbon method, the age of sediment is determined with an error of up to 300 years. In addition, to register the position of the dated shoreline in relation to contemporary edge, the material for dating (wood, peat, leaf mollusks, corals) are taken on the ancient border between ocean and land. It's hard to do, as the wood with the coastal sediments can be discarded by the waves above the water line or, alternatively, buried below it (especially in estuaries). Peat deposits are also not accurately fix the position of the basin level. Mollusk of the shell of which can be carried out determination of age, can live at different depths, which is not always possible to determine with sufficient accuracy, in addition, the waves or currents could move its shell to another vertical position.

V. Acknowledgment

The study was funded by RFBR according to the research project № 16-35-00441 мол_а.

VI. References

[1] N.V. Esin, V. Yanko-Hombach, O.N. Kukleva, and N.I. Esin, “Main regularities of the late Pleistocene–Holocene transgression of the Black Sea,” *Doklady Earth Sciences*, vol. 430, Part 2, DOI: 10.1134/S1028334X10020108, pp. 194–197, 2010.

[2] N.I. Esin, Dinamika urovnya Chornogo morya v poslednie 20 tysyach let [Dynamic of the Black Sea level during the last 20,000 years].PhD thesis, PP Shirshov Institute of Oceanology, Russian Academy of Sciences, Moscow, 2014, p. 156 http://www.ocean.ru/disser/index.php/dissertatsii/category/23-esin.html (in Russian).

[3] N.V. Esin, and N.I. Esin, “Mathematical modeling of the Black Sea level change for the last 20000 years,” *Quaternary International*, Elsevier Ltd and INQUA, DOI: 10.1016/j.quaint.2014.05.026, vol. 345, pp. 32-47, 2014.

[4] N.V. Esin, V. Yanko-Hombach, and O.N. Kukleva, “Mathematical model of the Late Pleistocene and Holocene transgressions of the Black Sea,” *Quaternary International*, Elsevier Ltd and INQUA, DOI: 10.1016/j.quaint.2009.11.014, vol. 225, pp. 180-190, 2010.

[5] N.V. Esin, N.I. Esin, and V. Yanko-Hombach, “The Black Sea basin filling by the Mediterranean salt water during the Holocene,” *Quaternary International*, Elsevier Ltd and INQUA, DOI: 10.1016/j.quaint.2015.05.011, in press.

[6] E. Jarosz, W.J. Teague, J.W. Book, and Ş. Beşiktepe, “On flow variability in the Bosphorus Strait,” *Journal of Geophysical Research*, vol. 38, issue 21, pp. 116-124, 2011..

[7] B. Alpar, and H. Yuce, “Sea-level variations and their interactions between the Black Sea and Agean Sea,” *Estuarine, Coastal and Shelf Science*, vol. 46, pp. 609-619, 1998.

[8] Ş. Beşiktepe, H.İ. Sur, E. Özsoy, M.A. Latif, T. Oğuz, and Ü. Ünlüata, “The circulation and hydrography of the Marmara Sea,” *Progress In Oceanography*, vol. 34, issue 4, DOI: 10.1016/0079-6611(94)90018-3, pp. 285-334, 1994.

[9] R.N. Hiscott, A.E. Aksu, P.J. Mudie, M.A. Kaminski, T. Abrajano, D. Yaśar, and A. Rochon, “The Marmara Sea Gateway since ~16 ky BP: Non-catastrophic causes of paleoceanographic events in the Black Sea at 8.4 and 7.15 ky BP,” in The Black Sea Flood Question: Changes in Coastline, Climate, and Human Settlement, V. Yanko-Hombach, A.S. Gilbert, N. Panin and P.M. Dolukhanov, Eds. Springer Netherlandsa, DOI: 10.1007/978-1-4020-5302-3_5, 2007, pp. 89-117.

[10] E. Jarosz, W.J. Teague, J.W. Book, and Ş. Beşiktepe, “Observed volume fluxes and mixing in the Dardanelles Strait,” *Journal of Geophysical Research: Oceans*, vol. 118, pp. 5007–5021, 2013.

[11] T. Oğuz, E. Özsoy, M.A. Latif, H.İ. Sur, and Ü. Ünlüata, “Modeling of Hydraulically Controlled Exchange in the Bosporus Strait,” *Journal of Physical Oceanography*, vol. 20, № 7, pp. 945-965, 1990.

[12] N.V. Esin, and N.I. Esin, “Change in the Level of the World Ocean in the Holocene,” *Doklady Earth Sciences*, vol. 448, part 1, DOI: 10.1134/S1028334X12120082, pp. 135–137, 2013.

[13] Y. Kanarska, and V. Maderich, “Modelling of seasonal exchange flows through the Dardanelles Strait,” *Estuarine, Coastal and Shelf Science*, vol. 79, issue 3, DOI: 10.1016/j.ecss.2008.04.019, pp. 449-458, 2008.

VERTICAL MOVEMENTS OF THE COAST AND SHELF OF THE BLACK AND MEDITERRANEAN SEAS DURING THE HOLOCENE

Nikolay V. Esin, Southern Branch of the P.P. Shirshov Institute of Oceanology, Russian Academy of Science, Russia
Nikolay I. Esin, Southern Branch of the P.P. Shirshov Institute of Oceanology, Russia
Olga Sorokina, Southern Branch of the P.P. Shirshov Institute of Oceanology, Russian Academy of Science, Russia

ovos_oos@mail.ru

Vertical movement of Earth crust can modify the shape of the eustatic sea level curves. A method allows calculation of the eustatic sea level course using the known local curves. We were able to divide a number of local curves of the Mediterranean Sea to the eustatic and tectonic components. The data about dynamics of the vertical crustal movements in 27 points of the Mediterranean coast and shelf during the Holocene were obtained. It was found that the velocities of raising and dipping are unstable over time and can reach value of 10 mm/year. Satellite measurements have recorded the velocities of vertical movements in the range of -10 to +20 mm/year for some parts of Black Sea coast. Such movements of the Earth's crust undoubtedly have a large impact on coastal processes and should be considered in designing coastal structures.

Key words: tectonic movements of the Earth's crust, local sea level changes.

I. INTRODUCTION

Studies of fluctuations in the level of the oceans and inland seas in the geological past, undertaken by many countries since second half of the last century, gave unexpected results. Processing of materials which are received at various parts of the coast and shelf of the same sea, showed that the curves of the sea level change differ significantly from each other, as if the level in different parts of the sea area changed in different ways.

By the end of the last century it became clear that in fact the previously obtained curves actually describe not the eustatic sea level course but the sea level change relatively to vertical movements of the Earth's crust. These curves, each of which is obtained by materials from a separate small area of the coast, are given the name "local curves". They show how the level of the reservoir was changed relative to the vertical movements of the Earth's surface in the past. The other curves are the compilation of the sea level markers obtained for different parts of the coast. In our opinion, such curves do not carry any useful information about the studied processes. Because in the Holocene the velocities of vertical movements of the Earth's crust as a rule were more than the velocity of eustatic change of the World Ocean level, then the contribution of tectonics to the local curves was significantly higher than the contribution of eustatic changes of the sea level.

II. RESULTS AND DISCUSSION

Local curves are the sum of the two curves, one of which describes the movement of the Earth's surface, and the other – the movement of sea level relative to its current vertical position. Thus, we have the problem of obtaining the curve of the eustatic sea level change using the local curves. The first attempt of obtaining the eustatic for the Mediterranean Sea was made by Australian scientists K. Lambeck [1]. His curve is shown in Fig.1 by green line.

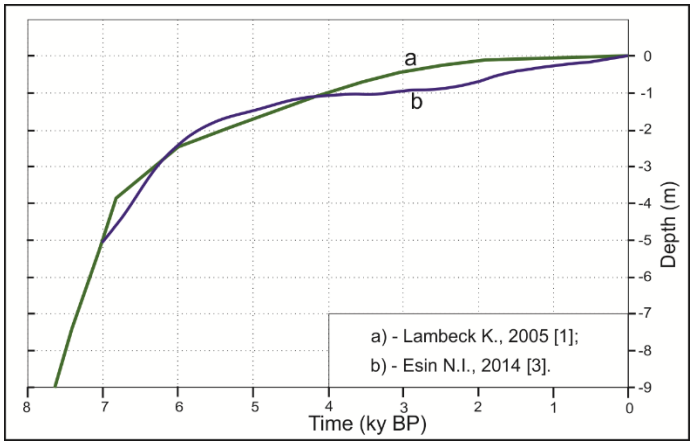

Fig. 1. The reconstructions of the Mediterranean Sea level eustatic change in the Holocene. The reconstructions were performed by different techniques and on the basis of different data [1; 2; 3].

Later we [4; 2] have developed an alternative method for extraction the eustatic component from the set of local curves. Using a set of 22 local curves, the curve of the Mediterranean Sea level change during the Holocene was calculated (Fig.1, blue curve) [3]. As can be seen from Fig. 1, our curve is very close to the Lambeck curve. For the Black Sea such calculations have not yet been done, because almost all available in the literature curves of its level are not local, but are built with using data from different parts of the coast.

Using the obtained eustatic component we calculated the dynamics of the vertical movements of the Earth's crust during the last 7 thousand years in the 27 points of the Mediterranean Sea coast. Fig. 2 and 3 show respectively schematic map indicating coastal areas with the known local curves, and local curves of the Mediterranean Sea level change obtained by different authors. Graphs of the absolute vertical displacement of the Earth's crust are presented in Fig. 4.

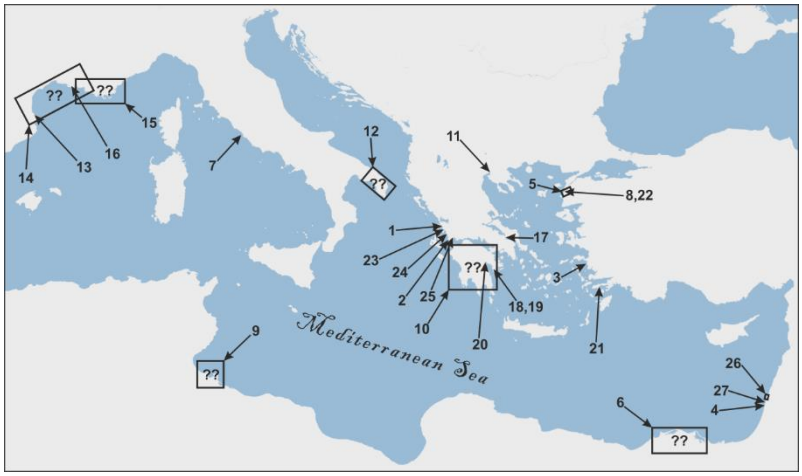

Fig. 2. Parts of the Mediterranean Sea coast, for which we have the local curves of the sea level change which are presented in Fig. 3 [3].

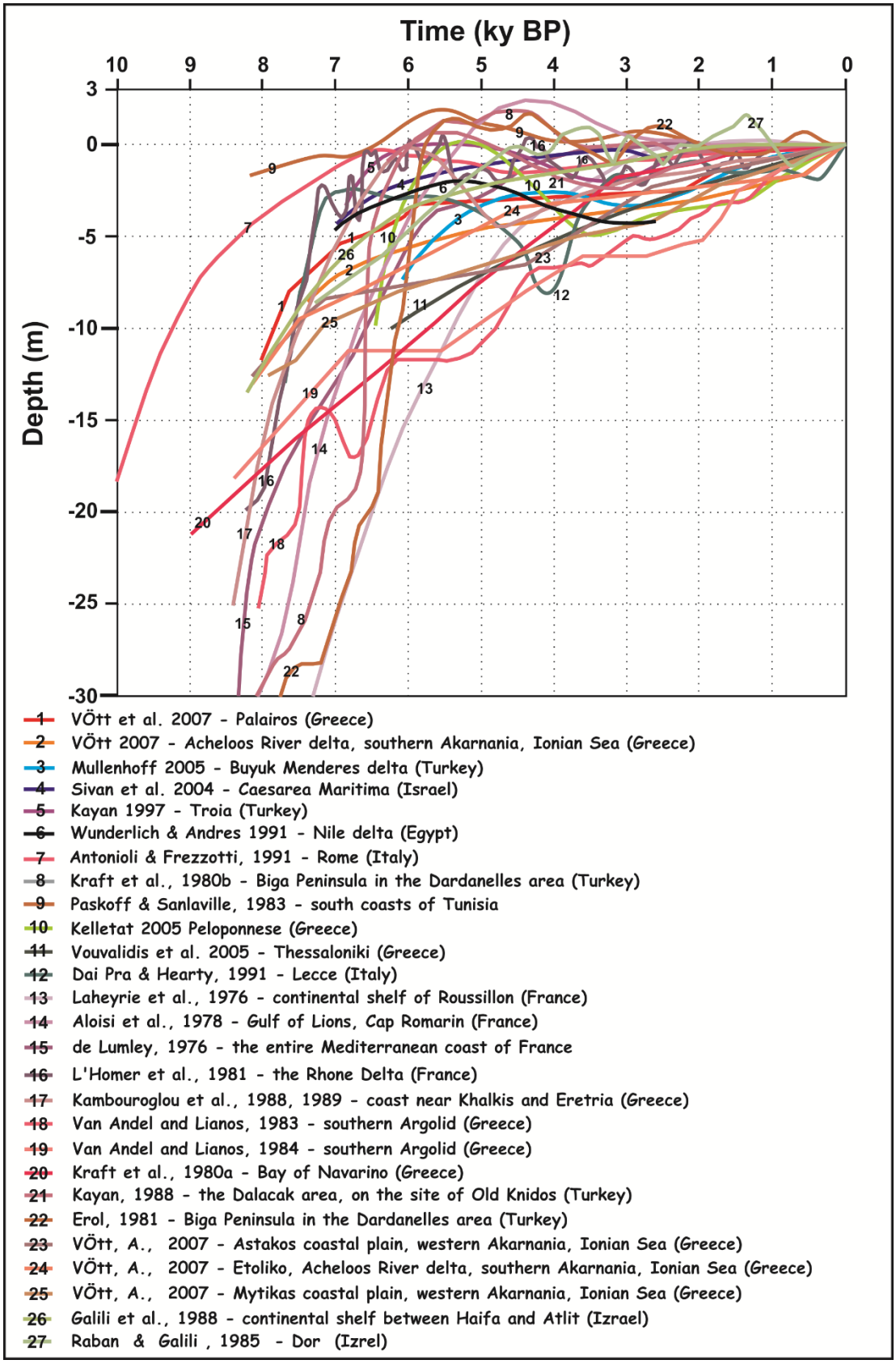

Fig. 3. The local curves of the Mediterranean Sea level change during the Holocene, obtained by different authors for different parts of the coast [3].

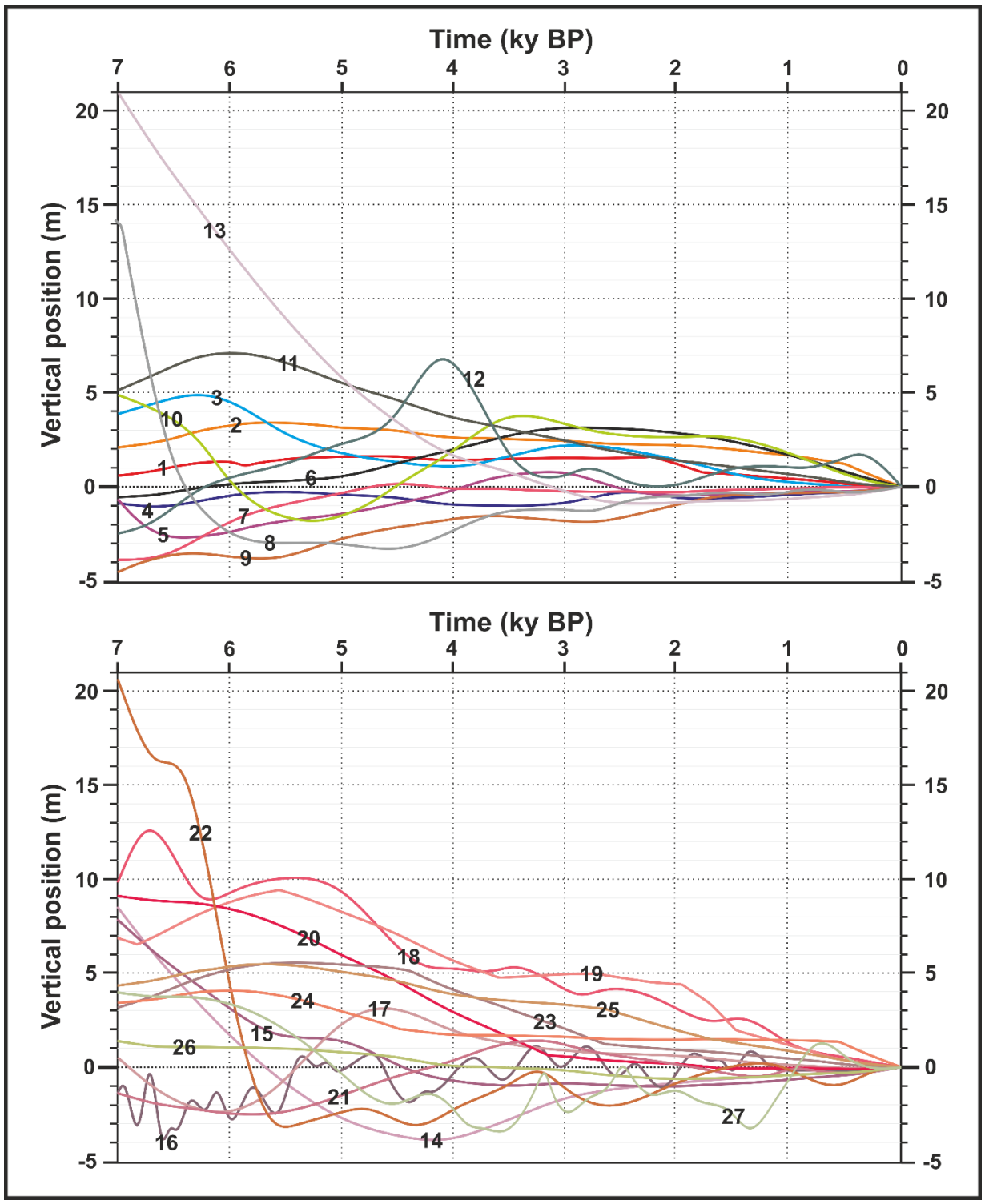

Fig. 4. The Graphs of vertical movements of the Earth's crust, calculated for the Mediterranean coast areas indicated in the Fig. 2.

Fig. 4 shows that the surface of the Earth is in constant motion. Figuratively speaking, it is as if "breathes". In some places it uplifts, in the other – falls, in the third periodically uplifts and lowers. In some areas, relatively short time fluctuations with relatively high velocities occur in the background of a more or less slow movement. Obviously, the movements of the Earth's crust are

caused by constantly acting factors: the movement of plates, compressing the Earth's surface, temperature change, exogenous processes and other.

Results comparable to ours, but for much shorter time intervals, are obtained by employees of the GNC FGUGP "YUZHMORGEOLOGIYA" for several places of the Russian area of the Black Sea coast [5]. Vertical movements of the Erth surface were measured by the method of differential interferometry based on the high-resolution satellite radar TERRASAR-X. Parallel measurements were performed on the geodynamic satellite points by the GPS/GLONASS. Measurements were performed in 2012 and 2013. Significant velocities of vertical movements of the Earth's crust and complex short-period fluctuations, as with the trend of decreasing or uplifting, and without trend were recorded. According to the results of measurements, the velocity of lowering of some coasts can reach 20 mm/year. Therefore, we can assume that the abrasion processes, for example, on the coast of the Imereti Valley (Russia), are the result of the coast lowering. If not for this factor, the canyons peaks were covered with detrital material coming from the coast. But for thousands of years this has not happened, because there was the significant velocity of the coast lowering, and the longshore sediment flow is not enough to compensate the lowering of detrital material.

A particularly important and poorly understood is the question about the size of the Earth's crust block subjected to its own movement. According to satellite interferometry [5], fundamental differences, namely, the opposite vertical movements of the Earth's crust with the difference in velocities of more than 15 mm/year can occur closer than 10 km. The area of unidirectional sections can be 10 – 100 km^2. This issue is extremely important. If, for example, there are two adjacent sections of the Earth's crust, the direction of movements of which is different, then on their border, we should expect the appearance of tectonic dislocations or the development of existing violations with possible catastrophic consequences.

III. Conclusion

Described in the report the various fluctuations in the Earth's crust, of course, have an impact on the infrastructure of a modern city. If to speak only about the widespread "slow" movements of the Earth's crust, they very weak, almost imperceptible impact on constructions accumulate over time and can lead to their destruction. In our opinion, the main reason for the destruction of many ancient cities could be weak crustal movements.

Considered vertical land movements can play a significant role in coastal processes. So, in areas of intensive lowering it will always be to develop the abrasion processes. Here all attempts to stop the abrasion of the coast through the creating of beaches will not be effective. These beaches will be washed away in the sea. A feature of such processes is that the cause of abrasion unknown, because the data on vertical movements of the coasts are almost absent. Therefore, experts will consider as a reason for the abrasion anything, but only not movement of the Earth's crust.

In the design of coastal economic facilities, recreational and other Human activities should pay attention not only to possible future eustatic changes in sea level, but also possible scenarios for the displacement of the Earth's crust, taking into account their temporal variability.

This article discusses only the vertical crustal movements directed along the normal to the Earth's geoid. But there's also horizontal movement of blocks, which in some cases are no less important and should be considered in the design of construction projects.

We can conclude that the dynamics of the vertical movements of the Earth's crust has a fractal nature. Previously this was not taken into account either in research or in applied research.

IV. Acknowledgment

The study was funded by RFBR according to the research project № 16-35-00441 мол_а.

V. References

[1] K. Lambeck, and A. Purcell, "Sea-level change in the Mediterranean Sea since the LGM: model predictions for tectonically stable areas," *Quaternary Science Reviews,* vol. 24, pp. 1969-1988, 2005.

[2] N.V. Esin, and N.I. Esin, "Mathematical modeling of the Black Sea level change for the last 20000 years," Quaternary International, Elsevier Ltd and INQUA, DOI: 10.1016/j.quaint.2014.05.026, vol. 345, pp. 32-47, 2014.

[3] N.I. Esin, Dinamika urovnya Chornogo morya v poslednie 20 tysyach let [Dynamic of the Black Sea level during the last 20,000 years]. PhD thesis, PP Shirshov Institute of Oceanology, Russian Academy of Sciences, Moscow, 2014, p. 156 http://www.ocean.ru/disser/index.php/dissertatsii/category/23-esin.html (in Russian).

[4] N.V. Esin, and N.I. Esin, " Change in the Level of the World Ocean in the Holocene," *Doklady Earth Sciences,* vol. 448, part 1, pp. 135–137, 2013.

[5] E.A. Glazyrin, A.A. Marfin, and E.G. Gross, "Sostojanie nedr pribrezhno-shel'fovoj zony Azovo-Chernomorskogo i Kaspijskogo bassejnov Rossijskoj Federacii" [The subsurface status of the coastal-shelf zone of the Azov-Black Sea and Caspian Sea basins in Russian Federation], Informacionnyj bjulleten', Gosudarstvennyj nauchnyj centr FGUGP «JUZHMORGEOLOGIJA». Gelendzhik, p. 97, 2013 (in Russian).

[6] A. Vött, "Relative sea level changes and regional tectonic evolution of seven coastal areas in NW Greece since the mid-Holocene," *Quaternary Science Reviews*, vol. 26, pp. 894-919, 2007.

[7] M. Müllenhoff, Geoarchäologische, sedimentologische und morphodynamischeUntersuchungenimMündungsgebiet des Büyük Menderes (Mäander), Westturkei: Dissertation … GeographischeSchriften: Marc Müllenhoff. – Marburg/Lahn: MarburgerGeograph, 2005. – 282 p.

[8] J.C. Aloisi, A. Monaco, N. Planchais, J. Thommeret, and Y. Thommeret, "The Holocene transgression in the Golfe du Lion, southwestern France: paleogeographic and paleobotanical evolution," *Geogr. phys. Quat*, vol. 32 (2), pp. 145-162, 1978.

[9] T.H. Andel, and N. Lianos, "High-resolution seismic reflection profiles for the reconstruction of postglacial transgressive shorelines: an example from Greece," *Quaternary Research*, vol. 22, pp. 31-45, 1984.

[10] T.H. Andel, and N. Lianos, “Prehistoric and historic shorelines of the southern Argolid Peninsula: a subbottom profiler study,” *Int. J. Naut. Archaeol. Underw. Explor,* vol. 12 (4), pp. 303-324, 1983.

[11] F. Antonioli, “Geomorfologiasubacquea e costieradellitoralecompresotra Punta Stendardo e Torre S. Agostino (Gaeta),” *Il Quaternario*, vol. 4 (2). pp. 257-274, 1991.

[12] G. Dai Pra, and P.J. Hearty, “VariazionidelLivello del Mare sulla Costa IonicaSalentinaduranteL'Olocene: Epimerizzazionedell'Isoleucina,” *Helix sp. Memoire Soc. Geol. d'Italia*, vol. 42, pp. 11-320, 1989.

[13] O. Erol, Summary report from Turkey. Sea-Level. Inf. Bull. IGCP Proj. 61. pp. 20-21, 1981.

[14] E. Galili, M. Weinstein-Evron, and A. Ronen, “Holocene sea-level changes based on submerged archaeological sites off the northern Carmel coast in Israel,” *Quaternary Research*, vol. 29, pp. 36-42, 1988.

[15] E. Kambouroglou, H. Maroukian, and A. Sampsos, “Coastal evolution and archaeology north and south of Khalkis (Euboea) in the last 5000 years,” *Archaeology of Coastal Changes*, Raban A. (Editor), Oxford: BAR Int. Ser., vol. 404, pp. 71-79, 1988.

[16] E. Kambouroglou, Eretria: Paleogeographic and Geomorphological Evolution During the Holocene - Relationship Between Ancient Environment and Ancient Inhabitation : Ph.D. Thesis, Univ. Athens. Publication of the Municipality of Eretria, Athens, p. 220, 1989.

[17] I. Kayan, “Bronze Age regression and change of sedimentation on the Aegean Coastal plains of Anatolia (Turkey),” Third Millennium BC Climate Change and Old World Collapse, Dalfes H.N., Kukla G., Weiss H. (Eds.). Berlin: NATO ASI, pp. 431-450, 1997.

[18] I. Kayan, “Late Holocene sea-level changes on the western Anatolian coast,” *Palaeogeography, Palaeoclimatology, Palaeoecology*, vol. 68, pp. 205-218, 1988.

[19] D. Kelletat, “A Holocene sea level curve for the eastern Mediterranean from multiple indicators,” *Zeitschrift fur Geomorphologie* N.F. 137 (Supplement), pp. 1-9, 2005.

[20] J.C. Kraft, I. Kayan, and O. Erol, “Geomorphic reconstructions in the environs of ancient Troy,” *Science*, vol. 209 (4458), pp. 776-782, 1980b.

[21] J.C. Kraft, G.R. Rapp, and S.E. Aschenbrenner, “Late Holocene palaeogeomorphic reconstructions in the area of the Bay of Navarino: Sandy Pylos,” *J. Archaeol. Sci.*, vol. 7, pp. 187-210, 1980a.

[22] J. Labeyrie, C. Lalou, A. Monaco, and J. Thommeret, “Chronologie des niveauxeustatiquessur la cdte du Roussillon de -33 000 ans BP h nosjours,” *C.R. Acad. Sci., D.*, vol. 282, pp. 349-352, 1976.

[23] A. L'Homer, F. Bazile, J. Thommeret, and Y. Thommeret, “Principalesetapes de l'edification du delta du Rhone de 7000 BP a nosjours; variations du niveaumarin,” *Oceani*, vol. 7 (4), pp. 389-408, 1981.

[24] H. Lumley, “Les lignes de ravage enFrsnce,” In book: La Prehistoirefrancaise. – Paris: CNRS, vol. 3, pp. 24-26, 1976.

[25] R. Paskoff, and P. Sanlaville, “Les côtes de la Tunisie. Variations du niveaumarindepuis le Tyrrhénien,” Lyon: Maison de l'OrientMediterraneen, p. 192, 1983.

[26] A. Raban, and E. Galili, “Recent maritime archaeological research in Israel,” A preliminary report. Int. J. *Naut. Archaeol. Underw. Explor*, vol. 14(4), pp. 321-356, 1985.

[27] K.G. Vouvalidis, G.E. Syrides, and K.S. Albanis, “Holocene morphology of the Thessaloniki Bay: impact of sea level rise,” *Zeitschrift fur Geomorphologie* N.F. 137 (Supplement), pp. 147-158, 2005.

[28] J. Wunderlich, and W. Andres, “Late Pleistocene and Holocene evolution of the western Nile delta and implications for its future development,” Von der NordseebiszumIndischenOzean. ErdkundlichesWissen, Bruckner H., Radtke U. (Eds.), pp. 105-120, 1991.

NUMERICAL SIMULATION OF MESO- AND SUBMESOSCALE FEATURES OF THE *NORTH-WESTERN* BLACK SEA *SHELF* CIRCULATION USING HIGH SPATIAL RESOLUTION

Natalia Evstigneeva, Marine hydrophysical institute RAS, Russia
Sergey Demyshev, Marine hydrophysical institute RAS, Russia

naevstigneeva@yandex.ru

A numerical experiment on reconstruction of currents was conducted with real atmospheric forcing data in autumn period of 2007 on the basis of Marine hydrophysical institute (MHI) hydrodynamic model, which was adapted to the coastal area of the Black Sea with an open boundary (north-western shelf). A high resolution (horizontal grid 500×500 m and 44 vertical layers from 1 m to 49 m) and detailed bathymetry with resolution ~1.6 km were used in the calculation. A higher spatial resolution allowed to get a detailed mesoscale and submesoscale structure of currents in the upper and deep layers of the north-western shelf and to obtain quantitative and qualitative characteristics of the eddies and jets more accurately in comparison with previous calculations.

Key words: *numeral modeling, high spatial resolution, north-western shelf, mesoscale and submesoscale features of circulation*

I. INTRODUCTION

A study of hydrodynamics of coastal regions has a practical importance in connection with intensive development of its resources. North-western shelf (NWS) of the Black Sea is a vast shallow water lying to the north of the northern latitude 45º. The main features of NWS are estuarine areas of the Black Sea rivers, shallow bays and estuaries, formation of seasonal pycnocline due to heating of the surface waters and freshening them under the influence of river discharge in spring and summer, domination of the wind component in the formation of water circulation, intense water exchange with the open sea. A large number of papers is devoted to the study of large-scale and synoptic variability of hydrophysical fields of the Black Sea north-western shelf by means of mathematical modeling. Influence of bottom topography, direction and magnitude of wind velocity, atmospheric disturbances, river discharge in the formation of circulation on NWS was studied in [1–5]. In [6] analysis of climatic current fields was conducted in the region of north-western shelf using z-coordinate model developed in MHI [7, 8] (horizontal grid 5×5 km, 45 vertical layers). It was obtained that the main features of shelf circulation were eddies of various generation and jet currents.

Along with numerical simulation of the dynamics of the coastal zones, investigations based on using instrumental measurements of currents [9, 10] and the satellite altimetry data [11] were

carried out. A high degree of variability in the horizontal and vertical structure of currents has been demonstrated.

Nowadays a study of spatio-temporal variability of sea shelf hydrophysical structure on the scale of a few kilometers and days is one of the urgent problems of modern oceanography. Small-scale eddies, regularly observed on satellite radar images, make a significant contribution to the circulation of the coastal zone and are an effective mechanism for the transport of various kinds of contaminants of natural and anthropogenic origin.

New results on meso- and submesoscale features of circulation in the variuos regions of the *World Ocean* were obtained in [12–21]. In [12] complex spatio-temporal variability of the monsoon system currents of **the Indian Ocean** was reconstructed using the σ-model of the Institute of Computational Mathematics, Russian Academy of Sciences, with a high spatial resolution $1/8° \times 1/12°$ in accordance with data observations and the main features of the ocean eddy structure were investigated. In [13] simulation results of meso- and submesoscale variability using the ROMS model with a horizontal grid size 3.5 km were compared with RAFOS observations and satellite altimetry for **the region of Pacific ocean** in Central California. In [14] a within-year variability of **World Ocean** circulation was reconstructed using eddy-resolving model of high horizontal resolution (1/10º). It enabled to reproduce spatio-temporal characteristics of the narrow boundary currents of World Ocean more accurately. In [15] a seasonal cycle of submesoscale flows in the upper ocean layers was investigated in an idealized model domain analogous to **mid-latitude open ocean regions**. It was shown that submesoscale processes became much stronger as the resolution was increased. In [16] characteristics of submesoscale eddies in **the White Sea** were mapped with the help of remote and contact observations. Areas of eddy activity were found on the basis of statistical analysis. In [17] five mesoscale eddy structures of different signs were observed in the coastal part of **the Russian sector of the Black Sea** according to the geological survey data in August 2004. Such a dynamic situation contributed to the intensive horizontal water exchange between the near-shore and open sea waters as well as to the redistribution of water masses over the vertical in the active sea layer. In [18] the results of observations of small-scale eddies (with a diameter of 2–8 km) **in the coastal zone of the Black Sea in the Gelendzhik region** were presented using various methods of hydrophysical investigations. The mechanisms of generation of such eddies were specified. In [19] a structure of Rim Current was analyzed in the upper 100-m layer near **the coast of the Crimea** on the basis of processing of tool data obtained in September 2008 with high spatial resolution. It was shown that a mesoscale variability of current field had ageostrophic character and essentially influenced circulation structure in the vicinity of Rim Current (visualized in the form of local eddies, as well as inertial currents). In [20] analysis of small-scale eddies of the **Baltic, Black and Caspian Sea** basins was conducted, according to satellite radar data. It was found that they were associated with either hydrologic fronts or peripheral areas of mesoscale eddies. In [21] simulation results of submesoscale variability and eddy generation of the **north-eastern shelf of the Black Sea** were presented on the basis of the numerical model with high spatial resolution. A comparison of these results with the data of direct measurements for September 2008, January 2011 and March 2013 were provided.

The aim of this investigation was to reproduce and analyze coastal circulation of the **north-western shelf of the Black Sea** on the basis of the z-coordinate three-dimensional non-linear model

[7, 8] with a horizontal resolution of 500 m and with real atmospheric forcing data in autumn period of 2007. Influence of high resolution on reconstruction of meso- and submesoscale features of coastal circulation was shown on the basis of a comparison with calculation with coarser grid size (~1.6 km).

II. STATEMENT OF THE PROBLEM AND DESCRIPTION OF NUMERICAL EXPERIMENTS

We considered a region of the Black Sea (Fig. 1) limited by latitude 45.5ºN located between meridians 29.5º and 33.5º E. We used more detailed presentation of bottom topography (with a resolution of ~1.6 km) obtained by digitization of navigation maps by staff of Shelf Hydrophysics and Waves Theory departments.

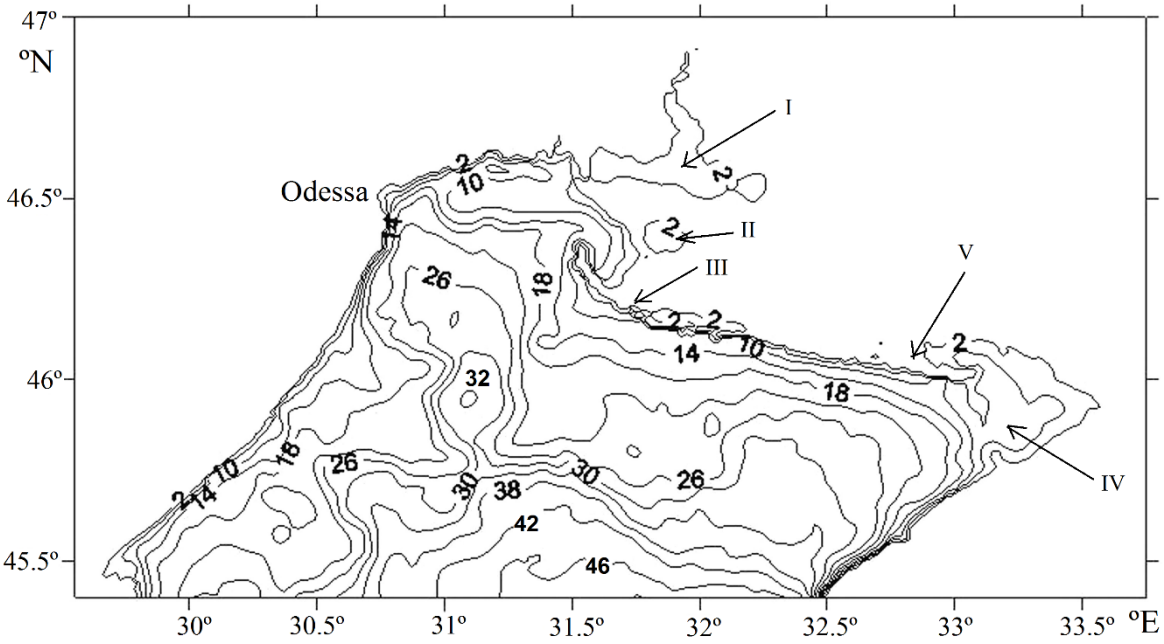

Fig.1. Bathymetry of the north-western shelf of the Black Sea (m). Roman numerals indicate: I – the Dnieper-Bug estuary, II – Yagorlytsky, III – Tendrovsky, IV – Karkinitsky and V – Dzharylgach bays

The system of model equations using the Boussinesq approximation, hydrostatic approximation and incompressibility of seawater in the Gromeko–Lamb form, the boundary conditions on the surface, at the bottom, on the solid lateral walls were written as follows [7, 8]. Note that a reduced sea level ζ was calculated from a discrete analog of the continuity equation taking into account the specification of the velocities at the open boundary of the domain [22].

In order to adapt the numerical model of the dynamics [7, 8] for the calculation of NWS circulation we made the following steps. Data array of the region bathymetry was processed, model parameters were chosen on the basis of preliminary experiments, river inflow locations and depths of estuaries were assigned, boundary conditions on the open boundaries of the region were selected and implemented, initial fields as well as fields of wind stress, heat flows, short-wave radiation, precipitation and evaporation were processed in order to be used in the model.

The numerical experiment 1 was carried out with resolution 500 m. The time step was equal to 10 s. The choice of values of horizontal and vertical turbulent viscosity coefficients was based on a series of specialized numerical experiments.

The numerical experiment 2 was carried out with resolution ~1.6 km. The time step was equal to 30 s. Horizontal coefficients of turbulent viscosity and diffusion were equal to $\nu_H = 5 \cdot 10^5 \mathrm{cm}^2/s,\ \kappa_H = 5 \cdot 10^5 \mathrm{cm}^2/s.$

The total period of integration of model equations for the two experiments was 30 days (from October 14 to November 12 of 2007). Along the vertical, horizontal components of the current velocity were computed at 44 depths: 0.5; 1; 1.5; 2; 2.5; 3;…; 32; 34; 49 m.

Fields of currents, temperature and salinity, obtained from model for the entire sea on a 5 × 5 km horizontal grid within the Operative Oceanography project [23], were used to specify initial and the boundary conditions at the open boundary of the domain.

The *u*, *v*, *T* и *S* values, calculated at depths of 2.5, 5, 10, 15, 20, 25, 30 and 40 m, corresponding to the latitude of the liquid boundary, were linearly interpolated on the selected grids (500×500 m и 1.6×1.6 km) at each time instant.

In order to specify conditions on the open southern boundary we used the results of [22], where an efficiency of combined approach was shown on the basis of the simulation numerical experiments. The components of the current velocity, temperature, and salinity (the Dirichlet conditions) were specified in the boundary regions where water flowed into the domain ($v > 0$); conditions $\partial u/\partial n = 0,\ \partial v/\partial n = 0$ for *u*, *v* and radiation conditions for *T* and *S* were specified in the boundary regions where water flowed out of the domain ($v < 0$).

The vertical coefficients of turbulent exchange of momentum and diffusion were calculated according to the Philander–Pacanowski approximation [24] with $R_0 = 1,\ \nu_0 = 5 \mathrm{cm}^2/\mathrm{s},$ $\nu_1 = 1 \mathrm{cm}^2/\mathrm{s},\ \kappa_1 = 1 \mathrm{cm}^2/\mathrm{s}.$

The fields of tangential wind stress, heat fluxes, short-wave irradiance fluxes, as well as precipitation and evaporation, obtained from data of the regional atmospheric model ALADIN and provided by the department of Marine Forecasts of MHI [23] and linearly interpolated to the selected grid, were specified for each day.

Used fields of wind stress were characterized by significant variability during the calculating period, wind velocity varied from values of 2.4 to 14.3 m/s .Northern, north-eastern, north-western and south-western winds with a maximum velocity 14.3 m/s (was recorded on October 16) dominated from 14 to 20 October, south-western winds with a maximum velocity 10.2 m/s (October 23) – from 21 to 25 October, northern winds with a maximum velocity 11.3 m/s (October 27) – from 26 to 28 October, western and south winds with a maximum velocity 7.1 m/s (October 29) – from October 29 to November 2, northern, north-eastern and western winds with a maximum velocity 11.3 m/s (November 5) – from 3 to 12 November.

We took into account the discharges of three rivers: Dnieper, Dniester, and South Bug.

III. ANALYSIS OF CURRENT FIELDS OF NORTH-WESTERN SHELF

The main direction of currents in the upper water layer changed from the south-west to the south, north, north-east, east, west and north-west. This was caused by changeable weather pattern that was observed during the calculating period.

Intense jets, directed to the south, were formed at depths of 10–26 m in case when currents in the upper water layer were directed to the south north, north-east and north-west. Intense jet currents, directed to the north, were observed at depths below 10 m in case of southern and south-eastern directions of currents dominated in the upper water layer. Fig. 2 shows current fields on October 29 (Fig. 2a) and November 3 (Fig. 2b), obtained in Experiment 1 at the depth of 10 m (every fifth arrow was drawn). We noted that trajectories of jets coincided with isobaths 19–28 m.

We compared the current fields obtained in Experiments 1 and 2 during the calculating period and found a qualitative correlation between the fields. The maximum values of currents, calculated in Experiment 1, were on average 5–10% higher than the values, obtained in Experiment 2.

Current fields of NWS had a complex mesoscale structure, characterized by eddies and jets. For the classification of obtained eddies we estimated a value of the local baroclinic deformation radius (R_d) for the selected coastal area of the Black Sea.

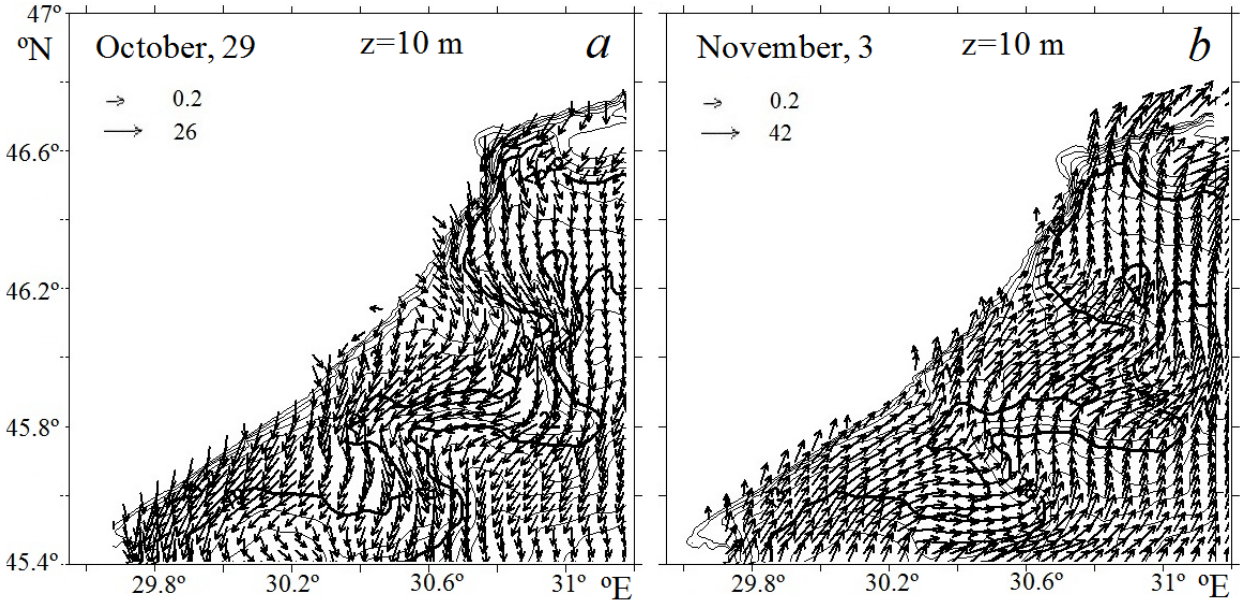

Fig. 2. Current fields (cm/c), calculated in Experiment 1: a – October 29 at the depth of 10 m;
b – November 3 at the depth of 10 m

As we know from [25], estimations of characteristic values of R_d for open areas of the Black Sea have a value of 15–20 km, for shelf and coastal areas – 5–10 km [18, 25].

The baroclinic Rossby deformation radius was calculated using the formula:

$$R_d=[g(\Delta\rho/\rho)H]^{0.5}f^{-1},$$

where g – acceleration of gravity, $\Delta\rho$ – density gradient in the thermocline (~$1.7*10^{-3}$ g/cm^{-3}), ρ = 1 g/cm^{-3}, H – the upper layer thickness for October 2007 (~24 m) , f – Coriolis parameter corresponding to 46° N (~10^{-4} s^{-1}). R_d was equal to ~6.4 km for the selected coastal zone. We assumed that mesoscale eddies had a radius bigger than local baroclinic Rossby deformation radius and Rossby number was much less than unity ($R>R_d$, $R_o<1$). We assumed that submesoscale eddies had a radius smaller than R_d and Rossby number was of the order of unity ($R<R_d$, $R_o\approx1$).

Mesoscale eddies with a spatial scale of 8–12 km and a temporal scale of a few days were reproduced in the upper water layer near Odessa, in areas of Tendrovsky and Karkinit bays, in the western, eastern and central parts of the region, as well as near the open boundary during the calculating period. Fig. 3 shows these features of circulation, recovered in Experiment 1 (every fourth arrow was drawn).

Cyclonic eddy ($R\approx12$ km $>R_d$, $R_o\approx0.18$) was generated in the western part near the open boundary (Fig. 3a), anticyclonic eddies (Fig. 3b) were formed near Odessa ($R\approx12$ km $>R_d$, $R_o\approx0.38$) and in Tendrovsky bay ($R\approx8$ km $>R_d$, $R_o\approx0.33$). Anticyclonic eddy ($R\approx8$ km$>R_d$, $R_o\approx0.3$) was obtained in Karkinitsky bay (Fig. 3c), two cyclonic eddies ($R\approx10$–12 km $>R_d$, $R_o\approx0.2$) and one anticyclonic eddy($R\approx12$ km $>R_d$, $R_o\approx0.12$) – in the central part of the region (Fig. 3d). Cyclonic eddy ($R\approx8$ km $>R_d$, $R_o\approx0.12$) was observed in the eastern part of the region (Fig. 3e), anticyclonic eddy ($R\approx12$ km $>R_d$, $R_o\approx0.22$) – in Dzharylgach bay (Fig. 3f). According to the classification these eddies can be attributed to the mesoscale eddies and quasigeostrophic. We noted that these features were also observed in the results of the Experiment 2.

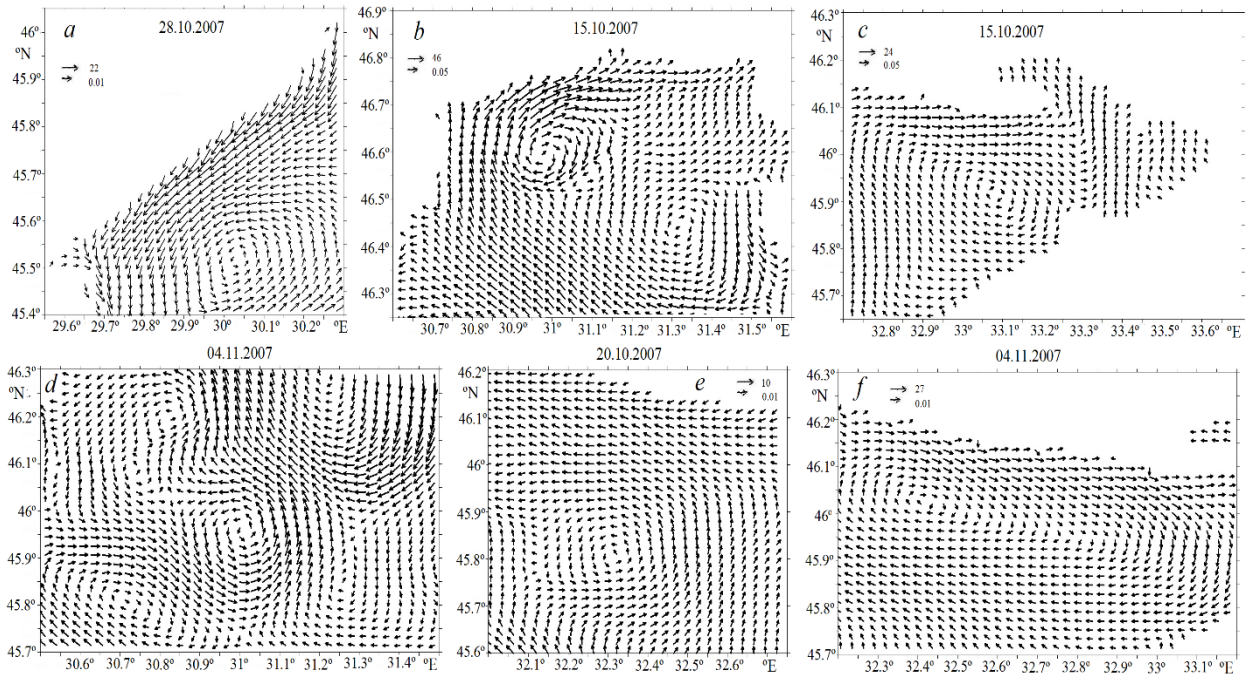

Fig. 3. Fragments of current fields (cm/c) at the depth of 5 m, calculated in Experiment 1: a – October 28; b – October 15; c – October 15; d –November 4; e – October 20; f – November 4

Mesoscale cyclonic eddy with a radius ~15 km, which was repeatedly registered in satellite observations, was generated in the period from 16 to 20 of October and from 1 to 5 of November, 2007 at depths of 1–24 m between the meridians 30.8° and 31.2° E. Fig. 4 shows the fields of

surface currents on October 17 and 18 of 2007 calculated in Experiment 1 and 2 (every fifth and second arrow were drawn respectively).

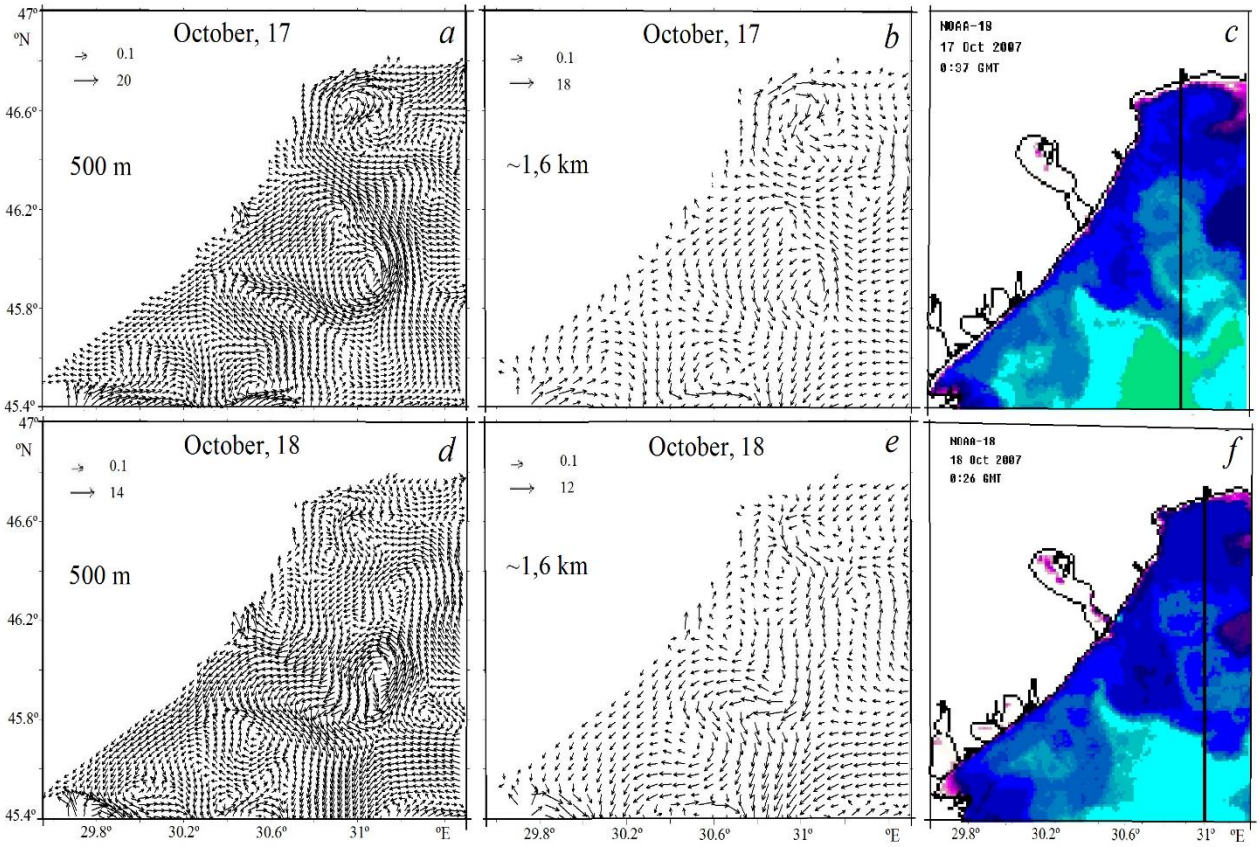

Fig. 4. Current fields (cm/c) in the upper water layer on October 17 and 18, calculated in Experiment 1 (a, d), Experiment 2 (b, e) and satellite images NOAA (c, f)

Intensification of currents inside the cyclonic eddy was observed in Experiment 1 on October 17 (Fig. 4a), and field structure was reproduced more accurately to the north of 46.4 °N compared with the results of Experiment 2 (Fig. 4b). This eddy wasn't reproduced in Experiment 2 on October, 18 (Fig. 4e) in contrast to the results of Experiment 1 (Fig. 4d). Two anticyclonic eddies with a radius ~8 km were formed to the west and east of the cyclonic eddy. Correspondence between the results of Experiment 1 (Fig. 4a and Fig. 4d) and satellite observations on October, 17 and 18 of 2007 NOAA with resolution 1 km (Fig. 4c and Fig. 4f) was obtained. Formation of this eddy was a result of the influence of inhomogeneity of the bottom topography on the jet current. As it was noted in [26], cyclonic eddies were predominantly formed over submarine depressions.

We compared the current fields obtained in Experiments 1 and 2 during the calculating period and found a qualitative correlation between the fields, however, a number of eddies was absent and a field structure was smoother in the experiment with a lower resolution. Fig. 5 presents current fields obtained in experiments with a resolution of 500 m and ~1.6 km at depths of 5, 10 and 24 m on October 19, 2007 (every fifth and third arrow were drawn respectively, we marked on Fig. 5a, b, c elements of circulation that were absent on Fig. 5d, e, f)

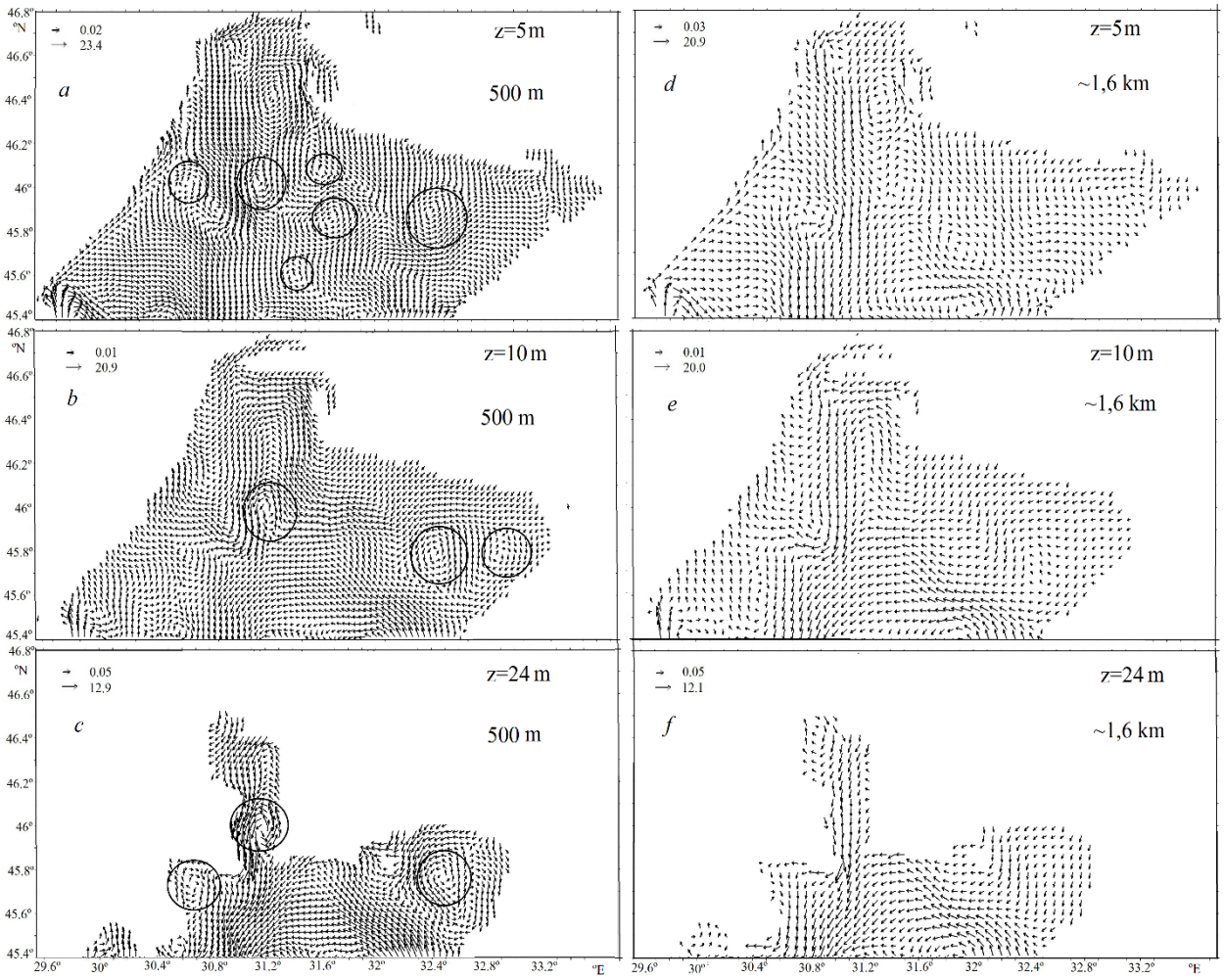

Fig. 5. Current fields (cm/c) at various depths on October 19, calculated in Experiment 1 (a, b, c) and Experiment 2 (d, e, f)

Cyclonic eddy was reconstructed in the entire water layer in the eastern part of the region (between meridians 32.3º and 32.6º E) in Experiment 1. Cyclonic eddy in the central part of the area between meridians 30.8º and 31.2º E (Fig. 5a, b, c) was described above. It was observed in the entire water layer and its radius was ~12 km (Fig. 5a, b, c). Anticyclonic and cyclonic eddies with radius from ~4 to ~12 km in the central region at the depth of 5m (Fig. 5a), anticyclonic eddy with a radius ~10 km at the depth of 10 m in Karkinit bays (Fig. 5b), anticyclonic eddy with a radius of ~8 km at the depth of 24 m between the meridians 30.4 and 30.8º E (Fig. 5c) were reconstructed. These features were reproduced only in Experiment 1.

Fig. 6 shows fragments of current fields obtained in Experiment 1 on November 1, 4 and 10 of 2007 (Fig. 6a, b, c, every sixth arrow was drawn) and in Experiment 2 (Fig. 6d, e, f, every second arrow was drawn). We marked on Fig. 6a, b, c elements of circulation that were absent on Fig. 6d, e, f.

From the analysis of the current fields, calculated in experiments 1 and 2, we noted that due to the smaller grid size eddies with a radius of ~5 km between meridians 30.4º and 30.8º E on November 1 (Fig. 6a), cyclonic eddy with a radius of ~7 km between the meridians 31,9 and 32.1º

E on November 4 (Fig. 6b), cyclonic eddies with a radius of ~12 km and anticyclonic eddy with a radius of ~5 km in the eastern part of the area on November 10 (Fig. 6c) were obtained .

Determining the type of small-scale eddies depends on the orbital velocity of an eddy. Analysis of the results of calculation of Rossby number R_o showed that values $R_o \approx 1$, as well as values $R_o < 1$, have been obtained for the eddies with $R < R_d$ during the calculating period.

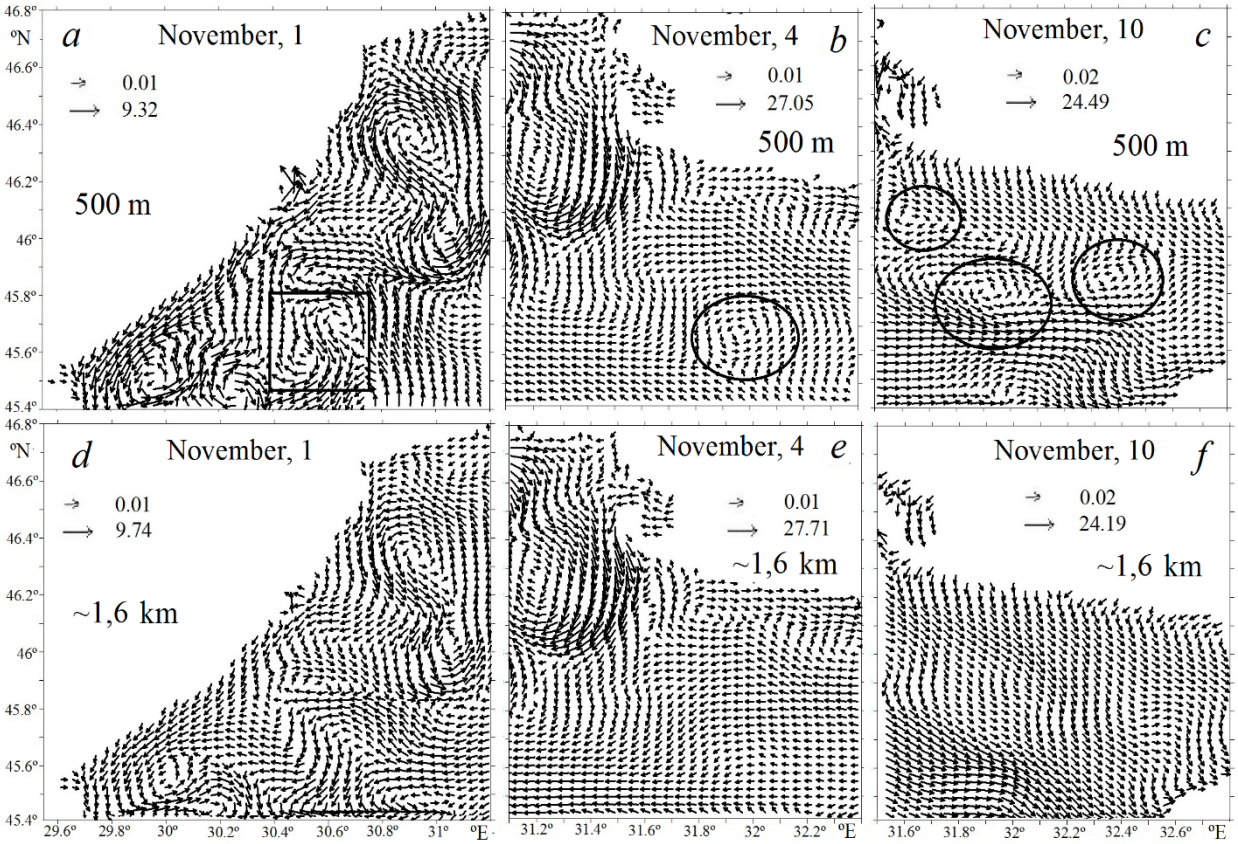

Fig. 6. Fragments of current fields (cm/c) at the depth of 5 m on November 1, 4 and 10, calculated in Experiment 1 (a, b, c) and Experiment 2 (d, e, f)

IV. CONCLUSIONS

Current fields of the north-western shelf of the Black Sea were reconstructed on the basis of numerical model with high spatial resolution, taking into account river discharge and real atmospheric forcing data in autumn period of 2007. It was shown that a field of currents had a complex meso- and submesoscale structure, characterized by eddies and jets. Bottom relief played a crucial role in their formation. Mesoscale eddies of various rotating signs were reproduced in the upper layer of water near Odessa, in areas of Tendrovsky and Karkinit bays, in the western, eastern and central parts of the region, as well as near the open boundary during the calculating period. Cyclonic eddy with a radius ~15 km was generated at the depth of 1–24 m between the meridians 30.8º and 31.2º E, which corresponded to the satellite observations. Intense jets, which trajectories coincided with isobaths 19–28 m, were formed at the depth of 10–26 m.

Due to the smaller grid size (500 m) meso- and submesoscale eddies have been obtained for the first time in the upper and deeper water layers of north-western shelf (anticyclonic and cyclonic eddies with a radius from ~4 to ~12 km in the central region, anticyclonic eddy with a radius of ~10

km in Karkinit bay, cyclonic eddies with a radius of ~12 km and anticyclonic eddy with a radius of ~5 km in the eastern part of the region).

These results convincingly confirm that a qualitative improvement in calculation accuracy of currents in the coastal zone requires the use of a few hundred meters of spatial resolution of numerical model.

This work was supported by the Russian Foundation for Basic Research (project no. 15–05–05423 A).

V. REFERENCES

[1] A.I. Androsovich, E.N. Mikhailova and N.B. Shapiro, "Numerical model and water circulation calculations in north-western part of the Black Sea," *Marine Hydrophysical Journal*, vol. 5, pp. 28–42, 1994 (in Russian).

[2] V.A. Ivanov, **A.I. Kubryakov,** E.N. Mikhailova and N.B. Shapiro, "Formation and evolution of eddies, caused by the river flow in the north-western shelf of the Black Sea," *Studies of the shelf zone of the Azov-Black Sea basin*, pp. 147–167, 1995 (in Russian).

[3] V.G. Alaev, Yu.N. Ryabtsev and N.B. Shapiro, "Adaptive calculation of current velocity on the shelf using a quasi-isopycnic model," *Marine Hydrophysical Journal*, vol. 4, pp. 64–79, 1999 (in Russian).

[4] D.V. Alekseev, V.A. Ivanov, E.V. Ivancha and L.V. Cherkesov, "Simulation of the evolution of wave fields on the north-western shelf of the Black Sea during a cyclone passage," *Marine Hydrophysical Journal*, vol. 1, pp. 42–54, 2005. (in Russian).

[5] V.A. Ivanov, E.N. Mikhailova and N.B. Shapiro, "Simulation of wind upwelling on the north-western shelf of the Black Sea in the vicinity of the local features of the bottom relief, " *Marine Hydrophysical Journal*, vol. 3, pp. 68–79, 2008. (in Russian).

[6] S.G. Demyshev, V.A. Ivanov, N.V. Markova and L.V. Cherkesov, "Construction of the current fields in the Black Sea on the basis of eddy-resolving model with assimilation of climatic temperature and salinity fields," *Ecological safety of coastal and shelf areas and complex use of shelf resources*, vol. 15, pp. 215–226, 2007. (in Russian).

[7] S.G. Demyshev and G.K. Korotaev, "Numerical energy-balanced model of baroclinic currents of the ocean on the C-grid," in *Numerical models and results of calibration calculations of currents in the Atlantic Ocean*, INM RAS, Moscow, 1992, pp. 163–231 (in Russian).

[8] S.G. Demyshev, "A numerical model of online forecasting Black Sea currents," *Izvestiya Atmospheric and Oceanic Physics*, vol. 48 (1), pp. 120–132, 2012.

[9] I.F. Gertman, "The thermohaline structure of the sea water," in *Hydrometeorology and hydrochemistry seas of the USSR*, vol. 4: Black Sea, Issue 1. Hydrometeorological conditions, S.Pb: Gidrometeoizdat, 1991, pp. 146–195 (in Russian).

[10] S.N. Bulgakov and V.M. Kushnir, "Features of current fields in the north-western part of the Black Sea," *Marine Hydrophysical Journal*, vol. 5, pp. 66–78, 1996 (in Russian).

[11] G.K. Korotaev, T. Oguz, A.A. Nikiforov, B.D. Beckley and C.J. Koblinsky, "Dynamics of the Black Sea anticyclones derived from spacecraft remote sensing altimetry," *Earth Research from Space*, vol. 6, pp. 1–10, 2002 (in Russian).

[12] N.A. Diansky, V.B. Zalesny, S.N. Moshonkin and A.S. Rusakov, “High resolution modeling of the monsoon circulation in the Indian Ocean,” *Oceanology*, vol. 46 (6), pp. 608–628, 2006.

[13] L.M. Ivanov, C.A. Collins, P. Marchesiello and T.M. Margolina, “On model validation for meso/submesoscale currents: Metrics and application to ROMS off Central California,” *Ocean Modelling*, vol. 28 (4), pp. 209–225, 2009.

[14] R.A. Ibrayev, R.N. Khabeev and K.V. Ushakov, “Eddy-resolving 1/10° model of the World Ocean,” *Izvestiya Atmospheric and Oceanic Physics*, vol. 48 (1), pp. 37–46, 2012.

[15] L. Brannigan, D. Marshall, A. Naveira-Garabato and A. GeorgeNurser, “The seasonal cycle of submesoscale flows,” *Ocean Modelling*, vol. 92, pp. 69–84, 2015.

[16] A.A. Rodionov, D.A. Romanenko, A.V. Zimin, I.E. Kozlov and B. Chapron, “Submezoscale structures of the White Sea waters and their dynamics. State and direction of the investigations,” *Fundamental and Applied hydrophysics*, vol. 7 (3), pp. 29–41, 2014 (in Russian).

[17] V.G. Krivosheya, V.G. Yakubenko, A.Yu. Skirta and V.M. Shishkin, “Circulation and hydrological structure within the active layer of the 50-mile coastal part in the Russia sector of the Black Sea in August 2004,” *Oceanology*, vol. 47 (2), pp. 147–153, 2007.

[18] *A.G. Zatsepin, V.I. Baranov, A.A. Kondrashov, A.O. Korzh, V.V. Kremenetskiy* et al., “Submesoscale eddies at the Caucasus Black Sea shelf and the mechanisms of their generation,” *Oceanology*, vol. 51 (4), pp. 554–567, 2011.

[19] G.F. Dzhiganshin and A.B. Polonsky, “Kinematic structure and mesoscale variability of the rim current near the coast of Crimea (according to the data of instrumental measurements in September 2008),” *Marine Hydrophysical Journal*, vol. 1, pp. 25–35, 2011 (in Russian).

[20] S.S. Karimova, “Statistical analysis of the submesoscale eddies of the Baltic, Black and Caspian seas by satellite radar data,” *Earth Research from Space*, vol. 3, pp. 31–47, 2012. (in Russian).

[21] B.V. Divinsky, S.B. Kuklev, A.G. Zatsepin and B.V. Chubarenko, “Simulation of submesoscale variability of currents in the Black Sea coastal zone,” *Oceanology*, vol. 55 (6), pp. 814–819, 2015.

[22] S.G. Demyshev and N. A. Evstigneeva, “Numerical analysis of hydrophysical fields on the north-western shelf of the Black Sea,” *Oceanology*, vol. 53 (3), pp. 511–524, 2013.

[23] Yu.B. Ratner, M.V. Martynov, T.M. Bayankina and S.V. Borodin, “Information flows in the real-time system of rapid monitoring of hydrophysical fields of the Black Sea and automation of their processing,” *Environmental control systems*, pp. 140–149, 2005 (in Russian).

[24] R.C. Pacanowski and S.G.H. Philander, “Parameterization of vertical mixing in numerical models of tropical oceans*,” J. Phys. Oceanogr*., vol. 11 (11), pp. 1443–1451, 1981.

[25] A.S. Blatov, N.P. Bulgakov and V.A. Ivanov, *The variability of hydrophysical fields of the Black Sea*, – Leningrad: Gidrometeoizdat, 1984, 240 p. (in Russian).

[26] V.F. Kozlov and M.A. Sokolovskiy, “Stationary motion of a stratified fluid above a rough bottom,” *Oceanology*, vol. 18 (4), pp. 383–386, 1978.

MONITORING OF COASTAL ECOSYSTEMS BY METHOD OF REMOTE SENSING IN THE SHORT-WAVE RANGE OF RADIO WAVES

Sergej Belov, M.V. Lomonosov Moscow State University, Russia
Ija Belova, A.M. Obukhov Institute of Atmospheric Physics Russian Academy of Sciences, Russia
Stepan Falomeev, SBEI-149 of Moscow, Russia

Belov_Sergej@Mail.Ru

A new method for estimating the parameter noncoherent signal/noise β_K of ionospheric signal is offered. A comparative analysis is carrying out. This new method exceeds an order of magnitude widely used standard one by analytical (relative) accuracy of determining a parameter β_K. It has the same order as the well-known coherent methodology.

Key words: remote sensing, measurement technique, the scattering parameter signal/noise ratio. vertical sounding, Earth Surface Scattering Power β_K.

I. INTRODUCTION

Parameter of returned partially scattered ionospheric signal β_K is of interest to an important characteristic of the "perturbation" and "turbidity" of statistically inhomogeneous ionospheric plasma and to the work index of reliability of ionospheric communication channels including diagnostic one. Prompt and reliable estimate of the parameter β_K is of interest to radio physics, geophysics, and optics. Specification for ionospheric case is implemented.

This range allows us to diagnose sub-surface layer of the earth because scattering parameter is formed by inhomogeneities dielectric permittivity of the subsurface structures.

The problem of measuring and accounting of scattering power of the earth's surface in the short-range radio waves is an important for solving such challenges as diagnostic properties of the environment by means of methods that use this radio band, when in the channel there is an intermediate reflection (scattering) of the earth's surface, which is of interest for exploration and environmental studies.

Selection of the working sensing range and the impact of environment on the passing radiation are an important issues for using space-based tools, for environmental management and environmental monitoring.

The most important aspects of using space-based tools for environmental management and environmental monitoring are the choice of the operating range and probing questions about the influence of media on the passing radiation [1]. The problem of this discussion is the "rough" remote diagnostics of the earth's surface and subsurface of the dielectric structures in the SW range [2]. Selection of SW range takes into account the subsurface layer (thickness of the order of the wavelength of the incident signal). Interpretation of the data is based on a statistical multiplicative model of the signal [3]. Testing the method of obtaining a signal/noise ratio in this model was

produced by the example of a double reflection of the probe signal from the SW ionosphere in a vertical sounding (remember that when using a satellite, the signal passes twice through the atmosphere and ionosphere). The work addressed issues of sensitivity of the model parameters that were studied.

The measurement, mapping, and computation of the "rough" Earth Surface Scattering Power (ESSP) in the SW range are of interest for a set of problems (communication, geology, etc.). The ESSP parameter is the signal/noise ratio of the β_K waves reflected from the earth's "rough" backing. There is the back of the β_K-data and measuring method is in SW range. [4] presents the experimental method of β_K determination.

In this paper, this method is tested on the parameter of β_K sensitivity. According to the statistical model (SM), a database ("records" for the numerical experiment) adequate to the real conditions was created. The properties of the "rough" earth area were defined by the theoretical β_K value. Based on the method of [5], β_K (numerical experiment) was determined. Then, the arrays of the β_K and β_K^t were compared and analyzed. In this paper, the admissible sensitivity and stability of the method [6] were justified. The comparative analysis of the real experimental data and adequate numerical ones were fulfilled. As a result, the plausibility of the ionosphere echo statistical structures used were justified [7].

In this paper, we propose a new method for estimating the parameters of noncoherent signal/noise ratio β_K ionospheric echo [8]. A comparative analysis shows that the analytical (relative) accuracy of the determination of the parameter β_K using the new method exceeds the widely-used standard, and the same order of known coherent methodology [9].

The paper presents the results of comparison of the measurement method from the point of view of their admissible relative analytical errors. The new method is suggested.

II. CALCULATION METHODS

Narrowband random process E(t) in fixed point of reception in the ground in scalar approximation is the superposition of mirror $E_0(t)$ and scattered $E_P(t)$ components distributed by the normal law:

$$\begin{aligned} \mathcal{E}(t) &= \mathcal{E}_0(t) \ + \ \mathcal{E}_P(t) \ = E_{00}\cdot e^{i\cdot\left(\omega_0\cdot t-\varphi(t)\right)} + \mathcal{E}_P(t) = \\ &= R(t)\cdot e^{i\cdot\left(\omega_0\cdot t-\Phi(t)\right)} = \left[E_C(t)+i\cdot E_S(t)\right]\cdot e^{i\cdot\omega_0\cdot t}, \end{aligned} \tag{1}$$

where $\varphi(t)$, $\Phi(t)$, $R(t)$, $E_m(t)$, m=c,s – shown to slow random processes on the period $T=\frac{2\cdot\pi}{\omega_0}$; E_{00} = Const.

Scattering parameter is the ratio:

$$\beta_k^2 = \frac{\text{power of mirror components}}{\text{power of scattered components}} = \frac{E_{00}^2}{2\cdot\overline{E_P^2}} \ . \tag{2}$$

Here and below, "— " means statistical averaging. $E_C(t) = R(t)\cdot\cos\Phi(t)$ and $E_S(t) = R(t)\cdot\sin\Phi(t)$ are low-frequency quadrature of the ionospheric signal, R(t) is envelope, Φ(t) is total phase.

The subscript k = E4, R2, R4 means experimentally recorded primary random processes and appropriate method of their registration: E4 – coherent; R2, R4 – noncoherent amplitude. Index k indicates the primary parameter recorded: E – quadrature, R – envelope of the ionospheric signal.

Standard noncoherent R2-method based on the relationship (3) is widely used for estimating β_K (2) [1]:

$$\frac{\overline{R^2}}{\left(\overline{R}\right)^2} = f\left(\beta_{R2}\right) = \frac{4}{\pi}\cdot\frac{\left(1+\beta_{R2}^2\right)\cdot\exp\left(\beta_{R2}^2\right)}{\left[\left(1+\beta_{R2}^2\right)\cdot I_0\left(\beta_{R2}^2/2\right)+\beta_{R2}^2\cdot I_1\left(\beta_{R2}^2/2\right)\right]^2}. \qquad (3)$$

$I_n(x)$ is Bessel function of n^{th} order of a purely imaginary argument [10].

Using coherent E4-method and estimating β_{E4} by γ_{E4} kurtosis of quadrature [11]:

$$\gamma_{E4}\left(\beta_{E4}\right) = \frac{\overline{E_m^4}}{\left(\overline{E_m^2}\right)^2} - 3 = -\frac{3}{2}\cdot\frac{\beta_{E4}^4}{\left(1+\beta_{E4}^2\right)^2}; \quad m=c,s. \qquad (4)$$

It should be noted that measured primary parameters are the ratio of moments $\overline{R^2}\Big/\left(\overline{R}\right)^2$, $\overline{E_m^4}\Big/\left(\overline{E_m^2}\right)^2$ respectively. Relations (3), (4) are obtained by taking into account the specific models of structure of the ionospheric signal.

Probabilistic properties of the ionospheric signal (1) of the first multiplicity response is well described by Rice model with a displaced spectrum (RS-model) [12, 13]. Expressions (3) and (4) are obtained based on Rice model with a displaced spectrum.

A priori expression (4) of coherent method E4 contributes an order of magnitude higher relative analytical accuracy of the estimation of parameter β_K [14, 15].

In this paper, we propose new noncoherent R4-method of determination β_{R4} by γ_{R4} kurtosis of envelope for RS-model [16]:

$$\gamma_{R4}\left(\beta_{R4}\right) = \frac{\overline{R^4}}{\left(\overline{R^2}\right)^2} - 3 = \gamma_{R4}\left(\beta_{R4}\right) = -1 - \frac{\beta_{R4}^4}{\left(1+\beta_{R4}^2\right)^2}. \qquad (5)$$

For compare the given methods in the sense of relative errors permitted in calculating β_K resulting view of functional dependencies $f(\beta)$, $\gamma_{E4}(\beta)$ and $\gamma_{R4}(\beta)$, we obtain expressions (6):

$$\varepsilon_k = \left|\frac{\Delta\beta_K}{\beta_K}\right| = \left|\frac{1}{\beta_K}\cdot\frac{dG_K}{dZ_K}\cdot\Delta\left(Z_K\right)\right|, \qquad (6)$$

where K = R2, E4, R4; $G_K = f, \gamma_{E4}, \gamma_{R4}$; $\Delta(Z_K)$ – absolute statistical errors of measured values: $Z_K = \dfrac{\overline{R^2}}{\left(\overline{R}\right)^2}, \dfrac{\overline{E_m^4}}{\left(\overline{E_m^2}\right)^2}, \dfrac{\overline{R^4}}{\left(\overline{R^2}\right)^2}$.

Measures of inaccuracy including statistics for the different techniques of determination β_K are:

$$\varepsilon_{R2}(\beta) = \frac{\pi}{8} \cdot \frac{\left[\left(1+\beta^2\right)\cdot I_0\left(\beta^2/2\right) + \beta^2 \cdot I_1\left(\beta^2/2\right)\right]^3}{\beta^2 \cdot \exp\left(\beta^2\right)\cdot I_1\left(\beta^2/2\right)} \cdot \Delta\left(Z_{R2}\right); \tag{7а}$$

$$\varepsilon_{E4}(\beta) = \frac{\left(1+\beta^2\right)^3}{6\cdot\beta^4} \cdot \Delta\left(Z_{E4}\right); \tag{7б}$$

$$\varepsilon_{R4}(\beta) = \frac{\left(1+\beta^2\right)^3}{4\cdot\beta^4} \cdot \Delta\left(Z_{R4}\right). \tag{7в}$$

Statistical error $\Delta(Z_K)$ depends on the sample volume N. It may be different at identical sample volume for each of the methods. We normalize (7) on $\Delta(Z_K)$ for focusing on the errors due to differences in functional dependencies (3) – (5).

Dependency Graphs $\varepsilon_K^* = \dfrac{\varepsilon_K}{\Delta\left(Z_K\right)}$ for β_{R2} , β_{E4} and β_{R4} are shown in Fig. 1. ε_K^* will be called analytic (relative) error method.

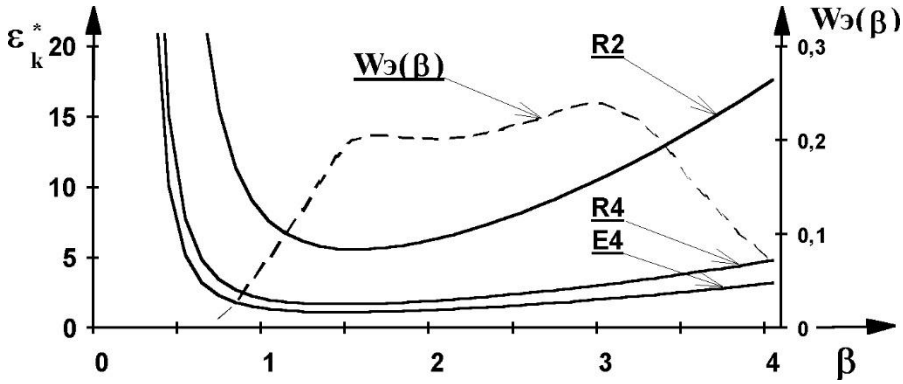

Fig. 1. Dependency Graphs ε_K^*, K = R2, R4, E4 (solid curves) and the experimental distribution $W_Э(\beta)$ (dashed curve) (F2-layer, 4,5 – 9,5 MHz, single signal).

Experimental distribution $W_Э(\beta)$ determines the range of variation of □.

From equation (4) and (5) we conclude that $\varepsilon_{E4}^* = \dfrac{2}{3}\cdot\varepsilon_{R4}^*$ have the same order and significantly (by order) exceed measurement accuracy of standard R2-method [17, 18].

Analysis of analytical error of estimation of the parameter β_K allowed to recommend R4-method instead of standard R2-method. Sufficiently high analytical (relative) accuracy of parameter estimation β_K can be achieved using noncoherent apparatus using (5) of R4-method [19]. Naturally, the ability to optimize the statistical error by the relevant special digital processing of ionospheric signal is keep on coherent methodology E4 [20].

III. Conclusion

The comparative analysis of the normalized relative analytical errors ε_K^* of the known methods and the new one was performed [9]. It was shown that errors δ_E and δ_{R4} have the same order, and both errors significantly exceed the error δ_{R2} in comparison with the standard R2-method by a measurement accuracy of β_K [14].

Environmental monitoring of the earth's surface by remote sensing in the short-wave band can provide quick identication of some ecological characteristics. This band range allows one to diagnose subsurface aspects of the earth, as the scattering parameter is affected by irregularities in the dielectric permittivity of subsurface structures. This method based on the organization of the monitoring probe may detect changes in these environments, for example, to assess seismic hazard and seismic risk [17]. The problem of measuring and accounting for the scattering power of the earth's surface in the short-range of radio waves is important for a number of purposes, such as diagnosing properties of the medium using the radio band when going on the road to interpret the intermediate reflection (scattering) from the earth's surface, which is of interest for geological and environmental studies [4].

As a result, it was found that sufficient β_K analytical measurement accuracy can be achieved when using an noncoherent apparatus [13] using a new R4-method. But the coherent E-method reserves the possibility of statistical error optimization with a special processing of the ionospheric signal [20].

IV. References

[1] Ya.L. Alpert, “Rasprostranenie radiovoln v ionosfere.” [Distribution of radio waves in an ionosphere.] AN USSR, Moscow, 1960, 480 p.

[2] S.F. Mirkotan, S.Yu. Belov, and V.I. Zaharov, “Distancionnaia diagnostika rasseivayushei sposobnosti "sherohovatoi" zemnoi poverhnosti v korotkovolnovom diapazone radiovoln.” [The distant diagnostics of the “rough” Earth Surface Scattering Power in the SW range.] // *Radiotechnika i electronika*, vol. 44, № 10, 1999, pp. 1190–1194.

[3] S.F. Mirkotan and S.Yu. Belov, “O parametre vozmushennosti neodnorodnoi fluktuiruyushei ionosfernoi plazmy.” [On disturbance parameter of the irregular, fluctuating ionosphere.] // *Radiotechnika and electronika*, vol. 43, № 11, 1998, pp. 1382–1383.

[4] S.Yu. Belov, “Metody otsenki parametra signal/shum v korotkovolnovom diapazone radiovoln.” [Parameter assessment methods signal/noise in the SW range of radio waves]. In *Fizicheskie problemy ekologii (Ekologicheskaya fizika) [Physical Environmental Problems (Ecological Physics)]*, V.I. Trukhin, Yu.A. Pirogov, K.V. Pokazeev, Eds. Moscow: MAKSPress, vol. 16, 2010, pp. 31–38.

[5] S.Yu. Belov, “Chislennoe modelirovanie v zadache testirovaniya metoda distancionnoi diagnostiki rasseivayushei sposobnosti zemnoi poverhnosti v KV-radiodiapazone.” [Numerical simulation test in the problem of remote diagnostics scattering power of the earth's surface in the SW range.] *Proceedings of the International Youth Scientific Forum "Lomonosov-2015"*, A.I. Andreev, A.V. Andrianov, E.A. Antipov, Eds. [Electronic resource] Moscow: MAX Press, 2015.

[6] S.Yu. Belov, “O metodah opredeleniya parametra signal/shum na primere rasprostraneniya radiosignala v kanale Zemlya – Ionosfera.” [On the methods of determining the parameters of the signal/noise ratio at the example of propagation of radio channel Earth–Ionosphere.] *Proceedings of the International Youth Scientific Forum "Lomonosov-2013"*, A.I. Andreev, A.V. Andrianov, E.A. Antipov, M.V. Chistyakov, Eds. [Electronic resource] Moscow: MAX Press, 2013, p. 73.

[7] S.Yu. Belov, “Distantsionnaia diagnostika rasseivayushei sposobnosti zemnoi poverhnosti v dekametrovom diapazone radiovoln.” [The distant diagnostics of the Earth Surface Scattering Power in the decameter radio waves]. *XVI International Symposium with the Elements of Scientific School for Youth "Optics of Atmosphere and Ocean. Physics of Atmosphere."* Tomsk, 2009, pp. 279-280.

[8] S.Yu. Belov and I.N. Belova, “Vyyavlenie ekologicheskogo riska pri monitoringe poverhnosti zemli metodom distantsionnogo zondirovaniia v korotkovolnovom diapazone radiovoln.” [Identification of environmental risk in monitoring land surface remote sensing in the SW range]. *Proceedings of the II All-Russia Scientific Conference "Ecology and Space"* Academician K.Y. Kondratyev, Y. Kuleshov, Ed. Saint–Petersburg: WCA name Mozhaiskii, 2015, pp. 70-76.

[9] S.Yu. Belov and I.N. Belova, “On the signal/noise ratio of the measurement method of the inhomogeneous fluctuating diffraction screen.” *International Symposium «Atmospheric Radiation and Dynamics» (ISARD-2015)*, Saint–Petersburg, 2015, p. 104.

[10] S.Yu. Belov, “Distantsionnaia diagnostika rasseivayushei sposobnosti zemnoi poverhnosti v KV-diapazone.” [The distant diagnostics of the Earth Surface Scattering Power in the SW range.] *Prospects of Development of Scientific Research in the 21st Century: Proceedings of the 6th International Scientific and Practical Conference*, Makhachkala, 2014, p. 43.

[11] S.Yu. Belov, “New measurement method of estimation signal/noise parameter.” *European Geosciences Union General Assembly 2010 Vienna*, Austria, Geophysical Research Abstracts. 2010, vol. 12, p. 2233.

[12] S.Yu. Belov and I.N. Belova, “Eksperimentalnaya apparatura kogerentnogo priema v zadachah monitoringa poverhnosti zemli metodom distancionnogo zondirovaniya v korotkovolnovom diapazone radiovoln.” [The experimental apparatus coherent reception in the tasks of monitoring land surface remote sensing in the short-range radio waves.] *II International Conference of Young Scientists "Modern Problems of Geophysics, Engineering Seismology and Earthquake Engineering."* Erevan, 2015.

[13] S.Yu. Belov and I.N. Belova, “Funkcional'naya shema eksperimentalnoi apparatury kogerentnogo priema v zadachah monitoringa poverhnosti zemli metodom distancionnogo zondirovaniya v korotkovolnovom diapazone radiovoln.” [Functional diagram of the experimental

apparatus coherent reception in the tasks of monitoring land surface remote sensing in the short-range radio waves.] *III International scientific-practical conference "Applied aspects of geology, geophysics and geo-ecology, using modern information technology."* Maikop, ISBN 978-5-906696-22-9, 2015, pp. 53-58.

[14] S.Yu. Belov and I.N. Belova, "Monitoring poverhnosti zemli metodom distancionnogo zondirovaniya v KV-radiodiapazone." [Monitoring of the Earth's surface by method of remote sensing in SW range.] // *V International Youth Scientific Conference "Ecology-2015"*, Arkhangelsk. ISBN 978-5-91378-098-0, 2015, pp. 6-7.

[15] S.Yu. Belov, "O nekotoryh harakteristikah rasseivayushei sposobnosti zemnoi poverhnosti pri distancionnom zondirovanii v korotkovolnovom diapazone radiovoln." [On some characteristics of the scattering of the earth surface for remote sensing in the short-wave band.] *II International Conference «Regional problems of remote sensing of the Earth» (RPDZZ-2015)*, Krasnoyarsk, E.A. Vaganov, M.V. Noskov, Eds. Sib. Feder. University Press, ISBN 978-5-7638-3306-5, 2015, pp. 101-104.

[16] S.Yu. Belov, "O vozmozhnosti povysheniya tochnosti izmereniya rasseivayushei sposobnosti zemnoi poverhnosti pri distancionnom zondirovanii v korotkovolnovom diapazone radiovoln." [About a possibility of increasing the accuracy of measurements of the Earth's surface scattering ability at remote sensing in the short-wave range of radio waves.] // *24th Scientific Conference "The structure of the substance, the history of the lithosphere Timan-Severouralsk segment"*, Syktyvkar, Geoprint, 2015, pp. 28-31.

[17] S.Yu. Belov and I.N. Belova, "Environmental aspects of the use of remote sensing of the earth's surface in the short-wave range of radio waves." // *IGCP 610 Third Plenary Conference and Field Trip "From the Caspian to Mediterranean: Environmental Change and Human Response during the Quaternary"* 22-30 September 2015, Astrakhan, Russia. A. Gilbert, V. Yanko-Hombach, T. Yanina, Eds. Moscow, MSU, 2015, pp. 29-31.

[18] S.Yu. Belov and I.N. Belova, "On the possibility of more informative methods of determining the parameters of the signal/noise ratio at the example of propagation of radio short-wave radio waves." // *XVII Scientific School "Nonlinear Waves 2016"*, A.V. Slyunyaev, Ed. Nizhny Novgorod, 2016, p. 170.

[19] S.Yu. Belov, "Kogerentnyy i nekogerentnyy metody opredeleniya parametra signal/shum v zadachakh rasprostraneniya radiosignala korotkovolnovogo diapazona radiovoln." [Coherent and incoherent methods of determining of the parameter signal/noise in problems of propagation of radio waves of the short-wave range.] // *XXIII International conference of students, graduate students and young scientists on fundamental sciences "Lomonosov-2016"*, vol. 1. - Moscow, MSU. ISBN 978-5-8279-0127-3. 2016, pp. 171-173.

[20] S.Yu. Belov, "Programma registracii kvadraturnyh komponent n-kratnogo otrazhennogo ot zemnoi poverhnosti radiosignala." [The program of registration quadrature a component of the n-fold reflected radio signal from a terrestrial surface.] The certificate on registration of the right to the software No. RU.2016612172 of 19.02.2016.

THE IMPACT OF WIND CONDITIONS ON THE LEVELS OF TOTAL IRON CONTENT IN THE SEA OF AZOV

Yuri Fedorov, Southern Federal University, Perm State University, Russia
Irina Dotsenko, Southern Federal University, Russia
Leonid Dmitrik, Southern Federal University, Russia
Anna Mikhailenko, Southern Federal University, Russia

fed29@mail.ru

The distribution and behavior of certain of trace elements in sea water is greatly affected by both physical, chemical and hydrometeorological conditions that are showed in the scientific works of prof. Yu.A. Fedorov with coauthors (1999-2015). Due to the shallow waters last factor is one of the dominant, during the different wind situation changes significantly the dynamics of water masses and interaction in the system "water – suspended matter – bottom sediments".Therefore, the study of the behavior of the total iron in the water of the sea at different wind situation is relevant. The content of dissolved iron forms migration in The Sea of Azov water (open area) varies from 0.017 to 0.21 mg /dm^3 (mean 0.053 mg /dm^3) and in Taganrog Bay from 0.035 to 0.58 mg /dm^3 (mean 0.11 mg /dm^3) and it is not depending on weather conditions.The reduction in the overall iron concentration in the direction of the Taganrog Bay → The Sea of Azov (open area) is observed on average more than twice. The dissolved iron content exceeding TLV levels and their frequency of occurrence in the estuary, respectively, were higher compared with The Sea of Azov (open area).There is an increase in the overall iron concentration in the water of the Azov Sea on average 1.5 times during the storm conditions, due to the destruction of the structure of the upper layer and resuspension of bottom sediments, intensifying the transition of iron compounds in the solution.

Key words: The Sea of Azov, the Taganrog Bay, iron, wind activity.

I. INTRODUCTION

Iron is one of the most common elements in nature, which is approximately 4% of the total mass of the earth's crust. As a result of chemical weathering of rocks the iron is in natural water in which it is migratory in three forms: dissolved, colloidal and suspended. Dissolved iron are in the water in ionic form (Fe^{2+} and Fe^{3+}), in the form of hydroxocomplexes ($Fe(OH)_2$, $Fe(OH)_3$ etc.) and complex compounds with mineral and organic substances water. This element in addition to dissolved and suspended forms of migration may be present in the following conditions: colloids and pseudocolloid, simple and complex ions with a positive charge and the complex ions that carry a negative charge, and neutral complex molecules. To denote the total concentration of all dissolved forms of iron in water we used the term "total iron". The term "total concentration" or "total content" is used when talking about the total content in water as dissolved and suspended forms of iron [1]. Iron plays an important physiological and biochemical role in living organisms. Its hydroxides are

active sorbents of heavy metals. This contributes to their co-deposition and removal of sediment in promoting self-purification of water. On the other hand, high concentrations of this element can have toxic effects on organisms. In [2] on the example of the distribution of suspended matter, methane, and sulfur isotopic composition of sulfate ions, and in communications [3-9] – organic matter of some priority heavy metals, values of Eh and pH, was demonstrated the important role of weather conditions in the change of these characteristics in shallow water in the Azov sea. The study of the distribution, modes of occurrence and migration of iron in surface and mine waters of the Azov seas basin were devoted to the work [10-12]. In the present communication will focus on the distribution of total dissolved iron in the water column of the Sea of Azov and his behavior in conditions of permanent changing wind situations.

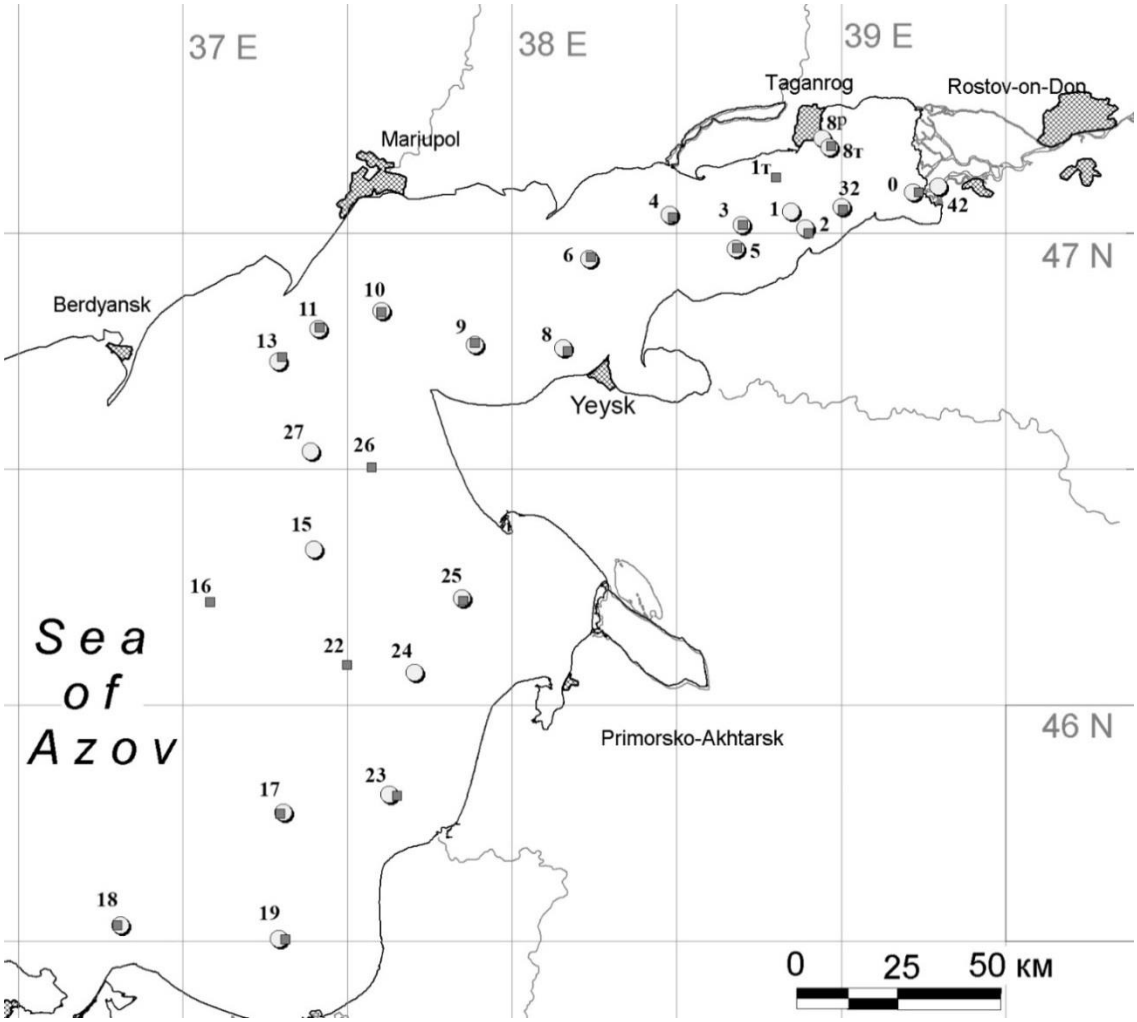

Fig. 1. Map-scheme of location of sampling stations during expeditions in summer (○) and autumn (■)

II. MATERIALS AND METHODS

The study was conducted in the Taganrog Bay and in the Russian area of Azov Sea (Fig.1). During the expedition, samples were sampled in different weather conditions, methods of selection and identification of samples is presented in [4]. In the process, made 22 oceanographic stations (Fig.1). At each station held vertical exploring of temperature, salinity, O_2, pH, Eh from surface to

bottom by probe "Hydrolab". Samples were taken from two horizons from the surface and the bottom layers. In each sample held determining dissolved oxygen, ammonia, nitrite, nitrate nitrogen, phosphates, silica, organic forms of nitrogen and phosphorus, iron (Fe^{+2}) and (Fe^{+2} + Fe^{+3}), quantitative and qualitative composition (proteins, lipids, carbohydrates) dissolved and suspended organic matter [4,5].

III. RESULTS AND DISCUSSION

The values of total iron content in the Taganrog Bay of the fall in calm weather fluctuate from 0,035 mg/dm^3 to 0,21 mg/dm^3 (on the average 0,084 mg/dm^3), and in the Sea of Azov - from 0,021 mg/dm^3 to 0,07 mg/dm^3 (on the average 0,04 mg/dm^3). In the Taganrog Bay, concentrations varies from 0 to 0.05 mg/dm^3 in 34.6% of samples, from 0,05 to 0,1 mg/dm^3 – 30,8%, from 0,1 to 0,15 mg/dm^3 – 26,9%, from 0,15 to 0,2 mg/dm^3 – 3,85%, from 0,2 to 0,25 mg/dm^3 – 3,85%. In the Sea of Azov (fig.2B) on the interval 0-0.05 mg/dm^3 accounted 77.8% of all values, and the interval 0.05-0.1 mg/dm^3 - 22.2%.

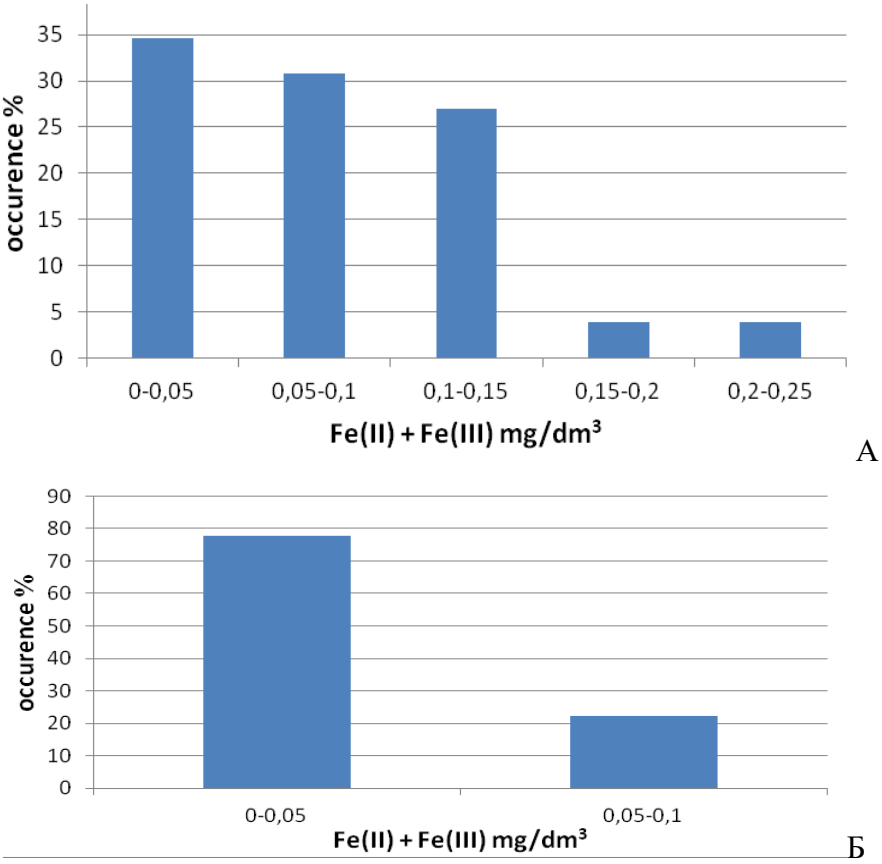

Fig. 2. The frequency of occurrence of the total iron content in the Taganrog Bay (A) the Sea of Azov (B) in calm weather

In summer, during a storm in the Taganrog Bay of the total iron content varies from 0.044 mg/dm^3 to 0.58 mg/dm^3 (on the average 0,13 mg/dm^3). In the Sea of Azov content varies from 0,017 mg/dm^3 to 0,21 mg/dm^3 (on the average 0,067 mg/dm^3). In the Taganrog Bay (Fig. 3 A) on the interval 0-0.05 m /dm^3 falls 3.85%, at an interval of 0.05-0.1 mg / dm^3 - 38.5%, in the range 0,1-0 15 mg/dm^3 - 23.1% at the interval of 0.15-0.2 mg / dm^3 - 26.9% at the interval of 0.2-0.25 mg/dm^3 - 3.85%, on the interval 0,55-0,6 mg / dm^3 - 3.8%. And in the Azov Sea (Fig. 3 B) on the interval 0-

0.05 mg/dm^3 accounted for 50%, in the range of 0.05-0.1 mg / dm^3 - 31.25%, in the range 0,1-0, 15 mg/dm^3 - 6.25%, at an interval of 0.15-0.2 mg/dm^3 - 6.25% and the interval of 0.2-0.25 mg/dm^3 - 6.25%.

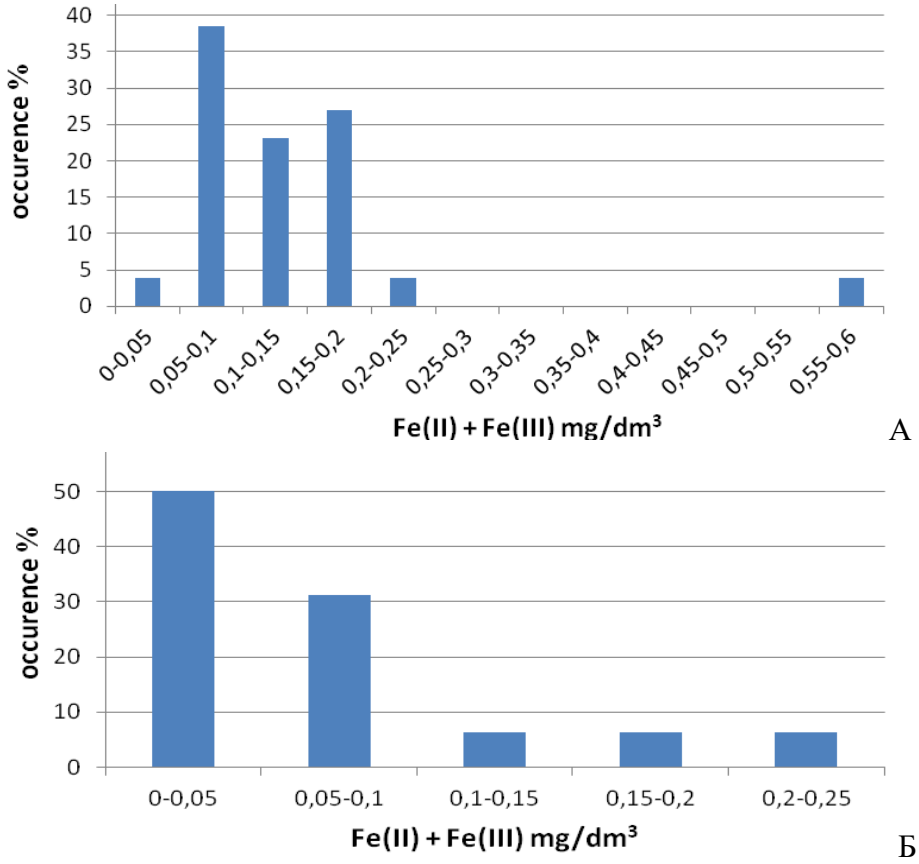

Fig. 3. The frequency of occurrence of the total iron content in the Taganrog Bay (A) and the Sea of Azov (B) during a storm

In Taganrog Bay for the entire observation period of total iron content ranged from 0.035 mg/dm^3 to 0.58 mg/dm^3, on the average 0,11 mg/dm^3, it is 2.5 times higher than the MPC for marine water bodies of fishery (0.05 mg/dm^3). In the Sea of Azov total iron content ranged from 0,017 mg/dm^3 to 0,21 mg/dm^3, on the average 0,053 mg/dm^3. The average content of $Fe_{общ}$ in the Taganrog Bay approximately 2-fold higher than in the Sea of Azov.

In the autumn iron concentrations was distributed in the Sea of Azov as follows: in the surface layer (Fig.4A) in the open sea of the metal content ranged from 0,5 to 1,1 μM (0,03 – 0,06 mg/dm^3). In the estuary the concentration was changed from 0.7 to 2.8 μM (0,04 – 0,16 mg/dm^3). The iron content in the bottom layer (Fig.4B) of the open part of the sea ranged from 0.4 to 1.2 μM (0,02 – 0,07 mg/dm^3), in estuaries concentrations ranged from 0,8 to 3,4 μM (0,04 – 0,19 mg/dm^3).

In summer on the surface (fig. 5A) iron content in the sea ranged from 0.6 to 3.0 μm (0.03 to 0.17 mg/dm^3), in the Taganrog Bay of from 1.6 to 3.0 μm (0.09 to 0.17 mg/dm^3) and in the bottom layer (Fig.5B) in the sea from 0.4 to 1.2 μm (0,02 – 0,07 mg/dm^3), in the Taganrog Bay from 1.4 to 2.6 μm (0,08 – 0,15 mg/dm^3). Thus, it was found that during calm weather a higher concentration of dissolved iron are characterized by near-bottom layers of water, whereas with increasing wind activity increased contents of this element are recorded in the surface layers of the water column.

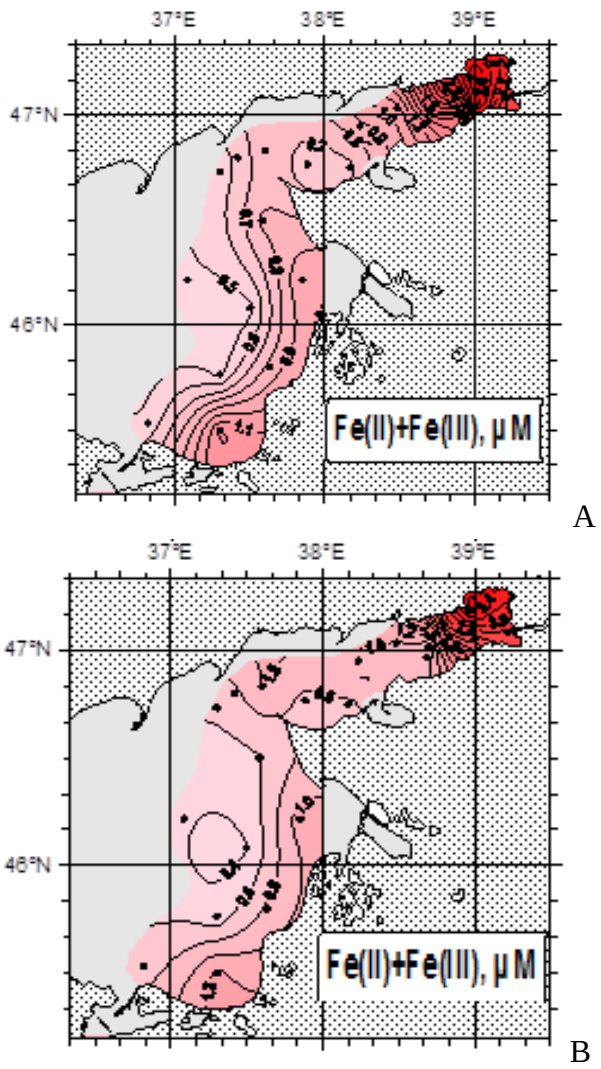

*Fig.*4. *Distribution of total iron in the surface (A) and bottom (B) layers of water, autumn*

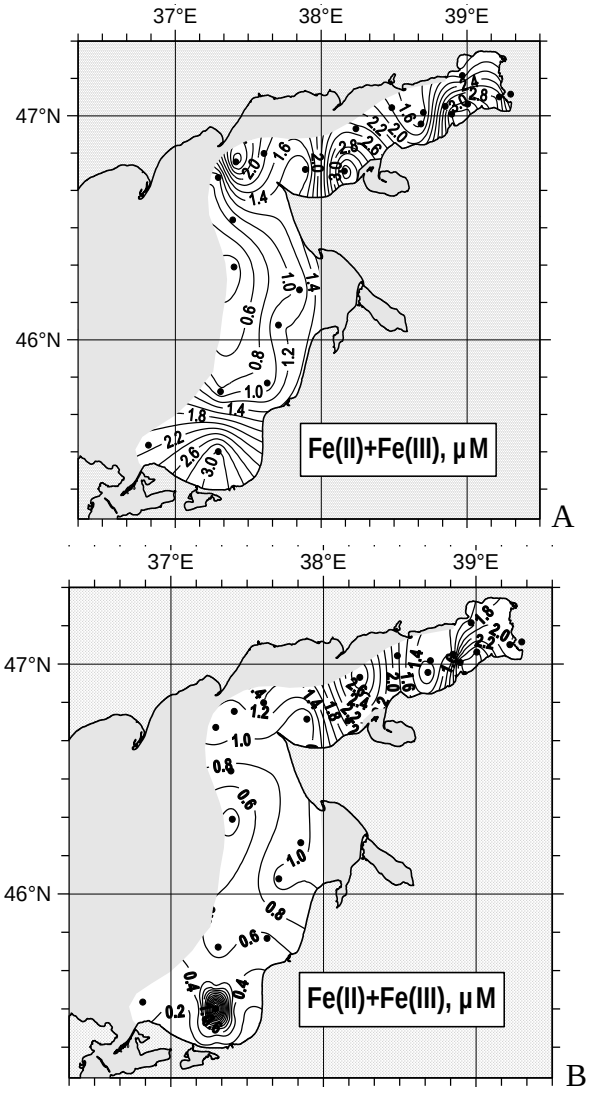

Fig.5. Distribution of total iron in the surface (A) and bottom (B) layers of water, summer

In summer (Fig.5A) iron content in the surface layers of open part of sea ranged from 0.6 to 3.0 µm (0.03 to 0.17 mg/dm^3). In the Taganrog Bay concentration of iron changed from 1.6 to 3.0 µm (0.09 to 0.17 mg/dm^3). In the bottom layer (Fig.5B) content varied from 0.4 to 1.2 µm (0,02 – 0,07 mg/dm^3), in the Taganrog Bay - from 1.4 to 2.6 µm (0,08 – 0,15 mg/dm^3). Thus, it is determined that during calm weather a higher concentration of dissolved iron are characterized by near-bottom layers of water, whereas with increasing wind activity increased contents of this element are recorded in the surface layers of the water column of the sea.

We studied the change based on the content of dissolved protein from the dissolved iron (Fig.6A and B).

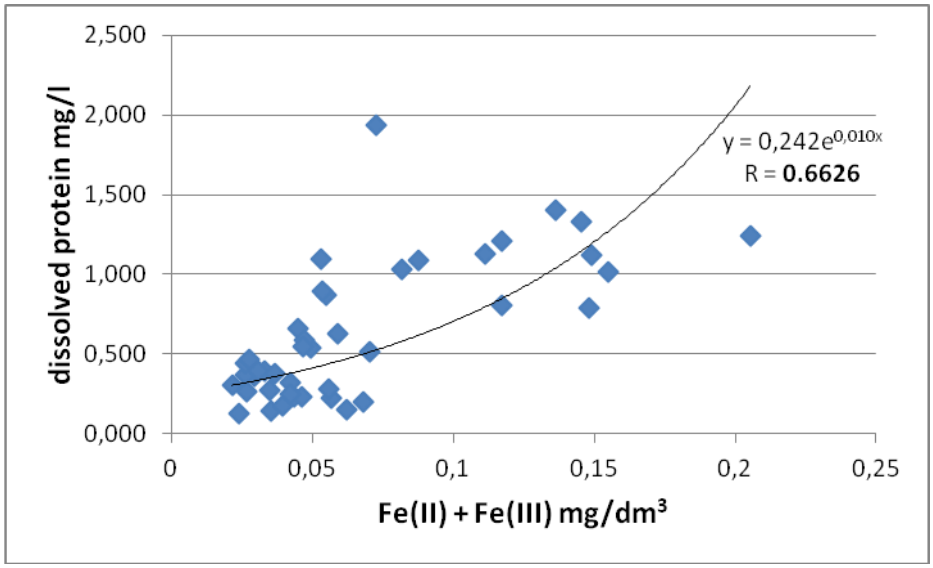

Fig. 6 A. The dependence between the total iron content and dissolved protein in the Sea of Azov and the Taganrog Bay during a calm weather

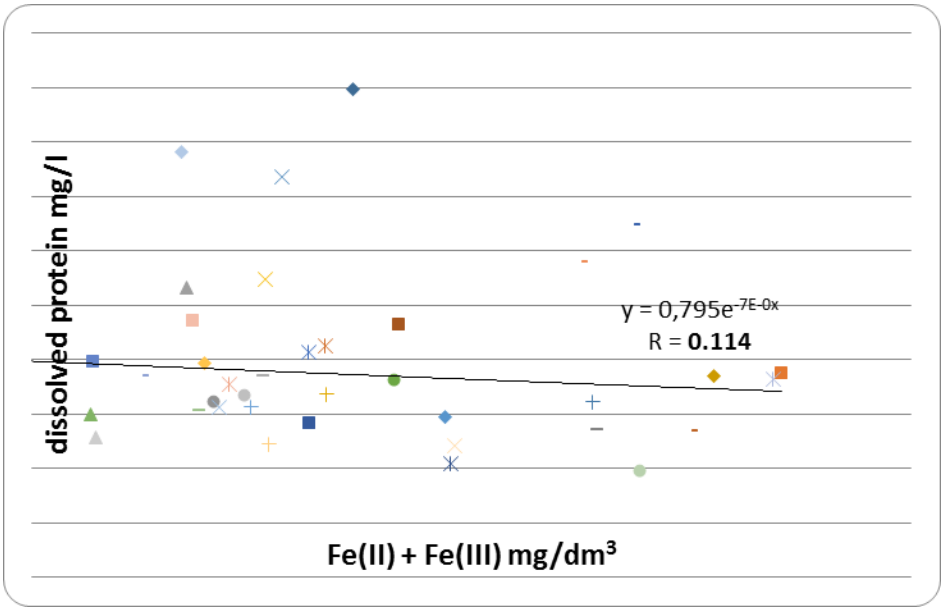

Fig. 6 B. The dependence between the total iron content and dissolved protein in the Sea of Azov and the Taganrog Bay during a storm

In calm weather (Fig.6A) there is a clear exponential relationship with a correlation coefficient of 0.66, while increasing wind activity, this dependence is disappear practically (Fig.6B).

IV. CONCLUSION

The study showed that the average content of total dissolved iron during the storm was 1.5 times higher as compared to those during a calm. Such an increase in the dissolved iron content may be due to his transition into the water column due to resuspension bottom sediments with increasing wind activity. During calm weather, the higher concentration of dissolved iron is observed in the bottom layer of water. During wind activity higher levels recorded in the surface water layer. Noteworthy is the fact that in calm weather between the content of dissolved protein and iron takes place a significant exponential relationship is direct, while in windy weather, it is almost absent. This may indicate the prevailing role of iron associated to organic and organic-mineral complexes in the period of quiet water. With increasing excitement of the water masses, they are more rapidly destroyed, which leads to the transition element into the water and reduce the closeness of the connection between these ingredients. The concentration of dissolved iron was higher in the Taganrog Bay than in the open part of the Sea of Azov irrespective of weather conditions that relate to the acquisition of iron from flowing into the Taganrog Bay of the rivers.

V. ACKNOWLEDGMENT

The work was supported by project №5.1848.2014/K

VI. REFERENCES

[1] Yu. A. Fedorov, L. M. Predeina, L. Yu. Dmitrik Iron: distribution, forms of occurrence and migration in surface and mine waters of the Eastern Donbass and the Sea of Azov // Proceedings of the VII International scientific-practical conference "Ecological problems. A look into the future". Rostov-on-don: Publishing southern Federal University, 2015, P. 332-336.

[2] Yu.A. Fedorov Stable isotopes and evolution of the hydrosphere. – Moscow: MO RF CENTER Istina, 1999, 370 p.

[3] Yu.A. Fedorov, I.V. Dotsenko, A.N. Kuznetsov, A.A. Belov, E.A. Loginov, Regularities of Organic Carbon Distribution in Bottom Sediments of the Russian Part of the Sea of Azov. Oceanology. 2009, vol. 49, No 2, p. 211 – 217

[4] Yu.A. Fedorov, V.V. Sapozhnikov, A.I. Agatova, N.V. Arzhanov, A.A. Belov, A.N. Kuznetsov, N.M. Lapina, E.B. Loginov, L.M. Predeina, T.B. Semochkina, N.I. Torgunova Comprehensive ecosystem studies in the Russian part of the Sea of Azov (18-25 July 2006) // Oceanology, 2007, vol.47, No. 2, pp. 316-319.

[5] Yu.A. Fedorov, I.V. Dotsenko, A.V. Mikhailenko Mercury and organic matter in bottom sediments in the profile Don river − Sea of Azov // Conference Proceedings of 14-th International Multidisciplinary Scientific GeoConference &EXPO Modern Management of Mine Producing, Geology and Environmental Protection, SGEM 2014. Bulgaria, 2014, Vol.II, pp. 717-723

[6] Yu.A. Fedorov, I.V. Dotsenko, A.V. Mikhailenko Regular patterns of distribution and behavior of trace elements in aquatic landscapes along the continuum of «the mouth of the Don River − Sea of Azov» // Conference Proceedings of 15th International Multidisciplinary Scientific GeoConference, SGEM 2015. Bulgaria, 2015, vol. I, pp.721-726.

[7] Yu.A. Fedorov, I.V. Dotsenko, A.V. Mikhailenko The role of the hydrological factors in the formation of field concentrations and fluxes of reduced gases and mercury in the Sea of Azov // Conference Proceedings of 11-th International Multidisciplinary Scientific GeoConference&EXPO Modern Management of Mine Producing, Geology and Environmental Protection, SGEM 2011. Bulgaria, 2011, Vol.III, pp. 717-723.

[8] A.A. Zimovets, Yu.A. Fedorov, A.E. Ovsepyan, A.V. Mikhailenko, I.V. Dotsenko About the features of the mercury levels formation in precipitation of the Azov Sea and White Sea // Conference Proceedings of 15th International Multidisciplinary Scientific GeoConference, SGEM 2015. Bulgaria, 2015, vol. I, pp.19-24.

[9] Yu.A. Fedorov, I.V. Dotsenko, A.V. Mikhailenko Behavior of heavy metals in water of the Azov sea during wind activity // Izvestiya vuzov Severo-Kavkazskiy region. Natural science. No. 3. Rostov-on-don, 2015, p. 108 – 112.

[10] L.Yu. Dmitrik, Yu.A. Fedorov The levels and distribution of iron on geochemical barriers in the system "mine water – river – pond" // Actual problems of Earth Sciences. Proceedings of the scientific conference of students and young scientists with international participation; southern Federal University. Rostov-on-don: Publishing southern Federal University, 2015, 518 p.

[11] Yu.A. Fedorov, Y. L. Dmitrik Behavior of iron in the system "Mine water-river-sea of Azov" // Topical issues of modern physics, mathematics and natural Sciences: proceedings of the international scientific e-Symposium. Russia, Moscow, June 29-30, 2015 [Electronic resource] / under the editorship of Professor Yu. a. Fedorov. – Electron.text. Dan. (1 file is 5.6 MB). Kirov: MCNIP, 2015, p. 145-151.

[12] Yu.A. Fedorov, L.Yu. Dmitrik, M.P. Galushko Behavior of iron on geochemical barriers in the system "Mine water-river-pond" // Materials of scientific conference with international participation "Modern problems of hydrochemical monitoring of surface water quality". Part 1. Rostov-on-don, 2015, p. 175-178.

DYNAMICS OF THE ANAPA BAY-BAR SUBMERGE SLOPE

Elena Fedorova, The Southern Branch of the P.P. Shirshov Institute of Oceanology of the Russian Academy of Sciences, Russia

elalfe555@gmail.com

The planning of exploration and socio-economic development of coastal regions is impossible without the knowledge of coastal processes and scientifically based forecast of the evolution not only the shoreline, but the submerge slope also. Laboratory of lithodynamic and geology of the Southern Branch of the P.P. Shirshov Institute of Oceanology RAS since 2010 surveys bottom topography within Anapa Bay-Bar. Along Anapa Bay-Bar the presence of two longshore underwater bars is clearly observed. The first underwater bar is narrower than another one. His width is up to 40 m and it is located at the depth of 1.5-2.0 m. The second underwater bar is wider (up to 150 m) and it is located at the depth of 3.5-4.0 m. The both bars have the height, approximately, of 2.0-2.5 m. Both bars are well expressed in the central part of Anapa spit. Modern dynamics of the submerge slope changes will be considered in the paper.

Key words: Anapa Bay-Bar, evolution of the submerge slope, longshore underwater bars.

I. INTRODUCTION

The Anapa bay-bar is an accumulative sand body approximately 47 km long, located in the North-West part of the Russian coast of the Black Sea. The Anapa bay-bar is a narrow spit (its width ranges from 80 m in the northern part to 1.5 km in the south) which isolates a system of lagoons from the Black Sea (Fig. 1). The entire bay-bar and especially its southern part with sand beaches 50-200 m wide is intensely used in recreation.

The Anapa bay-bar is a polygenetic accumulative coastal form, combining in its development the properties of an accumulative body of the barrier type with the transversal motion of sediments and longitudinal type with alongshore displacement. The configuration of the shore and topography of the shelf actually formed the closed lithodynamic system of the Anapa bay-bar (Fig. 1), which has a form of a concave arc [1, 2].

The first scientific data on the geological and geomorphological structure of the Anapa bay-bar appeared in the 19th century. In 1838-1865, E. Verneil and I. Guyo, and others considered the problems of the geological structure and topography forms of the Anapa region [3]. Beginning from 1948, V.V. Longinov, A.A. Popov, E.N. Nevessky, E.N, Egorov and other carried out scientific researches in the region of the Anapa bay-bar. A publication by V.P. Zenkovich [4] is one of the most complete descriptions of the Anapa bay-bar. N.A. Aibulatov repeatedly addressed the Anapa bay-bar as an object of the scientific research. The monograph by Ya.A. Izmailov published in 2005 [3] presents a paleo-geographical reconstruction of the history of Anapa bay-bar formation based on the analysis of the geological and geomorphological data. Since 2010, the scientists of the Southern

Branch of the P.P. Shirshov Institute of Oceanology of the RAS have been conducting annual multidisciplinary investigations of the Anapa bay-bar [5]. Current state of the Anapa bay-bar coastal zone more detail described in the papers of R.D. Kosyan, et al [1, 2, 5, 6, 7].

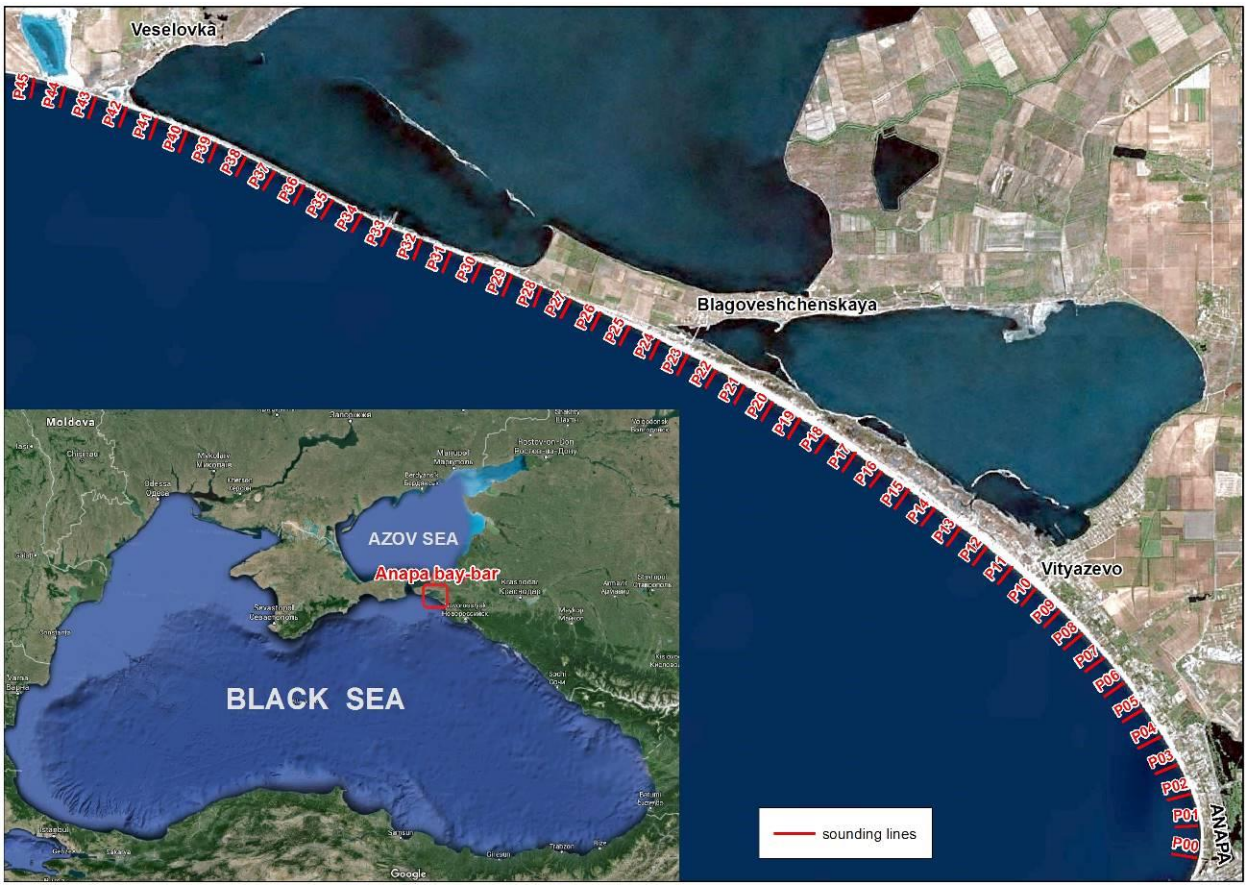

Fig. 1. The scheme of the Anapa bay-bar and sounding lines for measurement of depths.

II. Methods and Results

The issue of the underwater sand bars formation and dynamics is not new for the Black Sea coast. However, a complete theory of formation and dynamics of the underwater sand bars did not create and also a method for the forecasting of the natural phenomena, like the underwater sand bars, did not developed. While the issues of forecasting dynamics and control of the submerge slope are very important and practical interest to these issues are actual up to now.

The submerge slope along Anapa bay-bar is slightly convex, as for the area of underwater sand bars should be a slight increase in the incline. The average slope to 5 m depth is 0.01; followed to a depth of 5-12 m slope is 0,015-0,018, and then slope sharply decreased to 0.003 at depths exceeding 12-15 m.

The underwater bars are relatively stable. Their moving either to the beach or to the sea during a wide variety of storms is negligible. Three underwater bars were discernible in the studied area according to data of 1955 [4]. The tops of the underwater bars in 1955 were located from the shoreline at 63-84, 157-177 and 272-319 meters. The depths over the tops of the bars were, respectively, 0.9-1.4, 2.0-2.3 and 3.9-4.0 m. The middle bar was the most well marked for height and was more constantly in comparison with first and second bars. The first bar (located closer to

the shore) was quite movable - sometimes this bar was closer to the shoreline, sometimes it was become further. The third bar was the lowest.

At the present time, there are two bars only, identified according to observation of 2010-2015. The underwater bars are at the distances of 100-120 and 250-350 meters from the shoreline. Depths over the tops of the bars are 1,5-2,2 and 3,8-5,0 m. The first bar is more steep and narrow in comparison with the second one, the height of the both bars are average out at 1-2 m (Fig. 2-12).

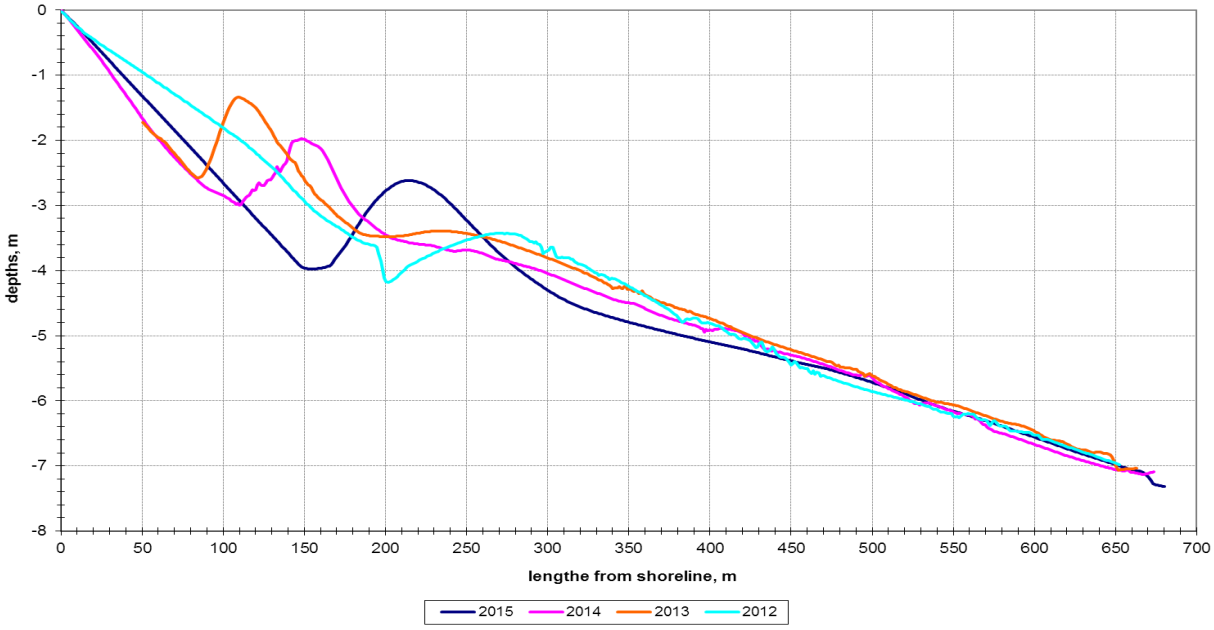

Fig. 2. Changing of the bottom profile at different times for the sounding line P44.

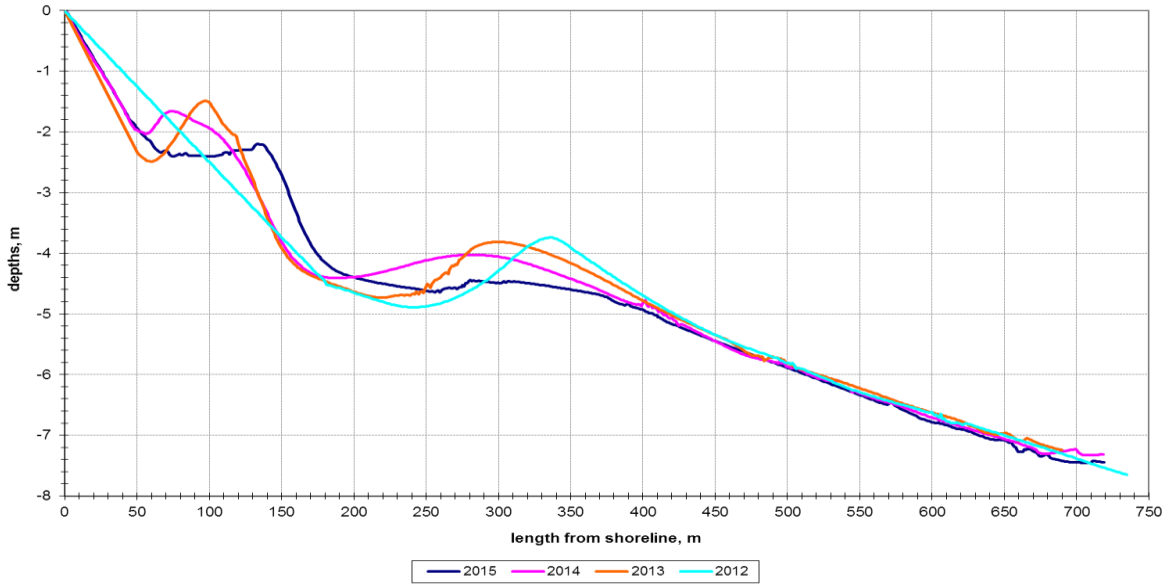

Fig. 3. Changing of the bottom profile at different times for the sounding line P41.

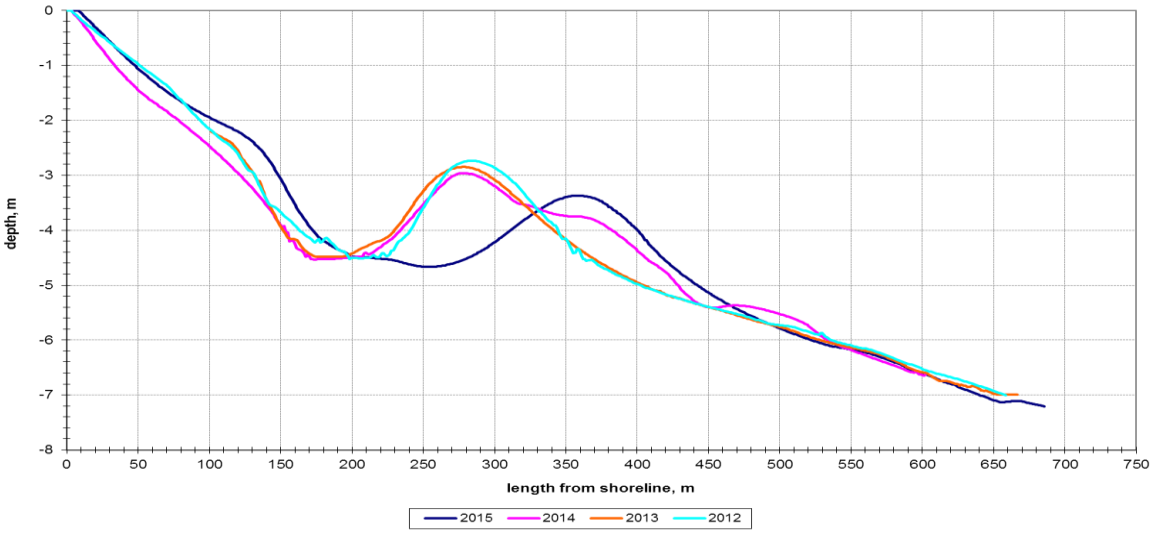

Fig. 4. Changing of the bottom profile at different times for the sounding line P36.

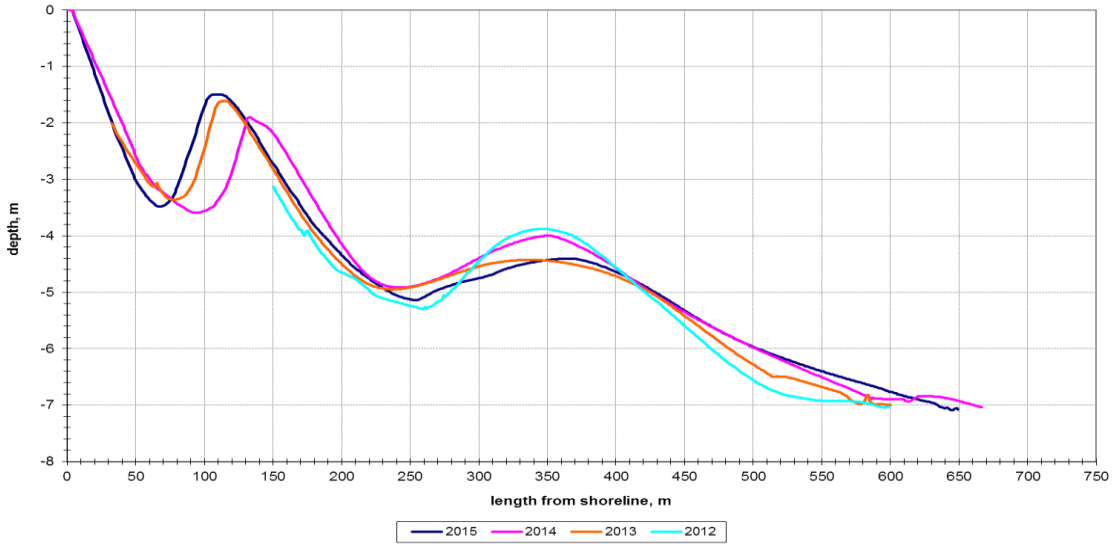

Fig. 5. Changing of the bottom profile at different times for the sounding line P31.

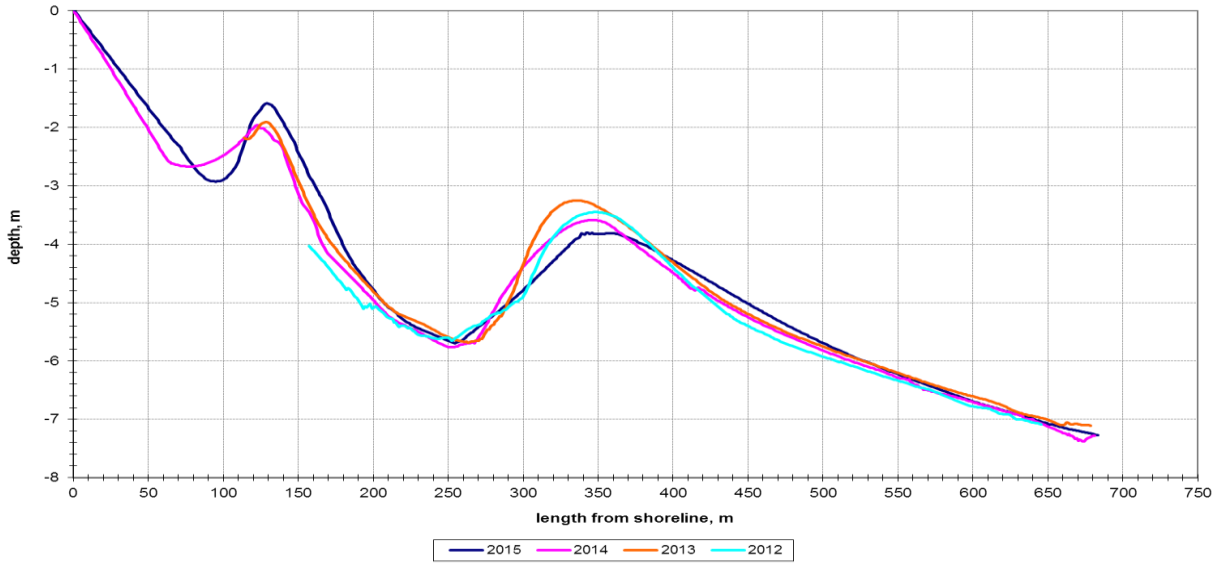

Fig. 6. Changing of the bottom profile at different times for the sounding line P26.

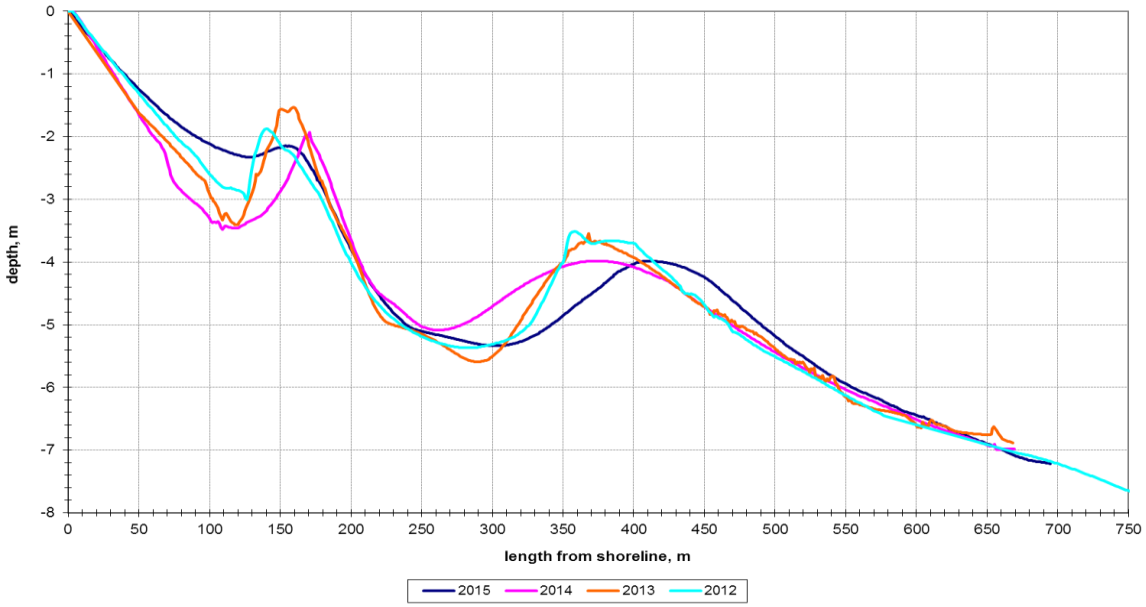

Fig. 7. Changing of the bottom profile at different times for the sounding line P14.

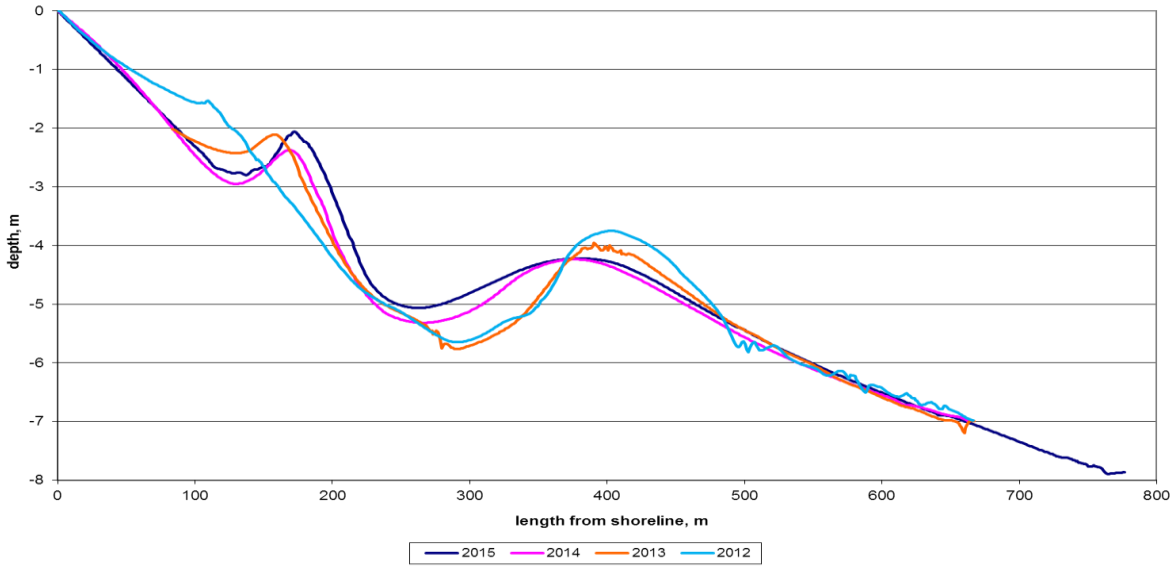

Fig. 8. Changing of the bottom profile at different times for the sounding line P15.

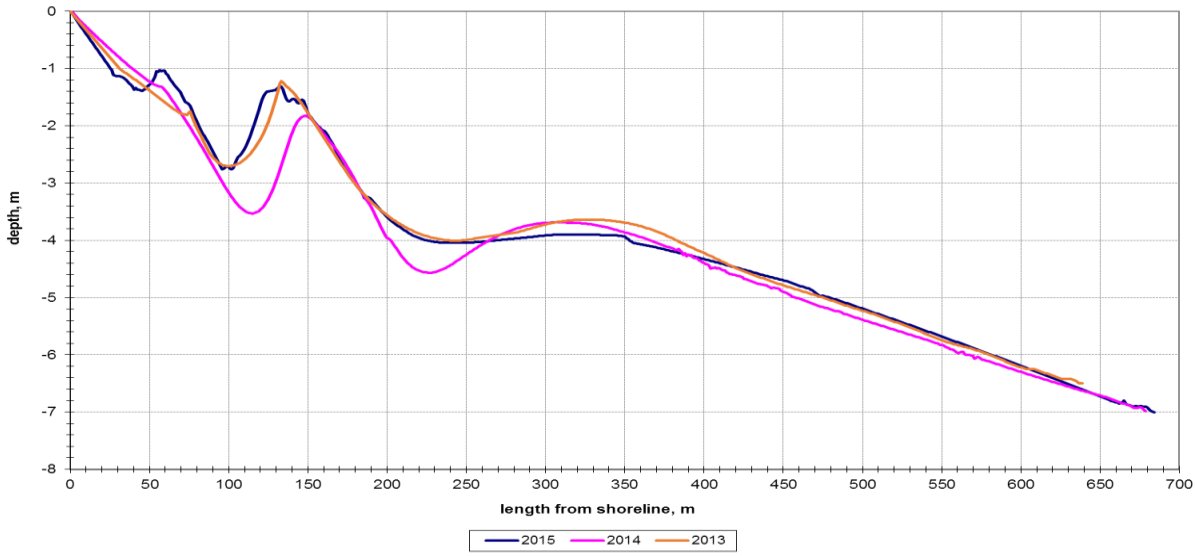

Fig. 9. Changing of the bottom profile at different times for the sounding line P08.

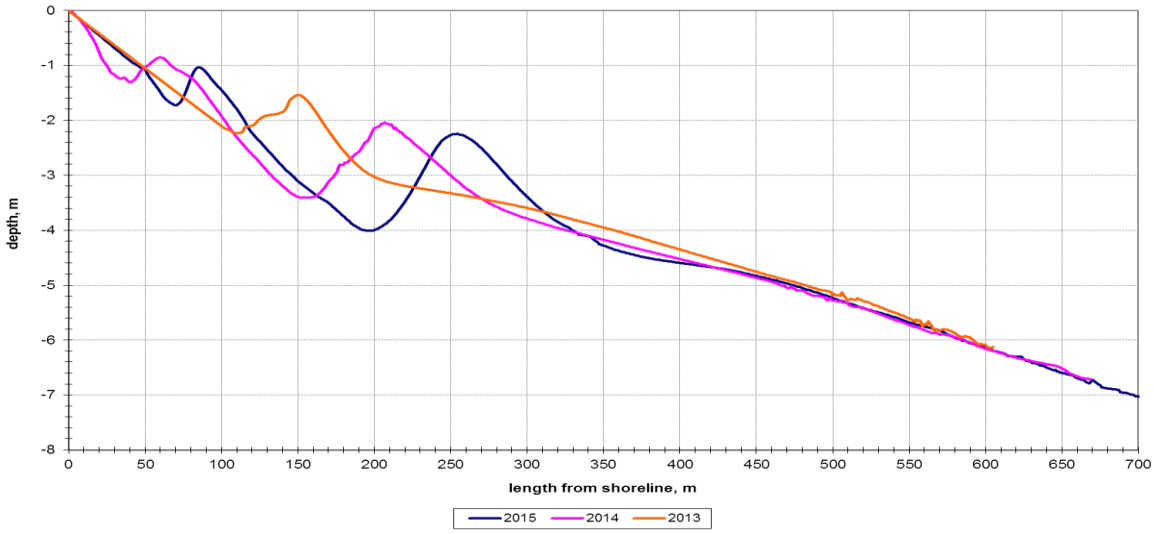

Fig. 10. Changing of the bottom profile at different times for the sounding line P06.

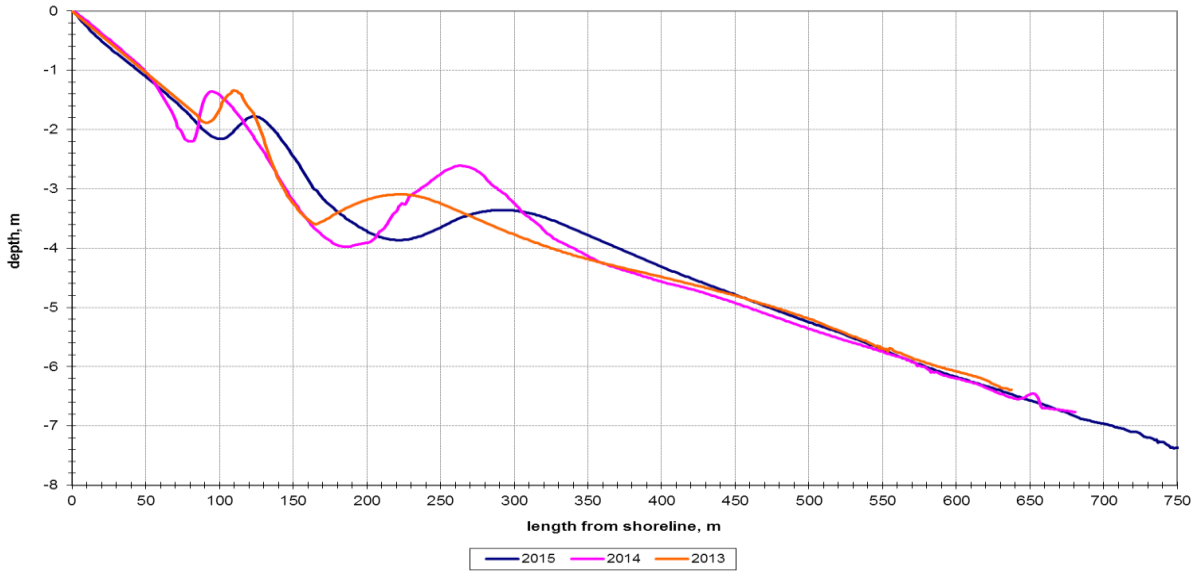

Fig. 11. Changing of the bottom profile at different times for the sounding line P04.

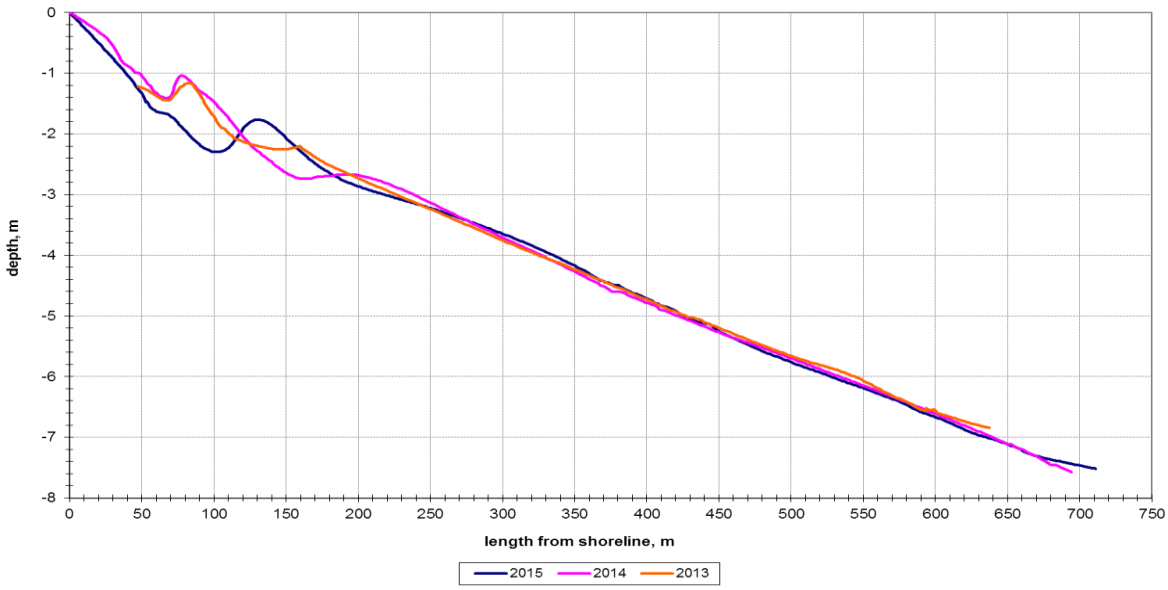

Fig. 12. Changing of the bottom profile at different times for the sounding line P01.

The bars gradually became smaller, lower and closer in the direction from the central part of Anapa bay-bar to its edges, according to data of 1955 [4]. The observations of 2010-2015 showed the same trend of the longshore underwater bars changes.

The contour of the first underwater bar has an influence on the shoreline contour. A specific cape was formed opposite this bar (Fig. 13). The water is usually catching up between two such capes during storms. The undertow currents formed and washed the hollow in the underwater bar surface. Accordingly, the first bar has fairly frequent bends and breaks. The shoreline contour is changing, when the waves are approaching to the shore with the narrow angle and the capes are migrating along the shoreline. The orientation of the underwater bars is changing, when the west storms are dominate. The first underwater bar is disintegrated to few small bars in the eastern and central parts of the Anapa bay-bar. These small bars have usually narrow angles with the shoreline (Fig. 13). However, the position of the underwater bars is restored after several southern storms.

Fig. 13. The capes formed opposite the first broken underwater bar (Modified from [7]).

As can be seen from Figures 2-12 the position of underwater bars relative to each other for 2012-2015 has changed slightly. The most stable underwater bars are located in the central part of the Anapa bay-bar (Fig. 5-7). On the eastern and western ends of the Anapa bay-bar the underwater bars change its shape, height and distance from the coastline in different years (Fig. 2-4 and 8-12). These observations demonstrate significant instability of the underwater relief near the capes that corresponds to the basic concepts of the coastal zone development [4].

III. Conclusions

Laboratory of lithodynamic and geology of the Southern Branch of the P.P. Shirshov Institute of Oceanology RAS since 2010 surveys bottom topography within Anapa Bay-Bar. Along Anapa Bay-Bar the presence of two longshore underwater bars is clearly observed. The first underwater bar is narrower than another one. His width is up to 40 m and it is located at the depth of 1.5-2.0 m. The second underwater bar is wider (up to 150 m) and it is located at the depth of 3.5-4.0 m. The both bars have the height, approximately, of 2.0-2.5 m. Both bars are well expressed in the central part of Anapa spit. During calm weather of the summer period the submerged slope becomes less steep as compared with the profile generated during winter storms. It seems necessary to link the main changes in the morphology and morphometry of the underwater bars with different storms and sediments grain size to make accurate predictions of the bottom relief reformation. It is also necessary to make some series sounds of the submerge slope before and after the different storms.

IV. Acknowledgments

This work was initialized by the Russian Foundation for Basic Research (Project no. 16-35-00533). The performing of experimental works was supported by the Russian Science Foundation, project no. 14-17-00547. The calculations and analysis of the results were supported by the Russian Science Foundation, project no.14-50-00095.

V. REFERENCES

[1] V.V. Krylenko, R.D. Kos'yan, A.D. Kochergin, "Regularities of the Formation of the Granulometric Composition of the Bottom and Beach Deposits of the Anapa Bay-Bar" *Oceanology* 51(1), 1061–1071 (2011).

[2] R.D. Kosyan, S.B. Kuklev, V.V. Krylenko, "Brittle equilibrium of the Anapa bay-bar" *Priroda 2*, 2012, pp. 19-28. (in Russian).

[3] Ya.A. Izmailov, "Evolutionary Geography of the Azov and Black Sea Coasts. Anapa Bay-Bar", 2005, pp. 1-174. (in Russian).

[4] V.P. Zenkovich, "Coasts of the Black and Azov Seas", 1958, 150 p. (in Russian).

[5] R.D. Kosyan, Yu.N. Goryachkin, V.V. Krylenko, V.V. Dolotov, M.V. Krylenko, E. A. Godin, "Crimea and Caucasus Accumulative Coasts Dynamics Estimation using Satellite Pictures" *Turkish Journal of Fisheries and Aquatic Sciences* 12, 2012, pp. 385-390.

[6] M. Krylenko, V. Krylenko, R. Kosyan "Accumulative coast dynamics estimation by satellite camera records" *Third international conference on remote sensing and geoinformation of the environment (RSCY2015)*. Book Series: Proceedings of SPIE. Vol. 9535. Hadjimitsis, DG; Themistocleous, K; Michaelides, S; et al, 2015, P. 95351K. http://dx.doi.org/10.1117/12.2192495.

[7] R.D. Kosyan, V.V. Krylenko, "Modern status of marine accumulative shores of Krasnodar region and their use", Nauchnyi Mir, Moscow, 2014, 256 p. (in Russian).

ESTIMATION OF RECREATIONAL POTENTIAL BASED ON THE DYNAMIC PROCESSES, NATURAL AND ANTHROPOGENIC FACTORS

Filobok Anatoly, Kuban State University, Russia
Volkova Tatiana, Kuban State University, Russia
Minenkova Vera, Kuban State University, Russia
Belikov Michael, Kuban State University, Russia
Voronina Victoria, Kuban State University, Russia

econgeo@mail.ru

This article is devoted to the estimation of recreational potential based on the dynamic processes, natural and anthropogenic factors of the Azov-Black Sea coast of Krasnodar region as an example. Bioclimatic figures are considered as the dynamic processes and natural factors, the degree of the development of exogenous geological processes. Anthropogenic factors are represented by the multi aspect business activities in the coastal zone.

Keywords: recreational potential, recreational natural management, coastal ecosystems, the Azov-Black Sea coast, Krasnodar region.

In up to date sircumstances more attention is given to recreational nature management. This is quite justified, because the efficient use of the recreational areas can be a source of funds to supplement the budget at a certain stage of an economic development of regions.

The presence of the recreational potential on the territories is an important condition for the tourism development. The recreational potential of the territory is often stands for the totality of natural, cultural, historical and socio-economic conditions for the organization of recreational activities in a particular area.

The recreation potential very often refers to the existence of certain objects that are unique or at least attractive not only for locals. The recreational potential of the territory is very variable and depends on the specific socio-cultural knowledges it is located in. Identification of the existing tourism potential is not the most difficult task, because nowadays almost every old-cultivated territory has monuments of history and culture, natural protected sites, including a detailed information about the objects of social and cultural facilities - museums, hotels, restaurants, health resorts and recreation centers, etc. [1].

There are some complex methods of exploration of recreational resources, including their identification and a natural, historical, cultural potential, infrastructure and personnel detection. Revealing of recreational resources is primarily associated with the study of natural and cultural systems and human resources to involve in some tourist and recreational activities. Several common approaches to the evaluation of recreational resources have been currently developed, in this case the following is primary evaluated: the functional serviceability for a particular type of tourism (technology evaluation); the degree of comfort (physiological evaluation); aesthetic qualities

(psychological evaluation) [2]. An economic and environmental evaluation, by the way, integrated in the definition of a resourse of recreational value. The evaluation of dynamic natural and anthropogenic processes on the level of the recreational potential of the territory is of a key importance lately. It is not enough to detect the presence of certain recreational resources to assess the recreational potential of the territory, it is important to identify and predict the impact of these resources in terms of different types of geosystems. The evaluation of the recreational potential of coastal geosystems and its efficient use is one of the relevant problems of modern natural management [3].

The target of research in this case is the Azov-Black Sea coast of Krasnodar region.

In order to clarify the understanding of the nature and description of the study area, different approaches to the definition of coastal areas should be taken into account. The main difficulties of the conceptual construct of the coastal zone are determined by two factors:

1. The absence of a clear legislative framework, which contains clear terms such as coastal zone, its components, coastal zone management, etc.;

2. The lack of a uniform terminology in the science sidelines concerning the coastal zone (geomorphology, biology, geology, management and so on.). Moreover, the ambiguous use of certain terms in different fields of science. For example, there is a term "waterside or littoral zone" in geology, geomorphology, coast survey and it is "coastal zone" in biology and management.

The territory and boundaries of this area differ from each other sometimes fundamentally due to the variety of applied approaches.

In general, coastal areas can be described as complex spatial-territorial objects, which include geographical, ecological, economic and social components.

The definition that reflects the essence of the concept of "coastal area" or "coastal zone", was proposed by the European Commission: coastal zone is a contact area of land to the sea, including natural systems both the coast and the adjacent marine area within the boundaries, allowing to provide ecologically balanced development of coastal areas, conservation of coastal and marine landscapes and ecosystems from pollution and destruction, a territory with a limited and regulated regime of economic and other activities [4].

A "coastal zone" term had already appeared in the 60-70-s of the XX century in developed coastal countries and a furhte term "integrated coastal zone management" as a result. We can say now that the study of integrated coastal zone management contributes to understanding the relationships formed within the socio-economic system of the coastal zone, as well as the conditions in which methods and approaches of planning and management have been developed.

There is no definition of coastal areas in the Russian Federation regulation. The Water Code of the Russian Federation reveals the concept of the water protection zone, which can be considered as a component of the territory (land) of the coastal zone.

Many authors have noted the concept of coastal zone in russian encyclopedia is firstly defined with the help of the principle formulated by the United States and outlined in the Law on Coastal Zone Management US, and secondly, according to the principles set out in the Model Law of the EU Sustainable management of coastal zones. Analyzing different interpretations offered by these regulations we can generally conclude that in this study a coastal zone (territory) is advisable to be regarded as the geographical area consisting of both land and sea side, as well as the territory

of the local administrative units adjacent to sea. Land boundaries are determined by the coastal territory at such a distance from the sea, which provides control over the relevant area of the land, the use of which has a direct and significant impact on coastal waters. In the process of determining the boundaries it is also important to mention the relationship factors of activity in the coastal zone, the exchange of information on this issue, the possibility of formation of mechanisms of good governance, based on clear and common understanding by all participants of the process goals and objectives of this complex system.

Increasing anthropogenic pressure on the ecosystem of the Black and Azov seas associated with increased recreational activities in coastal areas, has a negative impact on the biological quality of water resources of the basin [5]. Industrial development of the coastal regions, increasing number of urban and coastal settlements, proliferation of resorts and the increase in the volume of industrial waste water, increasing the volume of congestion in ports and transportation of oil, fertilizer and other mineral resources, the growth of shipping, the expansion of sea ports, construction of new terminals, underwater exploration and production of oil and gas require the adoption of necessary measures to prevent the negative consequences of these changes [6].

Azov-Black Sea coast of the Rostov Region and Krasnodar Region is a unique natural complex with rich flora and fauna, within which the huge industrial and social potential is concentrated. The main specialization sectors of this areas are agriculture, recreation and port facilities. (Fig.1, Fig.2)

The coastal zone is the zone of important public interests. Natural management must be controlled strictly by the state here. The clash of interests of various branch departments, financial giants at the time of deficit at the all-Russian coastal areas leads to the competition functions; many natural resources are extremely sensitive to human impact, which may jeopardize the very existence of the most valuable natural complexes. Therefore, coastal resources should be involved in the use on the basis of federal programs, and integrated management, which should be based on scientific data [7].

Azov-Black Sea coast of a Krasnodar region seaside is a contact zone with the length of 950 km. Azov-Black Sea coast border is limited by the administrative border of the land of the coastal cities and districts. Thus, Azov-Black Sea coast is not a narrow strip of the land directly fitting to the sea and its width varies from 10 to 50 km [8].

At the same time, the study has found that the territory of the Azov-Black Sea coast of Krasnodar region is the subject to both anthropogenic impact and to the objective exogenous processes (Fig.3).

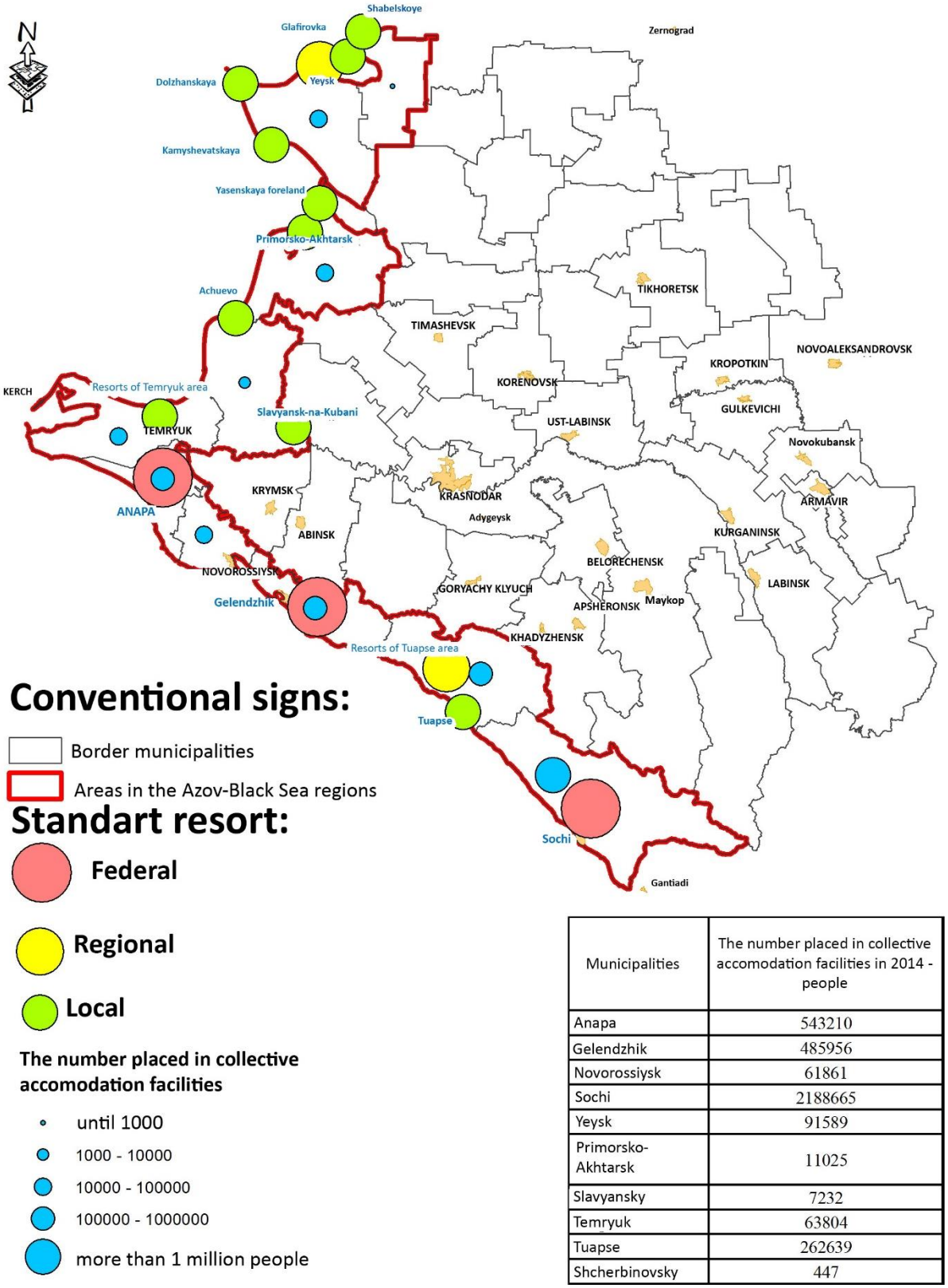

Municipalities	The number placed in collective accomodation facilities in 2014 - people
Anapa	543210
Gelendzhik	485956
Novorossiysk	61861
Sochi	2188665
Yeysk	91589
Primorsko-Akhtarsk	11025
Slavyansky	7232
Temryuk	63804
Tuapse	262639
Shcherbinovsky	447

Fig. 1 Health and Recreation areas and resorts of the Azov-Black Sea coast of Krasnodar region

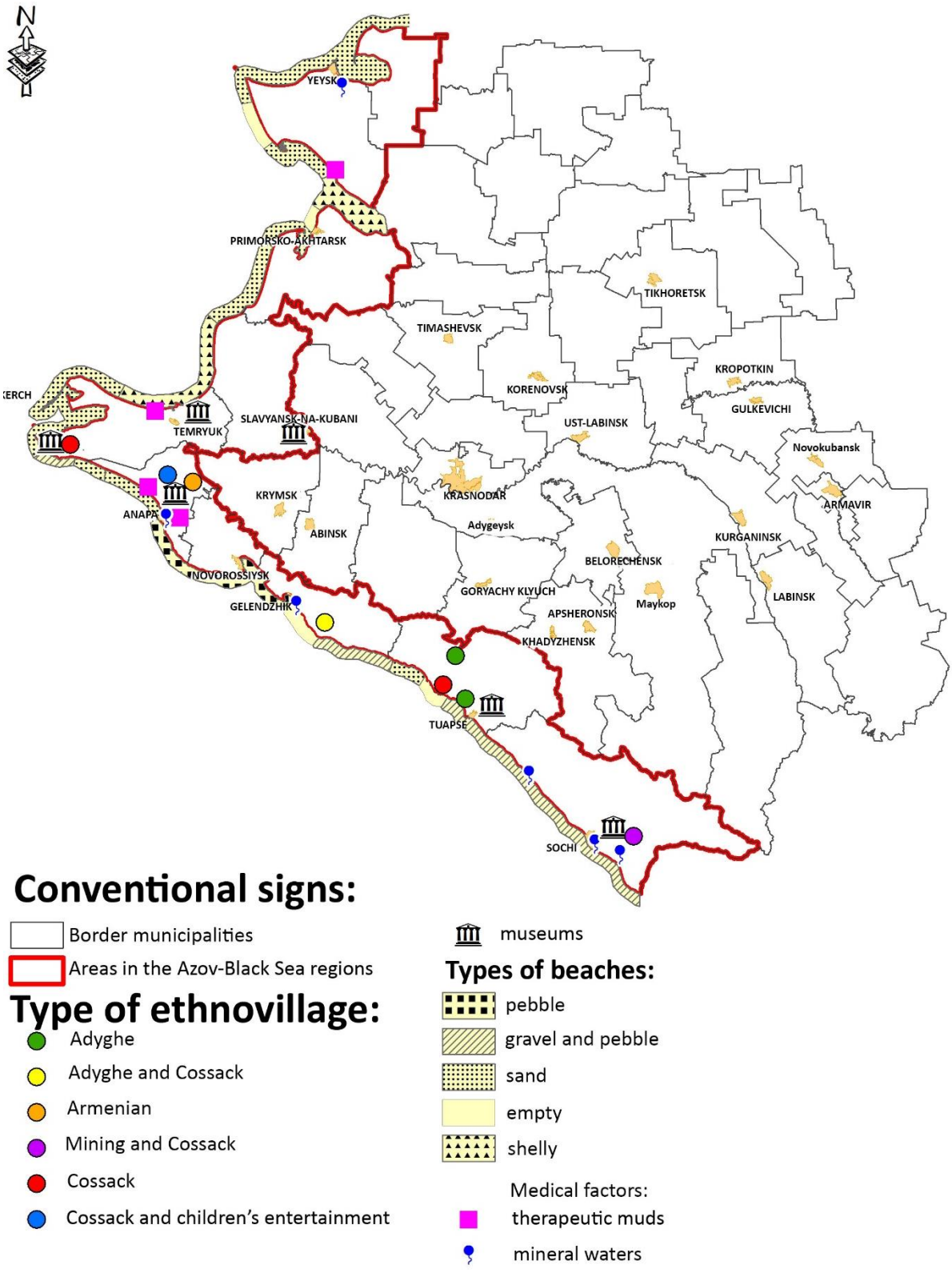

Fig. 2 Recreational Resources of the Azov-Black Sea coast of Krasnodar region

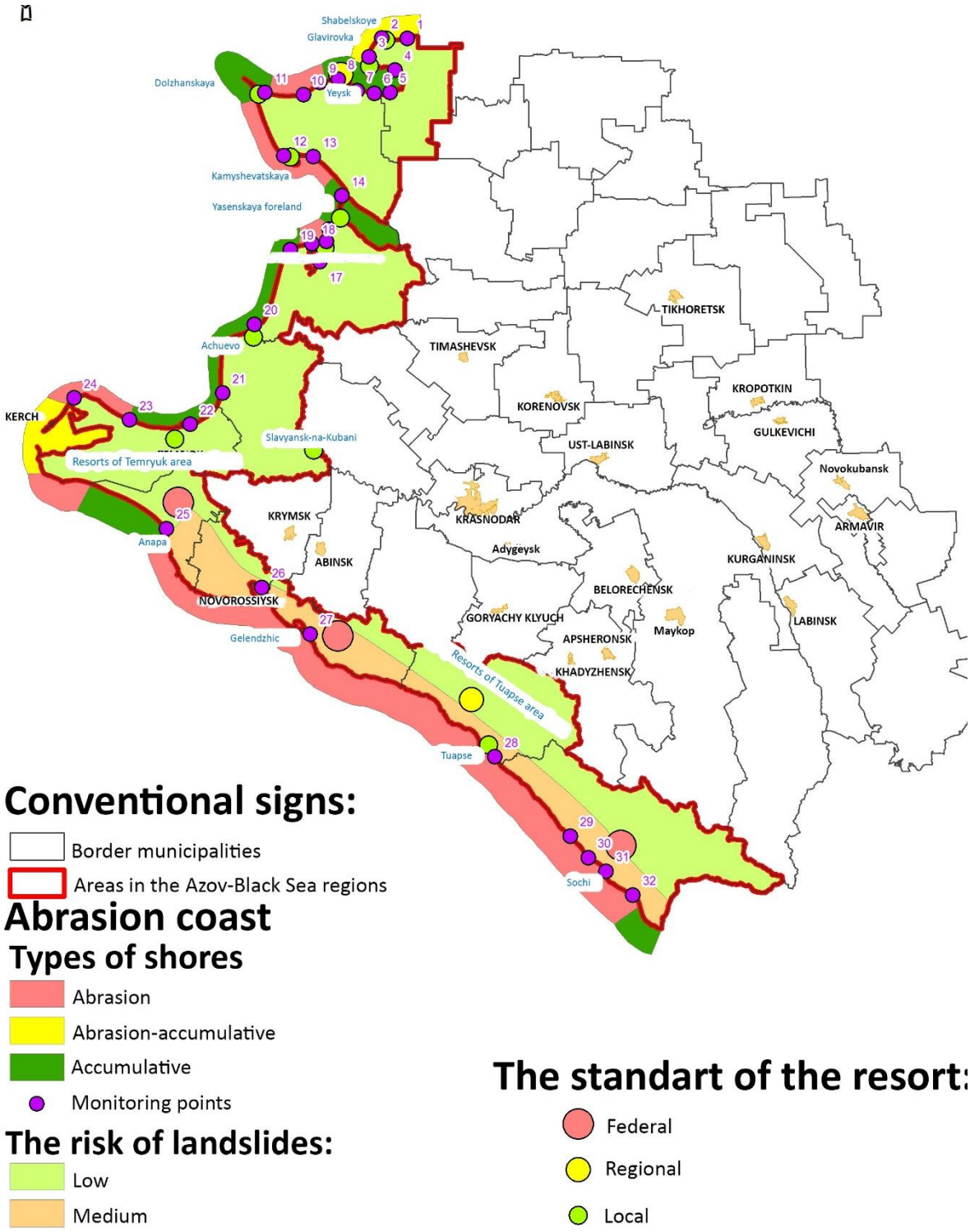

Fig. 3 Exogenous geological processes of the Azov-Black Sea coast

Based on the above mentioned, the target of the research means a totality of the subjects of the administrative-territorial division in the structure shown in Table 1.

Table 1 – Municipal structures of study area

№	Municipal structure	Administrative center	Square kilometers
1	Shcherbinovsky region	Staroshcherbinovskaya	1377,1
2	Yeisky	Yeisk	2120,3
3	Primorsko-Akhtarsky region	Primorsko-Akhtarsk	2503,6
4	Slavyansk-on-Kuban region	Slavyansk-on-Kuban	2198,6
5	Temryuk region	Temryuk	1956,5
6	Resort town Anapa	Anapa	981,9
7	Novorossiysk	Novorossiysk	834,9
8	Resort town Gelendzhik	Gelendzhik	1227,5
9	Tuapsinsky region	Tuapse	2399,2
10	Resort town Sochi	Sochi	3506,1

However, these exogenous geological processes are very irregular. The activity of slope processes increases in the sub-mountain areas of the region including the coastal zone. The part of the study area (most of the Black Sea region) goes in the zone of mudflow hazard. The process of coastal erosion has a great impact on recreation in the coastal zone and the absence of shore protection can lead to loss of beach areas. The monitoring of hazardous exogenous processes should be carried out continuously.

According to ecological and phytocenotic characteristics of coastal and adjacent areas flora and the studied recreation area is characterized by a high degree of diversity and exoticism of species and is attractive (including consumer tourism).

Bioclimatic rate of the Azov-Black Sea coast of Krasnodar region has been studied: the mode of solar radiation, atmospheric circulation, wind and thermal regime, the regime of humidity and precipitation (Fig.4). The first findings show that the study area belongs to the zone of discomfort according to some bioclimatic parameters and it should affect the specific features of the organization of some recreational activities.

Some synoptic phenomena have been identified with the help of the long-term recurrence of wind directions analysis: northeasterly strong winds reaching hurricane force (Novorossiysk, Gelendzhik, Anapa); the increase in repeatability of western moisture-laden flows in summertime increases greatly the amount of precipitation on the Black Sea coast, resulting in floods and overflowing; surges on the Azov coast; squally wind in autumn and winter period on the Taman peninsula. The estimation of wind-wave flows of the coastal zone has been conducted. The analysis of the factors influencing the development of the disturbances in the study area has been carried out. Zones of stagnation and siltation have been detected. Zones of active coastal erosion (due to wind conditions), stagnant zones and siltation have been educed. The recurrence of great flurry periods as a limiting factor for the beach-bathing recreation has been investigated.

There is a reallocation of tourist flows associated with the changes in geo-economical and geopolitical situation. Right from the beginning of economic sanctions of western countries deter the desire of Russian tourists to take holidays abroad. Attraction to the Russian resorts is artificially enhanced by the growth of the foreign currencies' rate against the Russian ruble, which reduced significantly the purchasing power of the Russian citizens in relation to the proposed foreign travel products. The accession of the Republic of Crimea to the Russian Federation transformed the market of tourist services of the Krasnodar region. The expected outflow of tourists did not happen due to problems of transport infrastructure (the absence of a bridge across the Kerch Strait and the low through-flow rate of the ferry line). At the moment the situation is redoubled by the unstable situation in the Crimea on the border territory with Ukraine and energy blockade of Crimea.

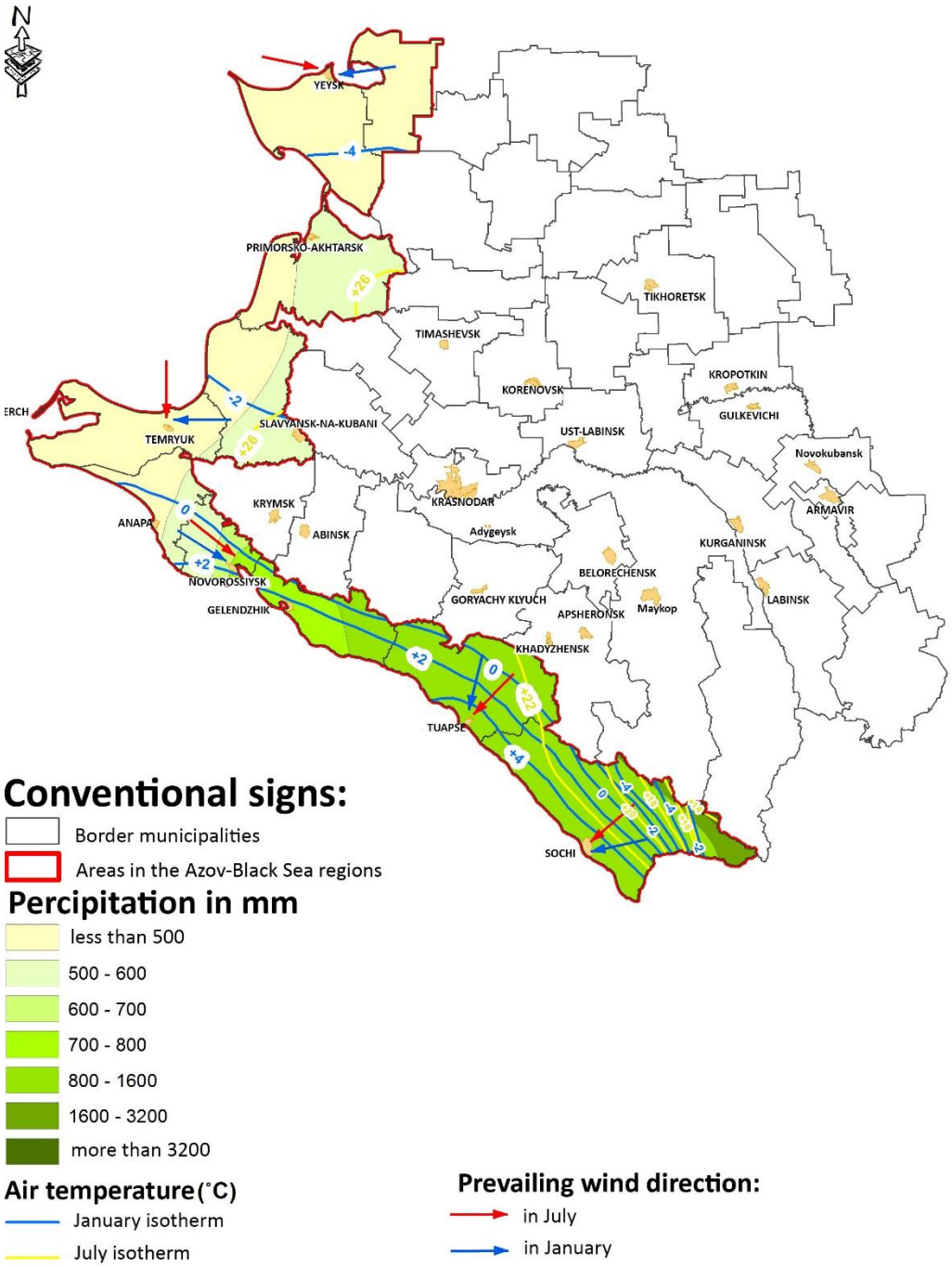

Fig. 4 Basic characteristics of the climate of the Azov-Black Sea coast

The escalation of the conflicts with Western countries and their policy towards the Russian Federation only strengthened the position of Russian tourists in the choice of their holiday destinations in 2014, 2015 and 2016. All these processes have led to the significant growth of the holidaymakers flow taken in coastal areas of Krasnodar region, which led to a considerable load increase not only on the natural recreational resources but also on the subsystems serving the tourist and recreational sector tourism infrastructure in particular. Thus, the observed processes can lead to irreversible effects, including the digression of natural systems, and therefore it is advisable to take immediate steps to redistribute the resulting load.

ACKNOWLEDGEMENTS

Supported by grant number 15-12-23010 (p) of the Russian Humanitarian Science Foundation and the Administration of Krasnodar Region

REFERENCES

[1] Kudelya E.V., Volkova T.A., Anisimova V.V., Karpova Y.I., 2013 Some of the defining characteristics of the recreational potential of the territory // Resort and recreation complex in the system of regional development: innovative approaches.2013. T. 1. pp. 176-178.

[2] Mishchenko T.A. The impact of tourism resources in the development of regional tourism and the problem of their recreational evaluation // Geographical research Krasnodar Territory: collection of scientific works. Krasnodar, 2009. pp. 237-241.

[3] Lipilin D.A., Volkova T.A., Mishchenko A.A., Minenkova V.V. Estimation of recreational potential of protected areas of the Western Caucasus via kosmosemok methods (for example, Tuapse district) // global scientific potential. 2015. № 9 (54). pp. 90-97.

[4] Kropinova E.G., Afanasyev E.P. Sustainable development of coastal areas as a basis for integrated coastal zone management // Herald Baltic Federal University. Kant. 2014. Вып. 1. pp. 140-147

[5] Volkova T.A., Filobok A.A., Belikov M.Y., Pinchuk D.S, Kalustova I.S. Sustainable development and vulnerability of coastal ecosystems Azov-Black Sea coast of Krasnodar region // Ecology and natural resources: applied aspects VI International Scientific and Practical Conference. Ufa. 2016. pp 82-89.

[6] Minenkova V.V., Voronina V.V., Filobok A.A. Azov-Black Sea coast of Russia in the structure of the new geopolitical space in the globalization // Polimasshtabnye system "center-periphery" in the context of globalization iregionalizatsii: theory and practice of socio-geographical research: Proceedings of the International Conference (Sixth Annual Scientific Assembly ARGO). Simferopol. 2015. pp. 305-310.

[7] Chistyakov V.I., Filobok A.A. Sustainable urban development of the Azov-Black Sea coast of Russia in the new geo-economic conditions. Monograph - Krasnodar. 2008. - 308 pp.

[8] Filobok A.A., Voronina V.V., Kudelya A.V. Transformation of population settlement of in the russain mountainius Black sea coastal area in post soviet period // The Caucasus and the Alps in the comparative aspect: Proceedings on the materials of the joint summer school "Caucasus and the Alps in the comparative aspect." Krasnodar. 2014. pp. 93-100.

DYNAMICS OF THE NEARSHORE ZONE OF KALAMITSKIY GULF (BLACK SEA) UNDER INFLUENCE OF WIND WAVES

Vladimir Fomin, Marine Hydrophysical Institute of RAS, Russia
Konstantin Gurov, Marine Hydrophysical Institute of RAS, Russia
Vladimir Udovik, Marine Hydrophysical Institute of RAS, Russia
Sergey Konovalov, Marine Hydrophysical Institute of RAS, Russia

fomin.dntmm@gmail.com

Coastal zone dynamics is especially interesting for interdisciplinary researchers. This is due to general retreat of the coast of the Western Crimea and the fast response in the beach area. This justifies the need for monitoring of morphodynamic processes in the coastal zone of Crimea with the aim of qualitative and quantitative assessments of modern coastal transformation, as well as forecasts of possible changes. XBeach model has been used to simulate dynamics of waves and currents, sediment transport and changes in bottom topography, as well as the processes of drying and flooding of coastal areas. Erosion and sedimentation processes for the bottom sediments of the coastal zone of the Western Crimea have been numerically studied. The bottom profile has been reconstructed on the basis of bathymetric investigations in the coastal zone of the Western Crimea. Numerical simulations have been performed for various parameters of the bed composition and wind waves. Two fractions of bottom sediments have been considered for numerical experiments. The obtained results show that XBeach model can be successfully applied to simulate the bed profile evolution and changes in bottom sediment fractionation.

Key words: Black Sea, Western Crimea, coastal zone, XBeach model, sediment transport and fractionation modelling.

I. INTRODUCTION

In shallow waters and coastal zones, waves and currents support redistribution of clastic material and subsoils presented in the form of suspended load and bed load. This results in erosion and accumulation of bottom sediment, affects transformation of bottom topography and changing coastlines [1]. While waves propagate from outer limits of the nearshore zone towards the shore they increasingly affect bottom sediments, especially in processes wave shoaling and breaking. In one to two day of coastal storm, a radical restructuring of the cross-shore profile is observed. Material is carried away from the beach and the fine fraction is set in motion. Changes in the intensity and spatial distribution of sediments transport parameters largely determine the main trends of reshaping the underwater coastal slope and coastline.

The coastal zone, investigated in this paper, extends from the shoreline to the depth of water where wave motion ceases to affect the seabed. Modelling will provide critical information on how changes of the wave period influence the redistribution of sediments with various grain sizes. For

Kalamitskiy Gulf beaches degradation problem is very relevant. Therefore, it is necessary to develop robust tools that enable accurate prediction of coastal system responses to storms in order to improve coastal management.

Kalamitskiy Gulf is situated at the west coast of the Crimean peninsula (Fig. 1). Wide and straight beaches are known for their clean and soft golden sand, clear sea water and gently sloping bottom of the gulf. The study area is located in the northern part of the gulf and extends approximately 600 meters longshore and 500 meters seaward.

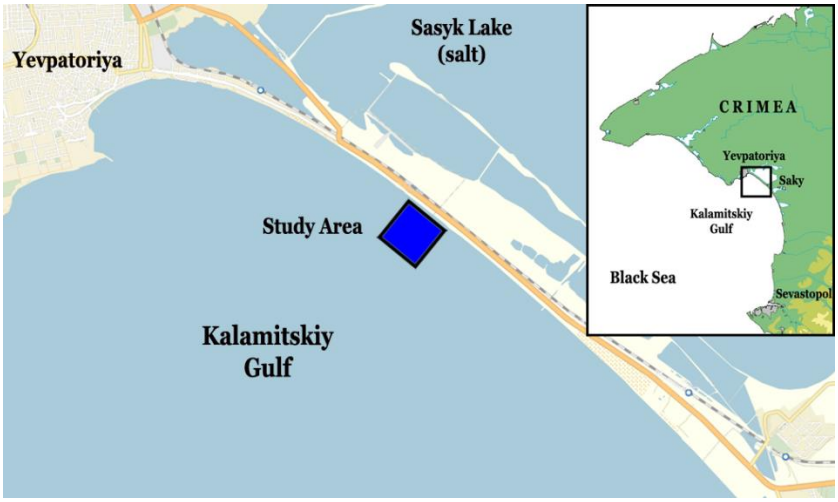

Fig.1. Area of investigation showing the location of the study area chosen for modelling.

Sandy beaches constantly adjust their morphology in response to changing hydrodynamic conditions. The Black sea is a tideless basin and sediment transport in littoral zone of Kalamitskiy Gulf induced primarily by wind waves. Anthropogenic influences, including dam construction during the 20th century, have had significantly affected the natural sedimentary dynamics in the Kalamitskiy gulf. As a result, the northern part of the gulf has become limited in sediment supply. Seasonal variations in wave parameters results in specific winter and summer profiles in nearshore zone.

The position of shoreline over the last decades is quite stable in the study area [2]. But, during strong storms, local beaches can be extremely dynamic, with the potential up to tens of meters of shoreline recession or propagation over hours to days. If so, waves can reach coastal constructions and cause a damage to infrastructure.

The purpose of this paper is to apply the XBeach model (1D) for modelling of changes of the beach and nearshore morphology within the region of Kalamitskiy Gulf at the west coast of Crimea. As sediments in the coastal area are presented by a variety of coarse and fine fractions [3], we used data from actual studies of sediments from the Kalamitskiy Gulf.

II. MODEL IMPLEMENTETION

The XBeach model [4] is applied in a 1D cross-shore setting with a constant grid size 1m. All calculations carried out for the storm period of about 48 hours. On the first stage of model adaptation to the region of Kalamitskiy Gulf the approximation of the summer profile is used as initial profile for numerical simulations (Fig. 2a).

Wave boundary conditions were implemented as time series of sea state (*instant=jonswap*) with perpendicular direction to the coast. The significant wave height H_s was set at 2 m. The wave peak period T_p = 6, 8 and 10 s. Further, default settings were applied, except from the avalanching parameters. The critical slope for avalanching above water (*dryslp*) and the critical slope for avalanching below water (*wetslp*) had values 0.1. The two sediment classes (*ngd* = 2) were considered (see Table 1).

Table 1. Grain size of the sediment fractions [mm]

Coarse fraction		Fine fraction	
$d_{50}(1)$	$d_{90}(1)$	$d_{50}(2)$	$d_{90}(2)$
0.635	1.370	0.115	0.175

The calculations were carried out for two types of initial bed composition (BC1 and BC2):

BC1: $p_1(x,z,0) = 0.5$ for $0 \le x \le L$; $p_2(x,z,0) = 0.5$ for $0 \le x \le L$.

BC2: $p_1(x,z,0) = 0.2$ for $0 \le x \le L_1$ and $p_1(x,z,0) = 0.8$ for $L_1 < x \le L$;
$p_2(x,z,0) = 0.8$ for $0 \le x \le L_1$ and $p_2(x,z,0) = 0.2$ for $L_1 < x \le L$

where $p_1(x,z,0)$ is the volumetric concentration for coarse fraction at the initial time; $p_2(x,z,0)$ is the volumetric concentration for fine fraction at the initial time; x is the cross-shore coordinate; z is the vertical coordinate; L = 555 m is the computational profile length and L_1 = 489 m (see Figure 1);

The value of mean grain size (D_{50}) is calculated by the following formula:

$$D_{50}(x,t) = \sum_{i=1}^{ngd} d_{50}(i) \cdot P_i(x,t). \quad (1)$$

Here P_i are weighting factors given by:

$$P_i(x,t) = \frac{\sum_{j=1}^{nd} p_{i,j}(x,z_j,t) \cdot \Delta z_j(x,t)}{\sum_{j=1}^{nd} \Delta z_j(x,t)}, \quad (2)$$

where *nd* = 3 is the number of bed layers; $p_{i,j}$ is the volumetric concentration of every sediment classes, per bed sediment layer; Δz_j is the vertical dimension of each bed sediment layer.

III. RESULTS AND DISCUSSION

Wave period and initial partitioning of fractions are two input parameters, which have been varied in numerical experiments. The evolution of the bed profile and redistribution of sandy factions in the littoral zone have been investigated in numerical simulations for six scenarios. We illustrate further mostly the results of experiments for the wave period of 8 seconds because all results are qualitatively similar.

The evolution of the profile for all types of the used wave conditions and sediment fractionations results in beach erosion and slope flattening in the foreshore zone. Eroded material moves in the seaward part of the nearshore zone to accumulate as a bar. With increasing of the wave period, the band of bottom topography is expanded. The beach erosion boundary is shifted toward

the shore, the bottom deformation absolute values are grown in the both erosion and accumulation area (Fig. 2b). The largest volume of sediment movement and accordingly the bottom relief change occur at the base of the ledge erosion.

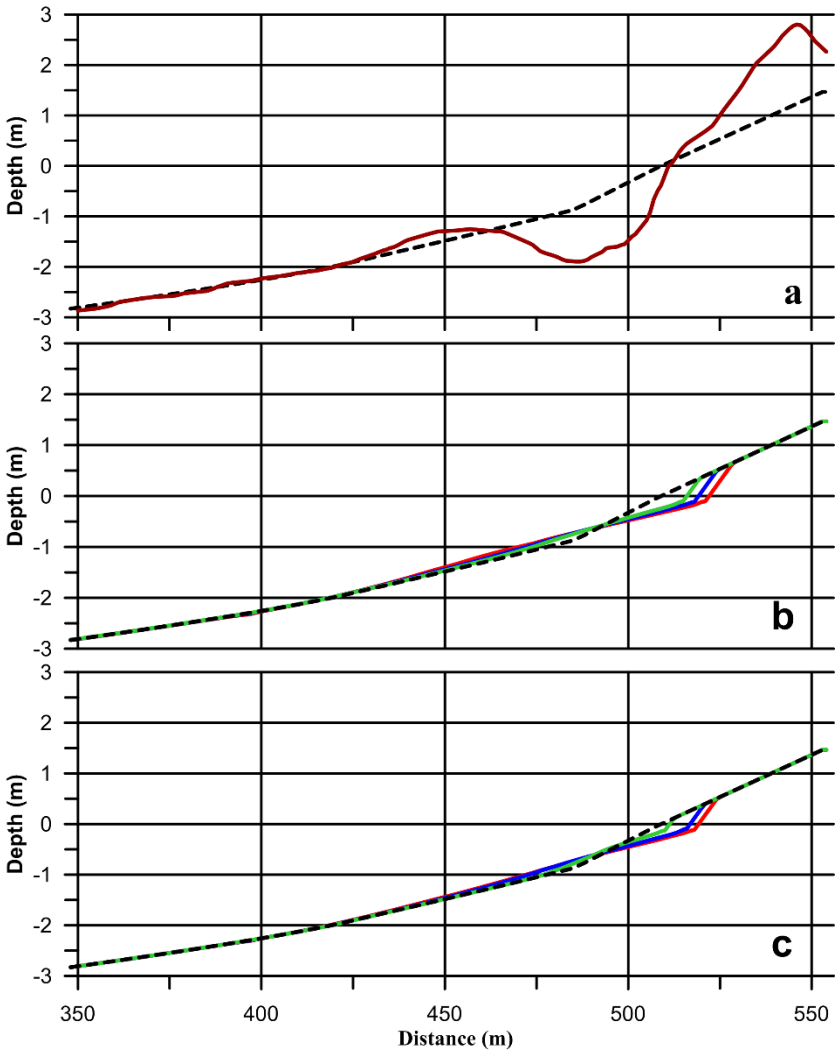

Fig. 2. (a) Measured profile (ruby red line) and its approximation (black dotted line). (b) Initial bed level for BC1 (black dotted line), bed level for Tp = 6s after 48h (green line), bed level for Tp = 8s after 48h (blue line), bed level for Tp = 6s after 48h (red line). (c) Initial bed level for BC1 (black dotted line), bed level for Tp = 8s after 3h (green line), bed level for Tp = 8s after 24h (blue line), bed level for Tp = 8s after 48h (red line).

The rate of shoreline retreat changes over time. The highest values are observed at the start of the storm and they reach about 1 meter per hour. By the end of simulation, the beach erosion rate is significantly reduced and does not exceed 0.1 m/h (Fig. 2c).

Position of zero sea-level mark for wave period of 8 seconds is shifted shoreward by 11 m for BC1 and by 8.5 m for BC2 (Fig. 3c, 4c). The erosion layer thickness increases with decreasing of D50. Using of avalanching parameters in numerical experiments results in erosion of the beach profile above water. The width of the erosion zone for the aerial part of the beach is about 4 m.

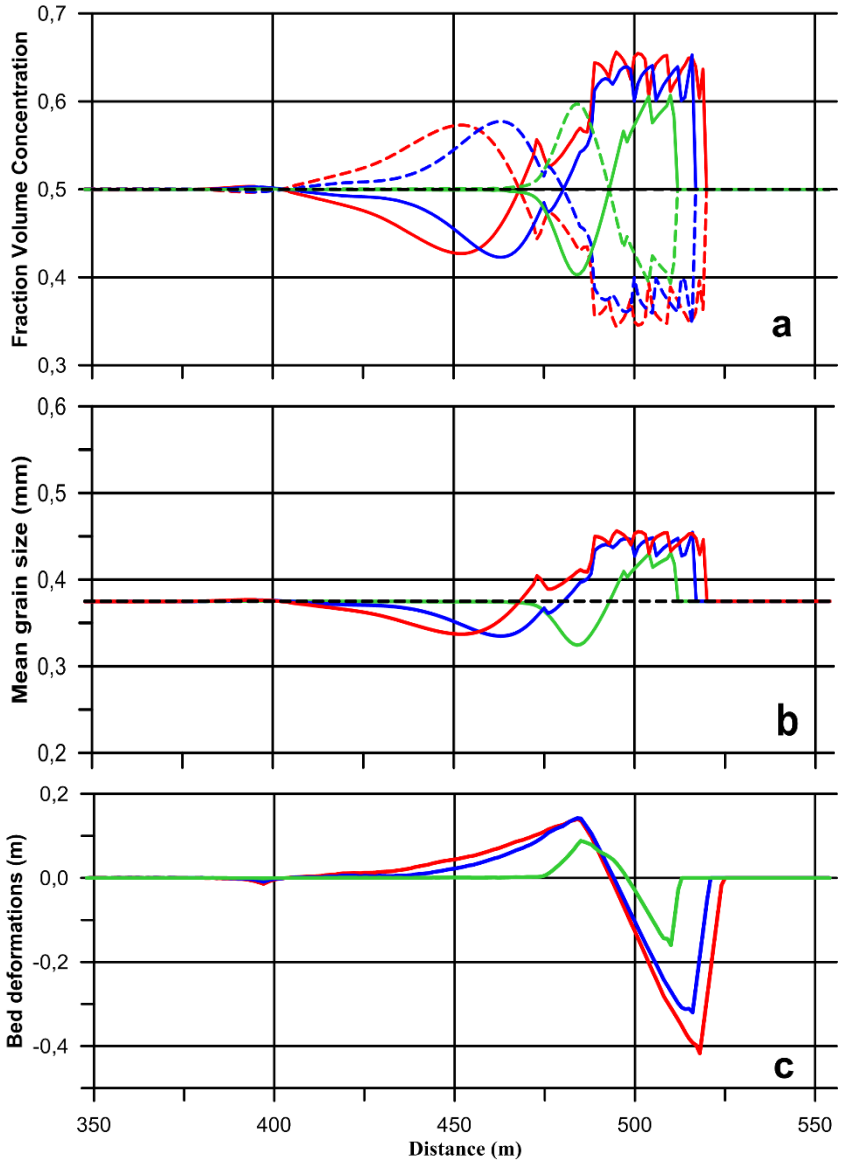

Fig. 3. (a) Distribution of the fraction volume concentration for BC1(Hs = 2m, Tp = 8s), initial fraction volume concentration (black dotted line), fraction volume concentration after 3h (coarse fraction – green line, fine fraction – green dotted line), fraction volume concentration after 24 h (coarse fraction – blue line, fine fraction – blue dotted line), fraction volume concentration after 48h (coarse fraction – red line, fine fraction – red dotted line); (b) Distribution of mean grain size (D50) for BC1(Hs = 2m, Tp = 8s), initial D50 (black dotted line), D50 after 3h (green line), D50 after 24 h (blue line), D50 after 48h (red line); (c) Bed deformations for BC1 (Hs = 2m, Tp = 8s), bed deformation after 3h (green line), bed deformation after 24 h (blue line), bed deformation after 48h (red line).

At the beginning of storm, the bar profile is rather symmetric. Exposure of waves, the position of the bar crest moves seaward, and then remains stable. During this time, the height of the bar crest is also stable. At the same time, the bar width essentially depends on the particle size distribution. The slope of the bar towards the shore has a greater inclination and shorter length than

the backcourt slope. This asymmetry increases over the period of wave action. Sandy material moves seaward and leads to an increase in the width of the bar and its more acclivous slope. The increase of the period of wave influence changes the amount of transported material, causing the increase in the height and width of the bar.

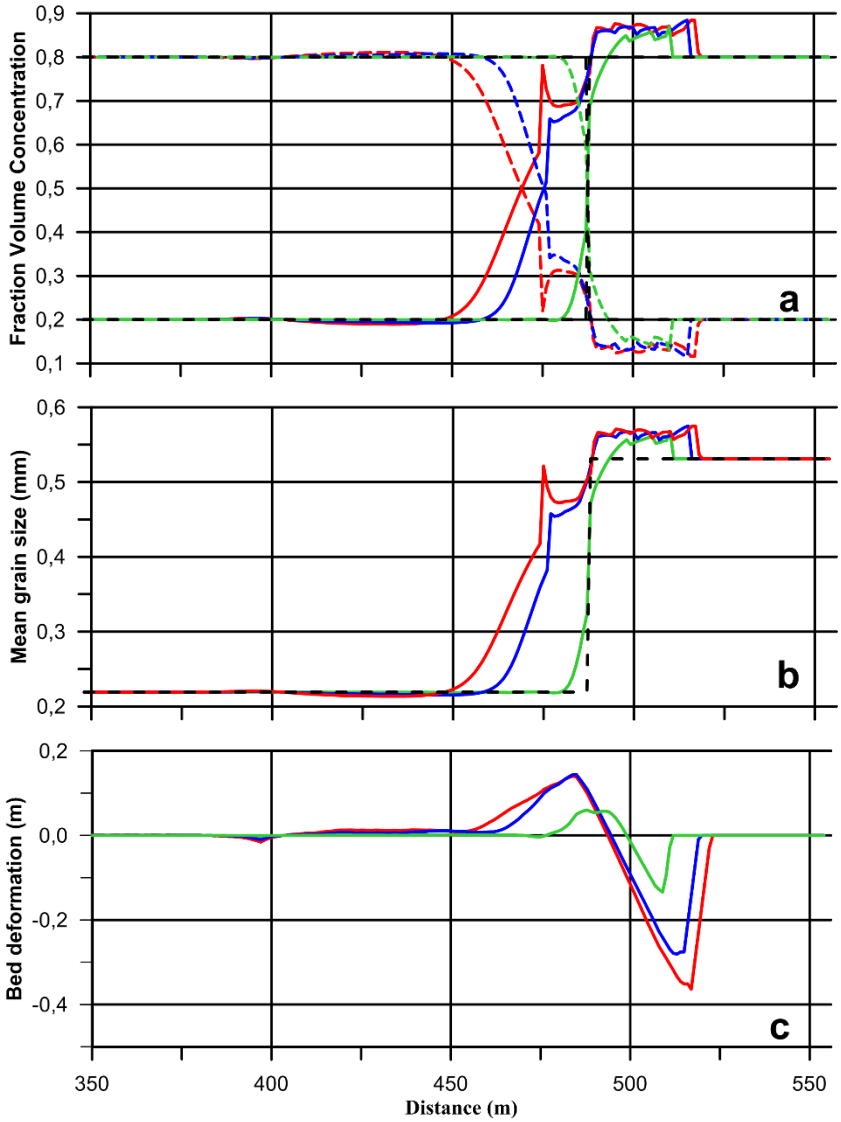

Fig. 4. (a) Distribution of the fraction volume concentration for BC2 (Hs = 2m, Tp = 8s), initial fraction volume concentration (black dotted line), fraction volume concentration after 3h (coarse fraction – green line, fine fraction – green dotted line), fraction volume concentration after 24 h (coarse fraction – blue line, fine fraction – blue dotted line), fraction volume concentration after 48h (coarse fraction – red line, fine fraction – red dotted line); (b) Distribution of mean grain size (D50) for BC2 (Hs = 2m, Tp = 8s), initial D50 (black dotted line), D50 after 3h (green line), D50 after 24 h (blue line), D50 after 48h (red line); (c) Bed deformations for BC2 (Hs = 2m, Tp = 8s), bed deformation after 3h (green line), bed deformation after 24 h (blue line), bed deformation after 48h (red line).

Redistribution of individual grain fractions of sediments starts immediately with the wave action. The results of simulations for both BC1 and BC2 types reveal movements of coarser particles towards the coast and movements of finer particles seaward (Fig. 3a, 4a). At the same time, the mean diameter of grain size D50 grows in the area of beach erosion and coastline retreat (Fig. 3b, 4b). With increasing the waving exposure, the total width of D50 changing band is expanded. As the result, a stable zone is formed near the coastline, in which the coarser sediments are concentrated. This zone is expanded mainly due to displacement of the water boundary due to erosion of the beach. Results of modeling indicate that the width of this zone does not depend on the initial distribution of grain fractions. Only wave parameters are important.

Processes of sediments redistribution for BC1 and BC2 reveal significant differences in the seaward part of the profile. The initial distribution of the sand fractions by the type BC1 is extremely rare in the nature. Homogeneous conditions may occur mainly for artificial beach nourishment. As a result, after 48 hours of storm for BC1, the distribution of D50 significantly different in comparison to initial (Fig. 3b). Deposition of fine factions take place in the seaward part of the profile . An increasing number of fine particles and decreasing D50 from 0.375 to 0.337 mm are observed. The offshore part of the profile is characterized by differentiation and transition to the originally specified distribution of sediments.

The initial distribution of sand fractions by type BC2 is similar to the field observations in the coastal zone of the Kalamitskiy Gulf. In this case, the initial sediment distribution is largely preserved in the seaward part of the profile (Fig. 4b). A monotonic decrease of D50 values is formed in the transition zone. Within the area of coarse material, the mean grain size increases from 0.53 to 0.57 mm. This demonstrates that redistribution of sediments under the wave action is insignificant in case the initial sediment composition is close to the nature.

IV. CONCLUSION

The XBeach model has been applied for the region of the Kalamitskiy Gulf at the west coast of Crimea. The obtained results show that the XBeach model can successfully simulate the bathymetry evolution and sand fraction redistribution.

The results of numerical experiments indicate that beach erosion and slope flattening in foreshore zone occur for all types of used wave conditions and sediment fractions distributions.

The increase of the period of wave action changes the amount of transported material, resulting in lengthening of the reformation zone and rising in the height and width of the forming bar. The bar width depends on the initial particle size distribution.

A sufficiently stable zone is formed near the coastline, in which the coarser sediments are concentrated. Yet, redistribution of sediments is insignificant in case the initial composition is close to the nature.

V. REFERENCES

[1] V.A. Ivanov, V.V. Fomin, “Mathematical Modelling of Dynamical Processes in the Sea-Land Area”, Kyiv: Akademperiodyka, 2010, 286 p.

[2] Yu. N. Goryachkin, V.V. Dolotov “Variations of shoreline of accumulative coast of the Western Crimea”, *Ecological safety of coastal and shelf zones and comprehensive use of shelf resources*: Collected scientific papers. 2011, Iss. 25, vol. 1, pp. 8 – 18. (in Russian).

[3] K.I. Gurov, E.I. Ovsyany, E.A. Kotel’yanets, S.K. Konovalov, “Geochemical characteristics of bottom sediments in the Kalamita Bay water area in the Black Sea”, *Marine Hydrophysical Journal*, 2014, vol. 5, pp. 69 – 80. (in Russian).

[4] “XBeach Manual”, Deltares, UNESCO-IHE Institute of Water Education and Delft University of Technology, 2015, 138 p.

MORPHODYNAMICS OF THE BAKALSKAYA SPIT OF THE BLACK SEA

Vladimir Fomin, Marine Hydrophysical Institute of RAS, Russia
Ludmila Kharitonova, Marine Hydrophysical Institute of RAS, Russia
Dmitrii Alekseev, Marine Hydrophysical Institute of RAS, Russia
Elena Ivancha, Marine Hydrophysical Institute of RAS, Russia

v.fomin@ukr.net

Studies of shape dynamics of the Bakalskaya Spit based on observation and numerical simulation are carries out. The Bakalskaya Spit is a dynamically active sand formation on the north-west coast of the Crimea Peninsula. Field observations and satellite image analyses showed that the erosion of spit west coast, eastward displacement of spit distal part and separation of distal part from the spit main part are the most significant processes. After the autumn storms in 2010 the isthmus between the distal part of spit and its main part was eroded and had not recovered till now. So the distal part of the Bakalskaya Spit turned into island. Dynamic of sediments depends on wind wave parameters and sea level oscillations. Effect of changing of wind wave direction and storm surge height on erosion and deposition processes in the Bakalskaya Spit region of the Black Sea is studied by using of XBeach numerical model. Dependencies of location and space dimension of erosion and deposition areas of sediments on characteristics of waves and surges are obtained. It is found that the most intensive erosion of spit isthmus occurs in case of wave running from the west in comparison of cases of wave running from the south-west and north-west if there are no surges. Presence of surges may results in increasing or decreasing of erosion process intensiveness depending on wave direction.

Key words: wind waves, wave currents, sediments, erosion, numerical simulation

I. INTRODUCTION

The Karkinitsky Bay of the Black Sea due to its morphological features (10 – 35 m depths, sandy and muddy bottom structure with the addition of shell limestone, the presence of islands and spits) is an area of intense morphodynamic processes. The Bakalskaya Spit which juts out into the Karkinitsky Bay at 8 km distance is characterized by special dynamic activity. The width of the spit western branch is 30 – 80 m, of the eastern branch – 1200 – 2000 m [1]. A narrow underwater sandbank (the Bakalskaya Bank) extends at up to 40 km distance to the North. The depths above its peak reach 3.5 – 4 m.

According to [2], the main morphodynamic processes in the area of the Bakalskaya Spit are the following: the erosion of the spit western coast; the extension of its distal part into the Karkinitsy Bay water area in the north-east direction; reduction of the spit width in the area of the isthmus, which connects the main part of the spit with its distal part; separation of distal part from the main

part of the spit. After the storms which took place in autumn, 2010 the isthmus was eroded and has not recovered yet, and the distal part of the spit became an island.

The dynamics of sediments in the Bakalskaya Spit region depends on wind waves and sea level oscillations [1], which should be reasonably taken into account during the numerical simulation. However, the setting of these parameters based on the field data or numerical calculations always contain some uncertainty [3]. So the estimation of the dependence of morphodynamic process simulation results in the Bakalskaya Spit region on the variations of wind wave parameters and the sea level is of interest. In this work such estimations are carried out on the basis of XBeach (eXtreme Beach behavior) [4] numerical hydrodynamic model.

II. Mathematical statement of the problem and solution method

XBeach model includes the interacting blocks on the calculation of short wind waves, barotropic currents and sediment dynamics. Short waves in the model are described by non-stationary equation of wave energy balance in the spectral form [4]. An angular distribution of wave spectrum is considered and one peak frequency is used, that is corresponded to the assumption of narrow-band spectrum in the frequency space. The equation of wave energy balance has the following form

$$\frac{\partial A}{\partial t}+\frac{\partial (c_x A)}{\partial x}+\frac{\partial (c_y A)}{\partial y}+\frac{\partial (c_\theta A)}{\partial \theta}=-\frac{D_w}{\sigma}, \qquad (1)$$

where t is the time; x and y are the horizontal coordinates; $A=E_w/\sigma$ is the wave action density; E_w is the wave energy; σ is the eigen wave frequency; θ is the direction of wave propagation; D_w is the energy dissipation rate due to the wave breaking; c_x, c_y and c_θ are the velocities of energy transfer in the direction of x, y and θ axes. The second and the third terms in the equation (1) describe energy transfer along the coordinate axes x, y, and the fourth term describes the effects of wave refraction on the bottom inhomogeneities and currents.

To describe the energy transfer from breaking waves to the rollers the equation of roller energy E_r balance is used [5]

$$\frac{\partial E_r}{\partial t}+\frac{\partial (c_x E_r)}{\partial x}+\frac{\partial (c_y E_r)}{\partial y}+\frac{\partial (c_\theta E_r)}{\partial \theta}=D_w-D_r\,. \qquad (2)$$

Here the energy source is D_w, and D_r is the dissipation rate of rollers.

The currents induced by short waves are described by non-linear shallow water equations

$$\frac{\partial u}{\partial t}+u\frac{\partial u}{\partial x}+v\frac{\partial u}{\partial y}-fv+g\frac{\partial \eta}{\partial x}-\mu\left(\frac{\partial^2 u}{\partial x^2}+\frac{\partial^2 u}{\partial y^2}\right)=\frac{F_x-\tau_{bx}}{\rho h}, \qquad (3)$$

$$\frac{\partial v}{\partial t}+u\frac{\partial v}{\partial x}+v\frac{\partial v}{\partial y}+fu+g\frac{\partial \eta}{\partial y}-\mu\left(\frac{\partial^2 v}{\partial x^2}+\frac{\partial^2 v}{\partial y^2}\right)=\frac{F_y-\tau_{by}}{\rho h}, \tag{4}$$

$$\frac{\partial \eta}{\partial t}+\frac{\partial (hu)}{\partial x}+\frac{\partial (hv)}{\partial y}=0, \tag{5}$$

where η is the elevation of level; u, v are the current velocity components; f is the Coriolis parameter; g is the acceleration of gravity; μ is the turbulent viscosity coefficient; ρ is the water density; h is the dynamic depth; τ_{bx}, τ_{by} are the components of bed shear friction stresses which are squarely dependent on the velocities of currents; F_x, F_y are the components of wave-induced additional momentum. These values have the following form

$$F_x=-\frac{\partial (S_{xx}+R_{xx})}{\partial x}-\frac{\partial (S_{xy}+R_{xy})}{\partial y}, \quad F_y=-\frac{\partial (S_{xy}+R_{xy})}{\partial x}-\frac{\partial (S_{yy}+R_{yy})}{\partial y}. \tag{6}$$

In the formulas (6) S_{ij} and R_{ij} ($i, j = x, y$) are the stresses due to the presence of waves and rollers, respectively, and depending on E_w and E_r.

In *XBeach* model the flows of sediments are determined by expressions [5]

$$Q_x=hCu-\mu_c h\frac{\partial C}{\partial x}, \qquad Q_y=hCv-\mu_c h\frac{\partial C}{\partial y}, \tag{7}$$

here C is the depth-averaged concentration of sediments; μ_c is the turbulent diffusion coefficient. Changes of C are described by advection-diffusion equation of the following form

$$\frac{\partial (hC)}{\partial t}+\frac{\partial Q_x}{\partial x}+\frac{\partial Q_y}{\partial y}=h\frac{C_{eq}-C}{T_{eq}}, \tag{8}$$

where C_{eq} is the equilibrium concentration; T_{eq} is the adaptation time of concentration to the equilibrium state. Further, using the known Q_x and Q_y values the bed deformations are calculated from the equation [5]

$$(1-p)\frac{\partial z_b}{\partial t}+\frac{\partial q_x}{\partial x}+\frac{\partial q_y}{\partial y}=0, \tag{9}$$

where $q_x=Q_x+\alpha|u|\frac{\partial z_b}{\partial x}$; $q_y=Q_y+\alpha|v|\frac{\partial z_b}{\partial y}$; z_b is the bed surface coordinate; p is the soil porosity; $\alpha = 1–10$ is the setup parameter.

Solving the equation (1) it is assumed that at the rigid lateral boundaries $E_w = 0$. By the angular variable $E_w(\theta = 0) = E_w(\theta = 2\pi)$ periodicity condition is used, by the frequency variable for minimum $\sigma_{\min}$ and maximum $\sigma_{\max}$ frequencies – $E_w(\sigma_{\min}) = E_w(\sigma_{\max}) = 0$ condition is used. In *XBeach* model for the specifying of boundary conditions at the seaward boundary a 2-D frequency-angular spectrum of the following form is used

$$E_w(\sigma,\theta) = F(\sigma)\psi(l)\cos^{2l}\left(\frac{\theta-\bar{\theta}}{2}\right), \qquad \psi(l) = \frac{2^{2l-1}}{\pi}\frac{\Gamma^2(l+1)}{\Gamma(2l+1)}, \tag{10}$$

where l is the index of angular wave dissipation; Γ is the gamma function; $F(\sigma)$ is the *JONSWAP* (*Joint North Sea Wave Project*) frequency spectrum calculated by the following formula

$$F(\sigma) = 0{,}307\,\alpha_F \frac{h_s}{\sigma_p}\frac{\exp(-1{,}23a^{-4})}{a^5}\gamma^{\beta}, \tag{11}$$

where $a = \sigma/\sigma_p$; $\beta = \exp\left(-\frac{(a-1)^2}{2b}\right)$; $b = \begin{cases} 0{,}07 \text{ at } a \le 1 \\ 0{,}09 \text{ at } a > 1 \end{cases}$; h_s is the significant wave height; σ_p is the wave frequency corresponding to the spectral peak ($\tau_p = 2\pi/\sigma_p$ is the spectra peak period); γ is the spectral peakedness parameter; α_F = 0.0131 is the generalized Phillips parameter.

In the shallow water equations (3) – (5) and in the sediment transport equation (8) the absence of fluid flows and sediment ones at rigid lateral boundaries is assumed. At the open boundaries a condition of weak reflection based on the Method of Characteristics [4] is assumed.

In the XBeach model for difference approximation of (1) – (9) equations a rectangular staggered grid is used. Depth, level, sediment concentration, wave and roller energy are determined in cell centers, and current velocity components, sediment flows and right parts of (3) and (4) equations are determined in the middle of lateral boundaries. The integration is performed on the basis of explicit scheme with an automatic time step selection. In the difference scheme, utilized in the XBeach model, a drying/flooding algorithm is implemented [4].

III. INPUT PARAMETERS

Digital model of the studied region relief is developed on the basis of the Karkinitsky Bay 1:200 000 scale navigation chart and the data obtained as a result of Marine Hydrophysical Institute expeditions in July, 2007. During the expedition on July, 21 a bathymetric observation of the Bakalskaya Spit coastal zone from a small vessel was performed. Coastline contour and cross section profiles of spit isthmus and head were obtained during the expedition on July, 27 – 28 according to high-precision GPS-observation data (Fig. 1, *a*). The analysis of cross section profiles across the main part of the spit showed that beach excess over the sea level in the area of the isthmus (which separates the head from the main part of the spit) is up to 0.9 m.

The seabed relief of computational domain, which covers the northern part of the Bakalskaya Spit and Bakalskaya Bank and has 2.2 × 2.9 km dimensions, is represented in Fig. 1, *b*. Grid steps for *x* and *y* axes are 17 and 19 m, respectively. Inasmuch as the Bakalskaya Spit is a sandy formation [1], we will assume that the spit and the seabed near it consist of medium sand with $D_{50} = 5 \cdot 10^{-4}$ particle size and 2650 kg/m^3 density [6].

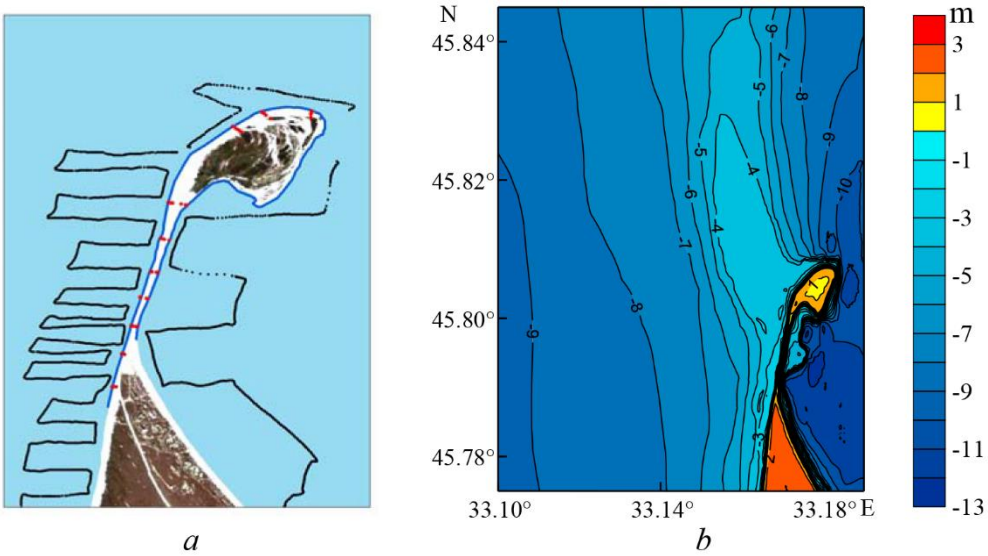

Fig. 1. Observation work diagram in the Bakalskaya Spit region in July, 2007 (black points – depth measurements, red points – cross section profiles across the main part of the spit, blue line – coastline measured contour) (a) and also a schematic map of computational domain land and seabed relief (m) (b)

IV. Analysis of numerical experiment results

It is known [7] that morphodynamic processes in the sea coastal zone are mainly effected by wind waves and wave currents (caused by wind waves). The direction of wave propagation and wave intensity are determined by wind effect and also by shoreline and seabed features. Besides, wave transformation near the coast is effected by local hydrodynamic processes such as surges, which can lead to sufficient increase of dynamic depth. For example, in the apex of Karkinitsky Bay storm surges can reach 4 m height [8]. Therefore, we are to study the effect of wind wave direction and storm surge magnitude on the process of Bakalskaya Spit erosion.

At first let's consider a sediment transport in case of the storm wave running from the south-west, west and north-west in the absence of storm surges. At the northern, eastern and southern boundaries of computational domain the free passage conditions for the waves were specified. At the western boundary the incoming wave parameters were determined on the basis of (10), (11) relations. So far as the *XBeach* model is applied for the small coastal zone regions, the model does not take into account a spatial variability of wave spectrum specified at the western boundary. *JONSWAP* frequency spectrum parameters in the numerical experiments were considered as the following: the significant wave height h_s = 4 m; the wave peak period τ_p = 6 s; the spectral peakedness γ = 3.3; the index of angular wave dissipation l = 10. These parameters correspond to

the developed storm wind waves and are obtained from the preliminary numerical experiments using spectral wave model *SWAN* (*Simulating Waves Near Shore*) [9].

The directions of steady wave currents (in 10 hours after the start of wind wave effect) generally correspond to the directions of running waves in all considered cases. Local features are manifested in the field of wave current velocities near the Bakalskaya Spit and above the Bakalskaya Bank. Thus, when waves run from the south-west in the narrow band along the spit western coast an increase of current velocities takes place, and when waves run from the north-west at the northernmost tip of the spit a cyclonic eddy is observed. Above the Bakalskaya Bank the wave currents in these cases are directed almost meridionally.

An erosion of isthmus between the distal part of the spit and its main part and the occurrence of scour are observed at all considered wave directions (Fig. 2, *a* – *d*). This process occurs most intensively when the waves run from the west (Fig. 2, c). In 4 hours a spit segment in the isthmus area appeared to be flooded, and after 24 hours the depths in this place reach 2 – 3 m (Fig. 3, *c*). In case of wave running from the south-west and north-west the isthmus appeared to be eroded in 8 hours and in 24 hours it appeared to be flooded at 1 – 2 m depths (Fig. 3, *a*, *e*). In all considering cases in the formed scour zonal component of wave current increases. Besides, in case of the wave running from the west in the scour a local intensification of wave currents takes place.

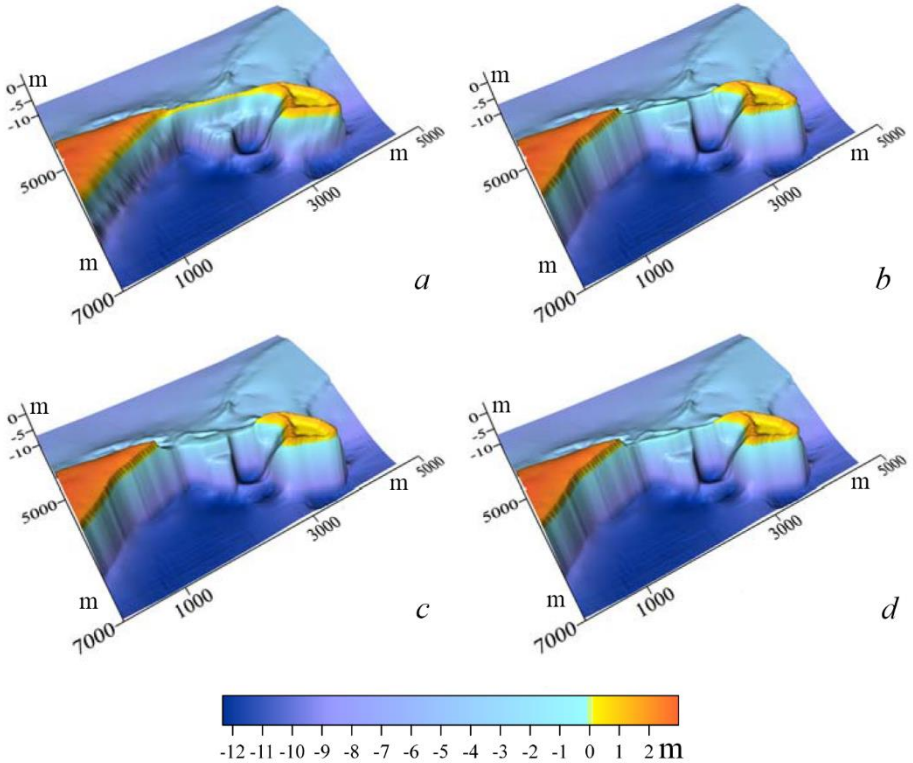

Fig. 2. The Bakalskaya Spit profile prior to the effect of waves and currents (a) and after 24 hours of wave running from the south-west (b), west (c) and north-west (d)

In the considering cases of wave running erosion occurs along the entire Bakalskaya Spit coastal zone (Fig. 3, *b*, *d*, *f*). The intensity of this process reaches its maximum along the west coast in the isthmus area, near the north-east segment of the head and also near the eastern shore,

southward and northward of the scour occurred at the site of isthmus. When the waves run from the west the erosion areas directly in the isthmus region are the most extensive both in the zonal and meridional directions (Fig. 3, *d*). In case of wave running from the south-west erosion occurs at depths which are slightly greater than in case of wave running from the north-west (Fig. 3, *b*, *f*).

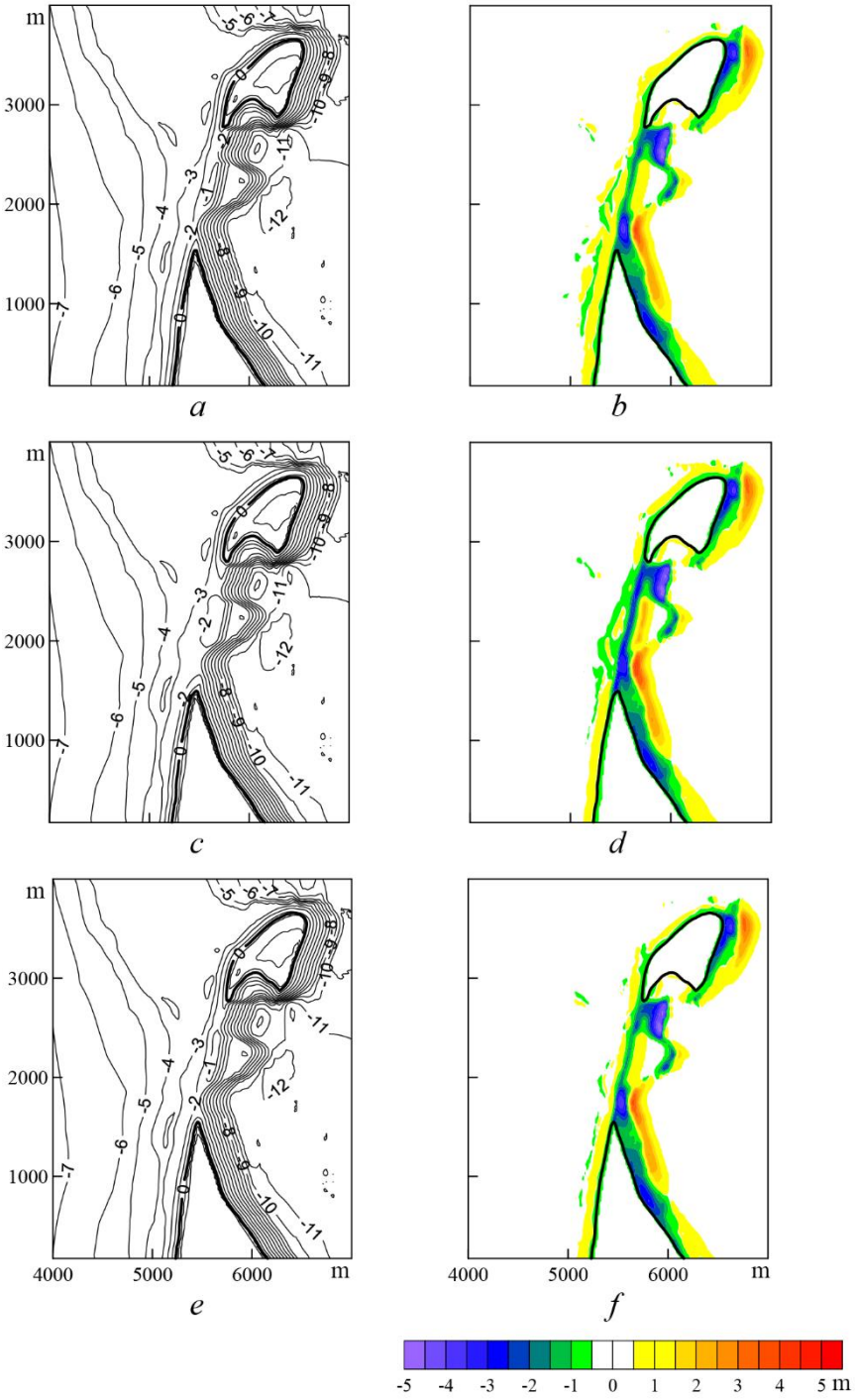

Fig. 3. Land and seabed relief (m) in the Bakalskaya Spit region after 24 hours of 4 m height wave running from the south-west (a), west (c) and north-west (e) and also the corresponding relief changes (b, d, f)

The sediment accumulation on the seabed occurs seawards of erosion areas in a close proximity to them (Fig. 3, *b, d, f*). However, it doesn't take place along the entire Bakalskaya Spit coastline. So, when the waves run from the west there is practically no accumulation zone occurrence to the west of the isthmus. In all considering cases the most significant sediment accumulation takes place to the east of the spit head and to the south-east of the scour along the eastern coast of the spit. An accumulation zone westward from the spit appears to be the most significant in case of wave running from the south-west, and eastward from the spit – in case of wave running from the west (Fig. 3, *b, d*). In the latter case the amount of accumulated sediments eastward from the spit also appears to be the most significant.

Now let us consider morphodynamic processes in the presence of storm surges. The calculations were carried out for four constant in time values of surges: 0.25; 0.50; 0.75; 1.00 m. Whereas the height of the Bakalskaya Spit isthmus in the applied digital relief doesn't' exceed 0.6 – 0.7 m, it was completely flooded at surges with 0.75 and 1.00 m values.

The spatial structure of steady wave currents in the presence of surges largely remains the same as it was without them. Changes of erosion characteristics are manifested in the areas with depths up to 3 m in close proximity to the Bakalskaya Spit and depend on the direction of wave running. Particularly, when the waves run from the south-west and north-west the intensity of erosion processes in the isthmus area increase with the growth of surge height (Fig. 4, *a, e*). At the same time the difference in intensity and spatial localization of erosion becomes noticeable in these two cases. In case of wave running from the north-west the isthmus is eroded somewhat intensively than in case of wave running from the south-west. For example, in the first case after 24 hours at 0.75 m height surge the depth of erosion in certain isthmus areas reaches 3 m below the undisturbed sea level, and in the second case the same depth of erosion is reached at the surge with 1 m height. When integrating the model equations at longer time intervals these differences become noticeable at lower surge heights. In case of wave running from the west, on the contrary, the depth of isthmus erosion decreases with the increase of surge height (Fig. 4, *c*). Thus, after 24 hours the erosion up to 3 m below the undisturbed sea level at 0.25 m surge occurs in the north and the south of the isthmus except for its central part. At 0.50 m surge such magnitude of erosion is observed only in the south, closer to the main part of the Bakalskaya Spit.

Thus, the obtained results are consistent with the conclusions made when carrying out the calculations at a coarse grid without taking into account the modern measurements of the Bakalskaya Spit topography [10]. These conclusions are the following: in the presence of storm surges hydrodynamic processes, caused by wave running in direction range from western to the north-western, are most conducive to separation of the Bakalskaya Spit head from its main part.

The presence of storm surges doesn't effect the localization of erosion areas along the Bakalskaya Spit shore, but it effects characteristics of sediment accumulation areas. This effect is the most significant along the western shore. With the increase of surge height, the accumulation areas extend seaward, exceeding the erosion areas by the width in several regions (Fig. 4, *b, d, f*). The most extensive accumulation areas are formed at wave running from the south-west. In case of wave running from the west (after 24 hours and with the absence of surges) accumulation areas in

the isthmus zone are insufficient, and in the presence of surges higher than 0.5 m they become sufficient and their areas exceed the ones of erosion zones.

V. Conclusions

In conclusion we will briefly formulate the main results of study of morphodynamic process dependences in the Bakalskaya Spit region on the wind wave and storm surge parameters.

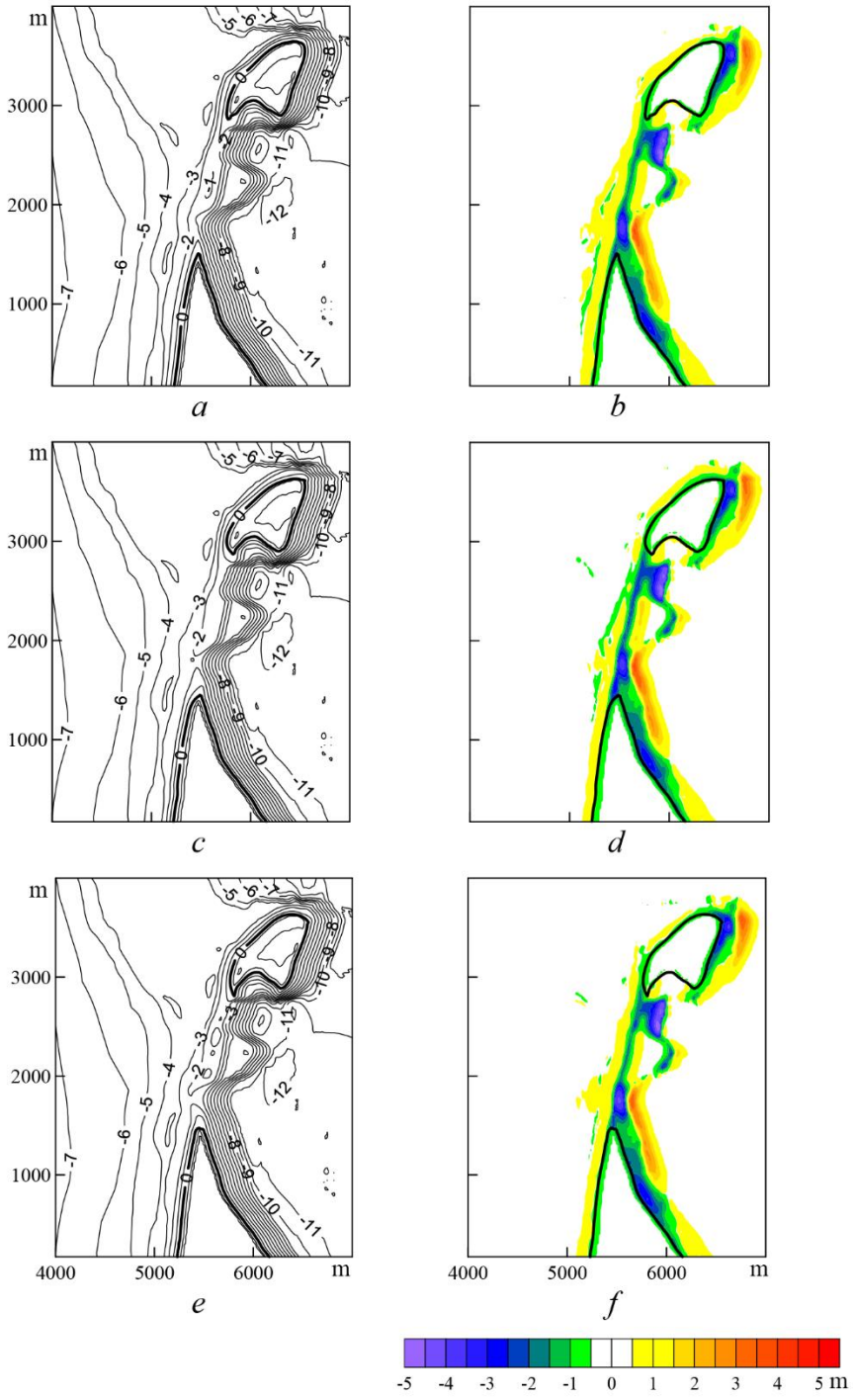

Fig. 4. Land and seabed relief (m) in the Bakalskaya Spit region after 24 hours of 4 m height wave running from the south-west (a), west (c) and north-west (e) and corresponding relief changes (b, d, f) in the presence of surge with 0.75 m height

In all considered cases the *XBeach* model reproduces basic characteristics of the Bakalskaya Spit dynamics, obtained from the observational data analysis [2]. These characteristics could include: spit head displacement in the north-west direction due to erosion of its western part and sediment accumulation near its north-eastern part; spit erosion in the area of the isthmus, which connects the main part of the spit with its distal part up to its separation.

The most intensive erosion of the isthmus between the Bakalskaya Spit head and main part in the absence of surges occurs at wave running from the west. The wave running from the south-west and north-west causes erosion processes of almost equal intensity. Seabed erosion occurs along the entire coastline of the spit with different intensity. Sediment accumulation takes place seawards of erosion areas, but not continuously along the entire coast. The areas of most significant sediment accumulation are located to the east from spit head and to the south-west from the scour, along the eastern shore of the spit.

Storm surge effect on the morphodynamic process characteristics depends on the direction of wave running. In case of wave running from the south-west and north-west, seabed erosion intensity in the isthmus area increase with the surge height rising. At wave running from the north-west the isthmus erosion is somewhat more intensive than at wave running from the south-west. In case of wave running from the west, the increase of surge height results in the decrease of isthmus erosion depth. The presence of surges has no effect on the location of erosion areas. Sediment accumulation areas at that extend seawards.

VI. References

[1] V.A. Ivanov, Yu.N. Goriachkin, V.F. Udovik, L.V. Kharitonova, and S.A. Shutov, "Current state and evolution of the Bakalskaya Spit," *Ecological Safety of Coastal and Shelf Areas and Comprehensive Use of Resources Shelf*, vol. 1, no. 26, Sevastopol: ECOSI-Gidrofizika, 2012, pp. 8-15.

[2] Yu.N. Goriachkin, L.V. Kharitonova, and V.V. Dolotov, "Changeability of the coastline of the North-West Crimea," *Ecological Safety of Coastal and Shelf Areas and Comprehensive Use of Resources Shelf*, no. 20, Sevastopol: ECOSI-Gidrofizika, 2009, pp. 18-26.

[3] R. McCall, *The longshore dimension in dune overwash modelling. Development, verification and validation of XBeach*, Thesis: Delft University of Technology, 147 p.

[4] *XBeach model description and manual*, Unesco-IHE Institute for Water Education, Deltares and Delft University of Technology, 2010, 106 p.

[5] D. Roelvink, A. Reniers, A. van Dongeren, J. van Thiel de Vries, R. McCall et al., "Modeling storm impacts on beaches, dunes and barrier islands," *Coastal Engineering*, vol. 56, 2009, pp. 1133-1152.

[6] A.F. Blumberg, *A primer for ECOMSED, Version 1.3*, Mahwah New Jersey: HydroQual, Inc., 2002, 188 p.

[7] A.S. Blatov and V.A. Ivanov, *Hydrology and hydrodynamics of the Black Sea shelf zone*, Kiev: Naukova Dumka, 1992, 244 p.

[8] Yu.N. Goriachkin and V.A. Ivanov, "Current state of the Crimea Black Sea coast," *Reports of the NAS of Ukraine*, no. 10, 2010, pp. 87-92.

[9] http://www.swan.tudelft.nl.

[10] V.V. Fomin, D.V. Alekseev, and L.V. Kharitonova, "Modelling of the morfodynamic of the Bakalskaya Spit," *Ecological safety of coastal and shelf areas and comprehensive use of resources shelf*, Sevastopol: ECOSI-Gidrofizika, no. 27, 2013, pp. 374-380.

NUMERICAL MODELING OF STORM SURGES, WIND WAVES AND FLOODING IN THE TAGANROG BAY

Vladimir Fomin, Marine Hydrophysical Institute of RAS, Russia
Dmitrii Alekseev, Marine Hydrophysical Institute of RAS, Russia
Dmitrii Lazorenko, Marine Hydrophysical Institute of RAS, Russia

fomin.dntmm@gmail.com

Storm surges and wind waves are ones of the most important hydrological characteristics, which determine dynamics of the Sea of Azov. Extreme storm surges in Taganrog Bay and flooding in the Don Delta can be formed under the effect of strong western winds. In this work the sea level oscillations and wind waves in the Taganrog Bay were simulated by means of the coupled SWAN+ADCIRC numerical model, taking into account the flooding and drying mechanisms. The calculations were carried out on an unstructured mesh with high resolution. The wind and atmospheric pressure fields for the extreme storm from 20 to 28 of September, 2014 obtained from WRF regional atmospheric model were used as forcing. The analysis of simulation results showed the following. The western and northern parts of the Don Delta were the most flood-prone during the storm. The size of the flooded area of the Don Delta exceeded 50%. Interaction of storm surge and wind wave accelerated the flooding process, increased the size of the flooded area and led to the intensification of wind waves in the upper of Taganrog Bay due to the general rise of the sea level.

Key words: the Sea of Azov, storm surge, wind waves, flooding, SWAN, ADCIRC, wetting/drying, parallel computing.

I. INTRODUCTION

Storm surges and wind waves are ones of the most important hydrological characteristics, which determine dynamics of the Sea of Azov on synoptic scales. Extreme storm surges of 2–3 m height in Taganrog Bay [1, 2] and flooding in the Don Delta can be formed under the effect of strong western winds. There have been several such cases over the past 20 years: April 12, 1997; March 1, 2005; September 30, 2010; March 24, 2013; September 24, 2014. The two latter cases are described in [2, 3].

In [4], a numerical simulation technology of storm surges and wind waves in the Sea of Azov is presented by means of tightly-coupled SWAN+ADCIRC model [5]. The model validation has shown that it adequately describes the Sea of Azov level variations during intense storms.

Characteristics of storm surge and wind waves in the Taganrog Bay during the extreme storm of September 24–25, 2014, are studied in this work with the mesh of abovementioned technology. High resolution unstructured computational mesh has been created for this purpose. The mesh describes bathymetry and topography of the Don Delta in detail.

II. MODEL DESCRIPTION

The coupled model SWAN+ADCIRC integrates two models – SWAN (Simulation Waves Nearshore) [6, 7] and ADCIRC (Advanced Circulation Model for Shelves Coasts and Estuaries) [8, 9]. Both models are used to simulate the wind waves and storm surge.

The ADCIRC model basic equations are defined as follows

$$\frac{\partial U}{\partial t}+U\frac{\partial U}{\partial x}+V\frac{\partial U}{\partial y}-fV=-g\frac{\partial}{\partial x}\left[\eta+\frac{P_a}{g\rho_0}\right]+\frac{\tau_{sx}-\tau_{bx}}{\rho_0 H}+\frac{M_x-D_x}{H}, \quad (1)$$

$$\frac{\partial V}{\partial t}+U\frac{\partial V}{\partial x}+V\frac{\partial V}{\partial y}+fU=-g\frac{\partial}{\partial y}\left[\eta+\frac{P_a}{g\rho_0}\right]+\frac{\tau_{sy}-\tau_{by}}{\rho_0 H}+\frac{M_y-D_y}{H}, \quad (2)$$

$$\frac{\partial^2\eta}{\partial^2 t}+\tau_0\frac{\partial\eta}{\partial t}+\frac{\partial J_x}{\partial x}+\frac{\partial J_y}{\partial y}-Q_x\frac{\partial\tau_0}{\partial x}-Q_y\frac{\partial\tau_0}{\partial y}=0. \quad (3)$$

Where t is time; x, y are horizontal coordinates; U, V are current velocity components; η is the free surface elevation; f is the Coriolis parameter; g is the gravitation acceleration; P_a is the atmospheric pressure at the surface; ρ_0 is the reference density of water; $H = h + \eta$ is the total water depth; h is the sea bottom; M_x, M_y are the horizontal eddy-viscosity terms; D_x, D_y are terms, obtained after differential transformations of the original system of equations [9]; τ_{bx}, τ_{by} are bottom stress components; τ_0 is the weighting factor that optimizes the phase propagation properties [10]; $Q_x = UH$, $Q_y = VH$ are fluxes per unit width;

$$J_x=-Q_x\frac{\partial U}{\partial x}-Q_y\frac{\partial U}{\partial y}+fQ_y-\frac{g}{2}\frac{\partial\eta^2}{\partial x}-\frac{H}{\rho_0}\frac{\partial P_a}{\partial x}+\frac{\tau_{sx}-\tau_{bx}}{\rho_0}+(M_x-D_x)+\tau_0 Q_x+U\frac{\partial\eta}{\partial t}-gH\frac{\partial\eta}{\partial x};$$

$$J_y=-Q_x\frac{\partial V}{\partial x}-Q_y\frac{\partial V}{\partial y}-fQ_x-\frac{g}{2}\frac{\partial\eta^2}{\partial y}-\frac{H}{\rho_0}\frac{\partial P_a}{\partial y}+\frac{\tau_{sy}-\tau_{by}}{\rho_0}+(M_y-D_y)+\tau_0 Q_y+V\frac{\partial\eta}{\partial t}-gH\frac{\partial\eta}{\partial y}.$$

The following notations are used in (1) – (3):

$$\tau_{sx}=\tau_{sx,wind}+\tau_{sx,wave},\quad \tau_{sy}=\tau_{sy,wind}+\tau_{sy,wave}, \quad (4)$$

$$\tau_{sx,wind}=\rho_a C_a W_x\sqrt{W_x^2+W_y^2},\quad \tau_{sy,wind}=\rho_a C_a W_y\sqrt{W_x^2+W_y^2}, \quad (5)$$

$$\tau_{bx}=\rho_0 C_d U\sqrt{U^2+V^2},\quad \tau_{by}=\rho_0 C_d V\sqrt{U^2+V^2}, \quad (6)$$

where ($\tau_{sx,\,wind}$, $\tau_{sy,\,wind}$) and ($\tau_{sx,\,wave}$, $\tau_{sy,\,wave}$) are surface stresses due to wind and waves, respectively; ρ_a is the air density; W_x, W_y are wind velocity vector components; C_a is the surface stress coefficient; C_d is the bottom stress coefficient.

The stress coefficients in (5) and (6) are given by

$$C_a = 0{,}001\left(0{,}75 + 0{,}067\sqrt{W_x^2 + W_y^2}\right), \qquad C_d = gn^2 / H^{1/3}, \tag{7}$$

where n is Manning's roughness. In general, n is a function of the spatial coordinates and it depends on the type of the underlying surface and the properties of soil and vegetation cover.

SWAN predicts the evolution in geographical space and time of the wave action spectral density $N(x, y, t, \theta, \sigma)$, where θ is the wave direction and σ is the relative frequency, by means of the following equation [6]

$$\frac{\partial N}{\partial t} + \frac{\partial}{\partial x}\left[(c_x + U)N\right] + \frac{\partial}{\partial y}\left[(c_y + V)N\right] + \frac{\partial}{\partial \theta}\left(c_\theta N\right) + \frac{\partial}{\partial \sigma}\left(c_\sigma N\right) = \frac{S_{tot}}{\sigma}, \tag{8}$$

where (c_x, c_y) is the group velocity, c_θ and c_σ are propagation velocities in the θ and σ spaces. The source term S_{tot} denote the wave growth by wind, the action lost due to white-capping, surf breaking and bottom friction, and the action exchanged between spectral components due to the nonlinear effects in deep and shallow water.

SWAN computes wave characteristics by using of fields of wind velocities obtained from atmospheric model, as well as sea level and currents obtained from ADCIRC. In its turn, in ADCIRC wave stresses obtained from SWAN is used, which are given by

$$\tau_{sx,waves} = -\frac{\partial S_{xx}}{\partial x} - \frac{\partial S_{xy}}{\partial y}, \qquad \tau_{sy,waves} = -\frac{\partial S_{xy}}{\partial x} - \frac{\partial S_{yy}}{\partial y}, \tag{9}$$

where S_{xx}, S_{xy}, S_{yy} are wave radiation stresses.

In SWAN model the Grant-Madsen method [11] is used for parameterization of the bottom friction. In this method the bottom roughness scale k_N depends on Manning's roughness n values used in ADCIRC. This is achieved by using relationship $k_N = 30z_0$, where z_0 is defined as [12]

$$z_0 = H \exp\left[-\left(1 + 0{,}4\frac{H^{1/6}}{n\sqrt{g}}\right)\right]. \tag{10}$$

SWAN and ADCIRC are executed sequentially on the same unstructured grid and use the same set of computational cores. Both models use Message Passing Interface (MPI), which allows the use of parallel computing.

The coupled model allows to introduce the total sea level (TSL) as a sum:

$$\mathrm{TSL} = \mathrm{SL} + \mathrm{CW}, \tag{11}$$

where $\mathrm{SL} = \eta$ is the sea level variations due to the combined effect of wind stresses, atmospheric pressure and wave stresses; $\mathrm{CW}=H_s/2$ is the height of wind wave crests; H_s is the significant wave height (SWH) from SWAN. Actually, the TSL gives more adequate estimation of the sea level variations, since it includes both low- and high-frequency components.

III. RESULTS OF NUMERICAL EXPERIMENTS AND DISCUSSION

In numerical experiments a finite element mesh comprised of 178 565 nodes (348 735 triangular elements) was utilized. The mesh included the Sea of Azov and Kerch Strait (Fig. 1). The size of triangular elements edges varies from 50 to 800 m. Integration time steps in ADCIRC and SWAN were 1 s and 600 s respectively. The angular resolution in SWAN was set to 10°. A grid with 40 nodes was used for frequency coordinate in the range of 0.03 – 1.4 Hz. Two values were used for Manning's roughness: 0.025 for the sea bottom; 0.10 for the land. The weighting coefficient τ_0 is defined by: $\tau_0 = 0.03+1.5C_d\sqrt{U^2+V^2}/H$.

ADCIRC has 2 tuning parameters: $H_{\min}$ is the minimal water depth at which the calculated cell is inactive and removed from the calculations; $U_{\min}$ is the minimal velocity at which the cell is opened for flooding. According to [13], these parameters are set to be 0.1 m and 0.01 m/s respectively. The impact of the river discharge on the Don Delta flooding was not considered. A radiation condition was used on the southern border of the Kerch Strait.

A series of numerical experiments on modeling of wind waves and the Sea of Azov level was carried out for the extreme storm situation, which happened on September 24–25, 2014, and was caused by the passage over the sea of fast and deep cyclone, which was formed in the western part of the Black Sea.

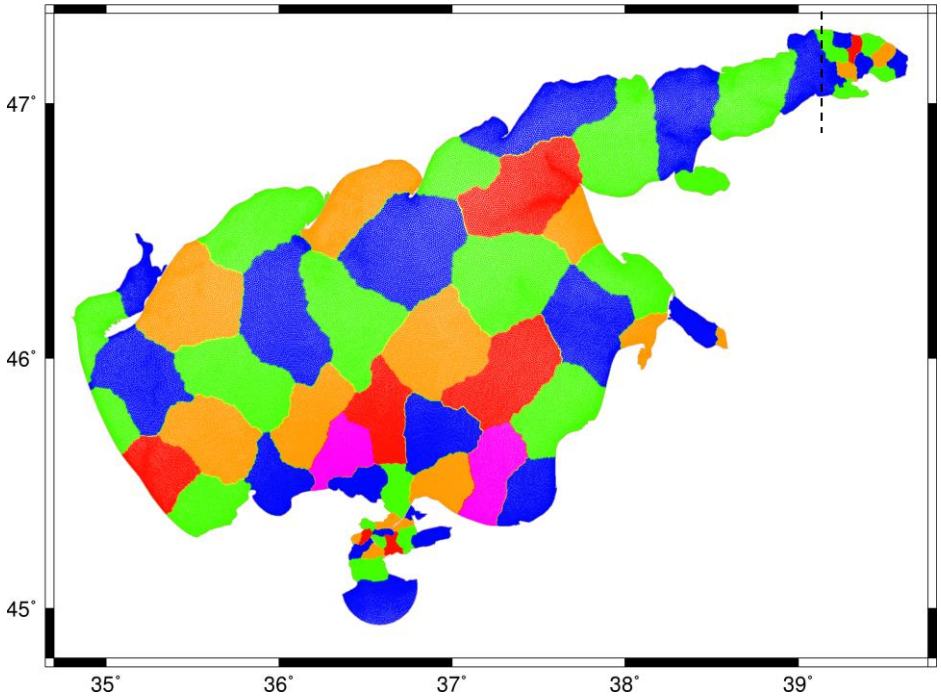

Fig. 1. Finite element mesh for the Sea of Azov. Colors indicate local sub-meshes and shared boundary layers (domain decomposition for 64 computational cores).

Surface wind and atmospheric pressure fields with spatial resolution of 7 km and time resolution of 3 hours from the WRF regional model (ecobase.org.ua) for the period from 20 to 28 of September 2014 were used as atmospheric forcing. According to the WRF data, the maximum wind speed in the Taganrog Bay during the specified time period varied from 17 m/s in the Don Delta area up to 21 m/s in Dolzhansky Strait.

Figure 2 shows the time variations of wind speed and wind direction from the WRF model for the Don delta for the period from 20 to 28 of September 2014. The wind direction is measured counter-clockwise in relation to the *x*-axis, which points to the east. As it can be seen, during the first 90 hours the wind was predominantly eastern and south-eastern with the velocity of 7.5 m/s. Next day the wind velocity increased to 17 m/s. Then there was a sharp change of wind direction from south-eastern to western, which created suitable conditions for the formation of strong storm surge at th**e** upper of Taganrog Bay.

Numerical experiments were carried out with zero initial conditions. In the first experiment (E1), the coupling between ADCIRC and SWAN was off, and thus, mechanisms of interaction between currents, sea level and wind waves were not taken into account. These mechanisms were accounted for in the second experiment (E2). In the experiment E1 bottom roughness scale $k_N = 0.01$ m was used. In the experiment E2 $k_N = 30z_0$, where z_0 is defined by the relationship (10).

The analysis of the results of numerical experiments shows that overall sea level decrease and damped oscillations on its background took place in the bay during the first 3,5 days. Sea level rise began in the first half of September, 24, due to a sharp change in wind direction from offshore to onshore. Starting from September, 25, the wind velocity began to decrease, leading to a gradual sea level fall in the bay.

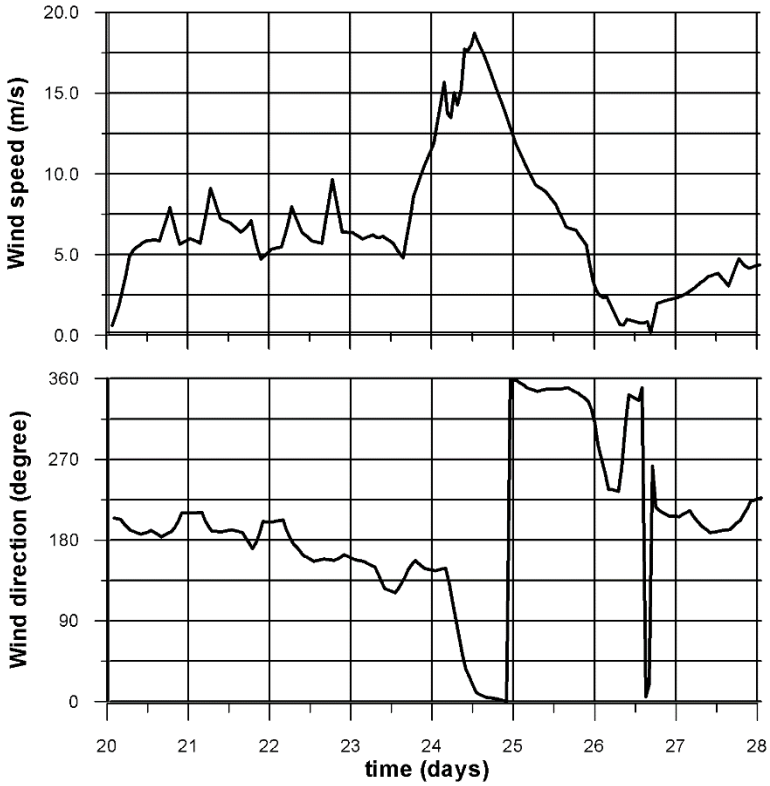

Fig. 2. Time series of the simulated wind velocity and wind direction in the Don delta for the period 20–28 of September 2014.

Fig. 3 shows the Don Delta flooding extent for four characteristic moments of time. The following procedure was developed for construction of these fields. The dynamic depth H in all cell points was compared with constant $H_{\min}$ at any time. If all three cell nodes satisfied the condition $H > H_{\min}$ at the same time, than the cell was considered to be flooded. As can be seen, notable flooding regions in the Don delta began to appear, starting from September, 25. Western and northern parts of the delta turned out to be more vulnerable to flooding.

The flooding index (FI) was used to evaluate changes of the flooded area size in the Don Delta over time:

$$\mathrm{FI}(t) = \left(1 - \frac{S(t)}{S(0)}\right) \cdot 100\%, \quad S(t) = \iint_{\Omega} \delta_d(x,y,t)\,dxdy, \quad \delta_d(x,y,t) = \begin{cases} 1, & H(x,y,t) \le H_{\min} \\ 0, & H(x,y,t) > H_{\min} \end{cases}, \quad (12)$$

where $S(t)$ is the size of dry land at a moment t in time; $S(0)$ is the area of dry land at initial time. $H_{\min}$ is the minimum depth in the wetting and drying algorithm. In (12), the integration is performed in the Ω region, the western boundary of which is represented by a vertical dashed line on Fig. 1. The flooding index represents variation of the sum of all dry areas in the Don delta over time in percentage. If bottom dries, then $S(t) > S(0)$ and the flooding index becomes negative.

Fig. 4 shows the dependence of the flooding index on time for the period from 20 to 28 September, 2015. The blue curve represents the E1 experiment, the red curve represents the E2 experiment. As it can be seen, the sea level decreased from 20 to 23 September. This manifested

itself in a periodic increase of the dry land area by 5–8%. Then, after the change of wind direction, a sharp flooding of the delta began, and in the next 24 hours the delta area decreased by about 40%. Following that, the flooding rate decreased and the dry land area dropped by 10% within next two days. Comparison of the curves in Fig. 4 shows that the coupling accelerates the process of flooding and increases flooding of the delta area by 4%.

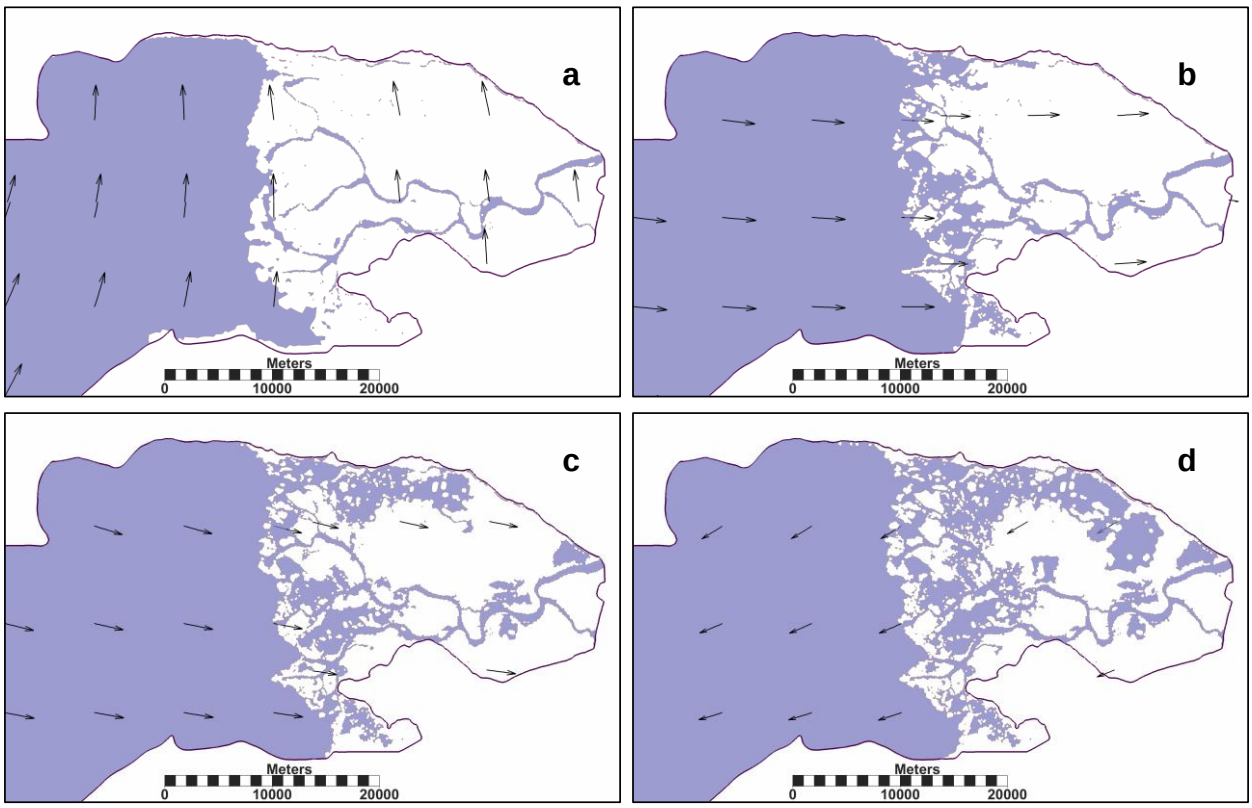

Fig. 3. Flooding extent of the Don Delta and wind directions: (a) September,24, 2014 at 00:00; (b) September, 25, 2014 at 00:00; (c) September 25, 2014 at 12:00; (d) September 27, 2014 at 00:00.

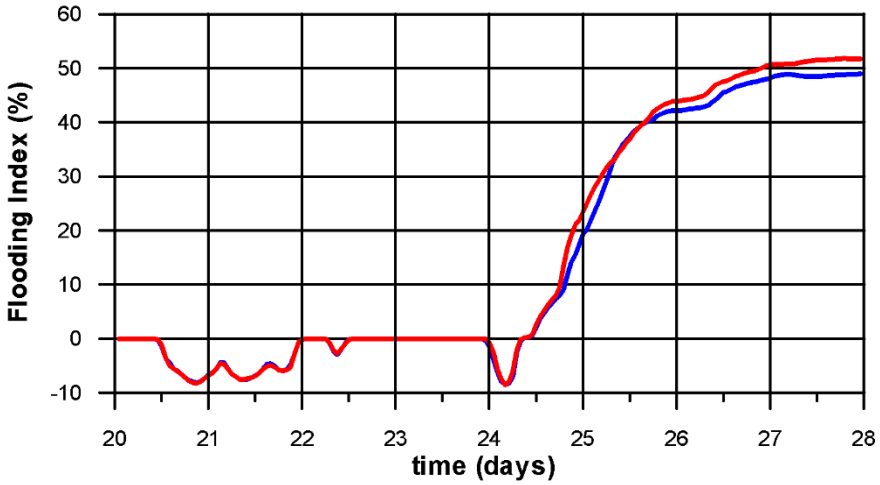

Fig. 4. FI *time series for the period 20–28 of September 2014 (blue line – E1 experiment, red line – E2 experiment).*

The following formulas are used for the estimation of mean values SL, SWH and TSL:

$$\mathrm{SL}_{\mathrm{m}}(t)=\frac{\iint\limits_{\Omega}\mathrm{SL}(x,y,t)\cdot\delta_w(x,y,t)dxdy}{\iint\limits_{\Omega}\delta_w(x,y,t)dxdy}, \tag{13}$$

$$\mathrm{SWH}_{\mathrm{m}}(t)=\frac{\iint\limits_{\Omega}\mathrm{SWH}(x,y,t)\cdot\delta_w(x,y,t)dxdy}{\iint\limits_{\Omega}\delta_w(x,y,t)dxdy}, \tag{14}$$

$$\mathrm{TSL}_{\mathrm{m}}(t)=\frac{\iint\limits_{\Omega}\mathrm{TSL}(x,y,t)\cdot\delta_w(x,y,t)dxdy}{\iint\limits_{\Omega}\delta_w(x,y,t)dxdy}, \tag{15}$$

where $\delta_w(x,y,t)=\begin{cases}0, & H(x,y,t)\le H_{\min}\\ 1, & H(x,y,t)>H_{\min}\end{cases}$.

Fig. 5 shows SL_m functions of time for the E1 experiment (blue curve) and the E2 experiment (red curve). In the E2 experiment, SL_m values at all points are 5–6 cm higher than the corresponding SL_m maximum values in the E1 experiment. Thus, the contribution of wave stress to the sea level elevation is insignificant for the given water area.

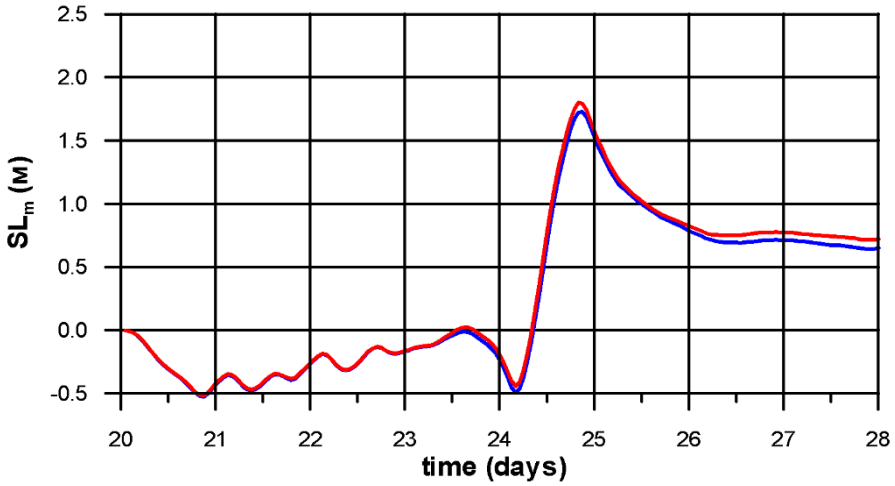

Fig. 5. SL_m *time series for the period 20–28 of September 2014 (blue line – E1 experiment, red line – E2 experiment).*

Fig. 6 shows SWH_m functions of time for the E1 (blue curve) and E2 (red curve) experiments. As it can be seen, the E2 experiment gives more intense wind waves in comparison with the E1 experiment for the stormy period (24–25 of September). SWH_m maximum is 35% higher for the E2 experiment than for the E1 experiment. To determine the causes of this effect, an additional numerical experiment (E3) was carried out, in which SL was not taken into account in SWAN in contrast to the E2. The dependence of SWH_m on time for the E3 experiment is shown by the black dashed curve. It is almost the same as the curve for the E1 experiment.

The physical meaning of this result is obvious. There are areas with shallow depths at the top of the Taganrog Bay, where wind waves cannot be significant due to strong dissipative effects. At the same time, as the sea level rises by 1.5–2 m and more the dynamic depth can significantly increase in these areas. This will facilitate increase of wave heights as a result of bottom friction influence reduction.

Thus, the storm surge creates conditions for the intensification of wind waves in the bay due to the general rise of the sea level. It is natural to assume that it is the combination of strong wind surges and intense wind waves that creates one of the main mechanisms of the extreme level rises in the Taganrog Bay, which leads to the flooding of the Don Delta.

Time dependence of TSL_m for the E2 experiment is shown in Fig. 7. As it can be seen, the maximum value of $TSL_m = 2.25$ m is reached on September, 24, in the afternoon. This fits well with the measurements at hydro-meteorological station Taganrog, where the maximum level of 2.5 m was observed on September, 24, at 18.00. Comparison of the curves in Fig. 7 and Fig. 5 shows that contribution of wind waves to the full level reaches 20% during the maximum of the storm.

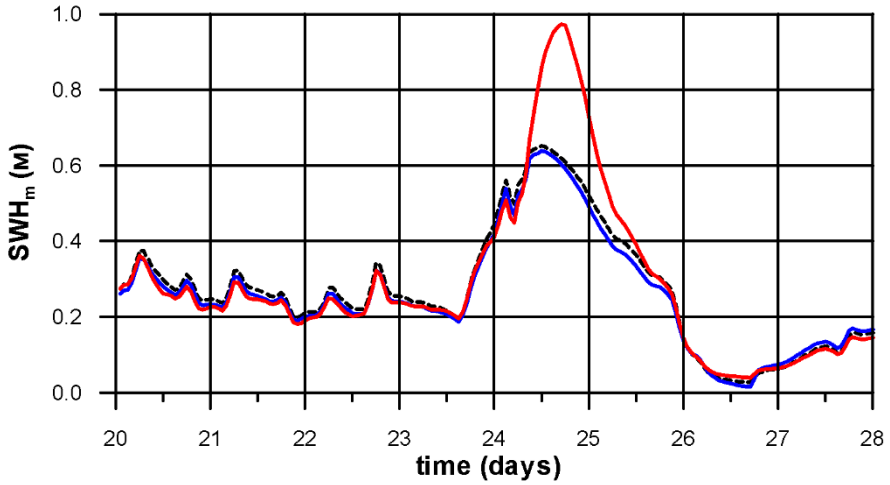

Fig. 6. SWH$_m$ *time series for the period 20–28 of September 2014 (blue line – E1 experiment, red line – E2 experiment, black dashed line– E3 experiment).*

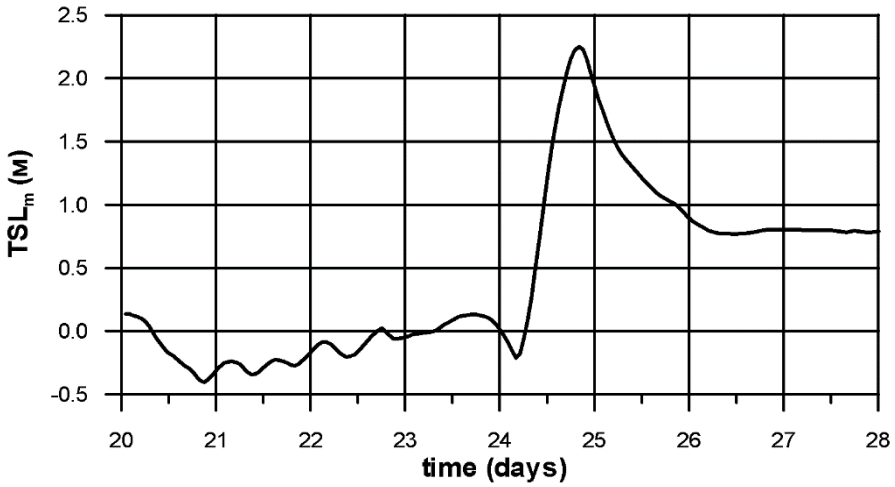

Fig. 7. TSL$_m$ *time series for the period 20–28 of September 2014 (E2 experiment).*

IV. Conclusion

The sea level oscillations and wind waves in the Taganrog Bay were simulated by means of the coupled SWAN+ADCIRC numerical model, taking into account the flooding and drying mechanisms. The calculations were carried out on an unstructured mesh with high resolution. The wind and atmospheric pressure fields for the extreme storm from 20 to 28 of September, 2014 obtained from WRF regional atmospheric model were used as forcing.

The analysis of simulation results showed the following. The western and northern parts of the Don Delta were the most flood-prone during the storm. The size of the flooded area of the Don Delta exceeded 50%. Interaction of storm surge and wind wave accelerated the flooding process, increased the size of the flooded area and led to the intensification of wind waves in the upper of Taganrog bay due to the general rise of the sea level. Wave stress did not contribute significantly to the value of storm surge.

V. Acknowledgment

This work was supported by RFBR, research project No. 15-05-06382 A.

The authors thank Crystal Fulcher from UNC-Institute of Marine Sciences for providing the source codes of SWAN+ADCIRC.

Calculations were carried out on a computing cluster of Marine Hydrophysical Institute and "Lomonosov" supercomputer of Moscow State University. Some ADCIRC visualizations were produced with FigureGen (Dietrich *et al.*, 2013).

VI. References

[1] V.A. Ivanov, V.V. Fomin, "*Mathematical Modelling of Dynamical Processes in the Sea-Land Area*", Kyiv: Akademperiodyka, 2010, 286 p.

[2] G.G. Matishov "The Kerch Strait and the Don Delta: the Security of Communications and Population", *Vestnik Yuzhnogo Nauchnogo Tsentra*, 11(1), 2015, pp. 6 – 15. (In Russian).

[3] G.G. Matishov, A.L. Chikin, S.V. Berdnikov, I.V. Sheverdyaev, A.V. Kleshchenkov et al., "Extreme flooding of the Don Delta in spring 2013: chronology, formation conditions, and consequences", *Vestnik Yuzhnogo Nauchnogo Tsentra*, 10(1), 2014. pp. 17–24. (In Russian).

[4] V.V. Fomin, A.A. Polozok, R.V Kamyshnikov, "Wave and Storm Surge Modelling for Sea of Azov with use of ADCIRC+SWAN", *Collection of articles of the II International conference «Geoinformation Sciences and Environmental Development: New Approaches, Methods, Technologies»*, Rostov-on-Don, 2014, pp. 111 – 116.

[5] J.C. Dietrich, M. Zijlema, J.J. Westerink, L.H. Holthuijsen , C. Dawson, et al., "Modeling Hurricane Waves and Storm Surge using Integrally-Coupled, Scalable Computations", *Coastal Engineering,* vol. 58, No. 1, 2011, pp. 45 – 65.

[6] N. Booij, R.C. Ris, L.H. Holthuijsen "A third-generation wave model for coastal regions. Model description and validation", *J. Geophys. Res.*, 104 (C4), 1999, pp. 7649 – 7666.

[7] M. Zijlema, "Computation of wind-wave spectra in coastal waters with SWAN on unstructured grids", *Coastal Engineering*, vol. 57, No. 3, 2010, pp. 267 – 277.

[8] R.A. Luettich, J.J. Westerink, "*Formulation and Numerical Implementation of the 2D/3D ADCIRC*", 2004, URL: http://adcirc.org/adcirc_theory_2004_12_08.pdf.

[9] R.A. Luettich, J.J. Westerink, N.W. Scheffner, "*ADCIRC: an advanced three-dimensional circulation model for shelves coasts and estuaries, report 1: theory and methodology of ADCIRC-2DDI and ADCIRC-3DL*", Dredging Research Program Technical Report DRP-92-6, U.S. Army Engineers Waterways Experiment Station, Vicksburg, MS, 1992, 137 p.

[10] J.H. Atkinson, J.J. Westerink, J.M. Hervouet, "Similarities between the wave equation and the quasi-bubble solutions to the shallow water equations", *International Journal for Numerical Methods in Fluids*, vol. 45, 2004, 689–714.

[11] W.D. Grant, O.S. Madsen, "Movable bed roughness in unsteady oscillatory flow", *J. Geophys. Res.*, vol. 87, 1982, pp. 469 – 481.

[12] P.C. Kerr, R.C. Martyr, A.S. Donahue, M.E. Hope, J.J. Westerink, et al., "U.S. IOOS coastal and ocean modeling testbed: Evaluation of tide, wave and hurricane surge response sensitivities to mesh resolution and friction in the Gulf of Mexico", *J. Geophys. Res. Oceans*, 118, 2013, pp. 4633 – 4661, doi:10.1002/jgrc.20305.

[13] J.C. Dietrich, R.L. Kolar, R.A. Luettich, “Assessment of ADCIRC's Wetting and Drying Algorithm”, Proceedings of the XV International Conference on Computational Methods in Water Resources, vol. 2, 2004, pp. 1767 – 177.

CRYOGENIC DYNAMICS IN THE COASTAL ZONE OF THE LAPTEV AND EAST SIBERIAN SEAS

Anatoly Gavrilov, Lomonosov Moscow State University, Faculty of Geology, Russia
Elena Pizhankova, Lomonosov Moscow State University, Faculty of Geology, Russia

a-v-g-37@yandex.ru

We consider the patterns of existence of thermo-abrasion, thermo-denudation and submarine permafrost degradation in the coastal zone of the Laptev and East Siberian seas. The key goal is to assess their role in changing the permafrost conditions along the coastal zone of a few tens of kilometers wide.

Keywords: thermo-abrasion, thermo-denudation, degradation of submarine (subsea) permafrost

I. INTRODUCTION

The major cryogenic processes in the coastal zone of the Laptev and East Siberian seas are thermo-abrasion and thermo-denudation. They lead to the rapid retreat of the ice-rich shores and degradation of subsea permafrost. Degradation is a consequence of the transition of coastal sediments into submarine environment.

Fig. 1. Research area.

The dynamics of the considerably extended shoreline was studied by the method of topographically accurate alignment of multitemporal and multiscale remote sensing data with the help of ScanEx Image Processor. The assessment of coastal retreat rates and interpretation of landscapes along the coastline was carried out in a GIS program MapInfo Professional. Degradation of submarine permafrost was studied using mathematical modeling of its evolution and synthesis of data on distribution and depth of the subsea permafrost roof.

II. PERMAFROST CONDITIONS

Continuous permafrost is developed onshore along the coastline of the Laptev and East Siberian seas. Average annual temperatures of coastal sediments are -11÷-15 °C, and its thickness reaches 500-700 m [1]. Submarine permafrost thickness varies from 150-200 to 500-700 m [2].

Syncryogenic ice-rich silts of Late Pleistocene Ice Complex with high ice wedges at the top (30-40 m) of the cross-section are exposed along the coastline. Ice wedges are 5-8 m wide and penetrate the entire thickness of the Ice Complex. Bulk ice content of sediments reaches 80-95% [1]. High coasts (up to 25-40 m) are composed of Ice Complex and often are represented by two bluffs. The lower one is destroyed by thermo-abrasion. The upper bluff is destroyed by thermo-denudation, and in fact, is separated from the lower one by a thermo-terrace 30-300 m wide. Thermo-abrasion and thermo-denudation are closely related to each other, activating the alternate retreat of both bluffs. The length of the coastline composed of the Ice Complex does not exceed 35% (for the Bol'shoy Lyakhovsky Island) and 20% (for the Oyogos Yar) of the total length of the eroded coastline.

Another relief-forming factor is the Holocene Alas Complex. It is comprised, from bottom to top, of the taber, lacustrine and boggy sediments with ice wedges. Ice wedges are 6-10 m height and up to 1.5-2 m wide. Ice content reaches 60-70%. Coasts composed of the Alas Complex are 8-12 m high. The marine and alluvial-marine coastal terraces height does not exceed 3-4 m.

The cliff structure depends on the areal distribution of neotectonic structures in the surrounding relief. The horst structures in the rift system of the Laptev Sea are usually represented by poor-ice sediments in the wave-breaking zone. Cliffs of the rift grabens are composed entirely of Ice and Alas Complexes. Here, the bottom of icy sediments goes underwater to a level 3.5-10 m deep.

Horsts and rift grabens vary considerably in the geothermal flux density (q), which influences the thickness and degradation rate of permafrost at the bottom. Characteristic values for horsts are 45-53 mW/m^2, and, presumably, for the graben they are 70-100 mW/m^2 [2].

III. COASTAL EROSION

The Eastern Siberia has the highest coastal retreat rate in the Northern Hemisphere. In recent years, due to a sharp drop in sea ice cover of the Arctic Ocean and rise of air temperatures, the retreat rates of the Laptev and East Siberian ice-rich shores have risen 1.3-2.9 times. Estimates for different years [3] have been made on the basis of comparison of the position of the Lyakhovsky Islands shoreline and the southern coast of Dm. Laptev Strait. The data showed that during the 50-year period (1951-2000), 27.2 km^2 of the Bol'shoy Lyakhovsky Island, 1.7 km^2 of the Maly

Lyakhovsky Island , and 12.4 km^2 of the Oyogos Yar mainland have been removed. Moreover, over the past 13 years (2001-2013), the eroded 10.3 km^2 area of the Bol'shoy Lyakhovsky Island and 6.5 km^2 area of the Oyogos Yar must be added to the above estimates. On average, the retreat rates for all the eroded coasts in the region have been estimated as 3.2 m^2/year over the period up to year 2000, and 6.4 m^2/year for the last 13 years.

Upon comparison between remote sensing images taken in different years, the data showed a significant spatial heterogeneity of the studied retreating shores. As a result of the remote and land-based studies, 4 morphostructural fields [4] and 10 types and subtypes of the coasts have been distinguished, based on the structure of the onshore cross-sections [5]. According to this classification, the retreat rates change from the minimum (0-0.5 m/year) in areas of stable uplifts (e.g., the Kigilyakh Peninsula, the Cape of Shalaurov, the Cape of the Holy Nose) to the significantly higher values of up to 5-7 m/year observed during the period 1951-2000, and 10-13 m/year during the period 2001-2013 in areas with a tendency to subsiding. The maximum rates were observed in the negative-relief structures where the bottom of ice sediments was located below a sea level.

Fig. 2 shows the values of the retreat rates in the areas composed of the Ice and Alas Complexes from the surface, and alluvium and alluvial-marine sediments. The plots are constructed for different periods for the Bol'shoy Lyahovsky Island and for the southern shore of the Dmitry Laptev Strait, named Oyogos Yar.

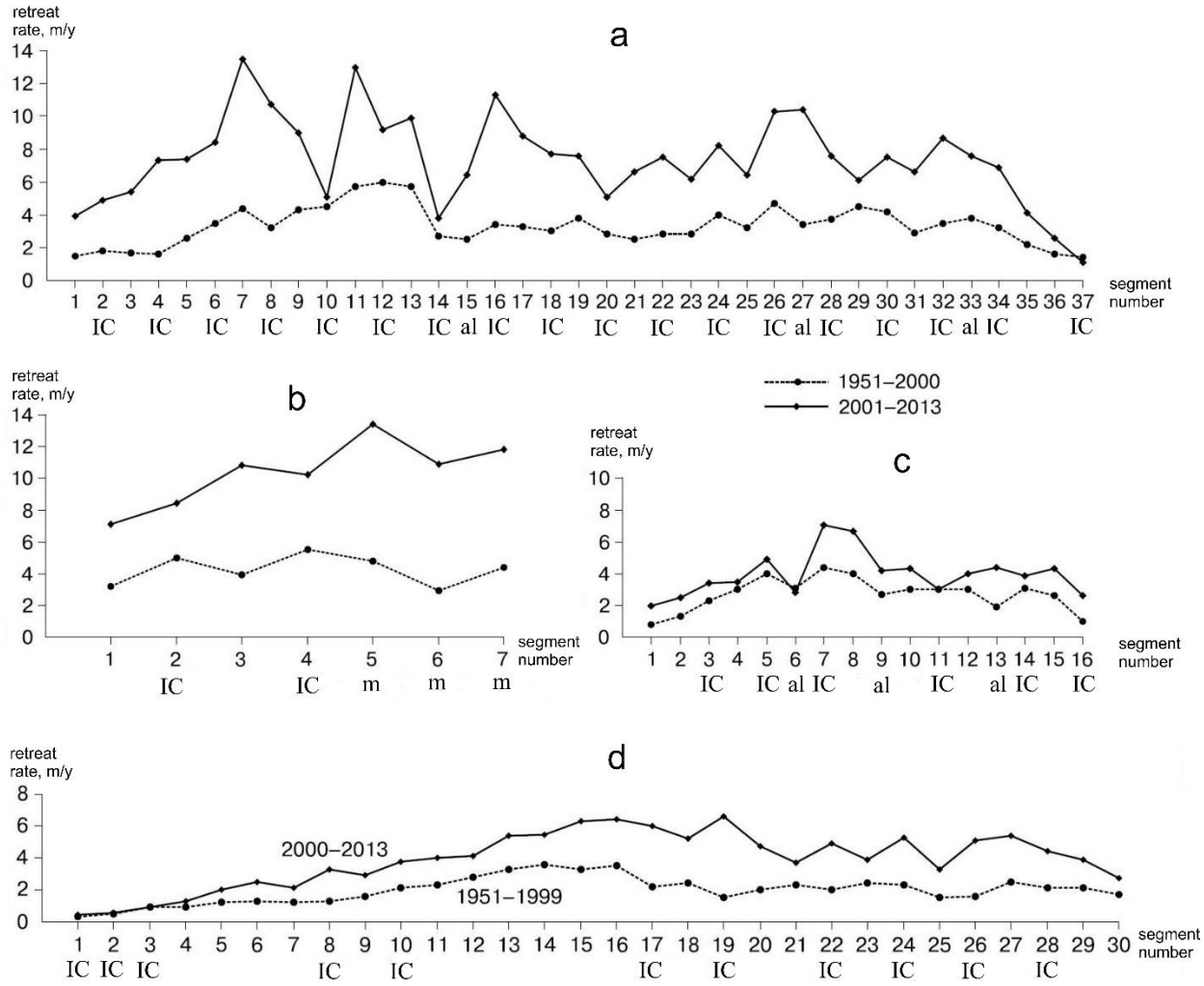

Fig. 2. Change of the retreat rates for the eroded coastlines of the Bol'shoy Lyakhovsky Island: the southern coast of 70 km long (a), the western coast of 48 km long (b), the north-eastern coast of 32 km long (c) and Oyogos Yar of 107 km long (d). IC - *segments of Ice Complex*, al - *segments of alluvial sediments*, m - *segments of marine and alluvial-marine sediments, no- symbol line there were allocated - segments of Alas Complex.*

The mechanism of the coastal erosion depends on the structure of the onshore cross-section. The first (block-type) mechanism is most typical for the coasts 8-12 m high, preferably occurring in the Alas Complex. Sea wave-cut coves are generated at a depth of 10-15 m at the base of the coastal cliff. The overlying sediments along the fractures crumble and are washed away by sea waves.

The second type of erosion is observed along the coasts of more than 15-20 m high, composed of Ice Complex. Thermal cirques with ice cliffs on its remote edge and thermo-terraces in the basement are found here (fig.3). Thermo-terraces are formed upon retreat of the ice cliffs at a rate exceeding the rate of thermo-abrasion. Such retreats are due to the processes of thermo-denudation of ice cliffs under the influence of air temperature, solar radiation and precipitation and resulting erosion of the coastal part of thermo-terraces. Comparison of multitemporal remote sensing data showed that thermo-denudation rate has been increasing by 1.7-1.9 times over the last 13 years.

Fig. 3. The Shore Oyogos Yar in 2007. Photo by A. Dereviagin

The third type of erosion is characteristic of marine and alluvial-marine terraces. Here, thermo-abrasive coves are not developed, but instead, thawing ice sediments are sliding down to the water edge, where they are being eroded.

IV. DEGRADATION OF THE SUBMARINE PERMAFROST AT THE TOP

Submerged below the sea level sediment sequences are initially frozen. Firstly, its subsea erosion is initiated by thawing. Summer warming of bottom water up to 10-12 °C as well as salinization of the bottom sediments are contributing factors to permafrost degradation. As a result of salinization and seasonal thawing at depth interval 0-2 m, and perennial thawing at depth interval 2-7 m, thickness of the degraded permafrost on the submarine coastal slope is increasing from 1-2 to 30-40 m [6]. The first value 1-2 m is characteristic of a distance 0.1-0.2 km from the coast, the second value 30-40 m is observed at a distance 3-10 km offshore. Sea waves carry upslope a smaller portion of thawed sediments. Approximately 2/3 to 1/2 of sediment mass is deposited on the coastal slope [7].

V. PERMAFROST DEGRADATION FROM BELOW

Permafrost degradation from below begins one-two millennia later than the processes of the degradation on top. It takes place under the influence of geothermal flux. This process starts when a temperature profile of submarine permafrost corresponds to a temperature of the bottom water. According to the mathematical modeling permafrost 500-700 m thick had been developed over a period 1500-2000 years with geothermal flow (q) equal to 50 mW/m^2 [2]. The degradation is

observed where there is a reduction of permafrost thickness from below, and ice-bonded permafrost is transformed into ice-bearing permafrost (with unfrozen water).

VI. THE CONTRIBUTION OF CRYOGENIC PROCESSES IN PERMAFROST COASTAL DYNAMICS

Assessing the contribution of cryogenic processes in permafrost dynamics of the coastal zone was carried out by constructing a conceptual model. It is based on the data of permafrost thickness reduction, changing of permafrost state and estimation of coastal retreat rates over the last 5 thousand years when a sea level rise had stabilized on modern altitudes.

Received data of permafrost degradation rate were used for assessment [8]. They show its dependence on the coast position in the certain morphological structure. The rate of permafrost degradation from below in the rift grabens at q = 70-100 mW/m^2 is 2.2-3 cm/year; in the horsts it equals 1.5 cm/year at q = 50 mW/m^2. The rate of permafrost thawing on the underwater coastal slope at the north-western end of the Muostakh Island in the Ust-Lensky graben (in the Buorhaya Bay) was 14-18.5 cm/year during the period of 30 years (1983 - 2013/2014.). Here bottom of Ice Complex goes under the sea level at 10 m. Thawing of poor-ice sediments underlying the Ice Complex is going 2.5-3 times slower (6 cm/year), what, in our opinion, corresponds to the horst conditions.

Data of the most extended borehole profile (11.5 km) near the Cape of the Mammoth Tusk (fig. 3) were used for paleogeocryological reconstructions. The bottom of the Ice Complex submerged under the sea level by 3.5 m. The thickness of thawed permafrost in the cross-section in the borehole C-2, located on the isobath 6 m, is 29 meters deep. If we consider that 1/3 of the sediment mass was eroded by waves, the thickness of thawed permafrost might have reached 35 m, and thus average rate of thawing equals 1.4 cm/year.

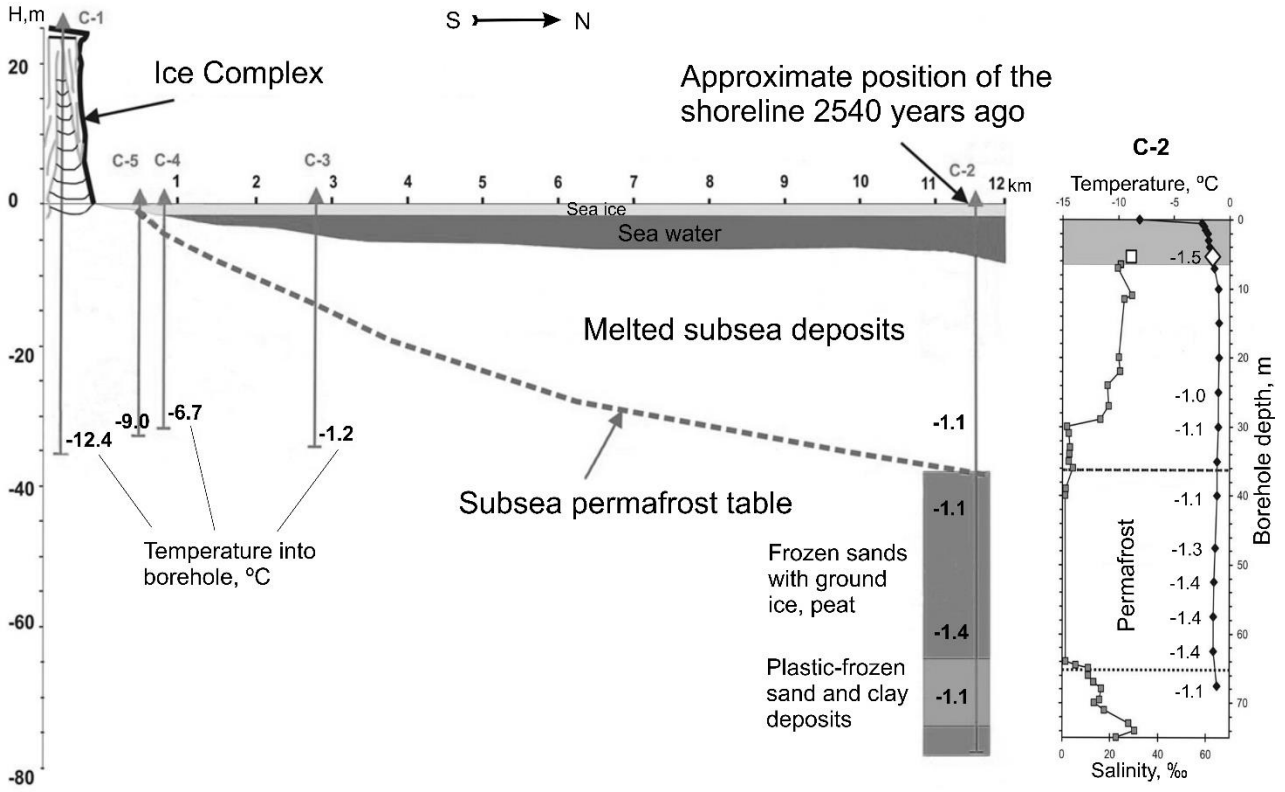

Fig. 3. The borehole profile next to the Cape of the Mammoth Tusk on the Anabar-Olenek near-shore zone and the distribution of temperature and salinity in borehole C-2 [by 6].

The cross-section in the borehole C-2 includes a layer of plastic-frozen sand and clay sediments (fig. 3). Temperatures of sediments in the borehole (-1.1÷-1.4 °C) expose gradientless distribution along the cross-section and correspond to a temperature of bottom water. Considering the distance from the coast and average coastal retreat rate (4.5 m/year), M.N. Grigoriev determined that permafrost at borehole C-2 area submerged under the sea level 2540 years ago [6].

The specified time period was estimated using mathematical modeling and paleogeographic data. It showed that permafrost from the borehole C-2 was land-based not less than 2000 years ago. During this period, the temperature of permafrost sequences 700 m thick assumes a value corresponding to the temperature of the bottom water. Since part of the permafrost sequence had been transformed into to the plastic-frozen state, an estimate of 2,500 years appears to be a reasonable value.

Paleogeographic data were used in the calculation of the coastal area submerged over the last 5 thousand years. In particular, we applied oxygen isotope GISP2 method [9], palynological data [10] and data on complexes of diatoms and foraminifera in the sediments of the Laptev Sea [11]. The results of calculation showed that the coastline in the western part of the cold-water Laptev Sea 5000 years ago was located 25 km away from its current position. In the rift grabens, where the bottom of Ice Complex was found at 10 m below modern sea level, the coastline could be found even further, while in the horsts it could be found closer. Earlier estimates obtained on the basis of the observed rates of coastal retreat suggested 30-36 km difference from the present position [12].

VII. CONCLUSIONS

G. High-rate retreat of the coastline of Eastern Siberia is caused by the predominance of ice-rich Quaternary sediments in its structure.

H. The rate of coastal retreat is influenced by the following factors: tectonic structures of the territory, expressed in certain morphological structures that define permafrost geology in the coastal cross-section; the duration of the ice-free period, the strength and direction of winds, snowdrift transfer; shore orientation relative to the direction of prevailing tides, storms and currents, solar radiation. The current climate warming, likely driving the reduction of sea ice cover in recent decades has led to an increase in coastal retreat rate 1.3-2.9 times in comparison with the second half of the XX century.

I. Top-down degradation of submarine permafrost formed from the subaerial permafrost as a result of sea-level rise, is due to the summer radiative warming of bottom water and thawing of the submarine permafrost on the isobaths 2-7 m, as well as salinization of the sediments on isobaths 0-2 m. The average degradation rate for periods within the first thousand years does not exceed 1-2 cm/year. The highest recorded thickness of the thawed sediments as a result of the coastal retreat is more than 50 m. During the period of 5 thousand years coastline has retreated up to 25-30 km.

J. The rate of degradation of submarine permafrost from below depends on the density of the geothermal flow and equals 1.5-3 cm/year. The greatest reduction in permafrost thickness submerged under the sea level as a result of coastal retreat, has been 45-90 m during the last 5 thousand years.

K. The rates of the coastal retreat and permafrost degradation are higher in the negative-relief structures compared to the positive ones.

VIII. REFERENCES

[1] Geocryology USSR. Eastern Siberia and the Far East (ed. Ershov, E.D.). M., Nedra, 1989. 515 p.

[2] N.N. Romanovsky, A.A. Eliseeva, A.V. Gavrilov, G.S. Tipenko, H.W. Hubberten, “Long-term dynamics of permafrost and stability zone of gas hydrate in the rift structures of the Arctic shelf of Eastern Siberia” (Note 2). The results of numerical modeling // *Earth's Cryosphere*, 2006, v. X, № 1, p. 29-38.

[3] E.I. Pizhankova, “Modern climate change at high latitudes and their influence on the coastal dynamics of the Dmitry Laptev Strait area” // *Earth's Cryosphere*, 2016, v. XX, № 1, pp. 51-64.

[4] V.K. Dorofeev, M.G. Blagoveshensky, A.N. Smirnov, V.I. Ushakov, New Siberian Islands. Geological structure and metallogeny // Ed. Ushakov, V.I., SPb, VNIIOkeanologiya, 1999, 130 p.

[5] E.I. Pizhankova, M.S. Dobrynina, “The dynamics of the Lyakhovsky Islands coastline (results of aerospace image interpretation)” // *Earth's Cryosphere*, 2010, v. XVI, № 4, pp. 66-79.

[6] M.N. Grigoriev, Kriomorfogenesis and lithodynamics of the coastal shelf zone of the seas of East Siberia. Author's abstract of Ph.D thesis, Yakutsk, 2008, 38 p.

[7] F.E. Are, The coastal destruction of the Arctic coastal lowlands. Novosibirsk, Geo, 2012, 291 p.

[8] F. Günther, P.P Overduin, I. A.Yakshina, T. Opel, A.V. Baranskaya, M.N. Grigoriev, "Observing Muostakh disappear: permafrost thaw subsidence and erosion of a ground-ice-rich island in response to arctic summer warming and sea ice reduction" // *The Cryosphere*, 9, 2015, p. 151–178.

[9] M. Stuiver, P.M. Grootes, T. Braziunas **"**The GISP2 $d^{18}O$ Climate Record of the Past 16,500 Years and the Role of the Sun, Ocean, and Volcanoes" // *Quatern. Res.*, 1995., Vol. 44., p. 341–354.

[10] A.A. Andreev, V.A. Klimanov, "Quantitative Holocene climatic reconstruction from Arctic Russia" // *Journal of Paleolimnology*, 2000, v. 24, p. 81-91.

[11] A.G. Matul, T.A. Khusid, V.V. Mukhina, M.P. Chekhovskaya, S.A. Safarova, "Modern and Late Holocene environmental conditions on the shelf of the south-eastern part of the Laptev Sea, according to the microfossils" // *Oceanology*, 2007. Т. 47. № 1., pp. 90-101.

[12] F.E. Are, Coastal thermo-abrasion. Nauka, Moscow. 1980, 158 p.

WAVE CLIMATE OF THE BLACK SEA'S COASTAL WATERS DURING THE LAST THREE DECADES

Fedor Gippius, Department of Oceanology, Lomonosov Moscow State University, Russia
Stanislav Myslenkov, Department of Oceanology, Lomonosov Moscow State University, Russia
Elena Stoliarova, Department of Oceanology, Lomonosov Moscow State University, Russia
Victor Arkhipkin, Department of Oceanology, Lomonosov Moscow State University, Russia

fedor.gippius@gmail.com

This study is focused on the alterations and typical features of the wind wave climate of the Black Sea's coastal waters since 1979 till nowadays. Wind wave parameters were calculated by means of the 3rd-generation numerical spectral wind wave model SWAN, which is widely used on various spatial scales – both coastal waters and open seas. Data on wind speed and direction from the NCEP CFSR reanalysis were used as forcing. The computations were performed on an unstructured computational grid with cell size depending on the distance from the shoreline.
Modeling results were applied to evaluate the main characteristics of the wind wave in various coastal areas of the sea.

Key words: wave climate, coastal areas, NCEP CFSR reanalysis, SWAN model, climate change

I. INTRODUCTION

Wind waves are of a crucial importance both to the coastal waters and to the coast itself. They influence nearly all processes occurring in the coastal zone – e.g. marine currents, mixing of freshwater form rivers with marine waters and others. Moreover, wind waves are one of the most hazardous phenomena on the sea and they must be considered during the construction and exploitation of engineering facilities both on the coasts and offshore, shipping and other kinds of human activities. Wind waves are also one of the possible sources of renewable energy.

During the recent decades much efforts were made to improve our understanding of wind waves and corresponding processes in the Black Sea. Wave climate studies corresponding to the entire Black Sea can be found in, e. g., [1], [2]. Another important study subject are storms and their long-term variability [3; 4] as well as waves related to them [5]. Numerous research projects are devoted to the interaction of wind waves with other natural and anthropogenic processes such as wave-current interactions [6], coastal transformations [7] and the influence of waves on the propagation of an oil spill [8]. A practical applications of wind waves is the transformation of their energy into electricity. Therefore, studies of the wave energy potential of the Black Sea and its coastal waters are more and more increasing (e. g. [9], [10] and [11]).

This study is focused on the evolution of parameters of wind waves in the coastal areas of the Black Sea during the recent 37 years. Wind waves were numerically simulated by means of the SWAN model using the NCEP-CFSR reanalysis and an original unstructured computational grid.

I. Data and Methods

Three components are necessary for any numerical study of wind waves – a computation grid, wind data and a numerical model.

The computation grid used in this study is an original unstructured mesh based on digitized nautical maps of the entire Black Sea and its coastal areas. General concepts related to the generation and application of unstructured grids is given in [12] and [13]. The distance between the grid points in this mesh depends on the water depth. In our case this distance varies from 10—15 km in deep-water offshore regions till 500 m in coastal areas (fig. 1, fig. 2). The grid consists of 42284 nodes and 77036 elements. The advantage of such unstructured grids is the possibility to obtain high-resolution data in coastal area and to perform computations in a relatively low amount of grid points at the same time. Previous studies of wind waves on the Black Sea with the use of unstructured grids can be found in e. g. [14] and [15].

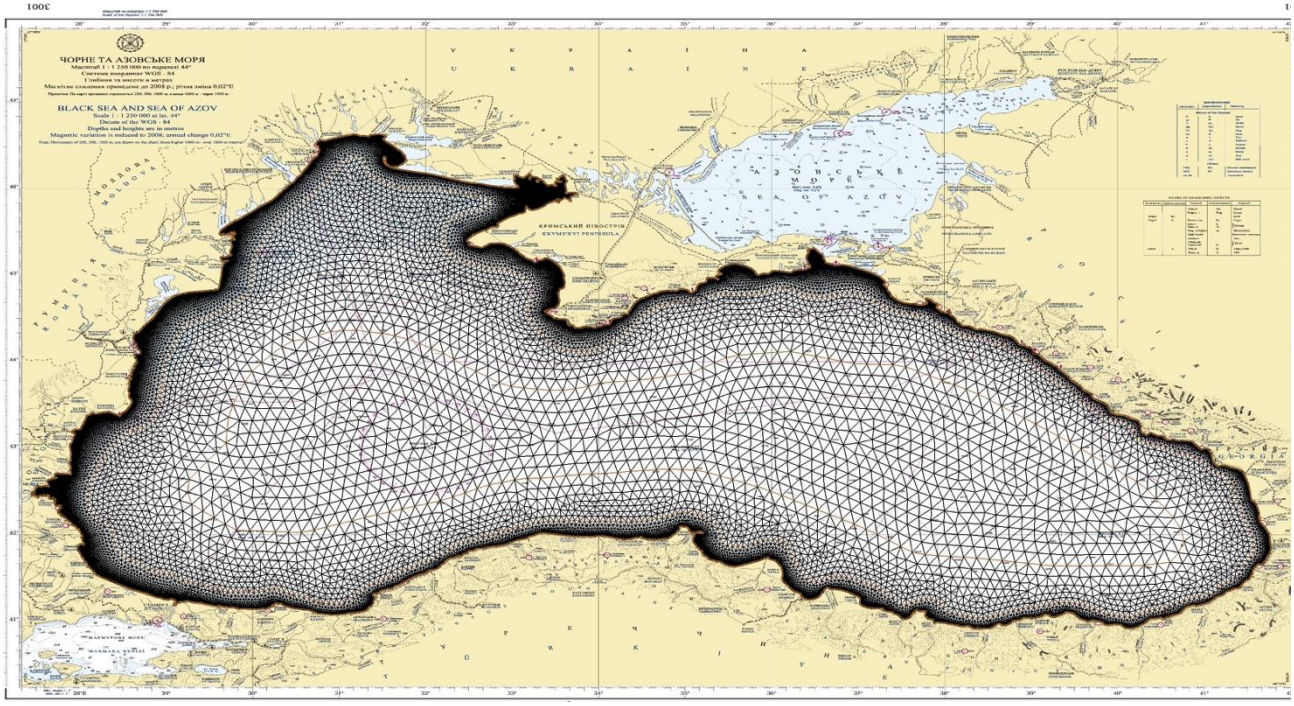

Fig. 1. The entire unstructured computation grid.

High resolution wind fields form the NCEP-CFSR reanalysis [16] were used as forcing for the computations covering the period from 1979 till 2010. For the period form 2011 till 2015 the 2nd version of this reanalysis [17] was used.

The third-generation spectral wind wave model SWAN (version 41.01) [18; 19; 20] was applied for computations of wind wave parameters.

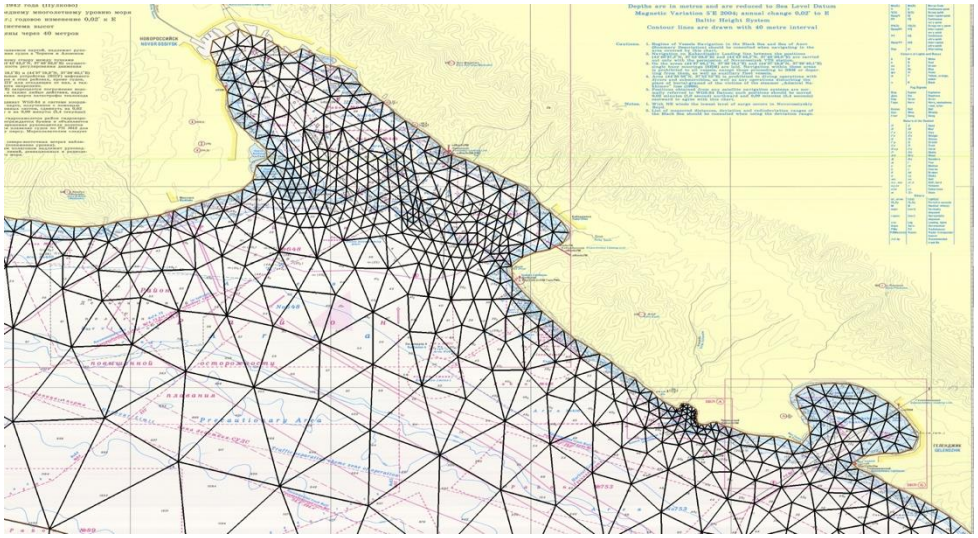

Fig. 2. Part of the unstructured computation grid corresponding to the coastal area between Novorossijsk and Gelendzhik cities (northeastern Black Sea).

The results of computations were validated against data of in situ measurements performed by a Datawell wave buoy. This buoy was installed within the NATO TU-WAVES program 7 km off the city of Gelendzhik (44° 30' 27" N, 37° 58' 42" E). The water depth at the installation point is 85 m. Measurements were carried out from 1996 till 2003 with several interruptions [21; 22].

The comparison of measured and modelled values of significant wave heights (SWH) shows a good agreement between these parameters (fig. 3). The average difference between measured and modelled SWH is 0.20 m; its standard deviation is 0.32 m.

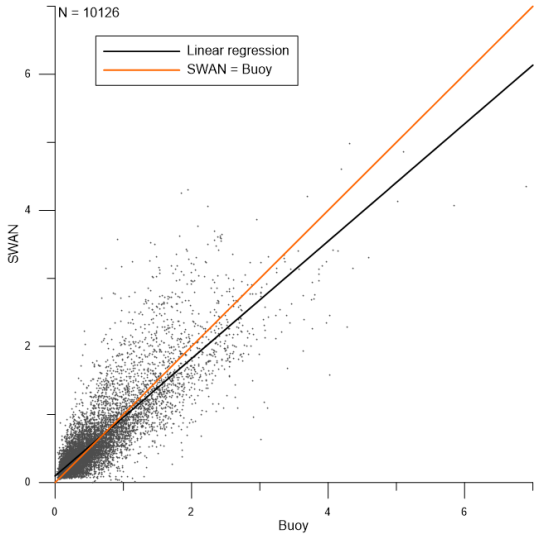

Fig. 3. Scatter plot of measured and modelled SWH at the Gelendzhik buoy.

III. Results and discussion

In this study we analyze timeseries of wind waves parameters corresponding to 5 locations in the coastal waters of the Black Sea – Gelendzhik, Katziveli, the Karkinitskaya Oil Platform, Sinop and Hopa (fig. 4, table 1). Instrumental observations of wind waves within the NATO TU-WAVES project were carried out at all these locations.

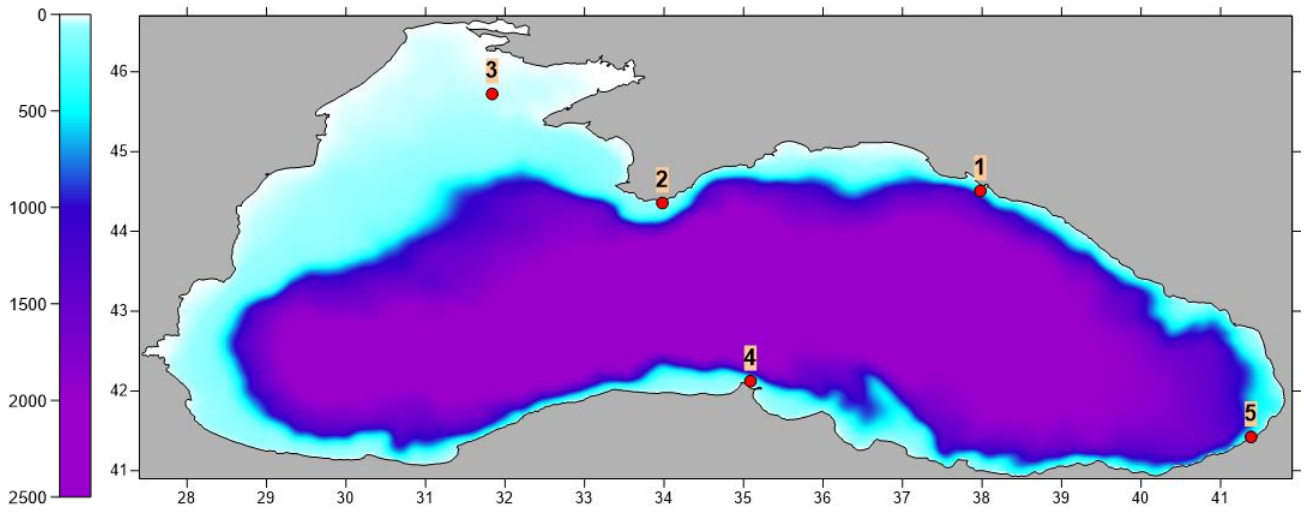

Fig. 4. Bathymetry of the Black Sea and location of study points (1 – Gelendzhik, 2 – Katziveli, 3 - Karkinitskaya Oil Platform, 4 – Sinop, 5 – Hopa).

Table 1. Coordinates of study points

Point		Location
1	Gelendzhik	44.5075° N, 37.9783° E
2	Katziveli	44.3557° N, 33.9787° E
3	Karkinitskaya Oil Platform	45.7231° N, 31.8378° E
4	Sinop	42.1233° N, 35.0867° E
5	Hopa	41.4233° N, 41.3833° E

Some basic statistics of SWH at these location are given in Table 2. Maximal SWH values correspond to Sinop (6.36 m). Maximal SWH at all other study points are at least 0.5 m lower. The lowest SWH maxima correspond to Hopa (4.39 m). The maximal SWH calculated for the Karkinitskaya Oil Platform, which is located at least 50 km off the coast, is also relatively small – 5.35 m. This value is lower than maximal SWH at all other points except Hopa. Such a distribution is in good agreement with the pattern of SWH maxima on the entire Black Sea shown in [1]. According to these results, there are two areas with maximal SWH in the Black Sea – its south-western and north-eastern areas. The relatively shallow north-western area including the Karkinitskaya Oil Platform as well as the south-eastern area including Hopa are the less stormy parts of the sea. Finally, the standard deviation at all locations except Hopa varies between 0.50 and 0.54 m. At the Hopa location it is of 0.40 m.

Table 2. Statistics of SWH in study points

Point	Maximal SWH (m)	Average SWH (m)	Standard deviation (m)
Gelendzhik	5.84	0.58	0.54
Katziveli	5.61	0.65	0.50
Karkinitskaya Oil Platform	5.35	0.73	0.54
Sinop	6.36	0.71	0.51
Hopa	4.39	0.47	0.40

Statistics of wave periods and lengths are given in tab. 3 and tab. 4 correspondingly. Maximal values of these parameters do not vary significantly form point to point. The only exception are these data at the Karkinitskaya Oil platform, where both the maximal wave period (8.03 s) and wave length (83.23 m) are notably lower than at other locations.

Table 3. Statistics of wave periods in study points

Point	Maximal period (s)	Average period (s)	Standard deviation (s)
Gelendzhik	9.44	3.28	1.47
Katziveli	9.71	3.60	1.25
Karkinitskaya Oil Platform	8.03	3.26	1.08
Sinop	9.65	3.95	1.25
Hopa	9.59	3.43	1.41

Table 4. Statistics of wave lengths in study points

Point	Maximal length (m)	Average length (m)	Standard deviation (m)
Gelendzhik	125.57	16.02	16.24
Katziveli	132.20	17.24	14.15
Karkinitskaya Oil Platform	83.23	14.82	10.85
Sinop	128.41	21.53	15.40
Hopa	129.83	16.43	15.37

The distribution of waves depending on their SWH and direction at the study locations is shown on fig. 5. The patterns of these distributions vary significantly form point to point. Thus, two predominant directions of waves can be derived in Gelendzhik – SSE and WNW. Another interesting feature of this distribution is a weak peak corresponding to NW. This peak may be induced by local orographic wind circulation common for the region between the cities of Novorossijsk and Tuapse on the northeastern coast of the sea [23]. In Katziveli there are also two predominant directions of waves – E and WSW. Unlike the pattern in Gelendzhik, there are practically no waves arriving from the shore. Southern waves are very rare as well. As the Karkinitskaya Oil Platform is located far from any coasts the pattern of the directional distribution is more uniform here. However, there are also two prevalent wave directions, namely the SSW and ENE ones. The amount of SE waves is very low here. At the Sinop location there are also two peaks

in the distribution of wave directions, namely NW and NNE. Finally, the most evident peak among all these distributions is observed in Hopa, where at least 50% of all waves arrive from WNW.

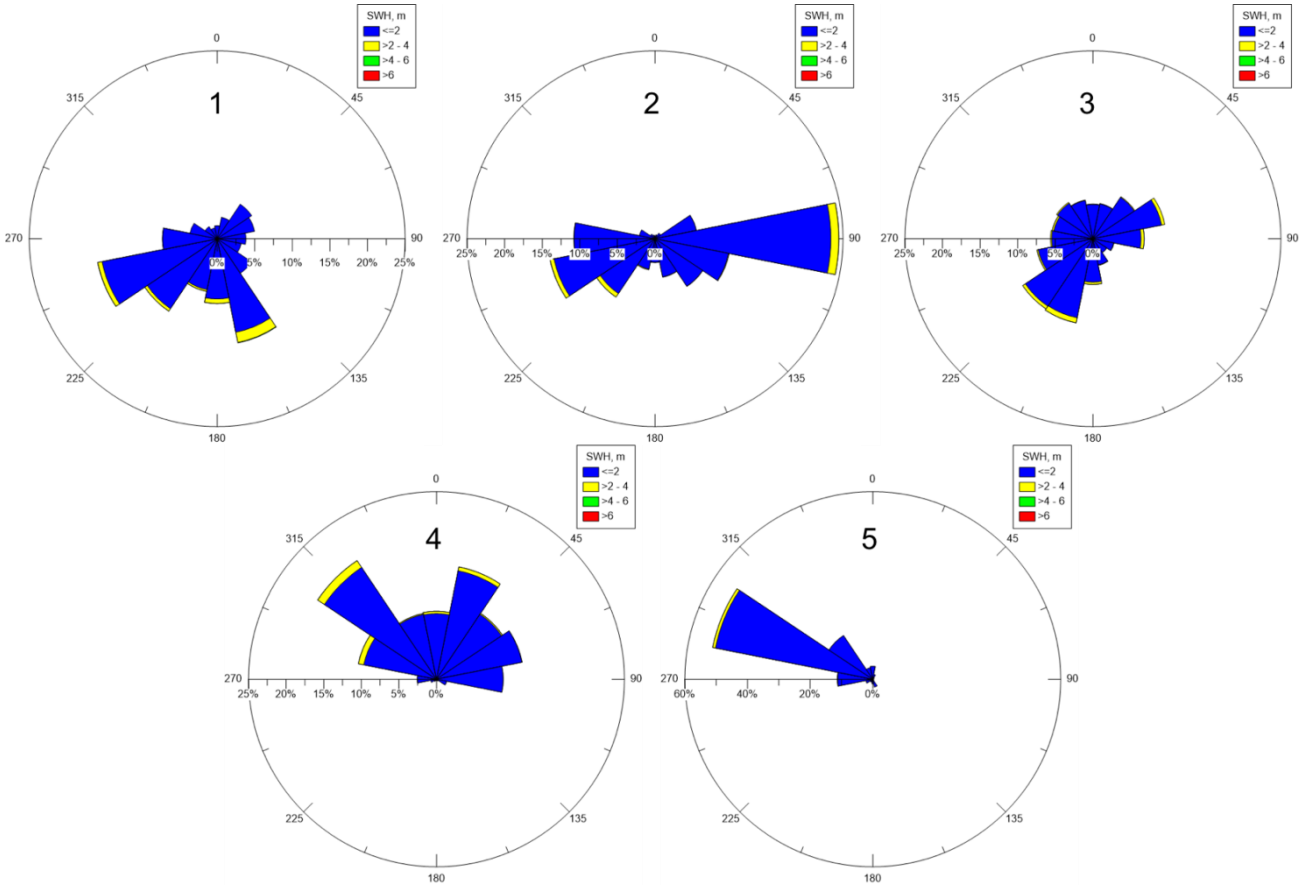

Fig. 5. Wave roses at the study locations. Numbers indicating study points correspond to fig. 4.

IV. Acknowledgments

The reported study was carried out by F.N. Gippius and E.V. Stoliarova within the project № 16-35-00488 funded by the Russian Foundation for Basic Research (RFBR) and by S.A. Myslenkov and V.S. Arkhipkin within the project № 16-08-00829 funded by RFBR.

V. References

[1] V.S. Arkhipkin, F.N. Gippius, K.P. Koltermann, and G.V. Surkova, “Wind waves in the Black Sea: Results of a hindcast study”, *Nat. Hazards Earth Syst. Sci.*, vol. 14, pp. 2883—2897, November 2014.

[2] A. Akpinar, G. Ph. van Vledder, and B. Bingölbali, “Wave climate simulation for the Black Sea basin”, *E-proceedings of the 36th IAHR World Congress 28 June – 3 July*, 2015, The Hague, the Netherlands.

[3] N.N. Valchev, E.V. Trifonova, and N.K. Andreeva, “Past and recent trends in the western Black Sea storminess”, *Nat. Hazards Earth Syst. Sci.*, vol. 12, pp. 961—977, April 2012.

[4] G.V. Surkova, V.S. Arkhipkin, and A.V. Kislov, "Atmospheric circulation and storm events in the Black Sea and Caspian Sea", *Central European Journal of Geosciences*, vol. 5 (4), pp. 548—559, 2013.

[5] V. Galabov, A. Kortcheva, A. Bogatchev, and B. Tsenova, "Investigation of the hydro-meteorological hazards along the bulgarian coast of the Black Sea by reconstructions of historical storms", *Journal of Environmental Protection and Ecology*, vol. 16, pp. 1005—1015, 2015.

[6] E. Rusu, "Modelling of wave–current interactions at the mouths of the Danube", *J. Mar. Sci. Technol.*, vol. 15, pp. 143—159, 2010.

[7] S. Dan, M.J.F. Stive, D.-J.R.Walstra, and N. Panin, "Wave climate, coastal sediment budget and shoreline changes for the Danube Delta", *Marine Geology*, vol. 262, pp. 39—49, 2009.

[8] L. Rusu, "Application of numerical models to evaluate oil spills propagation in the coastal environment of the Black Sea", *Journal of Environmental Engineering and Landscape Management*, vol. 18 (4), pp. 288-295, December 2010.

[9] A. Akpinar, and M.T. Kömürcü, "Wave energy potential along the south-east coasts of the Black Sea", *Energy*, vol. 42 (1), pp. 289—302, 2012.

[10] H. Keskin Citiroglu, and A. Okur," An approach to wave energy converter applications in Eregli on the western Black Sea coast of Turkey", *Applied Energy*, vol. 135, pp. 738—747, 2014.

[11] V.S. Arkhipkin et al., "Assessing the potential of wave energy in coastal waters of Crimea peninsula", *International scientific journal for alternative energy and ecology*, vol. 20, pp. 25—35, 2015 (in Russian).

[12] J.C. Dietrich et al., "Performance of the unstructured-mesh, SWAN+ADCIRC model in computing hurricane waves and surge", *Journal of Scientific Computing*, vol. 52 (2), pp. 468—497, 2012

[13] M. Zijlema, "Computation of wind-wave spectra in coastal waters with SWAN on unstructured grids", *Coast. Eng.*, vol. 57, pp. 267—277, 2010.

[14] S.A. Myslenkov, and V.S. Arkhipkin, "Analysis of wind waves in the Bay of Cemes of the Black Sea by means of the SWAN model", *Proceedings of Hydrometcentre of Russia*, vol. 350, pp. 58—67, 2013 (in Russian).

[15] E.V. Stoliarova, and S.A. Myslenkov, "High resolution wave forecast system in Kerch strait", *Proceedings of Hydrometcentre of Russia*, vol. 354, pp. 24—35, 2015 (in Russian).

[16] S. Saha et al., "The NCEP climate forecast system reanalysis", *Bulletin of the American Meteorological Society*, vol. 91 (8), pp. 1015—1057, 2010.

[17] S. Saha et al., "The NCEP climate forecast system version 2", *Journal of Climate*, vol. 27 (6), pp. 2185—2208, 2014.

[18] N. Booij, R.C. Ris, and L.H. Holthuijsen, "A third-generation wave model for coastal regions 1. Model description and validation", *Journal of Geophysical Research C: Oceans*, vol. 104 (C4), pp. 7649—7666, 1999.

[19] R.C. Ris, L.H. Holthuijsen, and N. Booij, "A third-generation wave model for coastal regions 2. Verification", *Journal of Geophysical Research C: Oceans*, vol. 104 (C4), pp. 7667—7681, 1999.

[20] *SWAN Technical Documentation, SWAN Cycle III version 40.51A*. Delft: University of Technology, 2007, 98 p.

[21] A.V. Boukhanovsky, B.V. Divinsky, R.D. Kos'yan, L.I. Lopatoukhin, and V.A. Rozhkov, "Typification of wind disturbance of the Black Sea under the instrumental data", *Oceanology,* vol. 40 (2), pp. 289—297, 2000 (in Russian).

[22] http://coastdyn.ru

[23] P.A. Toropov, S.A. Myslenkov, and T.E. Samsonov, "Numerical modeling of bora in novorossiysk and associated wind waves", *Vestnik Moskovskogo Universiteta, Seriya 5: Geografiya*, vol. 2, pp. 38—46, 2013 (in Russian).

ESTIMATE OF DEPENDENCE OF THE VERTICAL TRBULENT DIFFUSION COEFFICIENT FROM BUOYANCY FREQUENCY FOR COASTAL ZONE OF THE BLACK SEA

Globina Lubov, Federal State Budget Scientific Institution "Marine Hydrophysical Institute of RAS" FSBSI MHI, Russia

The article highlights the most important studies of oceanographic processes, such as horizontal convection, winter cascading on the shelf and continental slope, the processes in the bottom of the Black Sea. The results of the study of small-scale structure of the shelf upper active layer of the Black Sea in 2014 are discussed. The new information about the distribution of the eddy diffusivity with depth in the coastal part of the Heracleian peninsula is given. The investigated dependence vertical turbulent diffusion coefficient from buoyancy frequency at the active layer is found to be has a quadratic character for the entire shelf area and doesn't depend on the stratification.

Keywords: turbulent diffusion, energy dissipation rate, cold intermediate layer, cascading.

I. INTRODUCTION

In the stratified ocean interior there are variety physical mechanisms aimed at the exchange of energy, temperature, salinity between water masses of different scales. Each mechanism operates under certain hydrophysical conditions. Joint study of the processes taking place on different spatial and temporal scales, will set the boundary conditions for the operation of various physical mechanisms for simplifying and solving mathematical models of semi-empirical equation of turbulent diffusion.

The ocean interior is conditionally divided on the layers. Layers are divided according to the action type of some mechanism. For example, in the ocean there are three main layers on the distribution of buoyancy frequency: the upper mixed layer (or a layer of wind mixing), the active layer (up to a maximum frequency of buoyancy), the main pycnocline (or a layer of local mixing) and the bottom layer of the convective exchange.

For the active layer an additional cold intermediate layer can be identified. It is involved in the formation of seasonal thermocline and is formed in the coastal part of the sea (ocean). Coastal waters differ from the open ocean waters by uneven warming of the water surface, which depends on the breadth and depth of the water area, the difference of temporal variability, geothermal.

An important role in maintaining the turbulent exchange plays cascading. It makes contribution to the exchange of water between the shelf and the deep ocean. Its effect is enhanced in the marginal seas, due to the instability of the main pycnocline, impervious surface water on the depth [1].

II. THE MECHANISM OF FORMATION OF THE COLD INTERMEDATE LAYR FOR THE BLACK SEA

There are all conditions for the formation and stable presence of the cold intermediate layer in the Black Sea. The Black Sea separate from the world's oceans and has a circulation mode.

The northwestern part of the Black Sea is a broad continental shelf, which narrowing stretches along the western coast to the Bosporus. The annual river flow is an average of more than 310 km^3. 80% of this amount goes to the north-western shelf of shallow water, where the Danube and Dnieper empty into. Fresh water balance is positive, because the coastal runoff and precipitation exceeds evaporation of about 180 km^3 [2].

Thus, any temperature change in the north-western waters of the Black Sea create the preconditions for the formation of convective horizontal and vertical circulation, which is the main mechanism for the formation of cold sea water.

The cooling of water is begun with river runoff. It is considered the original source of the dense cold waters.

With a small difference of hydro-physical characteristics from surrounding waters, the river plume is a stable structure. This structure is a little stratified, and there may be a separate layer, involving the nearby water in the common stock process, thereby changing the initial geometry of the river plume and consequently - the buoyancy gradient [3].

Coastal waters are cooled, become denser and heavier. They flow down the slope to their isopycnic level and then are distributed as intrusion, thereby displacing the lighter water, resulting in convective motion of water nearby. This theory is applied to the shelf zone of the sea, when the angle between the sea level and the shelf is relatively small.

Taking into account the external effects for the formation mechanism of convective exchange: Earth's rotation, transfer the Ekman, also contributing to an increase of the environmental water in river plume, wind and given runoff direction, the horizontal-vertical convective exchange takes the form of alongshore current [4].

III. USED DATA

Small-scale characteristics of the upper active layer were obtained by a free-falling probe measuring complex *Sigma-1,* during the expedition in November 2014, on the research vessel *Nikolaev* in the conditions of the winter circulation of the Black Sea. Measurements were carried out along the coastal areas of the peninsula from Cape Chersonese to Aya [5,6].

IV. ANALYSIS AND METHODOLOGY

Based on the measurement data of the three vector velocity pulsation components, the estimation of dependence of the vertical turbulent diffusion coefficient on the stratification was obtained.

The applied values in the computation were averaged over the depth in increments of 0.1m, 0.3m and 0.5m. The turbulent energy dissipation rate was calculated using the following formula (1):

$$\varepsilon = \frac{15}{2}\nu\left(\frac{\partial u'^2}{\partial z} + \frac{\partial \upsilon'^2}{\partial z}\right) \quad (1)$$

where u' and υ' - the horizontal speed pulsations on X and Y axes, respectively, ν - molecular viscosity water coefficient. Buoyancy frequency was calculated as follows (2):

$$N = \sqrt{\frac{g}{\rho_0}\left(\frac{\partial \rho}{\partial z}\right)} \quad (2)$$

where g is the acceleration of free fall, ρ is the density, ρ_0 the density in the layer. Turbulent diffusion coefficient was calculated in accordance with the well-known Osborn [7] relation (3):

$$K = 0{,}2\frac{\varepsilon}{N^2} \quad (3)$$

The calculation example of the eddy diffusivity for a straight line along the stations is listed below.

station№6:

$$K = 2 \cdot 10^{-7} N^{-1{,}96}$$

station №7:

3-20 м.: $K = 3 \cdot 10^{-8} N^{-1{,}7}$

20-50 м.: $K = 4 \cdot 10^{-9} N^{-2{,}0}$

50-80 м.: $K = 6 \cdot 10^{-9} N^{-1{,}9}$

station №8:

4-30 м.: $K = 2 \cdot 10^{-7} N^{-1{,}98}$

30-59 м.: $K = 10^{-6} N^{-1{,}64}$

62-83 м.: $K = 10^{-7} N^{-1{,}99}$

station №9:

3-13 м.: $K = 2 \cdot 10^{-9} N^{-2{,}9}$

15-50 м.: $K = 9 \cdot 10^{-8} N^{-2{,}15}$

station №10:

3-21 м.: $K = 9 \cdot 10^{-8} N^{-2{,}15}$

21-28 м.: $K = 2 \cdot 10^{-7} N^{-1{,}85}$

28-47 м.: $K = 6 \cdot 10^{-7} N^{-1{,}74}$

For each station, the total layer is divided into sub-layers, depending on the buoyancy gradient sign. For example, three sub-layer were selected for the station №7: in the first one the decrease in the buoyancy frequency with depth was observed, in the second - the growth, in the third – the

decrease. This division was carried out to check for strict stratification and its influence on the mixing of the sea upper layers.

The presented equalities of the eddy diffusivity have the same index at buoyancy frequency, $K \propto N^2$, and does not depend from on the selected layer (independent from the division into sub-layers and stratification). This ratio remains everywhere up to bottom convective mixing layer.

If the sea shelf zone is characterized by intrusive stratification in the presence of horizontal exchange, after the cascading transition to the continental slope being the vertical exchange process intensification process consequence, the intrusions do not exist for a long time and the break up, keeping the temperature of the main cold intermediate layer constant.

Unlike the water circulation mechanism on the shelf, there are other mechanisms forming the vertical exchange on the continental slope. In the deep sea the convective exchange weakens and the main source of vertical mixing becomes instability and overturning *internal waves*, taking into account topographic features on the sloping bottom [8].

This fact is confirmed by the fact that the shelf temperature is changed in the horizontal direction, i.e. stratification adapts to external conditions, after crossing the *shelf - continental slope* boundary the temperature vertically changes (the external conditions are adjusted under stratification).

The change of one mechanism to another can be seen in the change of the exponent under *N* in the expression *K*(*N*). For example, data distribution analysis of the turbulent energy dissipation rate and buoyancy frequency, depending on the depth of the coastal part of the Southern Coast of Crimea from the article [9], showed the following expression for the stratified layer of the main pycnocline: $K \propto N^{-1,1}$.

In the given turbulent diffusion coefficient distribution with depth the studied value minimum was traced at 100 m depth and increased to its maximum at 400 m depth. The result obtained for the studied dependence under the in situ data from [9] showed good agreement with the previously obtained model of dependence of the turbulent diffusion coefficient on buoyancy frequency for the Black Sea.

Thus, due to the action of different mechanisms should be applied a different approach to the determination of the exchange ratios for the upper mixed layer on the shelf and in the deep sea. Cascading plays the main role in the redistribution of water masses on the shelf; it creates preconditions for involving of cold water into the deep sea, due to the formation of intrusions.

V. REFERENCES

[1] И. П.Чубаренко “Горизонтальная конвекция над подводными склонами,” Калининград : Терра Балтика, 2010, 255с.

[2] А.Н. Коршенко “Качество моских вод по гидрохимическим показателям,” Ежегодник, Москва, «Наука», 2013, 200с.

[3] F. M. Pimenta, A. D. Kirwan, P. Huq “On the transport of buoyant coastal plumes,” J. Phys.Oceanogr, 2011, 41, pp. 620–640.

[4] C. Moffat, S. Lentz “On the response of a buoyant plume to downwelling-favorable wind stress,” J. Phys.Oceanogr, 2012, pp.1083-1098.
[5] А.С. Самодуров, А.М.Чухарев, А.Г. Зубов, О.И. Павленко “Структурообразование и вертикальный турбулентный обмен в прибрежной зоне Севастопольского региона,” Морской гидрофизический журнал, 2015 № 6, с. 3-16.
[6] А.С. Самодуров, А.М. Чухарев, О.Е. Кульша “Режимы вертикального турбулентного обмена в верхнем стратифицированном слое Черного моря в районе Гераклейского полуострова,” Процессы в геосредах, 2015, № 3, с. 63 – 69.
[7] T.R. Osborn “Estimations of local rate of vertical diffusion from dissipation measurements,” J. Phys. Oceanog, 1980, 10, pp.83–89.
[8] T. Dauxois, A. Didier, E. Falcon “Observation of near-critical reflection of internal waves in a stably stratified fluid,” Physics of fluids, 2004, V.16, №6, pp.1936-1941.
[9] А.Н. Морозов, Е.М. Лемешко “Оценка коэффициента вертикальной турбулентной диффузии по данным CTD/LADCP-измерений в северо-западной части Черного моря в мае 2004 года,” Морской гидрофизический журнал, 2014, № 1, с.58-67

THE CURRENT STATE OF THE BLACK SEA COASTAL GEOSYSTEMS IN THE NORTH-EASTERN SECTOR

Eugeny Godin, Marine Hydrophysical Institute of RAS, Russia
Yury Goryachkin, Marine Hydrophysical Institute of RAS, Russia
Vyacheslav Dolotov, Marine Hydrophysical Institute of RAS, Russia
Sergey Dotsenko, Marine Hydrophysical Institute of RAS, Russia
Andrey Ingerov, Marine Hydrophysical Institute of RAS, Russia
Alexey Khaliulin, Marine Hydrophysical Institute of RAS, Russia
Sergey Konovalov, Marine Hydrophysical Institute of RAS, Russia
Alisa Kosyan, A.N. Severtsov Institute of Ecology and Evolution of RAS, Russia
Ruben Kosyan, Southern Branch of the P.P.Shirshov Institute of Oceanology of RAS, Russia
Marina Krylenko, Southern Branch of the P.P.Shirshov Institute of Oceanology of RAS, Russia
Elena Sovga, Marine Hydrophysical Institute of RAS, Russia

godin_ea@mail.ru

This work is a multi-disciplinary research aimed to develop common approaches to estimating the current state and forecasting evolution of coastal geosystems. From 2010 to now, the state of coastal zone geosystems of the Crimean and Caucasian Russian coast has been studied. The research tasks are solved using up-to-date IT based integrated analysis of historical and new observational data.

Key words: Black Sea, coastal zone, geosystems, sediments, database, natural disasters

I. INTRODUCTION

From 2010 to now, specialists of the Southern Branch of Shirshov Institute of Oceanology, Russian Academy of Sciences (SB IO RAS, Gelendzhik) and Marine Hydrophysical Institute (FSBSI MHI since May 2015, Sevastopol) have been conducting joint research of coastal zone geosystems of the Crimean and Caucasian Russian coast. The complex activity aims to work out general approaches to evaluation of the current state and forecast of the evolution of coastal geosystems having regard to variability of natural factors and anthropogenic pressure [1]. The research tasks are solved using up-to-date information technologies based on complex analysis which combined both the acquisition and analysis of new data of the field observations and systematization and analysis of archived data as well as materials of space sounding and aerial photographs. The paper presents results obtained in the course of this work.

Change of the Crimean coastline

From coastal zone geosystem state point of view, changes of the coast and coastal line are essential. In the long term, they occur either because of climatic changes of the sea-level and storm conditions or from human activities. To analyze the coastline changes we used data of contact and satellite observations. Old maps were also applied for the qualitative analysis.

The main natural process affecting coastline change during the last hundred years is the process of the Black Sea level rise, which began in the early 20's of the last century and is still going on. For this period, the relative sea level has risen by 20 centimetres. The main reasons are increase in the positive component of the water balance of the sea due to the rainfall growth and reduced evaporation from the sea surface, and also the tectonic subsidence of the coasts [2]. The storm activity by the Crimean coast, peaking in the middle of the twentieth century, began to decline significantly and reached a low in the end of the century. Since the beginning of the twenty-first century, there has been a tendency to the increase of the storm frequency especially in the western part [3].

The real picture of the development of the coast section under sea level changes is rather complicated and, in general, is not described by unambiguous causal relationships. The decisive role is often played by the rate of the sea level rise.

In the twentieth century, closing bays with bay bars and formation of lagoons (silted estuaries Andreevsky, Donuzlav, Bogayly, etc.) were typical for the Crimean coast. This process was characteristic of the Caspian Sea under the sea level rise conditions, where, along with passive flooding of land, a waterfront bar occurred in the wave breaking band and eventually separated a part of the sea as a lagoon [4]. The process of the insignificant (0.1–0.2 m/year) coastline retreat on the accumulative shores and its alignment (cutting capes and filling coast concavities) is typical for the Western Crimea. The maximum rate of the clay cliffs retreat on the scarp reached 1.5 m/year while its typical value is 0.5 m/year. The process of the spits growth and separation of their distal extremities followed by islands formation (the spits of Tuzla and Bakal) should be noted as well. At present, this process is also characteristic of the Sea of Azov.

However, the most notable changes of the shores were caused by human activities. So, large-scale construction works to protect the Southern and Western coasts of the Crimea were deployed in the second half of the twentieth century. As a result, a considerable stretch of beach was dressed in a concrete frame. The positive results of anthropogenic impact on the coast include reducing the damage caused by landslides; stabilization and abrasion protection of the coastal slope and the adjacent land area with constructions for different purposes and valuable natural landscapes; a significant expansion of the beach areas. However, the construction of protective structures has led to the definite environmental damage – the destruction of coastal marine communities and changes in the conditions of their habitats. As a result, the water area by the Southern Coast of the Crimea lost a number of flora and fauna species, such as: fish-swallow *Chromis chromis*, perch *Serranus scriba*, sea cock *Eulrigla gurnardus*; stone crab *Eriphia verrucosa*, seahorse *Hippocampus guttulatus*, etc. The damage caused to the landscape aesthetics seems to be also important. The

concrete shores stretching for many kilometers undoubtedly reduce the impression of the unique nature of the Southern Coast.

In contrast to the Southern Coast, the coastal protection strategy turned out to be a failure in the Western Crimea. It was caused both by an unreasonable desire to "improve" the shore with concrete structures and by mechanical transferring the building experience from the Southern Coast to the Western Crimea where the lithodynamic and geomorphologic features of the coastal zone are fundamentally different. As a result, a significant number of coastal protective constructions were destroyed by storms and now represent an emergency area where recreational activities are prohibited (fig.1).

Fig. 1 Ruins of coast protection in health resort Peshanoe.

These problem areas are located in the resort areas of Evpatoria, Nikolaevka, Peschanoe, and Beregovoe. The unreasoned construction led to a significant change in the natural dynamics of alongshore streams and to a whole series of negative consequences [5].In general, the essential problem in the Crimean coastal area is a shortage of beach forming material caused by the long-term negative anthropogenic impact and partly by the influence of natural factors.

Anapa bay-bar shoreline dynamics on satellite and aerial photographs

To study the Anapa bay-bar shoreline dynamics, data of aerial survey of 1941 (accomplished by the German AF during the II World War), satellite images of 1960ies (taken within the CORONA program), and satellite images with spatial resolution from 0.5 to 2.0 m for the period since 2003 till now have been used.

For the period of 1941–1966, the washout of the water edge did not exceed 15 m, and during 1941–2013 its average exceeded 37 m. The high accumulation values to the South of the current mouth of the Anapka river during 1941-1966 are probably explained by technogenic displacement of the mouth to the north in early 1960ies. A similar comparison of occasional surveys on 21.08.1966 and 21.11.2013 showed that the washout predominated on the most part of the bay-bar (more than 70 m at certain sections) but the accumulation (more than 20 m) was also observed. For the entire region, mean displacement of the water edge over 47 years was 23.3 m (towards the coast). To precise the results, the data were averaged for the water edge position in 1964–1966 (3 surveys) and 2012–2015 (7 surveys). The mean for the entire bay-bar displacement of the water edge was 22.1 m (towards the coast) for about 50 years, and the maximum washout exceeded 80 m.

This value is evidently out of limits of possible errors, so one can speak about the recession of the Anapa bay-bar sea shore. The sections with significantly different washout-accumulation regimes were found out within the Anapa bay-bar [6, 7].

A method for operational registration of sandy coast washouts

A method for operational registration of sandy coast washouts was worked out and tested using the satellite position control system manufactured by "LeicaGeosystems". It included two dual-frequency receivers (Leica GS10 and Leica GS15) processing signals from navigation satellites GPS (L1,L2), GLONASS (L1,L2), a receiving antenna and a field controller Leica CS 10 to control survey regimes and parameters. The system operation was supported by LeicaSmartWorxViva software [8].

Reasoning from the survey conditions and tasks, the system hard- and software configuration corresponded to RTK-cinematic regime and allowed conducting continuous cinematic survey in real time. For the GS15 receiving device functioning as a mobile receiver (RTK-rover), a special construction was prepared to allow locating the device on operator's shoulders and facilitating his walking about the survey area. To determine an error resulting from the irregularity of operator's movement, the measurement was done on an even surface.

Taking into account morphological peculiarities of the accumulative coast, an automatic coordinate counting was conducted with 2 m displacement in plan of with 20 cm relative displacement in height. The worked out technique was used to record the shoreline inter-storm dynamics of the accumulative coast in Krasnodar region(Fig. 2). Applying both the technique and the satellite position control system manufactured by "LeicaGeosystems" allowed executing a large scope of work in short time, quickly determining scale and speed of accumulative coast changes resulting from the storm activity, and passing users' data necessary to prevent washout consequences.

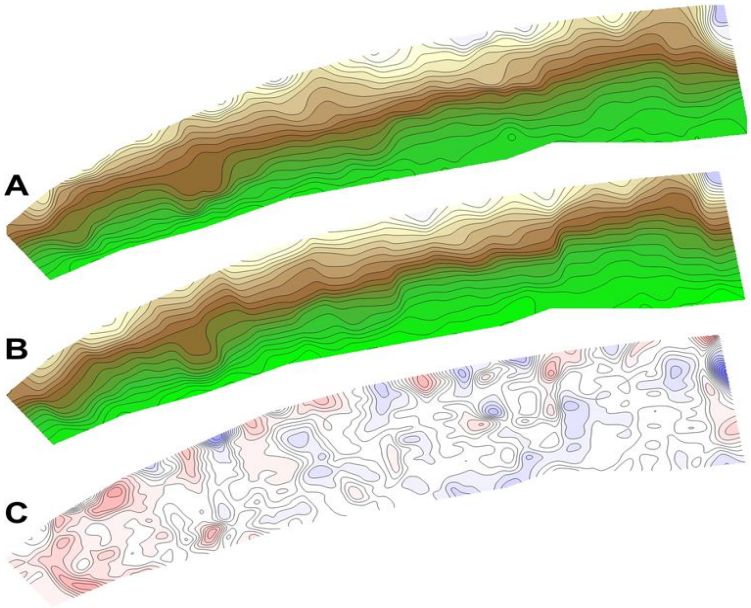

Fig. 2.Beach storm dynamics (A – beach elevation before storm, B – beach elevation after storm, C – change of beach elevation).

The Bay of Sevastopol

The Bay of Sevastopol (Fig. 3) is one of rare natural inland harbors at the coast of Crimea on the Black Sea that has being serving as a marine shelter and residence for sequencing human civilizations for over 25 centuries.

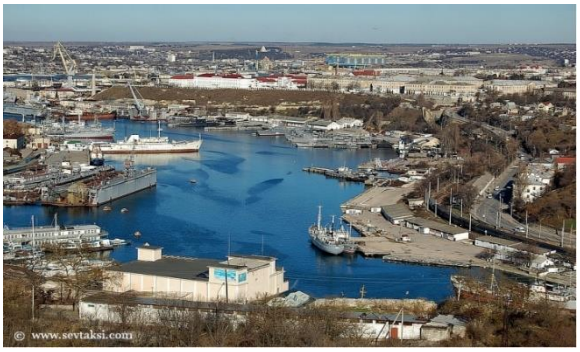

*Fig. 3 The Bay of Sevastopol (*http://gamelika.com/imaginator/1/4e5fa9dd2ed5a_sevastopol.jpg *and* http://www.sevtaksi.com/foto/0014-crimea-sevastopol-juzhnaja-buhta-foto.html*).*

Historically, this bay is a natural reason for the existence of Sevastopol, as a navy base and the city with its all maritime activities. The Bay has been intensively used since Sevastopol was founded in 1783. Currently, Sevastopol Bay is a place for a big and intensively growing seaport (the total length of place for ship docking and mooring is ~11 km), ship docking, sea-land transportation of various goods. The population of Sevastopol is about 400,000 permanent residents, but this number can easily double on summer time. Unfortunately, the major part of municipal and industrial sewage waters (~10,000 m^3 per day) are loaded to the bay from ~30 sewers without or after minimal treatment. The latter leads to increase of nutrients and organic carbon supply, supporting active oxygen consumption in the waters of the bay. Biogeochemical conditions in the bay's environment have become so extreme that hypoxia is a regular feature of the inner part of the bay on summer time [9]. Sediments have become sulfidic. To make matter worse, up to 40 μM of sulfide have been registered in the bottom layer of waters. This has drastic negative consequences for the ecosystem of the Bay of Sevastopol.

Yalta Bay

To estimate the ecological state in Yalta Bay including the Yalta port area, the trend of seasonal and interannual variability of data distribution for biogenic elements, oxygen and temperature was studied based on the comparison of data obtained in 1987–2004 and 2005–2010 [10, 11]. Dynamics of biogenic elements and dissolved oxygen on the background of variation in temperature, salinity of waters in the surface and near-bottom layers during all the seasons for the last decade (2003–2012) was also evaluated for the Yalta port area. It was found that the oxygen and temperature regimes in the areas under consideration are in antiphase that became particularly evident in 2005–2010. During this period the content of dissolved oxygen in the surface layer was decreasing especially from May to October while the temperature trend was positive for all the

seasons. It was shown that the hydrochemical regime in the Yalta port area since 2005 to 2010 was characterized, despite the temperature growth, by decrease in dissolved oxygen , inorganic phosphor and silicon, and significant increase in content of nitrogen salts (particularly, nitrates) when compared to the period of 1987 – 2004. It was ascertained that the anthropogenic pressure effects both dynamics of the biogenic elements and the oxygen regime in the area under investigation, and it is more pronounced in the surface layer than near bottom.

The Heracles peninsula coastal waters

The hydrochemical regime of the Heracles peninsula coastal waters was also studied. This water area is of particular interest because it is indirectly influenced by all of the bays of Sevastopol (Sevastopol, Kruglaya, Streletskaya, Kazachya, Kamyshovaya, and Balaklava) and undergoes a considerable anthropogenic pressure. The main sewer line is located in this area (more than a half of total city discharge) with a diffuser in a distance of 3.3 km from the shore, resulting in a sharp increase of phytoplankton production caused by an intense influx of biogenic matter and dissolved organics.

The accomplished analysis allowed evaluating the long-term variability in the surface and near-bottom layers for the following hydrochemical parameters: oxygen O_2 (ml/l); pH; nitrites NO_2 (mkM/l); nitrates NO_3 (mkM/l); phosphates PO_4 (mkM/l); silicon SiO_3 (mkM/l). At the same time, high silicon concentrations (80–167 mkM/l), regardless of the season, were found out especially in the near-bottom layer, and they were observed on the background of low salinity in the surface layer particularly in May and August. As a result of analyzing the annual course of the biogenic elements (phosphor and nitrogen), different from silicon seasonal variability was found, demonstrating evident dependence on biological processes (growth in winter and decrease in summer). At the same time, the research showed insufficiency of data on the Heracles peninsular coastal waters. It raises a question of necessity of continuous hydrochemical monitoring of the area. The priority should be paid to observing distribution of nitrates and ammonium during all the seasons as they are main pollutants in sewer and rainy flows.

IV. BIOLOGICAL STUDIES OF THE COASTAL SYSTEMS

It was found that biogenic carbonates comprise up to 90% of beach sand of Anapa Bay Bar. The main source of carbonates are dead shells of the bivalve *Chamelea gallina*, inhabiting mostly the depth range 5-10 m. Preliminary investigations of the sediment balance of Anapa bay bar and adjacent regions were conducted, and approximate annual income of the carbonates of biogenic origin was estimated as 350 kg/m2 [12] .

A biological assessment of the sea water pollution was conducted using the gastropod *Rapana venosa*. In two sites: Sevastopol Bay in Crimea and Blue Bay (2) in the Caucasian coast, imposex females of this whelk were found (see Table 1). Imposex is a phenomenon described for more than 150 gastropod species, when females develop male organs (penises, distal parts of the seminal duct and prostate gland) as a result of interaction with a pesticide tributyltin, a component of antifouling paints for marine vessels and immersed constructions. All imposex females of the rapa whelk examined were Stage 1, rarely 2 on the VDS scale [13], and were expected to function

normally in reproduction. It is interesting that imposex females in the small Blue Bay were only found under the pier with moored ships, while samples from the center of the bay (three sites about 200 m apart from each other, with about 300 specimens studied) were lacking imposex. No imposex was found in other investigated sites (ten sites from Sochi to Balaklava Bay, with total more than 1200 specimens analyzed). The presence of imposex in the two bays may be connected with higher shipping activity in these water areas and as a consequence, pollution with tributyltin.

Table 1. Sex distribution of *Rapana venosa* from sites with detected imposex

Sampling site and date	Males		Normal females		Imposex females	
	Number	Rw/Tw, %	Number	Rw/Tw, %	Number	Rw/Tw, %
Pier in Blue Bay. June 2010	10	19.3	21	27.7	0	-
Pier in Blue Bay, 16.05.2011	6	29.2	30	28.6	6 (50%)	30.0
Pier in Blue Bay, 27.06.2012	1	?	9	29	10 (91%)	27.6
Sevastopol Bay, June 2009	1	?	28	19.9	14 (33%)	18.9
Sevastopol Bay, June 2011	1	?	1	?	2 (66%)	?

? – insufficient data.

In collaboration with HCMR, Greece, the pollution assessment of *Rapana venosa* collected in Blue Bay (a region, suffering from high recreational pressure during summer time, with flowing mountain river releasing large volumes of sediments from land) and the Tuzla Spit (a reserve and protected area) using biomarkers acetylcholinesterase (AChE), catalase (CAT), glutathione S-transferase (GST) and metallothionein (MT) was conducted [14]. A several times higher concentration of MT in *R.venosa* from Blue Bay was shown (Table 2). This, together with the data on imposex, may indicate heavy metals pollution of the bay. Weight indices of rapa whelks from the sites under discussion also indicate much better condition of the population from the Tuzla Spit than those from Sevastopol and Blue Bays (Fig. 4).

Table 2. Biomarkers concentrations in *Rapana venosa* from Tuzla Spit and Blue Bay

Sampling site	CAT(Units/mg proteins)	AChE Units/mg proteins)	GST (nmoles/min/mg proteins)	MT(mg/g tissue)
Tuzla Spit	3.73 ±0.21	289.81 ±73.00	320.28 ±36.93	83.53 ±8.12
Blue Bay2	2.38 ±0.30	286.24 ±74.09	389.11 ±34.56	276.33 ±24.28

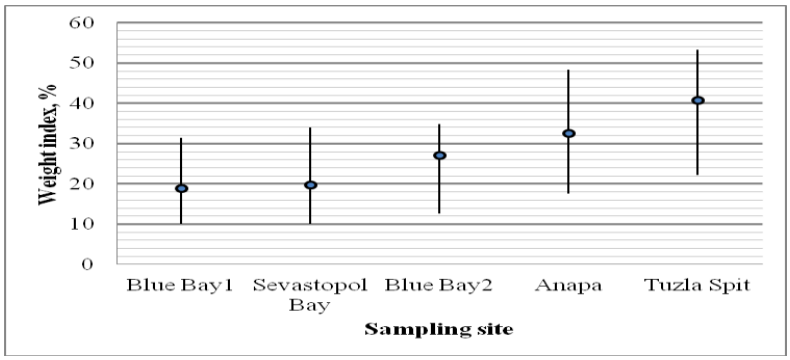

Fig. 4. Weight index of Rapana venosa in the Black Sea (raw weight of the soft body ratio to total raw weight).

The phenomenon of imposex in *R. venosa* was described in the Bohai Sea [15] and Chesapeake Bay [16]. In the Black Sea, pseudohermaphrodite females were discovered in Romania [17]. Russia joined the International Convention on the Control of Harmful Anti-fouling Systems on Ships in 2012. The presence of imposex in the Russian Black Sea reveals a necessity of tributyltin pollution monitoring.

V. DATABASES AND GIS

Oceanographic database for information support of the coastal zone study

In the framework of the joint research of coastal zone geosystems of the Crimean peninsula and the Russian Caucasian coast in the Black Sea, a specialized oceanographic database for information support of the coastal zone study has been prepared in the FSBSI MHI oceanographic data bank (MHI BOD). The database includes observations (up to 200 m isobath) along the Crimean and Caucasian coasts as well as on the north-west shelf of the Black sea (fig. 5). The database contains above 97,000 oceanographic and about 19,500 hydrochemical stations (about 20 hydrochemical parameters) and also data on hydrooptics, waves, currents, sea level, and some other parameters [18]. The database served as an information basis while analyzing the environmental state of a number of coastal water areas.

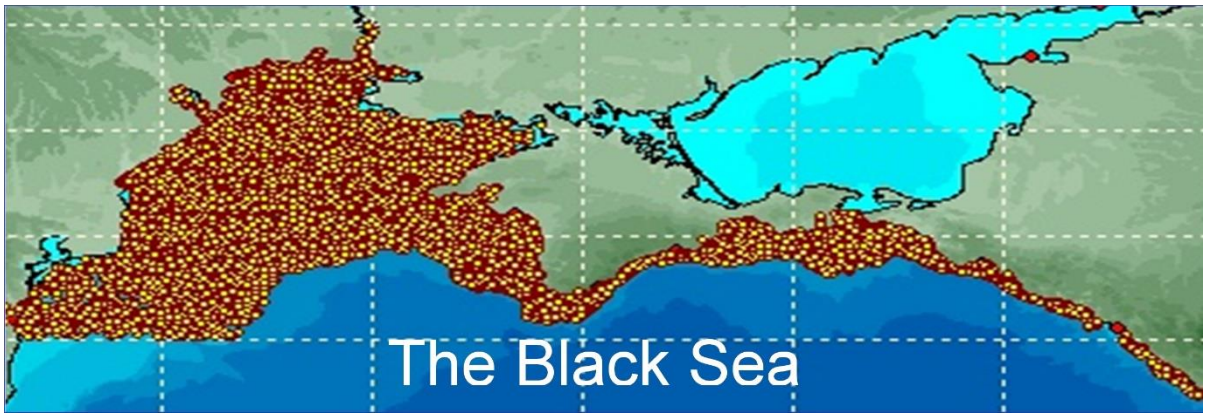

Fig. 5. Distribution of the oceanographic stations.

Database and the GIS-type tool for Sevastopol Bay

Sevastopol Bay has become the subject of regular oceanographic investigations and monitoring (regular observations at the regular locations/stations) since 1997. Regular oceanographic studies and monitoring of environmental conditions of the Sevastopol Bay are typically carried out at 32 oceanographic stations at a quarterly basis. Results of monitoring have been contributed to data bases of Marine Hydrophysical Institute of RAS and presented in publications [19]. This has made possible a detailed oceanographic description of Sevastopol Bay. Though these atlases are a valuable source of scientific information, their form has always limited utilization leaving stakeholders and managers with the problems of data accessibility and utilization of data of different nature for integrated coastal zone management. To resolve this problem, a digital atlas [20, 21] has been developed (Fig. 6).

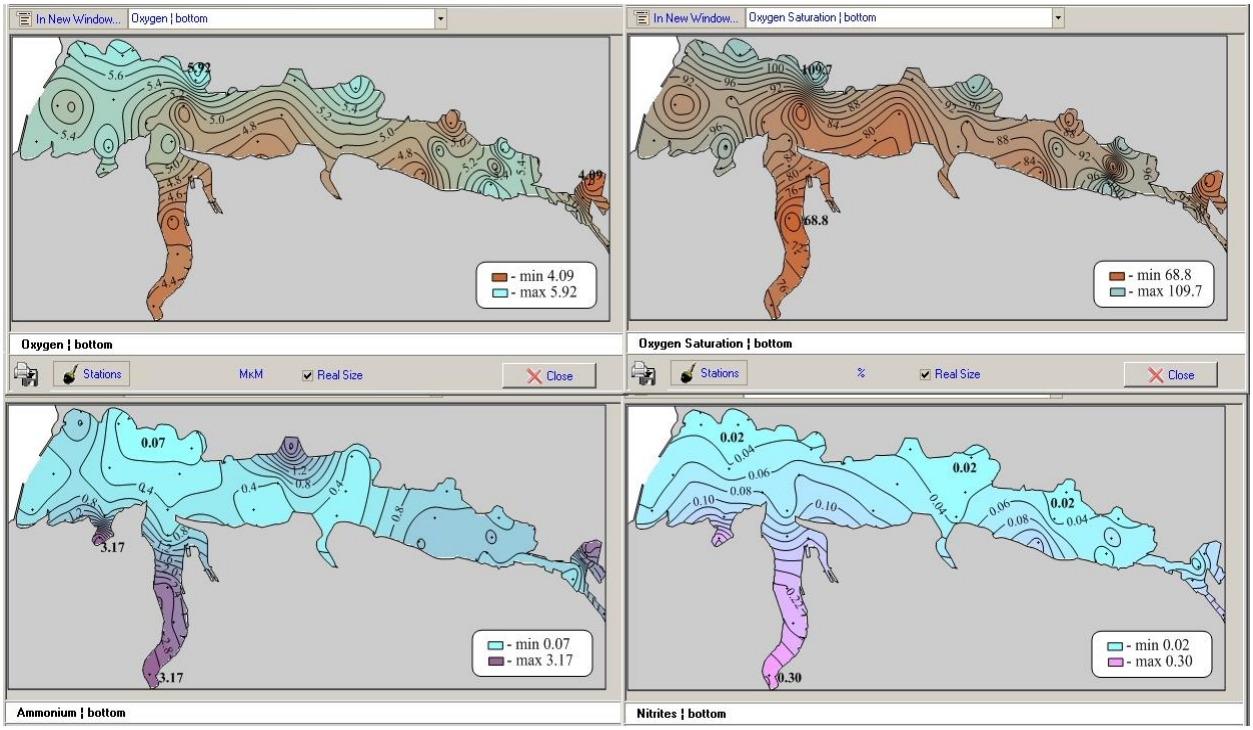

Fig. 6. The digital atlas of Sevastopol Bay.

There are several tools developed within this system. The major of these tools are GIS (Fig. 7) and indices (Fig.8). The GIS tool is basically an extended set of regular numerical grids for all considered properties that can be arranged as needed (scale of maps, color scheme, isolines and their format) and combined with other layers of information (municipal and industrial buildings, sources of pollutants and their properties, etc.). Though this tool is far more powerful for environmental assessment, it still provides basically scientific information, serving as a basis for calculation of indices [22].

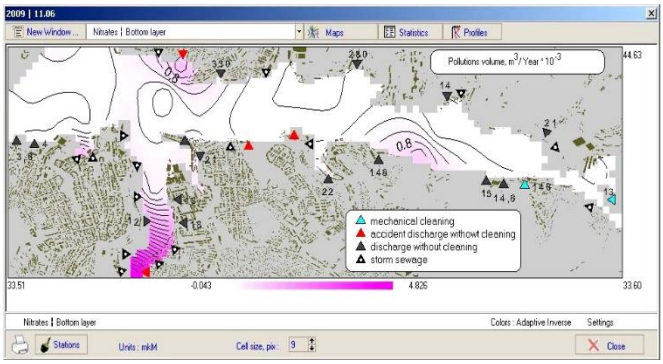

Fig. 7. The GIS-type tool for Sevastopol Bay.

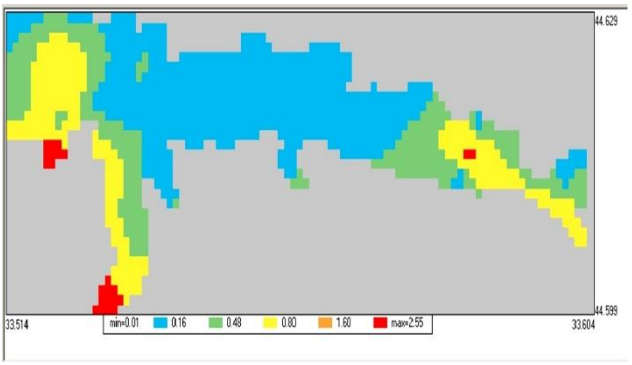

Fig. 8. The "traffic light" index for the average summer concentration of ammonium in Sevastopol Bay waters.

While interaction with gridded data makes possible to construct different maps, which have not been preloaded, indices make possible to evaluate the state of environment and achieve an integrated regional assessment and ICZM. Thus, for example, a "traffic light" index has been constructed and introduced into the system (Fig. 8). As an example, this index has been applied to assess average summer concentrations of ammonium in the surface layer of water. We have used 1-, 3-, 5-, and 10-fold the maximum allowed concentrations for coastal waters used for common purposes. The result clearly demonstrates that only the central part of the bay can be considered as "clean", but the inner part of the bay and that one under heavy municipal and maritime pressures are highly polluted.

Information on indices is generated in the form of tables and various maps and graphs. The most important advantage is that all indexes are calculated "on demand" for needed stations, areas, and periods of time. This makes possible to actually provide an integrated regional assessment, to monitor spatial and temporal variations in the state of coastal environment, to trace negative and positive trends due to changes in anthropogenic pressures or/and climate changes.

Database of the sea shore zone

In the framework of creating an up-to-date database of the sea shore zone current state, a universal data base in the ESRIShape format supposed to be used within a series of projects is concurrently worked out, detailed and corrected. The peninsula coastline location has been corrected so far according to its state in June 2014, including the description of all the coastal objects, particularly dikes, moorings, and retaining walls. An average density of the coastline points is about 6 meters and their general number is 185,000 [23]. At present, the above mentioned database is a basis for developing an interactive information system on the current state of the Crimean coast and also a GIS-tool for operational evaluating the coastal area pollution (Fig. 9).

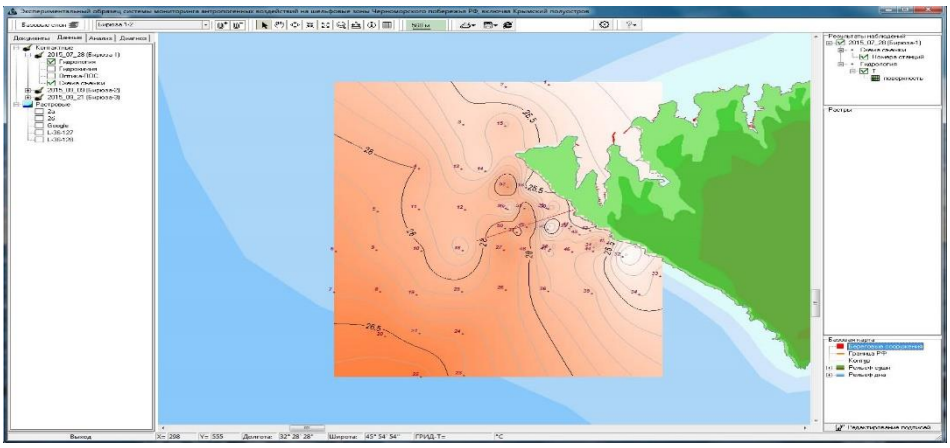

Fig. 9. An example of the database of the sea shore zone information spatial representation.

VI. NATURAL DISASTERS

Major types of natural catastrophes in the Black Sea coastal zone

Natural disasters in the Black Sea region which took place in the past, are happening in the present and may happen in future, causing death of people, significant economic losses and environmental damage. In the coastal zone of the Crimean peninsula and the Russian Caucasian coast the following natural events are considered the most important in terms of economic and environmental protection:

- abnormal sea level lifting and lowering of meteorological origin (surges, wind fluctuations and anemochore fluctuations of the sea level near the shore);
- gales, caused by Mediterranean cyclones;
- storm surges;
- tsunamis, caused by earthquakes and / or landslides;
- harbor oscillations;
- long-distance propagation of salt water in estuaries;
- abnormal ice conditions and early icing;
- upwelling in the summer period;
- abnormal temperatures and related phenomena (Novorossiysk boron, boron Crimean);
- tornadoes on land and sea, dust storms;
- heavy rains;
- fog over the Black Sea.

To quantify these phenomena, appropriate scientifically based magnitude scales and knowledge of the phenomena intensity thresholds are needed, as their violation may lead to emergency situations. The phenomena's critical magnitudes can be determined when sufficient data of instrumental observations of natural disasters are available. Unfortunately, information about the extreme manifestations of real events for many natural phenomena in the region is relatively scarce; it is limited in time and space. Descriptions of major natural disasters of the past were reflected in ancient books, myths and legends, historical manuscripts, chronicles; they contain little information about the exact quantitative characteristics of the phenomena, so it is not always possible to

determine physical causes of their occurrence and physical mechanisms of their development. Thus, continuous work of collecting and organizing data, conducting physic-statistical analysis of historical data, describing hazardous phenomena of different nature, are required. What is more, both types of data are valuable: of the distant past, and obtained in the instrumental observation period.

Insufficient observations severely limit the analysis based on instrumental data about real events. For this reason, mathematical modeling of ocean and atmospheric dynamic processes is currently being developed to study close to real conditions and determine extreme characteristics of hydrometeorological fields in the Black Sea region. To the greatest extent it relates to wind-level fluctuations surges, waves, tsunami, seiches, wind waves, barotropic and baroclinic currents, storm winds, eddies in the atmosphere, and pollutants and sediments transport. There is still much to do and improve in this area of research with the help of modern high-performance computing resources and numerical methods.

As an example, locations and times of tsunami observation along the coast of the Black Sea are shown (Fig. 10) for the cases when the events have not been registered instrumentally. The case of tsunami registration is shown on Fig. 11.

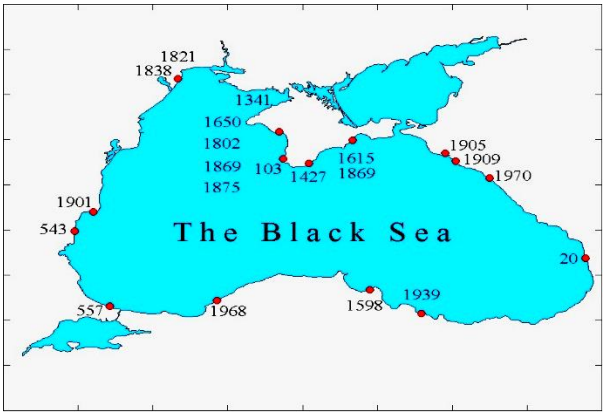

Fig. 10. Locations and times of tsunami observations along the coast of the Black Sea for the cases when the events have not been registered instrumentally.

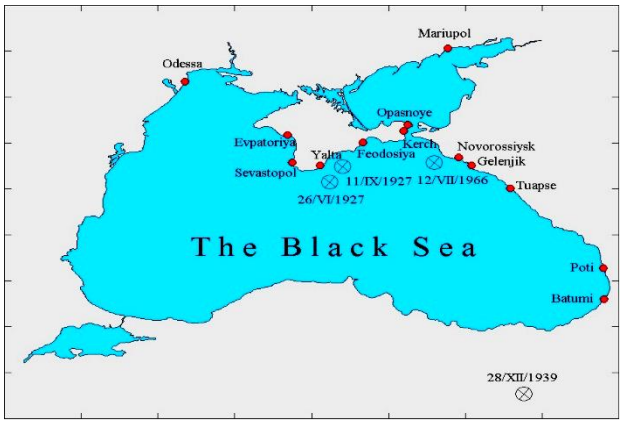

Fig.11. Tsunamigenic earthquakes epicenters and tsunami registration stations.

Research of the effect of an extreme rainfall on the state of the coastal zone

The effect of an extreme rainfall (06.07.2012) on the state of the coastal zone near the city of Gelendzhik was estimated. The abrasion of coast parts by the open sea where solid material entered directly in the surf area, and its immediate wave processing were studied. Numerous landslides have been formed on the sea coast as a resultof this extremely intensive rainfall.

About 20 large landslides of not less than 100 m3 occurred along 2 km line. Colluvium was presented by macrofragmental debris with insignificant amount of fine-grained material. The formation of debris cones (mainly crushed stone) with loam admixture was noticed in the places of narrow valleys joining, in mouths of temporary streams [24]. The extreme rainfall significantly changed the existing “natural” course of the coast evolution. The entered material contributes to a

certain increase of beaches and protect the cliff against the impact of small waves. On the other hand, this material will contribute to the cliff base abrasion during heavy storms.

VII. Acknowledgment

The work was financially supported by the Russian Science Foundation (RSF grant 14-50-00095)and study in Sevastopol bay was partially funded by the Russian Foundation for Basic Research (RFBR grant 16-35-60006 mol_a_dk).

VIII. References

[1] V. Eremeev, R. Kosyan, M. Krylenko, S. Dotsenko, E. Godin, A. Khaliulin, et al.. "Joint Investigations of the Coastal Zone of Ukraine and Russia in the Black Sea,"Proc. of the Int. Conference MEDCOAST – 2011 (Rhodes, Greece), no. 1, 2011, pp. 71-79.

[2] Yu.N. Goryachkin and V.A. Ivanov, *The Level of the Black Sea: Past, Present and Future,*Sevastopol: EKOSI-Gidrofizika, 2006 [in Russian].

[3] Yu.N. Goryachkin and L.N. Repetin, "Storm wind and wave conditions in the Black Sea coast of Crimea," in *Ecological Safety of Coastal and Shelf Zones and Comprehensive Use of Shelf Resources,* Sevastopol: EKOSI-Gidrofizika, vol. 19, 2009, pp. 56-69 [in Russian].

[4] E.I. Ignatov, *Coastal Morfosystems,* Moskow-Smolensk: Madzhenta, 2004 [in Russian].

[5] Yu.N. Goryachkin, *The Modern State of the Coastal Zone of Crimea,* Sevastopol: EKOSI-Gidrofizika, 2015[in Russian].

[6] M. Krylenko, V. Krylenko, R. Kosyan, "Accumulative coast dynamics estimation by satellite camera records", *Proc. of the Third International Conference on Remote Sensing and Geoinformation of the Environment (RSCY2015),* Book Series: Proceedings of SPIE. Vol. 9535. Hadjimitsis, DG; Themistocleous, K; Michaelides,S; et al, 2015. P.95351K. http://dx.doi.org/10.1117/12.2192495.

[7] V.V. Krylenko and M.V. Krylenko, "Evaluation of the accumulative edge dynamics using satellitephotographs",*Digests Intern. Conf. "Inter-Karto/InterGIS 21,"*Krasnodar, 16-19 November 2015, pp. 439-446 [in Russian].

[8] V.V. Krylenko, "Application of GLONASS LEICA GEOSYSTEMS equipment in scientific research", *Geoprofi,* vol.5, 2013, pp. 19-23 [in Russian].

[9] S.V. Svishchev, S. I. Kondrat'ev, S. K. Konovalov, "Regularities of seasonal variations in the content and distribution of oxygen in waters of the Sevastopol Bay,"*Physical Oceanography*, vol. 21, no. 4, 2011, pp. 280-293.

[10] E.E. Sovga, E.A. Godin, T.V. Plastun, and I.V. Mezentseva, "Evaluation of the hydrochemical regime of the coastal waters in Yalta Bay, "*Marine Hydrophysical Journal*, vol. 3, 2014, pp. 48-59, [in Russian].

[11] I.V. Mezentseva, E.E. Sovga, E.A. Godin, and T.V. Plastun, "Long-term variability of biogenic elements content in the Yalta port area," in *Ecological Safety of Coastal and Shelf Zones and Comprehensive Use of Shelf Resources,* Sevastopol: EKOSI-Gidrofizika, vol. 19, 2013, pp. 255-262 [in Russian].

[12] A.R. Kosyan, N.V. Kucheruk, and M.V. Flint, “Role of bivalve mollusks in sediment balance of Anapa bay bar”, *Oceanology*, vol. 52, no. 1, 2012,pp. 72-78.

[13] P. Gibbs, P. Pascoe, and G. Burt, “The use of the dog whelk Nucella lapillus as an indicator of tributyltin (TBT) contamination”, *J. Mar. Biol. Assoc. UK*, vol. 67, 1987,pp. 507-523.

[14] C. Tsangaris, V. Moschino, E. Strogyloudi, V. Coatu, A. Ramšak, A. Kosyan, et al., “Biochemical biomarker responses to pollution in selected sentinel organisms across the Eastern Mediterranean and the Black Sea, ”*Environmental Science and Pollution Research*, vol. 23, no. 2, 2015, pp. 1789-1804.

[15] H.H. Shi, C.J. Huang, S.X. Zhu, X.J. Yu, and W.Y. Xie, “Generalized system of imposex and reproductive failure in female gastropods of coastal waters of mainland China, ”*Mar. Ecol. Prog. Ser.*, vol. 304, 2005,pp. 179-189.

[16] R. Mann, J.M. Harding, and E. Westcott, “Occurrence of imposex and seasonal patterns of gametogenesis in the invading veined rapa whelk Rapana venosa from Chesapeake Bay, USA, ”*Marine Ecolology Progress Series*, no. 310, 2006,pp. 129-138.

[17] S. Micu, G. Comanescu, and B. Kelemen, “The imposex status of Rapana venosa population from Agigea littoral,”*l. Analele Ştiinţifice ale Universităţii „Al. I. Cuza” Iaşi, s. Biologie animal,”*vol. LV, pp. 133-137.

[18] A.Kh. Khaliulin, E.A. Godin, A.V. Ingerov, E.V. Zhuk, L.K. Galkovskaya, E.A. Isaeva,“Ocean data bank of Marine Hydrophysical Institute: information resources to support research in the Black sea coastal zone,” in *Ecological Safety of Coastal and Shelf Zones of Sea*, Sevastopol: EKOSI-Gidrofizika, vol. 1,2016, pp. 88-94 [in Russian].

[19] S.K. Konovalov, A.S. Romanov, O.G. Moiseenko, Yu.L. Vnukov, N.I. Chumakova, E.I.Ovsyany, *The Sevastopol Bay Oceanographic Atlas*, Sevastopol: EKOSI-Gidrophizika, 2010, 320p.

[20] S. Konovalov, V. Vladymyrov, V. Dolotov, A. Sergeeva, Yu. Goryachkin, Yu. Vnukov, et al., “Coastal management tools and databases for Sevastopol Bay (Crimea),”*Proc. of the Tenth International Conference on the Mediterranean Coastal Environment* (Ed. E. Özhan), MEDCOAST 11, 25-29 October 2011, Rhodes, Greece, MEDCOAST, Mediterranean Coastal Foundation, Dalyan, Muğla, Turkey, 2011, vol. 1, 145-156.

[21] S. Konovalov, V.Vladymyrov, V.Dolotov, O. Sergeyeva, Yu. Goryachkin, O. Moiseenko, et al.,“Environmental assessment tools in the PEGASO case – Sevastopol bay, ”*Proceedings of the Global Congress on ICM: Lessons Learned to Address New challenges* (Ed. E. Özhan), EMECS 10 –MEDCOAST 2013 Joint Conference, 30 Oct – 03 Nov, Marmaris, Turkey, MEDCOAST, Mediterranean Coastal Foundation, Dalyan, Muğla, Turkey, vol. 1, pp. 59-70.

[22] O.G. Moiseenko, N.A. Orekhova, A.V. Polyakova, E.V. Medvedev, S.K. Konovalov,“Indices and indicators of the environmental state of the Sebastopol bay,”*Moscow University Geography Bulletin,*no. 4, 2015, 41-48[in Russian].

[23] V.V. Dolotov and A.V. Dolotov, “Conception of constructing a system for monitoring anthropogenic impacts on the sea shore zone, ”*Marine Hydrophysical Journal*, vol. 6, pp. 34-42, 2015 [in Russian].

[24] V.V. Krylenko, M.V. Krylenko, R.D. Kosyan, and I.S. Podymov, “Solid material entering into the coastal zone in the area of Gelendzhik as a result of the extreme shower, ”*Oceanology,* vol. 54, no. 1, pp. 97-104, 2014 [in Russian].

THE PRINCIPLES AND ACTIVITIES OF THE NATIONAL SCIENTIFIC DEVELOPMENT STRATEGY IN THE ARCTIC ZONE OF THE RUSSIAN FEDERATION

George Gogoberidze, Russian State Hydrometeorological University, ggg@rshu.ru
Mikhail Bubynin, Federal Research Centre for Projects Evaluation and Consulting Services, bubynin-md@mon.gov.ru
Valery Abramov, Russian State Hydrometeorological University, val.abramov@mail.ru
Gennady Zabolotnikov, Russian State Hydrometeorological University, nis@rshu.ru
Alexey Krylov, Russian State Hydrometeorological University, a.krylov@rshu.ru

The paper considers the priorities of the state policy of the Russian Federation in the Arctic, from the point of view of the development of scientific research, identified by the main strategic documents of national policy and security in the Arctic zone of the Russian Federation. Measures for implementation of priorities in the development of scientific research in the Arctic can be divided into three main sections:

1. Scientific projects and expeditions in the Arctic;

2. International activities;

3. Coordination and implementation of integrated research in the Arctic.

Note that currently the Ministry of education and science of the Russian Federation develops the Analytical Coordination Program "Comprehensive research of the Arctic and Antarctic", in cooperation with the federal state bodies and Governance of the Subjects of the Arctic zone of the Russian Federation. The mechanism of the Program will ensure coordination between state bodies for integrated scientific researches in the Arctic in the interests of economic and scientific development of the region, and the creation of the scientific, technical and technological reserve in order to ensure of national security in the Arctic zone of the Russian Federation.

Key words: Arctic zone of the Russian Federation, development strategy, coordination of scientific research

I. INTRODUCTION

Today it has witnessed great interest to the Arctic zone. The Arctic contains a huge amount of energy sources, oil and gas, and proven reserves of oil in the Arctic (both offshore and onshore) are slightly less than 100 billion barrels. Through the Arctic the cross-polar air link (the shortest way between North America and Asia) the Northern Sea Route (the shortest sea route between East Asia and Europe) are passed.

The use of resources in the Arctic is extremely difficult and dangerous process from the environmental point of view, because due to the harsh Arctic climate the probability of accidents increases significantly. On the whole, the nature of the Arctic is one of the most vulnerable ecosystems on the planet. In 1991, Canada, Denmark, Finland, Iceland, Norway, Russian Federation, Sweden and the United States adopted the Arctic Environment Protection Strategy

(AEPS). In 1996, the Ministry of Foreign Affairs of the Arctic region have signed the Ottawa Declaration and formed the Arctic Council.

However, the Arctic is one of the few places on the planet, whose resources were not shared between countries. The Arctic areas are claimed at least five countries: Russia, Norway, Denmark, Canada and the United States who have access to the coast of the Arctic ocean. National claims may in the future be supported by different arguments, but it is clear that the main of them is practical – a real willingness of the country to actively explore the Arctic.

Russia has always been closely linked with the Arctic in its historical development. In the XI century Russian explorers came to the sea of the Arctic ocean, the middle of the XVII century is the time of development by Russian pioneers of the Eastern section of the Northern Sea Route from Lena river to the Kolyma river. Semen Dezhnev passed by sea from the mouth of the Kolyma river to the most easterly point on the mainland, and in 1648 he discovered the strait between Asia and America. The first Europeans who visited Alaska, were members of the team of "St. Gavriil" vessel. By the result of the great Northern expedition (1733-1743) in Russia, all the Siberian coast of the Arctic ocean was studied, described and mapped. Russia is the first country using the drifting polar station. The first drifting expedition called "North pole" was worked at the North pole at May, 1937. Due to the existence of the drifting polar station, Russian scientists got an opportunity to explore the Arctic year-round.

II. State policy of the Russian Federation in the Arctic

In the "Principles of State Policy of the Russian Federation in the Arctic for the Period till 2020 and Further Prospect" there were formulated the problem for use of the Arctic zone as the strategic resource base for socio-economic development, preservation of the Arctic as the zone of peace and cooperation and the conservation of local unique ecosystems.

Priority directions of development of the Arctic zone of the Russian Federation and national security are development of science and technology and security of international cooperation in the Arctic, in addition to the comprehensive socio-economic development of the Arctic zone of the Russian Federation and ensuring of ecological and military security, protection and safeguarding of the state border of the Russian Federation in the Arctic.

In the field of science and technology currently, there is shortage of technical means and technological possibilities for study, exploration and use of Arctic space and resources, with a simultaneous increase of technogenic and anthropogenic load on the environment. Development of science and technology of Arctic orientation in the Russian Federation conducts work on formation of a competitive scientific and technological sector in the development and introduction of advanced technologies and materials adapted to the climatic conditions of the Arctic, as well as the introduction of technical means and instrument base adapted for carrying out polar scientific research, particularly in the area of environmental management, development of offshore mineral deposits and water biological resources as well as the prevention and elimination of oil spills in ice conditions.

Russia seeks to increase the number of comprehensive scientific studies of natural hazards, technologies and methods of their forecasting in the context of climate change, including studying the impact on health of harmful environmental factors. In those aspects important to the

development of expedition activities in the Arctic, including international participation, and the use of international scientific and technological cooperation, ensuring the participation of Russian scientific and scientific-educational organisations in global and regional technological and research projects in the Arctic.

III. Development of scientific research in the Arctic

Measures for implementation of priorities in the development of scientific research in the Arctic can be divided into three main sections.

1. Scientific projects and expeditions in the Arctic
2. International activities
3. Coordination and implementation of integrated research in the Arctic

From this side, the Russian Federation expresses a particularly high degree of interest to participation in two topics:

1. Identifying Arctic-Science Challenges and their Regional and Global Implications.
2. Strengthening and Integrating Arctic Observations and Data-Sharing.

In the first subject it is necessary to allocate as the basic directions of research conducted in Russia, the following main works:

– Seismic geodynamic analysis and seismic zoning of the coastal-shelf region of the Russian Arctic;

– Comprehensive system for prospecting and exploration of mineral deposits in the shelf zone of the Arctic, based on seismic and electromagnetic (magnetotelluric) methods;

– The thermal state of the upper horizons of cryolithozone of the Russian Arctic and subarctic;

– Ecosystem evolution of thermokarst lakes in the context of climate change and anthropogenic load;

– Comprehensive assessment of the sustainability of coastal systems and coastal infrastructure in the tasks of spatial planning of maritime activities and socio-economic development of the Arctic zone of the Russian Federation;

– The expert system of forecasting of climate changes in the Arctic and the navigability of the Northern Sea Route;

– Dynamics of transport and transformation of carbon system in the Arctic land-shelf-atmosphere in the global warming and degradation of permafrost;

– Comprehensive monitoring and forecasting the state of the environment and creation the Arctic national system of environmental risk management due to climatic factors, including black carbon (black carbon).

In Russian State Hydrometeorological University successfully operating a unique Laboratory for Satellite Oceanography, which developed and maintains an information system for integrated monitoring of hydrometeorological state of the Arctic region on the basis of integrated analysis of satellite data, and created a fundamentally new approach to the study of Arctic cyclones.

In the Yamalo-Nenets Autonomous Okrug there are field-research hospitals which make detailed study of exogenous geological processes and phenomena.

A number of studies holds the Moscow State University, including study of integral factors determined by climate affect human activity in the Arctic region, and to develop recommendations to adapt and counter the negative influence of the specificity of the natural environment of the Arctic.

Within the second theme, it is first necessary to note the research activity, conducted by the Arctic and Antarctic Research Institute (AARI), having big international activity. Starting in 2012, it's implemented a joint Russian-German project "Transpolar system of the Arctic ocean", including a wide range of expeditionary marine and polar research in the Arctic. AARI continue monitoring in Tiksi Hydrometeorological Observatory, together with the United States and Finland. In 2015 in the framework of Russian-American cooperation on the project "Monitoring system for Nansen and Amundsen marine areas", the expedition studies the role of transformation processes of Atlantic water in the formation of modern climatic changes in the Arctic. In cooperation with the Finnish Meteorological Institute on the Ice Base "Cape Baranova" it's deployed complex of modern equipment for measurements of concentrations of greenhouse gases and aerosols in the surface layer of air.

In addition, AARI is the base a permanent research institute on the Spitsbergen archipelago of the Russian Scientific Arctic Expedition.

As for other organizations, leading its research activities, it is necessary to highlight the following works:

- Development of expert system to predict climate changes in the Arctic and the navigability of the Northern Sea Route;
- Development of integrated monitoring system in the coastal-shelf zone of the Russian Arctic seas;
- Development of methods and technologies of monitoring of the Arctic by space images and data of ground-based observations;
- Monitoring and forecast of extreme events in the Arctic;
- Development of comprehensive system for prospecting and exploration of mineral deposits in the Arctic shelf zone.

There is no doubt that for Russia the expansion of international scientific cooperation in the Arctic is one of the priorities. First and foremost, it needs to develop such research areas as:

- international project activities which are directly linked to the technology data exchange and collection of information;
- Russia's participation in international projects ("SIOS", "Inter-Act", "SAON", etc.);
- development of joint scientific expedition activities.

IV. Principles of the Analytical Coordination Program (ACP) "Comprehensive research of the Arctic and Antarctic"

Note that currently the Ministry of education and science of the Russian Federation develops the Analytical Coordination Program (ACP) "Comprehensive research of the Arctic and Antarctic", in cooperation with the federal state bodies and Governance of the Subjects of the Arctic zone of the Russian Federation.

The necessity of the ACP due not only to the importance of coordinating between Federal and Regional Authorities, but also the necessity of mutual coordination of activities with the research foundations, educational and scientific organizations which active in scientific and technological processes in the Russian Arctic, located in all regions of the Russian Federation.

The mechanism of the Program will ensure coordination between state bodies for integrated scientific researches in the Arctic in the interests of economic and scientific development of the region, and the creation of the scientific, technical and technological reserve in order to ensure of national security in the Arctic zone of the Russian Federation.

ACP is divided into 4 sub-programs by functional basis:

- Sub-program 1. Provision of monitoring and comprehensive analysis of state and prospects of scientific research development in the Arctic zone of the Russian Federation and the Antarctic;
- Sub-program 2. Monitoring and coordination of the comprehensive marine and coastal research in the Arctic and Antarctic;
- Sub-program 3. Monitoring and coordination of applied research aimed at solving tasks related to the strategic priorities of the Polar state policy of the Russian Federation;
- Sub-program 4. Activities of the regional research programs of the Arctic zone of the Russian Federation;

In the list of sub-programs, it is important the selection of individual regional components, which will allow to involve subjects of the Russian Arctic in the implementation of ACP activities. In addition, in frame of ACP it's possible to engage state programs and research funds and their financial resources for support of scientific, scientific-technical, innovative activities to the implementation of routines and specific activities of ACP.

As the participants in the implementation of ACP activities notes:

- the profile Federal Executive Authorities;
- scientific funds of support of scientific, scientific-technical and innovation activity;
- specialized scientific and educational organizations, which have active research and innovation activities in the Russian Arctic;
- enterprisers, including with state participation, supporting scientific and technological developments for the implementation of activities in the Russian Arctic;
- Arctic regional research centers.

The result of the ACP implementation will enhance the role and effectiveness of the Arctic scientific research, in the field of creation and development of technical means and instrument base for use in the Arctic, including the processes of import substitution, in implementing the policy of socio-economic development of the Russian Federation and increase of efficiency of use of budgetary appropriations for these purposes.

V. Acknowledgment

The Ministry of education and science of Russia provided financial support for this research, project 5.7.2016/NM.

COMPARATIVE CHARACTERISTIC OF SEA RADIANCE COEFFICIENT SPECTRA MEASURED REMOTELY IN COASTAL WATERS OF FIVE SEAS

Vera Rostovtseva, P.P. Shirshov Institute of Oceanology RAS, Moscow, Russia
Igor Goncharenko, P.P. Shirshov Institute of Oceanology RAS, Moscow, Russia
Dmitrii Khlebnikov, P.P. Shirshov Institute of Oceanology RAS, Moscow, Russia
Boris Konovalov, P.P. Shirshov Institute of Oceanology RAS, Moscow, Russia

goncharenko@ocean.ru

Sea radiance coefficient, defined as the ratio of the sunlight reflected by the water bulk to the sunlight illuminating the water surface, is one of the most informative optical characteristics of the seawater that can be obtained by passive remote sensing. We got the sea radiance coefficient spectra by processing the data obtained in measurements from board a moving ship. Using sea radiance coefficient optical spectra it is possible to estimate water constituents concentration and their distribution over the aquatory of interest.

However, thus obtained sea radiance coefficient spectra are strongly affected by weather and measurement conditions and needs some calibration. It was shown that practically all the spectra of sea radiance coefficient have some generic peculiarities regardless of the type of sea waters. These peculiarities can be explained by the spectrum of pure sea water absorption. Taking this into account a new calibration method was developed.

The measurements were carried out with the portative spectroradiometers from board a ship in the five different seas: at the north-east coast of the Black Sea, in the Gdansk Bay of the Baltic Sea, in the west part of the Aral Sea, in the Kara Sea with the Ob' Bay and in the Philippine Sea at the coast of Taiwan. The new method of calibration was applied to the obtained spectra of the sea radiance coefficient that enabled us to get the corresponding absorption spectra and estimate the water constituents concentration in every region. The obtained concentration estimates were compared to the values obtained in water samples taken during the same measurement cycle and available data from other investigations.

The revealed peculiarities of the sea radiance coefficient spectra in the aquatories under exploration were compared to the corresponding water content and some characteristic features were discussed.

Key words: optical passive remote sensing, sea radiance coefficient spectrum, sea water absorption, concentration of sea water phytoplankton, "yellow substance" and suspended matter, sea shelf, river mouths, inland seas

I. INTRODUCTION

Recently, investigation of oceans and seas by satellite remote sensing in visible is used for estimation of water content and main water constituents distribution. However, for thorough study of the coastal zones and inland seas the algorithms developed for open ocean are not valid and some

regional algorithms must be provided. That is why optical remote sensing from board a ship is of great importance. There have been a lot of works applying spectroradiometry from board a ship since the ninetieth of the last century (see, e.g., [1]-[4]). However, the results of such measurements are strongly affected by the wind, cloudiness and sea surface roughness as well as by experiment conditions. As a result one need either to restrict dramatically the suitable weather and experiment conditions (for instance, carry on measurements only with the clear sky and rather smooth water surface that is often impossible for some regions) or introduce some calibration method. The frequently used calibration method is based on the fact that water absorption in the long-wavelength range (more than 700 nm) makes the signal from the open ocean water bulk practically equal to zero, using it one can correct the coefficients in the sky reflecting part of the upward radiation. However, it is often not valid for the coastal zones and inland seas as the water scattering indices are much bigger there due to the enhanced suspended matter concentration.

In this article a new original calibration method is suggested. It gives the possibility not only to calibrate spectra measured in unsuitable weather conditions but also to obtain the estimates of sea water absorption spectra. After processing of thus obtained spectra we get the concentration of sea water main constituents in the region of interest. In this paper we show the application of such method for five different seas.

II. Details of measurements

This paper presents the results of the study of waters in five seas - the Black Sea, the Baltic Sea, the Aral Sea, the Philippine Sea at the coast of Taiwan and the Kara Sea - using the passive optical remote sensing of water surface. As a result of measurements we obtained some spectra of the sea radiance coefficient (Ro(λ)), defined as sea–water radiance referred to the horizontal white diffuse reflector radiance, which is proportional to the total sea surface irradiance. In the process of determining the sea radiance coefficient from the ship we used the spectrometer (AVANTES), operating in the spectral band 360-760 nm with 5.5 nm resolution. At each point we obtained the sea radiance coefficient spectrum by successive measurements of the three spectra: firstly, the radiance of the upward radiation (L_{sea}), which includes the intensity of the solar radiation backscattered by the sea water bulk and the intensity of light reflected by the sea surface; secondly, the radiance of the sky region, giving the largest contribution to the reflected radiation (L_{sky}); thirdly, the radiance of a white, horizontally disposed, diffuse reflector (L_{ws}), which characterizes the total sea surface irradiance. Every spectrum was measured with appropriate integration time (from tenths of a second to several seconds) with the intervals between the successive measurements at each point no more than 1-2 minutes. Other researchers use similar techniques for carrying out optical measurements, sometimes the white screen is substituted with cosine collector to estimate the total irradiance of the water surface [4].

After subtracting the reflection part ($r \cdot L_{sky}$, here r is Fresnel coefficient) from the upward sea surface radiance (L_{sea}) and dividing the result by the white-screen radiance (L_{ws}), which characterizes the total sea surface irradiance, the sea radiance coefficient spectrum is obtained:

$$Ro(\lambda) = \frac{L_{sea} - r \cdot L_{sky}}{L_{ws}} \qquad (1)$$

The sea radiance coefficient spectra obtained for 16 points using measurements from board a moving ship in the north-eastern part of the Black Sea are shown in Fig. 1.

The nadir angle was 25º-30º, azimuth angles provides the measurements from the board opposite to the sunlit one (the measurements were carried out from 8 a.m. to 3 p.m.) escaping the shade. The sky was partly clear and partly masked with fast moving clouds because of the windy day. The cloudy sky and the rough sea became the sources of the abrupt substantial changes of the spectra intensity.

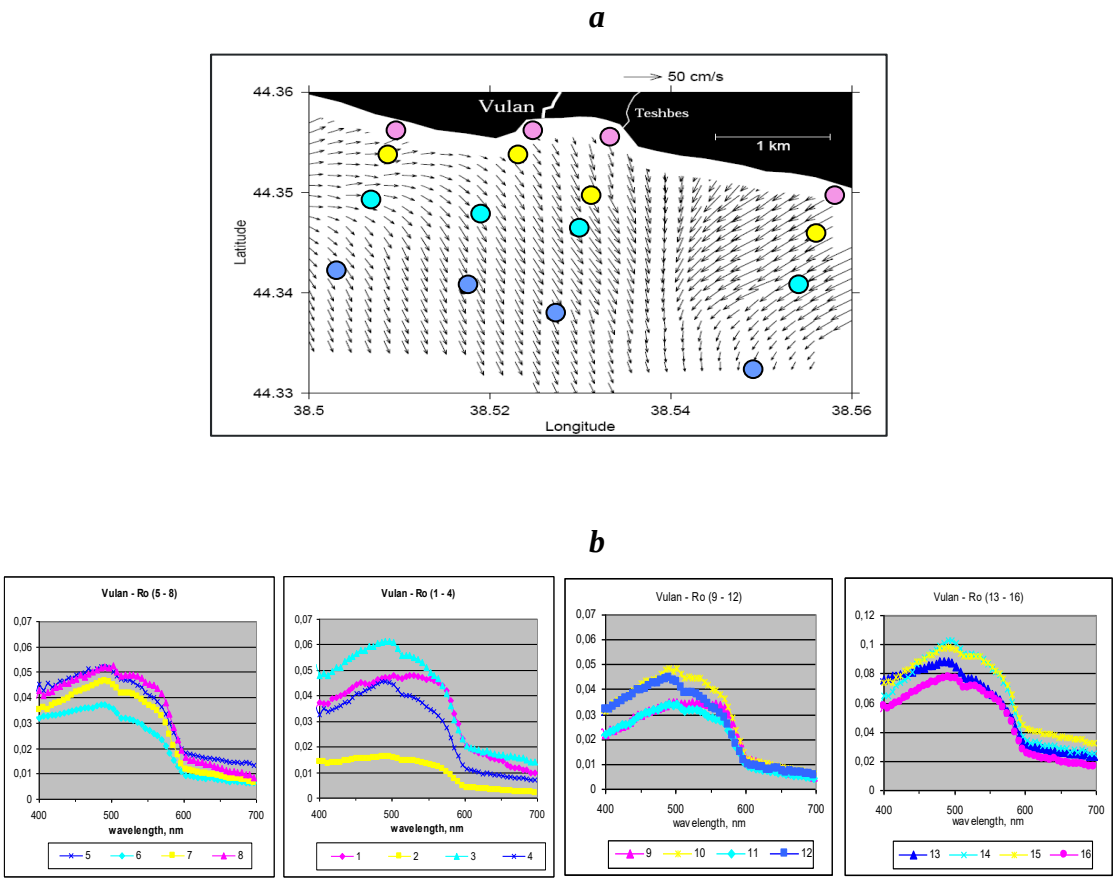

Fig. 1. Sea radiance coefficient spectra obtained for the Black Sea at 16 points at the Vulan and the Teshbes rivers mouth: position of the measurement points (a) and the sea radiance coefficient spectra obtained at every point (the colour of every curve corresponds to the number of the point and indicates the distance from the shore) (b).

Though the main water constituents concentration changes gradually from the rivers mouth to the open sea, one can see that the obtained Ro-spectra have rather chaotic appearance. That is the

result of the fast changes in the conditions of water surface illumination, reflectivity of the wavy surface and difference in radiance of cloudy and non-cloudy sky areas. It is obvious some calibration is necessary for this kind of the experiment data.

II. NEW CALIBRATION METHOD

By analyzing the sea radiance coefficient spectra demonstrated above and some other ones obtained by the same method in different aquatories, their common feature was revealed: regardless of the water content they all have so-called "step" – rapidly decreasing dependence in the section of the spectrum from 580nm to 600nm turns into less steep dependence from 600 nm to 700 nm. Since the main water constituents absorption and backscattering have no peculiarities in this spectral region (Fig. 2), the revealed "step" can be explained only by the peculiarities in pure sea water absorption spectrum (the review of the pure water absorption measurements is given in [5]). This explanation of the "step" appearance in the sea radiance coefficient spectra enables us to understand why practically all such spectra in coastal areas have abovementioned peculiarities. It should be mentioned that in open ocean waters such peculiarities also exist, however, they are practically not seen as the sea radiance coefficient value is negligibly small for more than 600 nm due to the relatively small backscattering index.

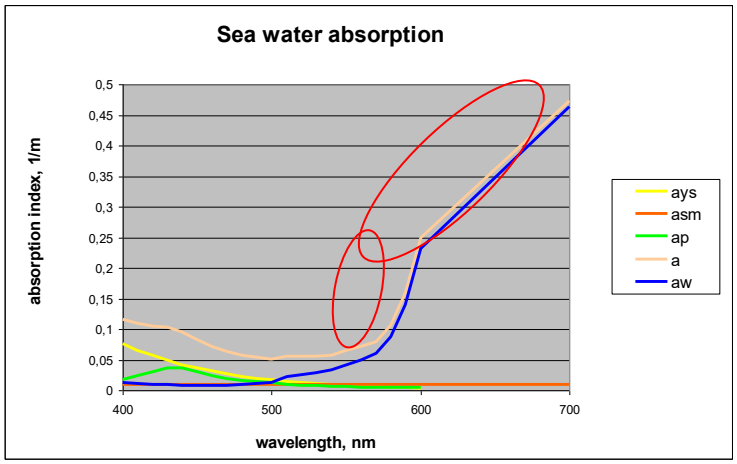

Fig. 3. Absorption spectrum of pure sea water – $a_w.(\lambda)$. For comparison an example of light absorption spectra by the three main natural water constituents ($a_{ys}(\lambda)$ - absorption of "yellow substance", $a_{sm}(\lambda)$ - absorption of suspended matter, $a_p(\lambda)$ - absorption of phytoplankton pigments) and total sea water absorption spectrum is given.

There are three main sources for Ro errors: the instrumental errors, errors from the alternation of light intensity during the set of three measurements (L_{sea} , L_{sky} , *and* L_{ws}) and errors from the uncertainty of the reflected from the water surface part of L_{sea} , the first one being much smaller than the two others. Our calibration is aimed at the two sources of larger error. The revealed properties of the spectrum enable us to calibrate sea radiance coefficient spectra obtained by measurements. We assumed that the true spectrum ($Ro^*(\lambda)$) is different from the measured one ($Ro(\lambda)$) and can be calculated with the help of two values:

$$Ro^*(\lambda) = k \cdot Ro(\lambda) - delR \qquad (2)$$

Here k is the coefficient responsible for the total irradiation changes and *delR* stands for the possible deviation in the reflectance part of the sea radiance signal ($r\,L_{sky}$).

Then, using the well-known dependence of the sea radiance coefficient upon the absorption and backscattering indexes of sea water ($a(\lambda)$ and $b_b(\lambda)$)

$$Ro^*(\lambda) = \frac{k_0 \cdot b_b(\lambda)}{a(\lambda) + b_b(\lambda)} \quad , \qquad (3)$$

we wrote the system of the three equations for *Ro(580), Ro(600) and Ro(700)* and resolved it for the three variables: $(a(600) + b_b(600))$, $\frac{k}{k_0 \cdot b_b(600)}$ and $\frac{delR}{k_0 \cdot b_b(600)}$. The detailed description of this process is given in [6]. It gives us the possibility to calculate some spectrum of the sea water under investigation in the whole visible (400 nm -:- 700 nm):

$$\frac{(a + b_b)}{b_b / b_b(600)} = \frac{1}{k/(k_0 b_b(600))Ro - delR/(k_0 b_b(600))} \qquad (4)$$

We claim that it is a good approximation for absorption in the case of backscattering being almost spectrally flat (it happens in some mesotrophic and eutrophic waters) and retrieve water constituents concentration from it. Of course, we can estimate only the sum of the suspended matter absorption and backscattering, however, as the backscattering index, as a rule, is much smaller than the absorption index, this sum can be accepted as an estimate of the suspended matter concentration. For simplicity from this point on we use “absorption” instead of “absorption plus backscattering” assuming that backscattering is spectrally flat and small in the whole wavelength range under consideration that is the case in coastal waters near river mouths.

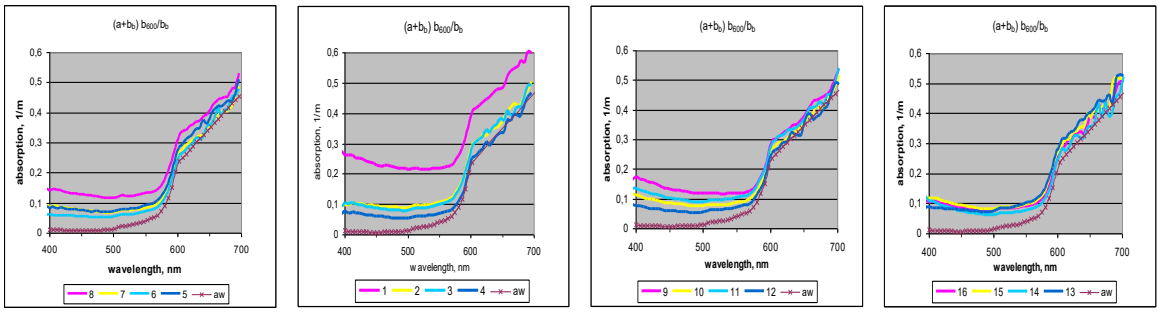

Fig. 3. Sea water absorption spectra calculated from the measurements of sea radiance coefficient in the Black Sea with the help of a new calibration method taking into account some inherent properties of pure sea water absorption.

The suggested method was applied to the above given spectra of the sea radiance coefficient measured in the Black Sea (Fig. 1). Comparing the initial spectra and the spectra of water absorption after calibration one can see the positive effect: despite the unfavorable meteorological conditions all the resulting spectra show the decreasing of absorption with increasing distance from the Vulan and the Teshbes mouth (see Fig. 3). For example, the spectrum in the second plot derived from the measurements at point 1 (see Fig.1a), which is the nearest to the Vulan river mouth, is significantly higher than others as the concentration of the suspended matter is the highest here.

III. ESTIMATION OF WATER CONSTITUENTS CONCENTRATION FROM ABSORPTION SPECTRA

The next step was processing the absorption spectra in order to reveal the water content at every point. Assuming that the main water constituents for this region of the Black Sea are phytoplankton, "yellow substance" and suspended matter and using the model spectra for their absorption (we got them averaging the data from [5]) we calculated their concentrations. The phytoplankton absorption model has a bell shape with the maximum at $\lambda_{p\max} = 440nm$, the "yellow substance" absorption is modeled by the exponential function with the index $g = -0.015nm^{-1}$ and both absorption and backscattering of the suspended matter do not depend on the wavelength. The illustration of this procedure is given in Fig. 4. After subtracting pure water absorption from the absorption spectrum obtained in the experiment we get the curve (dark triangles) representing the joint absorption spectrum of the water constituents. Varying the absorption values of the main water constituents we reach the best coincidence of the experimental and model total absorption curves and thus estimate the water constituents concentrations in terms

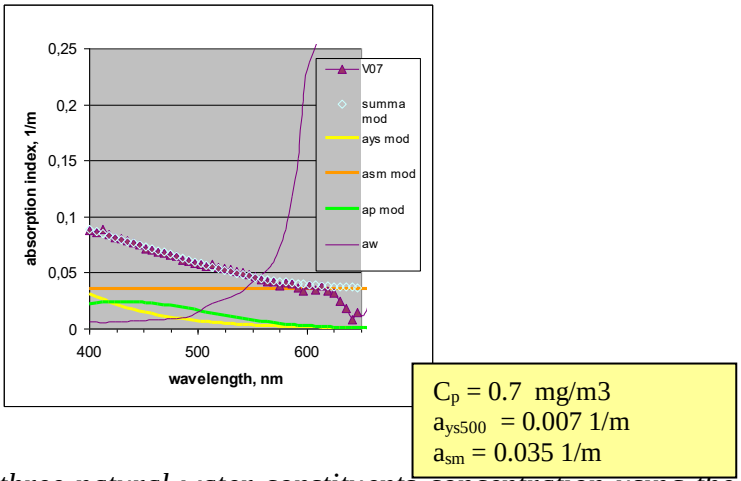

Fig. 4. Estimation of three natural water constituents concentration using the procedure of matching the experiment and the model absorption:

- *sea water admixtures absorption spectrum was derived from the remote measurements of sea radiance coefficient with the help of a new calibration method (dark triangles)*
- *model absorption spectrum was calculated as a sum of the water main constituents absorption by varying their concentration (light triangles).*

of their absorption indices at characteristic wavelengths: $a_p(\lambda_{p\max})$ for phytoplankton pigments, from which we calculate pigments concentration C_p, $a_{ys}(\lambda_{ys})$ for "yellow substance" ($\lambda_{ys} = 500nm$) and a_{sm} for suspended matter (it is assumed independent from the wavelength in the range of 400-700 nm).

IV. Comparison of Measurement Results in Five Seas

The analogical measurements were carried out with the same device in different seas and the same method of calibration was applied to the obtained spectra of the sea radiance coefficient that enables us to get the corresponding absorption spectra and estimate the water constituents concentration.

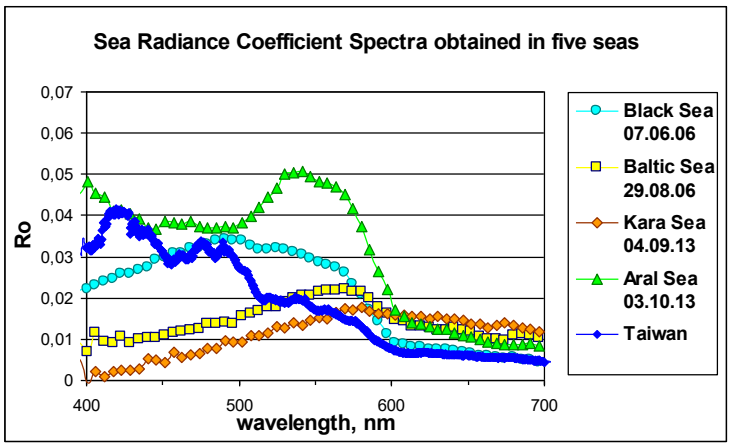

Fig. 5. Sea radiance coefficient spectra obtained for the Black Sea, the Baltic Sea, the Kara Sea, the Aral Sea and the Philippine Sea near Taiwan (the latter was obtained with a new spectroradiometer OCEAN OPTICS with spectral resolution of 1 nm)

All measurements were carried out from board of moving vessels (Fig. 5). The weather during the experiments was typical for the season: wind and roughness of the sea were average intensity, the sky was overcast for the Baltic and the Kara Seas, cloudless for the Aral and Taiwan and rather changeable for the Black Sea. As a result of the measurements and further calculations we received the following absorption spectra (Fig. 6). One can see that water types are quite different for the regions of exploration and even under unfavorable weather conditions our new method shows its operability. Using the main water constituents specific absorption we then estimated their concentration (Table 1).

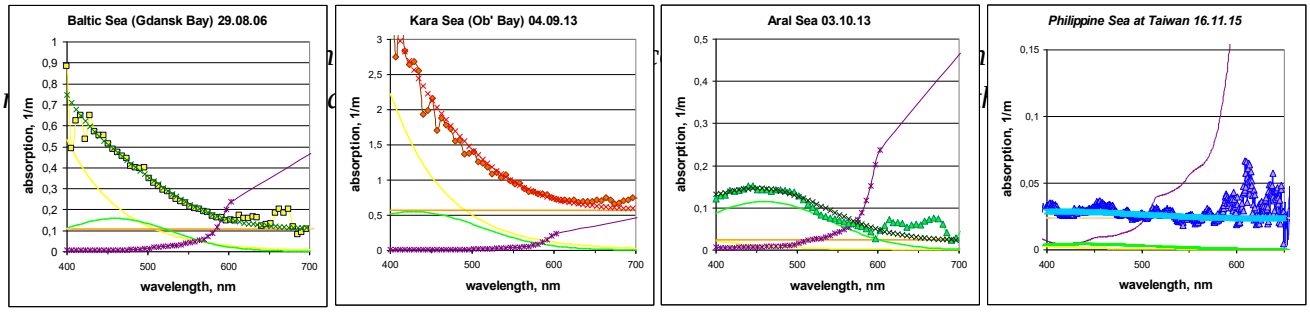

Table 1. Concentration of the main water constituents obtained by remote sensing

Concentration of	Black Sea	Baltic Sea	Kara Sea	Aral Sea	Taiwan
Suspended matter, 1/m	0.04	0.1	0.57	0.02	0.02
"yellow substance" at 500nm, 1/m	0.01	0.12	0.5	0.005	0.00
Phytoplankton pigments, mg/m^3	0.7	4.5	15.6	3.3	0.1

V. Discussion of the results and conclusions

The suggested calibration method enables one to get sea radiance coefficient spectra and water absorption spectra of the aquatory under investigation for wide range of the weather and measurement conditions. This possibility was confirmed during the measurements at the river mouth in the Black Sea. Firstly, the application of this method to the obtained sea radiance coefficient spectra, which were rather chaotic due to the unfavorable weather conditions, allowed to estimate the water absorption spectra, which showed a gradual decrease of water absorption with increasing distance from the river mouth and the shore. It should be stressed that as this method is based on the inherent properties of the pure sea water it can be applied for aquatories with various content of sea water constituents. Secondly, the obtained absorption spectra were successfully processed to estimate concentration of the three natural sea water constituents – phytoplankton pigments, "yellow substance" and suspended matter, the obtained values being in quite satisfactory coincidence with the measurements of phytoplankton pigments concentration in water samples. There is a possibility to add some more impurities with their absorption spectra to this list if necessary.

Application of the suggested remote sensing method with new calibration to the five different seas is shown to be quite useful. It showed that one can get proper results in the cases with the sky totally overcast, in the cases with the low solar elevation angle in the Kara Sea and therefore with low level of signals, in the cases of great variety of the sea water constituents concentration. The obtained values of sea water constituents concentration, such as phytoplankton pigments, "yellow substance" and suspended matter, fall within the range of concentrations, measured by other methods in the aquatories under investigation (see [7], [5], [8], [9]).

On the whole, using the new calibration method we got some encouraging results:

- the distribution of the water absorption values, which were obtained by remote sensing, is quite reasonable for the Black Sea polygon (decreasing with the distance from the river mouth and from the shore)
- for the wide range of weather and measurements conditions as well as for the great variety of water constituents concentration the estimates of the concentration obtained by remote sensing get within the range of the estimates obtained from sampling for every region.

Estimating of natural water constituents concentration from data of optical passive remote sensing of sea surface from board a ship combined with the new calibration enables to get some necessary data during ground truth measurements or explore the sea areas which are too close to the coastal line or are unseen from satellites because of cloudiness.

The future research is planned for further validation of this method with relevant results of water content determination on water samples and for investigation of other coastal and inland seas.

ACKNOWLEGEMENT

This work has been supported by Russian Scientific Fund Project N 14-50-00095.

REFERENCES

[1] V. A. Matyushenko, V. N. Pelevin and V. V. Rostovtseva. "Measurement of the Sea Radiance Coefficient with Three-Channel Spectrophotometer from board a Research Ship". *Atmospheric and oceanic optics,* vol. 9 (5): pp. 421-424. 1996.

[2] C. D. Mobley, "Estimation of the Remote-Sensing Reflectance from above-Surface Measurements". *Applied Optics,* vol. 38(36): pp. 7442–7455, 1999.

[3] V. N. Pelevin, and V. V. Rostovtseva. "Estimation of "Yellow Substance" Concentration in Sea Water by Various Contact and Remote Measurements Data". *Proceedings of SPIE,* vol. 4341: pp. 459-465, 2000

[4] A. Hommersom, S. Kratzer, M. Laanen, I. Ansko, M. Ligi, M. Bresciani, C. Giardino et. al. "Intercomparison in the Field between the New WISP-3 and other Radiometers (TriOS Ramses, ASD FieldSpec, and TACCS)". Journal of Applied Remote Sensing vol. 6: 063615-1 – 063615-21, 2012.

[5] B. Wozniak, and J. Dera. *Light Absorption in Sea Water*. New York: Springer Science+Business Media, LLC, 2007.

[6] V. V. Rostovtseva "Method for sea water absorption spectra estimation on the basis of shipboard passive remote sensing data and pure sea water properties*", Atmospheric and Oceanic Optics,* vol. 29(2), pp.162-170, 2016.

[7] N. A. Aibulatov, P. O. Zavyalov and V. V. Pelevin. "Peculiarities of Hydrophysical Self-Cleaning of Russian Black Sea Coastal Zone near the Mouths of Rivers". [in Russian] *Geoekologiya,* no 4: pp. 301-310, 2008.

[8] P. O. Zavyalov, ed. *The Large Aral Sea at the Beginning of the 21th Century*. *Phisics, Biology, Chemistry*. [in Russian]. Moscow: Nauka. 2012.

[9] I. N. Sukhanova, M. V. Flint, S. A. Mosharov and V. M. Sergeeva. “Phytoplankton Community Structure and Primary Production in the Ob Estuary and Adjacent Kara Shelf”. *Oceanology* vol. 50(5): pp. 785-800. 2010.

ASSESSMENT OF NUTRIENT LOAD ON THE PREGOLYA RIVER BASIN (VISTULA LAGOON CATCHMENT) FROM THE ANTHROPOGENIC SOURCES

Julia Gorbunova, Atlantic Branch of P.P. Shirshov's Institute of Oceanology of the Russian Academy of Sciences, Russia
Boris Chubarenko, Atlantic Branch of P.P. Shirshov's Institute of Oceanology of the Russian Academy of Sciences, Russia
Dmitry Domnin, Atlantic Branch of P.P. Shirshov's Institute of Oceanology of the Russian Academy of Sciences, Russia
Jens Christian Refsgaard, Geological Survey of Denmark and Greenland (GEUS), Denmark

julia_gorbunova@mail.ru

The catchment area of the Pregolya River is about 65% of the Vistula Lagoon drainage basin and occupied by Russia and Poland in approximately equal proportions. Nutrient load from the catchment largely controls the eutrophication processes of the lagoon ecosystem. Open statistical data (2011-2014) were used for evaluating the nutrient loads. At present, the nutrient load from the major anthropogenic sources (population, livestock, poultry and crop production) is 53,267 tons N/year and 16,424 tons P/year in the Pregolya River catchment. This results in loads of 23,032 tons N/year and 2,819 tons P/year when the removal of nutrients by the harvest is taken into account. It was found that the load from anthropogenic sources in the Polish part of the catchment higher than in the Russian part by a factor of three times for nitrogen and two times for phosphorus. The reason for this is that Polish territory is relatively more agriculturally developed. In the Kaliningrad Oblast agriculture declined in the 1990-2000's and now about 50% of arable lands are not used, which creates a potential for development. Currently there is a positive trend of the agriculture development and the "Strategy of socio-economic development of the Kaliningrad Oblast until 2020" is expected to increase arable land by 70%, the number of cattle and pigs by factors of 3.5 and 9.5, respectively. This creates a potential for significant increases of the nutrients loading and eutrophication of the Vistula Lagoon. The nutrient load from the anthropogenic sources in the Russian part of the catchment can be compensated greatly by using the manure as organic fertilizer replacing mineral fertiliser, as at present time 40% of available arable land in the Kaliningrad Oblast is sufficient for utilization of all manure originated locally at the maximum fertilization rate recommended by HELCOM. At the same time more than 80% of the wastewater in Kaliningrad Oblast is not sufficiently treated. This poses a great potential for nutrient load reduction. The calculations showed that equipment of Kaliningrad city with the modern treatment facilities will reduce the nutrient load by 1,400 tons N/year and 290 tons P/year.

Key words: nutrient load, phosphorus, nitrogen, Pregolya River catchment area, Vistula Lagoon

I. INTRODUCTION

The Pregolya (Fig. 1) is the largest river that flows into the Vistula Lagoon of the Baltic Sea. Its basin is 65% of the Lagoon's catchment area and its runoff is 44% of the total [1]. Nutrient load with the Pregolya River flow determines the eutrophication level of the Vistula Lagoon ecosystem largely. At present, there are several expert assessments of nutrients removal with the Pregolya River runoff. It is estimated at about 3,700-4,250 tons N/year and 490-740 tons P/year [2] [3] [4]. Removal of nutrients from the catchment area is determined by the load on the basin area from various sources and their retention in the catchment and hydrographical network.

The aim of the study is to assess the nutrient load (nitrogen and phosphorus) in the Pregolya River Catchment from the major anthropogenic sources: population, livestock and poultry, crop production. It also takes into account the removing of nutrients by the harvest. The study does not include an assessment of nutrients input from the natural landscapes, atmospheric deposition and retention in the catchment and river network.

The actual nutrient load from the anthropogenic sources was assessed from 2014 data. In addition, the potential changes were analysed for two scenarios of human activity evolution (the preservation of trends and planned development).

The transboundary catchment position of the Pregolya River causes difficulties for the assessment. The Pregolya River flows through the territory of the Kaliningrad Oblast and its main tributaries (the Angrapa and Lava) originate in the Warminsko-Mazurskie and Podlaskie Voivodships of Poland. The catchment area is occupied by Russia and Poland in approximately equal proportions – 49% and 51% respectively. In addition, a small part of the Pregolya River catchment (about 0.5%) is in the territory of Lithuania. The transboundary position of the catchment causes diverse social and economic conditions within the basin, because different countries have developed different management and decision-making systems. To obtain reliable results, a unified methodological approach of evaluating human impact across countries was applied.

II. MATERIALS AND METHODS.

The same methods of calculation of nutrient load for different national parts of the catchment were used in the study.

The anthropogenic sources of nutrient load in the catchment area were identified. The data were obtained from archives and electronic databases of the Territorial Authority of the Federal State Statistics Service in the Kaliningrad Oblast and Statistical Office in Olsztyn (http://kaliningrad.gks.ru, http://olsztyn.stat.gov.pl) as well as from literature.

To calculate the emissions of nutrients from the population a complete list of all localities and their inhabitants number was produced (the data are geographically referenced). The gross emissions [5] of 13.5 g nitrogen/person per day and 2.1 g phosphorus/person per day were used.

In the calculations of nutrients input from livestock, the annual load of nitrogen and phosphorus were determined according to the daily manure production per animal, content of nutrients in manure, the number of livestock and poultry in the farms and enterprises and households. The following manure daily production per animal were used in the estimations: cattle - 50 kg, pigs – 5 kg, goats and sheep - 3 kg, chickens - 0.16 kg [6]. The approximate chemical

composition of manure for nitrogen and phosphorus, respectively, were assumed as follows: cattle - 0.5%, 0.2%; pigs - 0.6%, 0.2%; goats and sheep - 0.8%, 0.2%; chickens - 1.6%, 1.3% [6].

Fig. 1. The study area - transboundary catchment of the Pregolya River

An evaluation of the area actually used for arable land was carried out using the open access data for administrative districts [7]. With the existing map for zoning of the Kaliningrad Oblast [8] according to administrative district occupied by the sub-catchment area, the areas of arable land were calculated for these sub-catchment areas. The agricultural crop yield was estimated by statistical data [7, 9]. The following removal ratios were used for the main cultivated plants: crops – 3.3 kg/ha, potato – 0.15 kg/ha [6], rape and oilseeds – 1.6 kg/ha [10]. Most of the soils in the catchment are sod-podzolic.

III. Results and Discussion

The basin is located in an agriculturally developed area, especially the Polish part. The Russian part of the catchment is mainly rural area too. Large industry facilities, such as Kaliningrad pulp and paper mills, have not operated since 2000s. Agriculture, which came into decay in 1990s-2000s, has intensified slightly in recent years. Agricultural development is now one of the priorities of the Kaliningrad Oblast policy.

Thus, population, livestock including poultry breeding and crop production are the main anthropogenic sources of nutrients in the Pregolya River catchment area. Kaliningrad, the largest

city of the region, is situated in the mouth of the river. Kaliningrad sewages are discharged directly to the Vistula Lagoon bypassing the Pregolya River. Therefore, the population of the Kaliningrad is not considered for nutrient load in the Pregolya River catchment calculations. Instead, the nutrient load from Kaliningrad was assessed separately as this source is of great importance.

Population

There are 660,000 inhabitants in the Russian part and 330,000 inhabitants in the Polish part of the Pregolya River catchment. Most of the population in the Russian part lives in Kaliningrad city (450,000 people).

In the Russian part of the catchment 90% of urban population and 30% of inhabitants in the rural areas are connected to the sewerage network [11], while the corresponding numbers in the Polish part are 97% and 43%, respectively [12]. Three cities in the Russian part of the catchment have biological treatment systems: Guryevsk (50% of discharges), Krasnoznamensk (80%), Gusev (100%) [11]. In the Polish part nearly all wastewaters (98%) are treated [12]. For all treatment facilities, except Olsztyn, the values for the biological treatment (without chemical and denitrification) are adopted. The degree of removal of nutrients during treatment are: 17% for the total nitrogen, and 25% for the total phosphorus [13]. In the case of Olsztyn the treatment plants include phosphorus removal and a denitrification unit: the degree of removal of total N is 70%, total P is 98%. In the case of households that are not connected to the sewage system, the degree of purification of waste water is 13% for total nitrogen and 10% for total phosphorus, adopted as in the case of a septic tank [14].

The load of total nitrogen and total phosphorus from point sources (the part of population connected to sewerage system) and urban areas (population without the sewerage system) are presented in Table 1.

Livestock and poultry farming

The livestock (cattle, pigs, goats and sheep) and poultry number was estimated from statistical data for administrative districts [15, 16]. A geographically referenced list of livestock and poultry enterprises and farms was compiled for Russian part. Livestock in households was calculated according to the rural population number [17]. The number of cattle in the Polish part is almost 3 times larger than in the Russian part of the catchment (143,000 and 52,000, respectively). The number of pigs in the Polish part is almost 1.3 times larger than in the Russian part (165,000 and 128,000, respectively) [15, 16]. According to data of 2014, the largest number of cattle and pigs in the Russian part were in the agricultural enterprises, while previously (2011), the number of cattle in households was almost equivalent to the number in agricultural enterprises, 45% and 51%, respectively. The number of poultry in the Russian part is almost 2 times more than in the Polish part of the catchment area (1,990,000 and 1,060,000 respectively). Most of the poultry in the Russian part is chicken, while half of the number in the Polish part is turkey.

The loads of total nitrogen and total phosphorus from livestock and poultry in the Pregolya River catchment area are presented in Table 1.

Crop production

It was difficult to evaluate the area of the arable lands in Russian part of the catchment. Available cartographic materials and spatial planning schemes contain the information only on lands nominally attributed as arable. In reality, less than 50% of the available arable land is used in the Kaliningrad Oblast. To assess the area actually used as arable the open access data for administrative districts was used [7]. The area of arable land in the Russian part is about half of the area in the Polish part. The use of mineral fertilizers in agricultural land is on average 65.2 kgN/ha and 14.6 kgP/ha for the Warmińsko-Mazurskie Voivodship [16] and 18 kgN/ha and 2.7 kgP/ha for the Kaliningrad Oblast [18]. The load of nutrients from mineral fertilizers in the Pregolya River catchment is presented in Table 2.

For the nutrient balance the nutrient removal by the harvest is important as well as the load from anthropogenic sources (Table 1).

Chemical fertilizers and livestock waste are the most significant sources of nutrients. Poultry breeding is important for phosphorus emission in the Russian part of the catchment area. (Fig. 2, 3).

The nutrient load from the anthropogenic sources can be compensated greatly by using the manure as organic fertilizer replacing mineral fertiliser. In this respect, HELCOM recommends an upper limit of manure at 170 kg nitrogen and 25 kg of phosphorus per hectare per year. At present time 40% of available arable land in Kaliningrad Oblast is sufficient for utilization of all of the manure originated locally at the maximum fertilization rate recommended by HELCOM, considering limitation by phosphorus.

Table 1. The main components of anthropogenic nutrient load in the Pregolya River catchment for 2014 (RU – the Russian part; PL – the Polish part).

Component of the anthropogenic load	Total Nitrogen		Total phosphorus	
	RU	PL	RU	PL
	tons/year	tons/year	tons/year	tons/year
Point sources (population connected to the sewerage system)*	640	1,160	100	110
Total catchment area	1,800		210	
Urban areas (population without sewerage system)	540	500	90	75
Total catchment area	1040		165	
Mineral fertilizers	6,000	20,000	900	4,500
Total catchment area	26,000		5400	
Organic fertilizers (livestock waste)	6,698	14,882	2,508	5,827
Total catchment area	21,580		8,335	
Organic fertilizers (poultry waste)	1,859	988	1,510	803
Total catchment area	2,847		2,313	

Total nutrient load from the main anthropogenic sources	***15,737***	***37,530***	***5,109***	***11,315***
Total catchment area	***53,267***		***16,424***	
Removal of nutrients by harvest	8,920	21,315	4,020	9,585
Total catchment area	30,235		13,605	
Total nutrient load from the main anthropogenic sources after considering removal by harvest	***6,817***	***16,215***	***1,089***	***1,730***
Total catchment area	***23,032***		***2,819***	

Notes: * - Kaliningrad city is not taken into account

a *b*

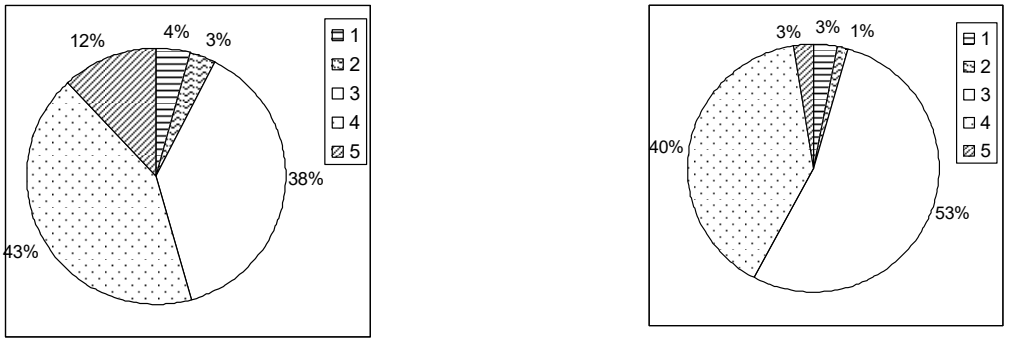

Fig. 2. Proportion of the main anthropogenic sources of total nitrogen in (a) Russian part and (b) Polish part of the Pregolya River catchment area: 1 – point sources (population connected to the sewerage system); 2 - urban areas (population without the sewerage system); 3 - mineral fertilizers; 4 - organic fertilizers (livestock waste); 5 - organic fertilizers (poultry waste).

a *b*

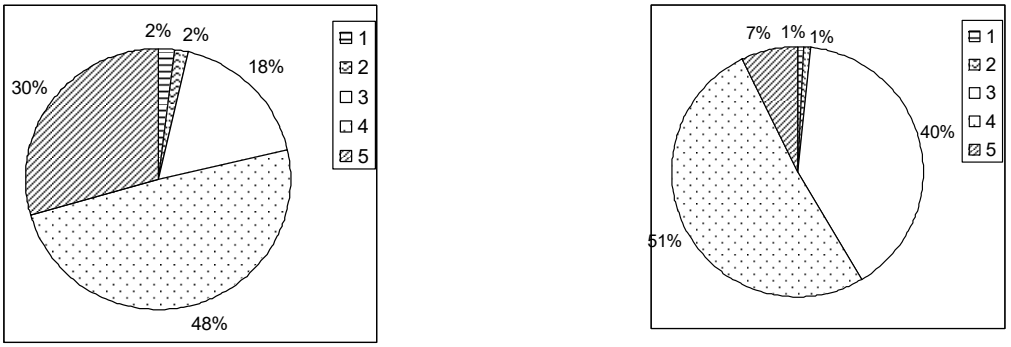

Fig. 3. Proportion of the main anthropogenic sources of total phosphorus in (a) Russian part and (b) Polish part of the Pregolya River catchment area: 1 – point sources (population connected to the sewerage system); 2 - urban areas (population without the sewerage system); 3 - mineral fertilizers; 4 - organic fertilizers (livestock waste); 5 - organic fertilizers (poultry waste).

Potential changes of the nutrient load due to different scenarios of human developments in the Pregolya River catchment

Two scenarios were formulated to assess possible changes of anthropogenic load as a result of alternative assumptions on human activities in the Pregolya River catchment.

Business as usual (BAU) - the scenario assumes preservation of the observed trend of development of agriculture and population. The last five years trends where analyzed for Russian and Polish parts of the Pregolya River catchment for arable lands, livestock of pigs and cattle and population (Table 2).

Documented future, official projections (DF). Further socio-economic development of Warmian-Masurian Voivodeship and environmental measures significantly depends on the implementation of the European Union program "Operational Program Eastern Poland 2014-2020". A significant increase in agricultural production is not expected [19, 20]. Analysis of the "Strategy of socio-economic development of the Kaliningrad Oblast in the long term" showed an expected increase in the area of arable lands by 70%, as well as cattle livestock and pigs by factors of 3.5 and 9.5, respectively (Table 2) [21]. As for population – a significant effect of the "Program of the Kaliningrad Oblast to assist the voluntary resettlement to the Russian Federation of compatriots living abroad" is expected. According the Strategy of Development of Kaliningrad Oblast the population in the Oblast is expected to increase up to 1.6 million people by 2020 [21].

Table 2. Quantitative assessment of agricultural developments for two different scenarios in the Pregolya River catchment.

	Business as usual (BAU)		Documented future (DF)	
	Russian part	Polish part	Russian part	Polish part
Arable	+5%	0%	+70%	+3%
Livestock				
Pigs	+15%	0%	+950%	+5%
Cattle	+15%	0%	+350%	+5%
Population	+25%	-6%	+70%	+3%

In the case of implementation of BAU scenario (development in accordance with the existing trends), the total load from anthropogenic sources will increase by 1,423 tons N/year and 438 tons P/year, i.e. less than 3% (Table 3). In the case of implementation of the plans of Kaliningrad Regional Government in accordance with the "Strategy of Economic Development of the Kaliningrad Oblast until 2020" (DF scenario) the significant rise of nutrient load by36,437 tons N/year and 12,317 tons P/year is expected, i.e. the total load from anthropogenic sources will double (removing by the harvest is not considered).

Table 3. Changes of the main components of the anthropogenic nutrient load in the Pregolya River catchment for Business as usual (BAU) and Documented future (DF) scenarios

Component of the anthropogenic load	BAU		DF	
	N total tons/ year	P total tons/ year	N total tons/ year	P total tons/ year
Point sources (population connected to the sewerage system)	+90	+18	+483	+73
Urban areas (population without the sewerage system)	+105	+18	+393	+65
Mineral fertilizers	+300	+45	+4,800	+765
Organic fertilizers (livestock waste)	+927	+357	+30,761	+11,414
Organic fertilizers (poultry waste)	0	0	0	0
Total nutrient load from the main anthropogenic source	**+1,423**	**+438**	**+36,437**	**+12,317**
Removing of nutrients by harvest *	+446	+201	+6,883	+3,102
Total nutrient load from all anthropogenic sources with considering removing by the harvest t	+977	+237	+29,554	+9,215

Note: * an increase in the runoff with the harvest is calculated in accordance with the increasing cultivation area, without taking into account changes in productivity.

A part of the increased load of nutrients will be removed by harvest (Table 3). Nutrient removal by harvest is calculated according to the extension of the arable lands and does not take into account the productivity increase. Hence the harvest removal is likely to be underestimated.

Kaliningrad wastewater

The wastewaters of Kaliningrad are mechanically treated only (mechanical filters operate with substantial overload) and it is discharged directly into the Vistula Lagoon through an open canal built as early as 1904 [22]. It is estimated that about 1,390-1,400 tons N/year and 240-400 tons P/year remove from the Kaliningrad sewage canal [2,4]. Based on the 2014 population number we estimated the load of 1990 tons N/year and 310 tons P/year.

The construction of a sewage treatment plant for the city of Kaliningrad began in 1976 but was not completed, and it was re-started in 2009. The operational scheme of the treatment facilities will provide full biological wastewater treatment with nitrogen and phosphate removal and advanced treatment in compliance with the standards of the Helsinki Commission [23]. Currently, the project is not yet complete. The completion date for the project was once again postponed.

Introducing the modern treatment facilities in the Kaliningrad city will reduce the nutrient load by 1400 tone N/year and 290 tone P/year (Table 4). But if the treatment facilities will not be completed, the nutrient load will increase by 220 tons N/year and 80 tons P/year in the case of the BAU scenario; and by 1,390 tons N/year and 500 tons P/year in the DF scenario.

Table 4. Changes in nutrient load from Kaliningrad in cases of the introducing of the waste water treatment plant for the 'Business as usual' and 'Documented future' scenarios.

Nutrients	Waste water treatment plants	BAU	DF
Total nitrogen	-1,400	+220	+1,390
Total phosphorus	-290	+80	+500

IV. Conclusions

1. The nutrient load from the major anthropogenic sources (population, livestock, poultry and crop production) is 53,267 tons N/year and 16,424 tons P/year on the Pregolya River catchment area at present. Total nutrient load from the main anthropogenic sources after considering removal by harvest is estimated as 23,032 tons N/year and 2,819 tons P/year. The nutrient load from the Kaliningrad wastewaters is about 1,990 tons N/year and 310 tons P/year (sewages are discharged directly to the Vistula Lagoon and only mechanically untreated at present).

2. The proportion of the anthropogenic nutrient load for the different national parts of the Pregolya River catchment is such that the nitrogen load is three times and the phosphorus is less than two times larger from the Polish part compared to the Russian part.

3. Chemical fertilizers and livestock waste are the most significant sources of nutrients. Poultry breeding is important for phosphorus emission in the Russian part of the catchment area. Nutrient load from the population is noticeable only from the city of Kaliningrad.

4. Potential changes of the nutrient load were calculated for two future scenarios (BAU scenario – development in accordance with current trends; DF scenario – the official plans of the local authorities). For the BAU scenario the total anthropogenic load of nutrients will increase slightly – less than 3%. For the DF scenario, a significant rise of nutrient load is expected. Hence, the load from the anthropogenic sources will double (removing by the harvest is not considered).

5. The nutrient load from the anthropogenic sources in the Russian part of the catchment can be compensated greatly by using the manure as organic fertilizer replacing mineral fertiliser. At present time 40% of available arable land in Kaliningrad Oblast is sufficient for utilization of manure originated locally at the maximum fertilization rate recommended by HELCOM.

6. The calculations showed that equipment of Kaliningrad city with the modern treatment facilities will reduce the nutrient load by 1,400 tons N/year and 290 tons P/year.

V. Acknowledgement

Data collection was made under support of the theme № 0149-2014-0017 of State Assignment of the P.P.Shirshov Institute of Oceanology of the Russian Academy of Sciences (2015-2017). Preparation of this article was made under the support of the grant RFBR-Bonus 14-05-9173015 "Reducing nutrient loadings from agricultural soils to the Baltic Sea via groundwater and streams (Soils2Sea)".

V. REFERENCES

[1] M.V. Silich, “Balance of the Lagoone”, *Hydrometeorological regime of the Vistula Lagoon*. Leningrad: Gidrometeoizdat, 1971, pp. 143-172.

[2] S.V. Aleksandrov, J.A. Gorbunova, ”Nutrient load for the Vistula Lagoon from the Pegoliy River flow”, *Water: chemistry and ecology*, vol. 1, pp. 4-8, 2010.

[3] S.I. Zotov, *Modeling of geosystems*. Kaliningrad: KSU, 2001.

[4] BASE project 2012-2014, “Assessment and quantification of nutrient load to the Baltic Sea from Kaliningrad Oblast and transboundary rivers, and the evaluation of their sources”. HELCOM, 2014.

[5] “What does domestic wastewater contain?”, *Swedish Environmental Protection Agency Report 4425*. Stockholm, 1995

[6] *The methodology of calculation of the removal of nutrients and evaluation of long-term state of pollution of small rivers*, vol. 331. Belarus: Ministry of Natural Resources and Environmental Protection of the Republic of Belarus, September1999.

[7] *The arable lands and gross harvest of agricultural crops in the Kaliningrad region in 2014: Statistical Yearbook.* Kaliningrad: Federal State Statistics Service, 2015.

[8] D.A. Domnin, B.V. Chubarenko, *Atlas of river basins of transboundary Kaliningrad Oblast*. Kaliningrad: Tera Baltika, 2007.

[9] “Kaliningrad Oblast and Warminsko-Mazurskie Voivodship in numbers 2014”, *Statistical Yearbook by Territorial Authority of the Federal State Statistics Service in the Kaliningrad Oblast and Statistical Office in Olsztyn*. Olsztyn: Statistical Office in Olsztyn, 2015.

[10] A. Shcherbakov, *The spring oil-bearing plants*. Minsk: FUAinform, 1999.

[11] “Sewerage in the Kaliningrad Oblast in 2014”, *Statistical Yearbook*. Kaliningrad: Federal State Statistics Service, 2014.

[12] *Statistical Yearbook of Warmińsko-Mazurskie Voivodship 2014*. Olsztyn: Statistical Office in Olsztyn, 2015.

[13] “Nutrient Loads to the Swedish Marine Environment in 2006”, *Sweden's Report for HELCOM's Fifth Pollution Load Compilation.* Stockholm: Naturvardsverket, 2009.

[14] B. Liss, “Quantification of nitrogen and phosphorus load from local on-site wastewaters treatment”. Degree dissertation, Uppsala: Universitet, 2003

[15] *Agriculture of the Kaliningrad Oblast: Statistical Digest*. Kaliningrad: Federal State Statistics Service, 2014.

[16] *Statistical Yearbook of Agriculture 2014*. Warszawa: Central Statistical Office, 2015.

[17] *Rural settlements: Statistical Digest*. Kaliningrad: Federal State Statistics Service, 2014.

[18] "Fertilisation and chemical land reclamation in 2014", *Statistical Yearbook*. Kaliningrad: Federal State Statistics Service, 2015 22p.

[19] "Regional Development Strategy of the Voivodeship of Warmia and Mazury until 2020", *Annex to Resolution, vol. XXXIV/ 474/05*. Voivodeship of Warmia and Mazury of 31 August 2005.

[20] *Population projection for Poland 2008–2035*. Warszawa: Central Statistical Office, 2009.

[21] *Strategy of socio-economic development of the Kaliningrad Oblast till 2020*, vol. 583. Kaliningrad: Governor of the Kaliningrad region, August 2012.

[22] *State of the environment and its impact on the health of the population of the Kaliningrad Region in 2007*. Kaliningrad: Federal State Statistics Service, 2008.

[23] *Baltic Sea Action Plan*, Krakow: HELCOM ministerial meeting. November 2007.

COASTAL EROSION IN THE GULF OF KALAMITA AS A RESULT OF LONG-TERM ANTHROPOGENIC INFLUENCE

Yuri Goryachkin, Marine Hydrophysical Institute of RAS, Russia

yngor@mhi-ras.ru

The Gulf of Kalamita is located in the Black Sea off the west coast of the Crimea and is known to be a major recreational area. However, in the last 30 years, its famous sandy beaches have drastically degraded. Degradation of sandy beaches was expressed in erosion of the coastal line (30-70 m) and reduction of the total area of beaches; disappearance of sand in a number of areas in the near-shore zone and openings of marl; sharp increase of fragments of limestone in the composition of beaches. In the last 60 years, the level of the Black Sea has risen by 14 cm. Only this factor, as the calculations show, has caused about 15 mln m^3 deficiency of deposits. According to direct observations, shoreline response to changes in the sea level at the inter-annual scale changes comproses 0,3 m per 1 cm. Climate changes in trajectories of passing cyclones have resulted in a 2-3 times increase in storm activity over the past 30 years. The contribution of natural factors into the shoreline changes do not exceed 10-15% according to our estimates. The main contribution is related to the background and point anthropogenic impacts. The first group includes overall reduction of sediment in the sea due to construction of reservoirs, cliffs closing with concrete embankments, reducing populations of benthic mollusks for various reasons, etc. The second group includes construction of hydraulic structures which do not address lithodynamics peculiarities in particular stretches of coastline.

Key words: Crimea, Kalamita gulf, degradation of sandy beaches, anthropogenic impacts.

Kalamita gulf is located in the Black Sea at the Western coast of the Crimean peninsula (fig. 1). The gulf is shallow, its depths increase gradually from the coast to the sea, and the maximum depth is about 30 m. In the Northern part of the gulf, the coast is low and sandy. In the Southern part, it is high, steep, formed by clays. At the coast of the gulf, there are many salty lakes separated from the gulf by sandy bay-bars. The lakes are of medical value. On the coast of the gulf the cities of Evpatoria (120,000 inhabitants), Saki (25,000) and a number of smaller settlements are located. The water area in the Southern part of the gulf is considered to be a natural object with unique water and land ecosystems and it is a reserve.

Kalamita gulf is known to be a major recreational zone of Crimea. Evpatoria is the most famous resort. The city was founded by the Greeks in VI century B.C. and it was called Kerkinitida (Κερκινίτις, Kerkinitis). In the XV century it was renamed as Gezlev (Gözleve) and it was governed by the Crimean khanate. In the end of the XVIII century it became a part of Russia and it got a new name, Evpatoria, in honour of the tsar of the Greek-Persian state Mitridat VI - Evpator (134-63 BC).

Up to the XX century, trade, fishery and salt extraction from the lakes were the basic occupations of those who inhabited the region. In this period, the population never exceeded 25,000

people. In the beginning of the XX century, resorts started to develop. Two factors triggered such development: medical dirt and brine in the salty lakes and the famous sandy beaches. Besides this, favorable climate in combination with shallow relief of the coastal line has created good conditions for development of the resorts.

By the end of the XX century, over 70 sanatoria worked only in Evpatoria, about 1,0 million visitors had a rest in the region annually. The only analogue to the quality and extent of

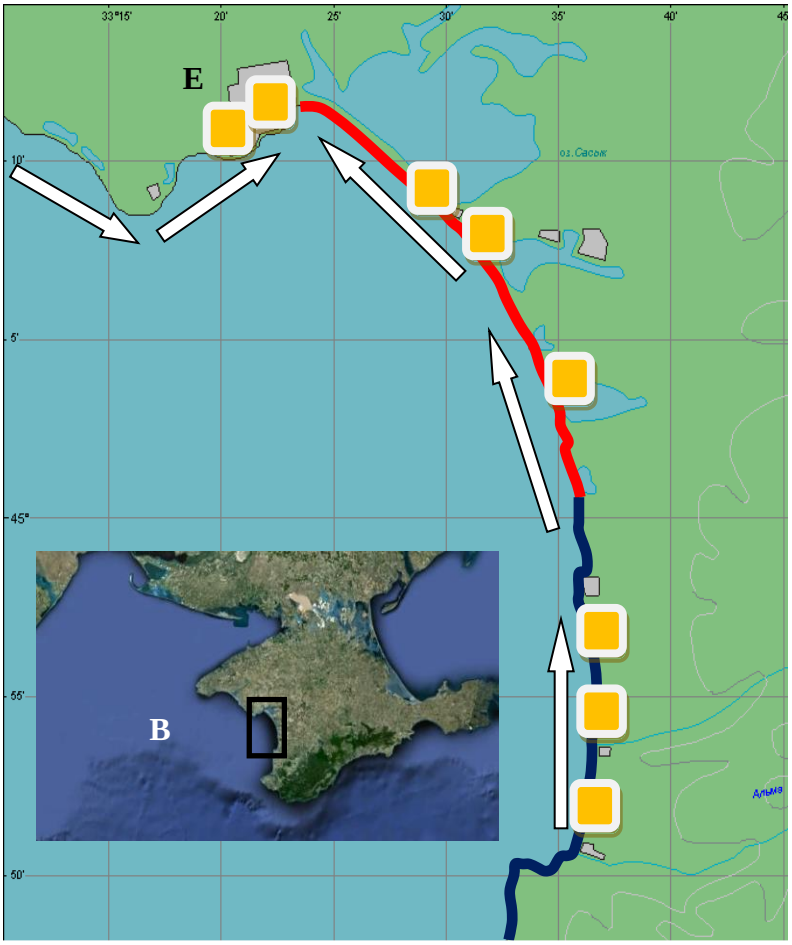

Fig. 1. Kalamita gulf. Red line – beaches of mainly longshore feeding; dark blue line - beaches of complex feeding. White arrows - direction of bottom deposits transfer. Numbers - locations mentioned in the text

Evpatorian beaches on the Black Sea is "Golden Sands" in Bulgaria. However, during the last 30 years the sandy beaches have sharply degraded. Degradation of beaches was expressed in:

- erosion of the coastal line (in some areas up to 30-70 m) and reduction of the total area of beaches;
- disappearance of a number of sand areas in the water level zone and opening of clay adjournment;
- sharp increase of fragments of bay-bars in the composition of beaches.

All this has considerably worsened the recreational attractiveness of the resort, which causes reasonable alarm among the city administration and heads of health resorts.

Before we pass to the reasons which have caused the degradation of beaches, we will mention some features of the coast structure and lithodynamics of the Kalamita gulf [1].

In the Northern part of the gulf the coast is accumulative, bay-bars of salty lakes are generated here. Beaches are formed mainly by fine-grained sand. In some places deposits mainly consist of fragments of modern cockleshells which are thrown out from the sea-bottom. The Southern part of the accumulative coast is formed by deposits which consist of 50 % pebbles and 50 % sand. The pebble part consists of alluvium brought by the rivers and temporary waterways of South-Western Crimea. The rest is formed by the product of coast destruction (ancient alluvial plain occurs in the cliffs of the Southern part of the Kalamita gulf). In the Southern part of the Kalamita gulf, the coast is abrasive with clay cliffs up to 15 m high.

In the Northern part, beaches are mainly formed by beach drifts (their mean annual direction is from the South to the North). In the Southern part of the gulf, the beaches have a complex supply (destruction of benches and cliffs, river deposits). According to the observational data, on average about 1 million m^3 arrive from cliffs to the coastal zone annually. The specific value of driftage is 21 m^3/m per year. Abrasion of benches is especially widely spread in the Southern part of the region. It is active up to 12 m deep, which was defined by direct observation with bottom reference points. Abrasion of coast and bottom combined delivers about 1,5 million m^3/year sedimentary material to the sea. Only about 0,3 million m^3 of this amount make the beach-forming fractions which remain in the coastal zone. The rest of the sedimentary material is taken to the sea in the form of suspension.

In our opinion, anthropogenous activity has had the greatest influence on changes in the coast line in the Kalamita gulf [2]. As historical photos show, in the end of the XIX century, there was a vast beach in the central part of Evpatoria. Storm surges made certain problems; therefore in the beginning of the XX century the first coast protecting construction in the form of an inclined wall about 500 m long was erected in the city centre. Further dynamics of beaches in this part of the city depended on presence or absence of this wall which was continually destroyed and restored. The most significant reconstruction of the downtown quay was made in 1968 – 1972. After the reconstruction was completed, it represented a vertical concrete wall with a breakwater 1,8 km long. Within only one year, beaches in the central part of the city have completely disappeared, and the depths in the Evpatoria bay have increased by 1 m on average. In other words, the stock of deposits was sharply reduced. The earlier measurements of depths in 1836, 1896 and 1923 showed that the bottom relief there had hardly changed.

In the early 1950-ies a sand open-cast mine was put into service on the bay-bar of the lake Sasyk (fig. 1, number 1). At that time nobody thought about the possible consequences. As the sand was extracted, the closing dike, which separated the open-cast mine from the sea, narrowed and under the influence of storms it curved towards the open-cast mine. At the coast of the Kalamita gulf a considerable bend of the coastal line was formed and a tendency to beach reduction was outlined in the sites adjoining to the open-cast mine. There was a real danger of increase in filtration of the sea waters into the lake and eventually a loss of medical properties of the dirt. Because of this danger, the open-cast mine on the bay-bar was closed and moved to the underwater slope of the sea (fig. 1, number 2). Nowadays, the site of the bay-bar where sandy dunes used to be is a bog.

While the open-cast mine was in action, over 15 million m^3 sand was extracted on the underwater slope in 1960-ies, in the period of about 10 years. During this period the beach drift was

almost completely intercepted. The filling of the underwater open-cast mine with the sand from the adjoint sites has caused considerable erosion in the coastal line (up to 11 m per year). In some places it has receded by 200-220 m. Open-cast mine was closed soon after it started to affect the beaches of Evpatoria, but it was too late.

In the 1970-ies a new phase of drama with the beaches of the Kalamita gulf began. Several factors came to action at once.

1. At this time, a medical procedure "sleep next to the sea" became popular. In order to fulfill this requirement, massive two-storeyed constructions with powerful ferro-concrete basements were built right on the sandy beaches (fig. 1, number 3; fig. 2). However, they have not justified their purpose. On the contrary, beaches began to recede quite quickly, washing away the basements. 10

Fig. 2. Concrete constructions on the beaches of Evpatoria (1969-1980).

years later, these buildings were pulled down.

2. On Quarantine cape a 200 m long pier was built for the needs of port; it was a monolithic concrete construction (fig. 1, number 4, fig. 3, a). Migration of deposits has changed and an extensive shallow was formed at the East side of the pier. In order to maintain the constant depth on the waterway, bottom dredging started**.** The sand was dumped into the sea according to the existing notion about the direction of movement of deposits. However, this notion was not proved. As a result, to the West of the port pier, the coastal line started to recede quickly, and the sand almost disappeared from the bottom. Nowadays, the beaches of this part of the city are the most troublesome.

3. At the same time on the bay-bar at the lake Kyzyl-Jar, a hydraulic engineering construction was built and it blocked the deposit drift (fig. 1, number 5; fig. 3, b). To the South from this construction, the material began to accumulate (mean annual speed of accumulation was 7,5 m/year), and the coastal line was put forward by length of this hydraulic engineering construction (120 m). To the North from the water intaking construction, intensive abrasion began, with the mean annual speed of 3,7 m/year.

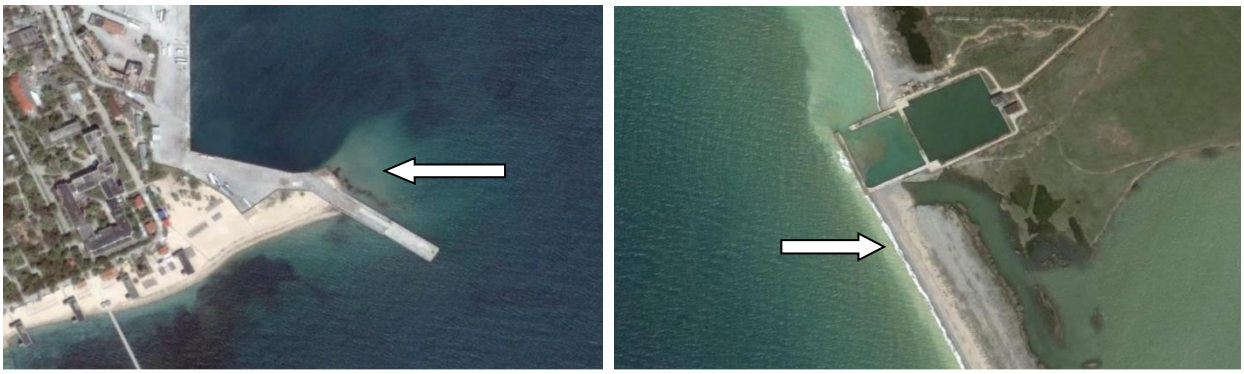

Fig. 3. Interception of longshore deposits. In the satellite pictures there is a mooring of Evpatoria port (left) and a water intake area (right). Arrows show the places of accumulation of deposits

4. During the same period, water basins were constructed on the basic rivers of the Western Crimea. As a result, the firm drain of the rivers was reduced by almost ten times.

5. In the Southern part of the Kalamita gulf quays in the form of ladders were built in order to create “aesthetic landscape”. Due to such fastening of coast by concrete constructions, wave processing of cliffs was reduced and, hence, the amount of firm deposits in the coastal zone was reduced as well. It should be mentioned that beaches before such constructions quickly disappeared, and the constructions have completely collapsed by now. The basic problem now is their recycling, since they are “stone chaos” (fig. 1, number 6, fig. 4).

Fig. 4 “Stone chaos” at the former seafront. Beaches have disappeared. In the background there is the groin which intercepted the stream of deposits.

Among other factors of anthropogenous influence on the coasts, we can also name uncontrolled (often illegal) building in the coastal zone, "piracy" extraction of sand at the beaches, etc.

In the end of the XX century – beginning of the XXI century adverse factors of change of environmental conditions had an influence on the coast, too. Within the last 30 years in the vicinity of the Kalamita gulf frequence of storms from the South and South-West directions has increased three times. It is connected with climate change of trajectories of the Mediterranean cyclones. Besides this, in the last 60 years the level of the Black Sea has risen by 14 cm. Only the latter factor, as the calculations show, has caused about 15 million m^3 deficiency of deposits in the Kalamita gulf [3].

According to direct observations, response of the coastal line to sea level changes at scales of interannual changes in the Kalamita gulf makes 0,3 m for 1 cm of sea level change, which confirms the famous Bruun rule. A certain contribution to deficiency of deposits also belongs to the inadvertent introduction from of mollusc *Rapana venosa* from the Pacific Ocean to the Black Sea, which has strongly reduced the local populations of molluscs. Anthropogenous water pollution and pollution of the bottom deposits by municipal drains has resulted in reduction of amount of cockleshells, too.

Thus, the greatest influence on degradation of beaches in the Kalamita gulf of the Black Sea was made by anthropogenous activity, with a certain contribution of changes in the environment.

Now a consistent question arises. Were any actions taken to change the unfortunate trends? Yes, they were. The city authorities have repeatedly initiated research with the purpose of creation and implementation of projects of beaches restoration. Research was made by various organizations of the former USSR, Russia and Ukraine. Due to these researches, unique banks of observational data were received. They cover the coastal zone dynamics, currents, meteorological parameters, which have allowed to verify mathematical models of lithodynamics and changes of the coastal line [4].

At the same time, in all these years, no real actions to prevent degradation of beaches were taken. The main reason for this is that various sites of coast belonged (and do now) to various departments. These are various ministries, the Navy, municipalities, private structures etc. All the attempts to join the efforts have failed. Suggestions of the scientists to disassemble the coast cross-section hydraulic engineering constructions and to transfer the port to another place did not find understanding. This decision was officially accepted in the beginning of the XXI century about 10 years ago, but it has not been implemented yet. Suggestions to use by-passing have led to the fact that the port authorities began to sell the sand after dredging to those organizations whose territory suffered most from the catastrophic state of beaches. The decision to pull down all constructions, fences etc. in the 100 meter zone has only partially been implemented. In 2011 the Law about prohibition of any building in 100 meter zone from the sea came into effect. At the same time, this law has a norm according to which it is possible to build coast protecting constructions in this zone. Unfair proprietors abused it. Under the official documents, a hotel 10 m from the sea is called "Coast protecting construction with rest rooms" that allows to bypass the law.

In order to solve the problem there are civil-engineering designs of artificial islands, but such projects are extremely costly. In our opinion, one of the ways to solve this problem is to create artificial beaches. According to our calculations, for initial feed of beaches only on the most troublesome sites it is necessary to pile 100-150 m^3 of sand per linear meter. These suggestions have been confirmed by one of the famous Dutch firms which was invited for consultations. However, the

problem (except for the finances) consists in the lack of sand deposits. Nowadays, many beaches are fed in order to rescue them in many sanatoria and boarding houses. Imported sand is used for this, and its quality is fundamentally different.

In 2012 the new phase in the struggle for preservation of the Kalamita gulf beaches began. The authorities received a project of erecting a complex of high-rise recreational buildings at the bay bar to the east of Evpatoria. According to the primary estimations, such construction can destroy the unique beaches of Evpatoria completely. Struggle for their preservation still proceeds.

Thus, we can ascertain that long-term unreasonable anthropogenous activity has led to degradation of beaches in the Kalamita gulf, an important recreational zone of Crimea. Egoism of proprietors has not allowed taking effective measures to prevent the negative consequences.

REFERENCES

[1] Zenkovich, V. P. 1960. "Morphology and dynamics of the Soviet Black Sea coast" (in Russian) Morfologiya i dinamika sovetskih beregov Chernogo morya, *Izd-vo AN SSSR, Moskva.* vol. 2, 216 p.

[2] Goryachkin Yu. N. "Coastal erosion and protection in Ukraine". In book *«Coastal erosion and protection in Europe»*, «Earthscan», London, editing A. Williams and E.Pranzini, 2012, 512 p.

[3] Kosyan R.D., Krylenko V.V., Goryachkin Y.N., Dolotov V.V., Krylenko M.V., Godin E.A. "Crimea and Caucasus Accumulative Coasts Dynamics Estimation using Satellite Pictures". *Turkish Journal of Fisheries and Aquatic Sciences,* 2012, 12: pp.385-390.

[4] Goryachkin Yu. N. "The modern state of the coastal zone of Crimea" (in Russian) Sovremennoe sostoyanie beregovoy zonyi Kryima *ECOSI-Hydrophysika*, Sevastopol, 2015, 252 p.

LANDSCAPE STUDY OF CHEBOKSARY AND KUYBYSHEV RESERVOIRS COASTS FOR RECREATIONAL USING

Anna Gumenyuk, Chuvash State University, Russia
Inna Nikonorova, Chuvash State University, Russia

annagumenuk@yandex.ru

The plot of study is Cheboksary and its suburbans and located on the joint of two landscape zones: a forest zone and a forest-steppe zone. The border between the zones goes along the Volga River, which establishes favourable environment for recreation. There has been observed slope type of areas on the right bank of the Volga River of the Cheboksary and Kuybyshev Reservoir. It has 3º and more incline, with washed-off soil and broadleaved woodland (relict mountainous oak woods), subjected to considerable land-clearing. In the immediate bank zone of the Volga River, where abrasive-soil-slipping and abrasive-talus processes mostly develop, the main types of natural areas have been marked out:

1) Abrasive landslide cliffs at the original slopes of Volga Valley of 60º steepness, more than 15 m high, with permanent watering as a result of underground waters leakage;

2) Abrasive cliffs of terraces above flood-plains of 2 m high;

3) Abrasive cliffs of original slope of the valley of the river Volga of 2 m high, with distinctive abrasive niches in the lower part of the slope or temporary concentration of caving demolishing material.

Left coast is lowland plain, the part of taiga landscape zone. Low terraces above flood plain of Volga are formed by sand with loam layers, with sod-podzol sandy and sandy loam soil in combination with marshy soil, with fir-pine forest, with from lichen bogs to sphagnum bog; in lowlands, on old felling plots, on abandoned peat mines deciduous forests with mostly birches and aspens prevail.

Key words: reservoirs coasts, landscape, water-dividing type, water-dividing natural area, recreational.

I. INTRODUCTION

The investigated site is on territory of the Chuvash Republic which features the part of physic-geographical country of the Russian Plain (East European Plain) and is located on the joint of two landscape zones: a forest zone and a forest-steppe zone. The border between the zones goes along the Volga river, and is mostly defined by climate, more specifically by heat and humidity ratio, which changes gradually from the north to the south [6]. Location of Cheboksary and its suburbans in two natural zones, i.e. forest and forest-steppe, establishes favourable environment for recreation.

Town planning pattern complies with terrain, formed by watershed of the Volga's tributaries: Cheboksarka, Sugutka, Trusikha, Kaybulka, which radiate fanwise in the meridian direction. As a result, main town constructions are located on watersheds and form arrow-headed (V-shaped) territories of administrative areas, tapering in amphitheatre at the Volzhsky Bay and widening southwards. All main traffic arteries lay on upper section of watershed's ridge and form a radial-type system of streets, coming together by the bay.

II. MATERIALS AND METHODS OF RESEARCH

Landscape differentiation of the territory under study has been researched on the basis of types of areas as structural landscape levels.

At the territory under study there have been observed such types of areas:

1) water-dividing type;

2) valley type of minor rivers;

3) slope type of the right bank of the Volga river;

4) terrace above flood-plain type (Fig. 1).

Water-dividing area type is located in-between the rivers Volga (Cheboksary Reservoir) and Cheboksarka, in-between the rivers Cheboksarka and Sugutka, in-between the rivers Sugutka and Trusikha, in-between the rivers Volga and Kukshum, represented by horizontal and sub-horizontal surfaces, industrial-straightened, with removal of native vegetation (maple-lime oak woods used to grow here), taken up by residential and industrial buildings and sites.

Slope type of the right bank of the Volga river of the Cheboksary Reservoir has 3º and more incline, with washed-off soil, and broadleaved woodland (relict mountainous oak woods), subjected to considerable land-clearing.

In the immediate bank zone of the Volga River, where abrasive-soil-slipping and abrasive-talus processes mostly develop, the main types of natural areas have been marked out:

1) abrasive landslide cliffs at the original slopes of Volzhskaya Valley of 60º steepness, more than 15m high, with permanent watering as a result of underground waters leakage;

2) abrasive cliffs of terraces above flood-plains of 2m high;

3) abrasive cliffs of original slope of the valley of the river Volga of 2 m high, with distinctive abrasive niches in the lower part of the slope or temporary concentration of caving demolishing material [5].

On the territory under study the key plots are located, e.g., "500 years of Cheboksary" Park (Pic. 1), with inclined surface with rugged topography on the slope with exposure to the north; then, such natural areas as: flat relief with 0-1º incline, and with lime-maple oak woods on light-grey forest soil; low-inclined surfaces of 1-3º with oak-elm-maple lime woods on light-grey forest soil; slightly sloping surfaces with 3-5º incline with oak-elm-maple lime woods on light-grey forest soil.

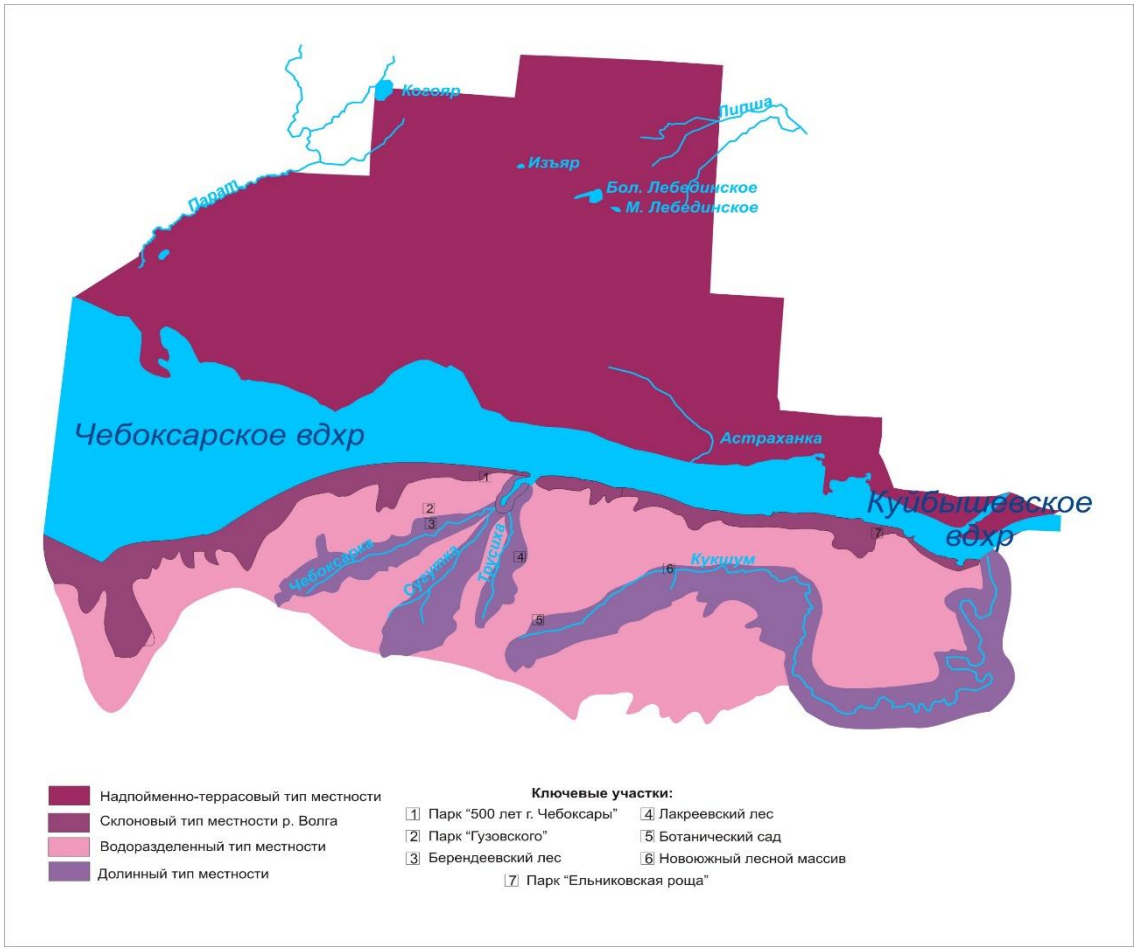

Fig. 1. Landscape layout on Cheboksary and Kuybyshev reservoir coast.

The territory of sanatorium-and-spa resort "Volzhanka" has been anthropogenically transformed, and is represented by *slope area type* with exposure to the east, with steep-slope gulley (20º), 60 m long, with washed-off soil.

The *slope type* of the relief is also presented in the Park Pobedy. The steepness of the slope is 20°, the length is 40 m with exposure to the north, on light-grey forest soil.

The *slope type* of the right bank area of the river Volga (Kuybyshev Reservoir) is presented by the key plot «Elnikovskaya Rosha». This plot is the natural landmark, which is represented by a sloping surface with rugged topography at the slope of northern exposition, steeply crumbling down to the valley of the Volga River, with absolute marks of the territory at 70-123 m, with difference of height at 50m and slope steepness from 9˚ to 24˚, and with near-Volga mountainous oak woods on light-grey forest soil. On the slope territory there are the following natural areas: slope surfaces with soddy-mesopodzol soil on loess loams with ferny oak woods and lime-hazel oak woods; slopes of hollows with exposure to the north with soddy-mesopodzol soil on loess loams with maple-lime-goutweed oak woods; slopes of hollows with exposure to the north-west with soddy-mesopodzol soil on loess loams with maple-lime-mercury oak woods; hollow bottoms with soddy-mesopodzol soil and ravine-hollow soil on alluvial-deluvial loess deposits with elm shrubs.

Water-dividing natural area "Rosha Guzovskogo" has the declining surface with the 4-7º incline, where the relief is of erosive character, and is represented by the closed type of landscape

with zonal crown closure of lime-maple oak woods, soil covering is mostly light-grey and dark-grey soil of loamy mechanical character, formed on deluvial and alluvial Perm clays and loams.

Valley type of the river Cheboksarka area is anthropogenically transformed. This area is represented by steep slope (15-20º) with exposure to the north-east, of 15-20m length; partially slopes are occupied by low-height housing or by dacha-gardening units. The natural area "Cheboksar creek" is represented by the slope with the exposure to south-east and south, steepness of 15-25º, islets with maple-lime copse on light-grey forest soil.

At the inflow of the river Cheboksarka in Cheboksar Creek, the creek basin is covered by bank-protecting structures; around the perimeter of the creek there is the pedestrian zone, where the population of the city takes part in diverse recreational activities throughout a year. During summer season the water area is used for catamaran and boat sailing, fishing, and during winter season it is used for winter fishing, ice-skating.

The index plot «Berendejevski Les» is situated on the left slope of the river Cheboksarka with the inclination from the north to the south-east, and lays at the elevation points 120-160 m, elevation difference from north to south-east is 40 m. Continuous gradient of Berendejevski Les to south-east at the whole territory of the area is about 3º. The following surfaces by a gradient of the slope have been observed: low angle (1-3º); slight-slanting (3-5º) with maple-lime oak woods on light-grey forest soil; slanting (5-7º) with maple-lime oak woods on light-grey forest soil; steep (more than 7º) with maple-lime oak woods on light-grey forest soil. This area is used for skiing, sportive orienteering, laying of terrainkurs, race-walking.

Valley area type of the river Trusikha is as following: the relief of the territory is presented by steep slopes (15-25º) with lime-maple oak woods on light-grey forest soils.

There has been pointed out the index plot «Lakreejevsky forest», which is a natural landmark. The slope of broken ground with the exposure to the east is divided into the following natural areas: steep (15-25º) slope of the river Trusikha with lime-maple oak woods of light-grey forest soils; slanting (8-20º) slope of the river Trusikha with lime-maple oak woods of light-grey forest soils; low-angle (8-12º) slope of the river Trusikha with oak birch wood on of light-grey forest soils, plant communities are under strong antropogenic pressure; slight-slanting (8-12º) slope of the river Trusikha with maple oak woods on light-grey forest soil; slanting slope of spring valley with oak woods on slight-grey soil; slanting (8-12º) slope with grassland vegetation on alluvion. The slope with exposure to the west is built up with low-height housing or by dacha-gardening units/properties.

Valley type of the river Kukshum has been mostly modified by antropogenic activities. The relief is represented by slanting surface of more than 3º of slope inclination, with deciduous forest on grey forest soil. The index plots are situated here: "Botanicheski Sad", Novojuzhny forest area and middle plot of the river Kukshum's valley.

Novojuzhny forest area is represented by inclined slope with broken ground of near-Volga mountainous oak woods on light-grey forest soil. There has been noted the following surfaces with exposure to north-east by slope gradient: plain, with the angle of slope 0-1º formed by loess loam; slight-slanting, low-arched slopes with the angle of slope 1-3°, formed by loess loam with low watering, with maple-lime-goutweed oak woods; slopes of hollows, which are slight-slanting concave surfaces (dell) with angle of inclination of 1-3°, formed by loess loams, more watered;

slight steep raised slopes, with angle of slanted surface of 3-5°, formed by loess loams; slight-slanting hollow slopes with exposure to south-west, with the angle of slanted surface of 5°-7°, formed by loess loams; slanted hollow slopes with the angle of slanted surface from 7° to 10°, formed by loess loams; penchant slopes of hollows with angle of slope 10-15° formed by loess loams with oakwoods with maple-lime underwood; bottoms of hollows with the angle of a slope no more than 2°, formed by alluvial-deluvial loess loams with flowing watering with elm shrubs. Slope inclination is from 5 º to 10-30 º and more. This index plot is characterized by advantageous conditions for skiing and sledging, and also for promenade and hiking.

The index plot «Botanicheski Sad» is represented by antropogenic landscape, and sloping (3º) surface with exposure to the south. Within the slope there have been observed anthropogenic natural areas: arboretum, preserved oakwood, rosary, shady garden, garden of riverian plants, the garden of continuous blossoming, exposition of plants of natural flora, Japanese garden, exposition of cultivated plants, plots of the natural forest and science research territories. This area is used for scientific and educational tourism.

The middle plot of the river Kukshum valley with hypsometric marks of slope shoulder of 138 m with exposure to south-west and north-east, with slope steepness of 10º and more, with washed-off soil, and here the farming lands of state owned farm «Kadykovsky» are located. This territory is used by the residents of the area for sledging and skiing in winter.

A terrace above flood-plain type of the area is located on the left bank of Cheboksary and its suburbs in the forest zone and belongs to the forest province of Nizmennoe Zavolgie. Forests of Zavolgie are mostly pinaceous. This is the part of the whole massif of Mariyski forest, which in its turn is the part of Nizhegorodskoe Zavolzhje. Rarely the plots of birch wood, aspen wood and lime wood are speckled among pinewood. In the west part an oak is met as subordinate species.

According to landscape zoning left bank area (Zavolzhje) belongs to the province of southern boreal forest of taiga zone. The Volga River separates it from the forest-steppe left bank area.

Left bank area (Zavolzhjye) of Ceboksary reservoir, city and suburbs are the part of taiga landscape zone, the south border of which goes along the Volga river. Here the balance of watering is positive. Terrain of Zavolzhje is lowland plain. True altitude does not exceed 150 m. Plainness of the territory and inconsiderable downcutting of rivers define low horizontal and vertical terrain roughness. Valleys of Zavolzhje rivers have aged and developed look. In Zavozhje eolian forms of terrain are widespread. Before afforestation of formed Volga terraces parabolic dunes of 10-15 m high and of 1-2 km long used to be formed here.

Horns of dunes are usually oriented on the east or north-east, pointing out the direction of prevailing winds. Dunes have been formed by eolian processing of Volga alluvia (Pic. 1). In topographic low of Zavolzhje marshes and lakes were formed.

According to the scheme of Middle Povolzhje physic-geographical zoning by F.N. Milkov and E.M. Rakovskaya (1953) the left bank suburban recreation zone of Cheboksary and its suburbs belongs to the forest zone, subzone of south taiga, province of lowland Zavolzhje.

According to A.V. Stupishin (1964) and E.G. Kolomyts (1995), Zavolzhje belongs within forest zone, subzone coniferous-deciduous (mixed) forest. In the atlas of agricultural sector of Chuvashia Republic, Zavolzhje is the forest zone, and the forest area of Zavolzhje lowland is Zavolzhje valley-terrace Polesye area.

High (third) terrace above flood plain of Volga (valley-outwashed) is gently undulating and flat, sometimes hummocky and pitted, greatly waterlogged, formed by sand and loams, with sod-podzol sandy and sandy-loam podzol soil in combination with marshy soil, with moss or myrtillus fir-pine forests in combination with moss, lichen or bog moss pine forests [1].

Low (first and second) terraces above flood plain of Volga are formed by sand with loam layers, with sod-podzol sandy and sandy loam soil in combination with marshy soil, with fir-pine forest, with from lichen bogs to sphagnum bog; in lowlands, on old felling plots, on abandoned peat mines deciduous forests with mostly birches and aspens prevail [5].

Natural areas here are flat-bottomed dry hollows, basins, drift hummocky sands, natural and homogenous/artificial pine forests and subors, with bayou lakes in near-bank area [2].

III. Conclusion

Analysis of differential landscape structure and recreation value of the district under study shows that this natural region has moderate variety of area types, but is defined by high sanitary-hygienic and aesthetic qualities, and therefore is foremost favourable for recreation of population of Cheboksary and its suburbs on Cheboksary and Kyubyshev reservoir coast.

IV. References

[1] Archikov, E.I. Location of the Chuvash Republic / E.I. Archikov. - Cheboksary: Chuvashia. Vol. Publishing House, 1998. - 94 p.

[2] Atlas of agriculture Chuvash ASSR. - M .: Main Department of Geodesy and Cartography under the Council of Ministers of the USSR, 1974. - 68 p.

[3] Gumenyuk, A.E. The use of intra-recreation area's. Cheboksary and Novocheboksarsk / A.E. Gumenyuk, I.V. Ilivanova // Ecological Bulletin of the Chuvash Republic. - Vol. 48, "Geo-ecological research in the Chuvash Republic" series. - Cheboksary: Chuvashia. Vol. Publishing House, 2008. Part 1. - Pp. 101-105.

[4] Kuskov, A.S., Lysikova, O.V. Balneology and wellness tourism: Textbook. pos. - Rostov-na-Donu: "Phoenix", 2004. - 320 p.

[5] Nikonorova, I.V. Geological and geographical features of the formation of the Chuvash plot Cheboksary and Kuibyshev reservoir. / I.V. Nikonorova, E.I. Archikov- Cheboksary: Chuvashia. state. University Press, 2000. - 104 p.

[6] Sirotkina, M.M. Geographical analysis of natural factors and the assessment of the current gully erosion in the territory of the Chuvash Autonomous Republic / M.M. Sirotkina // Thesis Cand. geographer. Sciences. – Kazan. 1971.

THE INFLUENCE OF SEA ICE ON THE SEA COAST OF SHANTAR ISLANDS

Margarita Illarionova, Far Eastern Federal University (FEFU), Russia

sticker96@mail.ru

The Shantar Islands is the group of islands satiated in the Sea of Okhotsk near the exit of Uda Bay, Tugur Bay and Ulban Bay. The islands separated from the mainland and started to exist only 6000 years ago. It happened under the influence of the sea transgression followed by flooding of some parts of the land surface and isolation of the most elevated mountain parts from the mainland.

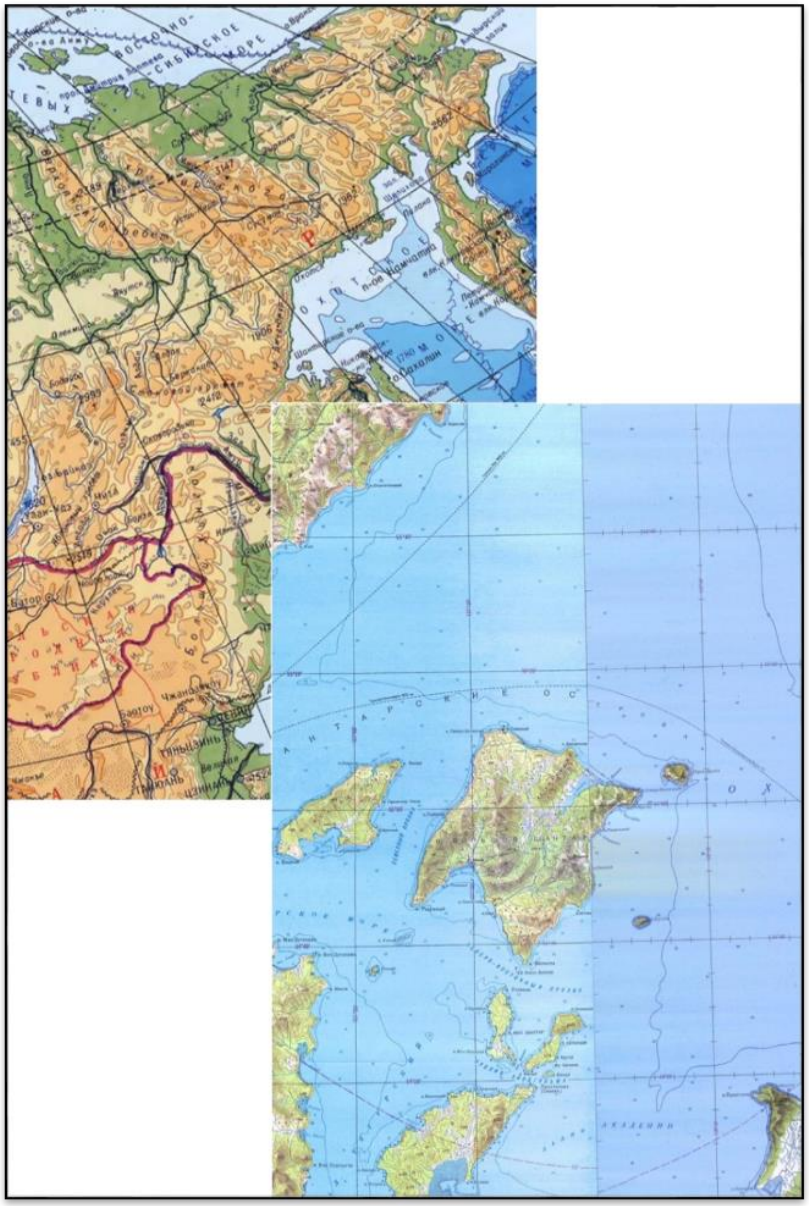

Fig. 1. Shantar Islands

The climate of The Shantar Island is more severe than the climate in the North part of the Sea of Okhotsk due to its proximity to cold regions of Yakutia, complex system of wind and tidal currents, the duration of the ice period, loads of fog and frequent storm winds. The height of tides on the islands can reach 8 meters, and these tidal currents are considered as one of the fastest tides of the World Ocean.

The ice near the islands appears in the beginning of November and doesn't melt for 8-9 months, usually, till mid-July, but some years – till mid-August. Such severe ice conditions cannot be observed anywhere else in the Sea of Okhotsk.

The variety of forms of the Shantar Islands is a consequence of severe ice conditions, unusual tidal currents and irregularity of the seashore. The most important seashores forming factor is considered to be the activity of sea ice.

Activities of sea ice in the coastal shelf zone of the Shantar sea, as an agent of relief formation, on a scale comparable to the waves and tides.

Landforms parameters created under the influence of sea ice can reach few meters in depth, a few tens of meters in width, and a few kilometers in length. The volume of sediment in some parts of the underwater slope comparable to or greater than the volume of sediment transported by the action waves and currents.

Thus, the external border of the coastal zone is advantageously draw at a depth from which the wave stops processing the ice-ekzaratsionny forms and ice-ekzaratsionny microrelief becomes dominant.

The Shantar islands shores divided into four main geomorphological types:

Pebble-sand beaches with a predominance of small soil fractions distributed at the tops of the large bays with low-lying coasts, where silty-sandy beaches with an admixture of pebble and stone are formed under influence of tidal fluctuations and weakened wave mode conditions.

The most striking example of this type coasts are drying in Yakshina Bay on the island of Grand Shantar and in Swan Bay on the Feklistov island.

A sufficiently strong surface layer of frozen pebbles are formed on the pebble beach at the negative temperatures; the ice sheet appears and completely stops abrasion, even under the action of strong waves.

Apparently, ice movement occurs in this case not on the surface of the soil, but between its upper and lower layers.

Rocky shores develop in areas where high mountainous land is located near the sea. The degree of inclination of the surface is diverse - from vertical walls to a relatively flat horizontal areas. There are many cracks and depressions in which water is at low tide, or cleft, stretching inland. These formations are a type of ecological niches, which are very different by composition and stratification of organisms from the adjacent flat portions of the rocks.

In the case of rocky coasts composed of strong bedrock, ice can develop enormous pressure directly on the surface of rocks, tear pieces of rock, delete surface parts, damaged by weathering. Grinding action of moving ice, surely, leads to depletion and the sparseness of the population exposed surfaces and to the concentration of the littoral in cracks, cavities, various kinds of baths. In such circumstances, the nature of the rocks microrelief becomes a factor directly influencing the biomass and population density in the dominant groups of organisms.

Rocky-pebble shores are represented by two types. In some cases, portions of the rocks are located on a short distance from the shore, and they account for, as a rule, only the average horizon shore, and the other horizons are occupied by small fractions of the soil with a predominance of pebbles and boulders in the lower horizon and coarse-grained material (gravel, stones, boulders, pebbles) in the upper horizon. Another version of this type is rocky outcrops shore-stacks quite far removed from the coast. All horizons littoral zone of such stacks account for rocky ground, and the main beach is characterized in most cases the development of block-boulder intertidal zone. Ice effect on that geomorphological type is peculiar. The floating ices in Yakshina Bay in spring and summer make regular migrations under the influence of tidal currents. Huge ice floes dug long furrows deeper than a meter with heaps of sand at the ends of the furrows. Usually the furrows are located in the middle horizon of the coast in the central part of the bay, where is the main track movement of such "icebergs".

It should also indicate the important transporting role of the ice at "ice-floe-marine accumulation." The coastal slopes under the influence of weathering and denudation in the winter give the ice freezing of detrital material. In the spring ice floes are detached from the coast, picked up and taken out over the sea. And fraction of this type are leading in the composition of littoral soils because of repetition of these processes annually.

Regarding the impact of the ice on littoral organisms, most biologists only indicate the fact of its mechanical action and explain the emergence of these "dead zones" in the littoral zone. It should be noted that this mechanical action produce only because of ice floes, pushing on the bedrock of the shore, or whole ice field when approaching the surface ridging beaches. It should be considered that the solid ice cover is almost neutralizes the impact factor of the wave for a long period of time, as shown in the example of the Shantar Islands.

Thus, the ice activity is the most important factor in the formation of the Shantar islands's shores. At the same time the ice activity affects in different degrees, and this affect is always strong.

REFERENCES

[1] P.F. Brovko, “Geomorphology of the mainland coast and the unique coastal complexes of the Sea of Okhotsk”, Structural transformation in the ecosystems of the North-East Asia, Vladivostok: Dalnauka, 2015, pp. 20-24.

[2] Ecological and economic rationale of establishing a national park “Shantar Islands”, Khabarovsk, 2012, vol. 1, p. 310.

[3] L.I. Krasnyy, G.S. Ganeshin, “Geological and geomorphological essay Big Island Shantar, Feklistov and Prokofiev (Report of field work in the summer of 1948)”, Leningrad, VSEGEI, 1949, p. 446.

[4] A.P. Nechayev, “Shantar Islands”, Questions of Geography of the Far East, Khabarovsk, 1955, vol. 2, pp. 18-35.

[5] S.D. Shlotgauer, M.V. Kryukova, “Flora coastal protected areas of the Russian Far East: Botchinsky, Dzhugdzhur reserves, Shantar National Park”, Moscow: Nauka, 2005, p. 264.

[6] V.A. Chetverova, A.S. Makarov, “Ice condition of the Laptev Sea and East-Siberian sea as a factor of formation the seas coastal zone”, Proceedings of the IV School-Conference of Young

Scientists with international participation (26-28 August 2011), Petrozavodsk: Karelian Research Centre of Russian Academy of Sciences, 2011, pp. 49-52.

THE MANAGEMENT OF HYDROMETEOROLOGICAL RISKS IN SOCIO-ECONOMIC SYSTEMS OF COASTAL AREAS

Istomin Evgeniy, Russian State Hydrometeorological University, Russia
Sokolov Alexander, Russian State Hydrometeorological University, Russia
Fokicheva Anna, Russian State Hydrometeorological University, Russia
Slesareva Ludmila, Russian State Hydrometeorological University, Russia
Popov Nikolay, Russian State Hydrometeorological University, Russia

biom@bk.ru

The article considers the problems of functioning and development of complex socio-economic systems of coastal areas in unstable weather-climatic conditions. It is known that the characteristics of the spatial organization of economy of coastal zones are defined industrial and trade specialization and tourism potential of the area It is shown that socio-economic systems are subject to a number of factors, including weather and climatic conditions, which can have both positive and negative effects on economic potential. development of the coastal areas. The density distribution and the economic activities should be considered. The classification of risks of socio - economic systems of coastal areas, due to the influence of hydrometeorological conditions are described. The need to incorporate the tasks of risk management function and the development of spatial distributed systems in the concept of integrated coastal zone management is justified. The model of management of hydrometeorological risks in the system "territory - economy - natural environment" in the space-time dimension is developed. Proposed methods of solving the problems of functioning and development of complex socio-economic systems are based on complex research carried out by the authors.

Key words: GIS, risk-management.

Functioning and development of socio-economic systems of coastal areas are characterized by features associated with the spatial organization of economy of coastal zones, high population density and the need to ensure optimal management.

The coastal areas are stressed by industrial and commercial activities. Considers tourist space, determining the existence of a number of social, environmental, traffic and other problems as a consequence of the conflict of interests of participants of economic activities.

Integrated Complex Zone Management (ICZM) is developed in the framework of the concept of sustainable development. World experience of implementation of ICZM shows that the main emphasis in management policy are made for the protection of the marine environment, scientific research of ecosystems, the sustainable use of fishery stocks, biodiversity conservation, tourism development in coastal areas. At the same time, there is the problem of coordination of the

countries in the coastal zone between individual activities, determining the desire for sovereign control of the industry, which increases the risks for the functioning and development of the coastal areas.

Risk assessment of the functioning of the coastal areas should contain not only the impact of socio-economic systems on the environment, which is defined as the restriction of economic activity, but effects of natural, including hydrometeorological environment on various components of socio-economic systems of coastal areas.

Hydrometeorological environment can have both positive and negative effects on the economic system: weather-climatic conditions are defined as natural resources in agricultural production, energy; at the same time unfavorable and hazardous hydro-meteorological conditions and phenomena of weather may be causing economic and social losses that should be investigated in the space-time dimension. The integral effect of the meteorological environment should be considered when assessing the economic development potential of the region. When this essential condition are the variability of weather-climatic conditions, density and types of economic activity in the territory.

At the present time hydro-meteorological information is widely used in the research, development and use of the space and resources of the oceans, seas and coastal areas. In the framework of the Federal target program "World ocean" has developed the unified state information system about the situation in the World ocean (ESIMO). ESIMO is an interdepartmental information system designed for the formation and maintenance of a common information space in the field of Maritime activities, providing comprehensive information about the situation in the oceans the bodies of state power of the Russian Federation and to persons engaged in Maritime activities, as well as information interaction with international systems. GIS systems allow for interactive assessment of hydrometeorological conditions of water areas of the seas and coastal areas, provide operational information on ice conditions, dangerous weather phenomena combined with information about location transport and fishing vessels, permits calculation of the distribution of contaminants in the areas of oil and gas platforms [1]. At the same time, the instability of weather-climatic conditions, in recent decades, and is characterized not only by the variability of calculated values of meteorological characteristics, but also the increase in the frequency of hazards and to adverse meteorological conditions, causes the growth of uncertainty of the results of weather-dependent economic activity that should also be reflected in the systems of decision support.

Because the negative impacts the uncertainty of economic performance is characterized by the notion of risk, we will use the term "hydrometeorological risk" to refer to the probabilistic characteristics of the costs of the entity associated with the uncertainty of the implementation of the weather conditions.

Considering the negative impact of the metocean environment on the economic activity socio-economic systems spatially distributed in coastal areas, we propose to distinguish the following groups of risks of economic systems, due to the influence of weather and climate [2]:

1. Current hydro-meteorological risks - risks from daily fluctuations in weather conditions that influence the activities of industrial facilities. Current risks exposed to all weather-dependent facilities located in coastal areas. When the deviation of weather conditions from the most

favourable for the implementation of this type of economic activity, business entities there are additional economic costs.

2. Catastrophic hydrometeorological risks - risks from extreme manifestations of weather and climate, influencing the functioning of the region as a whole. Catastrophic risks cause the problem of sustainability of socio-economic systems to the effects of hydrometeorological environment.

Risks of both types should be considered as strategic planning of territory development and operational management of the region. First of all, the analysis aimed at identifying in the economic system of the subjects of risk - modulating elements of the economy and the definition of these types of potential damage, and also risk identification (determination of threshold values of meteorological variables and weather conditions, the implementation of which may lead to a risk for the subject risk). Note that any socio-economic system has such characteristics as exposure and vulnerability to the negative impacts of hydro-meteorological environment[3].

Exposure is determined by features affecting the phenomenon or condition of the weather depends on the magnitude of the economic objects located in a given area, and their density. It is necessary to develop quantitative and qualitative characteristics of the exposure region, and the zoning on this criterion with consideration of peculiarities of economic activity. Note that in general, coastal areas will always have high exposure to negative manifestations of weather and climate. Exposure is a necessary but not sufficient determinant of hydrometeorological risk. Exposure characterizes the possible influence of weather conditions on economic activity and should be considered during development of strategic plans for development of the territory.

Actual the impact of the metocean environment on the socio-economic system characterizes the vulnerability of socio-economic system. Vulnerability is seen as the susceptibility of the subject to the impact of hydrometeorological elements of the system to adverse effects (economic and social losses from the dangerous manifestations of weather and climate). The degree of vulnerability is determined by the capabilities of this element of the socio-economic system to protect from the effects of adverse meteorological conditions.

Assessment of hydrometeorological risk assessment boils down to two components – risk assessment (probability of occurrence to adverse meteorological conditions) and vulnerability assessment (estimates of potential damages under the unfavorable meteorological conditions). Therefore, as noted above, is especially important to take into account the possible range of exposure to adverse meteorological conditions at the stage of making strategic decisions in the planning of development of territories. The distribution of values of hydrometeorological characteristics in coastal areas studied by several authors, for example [4], given in climatic handbooks, the increasing instability of the climate system is seen as a factor leading to the increase of risk in socio-economic systems.

Spatially distributed socio-economic system and its individual elements (production facilities, infrastructure, etc.) must implement continuous management process hydro-meteorological risks. This needs to be defined:

a) meteorological factors affecting the functioning of the socio-economic system;

b) values of meteorological factors leading to impaired functioning socio-economic system;

b) the economic impact of hydrometeorological conditions with varying degrees of intensity, expressed in monetary terms.

Exploring the dependence of economic performance and the influencing meteorological factors *X*, we assume that the damage *U* possible, if the realized value of *X* is greater than a preset threshold X_{nop} determined by the specifics of economic activity ($X>X_{nop} \rightarrow U>0$). Damage is a function of the value of meteorological factor of $U=U(X)$ depends on the intensity and duration of adverse meteorological conditions. The realization of *X* at time t is a random event, and the change in *X* in time is a random process *X(t)*, as shown in figure 1.

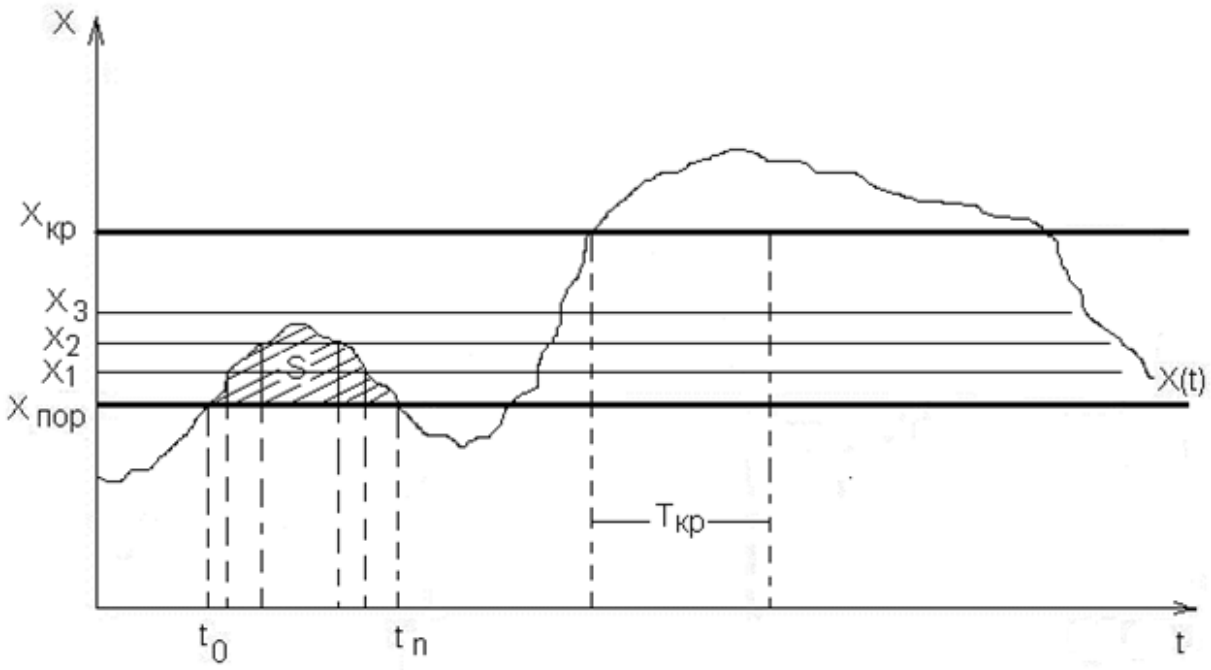

Fig. 1. Implementation of meteorological factor in time

Obviously, the damage can be seen as a process that will depend on the duration of the period of time t_1-t_n in which the condition $X>X_{nop}$ and the total gross positive deviations $\Delta X=X-X_{nop}$ affecting meteorological factor, i.e. the square *S*:

$$S = \int_{t_0}^{t_n} \left[X(t) - X_{nop}\right] dt . \qquad (1)$$

Then the damage assessment is described by the following expression:

$$U(X) = K \cdot A \cdot S , \qquad (2)$$

where: *K* – coefficient of proportionality, is set empirically; *A* is the parameter determined by the adaptive capacity of socio-economic systems to the effects of adverse meteorological factors, $A \in [0, 1]$. Values of *A* will vary for different levels of *X*i and the length of time values of meteorological factor is higher than a predetermined intensity.

If socio-economic system takes no action to reduce damage (A=1), then there is possible damage $U_{max}(X)$:

$$U_{max}(X) = K \cdot S \qquad (3)$$

If the system has a cardinal measure of protection against adverse weather influences, damage is determined only by the cost of implementation of protection measures ($A \rightarrow 0$).

We assume that extreme weather can lead to disturbances in the stability of the economic system, if the damage from their manifestations $U(X)$ beyond a certain level of $U_{кр}(X)$.

It is assumed that at A=1 catastrophic damage is possible if meteorological factor X exceeds a critical value $X_{кр}$ at the period of time t is not less than $T_{кр}$. The application of measures of protection (A<1) enables to prevent an increase in the interval of the $T_{кр}$.

Exploring the possible realization of the random process $X(t)$ in a given territory for a sufficient period of time, you can determine the most typical scenario of the process. Climate change will lead to deviations from the standard scenario and would require improvement measures.

Baseline risk assessment R may be given on the basis of accumulated information about the possible realizations of the random process and their economic consequences:

$$R = Q\left(X(t) > X_{пор}\right) \cdot U_{max}(X), \qquad (4)$$

where: $Q\left(X(t) > X_{пор}\right)$ - the probability of exceeding the threshold value of meteorological factor $X_{пор}$ random function $X(t)$ describing the behavior of this factor in time.

Under the condition of stationarity of the studied process in the time interval τ as risk assessment $Q\left(X(t_k) > X_{пор}\right)$ at the time t_k, can be used for prognostic evaluation [5]:

$$Q\left(X(t_k) > X_{пор}\right) = \left(1 - \Phi\left\{\frac{X_{пор} - m_X - r_X(\tau) \cdot [X_i - m_X]}{\sigma_X \sqrt{1 - r_X^2(\tau)}}\right\}\right) \qquad (5)$$

where: $\Phi\{...\}$ – Laplace function, m_X – the expectation of a random process $X(t)$, $r_X(\tau)$ – autocorrelation function, σ_X – standard deviation, X_i – the current (actual) value of meteorological factors at the time t_i, $X(t_k)$ – meteorological factors expected value at time t_k, τ – the width of the time interval

$$\tau = t_k - t_i, \qquad (6)$$

where $i<k$.

In general, hydrometeorological risks are associated not only with adverse weather conditions, but also with their expectation. The use of weather forecasts reduces the risk of damage by hydro-meteorological causes regarding climate assessments by reducing the uncertainty of the value of meteorological factor on a given time interval and the use of protective measures, but not avoiding it completely - there are risks management, which are caused by the problem of choosing the optimal management decisions in accordance with the principle of maximizing expected utility, taking into account the uncertainty of the realization of the forecast of the hydrometeorological state of the environment.

The management of hydrometeorological risks are managed in the system "territory - economy - natural environment" [6], an important role is played by the process of adaptation (adaptation) of economic activity possible negative manifestations of the hydrometeorological environment. In the process of adaptation is classified into the following stages:

- the stage of development of protective measures, differentiated depending on the intensities I ($I \sim \Delta X$) and the duration T of the influencing meteorological factors;
- the stage of implementation of protective measures in anticipation of inclement weather.

The task of operational management of risk of loss from adverse meteorological conditions is a cyclically repeating the process of making decisions on the basis of information about the expected state of weather. The solution to this problem is the development of algorithm of actions of decision-makers, management process of adaptation to the adverse weather conditions, aimed at mitigating the damage by hydrometeorological causes, and includes the following successive steps:

- determining the level of impact of meteorological factor X at a given time t_k: if it is expected that the value of meteorological factor exceeds the threshold ($X(t_k) > X_{пор}$), then define the processes aimed at reducing the consequences of exposure to a predetermined (minimum) level $U_{min}(X)$ is a selection control function;
- implementation of management functions - the implementation of the planned activities aimed at reducing the effects of adverse weather. Implementation of protective measures requires a lead time, at the time of the adverse weather t_k protection measures should be implemented;
- at the moment of time gathering information t_k about the actual condition of meteorological parameters and monitoring results obtained during the implementation of protective measures on the basis of quantitative indicators; identification and analysis of deviations of actual from expected results, determination of causes of deviations;
- the adoption of measures to eliminate the causes of deviations, change in planning and allocating resources for the next time t_{k+1} of the actual weather forecast and the adjusted forecast.

For effective management of hydrometeorological risks necessary to create information systems to support decision making, comprising:

- database correlation of predicted and actual weather over time and space;
- information about the possible economic consequences of management decisions, due to the influence of weather in their respective areas.

This approach to risk management will allow to optimize the process of selecting solutions that satisfy the objective function - the reduction of economic loss caused by adverse meteorological conditions in the study area, and will contribute to the achievement of sustainable results of financial and economic activity of the region.

REFERENCES

1. N.N. Mihajlov, E.D. Vjazilov, A.A. Voroncov, S.V. Belov Edinaja gosudarstvennaja sistema informacii ob obstanovke v Mirovom okeane i ee primenenie dlja informacionnoj podderzhki morskoj dejatel'nosti Rossijskoj Federacii// Trudy Vserossijskogo nauchno-issledovatel'skogo instituta gidrometeorologicheskoj informacii – mirovogo centra dannyh, Obnisk, 2014, vyp.177, s. 95-118.
2. Istomin E.P., Sokolov A.G., Fokicheva A.A. O nekotoryh voprosah upravlenija gidrometeorologicheskimi riskami // Materialy 9-j mezhdunarodnoj nauchno-prakticheskoj konferencii «Analiz, prognoz i upravlenie prirodnymi riskami v sovremennom mire, GEORISK-2015» , M.: RUDN, 2015, T.2 s.170-176.
3. Handozhko L.A., Korshunov A.A., Fokicheva A.A. K voprosu o gidrometeorologicheskoj ujazvimosti Rossii // Uchenye zapiski RGGMU . – 2006 , № 3 , s. 146-158.
4. N.V. Kobysheva, E.M. Akent'eva, M.V. Kljueva, A.V. Meshherskaja, Je.Ja. Ran'kova Osnovnye osobennosti klimata Rossii
5. Istomin E.P., Slesareva L.S. Primenenie stohasticheskih modelej dlja prognozirovanija riskov v geosistemah// Uchenye zapiski RGGMU. - 2011, №17, s.145-149.
6. Istomin E. P., Sokolov A. G., Abramov V. M., Gogoberidze G. G.,Fokicheva A.A. «Methods for external factors assessing within geoinformation management of territories» / 15th International Multidisciplinary Scientific GeoConference SGEM 2015, www.sgem.org, SGEM2015 Conference Proceedings, ISBN 978-619-7105-34-6 / ISSN 1314-2704,June 18-24, 2015, Albena, BULGARIA Book2 Vol. 1, 729-736 pp.

METHODOLOGICAL ASPECTS OF RISK MANAGEMENT. DEVELOPMENT OF THE COASTAL AREAS

Evgeniy Istomin, Russian State Hydrometeorological University, Russia
Alexandr Sokolov, Russian State Hydrometeorological University, Russia
Valery Abramov, Russian State Hydrometeorological University, Russia
Anna Fokicheva, Russian State Hydrometeorological University, Russia
Ludmila Slesareva, Russian State Hydrometeorological University, Russia
Nikolay Popov, Russian State Hydrometeorological University, Russia

biom@bk.ru

Risk management of a development of systems and territories is one of the key problems of managerial decision-making. This is due to the impossibility of carrying out model experiments and the complexity of formalization of characteristics. The necessity of considering the peculiarities of the spatial distribution of subjects and objects of management allows to speak about relevance of geoinformation management.

Compared with other classes of potentially hazardous systems, spatially distributed systems and areas characterized by a significant level of inertia that contributes to sustainability in development, but hinders the development management and allows the dynamics to determine the influence of threat factors. The effects of hazards on the territory are systemic. The article describes:
- analysis of dynamics of control conditions for the development of spatially distributed objects and territories;
- classification of risks for coastal management;
- principles of risk management development of the coastal areas;
- the system model (conceptual model) of risk management in its spatial aspect, as well as private models for risk management under the influence of natural factors.

Key words: Territorial organizational-technical systems, risks management, development of systems and territories, risk management model

I. INTRODUCTION

Risk management for development of coastal systems and territories is essential problem of geo-information management (GM) [1-8]. Coastal systems and areas characterized by a significant level of inertia that contributes to sustainability in development, but hinders the development management and allows the dynamics to determine the influence of threat factors. The effects of hazards on the coastal territory are greatly important. In article we present:
- dynamic analysis for control conditions while the development of spatially distributed objects and territories;
- risk classification for GM of coastal systems and areas;

- principles of risk management while development of the coastal areas;
- the conceptual model of risk management with spatial aspects;
-private models for risk management under the influence of natural factors.

The use of risk management in GM involves the use of complex techniques of planning and control, which includes several stages [4]: conducting strategic analysis of potential development of the territory, including analysis of the current state of the territory and the main trends (opportunities, threats, etc.) development; identifying existing, emerging and potential clusters of signs on site [2]; assessing of competitive advantages of the territory and the rationale for management strategy development on the basis of cluster analysis [2], using of environmental monitoring systems [8-10] including sophisticated techniques [11-18].

II. METHODOLOGY

The GM phenomenon in modern conditions leads to the need to consider and implement a system of management of human activities as a multidimensional spatial phenomenon, comprising certain way distributed objective and subjective factors, and feasible in the geo-space. From the GM point of view, geo-space can be structured to allocate the interconnected components of the solution space [1]. To solve these problems, well-known methodological developments of strategic management can be used, including identifying current, emerging and potential clusters of signs on site [2].

III. RESULTS AND DISCUSSION

Territorial organizational-technical systems (TOTS) function in space and time, performing the appropriate function, focusing on the appropriate goals. The choice of targets for the development of such systems is based on the principles of sustainable development and security. Security of the population, enhance shareholder value and social facilities and natural environment elements of the territorial system, is a very complex task which is impossible without improving the methodological apparatus in the field of reliability research, forecasting, and security systems of different levels of complexity and goal of. Modern trends of security suggest a change from the concept "to respond to threats and fix" approach to a "predict and prevent is to give." The implementation of preventive security requires the identification of dangerous functions, threats to the development of TOTS, risk assessment of management decisions and the formation of the system of risk management system development.

Dangers of developing OTS arise as a consequence of the effects of certain negative external and internal factors. Manifestations of risk can be assessed as non-compliance of characteristics of the influencing factors characteristics of the OTS, which can cause unintended consequences directly or indirectly. Implementation of threat factors can be realized in the form of:

- direct or indirect damage to the territory, manifested in time, gradually or suddenly, and involve a critical decline in the level of safety for the population, environmental, natural and technological disaster as a result of failures and accidents of technical systems, destructions, deaths, etc.;

- reduction potential of the system properties object, which does not lead to a complete loss of ability to function, but its effectiveness;

- loss of control, loss of diversity, trauma, partial loss of functional activity, reduced competitiveness, pollution etc.

The development of territorial systems is potentially dangerous because of the hidden implicit nature of the manifestation of dangerous factors mediated in certain conditions, and in the long run (delayed symptoms). For a comparison, as compared to other classes of potentially hazardous systems, spatially distributed systems and areas are characterized by a significant level of inertia that, on the one hand contributes to the sustainability in development, and with another – complicates development management and allows the dynamics to determine the influence of threat factors, and to realize effective and adequate solutions to the adaptation of the system and minimizing negative governmental impact.

The danger is based on potential and the dynamic characteristics of the territorial systems. The latter are formed and rely on the property of openness of systems – flows of substance, energy and information that the system exchanges with the external it environment and which exist within its borders. Therefore, the risk can be characterized by:

- acceptable threshold levels of hazardous factors (potential characteristics);
- excess flows of substance, energy and information of acceptable levels characteristics of these threads (dynamic characteristics).

Sources of hazards the development of TOTS may be:

- technical factors such as defects, malfunctions, unsuccessful, merely leading characteristics, misuse, etc.;
-economic growth – costs of implemented solutions, reducing competitiveness, consumer dissatisfaction, etc.;
- social factors (the rise in crime, decline in fertility, political instability and large-scale, the weakness of the culture, etc.);
- information factors (information overload, the willingness of the individual and society to perceive information, the impact of information on the education of youth, etc.);
- environmental factors (harmful effects on humans and the natural environment, the degradation of the natural environment, reduction of resource potential, etc.).

The effects of hazards on TOTS are systemic: they are implemented in a spatial system "man – the individual – society – techno-sphere – geo-system".

The dangers are in space and in time, which involves the allocation of certain areas and intervals of exposure, frequency of manifestation of risk factors-in particular, frequency of exposure and other indicators of danger. Spatial aspects of risk include the region of occurrence of natural hazards, industrial specific zones and negative consequences of human activities (e.g., waste-baskets, war zones etc. the Classification (taxonomy) of hazards may be conducted according to certain criteria presented in table.

Table. Classification for hazards to development of territorial systems

Classification sign	Hazards
Source (nature) the occurrence of	Natural, technological, human, informational, economic, environmental, political and mixed

Symptoms	Physical, chemical, biological, physiological, organizational
Time of symptoms	transient or impulsive, long-term or cumulative, with the accumulation of consequences
Localization	Atmosphere, hydrosphere, lithosphere, space, society: staff, company, family
Area of activity	domestic, industrial, sports, military, road traffic, etc.
Kind of damage	social, technical, economic, environmental, etc.
Kind of the human exposure	active (having a direct impact on the basis of internal energy) passive-active (activated by the energy of the person) passive (indirect manifest)
Reason	voluntary - the person chooses a dangerous activity, the danger zone, etc. forced - finding near a source of danger as needed, meta residence, etc.
Structure	simple - factors, complex - multiple factors, derivatives - of the indirect factors
Concentration	concentrated in space, time, object impact, etc. scattered - distributed in space, time, objects of impact: local, domestic, local, regional, global etc.

The dangers present in the general case of multidimensional phenomena, which are manifestations or consequences of systemic or combined character. As a rule, the risk of single accidents, incidents, phenomena quite low, but the risk implications of the object - large. For group events (processes), the opposite pattern – the danger increases with the complexity and size of the object, but the risk is reduced due to the increase of stability and reliability of a complex object and, therefore, the growth of acceptable levels of risk (threshold of risk acceptable level of the object characteristics and impact).

The formalization of hazards involves the use of several types of features: energy, temporal and spatial. The energy of the hazard show the distribution of dangerous phenomena on the power of manifestation that is determined by the levels of physical quantities of the factors (amplitude, speed change, pressure, energy, etc.) and frequency of occurrence (impact on target), which allows to characterize the integral levels of influencing factors. The temporal characteristics of risk based on consideration of the hazards as flow of random events. The spatial characteristics of hazard it is convenient to depict on the map in form of isolines of the frequency of occurrence or strength. To characterize the degree of hazard areas, using the concept of injury rate dangerous phenomenon – the ratio of the area of the emergence or spread of a certain dangerous process to the total area of the territory. Area of negative factors, the affected area depends on the strength of the dangerous phenomenon, factor, durability of the object of exposure, and other factors. It is estimated according to statistical data or using theoretical models.

We call hazardous areas the region where the there are development of hazardous and harmful factors of the environment. They are characterized by an increased risk of the occurrence of the incident or accident. However, even if the person is in the danger zone, but properly organize

their activities, to comply with the terms of the security, monitors the serviceability of technical systems, an accident occurs. Often accidents are the result of violations of security measures at the time of being in the danger zone.

The development of risk it is possible to present the relevant algorithms. The typical algorithm of impact on the object of threat of external factors: initiation, the accumulation of hazardous factors → the release and migration of hazardous factors on the object → the impact of hazardous factors on the object (interaction object) → object response to external stimuli → the violation of the processes of functioning of the object → the destruction of the object → internal threat factors → release of hazardous factors by the object itself → secondary effects of hazards, interaction, etc.

The typical algorithm of the impact of threat internal factors on the object: initiation, the accumulation of internal threat factors → the violation of the processes of functioning of object → object is destroyed → the release of hazardous factors by the object itself → secondary impact of hazardous factors on the object, interaction → transport of dangerous factors on other objects, etc.

Each such event can be put into correspondence with private indicator-probability event, which will formulate the logical-probabilistic model of the manifestation of risk – taking decisions in risk management for site development. For the realization of the danger, you need to meet several conditions:

- danger really exists, is present;
- the object is in a spatial or temporal region of existence for risk factor exposure conditions;
- the level of danger, exposure factor sufficient to disruption of the object, its destruction.

Measurement of hazards and the quantification is a quantitative expression of the relevant concepts via a scorecard. For the hazards the indicators are used:

- potential is evident in quantitative terms, using the maximum achievable value of the object characteristics, external and internal influences: noise, air dust level, the intensity of the electric current, needs, purchasing power, requirements for the level of personnel training, etc.;
- quality reflects the specific features of the object and impact the possibility of their interaction and adaptation: the physical composition of the inputs and outputs of the object, its purpose, accessibility to influence, etc.;
- damage is a quantitative measure of the impacts of danger. Can be measured quantitatively: the economic damage, the costs of elimination of consequences of realization of risk or qualitatively: implications for individual - psychological damage, social implications, changing socio – economic conditions of functioning of the object.

The dangers are unrealized potential, i.e. hidden, which suggests a solution to the problem of their identification - the detection and establishment of quantitative, temporal, spatial and other characteristics necessary and sufficient for the development of preventive and operational measures aimed at ensuring the normal functioning of the JTS of the quality of life of the population in the study area. To identify the range of hazards, the likelihood of their expression, spatial localization, coordinates, possible damage and other parameters required for solving specific tasks.

Danger threshold level is the one of external influence or change the internal factors for a system in which adverse reactions is not observed and the system stably operates within acceptable performance. The threshold levels depend on the stability margin of the system, its ability for

resisting to external factors, workloads, level of available reserves and the ability of the system to their completion. The threshold levels can be characterized by the magnitude of this factor and the exposure time, the system's ability to accumulate the negative effects of impacts and development of adaptive features of the system.

The flip side evaluation of the risk of developing TOTS is the estimation of the security level. The main indicators of safety TOTS is the system's ability to withstand the negative effects of external and internal factors can be divided into several groups.

Indicators of resistance include the critical loads or levels of negative factors which impact the object retain the ability to perform functions. The opposite characteristic is a conditional vulnerability. Rationing of indicators of resilience (vulnerability) takes into account the size of the prevented damage.

Security metrics characterize the possibility of harm to TOTS that can be prevented by conducting early protective measures. The modern concept of assessment - the so-called "barrier" concept based on the use to counter the negative factors, many barriers - layered protection [1, 2, 3]. To quantify the degree of protection can be assessed using the coefficient of resistance, which generally represents the ratio of the forces influencing factor before and after the respective barrier, the protective echelon. Barriers have different meaning – the physical, organizational, financial, institutional, psychological, etc. the Efficiency of protection can be estimated by the decrease in the level of this factor to an acceptable level.

The overall objective of the potential development areas is to occur, the estimated liabilities exactly matches the existing potential. Knowing the potential areas for strategic period, it is possible to calculate obligations for this period.. Task of strategic management of the potential site is not only the preservation of the past but also providing capacity building in the implementation of any activities.

The presence of high potential areas is necessary but not sufficient condition for its implementation, which is associated with the existence of certain risks the occurrence of events with negative consequences. Risk assessment the management of territories should be focused on identifying key factors or issues about timeliness of management decision-making and increase predictive power. The system of factors allows to group model management on a specific basis and use appropriate methods and management tools, extending their capabilities based on spatial information. In this sense, the logic of geographic information management development of TOTS needs to take into account the characteristics of the territories, a system of internal and external objects and relationships between them. Control logic development based on the selected control factors suggests the possibility of decomposition of management practices across levels, content, the specifics of the management tools and functions. Using the terminology and the most common technology of geographic information systems we can talk about the formation of the corresponding slices or layers of analysis of the system and detail of objects of each slice in space and the object space for management decisions. The set of the slices or layers, of events and objects is based on multidimensional knowledge bases with respect to general components of the TOTS. In the context of several slices or layers of decisions aimed at the development of specific control object, component areas, involving the integration of management tools to achieve the common goal of

developing the component TOTS for different levels of management in relation to significant events and dynamics attributes of the objects.

Within a single level of decision-making, the formation of several private sections in attribute space-oriented space of the respective characteristics or attributes, the TOTS needed for decision-making at the appropriate management level, and relevant events. Thus formed multi-level, at least three-dimensional spatially distributed system of decision making. Risk management in conceptual representation focuses on the main consequences of management decisions in appropriate situations.

IV. Summary and conclusion

Risk management within GM at a conceptual level largely depends on the organization of relevant information. We propose meaningful ways of generating and presenting information to the decision-makers. GM for TOTS focuses on a multidimensional view of spatial information flows. The authorities may define additional components and additional requirements for the development plan of the state sector of the economy. They can develop a long-term target programs, subject to approval by relevant representative bodies. Well-designed concept of development greatly facilitates the development and adoption of specific target programs for the development of the region. The target program links resources, performers and terms of implementation the complex of scientific-research, experimental, production, socio-economic, organizationally-economic and other activities providing effective solution of tasks in the field of state, economic, social and cultural development.

IV. Acknowledgment

The platform https://www.researchgate.net/profile/Valery_Abramov2/?ev=hdr_xprf was used as a tool for scientific communication while research. The Ministry of education and science of Russia provides financial support for this research with the state task 1223.2014/166.

V. References

[1] Istomin E. P., Sokolov A. G, Abramov V. M., Gogoberidze G.G., Popov N.N. Geoinformation management as a modern approach to the management of spatially-distributed systems and territories, International Multidisciplinary Scientific GeoConference Surveying Geology and Mining Ecology Management, SGEM, Bulgaria, vol. 1, issue 2, pp 607-614, 2015.

[2] Istomin E. P., Sokolov A. G, Abramov V. M., Fokicheva A.A., Popov N.N. CLUSTERS WITHIN GEOSPATIAL INFORMATION MANAGEMENT FOR DEVELOPMENT OF THE TERRITORY, International Multidisciplinary Scientific GeoConference Surveying Geology and Mining Ecology Management, SGEM, Bulgaria, vol. 1, book 2, pp 601-608, 2016.

[3] Sokolov A. G. decision Analysis in business management, St. Petersburg, Andrew's editing house, 2011, 189 p

[4] Karlin L.N., Abramov V.M. Environmental and ecological risks management, St.-Petersburg, RSHU, 2013, 332 p - DOI: 10.13140/2.1.1978.8482

[5] Istomin E. P., Sokolov A. G, Abramov V. M., Gogoberidze G.G., Fokicheva A.A. Methods for external factors assessing within geoinformation management of territories,

International Multidisciplinary Scientific GeoConference Surveying Geology and Mining Ecology Management, SGEM, Bulgaria, vol. 1, issue 2, pp 729-736, 2015

[6] Gogoberidze G.G., Karlin L.N., Abramov V.M., Lednova J.A., Malakhova J.A. Marine economic potential assessment for environmental management in the Russian Arctic and subarctic coastal regions, International Multidisciplinary Scientific GeoConference Surveying Geology and Mining Ecology Management, SGEM, Bulgaria, 2014.

[7] Gogoberidze, G., Karlin, L., Abramov, V., Lednova, J. Indicator method of estimation of human impact assessment for coastal local municipalities, Measuring and Modeling of Multi-Scale Interactions in the Marine Environment - IEEE/OES Baltic International Symposium, BALTIC 2014, Estonia, 2014.

[8] Lednova J., Gogoberidze G., Abramov V.M., Karlin L.N., Berboushi, S. Concept of environmental monitoring in the Russian arctic coastal regions, International Multidisciplinary Scientific GeoConference Surveying Geology and Mining Ecology Management, SGEM, Bulgaria, vol. 1, issue 5, pp 161-168, 2014

[9] Abramov V.M., Karlin L.N., Gogoberidze G.G., Golosovskaya V.A. On route to Integrated Water Resources Management for Russian arctic and subarctic rivers, International Multidisciplinary Scientific GeoConference Surveying Geology and Mining Ecology Management, SGEM, Bulgaria, vol. 1, issue 3, pp 495-501, 2014.

[10] Gogoberidze G., Abramov V.M., Lednova J., Karlin L.N., Isaev A., Khaimina, O. Main results of summer oceanographic surveys in the eastern gulf of Finland in the framework of the Topcons project, International Multidisciplinary Scientific GeoConference Surveying Geology and Mining Ecology Management, SGEM, Bulgaria, vol. 3, issue 5, pp 253-260, 2014.

[11] Abramov V.M., Karlin L.N., Gogoberidze G.G., Alexandrova L.V., Popov N.N. Water exchange between the Pacific and the Bering sea with impact on climate change in the Arctic and Subarctic, International Multidisciplinary Scientific GeoConference Surveying Geology and Mining Ecology Management, SGEM, Bulgaria, vol. 2, issue 3, pp. 701-708, 2014

[12] Abramov V.M., Karlin L.N., Gogoberidze G.G., Alexandrova L.V., Bournashov, A.V. On Atlantic water inflow to Arctic ocean: Unique Argo buoy trip across Atlantic and Barents sea, International Multidisciplinary Scientific GeoConference Surveying Geology and Mining Ecology Management, SGEM, Bulgaria, vol. 2, issue 3, pp. 661-668, 2014.

[13] Karlin L.N., Abramov V.M., Ovsyannikov A.A. THE TEMPORAL STRUCTURE OF THE ICEBERG HAZARD IN THE CENTRAL PART OF THE BARENTS SEA, Oceanology, 2009, vol. 49, No 3.

[14] Abramov V.M., Karlin L.N., Lednova J.A., Gogoberidze G.G., Popov N.N. Clean technologies development strategy for the national black carbon controlling system in the Russian Arctic, International Multidisciplinary Scientific GeoConference Surveying Geology and Mining Ecology Management, SGEM, Bulgaria, vol. 2, issue 4, pp 313-320, 2014.

[15] Abramov V.M., Gogoberidze G.G., Popov N.N., Isaev A.V., Berboushi S.V. Method of assessment for black carbon random fields within Russia for climate management in the Arctic, International Multidisciplinary Scientific GeoConference Surveying Geology and Mining Ecology Management, SGEM, Bulgaria, vol. 1, issue 4, pp 953-960, 2015.

[16] Abramov V.M., Karlin L.N., Lednova J.A., Malakhova J.A., Gogoberidze G.G., Berboushi S.V. Variability of particulate matter in Saint-petersburg megacity air within climatic time scale, International Multidisciplinary Scientific GeoConference Surveying Geology and Mining Ecology Management, SGEM, Bulgaria, vol. 2, issue 4, pp 599-606, 2014.

[17] Abramov V. M., Popov N.N., Bachiev R.I. DECADAL VARIABILITY OF PARTICULATE MATTER IN MOSCOW MEGACITY AIR, International Multidisciplinary Scientific GeoConference Surveying Geology and Mining Ecology Management, SGEM, Bulgaria, vol. 2, book 4, pp 323-330, 2016.

MODELING AND MONITORING OF THE PROCESSES IN THE COASTAL ZONE OF IMERETINKA LOWLAND, BLACK SEA, SOCHI

Izmail Kantarzhi, Moscow State Civil Engineering University, Russia
Mark Zheleznyak, Fukusima University, Japan
Igor Leont'yev, P.P.Shirshov Institute of Oceanology, Russian Academy of Sciences, Russia

kantardgi@yandex.ru

The interest to study the processes in the Imeretinka lowland increases in the last years due the few reasons. The main structures of so-called "coastal cluster" of Olympic Games 2014 built in this area. Some of planned structures effected significantly the coastal processes; they are the seaport near the river Mzimta mouth and coastal protection. The natural coastal processes in the area complicated by the effects of the underwater canyons. The natural-technogenic system requires the study with using the methods of modeling and monitoring. Wave climate of Imeretinka lowland coast estimated based on long-term data of meteorological fields above Black Sea with modeling of wave transformation in nearshore zone by the gentle slope equations. Such approach provides possibilities to assess the effect of the designed coastal protection structures on the changes of the wave parameters in nearshore zone. Numerical modeling of currents in the Black Sea using 3D circulation model with refinement in the region of canyons of the Imeretinka coast obtained. To estimate the sediment transport, 3D Lagrangian multifraction sediment transport model LagrSed is used. 2D flow fields, free-surface level and wave characteristics calculated, using 2D hydrodynamic model of the coastal zone. It has presented the few years story of modeling and monitoring of the coastal processes with the important lessons.

Key words: coastal zone, Black Sea, Sochi region, Imeretinka lowland, coastal protection project, coastal processes, mathematical and physical modelling, monitoring

I. INTRODUCTION

The important area of the Russian Black Sea coast is the Sochi region, the Olympic Games 2014 city. The serious part of the Olympic Games infrastructure is built in the Imeretinska lowland. That is the very special area of the Sochi city coast with duration along shore in about 8 km (Fig.1). The lowland had been generated historically by the flow of solid matter of the two rivers: Mzimta and Psou. Due the good supply by the sediments from rivers the coast had the stable fine gravel beach with the wide of the overwater part about 50 m. The actual solid matter flow of Mzimta river is about 20-45 thousand cubic meter per year. About 80-85% of the total flow had been transported by the longshore currents to the east and nourishes the beaches of the area.

To supply the global construction works it was decided to build the new cargo port in the area of river Mzimta mouth, at the western bound of the area (Fig.2). The protective piers of the port are reached the water depth in 10 m, and, as the result, the longshore flow of sediments from river to

beaches had been interrupted. That is the classical mistake in shore management and the repeat of the similar mistake have been made in 1930-1935, when the main Sochi sea port had been placed in the month of the river Sochi. As the result, the area has the very serious problems with beach erosion until this time.

Fig 1. General view of the Imeretinska lowland, stage of construction the sport and infactructure structures. Port structures at the left side of photo

Fig.2. Mzimta port under construction, Mzimta river at the right side of the port

II. STUDY OF THE COASTAL PROCESSES

The situation of the Imeretinka lowland coast is complicated by the effect of the underwater canyons in the coastal zone. In the Fig. 3, it has shown the underwater relief of the sea bottom, from which the very close position of the canyons to shore is understandable. The canyons work as the traps for the beach material what can moves to the deep water by the gravitational flow.

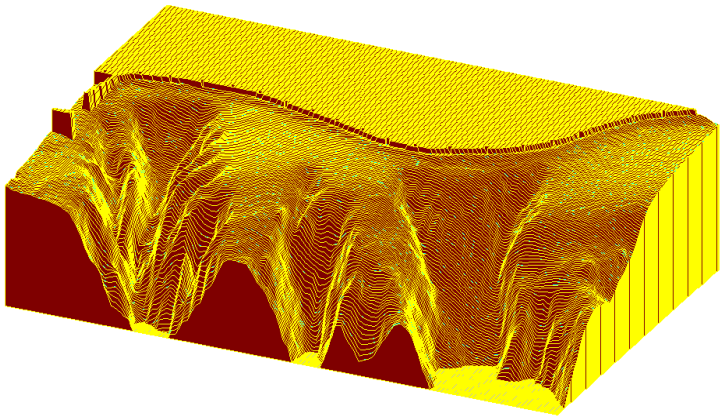

Fig.3. Bottom relief of Imeretinka coastal zone. Numerical reconstruction by Dr.V.Shakhin

The authors with colleagues carried out the complicated mathematical modeling of the coastal processes. That includes the following study: beach stability and effect of the protective moles on the lytodynamic processes; wind and deep water waves; waves and water set up at the sea edge of the coastal area; waves in the shallow water; longshore currents, transport of sediment, changes of bottom and beaches; current field in the area of canyons; stability of the shore protection structures.

The modeling based on the monitoring of the natural coastal processes what carried out in previous years.

Heterogeneity of bottom topography, rugged by deep-sea canyons, defines the feature of formation of wave regime. Therefore, the most dangerous to the coast near Canyon “Novyi” (New), storms from the southern and southwestern directions, which are suitable to the shore along the canyon.

Within the framework of the project on modelling of hydrodynamic and litodynamic coastal zone regime before and after the construction of the coastal protection structures [1], transformation of wave fields in deep water areas and near shore to shoreline studied by applying models SWAN and HWAVE [2].

Important problem of modeling of run-up of the extreme waves on protected dam and erosion of gravel-pebbles beach in splash zone under the influence of the dynamics of the overtopping stream. Simulation of these processes was based on models COASTOX-MORPHO [2,3] that can be used to calculate the longshore currents generated by the waves, the waves are considered as undergrid processes magnitude affecting the hydrodynamics only through stresses (through radiation stress and bottom friction) [3] and to directly describe the equations of shallow water waves run-up on the shore processes [2].

The results of the integrated modeling of the coastal processes are very helpful and may be used for searching of the optimal solution. Unfortunately, the modeling has been done not before the construction works, but after them.

As an example, the numerical modeling of the coastal waves in the canyon area is shown in Fig.4.

During the storm impact shore profile strives to take equilibrium form, which satisfies the minimum gradients of sediment discharges [4]. Bottom deformation reflects the process of the formation of the equilibrium profile. The closer the initial profile to equilibrium one, the smaller changes it is experiencing.

The alongshore distribution of the integral sediment discharges are shown in Fig.5.

Distribution of the storm deformations on some profiles under the action of southwestern directions storms of varying frequency of occurrence are shown in Fig. 6. A common feature of derived distributions is that in all cases indicated dredging near the line, moving material down the slope and its accumulation in the bottom of the profile. These trends are quite consistent with observations for storm changes pebbly beaches.

In the light of the results obtained, the most vulnerable are the cross sections of the shore 18 and 28, where the coastal slopes breaks to the canyons in offshore direction. When storm impacts sediments washed off the beach, move down and irretrievably lost.

In other areas, in general, more favorable conditions and do not cause fear. Cross section profiles 22, 32 and 41 storm washouts in total do not exceed 0.4 m. Cross section profile 30 underwater slope may be eroded to a considerable depth, but the beach at the same time is growing.

To maintain the beaches at designated sites will require regular filling pebble material in the volume shortfall, determined based on the results of monitoring.

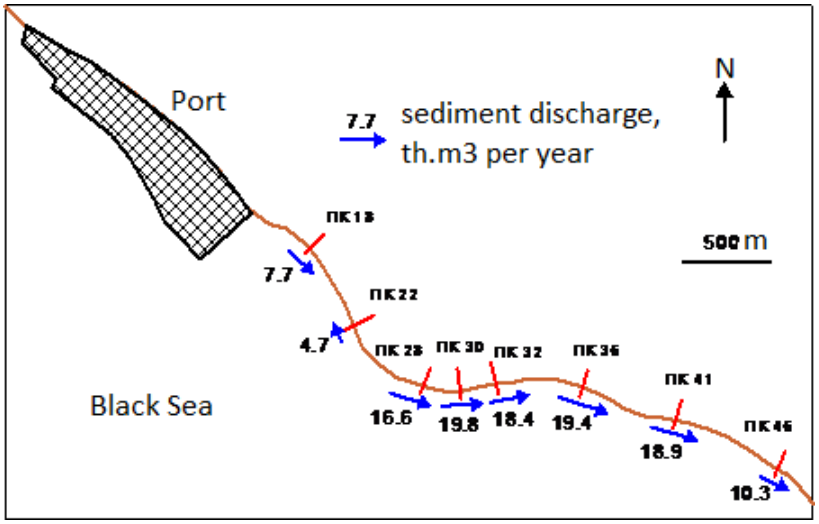

Fig.4. Result of numerical modeling of the waves in the coastal zone. The effect of canyons onto the waves

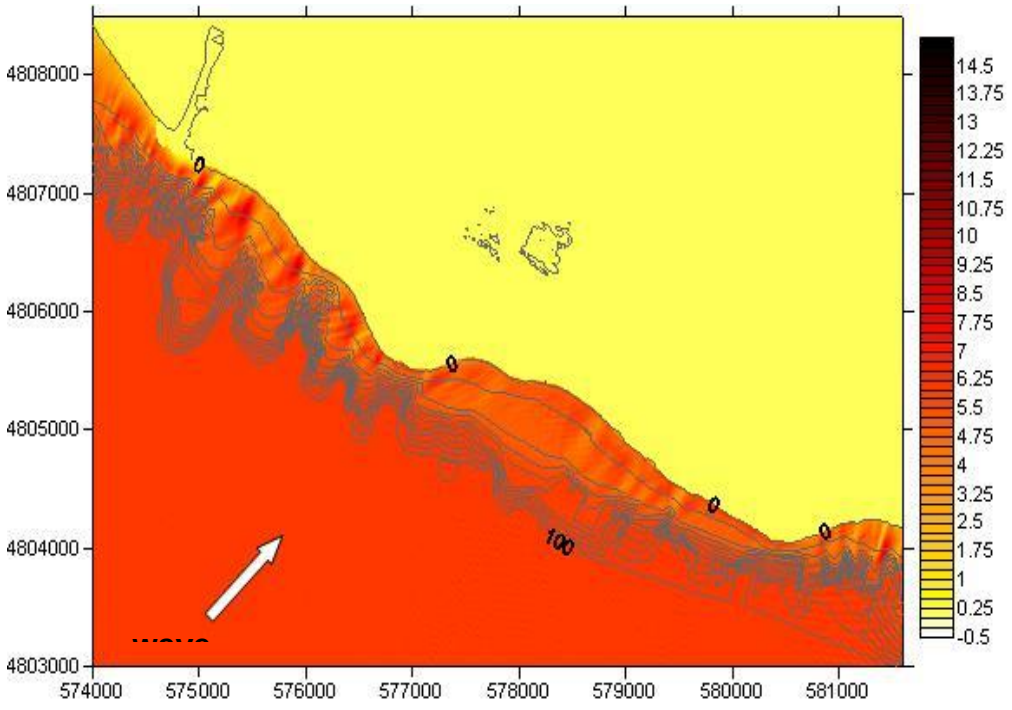

Fig.5. Scheme of the alongshore sediment transport with estimation of the rates

Experimental research on determination of coastal protection ability of dam constructions for Imeretinka lowland were held at the wave basin (Fig.7). In accordance with the chosen scale: 1 : 80 in the wave pool was built model reporting plot shore and bottom up to 70 m water depth, with longshore length 1600 m, from cross section 16 to 32.

Projected coastal protection structures with the beach 50 m wide, explored in the second series of experiments, not fully clearing waves in the zone of canyons at storm the southern and West-South-West directions. Surf zone flow with breaking of these waves crosses the shingle beach and overflowing on high mount and poured through it.

III. REALIZED COASTAL PROTECTION

Currently, the beaches of Imeretinka lowland coast located to the East coast from the mouth of r. Mzymty, lack of sediment nutrition. Particularly dangerous situation created in areas of canyons Novyi and Constantin, which absorb sediments and move deeper into shore. The existing situation, to some extent, can be corrected by adding a certain amount of beach material to the litodynamic system. It is this way to reinforce the shore will be offered for sale because of the construction of coastal protection dam (Fig. 8). At the top of the stacked concrete blocks, but below 2.5 m the pebble beach 50 m wide is built.

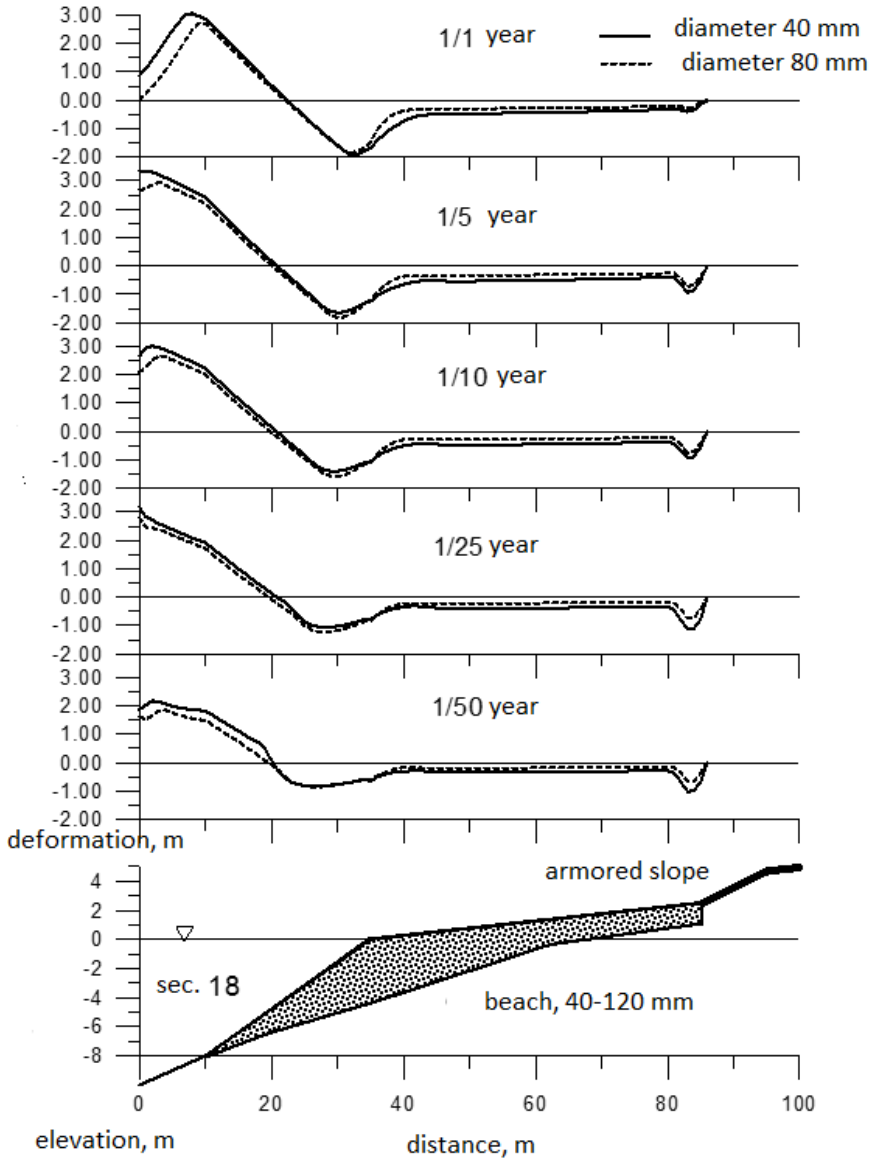

Fig.6. Erosion and accumulation of the coast profile, section 18, mathematical modeling

The natural result of the sediment balance disturbance is the shore erosion to the east of the port structures. The area is planned as the recreation area for the Olympic Games and for the region. So it was decided to construct the shore protection to conserve the beaches.

The proposed shore protection includes the along shore dam what includes the beach 50 m wide, concrete slope protected by perforated units or concrete desks with slope 1:5 and with based by the sea end on the concrete cushion (Fig.8).

Due the absence of the correct date on the dynamic behavior of the canyons, the level of risks of coastal damage is not understandable. By that it was decided to strange the coastal protection in the dangerous areas, which are connected with the canyon mouths.

Rubble mound dam with stones 3-5 tons – Fig.9, covered about 200 m of the coast near port mole. Moreover, few areas opposite the canyon mouths are strange by stones 10-30 kgs – Fig.10.

Fig.7. Physical modelling of the stability of the coastal protection dam (Scientific Center "Sea Coasts", Sochi)

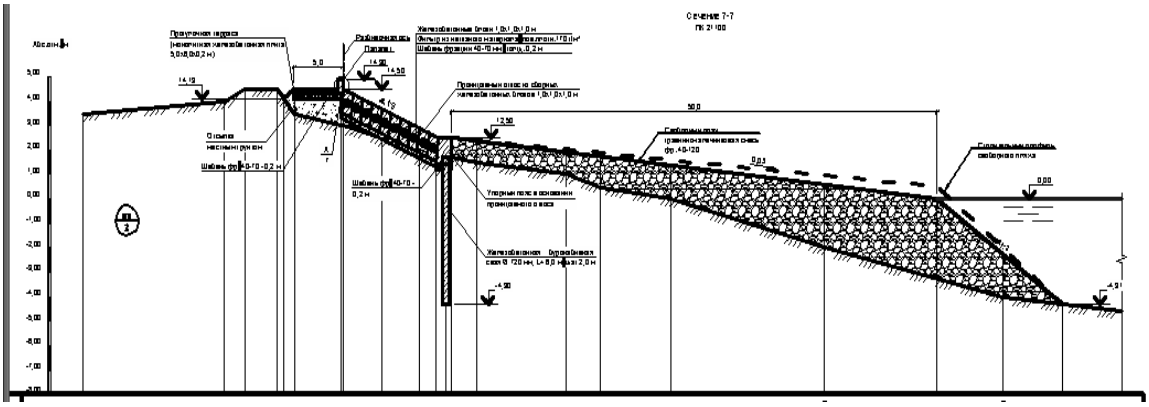

Fig.8. General scheme of the coastal protection dam

IV. MONITORING PROJECT

A very brief description of the project developed on coastal protection integrated monitoring for Imeretinka lowland is presented below. Comprehensive monitoring on the territory of the Imeretinka lowland is composed of:

1. Geotechnical monitoring for changes in the physic-mechanical characteristics of natural and anthropogenic soils in process engineering protection activities.

2. Hydrogeological monitoring and regime-formatted factors of groundwater territory and changes forecasting hydrogeological conditions in time under the influence of engineering activities.

3. Monitoring the safety and reliability of protecting structures.

4. Monitoring of the coastal protection before, during, and in the period of operation of the structures, with the aim of identifying the early stages of development of dangerous existing lithodynamic processes.

5. Environmental monitoring during the works on engineering protection of territory of Imeretinka lowland.

Fig.9. Coastal protection rubble mound dam in the area near the port mole

Fig.10. Coastal protection dam reinforced by rubble mound breakwater in the area of underwater canyon mouth

For the prediction of the conditions of nature and man-caused geological system and structures of artificial protection, it is planned the mathematical modeling of stress-strain state of ground array and its changes over time in the zones of most responsible sites of geo-systems and installations of artificial protection.

Comprehensive project monitoring is designed based on data from geotechnical surveys, based on the terms of the construction and initial data for project development. Integrated monitoring you intend to in two phases over four years (first period).

The first stage is preparatory one and includes the following works:

Adjustment of the integrated monitoring programme;

The creation of the locomotive and observation network device with wells and geodetic marks;

The establishment of mathematical models;

Organization of integrated monitoring.

Second stage - observations includes works by:

Measurements of parameters to be monitored;

Operational control;

The collection and analysis of information, the creation of a database;

Evaluation of stress-strain state of inhomogeneous ground array and state of environment and forecast natural and technogenic geosystem and engineering protection and constructions;

Preparation of accounting documentation.

Safety monitoring tasks of protecting structures.

1. Development of monitoring programmes.

2. Monitoring of local deformations of slopes and ridges structures.

3. Conducting geodetic control values by definition of vertical offsets (sludge, drawdowns, and upgrades) and horizontal offsets of the shifts and the banks structures.

4. Conduct a comprehensive assessment of the state of installations and their operational reliability, to develop recommendations to ensure the safety of structures.

Litodynamic monitoring tasks.

1. Litodynamic monitoring program development, taking into account the planned technical solutions and assess the possible impact of protecting structures on the progress of existing lithodynamic processes in the coastal zone of the sea.

2. Measurements of the width of the beach on a stretch of coastal protection, sampling and analysis on granulometric analysis of beach sediments.

3. Conduct a survey of the beach surface to a depth of 1 m, bathymetric shooting from the water line to a depth of 20 m.

4. Diving survey of the bottom surface to a depth of 20 m with a sampling of surface sediments for granulometric analysis, as well as diving survey tops canyons "Mzymta River", "New" and "Constantine" with a view to assessing the dynamics of sediment in their upper reaches.

5. Evaluation of existing lithodynamic processes features and effectiveness of the project on engineering protection of coast activities during construction and operation of the coastal structures. Validation and adjustment of the existing lithodynamic predictions of dangerous existing lithodynamic processes during construction and operation of the coastal protection.

V. Conclusion

Coastal protection for complex projects, such as the complex of buildings in the Imeretinka lowland, the project must provide for integrated monitoring of coastal processes and structures under construction. Such monitoring allows you to monitor the situation during the operation of the facilities and make the better decisions.

To implement an integrated dashboard, you must at the design stage to develop the necessary tools for monitoring of natural processes and state of structures. Information obtained through such monitoring, is used for the development of mathematical models of processes.

Coastal protection complex for Imeretinka lowland, created in 2011-2014, not fully implements this principle. In the design phase the mathematical models of coastal processes have been created, which take account of the real characteristics of the area. Including the effect of submarine canyons and seaport facilities. Using physical modelling and comparison with existing data studies it has been shown that models adequately reflect real processes.

However, the developed project of monitoring was not implemented, resulting in the need to make intuitive decisions on protection of dangerous sections of coast. The degree of risk is uncertain.

VI. Acknowledgment

We thank to our colleagues and assistances: Natalia Shunko (Moscow State Civil Engineering University), Igor Brovchenko, Pavel Dikiy, Natalia Dzyuba, Maxim Sorokin, and Pavel Kolomiets (Ukrainian Center of Environmental and Water Projects) who contribute to the present research.

VII. References

[1] I. Kantardgi and K. Mordvincev, "Mathematical modelling of the coastal processes to support the shore protection of the Imeretinsky lowland," *Int. J. for Computational Civil and Structural Eng.*, vol.7, issue 2, pp. 64-71, 2011.

[2] P. Dikiy, N. Dzyuba, M. Zheleznyak, and M. Sorokin, "Modelling of wave climate of Imeretinsky lowland coast," *Int. J. for Computational Civil and Structural Eng.*, vol.7, issue 2, pp. 54-63, 2011.

[3] S.Kivva and M. Zheleznyak, "2-D modelling of water yield and sediment transport from the small aquilegia," *Applied Hydromechanics*, vol. 4(76), issue 1, pp. 67-89, 2002

[4] I. Leont'yev, "Dynamics of the sand coast profile on the various time scales," *Fundamental and Applied Hydrophysics*, no.4 (10), pp.78-89, 2010.

LONG-TERM DYNAMICS IN LOCATIONS OF COASTLINE OF THE VISTULA SPIT BY RESULTS OF THE SATELLITES IMAGES ANALYSIS

Konstantin Karmanov, State Organization of the Kaliningrad region "Baltberegozaschita", Atlantic Branch of P.P. Shirshov Institute of Oceanology of Russian Academy of Sciences, Russia
Boris Chubarenko, Atlantic Branch of P.P. Shirshov Institute of Oceanology of Russian Academy of Sciences, Russia

mr.pocketoff@rambler.ru

Images of satellites OrbView-3 for 2004 and 2005 years (spatial resolution 1 m/pixel) and Pleiades for 2014 year (spatial resolution 0.5 m/pixel) for the Vistula Lagoon (the Baltic Sea) were used. In contrast to shoreline location often used as an indicator of a shore retreat the paper recommends to use the changes in location of dune edge as an indicator of shore dynamics.

Nine well identified mark points were selected for the northern Russian part of the Vistula Spit as control ones. The average difference in locations of these points obtained by geodetic survey and satellite images was 0.4 m.

The lines of the foredune edge for 25 km northern part of the Vistula Spit (from the Polish-Russian border to the Strait of Baltiysk) for 2004-2005 and 2015 were digitized with the step of 10 m and compared. Introducing the level of confidence ± 1.5 m per 10 years, we considered that eroded, stable and accreted parts of the shore have the total length 15.4, 4.9, 5.2 km (60.4%, 19.1%, 20.5%). The average (10 years) erosion rate for the marine shore on the Russian side of the Vistula Spit is 0.6 m/year, and accretion rate is 0.3 m/year.

Maximum erosion rate (2.2 m/year) was revealed on the shore segment to south from the Strait of Baltiysk, which is under permanent erosion during last one century and a half after construction of the entrance jetties.

The comparison of result of geodetic instrumental monitoring and estimation using satellite images showed that the second method slightly underestimates the shoreline displacement. Also it was shown that instrumental monitoring measurements at the profiles with spatial step of several kilometers are not optimal enough to reveal erosion/accretion processes for the shore of South-Eastern Baltic, which is characterized by alongshore nonmonotonic variations of shoreline dynamics parameters.

I. INTRODUCTION

The Vistula Spit is located in the south-eastern part of the Baltic Sea and borders the Vistula Lagoon (Fig. 1). It is transboundary sandy barrier peninsula, southern 40 km belong to Poland and northern 35 km belong to Russia (Kaliningrad Oblast). The single inlet to the Vistula Lagoon (the

Strait of Baltiysk[4]) cuts the spit in 2 parts on Russian territory (25 to south and 10 km to north from the inlet).

Sandy beaches on the marine shore have width of 40-50 m in the central part and 20-25 m in the northern part of the spit. The continuous alongshore foredune borders the beach and forested area, it was formed by natural eolian accumulation. The ancient dunes are located at the lagoon shore, they have a height 7-12 m at the northern part and up to 30 m at the southern and central parts. The beaches at the lagoon shore are very narrow – 5-15 m [1].

Instrumental geodesic monitoring [2] was started on the marine and lagoon shore by AB IO RAS[5] in 2002, while some test measurements were done in 2000. This type of monitoring has rather good accuracy but doesn't cover the whole shore. It is fulfilled via measurements along the profile perpendicular to the shoreline, and doesn't consider what happened with the shore between the measuring profiles. It appeared that the method is not optimal enough for the shore of South-Eastern Baltic, characterized by alongshore nonmonotonic variations of shoreline dynamics parameters.

Nowadays step in development of coastal monitoring is connected with satellite images [3,4,5]. This method became applicable for the Baltic Sea shore only recently, once the satellite images with resolution about 1-2 m became accessible, as the crucial point to apply this method is the comparability between satellite image resolution and rate of shore erosion.

The aim of the study – to estimate quantitatively the dynamics of marine shore of the Russian part of the Vistula Spit (erosion or accretion) and changes of coastline location in space and time using the satellite images of high resolution.

[4] Some studies call it the 'Baltiysk Strait'

[5] - *Atlantic Branch of P.P.Shirshov Institute of Oceanology of Russian Academy of Sciences, Kaliningrad, Russia*

a)

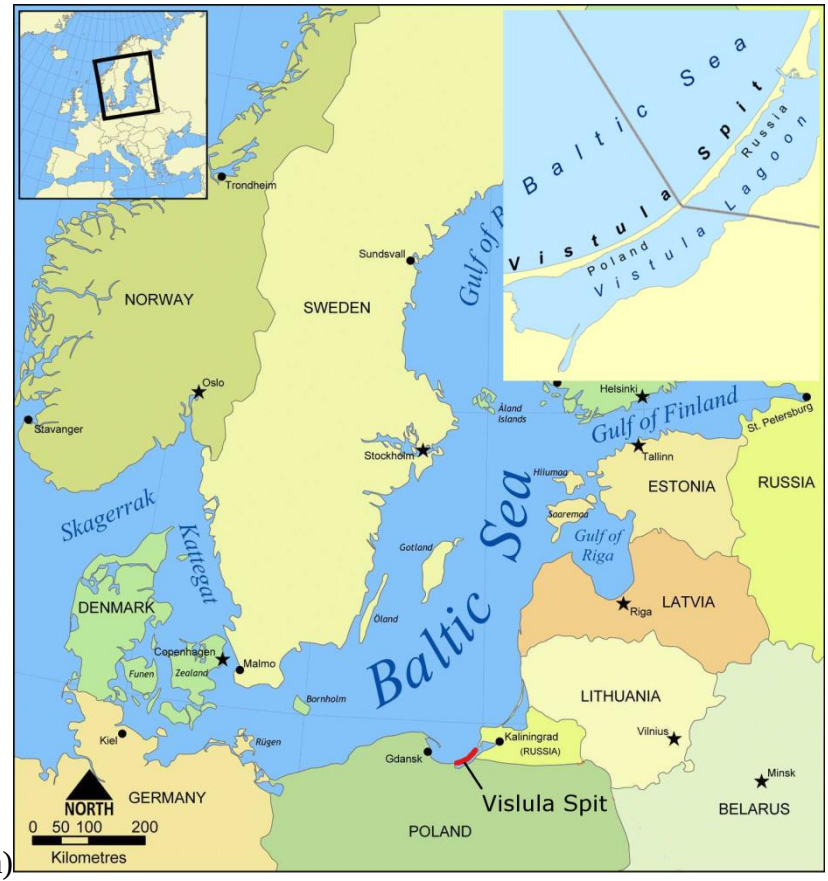

Fig. 1. Location of the Vistula Spit in the south-eastern part of the Baltic Sea.

II. MATERIALS AND METHODS.

The images of extra high spatial resolution from the satellites OrbView-3 and Pleiades were used to estimate quantitatively the dynamics of marine shore of the Vistula Spit (erosion or accretion) and changes of coastline location in space and time.

Satellite images of the OrbView-3 is panchromatic images with spatial resolution 1 m/pixel. Four images of the OrbView-3 satellite were used: 1 image for August 2005 and 3 images for August-September 2004 (Fig. 2). Due to absence of the images of the same year to cover the whole research area, the image for 2004 was combined with image 2005 for northern part of the area. The uncertainty caused by this combination of initial location of the coastline was supposed to be within the uncertainty of estimation made in this paper, and gave the little underestimation of erosion rate in the northern part of the area.

Satellite natural color images of the Pleiades with spatial resolution 0.5 m/pixel (five images for September 2014) were used.

In the paper we considered the change in location of the foredune scarp as an indicator of the coastline erosion if the foredune scarp retreated or the accretion if the foredune scarp moved forward towards to the sea.

Foredune scarp (Fig. 3a) is the line between upper part of a beach and lower part of a sea slope of the foredune. It is better visible on the satellite images than the foredune crest, which is usually used as an indicator for coastal retreat [2]. These two approaches to estimate the coastline retreat via the change of location of the lines of both dune scarp or dune crest may lead to different estimation of erosion/accretion rate for the same point of the shore. Dune crest may be stable, but dune scarp may retreat due to wave erosion, or vice versa, the dune scarp may be stable, but dune crest retreat due to wind deflation. We are expected that in long-term perspective these two approaches should give the same result.

Foredune scarp is easy visible on the satellite image as the border between beach and vegetation if the seaward slope of the foredune is covered by vegetation. Otherwise the foredune scarp is visible as the border between the area with maximal brightness on the satellite images (it is a beach) and neighbor area landward having less brightness or another texture (Fig. 3).

The following steps were made to estimate quantitatively the dynamics of marine shore of the Vistula Spit (erosion or accretion) via changes of coastline location in space and time:

- To make georeference of the satellite images using control points method. Images for 2004 were superposed with images 2014 by control points (crossroads, corner of buildings and detached trees).
- To digitize the positions of the foredune scarp on images with an accuracy of 1 pixel.
- To measure the distance between positions of the foredune scarp in 2004 and 2014 years, as the indicator of the dynamics of marine shore. The distance between locations of the foredune scarp in 2004 and 2014 years were measured at the points selected with 10 meters interval along the line of the foredune scarp in 2014. So, the shore displacement was measured as the distance from points on foredune scarp line in 2014 to the line of the foredune scarp in 2004. In the GIS instrument the lines were parameterized from north to south, and therefore, the points of 2014 located to left from foredune scarp line in 2004 were attributed as erosion points while points locate to right from foredune scarp line in 2004 were attributed as the accretion ones.

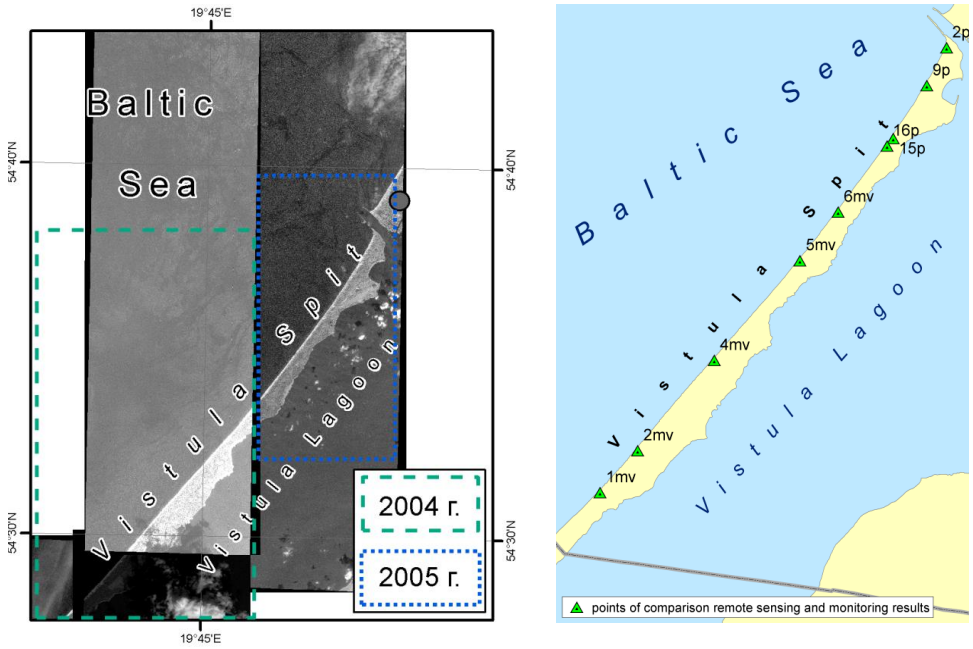

Fig. 2. The coverage of the Russian part of the Vistula Spit by satellite images of the OrbView-3 of 2004 and 2005 (a), and locations of the monitoring points at the marine shore of the Vistula Spit (b).

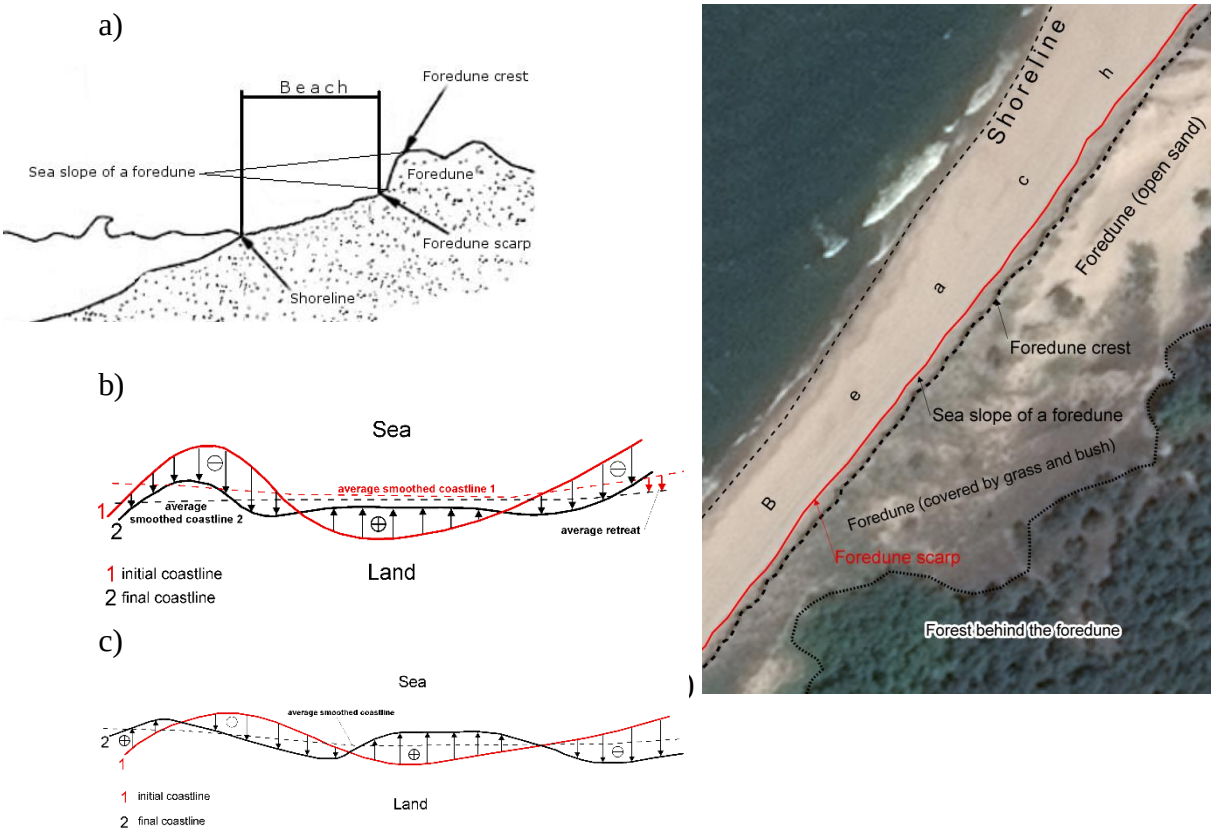

Fig. 3. Scheme of morphological structure of the dune marine shore of the Vistula Spit and the same morphological elements on the fragment of the satellite image (d), as well as principle drawing of coastline changes with presence (b) and absence (c) of average retreat.

The confidence range was introduced for more accurate estimation of shore dynamics – the shore segment was attributed as stable if the value of the displacement was lees then confidence range. We considered the confidence level of coastline retreat between -1.5 m and +1.5 m for given period 2004-2014 as the spatial resolution of the images were 1 m/pixel and 0.5 m/pixel, and the maximal error could be equal to 1.5 m. It followed by the confidence range (from -0.15 m/year to +0.15 m/year.) for the average annual shore dynamic rate.

The values of coastline displacement during 10 years period (2004-2015) obtained both from instrumental monitoring [6,7] and satellite images are presented in Table 1. The comparison was made for 9 monitoring profiles of the AB IO RAS monitoring network (Fig. 2). Mean difference between monitoring and satellite data was -0.7 m, i.e. it seems, that method based on the satellite images underestimates the coastline retreat. The maximal difference of 2-2.5 m was observed for profiles 16p, 5mv, 4mv. Partly it may be the consequence of refereeing the initial data of 2005 (profiles 5mv, 6mv, 16p, 15p, 9p, 2p) to 2004.

Table 1. The coastline displacement at the monitoring profiles during 10 years period 2004-2015 obtained from satellite images and instrumental monitoring. Retreat is marked by negative displacement, accretion – by positive.

№ of profile	Displacement by monitoring, m	Displacement by satellite image, m	Difference between 'monitoring' and 'image', m
2p	-11,0	-10,0	-1,0
9p	0,5	1,0	-0,5
15p	3,0	2,0	1,0
16p	-11,0	-8,5	**-2,5**
6mv	5,1	4,5	0,6
5mv	-4,8	-2,5	**-2,3**
4mv	-11,0	-9,0	**-2,0**
2mv	-1,0	-2,0	1,0
1mv	-7,5	-7,0	-0,5
		Average	-0,7

To investigate the differences in coastal changes caused by average coastal retreat and change of coastline tortuosity (Fig. 3 b,c) the GIS based procedure of average smoothing (30 m window) of both digitized coastlines of 2004 and 2015 was applied. The tortuosity (dimensionless value) is expressed by arc-chord ratio of the length of the coastline (L) to the distance between the ends of it (C): $\tau = L/C$ [8].

III. Results and discussion

Considering the series of 10-years displacement for all points of the studied shore, one may represent this series in terms of distribution of the total length of all shore segment against the erosion (-) or accretion (+) rate (ranges with the step of 0.15 m/year) (Fig. 4). The inset of Fig.4 presents the same information (sorted by rate) but along the cumulative length. The characteristic feature is that the shore segments of nearly the same total length (2000 – 2650 m) are attributed to the ranges of the erosion/accretion rate within the limits of -0.9 – 0.3 m/year (linear relationship on the insert of Fig. 4) and occupy the major part of the spit shore.

Fig. 5 demonstrates the variations of 10-years average shore dynamics rate for the marine shore of the Vistula Spit from the Polish-Russian border up to the Strait of Baltiysk for the period 2004(2005) – 2014. Erosion and accretion segments change each other rather irregularly. This is absolutely new level of understanding of shoreline dynamics, as results of instrumental monitoring [6,7] gave the uncertain picture: no one from monitoring profiles (they are indicated in Fig. 5) locates at the shore segment of high rate of changes, most of them are within the zones of a low rate of erosion/accretion. That is why the very general conclusion came from the instrumental monitoring program [6,7]: the segment of 4-5 km south from the Strait of Baltiysk is intensively eroded while the rest shore to south is in stable conditions in general.

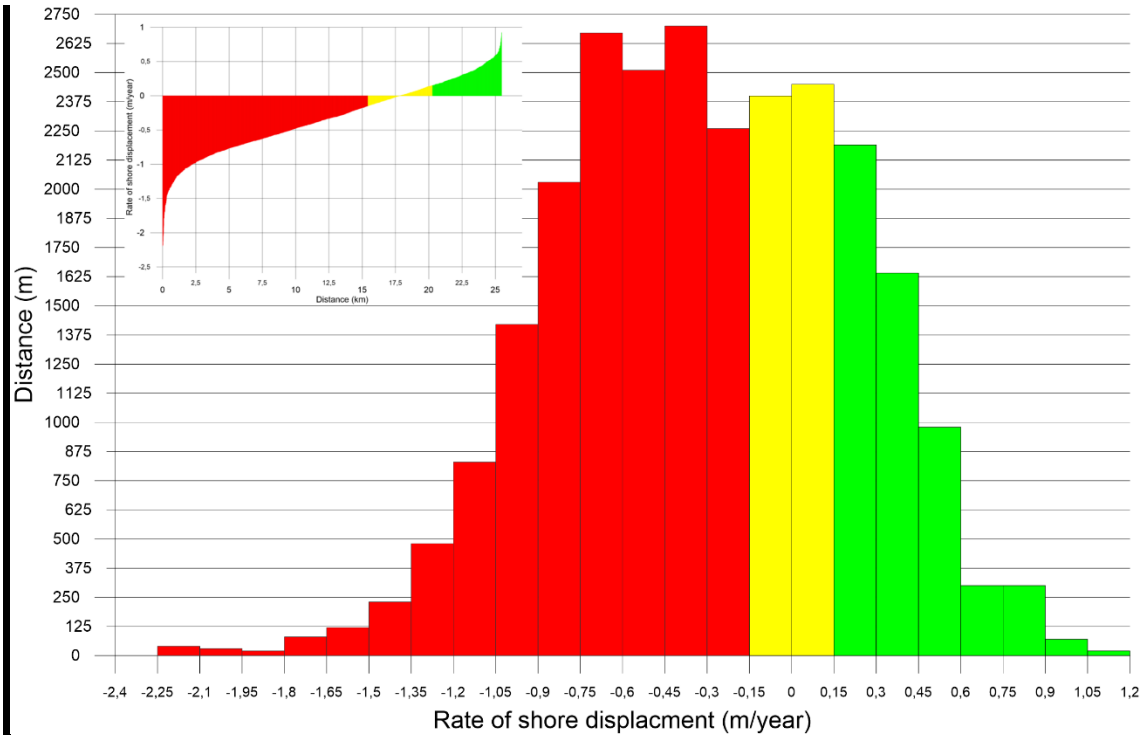

Fig. 4. Distribution of the length of the shore segment against the erosion (-, red color) and accretion (+, green color) rate assigned with the step of 0.15 m/year. The inset presents the same information but sorted by rate and cumulative length. The stable segments are yellow.

As it is seen from the Fig. 4 and 5, the significant part of shore of the Vistula Spit is under erosion of different extent. The average 10-years erosion rate (2014-2014) for the marine shore on the Russian side of the Vistula Spit is 0.6 m/year, and accretion rate is 0.3 m/year.

The length of eroded coastline is 15.4 km (60.4%): 5.8 km (22.7%) has the rate less than 0.5 m/year, 7.4 km (29.1%) has the rate 0.5-1.0 m/year, 2.1 km (8.4%) has the rate 1.0-2.0 m/year, 0.07 km (0.3%) has the rate higher than 2.0 m/year. The length of single eroded shore segment varies in a range 20-1450 m, 390 m is the average length.

The total length of the stable shore segments is 4.9 km (19.1%), they are characterized by the rate of erosion or accretion not less 0.15 m/year, as this rate is less than resolution of our method. The length of single stable shore segment varies in a range 20-240 m, 70 m is the average length.

The accretion was identified at 5.2 km (20.5%) in total, where 3.8 km (15%) was characterized with accretion rate 0.15-0.5 m/year, and nearly 1 km (4.2%) had accumulation with the rate 0.5-1 m/year. The length of single accreted shore segment varies in a range 20-530 m, 150 m is the average length.

Considering the rate 1 m/year as the threshold of erosion for the shores of South-Eastern Baltic, someone may define 3 shore sections (A-B-C) with the rate higher this threshold (Fig. 5). The longest one (A) is 7 km south from the Strait of Baltiysk. Here the maximum erosion rate (2.2 m/year) was identified. The shore segment with this rate has a length 70 m and is located at the southern end of the 2-kilometers shore segment belonged to the territory of the Kosa Settlement.

The length of the single eroded and accreted segment of the section A varies in a range 70-570 m and 30-180 m respectively. For sections B and C the length of single eroded and accreted segment varies in a range 200-1800 m and 50-700 m respectively, i.e. not so often as for the section A.

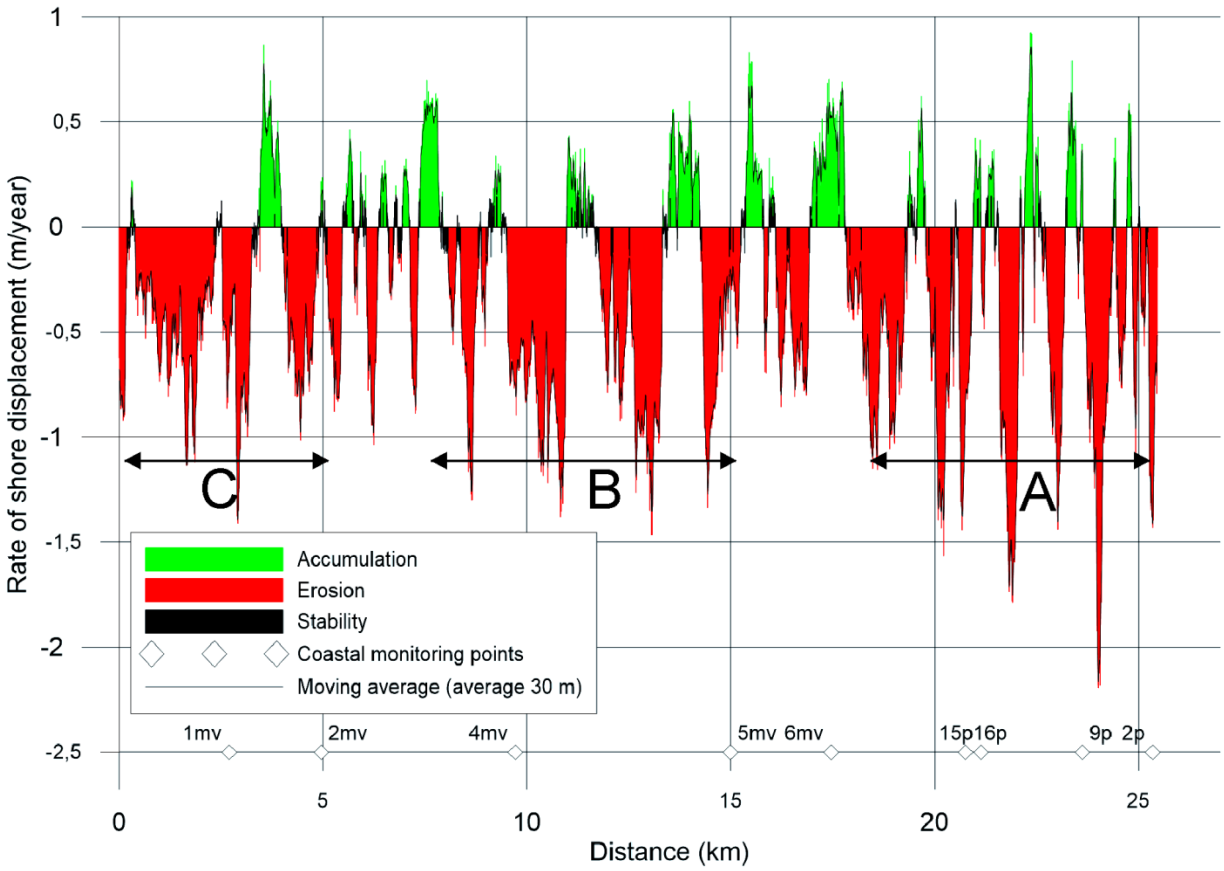

Fig. 5. Rate of shore displacement for the Russian side of the marine shore of the Vistula Spit averaged through the period 2004-2014. Three shore segments (A,B,C) with erosion rate higher than threshold of 1/year were identified. The rate obtained by analysis of displacements of smoothed coastlines (30 m window) very well fits to the rate basing on unsmoothed data.

Analysis of the coastline tortuosity for 2004 and 2015 (Table 2) showed that the coastline of 2014 became tiny more variable in space. The analysis of changes of coastline basing on averaged smoothed coastlines of 2004 and 2014 gave the same result for average length of eroded and accreted segments. The erosion/accretion rate estimated by displacement of averaged smoothed coastline very well fits to the one estimated by unsmoothed data (Fig. 5). It means that smoothed data well present the real situation and may be compared with any satellite image of rough resolution (up to 30 m per pixel).

Table 2. Tortuosity for coastlines 2004 and 2014.

Year	Total length of coastline, m	Total length along the chord, m	Tortuosity
2004	25273	25050	1.008902196
2014	25474	25043	1.017210398

IV. CONCLUSIONS

The uncertainties of the analysis of coastal dynamics using satellite images depend on ratio between the image resolution and rate of shore displacement. For the marine shore of the Vistula Spit located in the South-Eastern Baltic we have used the images with resolution 0.5-1 m/pixel for 10 years period (2004-2014). The change in location of the foredune scarp was used as an indicator of the coastline erosion/accretion. Introducing the level of confidence for displacement rate as ± 1.5 m per 10 years, we considered 19.1% (4.9 km) of length of coastline as stable (displacement was not higher than level of confidence).

Comparison of results of coastline displacement obtained by direct geodesic measurements and from satellite images at the 9 test profiles showed:

- for the shore segments where accretion dominates (3 profiles) the data obtained from satellite images gave less positive displacement than geodesic data (for 2 profiles among 3 ones);
- for the shore segments where erosion dominates (6 profiles) the data obtained from satellite images gave less value of displacement than geodesic data (for 5 profiles among 6 ones), the difference varies in the range 0.5-2.5 m per 10 years.

No one from monitoring profiles coincide with shore segment with high rate of shoreline displacement, most of them are located within the zones of medium and low rate of erosion/accretion. It means that monitoring results doesn't include important information about high value of changes happened at the shore segment between the monitoring profiles. The result once more showed that nowadays instrumental monitoring by measurements at the profiles with spatial step of several kilometers is not optimal enough for the shore of South-Eastern Baltic, which is characterized by alongshore nonmonotonic variations of shoreline dynamics parameters. New monitoring system with profiles each 500 m introducing by the State Organization of the Kaliningrad region "Baltberegozaschita" will better present the variability of coastal dynamics, but the using of satellite images anyway is the best method to get information about whole shoreline dynamics.

Erosion is the predominant process on the marine shore of the Vistula Spit in terms of both eroded length of shoreline and rate of displacement. Eroded, stable and accreted parts of the shore have the total length 15.4, 4.9, 5.2 km (60.4%, 19.1%, 20.5%). The average (10 years) erosion rate for the marine shore on the Russian side of the Vistula Spit is 0.6 m/year, and accretion rate is 0.3 m/year. Analysis of tortuosity and retreat of averaged smooth coastline showed that for the Russian side of the marine shore of the Vistula Spit the displacement of coastline is caused by average retreat and shift, not by increasing the tortuosity.

Spatial variability of erode/accreted segments of the shore is high. Using threshold of 0.6 m/year and 0.3 m/year for eroded and accreted segments we may reveal 19 eroded ones and 14 accreted ones, which change each other (there are stable segments also). The length of these segments varies in the ranges 70-1800 m (eroded ones), 20-160 m (stable ones), 30-700 m (accreted ones). It is expected that these segments are not stably located in space otherwise the shore will be extremely meandering through thousands of years of existence of the spit.

Maximum erosion rate (2.2 m/year) was revealed on the shore segment to south from the Baltiysk Strait, which is under permanent erosion during last one century and a half after construction of entrance moles.

V. Acknowledgement

Technical facilitation of the study and problem identification were made under support of the theme № 0149-2014-0017 (supervisor – B. Chubarenko) of State Assignment of the P.P.Shirshov Institute of Oceanology of the Russian Academy of Sciences (2015-2017). The preparation of this article was made under the support of the Project No 14-17-00547 "A forecast development for evolution of accumulative Russian coasts of tide less seas"

VI. References

[1] E. N. Badyukova, L. A. Zhindarev, S. A. Luk'yanova, and G. D. Solov'eva, "The geological-geomorphological structure of the Baltic (Vistula) spit," *Oceanology,* vol. 51, No 4, pp. 632-639, August 2011.

[2] V.P. Bobykina, V.L. Boldyrev, "Methods of monitoring of the Kaliningrad Oblast," *Proc. XXII Int. Conf. Problems of management and sustainable development of marine coastal zone*, Gelendzhik (Russia), p.52, 16-20 May 2007. In Russian.

[3] A.E. Tsygankova, "Mathods of analysis of satellite images for study of the shore of the northern-east part of the White Sea," *Proc. Int. Conf. devoted to 100 years anniversary of V.V. Longinov "Lithodynamics of the bottom contact zone of the ocean*," Moscow (Russia), Moscow: GEOS, p. 168, 14- 19 September 2009. In Russian.

[4] R. D. Kosyan, Y. N. Goryachkin, and E. A. Godin et al., "Crimea and Caucasus accumulative coasts dynamics estimation with using satellite pictures," *Turkish Journal of Fisheries and Aquatic Sciences.* Vol. 12, pp. 385–390, 2012.

[5] A. Santra, Mitra S. Santra, and D. Mitra, "Change detection analysis of the shoreline using Toposheet and Satellite Image: A case study of the coastal stretch of Mandarmani-Shankarpur, West Bengal, India," *Int. J. of Geomatics and Geosciences*, Vol. 3, Issue 3, pp. 425-437, 2013.

[6] V.P. Bobykina, K.V. Karmanov, "Dynamics of the shore of the Gulf of Gdansk and relations with anthropogenic influence," *Proc. Int. Conf. "Construction of artificial beaches, islands and other constructions in coastal zone of seas, lakes and reservoirs*," Novosibirsk, SB RAS, pp. 119-124, 20-25 July 2009. In Russian.

[7] V.P. Bobykina, K.V. Karmanov, "To Geoecology of the Kaliningrad Region's Coast (according to the monitoring results)", *Transactions of the Kaliningrad State Technical University*, No 35, pp. 44-54, 2014. In Russian.

[8] Tortuosity in 2D. *Tortuosity: article in Wikipedia*. [https://en.wikipedia.org/wiki/Tortuosity] 23.05.2016.

CHANGES IN BACKGROUND CONCENTRATIONS OF METALS IN THE SEDIMENTS OF MARSH-LAGOON LANDSCAPES OF THE WESTERN CASPIAN

Maria Kasatenkova, Moscow State University, Russia
Nicolay Kasimov, Moscow State University, Russia
Mihail Lychagin, Moscow State University, Russia

kasatenkova2010@yandex.ru

The last 1978-1995 transgression of the Caspian Sea caused the development of marsh-lagoon system along the Western Caspian seashore. Due to salt marshes are very vulnerable to sea-level fluctuations, complex and dynamic system, they may be considered as a regional model of rapid environmental transformation.

Changing conditions of migration in the soils of marsh-lagoon landscapes during the sea-level rise influenced on the migration of elements of variable valency, primarily Fe and Mn, but also Zn, Cu, Pb, Ni, Co, leading to their mobilization in slightly alkaline and neutral reducing conditions and subsequent deposition on the geochemical barriers.

That led to the emergence of landscape-geochemical anomalies of Fe and heavy metals in the soils of salt marshes with a characteristic time of formation of any persistent anomalies during 5-10 years.

Key words: Caspian Sea, fluctuations of the sea level, salt marshes, regional changes, landscape-geochemical anomalies, transport and accumulation of metals

I. INTRODUCTION

Recent climate changes have had widespread impacts on human and natural systems [9]. The rise of the world ocean's level is among the most important present-day environmental problem. Many coastal areas experience inundation and waterlogging by sea-water. Global mean sea level rose by 0.19 m over the period 1901 to 2010. The rate of sea level rise since the mid-19th century has been larger than the mean rate during the previous two millennia [9].

Coastal areas are very dynamic regions and they are of immense ecological and economic importance. Coastal wetlands, which are comprised of marshes, swamps, mangroves and other coastal plant communities, provide a large number of goods and services . Nowadays they face a number of hazards including rise in sea-level, increased atmospheric concentration of carbon dioxide, rise in air and water temperature, and changes in the frequency and the intensity of precipitation and storm patterns [2]. Sea-level rise can disrupt wetlands in three significant ways: inundation, erosion, and salt water intrusion. By the 2080s, sea-level rise could cause the loss of up to 22% of the world's coastal wetlands [18]. The threat posed by the rise in sea level has received increased attention [2, 3,18, 19].

The Caspian Sea is well known for large and rapid sea-level fluctuations. The most recent cycle lasted only 65 years [10,13]. Sea-level fell by over 3 m between 1929 and 1977 and rose again

by 2,4 m until 1995, when it started falling again [5,21]. Today it is stable at – 27.74 m below global sea-level [4]. The new method of forecasting the Caspian sea level shows, that in the coming years the sea level will rise again [17].

The Caspian Sea shores are perhaps the best sites to study the effect of sea-level changes on coasts [6,8,10, 11,12,15]. Understanding the consequences of Caspian sea-level changes is very important as they threat large areas with inundation, pollution and environmental changes [11,22].

Conducted researches have shown that different types of the Caspian Sea shores had various reactions on sea-level changes [6,8,11,12]. During transgression the intensity of coastal processes depend on the steepness of the coastal slope. The most dramatic consequences of the influence of rapid transgression were experienced by accumulative coasts [8].

Along accumulative shores transgression increases the geomorphological, lithological, soil, biotic, as well as geochemical diversity of the coastal landscapes. This is caused by the formation and landwards movement of a barrier-lagoon system, with a corresponding rise of the groundwater table, and also simultaneous vigorous development of vegetation in newly-formed hydromorphic and semi-hydromorphic areas.

The formation of the barrier-lagoon system during the last transgressive coastal cycle is typically for different regions of the Caspian shore [8,14]. Lagoon coasts occupy about 32% of the world ocean accumulative shores [20]. The domination of accumulative coasts reflects the eustatic sea-level rise in postglacial period [16]. Thus, the evolution of the Caspian coasts under the sea-level changes serves as natural model that can be used for understanding the general features of development of the world ocean coasts. Our local study of geochemical changes of the Caspian marsh-lagoon landscapes describes the regional environmental changes of the coastal zone.

The most contrasting landscape-geochemical changes of the coastal zone of the Caspian sea occurred within the lagoon shores, where a marine terrace has a small width (a few hundred meters), being replaced New-Caspian Holocene terrace outside the zone of influence of the modern sea level fluctuations. Within the modern marine terraces during transgression occurred contrasting changes in alkaline-acid and redox conditions and salinity of soils [6,11,12]. The fluctuation of the sea-level caused changes of the natural background concentrations of chemical elements in the coastal soils. The studying of such natural changes of the local geochemical background may help correctly to estimate the real level of the human-induced contamination of the coastal zone.

Our previous investigation showed that during the transgressive phase many heavy metals (Cu, Co, Zn, Ni, Cr, Fe, Pb) accumulated at geochemical barriers in the marsh-lagoon landscapes of Central Dagestan [11,12]. Their concentrations in the marsh zone became higher than in the soils of the adjoining territory. So the natural background concentrations of the heavy metals in the coastal soils were lower during the regression period and it has increased after the beginning of the Caspian sea-level rise.

In this paper we describe the changes of background concentrations of metals in the sediments of marsh-lagoon landscapes along the western coast of the Caspian sea. Our study shows that the intensity of geochemical processes, accumulation and transport of metals in soils and bottom sediments of marsh-lagoon landscapes has differences in the variety of key sites.

II. MATERIALS AND METHODS

Geochemical studies of marsh-lagoon landscapes were conducted on the 4 sites located on the west coast of the Caspian Sea. The first site is located on the coastal plain of Dagestan, the second - the north shore of the Apsheron peninsula, the third site was on Kur-Araz lowland and the fourth site - Lenkoran lowland. Landscape-geochemical catenas, crossed the main elements of the relief from the New-Caspian terrace through modern terrace to the beach, were studied using the profiling method.

Field works on the first site were conducted near the Turali research and training station, which belongs to the Moscow State University and is located 30 km to the south of Makhachkala, the capital of Dagestan. The investigations were carried out in 1995-1996 when the sea-level rose [6,11,12] and they were continued in 2001-2005 when it became stable.

The *Turali key site* stretches from the waterline across a modern constructional plain to the scarp of the New-Caspian Holocene terrace. The New-Caspian terrace is separated from the modern terrace by a relatively low scarp (up to 2 m high). The level of the terrace is 3.5 m higher than the sea level now.

The modern constructional plain varies in width from 100 to 500 m; a series of low bars of 1929, 1941, and 1956 can be distinguished within this plain. They were formed during different stages of the Caspian Sea retreating that started in 1929 (when the waterline was at 25.5 m below sea level) and continued until 1978. From 1978 till 1995 a considerable part of the 1956 terrace was inundated. At the present time, this part is occupied by 0.8-1.0 m deep and several hundreds of meters wide lagoon separated from the sea by a modern barrier beach with a height of 1.0-1.2 m and a width of 10-30 m.

The field work was carried out at a cross-section (150×400 m) stretched from the New-Caspian terrace to the sea shore through the modern strand flat. The landscape-geochemical, geomorphological, soil and geobotanical investigations were fulfilled at four parallel transects (T, 2D, 2N, 2M) located across the coastal plain (perpendicular to the shoreline).

The main transect is “T”. The study of soil pits along this transect was carried out in 1995-1996 and 2001-2005. During the fieldworks about 500 soil samples, 100 samples of bottom sediments, 100 samples of natural waters were collected.

The other key sites along the western coast of the Caspian Sea have been studied once in 1999.

The *Apsheron key site* is located near Gaia village that is 2 km to the north-north-west from the port of Apsheron. The main transect here is “Ar” (7 soil profiles), crossing the main forms of relief from the edge of the sea of modern marine terrace to the New-Caspian terrace at a distance of about 300 m.

The *Kura key site* is located on the left bank of the Kura river, 8 km from its bed, and 5 km to the north of the Bund village. Landscape and geochemical studies were conducted on the profile “K” (7 soil profiles), that intersects a system of "modern barrier beach - coastal lagoon".

The *Lenkoran key site* is located 5 km to the north of the city of Lankaran near the village Olkhovka. The length of the profile L (13 soil profiles) is about 700 meters. It crosses the main elements of relief: New-Caspian terrace - modern constructional plain - lagoon - modern barrier beach.

During the fieldworks along the Azerbaijani coast of the Caspian Sea about 160 soil samples and 24 samples of bottom sediments were collected.

The most important physical and chemical parameters of surface and ground waters and of each selected soil horizons were defined immediately at the sampling points: pH, Eh, total dissolved salts (TDS), the sodium content. The measurements were made with the help of portable devices (HANNA Instruments, Italy), providing the automatic temperature corrections of parameters. For bottom sediments and soil horizons below the ground water table the measurements were done directly and under their natural moisture. For determination of physical-chemical parameters in the soil horizons above the groundwater table, distilled water was added to each soil sample with 1:1 ratio, the mixture was stirred by plastic stick, and measurements were made in the obtained suspension.

The bulk content of chemical elements was determined by quantitative spectral method in Bronnitskaya geological and geochemical expedition.

The cation content analysis of water samples and mobile forms of chemical elements in soils were done by the atomic-absorption method using the spectrophotometer Hitachi 180 (Japan). The content of sodium, potassium, calcium, and manganese were defined without background correction, and the content of Fe, Mn, Ni, Cr, Co, Zn, Pb, Cd, Mo were defined with correction based on the Zeeman effect. For analysis of mobile forms of elements in soils and bottom sediments 1N (2N) HCl was used as the extraction agent. Water-soluble, exchangeable and amorphous forms of elements passes are extracted in this way, and also, in part, organic-mineral connections.

III. RESULTS AND DISCUSSION

Background content of trace elements in the beach sediments

Average contents of trace elements in the beach sediments change significantly along the coastal zone of the Caspian sea. The coast of Azerbaijan is characterized by a high geochemical background in comparison with the Russian coast of the Caspian sea (Table 1).

Minimal values of elements are observed in the beach sediments of the Turali key site [1], that folded by the material of Sulak river, with the participation of scattered Terek material (hornblende, pyroxene, mica).

The deposits of the modern barrier beach of the Turali site (Fig.1) are depleted in most elements in comparison to Clark [24], except for Sr that is participating in the evaporatortive concentration in the steppe and desert landscapes.

When moving to the south in areas of Apsheron and Kura there is a slight increase in the content of chemical elements, which is associated with erosion of the deluvial sediments of the Caucasus mountains with a predominance of augite, epidote, micas, pyroxenes, in co-organizing the contents of Sr, Pb, Co, Cu and Ni exceed the Clark values.

The contents of almost all trace elements (except Sr) show the maximal values in the beach sediments of Lankaran key site, due to their high content in mafic minerals (augite and titan-augite, ilmenite, magnetite, etc.) in the deluvial sediments of the Talish mountains [1].

Table 1. Average contents of trace elements in the beach sediments of West coast of the Caspian sea (mg/kg)

Key site (n-number of samples)		*Fe*	*V*	*Cr*	*Co*	*Ni*	*Cu*	*Zn*	*As*	*Pb*	*Sr*
Turali (6)	*1**	5895	*13,9*	*21,9*	*3,0*	*5,6*	*5,8*	*18,8*	--	*7,5*	*1159*
	2	1382	--	0,7	0,5	0,3	1,1	4,6	--	2,6	225
Apsheron (3)	*1*	*27000*	*22,9*	*55,3*	*31,6*	*39,7*	*64,9*	*48,9*	*9,3*	*24,8*	*838,7*
	2	5527	--	1,3	3,1	5,3	0,9	15,1	--	4,6	351
Kura (2)	*1*	*33000*	*37,9*	*73,2*	*33,3*	*54,5*	*84,7*	*73,2*	*15,1*	*62,0*	*1472,8*
	2	*6176*	--	*3,2*	*4,4*	*9,3*	*6,1*	*15,8*	--	*4,2*	*436*
Lenkoran (3)	*1*	*80000*	*205,9*	*414,4*	*76,2*	*102,6*	*117,7*	*90,4*	*13,0*	*55,3*	*763,4*
	2	*19670*	--	*8,1*	*7,0*	*28,1*	*32,0*	*61,3*	--	*11,2*	*96*
[1] Vinogradov, 1962	*1*	*46500*	*90*	*83*	*18*	*58*	*47*	*83*	*1,7*	*16*	*340*
[2]Turekian, Wedepohl, (1961)	*1*	*9800*	*20*	*35*	*0,3*	*2*	*X*	*16*	*1*	*7*	*20*

**1-bulk content, 2- mobile forms (2нHCl).*

[1] – Clark of the element in the earth's crust; [2]- the average content of chemical elements in sandstones.

The beach sediments of Turali key site are depleted in Fe, V and Cr in comparison with the average content of chemical elements in sandstones [23]. The contents of Co, Ni, Zn, Pb, Sr are higher than the average content in the sandstones. In the beach sediments of other key sites the background content of elements are above the average contents in the sandstones, while the Sr content is more in 38-74 times, Ni – 20-51 times, and Co – 100 - 250 times.

Thus, the average contents of most trace elements in the beach sediments of the coastal zone generally increase in the direction from the North to the South. The high content of Sr in the sediments of Turali and Kura key sites is due to the evaporative concentration and a large proportion of shell detritus. Sometimes it exceeds 1100 mg/kg, which is 3-4 times higher than the Clark value and its content in coastal sediments of the Lankaran key site is only 763,4 mg/kg, which is associated with a predominance of pebble material.

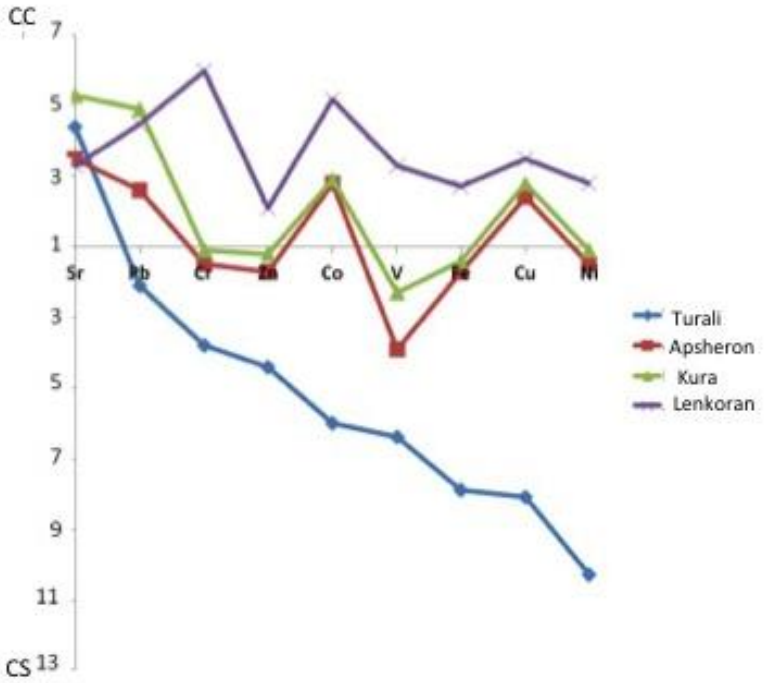

Fig. 3.4 Geochemical spectra of beach sediments along the Western coast of the Caspian sea (CC- Clark of concentration; CS - Clark of scattering)

Oxidative alkaline environment in beach sediments determines the low mobility of many cationogenic elements in soils and waters (Fig.2).

The portion of mobile forms of chemical elements does not exceed 40% in these sediments in different parts of the west coast. The portion of mobile forms of Zn (up to 67%), Cu and Ni (27 %) increases in the sediments of the Lenkoran lowland that is associated apparently with the increase in the proportion of organo-mineral complexes of these elements in the soils of variable-humid subtropics.

Thus, the migration and accumulation of chemical elements in the coastal zone occur in different geochemical background, which is determined by lithological and geochemical specialization of supply provinces.

Radial geochemical differentiation of coastal landscapes

Sea-level rise caused the transformation of migration flows. Landscape-geochemical processes in the marsh-lagoon landscapes led to the redistribution of chemical elements in coastal soils with the accumulation of certain associations of elements on geochemical barriers.

The geochemical transformation of coastal soils is related to a complex combination of landscape-geochemical processes, such as sulfidogenesis, gleyzation, iron accumulation (ferrugination), accumulation of humus and peat, halogenesis, and changes in redox conditions [11,12].

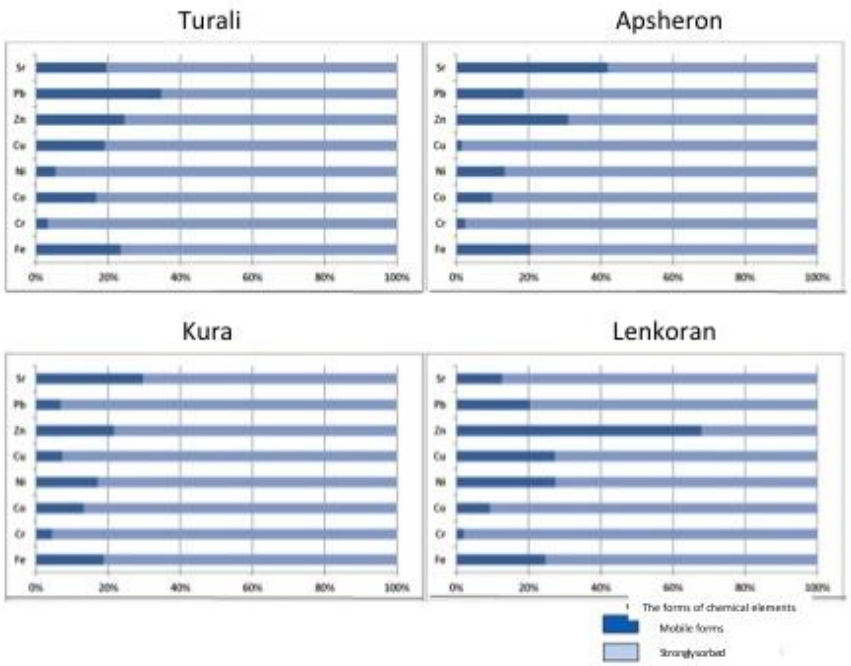

Fig. 2. The forms of chemical elements in the beach sediments of the west coast of the Caspian sea

A set of radial geochemical barriers, as well as their capacity differ in different parts of the western coast of the Caspian sea, which is associated with the heterogeneity of the migration conditions due to lithological and granulometric composition of rocks, as well as differences in bioclimatic conditions.

The main geochemical barriers in coastal landscapes with the accumulation of heavy metals are: oxygen − Fe, Mn, Co, biogeochemical − Zn, Cu, Cr, Ni, Cr, Cd, and sulfide − Fe, Mn, Zn, Cu, Co, Mo. The intensity of the oxygen barrier (accumulation ratio Fe) decreases along the west coast from north to south. Biogeochemical barriers most pronounced in soils of the Lenkoran, due to the great biological productivity of plant communities and nutrient accumulation of trace elements. The degree of appearance of sulfide barrier is the greatest in marsh soils and bottom sediments of the lagoon area of the Turali key site, the lowest –in layered marsh soils of Kura key site.

Gley, alkaline, acidic and evaporative barriers are common locally in meadow, marsh and saline landscapes. On Turali key site the contents of Mo and Cu increase on the gley barrier; of Mn, Co, Ni - on alkaline; of Mo – on acidic; of Sr - on evaporative.

Lateral differentiation of coastal landscapes

Lateral differentiation of marsh-lagoon landscapes of the Caspian sea is determined by hydrogeochemical features of groundwater flow with the chloride-sulphate-sodium composition.

There are two zones of the lateral differentiation of chemical elements within modern marine terrace. In meadow landscapes with poorly developed hydromorphic soils as the result of nutrient absorption, the mobility of cationogenic and anionic elements increases. In alkaline conditions the cationogenic elements don’t migrate, so the lateral migration which is typical only for anionic elements.

Active migration of anionic elements promotes the soda geochemical environment in the soil on the coastal shafts. The contrasting geochemical anomalies of Mo and Cr form in the wet-meadow and marsh soils.

The transformation of redox and alkali-acid conditions leads to a redistribution of cationogenic elements in the marsh zone. The mobility of Fe, Mn and Co increases in the reducing conditions that lead to their migration and accumulation on the geochemical barriers with the formation of the geochemical anomalies of these elements.

Thus, the two paragenetic associations of migration elements distinguish in the coastal landscapes, the first – the mobile forms of anionic elements (Mo and Cr) and the second – cationogenic elements (Fe, Mn, Co, Zn, Cu, Ni).

The contrast of lateral differentiation of mobile forms of Fe, Mn, Zn, Cu, Ni, Cr and Pb in soils and sediments of coastal landscapes is higher on the Lenkoran key site than in areas of Apsheron and Kura.

On the Lenkoran key site in subordinate positions of the marsh-lagoon landscapes the geochemical anomalies of Mn (up to 3.6 L), Pb and Ni (L to 3.1) are formed. In organogenic horizons of wet-meadow and marsh soils the contents of Cu, Ni, Zn increase because of biogenic accumulation. Accumulation of heavy metals and Fe also occurs in sulfide and gley barriers in marsh zone.

The coefficients of the lateral differentiation of Fe, Cr, Cu, Ni and Zn increases to 2-2,5 in the soils and sediments of the marsh zone in the Apsheron and Kura key sites.

IV. Conclusion

Geochemical features of migration and concentration of mobile forms of heavy metals and Fe in the coastal landscapes of the western Caspian region have much in common, due to the uniformity of the geochemical conditions of migration and the similar system of geochemical barriers formed in subordinate landscapes. The intensity of mobilization of cationogenic elements is determined by nutrient absorption, especially in Turali and Lenkoran key sites.

The changing conditions of migration in the marsh zone under the sea level rise significantly affected the migration of elements with variable valence, primarily Fe and Mn, but also Zn, Cu, Pb, Ni, Co, leading to their mobilization in slightly alkaline and neutral reducing conditions and subsequent deposition on a number of geochemical barriers. The geochemical anomalies of several elements formed in the marsh zone as the result of their radial and lateral migration. So, in bottom sediments of lagoons the contents of the Fe and Co increased from 1.5 times on the Lenkoran key site up to 4-5 times on the Turali key site; the content of Zn is more average in 1.5 times on all sites, and the content of Cu increased from 1.5 times at the site of Turali up to 5 times on the Apsheron key site.

Due to the sea level rise the geochemical structure of the coastal area complicated because of the formation of the marsh-lagoon landscapes that led to the emergence of landscape-geochemical anomalies of Fe and heavy metals in the soils of the marsh zone with a characteristic time of formation of any persistent anomalies of approximately 5-10 years.

V. Acknowledgements

This research was performed within the framework of the international INTAS project 94-3382 ("Geochemical changes in soils and bottom deposits caused by rapid rise in the Caspian Sea level"), the NWO project 047-009-003 ("Holocene sea-level change and mollusc biodiversity in the Caspian Sea: a proxy for the North Atlantic Oscillation"), and the projects of the Russian Foundation for Basic Research (№ 97-05-65731, 03-05-643060, 04-05-65073 and others).

VI. References

[1] S. A. Azhibekov, A. E. Bagirov, "*Geology and volcanism of the Talysh."* Baku: ELM, 1979, 245 p.

[2] D. Alongi, "Mangrove Forests: Resiliance, Protection from tsunamis and responses to global climate change", *Estuarine, Coastal and Shelf Science*, 76, 2008, pp.1-13.

[3] B. Blankenspoor, S. Dasgupta, B. Laplante, "Sea-level rise and coastal wetlands:impacts and costs", *Policy research working paper 6277*, 2012, 25 pp.

[4] "*Bulletin of the hydrometcentre of Russia*', № 36 from 28 April 2015.

[5] A. Cazenave, P. Bonnefond, K. Dominh, P. Schaeffer, "Caspian sea-level from Topex-Poseidon altimetry: level now falling", *Geophysical Research Letter* 24(8), 1997, pp.881-884.

[6] A.N. Gennadiev, N.S. Kasimov, D.L. Golovanov, M.Yu. Lychagin, T.A. Puzanova, "Soil evolution in the coastal zone under rapid changes in the Caspian sea level", *Eurasian soil science*, 31 (9), 1998, pp.929-936.

[7] "Geochemical changes in soils and sediments upon rapid rise of the Caspian sea level, and their environmental consequences", *INTAS project 94-3382*, scientific report, part 1, 1997, 200 p.

[8] E.I. Ignatov, P.A. Kaplin, S.A. Lukyanova, G.D. Solovyova, "Influence the recent transgression of the Caspian Sea on its coastal dynamics", *Journal of Coastal research*, 9(1), 1993, pp.104-111.

[9] "*Climate Change 2014: Synthesis Report."* Contribution of Working Groups I, II and III to the Fifth Assessment Report of the Intergovernmental Panel on Climate Change. Core Writing Team, R.K. Pachauri and L.A. Meyer (eds.). IPCC, Geneva, Switzerland, 2014, 151 pp.

[10] P.A. Kaplin, A.O. Selivanov. "Recent coastal evolution of the Caspian sea as a natural model for coastal responses to the possible acceleration of the global sea-level rise.", *Marine Geology*, 124, 1995,pp. 161-175.

[11] N.S.Kasimov, A.N.Gennadiev, M.Y. Lychagin, S.B. Kroonenberg, V.V. Kucheryaeva, "Geochemical transfomation of coastal soils in Central Dagestan upon the rise in the level of the Caspian Sea", *Eurasian soil science*, 33(1), 2000, pp.11-22.

[12] N.S. Kasimov, A.N. Gennadiev, M.S. Kasatenkova, M.Y.Lychagin, S.B. Kroonenberg, "Geochemical changes of the Caspian salt marshes under conditions of sea-level fluctuations", *Earth Science Research*, v. 1 (2), 2012, pp. 262-278.

[13] R.K. Klige, M.S. Myagkov, "Changes in the water regime of the Caspian sea", *Geological Journal*, 27(3),1992, pp.299-307.

[14] V.I. Kravtsova, S.A. Lukyanova, "Transgressive changes of the Russian cost of the Caspian sea', *Geomorphology*, 2,1997, pp.35-46.

[15] S.B. Kroonenberg, E.N. Baduykova, J.E.A. Storms, E.I. Ignatov, N.S. Kasimov, "A full sea-level cycle in 65 years: barrier dynamics along Caspian shores", *Sedimentary Geology*, 134, 2000, pp.257-274.

[16] O.K. Leont'ev, S.A. Luk'yanova, L.G. Nikiforov, G.D. Solov'eva, N.A. Holodilin, "*Map of type of the World Ocean coasts. Relief and landscapes*",1977, pp. 116-126.

[17] S.K. Monahov, I.N. Volkov, A.V. Suslov, "New method for prediction of Caspian sea level for a period of one year to ten years", *Conf. "Hydrometeorological and environmental security of marine activity"*, (16 – 17 October 2015, Astrakhan, Russian Federation). Astrakhan, Publisher, Sorokin Roman Vasilievich, 2015, pp.24-26.

[18] R.J. Nicholls, F.J.M. Hoozemans, M. Marchand. "Increasing flood risk and wetland losses due to global sea-level rise: Regional and global analyses", *Global Environmental Change*, 9, 1999, S69-S87.

[19] R. J. Nicholls, "Coastal flooding and wetland loss in the 21st century: Changes under the SRES climate and socio-economic scenarios", *Global Environmental Change*, 14, 2004, pp.69-86.

[20] "*Recent global changes of the natural environment*", v.2, Moscow, Scientific world, 2006.

[21] G.I. Rychagov, "The sea-level regime of the Caspian sea during the last 10,000 years", *Bull. Moscow State Univ.*, Ser. 5, 2, 1993, pp. 38-49

[22] "*TED Caspia. Main conclusions of the Technical Economical Report*", Moscow, 2000.

[23] K.K. Turekian, K.H. Wedepohl, "Distribution of the Elements in some major units of the Earth's crust", *Geological Society of America, Bulletin*, 72, 1961, pp.175-192.

[24] A.P. Vinogradov, "Average content of chemical elements in the main types of igneous rocks of the Earth Crust", *Geochimiya* 7, 1962, pp. 555-572.

SPECIALIZED OCEANOGRAPHIC DATABASE FOR INFORMATION SUPPORT OF THE BLACK SEA COASTAL ZONE STUDY

Alexey Khaliulin, Marine Hydrophysical Institute of RAS, Russia
Andrey Ingerov, Marine Hydrophysical Institute of RAS, Russia
Elena Zhuk, Marine Hydrophysical Institute of RAS, Russia
Eugeny Godin, Marine Hydrophysical Institute RAS, Russia
Elena Isaeva, Marine Hydrophysical Institute of RAS, Russia
Igor Podymov, Southern Branch of Shirshov Institute of Oceanology of RAS, Russia

khaliulin@yahoo.com

The information resources of the Federal State Budget Scientific Institution "Marine Hydrophysical Institute of RAS" (FSBSI MHI) oceanographic data bank (MHI BOD), which contains about 115,000 oceanographic and more than 27,000 hydrochemical stations accomplished in the Black Sea coastal zone, as well as experience accumulated while providing information support of the coastal zone research, main directions of activities, and short-term plans are considered.

Key words: *Black sea, coastal zone, databases and data banks, oceanographic data, quality control*

I. INTRODUCTION

The coastal zone of seas and oceans has been exploited by mankind for a long time. The state of the coastal zone environment and processes taking place here have a significant influence on human being and marine economy of seaside countries. Solving problems of the integrated coastal zone management, study and analysis of the processes determining its evolution, and forecast of possible changes need reliable information support. All this predetermines the most important role of oceanographic data and knowledge while conducting ecological and oceanographic research, project exploration in the coastal zone, working out different recommendations for its sustainable use and for making managerial decisions.

A significant experience of creating oceanographic databases and banks, maps, atlases, geoinformation systems, and other products aimed at providing information support of oceanographic research and practice, including those in the coastal zone, was accumulated in the Department of Marine Information Systems and Technologies (MIST) of FSBSI MHI for its more than twenty years' history, while conducting national and international projects.

At present, these activities, in cooperation with other scientific institutions, are carried out in the following main directions:

- working out and forming specialized databases and banks;
- improving data quality check systems;

– creating maps and atlases for different marine environmental parameters;
– working out and creating information systems;
– designing and creating web-sites.

Let us discuss in detail some of the directions mentioned above.

II. WORKING OUT AND FORMING DATABASES

MHI BOD includes oceanographic and meteorological data obtained in cruises of research vessels of MHI and other institutions in the Black, Azov, and Mediterranean seas and also in the Atlantic, Indian, and Pacific oceans. "The Black Sea" specialized database has a special position in the BOD and contains data on more than 160,000 oceanographic (since 1890) and 43,000 hydrochemical (since 1923) stations made by research vessels of Russia, Ukraine, Bulgaria, Turkey, USA, France, Romania, Denmark, and other states, as well as data on a number of other parameters [1].

It should be noticed that a considerable part of the Black sea oceanographic and hydrochemical stations was accomplished in the coastal zone (Table 1) and most of them were in the coastal zone of Russia and Ukraine (Table 2, Fig.1 and 2).

Table 1. The number of hydrological and hydrochemical stations in the Black sea

Parameters	Black sea	Isobath, m				
		20	50	100	150	200
	Number of stations					
Hydrology	160085	53253	91336	108309	112886	114972
Hydrochemistry	43231	10219	18106	25161	26417	27117

Table 2. The number of hydrological and hydrochemical stations in the Black sea coastal zone of Russia and Ukraine

Parameters	Isobath, m				
	20	50	100	150	200
	Number of stations				
Hydrology	48255	81079	92096	95819	97419
Hydrochemistry	8389	13950	18187	18988	19461

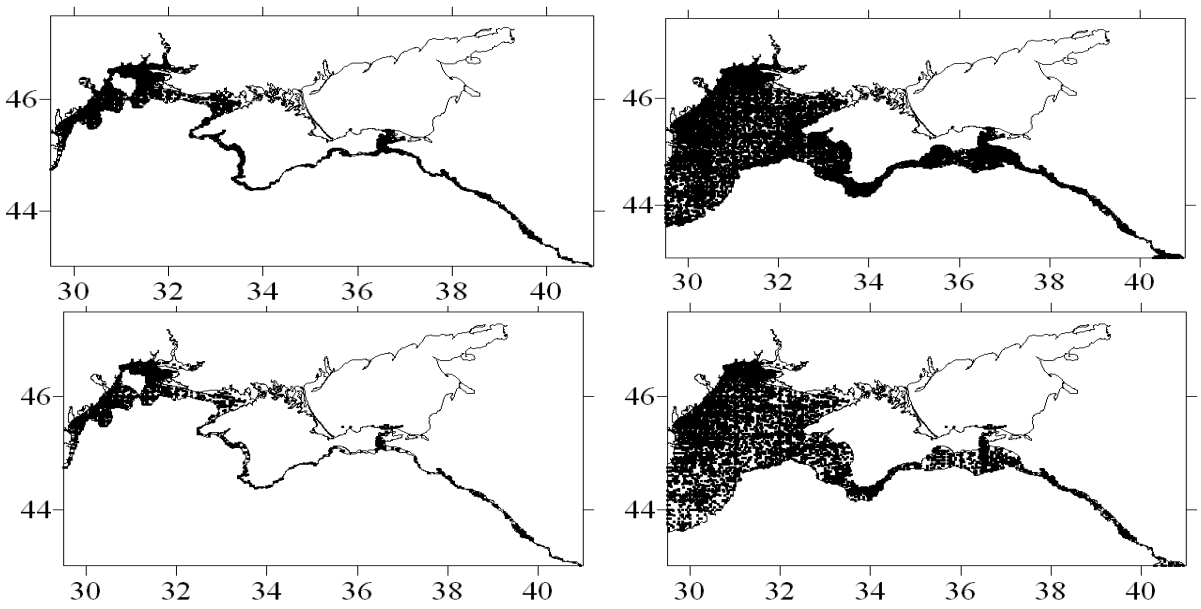

Fig.1. Distribution of hydrological stations in the Black sea coastal zone of Russia and Ukraine: up to 20 m isobath (a), up to 200 m isobath (b) and hydrochemical stations up to 20 m isobath (c), up to 200 m isobath (d).

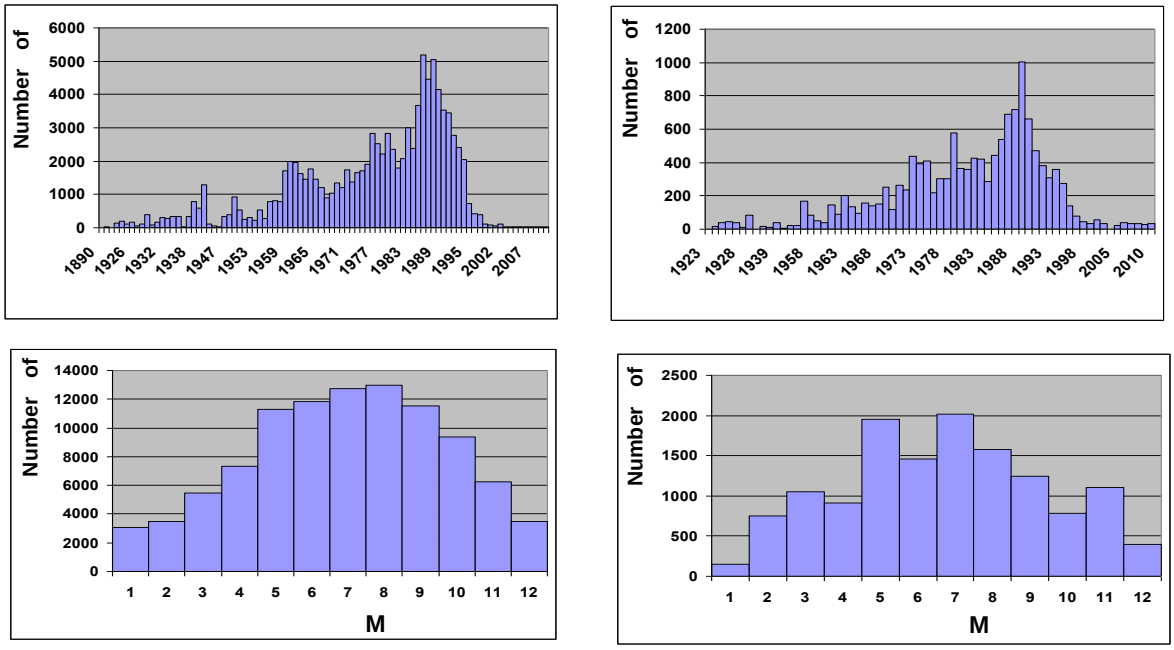

Fig. 2. Distribution of hydrological stations on years (a) and on months (c) and hydrochemical stations on years (b) and on months (d) in the Black sea coastal zone of Russia and Ukraine.

At present, MHI BOD receives data obtained with the use of such equipment for oceanographic observation as drifters and towed devices of different types. Depending on the type, the devices provide obtaining such data as seawater temperature distribution in depth and on the surface, air temperature and atmospheric pressure, currents, certain hydrochemical parameters, etc.

These data are contained in special arrays in MHI BOD. Table 3 gives information on their number for the Black sea coastal zone.

Table 3. Number of measurements accomplished using towed devices and drifters in the Black sea coastal zone

Water area	Device	Isobath, m				
		20	50	100	150	200
		Number of measurements				
Black sea coastal zone	Thermistor chain drifter	1015	3049	13462	14466	14940
	Drifter	4085	11932	35857	41015	43338
	Towed	3241	5094	7064	7514	7664
Coastal zone of Russia and Ukraine	Thermistor chain drifter	0	523	4647	5232	5453
	Drifter	931	5296	15420	18906	20323
	Towed	3241	5094	7064	7514	7664

MHI BOD also stores data obtained at the oceanographic platform in the village of Katsiveli (meteorological measurements, waves, water temperature, salinity, currents, hydrochemistry, etc.) and at the Golitsyn platform (meteorological measurements, water temperature).

Depending on the problems under solution, the specialized databases for the coastal zone study can contain hydrological data on temperature and salinity, hydrochemical data, including alkalinity, pH, oxygen, silicates, nitrates, nitrites, phosphates, hydrogen sulphide (about 20 parameters in total), data on hydrooptics, waves, currents, sea level, and other parameters. The databases can be created both for the entire coastal zone and for its significant parts or certain water areas. As examples one can take the prepared in MHI BOD specialized databases on the Black sea coastal zone of Russia and Ukraine, the databases intended to study the hydrochemical regime of Yalta bay, environmental state of Sevastopol bay, coastal waters of the Heracles peninsula, etc.

III. DATA QUALITY CHECK

While creating databases, the MHI BOD specialists pay great attention to data and metadata quality. The work aimed at developing and improving data quality check systems has been conducted at the MIST department for a long time [2]. The results of the activities were acknowledged both at the national and international levels.

Taking into account the coastline proximity, complicated interaction of various factors effecting generation of hydrophysical and hydrochemical fields in the coastal zone, the data quality check becomes of particular importance. To solve the posed question, the following step-by-step procedure is realized in MHI BOD:

1) data import and conversion into the necessary format;
2) metadata check:
   - location check;
   - date/time (including velocity and chronology) check;
   - sea depth/last sounding value check;

3) automated quality flags setting.

Some examples of metadata and data errors detected as a result of applying the data quality check procedure while forming a specialized database for information support of the coastal zone research are presented in Fig. 3.

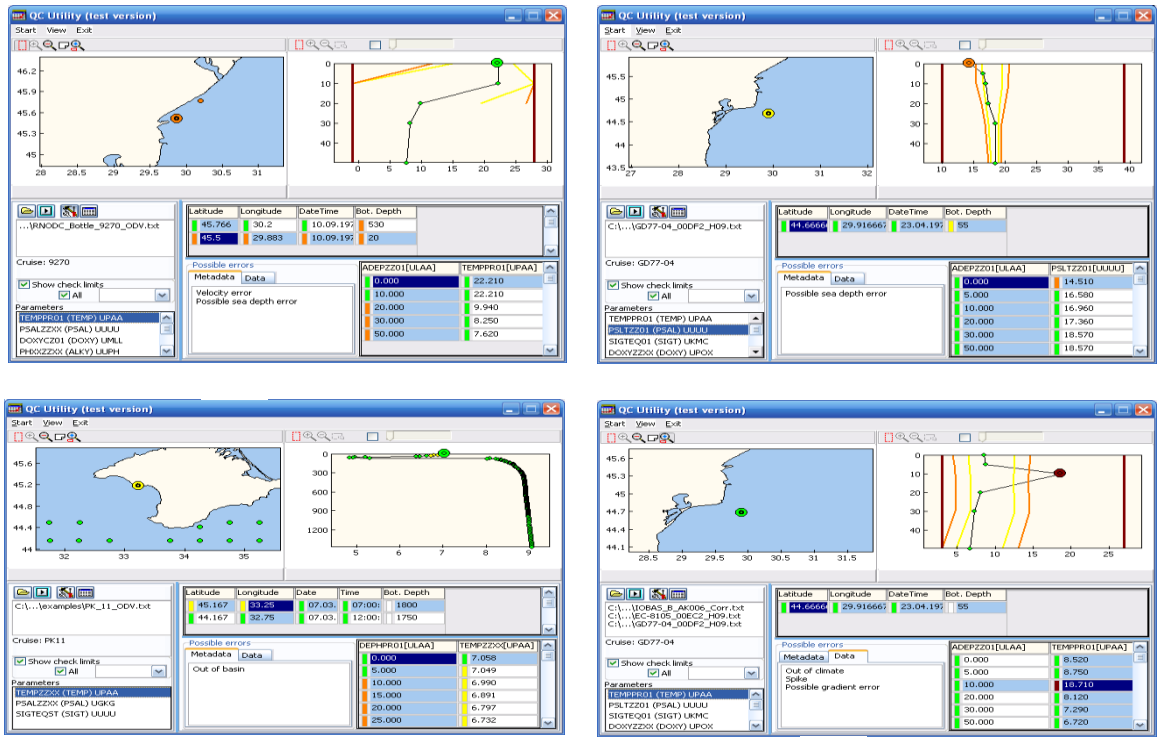

Fig. 3. Data quality check procedure. Examples of metadata and data errors: ship velocity error (a), depth error (b), station location error (c), data error – spike (d).

IV. EXAMPLES OF THE DATABASE USE

The database is in active use while studying natural processes and environmental state of certain water areas in the framework of both national and international projects. Applying this database in realization of the PEEX "Pan-Eurasian Experiment" project can serve as an example [3].

The successful realization of the PEEX "Pan-Eurasian Experiment" Program is impossible without reliable information support both on the global and regional levels.

MHI accumulated a considerable experience in creating data banks and specialized databases and developing on this information basis a wide range of differently targeted information products.

Due to the unique location of the Crimean peninsula, the information on the state of individual environmental components (in particular, the atmosphere), obtained there, is undoubtedly valuable for successful realization of the project tasks.

Creating, in the framework of the PEEX Project, the proper regional specialized databases and software to provide their management and data quality control is of current importance. At the first stage, it seems to be expedient to include into the database the information obtained in a number of observation points located both in the sea-land interactive zone (Golitsyn platform,

Sevastopol bay, the oceanographic platform and the set of sensors in the village of Katsiveli, Tuzla spit, and the coastal area of Lubimovka village) and in the central part of the Crimean peninsula (e.g., Simferopol).

It is also planned to include drifter and solar radiation data into the database. The location of observation points and drifter paths in the Black Sea are shown in Fig. 4.

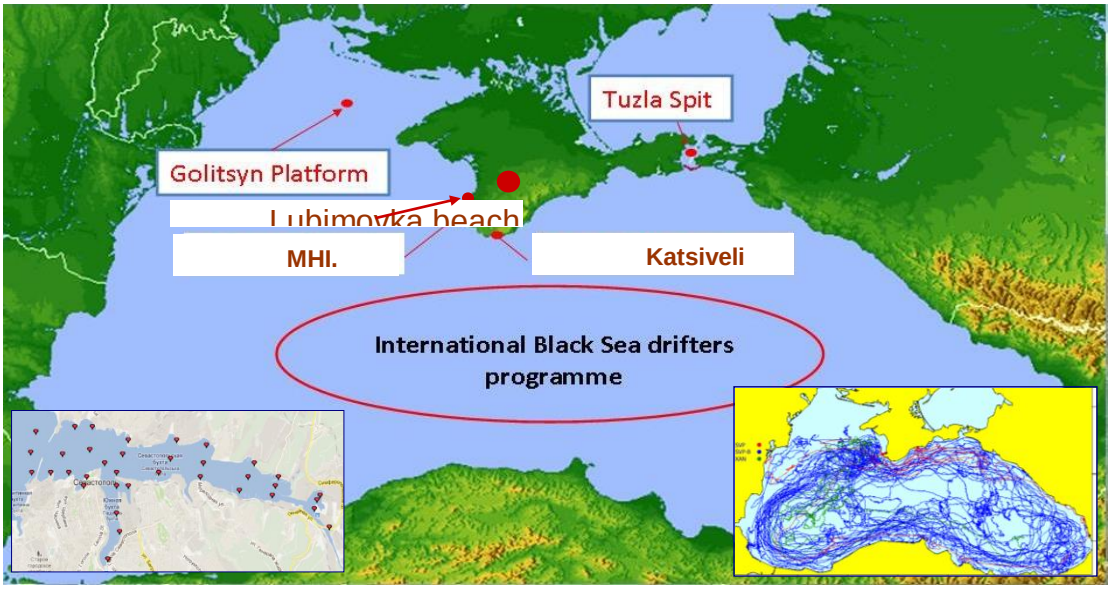

Fig. 4. Location of observation points. The insets show the location of observation points in Sevastopol bay and drifter paths in the Black Sea.

The database creation will allow more proper solving tasks of modeling in the sea-land interface area, as well as estimating the situation in the area of the Crimean peninsula and obtaining integrated characteristics of the environment.

The list of the parameters to be included into the database is shown in Table 4.

Table 4. The parameters to be included into the database

Station	Coordinates	Observation Parameters	Equipment	Period
Golitsyn Platform	45°43'23"N 31°50'16"E	Wind and Wave Parameters	Hydrometeorological complex KCTD + waverecorder	1995-2005
EB MHI NAS Ukraine	44°23'42"N 33°58'28"E	Wind and Wave Parameters	Hydrometeorological complex KCTD + waverecorder	2003-2014
		Temperature Chain	Temperature Chain	
		Sea Level	MedGLOSS Station	
Tuzla Spit	45°16'13"N 36°32'49"E	Wind and Wave Parameters	Hydrometeorological complex KCTD + waverecorder	2007-2013
MHI NAS Ukraine	44°36'56"N 33°31'1"E	Direct and Scattered Radiation of the Sun	Solar Spectrophotometer CIMEL380N	2006-2014
Drifters	Black Sea	Sea Surface Temperature, Temperature Chain	SVP Drifters with Temperature Chain	1999-2014
Lubimovka beach		Beach characteristics (length of beach, length of coastline, perimeter and area, coastline curvature, height and slope of cliff - average slopes of berm and bench and etc.)		2009-2015
Sevastopol bay		Chemical characteristics (concentration of Oxygen, Nitrates, Nitrites and etc.)	CTD, Laboratory analyze	2006-2014

The work will result in the database and software providing online access for its users.

In future, the database development will allow more proper solving tasks of modeling and estimating the situation in the area of the Crimean peninsula. It is also planned to create GIS of the Crimean region using this database and including regional models of the sea-land interface area.

V. Prospects of the database development

Taking into account the necessity of further improving the information support of research and practice in the coastal zone, perfecting the structure and updating the oceanographic database for the coastal zone seem to be the main tasks for the nearest future. The new data will be obtained as a result of further research accomplished by research vessels and other facilities in the coastal zone including a new hydrophysical polygon at the area of Gelendzhik. The up-to-date research equipment is used at the polygon, such as ADCP bottom stations; AQUALOG diving buoys with a large number of gauges for measuring oceanographic parameters; thermistor chains. Hydrological and hydrochemical surveys are regularly carried out by the research vessel.

VI. Acknowledgment

The research was accomplished under the support of the Russian Science Foundation (RSF grant 14-50-00095).

VII. References

[1] A.Kh. Khaliulin, E.A. Godin, Yu.N. Tokarev, I.V. Mezentseva, and S.S. Smirnov, "Information resources of Crimean oceanological institutions," *Digests Intern. Conf. "Current State and Prospects of Marine Resource Capacity Building in the South of Russia,"* Sevastopol: EKOSI-Gidrofizika, 2014, pp. 170-173 [in Russian].

[2] V.N. Eremeev, A.Kh. Khaliulin, A.V. Ingerov, E.V. Zhuk, E.A. Godin, and T.V. Plastun, "Current state of the oceanographic data bank, MHI NAS of Ukraine: software," *Marine Hydrophysical Journal*, no. 2, pp. 54-66, 2014 [in Russian].

[3] PEEX "Pan-Eurasian Experiment" https://www.atm.helsinki.fi/peex/

[4] V.A. Soloviev, D.A. Shvoev, S.B. Kuklev, O.N. Kukleva, O.I. Podymov, et al., "Subsatellite polygon for studying hydrophysical processes in the Black Sea shelf-slope zone," Izvestiya. Atmospheric and Oceanic Physics, vol.50, no. 1, pp.13–25, 2014 [in Russian].

ACCUMULATION OF PLASTIC FRAGMENTS AND MICROPLASTICS ON THE BEACHES IN THE SOUTH-EAST BALTIC SEA

Lilia Khatmullina, ABIORAS, Russia
Elena Esiukova, ABIORAS, Russia

liliakhatmullina@gmail.com

The sediment sampling from different areas of the beaches in the south-eastern part of the Baltic Sea (in Kaliningrad region) was executed for the purpose of studying the quantitative and qualitative composition of the microplastics particles (range 0.5-5 mm). Preference is given to those beaches that are exposed to maximum anthropogenic pollution. From June, 2015 to January, 2016, there were 14 expeditions along the coastline of the Baltic Sea (in Kaliningrad region) to collect experimental materials. The majority of samples were collected on the most recent flotsam deposited at "wracklines", in the supralittoral zone. The primary examination of those samples revealed the presence of abundant microplastic particles of the required size range (0.5-5 mm). Quantitative distribution of microplastics in beach sediments was obtained in milligrams per gram of sediment and milligrams per m^2: on average 0.05-2.89 (mg per gram of sediment) and 370-7330 (mg per m^2), accordingly.

Key words: microplastics, beach, the Baltic Sea, pollution, wracklines, particles, sample, fraction

I. INTRODUCTION

The sea and ocean waters have accumulated hundreds of thousands of tons of polymer litter (for instance, [1, 2, 3]). But the most dangerous kind of all polymers found in the ocean is microplastics – tiny particles of plastic, less than 5 mm [1, 2, 4]. Microplastics are formed when large man-made plastic objects are broken and degraded under the influence of the sun, waves or other factors. They are also ingredients of personal healthcare and beauty products which contain thousands of microscopic plastic spheres (microbeads) and fibers. An alarming feature of microplastics is the ability to effectively accumulate toxins on the their surface, which in the end get inside fish, sea animals, birds, and further on along the food chain – inside human bodies [1, 4, 5]. Not only does plastic float on the surface once it gets in the water; a large part of it sinks to the sea bed or accumulates on the beaches in the form of microplastics.

Plastic pollution in the Baltic Sea has been accumulating for years and just recently it has become obvious that only multidisciplinary approach (geographical, biological, chemical, etc.) to the issues related to the processes of transformation of properties and propagation of plastic particles will allow the study of physical aspects of the problem.

The aim of our study is to give an initial assessment of the distribution of microplastics on the beaches in the south-eastern part of the Baltic Sea (in Kaliningrad region) to show the qualitative

and quantitative composition of the microplastics as well as accompanying objects (macroplastic, amber, paraffin). During the first stage of the study, samples were selected from different areas at the beaches.

Sampling sites were chosen near the distributed and point sources of plastic pollution. Preference was given to those beaches that are exposed to maximum anthropogenic pollution: areas around the town of Baltiysk, the northern part of the Vistula Spit (near the settlement of Kosa), and the Sambian peninsula coast (settlements of Yantarny, Donskoye, Primorye, Kulikovo, and towns of Svetlogorsk, Pionersky, Zelenogradsk - in the field of active recreation) as well as rather solitary locations of the coast (Fig. 1).

II. MATERIALS AND METHODS

There is no universally agreed definition of microplastic size, but most commonly, microplastics have been defined as synthetic organic polymer particles with a size (or, more specifically, largest dimension) <5 mm [5, 6, 7, 8]. There is little consensus on the lower size boundary [1], but most studies reported main size ranges of microplastics to be 0.5-5 mm [3, 7, 9, 10, 11]. Separation of the particles ranging in size from 0.5 to 5 mm in a special group is not accidental. It is caused by considerable technical difficulties existing in the analysis of particle sizes less than 0.5 mm [7]. In cases where sampling included microplastics, but the upper size limit of the sampled plastics is somewhat above 5 mm (e.g. 10 mm), the term 'small plastic items' is employed. Plastic items larger than 5 mm frequently are designated as macroplastics [8]. But also plastic particles can be classified into "meso plastic particles" (5-25 mm) and "macro plastic particles" (>25 mm) [4]. Particles in the size range 0.5-5 mm were considered as "microplastics" for the purposes of this assessment. We use the term "meso/macro plastic" for particles with a size greater than 5 mm.

First stage of the work was aimed at sediment sampling from different areas of the beaches in the south-eastern part of the Baltic Sea to study the quantitative and qualitative composition of the microplastics particles (range 0.5-5 mm) in different seasons. Preference was given to those beaches that are exposed to maximum anthropogenic pollution: areas around the town of Baltiysk, the northern part of the Vistula Spit (near the settlement of Kosa), and the Sambian peninsula coast (settlements of Yantarny, Donskoye, Primorye, Kulikovo, towns of Svetlogorsk, Pionersky, Zelenogradsk) (Fig. 1). During this stage of the study samples were selected from different spots at the beaches (with the highest accumulation of so-called "litter") – "wracklines". In these places there is the accumulation of all sorts of objects of different nature and density, which are concentrated in the coastal zone after they have been thrown by sea on the beach. These are typically algae, beach grass, wood chips, branches, charcoal, feathers, shells, amber, paraffin, fish bones, and of course diverse anthropogenic debris (mostly plastic).

From June, 2015 to January, 2016 there were 14 expeditions along the coastline of the Baltic Sea (in Kaliningrad region) to take samples and collect experimental materials. Most parts of the expeditions were carried out after the gale episodes or series of storms. Altogether, 60 sediment samples were collected from thirteen beaches. At each beach, 2-7 positions were randomly selected along "wracklines", located in several beach zones. Sand samples were collected in a specific areal - a quadrat (0.15 m^2) within the top 2 cm of sediment, using a clean stainless steel spatula. Sediment

samples were transferred into the polyethylene packages. All sampling locations, sampling dates, sample sediment conditions were recorded.

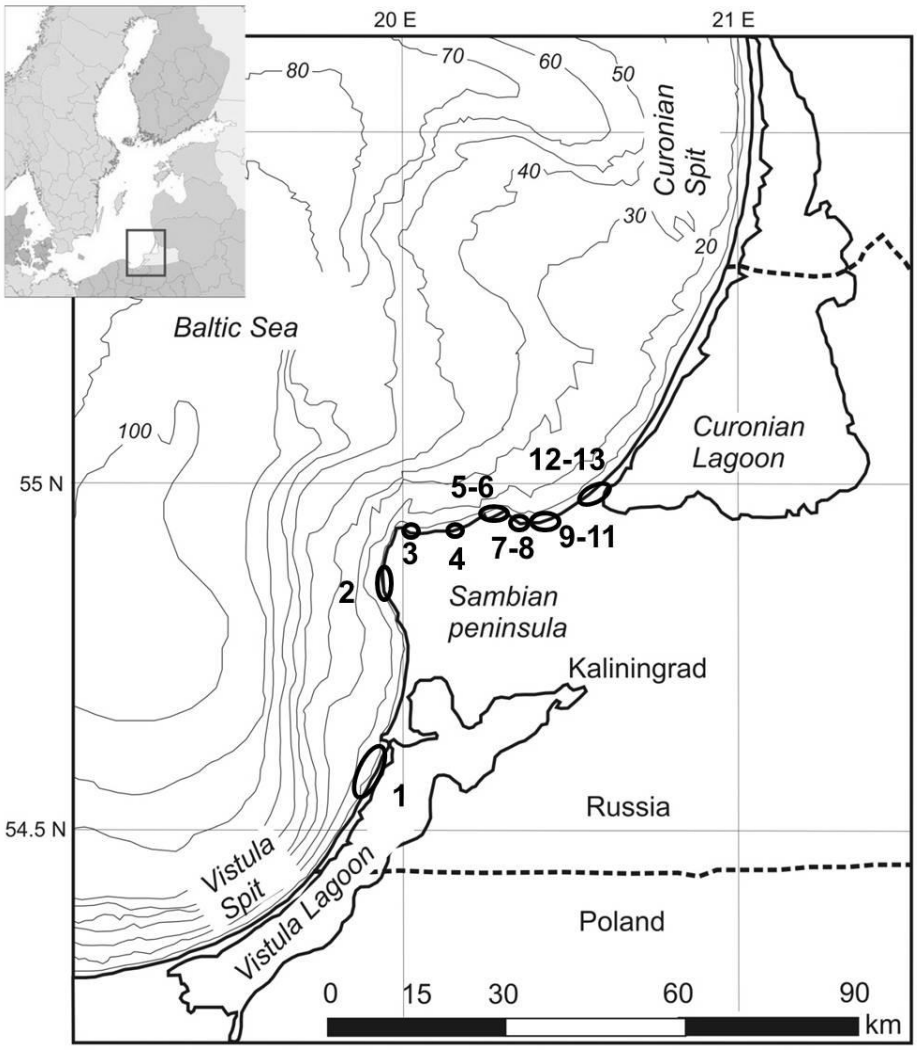

Figure 1. The sampling locations along the coastline of the Baltic Sea (in Kaliningrad region).

In the laboratory, the drying of the collected material happened at ambient conditions. The dried sample was weighed with an accuracy of 0.1 g. All sediments were separated using cascade of three sieves of mesh sizes: 5 mm, 1 mm, 0.5 mm. Materials saved in the sieve were sorted, while those that pass through were discarded. The following types of debris were selected from each site: macro-plastic, microplastics, paraffin and amber (close to plastic in terms of density). Then we weighed all sorted types of "litter". According to [6, 7, 8, 12], the visual differentiation of microplastic particles from other debris or sand is difficult and only suitable for microplastics ≥1 mm. So, the visual sorting has been used for particles ≥1mm. To separate microplastics from other material in the range 0.5-1 mm the visual inspection under the microscope was used. We used the criteria applied to define a plastic particle in studies of [13, 14] to avoid misidentification of microplastics: (i) no cellular or organic structures are visible, (ii) fibres are equally thick throughout

their entire length and should not be tapered at the end, (iii) coloured particles are homogenously coloured, (iv) fibres are not segmented, or appear as twisted flat ribbons, (v) particles are not shiny. These selection criteria are considered applicable only for the microplastic particles within the size range 0.5-5 mm [7, 9]. Visual sampling and sorting of small particles (<0.5-1.0 mm) and visual identification of microplastics are not considered reliable, since particles may be overlooked or wrongly classified as microplastics [8].

At this stage, we accomplished quite a rough estimation of the quantitative composition of microplastics (the visual differentiation of microplastic particles using the microscope) in the explored areas of the beach. For the technical reasons, we did not carry out the density separation of samples using $ZnCl_2$ solution and CaCl solution for separation of unaccounted particles of microplastics (where floating microplastics are picked up from the supernatant). But we plan to do additional processing of all saved sand samples in the range of 0.5-5 mm and to refine the obtained results.

III. Results and discussion

Large amount of debris of various nature was noted on the beach. Macro- and microplastics was found along the coast (from the Vistula Spit to the root of the Curonian Spit) regardless to the proximity of the sampling location to the human settlement area. Various kinds of anthropogenic debris were present even on the quite deserted and remote beaches. From the macro (>25 cm) and mega plastic objects (>1 m) we discovered a large number of plastic bottles, fishing nets, tackle, cables, fragments of boxes, plastic barrels, bags, and pieces of synthetic materials (made of polypropylene, polyethylene, foamed polyethylene, foamed polystyrene, foamed polyurethane, PVC, etc.), pieces of styrofoam, fragments of foamed plastic, reinforced hoses, nets, pieces of insulation, etc. The remnants of debris from earlier buried dumps were located on the slopes of dunes and cliffs.

Also visually we marked colored micro-fragments with size range <5 mm (micro particles) and fragments with larger size range (meso/macro particles >5 mm). Most of them were fragments of cigarette butts and cigarette filters, fishing nets, plastic bottles and plates, polyurethane foam, plastic films, foamed plastic, construction garbage, plastic fragments, granules, synthetic fibers, styrofoam, industrial pellets.

We collected, sifted, sorted, and weighed samples of various kinds of micro and macro particles of plastic, paraffin and amber from 60 beach sediments. We calculated the content of meso/macro plastic, microplastics, paraffin, and amber in the collected samples (percent from the total mass of the sample). Several samples were selected (2-7 points randomly selected) for each location of the beach. The diagrams show the content of meso/macro plastic, microplastics, paraffin, and amber in the collected samples (percent from the total mass of the sample) (Fig. 2). Each legend in Fig. 2 indicates the number of samples (2-7) taken from this location.

It was noted that fragments of dried “tired” meso/macro plastics become brittle. At the screening of the dry brittle material, some fragments broke up to smaller pieces, getting to a different size range - to microplastics. “Tired” plastic is plastic that has been on the beach for a long time and has been exposed to significant influence of the environment, such as: the effect of solar radiation, mechanical abrasion, impact of waves and wind, biofouling, etc. This effect particularly

concerns the fragments of disposable dishes (made of polystyrene PS, polystyrene, PP polypropylene), polystyrene films and some types of fibers.

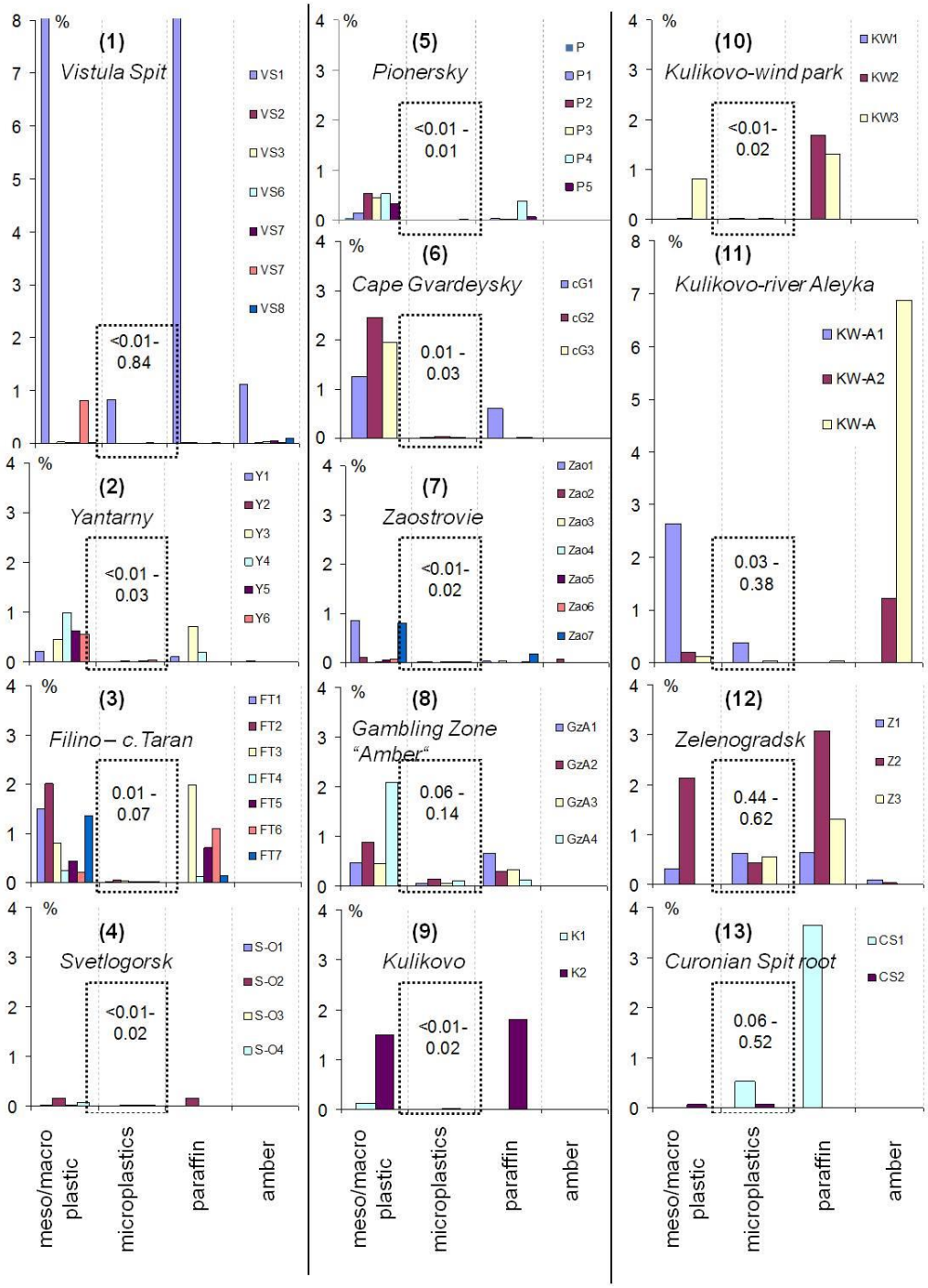

Figure 2. The content of meso/macro plastic, microplastics, paraffin, and amber in the collected samples (percent from the total mass of the sample) from 13 locations (numbers in round brackets corresponding to the areas indicated in Fig.1). Each legend indicates the number of samples (2-7) taken from every sampling location (see Fig. 1). The numbers in the dotted squares point out microplastics content in the samples.

Most meso/macro plastic particles in selected samples (percent from the total mass of the sample) (Fig. 2) was recorded in the following areas (according to Fig. 1): №1 – on the Vistula Spit (8.9%), №11 – between the Kulikovo village and the Aleyka river (2.7%), №6 – at Cape Gvardeysky (2.5%), №8 – in Gambling zone "Amber" (2.1%), №12 – in Zelenogradsk (2.1%), №3 – close to Cape Taran (2%), №9 – in the village of Kulikovo (1.5%). Most microplastics was observed in (Fig. 2): №1 – on the Vistula Spit (0.84%), №12 – in Zelenogradsk (0.44-0.62%), №13 – at the root of the Curonian Spit (0.52%), №11 – between the Kulikovo village and the Aleyka river (0.38%), №8 – in Gambling zone "Amber" (0.14%). We also evaluated the number of paraffin, which congregates well various particles and contaminants of the coast on its surface. Most paraffin was observed in (Fig. 2): №1 – on the Vistula Spit (8.7%), №13 – at the root of the Curonian Spit (3.6%), №12 – in Zelenogradsk (3.1%), №3 – near Cape Taran (2%), №9 – in the village of Kulikovo (1.8%), №10 – near the wind park (1.7%). We marked the presence of amber in samples as well. Most amber in samples was found in: №11 – between the Kulikovo village and the Aleyka river (6.9%), №1 – on the Vistula Spit (1.1%), №12 – in Zelenogradsk (0.1%), №7 – the village of Zaostrovye (0.08%), №2 – in Yantarny (0.01%), №5 – near Pionersky (0.004%).

Baltic amber (density of 1.05-1.09 g/cm^3) is within the range of plastics densities (0.05-1.61 g/cm^3). Microplastics may behave in the same way as the pieces of amber. Such a comparison of amber with microplastics allows us to use the patterns of behavior of amber in the coastal zone in order to understand the behavior of microplastics.

Beach sediments are moved under the influence of the wind and waves. Wind and wave action leads to breakage of plastic into microparticles. Generation of microparticles occurs on the shoreline during storms. The natural migration of sand during the storm should provide transfer of plastic from beaches to the underwater slope (through the grinding of plastic in the surf zone). This process can occur repeatedly, breaking up large items to smaller and smaller fragments.

Distribution of microplastics along the coast (from point 1 to point 13, according to the map in Fig. 1) in units of milligrams of microplastics per gram of sediment and milligrams of microplastics per m^2 are shown in Fig. 3. The figure shows the average and maximum values. Quantity distribution of microplastics in beach sediments (milligrams per gram of sediment and milligrams per m^2) with the average values with an error of random measurements, maximum and minimum values are shown accordingly in Table 1. Presentation of the obtained results in these units corresponds to the results of some studies [7, 15].

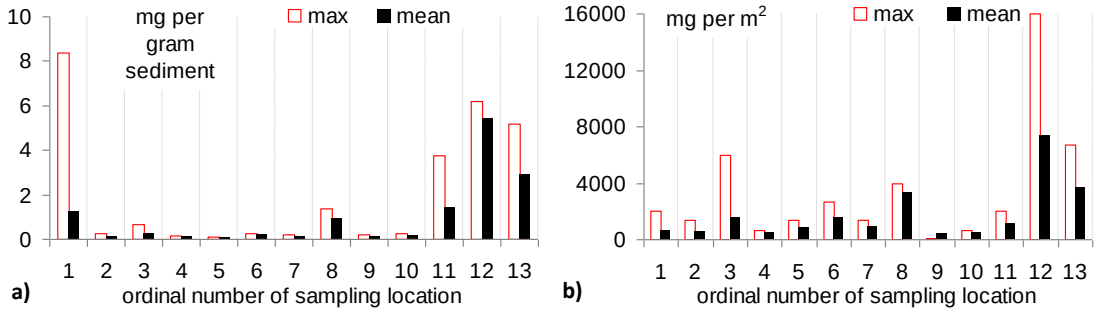

Figure 3. Distribution of the microplastics along the coast (from point 1 to point 13, according to the map in Fig. 1) in terms of: a) milligrams of microplastics per gram of sediment, b) milligrams of microplastics per m^2.

Table 1. Measured microplastics quantities in beach sediments

ordinal number of sampling location		mg per gram of sediment	mg per m^2
1	Mean ± Δ	1.23±2.92	690±590
	Min.–max.	$6.80 \cdot 10^{-3}$–8.38	67–2000
2	Mean ± Δ	0.10±0.10	580±500
	Min.–max.	$5.17 \cdot 10^{-3}$–0.25	67–1333
3	Mean ± Δ	0.23±0.20	1520±1840
	Min.–max.	0.09–0.67	666–6000
4	Mean ± Δ	0.11±0.11	520±480
	Min.–max.	0.01–0.17	67–667
5	Mean ± Δ	0.05±0.02	780±280
	Min.–max.	0.04–0.08	667–1333
6	Mean ± Δ	0.20±0.16	1560±2530
	Min.–max.	0.14–0.27	667–2667
7	Mean ± Δ	0.12±0.06	870±450
	Min.–max.	$7.83 \cdot 10^{-3}$–0.22	67–1333
8	Mean ± Δ	0.92±0.60	3330±870
	Min.–max.	0.58–1.38	4000–2667
9	Mean ± Δ	0.11±0.43	370±1290
	Min.–max.	0.01–0.21	67–667
10	Mean ± Δ	0.14±0.28	460±860
	Min.–max.	0.02–0.24	67–667
11	Mean ± Δ	1.44±5.04	1130±2440
	Min.–max.	0.20–3.78	67–2000
12	Mean ± Δ	5.42±2.27	7330±18800
	Min.–max.	4.4–6.2	2000–16000
13	Mean ± Δ	2.89±9.94	3660±12900
	Min.–max.	0.58–5.20	667–6667

Microplastics were found in all 60 beach sediment samples. Figures for each location are given within a range, because maximum and minimum densities were consistently found in different points on the beaches (Table 1). Most of the plastic particles were found near the popular recreation areas. But probably the action of sea and strong gales is the main explanation for the greater density along beaches.

Examples of detected particles of meso- and microplastics are shown in Fig. 4: polyurethane foam, plastic films, foamed plastic, plastic fragments, granules, synthetic fibers, styrofoam, industrial pellets, as well as pieces of paraffin and amber.

Figure 4. Beach samples of the micro- and mesoplastic particles: plastic fragments, industrial pellets, beads, fibres, plastic films, foamed plastic, granules, styrofoam, as well as paraffin that accumulates multiple pieces of everything in question, and amber (photos by Esiukova Elena).

IV. CONCLUSIONS

Micro-sized primary plastic litter from consumer products with degraded secondary micro-fragments leads to an increasing amount of small plastic particles on the beach. There are a great number of sources of primary and secondary microplastics in the environment (widespread consumer plastic products, plastic fragments, fishing nets, raw industrial pellets, etc. [1, 7, 16]). Abrasion and fragmentation of larger plastic items and of materials containing synthetic polymers is very relevant.

After the storm events the concentration of plastic on the beach along “wracklines” is increased. We noted that there is an unevenness of distribution and heterogeneity of plastic fragments along the coast of the south-eastern Baltic (in Kaliningrad region).

- Microplastics (0.5-5 mm) in samples taken from the top 2 cm of sandy beach make from <0.01% to 0.84% of the total sample’s mass. The areas of the Vistula Spit (0.84%), Zelenogradsk

(0.44-0.62%), the root of the Curonian Spit (0.52%), between the village of Kulikovo and the Aleyka river (0.38%), in Gambling zone "Amber" (0.14%) revealed its highest concentrations.

- Measured microplastics densities in beach sediments on average (with an error of random measurements) are from 370±1290 to 7330±18800 (mg per m^2), and from 0.05±0.02 to 2.89±9.94 (mg per gram of sediment).

- Macro- and mesoplastics were found all along the coastline of the Baltic Sea (in Kaliningrad region) (from 0.01% to 8.94% of the total sample mass).

- Paraffin in the samples makes up to 8.7%. Highest concentrations were found in the areas of the Vistula Spit (8.7%), the root of the Curonian Spit (3.6%), Zelenogradsk (3.1%), near Cape Taran (2%), the village of Kulikovo (1.8%) and near the wind park (1.7%).

- Small fractions of amber (mainly 0.5-2 mm) were detected in the samples at low concentrations (<0.01%). The exceptions were samples taken after heavy storms in the area of Kulikovo and the Vistula Spit (coarse fractions up to 1-3 cm) in the "wracklines" area.

- The greatest number of the micro-, meso-, and macroplastics was found in the band "wracklines" and under the foredune ridge.

Beaches are dynamic systems, so probably microplastics may become buried in deeper sediment layers during periods of accumulation of additional matter [7]. This should be further examined with stratified samples using cores [17, 18, 19].

The research is supported by the Russian Science Foundation grant number 15-17-10020.

V. References

[1] M. Bergmann, L. Gutow, M. Klages (Eds.). *Marine Anthropogenic Litter*, Springer, 447 p, ISBN 978-3-319-16509-7 ISBN 978-3-319-16510-3 (eBook) DOI 10.1007/978-3-319-16510-3, 2015.

[2] T. Rocha-Santos, A.C. Duarte, "A critical overview of the analytical approaches to the occurrence, the fate and the behavior of microplastics in the environment," *TrAC Trends in Analytical Chemistry,* vol. 65, pp. 47-53, 2015.

[3] M. Cole, P. Lindeque, C. Halsband, T.S. Galloway, "Microplastics as contaminants in the marine environment: A review," *Marine Pollution Bulletin,* vol. 62. pp. 2588-2597, 2011.

[4] P. Sundt, P-E. Schulze, F. Syversen, "Sources of microplastic-pollution to the marine environment," *Report no M-321/2015*, Asker: Mepex Consult, 2014.

[5] GESAMP, "Sources, fate and effects of microplastics in the marine environment: a global assessment," (P.J. Kershaw, eds.), (IMO/FAO/UNESCO-IOC/UNIDO/WMO/IAEA/UN/UNEP/UNDP Joint Group of Experts on the Scientific Aspects of Marine Environmental Protection), *Rep. Stud. GESAMP*, No. 90, 2015.

[6] European Commission, "Guidance on monitoring of marine litter in European seas. A guidance document within the common implementation strategy for the Marine Strategy Framework Directive," Ispra: European Commission, Joint Research Centre, MSFD Technical Subgroup on Marine Litter, 2013.

[7] V. Hidalgo-Ruz, L. Gutow, R.C. Thompson, M. Thiel, "Microplastics in the marine environment: a review of the methods used for identification and quantification*," Environ. Sci. Technol*., vol. 46. pp. 3060-3075, 2012.

[8] K. Duis, A. Coors, "Microplastics in the aquatic and terrestrial environment: sources (with a specific focus on personal care products), fate and effects," *Environ. Sci. Eur*., vol. 28:2 DOI 10.1186/s12302-015-0069-y, 2016.

[9] M.F. Costa, J.A. Ivar do Sul, J.S. Silva-Cavalcanti, M.C.B. Araújo, A. Spengler, P.S. Tourinho, "On the importance of size of plastic fragments and pellets on the strandline: a snapshot of a Brazilian beach," *Environ. Monit. Assess*., vol. 168. pp. 299-304, 2010.

[10] S.L. Wright, R.C. Thompson, T.S. Galloway, *"*The physical impacts of microplastics on marine organisms: A review," *Environ. Pollut*., vol. 178. pp. 483-492, 2013.

[11] I. Chubarenko, A. Bagaiev, M. Zobkov, E. Esiukova, **"**On some physical and dynamical properties of microplastic particles in marine environment," *Marine Pollution Bulletin*, DOI: 10.1016/j.marpolbul.2016.04.048, 2016.

[12] Y.K. Song, S.H. Hong, M. Jang, G.M. Han, M. Rani, J. Lee, W.J. Shim *"*A comparison of microscopic and spectroscopic identification methods for analysis of microplastic in environmental samples," *Marine Pollution Bulletinvol,* vol. 93(1-2), pp. 202-209. doi: 10.1016/, 2015.

[13] F. Norén, "Small plastic particles in Coastal Swedish waters," *KIMO report*, 2007.

[14] N.H.M. Nor, J.P. Obbard, *"*Microplastics in Singapore's coastal mangrove ecosystems," *Marine Pollution Bulletin,* vol. 79. pp. 278-283, 2014.

[15] F. Faure, C. Demars, O. Wieser, M. Kunz, L. de Alencastro, "Plastic pollution in Swiss surface waters: nature and concentrations, interaction with pollutants," *Environ. Chem.*, http://dx.doi.org/10.1071/EN14218, 2015.

[16] A.L. Andrady, "Microplastics in the marine environment," *Marine Pollution Bulletin*, vol. 62. pp. 1596-1605, 2011.

[17] J. Martins, P. Sobral, "Plastic marine debris on the Portuguese coastline: A matter of size?" *Marine Pollution Bulletin,* vol. 62, pp. 2649-2653, 2011.

[18] H.S. Carson, S.L. Colbert, M.J. Kaylor, K.J. McDermid, "Small plastic debris changes water movement and heat transfer through beach sediments." *Marine Pollution Bulletin*, vol. 62, pp. 1708-1713, 2011.

[19] A. Turra, A. Manzano, R. Dias, M. Mahiques, L. Barbosa, D. Balthazar-Silva and F. Moreira, "Three-dimensional distribution of plastic pellets in sandy beaches: shifting paradigms," *Scientific Reports*, vol. 4: 4435, DOI: 10.1038/srep04435, 2014.

EXPERIMENTING ON SETTLING VELOCITIES OF NEGATIVELY BUOYANT MICROPLASTICS

Liliya Khatmullina, Shirshov Institute of Oceanology Russian Academy of Science, Atlantic branch (ABIORAS), Russia
Igor Isachenko, ABIORAS, Russia
Elena Esiukova, ABIORAS, Russia
Irina Chibarenko, ABIORAS, Russia

liliakhatmullina@gmail.com

Presence of small plastic particles (< 5 mm), defined as microplastics, in the ocean and, especially, in coastal areas became evident in the last decade. From physical point of view, this fact indicates emergence of a new type of particles in the ocean. In contrast to the abundance of studies concerning sources, actual distribution and ecological effects of those particles, there are almost no detailed descriptions of physical mechanisms determining their distribution and behavior in the water column. Settling velocities of microplastics were measured in a series of experiments conducted in a 1-meter high glass tank filled with distilled water, in accordance with the typical methodology used in sedimentology. At first approximation, we supposed that the semi-empirical formulations developed for the natural sediments would be applicable to the microplastics. Results of preliminary experiments on microplastics of simple shapes justified this hypothesis. The majority of the implemented equations of settling velocity fitted well with the experimental data. Next step would be to test these formulations on the marine microplastic particles with greater variability in shapes. ***The research is supported by the Russian Science Foundation, project number 15-17-10020.***

Key words: microplastics, settling velocity

I. INTRODUCTION

Microplastics, defined as small plastic particles (< 5 mm), have been raised in popularity among the scientific society in recent years. Predominant amount of studies concentrate on the sources of microplastics, their actual concentration in the marine environment and ecotoxicity [see reviews by 1, 2, 3], while only a few describe marine microplastics from the physical point of view [4, 5, 6]. Better understanding of vertical transport of microplastics is fundamental for improving estimates of their concentration, size distribution, and dispersal in the world ocean [4, 5, 6, 7].

Once a plastic particle gets into the ocean, it either stays at the surface or subsurface (if it is less dense than the water), or it sinks (if it is denser than water and if it has overcame the surface tension). Reisser et al. [6] have experimentally revealed different relationships between the shape, size and rising velocity of buoyant microplastics. As for the plastics with negative buoyancy, we should firstly notice that, since any plastic particle in the ocean represents a substrate for the bacteria and algae growth, density of initially buoyant particle could subsequently increase due to the biofilm

formation and fouling so that it becomes dense enough to sink below the sea surface [7, 8]. To our knowledge, the fate of these fouled microplastics is unknown, as well as the settling process of initially non-buoyant particles in general.

Our study is focused on the sedimentation process of non-buoyant artificially made microplastics, which was studied through the series of laboratory experiments. We aim to test the applicability of existing semi-empirical formulations of settling velocity by comparing the theoretical predictions with the experimental data.

Theoretical assumptions

Particle sedimentation has been a subject of numerous investigations. Noticeable success was achieved in formulating the natural grains settling velocity [e.g. 9, 10, 11, 12, 13], which is regarded as one of the basic terms in sedimentology [14]. Terminal settling velocity (w_s) of a particle falling in the fluid implies the movement without acceleration and thus the balance between the gravitational force and hydrodynamical drag,

$$\frac{1}{2}C_d S w_s^2 = (\rho_s - \rho) g V, \tag{1}$$

where C_d denotes drag coefficient; ρ and ρ_s – fluid and particle density, respectively; g – acceleration due to gravity; S and V – the cross-sectional area and volume of the particle.

Giving the following equation of settling velocity for a spherical particle of diameter d,

$$w_s^2 = \frac{4}{3C_d}\Delta g d, \tag{2}$$

where $\Delta = \rho_s/\rho - 1$.

Well-known analytical solution for the settling velocity and drag coefficient of a perfect sphere was proposed by Stokes (1851) on the assumption of laminar flow,

$$w_s = \frac{1}{18}\frac{\Delta g d^2}{\nu}, \tag{3}$$

$$C_d = \frac{24}{\mathrm{Re}}, \tag{4}$$

where ν is kinematic viscosity of the fluid, and Re denotes Reynolds number, calculated as $\mathrm{Re} = w_s d/\nu$ and lower than 1 for laminar flow.

However, turning to the natural particles and microplastics, it becomes challenging to acquire a fully analytical settling velocity equation due to the not constrained regime and complexity of particle forms. Spread of Reynolds values yielded by the small natural or microplastic particles implies that inside the selected size group (0.5-5 mm in particular) the settling process of particles represents laminar, transitional and turbulent regimes, which as such are distinct from physical point of view and could not be described by one general equation. The possible measure to combine these distinct behaviors in one formula is to use the function of two asymptotic solutions (for high and low Re), which was suggested by different researchers (enumerated in ref. [12]). Relationships of the settling velocity for the particles of different shapes are usually based on those for spheres with implementation of various coefficients accounting for the effects of the shape [11, 13, 16].

Dietrich [17] did a comprehensive work concerning the settling velocity of sediment particles based on an extensive dataset. His approach had no explicit relation to the regime of the flow and was basically an attempt to fit the data (with broad range of Re numbers and shapes) to the 4-order polynomial function in terms of dimensionless velocity (W_*) and dimensionless diameter (D_*) calculated as follows,

$$W_* = \frac{\rho w_s^3}{(\rho_s - \rho) g \nu}, \tag{5}$$

$$D_* = \frac{(\rho_s - \rho) g D_n^3}{\rho \nu^2}, \tag{6}$$

where D_n is nominal diameter of the particle, equal to the diameter of a sphere of the same volume as the particle [14].

His approximations account for the roundness and shape of a particle, expressed by Powers [18] roundness coefficient (P) and Corey [19] shape factor (csf), calculated as follows,

$$csf = \frac{c}{\sqrt{ab}}, \tag{7}$$

where a, b, and c are the longest, intermediate, and shortest axes of the particle, respectively.

Dietrich's formulas (for exact equations and coefficients see [17]) could be regarded as a continuous representation of the data set he employed, thus they were consequently used by other researchers for calibration of their semi-empirical equations and data comparison [11, 13, 20].

Cheng [9] generalized previously proposed semi-empirical equations in a simplified relation between the drag coefficient and the Reynolds number, using the aforementioned "two-asymptotes approach",

$$C_d = \left[\left(\frac{A}{\mathrm{Re}} \right)^{1/m} + B^{1/m} \right]^m, \tag{8}$$

where A, B, and m denote semi-empirical coefficients, which account for the shape and are calibrated using the experimental data. For example, a spherical particle yields A=24, B=0.4, m=2 [11]. Therefore, in the laminar flow regime (Re<1) $C_d \rightarrow 24/\mathrm{Re}$ in accordance with (4), and in the developed turbulent flow regime (Re>10^5) C_d approaches a constant value, B.

Using (8), terminal settling velocity is expressed as follows,

$$w_s = \frac{\nu}{d} \left[\sqrt{\frac{1}{4} \left(\frac{A}{B} \right)^{2/n} + \left(\frac{4}{3} \frac{d_*^3}{B} \right)^{1/n}} - \frac{1}{2} \left(\frac{A}{B} \right)^{1/n} \right]^n. \tag{9}$$

Zhiyao et al. [12 and references therein] expressed settling velocity equations from 19 studies in the notation which is idem or close to the Cheng's formulation (8) to compare the resulting A, B, and m coefficients and to propose their own expression. Our experimental microplastics settling velocities were compared to some of those predictions. Camenen [11] *enhanced (8)* and, instead of constant coefficients, proposed a set of additional equations for A, B, and m, which implement csf shape factor and P roundness. Ahrens [10] suggested another asymptotic approach (10), which was calibrated on natural sand grains and thus could account for the effects of angularity, without, however, defining the relation to the shape explicitly,

$$w_s = \frac{C_1 \Delta g d^2}{\nu} + C_t \sqrt{\Delta g d}, \tag{10}$$

where the first and second terms are associated with laminar and turbulent flow regimes, respectively. The coefficients C_1 and C_t were calibrated [10] using the data on natural sediments settling.

II. MATERIALS AND METHODS

To date, there is no common definition of microplastic size [1, 3]. In this study, we focused on the plastic particles within the 0.5-5mm size range, upper limit is set in accordance with majority of publications [2, 3, 21], and the lower limit is conditioned by the employed experimenting facility. It is noteworthy that the settling characteristics of smaller particles could be fundamentally different owing to their Reynolds numbers.

Sample collections

Microplastic particles were prepared by hand from the Polycaprolactone (PCL) plastic (measured density $\rho_s = 1.131 \pm 0.005$ g cm^{-3}), which softens during heating (up to 60˚C) and stiffens in room temperature, and thus allows to produce granules of different shapes and sizes. We concentrated on two groups of artificially made plastic particles, which have not been influenced by any natural factors (e.g. sun radiation, bio-fouling, etc.): a) quasi-spherical particles fabricated from PCL; b) cylinder-shaped granules with equal height and diameter cut from circular rods of PCL (further referred as PCL cylinders). We aimed to make the rods with equal diameter along their length ranging from 0.5 to 5 mm. The obtained rods were cut into segments in such a way that the length of resulting cylinder would equal its diameter, giving length to diameter ratio of around unity.

Experimental facility and procedure

Our method of settling velocity measurement is consistent with the experiments described by Ref. [22, 23, 24]. We used a glass column 10 mm thick, of square section (180x180) mm^2 (inner size), and height of 110 cm. Marking lines were painted over the tank 11 cm from the top, and 12 cm from the bottom, giving 87 cm of working distance. The depth of the upper marking line was determined in such a way that the particles would already achieve the terminal settling velocity (no acceleration) by the time of crossing the mark.

The tank was filled with distilled water. Air temperature outside the tank and temperature of water near the surface and at the bottom of the tank was measured before and after each series of drop experiments to confirm the relative thermal stability (±0.5˚C) and thus the absence of significant convection in the water during the experiment.

Obvious inaccuracy in respect to the fabrication process was anticipated, thus, the diameter and length of each PCL cylinder and diameters of quasi-spherical particles were measured beforehand. Particles were placed approximately 1 cm below the surface of water (so that particles are not restrained by surface tension) in the center of the tank by forceps, and then let go of without inducing any additional acceleration. Finally, the time a particle took to cover the working distance (87 cm) was measured with a stopwatch and terminal settling velocity was calculated as a ratio of working distance to the duration of fall. Experimental results were presented in terms of dimensionless settling velocity and dimensionless diameter according to (5, 6) and compared to the

number of semi-empirical predictions. Goodness of fit was estimated by calculating average value of the relative error defined as

$$E = \frac{1}{N}\sum_{i=1}^{N}\left|\frac{W_s(\text{predicted})_i}{W_s(\text{experimental})_i} - 1\right|, \quad (11)$$

where N denotes the number of individual measurements.

III. SPHERICAL PARTICLES

Spherical particles were relatively well-studied in a vast number of works [9, 11, 16 and references therein]. Obviously, physical processes related to the settling of plastic spheres could not be fundamentally different from those of spheres of any other material. Thus, the main aim of drop experiment with PCL spheres was to test the experimental facility by comparing obtained data with the already existing datasets. However, owing to the peculiarities of fabrication process (particles were made by hand), it was unattainable to produce ideal spheres of different diameters from PCL, but rather ellipsoids, which could be seen from the resulting histogram of *csf* (Fig.1). The values of *csf* (0.8-1) were close to but not equal unity, which is characteristic of ideal spheres. Nevertheless, we assume that this discrepancy is minor and the intended test on our PCL spherical particles is credible.

Dietrich's [17] curves could be regarded as a compact representation of a wide set of experimental data, analyzed in his study. Thus, by comparing our data to the Dietrich's approximation for smooth spheres, we analyze their consistency to the previously obtained dataset and consequently the validity of employed experimental procedure (Fig.1).

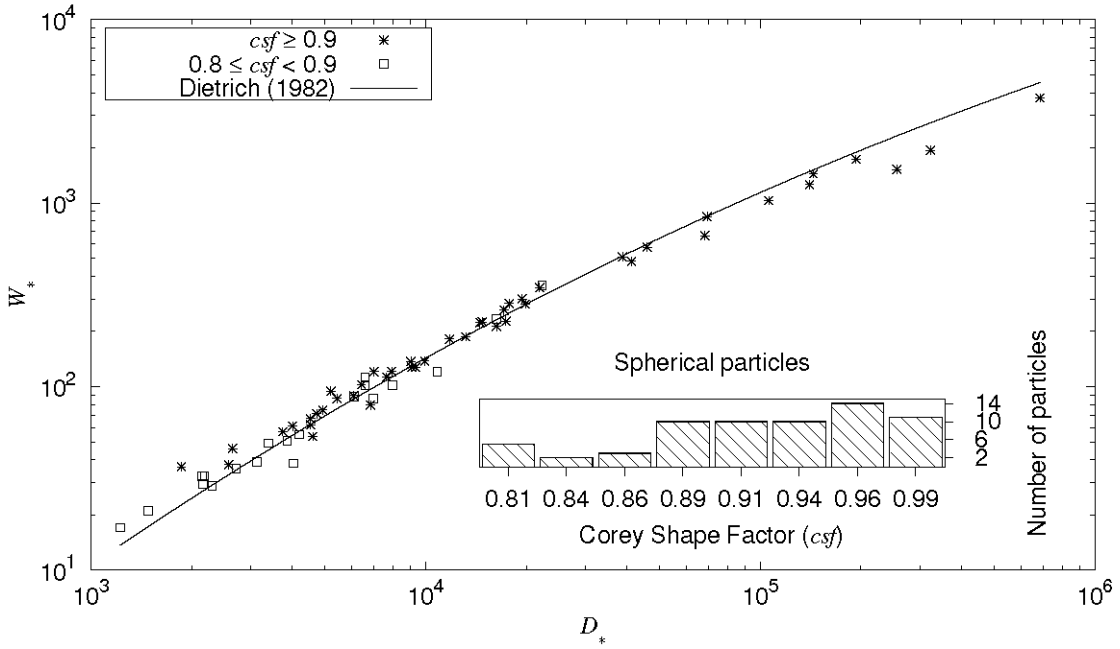

Figure 1. Spherical PCL particles. Corey shape factor (csf) and settling velocity of particles within two csf-groups (labels according to the legend). Curve is a fourth order polynomial fit for smooth spheres, given by Dietrich [17].

Figure 1 shows that although smaller particles are commonly less equal to spheres (*csf*=0.8-0.9), they correspond well with the approximation curve. For bigger particles, which on the contrary have relatively better concurrence to the spherical form, this minor divergence from sphericity results in slightly lower settling velocities compared to those of perfect spheres. Overall, experimental data is in good agreement with Dietrich's results, with relative error of 4% (Table 1). This is in accordance with [11, 13, 24], who stated that the effect of shape is more pronounced for bigger particles/higher Reynolds numbers.

IV. CYLINDER-SHAPED PARTICLES

Drop experiments with PCL cylinders revealed the presence of various secondary movements during the particle sedimentation in water. Surface curvature of non-spherical particles induces flow separation, resulting in higher drag coefficient, and makes the settling more instable with occurrence of rotation, oscillation and tumbling. As noticed by [17] and [24], this effect becomes more pronounced with higher Reynolds numbers. Additionally, during falling PCL cylinders did not always follow a rectilinear trajectory. Hazzab et al. [17] suggested that the frequency of these secondary movements is attenuated with the increase in Reynolds numbers. In this study, we did not analyze such characteristics quantitatively, which, however, would be of interest in the future estimations on real marine microplastics.

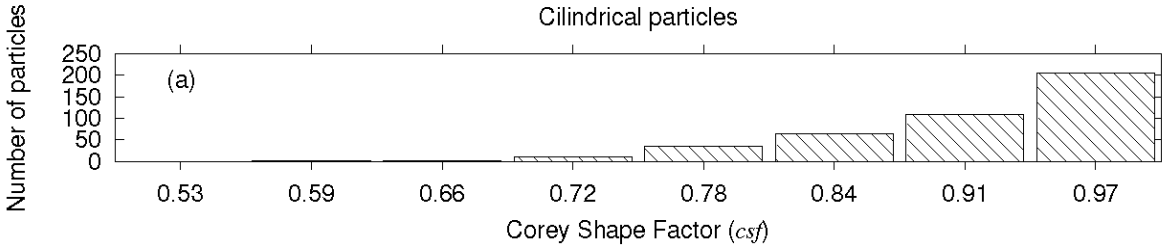

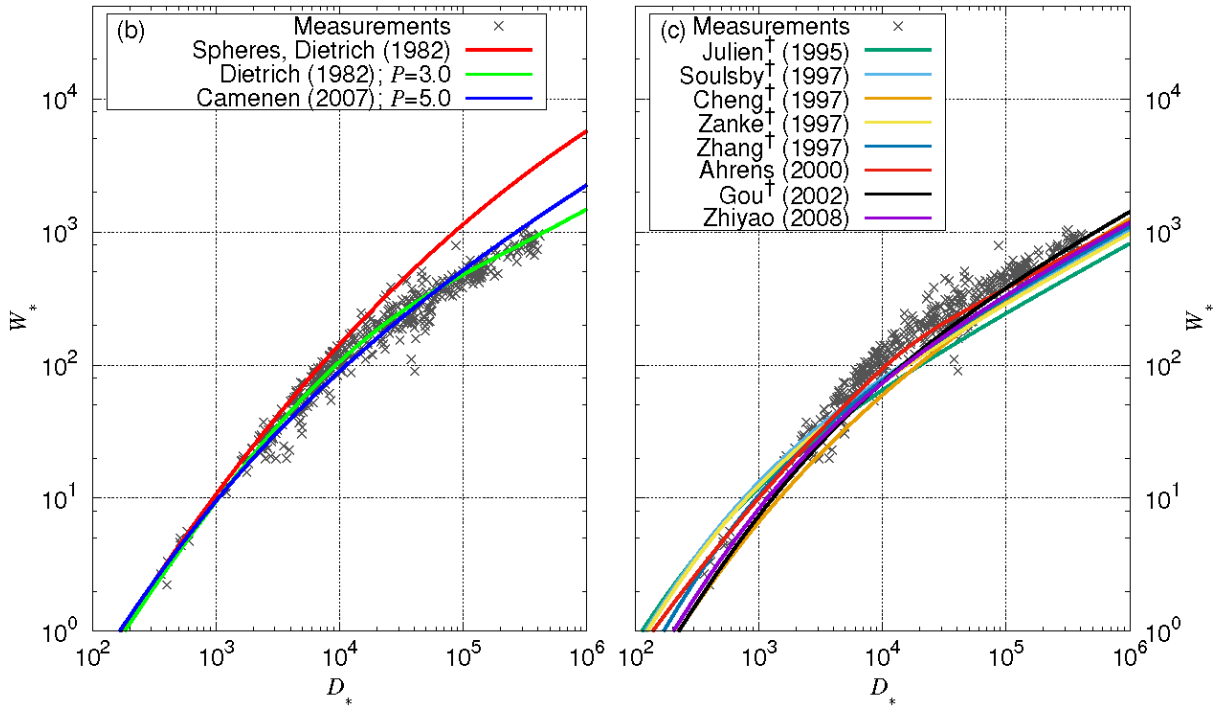

Figure 2. Cylinder-shaped particles. a) csf histogram, and b), c) experimental and predicted settling velocities in dimensionless terms (5, 6). Grey crosses represent experimental data; lines show the semi-empirical curves from different publications, colored according to the legend. † marks publications, which were used in comparative analysis by Zhiyao et al. [12] and are not directly referenced in this paper

We compared the experimental data with several existing semi-empirical formulations calibrated by using data on settling velocities of angular or naturally shaped grains (Fig.2, Table 1). Figure 2b represents two equations: Dietrich's [17] approximation of naturally shaped grains, and Camenen [11] formulation, – that explicitly account for particle shape and roundness. Both approaches involve defining *csf*, which formula (7) is comprehensible (for PCL cylinders we used mode value of *csf*=0.97, Fig. 2 a), and Powers roundness, *P*, which estimation is on the contrary rather subjective and could vary by around ±1 between two observers of the same grain [17]. Herein, we have not assigned the *P* value to our particles, but have selected the best curve fitting to our data points by changing *P* with 0.5 step as it is unrealistic to estimate *P* with higher resolution. Interestingly, the resulting *P* value was different for Camenen (5.0) and Dietrich (3.0) predictions, despite the fact that Camenen inter alia calibrated his formula on the Dietrich's approximation (and so it was more logical if roundness would be identical). Therefore, although these two formulas have in general better predicting ability as they directly consider the effect of shape and fit the data well (relative error of 7.4 and 5.3% for Camenen and Dietrich, respectively), the lack of clarity in roundness estimation reduces the applicability of these approaches. This problem becomes more striking considering the microplastic particles, which forms could be far from those of naturally occurring grains, thus indicating a need of development of a more quantitative approach to define

roundness. Ref. [13, 20] also noticed the complexity of Dietrich's formulas and the fact that Powers roundness factor is rarely measured in practice.

Dietrich approximation of smooth spheres is also plotted in Fig.2b. It could be seen that starting from $D_* \approx 10^4$, which corresponds to Re≈100, settling velocity of angular particles noticeably diverges from that of spheres in agreement with the aforementioned statement that angularity of shape increases the drag and reduces the settling velocity for the same D_* as a sphere.

Table 1. Accuracy of fit of several existing formulations against the experimental data. Average value of the relative error, *E*, was calculated by (11). † marks publications, which were used in comparative analysis by Zhiyao et al. [12] and are not directly referenced in this paper

Experimental dataset	**Authors**	**E**
Spherical particles	Dietrich, 1982	4.0%
Cylinder-shaped particles	Dietrich (1982); csf=0.97, P=3.0	5.3%
	Camenen (2007); csf=0.97, P=5.0	7.4%
	Julien† (1995)	15.2%
	Soulsby† (1997)	10.4%
	Cheng† (1997)	14.5%
	Zanke† (1997)	11.7%
	Zhang† (1997)	10.2%
	Ahrens (2000)	6.6%
	Gou† (2002)	9.5%
	Zhiyao et. al (2008)	10.6%

In general, all the other settling velocity predictions used for comparison in this study (Fig.2c), in which shape is incorporated in general by a set of coefficients that does not vary, were able to predict the experimental values with a good degree of consistency (within 15.2% of relative error). Among them Ahrens curve represented the best fit to data (6.6% error, Table 1).

The studied group of particles is characterized by a quite simple form, which is comparable to that of the natural sediments. However, as reported by some authors [25], significant part of the microplastics found in sediments is devoted to fibers. Settling process of such specific particles will be the scope of future investigations.

V. CONCLUSIONS

In this study, we made an attempt to incorporate microplastics as a distinct type of particles in the already existing body of sedimentology research. Terminal settling velocity, being a major sedimentology term, provides not only a fundamental view of the matter sinking in the ocean, but in our case can consequently shed light on the problem of microplastic transportation/distribution in the ocean and uncover why and how ocean sediments act as a sink of microplastics [1, 25]. In a set of experiments on the microplastic particles of simple forms, we have successfully tested the experimental facility and procedure, which could be further used in the experiments on real marine microplastic.

Measured settling velocity was in accordance with available experimental data. When applied to microplastics, the existing semi-empirical models predict the settling velocity of spherical and cylinder-shaped particles in the intermediate range of Reynolds numbers quite accurately. We pointed the potential of Dietrich and Camenen approximations to estimate the settling velocity of microplastics of different shapes with a good degree of consistency on a stipulation that the roundness coefficient would be calculated in a quantitative way.

In accordance with several existing studies, shape of a particle was found to be the major term in determining the character of settling and corresponding settling velocity, which is of great concern for marine microplastics which represents variety of forms.

VI. REFERENCES

[1] A.L. Andrady, "Microplastics in the marine environment," *Marine pollution bulletin*, vol. 62, pp. 1596-1605, 2011.

[2] M. Cole, P. Lindeque, C. Halsband, C., and T.S. Galloway, "Microplastics as contaminants in the marine environment: a review," *Marine pollution bulletin*, vol. 62, pp. 2588-2597, 2011.

[3] R. Thompson, "Microplastics in the Marine Environment: Sources, Consequences and Solutions" in *Marine Anthropogenic Litter* , M. Bergmann, L. Gutow, and M. Klages, Eds. Springer International Publishing, pp. 197-212, 2015.

[4] T. Kukulka, G. Proskurowski, S. Morét-Ferguson, D.W. Meyer, and K.L. Law, "The effect of wind mixing on the vertical distribution of buoyant plastic debris," *Geophysical Research Letters*, vol. 39, 2012.

[5] A. Isobe, K. Kubo, Y. Tamura, E. Nakashima, and N. Fujii, "Selective transport of microplastics and mesoplastics by drifting in coastal waters," *Marine pollution bulletin*, vol. 89, pp. 324-330, 2014.

[6] J. Reisser, B. Slat, K. Noble, K. du Plessis, M. Epp, M. Proietti, et al., "The vertical distribution of buoyant plastics at sea," *Biogeosciences Discuss.*, vol. 11, pp. 16207-16226, 2014.

[7] K.L. Law, S.E. Morét-Ferguson, D.S. Goodwin, E.R., Zettler, E. DeForce, et al., "Distribution of surface plastic debris in the eastern Pacific Ocean from an 11-year data set," *Environmental science and technology*, vol. 48(9), pp. 4732-4738, 2014.

[8] F.M. Fazey and P.G. Ryan, "Biofouling on buoyant marine plastics: An experimental study into the effect of size on surface longevity," *Environmental Pollution*, vol. 210, pp. 354-360, 2016.

[9] N.S. Cheng, "Simplified settling velocity formula for sediment particle," *Journal of Hydraulic Engineering*, vol.123(2), pp. 149–152, 1997.

[10] J. P. Ahrens, "A fall-velocity equation," *Journal of Waterway, Port, Coastal, and Ocean Engineering*, vol. 126(2), pp. 99–102, 2000.

[11] B. Camenen, "Simple and general formula for the settling velocity of particles," *Journal of Hydraulic Engineering*, vol.133, pp. 229-233, 2007.

[12] S. Zhiyao, W. Tingting, X. Fumin, and L. Ruijie, "A simple formula for predicting settling velocity of sediment particles," *Water Science and Engineering*, vol. 1(1), pp. 37-43, 2008.

[13] J.A. Jimenez, and O.S. Madsen, "A simple formula to estimate settling velocity of natural sediments," *Journal of Waterway, Port, Coastal, and Ocean Engineering*, vol. 129(2), pp. 70–78, 2003.

[14] Interagency Committee, "Some fundamentals of particle size analysis: A study of methods used in measurement and analysis of sediment loads in streams," Subcommittee on Sedimentation, Interagency Committee on Water Resources, St. Anthony Falls Hydraulic Laboratory, Minneapolis, Rep. No. 12, 1957.

[15] G. Stokes, "On the effect of internal friction of fluids on the motion of pendulums," *Trans. Cambridge Philos. Soc.*, vol. 9, pp. 8–106, 1851.

[16] A. Terfous, A. Hazzab, and A. Ghenaim, "Predicting the drag coefficient and settling velocity of spherical particles," *Powder technology*, vol. 239, pp. 12-20, 2013.

[17] W.E. Dietrich, "Settling velocity of natural particles," *Water resources research*, vol. *18*(6), pp.1615-1626, 1982.

[18] M.C. Powers, "A new roundness scale for sedimentary particles," *Journal on Sedimentary Petrolology*, vol. 32, pp. 117-119, 1953.

[19] A. Corey, "Influence of the shape on the fall velocity of sand grains," Master's thesis, Colorado A&M College, Fort Collins, Colo, 1949.

[20] W. Wu, and S.S. Wang, "Formulas for sediment porosity and settling velocity," *Journal of Hydraulic Engineering*, vol. 132(8), pp. 858-862, 2006.

[21] C. Arthur, J. Baker, H. Bamford, "NOAA Technical Memorandum NOS-OR&R30," *Proceedings of the international research workshop on the occurrence, effects and fate of microplastic marine debris*, September 2008.

[22] R.J. Gibbs, M.D. Matthews, and D.A. Link, "The relationship between sphere size and settling velocity," *Journal of Sedimentary Research*, vol. *41*(1), pp. 7-18, 1971

[23] J. R. L. Allen, "Physical sedimentology", Allen & Unwin, 1985

[24] A. Hazzab, A. Terfous, and A. Ghenaim, "Measurement and modeling of the settling velocity of isometric particles", *Powder Technology*, vol. 184(1), pp. 105-113, 2008

[25] L.C. Woodall, A. Sanchez-Vidal, M. Canals, G.L. Paterson, R. Coppock, et al., "The deep sea is a major sink for microplastic debris," *Royal Society open science*, vol. 1(4), 2014.

COMPLEX MONITORING OF GEOCRYOLOGICAL STRUCTURE AND GROUND TEMPERATURE REGIME OF THE ARCTIC COASTAL ZONE IN THE AREAS OF INFRASTRUCTURE CONSTRUCTION

Osip Kokin, Lomonosov Moscow State University (MSU), State Oceanographic Institute (SOI), Russia
Stanislav Ogorodov, Lomonosov Moscow State University (MSU), Russia
Nataliya Belova, Lomonosov Moscow State University (MSU), University of Tyumen (UT), Institute of the Earth Cryosphere (IEC SB RAS), Russia
Dmitry Kuznetsov, Lomonosov Moscow State University (MSU), Russia
Natalia Shabanova, Lomonosov Moscow State University (MSU), Russia

osip_kokin@mail.ru

The research of geocryological structure of the coasts is important in the planning and construction of infrastructure in permafrost zone. Long-term monitoring of temperature regime of the Arctic coastal zone soils needs to predict the steady state of the object during its operation and prevent possible negative consequences resulting from interruption of the steady state. It is especially important in conditions of today's climate change, as well as the possibility of warming effect of engineering facilities (for example pipelines). The results of a study of the coastal seasonally frozen cap, formed in the contact zone of freezing fast ice to the bottom are presented by the examples of the Mys Kamenniy settlement at the Gulf of Ob coast (Kara Sea) and Varandey settlement at the Pechora Sea areas. The technology of the monitoring station establishment for the geocryological statement and temperature regime of the Arctic coastal zone observations is proposed based on the conducted field works experience.

Key words: cryolithozone, sea coast, permafrost, coastal thermoerosion, accumulative shores, cryopeg, talik

I. INTRODUCTION

The research of geocryological structure of the coastal zone is important in the planning and construction of infrastructure Arctic coastal zone in order to reduce the financial losses at the construction phase of these objects.

An example of the negative consequences of ignoring of the coastal zone geocryological structure is the first phase of construction of an underwater pipeline to the Varandey Oil Export Terminal (Pechora Sea). The builders did not move "plough" (Fig. 1a) used to trench dredging that drove in coastal seasonally frozen cap which has formed in the contact zone of freezing fast ice to the bottom (so-called “visor of seasonally frozen ground” in literal translation from Russian into English). The presence of this cap was a surprise [1]. As a result of bad buried in the ground (Fig.

1b) 4 km long pipeline in shallow water was pulled from the bottom under the influence of sea ice and through away on the coast as a thin straw [2].

Long-term monitoring of temperature regime of the Arctic coastal zone soils needs to predict the steady state of the object during its operation and prevent possible negative consequences resulting from interruption of the steady state. It is especially important in conditions of today's climate change, as well as the possibility of warming effect of engineering facilities (for example pipelines).


a)


b)

Fig. 1. The «plough» (a) and the exposed pipeline which was bad buried in the ground (b)

The greatest contribution to the study of the geocryological structure and temperature of soils of the Arctic coastal zone have works by N.F. Grigoriev [3], L.A. Zhigarev [4] and A.N. Khimenkov and A.V. Brushkov [5]. Most of these researches have short-term observations.

The aim of this paper is proposal of the technology of the long-term monitoring station establishment for the geocryological statement and temperature regime of the Arctic coastal zone observations after reviewing several examples of field investigations.

II. GEOCRYOLOGICAL STRUCTURE FEATURES OF THERMOEROSION AND ACCUMULATIVE SHORES

Reference [3] was one of the first work where the geocryologial structure differences which depend on the history of sea coasts evolution. N.F. Grigoriev [3] allocated three cryolithozones in Western Yamal coastal area: sub-aerial, sub-aerial-erosion and sub-sea (shallow waters).

Sub-aerial cryolithozone is typical for both thermoerosion and accumulative shores. It is not exposed to direct influence of the sea at the present time.

Sub-aerial-erosion cryolithozone is transitional zone between sub-aerial and sub-sea cryolithozones and typical only for thermoerosion shores. It is located at the foot of the coastal bluff both in sub-aerial and sub-sea (under modern ice-bonded permafrost and cryotic talik) positions and presented itself part of sub-aerial cryolithozone which was recently destroyed after coastal erosion and covered by beach deposits. The main characteristic of sub-aerial-erosion cryolithozone is proximity of the relict permafrost-table to the surface which is lowered with increasing distance from the shoreline. The temperature of deposits is increased in the same direction.

Sub-sea cryolithozone is typical for both thermoerosion and accumulative shores. Its development takes place in conditions of active processes of erosion and accumulation. There are two types of permafrost: modern (Holocene) ice-bonded permafrost and cryotic talik. The first type is formed as the pereletok during seasonal freezing of accumulative landforms of submarine coastal slope (beaches, coastal ridges, bars, barriers. spits, islands, fans and deltas) on the contact of the fast ice with the seabed (coastal seasonally frozen cap). Such freezing take place until the water depth which equal to the thickness of ice (generally it is less than about 1.5-2 m). Accumulation processes are lead to increasing thickness of the modern ice-bonded permafrost which underlain by a relict permafrost, or cryotic talik and can contain highly saline talik layers and lenses (cryopegs).

Cryotic talik has no ice despite the temperature below 0°C. This is due to saline pore-water (cryopegs) which contained in sediments instead ice-cement. It is located at the water depth more than 2 m and under the modern ice-bonded permafrost until 2 m water depth. Cryopegs in the cryotic talik can have the temperature below -8°C.

III. EXAMPLES OF FIELD INVESTIGATIONS

Investigations of permafrost and seasonal freezing in coastal zones in the areas of Mys Kamenniy settlement (west coast of fresh water Gulf of Ob, Kara Sea) and Varandey settlement (Pesyakov Island, Pechora Sea) included core and auger drilling, drill rods penetrating into active layer (by the compact portable rig UKB-12/25) and temperature measurements in boreholes with a thermistor strings. Both key sites have close geomorphological structure. Mys Kamenniy is lowland fine sand spits (3-5 m high). Pesyakov Island is also lowland sandy barrier island but it has dune belt facing sea side (5-12 m high).

Mys Kamenniy settlement (the Gulf of Ob coast, Kara Sea)

Drilling in the area of Mys Kamenniy was taken in May 2012 from fast ice to determine depth and width of the coastal "visor" under fast ice and depth of permafrost table under water layer [6, 7].

In order to determine the depth of seasonal freezing and the limit of its spread the drilling from the fast ice was carried out on two profiles at the end of the cold season (from 11 to 23 May 2012), when freezing up have a maximum depth. 5 boreholes were done for each profile (Fig. 2). Profile 1 was located at a relatively steep-bottom shore, and the profile 2 – at shallow shore. It is worth noting that although the Gulf of Ob is a part of the Kara Sea, the water is fresh. It imposes some specific to the freezing of the bottom sediments.

The thickness of the seasonal frozen layer (when the frozen deposits are underlain thawed ground) reaches 3 m. The width of the longshore zone of seasonal frozen ground is about 70 m. The temperature of the seasonal frozen layer varies from -0,3°C to -1,5°C.

Permafrost roof plunges from a depth of 3 m near the shore line to 11 below the bottom of the Gulf of Ob at a distance of 400 m from the shore line.

The width of the contact zone of fast ice with bottom depends on the topography and incline of the submarine coastal slope and snow cover and fast ice thickness. If the thickness of fast ice is about 2 m, width of contact zone varies from 100 m at a relatively steep-bottom shores up to 300 m on the shallow shores.

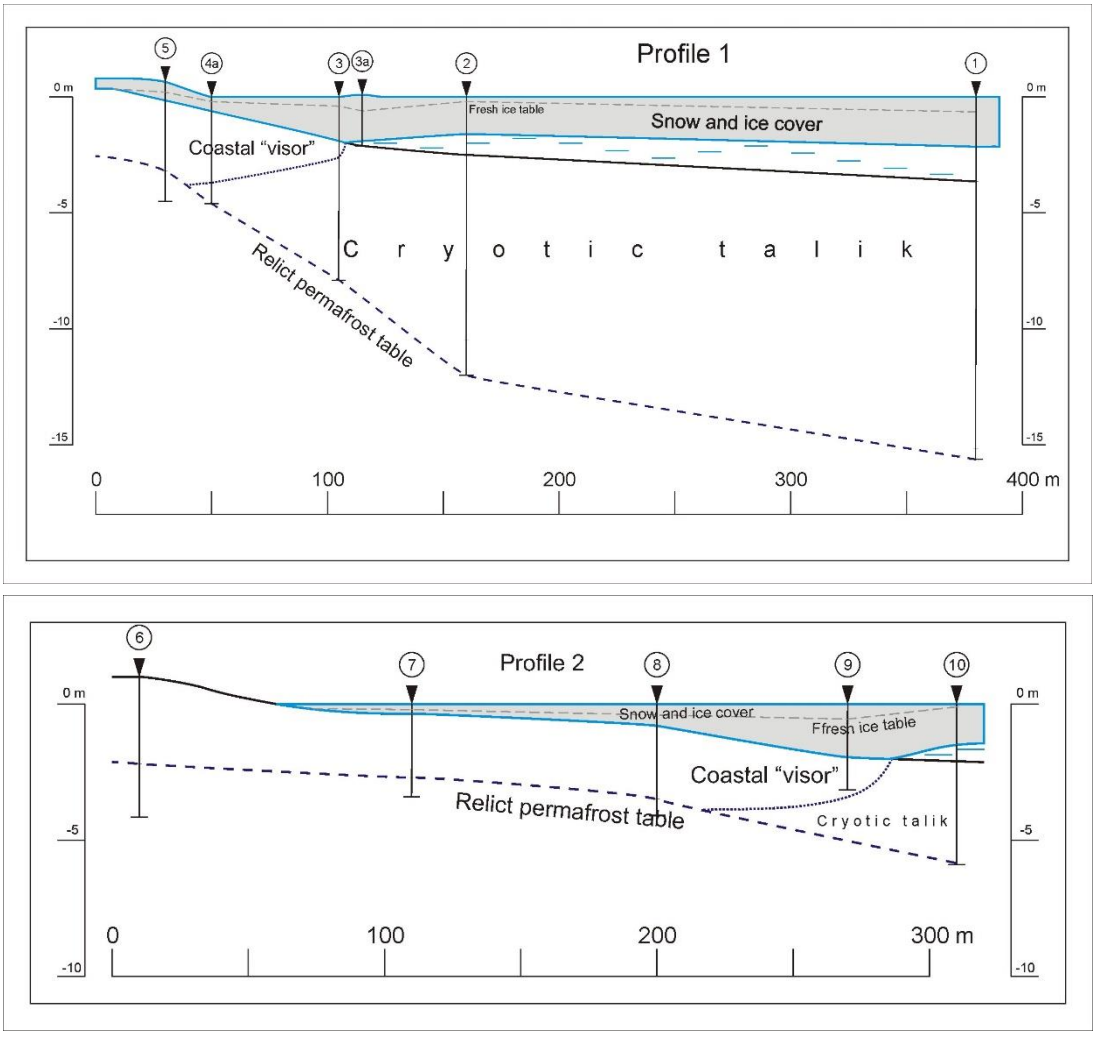

Fig. 2. Geocryological profiles near Mys Kamenniy: profile 1– relatively steep-bottom shore (a); profile 2 – shallow shore (b).

Varandey settlement (Pechora Sea)

Drilling in the area of Varandey was taken in July 2012 at different landforms of Pesyakov Island (beach, laida, coastal barrier and dune belt) to determine depth of permafrost table and temperature of frozen ground [7, 8].

Body of barrier (excluding laida) is composed from well-sorted and well washed mid-fine sands. Sediments of laida have higher content of fine graines (fractions smaller than 125 μm compose 2-12%), and have lower mid-grained sand fraction 250-500 μm (16-18%). Fine-grained fraction fraction 125-250 μm is dominating (76-82%).

The thickness of seasonally-thawed ground at the moment of drilling was 0.8 m on the upped laida, 2.2 m on the terrase barrier surface, 4 m on the top of dune belt, and more than 8 m on the tidal flat. The average elevation of permafrost table in barrier terrace is about 1-2 m higher than sea level. High of permafrost table raises at positive relief forms (on dune belt – up to 2.5 m about above sea level), and sinks below the sea level on the upper beach.

Horizons and lenses of cryopegs (lenses of saline water brine) were found below permafrost table. Cryopegs were found on the depth 0-2.5 and 3.5-7 m below sea level. Water in cryopegs were

under pressure. Water level in boreholes where cryopegs were found rised up on 4.5 m above the assumed level stratigraphy level of cryopegs [8].

The temperature of the top of permafrost at laida in summer is -1°C...-2°C. In the same time the temperature of the top of the permafrost at avandune (which located closer to open sea) in summer does not fall below 0°C. Probably, this is due to the warming effect of the sea.

For the time of drilling lenses of seasonally frozen ground were revealed in the barrier terrace (lower part of active layer) and on the upper part of beach (coastal seasonally frozen cap). They were 0.5-0.6 m thick on the depth 1.5 m, and on the upper part of beach lens was 0.3-0.5 m on the depth 2.2 m.

The lens of seasonally frozen ground at the barrier terrace was attached to permafrost table in some locations, but more often there was layer of unfrozen highly saturated soil between seasonally frozen ground and permafrost table. Lens of seasonally frozen cap, most probably adjoined to steep slope of permafrost core of barrier, and most probably present degraded remains of seasonally frozen ground which form due to adfreezing of land fast ice to the beach (Fig. 3).

Fig. 3. The strip of the wet deposits on the surge berm marks lense of seasonal frozen ground which still hasn't thawed (Pesyakov Island, Pechora Sea). 2012 July. The compact portable rig UKB-12/25 in the foreground.

IV. The technology of the long-term monitoring station establishment

Based on the conducted field works experience and previous investigations [3-5, 9-12] the technology of the long-term monitoring station establishment for the geocryological statement and temperature regime of the Arctic coastal zone observations is proposed. That technology is introduced in conceptual scheme for thermoersional coast (Fig. 4) because it has all three cryolithozones of the Arctic coasts. Besides, this scheme assumes that the drilling is carried out with the compact portable rig UKB-12/25 (Fig. 3).

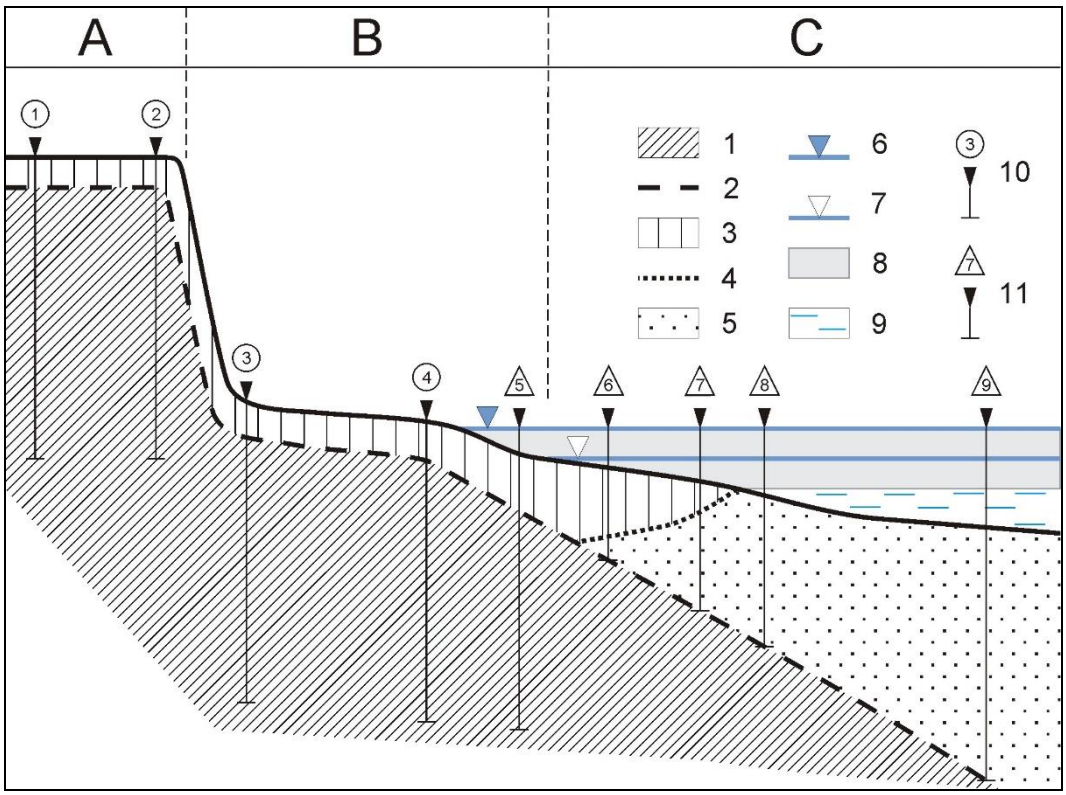

Fig. 4. The conceptual scheme of the long-term monitoring station for the geocryological statement and temperature regime of the Arctic thermoerosional coast observations: 1 – ice-bonded relict permafrost; 2 – table of ice-bonded relict permafrost; 3 – active layer (seasonally frozen and thawed grounds); 4 – bottom of active layer; 5 – cryotic talik; 6 – high tide; 7 – low tide; 8 – fast ice; 9 – sea; 10 – boreholes drilled from the ground (long-term year-round temperature measurements); 11 – boreholes drilled from the ice (repeated single temperature measurements in the winter season). Cryolithozones: A – sub-aerial, B – sub-aerial-erosion, C – sub-sea.

The long-term monitoring station for the geocryological statement and temperature regime of the Arctic coastal zone observations presents itself profile which consists of a series of boreholes. One part of boreholes can be drilled from the ground all year round. They are situated in sub-aerial and sub-aerial-erosion cryolithozones. A thermistor strings with data logger should be installed in each of them for long-term year-round temperature measurements. The number of boreholes depends on the complexity and variety of sub-aerial cryolithozone relief and extension of sub-aerial-erosion cryolithozone. If the sub-aerial cryolithozone is represented by a flat terrace then two boreholes are enough because in this case isotherms are parallel to ground surface and a large gradient is observed only near the coastal bluff. If the sub-aerial-erosion cryolithozone is represented by a narrow beach then two boreholes are also enough (near the foot of the coastal bluff and near the high tide level).

Another part of boreholes should be drilled only from the fast ice in the winter season. They are situated in sub-aerial-erosion and sub-sea cryolithozones. Only repeated single temperature measurements in winter season can be done here. The number of boreholes has defined by parameters of the coastal seasonally frozen cap. The minimum number of boreholes should be five.

Such monitoring station should be kind of coastal permafrost “meteorological station”.

V. Acknowledgment

The work was executed with the financial support of the Russian Science Foundation project No. 16-17-00034.

VI. References

[1] S.A. Ogorodov, V.V. Arkhipov, A.V. Baranskaya, N.G. Belova, A.P. Vergun, A.M. Kamalov, O.V. Kokin, N.V. Kopa-Ovdienko, D.E. Kuznetsov, N.N. Shabanova, "Technogenic factor of coastal dynamics of the Pechora and Kara seas under the conditions of climate and sea ice extent changes", in *Proccedings of the XXV International coastal conference "Coastal zone: a prospective into the future",* vol. 1. Moscow: GEOS, 2014, pp. 114-117 (in Russian).

[2] N.A. Chernikov, *Duga Barkova* (*Barkov's Arc)*. Publishing house of the magazine "Smena", 2006, 238 p. (in Russian).

[3] N.F. Grigoriev, *Cryolithozone of Western Yamal coastal area*. Yakutsk: IMZ of the SR AS USSR, 1987, 112 p. (in Russian).

[4] L.A. Zhigarev, *Oceanic Cryolithozone*. Moscow: Moscow State University Press, 1997, 319 p. (in Russian).

[5] A.N. Khimenkov, A.V. Brushkov, *Oceanic Cryolithogenesis*. Moscow: Nauka, 2003, 335 p. (in Russian).

[6] O.V. Kokin, A.S. Tsvetsinsky, "Geocryological structure of the underwater coastal slope in the Obskaya Bay in the contact area with the fast ice", *News of gas science,* № 3 (14). 2013, pp. 67-69 (in Russian).

[7] A. Abramova, A. Kirillova, O. Kokin, "Permafrost and seasonal frozen ground in coastal zones of Kara and Pechora seas" in *International Conference Permafrost in XXI century: basic and applied researches,* vol. 1. Pushchino: 2015, pp. 127–128.

[8] E. Guégan, A. Sinitsyn, O. Kokin, S. Ogorodov, "Coastal geomorphology and ground thermal regime of the Varandey area, Northern Russia", *Journal of Coastal Research,* in-press.

[9] V.P. Melnikov, V.I. Spesivtsev, *Geotechnical and geocryological conditions of Barents and Kara Sea shelf,* Novosibirsk: Nauka, 1995, 198 p. (in Russian).

[10] P. Overduin, S. Wetterich, F. Gunter, M.N. Grigoriev, G. Grosse, L. Schirrmeister, H.-W. Hubberten, A. Makarov. "Coastal dynamics and submarine permafrost in shallow water of the central Laptev Sea, East Siberia", *The Cryosphere Discuss.*, № 9, 2015, pp. 3741-3775.

[11] M.N. Grigoriev, *Cryomorphogenesis and Lithodynamics of the Coastal-shelf Zone of the Seas of Eastern Siberia,* doctoral thesis, Yakutsk Melnikov Permafrost Institute, 2008, 40 p.

[12] E.M. Chuvilin, B.A. Bukhanov, V.E. Tumskoy, N.E. Shakhova, O.V. Dudarev, I.P. Semiletov, "Thermal conductivity of bottom sediments in the region of Buor-khaya bay (shelf of the Laptev Sea)", *Earth Cryosphere,* 17 (2), pp. 32-40.

THE THEORETICAL BASES OF PORT AREAS AND ACCESS CHANNELS DEPOSITION CALCULATION

Konstantin Makarov, Sochi State University, Russia
Anastasiya Gorlova, Sochi State University, Russia

ktk99@mail.ru

The paper discusses the configuration options of port waters and channels affected by deposition in coastal flow of sediment transport (with/without waves). Performed typing the possible configuration options structures, hydro- and litho-dynamics conditions that lead to reducing the depth of areas and channels. Proposed the engineering method of port areas and channels deposition calculating depending on their configuration, nature and intensity of currents.

Key words: port waters, navigation channels, dredging, waves and currents alongshore sediment transport, deposition.

I. INTRODUCTION

When designing ports, one of the important tasks is to forecast deposition in port waters and approach channels, sandy or pebbly sediments. On the basis of the forecast are determined the frequency and volume of maintenance dredging works.

In the modern literature largely discussed the deposition of approach channels to ports [1-14] and several lesser the deposition of port areas [15-18].

In all the works it is noted that the deposition of approach occurs as a result of speed reduction of alongshore current over the channel due to the increase of depth and, respectively, reduce the carrying capacity of the water flow. In addition, port facilities solid structures may stop completely or partially of alongshore sediment transport with the formation of accumulative forms. In the number of works [9, 11-14, 17-18] for some configurations of hydraulic structures describes physics of the process. However, the classification (typing) options deposition in port waters and approach channels, as well as the general engineering method of calculation is missing.

II. CLASSIFICATION OF STRUCTURES CONFIGURATIONS, AT WHICH THERE IS A DEPOSITION OF WATER AREAS AND CHANNELS

Deposition in port waters and approach channels occurs for the following reasons:

1. The interception completely or partially of alongshore sediment transport by port moles of solid structure with the formation in the waters of the berths of accumulative forms of the type "incoming angle" – Fig. 1, *a*). In such instances when unidirectional sediment transport may occur

grassroots erosion of the shore. In the case of multi-directional sediment transport, incoming angles are formed on both sides of the mole.

2. Unloading of an alongshore sediment transport in a wave shadow of island port with formation of spit – Fig. 1 *b*). In such cases at the unidirectional alongshore stream of deposits, there is a local washout of the coast. In case of multidirectional streams of deposits, the spit can degenerate in tombolo (connected with breakwater).

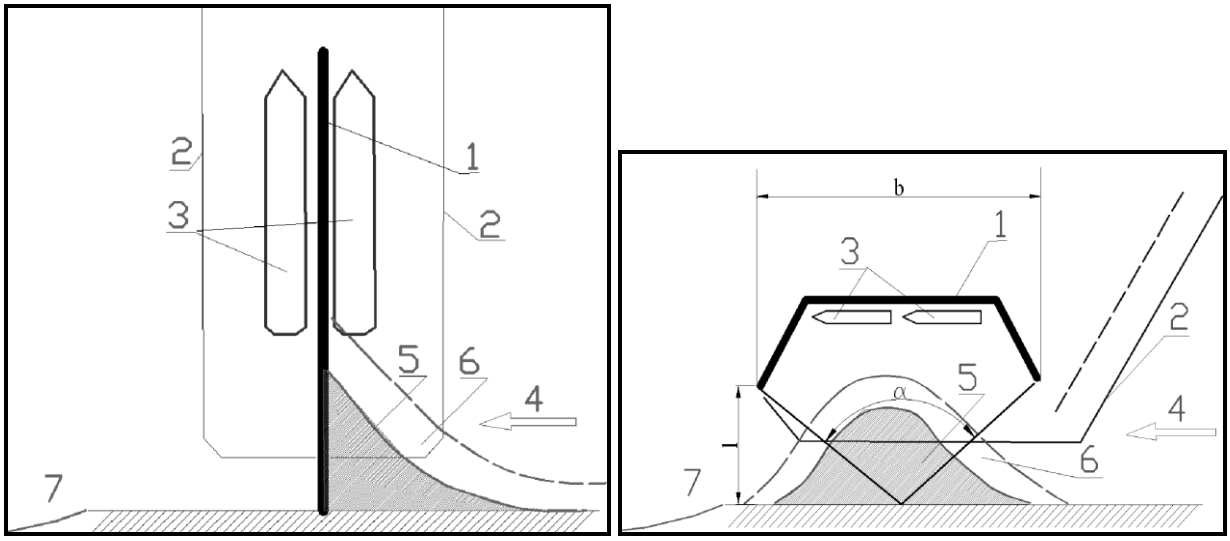

a) *b)*

Fig. 1. Deposition of water of the mole-pier of solid construction a) and water of the island port b); 1 – hydraulic structure, 2 – borders of dredging, 3 – ships, 4 - alongshore sediment transport, 5 – surface part of the sediment load, 6 – the underwater part of the sediment load, 7 – grassroots erosion of the shore.

3. Unloading of alongshore sediment transport on the approach channel when reducing the speed of current at the expense of increase in the area of its live section on dredging of the channel – Fig. 2 *a).*

4. Unloading of an alongshore sediment transport in the water area of dredging or on the approach channel at reduction of speed of an alongshore current as a result of at first its narrowing with increase in speed and, respectively, a stream turbidity, and then its expansion with reduction of speed and loss of deposits. Arises at considerable promotion of protective piers in the sea concerning the line of the coast - Fig. 2 *b).* Thus additional reduction of current is caused also by increase in depths in dredging zones.

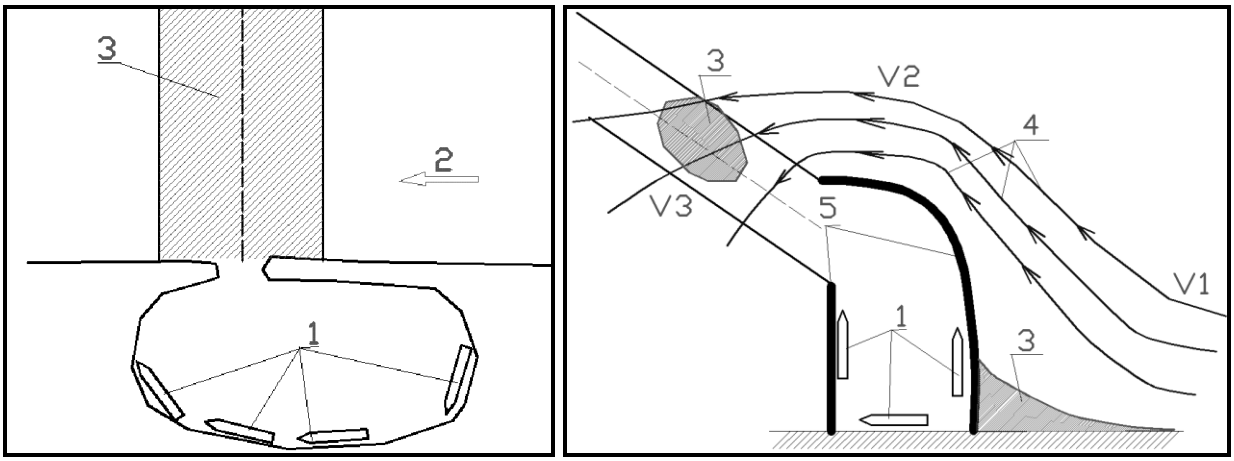

a) *b)*

Fig. 2. Deposition of approach channel as a result of decreasing flow velocity over the channel a) and as a result of expanding of current and increasing the depth on the channel; 1 – ships, 2 – alongshore sediment transport, 3 - accumulation of sediment, 4 – line of flow, 5 – moles.

5. Deposition of port water as a result of the ingress of sediment under the influence of wave and wind currents – Fig. 3 *a).*

6. Deposition of dredging water area, or of the approach channel by sediments of the river flood jet – Fig. 3 *b).*

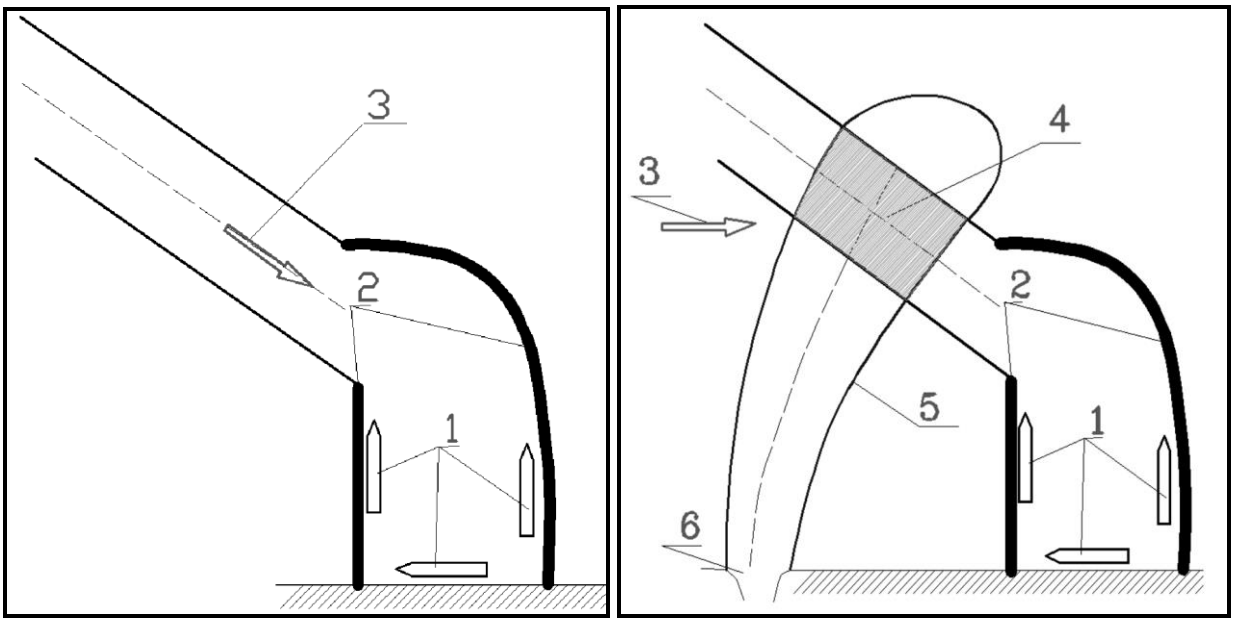

a) *b)*

3. Deposition of the port waters as a result of the total wave and wind currents a); deposition of the approach channel by flood stream of the river rejected by alongshore current b);1 – ships, 2 – moles, 3 – current, 4 – zone of deposition of channel, 5 – boundaries of the jet of river flooding, 6 – mouth of river.

It should be noted [23] that the waves and currents have the opposite effect on alongshore sandy sediment transport in the vicinity of cross shore constructions.

Under the influence of slantwise suitable waves sandy sediments tend to form a cross before the construction of the "incoming angle", that is accumulative form. At the grass-roots plot has place grass-roots erosion due to sediment deficit in alongshore current.

At the same time, current is forms of the cycle before the construction, seeking to erode the shore. Skirting the structure with sea side during "tapering" and its speed increases, it becomes saturated with suspended sediment. After bypass construction, the jet of flow expands, its velocity decreases and the sediment fall out in the head part of the structure on the leeward of him. With bottom-side of construction is formed the second cycle, seeking to form an accumulative form.

III. MODELS OF HYDRO- AND LITHO-DYNAMICS OF A COASTAL ZONE OF THE SEA

For modeling of port water areas deposition it is necessary to define the settlement equations describing the physical processes given above.

The estimated waves elements in the coastal zone can be determined in accordance with [29, 32].

For calculation of wave alongshore transport of pebble deposits the dependence recommended in the normative document [34] can be used. For deposits with an average diameter of $d_{50\%} \geq 2$ mm the transporting ability of a wave stream (capacity of an alongshore sediment transport) is determined by equation:

$$Q_e = 0.087 \frac{\rho}{\rho_s} g \frac{h_{cr1\%}^3 T \Delta t}{k_{ok} d_{50\%}} sin2\alpha_{cr} \quad (1)$$

where $h_{cr1\%}$ - height of a wave of 1% probability in system in the area of the last wave breaking, ρ_s - the volume weight of deposits, ρ - the volume weight of water, g – gravitational acceleration, T - the average period of waves, $d_{50\%}$ - the median diameter of beach material, Δt - time of action of waves, k_{ok} - coefficient of pebbles roundness [34], α_{cr} – angle of approach of waves to the line of the last wave breaking.

For the sand sediment in account with [35]:

$$Q_e = 0.035 \Delta t (\frac{h_{cr}}{d_{cr}})^2 \rho g d_{cr} V_{cp} \frac{tg\varphi_0 (1-(V_{ac}/V_{av})^{3/2})}{(1+3/8(h_{cr}/d_{cr})^2)}, \quad (2)$$

where d_{cr} – depth of wave breaking, V_{ac} - velocity of an alongshore current, average on depth, V_{av} – competent velocity, $tg\varphi_0$ - the slope of beach balance, determined by formulas:

$$tg\varphi_0 = \frac{tg\varphi_e}{1+\left[ln\left(\frac{h_{cr}}{d_{50\%} cos\alpha_{cr}}\right) lg\left(10^5 \frac{h_{cr}}{gT^2} cos\alpha_{cr}\right)\right]}, \quad (3)$$

$$tg\varphi_e = 1 - 0.8 ln \frac{1}{d_{50\%}\left(\frac{\rho_s}{\rho} - 1\right)}, \quad (4)$$

where $tg\varphi_e$ - average bias of a natural slope of material of deposits in quiet water; h_{cr} - height of waves of 30% probability in system of estimated storm at the first wave breaking

Pebble deposits move along the coast in slip or saltation. That is, practically, without coming off a bottom. Thus movement of deposits happens between the line of the last waves breaking and border of their run up on the coast. The maximum of movement of deposits takes place on shoreline

and linearly decreases to the line of waves breaking and border of a run up – Fig. 4. Width of the front of transfer of pebble deposits usually doesn't exceed 100 – 150 m from shoreline.

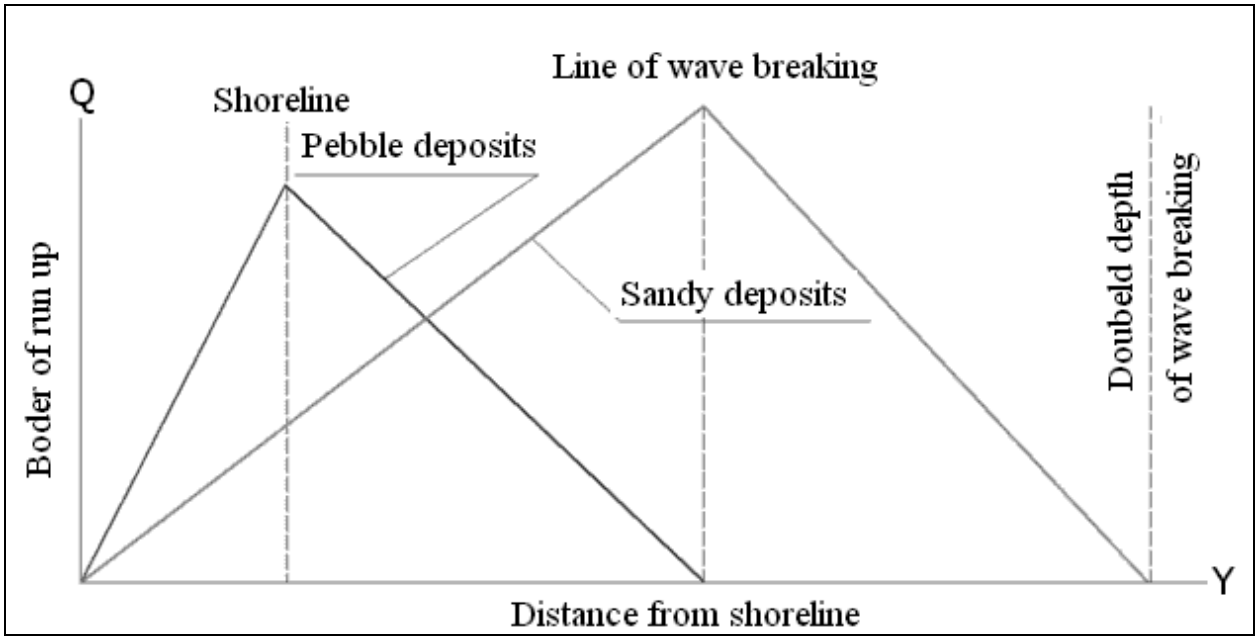

Fig. 4. The schematized diagrams of alongshore transport of pebble and sandy deposits.

Sandy deposits move at the front between border of wave run up and distance from the coast where depth makes the doubled depth of the first wave breaking (width of the front of transfer of sandy deposits can reach 1 km and more). The maximum of movement of sandy deposits by excitement is concentrated on the line of wave breaking – Fig. 4.

Influence of a breakwater of island port (Fig. 1 b) on alongshore wave sediment transport can be estimated by calculation of coefficients of diffraction of waves behind a breakwater [32]:

$$k_{dif} = \sqrt{k_{dif1}^2 + k_{dif2}^2}\ , \qquad (5)$$

where k_{dif1}, k_{dif2} - coefficients of diffraction of waves on head parts of breakwater. In formulas (1) - (3) it is necessary to substitute $h_{dif} = k_{dif}h_{cr}$ and the corresponding depth of wave breaking. Detailed research of this question is executed in work [36].

Surface velocity of drift (wind) currents V_{sf} in the coastal zone are calculated by the method proposed by Ekman and recommended in normative literature [29]. Average in vertical velocity of drift currents in the coastal zone can be defined based on the availability of surface waves by the formula:

$$V_{av} = 0.35V_{sf}\,[2 - lg\left(\frac{d}{\lambda}\right)], \qquad (6)$$

where d is the depth, λ - the average length of surface waves. Approximately $V_{av}/V_{sf} \approx 0.3$.

The transfer (Stokes) wave current in a shallow zone extends in the direction of a wave ray with velocity (formula by Longe-Higgins) [30]:

$$V_{tr} = \left(\frac{5}{4}\right)(a^2 mk)/(sh(md)^2), \qquad (7)$$

where $a = h/2$ - wave amplitude, d - depth, $m = 2\pi/\lambda$, $k=2\pi/T$, T - wave period, λ – wave length.

In the surf zone velocity of transfer current can be calculated according to empirical relationship:

$$V_{tr} = \sqrt{0.333d\left(\frac{h}{d}\right)^2}. \quad (8)$$

The currents caused by various height of wind and wave onset in a coastal zone are called gradient. Gradients of level and, respectively, pressure result. Pressure gradient actually is also the reason of gradient currents. After definition of marks of level of a free surface, calculation of gradient currents can be executed according to recommendations of Shadrin [31].

At calculations of a turbidity of water (the maintenance of a suspension) the limit turbidity of water C, average on depth, kg/m^3 can is determined by a known formula of Rossinsky [26]:

$$C = K_m V^3/(gdW_d), \quad (9)$$

where K_m - empirical coefficient, K_m = 0.24, V - depth-averaged horizontal fluid velocity, d - depth at the point or depth where the average depth velocity is not less than 20% of the surface velocity, W_d – settling velocity of sediment.

Discharge of bottom and suspended sediments from the total currents (Stokes, drift and gradient) per unit width of the front of their transport (m^2/s) is defined by I. Levi [36].

To calculate the distribution of the river flow in the coastal zone in the presence of alongshore current, the special method is developed [37], which implements the theory of turbulent planar jet in a drifting stream [28].

IV. Engineering Calculations of Deposition of Port Waters and Channels

Deposition of port water areas with formation of "incoming angle". To evaluate the deposition of moorings water area by wave long shore sediment transport in the presence of cross structures impenetrable construction (Fig. 1 *a*), it is necessary to calculate the sediment discharge $Q_{m,i}^j$ from the formulas (1) - (4), for each *i* wave dangerous direction and *j* gradation of wave height which has a length Δt_i^j and determine the amount of sediment runoff in an average year:

$$W_{ay} = \sum Q_{m,i}^j \Delta t_i^j. \quad (10)$$

At the same time duration in days of waves from every directions and gradation of wave height is determined by the wind rose:

$$\Delta t_i^j = P_i^j N, \quad (11)$$

where P_i^i - the repeatability of the unrest in the unit shares on average per year, N - the length of the ice-free period in days on average per year.

Next, the width of the front sediment transport (the distance to the last line of wave breaking for gravel deposits or distance to twice the depth of the first wave breaking for sandy sediment) and sediment discharge the diagram (Fig. 4) estimated the average annual share of that falls into the waters of berths W_{ak}. When the area of water recorded as S_{wa}, the average reduction of the depth will be

$$\Delta d_w = \frac{W_{ak}}{S_{wa}}. \quad (12)$$

If necessary, according to formulas (10) - (12) it can be determined the deposition in storms of rare repeatability.

Deposition of island port water areas. As shown in [36], deposition of water of the island by alongshore sediment transport occurs at $l<3b$, where l - the distance from the shoreline to breakwater of island port, b is the length of the breakwater along the coast (Fig. 1 *b*).

If this ratio indicates the possibility of deposition waters of island port, it must first be calculated the coefficients of diffraction of waves for each gradation in each direction - $K^j_{dif,i}$ using the formula (5), Next, calculate the amount of the average annual inflow W_{ayi} by the formula (10) and removal of sediment from the water area of the port of the island:

$$W_{ayr} = \sum Q^j_{m,b,i} \Delta t^j_i, \quad (13)$$

where $Q^j_{m,b,i}$ - the discharge of sediment taking into account diffraction of waves on breakwater of island port. The volume of deposition and depth reduce of the waters in the port area of the island S_{ak} is determined by formula:

$$\Delta W_{ay} = W_{ayi} - W_{ayr}, \quad (14)$$

$$\Delta d_{is} = \frac{\Delta W_{ay}}{S_{ak}}. \quad (15)$$

Deposition of berths or approach channel waters not narrowing of alongshore current by cross structure. When calculating the deposition of berths or approach channel waters not hesitate of alongshore current by cross structure (Fig. 2 *a*), it is assumed that to it is approach the alongshore current with discharge of water per unit width:

$$q_n = V_n d_n, \quad (16)$$

where V_n - total rate of alongshore current on the way to the waters of dredging (channel) with a depth d_n.

Above the water area dredging with a projected depth of $d_{dr} = d + \Delta d$, where Δd - the volume of dredging, velocity of current with same discharge is rate falls to:

$$V_{dr} = \frac{q_n}{d_{dr}}. \quad (17)$$

Consequently, the sediment discharge in dredging zone defined by taking into account the velocity V_{dr} is set to q_{dr}. The difference of sediment discharge, which determines the deposit of water area:

$$\Delta q_{dp} = q_n - q_{dr}. \quad (18)$$

Then the volume of deposition ΔW_{dp} and the average reduction in the depth Δd_{dp} the waters wide flow of sediment B in an area S_{ak} during time T will be:

$$\Delta W_{dp} = \Delta q_{dp} B T, \quad (19)$$

$$\Delta d_{dp} = \frac{\Delta W_{dp}}{S_{ak}}. \quad (20)$$

Duration T of alongshore currents varying speeds from each direction is determined by a rose flows according to field observations or calculated by the wind rose.

Narrowing of alongshore current by cross structure. In case of narrowing of alongshore current by cross structure (Fig. 2 *b*), it is necessary to estimate the width of stream (front of sediment transport) B_{fr}, testing influence of building. In hired from data of model supervisions on the Kaliningrad coast of the Baltic sea, this size is accepted equal $B_{fr} = 1.5L_{cc}$, where L_{cc} is length of continuous part of construction.

Calculation of water deposition as a result of the narrowing and subsequent expansion of

alongshore current execute the following statement. To the pier area with width of front B_{fr} enters the alongshore current at a speed V_n. Flow rate:

$$Q_n = V_n B_{fr} d_{av}, \quad (21)$$

where d_{av} – average depth on width of front.

When approaching the head portion of a structure the velocity of flow is increased to the value:

$$V_s = \frac{Q_n}{0.5 L_{cc} d_{dr}}, \quad (22)$$

where d_{dr} – depth at the head of the structures based on dredging.

The specific consumption of the sediment surrounding the construction of the flow will be q_c. Full sediment discharge:

$$Q_c = 0.5 q_c L_{cc}. \quad (23)$$

After crawling head part of the construction, the stream expands to a width of L_{cc}, while its speed drops to a value

$$V_o = \frac{Q_c}{L_{cc} d_a}, \quad (24)$$

where d_a is water depth after structure with subject to dredging.

Accordingly, the specific sediment discharge in the stream after bypass their structures will be equal to q_o, the total sediment discharge:

$$Q_o = q_o L_{cc}. \quad (25)$$

Then the value of deposition ΔW_d and an average reduction of the depth of the waters Δd_{dp} , located on the leeward side of the pier width X_s, length L_{cc} during time T will be:

$$\Delta W_d = (Q_c - Q_o)T, \quad (26)$$

$$\Delta d_{dp} = \frac{\Delta W_d}{L_{cc} X_s}. \quad (27)$$

Deposition in waters through the gates of the port. Deposition in port waters via its gate (Fig. 3 *a*) is considered for two cases. The entrance gate of the port width of B_p with depth d_p may be located outside the surf zone (major ports), protection structure when submitted to a considerable depth, and in the surf zone (small ports and yacht harbours).

In the first case, deposition of the port water area is determined mainly by the amount of drift and Stokes wave flow V_{sum}, which are calculated by formulas (6), (7).

The specific sediment discharge q_p, penetrating to the waters of the port and the calling deposition in its water area S_p is defined by the formula I. Levy. The full sediment discharge Q_p, and their volume W_p and reducing the depth at the port Δd_{dp} after time T given the action of the hydrometeorological situation (speed and wind direction) are determined by the expressions:

$$Q_p = q_p B_p, \quad (28)$$

$$W_p = Q_p T, \quad (29)$$

$$\Delta d_{dp} = \frac{W_p}{S_p}. \quad (30)$$

To determine the average deposition in the port water area it is necessary to calculate the duration of action of various meteorological situations using the wind rose and summarize the results obtained for them by the formulas (28)-(30).

If it place the entrance gate of the port in the surf zone to pebbly sediments or within the

riparian zone width to twice the depth of the first caving of the waves to the sandy sediment, their long-term average flow is determined by the formulas (1), (2). Further be plots which are shown in Fig. 4 is determined by the volume of sediment transported W_p entering the gate port and the equation (30) calculated a mean annual decrease of the depth in the port basin as a result of deposition.

Deposition of port waters and channels by the solid runoff of rivers. Deposition of port waters and approach channels by the solid runoff of the rivers (Fig. 3 *b*) occurs typically during major floods on the rivers flowing into the sea near the location of port facilities.

Therefore, to calculate the deposition in the port water area is necessary, first, to calculate the discharge Q_0 of the liquid and solid *Qs* flow [25], and velocity of flows of river at its confluence into the sea U_0. Turbidity jet of C_0 at the mouth of the river is determined by the formula (9). In addition, it is necessary to determine the duration of the flood T_r.

On the sea the river turns into a turbulent inertial jet. Friction on the bottom and the interaction with sea water leads to an overall reduction in jet velocity and its spread. River deposits, falling into the region of speeds, lower shift speed, start to accumulate in the form of the alluvial cone. The growth of accumulative the body, the flow meets increasing resistance, loses the stability under the action of waves and coastal currents strays to one side depending on the direction of alongshore current.

Calculation of distribution of the river flow near the port water area to estimate average annual deposition of its water area should be made for flood of annual repeatability, in combination with the most adverse speed and direction of alongshore current carrying flood stream toward the port.

Velocity of alongshore currents can be defined as according to direct observations, as calculated on the wind speed. In the latter case, the calculation is performed according to the formulas (6) to (8).

Next is calculated the trajectory of the river jet in the coastal zone [28, 37]. Turbidity in a jet is determined at any point by the formula (9). Therefore, in the area of dredging in connection with increasing depth of the turbidity in the part of the jet, which lands on the waters, will decrease the value of C_{jet} on the approach to the area of dredging, to the value C_{dr} in this area. Then the volume of deposition in area of dredging, which crosses the jet will be determined by the formula:

$$W_{dr} = \frac{Q_{dr}(C_{jet} - C_{dr})T_r}{\rho_s}, \quad (31)$$

where ρ_s - density of river sediment.

Reducing the depth Δd_s in area of S_{jet} in the zone of penetration of the river jet is determined by the formula (30).

On the elaborated methods was calculated deposition approach channels and operating water areas of the coal port "Sukhodol" in the Bay of Telyakovskiy, Peter the Great Bay sea of Japan (Vladivostok), port for small vessels on the Northern coast of the Kaliningrad region (Pionerskiy) [23], a new yacht Marina in port Sochi, berths of 1A and 1B in the port of Tuapse [37].

V. CONCLUSIONS

1. Classified configurations of the port waters and approach channels from the point of view of their deposition by sediment wave field or not wave currents.

2. Defined theoretical principles and computational formulas, allowing to estimate the deposition of water area and approach channel of the port having the configuration of structures according to Fig. 1 - 3, or their combinations.

3. Developed engineering calculation methods of deposition of water areas and approach channels.

4. Developed methods were applied for calculations of deposition of water areas and approach channels to a set of ports.

Work performed within the state budget scientific research work № 2614 "Development of mathematical models of interaction between waves and hydraulic structures" of Sochi state University.

VI. REFERENCES

[1] Abd El-Halim Mohamed Deabes E. Sedimentation Processes at the Navigation Channel of the Liquefied Natural Gas (LNG) Port, Nile Delta, Egypt // International Journal of Geosciences, 2010. http://www.SciRP.org/journal/ijg.

[2] Approach Channels: A Guide for Design. PIANC Working Group. 1997. 108 Pp.

[3] Vinogradov K. A., Bogatova, Y. I., Sinegub I. A. Approach channels and their importance in the ecosystem function of seaports // *Odessa branch Institute of biology of Southern seas of NAS of Ukraine*, 2012.

[4] Gagoshidze S. N. To assess the impact of alongshore waves on coastal slopes of open sea and river channels // *Proc. scientific papers of St. Petersburg scientific center of RAS*. St. Petersburg: 2011. No. 4, pp. 102-113.

[5] Gubina N.A. The use of storage slots to protect the sea approach channel from sinoimeri // *Hydraulic engineering*, 2007. No. 3. pp. 30-34.

[6] Gubina N.A. Modeling protection from sinoimeri sea approach channel // *Vestnik MGSU. Special issue.* 2010. No. 1. pp. 116-121.

[7] Ilyushin V.Y. Statistical evaluation of the sediment budget of the area of the Kerch Bay and sinoimeri the approach channel of the Kerch sea trading port (KSTP). // *Ukrainskii hudrometeorological journa*l, 2008, № 3, pp. 213-220.

[8] Kozhukhov I.V. Movement of sediment and sensimet approach channels near shallow sandy beaches. *Dis. candidate of geography Sciences*. L., 1980.

[9] Kozlov S.G. Channels, fairways and maneuver areas – problems and solutions // *Hydraulic engineering*, 2011, № 2. pp. 24-27.

[10] Kozlov, S. G. Determination of optimal parameters of navigation channels, fairways and manoeuvring areas and associated problems of safety of navigation // *Sea port hydraulic structures*. Moscow. 2011.

[11] Kuklev S.B., Divinsky B.V., Kozachinsky Y.S. The forecast of sinoimeri sea approach channels methods mathematical modeling // *Hydraulic engineering*, 2012. No. 3. pp. 55-57.

[12] Miroshnichenko V. G. Exploitation of marine channels. M.: Transport, 1982. 136 Pp.

[13] Chikin A.L., Chikina L.G. Modeling transport processes and sedimentation of silt in the approach navigation channels (on the example of the Taganrog Bay) // *Bulletin of the southern scientific center of Russian Academy of Sciences*, 2011. T. 7. No. 2. pp. 45 – 48.

[14] Sepsis V., Klein, A. L. Study of the distribution of sediments along the profile of the Maritime channel // *Problems of operation of sea channels.* M: CRIA the Navy, 1982 (proceedings of Chernomorniiproekt), pp. 62-69.

[15] Van Rijn. Basics of Channel Deposition/Siltation // www.leovanrijn-sediment.com. 2013.

[16] M. Chen, F. De Smedt, Wartel S. Sediment Transport Around Port Development Area in Estuary. *Proceedings of the 7th International Conference on Asian and Pacific Coasts. APAC* 2013. Bali, Indonesia, September 24-26, 2013. pp. 204-213.

[17] Liu J. Study on Sediment in Sea Ports and Coast Protection // *International Conference on Estuaries and Coasts*. November 9-11. 2003. Hangzhou. China. pp. 436-444.

[18] Lumborg U., Windelin A. Hydrography and Cohesive Sediment Modelling: *Application to the Romo Dyb Tidal Area // Journal of Marine Systems*. 2003, vol. 38. Issues 3-4. pp.287-303.

[19] Pandoe W.W., Edge B. L. Cohesive Sediment Transport in the 3D-Hydrodynamic-baroclinic Circulation Model, Study Case for Idealized Tidal Inlet // *Ocean Engineering*. 2004. vol. 31. Issues 17-18. pp. 2227-2252.

[20] Zuo S., Key B.K. Selection of Sediment Parameters and its Application in the Suspended Sediment Concentration Research of the Yangshan Deep-water Port in Shanghai, China // *Proceedings of the Twenty-third (2013) International Offshore and Polar Engineering*. Anchorage, Alaska, USA, June 30–July 5, 2013. p. 1383.

[21] Wang X. H., Andutta F. P. Sediment Transport Dynamics in Ports, Estuaries and Other Coastal. Environments Earth and Planetary Sciences // *Sediment Transport Processes and Their Modelling Applications*. Editor by A. J. Manning, 2013 under CC BY 3.0 license.

[22] Lebedev V.V., Galibin P.A., Belyaev N.D. Engineering Geology. Sensimet coastal engineering. SPb.: Izd-vo SPbSTU, 1996. 53 Pp.

[23] Makarov K. N. Sensimet approach channels and port water areas on the sandy shores // *Lithodynamic bottom surface area of the ocean. Proceedings of the international conference, devoted to 100 anniversary of birthday of Professor V. V. Longinov*. 2009. M.: GEOS. pp. 110-114.

[24] A guide to the methods of research and calculations of sediment movement and the dynamics of the banks for engineering surveys. Moscow: Gidrometeoizdat, 1975. 239 Pp.

[25] SP 33-101-2003. Determination of basic design hydrological characteristics. Moscow: the Gosstroy of the Russian Federation, 2003. 70 Pp.

[26] Rossinsky K. I., Debolsky V. K. Riverine sediments. M.: Nauka, 1980. 218 Pp.

[27] Makarov K. N. Mathematical modeling in marine hydraulic engineering. Sochi: SUTR, 2008, 397 Pp.

[28] Altshul A. D., Zhivotovsky, L. S., Ivanov I. P. Hydraulics and aerodynamics. M.: Stroiizdat, 1987. 414 Pp.

[29] Guide to the marine hydrological forecasts. St. Petersburg: Gidrometeoizdat, 1994. 525 Pp.

[30] Longuet-Higgins M. S. Mechanics of the surf zone Mechanics. *Period. sat. transl. articles*, 1974. No. 1. M.: Mir. pp. 84-103.

[31] Shadrin I. F. Coastal wind and currents of the gradient of the Coastal zone of the sea. M.: Nauka, 1981, pp. 40-46.

[32] SP 38.13330.2012. Loads and impacts on hydraulic structures (wave, ice and from vessels). Moscow: Ministry of regional development, 2012. 112 Pp.

[33] Makarov K. N., Makarova I. L. Simulation of the spreading of suspended solids and bottom sediments during dredging in the port of Tuapse // *Review of applied and industrial mathematics*, 2011, volume 18, issue 1. pp. 128 – 129.

[34] SP 32-103-97. The design of coast protection structures. – M., Transstroy, 1998, 166 Pp.

[35] Recommendations for the calculation of free artificial sandy beaches. – M., Ministry for transport construction of the USSR, 1982, 25 Pp.

[36] Abakumov O.L. Development of Express methods for the calculation of lithosphere dynamics of the coastal zone for the longitudinal hydraulic structures. – Diss. candidate. of tech. Sciences. – St. Petersburg, VNIIG im. B. E. Vedeneeva, 2002.

[37] Ivanov A. V. Mathematical modeling of the pollution distribution in the coastal area for the design of hydraulic structures. – Diss. candidate. of tech. Sciences. Moscow, MGSU, 2012.

MODELING STORM SURGES AND WAVE CLIMATE IN THE WHITE AND BARENTS SEAS

Anastasia Korablina, Lomonosov Moscow State University, Russia
Victor Arkhipkin, Lomonosov Moscow State University, Russia
Sergey Dobrolyubov, Lomonosov Moscow State University, Russia
Stanislav Myslenkov Lomonosov Moscow State University, Russia

jacksparrow91@bk.ru

Russian priority - the study of storm surges and wave climate in the Arctic seas due to the active development of offshore oil and gas. Researching the formation of storm surge and wave are necessary for the design and construction of facilities in the coastal zone, as well as for the safety of navigation. An inactive port ensues considerable economic losses. It is important to study the variability of storm surges, wave climate in the past and forecast the future. Consequently, this information would be used for planning the development of the Arctic in accordance with the development programme 2020. Mathematical modeling is used to analyze the characteristics of storm surges and wave climate formation from 1979 to 2010 in the White and Barents Seas. Calculation of storm surge heights in the seas is performed using model AdCirc on an unstructured grid with a 20 km pitch in the Barents Sea and 100 m in the White Sea. The model AdCirc used data of wind field reanalysis CFSv2. The simulation of storm surge was conducted with/without pressure, sea state, tides. A non-linear interaction of the surge and tide during the phase of destruction storm surge was detected. Calculation of the wave climate performed using SWAN spectral wave model on unstructured grids. Spatial resolution is 500 m-5 km for the White Sea and 10-20 km for the Barents Sea. NCEP/CFSR (~0.3°) input wind forcing was used. The storminess of the White Sea tends to increase from 1979 to 1991, and then decrease to minimum at 2000 and increase again till 2010.

Key words: Arctic, storm surge, wave climate, ADCIRC, SWAN

I. INTRODUCTION

Currently, there are virtually no scientific studies on the features of the spatio-temporal variability of storm surges and wind waves of the White Sea. Some aspects of storm surges and wind waves of the White Sea were touched upon only in a few works published quite a long time ago [1, 2, 3, 5,6,12, 14].

II. MATERIALS AND RESEARCH METHODS

A new method of calculating wind fluttering of the White Sea is proposed. Unstructured settlement area, which covers the entire area of the Barents and White Seas, was built to avoid the

boundary conditions on the open boundary of the computational grid and to reduce the computational cost by using the method of nested grids (Fig. 1, left). Using the unstructured grid with a pitch of 20 km in the Barents Sea and up to 500 m in the White helped to keep the small features of the coastline of the White Sea, small islands and shallow banks and helped to assess their impact on the development and transformation of wind-generated waves. It has to be noted that this area was based on the guidelines of the work [9]. In this paper, we present the evaluation of the effect of the swell generated either in the North Atlantic or in the Barents Sea, on the waters of the White Sea. It turned out that the effect on the White Sea from the North Atlantic swell slightly (height up to 0.2 m) for the area.

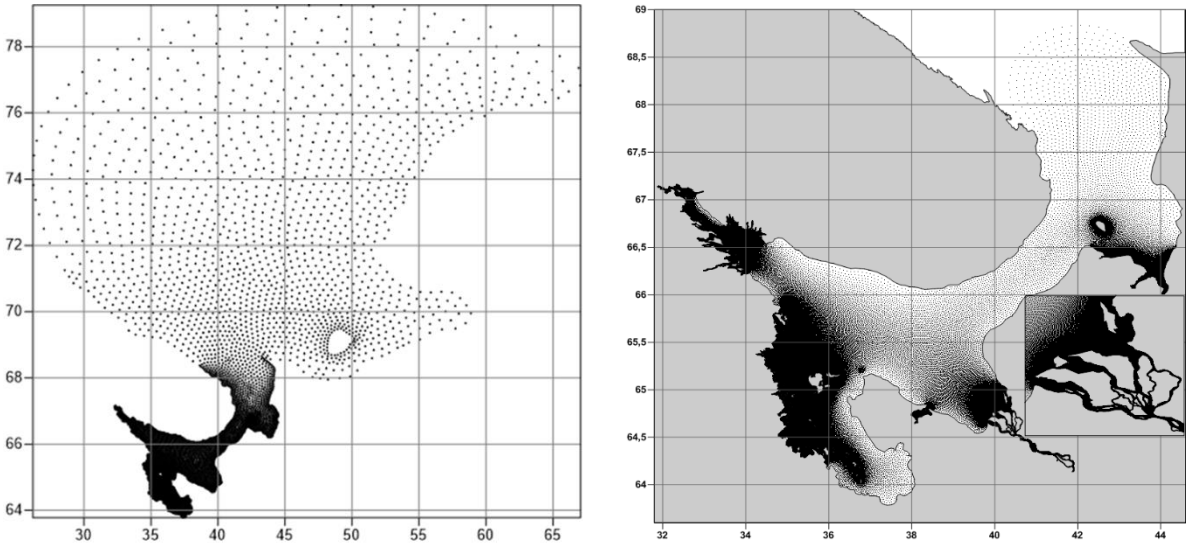

Fig.1. The nodes of the computational grid for calculation wind wave in the Barents Sea (left) and storm surges in the White Sea (right)

Other unstructured triangulation grid for the dynamic system has been created to simulate the storm surge with a system Surface Modeling System (SMS 11) Aquaveo for the White Sea - mouth area (Fig. 1, right) [10]. The grid was created by «paving», i.e. grid construction is based on the number of points on the shoreline [11]. Spacing on the coast in areas of the Gorlo (Fig.2) and the Onega Bay is 3 km away, Voronka - 5 km, on the whole west coast skerries - 150 m, punctuated by a rectilinear portions in increments of 200 m; in Mezenskaya Bay - 150 m, in the Dvina Bay, Delta, mouth area and on the site of the Northern Dvina estuary to the village of Ust-Pinega - 50 m; for the rest of the islands - 75 m (exception: Bolshoy Solovetsky Island, The Velikiy and Morzhovets - 100 m). Thus, the calculated unstructured grid with a minimum resolution of 50 m and a maximum of 5 km was constructed. However, for the second case - storm surge modeling, the calculated mesh has two outer liquid boundaries: at the entrance to Voronka of the White Sea and the Northern Dvina River near the mouth of the Pinega River. At the entrance to Voronka of the White Sea tidal fluctuations of sea level were specified in increments of 1 hour for a period of surge, calculated from the harmonic constant with hydrometeorological station Guba Saviha (39° 7.00 'E, 68° 11.00' N) and Tarkhanovo (43° 39.00 'E, 68° 30.00 'N). At 100 km from the mouth of the Northern Dvina (mouth of the river Pinega) the average river flow (data taken from gauging the village of Ust-Pinega) was indicated.

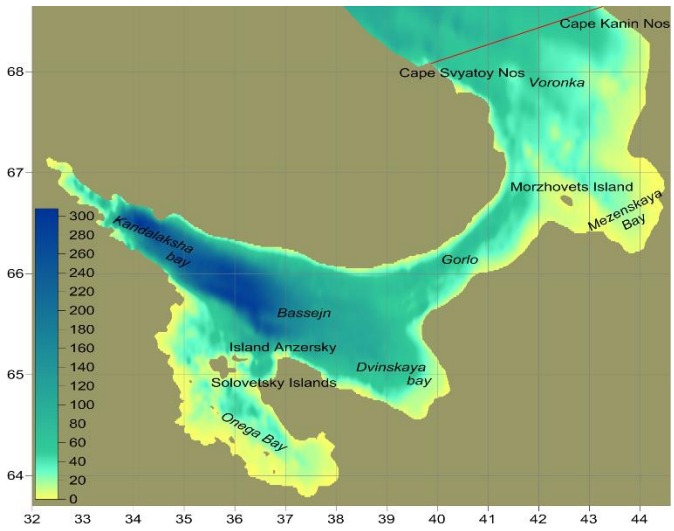

Fig.2 Bathymetry of the White Sea

The spectral wind-wave model SWAN 41.01 third generation was used to calculate the excitement. It is one of the most modern models existing that allows to make calculations of parameters of wind waves in the coastal zone for specified fields of wind and currents, topography of the seabed [13]. This model is being developed and freely distributed by Delft University of Technology. SWAN model is not inferior to the quality of the calculations in deep water on the seas [4] compared to other models (WAM and WATCH III), SWAN can estimate the waves in shallow water, which is especially important for the White Sea. The following characteristics of waves were calculated: height of significant waves (corresponding to 13% probability), the direction, the average period length and the wave height of the swell, the transfer of wave energy. Parameters of the mechanisms that were used in the model were set by default.

Barotropic model ADvanced CIRCulation model for oceanic, coastal and estuarine waters (ADCIRC) was selected to calculate the storm surge in the mouth area of the Northern Dvina River. This model is being developed at the University of North Carolina (USA). The model has a time-dependency, is non-linear, on the f-plane, takes into account wind pressure, atmospheric pressure, tides, rivers influence. The properties of the underlying surface can be defined in the model. It works with an unstructured computational grid that is needed for the seas with a complex configuration of the shoreline. In addition, it takes into account the flooding and drainage of adjacent land. This is the only licensed model to calculate the storm surge in the United States. It can be used in conjunction with a spectral wave model SWAN for the account of the wave surge, which is absent in all other models.

As input wind fields for numerical calculations high-resolution data reanalysis NCEP/CFSR (Climate Forecast System Reanalysis) for the period from 1979 to 2010 was used. This reanalysis is selected for the reason that it has a high spatial (~ 0.3°) and temporal resolution (1 hour), and a comparison of data on wind speed and direction reanalysis CFSR, MErra, JRA, Era Interim data of weather stations in the Arctic basin showed that the reanalysis CFSR has minimal error and a good correlation with the observed data [7].

As input data on topography and configuration of the coastline of the White Sea and Barents Sea open maps of the General Staff and GosGisTsentr of different scales depending on the study

area were digitized. Due to the presence of sea ice analysis of wind waves was conducted only during the ice-free season (May to December).

III. WAVE CLIMATE RESULTS AND DISCUSSION

From Fig. 3 it can be defined there exist two areas where the highest waves are formed throughout the year in the White Sea. These are the areas Bassejn and Voronka. In these areas, there is an increased intensity of emotion from spring to autumn. For example, in May in the Bassejn wave height 13% of the supply reaches 3.5 m in November — already 5.5 m. In Voronka in May wave height is about 5.5 m, in November - 10.5 m. In the first case the intense development of the waves is due to the presence of relatively large distances to disperse the wind, in the second area the presence of large wave heights is due to their spread from the Barents Sea.

The Gorlo plays a special role. This strait is a barrier on the way of spreading of high waves from a Voronka as well as from the Bassejn. For example, in November to the northern part of the Gorlo waves of heights of 5 m come from the Voronka. Wave height is slightly lower - up to 4 m coming into the southern part of the Strait from Bassejn. However, in the Strait wave heights are reduced to 3 m and, interestingly, these tongues of high waves spreading from different sources do not reach each other.

Onega Bay spatial structure of heavy sea is due to its large reserve, the presence of the Solovetsky Islands at the entrance to the bay. However, spreading of the high waves of the Bassejn through the Strait East Solovetsky Salma was observed despite the isolation. Wave height of 13% probability in the Gulf does not exceed 2.5 m.

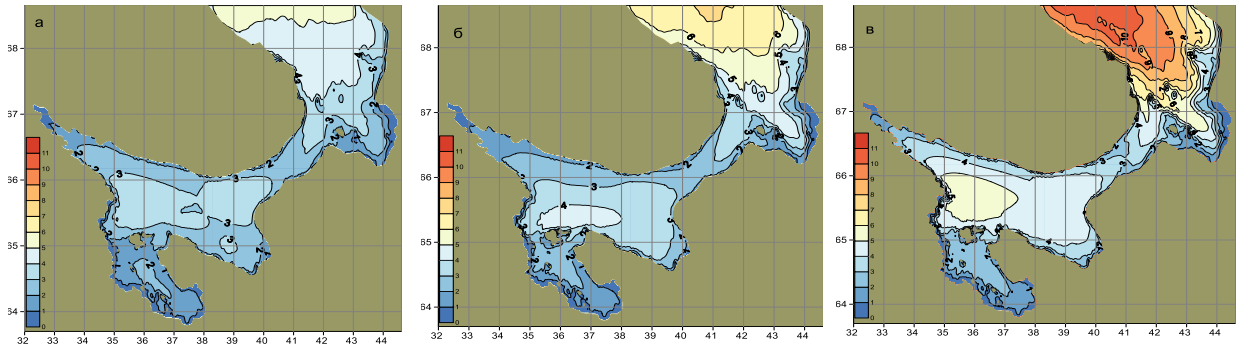

Fig.3. Significant wave height (meter) in May (1), August (2), November (3)

Fig.4 shows the extreme wave height 13% probability (significant wave) possible once in 100 years. It can be seen that in the Bassejn there may be significant waves up to 7 meters, in the Voronka up to 13 m, in the Onega Bay of up to 3 m.

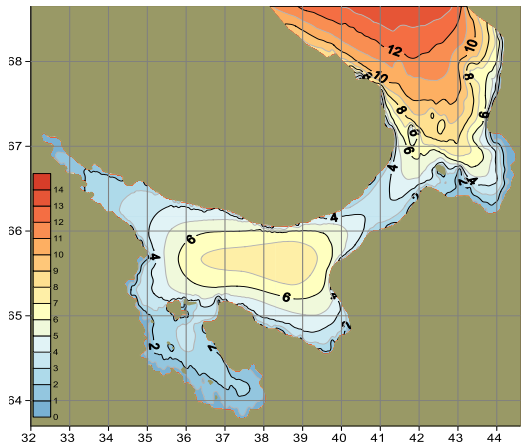

Fig.4 Extreme wave heights characteristics 13% probability possible once in 100 years

The maximum calculated average periods of T-10 waves are shown in Fig. 5. It can be seen that in May the average wave period in the Onega Bay reaches 5 seconds, Bassejn 6-7 seconds, in the Voronka — 9 seconds. By November, the average wave period in the White Sea is greatly increasing, especially in the Voronka. Thus, the average period of the waves in the Onega Bay is of approximately 6 seconds, 8 seconds in the Bassejn, and in the Voronka for 12 seconds.

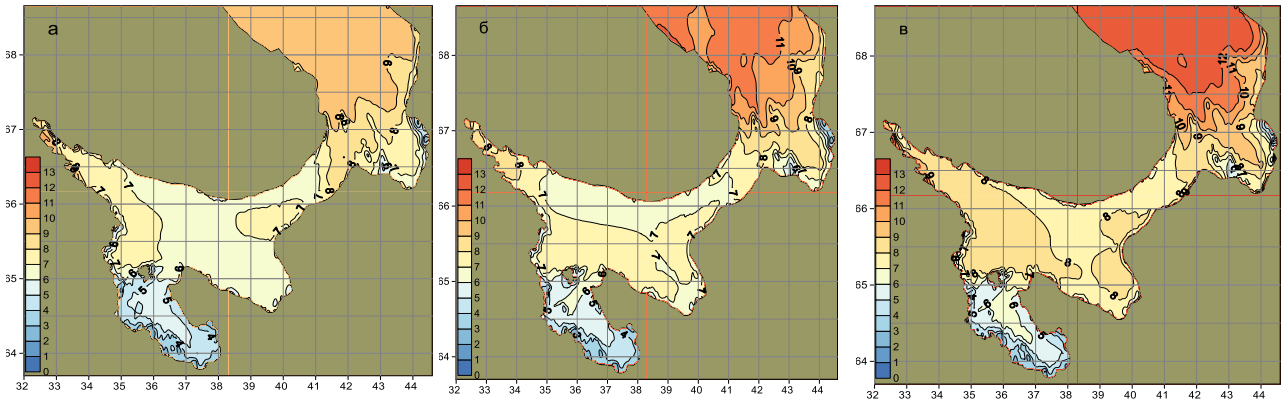

Fig.5. Period T-10 (seconds)in May (1), August (2), November (3)

The maximum calculated wavelengths in the White Sea are shown in Fig. 6. The smallest wavelength occurs in May in the Onega Bay. Here, it reaches only 25 meters In the Bassejn — wavelength increases up to 50 m The largest wavelengths were observed in the Voronka - 100 m The wavelength in the Bassejn (especially in the western part) and the Voronka significantly increased in November to 75 and 200 m, respectively. In the Onega Bay, it is about the same, but the occupied area increases. No wavelength greater than 60 m is observed in the Gorlo of the White Sea.

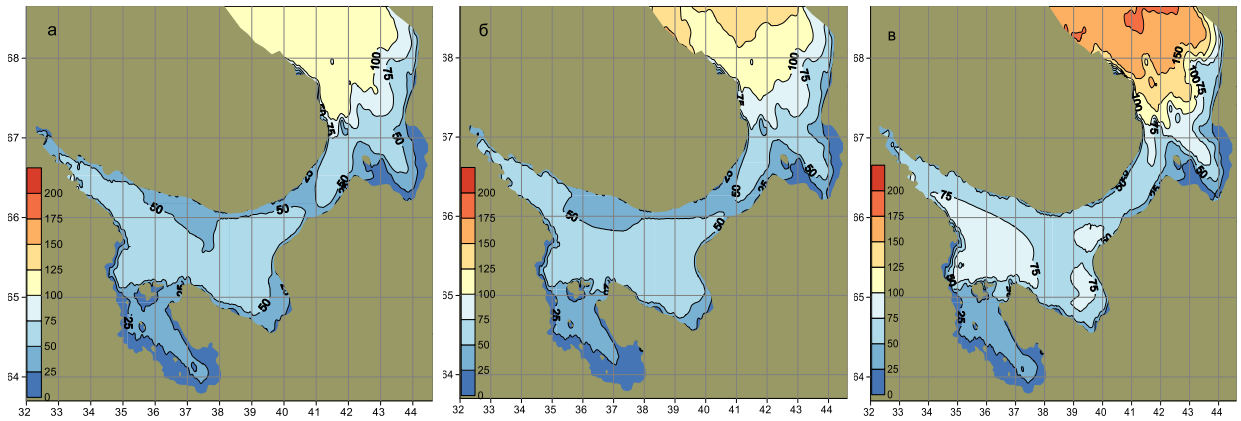

Fig.6. Wavelength (meter) in May (1), August (2), November (3)

The spatial distribution of swell height in the White Sea is very interesting (Fig. 7). In May, in the Onega Bay, Bassejn and Gorlo swell height does not exceed 1 m. Only in the Voronka, it increases up to 3 meters. By November, the height of the swell increases up to 3 m in the western part of the Bassejn and up to 9 m in the Voronka. In the central part of the Gorlo, it remains the same, indicating the inability of swell transit through the Gorlo into the White Sea. It also can be noted that Mezenskaya Bay, despite the presence shallow banks on the north and Islands Morzhovets, is still under the influence of wave processes, formed in the Barents Sea.

Temporal variability of wind waves in the White Sea was calculated to study the number of synoptic situations with different wave heights (more than 2, 3, 4 and 5 m) in the Bassejn and the Voronka (Fig. 8).

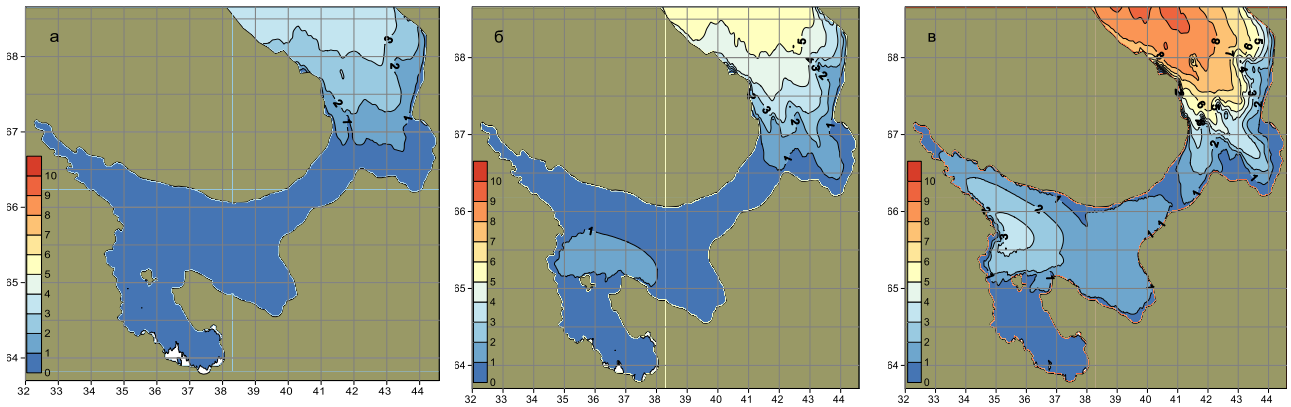

Fig.7. Swell height (meter) in May (1), August (2), November (3)

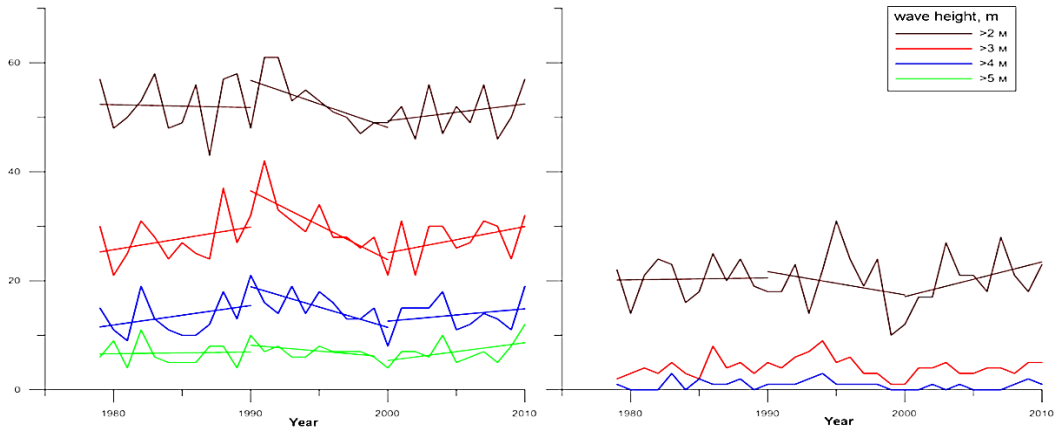

Fig.8. Number of synoptic situations with different height of wave in the Voronka and Bassejn

The number of synoptic situations of wave height of more than 2 m (50-60 events) in the Voronka is about 3 times more than in the Bassejn, of heights of more than 3 m (25-40 events) already5-6 times more. Cases with wave heights greater than 5 m in the the Bassejn are rarelynoted, while in the Voronka they occur 10 times a year.

Temporal variability of the number of synoptic situations clearly stands out in the Voronka of the White Sea. In the decade, 1979-1989 there is an increase in weather patterns. In 1992-1994 is the maximum of such cases. Then their sharp decrease until 2000. Then a gradual increase until 2010. A similar picture is observed in the Bassejn.

On average over the period from 1979 to 2010, trends to increase or decrease the amount of storm situations were not noted.

In conclusion, the wave climate of the White Sea is characterized by increased storm activity in autumn and winter months, a significant spatial and temporal heterogeneity of the properties of wind wave fields, the determined areas with different wave mode: Onega Bay, Bassejn, Gorlo, and Voronka.

IV. STORM SURGE RESULTS AND DISCUSSION

Storm Surges in the White Sea are mainly caused by the release of deep cyclones of two types - "diving" (repeatability about 88%) and Atlantic. "Diving" cyclone - an extratropical cyclone, characterized by a special path, for example, from north to south, and high travel speeds. Such cyclones move from the Barents Sea through Finland into the central western area of the county to the lower Don, from Cape Kanin Nos through Kirov to Tatarstan and then to the lower fieldsof the Ural River.

Due to the tidal character of the White Sea preliminary numerical calculations of tids were made using ADCIRC model. Te comparison of numerical calculations with field measurements of sea level of Solombala showed that systematic error was about 10% (Fig. 9). Points shown in Fig. 10 were chosen for analysis of storm surge.

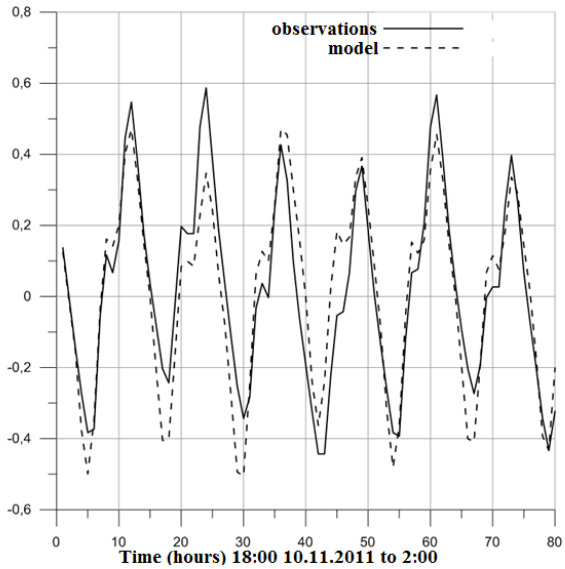

Fig.9. Comparison of the calculated and observed sea level (m) Solombala (point №8, Fig. 10)

Let's consider the use of mathematical modeling techniques to study the characteristics of the formation of storm surges in the dynamic system of the White Sea - mouth area of the Northern Dvina River on the example of storm surge in November 15, 2011. This storm surge was of the largest height level, flooding area and duration of standing.

Fig. 10 shows the spatial distribution of the height of the storm surge in the mouth area of the Northern Dvina in the phase of maximum development. The height is calculated as the difference between the height of the level obtained by the models and precomputed level tide (tide level fluctuations are excluded). Fig. 10 shows that storm surge extends from the north-north-west of the Dvina Bay. This causes a difference in height of storm surge as it enters the channels of the river delta. Thus, in Korabel'nom estuary surge height is 0.8 m, and in the mouth Pudozhemskom – 0.6 m. As the storm surge moves from seaside wellhead to the mouth of the Northern Dvina (district Solombala) its height increases from 0.5 to 2 m.

Features of water circulation (tidal currents are excluded) in the Dvina Bay in the mouth area of the Northern Dvina in the different phases of the storm surge are shown in Fig. 11, 12. In the phase of maximum speed raising of sea level (up to 8 hours maximum) the flow of water in all the channels is directed to the river mouth, and in the structure of the flows in the channels there are significant differences in flow velocity, and the spatial distribution (Fig. 11). Maximum flow rate (1.2 m/s) is indicated in the Korabelnoe channel with about the same speed on the width of the channel. In Murmansk and Nikolskij channels flow rate reaches 0.7 m/s, there are differences in flow velocity along the width of the channels. It is also shown that in Pudomzheskij, Murmanskij and Korabelnoe estuaries there are small cyclonic circulations of water.

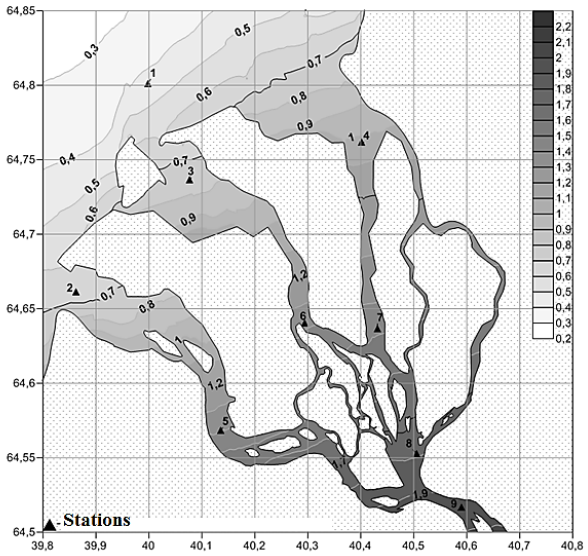

Figure 10. The height of the storm surge (m) in the mouth area of the Northern Dvina in the phase of maximum development. Stations for the analysis of time course the level 1 - near the wellhead coast of the delta of the Northern Dvina, 2 - Pudozhemskoe estuary, 3 - Murmanskoe estuary, 4 - Korabelnoe estuary, 5 – Nikolskij channel, 6 – Murmanskij channel, 7 – Korabelnoe channel, 8 - near the post Solombala, 9 – Bakaritsky channel.

In the period of greatest decreasing rate of sea level (7 hours after the surge peak) a complex spatial structure of water circulation is formed. In the Korabelnoe channel flow is directed towards the mouth of the river to Murmanskij channel, here it turns to Murmanskij channel, where the opposite flow happens - in the direction of the seaside wellhead of delta of the Northern Dvina river at an average speed of 0.7 m/s (Fig.12). Water circulation becomes complicated in structure taking the form of cyclonic and anticyclonic eddies in the mouth of the Murmansk. The flow in the Nikolskij channel is directed towards the seaside wellhead directly from the mouth of the river at an average speed of 0.5 m/s. The flow's direction is from east to west with an average speed of 0.6 m/s in the Dvina Bay.

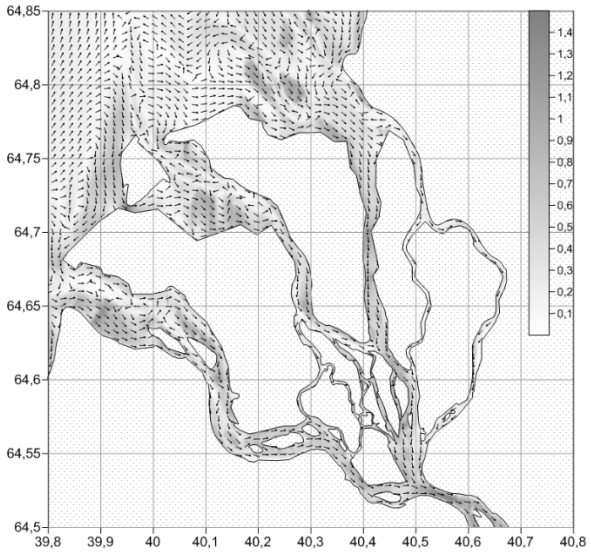

Fig.11. Waters circulation in the Northern Dvina estuarine area in the growth

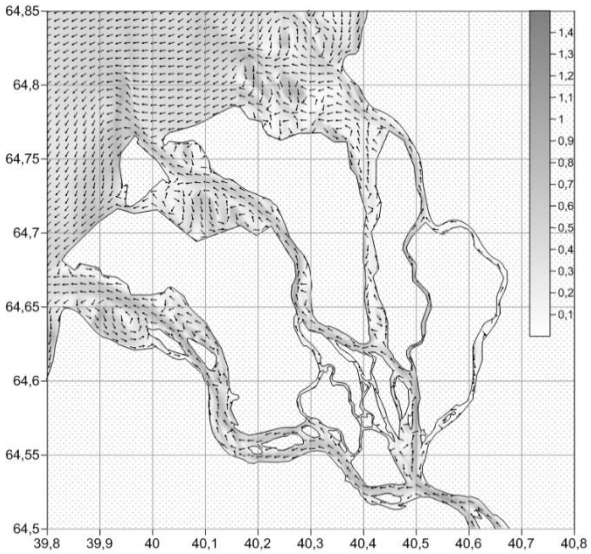

Fig.12. Waters circulation in Northern Dvina the estuarine area after the maximum

phase storm surge (grayscale – flow speed, m/s)

phase storm surge (grayscale – flow speed, m/s)

Fig. 13 shows a comparison of the height of the storm surge observational data and simulation results. (The height of the storm surge from observational data obtained as the difference between the observed level and the height of the tide precomputed.). The height of the surge in model data and field are the same, but as far as the phase is concerned, model time of the onset of the greatest height of surge is ahead of the largest maximum of observations for about 10 hours. This difference is likely due to the characteristics of the wind field of reanalysis data.

For the study of nonlinear interaction between high tide and storm surge it is common to use the difference between the level calculated on the full model, followed by net Precomputing tide level, and the level calculated by the model without considering the tide [8]. It was revealed that in the initial phase of development of surge nonlinear interaction is absent (the difference between the levels is negligible). In the phase of destruction the nonlinear interaction of the greatest surge is during the period of low water level and the lowest during the period of high water (Fig. 13).

For the study of the propagation of the storm surge from the seaside to the top of the Northern Dvina delta graphs of the height of the storm surge changes at different points of the river mouth area on the data model (Fig. 14) are drawn. At all points of the mouth area the speed level rise substantially more than its speed reduction. The rate of level rise in the region Solombala reached 1 m for 5 hours and lowering speed - 0.3 m for 5 hours. Therefore, there exists the asymmetry in the rate of change in sea level during rise and fall of sea level during the storm surge. Model results showed that the time of the maximum surge from the seaside wellhead to the mouth of the river is 2 hours (Fig. 14).

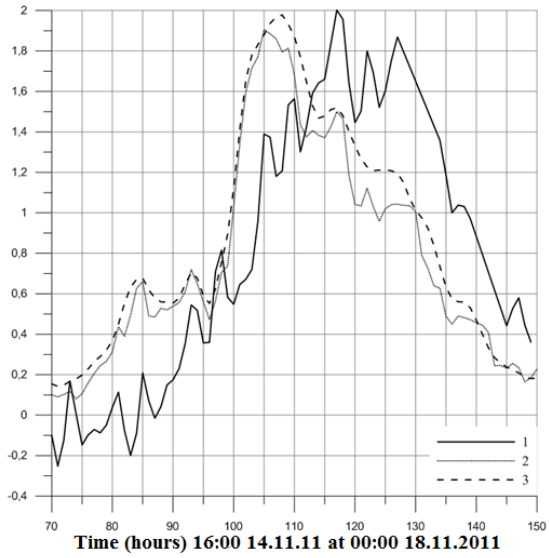

Fig.13. Storm Surge height (m) in the Solombala (point No. 8, Fig. 3): 1 – observations; 2 –the difference between the level calculated by the model, and the pre-calculated tide level; 3 – calculated by the model without considering the tide

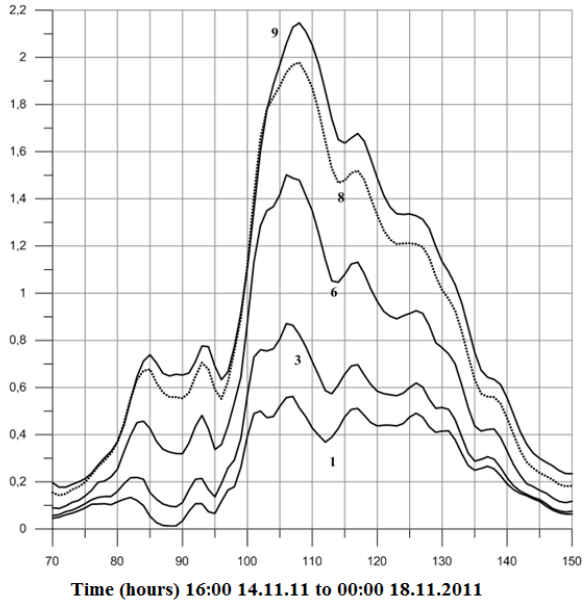

Fig.14. Change the height of storm surge (m) at its mouth of the Northern Dvina (the numbers station, see Fig. 10)

V. ACKNOWLEDGMENT

The study was performed in the framework of the Russian Science Foundation (project 14-37-00038).

VI. REFERENCES

[1] *Atlas of wave and wind of the White Sea,* Arhangelsk: Sev. UGKS, 1965.

[2] Belov V.P., Filippov Ju.G., "Numerical simulation of total fluctuations in the White Sea", *Meteorology and Hydrology*, №7, 1985, pp. 63–69 (in Russian).

[3] Inzhebejkin Ju.I., *White Sea level fluctuations,* SPb, RGGMU, 2004 (in Russian).

[4] Gusdal Y., Carrasco A., Furevik B.R., Sætra Ø. "Validation of the operational wave model WAM and SWAN". Norwegian Meteorological Institute, *Oceanography,* report no. 8/2010, Oslo, 2010, 24 p.

[5] Korobov V.B. "Storms in the White Sea", *Sbornik rabot Gidromettsentra Severnogo UGKS,* Arhangelsk, vol. 1, 1987. pp. 59–75 (in Russian).

[6] Korobov V.B. "Maximal wind waves White Sea", *Meteorology and Hydrology*, №1, 1991, pp. 86–91 (in Russian).

[7] Lindsay, R., Wensnahan M., Schweiger A., Zhang J. "Evaluation of Seven Different Atmospheric Reanalysis Products in the Arctic", *J. Climate,* V. 27, 2014, pp. 2588–2606

[8] Murty T.S. *Storm surges - Meteorological ocean tides,* Department of fisheries and oceans, Ottawa, 1984.

[9] Myslenkov S.A., Arkhipkin V.S., Koltermann K.P. "Evaluation of swell height in the Barents and White Seas", *Moscow University Bulletin*, Series 5. Geography. 2015. №5 (in Russian)

[10] Resio D.T., Westerink J.J. "Modeling the physics of storm surges", *Physics Today*. 2008, pp.33–38.

[11] *SMS Surface-water Modeling System User Manual* (v11.1), 2013.

[12] *The "Sea of the Soviet Union". Hydrometeorology and hydrochemistry of USSR seas*. Vol. 2. White Sea. Vol.1 Hydrometeorological conditions, edited by B.H. Gluhovskij, Leningrad, Gidrometeoizdat, 1991 (in Russian).

[13] *User manual SWAN Cycle III version 41.01AB*. 2015. http://swanmodel.sourceforge.net/

[14] *Wind and waves in the oceans and seas. Reference data. Register USSR*. – L.:Transport, 1974, 359 p., (in Russian).

INVESTIGATIONS OF THE BALTIC SEA COASTAL ZONE ABOVE-WATER PART TOPOGRAPHY DYNAMICS BY MEANS OF TERRESTRIAL LASER SCANNER (SVETLOGORSK CITY, KALININGRAD REGION)

Nikolay Lugovoy, Lomonosov Moscow state university, Immanuel Kant Baltic Federal University, Russia
Askar Ilyasov, Lomonosov Moscow state university, Russia
Elena Pronina, Lomonosov Moscow state university, Russia
Vladimir Belyaev, Lomonosov Moscow state university, Russia

lugovoy-n@ya.ru

The paper describes application of the terrestrial laser scanner for investigation of coastal dynamics of the Svetlogorskaya Bay, Baltic Sea. Methods of investigation and results of surveys repeated over the two consecutive years for quantification of coastal erosion and slope processes within the coastal zone are presented.

Keywords: Baltic Sea, coastal geomorphology, geoinformatic methods of investigation, terrestrial laser scanner.

I. INTRODUCTION

Northern coastline of the Sambiyskiy Peninsula (Kaliningrad Region, Russia) is characterized by actively eroded cliff from 5 to about 60 m high above the sea level. It is a subject of active hillslope processes provoked by wave erosion of the cliff base. The existing protective and enforcing constructions in the coastal zone are in unsatisfactory conditions and cannot provide necessary protection of the eroded cliffs from hazardous processes. It is therefore important to determine spatial distribution and dynamic variability of coastal erosion. This task requires regular morphometric observations by means of cartographic and geodetic methods. Combined use of the existing maps and remote sensing data can provide general understanding for longer time intervals between dates of the information sources available, or for zones where coastal retreat has catastrophic rates. This can be explained by absence of the detailed-scale maps (larger than 1:10000) for the coastal zone. Problem for detailed measurements from the remote sensing data sources is widespread forests along the cliff break within the studied areas. The most effective approach for quantification of coastal dynamics is in most cases regularly repeated geodetic surveys. Local researchers from the “Baltberegozaschita” have installed a network of fixed geodetic points used for regular surveys of cliff profiles at a number of locations [1]. Authors have attempted to use the same network for organization of cliff surveys by means of the terrestrial laser scanner (further – TLS) system (Fig. 1).

II. FIELD SURVEY METHODS

The TLS technology is actively used for large-scale geomorphic monitoring in various environments. It is particularly useful for the coastal zones dominated by eroded retreating cliffs. [2, 3]. Its major advantage is in its detailness and automation as survey (after the scanner is appropriately configured) is carried out automatically and covers the entire area of interest with required density of the survey points. TLS application also allows carrying out distant measurements for the locations unreachable by surveyors (such as extremely steep cliff faces). Its disadvantage, however, is in complexity of the post-processing caused by large number of survey points and necessity of their filtration due to possible presence of reflective objects unrelated to the topographic surface, such as vegetation.

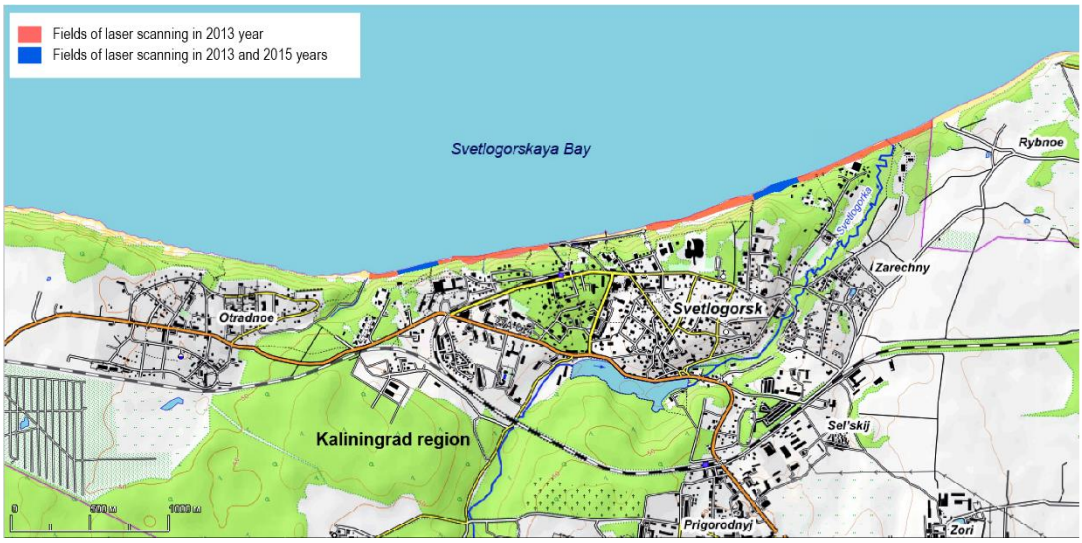

Fig. 1. Location of surveyed cliff sections along the Svetlogorsk coastline.

The first field survey was carried out in February, 2013 along the Svetlogorsk City coastal cliff sections with total length of survey about 3 km (Fig. 1). The TLS system used was MDL LaserAce 600P. Fieldworks were carried out during wintertime when deciduous trees were devoid of leaves, thus decreasing their reflectance and making the post-processing point filtering less laborious. In order to guarantee complete coverage of the surveyed coastline area, scanning was carried out from seven geodetically fixed position. Their locations were arrange to allow partial mutual coverage of the adjacent survey scenes. At least 4 orienting target points were used within every survey scene. Prior to the scanning, geodetic coordinates of the survey point and orienting target points were determined by means of the differential GPS (further – DGPS) survey by pair of the Trimble 5700 receivers. Measurements were obtained in the static regime allowing the spatial accuracy within 2 cm. Obtained geodetic coordinates of the survey point and orienting target points in unified coordinate system were later used for orienting each of the TLS survey scene within the same coordinate system. That allows integration of several separate survey scenes into a single point cloud.

Repeated survey of active cliffs along the same coastal section was carried out in November, 2015 (Fig. 1). In this case survey points were located in areas where maximum visibly evident cliff deformations occurred during the time interval passed since the first survey (22 months). As during

the first survey, DGPS survey in static mode was used for obtaining geodetic coordinates of the survey point and orienting target points with the accuracy required.

III. Geoinformatic methods of the TLS survey data post-processing

Post-processing of the TLS survey spatial point clouds was carried out using the software package CloudCompare version 2.6.1. The raw scanning schemes for the two survey dates initially represented in the local polar coordinate system from the survey points were recalculated basing on the DGPS measurements into a single local rectangular coordinate system. Having the control points measured both by DGPS and TLS made it possible to check the orientation precision. It was found out that discrepancies of control points coordinates between DGPS and TLS surveys does not exceed 2-3 cm.

Raw point clouds of the TLS survey characterize different types of objects. As our survey purpose was to investigate topographic surface dynamics, it was required to remove all raw points unrelated to reflections from the topographic surface. This post-processing operation is required to minimize distortion of final output. The filtration procedure was carried out semi-automatically using the CloudCompare software package algorithm Canupo described in details elsewhere [4]. Firstly the training samples were selected for points representing reflections from non-topographic surfaces. Secondly the software algorithm automatically removed all the points falling into the training samples selection criteria. Example of the raw point cloud filtration for vegetation is shown on Fig. 2.

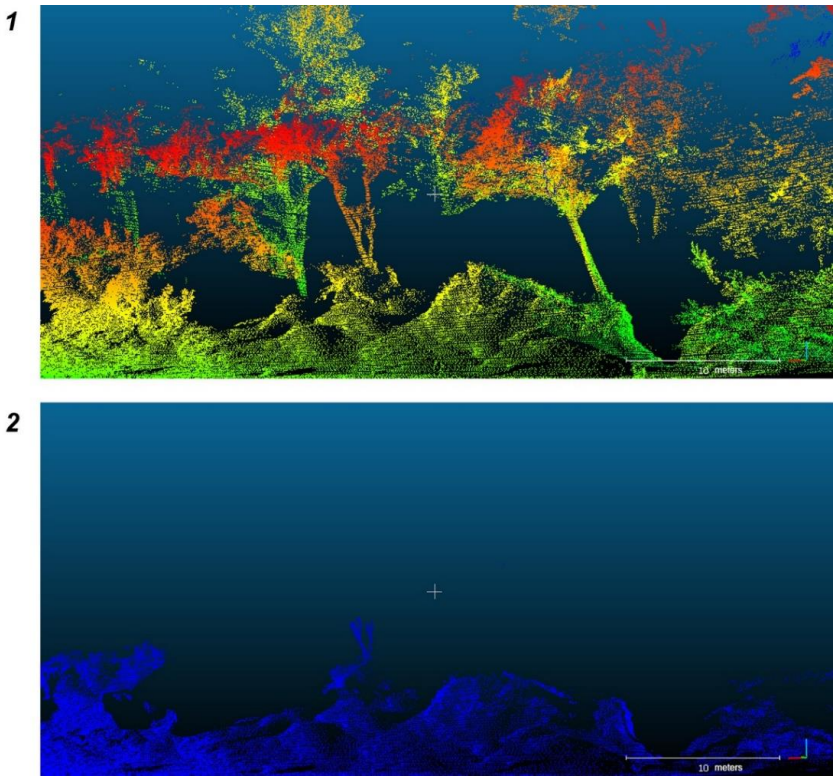

Fig. 2. Examples of the Canupo cloud filtration algorithm performance for vegetation (1 – raw points cloud with visible vegetation reflections; 2 – filtered cloud with vegetation reflections removed).

IV. RESULTS

After post-processing and integration into a single coordinate systems of the 2013 and 2015 survey point clouds they were compared by the Cloud Compare software package. The algorithm used for that purpose measures orthogonal distances between the point clouds being compared. The resulting point cloud with values representing the orthogonal distances between the source point clouds can be used directly for quantification of the relief dynamics. Example of such derivative point cloud visualization for one (eastern) of the surveyed coast sections containing 309036 survey points is shown on Fig. 3. Zones of dominant coastal cliff denudation and deposition along its base are clearly visible. Voids in the image represent partial data loss in one of the initial survey scenes. Possible reasons for that are either data filtering of vegetation reflections or partial lack of coverage due to some obstacles related to differences of the scanner orientation between the two surveys.

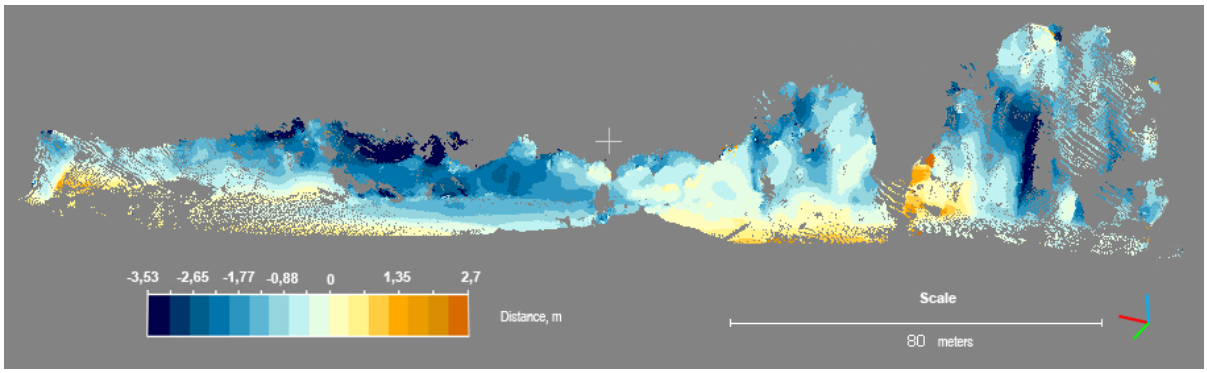

Fig. 3. Results of the two year survey point clouds (2013 and 2015) comparison for one of the monitoring sections.

Another possible way of quantitative analyses is based on histogram of distribution of the derivative point cloud values showing negative or positive distances between the two source point clouds from 2013 and 2015 surveys. Example of such histogram for the same survey section is shown on Fig. 4. Even from simple visual analysis it is evident that this particular section of the coastal cliff is dominated by denudation, with cliff retreat values exceeding 1 m over the 2013-2015 period for about 30% of the total number of the survey points.

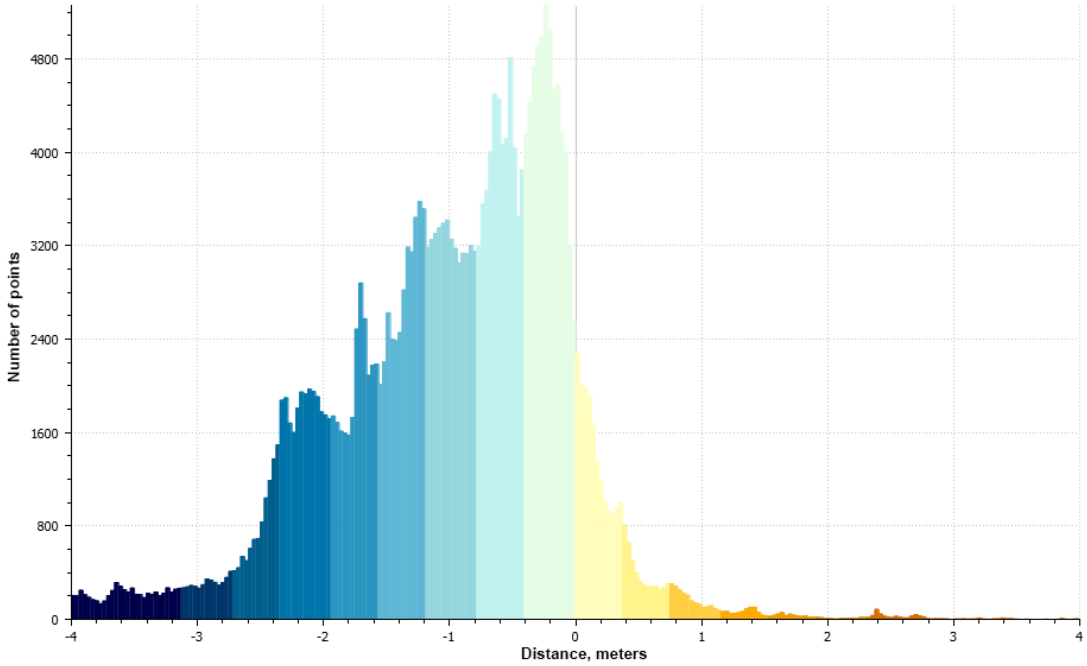

Fig. 4. Histogram of distances distribution between the two year survey point clouds (2013 and 2015).

Calculations of morphometric characteristics and volumetric assessment of coastal cliff dynamics were performed by the Autodesk Civil 3D software package with the Volumes Dashboard module. Thus module employs the calculation algorithm comparing triangulation surface models for each of the source survey point clouds and constructing a derivative composite surface used for volumetric differences estimation. Total area of scanning scenes being compared is 6987 m^2. According to the survey results, total volume of the coastal cliff retreat over the 22 months passed between the consecutive surveys was estimated as 7512 m^3, while volume of deposition along the cliff base and on the adjacent beach surface – 1173 m^3. Mean value of cliff retreat from the derivative point cloud representing orthogonal distances between the source survey point clouds is -1.68 m.

V. Geomorphic interpretation of the TLS survey results

The 250 m long surveyed coastal section is located at the eastern outskirt of the Svetlogorsk City between the two pedestrian descents (staircases) to the sea from the “Rus” hotel and the “A.P. Gaidar” children rest house. Of its total length the easternmost 150 m are characterized by coastal cliff height about 7-10 m composed of dense glacial loams overlain by layers of loose alluvial and aeolian sands [5]. The western 100 m of the surveyed section is characterized by sharp increase of the cliff height up to 30 m. Higher part of the cliff is composed of interbedded dense glacial boulder loams and loose glaciofluvial sands and silts. Lithological composition of the higher cliff section favors active development of landslides, screes and earthfalls. Further to the west of the scanned section protective construction represented by gabion wall 4 m high was installed at the cliff base in 2008. This construction unsuitable for high cliff protection is already in damaged conditions. Its presence, nevertheless, results in declined volume of beach-forming sediment eroded from that part

of cliff and available for longshore drift further eastward. This causes increased erosion of sand beaches along the gabion wall and downdrift, i.e. at the surveyed section. Average width of sandy beach along the gabion wall decreased from 30 to 5 m since 2008. Beach width along the scanned cliff section is 10-15 m under the high western part of the cliff and up to 30 m under the eastern part.

Analyzing the comparative orthogonal distances derivative point cloud visual representation (Fig. 3) and histogram (Fig. 4) the following methodic shortcomings must be noted. Firstly we have attempted to compare the scanning scenes surveyed from not exactly the same points with slightly different orientations of the scanner. This results in different detailness of surveys in the most problematic parts, potential presence of no-data zones obscured by cliff face irregularities, vegetation or other obstacles, seriously decreasing the quality of final results. Scanning of the cliff sections covered by bushes and trees, even devoid of leaves and not very dense, has not produced geomorphically meaningful results. Most of such zones on the visual representation of derivative point cloud are represented by voids (no-data zones in at least one of the source point clouds).

Nevertheless, the obtained results allow certain geomorphic interpretation. Firstly, it has been shown that average cliff retreat rate along the studied coastal section is about 0.9 m/year. Retreat of the lower part of the cliff is more spatially uniform with maximum values of 3 m per 22 months observed along its upper break with developed aeolian microtopography. At the same time, along the higher cliff section spatial variability of retreat rates is much higher with evident relatively stable zones separated by abruptly retreating areas of freshly collapsed landslide and earthfall scars with maximum retreat rate up to 4 m per 22 months. Colluvial deposits along the high cliff base are represented by zones of its temporary advance towards the sea up to 3 m. At the low cliff base, in contrast, there are only limited zones of ephemeral beach and aeolian sedimentation with amplitude up to 1 m. Average volume of material delivered on the beach surface by complex denudation of the cliff has also been estimated as about 15 m^3 per 1 m of the coast length over the 22 months observation period.

The work was partly financed by the Russian Scientific Fund (grant 14-37-00047).

VI. References

[1] Burnashov E.M. Modern dynamics and environmental conditions of the Kaliningrad Region coastline. Ph.D. in Geography Thesis. Barnaul-2011.

[2] Olsen, M.J., Johnstone, E., Kuester, F., Driscoll, N., Ashford, S.A. New automated point-cloud alignment for ground-based light detection and ranging data of long coastal sections // Journal of Surveying Engineering 137(1), 2011, pp. 14–25.

[3] Rosser, N.J., Petley, D.N., Lim, M., Dunning, S.A., Allison, R.J. Terrestrial laser scanning for monitoring the process of hard rock coastal cliff erosion // Quarterly Journal of Engineering Geology and Hydrogeology 38 (4), 2005, pp. 363–375.

[4] Brodu N., Lague D. 3D terrestrial lidar data classification of complex natural scenes using a multi-scale dimensionality criterion: Applications in geomorphology // ISPRS Journal of Photogrammetry and Remote Sensing. 68, 2012, pp. 121-134.

[5] Zhindarev L.A., Habidov A.Sh., Trizno A.K. Dinamika peschanyh beregov morej i vnutrennih vodoemov (The dynamics of the sandy shores of the seas and inland reservoirs). Novosibirsk, Nauka Publ., 1998. 271p.

CONCENTRATION OF HEAVY METALS AND OIL PRODUCTS IN THE SEABED SEDIMENTS OFF THE COAST OF THE CURONIAN SPIT (THE SOUTHEASTERN PART OF THE BALTIC SEA)

Alexander Krek, Immanuel Kant Baltic Federal University, Atlantic Branch of P.P. Shirshov Institute of Oceanology, Russian Academy of Sciences, I. Kant Baltic Federal University, Kaliningrad, Russia

alexander.krek@gmail.com

During spring and summer (2014) environmental investigations of the sea coastal zone, conducted in the frameworks of the Baltberegozaschita (Kaliningrad) program, determinations of content of heavy metals and oil products in the bottom sediments along the shore of the northern coast of the Kaliningrad Region were performed. The highest values of their contents were found in the middle part of the Curonian Spit (near the border with Lithuania). According to Swedish classification WGMS 2003-SSQC these values correspond to the highest 4 and 5 Classes of Contamination. At the Curonian Spit, which is a protected area, unknown any significant sources of anthropogenic pollution. Supposedly, the origin of the detected anomaly is connected with influence of along shore bed load, directed from abrasive coast of the Sambia Peninsula along the Curonian Spit, to its middle part, where accumulation of sedimentary material is dominated. The shore of the Sambia Peninsula is much more populated and used for recreational purposes, and can therefore be considered as a possible source of contamination.

Key words: Southeastern Baltic Sea, alongshore suspended sediment transport, seabed sediments contamination by heavy metals and oil products

I. INTRODUCTION

Coastal zones are characterised by intensive urbanization [1]. Consequently, they suffer from considerable anthropogenic impact. In addition, coastal waters due to active hydrodynamic factors are the most dynamic in comparison to other parts of the sea basin. Here, sedimentation in occurs more rapidly as a result of numerous processes: winds and waves as well as local atmospheric circulation patterns [3, 4].

As a result of the active circulation, an intense mechanical separation of polydisperse solid particles occurs [5] together with redistribution of contamination, which depends on the sorption capacity of the sediment and the size of the particles.

The present research is particularly relevant taking into account the fact that the Curonian Spit is a unique nature site, which is on the UNESCO World Heritage list.

II. MATERIALS AND METHODS

Samples from the underwater coastal slope and beaches of the northern coast of the Sambia Peninsula and the Curonian Spit were taken from a regular sampling uniform grid of profiles with 2 km interval (Fig. 1). In each profile, samples of sediment were collected from the sea botom at a depth of 10 m by a "Van Veen" grab during the period 19-31.05.2014. The beach sediment samples were collected in the period 10-18.06.2014 and comprised samples collected from the whole width of the beach starting from the water edge. To identify possible sources of contamination samples were also collected near coastal settlements Primorye, Otradnoe, Svetlogorsk, Pionersky, Zaostrovye, and Lesnoy.

In order to determine the content of heavy metals (Cd, Cu, Pb, and Hg) and oil products (OP) in coarse sediments, the data of environmental monitoring during oil extraction at the "Kravtsovskoye" (D-6) platform were used. The data obtained from the engineering and environmental surveys, and exploratory drilling in the promising oil-bearing structures (158 values in total) were also used (see. Fig. 1).

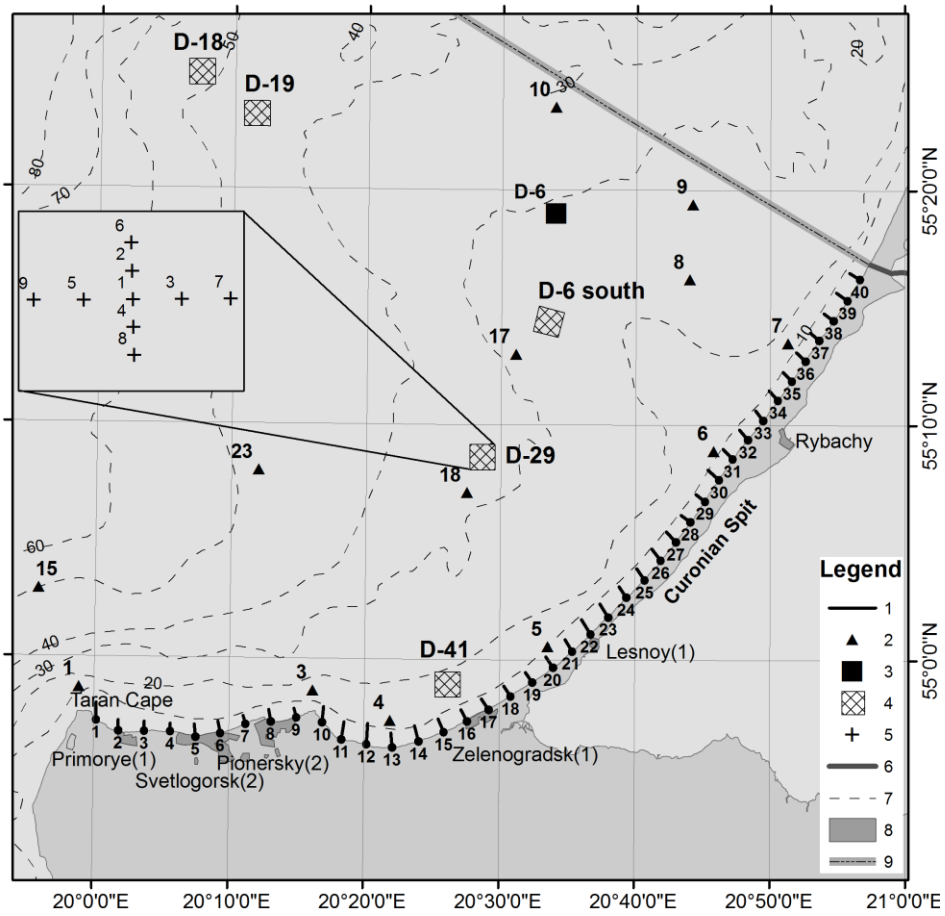

Figure 1. Area of investigations. Legend: 1 – Sampling profiles in 2014; 2 - Background points; 3 - The sea ice-resistant fixed platform D-6; 4 – Sites of engineering and environmental surveys, environmental monitoring during exploratory drilling in the oil-bearing structures; 5 - Sediment sampling points in the oil-bearing structures (background); 6 - The state border with Lithuania; 7 - Isobaths, m; 8 - Coastal settlements (in parentheses - the number of samples taken in the residential areas); 9 - Exclusive Economic Zone (EEZ).

The physical property analysis - the particle size analysis - was done by sieve tests, using the Krumbein phi scale [7]; the mesh sizes of the sieve were 4.0; 2.8; 2.0; 1.4; 1.0; 0.71; 0.5; 0.355; 0.25; 0.18; 0.125; 0.09; and 0.063 mm.

The chemical analysis of soils and sediment samples was carried in the "Centre of laboratory analysis and technical measurements of the Kaliningrad region". The concentrations of Pb, Cd, Cu, Ni, Zn were determined by atomic emission spectrometry; Hg concentration was identified using the flameless atomic absorption and the content of oil products - by the IR spectrometry.

The Swedish classification WGMS 2003-SSQC was used to assess sediment contamination [8]. The general direction of the alongshore sediment transport was determined according to [9]. It helped to identify the prevailing vectors of sediment contamination. Calculation of the alongshore sediment-driving force was performed for the period of October-March of 2013-2014. The data on the wind speed and wind direction were obtained from Automatic Hydro-Meteorological Station Minikrams-4, located on the off-shore D-6 oil platform at a height of 27 m. The wind speed was calculated for the height of 10 m [10].

The particle size analysis [11] was used to confirm direction of the last significant bed load in the linear sector of the underwater coastal slope of the Curonian Spit (profiles 19-40).

III. RESULTS

Seabed sediment

Seabed sediments in the studied area were mainly composed of sands of different grain size having a median diameter of 0.26 ± 0.36 mm. Coarse sediments (boulders, pebbles, gravel at profiles 15, 16 and 18, respectively) were found only at the base of the Curonian Spit. This sediment distribution pattern is typical of coastal zones [12]. Generally speaking, a decrease in the median particle diameter and, as a consequence, a change in the sediment types were observed from the Taran Cape, and eastward, along the Curonian Spit to its middle part.

Toxic substances were found in almost all industrial discharges and household runoffs [12], the main source of contamination being seaside settlements, rivers and transboundary transport [13]. The average concentration of heavy metals was usually higher than the background level of contamination (Table 1).

The Sambia Peninsula is densely populated; it is a seaside resort visited by many tourists. The density of the population and the number of tourists result in contamination. However, the maximum concentration of pollutants (Hg, Cu, Ni, Pb, Zn and OP) was registered along the underwater slope of the Curonian Spit (Table 2). The reason for such substantial differences may be the alongshore transport of suspended sediment, which drifts from the deeply eroded coastline of the Sambia Peninsula along the Curonian Spit, to its middle part, where sediment accumulation prevails [14-18].

The Cu distribution pattern is of particular concern. The Cu concentration corresponding to Contamination Class 5 was registered near the Rybachy settlement (profiles 28, 32, 34, 35, 38 and 40 having 240, 170, 340, 150, 160, 240 mg/kg, respectively). It should be noted that during the 2013-2014 environmental monitoring of “Kravtsovskoye” D-6 oil platform, the Cu concentration corresponded to Contamination Class 4 and 5 (in 2013–110 mg/kg and 200 mg/kg; in 2014 - 110 mg/kg and 300 mg/kg in the background points 7 and 6, respectively).

The Ni and Pb content matched Contamination Class 5 in some tests at profile 32 (Ni - 120 mg/kg) and profile 33 (Pb - 130 mg/kg); Zn – Contamination Class 4 only at profile 33 (230 mg/kg). The highest concentrations of oil products were registered at profile 33 (650 mg/kg) and profile 35 (1380 mg/kg), with a average of 59.8 ± 45.9 mg/kg, significantly exceeding the background value (<40 mg/kg).

Table 1. The average content of heavy metals in the seabed sediments compared to their background values

Heavy metal	The content of toxic metals in the coastal zone (2014)				Contamination class according to [8]	Background value	σ	Contamination class according to [8]
	Min	Max	Average	σ				
	mg/kg							
Cd	<0.05	0.96	0.42	0.25	2	0.36	0.63	2
Cu	0.98	340	67.8	74.6	4	10.3	31.4	1
Ni	<0.5	120	7.1	19.2	1	-	-	-
Pb	<0.5	130	5.4	21.0	1	1.64	2.35	1
Zn	4	230	13.7	13.5	1	-	-	-
Hg	<0.005	0.01	0.005	0.002	1	0.005	0.007	1

Table 2. The ratio of pollutants in the seabed sediments of the Sambia Peninsula and the Curonian Spit underwater slopes

Pollutant	The Sambia Peninsula (profiles 1-17)				The Curonian Spit (profiles 18-40)			
	Min	Max	Average	σ	Min	Max	Average	σ
	mg/kg				mg/kg			
Hg	<0.005	0.007	<0.005	-	<0.005	0.01	0.005	0.002
Cd	<0.05	0.96	0.46	0.26	<0.05	0.86	0.40	0.23
Cu	0.98	56	25.3	18.6	20	340	98.7	84.7
Ni	0.67	12	5.41	4.02	<0.5	120	8.41	25.24
Pb	<0.5	19	1.71	4.64	<0.5	130	8.03	27.34
Zn	5.7	24	14.7	4.6	4	230	26.1	48.7
OP	<40	120	52.6	36.3	<40	1380	151.8	305.4

Coastal research

The average content of pollutants on the beaches (Table 3) is multiply lower than that of the underwater coastal slope. The exception was Zn, the concentration of which was comparable to that in the seabed sediments. The most polluted beaches were those of the Sambia Peninsula (Table 4), suffering from direct anthropogenic impact as well as from both municipal and non-municipal (untreated) sewage water runoffs from the coastal settlements [13].

Table 3 - The content of pollutants in the beach sediment

Pollutant	The minimum concentration	Maximun concentration	The average concentration	σ
	mg/kg			
Cd	0.06	0.54	0.2	0.12
Cu	<0.5	85	14.47	19.32
Ni	<0.5	4.8	1.76	1.26
Pb	<0.5	5.8	0.96	1.06
Zn	1.4	190	11.31	30.21
Hg	<0.005	0.008	<0.005	-
OP	<40	72	<40	-

Table 4. Pollution of the Sambia Peninsula and the Curonian Spit beaches: a comparative analysis

Pollutant	The Sambia Peninsula				The Curonian Spit			
	Min	Max	Average	σ	Min	Max	Average	σ
	mg/kg				mg/kg			
Hg	<0.005	<0.005	<0.005	-	<0.005	0.008	<0.005	-
Cd	0.08	0.54	0.24	0.14	0.061	0.39	0.16	0.08
Cu	0.88	89	21.2	24.4	<0.5	45	9.0	11.9
Ni	0.86	4.2	1.83	0.72	<0.5	4,8	1.7	1.6
Pb	<0.5	3.5	0.95	0.84	<0.5	5,8	0.96	1.24
Zn	2.1	190	19.8	44.2	1.4	8.1	4.4	2.0
OP	<40	72	<40	-	<40	50	<40	-

As it was expected, the average content of pollutants in the settlements of the Sambia Peninsula was much higher than on the beaches: Cd - 0.53 ± 0.19 mg/kg; Cu - 28.43 ± 7.76 mg/kg; Ni - 2,63 ± 2.03 mg/kg; Pb - 5.36 ± 4.44 mg/kg; Zn - 28.43 ± 28.86; Hg - 0.28 ± 0.51 mg/kg; OP - 181.29 ± 157.76 mg/kg.

The study identified potential contamination sources (settlements on the northern coast of the Sambia Peninsula) and the area of accumulation of contamination (underwater coastal slope near the Rybachy settlement) in many indicators (Fig. 2).

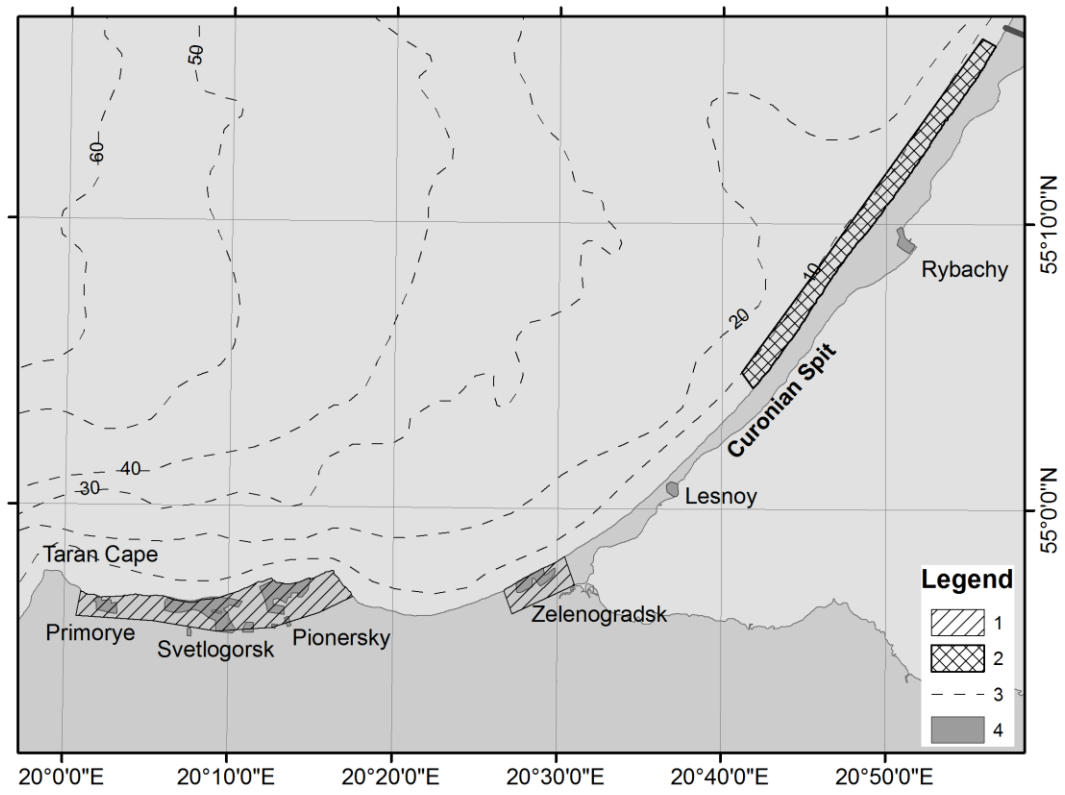

Fig. 2. Areas of potential contamination and accumulation of pollutants.
Legend: 1 – Pollutants input areas; 2 – Areas of massive contamination (Contamination Class 4-5 for Zn, Ni, Pb, Cu calculated according to WGMS 2003-SSQC [8] and oil products multiply exceeding the background values); 3 - Isobaths, m; 4 - Coastal settlements.

IV. Discussion

On the Curonian Spit, a protected nature reserve, there are no sources of anthropogenic pollution. Presumably, the reason for the identified deviations from the norm is the impact of the alongshore suspended sediment transport. Many authors [14-26] confirmed the presence of the alongshore transport of suspended sediment. It is important to note that the recent works [25-26] have been carried out using the meteorological data of the second half of the XX century. Given climate change [27-31], meteorologists have observed changes in wind and wave patterns, which in their turn, lead to changes in the characteristics of the alongshore transport of sediment.

Storms play a dominant role in the transport of sediment [26]. The autumn-winter season in the Southeastern Baltic is characterized by the highest frequency of gale-force winds [32], resulting in active lithodynamic processes.

Contemporary calculations done for the previous period of storms helped to identify the general direction of the alongshore bed load (Table 5). The positive sign of the relative sediment-driving force (τ) (see. Table 5) indicates a unidirectional general transport of the sediment from the Taran Cape along the Curonian Spit.

Table 5. Results of calculation of the sediment-driving force components T_1 and T_2, sediment transport scale A; resultant sediment-driving force T; breaking waves force B, energy vectors values of the general sediment-driving activity E; relative sediment-driving force τ (conditional kilo-units)

Profile	T_1	T_2	A	T	B	E	τ
1	51.9	-7.5	59.4	44.3	53.8	69.7	0.82
3	28.4	-5.1.	33.6.	23.3	30.1	38.1	0.77
5	29.7	-6.6.	36.3	23.1	37.6	44.1	0.61
7	31.2	-4.9	36.1.	26.3	37.4	45.7	0.70
9	27.4	-7.7	35.1.	19.7	40.0	44.6	0.49
11	30.7	-12.0	42.7	18.7.	43.9	47.7	0.43
13	41.4	-8.8	50.2	32.6.	51.2	60.7	0.64
15	14.3	-9.9	24.1	4.4	21.0	21.5	0.21
17	32.5	-5.0	37.5	27.6	34.7	44.3	0.79
19	33.9	-7.1	41.0	26.7	44.9	52.3	0.60
21	36.4	-9.0	45.4	27.4	52.4	59.1	0.52
23	45.9	-12.6	58.5	33.3	64.8	72.9	0.51
25	79.9	-12.1	92.0	67.8	88.3	111.4	0.77
27	76.9	-14.1	91.0	62.8	93.1	112.3	0.68
29	80.4	-14.2	94.6	66.3	95.5	116.3	0.69
31	75.7	-24.0	99.8	51.7	106.6	118.5	0.48
33	79.3	-24.0	103.3	55.3	108.9	122.1	0.51
35	85.0	-24.0	109.0	61.0	113.5	128.8	0.54
37	84.8	-23.9	108.7	60.8	113.2	128.5	0.54
39	88.1	-23.9	112.0	64.2.	115.5	132.2	0.56

Within the area with shallow water and jagged coastline, there are no prerequisites for an extended unidirectional alongshore drift of loose sediment [33]. It should be noted that sediment transport scale A (see Table 5) reaches its maximum values near the middle part of the Curonian Spit, which leads to an increased probability of multidirectional drifts of sediment.

Calculation of the granulometric characteristics (reflecting the direction of the last sediment transport), allowed to identify the most probable vector of sediment transport and, consequently, contamination spots (Table 6). The results of the calculation do not contradict the ones obtained by other authors [25, 34] and confirm the general vector of transport of sediment material from the Sambia Peninsula along the Curonian Spit.

Table 6. Probability of the direction of the last significant sediment transport

Sediment transport direction	The number of pairs that meet the specified conditions		Z		Significance level	
	Case 1	Case 2	Case 1	Case 2	Case 1	Case 2
19 → 40 North-East	69	11	7.98	-3.56	0.01	-
40 → 19 South-West	4	26	-4.95	-0.57	-	-

Concentration of pollutants in the sediments near the Rybachy settlement indicates the weakening of the alongshore transport at the analysed site, and the formation of a sediment accumulation zone.

V. Conclusions

Deviations from the norm in the content of heavy metals and oil products along the underwater coastal slope of the Curonian Spit are caused by the redistribution of solid sediment as a result of coastal lithodynamic processes. The prevailing direction of sediment transport is from the northern coast of the Sambia Peninsula, which experiences the heaviest anthropogenic impact, thus significantly contributing to the distribution of pollutants. The coastal zone of the Curonian Spit is vulnerable to the anthropogenic impact coming from even fairly remote areas (20-50 km away from the coast), yet located within the boundaries of the same lithodynamic system. It is necessary to note that previous tests done at the site of the underwater disposal of dredged material, located near the port of Pionersky, showed a higher content of Cu [35], which could be another source of pollution of the coastal zone.

The beaches of the northern coast of the Kaliningrad region, being influenced by high dynamic waves, mainly play a transit role in the spreading of contamination.

VI. Acknowledgment

The work was performed within the Federal Task Programme of the Ministry of Education and Science of Russia “Investigations and elaborations on priority tendencies of scientific-technological complex development in Russia for 2014-2020” with unique identifier RFMEFI57414X0091.

VII. References

[1] R.D. Kos'yan and N.V. Pyhov, *Hydrogenous sediment transport in the coastal zone of the sea*, Moscow: Nauka, 1991, 280 p.

[2] Saf'yanov G.A., *Coastal ocean zone in the XX century*, Moscow: Mysl', 1978, 263 p.

[3] Yu.S. Dolotov, *Dynamic conditions for coastal marine relief formation and sedimentation*, Moscow: Nauka, 1989, 269 p.

[4] N.A. Aybulatov, *The dynamics of solids in the offshore zone*, Leningrad: Hydrometeoizdat, 1990, 271 p.

[5] E.M. Emel'yanov "The distribution of chemical elements and components in the sediment and some features of their diagenesis", *Sedimentation in the Gdansk Basin (The Baltic Sea)*. Ad. E.M. Emel'yanov, Moscow, AS USSR. 1987. pp. 217-242.

[6] V.T. Trofimov and D.G. Ziling, *Environmental geology*, Moscow Geoinformmark, 2002, 415 p.

[7] W.C. Krumbein, "Size frequency distributions of sediments", *Journal of Sedimentary Petrology*, 1934, vol. 4, pp. 65-77.

[8] WGMS 2003, "Report of the Working Group on Marine Sediments in Relation to Pollution", ICES CM 2003 / E:04.

[9] R.Ya. Knaps, "On the method of determining the movement characteristics of the sediment in non tidal seas", Scientific Reports of the Institute of Geol. and Geogr. AS LitSSR. Geofisics, 1956. vol. 3. Vilnus, pp. 141-143.

[10] "Manual to Meteorological Instruments and Methods of Observations", 5th ed., Secretariat of the World Meteorological Organization, Geneva- Switzerland, 1983. N 8, 1988, Obninsk: VNIIGMI-MCD.

[11] P. MacLaren and D. Bowles, "The effects of sediment transport on grain-size distributions", *Journal of Sedimentary Petrology*, 1985, vol. 55, N 4, pp. 0457-0470.

[12] E.M. Emel'yanov, V.A. Kravtsov, V.V. Sivkov, and E.V. Dorokhova, "Toxic substances in the bottom sediments", In: *Oil and environment of the Kaliningrad Region*, vol. 2: TheSea, Ad. by V.V. Sivkov, Kaliningrad: Terra Baltica, 2012, pp. 304-314.

[13] O.V. Bass, "Introducing of oil products from the coast", In: *Oil and environment of the Kaliningrad Region*, vol. 2: The Sea, Ad. by V.V. Sivkov, Kaliningrad: Terra Baltica, 2012, pp. 174-181.

[14] N.A. Bogdanov, V.A. Sovershaev, L.A. Zhindarev, A.P. Agapov, "The evolution of ideas about the dynamics of the south-eastern shores of the Baltic Sea", *Geomorphology*, 1989, N 2. pp. 62-69.

[15] O.K. Leont'yev, L.A. Zhindarev, O.I. Ryabkova, "The origin and evolution of large coastal accumulative forms", *Theoretical problems of development of the sea coasts*, AS USSR. Moscow: Nauka, 1989, pp. 83-91.

[16] Yu. D. Shujsky, "Features of coastal marine placers of Eastern Baltic in connection with the regime of the alongshore bed load", *Diss. cand. geogr. sciences*, in 2 vol., Moscow, IO AS USSR, 1969, 292 p.

[17] Yu. D. Shujsky, V.L. Boldyrev, B.V. Kochetkov, "On the conditions and characteristics of the formation of of coastal marine placers of the eastern part of the Baltic Sea", *DAS USSR*, vol. 194, N 1, 1970. pp. 187-190.

[18] O.I. Ryabkova, "The dynamics of the coast of the Sambia Peninsula and the Curonian Spit in connection with the problems of coastal protection", *Abstr. of diss. cand. geogr. sc*. Moscow: Geogr. dep. MSU, 1987, 17 p.

[19] R.Ya. Knaps, "Protecting structures such as moles and the movement of sediment on sandy coasts", *Proc. of AS Latv SSR*, 1952, N 6 (59), pp. 87-130.

[20] V.P. Zenkovich, "Some aspects of the dynamics of the Polish coast of the Baltic Sea", *Proc. VGO*, vol. 90, issue 3. Moscow, 1958.

[21] V.L. Boldyrev and V.P. Zenkovich, "The Baltic Sea", *The Far East and the shores of seas washing the territory of the USSR*. Moscow: Nauka, 1982, pp. 214-218.

[22] V.L. Boldyrev, V.K. Gudelis, and R.Ya. Knaps, "Currents of sand deposits in the Southeastern Baltic", *Studies of the dynamics of sea coasts relief, Moscow*: Nauka, 1979, pp. 14-18.

[23] V.G. Ul'st, "Differentiation of sandy material in accordance with form of grains in the coastal marine environment", *Baltica*, vol. 2, Vilnius, 1965, pp. 167-180.

[24] V.I. Kirlis, "Some features of the dynamics of coasts of Kursiu Nerija", *Proc. AS LitSSR*, 1971, is. B. vol. 4 (67), pp. 211-224.

[25] A.N. Babakov, "Spatial and temporal structure of migration flows and sediment in the coastal zone of Southeastern Baltic (the Sambia Peninsula and the Curonian Spit)", *Diss. cand. geogr. sc*. Kaliningrad: KSU, 2003, 273 p.

[26] A.N. Babakov, "The dynamics of sediments in the coastal sea area", In: *Oil and environment of the Kaliningrad Region*, vol. 2: The Sea, Ad. by V.V. Sivkov, Kaliningrad: Terra Baltica, 2012, pp. 37-59.

[27] BACC Author Group., *Assessment of climate change for the Baltic Sea basin*, Berlin: Springer-Verlag, 2008, 473 p.

[28] IPCC Fourth Assessment Report: Climate Change, 2008.

[29] IPCC, 2013: Climate Change 2013: The Physical Science Basis. Contribution of Working Group I to the Fifth Assessment Report of the Intergovernmental Panel on Climate Change [Stocker, T.F., D. Qin, G.-K. Plattner, M. Tignor, S.K. Allen, J. Boschung, A. Nauels, Y. Xia, V. Bex and P.M. Midgley (eds.)]. Cambridge University Press, Cambridge, United Kingdom and New York, NY, USA, 1535 p.

[30] HELCOM, "Climate change in the Baltic Sea Area: HELCOM thematic assessment in 2013", *Baltic Sea Environment Proceedings*, 2013, N 137. 66 p.

[31] N. Rangel-Buitrago, "Winter wave climate, storms and regional cycles: the SW Spanish Atlantic coast", *International Journal of Climatology*, 08/2013; 33:2142-2156. DOI: 10.1002/joc.3579.

[32] V.F. Dubravin and Zh. I. Stont, "Hydrometeorological regime, structure and circulation of waters", In: *Oil and environment of the Kaliningrad Region*, vol. 2: The Sea, Ad. by V.V. Sivkov, Kaliningrad: Terra Baltica, 2012, pp. 69-105.

[33] E.M. Emel'yanov, *The barrier zone in the ocean. Sediment- and ore formation, geoecology*, Kaliningrad: Yantarny skaz, 1998, 416 c.

[34] A.Yu. Sergeev, "Features of the direction of sand material transport in the coastal zone of Sambia Peninsula of the Kaliningrad Region", *Proc. of XVIII Intern. scient. conf. (school) in mar. geol.*, Moscow, GEOS, 2009, vol.5, pp. 145-150.

[35] E.M. Emel'yanov, A.I. Blazhchishin, O.I. Koblenc-Mishke, V.A. Kravtsov, D.K. Stryuk, and G.S. Kharin, "Ecological and geochemical conditions in the Eastern Baltic", *Problems in the Study and nature conservation of the Curonian Spit*, eds. by V.M. Slobodyanik and A.R. Manukyan, Kaliningrad: GP KST, 1998, pp. 148–185.

OIL POLLUTION OF THE SOUTHEASTERN BALTIC SEA SURFACE AND POSSIBLE DIRECTIONS OF ITS PROPAGATION

Alexander Krek, Immanuel Kant Baltic Federal University, Atlantic Branch of P.P. Shirshov Institute of Oceanology, Russian Academy of Sciences, Russia
Elena Bulycheva, Atlantic Branch of P.P. Shirshov Institute of Oceanology, Russian Academy of Sciences, Russia
Andrey Kostianoy, P.P. Shirshov Institute of Oceanology, Russian Academy of Sciences, Immanuel Kant Baltic Federal University, Russia

alexander.krek@gmail.com

Ships, seeps from the seabed, municipal and industrial waste waters, and the atmosphere are the main sources of sea water contamination with oil and oil products. During the satellite monitoring of the Kravtsovskoe oilfield (D-6) (2004-2015) the area west of Sambia Peninsula and anchorage in front of entrance to Kaliningrad Sea Canal were localized as the most polluted area of the Southeastern Baltic Sea. Oil spill drift forecast from these areas with a help of Seatrack Web model (SMHI, HELCOM) has shown that the average annual direction of oil pollution drift is directed to the North-East. In some cases, leakage of oil or oil products from ships west of Sambia Peninsula could be a reason of oil contamination of beaches of the "Curonian Spit" National Park.

Key words: Southeastern Baltic Sea, oil pollution, satellite imagery, oil spill drift forecast, Seatrack Web model

I. INTRODUCTION

The Baltic Sea is one of the busiest waterways in the World Ocean. It has about 40 ports and oil terminals. Increasing maritime transportation threatens fragile ecosystems and the livelihoods of the many people who depend on the sea. During the last decade shipping has steadily increased, reflecting intensifying co-operation and economic prosperity around the Baltic Sea Region. On average 2,000 ships are at sea every day, including 200 tankers carrying oil or other potentially harmful products. It is estimated that the transportation of goods by sea will double by 2017 in the Baltic Region [1].

The main sources of oil pollution in the sea are natural hydrocarbon seeps, rivers, waste waters, shipping and atmosphere [2-9]. In the Baltic Sea, ships play a key role in the transportation of goods, oil and oil products, passengers and cars, as well as in fishery. At the same time shipping activities creates operational environmental pressures in the form of exhaust gas pollution, illegal discharges of oil, sewage from passenger, ferry and fishery ships, as well as introduction of invasive alien species via ships' ballast water [10].

Oil production on the shelf of the Southeastern Baltic Sea also represents a risk of oil pollution and a potential threat to the environment.

II. DATA

Data on oil pollution of the Southeastern Baltic Sea surface were obtained during operational satellite monitoring of the Kravtsovskoye oilfield (D-6) from June 2004 to December 2015. The monitoring was based on the analysis of satellite images from the following satellites: ENVISAT (European Space Agency (ESA)), RADARSAT-1 (Canadian Space Agency (CSA)), RADARSAT-2 (McDonald, Dettwiler & Associates (MDA, Canada)), TerraSAR-X (German Aerospace Center (DLR), Germany), and four satellites of the Italian Space Agency (ASI) Cosmo-SkyMED-1, -2, -3, -4.

In total 1946 radar images were analyzed, and 1232 oil spills were detected during the analysis of satellite radar images (Fig. 1). “Tail”-shaped oil spills are prevailed, what means that these spills are originated from moving ships [11].

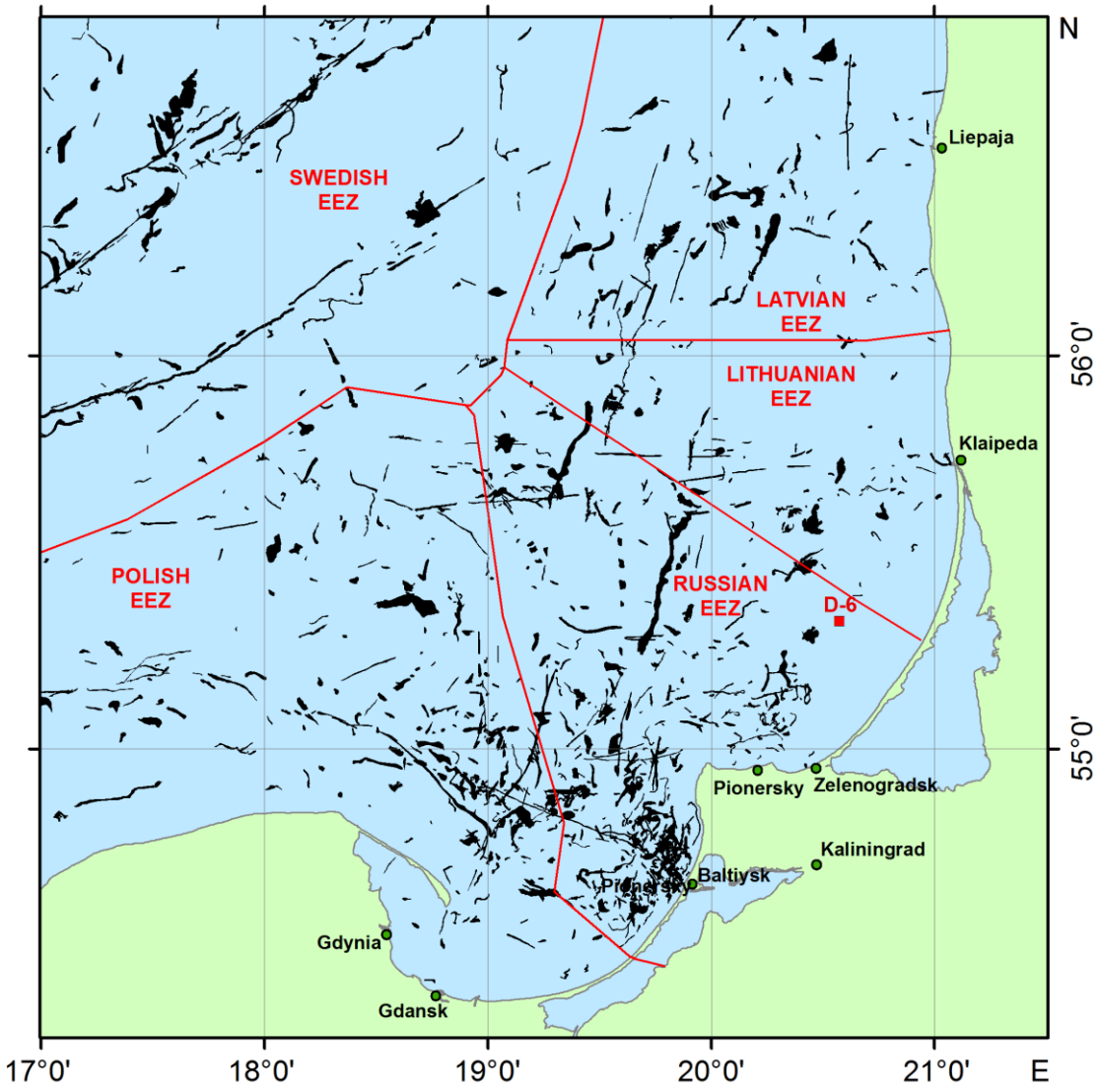

Fig. 1. Distribution of oil spills on the sea surface in the Southeastern Baltic Sea detected by satellite observations from June 2004 to December 2015.

III. NUMERICAL MODELLING

The Seatrack Web numerical model was used for prediction of drift and transformation of oil pollution. Seatrack Web is the HELCOM operational oil spill drift forecasting system which is based on operational weather and hydrodynamics forecasts. Oil spill drift model calculates the drift and spreading of oil spills using a Lagrangian particle tracking technique. Weathering processes such as evaporation, vertical dispersion and formation of water-in-oil emulsions are also calculated based on the standard formulae.

The system uses two different operational weather models ECMWF and HIRLAM (HIgh Resolution Limited Area Model, 22 km grid) and circulation model HIROMB (HIgh Resolution Operational Model for the Baltic Sea, 24 layers, driven by the two weather models respectively), which calculates the current field at 3 nm grid with 15 min time step. The model allows to forecast the oil drift for five days ahead or to make a backward calculation for 30 days for the whole Baltic Sea. Seatrack Web is in operational use in all the Baltic States [12-15].

Two modeling areas were selected west of Sambia Peninsula for numerical experiments of oil spill drift forecast (Fig. 2). The area #1 is the area of location of huge oil spill, composed of several separate parts, detected from ENVISAT (27.06.2008, 09:03 UTC) (Fig. 3). Results of forward calculations using Seatrack Web model showed, that this oil spill could be a source of observed oil pollution of the Curonian Spit beaches [12]. This is a reason why this area was selected as the modeling area #1. Area #2 is a 50 km long line along the main shipping route directed to Kaliningrad Sea Canal which corresponds to the concentration of the “tail”-shaped oil spills originated from moving ships (see Figs. 1 and 2).

Forecasts of potential oil spills drift originated from modeling areas #1 and #2 were calculated for every day of 2015 for 48 hours. 365 daily forecasts for both regions were combined in the probability maps of oil contamination of the sea surface during 48 hours after appearance of an oil slick (Fig. 4, 5). These maps show that during the first 48 h after a release of oil from ships, in most cases, oil pollution will drift to the North-East, what corresponds to the general wind direction in this region as registered at Autonomous Hydro Meteorological Station (AHMS) installed on D-6 platform (Fig. 6). The main direction of the contamination propagation is also in agreement with local currents and the direction of mean annual transport of substances in the Gdansk Basin [16-18].

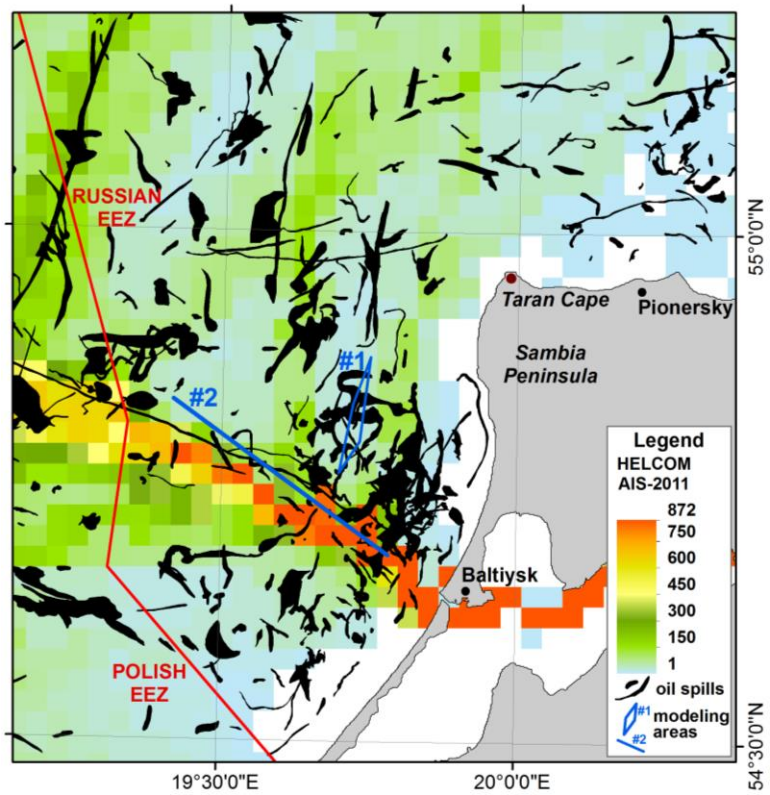

Fig. 2. Location of modeling areas #1 and #2 (blue lines) west of Sambia Peninsula.

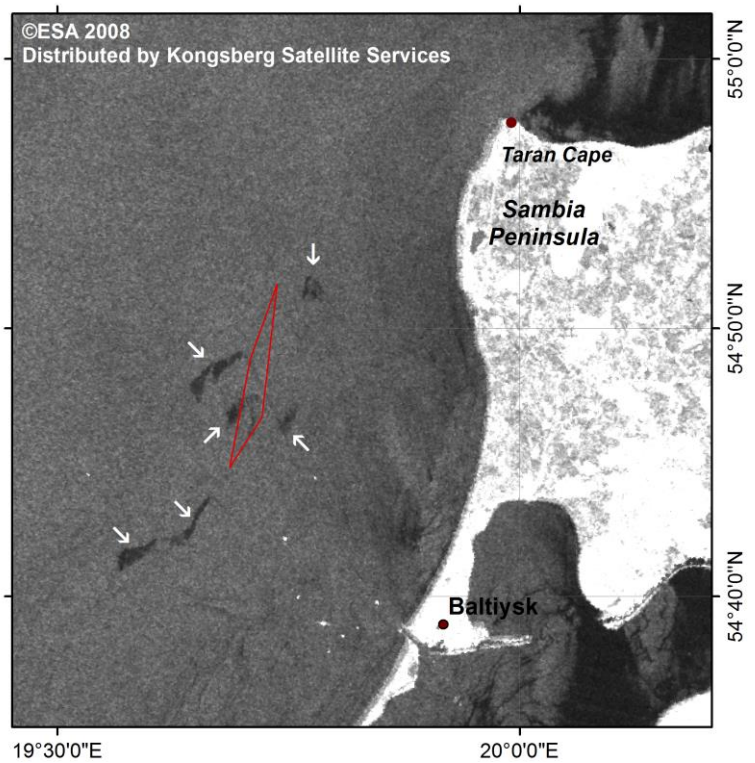

Fig. 3. Fragment of ENVISAT image on 27.06.2008 (09:03 UTC). Parts of oil spill are shown by arrows. Red area corresponds to the modeling area #1.

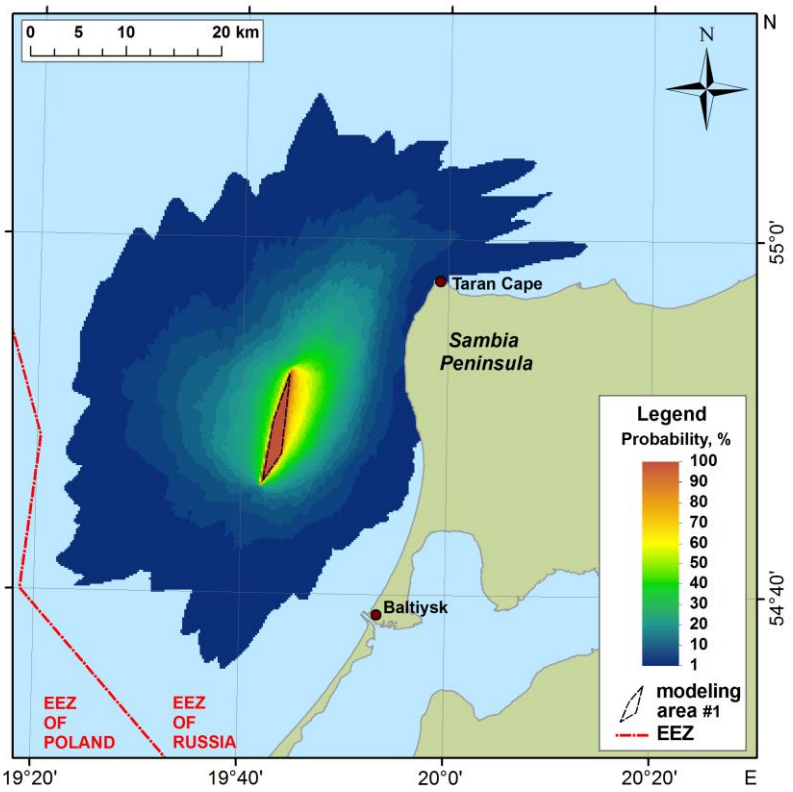

Fig. 4. Probability of propagation of oil pollution originated from the modeling area #1 for the next 48 h after leakage of oil for 2015.

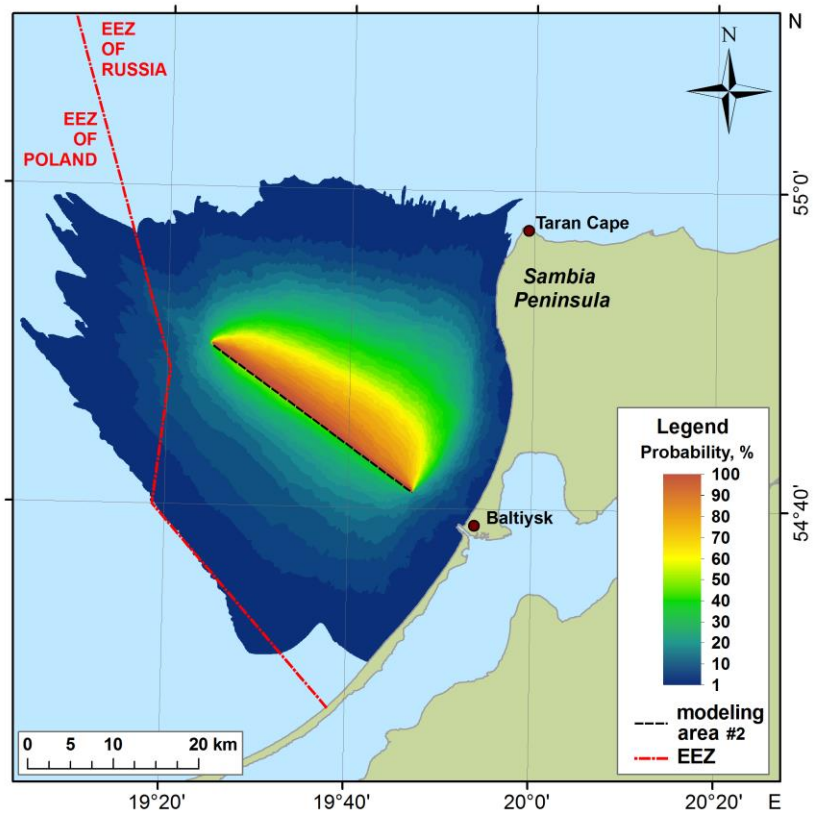

Fig. 5. Probability of propagation of oil pollution originated from the modeling area #2 for the next 48 h after leakage of oil for 2015.

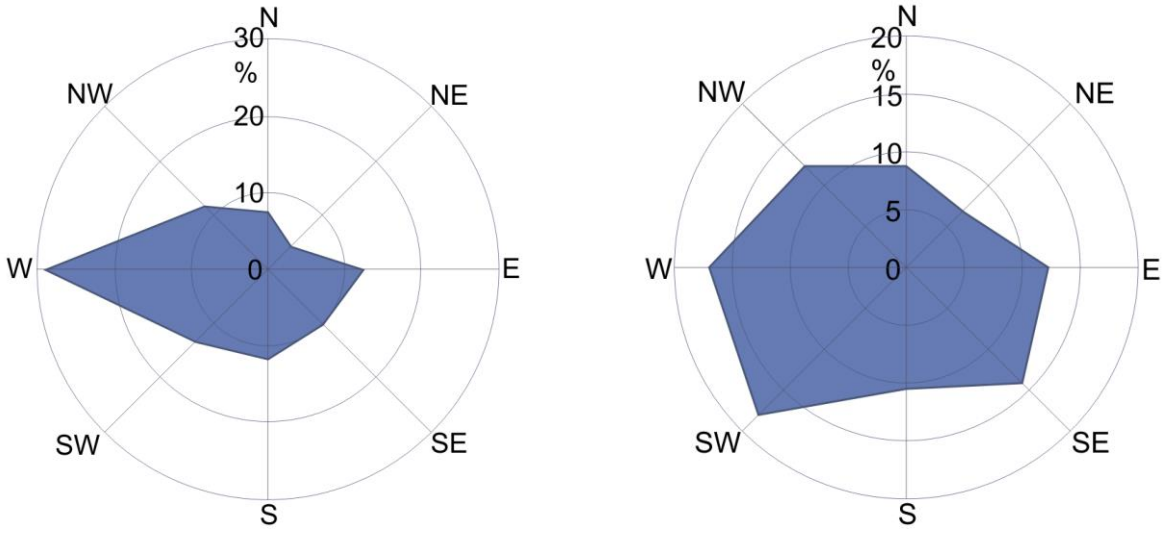

(a) **(b)**

Fig. 6. Wind rose calculated by data from AHMS installed on D-6 platform: a) for 2015; b) for 2006-2014.

In particular cases, oil pollution appearing from the modeling area #1 during 11 days after leakage may reach Curonian Spit beach (Fig. 7). Thus, at specific meteo and hydrological conditions for periods of 17-27 August and 20-30 August 2014 the oil spill could reach the Curonian Spit shore near Nida (Fig. 7a), or the area from Zelenogradsk to Lesnoy (Fig. 7b). These examples show that oil released west of Sambia Peninsula can be a reason of oil pollution of the Curonian Spit shore. For instance, during July 2008 oily sands were observed along the all Russian part of the Curonian Spit, i.e. several days – weeks after an oil spill was observed in the area #1 on 27 June 2008 [12].

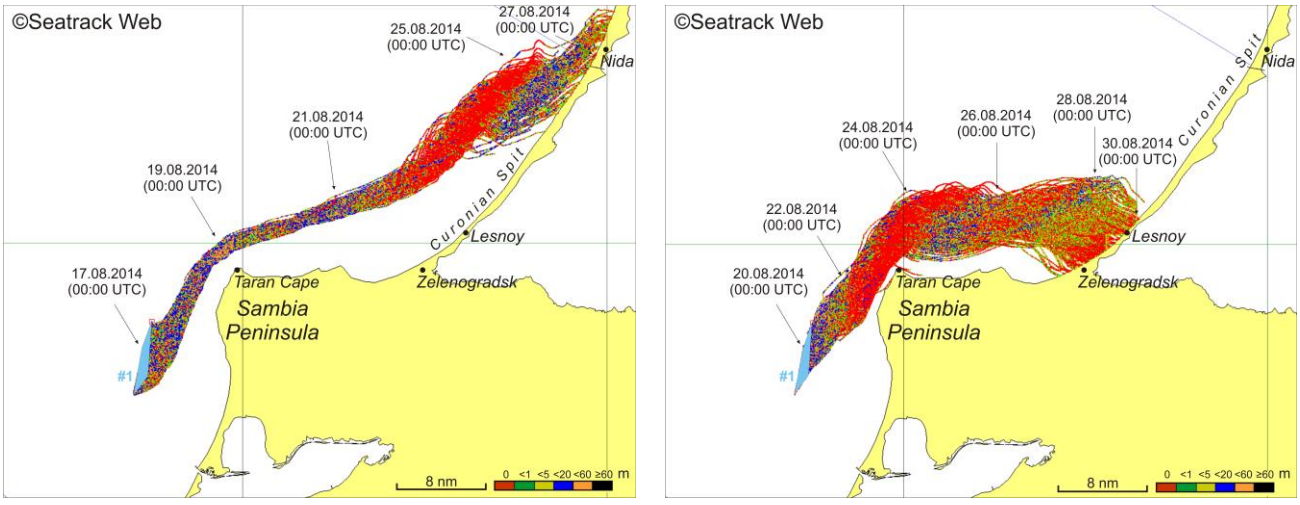

(a) **(b)**

Fig. 7. Propagation of oil pollution from the modeling area #1:
a) for a period of 17-27 August 2014; b) for a period of 20-30 August 2014.

As discussed in [19], the observed oil spills are shifted from the shipping route (area #2) northeastward (see Fig. 2). The results of numerical simulation of potential oil pollution from the shipping route leading to the Port of Baltiysk may explain this discrepancy by a general drift of oil spills to the North-East (see Fig. 5).

IV. Conclusions

Numerical simulations using Seatrack Web model for two areas of appearance of oil spills west of Sambia Peninsula allow to establish the main directions of their propagation. Oil products and other harmful substances released from ships in the area west of Sambia Peninsula will propagate to the North-East. In particular cases oil released in the area #1 can turn around Sambia Peninsula and washed ashore the Curonian Spit, the Natural and Cultural Heritage of UNESCO.

V. Acknowledgment

A.V. Krek performed the modeling of potential oil pollution using Seatrack Web model in the framework and with a support of the Russian Science Foundation Project N 14-37-00047. E.V. Bulycheva and A.G. Kostianoy conducted a study of oil pollution using satellite data in the framework and with a support of the Russian Science Foundation Project N 14-50-00095. Satellite radar data were provided by LUKOIL-KMN, Ltd.

VI. References

[1] http://www.helcom.fi/helcom-at-work/groups/maritime

[2] http://www.helcom.fi/action-areas/shipping

[3] I. A. Nemirovskaya. *Ocean Hydrocarbons: Snow, Ice, Water, Suspended Matter, and Bottom Sediments* (Nauchnyi Mir, Moscow, 2004) (in Russian).

[4] I. A. Nemirovskaya, “Oil hydrocarbons”, in *Oil and Environment of Kaliningrad Oblast*, Vol. 2: The Sea, Ed. by V. V. Sivkov (Terra Baltika, Kaliningrad, 2012), pp. 152–173 (in Russian).

[5] I. A. Nemirovskaya. *Oil in an Ocean: Pollution and Natural Flows* (Nauchnyi Mir, Moscow, 2013) (in Russian).

[6] S. A. Patin. *Oil and Ecology of the Continental Shelf* (VNIRO, Moscow, 2001) (in Russian).

[7] S. A. Patin. *Oil Spills and Their Impact on Marine Environment and Biological Resources* (VNIRO, Moscow, 2008) (in Russian).

[8] J. Burger, Oil Spills (*Rutgers University Press*, New Brunswick, 1997).

[9] A. G. Kostianoy and O. Yu. Lavrova (Eds.). *Oil Pollution in the Baltic Sea* (Springer-Verlag, New York, 2014), Vol. 27.

[10] A. Nelson-Smith. *Oil Pollution and Marine Ecology*, (Paul Elek, London, 1972).

[11] E.V. Bulycheva, A.G. Kostianoy, A.V. Krek. Interannual variability of the sea surface oil pollution in the Southeastern Baltic Sea in 2004-2015. *Modern problems of remote sensing of the Earth from space*, Vol. 13, N 3, 2016 (in press, in Russian).

[12] E.V. Bulycheva, A.G. Kostianoy. Results of the satellite monitoring of oil pollution in the Southeastern Baltic Sea in 2006-2009. *Modern problems of remote sensing of the Earth from space*, Vol. 8, N 2, 2011, P. 74-83 (in Russian).

[13] A.G. Kostianoy, O.Yu. Lavrova (Eds.). *Oil pollution in the Baltic Sea*. Springer-Verlag, Berlin, Heidelberg, New York. Vol. 27, 2014, 268 pp.

[14] A.G. Kostianoy, E.V. Bulycheva. Numerical simulation of risks of oil pollution in the Southeastern Baltic Sea and in the Gulf of Finland. *Modern problems in remote sensing of the Earth from space*, Vol. 11, N 4, 2014, P. 56-75 (in Russian).

[15] E.V. Bulycheva, A.V. Krek, A.G. Kostianoy, A.V. Semenov, A. Joksimovich. Oil pollution in the Southeastern Baltic Sea by satellite remote sensing data in 2004-2015. *Transport and Telecommunication*, 2016, V.17, N2, P. 155-163.

[16] Meier, H.E.M. (2007) Modelling the pathways and ages of inflowing salt- and freshwater in the Baltic Sea. *Estuarine, Coastal and Shelf Science*, N74, 610-627.

[17] E.V. Bulycheva, A.V. Krek, A.G. Kostianoy, A.V. Semenov, A. Joksimovich. Oil Pollution Of The Southeastern Baltic Sea By Satellite Remote Sensing Data And In-Situ Measurements - *Transport and Telecommunication*, 2015, V.16, N4, P. 296-304.

[18] E.V. Bulycheva, A.V. Krek, A.G. Kostianoy. Peculiarities of distribution of oil pollution in the Southeastern Baltic by satellite data and in-situ measurements. *Okeanologiya*, 2016, Vol. 56, N 1, P. 81-89.

[19] E. Bulycheva, I. Kuzmenko, V. Sivkov. Annual sea surface oil pollution of the south-eastern part of the Baltic Sea by satellite data for 2006-2013. *Baltica*, 2014. Vol. 27. Special Issue. P. 9-14.

METEOROLOGICAL CONDITIONS AFFECTING THE CURONIAN SPIT DUNE FORMATION (SOUTHEASTERN BALTIC COAST)

Zhanna Stont, I. Kant Baltic Federal University, Russia
Marina Ulyanova, Atlantic Branch of P.P. Shirshov Institute of Oceanology of RAS, Russia
Alexander Sergeev, A.P. Karpinsky Russian Geological Research Institute; I. Kant Baltic Federal University, Russia

ocean_stont@mail.ru

This article presents a study of the geomorphological changes of the Curonian Spit during last century. The analysis was conducted for both geological maps and satellite images. The eastward shift the southern part of the Curonian Spit dune ridge with velocity from 2 to 5 m per year takes place. The comparison of the slopes incline directions with denudation areas was done. In addition, the meteorological parameters affecting aeolian processes on the southeastern Baltic coastal were investigated for the period of 2005-2014. On average, dunes can be dispersed by wind throughout 36±17 days in a year. Velocity and direction of the wind, as well as precipitation, are of dominating importance for the dune shift.

Key words: Curonian Spit, Grand Dune Ridge, sandy dunes, geomorphological processes, hydrometeolrological regime

I. INTRODUCTION

The Curonian Spit was included into the UNESCO World Heritage List as a single cultural landscape of shifting and forested dunes of outstanding international importance, which is under constant threat from natural forces [1]. Practically this status was awarded for the human victory over the nature, as the man is responsible for the stop of sand movement. On the other hand, the remained movable dunes are the unique natural objects and represent the main attractive landscape of the Curonian Spit. Among other similar objects, the open ("white") dunes of Curonian Spit are marked out by their sizes. The Grand Curonian Dune Ridge is the third highest and the second longest shifting coastal dune ridge in Europe [2].

Hydrometeorological conditions (wind regime, precipitation amount, humidity, and air temperature) as well as economical activity (in general recreation) are the most significant factors determinating modern transformation of the Curonian Spit bottom landscape complex.

Aeolian processes are responsible for formation and development of all geomorphological zones of the spit. Stabilization by vegetation of the most part of its area sharply reduced expression of aeolian processes at the accumulative sandy plain and dune ridges. On the other hand, increase of the recreation activity resulted in destruction of the soil-vegetation covering, and, consequently, activation of the aeolian processes at some areas. Today the "white" dunes, especially their slopes, are the most unstable areas. The general geomorphologic trend of the entire Grand Curonian Dune

Ridge is the flattening of the highest shifting dunes and the lowering of the average height of the entire shifting dune ridge.

II. GEOLOGICAL AND METEOROLOGICAL SETTING

The Curonian Spit is a young geological formation, developed during Middle and Late Holocene as a result of sediment shift by coastal currents and winds [3, 4]. It presents a typical erosion-accumulative body, originated from the erosion of Sambian Peninsula cliffs and sediments of the Baltic Sea. Location and look, similar to present, the spit assumed about 3-5 thousands years ago in Litorina and PostLitorina stages. The present day parameters of the spit are as follows: total length 98 km, maximal width 4.2 km, and minimal width 0.38 km (Fig. 1). The Grand Dune Ridge was formed 150-200 years ago at the place of ancient parabolic dunes that are covered by thick layer of young sands. Its size varies depending of meteorological conditions: strong western winds contribute the dunes height, whereas eastern winds decrease it.

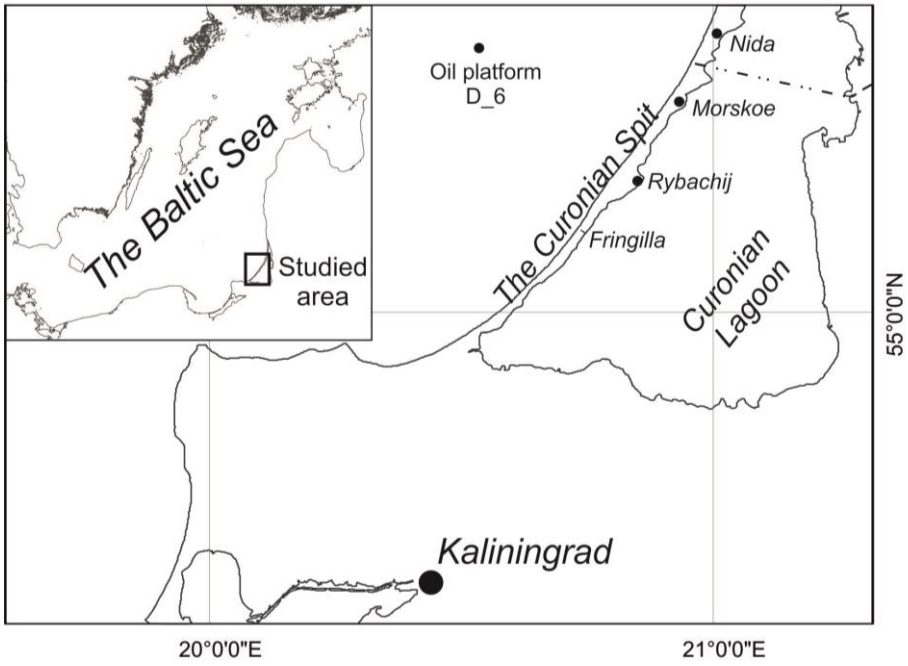

Fig. 1. Location of the studied area.

Shifting barchans are the relict formations. They formed in the period when the vegetation was practically annihilated, and the aeolian processes dominated. Curonian Spit dunes are of typical asymmetric form with steep slopes at the lagoon side and flat slopes sea-directed. Such asymmetric form proves the dune genesis by sand material shift from the seaside by western winds. Existence of different directed cross-bedded layers of sands (Fig. 2) indicates the alternation of sand accumulation with active deflation under wind direction change. Shifting dunes today are moving towards the lagoon somewhere entering the water and eroding [5]. Therefore, the total dune volume decreases.

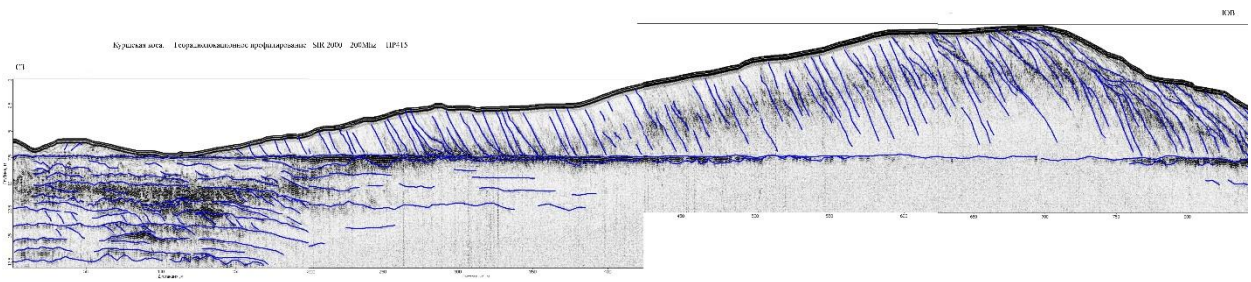

Fig. 2. Ground penetration radar profile of the Fringilla dune directed from the sea to the lagoon. The sandy layer thickness reaches 12-14 m. Profile location is showed at Fig. 1.

The studied area is located within the marine climate of temperate latitudes zone. Baric gradient is mostly all-year oriented from the south-east to the north-west. This determines the western winds domination above the Baltic Sea, and the warm and humid air masses transport from the Atlantic Ocean. Therefore, the following features are typical: relatively small fluctuations of the average monthly air temperature, high humidity and cloudiness during the whole year, significant amount of the precipitation, as well as frequent storms.

III. MATERIALS AND METHODS

Satellite images (SI) of low definition (cell size 30-60 m) for the period of 1985-2012 were used for the evaluation of the Curonian Spit dune ridge development. Data processing included an allocation of open and forested areas of dunes by typical optical features of raster image. Dedicated areas were vectorized by ArcGIS.

The comparison of the geological maps (scale 1:25000) of 1910 [6] and detailed SI of 2010 was used for detection of the average ranges of coastline and dune slopes movement. The scanning geological maps were georeferenced to SI using the stable infrastructure object that provides the comparison of the lagoon coastline and sandy dune contours changes with high degree of certainty.

The evaluation of dune surface transformation was done at two areas: southward the Rybachij settlement – Matrosova mt., and close to the Morskoe settlement – Skilvit Dune. For surface transformation analysis were used topographical plans of the 1:5000 scale (surveys of 1983-1984) and shuttle radar topographic mission (SRTM) data of 2000 (the raster resolution of data for this area is 30 m). The comparison of vectorizated topographical data of the maps and SRTM data allowed to evaluate a dune surface transformation. The calculation of the topography deformation thickness was done by the ArcGIS raster calculator tool.

Evaluation of the meteorological parameters influence on the recent dune transformation was based on the data for 2005-2014 from hydrometeorological stations, located on the offshore ice-resistant oil platform D-6, as well as in city of Klaipeda and Nida settlement (www.rp5.ru). The following conditions were taken as a basic for the investigation [7]:

– total precipitation in the period of five days cannot exceed 6 mm;

– average daily air humidity must be less than 95%;

– average daily wind velocity must exceed 6 ms-1, with wind directions within the range of 180–360° (from southern-western-northern rhumbs);

– average daily air temperature must be above 0°C or below –10°C [8].

Relative air humidity, velocity and direction of the wind, as well as air temperature were received from the meteostation, located at the offshore ice resistant platform D-6, at 27 m height. The wind velocity was reduced to standard 10 m. Precipitation was studied by data from meteostation at Nida settlement, located at the lagoon coast of the Curonian Spit (55°19′N 21°01′E), the height of the station is 2 m above the sea level. Absent dates were added by data from Klaipeda Hydrometcentre (55°42′N 21°09′E).

IV. RESULTS

Geomorphology

The main direction of the movement of dunes is the east along the whole dune ridge. The dunes moved by 300-400 m towards the lagoon for the period of 1910-2010, and by 70-130 m during 1985-2012. Maximum shift was revealed for the open dunes near the Morskoe settlement. Calculation of the movement average range by cartographic data as well as by data of SI analysis revealed similar results. Dune migration range was 3-4 m/year for the century measurement whereas for the last 27 years it was about 2.6-4.8 m/year.

Analysis of the vegetation development on the open dune areas revealed a foresting of the dune western slopes during 1985-2012 (Fig. 3). As a result, the reduction of sandy surface, exposed for winds, takes place. At that, the forested area at the western dune slope prevails over the area of dunes shift eastward towards the lagoon. Thus the tendency of open dune total area reduce is observed. The average annual decrease of the acreage of the shifting sand did not exceed 0.1% during the second half of the 20th century [9].

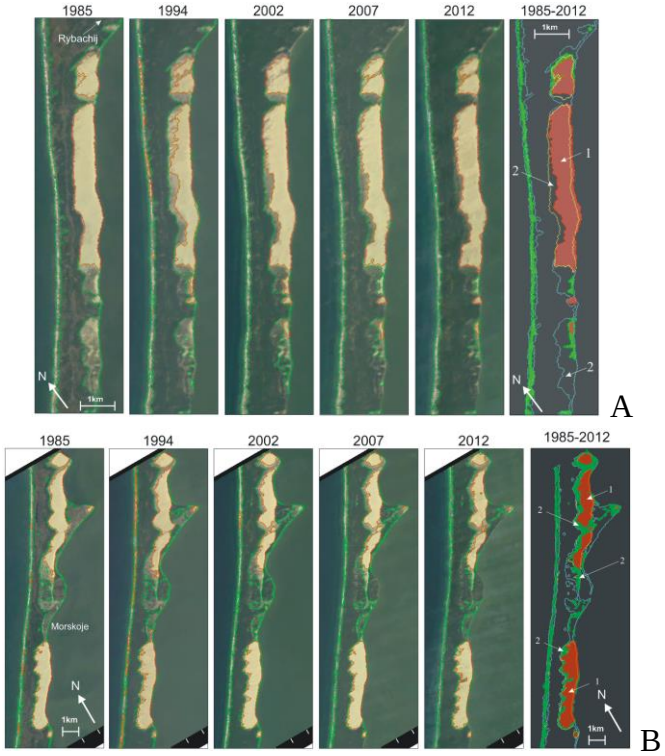

Fig. 3. The changes of vegetation cover on dune belt of Curonian Spit: A – dunes southward from Rybachij, B – dunes northward from Rybachij. 1 – areas of open dunes, 2 – areas of vegetation development during 1985-2012

Considerable part of the lagoon coasts of the Curonian Spit is eroded, especially in areas where the material supply from the sandy dunes is absent. Southward and northward from the Rybachij settlement the coast retreats with velocity of 0.5-2.0 m/year. Northward the Morskoe settlement the lagoon coast is most dissected part. On this coast, the washout of the sandy escarp takes place by 1-3 m/year at the southern side, and by 0.5-0.75 m/year at the eastern and northern sides. It is obvious, that the abrasion of dunes comes up also from the Curonian Lagoon waters activity. However, positive trend of dunes movement shows that range of sand supply from the dunes exceeds the washout velocity.

Tendency of active sand loss from the dunes and coastline shift is clearly observed by comparison of large open dunes topography for the 16-years period of 1984-2000 (Fig. 4).

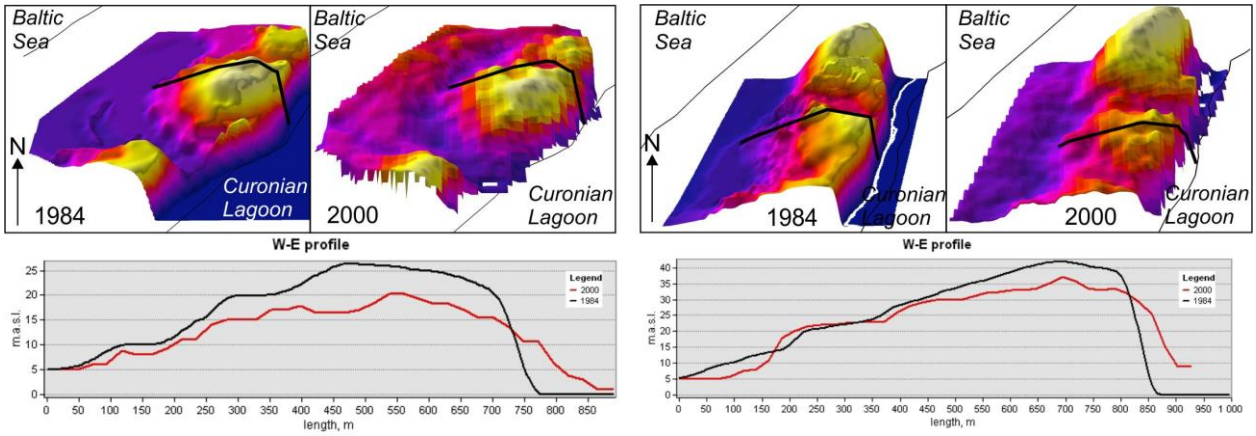

Fig. 4. Cross-section profiles of Matrosova mt. (left figure) and Skilvit mt. (right figure) based on digital elevation model of 1984 and 2000.

The comparison of the topography data, received from different sources, is rather approximate and cannot be used for exact calculations. However it makes possible to evaluate the general tendency and rough volumes of the transported material. Dune surface transformation more often takes place near its top and a leeward side slope. The windward side of the dune root remains virtually without any changes due to surface afforestation and slope stabilization.

The study of the dune located southward the Rybachij settlement (Matrosova mt.) revealed that its surface had shifted down by 5-10 m per 16-years. At the same time the eastern slope had entered the lagoon for 100 m and formed the sandy lens of 10 m thickness. The similar dynamics occurred for the dune located near the Morskoe settlement: the dune top had shifted down by 5-10 m, somewhere up to 15 m; the sandy lens length is about 100 m and thickness about 20 m. The western slope remains without any visible changes.

The comparison of the dune slopes angles and the areas of the maximal dune transformation revealed that the maximal decrease of sand thickness occurred for the western and north-western slopes. The growth took place at the opposite eastern and south-eastern slopes.

Meteorology

The favorable periods for the intensive generation of the aeolian land forms were marked out within an annual variation. Their features are the following: frequent and strong winds, minor

amount of atmospheric precipitation and low air humidity. Analysis of an average monthly meteorological data for 2005-2014 revealed (Fig. 5):

1. unfavorable by temperature are January and February, when average monthly temperatures vary from 0 to -10 °C;

2. average monthly wind velocities exceed 6 m/s during 7 months (September-March);

3. average monthly relative air humidity does not exceed 95 %, so by this value the aeolian forms may develop through the whole year;

4. average monthly precipitation sums were minimal in February-April (about 30 mm/month). The precipitation amount increases from June and reaches maximum in August.

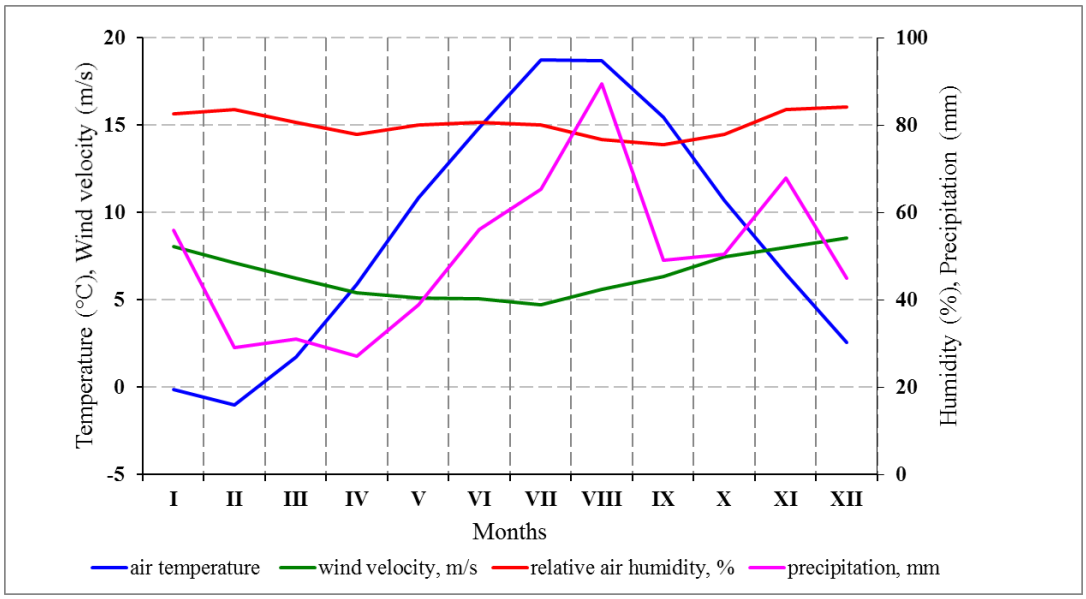

Fig. 5. Within year variation of different meteorological parameters (average monthly values for 2005-2014).

Detailed consideration of the average daily meteorological parameters revealed the following results (Table 1).

1. Temperature conditions at the Curonian Spit are unfavorable for aeolian forms development 52±38 days per year on average. In 2008 the air temperature promoted the aeolian processes through almost the whole year; minimal amount of days (221) was in 2005.

2. Total 10 days per year the annual daily relative air humidity was more than 95 %. This value varied from 330 days in 2011 to 357 days in 2005.

3. The Curonian Spit coast refers to the area with domination of the western winds of 5-6 points' strength by Beaufort scale. The winds with average daily velocity of 6 m/s dominates during half a year (180±10 days). The range varied from 161 days in 2006 to 196 days in 2011. The dominating wind direction varied from 180 to 360° by the wind rose within 219±21 days per year. 242 days with such winds were determined in 2011, whereas only 191 days were in 2014.

4. Despite the fact that the South-Eastern Baltic Region regards the area with excess humidity, about 45% (168±30 days) of all days the precipitation does not prevent the aeolian processes development. The most favorable year was 2014 (221 days), the less – 2012 (112 days).

Table 1 – Amount of days favorable for aeolian processes development at the Curonian Spit by different meteorological parameters and totally

Year	Air temperature	Relative humidity	Wind velocity	Wind direction	Precipitation sum	Total effect
2005	221	357	190	212	190	35
2006	312	355	161	230	189	35
2007	337	341	177	240	153	22
2008	355	349	178	240	146	29
2009	334	350	180	194	153	15
2010	278	343	183	194	162	26
2011	329	330	196	242	159	40
2012	326	350	177	238	112	27
2013	306	346	169	209	193	72
2014	330	333	189	191	221	58
av. ±σ	313±38	345±9	180±10	219±21	168±31	36±17

Analysis of the meteorological conditions in the aggregate revealed that the best conditions for the aeolian forms development at the Curonian Spit were in 2013 (72 favorable days). Only 15 such days were in 2009. The dunes were potentially formed by weathering during 36±17 days per year on average for the period of 2005-2014. The upward trend for the period with favorable days for the aeolian dunes forming took place (Fig. 6).

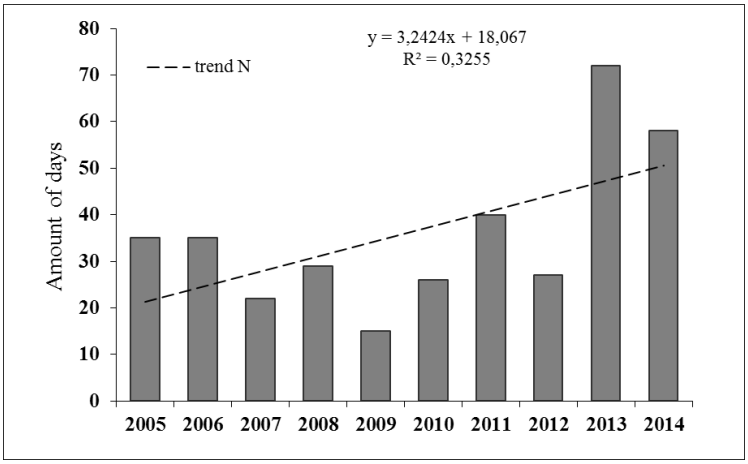

Fig. 6. Amount of days favorable for aeolian processes development at the Curonian Spit aggregate meteorological parameters.

Analysis of different meteorological parameters' revealed that the most significant influence over the weathering had wind conditions. The Curonian Spit is open for the dominating through the whole year winds of western rhumbs (from SW to NW), which are the strongest ones. The resulting transport vector in the region is directed from the SW to NE (230°), the value of the transport velocity module is 1.8 m/s [10]. The wind direction frequency is shown at the Fig. 7. Within year distribution of the days with wind velocity > 6 m/s had a seasonal character, maximal amount of the

days occurred in autumn-winter period: up to 23.6 days in December. This is confirmed by significant horizontal gradients of the air pressure. Decrease of the amount of the days with winds > 6 m/s begins in February and reaches its minimum in summer, especially in July (~6.5 days). Just in summer the horizontal gradients of the air pressure are the lowest. The increase of the winds > 6 m/s^{-1} frequency begins in August.

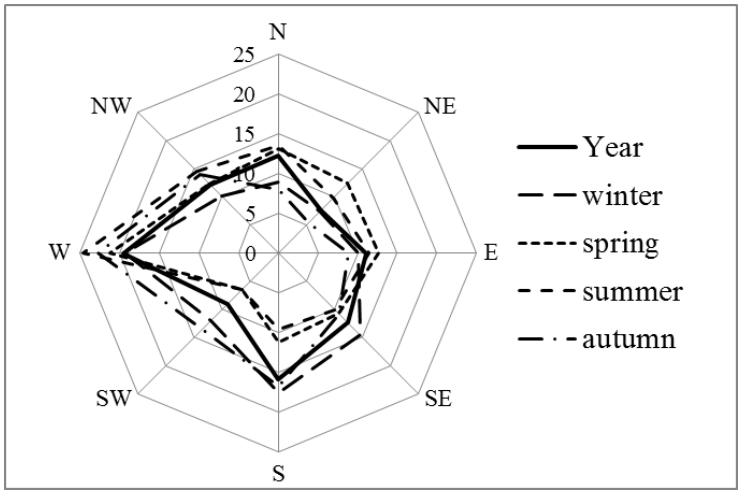

Fig. 7. Wind frequency by direction (%) during the year and by seasons.

The wind velocity at Curonian Spit depends on its direction. The alongshore wind direction from 180 to 360° (S–W–N) is typical for the most of the days with average velocity > 6 m/s^{-1}, and it assists the aeolian processes development. The spring-summer period is characterized by minimal amount of such days, whereas more than 2/3 of autumn-winter period is favorable for aeolian forms development (Table 2).

Table 2. Number of days with average wind velocity > 6 m/s^{-1}.
Means for the period 2005-2014

Month	I	II	III	IV	V	VI	VII	VIII	IX	X	XI	XII	Year
W > 6 m/s	21.8	17.8	14.6	10.9	9.0	7.8	6.4	12	14	20.3	22.1	23.6	180.3
(S-N) and >6 m/s	8.9	8.5	8.0	6.0	4.4	5.2	4.1	9.2	8.4	12.8	20.7	23.6	119.8

The precipitation regime is a limiting factor. The intensity of downpours increases in the summer and the amount of favorable days decreases up to 6.7 in August (Fig. 8). Maximal average monthly amount of the days was defined in March and April (17 days).

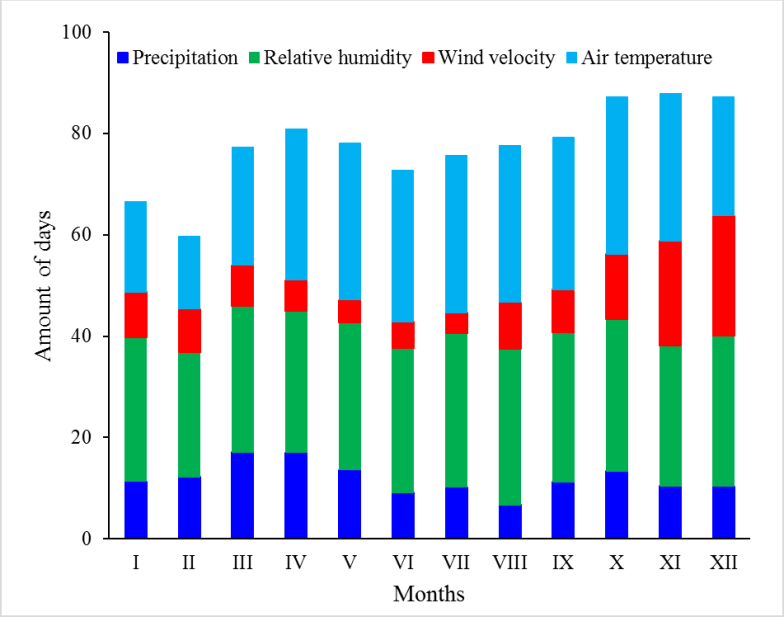

Fig. 8. Average monthly amount of the days (2005-2014) by separate meteorological factors, which influence the aeolian forms development.

The wind regime and precipitation amount are the main factors affected the forming and development of the dunes. Temperature conditions as well as relative humidity are not the obstacles for studied processes.

Variability of days' amount within the year is shown at Fig. 9. Maximal amount of days (12) by all parameters totality was defined in November. It is related to fact that in November the maximal velocities of western winds and considerable precipitation occur, and the air temperature rarely is below 0° (Fig. 9). Minimal days' amount is in the spring-summer period due to wind velocity and precipitation decrease. The amount of days increases in August when the maximal precipitation occurs; in autumn the wind velocity increases.

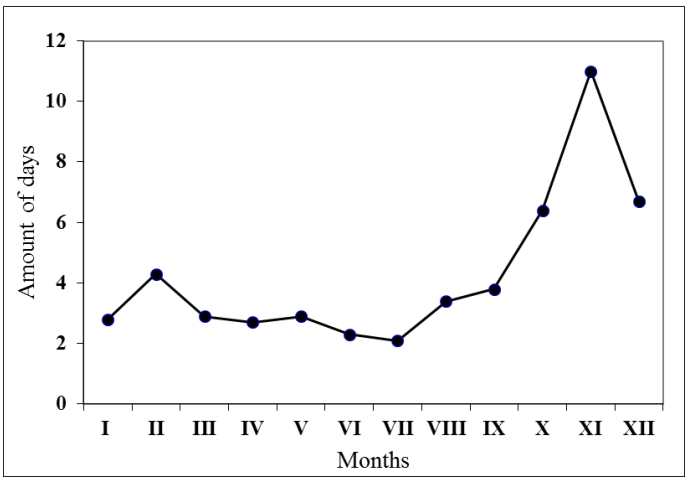

Fig. 9. Average monthly amount of days favorable for aeolian processes development (2005-2014).

V. CONCLUSION

Analysis of cartographic materials for the hundred years and satellite images for last decades revealed the eastward shift the southern part of the Curonian Spit dune ridge. The range in both cases is comparable – from 2 to 5 m per year.

An important feature is an existence of relatively reduction of the "white" dune area because of the western slope forestation what provides the common decrease of wind influence over sand transport.

Morphometric analysis of dune topography revealed the tendency to fixation of the western slope, denudation of the top, and partial flattening of the eastern slope with its entrance to the lagoon. Such tendency leads to gradual loss of the sandy material of dune ridge, and consequent decrease of dune migration range.

The comparison of the slopes incline directions with denudation areas revealed the domination of blowing-off from the western and northwestern slopes. Growth is typical for the opposite slopes – eastern and southeastern, what may be explained by prevalence of the western and northwestern winds.

Velocity and direction of the wind, as well as precipitation, are of dominating importance for the dune shift. On average, dunes can be dispersed by wind throughout 36±17 days in a year during the period of 2005-2014. The upward trend for the days with favorable days for the aeolian dunes forming took place.

VI. ACKNOLEDGEMENT

Geomorphological investigations were financed by the Russian Scientific Fund (grant 14-37-00047); analysis of meteorological data was financed by Basic Theme № 01201376666 of the Fundamental Study of Russian Academy of Sciences "Processes of formation and recent changes of the geological conditions in the Baltic Sea and within typical areas of the Atlantic Ocean".

VII. REFERENCES

[1] UNESCO, *Report on Monitoring Mission to the Curonian Spit (Lithuania / Russian Federation)*, 16–18 August 2001, ed. Henry Cleere, 2001.

[2] R. Povilanskas, H. Baghdasarian, S. Arakelyan, J. Satkūnas, J. Taminskas, "Morphodynamic trends of the Holocene dune ridge on the Curonian Spit (Lithuania/Russia)," *J. Coastal Res.*, vol. 25(1), 2009, pp. 209–215.

[3] E.N. Badyukova, L.A. Zhindarev, S.A. Luk'yanova, and G.D. Solov'eva, "Geological Structure of the Curonian Spit (of the Baltic Sea) and Its Evolution History (Revised)," *Oceanology*, vol. 47, No. 4, 2007, pp. 554–563.

[4] A. Sergeev, "The paleogeographic reconstruction of the Curonian Spit area in the Late Pleistocene-Holocene based on new geological data," *Reg. Geol. Metallogeny*, vol. 62, 2015, pp.34–44. (In Russian).

[5] E.N. Badyukova, L.A. Zhindarev, S.A. Luk'yanova, and G.D. Solov'eva, V.V. Scherbina, "Features of the recent dynamics of the lagoon coasts of the Curonian Spit, Southeastern Baltic," Lithodynamic of the bottom contact zone of the ocean, Moscow, GEOS, 2009, 168 p.

[6] Geologische karte von Preußen und benachbarten bundesstaaten. Ed. H. Heß v. Wichdorff. 1910

[7] M. Hojan and M. Więcław, “Influence of meteorological conditions on aeolian processes along the Polish cliff coast,” *Baltica,* vol. 27 (1), 2014, pp. 63–74.

[8] M. Hojan, “Aeolian processes on the cliffs of Wolin Island,” *Quaestiones Geographicae,* vol. 28A/2, 2009, pp. 39–46.

[9] R. Povilanskas, “Spatial diversity of modern geomorphological processes on a Holocene Dune Ridge on the Curonian Spit in the South–East Baltic,” *Baltica,* vol. 22 (2), 2009, pp. 77–88.

[10] V. P. Bobykina and Zh. I. Stont, “Winter storm activity in 2011–2012 and its consequences for the Southeastern Baltic coast,” *Water Resour.*, Pleiades Publishing, Ltd., vol. 42(3), 2015, pp. 371–377.

SUSPENDED MATTER CONCENTRATION ALONGSIDE THE NORTHERN COASTLINE OF KALININGRAD REGION (SOUTH-EASTERN PART OF THE BALTIC SEA)

Ekaterina Bubnova, Immanuel Kant Baltic Federal University, Kaliningrad, Russia
Victor Krechik, Immanuel Kant Baltic Federal University, Kaliningrad, Russia
Vadim Sivkov, Immanuel Kant Baltic Federal University, Kaliningrad, Russia

bubnova.kat@gmail.com

South-Eastern part of the Baltic Sea undergoes strong man-caused impact due to high level of shore usage. Suspended matter is an important carrying agent for pollutants. The Kaliningrad region has both the abrasion shore (Sambian peninsula) and the massive accumulative body (Curonian Spit), which is World Heritage site. The interannual and seasonal distribution of suspended matter concentration along the northern shore of Kaliningrad region against the hydrological conditions were studied. The research was made on five-year (2011-2015) monthly (April - October) data-array, consisting of surface and bottom water samplings. Two types of interannual and seasonal distribution of suspended matter concentration (SMC) revealed: Sambian type is defined by vertical gradient of SMC with descending of concentration from surface to bottom, while Curonian type – by horizontal gradient of latter.

Key words: suspended matter, coastal zone, the Baltic Sea

E. INTRODUCTION

In recent times, the coastal zone of the Baltic Sea to the north of the Kaliningrad region of the Russian Federation (fig. 1) experienced increase in usage for commercial purposes (e.g. waterworks building, recreation, fishery, oil exploration, etc.). At the same time, it is directly adjacent to the Curonian Spit which is the object of UNESCO natural and cultural heritage. Thus, there are increasing risks of negative impacts of marine natural management on the environment and growing urgency of research in this sea area.

Suspended in seawater mineral and organic particles (suspended matter) significantly affect the intensity of chemical elements migration, especially in the "coastal barrier zone" [1] where suspended matter concentration (SMC) is significantly higher than in the open sea. Therefore, suspended matter is one of the essential parameters of the marine environmental quality.

Suspended matter in the open part of the Baltic Sea is in a focus of research from 1960s [2], [3], [4]. However, the coastal zone, being so important for humanity, still remains insufficiently explored. Suspended matter data in the Gdansk Basin of the Baltic Sea was obtained during the 5-year period of research characterizes mainly open sea. Coastal erosion by wave action – is the main source of suspended matter in the studied area [5]. The vast majority of river discharge settles in

Curonian and Vistula lagoons; atmosphere aerosols can be neglected. Studies on suspended matter in the coastal zone of the Kaliningrad Region are rare and fragmentary [5], [6], [7].

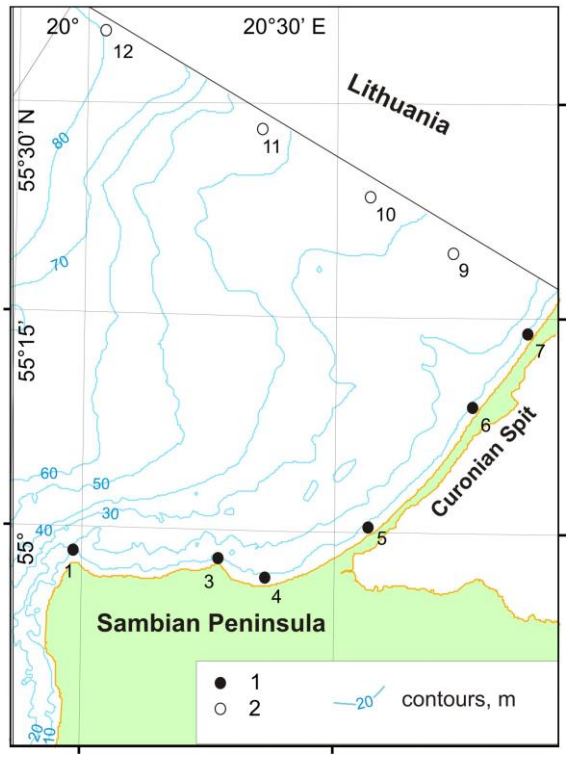

Fig. 1. Study area and location of stationary survey points of LUKOIL-KMN, Ltd. environmental monitoring: 1 – studied alongshore points; 2 – lateral profile points.

The aim of the present work is to summarize data on SMC collected over the last years along the northern coast of the Kaliningrad region as part of operational environmental monitoring of the marine oil production carried out by LUKOIL-KMN, Ltd.

F. MATHERIAL AND METHODS

The research was carried out on 5-year (2011-2015) monthly data-array, collected within spring-summer season (April to October) (fig. 1). The whole route length was about 70 km – from cape Taran to Lithuanian border. The sampling was made coastwise to the north from the Kaliningrad Peninsula and the Curonian Spit. As a result, 6 points (stations) with 2-horizonts (surface and sub-bottom) were made. Suspended matter was then separated from water samples by the mean of pressurized ultrafiltration with a use of previously weighted nuclear filters (0.45 μm membrane diameter) to determine concentration. Interannual and seasonal averaged SMC data were calculated. The simultaneous vertical CTD-profiling (Idronaut 316 probe) was made at all 6 route points, so water temperature and salinity averaged sections can be plotted.

The transition from individual profiling series to the averaged seasonal profiles was performed with the method of layer-by-layer median filtering [9]. The key point of the approach is to calculate the median value for a layer with arbitrary thickness (in this study this parameter was taken as 1m).

G. RESULTS AND DISCUSSION

In general, alongshore distributions of both annual averaged surface and near-bottom SMC demonstrate similarity (fig. 2). However, surface SMC is higher than near-bottom, and annual variations are more contrast. During entire period, increased SMC values with maximum in st. 4 were recorded at the Sambian Peninsula, while decreased values with minimum in st. 7 (close to Lithuanian border) were found at the middle of the Curonian Spit. Anyway, annual variability of SMC is quite high. Highest annual averaged SMC along almost whole investigated coastal zone were recorded in the 2015.

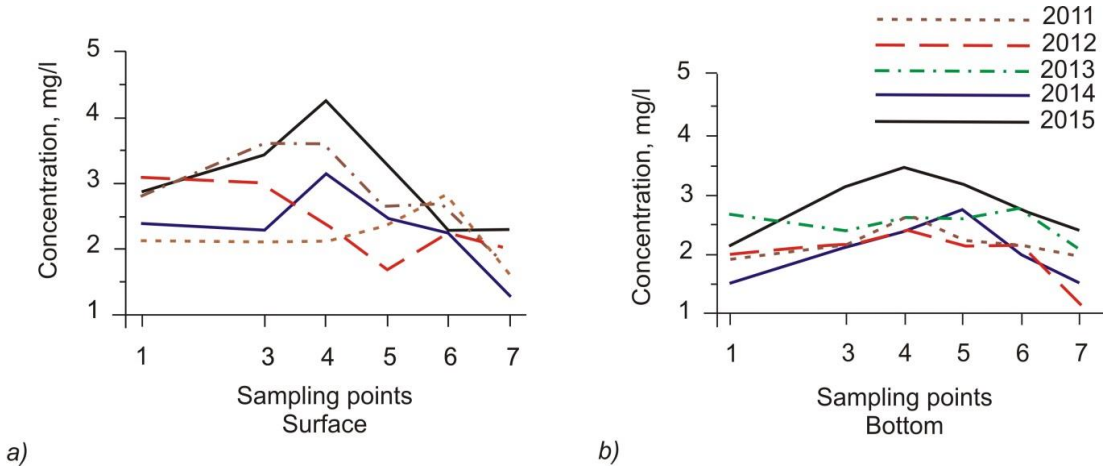

Fig. 2. Annual averaged suspended matter concentration at fixed survey points of monitoring along northern coast of Kaliningrad Region: a) surface layer, b) near-bottom layer.

Data discussed here corresponds with previously obtained results [8]. Maximum values within both near-bottom and surface layers were observed near eastern part of the northern coast of the Sambian Peninsula (fig. 3). However, our data demonstrates that SMC maximum moves to the east – from st. 3 (cape Gvardeysky) to st. 4. Anyway, this evidence do not contradict with an opinion that adjacent coastal area and underwater coastal slope are the main sources of suspended matter for the entire considered coastal area.

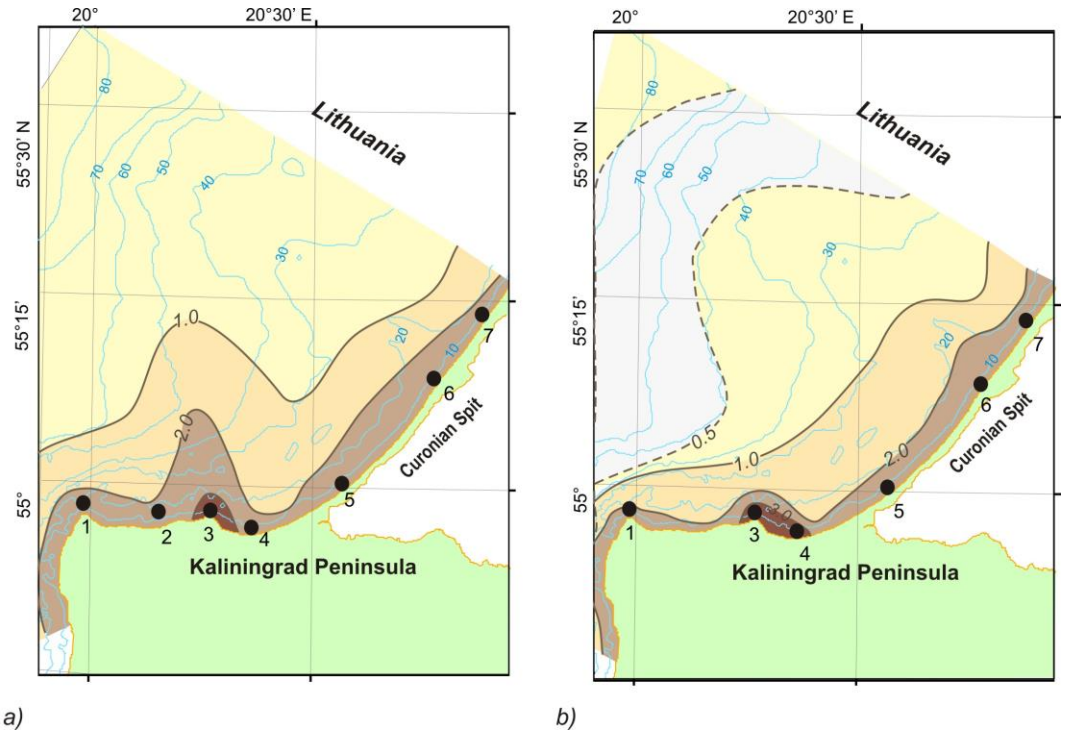

Fig. 3. Interannual averaged (2003-2008) surface suspended matter concentration (mg/l): a) surface layer (0-1 m); b) near-bottom layer (1-2 m from the bottom); black dots – studied alongshore points

The main features of the spatial distribution of suspended matter in the interannual time scale are clearly visible on the lateral profile along the Lithuanian border (fig. 4, after [8]). Seaward, coastal concentration maximum of the suspended matter transforms into subsurface "tongue" with the thickness 10-15 m which is visible at a distance of 50 km from the coastal zone. Near-bottom maximum is located close to center of the Gdansk Basin beginning from a depth 50-60 m.

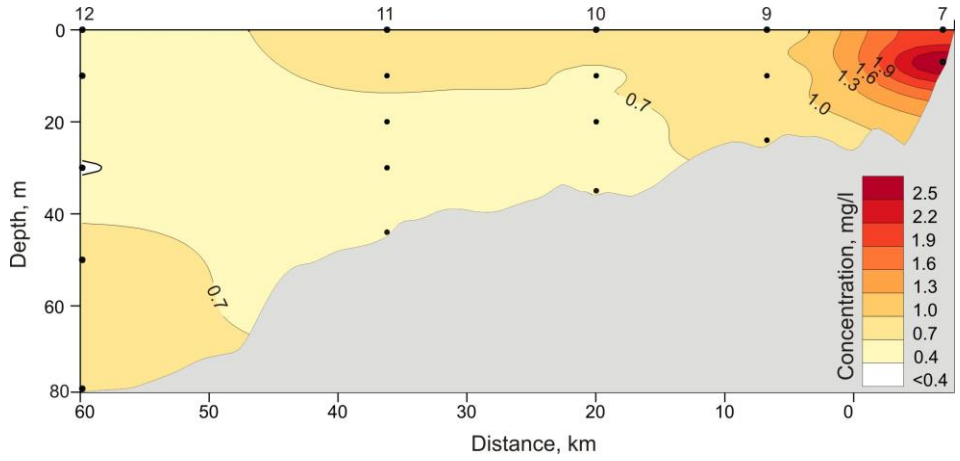

Fig. 4. Distribution of the interannual averaged suspended matter concentrations on the lateral profile from middle part of the Curonian Spit along the Russian-Lithuanian border (see fig. 1, after [8])

Our finding completes previous beliefs about suspended matter distribution in the studied area on the alongshore profiles. Interannual averaged and seasonal SMC data are shown on the hydrological section (fig. 5). For regional hydrological conditions the period from January to March is meant winter, April-June – the spring, July to September – the summer, October-December – autumn [10]. Therefore, there are two full seasons (spring and summer) and October during the time of observation.

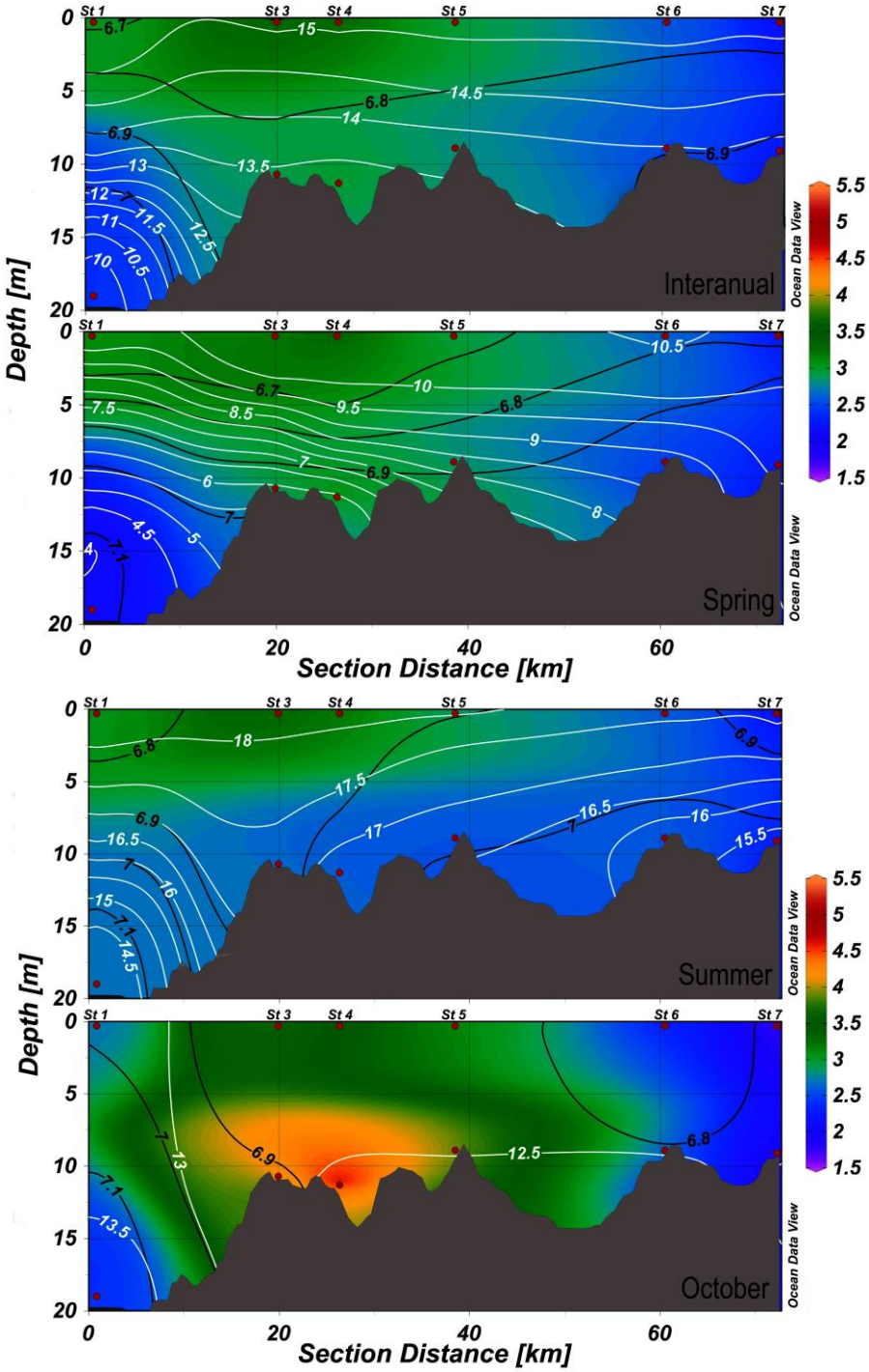

Fig. 5. Averaged SMC (color gradations) and hydrological conditions (white isolines – salinity (psu); black – temperature (°C); red dots – sample points of SMC.

The peak of suspended matter concentration appeared to be located at station 3 and 4, which are nearby the Kaliningrad peninsula. Both the interannual and seasonal pictures show this maximum, besides the highest concentrations occur in October. SMC tend to decrease significantly towards to the Curonian spit, which provides us to the following observation.

Two types of SMC vertical distribution is revealed on interannual section:

Sambian Peninsula coastal zone (stations 1, 3, 4) is characterized by vertical stratification of SMC, while Curonian Spit coastal zone (stations 5-7) – by homogenous distribution of latter. Transition from one stratification type to another takes place near eastern part of Sambian Peninsula (between st. 4 and 5).

Vertical stratification (first type) may maintain when vertical suspended matter movements prevailed, while homogenous distribution (second type) indicate prevailing of the horizontal transport of SMC.

Interannual hydrological structure appears to be less vertically stratified over the entire section; there are no strong gradient zones which can prevent suspended matter transport.

Spring distribution of SMC follows the same pattern as interannual one, along with hydrological structure. Total summer SMC are slightly lower, than in spring. Two types of vertical suspended matter distribution are not clearly visible during summer. In autumn (October) highest SMC values are recorded (influence of beginning of the storm season). Two types of SMC distribution are clearly visible.

It appeared, that summer data shows specific feature – signs of cellular circulation with border at station 3 (cape Gvardeysky). According to [5], circulating cells form inside bays during weak wind conditions. There are strong and storm winds, which destroy those cells and carry sediments towards an open sea. The main run-off of bed load takes place along skirts of bays, infront of capes. During west winds influence, compensating water and sediment outflow focus on eastern bay shores.

According to our data, we can assume that this process is vivid nearby the Gvardeysky cape (st. 3), where the concentration maximum is. The same maximum was observed in [10].

H. CONCLUSIONS

The maximum of SMC is situated alongside the Kaliningrad peninsula, the decrease in concentration takes place towards to the Cronian Spit. Consequently, two types of SMC vertical distribution is recorded on interannual and seasonal alongshore sections: Sambian Peninsula coastal zone is characterized by vertical stratification of SMC, while Curonian Spit coastal zone – by homogenous distribution of latter.

Our findings confirm that the main source of suspended matter for the northern coast area of the Kaliningrad region is located near the middle and eastern part of the northern coast of Sambian Peninsula (cape Gvardeysky).

ACKNOWLEDGEMENTS

The work was financed by the RSF grant 14-37-00047. Authors are grateful to L.D. Bashirova for language editing and help with artwork.

REFERENCES

[1] E.M. Emelyanov. “Sedimentogenesis in basin of the Atlantic Ocean”, Moscow: Nauka, 1982, pp.190 (in Russian).

[2] E.M. Emelyanov. “Geochemistry of suspended matter and bottom sediments of the Gdansk Basin and processes of sedimentation” in *Geology of the Gdansk Basin. Baltic Sea,* Kaliningrad: Yantarny skaz, 2002, pp. 220–302.

[3] E.M. Emelyanov. “Quantitative distribution of suspended matter along Kaliningrad Peninsula and Curonian Spit (Baltic sea)”, *Oceanological research,* no 18, 1968, pp. 203–213.

[4] V.V. Sivkov. “Suspended matter in the water”, in *Neft' i okruzhayushchaya sreda Kaliningradskoj oblasti. Tom II: More (Oil and the Environment of the Kaliningrad Region. Volume II: Sea),* Kaliningrad: Terra Baltica, 2012, pp. 120-128.

[5] A. N. Babakov. “Dynamics of Sedimentary Substances in the Coastal Zone of the Sea”, in *Oil and the Environment of the Kaliningrad Region. Volume II: Sea,* Kaliningrad: Terra Baltica, 2012, pp. 37-59.

[6] A.B. Kozhakhmetov, V. M. Latschenkov. “Preliminary results of determining of background turbidity on the aggradation area of free sandy beach loads at northern coast of Sambian Peninsula”, in *Problems of geomorphology and Quaternary geology of the shelf seas,* Kaliningrad: 1989, pp. 96-99.

[7] A.I. Blazhchishin, A.N. Babakov, V.A. Tschechko. “Concentration and contamination of suspended loads of the Kaliningrad near-shore zone”, in *Problems of studying and protection of the Curonian Spit,* Kaliningrad: AB IO RAS, 1998, pp. 31-58.

[8] V. Ph. Dubravin, E.V. Dorokhova, V.V. Sivkov, V.A. Smyslov, “Hydrochemical figures and suspended matter”, in *Oil and the Environment of the Kaliningrad Region. Volume II: Sea*, Kaliningrad: Terra Baltica, 2012, pp 276-291.

[9] I. M. Belkin, *Morphological and Statistical Analysis of the Ocean Stratification,* Leningrad: Gidrometeoizdat, 1991, 130 p.

[10] V. Ph. Dubravin, Zh. I. Stont, “Hydrometeorological Mode, Water Structure and Circulation,” in *Oil and the Environment of the Kaliningrad Region. Volume II: Sea*, Kaliningrad: Terra Baltica, 2012, pp. 69-105.

A DIFFERENT-SCALE VARIABILITY OF THE VERTICAL THERMAL STRUCTURE OF THE KALININGRAD REGION'S MARINE COASTAL WATERS

Viktor Krechik, Immanuel Kant Baltic Federal University, Kaliningrad, Russia
Maria Kapustina, The Atlantic Branch of the P. P. Shirshov Institute of Oceanology RAS, Russia
Vladimir Gritsenko, Immanuel Kant Baltic Federal University, Kaliningrad, Russia

myemail.gav@gmail.com

Baltic Sea hydrology is quite well explored. Nevertheless, the majority of classical and recent colligative research of Baltic Sea was focused on its off-lying part, shaping several regional databases – HELCOM, ICES. Thus data for 12-mile near shore zone in the Russian part of South-Eastern Baltic is nearly not represented.

IKBFU and ABIORAS employees have gathered an array of measurements, made by CTD probes in Kaliningrad region coastal area during the last 15 years. It was this fact, which make possible to examine a seasonal variability of thermal and halinic structure of shallow marine areas.

The pre-analysis revealed that there is only slight variability in salinity (at about 0.5 psu) in the region of interest. Therefore, the main aim of following work is to analyze a different-scale variability of the vertical thermal structure of Kaliningrad region's marine coastal areas.

This analysis showed two types of the variability – long-term and short-term. The long-term one is represented by seasonal cycle of meteorological features, affecting in a strong way on the hydrological behavior of Baltic sea. The short-term one are regarded as brief, but violent perturbations – storms.

While carrying out this research, the quantitative estimates of thermal structure alteration time were made along with features of thermal structure variability for marine coastal areas.

Key words: different-scale variability, stratification, thermohaline structure, Baltic sea.

I. INTRODUCTION

It is well known that hydrological conditions are the most important abiotic parameters of marine ecosystems functioning. On the one hand, the water area of the Baltic Sea has been well explored. On the another hand, attention of summarizing works on the Baltic Sea [2], [3], [5] are focused on its open part. Arrays of CTD-measurements in the Russian territorial waters of south-eastern Baltic are practically not represented in the global marine databases – for instance, HELCOM, ICES. The purpose of this paper is to describe the annual variability of thermal and salinity structure in shallow sea areas of the Baltic Sea alongshore the Kaliningrad region on the basis of the array of collected during 12 years CTD-measurements.

II. DATA AND METHODOLOGY

The outer limit of the Kaliningrad region coastal zone is signed along the 30 m isobath [7], [1]. There were carried out both single hydrological surveys and systematic long-term observations (Figure 1) in the area of interest from year 2003 to 2015. The measurements were made with a use of modern CTD-probes: CTD90M, Idronaut 316, STD-2a and YSI 600XLM. Data from 1278 hydrological stations was received and processed in total. Small vessels usage allowed conducting measurements from a depth of 3 m. In the area of oil platform D-6 (in Figure 1, it marked with the symbol ▲) measurements were made monthly since 2011.

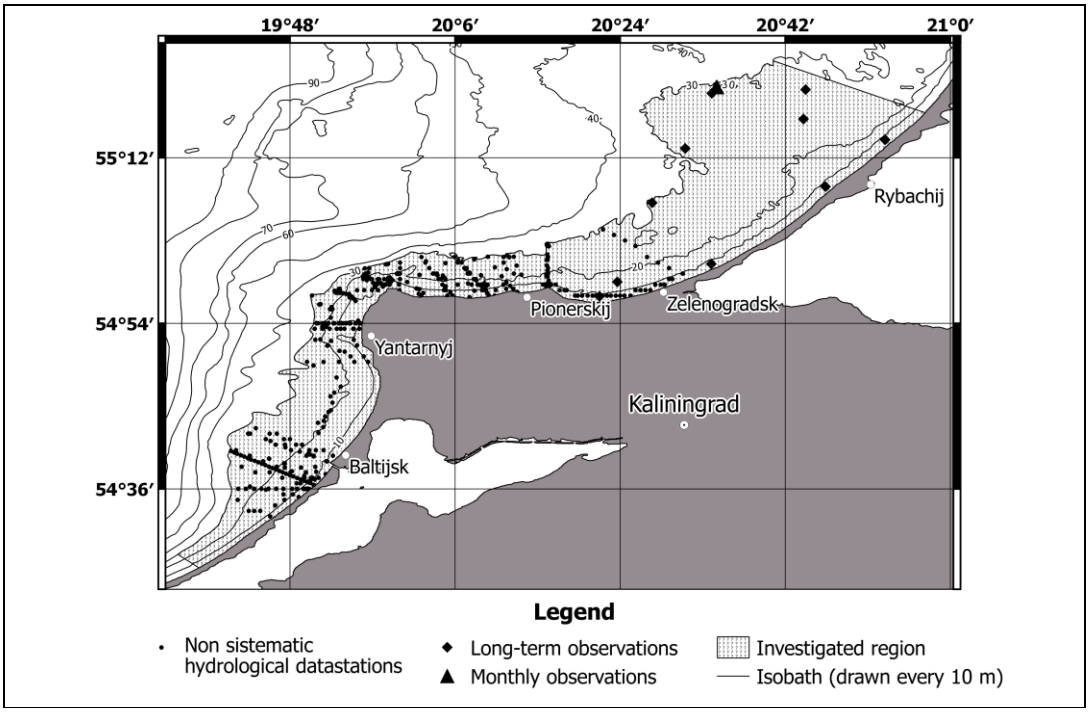

Fig. 1. The map of datastation distribution.

It should be noticed, that in the Gdansk basin seasons don't correspond with classical seasons due to regional climatic features, so by the period from January to March is meant winter, April-June – the spring, July to September – the summer, October-December – autumn [11].

Analysis of the variability of water structure of the area of interest was carried out on the basis of the averaged profiles of basic hydrological parameters vertical distributions. The transition from seasonal sampling series of the field data to the averaged seasonal profiles was performed by the method of layer-by-layer median filtering [6]. The key point of the approach is to calculate the median value for a layer with arbitrary thickness (in this study this parameter was taken as 1 m).

III. RESULTS

Features of the thermohaline structure of open part waters of the south-eastern Baltic are known [4]. The main factors here are the general atmospheric circulation, continental runoff, and water exchange with the North Sea. In the coastal zone of the sea an importance of the coastline exposure, the prevailing winds and the relief of the underwater coastal slope increases, while the effect of water exchange with the North Sea is weakening [8]. Such change in structure-forming

conditions, as well as a decrease in the volume and heat storage in coastal waters leads to occurrence of specific features in the thermal and salinity structure and characteristics of its variability.

For example, in the coastal zone in winter can be seen an inverse thermal stratification. Water temperature slightly increases with depth, reaching a maximum value (3 °C) at the bottom. There is a rising of the sea surface temperature in spring which is caused with the beginning of spring warming. The maximum values of surface temperature are observed in summer (up to 20-22 °C at the end of July-mid August). Autumn cooling of the surface activates the processes of the autumn-winter convection, gradually forming a mixed layer to a 30 m depth. Halocline lies at depths of wind mixing (5-15 m), regardless of the season. The maximum values of salinity are observed at the bottom, the minimum – at the surface.

Therefore, the most interesting periods (being interested in seasonal variability of the thermohaline structure of coastal waters) are spring and autumn, when there is an active restructuring of the water column of the area of interest.

In particular (Figure 2 a), the change in the spring vertical thermal and salinity structure is characterized by the following features: from April to June appears an increase in temperature throughout the entire water column – from 6.5 (in April) to 15 °C (June) on the surface and 2.5 (in April) to 7.5 °C (June) in the bottom layer. In April, the thermocline is at a depth of about 2 meters. It deepens to 15 m in June. Salinity demonstrates the general increase with depth, salinity values in the surface of the following: 6.25 psu – in April, 6.8 psu – in May, 6.55 psu – in June. The changes of salinity in the bottom layer: 7.15 psu – in April, 7.3 psu – in May, 7.6 psu – in June. Decrease in salinity of the surface layer in June is connected with an increase in precipitation.

In October the water temperature for the entire water column changes slightly: at a depth of about 2 m a thermocline is formed due to diurnal warming – a gradient is 0.1 °C/m. In November water of surface layer reaches a temperature about 9 °C, at a depth of about 5 meters and 12 are located temperature surges with range 0.25 °C. The mixed layer with the temperature about 10 degrees is located from 12 meters depth to the bottom (Figure 2 b).

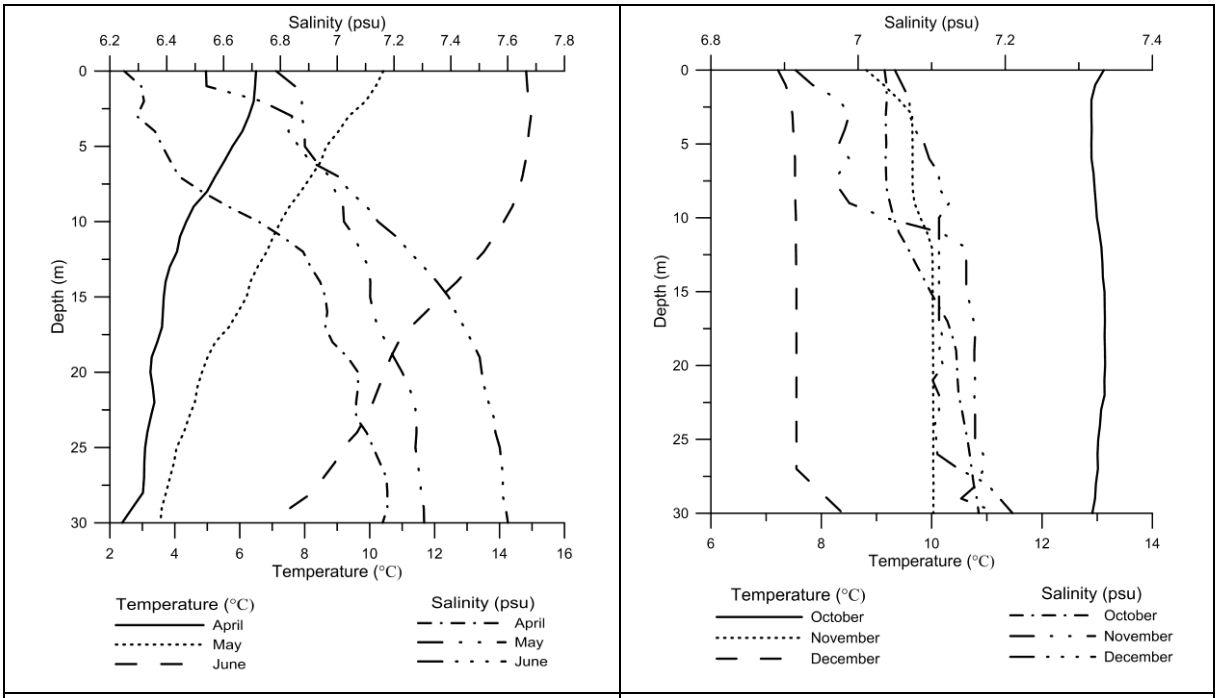

a. b.

Fig. 2. Profiles of the median values of temperature and salinity for spring (a) and autumn (b).

The temperature of the surface layer in December is within 7-7.5 °C, at a depth of about 27 meters thermocline is distinguishable, in the bottom layer temperature reaches 8.2 °C. In October, the salinity increases from 7.03 psu in the surface layer up to 7.1 psu – in the bottom, in November – from 6.9 to 7.18 psu, in December salinity varies with depth in the range 7.05-7.2 psu. In the autumn-winter season, the salinity of the surface layer increases slightly due to reduced river inflow. Low salinity value in November associated with an increase in rainfall.

The thermal structure variability of coastal waters not only follows slow within-year alteration, but also time to time experiences short-term (2-3 days) storm impacts. An example of such event was the 10-hours storm that was recorded on July 19, 2012 near the town of Pionerskij. Hydrological structure and weather conditions before the storm are shown in Figures 3a and 3b, after the storm – in Figure 4a and 4b.

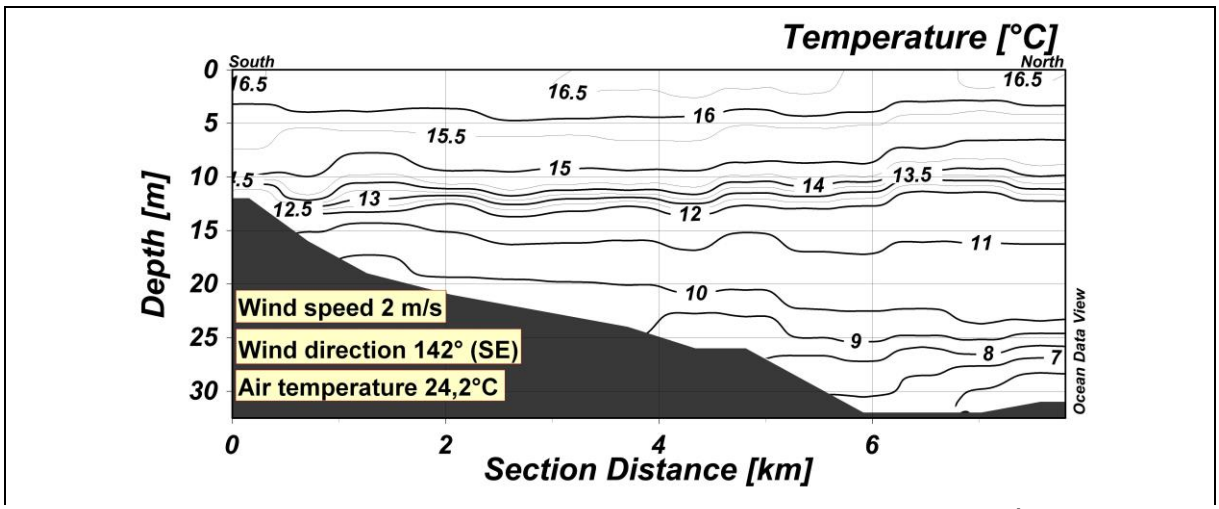

Fig. 3a. The distribution of temperature for section near Pionerskij on the 18th of July 2012

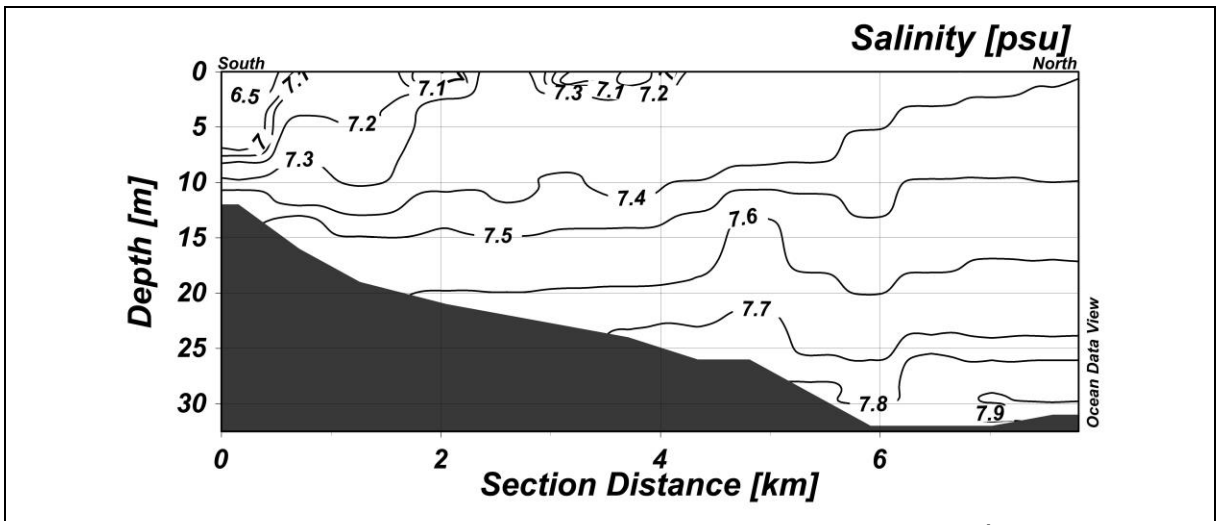

Fig. 3b. The distribution of salinity for section near Pionerskij on the 18th of July 2012

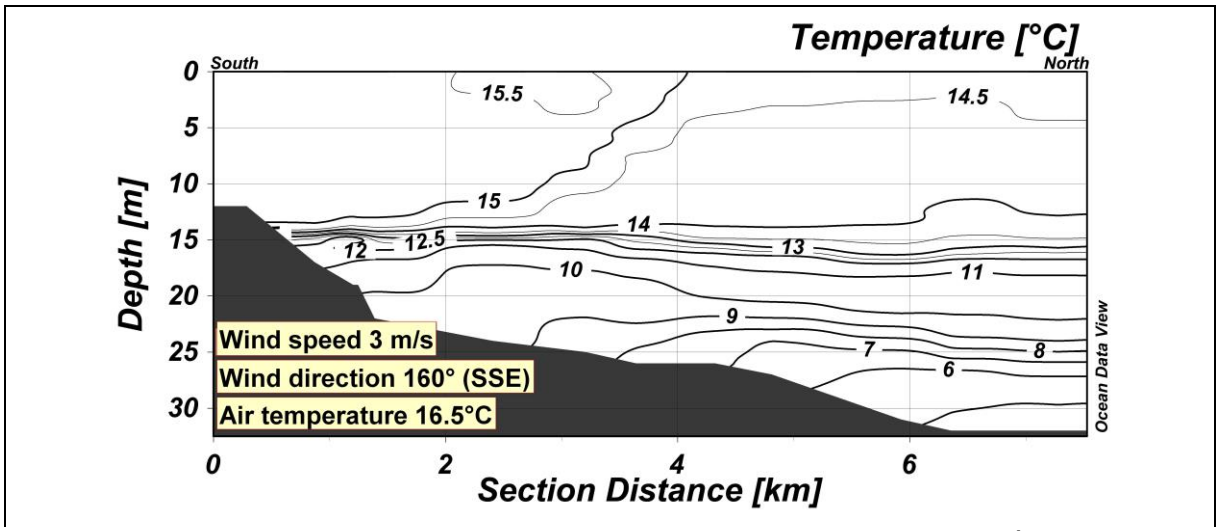

Fig. 4a. The distribution of temperature for section near Pionerskij on the 20th of July 2012

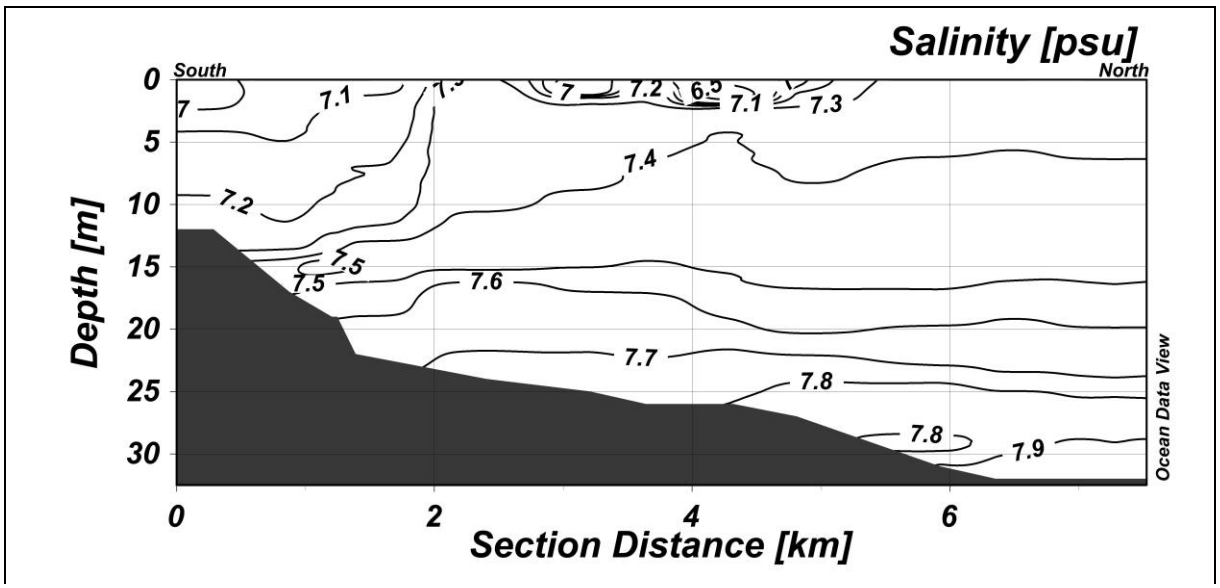

Fig. 4b. The distribution salinity for section near Pionerskij on the 20th of July 2012.

On July 19, 2012 in the study area were observed passing thunderstorm, which was accompanied by the wind direction change to north-west (310 °) and increase of its average speed to 8-9 m/s and gusts up to 12-14 m/s. Such wind disturbance lasted for 6 hours. The total duration of the storm was about 10 hours. The average air temperature during this period dropped to a value of 15.4 °C. The thermohaline structure in the area was rebuilt during the storm. Specifically, the heated upper surface layer (3-5 m thick) with 16-16.5 °C temperature disappeared. On 20 July there was a well-mixed layer of water with a 14.5-15 °C temperature and a 12-13 m thick in this place. The thickness of the thermocline has decreased from 5-6 m to 2-3 m. The bottom layer at a depth of 30 m has +5 °C temperature, which was 1 °C lower than before the storm. In the salinity distribution significant changes weren't noticed.

IV. CONCLUSIONS

Analysis of experimental data sets showed that seasonal variability of coastal waters, in general, corresponds to known climatic descriptions [9], [12]. However, distributions of the main hydrological characteristics in the profiles showed lower (by 1-3 °C) temperatures and higher salinity in the upper part (up to 15 m) in spring. Described in the atlas decrease in salinity values in autumn at 0.4-0.5 psu from the surface to depths of 20-25 m has not been confirmed by field observations.

This research has shown that the vertical thermal structure of the Baltic shallow waters alongshore the Kaliningrad region has two main time scale variabilities: slow seasonal variations and short-term (2-3 days) episodic changes, connected with storms passages, showing intensity and number increasing in recent years [11].

V. ACKNOWLEDGMENTS

This study was financed by the Russian Scientific Fund (grant 14-37-00047).

VI. REFERENCES

[1] A. N. Babakov, “Dynamics of Sedimentary Substances in the Coastal Zone of the Sea”, in *Neft' i okruzhayushchaya sreda Kaliningradskoj oblasti. Tom II: More (Oil and the Environment of the Kaliningrad Region. Volume II: Sea)*, Kaliningrad: Terra Baltica, 2012, pp. 37-59.

[2] A. Omstedt, J. Elken, A. Lehmann, M. Leppäranta, H.E.M. Meier, K. Myrberg, A. Rutgersson, “Progress in Physical Oceanography of the Baltic Sea during the 2003-2014 Period,” *Progress in Oceanography* , no. 128, 2014, pp.139-171.

[3] *Atlas of the Baltic Sea*, ed. by A. Majewska and Z. Lauer. Warsaw: Institute of Meteorology and Water Management, 1994, 214 p.

[4] D. Rak, P. Wieczorek, “Variability of temperature and salinity over the last decade in selected regions of the southern Baltic Sea,” *Oceanologia*, no. 54(3), 2012, pp. 339-354.

[5] *Hydrometeorology and Hydrochemistry of the USSR Seas. Volume III. The Baltic Sea. Issue I. Hydrometeorological Conditions*, ed. by F. S Terziev, V. A. Rozhkov, A. I. Smirnova, St. Petersburg: Gidrometeoizdat, 1992, 449 p.

[6] I. M. Belkin, *Morphological and Statistical Analysis of the Ocean Stratification*, Leningrad: Gidrometeoizdat, 1991, 130 p.

[7] I. O. Leontiev, *Coastal Dynamics: Waves, Currents, Sediment Flows*, Moscow: GEOS, 2001, 272 p.

[8] K. Bowden, *Physical oceanography of coastal waters*, Chichester: Ellis Horwood Ltd., 1983, 302 p.

[9] *State and Evolution of the Baltic Sea, 1952 – 2005. A Detailed 50-Year Survey of Meteorology and Climate, Chemistry, Biology, and Marine Enviroment*, ed. by R. Feistel, G. Nausch, N. Wasmund, 2008, [Electronic resource] Leibniz Institute for Baltic Sea Research Warnemünde [Official website]. URL: http://www.io-warnemuende.de/baltic2008/index.html (accessed: 25.02.2016).

[10] V. F Dubravin, Zh. I. Stont, “Hydrometeorological Mode, Water Structure and Circulation,” in *Neft' i okruzhayushchaya sreda Kaliningradskoj oblasti. Tom II: More (Oil and the Environment of the Kaliningrad Region. Volume II: Sea)*, Kaliningrad: Terra Baltica, 2012, pp. 69-105.

[11] V. P. Bobykina, Zh. I. Stont, “Winter storm activity in 2011–2012 and its consequences for the south-eastern Baltic coast”, *Water Resources*. vol. 42, no 3, 2015, pp. 371-377.

[12] *World Ocean Atlas 2014 Product Documentation*, [Electronic resource], National oceanographic data center of National Oceanic and Atmospheric Administration. [Official website], URL: http://www.nodc.noaa.gov/OC5/indprod.html. (accessed: 27.03.2016).

MAIN TRENDS OF THE SAMBIAN COASTAL SYSTEM (SOUTH-EASTERN BALTIC) DEVELOPMENT: HOLOCENE LITHODYNAMICS AND RECENT COASTAL PROCESSES

Daria Ryabchuk, A.P. Karpinsky Russian Geological Research Institute (VSEGEI), Immanuel Kant Baltic Federal University (BFU), Russia
Alexander Sergeev, A.P. Karpinsky Russian Geological Research Institute (VSEGEI), Immanuel Kant Baltic Federal University (BFU), Russia
Vadim Sivkov, Immanuel Kant Baltic Federal University (BFU), Atlantic Branch of P.P. Shirshov Institute of Oceanology (ABIO RAS), Russia
Vladimir Zhamoida, A.P. Karpinsky Russian Geological Research Institute (VSEGEI), Immanuel Kant Baltic Federal University (BFU), Russia
Olga Kovaleva, A.P. Karpinsky Russian Geological Research Institute (VSEGEI), Immanuel Kant Baltic Federal University (BFU), Russia
Eugenia Dorokhova, Immanuel Kant Baltic Federal University (BFU), Atlantic Branch of P.P. Shirshov Institute of Oceanology (ABIO RAS), Russia

daria_ryabchuk@vsegei.ru

Synthesis of long-term geological research on the Russian region of the southeastern Baltic and its coastal zone has allowed for the establishment of boundaries and determination of the time of formation and the structure of the Sambian morpho-lythodynamic marine and coastal system. The systems studied include the coastal zone (at a the water depth of 30 m according to longshore storm wave current impacts) and adjacent silty-clay sedimentation basins. The development of the Curonian Spit area in the Late Pleistocene – Holocene was reconstructed based on marine geological and geophysical study and modelling. Comparative analyses of the geological settings of the Curonian and Vistula Spits and lagoons has shown that the mechanisms for their development are significantly different. By the late Holocene, the southeastern Baltic Sea consisted of several lithodynamic coastal systems. By 5 ka BP, both lagoon systems had formed. Evolution of the spits and lagoons during the last 5000 years caused the development of similar morphological features. The Vistula and Curonian lagoons transformed into sediment traps for alluvial deposits of the Neman and Pregola Rivers. Smoothing of the shoreline as a result of longshore sediment drift is a dominant coastal process.

Key words: lithodynamics, morpho-lithodynamic system, Holocene, Sambian Peninsula, Baltic Sea

I. INTRODUCTION

The long history of investigations of the southeastern Baltic geology, geomorphology and coastal processes began in the late 19th and early 20th centuries, led by German scientists J. Schumann, G. Berendt, J. Abromeit, and A. Tornquist, and continued after the Second World War

under specialists from the P.P. Shirshov Institute of Oceanology of Russian Academy of Sciences (IO RAS) with Atlantic Branch (AB IO RAS) [1], [2], [3] and Lomonosov Moscow State University (MSU) [4], [5]. Considerable geological, geomorphologic and lithodynamic research on the Curonian Spit and lagoon was undertaken by Lithuanian scientists [6], [7], [8], [9], [10], [11], while the Vistula Spit and lagoon were studied by Polish specialists [12], [13], [14]. During the last decade, the Atlantic Branch of IO RAS, A.P. Karpinsky Russian Geological Research Institute (VSEGEI) and Immanuel Kant Baltic Federal University (BFU) carried out a significant number of marine geological and geophysical investigations, allowed to providing detailed information about the Quaternary geological settings, bottom and coastal relief and surface sediment distribution. A synthesis of the long-term geological research in the Russian region of the southeastern Baltic and its coastal zone provides the opportunity to develop an understanding of the evolution of the Sambian morpho-lithodynamic system.

The aim of this article is to summarize geological and geophysical data obtained in 2005-2015 in the Russian sector of the southeastern Baltic and compare the results with Polish and Lithuanian data to create a single regional model for coastal zone formation. Coastal zone evolution resulting from the long-term processes of sediment and energy interchange between land and sea can be examined using the concept of the morpho-lithodynamic system. The morpho-lithodynamic system of the southeastern Baltic includes the coastal zone (at a water depth of approximately 30 m according to longshore storm wave current impacts) and adjacent silty-clay sedimentation basins. The main task of such an approach is to establish boundaries and to determine the time of formation and the structure of the studied system.

II. MATERIALS AND METHODS

In 1993-2002 VSEGEI, ABIO RAS and Kaliningrad Hydrogeological Expedition carried out joint studies aimed at generalizing geological, geophysical and cartographic information concerning the geological structure of the seafloor of the southern Baltic Sea within the Russian Federation economic zone. The geological maps (at 1:200 000 and 1:500 000 scales) previously compiled for this area by the VNIIMORGEO Institute in 1970-1986 on the basis of the geological survey and geotechnical works have been substantially modified using modern geological and geophysical data obtained by VSEGEI and AB IO RAS. As a result of joint efforts, a set of maps (1:200 000), including Bedrock and Quaternary Geological maps combined with economic deposit maps, Distribution of Bottom Sediments maps and Environmental Geological maps, accompanied by Explanatory notes, was compiled [15]. This set of maps was not published, but was stored in the archives of VSEGEI and the Federal Agency for Mineral Resources of the Russian Federation. Further geological and geophysical studies have shown the high reliability of these maps, at least pertaining to sea depths of more than 5-10 m. In 2005-2008, geological studies by VSEGEI and AB IO RAS were concentrated in the Kaliningrad region coastal zone and adjacent offshore areas, as well as in the Curonian and Vistula lagoons, or the areas most variable in terms of bottom sediment distribution and transformation of bottom topography. Detailed maps of the bottom sediment distribution in the shallow key areas adjacent to the Sambian Peninsula, as well as the Vistula and Curonian spits, were developed based on data obtained by side-scan sonar profiling and sediment sampling. Extensive areas of bottom erosion marked by outcrops of glacial moraine and bedrock

were identified and mapped. The assumption that the lack of sediment load along the northern coast of the Sambian Peninsula is one of the main causes of beach degradation in this area was confirmed. Outcrops of relict lagoon sediments were identified and mapped along the coastal slope offshore of the Curonian Spit. Meanwhile, a pilot version of the electronic cadastre of the Kaliningrad region coastal zone has been developed. It contains modern information about the structure and dynamics of the coasts, as well as sets of multiscale combined (land - sea) geological and environmental geological maps.

New information about the geological structure of the sea bottom was obtained by AB IO RAS, VSEGEI and other organizations while conducting environmental research monitoring the offshore oil field "Kravtsovskoye" (D-6), within the framework of "LUKOIL-KMN", Ltd. As a result of this work, pockmark occurrence and underwater landslides on the slopes of the Gdansk Basin were identified. These investigations also included the assessment of the environmental geological conditions in the Russian region of the southeastern Baltic Sea, concentrating on the study of bottom sediment contamination by heavy metals, organic compounds and petroleum.

In 2010, VSEGEI together with AB IO RAS compiled and published the Atlas of geological and environmental geological maps of the Russian area of the Baltic Sea (1:700 000 scale) [16] and State Geological maps of the Kaliningrad Region (1:1 000 000 scale) [17], which compiled all of the newest information about the geological structure of the region.

In 2011-2015, VSEGEI and AB IO RAS began a new stage of geological exploration in coastal areas. High resolution materials were obtained by carrying out continuous aerial surveys of the seabed using side-scan sonar and multibeam, as well as a network of seismic-acoustic profiling and monitoring sediment sampling. To the west of the Sambian Peninsula, several scarps of ancient coastlines were traced and mapped; evidence of glaciotectonics was fixed; the accumulation of technogenic sediment dumped by the Amber Plant was located and the thickness of these sediments was measured; and underwater outcrops of the Paleogene rocks, including amber bearing layers, were differentiated. To the north of the Sambian Peninsula, some palaeovalleys were identified and areas of bottom erosion and outcrops of pre-Quaternary rocks were clarified. Outflow runnels and specific diapirs formed by relict lagoon muds were found in the area adjacent to the Curonian Spit. Near the Russian-Lithuanian border, an offshore area of ground water discharge, probably associated with deposits from the Palaeo-Neman River, was identified. This new geological and geophysical data allowed for the development of noncontradictory palaeogeographic schemes of regional development during the Late Pleistocene - Holocene, as well as forecasting the development of the coastal zone of the Kaliningrad region.

III. RESULTS AND DISCUSSION

Palaeogeographical analyses

The southeastern part of the Baltic Sea (within the boundaries of the Russian Federation) is located at the southwestern flank of the Russian Plate. The Archean-Proterozoic metamorphic basement is covered by the sedimentary cover of almost all Cambrian-Paleogene ages, except the Carboniferous [16]. The general contour of the shoreline is controlled by geology and tectonics. The Sambian Peninsula is located within a vast uplifted part of the “Kaliningrad megaswell”, where the Curonian and Vistula depressions are divided by cognominal lagoons [5].

The development of the Sambian Peninsula is the most self-evident since the time of the first paleogeographical reconstructions of the study area. Significantly shifted seaward and composed of easily erodible Paleogene-Quaternary deposits, it has been constantly eroded during postglacial history. Earlier, rather conflicting hypotheses regarding the location of submerged Holocene wave-cut cliffs (submerged coastlines) and terraces were presented by several authors based on bathymetric data analyses [8], [9], [18]. Recent detailed geophysical investigations and GIS analyses revealed several areas of maximum slope lines assumed to correspond to wave-cut cliff axes. A total of five axial lines of post-glacial wave-cut cliffs were identified: two dated to the Yoldia Sea (58–45 and 52–40 m), one assigned to the Ancylus Lake (38 m), and two dated to the Litorina Sea (29 and 21 m) [19]. All of the late-postglacial coastlines are located beneath the most recent sea level.

The question of the time and mechanism for the formation of the Curonian and Vistula spits is of fundamental importance in determining the age of the Sambian morpho-lithodynamic system. Before lagoon formation, alluvial deposits of the Neman, Vistula and Pregola Rivers discharged into the Baltic Sea Basin. Despite the morphological similarity of the Curonian and Vistula Spits, the results of geological investigations noted significant differences in their development caused by tectonic regime, pre-Holocene relief and sources of sediment material.

To the southwest of the Sambian Peninsula, the line of the Gardno end-moraines (Gardno Phase) is situated near the coast. It traces along the shore of the Vistula Lagoon, forming a landward curve in the area of the Vistula River delta and travels in the western direction within the Polish coastal zone [12], [14]. Within the Sambian Peninsula and further to the north-east, the end-moraine of the same stage (Mid-Lithuanian) [20], [21] changes direction, forming a large smooth landward curve. To the south-west of the Sambian Peninsula, all Late Pleistocene shorelines were located below the recent sea level. Deposits of the Baltic Ice Lake (BIL) were not found onshore. The young phase of the BIL was dated by the peat layers in the Pomeranian Bay; its transgressive phase was studied in the sediment complex of the Vistula River palaeodelta. The BIL level is estimated to be -30 - -25-22 m b.s.l. [14].

To the north-east of the Sambian Peninsula, the BIL clays are spread within glacial till depressions seaward from the Curonian Spit (at water depths of more than -25 m b.s.l.), from 12..-15 m b.s.l. in the southern part of the Curonian Lagoon [10] to 20 m b.s.l. in the central part and to -25..-28 m b.s.l. in front of Rybachy village. The thickness of the BIL deposits in the borehole from the central part of the Curonian lagoon is more than 10 m. In the northern (Lithuanian) part of the lagoon, BIL deposits are widespread, but their thickness is less [22]. Sandy facies of the BIL were mapped during the geological survey of the coasts of both the Curonian and Vistula lagoons. Taking into account the difference in the tectonic subsidence rates (Fig. 1), their occurrence can be easily explained for the Curonian Lagoon, but is rather contradictory with the existing hypothesis of the BIL sea level for the Vistula lagoon. Further research and dating is needed to solve this problem.

Late Pleistocene relief controls the land and sea bottom morphology, as well as the structure and composition of overlaying Holocene deposits. The results of geomorphological modelling revealed the conditions for the development and recent position of the Curonian Spit.

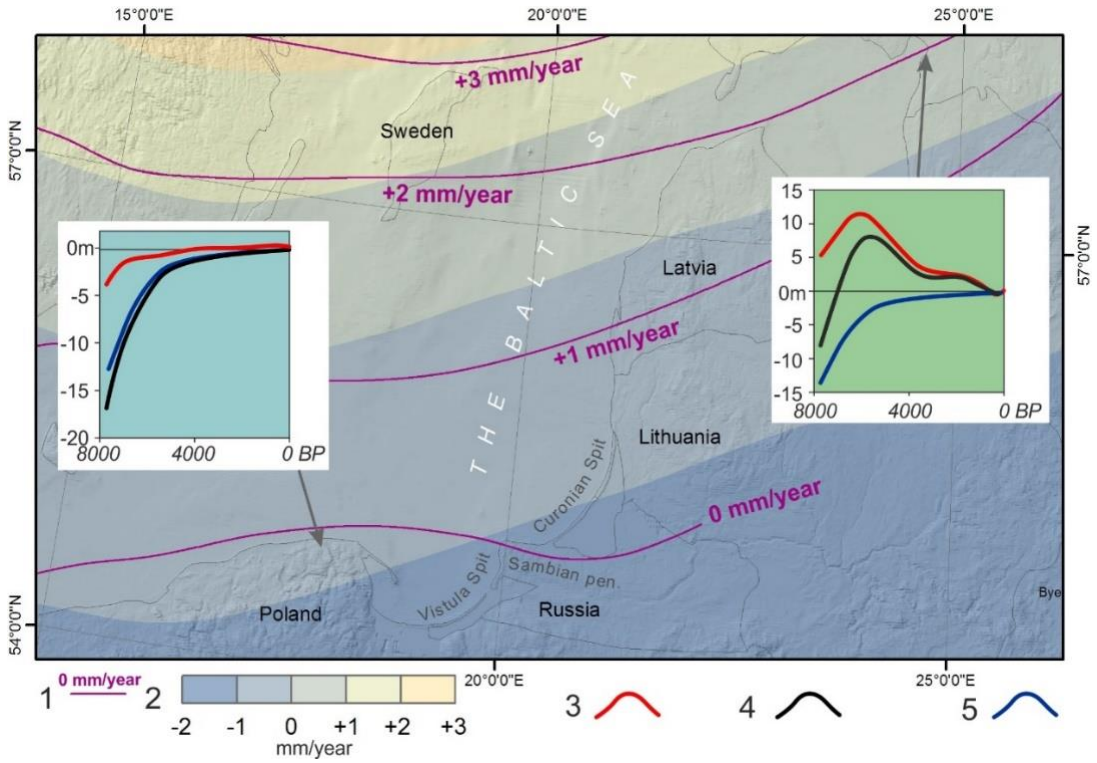

Fig. 1. Vertical crustal displacement (mm/year) for the twentieth century: 1 – isobases by [23]; 2 – isobases by [24]. Graphs: 3 – the isostatic component; 4 – relative sea level change; 5 – the eustatic curve.

The Late Pleistocene relief within the Baltic Proper in front of the Curonian Spit is rather dissected (Fig. 2), with several basins, ridges and narrow runnels. Runnels are up to 10 m in relative depth and are located within the Palaeo-Neman area and most likely have an erosion origin. The Late Pleistocene surface within the Curonian Lagoon is subdivided into two separate basins. Many modern relief features are inherited from the Late Pleistocene surface. GIS hydrological modelling allowed for the possible locations of palaeoriver valleys in the Early Holocene to be traced – linked with palaeo-Neman in the east, palaeo-Deima in the south and the third (southwestern) under the attached part of the Curonian Spit [25].

In the area of the Vistula Spit, deposits of Weichselian glaciation and Late Pleistocene postglacial basins were one of the few remaining occurrences of significantly reduced thickness, mainly sands with gravel. Their surface is eroded, and the degree of destruction increases in the eastern direction. Late Pleistocene deposits are identified in the Sztutowo area at -20-16 m b.s.l. and in the Przebrno area at -21-20.5 m b.s.l. [13].

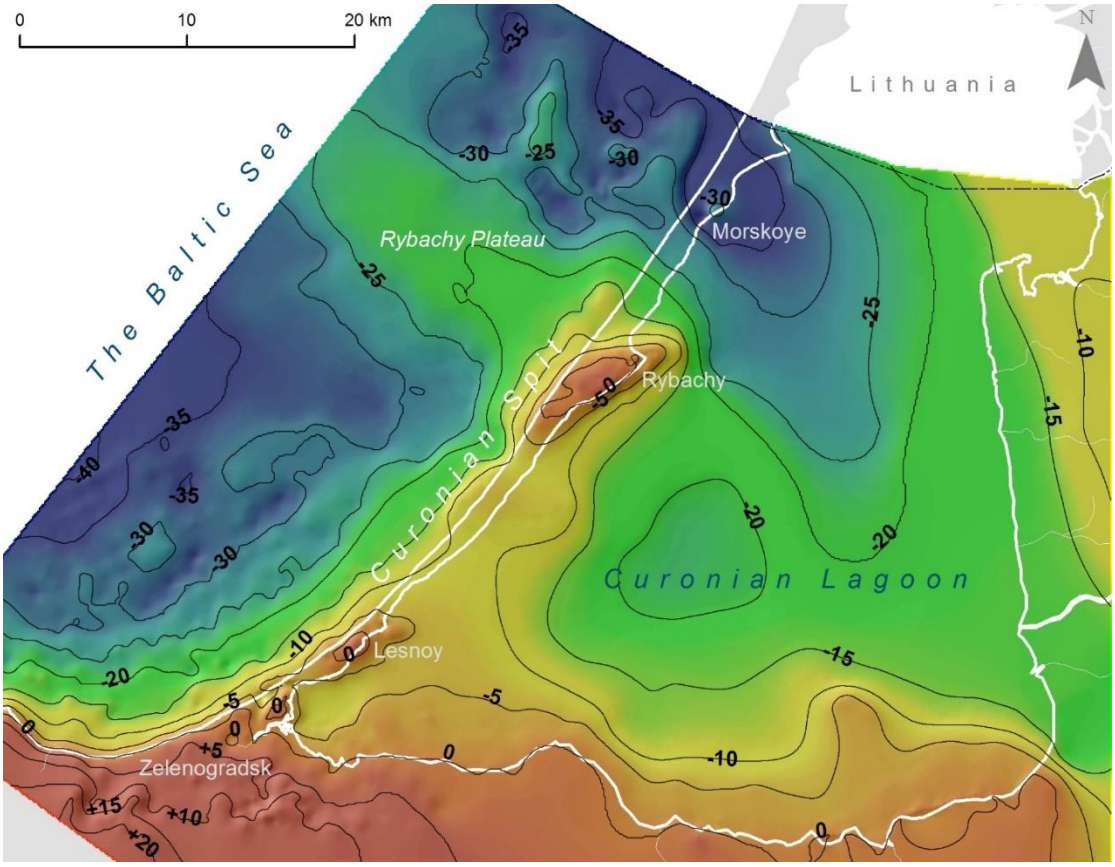

Fig. 2. Model of Late Pleistocene relief (m m.s.l.)

In the Early Holocene, as a result of the final drainage of the BIL, the water level dropped by -55-60 m b.s.l. within its southwestern part [12], [14] and the Baltic Basin was connected with the ocean, forming the Yoldia Sea. The next palaeobasin – the fresh-water Ancylus Lake – was formed after a 25 m transgression caused by a glacioisostatic rebound [12]. The level of Ancylus Lake in Gdansk Bay reached -20 m b.s.l. by the end of Early Holocene. To the north-east of the Sambian Peninsula, deep-water facies of Ancylus Lake are found at a sea water depth of -80 m b.s.l. [15], [16].

Significant differences were revealed in the Holocene geological settings of the Curonian and Vistula Spits. The thickness of Holocene deposits within the Russian part of the Curonian Spit increases from the southwest to the northeast from 1-5 m to 40-80 m (under dune massifs). Along some areas in the attached part of the spit and in the vicinity of Rybachy village, their thickness is less than 1 m [25]. On the contrary, Holocene deposits of the Vistula Spit are characterized by a consistent thickness of approximately 20 m.

In the boreholes located in the Russian part of the Curonian Spit, Early Holocene deposits are absent, with the exception of the southern part of the spit in the vicinity of Morskoye village [4], where they are represented by unsorted sands. In the Lithuanian part of the Curonian spit and the lagoon, a surface of Early Holocene deposits, submerging seaward, are located at a depth from -6 to -10 m b.s.l., with local valleys up to -15..-20 m b.s.l. [22].

The best preserved areas of Ancylus Lake deposits according to borehole data are found in the Curonian Lagoon [10]. They are represented by sand with the surface established at a depth from

-4 to -18 m b.s.l., with decreasing thickness in the eastern and southern directions. Along the eastern and southern coasts of the Curonian Lagoon, the thickness of Ancylus deposits is less than 1 m and completely absent within the Neman delta plain.

Palaeoreconstructions of the Curonian Spit area during the Holocene based on this research are shown in Fig. 3. According to the data on the Ancylus Lake level [1], [7], [14], it is can be concluded that palaeorivers were the main source of sediment material for deposition within the Curonian Lagoon basin during the Early Holocene within the Baltic Basin shoreline of the Ancylus Lake located near modern isobaths of -60 m. Small fresh-water lakes could have been located in the bottom depressions of the central part of the Curonian Lagoon. In the northern part of the Curonian Lagoon that was connected to the open part of the Baltic Basin during the period of the lowest water level, deltaic sand accumulation occurred.

During the first stage of the Litorina Sea development, the coast line was located at a depth of -25 m b.s.l. An isolated fresh-water lake occurred in the Curonian Lagoon Basin. During the maximal phase of the Litorina transgression (about +3 m a.s.l.), the Curonian Spit plateau and ridges and the Rybachy Plateau were submerged. The Curonian Lagoon area was an open bay of the Litorina Sea, possibly partly separated by several small islands. Due to active hydrodynamics, bottom erosion and redeposition of sediment material dominated within the study area after the maximal phase of the Litorina transgression.

Investigations of the Baltic Sea bottom along the southern half of the Curonian Spit using side-scan sonar, multibeam echosounder, seismic imaging, sediment sampling, and video observations allowed for the identification and mapping of a unique underwater landscape formed by extensive outcrops of laminated and folded lagoon marl at water depths of 5 to 15 m. The relict lagoon marl was deformed, compacted, and dehydrated by a massive dune-covered coastal barrier migrating landward (retrograding) over these sediments during the Litorina Sea transgression in a process termed “dune tectonics”. Offshore lagoon marl ridges form an extensive complex that was approximately 5 m (up to 8-10 m) thick; modern marine sands [26] cover the described complex. A conceptual palaeogeographic model of the relict lagoon marl extrusions (diapirs) on the underwater coastal slope of the Curonian Spit is shown in Fig. 3 (7500 ka BP).

Along the marine coast of the Curonian Spit in the vicinity of Zelenogradsk, Lesnoy and Rybachy, peat and palaeosols layers were found at a depth of approximately -1 m b.s.l. Radiocarbon dating results have shown that during the last 5000 years, slow shifting of the spit toward the lagoon due to the increasing sea level was the main Curonian Spit development trend [27].

Consequently, the Curonian Spit developed during the Holocene on a postglacial surface (e.g., glacial moraine ridges remain) as a polygenic accretion form. During the first stages of the Curonian Spit development (regressive phase after the Litorina transgression maximum), both cross-shore and longshore sediment transport were sources of sediment material, as a result of the erosion of the Sambian Peninsula, Rybachy Plateau and deltaic sediments. The smoothed contour of the spit shoreline formed during the last 5000 years as a result of longshore sediment drift.

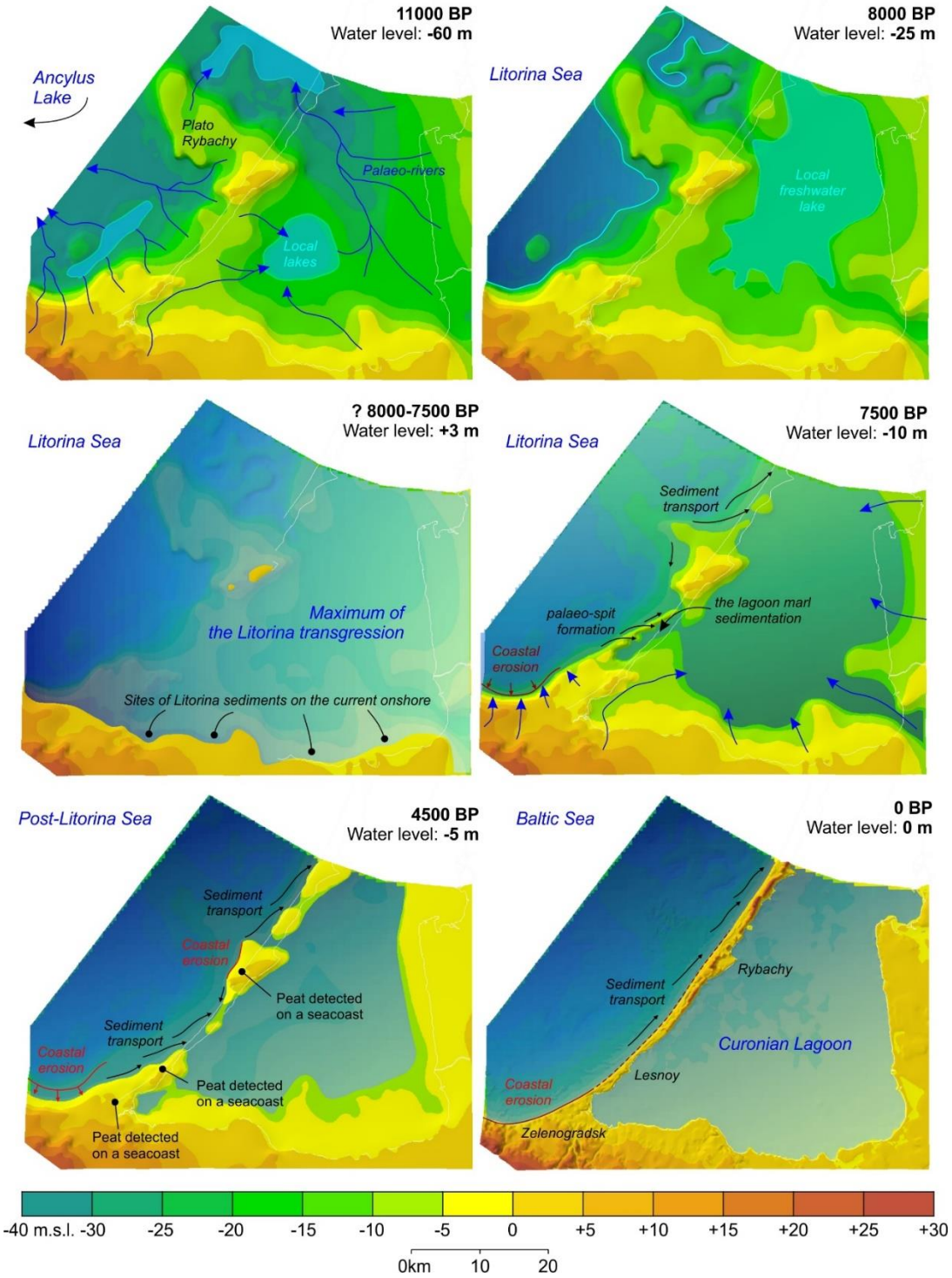

Fig. 3. Palaeogeographical reconstruction of Holocene development of the Curonian Spit area [25].

The geological setting and postglacial history of the Vistula Spit area, according to [12], [13], [14], are completely different, as was earlier mentioned by [28]. There are only subaerial lacustrine–swampy or alluvial–deltaic complexes beneath the modern silty sediments of the gulf, whereas marine complexes are completely absent. Therefore, the Vistula lagoon has never been open to the Litorina Sea. An important feature of the Vistula Delta Plain and area under the Vistula

Spit is a consistent biogenic layer, deposited between 9120 and 7330 kal years B.P. The palaeoenvironment of this long-term biogenic accumulation is interpreted as a large plain with channels and shallow swamps and peat logs in depressions. Within Vistula Spit, this layer is covered by marine Litorina sands and dunes [13].

According to detailed palaeoreconstructions [14], during the existence of Ancylus Lake, the coastline was situated below the recent sea level within the Gdansk Basin, forming a vast open bay with advanced palaeo-Vistula deltas. As a result of deltaic deposit erosion, extensive barrier beaches formed in the coastal zone and aeolian processes started. During Early Litorina time, the shoreline shifted landward within the central part of the recent Vistula Lagoon and the small, partly isolated lake occurred. During the Litorina transgression (by 8000 kal years BP), the coastline shape first became similar to the modern one. Hel Spit developed; the Vistula Lagoon became separated from the sea by the Vistula Spit, probably by several palaeostraits. Approximately 2500 kal years BP the area of the lagoon was larger than it is today [14].

It is noteworthy that numerous datings and other geological evidence support this concept. However, some geological survey results in the Russian part of the Vistula Lagoon coasts map marine Litorina sands at an altitude of 2 to 5 m, and hypotheses on the formation of the palaeo-lagoon marl of the Vistula Spit also differ. It should be mentioned that the Russian part of the Vistula Lagoon is much less studied in comparison with the Polish part. To fill in these gaps in knowledge, further investigation is needed.

Modern lithodynamic processes

Analysis of materials and data confirmed that most of the transported sediment forming the total sediment flux migrated within the coastal zone of the Sambian Peninsula and that the Curonian Spit consists of products of coastal and bottom erosion, although one of the particularities of the Gdansk basin is a predominance of the river load in its sediment balance. The explanation for this is that first, the equilibrium profile is still under formation and erosion processes are taking place there and, second, the Vistula and Curonian lagoons act as traps for fluvial sediments. As was previously observed, such fluvial sediment flux plays an important role in the Vistula Spit sediment balance.

Complex erosion and accumulation processes leading to the smoothing of irregularities along the coastline (bays, capes) is the modern development tendency of Kaliningrad region coasts. The common pattern of longshore sediment transport described in the literature depicts two sediment fluxes directed to the north-west and southeast from the Sambian Peninsula (Cape Taran). On an underwater slope of the northern part of the Sambian Peninsula and the Curonian Spit, sandy material migrates within so-called morpho-lithodynamic cells [29]. The McLaren method [30] was applied to determine the sediment transport direction of the underwater slope restricted by isobaths -30 m (zone of active wave influence) [31]. The results show that sediment movement depends on the morphological properties of the coastal zone – points of flux divergence are associated with capes; outcrops of moraine and pre-quaternary deposits are a source of material to be transported.

IV. CONCLUSIONS

Synthesis of long-term geological research in the Russian part of the southeastern Baltic and its coastal zone allowed for boundaries, the time of formation and the structure of the Sambian morpho-lythodynamic marine and coastal system to be established. New geological and geophysical

data enabled palaeogeographical schemes of the Holocene development of the Curonian Spit area to be produced. Comparative analyses of the Curonian and Vistula Spits areas revealed significant differences regarding their development in the Late Pleistocene and Early Holocene, when the coastal zone of the study area consisted of several morpho- lithodymanic systems.

The Curonian Spit developed during the Holocene on a postglacial surface (e.g., glacial moraine ridges remains) as a polygenic accretion form. During the first stages of Curonian Spit development (the regressive phase after the Litorina transgression maximum), both cross-shore and longshore sediment transport were sources of sediment material as a result of the erosion of the Sambian Peninsula, Rybachy Plateau and deltaic sediments. The smoothed contour of the spit shoreline was formed during last 5000 years, mostly as a result of longshore sediment drift.

The Vistula Spit area, according to [14], was located onshore by the time of the Litorina transgression when the coastline shape first became similar to the modern one. The Hel Spit developed and the Vistula Lagoon became separated from the sea by the Vistula Spit, most likely with several palaeostraits [14].

Consequently, the lagoon systems of the south-eastern Baltic became morphologically similar during the last 5000 years when the Curonian and Vistula Spits and lagoons had similar configurations; the lagoons became sediment traps for the alluvial material of the Neman, Vistula and Pregola Rivers; and longshore and sediment transport became one of the most important coastal processes of these marine shores.

The work was supported by the Russian Scientific Fund (grant 14-37-00047).

V. REFERENCES

[1] A.I. Blazhchishin, “Flooded Dunes and Deposits of Construction Materials on the Sea Underwater Slope of the Curonian Spit,” *Problems of Investigation and Protection of Nature at the Curonian Spit,* pp. 59-67, 1998, in Russian.

[2] V.L. Boldyrev and O.I. Ryabkova, “Coastal Zone Processes Dynamics of the Baltic Sea (Kaliningrad Region),” *Proc. Rus. Geographical Soc.*, vol.133. no.5, pp. 41-48, 2001, in Russian.

[3] G.S. Kharin and S.G. Kharin, “Geological Structure and Composition of the Curonian Spit (Baltic Sea),” *Lithology and Miner. Resources,* vol. 41, issue 4, pp.3 17-323, 2006.

[4] E.N. Badyukova, L.A. Zhindarev, S.A. Lukyanova and G.D. Solovyeva, “Curonian Spit: Genesis and Development,” *Quaternary International*, vol. 167, pp. 21-27, 2007.

[5] L.A. Zhindarev, O.I. Ryabkova and V.V. Sivkov, “Geology and Geomorphology of Marine Coasts,” *Oil and Environment of Kaliningrad Region,* vol. II: Sea, pp. 19-37, 2012, in Russian.

[6] A. Bitinas, R. Zaromskis, S. Gulbinskas, A. Damusyte, G. Zilinskas and D. Jarmalavicius, “The Results of Integrated Investigations of the Lithuanian Coast of the Baltic Sea,” *Geology, Geomorphology, Dynamics and Human Impact. Geological Q.*, vol. 49 (4), pp. 355-362, 2005.

[7] A. Damušytė, “Post-glacial Geological History of the Lithuanian Coastal Area,” Summary of doctoral dissertation, Vilnius, 84 p., 2011.

[8] Zh. Gelumbauskaite, “Methods and Results Study of Ancient Coastal Levels Deformations of the SE Baltic Sea,” *Baltica,* vol.7, pp. 95–104, 1982.

[9] V.K. Gudelis, L.S. Lukoshevichus, G.I. Klejmenova and E.M. Vishnevskaya, "Geomorphology and Late-after-glacial Bottom Sediments of the South-eastern Baltic," *Baltica,* vol.6, pp. 245–256, 1977, in Russian.
[10] M. Kabailienė, "Kursiu Nerija Spit and the Kursiu Marios Lagoon: Geological Structure, Origin and Development During Late Glacial and Holocene," *Abstr. Excursion Guide,* The fifth marine geological conference «The Baltic», pp. 134-142, 1997.
[11] O. Pustelnilovas, "The Development of Kursiu Marios Lagoon on the Sedimentological Data," *Abstr. Excursion Guide*, The fifth marine geological conference «The Baltic», pp. 149-155, 1997.
[12] J. E. Mojski, "The Evolution of the Southern Baltic Coastal Zone," *Oceanologia*, vol.42, no.3, pp. 285–303, 2000.
[13] A. Tomczak, "Geological Structure and Holocene Evolution of the Polish coastal zone," *J. Coast. Res.,* no. 22, pp. 15-32, 1995.
[14] S. Uscinowicz, "Relative Sea Level Changes, Glacio-isostatic Rebound and Shoreline Displacement in the Southern Baltic," *Pol. Geological Inst. Special Papers,* vol.10, 79 p., 2003.
[15] V.A. Zagorodnyh, T.A. Kunaeva, "Geology and Economic Deposits of Kaliningrad region," 171 p., 2005, in Russian.
[16] *Atlas of Geological and Environmental Geological Maps of the Russian Area of the Baltic Sea,* Editor O.V. Petrov, St. Petersburg, VSEGEI, 78 p., 2010, in Russian.
[17] N.V. Lukyanova, Y.B. Bogdanov, O.V. Vasiliev, G.P. Vargin, V.R. Verbitsky, N.R. Gorbatsevich, et al., "*State Geological map of the Russian Federation*," 1:1 000 000 scale (third generation). Central European Series. Sheet-N-(34) - Kaliningrad. Explanatory note, St. Petersburg, VSEGEI, 226 p., 2011, in Russian.
[18] A.I. Blazhchishin, V.L. Boldyrev, A.N. Efimov and I.A. Timofeev, "Ancient Coastal Levels and Formations in the South-eastern Baltic Sea," *Baltica,* vol. 7, pp. 57–64, 1982, in Russian.
[19] V. Sivkov, D. Dorokhov and M. Ulyanova, "Submerged Holocene Wave-Cut Cliffs in the South-eastern Part of the Baltic Sea: Reinterpretation Based on Recent Bathymetrical Data," *The Baltic Sea Basin, Cent. East. Eur.,* pp. 203-217, 2011.
[20] B.G. Anderson and H.W. Borns, *The Ice Age World,* Scandinavian University Press, Oslo, 208 p., 1994.
[21] I.I. Krasnov, K. Duphorn and A.Vogese, "*International Quaternary Map of Europe*," scale 1:2500000, 1971.
[22] L. Ž. Gelumbauskaitė, J. Šečkus, "Late–Glacial–Holocene History in Curonian Lagoon (Lithuanian sector)," *Baltica,* vol. 18, no.2, pp. 77-82, 2005.
[23] J. Harff and M. Meyer, "Coastlines of the Baltic Sea – Zones of Competition Between Geological Processes and a Changing Climate: Examples from the Southern Baltic," *The Baltic Sea Basin, Cent. East. Eur.,* pp. 149-164, 2011.
[24] O. Vestøl, "Determination of Postglacial Land Uplift in Fennoscandia from Levelling, Tide-gauges and Continuous GPS Stations Using Least Squares Collocation," *J. Geodesy,* no.80, pp. 248-258, 2006.
[25] A.Yu. Sergeev, "The Palaeogeographical Reconstruction of the Curonian Spit Area in the Late Pleistocene – Holocene," *Reg. Geology Metallogeny*, no. 62, pp. 34-44, 2015, in Russian.

[26] A. Y. Sergeev, V. A. Zhamoida, D. V. Ryabchuk, I. V. Buynevich, V. V. Sivkov, D. V. Dorokhov et al., "Genesis, Distribution and Dynamics of Lagoon Marl Extrusions along the Curonian Spit, Southeast Baltic Coast," *Boreas,* 10.1111/bor.12177. ISSN 0300-9483.

[27] A. Sergeev, V. Sivkov, V. Zhamoida, D. Ryabchuk, A. Bitinas and J. Mažeika, "Holocene organic-rich Sediments within the Curonian Spit Coast, the South-eastern Baltic Sea," *Baltica,* , vol.28, no.1, pp. 41-50, 2015.

[28] E.N. Badyukova, L.A. Zhindarev, S.A. Lukyanova and G.D. Solovyeva, "The Geological-geomorphological Structure of the Baltic (Vistula) Spit," *Oceanology,* vol. 51, no. 4, pp. 632–639, 2011.

[29] A.N. Babakov, "Evolution of Ideas about Structure of Long-shore Sediment Transport in the South-eastern Baltic," *Lithodynamics of Ocean Bottom Contact Zone,* pp. 56-58, 2009, in Russian.

[30] P. McLaren and D. Bowles, "The Effects of sediment transport on grain-size distributions," *J. of Sediment. Petrology*, vol.55, no.4, pp. 0457-0470, 1985.

[31] E.V. Dorokhova and D.V. Dorokhov, "Sediment Mapping and Transport Pathways in the Nearshore Zone of the Russian part of South-Eastern Baltic Sea," *EMECS'11 – SeaCoasts'26 Conference Proc.,* 2016, in press.

CONDITIONS FAVOURABLE FOR PROTECTION THE MARINE SHORE OF THE VISTULA SPIT AND SAMBIAN PENINSULA (THE BATIC SEA, KALININGRAD OBLAST) BY OFFSHORE DISPOSAL OF DREDGED MATERIAL

Andrei Sokolov, Immanuel Kant Baltic Federal University (IKBFU), Russia
Boris Chubarenko, Atlantic Branch of P.P. Shirshov Institute of Oceanology of Russian Academy of Sciences, Russia

tengritag@gmail.com

Three dumping sites located at the south-eastern part of the Baltic Sea (Kaliningrad Oblast) at shallow depths are considered. The first one is located to the south of the Vistula Lagoon inlet in front of a permanently eroded open marine shore segment. The second one is located to the north of the Vistula Lagoon inlet, and is used now for disposing of dredged material extracted from the Kaliningrad Seaway Canal. The third dumping site is located near the northern shore of the Sambian Peninsula to the east of the Cape Gvardeijski and assigned for disposing the dredged material extracted from the fairway to the Pionerskij Port located nearby. The last site is planned to be used for disposing of dredged material from the future port that should be constructed there before the beginning of the FIFA World Cup 2018. All three dumping sites are located not far from the eroded segments of the shore. The question behind the study is: would it possible that disposed material will naturally transported from the damping site to the shore and accumulate there to protect it from erosion? A numerical hydrodynamic-transport 3D model (MIKE) was used to model sediment transport under different wind actions. The winds with the speed stronger than 15 m/s complete wash out disposed material from the dumping site and spreading it over the wide area with a negligible layer thickness. Winds of about 7-10 m/s transport material along the shore at a distance of few kilometers that may be useful for shore protection. The first location of the dumping site (to the south of the Vistula Lagoon inlet) looks very ineffective for potential protection the shore nearby. At the other hand, the second and especially the third locations are favorable for transport of disposed material to the shore, the most favorable conditions are at onshore or alongshore currents.

Key words: dumping, sediment transport, numerical simulation, wind waves, near shore currents

I. INTRODUCTION

It is known [1-3] that the entrances to marinas and ports in the South-Eastern Baltic are regularly filling by sand and, therefore, require periodic dredging. On the other hand, construction of any port on the open sea shore usually negatively influences on sediment balance in the location and

coastal erosion very often becomes a problem after a port construction. Coastal protection would be the best use of the dredged material.

One of the places demanding constant deepening is the Baltijsk Strait, an inlet of the Vistula Lagoon (Figure 1), which hosts the main fairway connecting ports of Kaliningrad with the Baltic Sea. Entrance moles bounded this inlet from the marine side are obstacles for the alongshore sediment transport, and leeward erosion exists just to the south from the moles at a distance of 2.5-3 km [4, 5]. In June 2006 an experimental dumping of dredged materials were carried out in the vicinity of the eroded shore (insert of the Figure 1, site No 1). Unfortunately the result of the experiments was negative. Strengthening the coast at the Kosa Village, located opposite the dumping site No 1, did not happen. Detailed results of field measurements and numerical simulations given in [5] showed that the disposed material was transported along the shore and does not reach the shoreline under any landward wind conditions. It was concluded that the only effective suggestion which could strengthen the coast is to dispose dredged material directly onto the beach.

There are two regular offshore dumping sites (Figure 1, sites No 2 and 3) near the shore of the Kaliningrad Oblast that are used to dispose the dredged material. The dumping site No 2 is for the material dredged in the Baltijsk Strait. The dumping site No 3 is used to accumulate dredged material after the deepening of the marina near the town Pionerskij. This marina should be converted into a modern port before the beginning of the FIFA World Cup 2018. Consequently, the dumping site No 3 will be intensively used in the future.

The aim of the current paper is to analyze would the dredged material discharging on the dumping sites No 1, 2 and 3 be transported alongshore and serve to protect some part of the shore from erosion. The analysis is based on a numerical simulation.

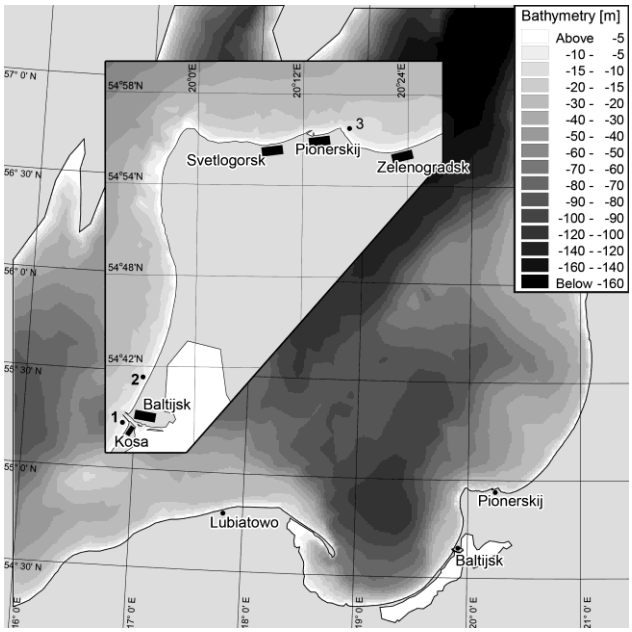

Figure 1. Computational domain and locations of offshore dumping sites in coastal waters of the Kaliningrad Oblast: 1 – the experimental dumping site in 2006 (just to south from the Vistula Lagoon inlet); 2 – the official dumping site for dredged material from the Baltijsk Strait; 3 – the official dumping site for dredged material from the marina Pionerskij.

II. METHOD

Simulations were performed using the software package MIKE, developed by DHI Software [6, 7]. A three-dimensional formulation (10 layers in depth, sigma-coordinate) was used for simulations. The computational domain covered a central part of the Baltic Proper (Figure 1). The depth field was taken from digital topography of the Baltic Sea [8]. Mesh sizes of irregular grid for the open sea were about 5-7 km, and in the vicinity of the dumping sites – about 100 m. All boundaries of the simulation area were closed, and wind was the only driving force in the model. It was assumed that wind measured in Baltijsk could be uniformly applied for the entire area of simulations. Such a model set-up showed its advantages for coupled hydrodynamic and wind waves simulations near the shore of the study area in [9, 10].

Three modules of the MIKE numerical models system were used. The Hydrodynamic Module gave the solutions (water level and currents) of 3-dimensional shallow water equations [7], the Spectral Wave Module solved the balance equation for the density of wave action [7], and the Mud Transport Module simulated the advection and dispersion of the admixture, including its settling and re-suspension [6]. All of them were used in coupled mode.

Calibration and verification.

The results of the calibration of the utilized model setup for the Hydrodynamic and Spectral Wave modules were presented in [9] and [10] respectively. The correlation coefficients between the measured and simulated currents and wave parameters were up to 0.8, and their maximal and average values were also comparable.

Utilized model setup is based on the assumption that wind speed and direction in computational area are uniform. Arguments behind are as follows: 1) satellite data [11] show that wind speed and direction over the Baltic Sea can be considered almost the same within the regions with a characteristic size from hundreds to thousands of kilometers; 2) the previous simulations [9, 10] showed a good agreement between field measured and simulated results for waves and currents while based on the same assumption. At last, the impressive results are shown in Figure 2. Solid line here represents field data obtained by the wave buoy of the IBW PAN[6] 1-31.07.2015 installed at the depth of 15 m opposite the Lubiatowo (see Figure 1). Dotted line represents simulation results. Simulations were performed for the point where the buoy was located but the wind speed and direction were measured by a meteorological station located in Baltijsk more than 200 kilometers far from Lubiatowo. In this case a good coincidence between field data and simulation results (correlation coefficient is higher than 0.8) shows that wind conditions over the Baltic Sea within hundreds of kilometers are similar.

[6] Institute of Hydroengineering of the Polish Academy of Sciences, Gdansk, Poland

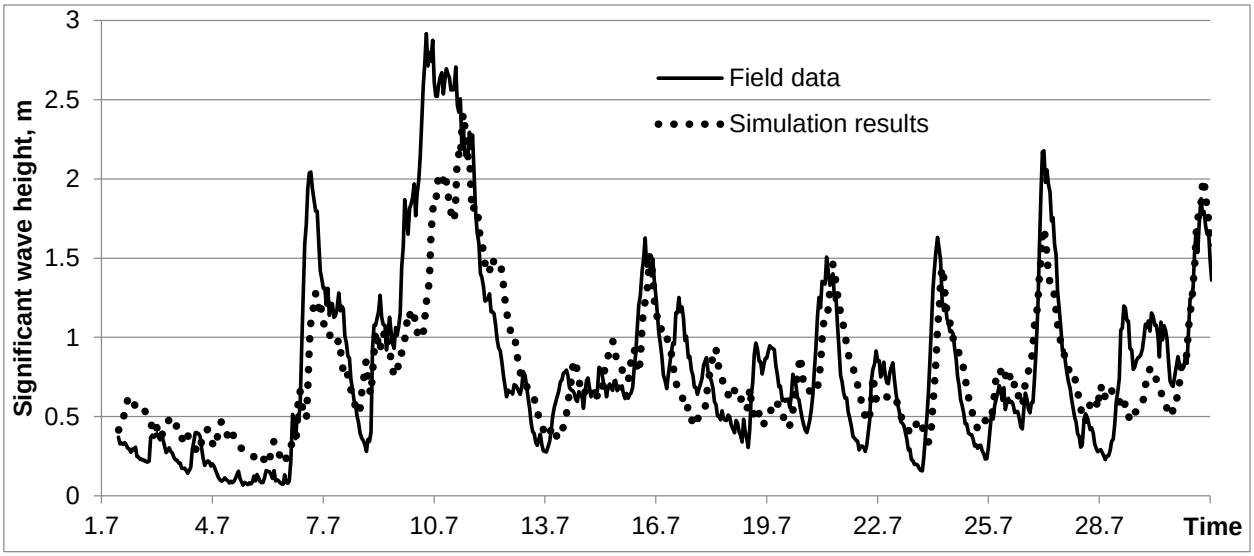

Figure 2. Significant wave height (field measurements and simulations) in July 2015. Solid line represents field data obtained by the wave buoy installed at the depth of 15 m opposite the Lubiatowo. Dotted line represents simulation results performed under atmospheric forcing based on wind speed and direction measured in Baltijsk located 200 kilometers east from Lubiatowo.

Calibration of parameters of the Mud Transport Module was based on field data obtained in this field experiment in June 2006 [4] at the dumping site No 1 (see insert in the Figure 1). The measurements of particle size distribution were conducted for bottom sediments around the dumping site No 1 before and after the discharge of about 17000 m^3 of dredged material with 70% of quartz sand with a median diameter of 0.7 mm. The measurements showed that a sediment spot was formed after the discharge and it was stretched along the southern entrance mole, then average thickness of the bed layer of the sediments was 15 cm. Related model parameters defining the settling and resuspension properties of the particles were the following: the settling velocity according to the Stocks formula was 0.004 m/s; critical shear stress for erosion was taken 0.01 N/m^2. Simulations reproduced the conditions of the field experiment, a calculated bed layer thickness was 17 cm and the calculated sediment distribution at the bottom was similar to the observed distribution (see details in [5]). All coefficients obtained during calibration were used in the simulations described below.

Model setup for dumping scenarios.

This paper presents the results of simulations of dumping events at all three dumping sites mentioned above. The amount of the material that was discharged in the model scenarios was 17000 m^3 (as in experimental dumping of 2006 on the site No 1). The dumping event lasts 20 minutes, i.e. the source with discharge of 14 m^3/s was assigned at the top computational sigma-layer. The depth of the sea at the dumping site locations was very similar: dumping site number No 1 – 8.1 m; dumping site number No 2 – 8.8 m; dumping site number No 3 – 8.8 m.

The model simulated first the settling of sediments on the bottom and formation of some spot of the deposits around the place of dumping, and then these sediments were resuspended by waves and transported by currents further from the dumping site. 24 model scenarios of constant wind

action were simulated: the wind of 5, 7, 10 and 15 m/sec blows from five main directions - SW (225°), W (270°), NW (315°), N (0°), NE (45°) and E (90°).

The wind speed varied during the scenario as following: it started at a rate of 3 m/sec (for all scenarios) and was constant within 12 hours from the beginning of the scenario. After that the dumping event occurred (20 minutes) but the wind speed remained 3 m/sec another 12 hours. Then the speed increased instantly up to the wind rate of the scenario and remained constant within 24 hours. Then a period of "calm" weather started, i.e. the wind speed dropped instantly to 3 m/sec (for all scenarios) and stayed constant within 24 hours. It was assumed that most of sediments will be settle down during the "calm" period.

III. Results and discussion

Simulations showed that for all dumping sites which have similar depth (8-9 m) a wind with 5 m/s is not strong enough to resuspend sediments and move it to another place. At the other hand a strong wind (more than 15 m/s) blowing about 24 hours completely washed out the initial sediment spot at the dumping site and spreads sediments to such a wide area that thickness of the layer after subsequent deposition is negligible (Table 1). So, the only winds in the range 5-15 m/s would be favorable for redepositing sediments from the dumping sites to the nearest segments of the shore.

Dumping site No 1.

It was shown [5] that no landward wind action bring sediments from dumping site No 1 to the shore opposite it, and therefore, the beach near the Kosa Village would not be protected by disposal of dredged material to this dumping site. Simulation of NE wind made in the current study showed that bottom currents are directed landward (Figure 3a) while the currents in the top layer are oriented mainly along the shore and a little bit seaward. This causes resuspended sediments to spread along the shore of the Vistula Spit and settle down along 10 km from the dumping site. In modeling simulations we obtained that near-bottom currents are capable to transport the particles of 0.7 mm. The same result was reported in [12] by comparison of POM modeling results with Hjulstrom diagram.

In addition, the N and NE winds produce the situation of upwelling near the shore of the Kosa Village. The upwelling itself is developing at some distance seaward from the shoreline [13], but the lateral strip of water near the shore traps sediments resuspensded from the dumping site.

Table 1. The fate of the sediments disposed at the dumping sites after the influence of different winds: “No” – there is no deposition near the shore, sediments are transported seaward but not very far from the dumping site; “Yes” – sediments are settled near the shore not far away from the dumping site, “0” – sediments are not washed from the dumping site due to low currents, “Far” - sediments are transported near the shore very far from the dumping site and are dispersed along the big distance, “∞” – sediments are washed out from the dumping site completely and spread over the huge area, the layer thickness is negligible.

Wind range	Probabi-lity, %	Modelled wind speed	Dumping site No 1	Dumping site No 2	Dumping site No 3
SW, 2-5 m/s	5.16	SW, 5 m/s	No	No	0
SW, 6-9 m/s	7.19	SW, 7 m/s	Far	Far	No
SW, 10-13 m/s	1.38	SW, 10 m/s	Far	∞	**Yes**
SW, 14-17 m/s	0.24	SW, 15 m/s	∞	∞	∞
W, 2-5 m/s	4.01	W, 5 m/s	0	No	0
W, 6-9 m/s	6.38	W, 7 m/s	No	Far	**Yes**
W, 10-13 m/s	2.76	W, 10 m/s	Far	Far	Far
W, 14-17 m/s	0.74	W, 15 m/s	∞	∞	∞
NW, 2-5 m/s	6.04	NW, 5 m/s	0	0	0
NW, 6-9 m/s	5.55	NW, 7 m/s	No	No	**Yes**
NW, 10-13 m/s	1.06	NW, 10 m/s	No	Far	Far
NW, 14-17 m/s	0.3	NW, 15 m/s	Far	∞	∞
N, 2-5 m/s	5.97	N, 5 m/s	0	No	**Yes**
N, 6-9 m/s	2.54	N, 7 m/s	0	Far	**Yes**
N, 10-13 m/s	0.22	N, 10 m/s	No	∞	**Yes**
N, 14-17 m/s	0.06	N, 15 m/s	Far	∞	Far
NE, 2-5 m/s	5.44	NE, 5 m/s	0	**Yes**	0
NE, 6-9 m/s	1.01	NE, 7 m/s	0	**Yes**	**Yes**
NE, 10-13 m/s	0.03	NE, 10 m/s	**Yes**	Far	Far
NE, 14-17 m/s	-	NE, 15 m/s	Far	∞	∞
E, 2-5 m/s	9.46	E, 5 m/s	0	0	**Yes**
E, 6-9 m/s	1.62	E, 7 m/s	0	**Yes**	**Yes**
E, 10-13 m/s	0.3	E, 10 m/s	0	**Yes**	∞
E, 14-17 m/s	-	E, 15 m/s	**Yes**	Far	∞

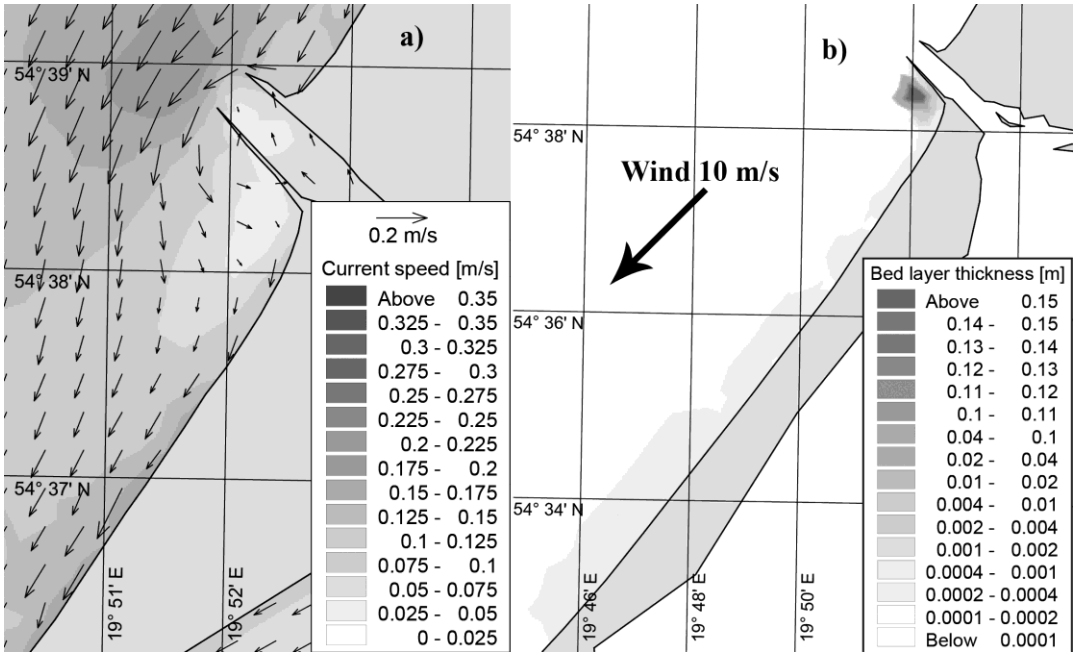

Figure 3. The scenario case of north-east (45°) wind with the maximum speed of 10 m/s (for the dumping site No 1): (a) the bottom currents at the end of wind action period and (b) the bed layer thickness of sediments redistributed from the dumping site.

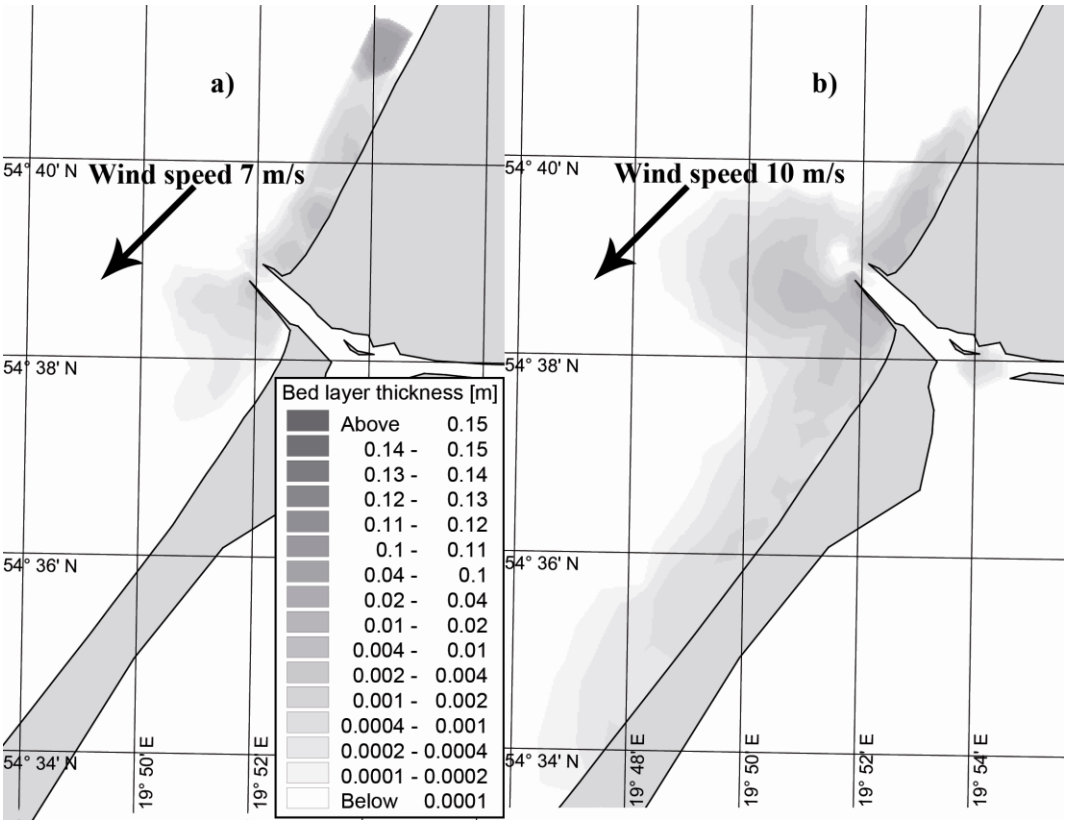

Figure 4. Bed layer thickness of sediments deposited at the dumping site No 2 for the scenario cases of north-east (45°) wind with the maximum speed of 7 m/s (a) and 10 m/s (b).

Dumping site No 2.

Simulations show that only in case of moderate winds (7-10 m/s) from the north (wind direction 0°) and north-east (wind direction 45°) we can see possible deposition near the shore (Figure 4a, b). Sediments spread significantly larger under wind with higher speed, they can settle down near the entrance to the Vistula Lagoon, round entrance moles and settle down along the shore, and even to come into the Vistula Lagoon.

This behavior can be explained by the same reason as in the previous case: for NE wind currents in bottom layer have a noticeable component that is oriented toward the shore. For other wind directions a seaward component of currents speed is dominated and no deposition along the shore was simulated.

Dumping site No 3.

Simulation showed that disposal of sediments at the dumping site No 3 is followed by their sedimentation along the shore (Figure 5). Moderate wind actions (7-10 m/s) from south-west, west, north and north-east lead to the export of the sediments towards the beach.

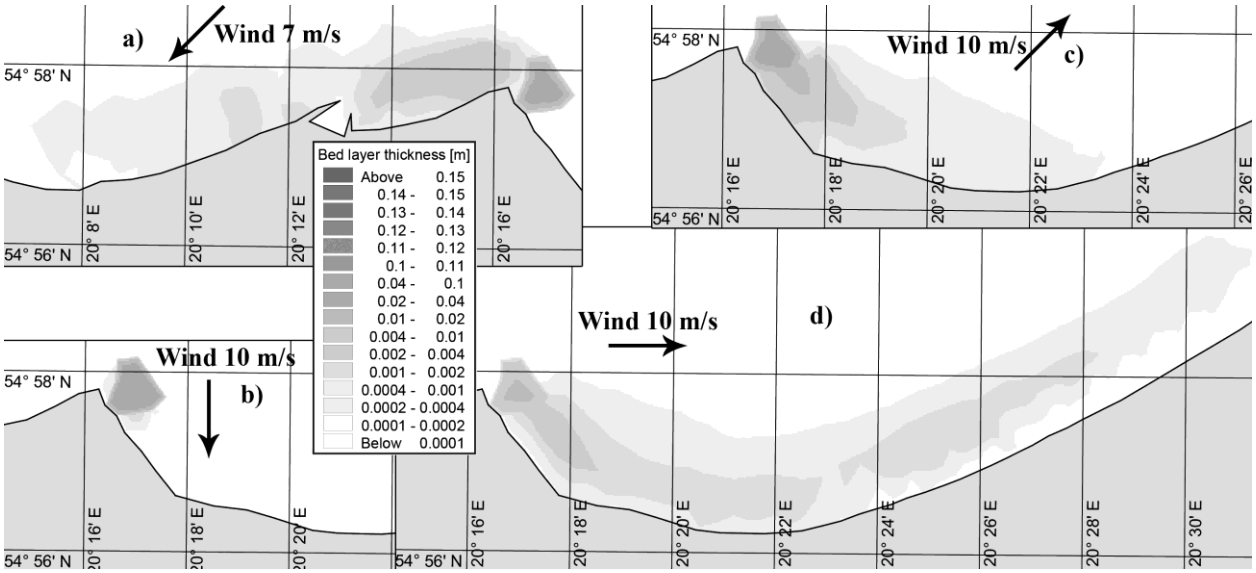

Figure 5. Bed layer thickness after the wind actions from (a) the north-east (45°), wind speed 7 m/s; (b) from the north (0°, 10 m/s); (c) from the south-west (225°, 10 m/s) and (d) from the west (270°, 10 m/s).

IV. CONCLUSIONS

1) Winds with the speed of about 5 m/s or less do not lead to resuspension of the sediments at the dumping sites located at the depths of about 8-9 m.

2) The winds with the speed stronger than 15 m/s lead to the complete washing out of disposed material from the dumping site and spreading it over the wide area with a negligible layer thickness.

3) From the point of potential protection of the shore near a dumping site the best option would be the winds of about 7-10 m/s, which wash out disposed material and transported it along the shore at a distance of few kilometers.

4) For the dumping sites located at the western shore of the Sambian Peninsula (sites No 1 and 2) the winds with alongshore (southward) and seaward components may transport sediments towards the shore; but the probability of such winds are rather low – not more than 8.4%.

5) For the dumping site at the northern shore of the Sambian Peninsula (site No 3), the probability of favorable wind is much bigger (in total 28.6%): SW, W, N, NE and E winds.

Acknowledgement

Authors thank colleagues from the Department of Coastal Engineering and Dynamics of the Institute of Hydroengineering of the Polish Academy of Sciences for providing the data for wave measurements for calibration of the model. Research and preparation of this article were supported by the Russian National Foundation: the study for the dumping sites No1 and 2, located at the Vistula Spit, – by the Project No 14-17-00547 "A forecast development for evolution of accumulative Russian coasts of tideless seas", and the analysis of situation around the dumping site No 3 – by the Project No. 14-37-00047 "Geoecological conditions of maritime use in the Russian sector of the South-Eastern Baltic".

References

1. Aibulatov, N.A., Bass, O.V., 1983. Anthropogenic factor in the development of Baltic Sea coastal zone. *Water Resources 3,* 127–134. [In Russian].
2. Basinski T., Zmudzinski L., 1988. Poland. *In* H.J. Walker (Ed.), *Artificial structures and shorelines,* Kluwer Academic Publishers, Dordrecht-Boston-London, 67–80.
3. Boldyrev, V.L., 1988. USSR – Baltic Sea. *In* H.J. Walker (Ed.), *Artificial structures and shorelines,* Kluwer Academic Publishers, Dordrecht-Boston-London, 47–52.
4. Chechko, V.A., Chubarenko, B.V., Boldyrev, V.L., Bobykina, V.P., Kurchenko, V.Yu., Domnin D.A., 2008. Dynamics of the marine coastal zone of the sea near the entrance moles of the Kaliningrad Seaway Channel. *Water Resources 35 (6).* 652–661.
5. Chechko, V., Sokolov, A., Chubarenko, B., Dikii, D., Topchaya, V., 2015. Dynamics of sediments disposed in the marine coastal zone near the Vistula Lagoon inlet, south-eastern part of the Baltic Sea. *Baltica 28 (2), 189–199.* Vilnius.
6. MIKE21&MIKE3, 2007. MIKE 21 & MIKE 3 Flow model FM. Mud transport module. Short description. *DHI software,* DHI Water and Environment, Horsholm, 12 pp. http://www.mikepoweredbydhi.com/upload/dhisoftwarearchive/shortdescriptions/marine/mudtransportmodulemt.pdf (last call 23.08.2015).
7. MIKE 3/21 model, 2004. MIKE 3/21 Flow model FM. Hydrodynamic and transport module: Short description (Hydrodynamic Module, Spectral Waves FM). *DHI Software,* DHI Water and Environment, Horsholm, 48 pp. http://naturstyrelsen.dk/media/nst/65583/54335_bluereef_actiona2_hyd_appendixa_short_descriptions.pdf (last call 23.08.2015).
8. Seifert, T., Kayser, B., 1995. A high resolution spherical grid topography of the Baltic Sea. *Meereswissenschaftliche Berichte 9,* 72–88.
9. Sokolov, A.N, Chubarenko, B.V., 2012. Wind influence on the formation of nearshore currents in the Southern Baltic: numerical modelling results. *Archives of Hydroengineering and Environmental Mechanics 59 (1–2),* 37–48.

10. Sokolov, A.N, Chubarenko, B.V., 2014. Analysis of possible influence of climate changes on the wind wave parameters in the nearshore zone of the South-Eastern Baltic. *Transactions of Kaliningrad State Technical University 34,* 43–52. [In Russian].
11. The Ocean Surface Winds Team (OSWT) of the Center for Satellite Application and Research, http://manati.star.nesdis.noaa.gov/index.php (25.04.2016)
12. Golenko M. N., Golenko N. N., Emelyanov E. M., Nekrasov M. A. Influence of Quasi-Geostrophic Currents and Inertial Waves on the Elution of Fine Sediments in the Southeast Baltic // Oceanology, 2016, Vol. 56, No. 2, pp. 200–204. DOI: 10.1134/S0001437016020077
13. Esiukova E.E, Chubarenko I.P., Sinyukhin A.O. How to differentiate between coastal cooling and upwelling events on SST images? // Baltic International Symposium (BALTIC), 2014 IEEE/OES, 27-29 May 2014, Tallinn, Estonia. - Publisher: IEEE. - p. 1-7. - Print ISBN: 978-1-4799-5707-1, DOI:10.1109/BALTIC.2014.6887839

MODERN STATE AND DYNAMIC OF THE BEACHES OF KALAMITSKIY GULF IN THE WESTERN CRIMEA

Svetlana Rubtsova, Institute of Natural and Technical Systems, Russia
Iryna Agarkova-Lyakh, Institute of Natural and Technical Systems, Russia
Natalya Lyamina, Institute of Natural and Technical Systems, Russia
Aleksey Lyamin, Institute of Natural and Technical Systems, Russia

rsi1976@mail.ru

In 1980-th the average width of beaches of Kalamitskiy Gulf on the Western coast of Crimea was 40 m on accumulative part and 10 m on abrasion. Now they are reduced more than 2 times. Depletion of beaches, abrasion of coasts and erosion of underwater slope accompany these processes. Activation of mentioned processes is caused by deficit of beaches material due to intense anthropogenic impact on the coast. The main factors of human activity in that area are quarrying of sand and pebbles on the beaches; regulation of solid runoff of rivers; unwarranted hydrotechnical construction; dredging; pollution of sea waters and bottom sediment. Between natural factors the Black Sea level rise, sinking down of described coast, wind-wave conditions, beaches lithology and activation of extreme storms facilitate beaches reduction.

Key words: beaches reduction, coastal deposits reduction, economic activity, coastal erosion, Kalamitskiy Gulf , Western coast of Crimea.

The coastal zone is an arena of modern interaction of the sea and the land, and one of the brightest contact zones on the Earth. Its specificity is determined by an active matter-energetic exchange between the sea and the land that is expressed in character and direction of coastal processes. Modern dynamic of the coasts is characterized by coasts stepping back that is correlated with the eustatic rising of World Ocean level with an average speed of 1.7 mm/year [4]. As a whole sea level rise activates abrasion and weaken accumulative processes in the coastal zone. About 41% of Russia coasts are actively demolished [9]. Intense economic activity in the most parts of the coastal zone promotes to the strengthening of those processes. It scale is comparable or prevail under the natural factors. The economic activity is mostly influence on the coasts consisted of loose materials. They are extremely dynamic and any interference of man into the natural coastal processes fraught with serious consequences. One of such problem takes part in the Western coast of Crimea in Kalamitskiy Gulf.

The goal of the article is to describe modern state of dynamic of the beaches in Kalamitskiy Gulf. To achieve the goal the following tasks have been solved: (1) modern state of long-term dynamic of the beaches is shown, (2) main reasons of beaches reduction and coasts retreat are detected.

MATERIALS

Analysis of modern state and dynamic of beaches is based on published data [1-3, 8, 11, 15, 19-22] and on long-term research data collected by Institute of Mineral Resources (Simferopol), Crimean State Hydrogeological Expedition, Yaltinskaya engineering-geological group, Crimean Republican Counterlandslide Board.

RESULTS AND DISCUSSION

Kalamitskiy Gulf is located on the Western coast of Crimea and bordered by cape Evpatoriyskiy on the north, and cape Lukull on the south (Fig. 1). The total length of the gulf coast is about 66 km (map with the scale 1:200 000). Coasts are an example of abrasion-accumulative system (pair) [24]. They consist of two genetically different parts: accumulative part from cape Evpatoriyskiy till lake Kyzyl-Yar, and abrasion part from lake Kyzyl-Yar till cape Lukull. The parts are binded together into single lithodynamic system. Beaches of accumulative parts take material transported by along-shore sediments flow from Sevastopol to Evpatoriya. Beaches of abrasion part has complex feeding: they take material from coastal and bench abrasion, rivers discharge, along-shore sediments flow, and biota functioning [14] (Fig. 1).

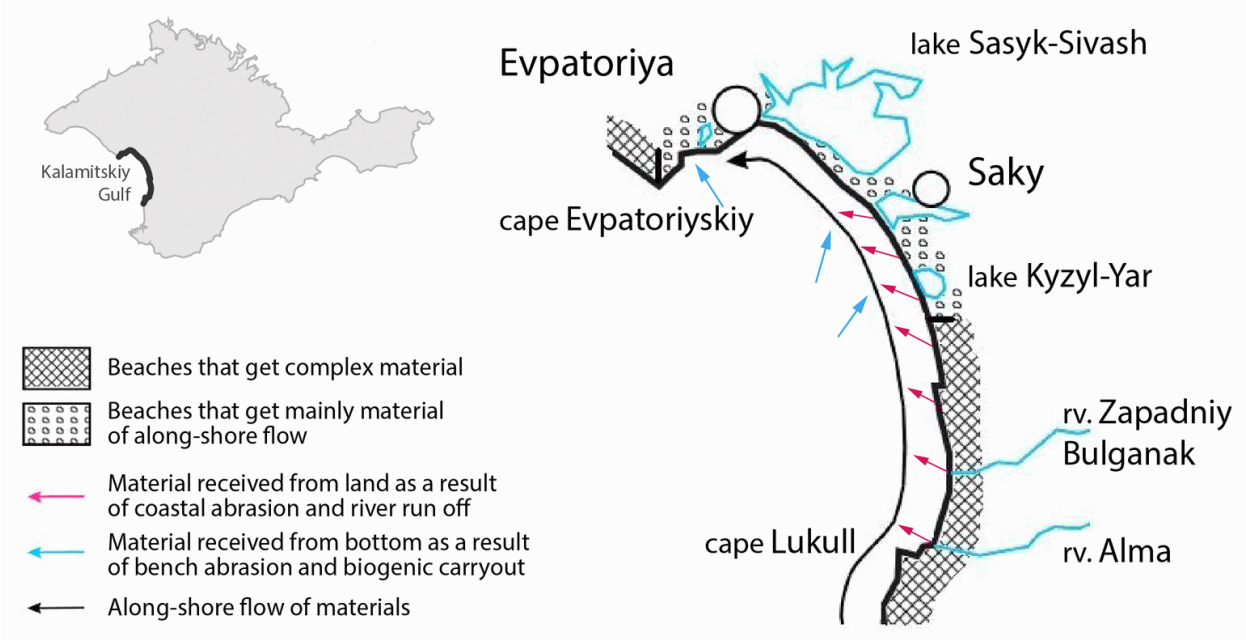

Fig. 1. Material flows and genetic type of beaches of Western Crimea.

We consider in detail the dynamic of beaches reduction from the middle of 1980-th. We describe beaches from south to north – from cape Lukull to cape Evpatoriyskiy.

In the middle of 1980-th there were a natural 8-10 m width beach in the mouth of rive Alma, and an artificial beach with the same width near Peschanoye settlement [20]. After 20 years the width of beach near sanatorium “Lukomorye” in Peschanoye was 0-6 m [19]. At the same time the coastal-protection construction near pension “Volna” in Peschanoye near “Lukomorye” had been destroyed by the sea.

In the middle of 1980-th beaches northward Peschanoye and near Beregovoye were 5-8 m width, northward Beregovoye were 10-15 m [20]. After 20 years those beaches reduced till 4-7 m width, and the distance from buildings of recreation complex "KSU Shevchenko" to coastal cliff was 2.5-5.0 m [19].

In the middle of 1980-th beaches southward Nikolaevka were 30 m width [20]. After 10 years there was a sharp reduction of beaches width southward of coastal-protection constructions. Beaches near pensions "Bolshevik", "Gornyak", "Yuzhniy" and "Izumrud" were absolutely vanish. Now sea washes the base of embankment here [19].

In 1990 in the central part of Nikolaevka the width of beaches was 23-34 m, now it is 3-5 m near pensions "Polymer", "Solnechniy", "Luchezarniy", and 10-18 m near "Energetic" and "Skif-88" [19].

In the middle of 1980-th northward of Nikolaevka there was a 10 m beach [20]. In last years that beach from pensions "Solnyshko" to pension "Polet" grows till 22-30 m because of building of coastal-protected constructions. Now its width seasonally vitiates on 5-7 m [19].

In the middle of 1980-th a beach southward of lake Bogayly bank was 18 m width [20]. From 1994 till 2005 the part of the coast northward of bank near recreation center "Volna" (Frunze settlement) retreat on 15 m. As a result the hangar and boat-berth of the recreation center were destroyed, and its cottages approaches to coastal step on 12 m [19].

In the middle of 1980-th the width of beaches between lakes Bogayly and Kyzyl-Yar was 7-12 m, and 10 m near Krasnaya Gorka [20]. The width of Kyzyl-Yar bank was reduced 1.5 times from 200 m [19]. In the northern part of Kyzyl-Yar bank since 1983, after the water intake had been constructed here, the beaches material began to accumulate.

In the middle of 1980-th beaches of the southern part of Saky bank had 60 m width. In 2000-th the width of the beaches is only 5-15 m. The maximal average speed of beaches reduction from 1983 till 2005 has been registered near child's sanitary camp "Zvezdniy" im. kosmonavta G. Titova and recreation center "Uyut". During that time the quay built here in 1986 had been completely destructed. Similar coastal processes and similar beaches width are registered everywhere between camp "Zvezdniy" and rest home "Prybrezhniy". The formed here wash-out step has the height 0.1-2.0 m [3] .

The beach near rest home "Prybrezhniy" is relatively stable. The beach width is varied from - 3.0 to 5.0 m during 20 years [19]. Near recreation center "Priboy" and pension "Golubaya volna" the width of beaches is changed a little and it is more than 50 m.

In the middle of 1980-th the average width of beaches between Saky bank and Evpatoriya was 30-50 m. Maximal beaches width was registered opposite to Pribrezhnoye settlement. It is a cause of changing coastal line direction that favor to accumulation of beaches material.

In the beginning of 1980-th the width of Evpatoriya beaches in the southern part of city was 30-50 m. After the strongest storm in November 1981 the sea started to destroy beaches [15]. In that year the quay and part of the street on south outskirts of the city were destroyed. At the beginning of XX century the width of beaches near quay Gorkogo was 20-85 m, and in 2005 it was reduced to 15-35 m. At the beginning of XX century in the central part of Evpatoriya (near park Frunze and pension "Zolotoy bereg") the width of the beaches was 50-80 m, in the middle of 1980-th it was 30-40 m, and in 2005 it was 6-15 m. The beaches degradation is increased during the last 20 years on

the part of coast from cape Karantinniy to cape Evpatoriyskiy. The 0.8 m steep of wash-out is formed at the beaches near pensions “Planeta”, “Magnat”, “Almazniy”, “Rossiya”. The width of lake Moynaky bank was reduced from 125-150 m in 1989 to 90-100 m in 2005 [19].

The reduction of beaches width leads to exhausting of beaches sediments on the studied coast. Average volume of beaches sediments increases from south to north according to the movement of along-shore sediments flow. In the southern part of Kalamitskiy Gulf it is 7.4-12.0 m^3/m of sediments. They are increased towards lake Bogaily till 42.0 m^3/m, and near Evpatoriya they equal to 85 m^3/m. Near Evpatoriya capes average volume of beaches sediments decreases from 28.0 m^3/m near cape Evpatoriyskiy to 17.6 m^3/m near cape Karantinniy [11]. Total reduction of beaches sediments increases the vulnerability of beaches in relation to washing-out and activates the development of exogenous processes on the coast.

The coastal erosion dominates between coastal processes in Kalamitskiy Gulf. During the last 100 years average speed of erosion is 1.3 m/year, maximal 7.8 m/year [19]. Beaches on abrasion part of Kalamitskiy Gulf have the maximal speed of erosion in Crimea. However different researches give different values of that speed. According to data [8] the speed of beaches erosion in the mouth of Alma river near settlements Peschanoye and Beregovoye is 3 m/year; on the southern parts of lakes Kyzyl-Yar and Bogaily is 5.0 m/year; northward to Nikolaevka settlement is 6.0 m/year. The speed of erosion decrease to 0.6-1.0 m/year on places where clay sediments armor pebble conglomerates, e. g. near Nikolaevka [8]. The speed of destruction of Krasnaya Gorka and the part of coast between end of Bogaily bank and cape Lukull is 2.0-2.8 m/year [11]. Romaniuk O. S. et al. [15] found that the speed of erosion on the part of coast between lake Kyzyl-Yar and Nikolaevka for the period 1940-1973 was 1.46 m/year. The coastal erosion brings into the sea about 350 thousand m3/year of material [11].

Beaches erosion on the accumulative part near and on Saky bank was registered since 1930-th [7]. Dzens-Litovskiy A. I. and Zenkovich V. P. mentioned that Saky coast retreated with the same speed as abrasion clay slope near lake Kyzyl-Yar [7, 23]. In 1941-1963 the width of beaches in the southern part of Saky bank decreased by 47.0 m and the mean annual speed of erosion was 2.1 m/year [15]. In 1970-th Shuisky Yu. D. calculated the speed of erosion on Evpatoriya part as 3.75 m/year, on Saky part as 1.0 m/year [16]. The speed of erosion of Saky bank in 1979-1982 was 2.6 m/year [22]. Maximal average speed of erosion on Saky bank for the period 1984-1998 was 3.76 m/year near camp “Zvezdniy” [1]. Total coastal line regression from the middle of 1980-th till 2005 was 31 m near camp “Zvezdniy”, 24-33 m near recreation center “Uyut”, and 18 m on the part of a coast from camp “Zvezdniy” to pension “Parus” [19]. The average speed of erosion near camp “Zvezdniy” in 1983-2005 was 1.5 m/year, in 1998-2005 was 1.8-2.0 m/year [2, 19]. Average speed of erosion of Evpatoriya beaches was 1-2 m/year [19].

The speeds of beaches erosion are changed in seasons and years. They increase in the years of active storms, and during winter season from November till March. Above mentioned speeds of erosion on abrasion parts of Kalamitskiy Gulf take into account exogenous processes, which stimulates coasts destruction and includes landslides, landslips, collapses [20]. Landslides are formed near Beregovoye settlement between mouth of river Alma and cape Lukull. Landslips are more intense on the parts of coasts without conglomerates. Along valleys of rivers Zapadniy Bulganak, Alma and other temporal streams of water the erosion is formed. Eolian processes are

active on accumulative parts of the banks of salt lakes Sasyk-Sivash, Sakskoye, Kyzyl-Yar and Bogaily. NE winds prevailing here in cold period of year carry away sand from shore on to the underwater slope.

When beaches sediments are exhausted and edge of coastal step moved towards land, bottom abrasion become stronger. Speed of abrasion is 2.0-14.0 cm/year in the northern part of the Gulf, and 23.0-26.0 cm/year in the southern [11]. Absence of sediments between cape Evpatoriyskiy and cape Karantinniy at depth 2-5–10 m confirms deficit of beaches sediments. For example in underwater part of sanatoriums "Smaragdoviy", "Smena", "Dnepr", "Druzhba", "Rodina" the volume of sand sediments sufficiently reduced and limestones were uncovered [19]. Insignificant bottom accumulation of 13.0 cm/year is observed near cape Evpatoriyskiy, which is explained by underwater submerging of along-shore sediments flows [11].

Shuisky Yu. D. calculates the capacity of Belbek-Evpatoriya sediments flow which is equal to 72.6 thousands m^3/year [17]. All sources of beaches material in Western Crimea have capacity of 300 thousands m^3/year that is equal to 3.6 $m^3/m \cdot$year. To keep a stable state of beaches it is necessary of 30-50 $m^3/m \cdot$year of coastal material [17], or 8,5-14 times more than exists. Therefore along-coast flow in Kalamitskiy Gulf feels a need in coastal material, and compensates it by washing relict gravel-pebble deep-water banks and beaches [22].

The modern deficit of material in the coastal zone of Western Crimea is the case of unreasonable economic activities. Through them the main role belongs to sand and pebble quarries, regulated rivers streams, unfounded hydrotechnical constructions, dredging, pollution of marine waters and bottom sediments [1-3]. Below we consider their deposit in forming of the beaches of Kalamitskiy Gulf.

The first sand quarries were founded in the northern part of Kalamitskiy Gulf near Pribrezhnoye in 1920-1930-th. The sand was used for building of DneproGES. Apparently from that time the intervention of man into natural dynamic of coastal processes starts the mechanism of Kalamitskiy Gulf beaches reduction. In 1952-1972 quaries moved underwater to depth 2.5-5.0 m. During those period about 15 millions m^3 of sand and pebble were withdrawn [22], and the along-shore sediments flow was completelly catched. According to data collected in [12] till 1985 sand was querred from abovewater parts of coast near Beregovoye and Peschanoye. After 1985 beaches material was mined near lake Kyzyl-Yar and from the bottom of Evpatoriyskiy Bay. Now it is prohibitted to quarry sand on Saky bank, but the facts of its unaproved mining are presented.

The first reservoirs in Crimea were made on rivers Alma and Kacha in 1920-1930-th. They held significant part of river alluvium. Further building of hydrotechnical constructions on rivers Belbek, Alma and Kacha in 1960-1980-th exacerbate the problem of along-shore sediments flow forming that negatively influence on stability of accumulative beaches in the northern part of Kalamitskiy Gulf.

In 1979-1982 a hydrotechnical construction 120 m length was built near lake Kyzyl-Yar. It blocks along-shore flow of sediments moved from south to north towards Saky and Sasyk-Sivash banks. According to calculations the hydrotechnical construction completely catch gravel-pebble flow (about 27.8 thousands m^3/year), and about 50 thousands m^3/year of suspended sand miss the construction and only partially come onto the Saky coast [21]. Together with quality-quantitative changes in sediments flow, the accumulative and abrasion parts of coasts are redistributed. Before

1979 the northern part of Kyzyl-Yar bank retreats back with the same temp as neighbour abrasion part of coast – 1.5 m/year. After the construction had been built the downstream wash of the northern part of the bank was started, and south part began to accumulate sediments. Now the coastline advance to the length of the construction, therefore we could forecast that along-shore flow will bring material into the northern part of the Gulf.

The clearing of passages for ships mooring in a marine port area affects on Evpatoriya beaches reduction. An annual volume of such clearing since 1986 was more than 50 thousands m^3/year. Extracted sand-gravel-pebble material was used for building. As a result the deficit of sediments in underwater area was compensated by an intensification of beaches erosion. After every clearing the edge of existed beaches from Evpatoriya marine port to lake Moynaki stepped back by 14 m. Only after the sea fills up ships passages by beaches material, it restores the beaches width [15].

Because coast-protection offices did not provide any actions to prevent beaches erosion, the recreation objects on Saky bank like "Poltava-Krym" sanatorium, child's sanitary camp "Zvezdniy" im. kosmonavta G. Titova, recreation center "Uyut" started to construct coast-protection objects, which, as it seemed, could retake the declining beaches from the sea. Unfortunately those construction were doomed to destruction. The fact is that concrete walls built in the zone of wave flow prevented the free moving of waves. Waves mirrored from the walls and washing away walls bases actively drawn beaches sediments back into the sea. As a result the walls crushed and generated a chaotic conglomerate of concrete constructions. For example the walls in child's sanitary camp "Zvezdniy" im. kosmonavta G. Titova begun to destruct after 6 years. However after crushing those constructions served as block heap that protected coast from erosion, and after about 10 years their remains were buried under the sand or go under the water.

Anthropogenic municipal and industrial drainages near human settlements, especially near Evpatoriya and Saky, pollute coastal area, biota, and bottom sediments. Comparative analysis of bottom vegetation in 1964 and 1988 reveals change in their saprophic state. In 1964 the oligosaprobic algae species were dominated and polysaprobic algae were absent. In 1988 the meso- (48%) and oligosaprobic (33%) algae species prevail, and polysaprobic species constitutes 19% [6]. The green algae *Enteromorpha intestinalis* and red algae *Ceramium rubrum* were found here that indicates the pollution of sea waters. In 1991-1992 researchers of zoobenthos of Kalamitskiy Gulf found that in bottom zoocenoses mussel *Mytilus galloprovincialis* predominated by biomass. The comparison of obtained data with the results of previous works showed enlargement of macrozoobenthos biomass and replacement of small detritophages (Polychaeta) by large sestonophages (mollusks, mainly mussels) [6]. Furthermore the pollution leads to reduction of abundance and productivity of marine hydrobionts which form granulometric and material composition of beaches. As a result the strength and dimension of beaches sediments were increased. A granulometric composition of beaches, instead of fine-grained in 1960-th, becomes medium-grained in 1990-th [15]. In the middle of 1990-th the Saky chemical factory, that supplied the most part of pollutions, stopped activity. For that reason we establish a fact that quality of waters near Saky coast gradually improves and communities of phyto- and zoobenthos restore.

In spite of convincing negative role of human activity in the coastal zone of Kalamitskiy Gulf, we try to analyze a role of natural factors in beaches degradation.

The most part of Kalamitskiy Gulf is located in Alminskaya sineclise, which sinks down with the average speed of 2.5-3.0 mm/year [13]. At the same time the average speed of the Black Sea level rise is about 1.6 mm/year [5], from the end of 1940-th it equals to 2.5 mm/year [12], and from that period the level rises up to 15.0 cm. The response of accumulative Crimean coasts on that process is their retreat: when a sea level rise on 1.0 cm, the Saky coasts retreat on 30.0 cm [12]. Therefore the coast of the northern part of Kalamitskiy Gulf retreat by 4,5 m for last 70 years.

Lithological structure of the coasts of Kalamitskiy Gulf favors to wash out, because they consist of material yielding and very yielding to abrasion [18]. Accumulative part of the coasts consists of loose marine Quaternary sediments of sand, gravel, pebble and shells. Abrasion part of the coasts consists of foxy Pliocene-Quaternary clays.

Hydrodynamic and hydrometeorological factors form unfavorable wind-wave situation in the gulf. Owing to comparative shallow-waters in the northern part of Kalamitskiy Gulf, the strength of sea waves is directly correlated with wind. The monitoring discover that NE, W and SW winds are the most frequent in Saky region. NE winds dominate in autumn-winter seasons and produce set-down of sea waters [21]. SW winds cause rough sea. Regular observations on Saky bank show that when waves are directed from south to south-west, the sea takes away beaches sediments and wash out a coastal step; western waves wash ashore sediments that protect coast from erosion. Comparison of wind characteristics in 1986-1990 and in 1991-1995 shows that the repeatability of SW winds, that facilitate coastal erosion, increased by 10%. Specialists from Marine Hydrophysical Institute confirm that tendency and indicate that since 1990-th the repeatability of SW and S storms increases. Those winds are dangerous for beaches in that region [19]. Beaches erosion is increased during storms because of sea onset and sea level rise. For example during storms sea water penetrates into cellars of sanatorium “Poltava-Krym” located on Saky bank [19].

Active destruction of marine coasts depended on extreme exogenous processes in the Black Sea region like cyclonic and rare strong storms activity [10]. The bright examples of those processes are the strongest Black Sea storms in November 1981, November 1992, January 2000, November 2007. For example during some days in January 2000 the 6-7 balls storm raves on Saky coasts. It strength is confirmed by biogenic emission from sea bottom. There were algae *Phyllophora nervosa*, vegetated at depth 10-20 m; live crustaceans *Upogebia* sp. or *Callianassa* sp.; eggs of rayfishes *Raja clavata*; living mollusks *Solen marginatus* and *Anadara* sp. [2].

The beaches of Kalamitskiy Gulf are the main natural resource in the Western Crimea and the main object that attracts tourists. Therefore their protection and conservation should be the priority task for all region. To solve the task the complex decisions are needed that takes into account coastal-protection, ecology and legal aspects of nature management [3, 8, 11, 15, 22], which need a governmental support. Beaches restoration and improvement will positively influence on tourists flow to Evpatoriya, Saky, and in the Western Crimea. That leads to the appearance of funds to support normal states of beaches in the region.

CONCLUSIONS

The coasts of Kalamitskiy Gulf are characterized by the tendency of beaches width reduction and shoreline retreat. Activation of economic activity on the coasts since middle of 1980-th leads to intensification of beaches reduction. As a result width of beaches in the accumulative part of the gulf

reduced more that 2 times from 40-50 m in 1980-th to 15-20 m at 2010-th. Those processes are accompanied by the depletion of beaches sediments, shift of coastal line towards land, and activation of abrasion on underwater slope. Parts where hydrotechnical constructions have been built or parts near them are exceptions because constructions upset natural lithodynamic conditions. The deficit of beaches material in the Western coast of Crimes is the cause of intense economic activities in the coastal zone. Through them the main role belongs to sand and pebble quarries, regulated rivers streams, unfounded hydrotechnical constructions, dredging, pollution of marine waters and bottom sediments. Through the natural factors the beaches reduction is facilitated by Black Sea level rise, newest sinking down of described coast, wind-wave conditions, beaches lithology and activation of extreme storms. Beaches of Kalamitskiy Gulf are the main recreation resource of the Western Crimea. To restore beaches it is necessary to minimize consumer attitude to nature and to realize costal-protection, ecological and legal aspects of coastal zone management with the support of government.

REFERENCES

[1] Agarkova I.V. Influence of economic activity on the dynamics of the Saky coast // Scientific notes of Taurida National University V.I. Vernadsky. - 1999 - 12 (51). - № 1. – P. 15 - 19. *(In Russian).*

[2] Agarkova-Lyakh I.V. Anthropogenic and natural factors of Saky beaches reduction // Notes geoecologists society. - Simferopol, 2007. - Vyp.9. - P.24 – 30. *(In Russian).*

[3] Agarkova-Lyakh I.V. Modern state of the beaches of the West Coast of Crimea and actual questions of coast using // Ecological safety of coastal and shelf zones and complex use of shelf resources: Coll. Scien. tr. - Vyp.29 / NASU, MHI, IGN, OB IBSS. The Editorial .: Ivanov V.A. (Gl.red.) and others. - Sevastopol, 2014. - P.50 - 60. *(In Russian).*

[4] Andrianova O.R. Patterns of variation in the level of the Black and Azov seas in the last 100 years / Ed. Zhindarev L.A. Sea coast – evolution, ecology, economy: Proc. XXIV Int. Coast Conf. dedicated to the 60th anniversary of the founding of the Working Group "Sea coast" (Tuapse, on October 1-6, 2012): in 2 Volumes. – Krasnodar: Publishing House-South., 2012. – 1. – P. 37-41. *(In Russian).*

[5] Boguslavsky S.G., Cubreacov A.I., Ivashchenko I.K. Black sea level changes // Marine Hydrophysical magazine. - 1997. - №3. - P. 47-56. *(In Russian).*

[6] Boltacheva N.A., Milchakova N.A., Mironova N.V. Changes in benthos near the Gulf Kalamitsky under the influence of eutrophication of the sea // Ecology. - 1999. - Vol. 49. - P. 5-9. *(In Russian).*

[7] Dzens-Litovskiy A.I. Banks and spits of the Crimean salt lakes // IZV RGO. -1938. - T.65. -Vyp.6. – P. 11-35. *(In Russian).*

[8] Erysh I.F. et al. Report on the study of landslides Crimea region in1976-1980 and 1981-1982. KGGE. - Simferopol, 1983. *(In Russian).*

[9] Glushko A.Y., Razumov V.V. Degradation of the lands of coastal territory of the subjects of the south of Russia under the influence of processes of abrasion // Bulletin of Moscow State Open University. "Science" series. - 2010. - № 3. - P. 161 - 170. *(In Russian).*

[10] Klyukin A.A. Extreme manifestations of exogenous processes in the twentieth century // Pontida. Electronic scientific journal. - Simferopol. - 2000 - Vol. 2. *(In Russian).*

[11] Lukyanov Yu.P. Report "Study of the conditions of development of exogenous geological processes of the coastal zone of the Crimean peninsula". - Yalta, 1993. *(In Russian).*

[12] Modern state of the coastal zone of Crimea / Ed. Yu.N. Goryachkin. - Sevastopol: ECOSI-Hydrophysics, 2015. - 252 p. *(In Russian).*

[13] Nevessky E.N. Evolution of the waters in Kalamitsky Gulf // Bulletin of the Oceanographic Commission of the Presidium of the USSR Academy of Sciences. - 1960. - № 5. - P. 54-59. *(In Russian).*

[14] Romaniuk O.S. Crimean beaches, their genesis and perspectives of practical use: Abstract. diss. ... Cand. geogr. Sciences. - Simferopol, 1968. *(In Russian).*

[15] Romaniuk O.S., Lushchyk A.V., Morozov V.I. The conditions of formation and dynamics of the sea coast in the region of the Saky resort area. - Simferopol: IMR, 1992. *(In Russian).*

[16] Shuisky Yu.D. The feeding of NW and Crimean areas of the Black Sea shelf by clastic material / Study of the dynamics of sea coasts relief. - Moscow: Nauka, 1979. - P. 89 - 97. *(In Russian).*

[17] Shuisky Yu.D. Modern sediment balance in the coastal zone of the seas: Abstract. diss. ... Doctor. geogr. Sciences. - M., 1983. *(In Russian).*

[18] Shuisky Yu.D. The problems of study balance of sediments in the coastal zone of the seas. - AL: Gidrometeoizdat, 1986. - 240 p. *(In Russian).*

[19] The report "State of the West Coast of the Crimea". "Crimean Republican landslide management". - Yalta, 2006. *(In Russian).*

[20] To create an inventory of abovewater parts of Crimean coasts in relation to the scale of 1:200000 / Ed. O. Romanyuk. - Simferopol: KGGE, Institute of Mineral Resources, 1988. *(In Russian).*

[21] Ukrainian State Institute of Design Cities "Giprograd". Evpatoria and Saki resort and recreation sub-area. Territory. complex. Nature Conservation resorts of national importance circuit. Annex 14: Ukryuzhgiprokommunstroy. - Yalta, 1986. - K., 1988. *(In Russian).*

[22] Ukrainian State Institute of Design Cities "Giprograd". Evpatoria and Saki resort and recreation sub-area. Territorial complex scheme of nature protection resort of national importance. – 1. – K., 1988. *(In Russian).*

[23] Zenkovich V.P. Studying of dynamics of coast of the Western Crimea // Voprosy Geographii. – M.: Mysl, 1948. -V.3. - P.28-32. *(In Russian).*

[24] Zenkovich V.P. Morphology and dynamics of the Soviet coast of the Black Sea / In 2 Volumes. Vol. 2. – M.: Academy of Sciences of the USSR, 1960. - 216 p. *(In Russian).*

ANALYSIS OF THE FUNCTIONING OF MARINE ECOSYSTEMS ON CHANGING THE PARAMETERS OF THE BIOLUMINESCENCE FIELD ON THE CRIMEAN BLACK SEA SHELF

Svetlana Rubtsova, Institute of Natural and Technical Systems, Russia
Natalya Lyamina, Institute of Natural and Technical Systems, Russia
Aleksey Lyamin, Institute of Natural and Technical Systems, Russia

rsi1976@mail.ru

The concept of a new approach to environmental assessment is offered in the system of integrated management of the resource and environmental safety of the coastal area of the Black Sea. The studies of the season and daily changeability in the bioluminescence field in the Sevastopol coastal waters has been conducted. For the first time considerable differences in the bioluminescence field seasonal changes in the surface and deep water layers and the reasons conditioning this phenomenon have been shown, using a method of multidimensional statistical analysis. The bioluminescence field vertical profile change in the Black sea coastal waters in the autumn period at night has been studied. It has been shown that according to the character of bioluminescence parameters dynamics a water column can be divided into layers: upper (0 – 35 m) and deep water (36 – 60 m). It has been revealed that life rhythms of the plankton community are the main reason for the bioluminescence field intensity variability. It has been revealed that 14-hour periodicity of the bioluminescence field is related to the changes in light and its variations with 2,5…4,5 hours are conditioned by planktonts endogenous daily rhythms. And here biotic factors effect mostly periodicity of the bioluminescence field intensity increase and fall down at the dark time of the day. Abiotic factors are of less importance in circadian rhythmic of the bioluminescence field in the neritic zone.

Key words: ecosystem, plankton, seasonal and daily changeability of the bioluminescence field, temperature, salinity.

An ecological system, or an ecosystem, is a basic functional unit in ecology, as it comprises organisms and inorganic environment, i.e. the components interfering with one another's properties and the conditions required for maintaining life in that very form which exists on the Earth. An ecosystem is understood to be a community of living organisms (communities) and their habitat, which form a stable life system thanks to the circuit of substances. Coastal ecosystems occupy a special place in ecology. At present the coastal zone is an important target of ecological, economic and hydrobiological researches because of its special geopolitical value within the framework of environmentally sustained development and national security.

The specificity of the Black Sea ecosystem is determined by weak water exchange with the adjacent seas through narrow straits, the hydrogen sulfide layer elongated vertically and by a large freshwater inflow from the rivers.

Figure 1. provides the block diagram of a new approach to the environmental assessment in the system of integrated management of the resource and environmental safety of the coastal area of the Black Sea [3].

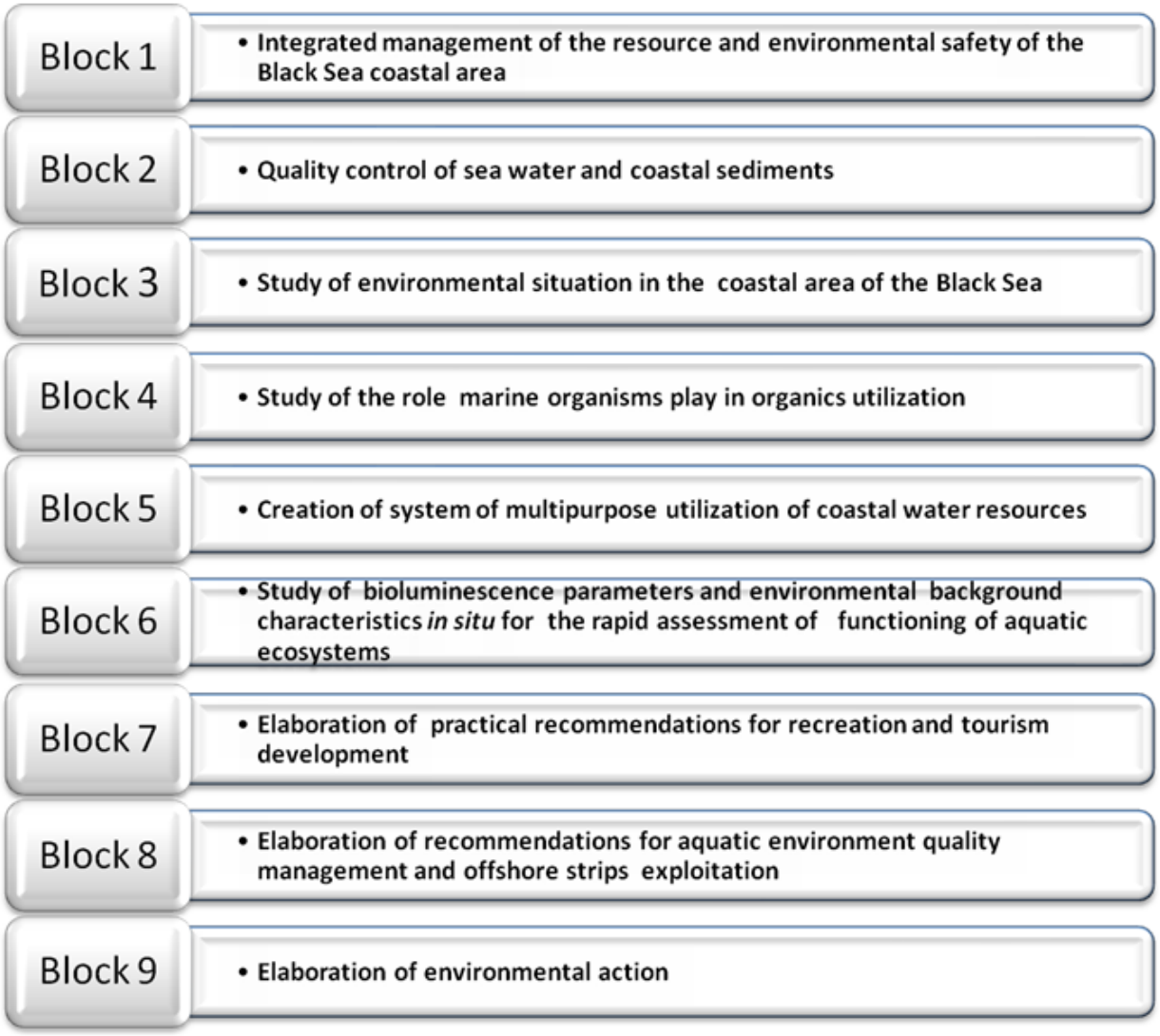

Fig. 1. Block diagram of a new approach to the environmental assessment in the system of integrated management of the resource and environmental safety of the coastal area of the Black Sea.

The dynamic study of the water layer bioluminescence characteristics is of vital importance for revealing a common pattern of functioning of plankton communities, as well as the reasons for their space-time variability [2]. The planktonic bioluminescence parameters can serve as a sensitive express-indicator of the degree of plankton resistance to pollutant exposure and as an expressive indicator of regional marine pollution [4].

The method is based on instrumental measurements *in situ* in a real time scale (vertical depth probing) of bioluminescent intensity, as well as on its spatial conjunction and correlation ratios with biological and hydrophysical characteristics of water masses.

Bioluminescent potential is an amount of light energy which can be emitted by the aggregate of organisms placed into a definite water volume or distributed on a definite area of the sea-bed during their saturating excitation by external irritants. The bioluminescent potential realization is a bioluminescence field [1]. A bioluminescence field is a total lighting effect created by the aggregate of marine bioluminescent organisms in the water layer [2, 4].

The primary role in creating a bioluminescent potential of the sea belongs to planktonic organisms [2, 4].

The bioluminescent potential in the Black Sea is formed by thirty six algae belonging to the Class Dinophyceae of the genera Neoceratium, Protoperidinium, Scrippsiella, Gonyaulacaceae, Noctilucaceae, Lingulodinium, as well as by three species of comb-bearers, some species of Copepoda and two genera of luminescent bacteria [2, 4]. The light-emitting properties of thirty 30 algae belonging to the Class Dinophyceae have been determined instrumentally under conditions of the Black Sea by the employees of the Biophysical Ecology Department of the A.O. Kovalevskiy Marine Biological Investigations Institute [2, 4].

The bioluminescence field (BF) in the Black Sea exists everywhere over the entire circadian period in essential regional and seasonal diversity. Fig. 2 shows a small-scale spatial inhomogeneity of the bioluminescence field in the seashore of Sevastopol (September).

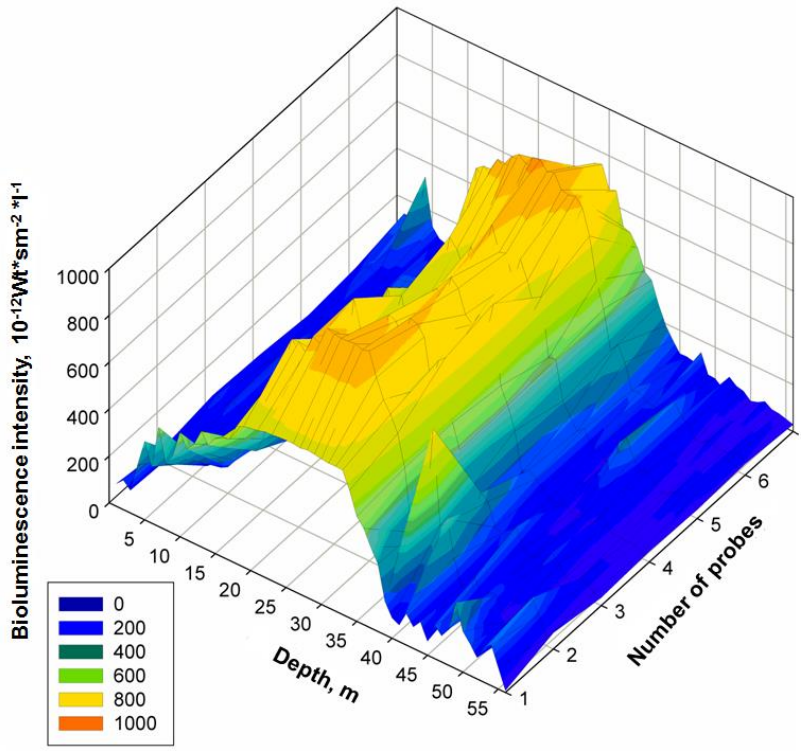

Fig. 2. Small-scale spatial inhomogeneity of the bioluminescence field in the seashore of Sevastopol (September)

When analyzing BF vertical intensity profiles of the open and closed areas of sea we found out that there are two BF highly intensive areas, the seasonal processes in which pass according to different consistent patterns (Fig. 3). In general, common features of the annual BF intensity dynamics are preserved in the surface layers of the investigated region.

Seasonal changes in bioluminescence field (BF) intensity have been analyzed. The seasonal changes in bioluminescence field (BF) intensity in the surface layer of different areas inside the Sevastopol Bay are characterized by rather high contingency, which is confirmed by a high paired correlation coefficient r = 0.83. The contingency of BF seasonal variation in the surface layer of open and closed areas of sea, on the contrary, are characterized by the average correlation relationship level (r = 0.56 – 0.63), which can give evidence, in particular, of different ecological state of the given regions [2].

The seasonal variation in the BF vertical structure in the surface layers of neritic area differs essentially from that in the deep-sea layers. The maximum BF intensity in the surface layer of the near-shore waters of Sevastopol was registered in autumn period (September-October). The maximum BF intensity in the deep-sea layer was registered in the open area of sea at depths located under thermal layer. BF intensity in the near bottom layer of the Sevastopol Bay in this period is about one – two orders lower than in the open water area [2].

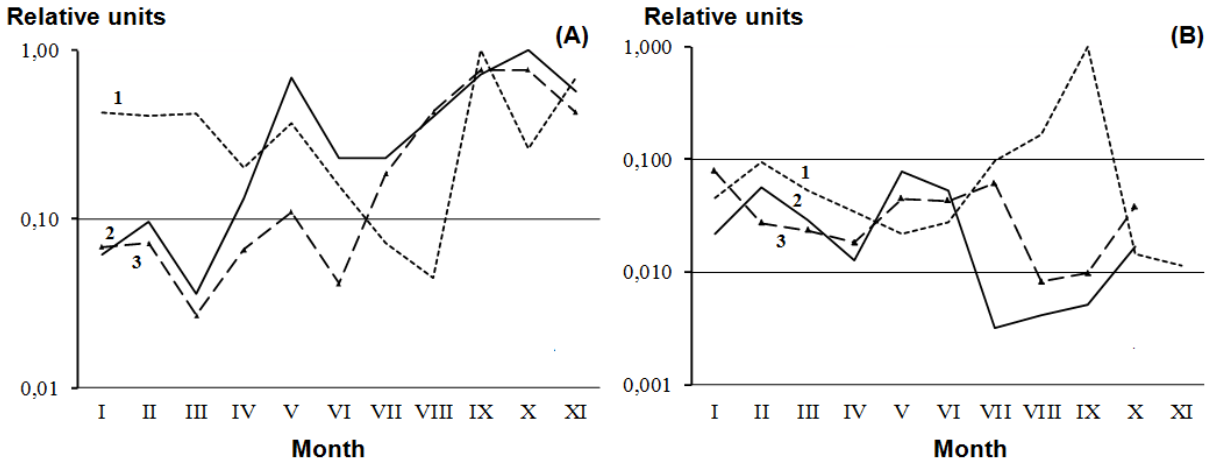

Fig. 3 Seasonal changes of BF intensity in the surface layer (A) and near bottom (deep-sea) layer (B) averaged and normalized by maximum annual value: 1 – at the st. 1(open area of sea); 2 – at the st. 2; 3 – at the st. 3 (closed area of sea).

The correlation relationship in the upper ten-meter layer between the bioluminescence field intensity and temperature (correlation coefficient r = -0,61), as well as the correlation relationship between the bioluminescence field intensity and salinity (r = 0,60) was obtained for the open water area (st. No 1, the beam of Kruglaya Bay) after the analysis and statistical data processing [2]. (Fig.4).

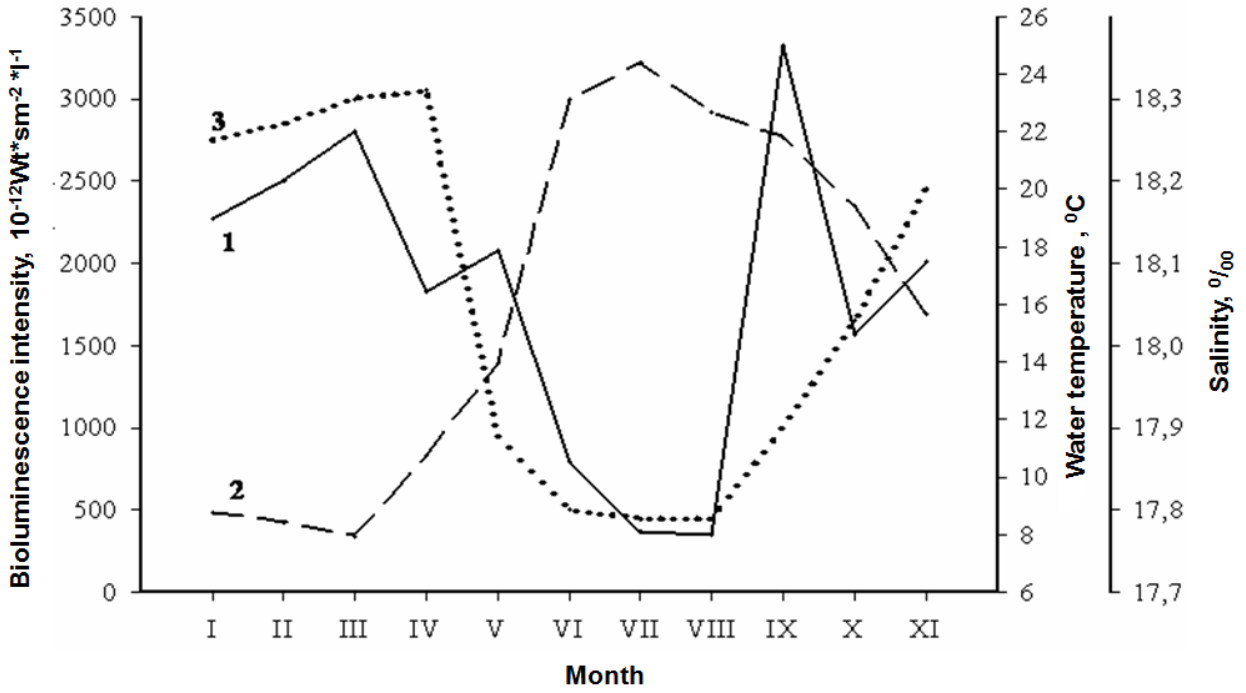

Fig. 4 Seasonal variations in bioluminescence field intensity (1), temperature (2) and salinity (3) in the surface water layer at the st.1 (open area of sea).

Two layers with different dynamics of bioluminescence field intensity have been discovered in the neritic area of the Black Sea during hours of darkness by cluster analysis method [2] (Fig. 5).

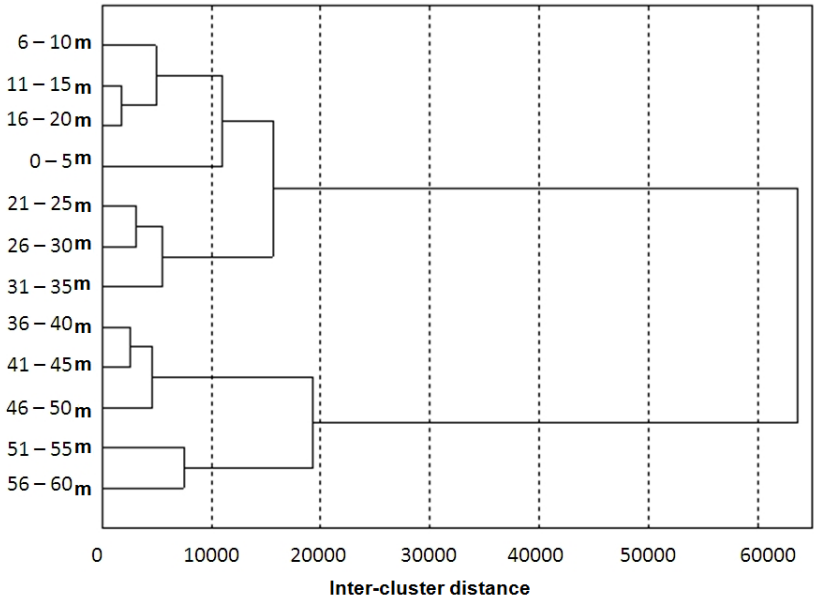

Fig. 5 Dendrogram of water layer clusterization and inter-cluster distances.

The bioluminescence field within the depths of 0 – 35 m is characterized by intensity peaks (at 7 pm, 11-12 pm, 3 am) and drops in intensity (at 8 pm, 1 am and 5-6 am) [2] (Fig. 6).

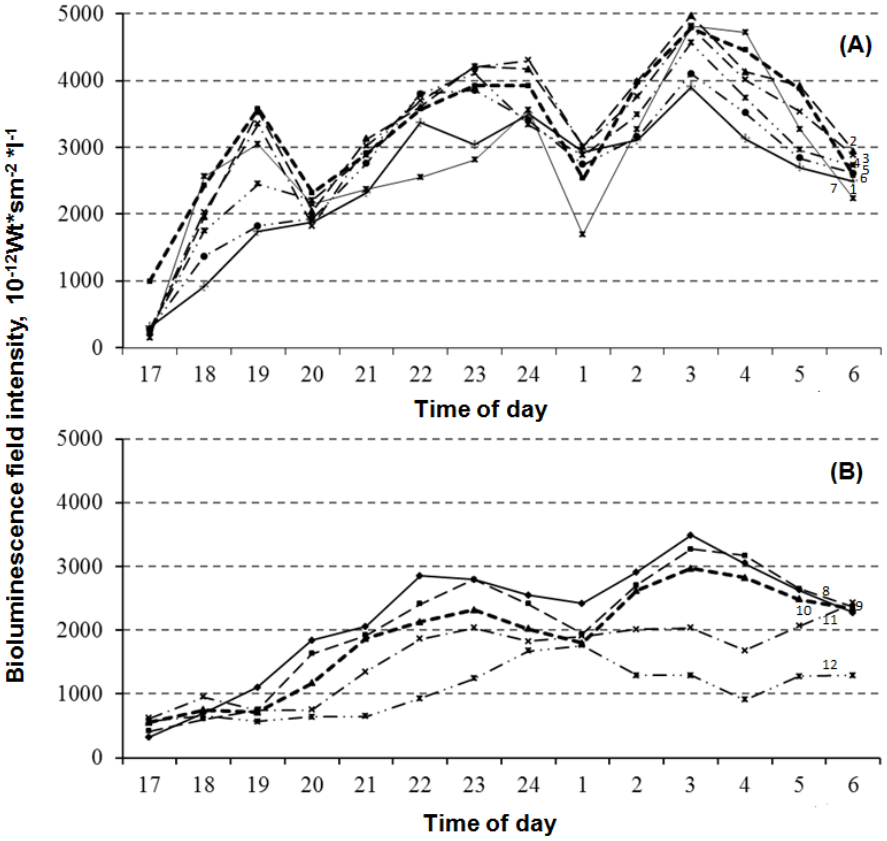

Fig. 6 Diurnal variations in BF intensity: A – in the upper layer: 1–0-5 m; 2–5-10 m; 3–10-15 m; 4–15-20 m; 5–20-25 m; 6–25-30 m; 7–30-35 m; B – in the deep-sea layer: 8–35-40 m; 9–40-45 m; 10–45-50 m; 11–50-55 m; 12–55-60 m

The methods of factor analysis show that the changes in BF intensity during hours of darkness can be described by three factors explaining 96,3% of total BF variance. It was shown that the basic factors determining the BF variability during hours of darkness are the cell division intensity of luminescent plankton and its grazing by zooplanktonic organisms [2].

The harmonic components of the change in BF intensity in coastal waters during hours of darkness were marked out and their gain-phase characteristics were calculated. It was shown that the 14-hour periodicity of variations of light produced by bioluminescent organisms related to the changes in illumination, and variations with 2,5…4,5 hours were conditioned by endogenous circadian rhythms of ethological nature [2].

The circadian dynamics of the BF parameters in the Black Sea gives evidence of the prevailing contribution of biotic factors (83,7 %) to its variability, the abiotic factors' contribution is 12,6 % [2].

CONCLUSIONS

The results of studying seasonal and circadian dynamics of the bioluminescence field parameters can be used for the express-methods of marine ecosystem functioning assessment.

The forecast of the nearshore ecosystem development, its protection against adverse natural and anthropogenic processes are the most important tasks during the coastal development. The

execution of the present work will make it possible to realize an integrated approach to solving problems of using Crimean coastal zones and to outline the ways to develop the promising directions of coastal management in the Russian Federation and to bring them closer to the international level.

ACKNOWLEDGMENT

The authors express gratitude and appreciation to Professor Mironov Oleg Glebovich, Doctor of Biological Sciences and to Professor Tokarev Yuri Nikolayevich, Doctor of Biological Sciences for their valuable scientific advice and commentaries, consultations when developing new hypotheses and for their pretentions to their approbation.

REFERENCES

[1] Gitelzon I.I. Bioluminescent Field of Ocean. / I. I. Gitelzon, L.A Levin, A. P. Shevyrnogov et al. / Abstracts of the IV International Congress "The Weak and Ultraweak Fields and Radiation in Biology and Medicine" - www.biophvs.ru/archive/consress2006/abs-p 109.pdf (In Russian)

[2] Lyamina, N. V. Dynamics of Parameters of Bioluminescence Field in the Black Sea and Their Association with Environmental Factors: Ph.D. Thesis in Biological Science: Speciality 03.02.10 "Hydrobiology" / Natalya Viktorovna Lyamina. – Sevastopol, 2014. – 133 p. (*In Russian*).

[3] Rubtsov S.I. Environmental Aspects of the Integrated Management of the Coastal Zone of Crimea. - Sevastopol: ECOSI-Hydrophysics, 2013. - 200 p. (In Russian).

[4] Tokarev Yu. N. Fundamentals of Biophysical Ecology of Aquatic Organisms / Yuriy Nikolayevich Tokarev - Sevastopol: ECOS-Hydrophysics, 2006. - 342 p. (In Russian).

DEVELOPMENT OF SCIENTIFIC FOUNDATION FOR SOLVING ENVIRONMENTAL AND HYDROBIOLOGICAL PROBLEMS OF INTEGRATED COASTAL ZONE MANAGEMENT

Svetlana Rubtsova, Institute of Natural and Technical Systems, Russia
Natalya Lyamina, Institute of Natural and Technical Systems, Russia
Aleksey Lyamin, Institute of Natural and Technical Systems, Russia

rsi1976@mail.ru

The work is dedicated to the development of the system of coastal zone environmental assessment, grounding on the principles of integrated approach to the management of resource and environmental safety in the Azov and Black Sea region. The methodological approaches and applied assessments of the quality control analysis of sea water and benthic sediment according to the monitoring data were formed. The methods of the marine environment biomonitoring were offered; its results have a universal basis and can serve both as the index of investigated cenosis structure and its physiological state.

Key words: ecosystem, integrated management, the coastal zone

The problem of environmental conservation is of crucial importance at present. The intensive natural resources development by Man, the further development of navigation, hydro-electric engineering take place in the coastal area. The aquatic bioresources' contribution to the maritime regions' economy under these conditions turns out to be rather insignificant in comparison with oil, gas or recreational resources. Furthermore, different users of resources enter into various conflicts with one another by creating spatial interferences and competition, polluting the environment and leading to the degradation of water ecosystems in general. In this connection the knowledge of biology of hydrobionts only is not enough any longer for their protection and rational use. The holistic approach to solving coastal zone problems of the Russian Federation is required.

The coastal management is a new trend which is determined as a coordinated activity aimed at the coastal zone management and administration. The integrated coastal zone management is a continuous process of elaborating and taking decisions aimed at harmonizing socio-economic development of coastal regions for the purpose of their sustained development. The development is sustained, if it guarantees economic growth, improvement of the quality of life of population, establishment of the democratic forms of social influence on the development process, cultural preservation and if it does not lead to the environmental deterioration of territories, habitat quality, water (sea water and continental waters) and air quality, biological diversity and variety of terrains. [16].

The task of the integrated coastal zone management is to find an effective balance among different kinds of activity in the coastal zone, to work out the strategy aimed at creating such its

economic and social structure, which would correspond to the fullest extent to the common interests of the territory development and would minimize conflict situations arising among different participants of this activity.

The increase in the anthropogenic effect on the ecosystem of the Black and Azov Seas becomes apparent in the degradation of biological, recreational and other resources. The measures taken for protecting the environment have led to the equalization of marine environment pollution and the uptrends emerged. However, the pollution level of benthic sediment, which is the source of secondary pollution in the water column, remains high as before. As a result of it, it is long past time to look for the ways of improving the natural resource exploitation and recreating the reproduction in the ecosystem of the Black and Azov Seas. The urgency of the chosen topic is determined by the necessity of creating the integrated system of environmental assessment of the coastal zone, grounding on the principles of integrated approach to the management of resource and environmental safety of the Azov and Black Sea region [16].

The environment status observations are made in the coastal zone of the Black Sea, but the works are not of a systemic nature: territorial one, by typology and networks for monitoring, parametric one, comparing indices, chronological, metrological, informative ones and the ones having other aspects. The absence of the integrated monitoring system does not make it possible to assess correctly the ecological state of territories in order to take important management decisions in the economic activity. Therefore, the maximum monitoring utilization is required, as well as its integration into the integrated system to provide assessments, predictions, recommendations. The creation of the integrated eco-monitoring system, in which the regional subsystems are provided for, will make it possible to give information and analysis support at regional and local levels. In this connection, the development of the system of environmental assessment of the coastal zone of the Sevastopol region, grounding on the principles of integrated approach to the management of resource and environmental safety in the Azov and Black Sea region is one of the up-to-date sectors of hydrobiological research for the moment.

The ever-growing demands of society for the development of new materials lead to the increase in the number of chemical compounds of anthropogenic origin which affect the biota. [7; 17]. It reduces the value of numerous laboratory experiments related to the toxicant effect upon model communities, as they, firstly, cannot “trace” the full range of toxic compounds and, secondly, do not take into account the synergetic effects which appear because of their influence.

The off-shore strip is characterized by high dynamism, as well as by the presence of alongshore circulation. The shallow household wastewater outlet with organic pollutants, and also the secondary pollution coming from the benthic sediment, present in the off-shore strips, are involved into the interconnected system of coastal flows, which results in the degradation of any integral part of its water area and may irreversibly affect the ecological situation of the sea in general [2 – 4; 18].

It is necessary to find new methods of marine environmental biomonitoring, whose results would be of universal (integral) nature and could serve as an index of both the chorologic structure of investigated cenosis and its physiological state. [7; 14; 19 – 21]. At that, the responses which, firstly, manifest themselves already within the first tens of minutes after the pollutant exposure and, secondly, the ones which are determined using instrumental control of registration of the observed

effects out of all diversity of populations' "post-impact" responses, undoubtedly, are of the greatest interest [13; 15; 17]. So, biophysical methods can serve as a sensitive indicator of the degree of resistance of plankton to pollutant exposure and as an express-indicator of regional marine pollution [5; 6; 18]. One of the tasks of our work is to assess the possibility of application of bioluminescent properties of plankton organisms and the light field created by them for the express assessment of neritic water area pollution.

An ecological system, or an ecosystem, is a basic functional unit in ecology, as it comprises organisms and inorganic environment, i.e. the components interfering with one another's properties and the conditions required for maintaining life in that very form which exists on the Earth. An ecosystem is understood to be a community of living organisms (communities) and their habitat, which form a stable life system thanks to the circuit of substances. Coastal ecosystems occupy a special place in ecology. At present the coastal zone is an important target of ecological, economic and hydrobiological researches because of its special geopolitical value within the framework of environmentally sustained development and national security.

Figure 1. provides the block diagram of a new approach to the environmental assessment in the system of integrated management of the resource and environmental safety of the coastal area of the Black Sea.

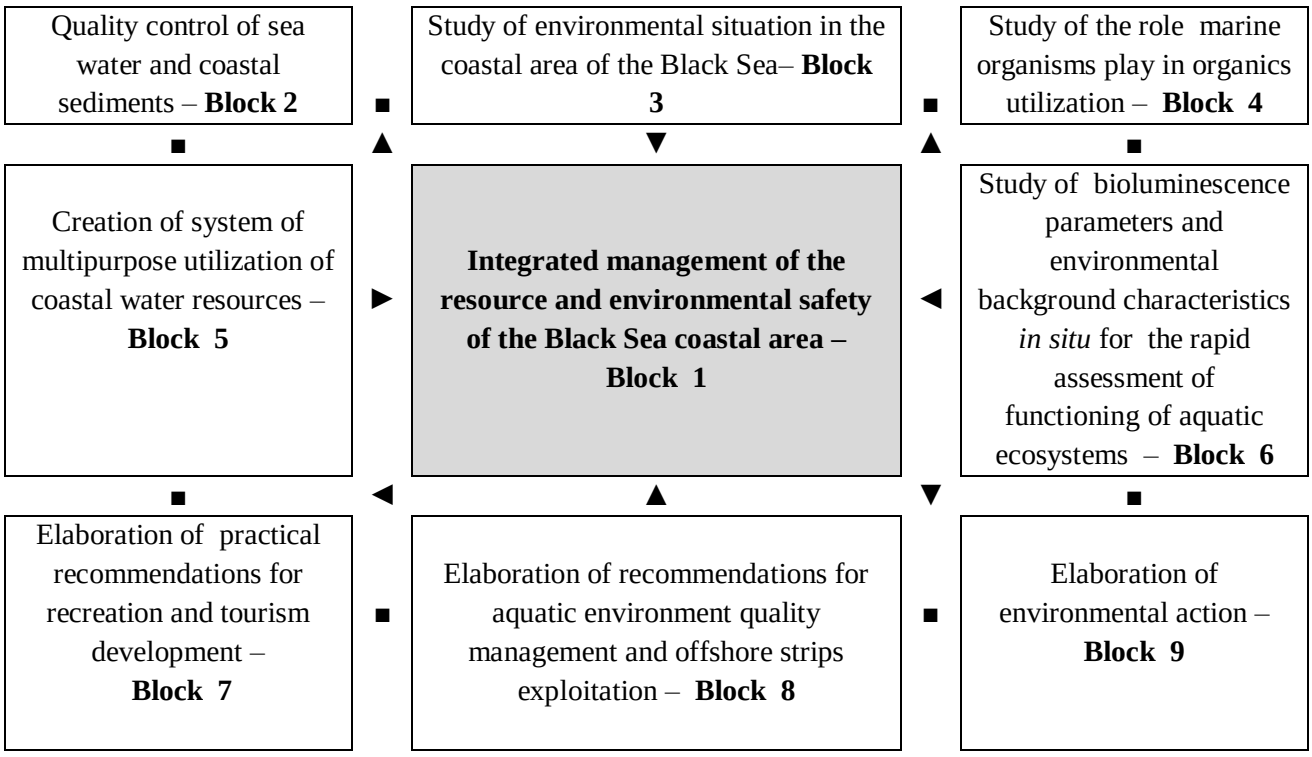

Fig. 1. Block diagram of a new approach to the environmental assessment in the system of integrated management of the resource and environmental safety of the coastal area of the Black Sea

Block 1, or coastal management, unites the rest of the blocks. The coastal management is defined as a coordinated activity on the coastal zone management and administration. The integrated coastal zone management is a continuous process of elaborating and taking decisions aimed at the harmonious development of coastal regions for the purpose of their sustained development. A coastal zone is understood to be a land-sea contact zone, including natural complexes, both coasts and adjacent sea surface within the borders that ensure environmentally balanced development of coastal territories, prevention of pollution and destruction of coastal landscapes, seascapes and ecosystems; it is the territory where economic and other activities are limited and regulated. A coastal zone is an area, where human interaction with the environment is particularly intensive.

Block 2 - quality control of sea water and coastal sediments. It is planned in this block to investigate routinely the pollutant dynamics, including oil and oil products, on the predetermined grounds of the coastal area of the Black Sea, as well as the number of main groups of organisms taking part in the transformation of pollution.

Block 3 – study of environmental situation in the coastal area of the Black Sea, it will make it possible to assess the ecological state of the littoral environment of the recreation zone. At that, such points as pollution, coastal wastewater flow are considered; the pollution sources are controlled, the amount of floating craft pollution and the pollution resulted from dumping rubbish is studied, pollutants are assessed and monitored.

Block 4 - study of the role marine organisms play in organics utilization; it is aimed at studying and further usage of marine organisms for organics utilization. The organics getting into the water serve as food for microorganisms; therefore the water enrichment with these substances definitely results in increasing growth of microflora. Microorganisms are bioindicators of the presence of different types of pollutants in the sea water. Heterotrophic bacteria use readily available organics as their food. The quantitative content of oil oxidizing microorganisms evidences the process in progress of natural self-purification from oil and oil products in the marine environment [11; 12; 16].

Block 5 – creation of system of multipurpose utilization of coastal water resources, in this block we consider the issues of industrial exploitation of resources, biological diversity conservation, habitat and landscape protection, estimation of environment impact level and integrated coastal zone management.

Block 6 – Study of bioluminescence parameters and environmental background characteristics in situ for the rapid assessment of functioning of aquatic ecosystems. Planktonic organisms play the main role in creating bioluminescent potential of the sea. The bioluminescent potential in the Black Sea is formed by thirty six algae belonging to the Class Dinophyceae of the genera Neoceratium, Protoperidinium, Scrippsiella, Gonyaulacaceae, Noctilucaceae, Lingulodinium, as well as by three species of comb-bearers, some species of Copepoda and two genera of luminescent bacteria (Fig.2) [8; 10; 17]. The planktonic bioluminescence parameters can serve as a sensitive express-indicator of the degree of their resistance to the impact of pollutants and as an expressive indicator of the degree of the regional marine pollution [1; 8; 10; 17; 18]. In this connection, the study of the dynamics of bioluminescence parameters and environmental background characteristics in situ is of current importance for the rapid assessment of functioning of aquatic ecosystems [8;10;17].

Blocks 7, 8, 9 make it possible to elaborate and propose practical recommendations for providing ecological safety of the population in the recreational zone of the Black Sea.

The constant growth of anthropogenic ecosystem load in the coastal zones results in the irreversible processes of exhaustion and deterioration of quality of natural resources, in more frequent and large-scale manifestation of crisis economic-environmental situations in the Black and Azov Seas. The results of the proposed study in the aggregate solve the scientific development of the system of environmental assessment of the coastal zone of the Black Sea, grounding on the principles of integrated approach to the management of resource and environmental safety in the Azov and Black Sea region.

The forecast of the nearshore ecosystem development, its protection against adverse natural and anthropogenic processes are the most important tasks during the coastal development. The execution of the present work will make it possible to propose an integrated approach to solving problems of using Crimean coastal zones and to outline the ways for the development of the promising directions of coastal management in the Russian Federation and to bring them closer to the international level.

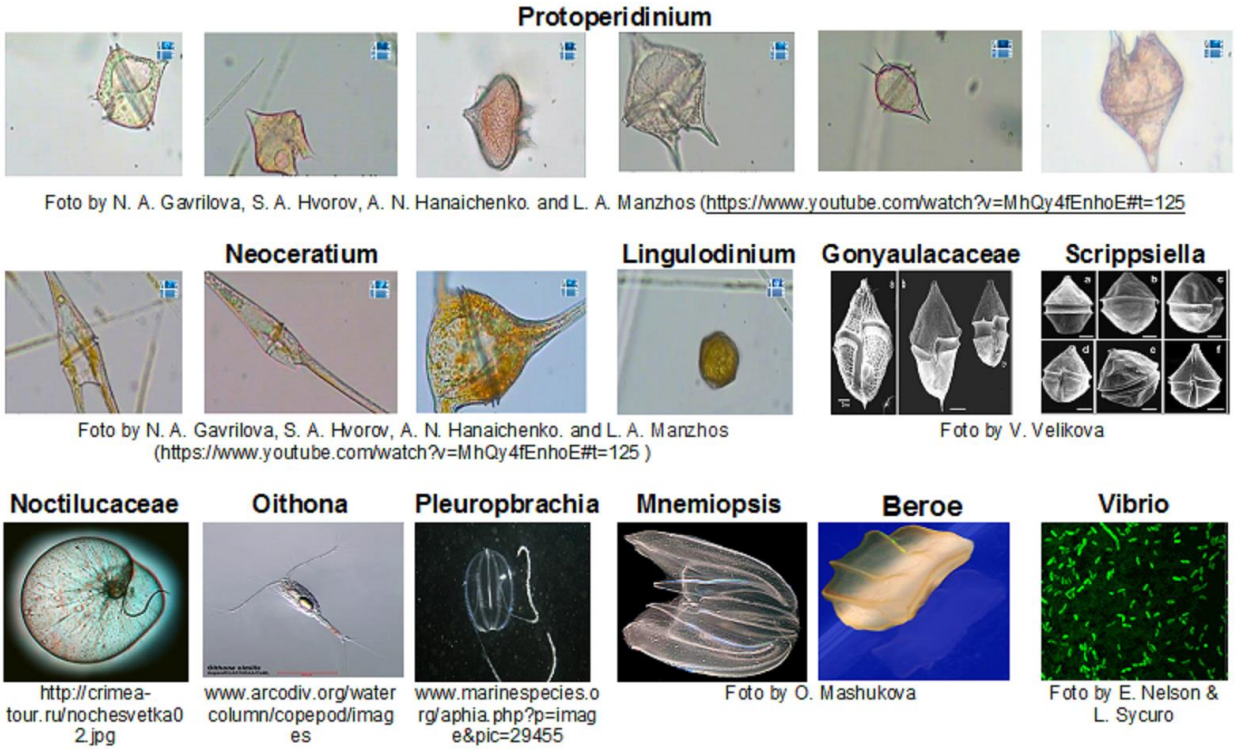

Fig. 2. Planktonic bioluminescent organisms of the Black Sea.

CONCLUSIONS

1. The proposed approach to the environmental assessment of the Crimean coastal zone in the system of integrated management of resource and environmental safety in the coastal zone will make it possible to elaborate practical recommendations for managing the aquatic habitat quality and exploiting off-shore strips, as well as for developing recreation and tourism in the Black Sea region.

2. The biota participation in the process of self-purification makes it possible to use marine organisms purposefully for the biomonitoring and pollution prevention, as well as for developing hydrobiological systems of conditioning of polluted sea waters.

3. The planktonic bioluminescence parameters can serve as a sensitive express-indicator of the degree of their resistance to the impact of pollutants and as an expressive indicator of the regional marine pollution.

ACKNOWLEDGMENT

The authors express gratitude and appreciation to Professor Mironov Oleg Glebovich, Doctor of Biological Sciences and to Professor Tokarev Yuri Nikolayevich, Doctor of Biological Sciences for their valuable scientific advice and commentaries, consultations when developing new hypotheses and for their pretentions to their approbation.

REFERENCES

[1] Bitjukov, E. P. Results and Prospects of Bioluminescent Research in the Black Sea/ E. P. Bitjukov, V. I. Vasilenko, I. M. Serikova, Yu. N. Tokarev // Ekologiya Morya –1996. – No 46 – P. 19 – 24. (*In Russian*).

[2] Bitjukov, E. P., Evstigneev, P.V. and Tokarev, Yu.N., "Dinoflagellata Black Sea and Influence on Them of Anthropogenous Factors", Gidrobiologicheskii Jurnal – 1993, No 29, P. 27-34. (*In Russian*).

[3] Bryantsev, V. A. and Bryantseva, Yu. V., "Long-Term Change in Phytoplankton of the Black Sea Deep-Water Part in Connection with Natural and Anthropogenic Factors", Ekologiya Morya – 1999, No 49, P. 24-28. (*In Russian*).

[4] Georgieva, L. V. "Specific Structure and Phytocen Dynamics", Naukova Dumka, Kiev, – 1993, P. 205-207 (*in Russian*).

[5] Gitelzon, I. I., "Ecological Biophysics and Its Role in Studying of the Water Ecosystem" / I. I. Gitelzon, M. I. Gladyshev, F. G. Degermendzhi, L. A. Levin and F. Ja. Sidko // Biophysics, – 1993, Vol. 38, No 6, P. 1069-1078 (*in Russian*).

[6] Gladyshev, M. I., "Basic of the Water Systems Ecological Biophysics", Science, Novosibirsk, – 1999, 113 p. (*In Russian*).

[7] Konovalov, S. M., "Anthropogenic Impact and Ecosystems of the Black Sea", CIESM Sci. Ser., – 1995, 1, P. 53-83

[8] Lyamina, N. V. Dynamics of Parameters of Bioluminescence Field in the Black Sea and Their Association with Environmental Factors: Ph.D. Thesis in Biological Science: Speciality 03.02.10 "Hydrobiology" / Natalya Viktorovna Lyamina. – Sevastopol, 2014. – 133 p. (*In Russian*).

[9] Marine Sanitary Hydrobiology / Under the general editorship of O.G.Mironov: Southern Seas Biology Institute of the National Academy of Sciences of Ukraine. – Sevastopol, 1995. – 102 p. (*In Russian*).

[10] Mashukova, O. V. Bioluminescence of the Black Sea Invading Comb-Bearers as a Test of Their Physiological State: Ph.D. Thesis in Biological Science / Olga Vladimirovna Mashukova. Sevastopol, 2011 – 183 p. (*In Russian*).

[11] Mironov, O. G. Oil Oxidizing Microorganisms in the Sea. – Kiev, 1971. – 226 p. (*In Russian*).

[12] Mironov, O. G. Scientific Basis of the Soviet International Project of Biological Monitoring of Oil Pollution of the Mediterranean Sea Basin // Herald of the Academy of Sciences of USSR. – 1978. - **8.** – P. 84 - 87. (*In Russian*).

[13] Narusevich, T. F., Shaida V. G., Yevstigneyev P. V., Davydov V. V. Interconnection of Plankton Structure and Bioluminescence as a Method of Biomonitoring of the Black Sea. In the book: V.I. Belyayev (edit.). Ecology and Rational Use of Natural Resources of South Region of Ukraine.- Sevastopol, Publishing House of MHI of National Academy of Sciences of Ukraine, 1985.- P. 273-276. (*In Russian*).

[14] Narusevich, T. F. and Tokarev, Yu. N. "Phytoplankton and a Bioluminescence in Mediterranean Sea During the Summer Period", Hidrobioljgicheskii Jurnal., – 1989, Vol. 25, No 6, P. 10-16. (*In Russian*).

[15] Patin, S. A. Chemical Pollution and Its Impact on Hydrobionts.- In the book: Oceanology. Biology of Ocean. - **2**. – M.E. Vinogradov (edit.).- M.: Nauka, 1977.- P. 322-331. (*In Russian*).

[16] Rubtsova, S. I. Environmental Aspects of Integrated Management of the Crimean Coastal Zone. – Sevastopol: ECOSI-Hydrophisika, 2013. – 200 p. (*In Russian*).

[17] Tokarev, Yu. N. Basic Principles of Biophysical Ecology of Hydrobionts / Yuri Nikolayevich Tokarev – Sevastopol: ECOSI-Hydrophisika, 2006. – 342 p. (*In Russian*).

[18] Tokarev, Yu. N. Bioluminescence of Plankton Organisms As an Index of the Neritic Aquatoria Pollution / Yu.N. Tokarev, P.V. Evstigneev, V.I. Vasilenko, O.V. Mashukova, N.V. (Burmistrova) Lyamina // Proceedings of the Eighth Intern. Conf. on the Mediterranean Coastal Environment, MEDCOAST 07, 13 – 17 November 2007, Alexandria, Egypt, Middle East Technical University, Ankara, Turkey. – Vol. 2. – P. 925 – 936.

[19] Tokarev, Yu. N., "The Bioluminescence Field As an Indicator of the Spatial Structure and Physiological State of the Planktonic Community at the Mediterranean Sea Basin", / Yu. N. Tokarev, E. P. Bityukov, R. Williams, V. I. Vasilenko, S. A. Piontkovski and B. G. Sokolov // Kluwer Academic Publishers, the Netherlands, – 1999– P. 407-416.

[20] Tokarev, Yu. N., "Influence of Various Dozes of Gamma Irradiation on Black Sea Noctiluca Bioluminescence", Interaction Between Water and Alive Substance: Proc. Inter. Symposium., Odessa, 6-10, Oct. 1979. M. : Vol.2., – P. 38-41.

[21] Tokarev, Yu. N., Shulman G. E., "Biodeversity in the Black Sea: Effects of Climate and Anthropogenic Factors", Hydrobiologia, – 20

AGGREGATION IMPACT ON THE FILTRATION AND GROWTH RATES OF MUSSELS *MYTILUS GALLOPROVINCIALIS* LAM.

Elena Vasechkina, Marine Hydrophysical Institute RAS, vasechkina.elena@gmail.com
Irina Kazankova, Institute of Natural and Technical Systems RAS, ikazani@ua.fm

Abstract. This study presents the results of field and laboratory-based experiments performed to determine the mussel density effect on an individual mollusk's growth and clearance rates. We measured the weight and length growth rates of single and aggregated mussels exposed into the sea for three monthly periods in summer and autumn 2015. The sample group contained 140 mollusks from natural populations within the length range of 15-20 mm. The average growth rate of aggregated mussels was almost the same as the growth rate of single ones. Clearance rate of single and aggregated mussels was measured in the laboratory using indirect method. There were selected 5 groups of mussels within the length ranges: 12-16 mm, 17-18 mm, 18-25 mm, 22-23 mm, and 35-38 mm. The clearance rate was measured for each mussel from the group and then for the whole group aggregated in a clump. Water temperature and seston concentration were the same for single and clumped mollusks. The volume of water in chambers was proportional to the weight of mussels put in water. The ratio of aggregated and single mussels' clearance rates varied from 0.48 to 0.85 at the same density of aggregation and without regard to the animal size. Significant individual variability was recorded in all field and laboratory-based experiments.

Key words: mariculture, Bivalvia, growth in aggregation, clearance rate, laboratory experiments

I. INTRODUCTION

FAO estimates that the world production of aquaculture increases almost twice every 10 years. Sustained development of aquaculture depends on effective minimizing of the mariculture harmful effect on the environment. Most of scientists agree that problem can be solved by passing from monocultures to integrated polyculture that means simultaneous cultivation of several species with different trophic level like fish, macrophytes, filter-feeders and detritophags. Cultivated species should be chosen to make excretory products of one species consumed by other species.

With the right choice of integrated polyculture components, their disposition and total weight according to the ecological capacity of the district, system comes to a balance thus minimizing any environmental impact. In fact the artificial ecosystem is created inside the natural one and it functions without making any harm. Practical biotechnology development must be preceded by creating information technology including the simulation model and the system collecting and processing information about the real system functioning [1]. Earlier we developed such simulation model including the description of the cultured mollusks and macroalgae, hydrochemical unit and comparatively simple hydrodynamic model [2, 3]. This paper reveals only one component of this model such as the unit reproducing the growth of mussel *Mytilis galloprovincialis* on artificial

substrate [4]. Empirical relations used in this unit were obtained in the laboratory-based conditions and need to be verified to imitate the cultivated species functioning within natural environment. Dense clumps of mollusks are formed on collectors of marine mussel plantations. There are reasons to suppose that physiological functions of specimen in such aggregations differ from physiological functions of specimen in laboratory. In this connection, to have these functions described adequately in the model we have to assess the influence of aggregation and adjust the empirical relations obtained in the laboratory for isolated mussels.

Studies on physiological characteristics changes of bivalves in clumps are very limited. The process of clump-forming itself is not studied well yet. Number of researchers supposes this process to be of random nature. Their opponents claim the forming of clumps to be the result of active behavior responses of mollusks [5]. We can assume that aggregative changes in physiological processes are one of the most important reasons of aggregation forming. One of the earliest studies of aggregation impact on mollusks' oxygen consumption rate was the research [6]. The laboratory-based experiments conducted in [6] revealed that specific oxygen consumption rate diminishes in relation to the number of mollusks in one chamber. Similar study was made in [7]. Researchers held experiments in the laboratory with the fresh-water bivalve mollusk *Elliptio complanata* and came to the same conclusion.

Density impact on the effective clearance rate of the bivalves was studied in [8, 9]. The authors of [8] fixed that the average effective clearance rate for isolated individuals was higher than that for those in clumps. They explain decrease of the clearance rate in dense aggregations by increased refiltration in the cores of the clumps. The results of [9] showed the significant effects of mussel density and the seston concentration on the effective clearance rate of mussels. As opposed to [8], the higher clearance rates in experiments were obtained at denser mussel clumps. The authors suppose that obtained results were connected with the high concentration of food particles used in the experiments. They hypothesized that refiltration could have an opposite effect and reduced negatively high food concentrations down to a more favorable range for less exposed mussels. But some other experiments should be carried out to check this hypothesis. Authors of [10] measured the ingestion rate in dense colonies of bivalves and came to conclusion that ingestion of mussels located within middle and bottom layers of the colony was less due to the suffering from reduced access to food resources. There were no information about ingestion or filtration abilities of a colony as a whole compared to the isolated mussels.

We failed to find another papers concerning aggregation impact on filtration and growth rates of mussels in the literature that is why we had held mussels' growth monitoring on collectors at the nearshore zone and laboratory-based study of density influence on mussels' filtration rate. The results of our work are described below.

II. Aggregation impact on the growth rate of mussels

Natural experiment was carried out in Martynova Bay, Sevastopol to study the aggregation impact on mussels' growth rate. We chose 140 mollusks from natural populations within the length range 15-20 mm. Length, width and wet weight of mollusks were measured, and then samples were divided into 7 groups by 20 specimens. Two groups were used for measuring the growth rate of mollusks growing separately to be referred to as "isolated" mussels hereinafter. Other groups were

meant to evaluate the mussels' growth rate in clumps. While exposing at sea, isolated mussels were arranged in cages by two specimens in each. Other groups of mussels were placed in cotton mesh bags where mollusks formed clumps of approximately the same density. All groups were exposed in the sea coastal zone on experimental collectors for the period from June till November.

Averages, standard deviations and coefficients of variation were calculated upon the results of monthly measurements of mussels' linear and weight growth. Average growth rates of isolated mussels and those in clumps had been compared. During the first monthly period (from June, 12 to July, 13) we used plastic cages but they malformed the shells of mussels and curbed the linear growth of mollusks so the results of that period had to be rejected.

Diagrams on Fig. 1 show average linear growth rates for different periods of time. Linear growth rate of mussel was counted according to the formula:

$$dL = \frac{30}{\Delta t}\sqrt{(\Delta L_1)^2 + (\Delta L_2)^2}, \qquad (1)$$

where L_1 and L_2 – length and height of mollusk's shell, Δt – time when collectors were exposed in the sea.

Specific weight rate was calculated upon the wet weight measurements:

$$dW = \frac{30}{\Delta t}\frac{\Delta W}{0.5(W_b + W_e)}, \qquad (2)$$

where W_b and W_e – original and terminal measurement of specimen's wet weight.

Diagrams on Fig. 2 demonstrate specific weight rates for different periods of time in comparison.

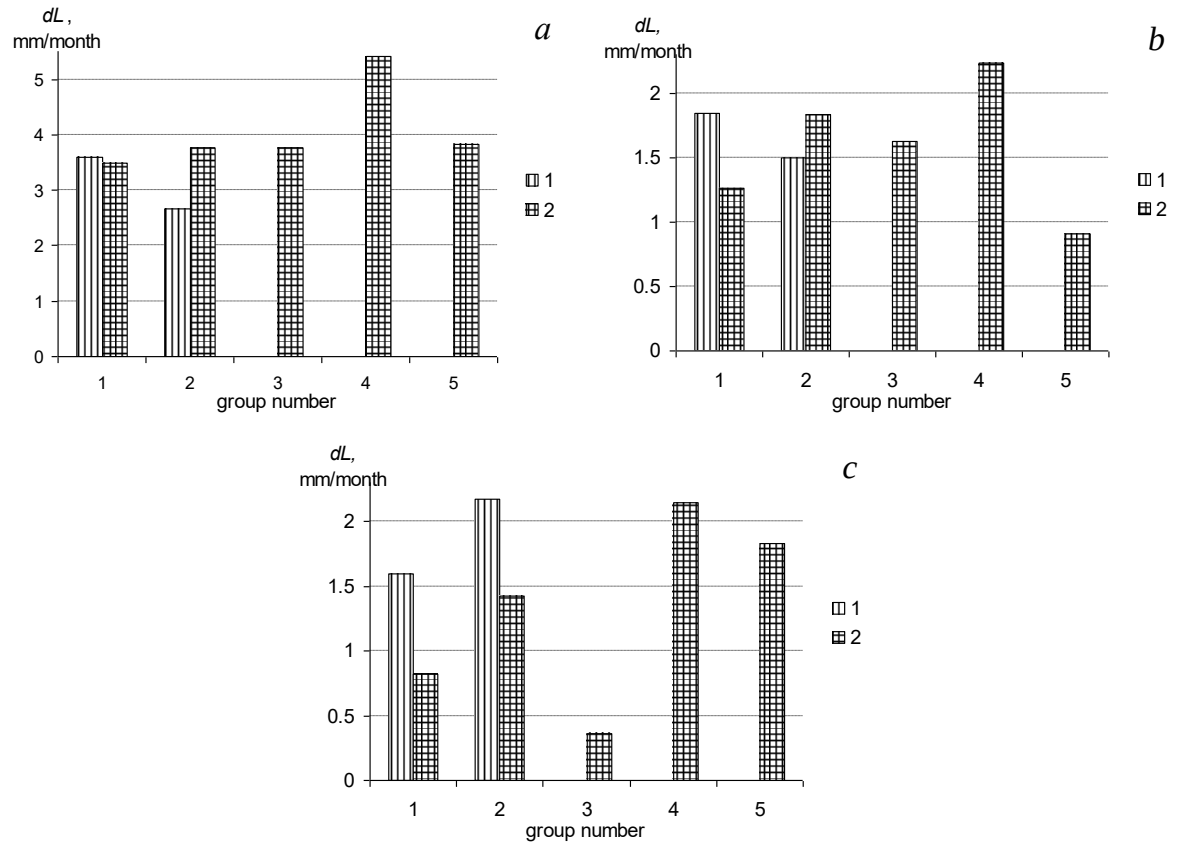

Fig.1. Average linear growth rates (1) in groups of isolated mussels – 1 and mussels in clumps – 2 during the time periods: a – July-August; b – August-September; c – September-November.

Diagrams on figs. 1 and 2 are qualitatively similar that proves sufficient accuracy of measuring mollusks' wet weight (mollusks were scaled with the water inside their shells). Great intergroup variation of rates draws our attention because it means that individual living characteristics of mollusks vary greatly as conditions of mussel groups on collectors and their food supply were almost the same.

It was supposed that isolated mussels would grow faster as they are provided with oxygen and food better and do not compete with their neighbors for resources. However, comparison of average growth rates of isolated mussels and mussels in clumps didn't give expected results.

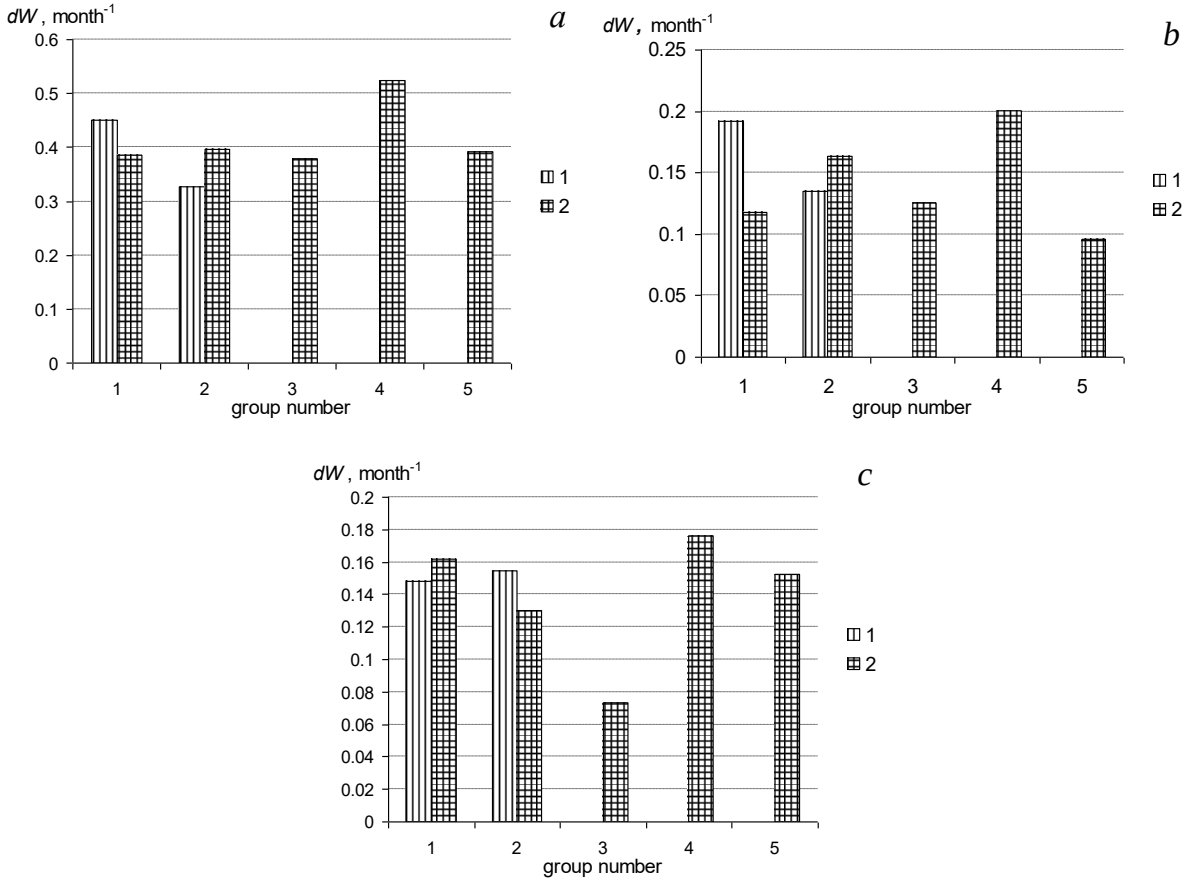

Fig.2. Average specific weight rate (2) in groups of isolated mussels – 1 and mussels in clumps - 2 during the time periods: a – July-August; b – August-September; c – September-November.

Fig. 3 demonstrates linear and weight growth rates averaged for all groups and for the whole time of experiment in comparison. In the first period of the experiment linear growth rate of isolated mussels was even smaller than for aggregated mussels. Average specific weight rates of mussels almost match not depending if mussels are isolated or aggregated. The relation between isolated mussels and mussels in clumps is 0.98 for linear growth and 0.95 for specific weight growth rate.

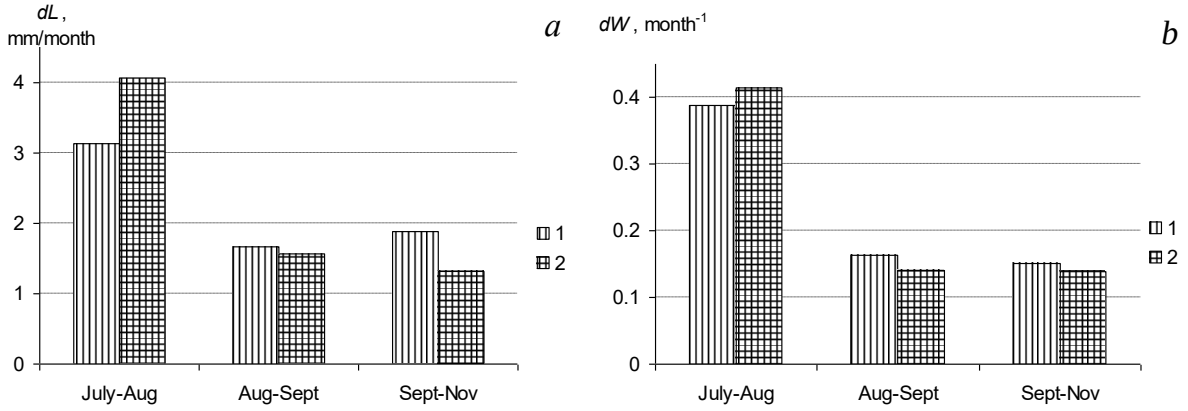

Fig.3. Average linear growth rate of mussels – a and average specific weight rate – b for the whole time of experiment. Growth rate of isolated mussels – 1, of mussels in clumps – 2.

The mortality coefficient of mussels *m* (month^{-1}) was also under control. Fig. 4 shows the average meaning in groups of this coefficient.

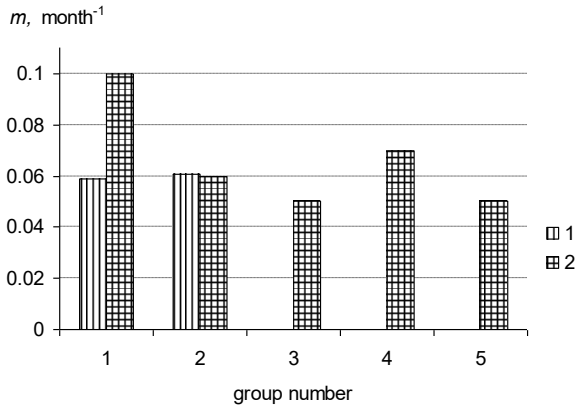

Fig. 4. Average mortality coefficient calculated for the whole period of sea exposition for groups of isolated mussels – 1, in clumps – 2.

The relation between average mortality coefficients of isolated mussels and mussels in aggregation is 1.10 (aggregated mussels – 0.066, isolated – 0.060). Considering high individual variation and limited sample we can accept a hypothesis that disposition of mussels in clumps doesn't augment the mortality coefficient under otherwise equal conditions.

III. LABORATORY STUDY OF DENSITY INFLUENCE ON MUSSELS' FILTRATION RATE

The filtration rate was estimated by the clearance rate defined as the amount of water cleared from food particles per unit of time. Microalgae *Tetraselmis viridis* was used to prepare food suspension for experimental mollusks. Optical density with the wave length 750 nm was used as indirect indicator of microalgae biomass. Measurements were held with photoelectric colorimeter

PC-3 and a 10 cm cuvette. Transition from optical-density units to absolute dry weight of biomass D was pursued by means of empirical coefficient equal to 0.0375 $g \cdot l^{-1} \cdot$unit of optical density^{-1} [11].

Five samples of mollusks with similar length parameters were selected from natural populations. The size ranges within groups were: 12 – 16 mm (12 spc.), 17-18 mm (15 spc.), 22-23 mm (15 spc.), 18-25 mm (22 spc.), and 35-38 mm (10 spc.). Each group was used in experiments in two replications to define the filtration rate of mussels separately and in clumps. The studied mussels were placed by one in chambers of equal volumes with sea-water containing food particles. Exposition lasted one hour. Optical density of sea water was measured before and after the exposition. The change of optical density was used to calculate the clearance rate of every mollusk. After the experiment mussels were placed in cotton mesh bags and hung in a container with filtrated sea water for one day. During this time mussels clung to each other forming a clump. Next day that clump was placed in the experimental chamber with food suspension of the same optical density. Water volume was more than in experiments with isolated mussels in proportion to the weight of mussels in the clump. So, the initial phytoplankton density D_0 and the relation V/W were the same as in a previous experiment with isolated mussels, where V – water volume, and W – wet weight of mussels in a chamber. Exposition also lasted one hour with following measuring of water optical density and filtration rate calculation. Water temperature in the experiment varied in a range 23 – 26°C, initial concentration of phytoplankton was 15.6 - 17 $mg \cdot l^{-1}$.

To derive the filtration rate formula C ($l \cdot h^{-1}$) we use the equation describing decrease of seston concentration in a chamber of volume V(l) containing n mussels [12]:

$$\frac{dD}{dt} = -D\left(\frac{Cn}{V} + \alpha\right), \tag{3}$$

where D – seston concentration in an experimental chamber, α is the rate at which particles settle out from suspension. The general solution of (3) can be written as

$$D_t = D_0 \exp(-(Cn/V + \alpha)), \tag{4}$$

and

$$C = \frac{60V}{nt}\left(\ln(\frac{D_0}{D_t}) - \alpha\right), \tag{5}$$

where D_0 and D_t – initial and final seston concentration ($g \cdot l^{-1}$), t – time of exposition in minutes.

The rate α can be estimated by the control experiment on measuring changes of seston concentration in a chamber without mussels D':

$$\alpha = \frac{60}{t}\ln\left(\frac{D'_0}{D'_t}\right). \tag{6}$$

Our experiment showed this rate to be close to zero so we used the following formula to calculate the average specific filtration rate in clumps (l $g^{-1} \cdot h^{-1}$):

$$C_a = \frac{60V}{W_a t}\left(\ln\left(\frac{D_0}{D_t}\right)\right), \quad (7)$$

where W_a – wet weight of mussels placed in the chamber (g). Specific filtration rate of isolated mussels (l $g^{-1} \cdot h^{-1}$) was calculated according to the formula:

$$C_u = \frac{60V}{W_u t}\left(\ln\left(\frac{D_0}{D_t}\right)\right). \quad (8)$$

Fig. 5 demonstrates average filtration rates of isolated mussels and the same mussels joined in clumps in comparison. The relation of aggregated mussels' filtration rate to the average filtration rate of isolated mussels turned out to be less than 1 and varied from 0.48 to 0.85. Apparently variability of this parameter was influenced by the water temperature and high individual variation of physical characteristics of mussels.

Laboratory experiments let us suppose that filtration rate of aggregated mussels is 15-50% lower than filtration rate of isolated mussels. At the same time we didn't observe substantial decrease of the growth rate of mussels in clumps. According to the energy balance equation of living organisms, productive energy could be estimated as $P = A - R - E$ (cal·day^{-1}), with A – assimilated energy, R – metabolic costs, E – excretion energy. The assimilated energy is proportioned to the consumption $I = CK_dD$, with C – filtration rate, D – concentration and K_d – calorific value of food suspension. In this case we can write down $P = A_eCK_dD - R - E$ with A_e – assimilation coefficient.

One can write

$$(R + E)_a < (R + E)_u \quad (9)$$

keeping in mind that productive energy of isolated and aggregated mussels seems to be almost equal (as it was showed by our investigation of growth rate of mussels on collectors), initial concentrations of suspension were equal, assimilation coefficients were the same (as experiment was held with the same mussels), and filtration rate of aggregated mussels was lower than that of isolated mussels.

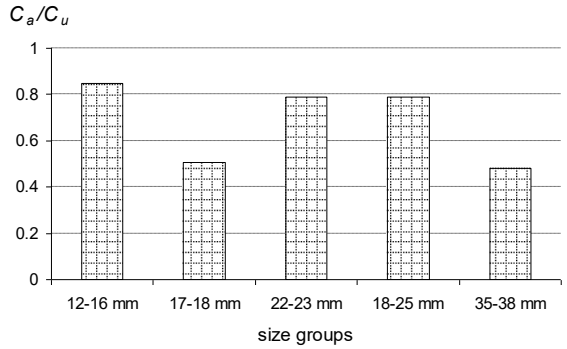

Fig. 5. Relations obtained in the experiment between aggregated mussels filtration rates and the filtration rate of isolated mussels averaged for all the groups.

Excretion energy (E) is still under-explored. According to [13], excretion depends on mollusk's weight and concentration of food particles in water. Excretion energy is smaller by an order of magnitude than metabolic costs, therefore with sufficient precision the relation (9) can be rewritten as $R_a < R_u$. That conclusion agrees with previously performed studies. Influence of mussels' stocking density in a respirometer on the oxygen consumption rate was studied in [6]. At first experimental mollusks were placed in separate respirometers and then they were replaced into one big respirometer with parallel measuring of oxygen consumption. Water volume per one specimen was 312 ml for mussels in aggregations and 250 ml for isolated mussels. Fig. 6 demonstrates the results of that experiment. 80% of measurements revealed the relation R_a/R_u to be less than 1, average obtained meaning was 0.92. Experiments when aggregated mussels had half as much water volume as isolated ones showed that oxygen consumption rate of the first was sufficiently lower than that of the second. In that case average ratio R_a/R_u decreased to 0.77 [6].

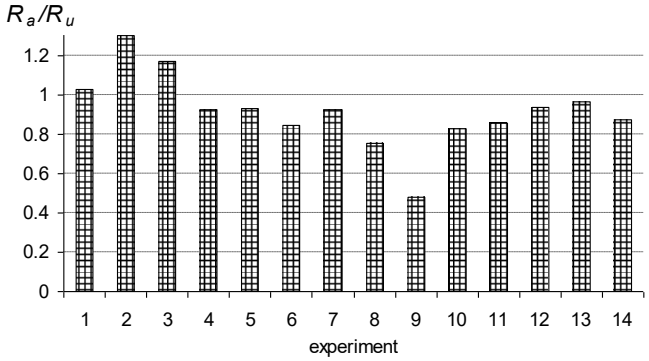

Fig. 6. The ratio of oxygen consumption rates of aggregated and isolated mussels [6]. Water temperature 22 – 23 °C.

Dependence of hydrobionts' specific basic metabolic costs on patch density is known for many kinds of aquatic organisms (physiological activities decrease in aggregations). In the case of mussels clumps, this can be explained by the limited (comparing to the isolated mussels) life space available for a mussel in a clump to take necessary nutrients and energy from the ambient water. It's reasonable to assume that mollusks from biofouling cenosis would experience this effect much bigger as they form very dense aggregations. Physical activity of mussels in aggregation decreases much more under the low current velocity because of metabolic products accumulation and oxygen depletion as the result of mussels' oxygen consumption. This phenomenon must be taken into account in the simulations of mussels' functioning on collectors of a mussel farm. It should be considered for accurate description of matter interchange between the artificial and natural ecosystems and estimation of ecological capacity of marine area planned for mariculture. To develop reliable empirical relations some additional laboratory-based experiments are needed to calculate the filtration rate and the oxygen consumption rate of mollusks under the variable environmental conditions, such as temperature, concentration of feeding suspension and the density of clumps.

V. REFERENCES

[1] E. F. Vasechkina, “Concept of informational technology of sustainable development support of mariculture in the nearshore zone of Crimea”, *Environmental control systems,* 2014, vol. 20, pp. 220-225.

[2] E. F. Vasechkina, “Multi-element model of the pelagic plankton community”, *Environmental control systems*, 2013, vol. 19, pp. 247-252.

[3] E. F. Vasechkina, “Simulation of an integrated multi-trophic aquaculture”, *Proc. of Conf. MARESEDU – 2015,* Moscow, MSU, October 2015, pp. 463-466.

[4] E. F. Vasechkina, I. I. Kazankova, “Mathematical modeling of the growth and development of the mussel *Mytilus galloprovincialis* on artificial substrates”, *Oceanology*, 2014, vol. 54, № 6, pp. 763-770.

[5] P. A. Lezin, “Peculiarities of aggregative behavior and spatial organization of mussels *Mytilus edulis* in the White Sea”, *PhD thesis in biology,* Institute of Zoology RAS, S.-Petersburg, 2009.

[6] V. D. Brajko, “Dependence of mussels’ breathing on the size of respirometers”, *Biologiya morya,* 1979, vol. 48, pp. 15-21.

[7] C. G. Paterson, “Effect of aggregation on the respiration rate of the freshwater unionid bivalve *Elliptio complanata* (Solander)”, *Freshwat. Inv. Biol.*, 1983, № 2, pp. 139-146.

[8] N. Yu, D. A. Culver, “Estimating the effective clearance rate and refiltration by zebra mussels, Dreissena polymorpha, in a stratified reservoir”, *Freshwater Biology*, 1999, vol. 41, pp. 481-492.

[9] A. Zaiko, D. Daunys, “Density effects on the clearance rate of the zebra mussel *Dreissena polymorpha*: Flume study results”, *Hydrobiologia,* 2012, vol. 680, pp. 79–89.

[10] N. C. Tuchman, R. L. Burks, C. A. Call, J. Smarrelli, “Flow rate and vertical position influence ingestion rates of colonial zebra mussels (Dreissena polymorpha)”, *Freshwater Biology*, 2004, vol. 49, pp.191–198.

[11] A. B. Borovkov, R. G. Gevorgiz, “Productivity of *Spirulina platensis* and *Tetraselmis viridis* under various methods of cultivation”, *Ecologiya morya,* 2005, vol. 70, pp. 9-13.

[12] J. Coughlan, “The estimation of filtering rate from the clearance of suspensions”, *Mar. Bio.*, 1969, № 2, pp. 356-358.

[13] V. I. Kholodov, A. V. Pirkova, L. V. Ladygina, “Functional characteristics of a typical mussel farm”, *Rybnoye khozyajstvo Ukrainy*, 2011, № 5, pp. 48-55.

LUMINESCENCE OF THE BLACK SEA MICROSCOPIC FUNGI CULTURES

Olga Mashukova, The Kovalevsky Institute of marine biological research (IMBR), RAS, Russia
Yuriy Tokarev, The Kovalevsky Institute of marine biological research (IMBR), RAS, Russia
Nadejda Kopytina, The Kovalevsky Institute of marine biological research (IMBR), RAS,Russia

olgamashukova@yandex.ru

We studied for the first time luminescence characteristics of the some micromycetes, isolated from the bottom sediments of the Black sea from the 27 m depth. Luminescence parameters were registered at laboratory complex "Svet" using mechanical and chemical stimulations. Fungi cultures of genera *Acremonium, Aspergillus, Penicillium* were isolated on ChDA medium which served as control. Culture of *Penicillium commune* gave no light emission with any kind of stimulation. Culture of *Acremonium* sp. has shown luminescence in the blue – green field of spectrum. Using chemical stimulation by fresh water we registered signals with luminescence energy (to $3.24 \pm 0.11)\cdot10^8$ quantum·cm^2 and duration up to 4.42 s, which 3 times exceeded analogous magnitudes in a group, stimulated by sea water ($p < 0.05$). Under chemical stimulation by ethyl alcohol fungi culture luminescence was not observed. Culture of *Aspergillus fumigatus* possessed the most expressed properties of luminescence. Stimulation by fresh water culture emission with energy of $(3.35 \pm 0.11)\cdot10^8$ quantum·cm^2 and duration up to 4.96 s. Action of ethyl alcohol to culture also stimulated signals, but intensity of light emission was 3–4 times lower than under mechanical stimulation. For sure the given studies will permit not only to evaluate contribution of marine fungi into general bioluminescence of the sea, but as well to determine places of accumulation of opportunistic species in the sea.

Key words: microscopic fungi (micromycetes), luminescence characteristics, chemical stimulation.

I. INTRODUCTION

Despite the fact that bioluminescence is known for many vegetable and animal systematic groups for several thousands of years, contribution of marine fungi into the seas and oceans luminescence has not been studied [3, 8, 15]. Moreover practically nothing is known about marine mycobiota luminescence. Two alternative ideas are under discussion: first, land tree fungi luminescence is provided by the classic enzyme – substrate system of luciferase – luciferine and, to the contrary, an idea that fungi luminescence causes oxidation of the organic substrates without specialized enzyme participation. Fungi represent by themselves the third kingdom of the living nature, evolutionary distanced from the plants and animals that is why learning of their luminescence mechanism is fundamental interest. Biochemistry of the fungi is quite peculiar and gives us opportunity to expect that their bioluminescent system can appear to be principally another [1]. By the present time 1500 microscopic fungi species have been isolated from the marine

environment, among them about 500 are higher obligate marine fungi known only for marine or water habitats. Representatives of Ascomycota section dominate in their species composition – 97% (including their anamorph forms, according to old classification group of Anamorphic Fungi (17%) [5].

Actuality of the studies of micromycetes different groups living in the sea is proved by their role in the ecosystem. Some widely spread in environment saprophyte fungi cause secondary mycoses and allergic diseases in men and hydrobionts. Such fungi are called opportunistic, representatives of genera *Aspergillus* (*A. flavus*, *A. fumigatus*, *A. terreus*), *Fusarium* (*F. moniliforme*, *F. oxysporum*), *Alternaria*, *Cladosporium*, *Penicillium* belong to them [6]. In the ecosystems of moderate altitudes with high anthropogenic load they clearly observe a tendency of the potentially pathogenic fungi accumulation with high rate of growth. It has been stated that often the same fungi species are resistant to several anthropogenic factors [10]. Just these fungi species inhabit different substrates and they are revealed by luminescent methods.

Eutrophication and pollution of the sea facilitate micromycetes development: on one hand they participate in decomposition of the organic and chemical substances, on the other hand they parasite on hydrobionts immunity of which is weaken by the unfavorable environmental conditions [14, 16]. At present time known hundreds of substances (toxins, growth stimulators, organic acids, hormones, vitamins etc), which are synthesized and accumulated in the microscopic fungi cells (micromycetes) and in the culture medium (liquid). As a rule they are specific for separate species and are called secondary metabolites. Obligate marine fungi are mostly connected with cellulose – containing substrates, thus resembling luminescent land fungi. Considering all above mentioned we aimed our work on determination of luminescent ability and the biophysical parameters of bioluminescence studies in separate species of the micromycetes and their complexes, isolated from the marine habitats.

II. MATERIALS AND METHODS

Beginning from 30-ties of the last century in medicine, veterinary and food industry fluorescent diagnostics use for revealing microscopic fungi and their metabolites on the skin and hair coverings of the animals and man, books, plastics, meat, fish, vegetables, corns, milk products, wine. Diagnostics is based on ability of fungi and substances they synthesize to produce light under the long-wave ultraviolet rays influence. The studies of the fungi metabolite products and their ability to produce light are conducted in mycelium cells and cultural medium [7, 9, 12]. To create ultraviolet radiation they use practically different devices (Wood lamp, hand lamp Vista UV handle etc) [18, 19, 21, 22, 23].

Using such methods in the Institute of marine biology, National Academy of Science of Ukraine were isolated cultures of microscopic fungi from marine environment. Characteristics of the micromycetes luminescence were studied in the biophysical ecology department of the Kovalevsky Institute of marine biological research of the Russian academy of sciences (IMBR RAS). Micromycetes were isolated from the samples of water and bottom sediments, taken during the expedition cruise № 70 (August 18 – 19, 2011) of the R/V “Professor Vodyanitsky” (Fig. 1). 56 water samples and 32 bottom sediments samples have been taken at 30 stations. Seeding was conducted by generally accepted methods [12]. Fungi species determination was conducted

according to [4]. 62 micromycetes species were identified; in species composition representatives of genera *Aspergillus* – 19, *Alternaria* – 8, *Penicillium* – 7, *Acremonium* – 7 dominated. Domination of the terrigenic fungi species in water and bottom sediments of the marine water reservoirs is general peculiarity. To study luminescent ability pure cultures of the most distributed species *Aspergillus fumigatus* Fresen, 1863, *Acremonium* sp., *Penicillium commune* Thom, 1910, *Penicillium* sp., represented by the anamorph fungi stages have been chosen.

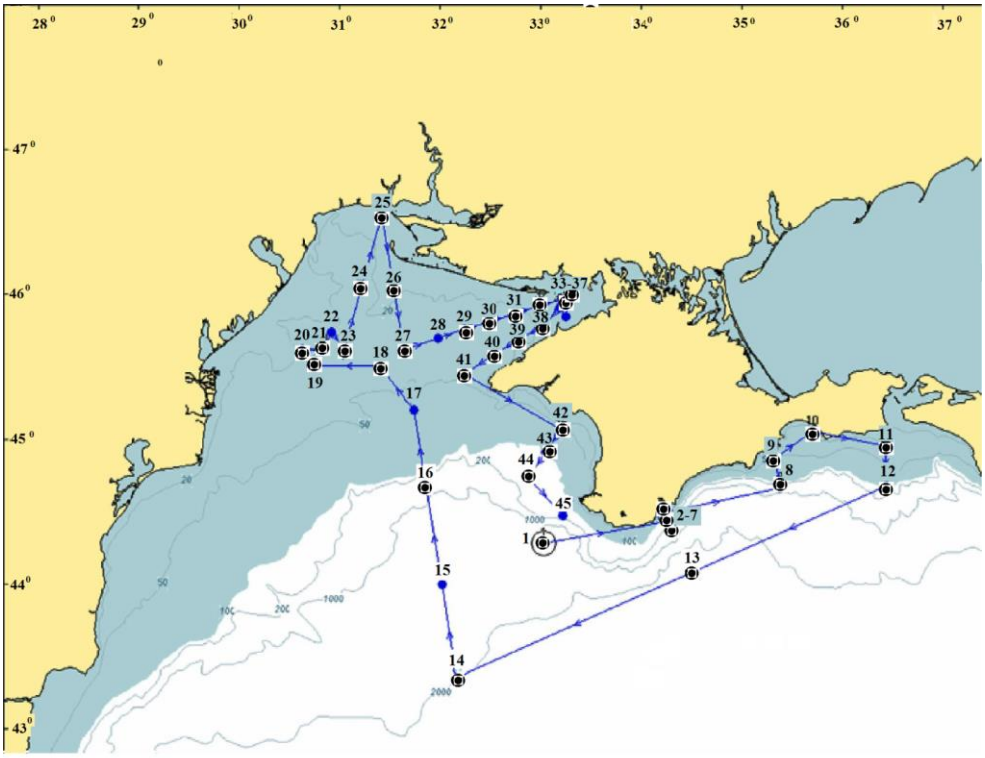

Fig. 1. Route and scheme of the stations location in the 70-th expedition cruise of R/V "Professor Vodyanitsky". Remark: – marking the stations at which they took samples for studying mycobiota

To compare characteristics of the facultative and marine fungi luminescence we studied also cultural liquid of the fungi complexes isolated from the Black sea scallop valves, crab carapax and fragments of wood gathered at the coast (Table 1). Fungi complexes were chosen according to the greatest fluorescence under ultraviolet lamp EVT – 01 irradiation (light flow 780 lm, wave length 360 nm) (Fig. 2). Substrate and culture of micromycetes were separated from the cultural liquid by filtration through the paper filter "white band" (specific weight – 80 g $*m^{-2}$; filtration time – 20 s; properties: average pores size, high rate of filtration) into clean sterile vessels, which were sent by the courier mail to Sevastopol for further spectral studies.

Obligate and facultative fungi species from Ascomycota section, represented by the anamorph and teleomorph stages made part of the mycocomplexes. Anamorh is an organ of sexless or vegetative reproduction of fungi. Teleomorph is a form of sex spore – containing in fungi, its purpose – genes recombination and fungus protection under unfavorable conditions or wintering. Anamorph and teleomorph have different names and morphologically and cariologically clearly differ one from another. Some fungi species are known only at one of reproductive stages.

Table 1. Species composition of the micromycetes complexes

Micromycetes species	Substrate, medium										
	SG	K	W	W	W	W	W	W	W	W	ChDA
	Age of a complex, months										
	22	25	24	33	12	7	10	18	7	15	1.2
Anamorph stages											
Alternaria alternata (Fr.) Keissl, 1912	+	–	–	–	–	–	–	+	–	–	+
Dendryphiopsis sp.		–	–	–	–	–	–	+	+	–	–
**Dictyosporium pelagicum* (Linder) G. C. Hughes, 1963		–	–	+	–	–	–	–	–	–	–
**Cirrenalia macrocephala* (Kohlm) Meyers, R. T. Moore, 1960	–	–	–	+	+	–	–	–	+	–	–
Cumulospora sp.	–	–	–	–	–	–	+	–	–	–	–
Cyphellophora sp.	–	–	–	–	–	–	–	–	–	–	+
Hormographiella sp.	–	–	–	–	–	–	–	–	–	–	+
**Monodictys pelagica* (Johnson) E. B. G. Jones	–	–	–	+	–	–	–	–	–	–	–
Stemphylium tomatonis E.G. Simmons, 2001	–	–	–	–	–	–	–	–	+	+	–
Stachybotrys chartarum (Ehrenb.) S. Hughes, 1958	+	–	–	–	–	–	–	–	+	+	–
Teleomorph stages											
Chaetomium globosum Kze, 1817	+	+									
**Corollospora trifurcata* (Höhnk) Kohlm,1962	–	–	+	–	–	–	–	–	–	–	–
**Corollospora maritima* Werdermann, 1922	+	–	+	–	–	–	+	+	–	–	–
**Corollospora* sp.		–	–	–	–	–	+	–	–	–	–
**Haligena elaterophora* Kohlm, 1961	–		–	+	–	–	–	–	–	–	–
**Halosphaeriopsis mediosetigera* (Cribb & J.W. Cribb) T.W. Johnson, 1958	–	–	+	–	–	–	–	–	–	–	–
**Remispora maritima* Linder, 1944	–	–	–	–	–	+	–	–	–	–	–
**Torpedospora radiata* Meyers, 1957	–	–	–	–	–	+	–	–	–	–	–

*Remark: SG – mycocomplex on the valves of the Black sea scallop Flexopecten ponticus Bucquoy Dautzenberg & Dollfus 1889; K – mycocomplex on crab; ChDA – mycocomplex on Chapek – Dox agar medium; * – obligate marine species of micromycete.*

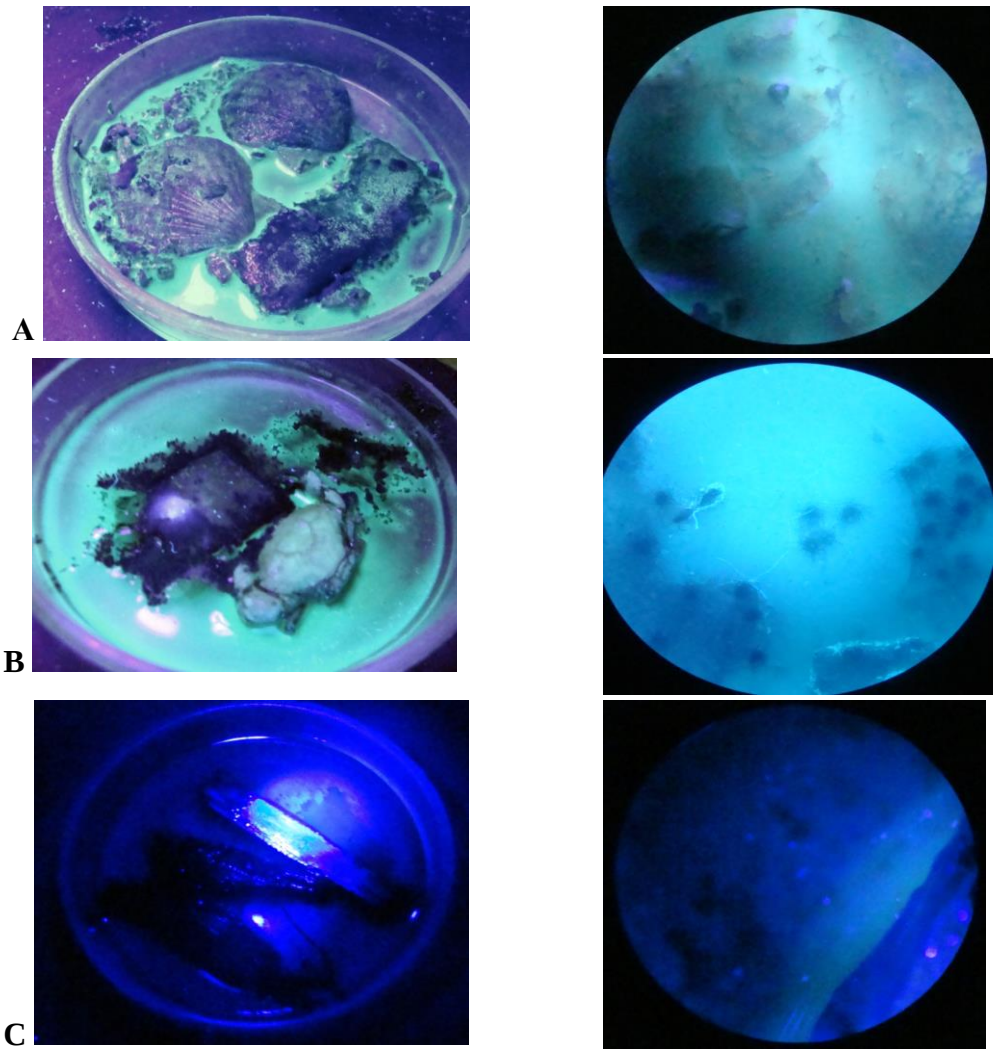

Fig. 2. A. On the left – general view of the fungi complex on the Black sea scallop Flexopecten ponticus valves (near the base of mollusk valves there is filtering paper, used as a substrate for fungi isolation); on the right – microphoto (16x). Mycocomplex species composition: Chaetomium globosum, Corollospora maritima, Alternaria alternata, Stachybotrys chartarum;
B. On the left – general view of the fungi complex on the crab carapax (in the upper part of Petri dish there is filtering paper used as a substrate for fungi isolation0; on the right – microphoto (16x). Culture: Chaetomium globosum; C. On the left – general view of the wood sample, on the right – microphoto (16x). Species composition of mycocomplex on wood: Corollospora maritima, Corollospora sp., Cumulospora sp.

Before an experiment on availability of fungi culture luminescence was kept under temperature of 18 ± 2ºC, adapting for 2 h to the experiment conditions. In the studies of cultural liquid sterile mixture of the brine (16 S‰) and fresh water in correlation 1 : 1 was a control; dish with clean medium was a control for fungi grown on ChDA medium. The studies were conducted at the day time under complete darkness. Biophysical parameters of luminescence in micromycetes and their complexes were registered at the laboratory complex IMBR RAS “Svet” [11]. Device

complex included high voltage power pack (HV-22), luminescope, consisting of an acceptor of light emission (FEU – 71) and dark camera for an object, as well as registration device – digital interface. Into dark camera of the luminescope they put specially made cuvette of 50 cm^3 volume for mechanical and chemical stimulation of the bioluminescent organisms. The cuvette is made of transparent organic glass, into which they placed control organisms and organisms under experiment. They used mechanical and chemical stimulations of mycelium or cultural liquid for studying the main luminescence characteristics: energy and duration of their signals. Mechanical stimulation was conducted by quick putting in marine water into cuvette with cultures. As a chemical reagent fresh water and ethyl alcohol in 0.96% concentration, administrated with syringe into cuvette were approbated [17].

III. RESULTS AND DISCUSSION

On the ChDA medium cultures of the facultative marine micromycetes anamorph stages with 4–6 weeks age have been received. Mycelium ability to emit light was revealed in species *A. fumigatus*, *Acremonium* sp. and in complex of *A. alternata*, *Cyphellophora* sp., *Hormographiella* sp. (Fig. 3). In this group of cultures only *A. fumigatus* species appeared to be active under effect of all types of stimulation, and characteristics of luminescence energy (E) were maximum (Table 2).

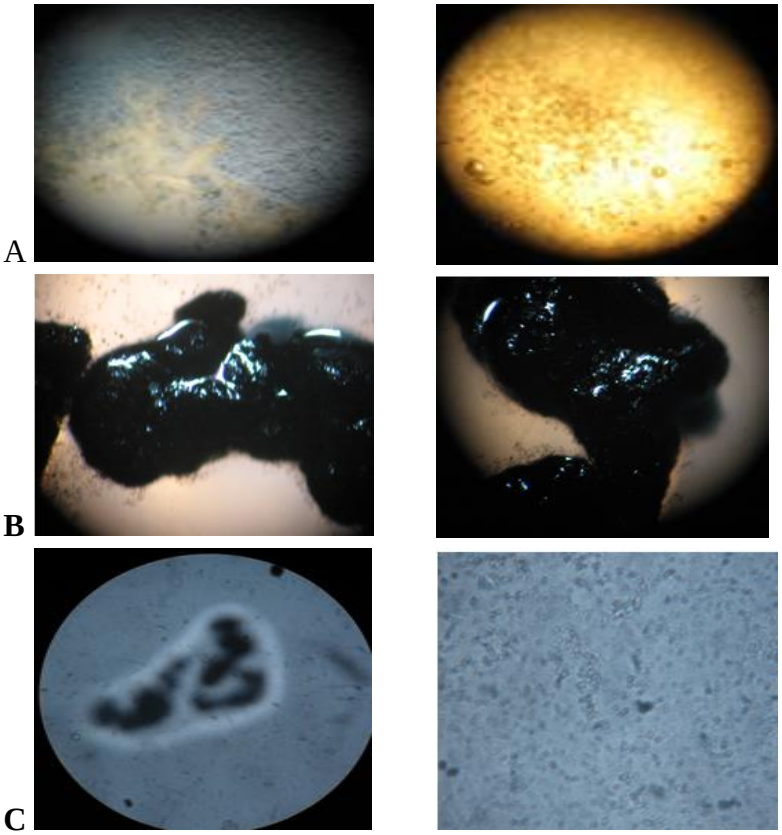

Fig. 3. A. – Colony of Aspergillus fumigatus in ChDA medium (magnification 16x); B. – Fungi complex on ChDA medium: Alternaria alternata, Cyphellophora sp., Hormographiella sp. *(magnification 16x); C. – Culture of Penicillium sp. On ChDA medium, on the left magnification 16x, on the right magnification 40x.*

Table 2. Mycocomplex composition, or fungus species (E – light-emission energy, 10^8 quantum·cm^{-2}; T – light-emission duration, s)

Mycocomplex composition, or fungus species	Mechanical stimulation (the marine water)		Chemical stimulation			
			Fresh water		Ethyl alcohol	
	E	T	E	T	E	T
Corollospora maritima, *Corollospora* sp., *Cumulospora* sp.	1.77 ± 0.08	4.49 ± 0.21	3.44 ± 0.17	4.57 ± 0.22	0.48 ± 0.02	4.39 ± 0.21
Alternaria alternata, *Cyphellophora* sp., *Hormographiella* sp.	1.14 ± 0.05	4.47± 0.22	2.24 ± 0.11	4.94 ± 0.24	–	–
Acremonium sp.	1.12 ± 0.05	4.46 ± 0.22	3.35 ± 0.11	4.53 ± 0.22	–	–
Aspergillus fumigatus	1.87 ± 0.08	4.59 ± 0.21	3.24 ± 0.11	4.96 ± 0.24	1.04 ± 0.05	4.38 ± 0.21

The cultures of *Acremonium* sp. and mycocomplex (*A. alternata*, *Cyphellospora* sp. and *Hormographiella* sp.) did not emit light under stimulation by alcohol. Fungi complex had less expressed light emission if compared with *A. fumigatus* and *Acremonium* sp. In *Penicillium* sp. and *P. commune* luminescent ability has not been revealed under such means of stimulation.

The second series of experiments was conducted with the cultural liquids of mycocomplexes consisting of anamorph and teleomorph stages of the obligate and facultative marine fungi species, isolated on the scallop valves, crab carapax and wood fragments. Liquid age was of 7 – 33 months. Positive result has been received only for the mycocomplex of *C. maritima*, *Corollospora* sp., *Cumulospora* sp., isolated on the wood fragments. The given complex reacted positively to all stimulation types. For all cultures able to emit light common peculiarity has been revealed: maximum average magnitudes of luminescence energy under chemical stimulation by the fresh water were more than under mechanical one 1.7 – 2.9 times. Duration of luminescence in all cultures under study remained to be relatively constant not depending on stimulation type, making averagely 4.35 – 4.96 s.

Comparison of typical luminescent signals of the mycocomplex *C. maritima*, *Corollospora* sp., *Cumulospora* sp. cultural liquid under mechanical stimulation and chemical way of the fungi luminescent system irritation by the fresh water has shown that their luminescence differed (Fig. 4). For example luminescent signal caused by marine water represents itself as a flash of average amplitude, which first decreases and then grows, reaching its amplitude maximum with $3.44 + 0.17 \cdot 10^8$ quantum·cm^{-2}. Under mycocomplex chemical stimulation they observe one – two weak signals of small amplitude with sharp front of growing and with the same decrement of descending.

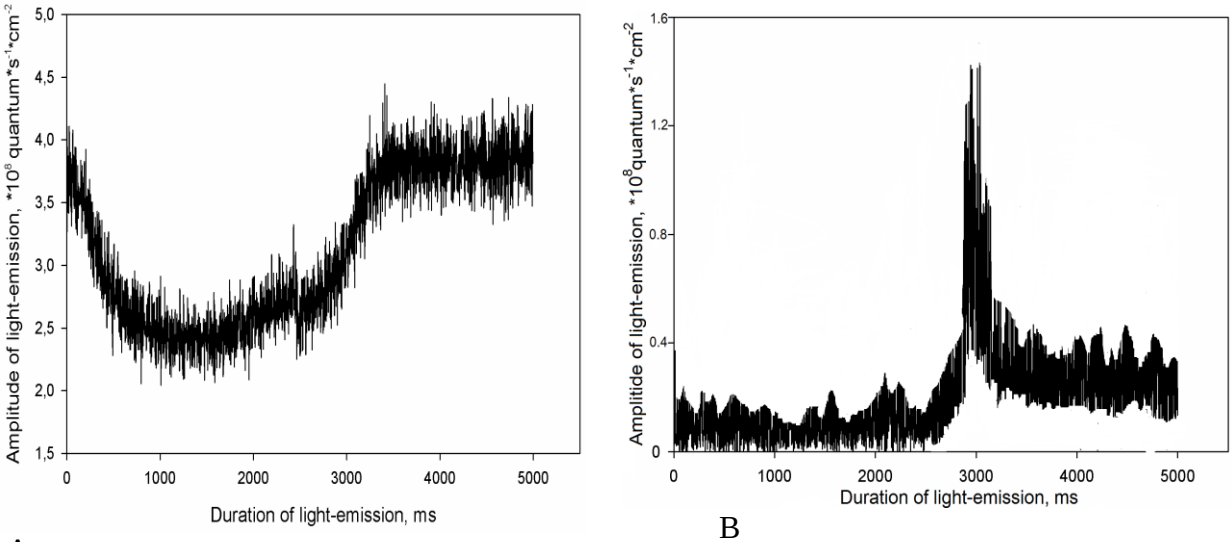

A B

Fig. 4. Typical luminescent signal under: A) mechanical stimulation by the brine and B) chemical stimulation by the fresh water of the cultural liquid in the complex of obligate marine fungi (Corollospora maritima, Corollospora sp., Cumulospora sp.)

Typical signals of *A. fumigatus* under effect of the marine water represent non-considerable in amplitude flashes with sharp peak of growth with maximum at the third second after stimulation. Effect of the fresh water for mycomycetes is analogous to this in the mycocomplex *C. maritima* (Fig. 5).

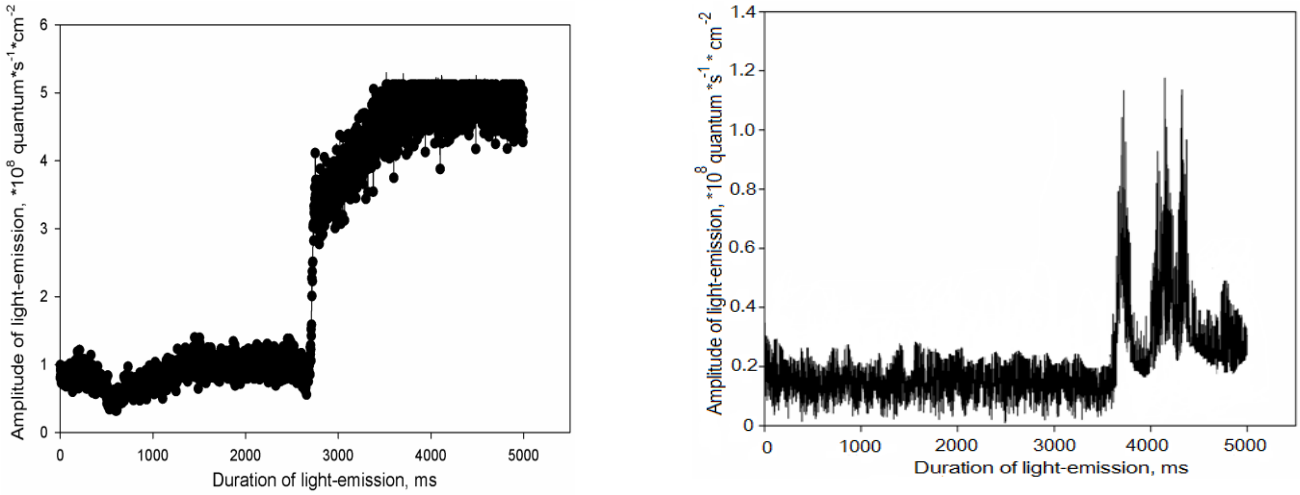

A B

Fig. 5. Typical luminescent signal under: A) mechanical and B) chemical stimulation of the Aspergillus fumigatus culture by the fresh water.

According to the character of luminescence in the mycomycetes under study we can determine that culture signals with both types of stimulation are more durable than those we registered in the other bioluminescent species. Really, while majority of the known bioluminescent

organisms (marine algae, coelenterates, ctenophores) emit light as impulses, fungi luminescence due to its character resembles bacteria luminescence [2, 13, 20].

Lighting mycocomplexes by the ultraviolet light on the ChDA medium, hydrobionts and wood fragments have shown that “old cultures” (5–6 weeks on ChDA, 7–33 months on another substrates) were fluorescent; on ChDA anamorph stages dominated in the species composition, marine species at the teleomorph stage dominated on hydrobionts and wood. It is also possible that like the land wood luminescent fungi from the Basidiomycota section, marine mycomycetes get ability to emit light after mycelium stops to grow, which takes place after starvation of substrate they grow on [1]. The ChDA medium dries and becomes poor soon that is why ascomata of fungi have no time for formation. Obviously in the cultural liquid without micromycetes there takes place decomposition of the substances, which provide an effect of luminescence that is why light emission has been revealed only in one variant of experiment. We suppose that character of the micromycetes luminescent response is determined by their trophic specialization, growth rate, different relation to the temperature and another factor. All this will be a subject of the further investigations.

IV. REFERENCES

[1] Bioluminescent analysis of the molecular processes in cells and their physical-chemical models; Creation on their basis of a new generation of bioluminescent sensors for biology and medicine. Report about scientific-research work in the frame of the federal target program “Scientific and scientific – pedagogical cadres of the innovational Russia” for 2009 – 2013 (intermediate stage № 2). The title of the stage: “The studies of molecular – cell mechanism of the bioluminescent fungi”. Head of SRW, academician, doc. of med. sci., prof. I.I. Gitelzon. Krasnoyarsk, 2010, 87 pp.

[2] I.I. Gitelzon, E.K. Rodicheva, S.E. Medvedeva, G.A. Primakova, S.I. Bartsev, G.A. Kratasyuk et al., *Luminescent bacteria*. Novosibirsk: Nauka, 1984, 386 pp.

[3] S.H.D. Haddock, M.A. Moline, and J.F. Case, “Bioluminescence in the Sea,” *Annu. Rev. Marine. Sci.,* vol. 2, pp. 443-493, 2010.

[4] G.S. De Hoog, J. Guarro, J. Gene, and M.J. Figueras, *Atlas of clinical fungi,* 2rd ed., Centraalbureau voor Schimmelcultures, 2000, 1126 pp.

[5] K.D. Hyde and S.B. Pointing, “Marine mycology”, *A Practical Approach,* Hong Kong: Fungal Diversity Press, 2000, 370 pp.

[6] A.E. Ivanova and O.E. Marfenina, “Life – ability of mycelium fragments and vegetation of spores of some species of the microscopic fungi in different ecological conditions,” *Modern problems of mycology, algology and phytopathology*, pp. 216-217, 1998.

[7] D. Khundzhua, E. Fedoseeva, S. Patsaeva, V. Terekhova, and V. Yuzhakov, “Spectroscopy of chromophoric organic substances released by soil microscopic fungi into aqueous medium,” *Czech Republic*, pp. 56-49, June 2011 [*Digests* 5th EARSeL Workshop on Remote Sensing of the Coastal Zone Prague, Czech Republic, p. 301, 2011].

[8] D. Lapota, “Bioluminescence – Recent advances in oceanic measurements and laboratory applications,” in *Tech Janeza Trdine*, vol. 9, 2012, 190 pp.

[9] Luminesent analysis. Eds. M.A. Konstantinova-Shlezinger, Moscow: The State editorial of physical-mathematical literature, 1961, 400 pp.

[10] O.E. Marfenina, “Opportunistic fungi in the anthropogenically disturbed ecosystems,” *Modern problems of mycology, algology and phytopathology*, pp. 249-250, 1998.

[11] O. Mashukova and Yu. Tokarev, “Variability of the bioluminescence characteristics of the Black Sea ctenophores-aliens in connection with different conditions of nutrition,” Open journal: *Adv. Biosci. Biotechnol. (ABB)*, vol. 4, № 11, pp. 968-973, 2013. . http://www.scirp.org/journal/abb/

[12] Methods of experimental mycology. Manual. Kiev: Nauk. Dumka, 1982, 552 pp.

[13] J. Poupin, An.-Sop. Cussatlegras, and P. Geistdoerfer, “Plancton Marin Bioluminescent. Inventaire documenté des espèces et bilan des formes les plus communes de la mer d’Iroise,” Rapport scientifique du Loen, Laboratoire d’Océanographie de l’École Navale, LOEN, 1999, 64 pp.

[14] K.L. Rypien, J.P. Andras, and C.D. Harvell, “Gliobally panmictic population structure in the opportunistic fungal pathogen *Aspergillus sydowii*”, *Molecular Ecology*, vol. 17, № 18, pp. 4068-4078, 2008.

[15] O. Shimomura, “Bioluminescence: Chemical principles and methods”, *World Scientific*, 2006, 470 pp.

[16] H. Souheil, A. Vey, P. Thuet, and J.P. Trilles, “Pathogenic and toxic effects of *Fusarium oxysporum* (Schlecht.) on survival and osmoregulatory capacity of *Penaeus japonicus* (Bate)”, *Aquaculture*, vol. 178, № 3-4, pp. 209-224, 1999.

[17] Yu.N. Tokarev, “The bases of the hydrobionts biophysical ecology”, Sevastopol: ECOSI-Hydrofizika, 2006, 342 pp.

[18] E.S. Trepova and A.G. Goryaeva, “Bioluminescent method for determination of polymer materials infection. Complex checking of the book-storages”, *Methodical manual*, Composed by T.D. Velikova, Eds. E.G. Vershinina, Sankt-Peterburg, pp. 147-153, 2013.

[19] E.S. Trepova and T.D. Velikova, “Express-method for determination of the documents degree of being invaded. Complex checking of the book-storages”, *Methodic manual*, Composed by T.D. Velikova, Eds. E.G. Vershinina, Sankt-Petersburg, pp. 142-146, 2013.

[20] Y.D. Tsviatkova, D.I. Voropaeva, and O.V. Povorova, “Cultivation and study of morphological and biochemical features of the luminescent bacterias”, *International Research Journal*, *Biological Scienses*, vol. 5-1 (12), pp. 54-56, 2013.

[21] Wenli Chen, Da Xing, Weigui Chen, and Yingliang Li, “View Author Affiliations Changes of delayed luminescence spectra in rice of different polluted degree by *Aspergillus flavus*”, *Chinese Optics Letters*, vol. 3, Issue S1, pp. S188-S190, 2005.

[22] Luminescent analysis of the food products http://biobloc.ru/lyuminescentnyy_analiz__pischevyh_p

[23] Optical methods of researches. Electronic document. http://veterinary.academic.ru/3473

SELF-PURIFICATION OF SEA COASTAL WATER AREAS UNDER CLIMATIC AND ANTHROPOGENIC CHANGE

Irina Mesenzeva, Sevastopol Branch of N.N. Zubov State Oceanographic Institute, Russia
Elena Sovga, Marine Hydrophysical Institute RAS, Russia
Tatyana Khmara, Marine Hydrophysical Institute RAS, Russia
Marina Tsyganova, Marine Hydrophysical Institute RAS, Russia

m.tsyganova@mhi.ras.ru

The ability of a bay and gulf ecosystems to self-purification was estimated and the current ecological state of the Sevastopol Bay in whole and the separated parts of the bay was given as an example. A zoning by type of anthropogenic impact subject to the water exchange with the open sea and an influence of the Chernaya River run-off were taken into account. A comparative analysis of assimilation capacity of the most environmentally disadvantaged part of the Sevastopol Bay (the Southern Bay) and the clean water area, bordering on the open sea, was carried out. The hydrodynamic regime of the Sevastopol Bay was described using numerical modelling. The prospect, opportunity and examples of the methodology for assessing the assimilation capacity of marine ecosystems are demonstrated.

Key words: ecosystem, the Sevastopol Bay, inorganic nitrogen forms, assimilation capacity, hydrodynamic regime.

I. INTRODUCTION

The threat to environment safety of the shallow water areas with high anthropogenic impact and limited water exchange comes not only from the high concentration of pollutants but also the formation of spots of “chronic” pollution. Different pollutants have negative effect on the sea ecosystem state that causes the need to improve the situation.

The Sevastopol Bay is one of the areas with high anthropogenic loading. This bay is the semi-enclosed estuary with limited water exchange. It is exposed to the constant anthropogenic impact because it is active shipping and water engineering area and also the Russian Navy placement with the industrial and economical infrastructure. A river runoff (the Chernaya River flows into the eastern part of the bay) and terrigenous runoff have a great impact on the hydrochemical water structure. Also municipal waste water and stormwater runoff negatively affect on the bay because with them an addition amount of biogenic elements get into the bay water.

Current ecological state of the Sevastopol Bay is considered as critical and it requires research-based approach to normalize. The calculation of assimilation capacity towards the specific contaminant is one way to analyze the sea ecosystem capacity to self-purification. The methodology implemented for the Sevastopol Bay conditions will allow regulating routine discharges of pollutants into the bay water on the scientific basis depending on the ecological state and hydrodynamic characteristics.

The aim of this paper is to compare the assimilation capacity of the most polluted Sevastopol Bay part (the Southern Bay) and the clearest part of bay which borders on open sea. On calculation a long-term monitoring of ecological state of the Sevastopol Bay waters was used and the hydrodynamic regime was taken into account. The methodology of the assimilation capacity calculation in the other shallow water areas of the Black Sea is demonstrated.

II. MATERIALS AND METHODS

This research is based on the long-term monitoring carried out by the Marine Hydrophysical Institute (MHI) in the Sevastopol Bay on 36 stations for 1998 – 2012 (a network of stations on Fig.1). The MHI bank of oceanographic data (BOD) contains such hydro-chemical parameters as dissolved oxygen, salinity, phosphates, inorganic nitrogen (nitrates, nitrites, ammonium) and silicon.

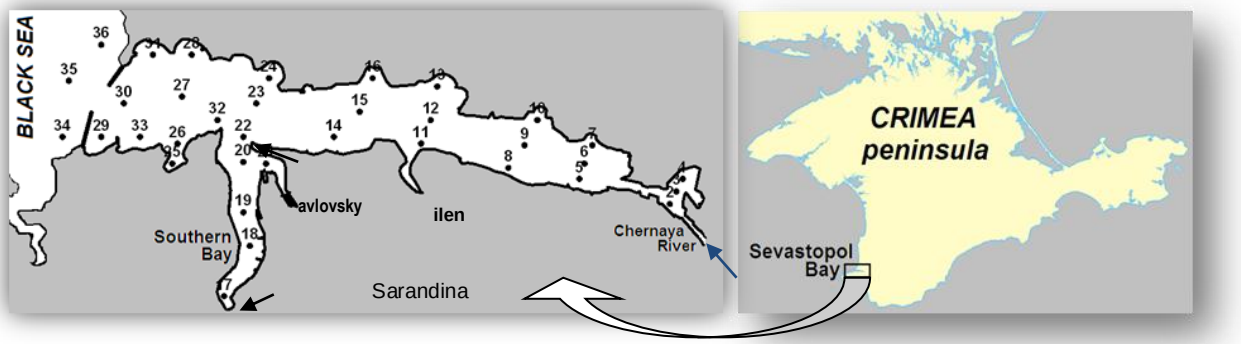

Fig.1. A network of stations for monitoring in the Sevastopol Bay.

The bay zoning were used as a scientific justification for the choice of the most and less polluted areas in the Sevastopol Bay by the anthropogenic impact [1] and by the peculiarities of morphological structure [2]. The bay is divided on four areas: of low, of moderate, of strong and of very strong pollution. Interesting fact is that the dedicated areas coincide with the bay zoning according the morphological parameters [2]: zone 1 is of low pollution; zone 5 (with the area of oil harbor) is of moderate pollution; zones 3 and 4 are of strong pollution; zone 2 (the Southern bay) is of high level of contamination.

To carry out the effective actions of improvement of ecological bay water state it is important to evaluate the dynamic in this area using modeling, to estimate quantitatively and to forecast the different external influences on the ecosystem. The main model component should be the hydrodynamic model which describes the circulation dynamic in the region.

The hydrodynamics in the bay was calculated using the unsteady 3D version of hydro-thermodynamic model MECCA (Model for Estuarine and Coastal Circulation Assessment) [3]. The environment bay was approximated to the horizontal grid 47 × 97 nodes with pitch at 80 m to which the model was adapted. The six levels were calculated in depth in σ-coordinate system.

The assimilation capacity method was used to evaluate sea water self-purification. The assimilation capacity is ability the sea ecosystem to sustain the addition of some pollutants without the development of irreversible biological consequences [4]. The assimilation capacity has a dimension of a flow of matter, namely, a mass of matter in a volume unit per a time unit.

The problem of the assimilation capacity estimation has two aspects. The first one is that is difficult to determine the cause-and-effect relationships between the pollution and biological impact. The second one is connected with the difficulties of the forward and reverse transition from the unit of flow (how the assimilation capacity is measured) and the unit of mass how the environment pollution is measured.

To overcome difficulty of the first aspect the weakest link in ecosystem should be found. On that basis the threshold of vulnerability of the whole ecosystem is determined [5]. To overcome difficulty of the second aspect the balance method is used [4]. But it is not always possible to use this method because the observing over the sea pollution is not constant and the intervals between the observing are longer than the time of the inner environmental remediation of object under study.

This balance method was successfully used for the evaluation of assimilation capacity in the port of Odessa and the port of Nikolayev in relation to oil and phenol [6, 7], as well as in the Dnieper estuary ecosystem subject to zoning of water areas according to the anthropogenic loading [8].

In case of lack of long-term monitoring to evaluate the assimilation capacity of sea waters it is possible to use "synoptic" method [9]. Long and repeated observations are not needed for the application of this method. We need only data of one oceanographic survey. This method is based on the assumption of the survey results that the inhomogeneous distribution of pollutants in homogeneous water mass according to the physical parameter is the result of self-purification in water. The last storm is the reference point of this process (that is why this method called "synoptic").

This method is based on the analyses of the inhomogeneous distribution of pollutants in hydrologically homogeneous water. The point T,S-charts were made according the results of each survey. The water mass is shown on these charts as a "cloud" of points. Each point means the water sample under chemical analysis (a data of temperature, water salinity in bottom and surface layers is needed for plotting these charts).

The assimilation capacity of the Sevastopol Bay was evaluated by the balance method [4]. This method was used both for the zone of very strong pollution (the Southern Bay) and more clear part near the open sea (further – zone 1 following [2]). To evaluate the assimilation capacity it is most difficult to calculate the integral time of being the pollutants in the ecosystem under study. It depends on physicochemical properties of a particular pollutant, the water hydrodynamics and the complex of processes (physical, chemical, microbiological ones) that promote the destruction of pollutants and its spread out of the researching water area.

The final formula for the evaluation of mean $\overline{A}_{mi}$ and mean square deviation $\sqrt{D[A_{mi}]}$ of the assimilation capacity of sea ecosystem (*m*) against *i*-pollutant is following:

$$AE_{mi} = \overline{A}_{mi} \pm \sqrt{D[A_{mi}]},$$

$$\overline{A}_{mi} = \frac{Q_m \cdot C_{thr\,i}}{C_{\max i}} \cdot \overline{v}_i, \qquad D[A_{mi}] = \left(\frac{Q_m \cdot C_{thr\,i}}{C_{\max i}} \right)^2 \cdot D[v_i],$$

where Q_m is a volume of water in the calculated domain; $C_{thr\ i}$ is a threshold limit of pollutants; $C_{max\ i}$ is a maximum pollutant concentration in ecosystem; v_i is a rate of pollutant elimination from the ecosystem; a mean value $\bar{v}_i$ and a dispersion $D[v_i]$ of the rate is defined by the original algorithm [10].

The data set about three forms of nitrogen was used for the evaluation of assimilation capacity of the Southern Bay. This data is obtained from 1998 to 2012. It composes 714 definitions for the Southern Bay and 1117 definitions for the zone 1.

III. Results and discussion

Modeling of hydrodynamics in the Sevastopol Bay and the Southern Bay.

It is insufficient to pay attention the bay water dynamics despite the fact that exactly the flows have an influence on the exchange with the open sea and determine the ecological situation in the water area. The different aspects of the bay water dynamics were fully researched using mathematical modeling [11]. *In situ* measurements of currents are less presented in literature [12].

Special dynamic conditions were in the zone 1 (sea depth is 19 m). The two-layer multidirectional flows are seen here. The western flows prevail in upper 10 m layer. These are the runoff flows caused by the Chernaya River. In summer the depth of layer covered with the western flows is reduced and increases to 12 m or 13 m in spring or after the rains. The eastern flows prevail in the layer deeper than 13 m. The average current is higher in this layer than in the upper. The midstream is in the depth of 15 to 16 m. Only in two cases there are one-layer flows in the all depth [13]:

a) The first case happens in spring and after continuous pouring rains (about 4 days). These increases runoff flows. In this case we see the western flows in the whole 19 m layer.

b) One-layer flow is also in the second case. But it has another direction (into the bay). The observations were made in early summer after strong offshore winds (up to 14 or 16 m/s).

The modeling of pollutants spreading in the Southern bay is showed [14] that the pollutants will be accumulated in water by typical water volume of rain runoff and sewage at the north winds. This worsens water quality. The pollutants are carried by wind currents of other directions outside the Southern bay. The relatively fast purification of the Southern bay occurs on condition of sewage stopping.

The patterns of current are shown on Fig.2 which was obtained using model MECCA [3]. As initial conditions *in situ* data for July 2002 was chosen. As a boundary conditions we have used data on weather conditions (air temperature, wind current and direction, precipitation, etc.), the surface water temperature and sea level, measuring on the hydrometeorological station "Sevastopol", located in the center of the bay on the Pavlovsky Cape, and an average discharge of the Chernay River (flow rate 1.2 m^3/sec, flow rate of 0.2 m/sec).

The patterns of surface current is given on Fig.2, *a* and of bottom current – on Fig.2, *b* from 8 to 12 July, when the wind direction was suddenly changed, even during the day. Fig.2, *c* shows the actual wind at 6-hours discreteness at 8 – 12 July.

The current changes cardinally after the wind direction changing. In zone 1 the water exchange is quite intensive due to close location with the open sea. Under certain wind conditions the flow current is 40 – 60 cm/sec in the input channel; and 15 – 20 cm/sec in the bottom layer. A 2

– 3-layer structure of flow of different directions is observed in the strait.

The Southern Bay is comparative shallow water area; therefore currents are determined mainly by wind. The south wind contributes the water exchange from the Southern bay to the Sevastopol Bay. The flow current is lower than in the Sevastopol Bay. The wind currents can be observed under wind condition 5 – 10 m/sec and more. In the bottom layer the flow is directed to south in the inner bay.

The assimilation capacity of the Southern bay ecosystem and the Bay ecosystem adjoin the open sea towards the inorganic nitrogen, based on long-term monitoring of ecological state.

The southern part of the Sevastopol Bay which includes the Southern Bay and the Kilen Bay is characterized by difficult water exchange with the main water area. The Southern Bay is the most polluted bay among the others because of difficult water exchange with the main waters; the location of numerous ship moorages; the volume of industrial, household and storm water. The freshened areas are typical for the inner Southern Bay but the intensity of spreading water is not constant throughout the year. The south-west coast of Sevastopol Bay adjoins the developed net of faults in the Chernaya River basin and the Sarandinaki beam where the underground runoff is drained from large areas with significant reserves of groundwater. Great among of runoff water gets into the Southern Bay as a result of the submarine unloading. This is registered by decreasing of salinity and increasing of silicon.

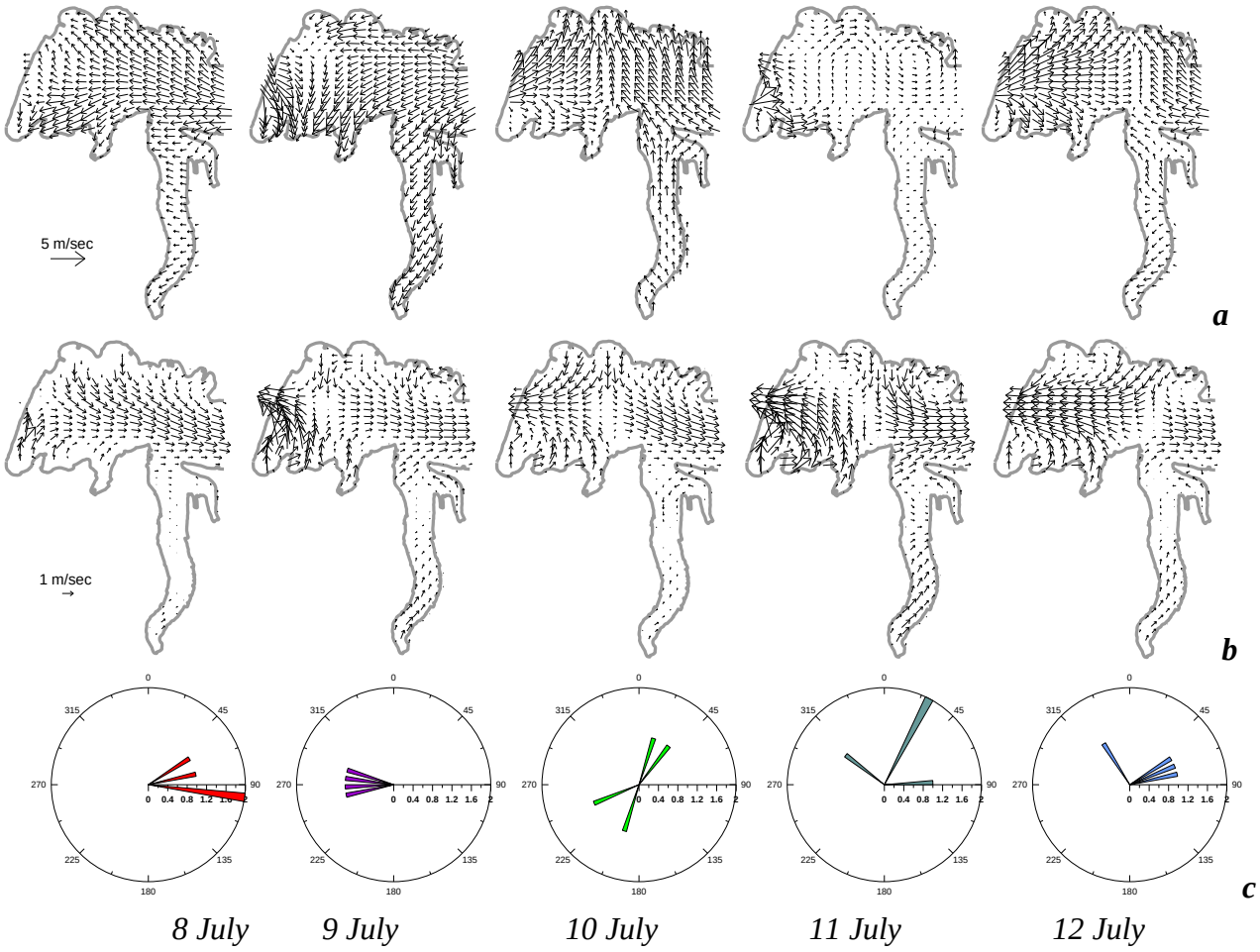

Fig. 2. The patterns of the surface (a) and bottom (b) currents in real winds (c) in the west part of

the Sevastopol Bay from 8 to 12 July 2002.

In the surface layer the water (especially in the inner part) is characterized by the maximum concentrations of nitrogen. At the same time on nitrates the 20-fold increase over the average values is seen in the Sevastopol Bay [14]. The untreated sewage, storm runoff gets into the Southern Bay according to the information given in [14]. Also floats are located here.

The self-purification capacity towards inorganic nitrogen (nitrites, nitrates and ammonia nitrogen) as a priority pollutant in municipal wastewater and storm water was evaluated for the Southern Bay and a part of the Sevastopol Bay adjoin the open sea. Also the inorganic forms of nitrogen are involved in the productive and destructive processes in the marine ecosystem.

The mean inorganic nitrogen for observing period did not exceed the corresponding maximum permissible concentration (MAC) which was used as threshold. The calculated specific (per 1 liter) values of the assimilation capacity for each form of inorganic nitrogen differ from the corresponding MAC (Table). This makes possible to estimate the limit of each ecosystem to self-purification capacity.

Comparative values of the assimilation capacity for the Southern Bay ecosystem and the water area adjoin the open sea (zone 1) for inorganic nitrogen are given in Table. For calculation of the assimilation capacity the morphometric parameters of areas under study were used from [2].

For the Southern Bay the maximum specific rate of pollutant elimination from the ecosystem reached 0.03 μM/l day for nitrites; 2.10 μM/l day for nitrates and 0.32 μM/l day for ammonium nitrogen that exceeds the average rate of elimination in 3 – 4 times. For zone 1 the maximum specific rates of elimination were 0.066 μM/l day for nitrites, 1.28 μM/l day for nitrates and 0.94 μM/l day for ammonium. For more clear water area the average rate of elimination were from 4.5 to 5.5.

Table. The assimilation capacity of the Southern Bay ecosystem and the ecosystem of the Sevastopol Bays adjoin the open sea (zone 1) for inorganic nitrogen.

Parameter, units	NO_2		NO_3		NH_4	
	Southern Bay	zone 1	Southern Bay	zone 1	Southern Bay	zone 1
Number of measurements	240	373	225	351	249	393
Threshold value of concentration, μM/l	1,43		221,43		20,71	
Average concentration, μM/l	0,23	0,12	12,59	2,45	0,95	0,57
Max concentration, μM/l	1,48	0,42	142,79	13,31	8,17	8,18
Average rate of elimination, μM/l day	0,008	0,012	0,49	0,28	0,10	0,21

Specific assimilation capacity, μM/l year	1,77	15,57	212	1863	48	197
Volume of Southern Bay, m^3	10253990					
Volume of zone 1, m^3	33825650					
Assimilation capacity, t/year	**0,25**	**7,4**	**30**	**880**	**7**	**93**

The Southern Bay is characterized by high values of maximum concentrations with respect to zone 1 (Table). The nitrates and nitrites concentration exceeds in 10 times and 3 times, respectively and the ammonium concentration is in the same range for these two zones.

According to the above mentioned estimations of the Southern Bay ecosystem capacity to the self-purification amount of inorganic nitrogen must not exceed 0.25 ton for nitrites, 30 ton for nitrates and 7 ton for ammonium nitrogen. Note, the quantitative limit of inorganic nitrogen conforms uniform discharge of pollution. In case of the emergency discharge to estimate the ecosystem self-purification capacity, we should consider the specific value of assimilation capacity for nitrites, nitrates, ammonium 0.0048, 0.58, 0.13 μM/l day respectively. Because we do not have exact information about total volume of inorganic nitrogen which get in the Southern Bay by municipal and storm water than it is impossible to estimate how many times this level is exceeded now. In zone 1, the threshold value is 7.4 ton for nitrites, 880 ton for nitrates and 93 ton for ammonium nitrogen. Note, differences take place with respect to overestimation of average rate of elimination which were lower in the Southern Bay (3,5 – 4 times) than in zone 1 (4,5 – 5,5 times). Probably this is connected with the dominance of biological processes in clear zones (recirculation of inorganic nitrogen) over anthropogenic impacts. However, the problem demands additional study.

IV. CONCLUSIONS

The Sevastopol Bay ecological state, which is depended on economical activity and anthropogenic impacts, is analyzed using multi-year *in situ* study.

The possibilities of the previously developed method for the assimilation capacity calculation to normalize of pollutant discharges were estimated for marine ecosystem. Firstly the comparative estimations of the assimilation capacity in the Southern Bay as the most polluted part of the Sevastopol Bay and the bay area adjoin the open sea as more clear to inorganic nitrogen forms (as main pollutants in municipal and storm water runoffs) were obtained. We showed that at the balanced discharge amount of inorganic nitrogen pouring in the Southern Bay during a year should not exceed 0.25 ton for nitrites, 30 ton for nitrates and 7 ton for ammonium nitrogen. In zone adjoin the open sea at above mentioned wind conditions the self-purification has higher value such as 7.4 ton per year for nitrites, 880 ton per year for nitrates 93 ton per year for ammonium nitrogen

We showed that the self-purification capacity of the Southern Bay ecosystem depends mainly on the anthropogenic impact level while for the ecosystem adjoin the open sea (zone 1) this capacity depends on both anthropogenic impact and biological productively-destructive processes which are connected with recirculation of inorganic nitrogen.

Considering the mentioned quantitative limits in which all the recycling processes considered

a standardization of discharges will make a contribution to the improvement of ecological situation both in the Southern Bay and area adjoin open sea. As a result it decreases the load on the Sevastopol Bay as a whole.

V. References

[1] V.A.Ivanov, E.I.Ovsianyi, L.N.Repetin, A.S.Romanov, and O.G.Ignateva, *Hydrological-hydrochemical impact of Sevastopol Bay and its changes caused by climate and anthropogenic influences*, 2006, 90 p. (in Russian)

[2] N.A.Stokozov, "The morphometric characteristics of Sevastopol and Balaklavskaya bays," *Ecological safety of coastal and shelf zones and complex usage of shelf resources*, vol. 23, pp.198-208, 2010. (in Russian)

[3] V.A.Ivanov, and Yu.S.Tuchkovenko, *Applied mathematical water-quality modeling of shelf marine ecosystems*, 2008, 311 p.

[4] I.A.Israel, and A.V.Tsyban, *The anthropogenic ecology of ocean*, Hydrometeoizdat, 1989, 528 p. (in Russian)

[5] S.K.Monakhov, A.A.Kurapov, and N.V.Popova, "The estimation of assimilation capacity of a water area and ecological regulation of pollutant discharge at the sea", *Vestnik DSC RAS*, vol.20, pp.58-65, 2005. (in Russian)

[6] I.V.Mezentseva, E.E.Sovga, and S.P.Lyubartseva, "Estimation of capability of Odessa port ecosystem for self-purification capacity in relation to oil products and phenols," *Ecological safety of coastal and shelf zones and complex usage of shelf resources*, vol.22. pp. 303-309, 2010. (in Russian)

[7] I.V.Mezentseva, "Complex characteristic of water quality of Nikolaev marine commercial port at 2008 – 2012," *Ecological safety of coastal and shelf zones and complex usage of shelf resources*, vol.28, pp.220-224, 2014. (in Russian)

[8] E.E.Sovga, I.V. Mezentseva, and S.P. Liubartceva, "Assimilation capacity of the Dnieper estuary ecosystem in relation to oil products as method of discharge regulation in the estuary," *Report of NAS of Ukraine*, vol.10, pp.105-109, 2011. (in Russian)

[9] G.A.Monakhova, G.M.Abdurakhmanov, and G.A.Akhmedova, et al. "Estimation of assimilation capacity of licensed water area "North-Caspian area" in relation to hydrocarbons using "synoptical" method," *Geography and geoecology of the south of Russia*, vol.4. pp. 207-212, 2011. (in Russian)

[10] E.Sovga, I.Mezentseva, L.Verzhevskaia, *Assimilation Capacity of the Ecosystem of Sevastopol Bay //* Proceedings of the Twelfth International Conference on the Mediterranean Coastal Environment MEDCOAST' 2015, 6-10 October 2015. Varna, Bulgaria, 2015. (Ed. E.Ozhan). vol. 1. pp.317-326.

[11] N.B.Shapiro, and S.A.Yushchenko, "Modelling of wind currents in Sevastopol Bays," *Marine Hydrophysical Journal*, vol. 1, pp.42-56, 1999. (in Russian)

[12] E.M.Lemeshko, A.N.Morozov, S.A.Shutov, V.V.Zima, and A.A.Chepyzhenko, "Currents in Sevastopol Bay according to ADCP-data, November 2014," *Ecological safety of coastal and shelf zones and complex usage of shelf resources,* vol. 28, pp. 25-30, 2014. (in Russian)

[13] M.S.Nemirovsky, and I.Y.Eremin, “Water dynamics of the Sevastopol roads,” *Ecological safety of coastal and shelf zones and complex usage of shelf resources*, vol. 9, pp. 59-66, 2003. (in Russian)

V.A.Ivanov, I.V.Mezentseva, E.E.Sovga, K.A.Slepchuk, and T.V.Khmara, “Estimations of self-purification capacity of the Sevastopol Bay ecosystem in relation to inorganic nitrogen,” *Processes in GeoMedia*, v.2. pp. 55-65, 2015. (in Russian)

CLIMATIC REGIME CHANGE IN THE ASIAN PACIFIC REGION, INDIAN AND SOUTHERN OCEANS AT THE END OF THE 20TH CENTURY

Vladimir Ponomarev, V.I. Il'ichev Pacific Oceanological Institute, FEB RAS, Russia
Elena Dmitrieva, V.I. Il'ichev Pacific Oceanological Institute, FEB RAS, Russia
Svetlana Shkorba, V.I. Il'ichev Pacific Oceanological Institute, FEB RAS, Russia
Irina Mashkina, V.I. Il'ichev Pacific Oceanological Institute, FEB RAS, Russia
Alexander Karnaukhov, V.I. Il'ichev Pacific Oceanological Institute, FEB RAS, Russia

pvi711@yandex.ru

Multiple scale climate variability in Asia of temperate and high latitudes, Pacific, Indian and South Oceans, their features and linkages are studied by using statistical analyses of monthly mean time series of Hadley, Reynolds SST, surface net heat flux (Q), atmospheric pressure (SLP), air temperature (SAT) from NCEP NCAR reanalyses (1948-2015). Three multidecadal climatic regimes were revealed for the whole area studied by using cluster analyses via Principal Components of differences between values of Q, SLP, SAT in tropical and extratropical regions of the Asian Pacific, Indian and Southern Oceans. The climate regime change in 70s of the 20th century in this area is confirmed by this method. It is also found that the climate regime is significantly changed at the end of the 20th century in both same area and World Ocean. The characteristic features of recent climate regime after 1996-1998 are SLP increase in the central extratropic area of Indian Ocean, North and South Pacific being prevailing in boreal winter. It is accompanying SLP increase and precipitation decrease in South Siberia and Mongolia prevailing in boreal summer. Inversed SLP and precipitation anomaly associated with increase of cyclone activity and extreme events in the land-ocean marginal zones including Southern Ocean, eastern Arctic, eastern Indian, western and eastern Pacific margins. It is known that low frequency PDO phase is also changed at the same time.

Key words: climatic, anomaly, regime, change, Pacific, Indian, Arctic, Southern, ocean, marginal seas, Asia, Mongolia, China, Siberia, Russian Far East, coastal zone, river basins, sea level pressure, surface, sea, air, temperature, heat fluxes, precipitable water content, precipitation, extreme events, flood, drop, level of lake, Lake Baikal, Lake Khanka

I. INTRODUCTION

The multidecadal oscillation of period 65-70 years was determined as a typical phenomenon in the global climate system [1]. Features of similar scale oscillations with period 50-60, 50-70 years were revealed in various meteorological and oceanographic characteristics in the North Pacific [2, 3, 4], Arctic [4, 5, 6, 7, 8] and Atlantic Oceans [8, 9]. Cause and possible mechanism [1 - 4, 5 - 7] of this oscillation suggested by various authors are quite different and not yet proven. Well expressed

transitional periods between the positive and negative phases of the multidecadal or interdecadal oscillation are usually characterized by very rapid change in parameters of the ocean-atmosphere system [1]. The transition period named as climate regime shift in late 70s of the 20th century was clear shown in both North Pacific [10] and North Atlantic [11] in many studies.

The recent climate regime shift in late 90s - 2000 is also shown in the state of North Atlantic [11], North Pacific [12, 13, 14]. In the North Atlantic it is shown in terms of phase trajectory of Sea Level Pressure (SLP), Sea Surface Temperature (SST) differences between its values in the Azores High area and Icelandic Low region [11]. Similar recent shift in the state North Pacific from 1996 to 1999 [12] is determined in terms of phase trajectory of the first two principal components (PC) of SST anomalies in the North Pacific The PC2 rapidly rises from negative value -1 in 1996 to 0,2 in 1998 and 0.9 in 1999. During four years 1999 - 2012 PC2 was in a stable positive phase with unusually high values 1.4 - 1.5. It is also manifested that physical devises of the transitions of the winters 1988, 1989 and 1976, 1977 are different and related to impact of anomalies in Arctic and tropical regions correspondently [13]. In this case a phase of different scale oscillations decadal and multidecadal was changed.

The climate regime change in late 90s in the Asia, Indian, North and South Pacific Oceans is also determined in terms of phase trajectory of Sea Level Pressure (SLP) and surface net heat flux (Q) differences between its values in selected large-scale areas of the Asia of temperate latitudes, Pacific and Indian Oceans [15]. The recent changes in the SLP and ocean-atmosphere interaction are associated with the increase in the frequency of occurrence of extreme events, severe storms, floods in some areas and droughts in others observed in the world in the first 15 years of the 21 century including extremes in 2014, 2015. In Russia the extremely low total rivers discharge in the Lake Baikal Basin and extremely low the lake water level are observed in summer and fall 2015 despite of some adjustment of the lake level change using dams of hydropower plants reservoirs on the Angara River. At the same time, an inverse extreme anomaly is observed in the Lake Khanka situated in the south of Russian Far-East (Primorskii Krai). The flood of the Lake Khanka has reached catastrophic level in the fall of 2015 that has led to destruction of the shores of the lake, buildings and the entire coastal infrastructure, as well as flooding of agricultural grounds. The problem is that the Lake Khanka is a transboundary lake. The border between Russia and China, crossing the lake near the sand spit that divides the lake into Small Lake Khanka (China) and a Big Lake Khanka. The main goals of our study are to identify the various features of the recent climate regime change in SLP, Q, precipitation (Pr), Precipitable Water Content in the atmosphere (PWC, kg/m2) over the continent, ocean, and their marginal zone using observation data from various data sets and different statistical methods, including cluster analyses via PCA. Objectives of our work are also to define scenarios of significant anomalies and extreme events in precipitations in South of Siberia, Mongolia, Lake Baikal Basin, as well as in the subarctic coastal area of the Japan (East) Sea, South of Russian Far East and Khanka Lake Basin in the Primorskii Region.

II. DATA AND METHODS

We use observation data from different from various sources, particularly gridded monthly mean time series of Hadley Sea Surface Temperature (SST) from 1870 to 2015, Reynolds SST, Sea Level atmospheric Pressure (SLP), air temperature (SAT), surface net heat flux (Q), precipitation

(Pr), Precipitable Water Content (PWC, kg/m2) in the atmosphere from NCEP NCAR meteorological reanalyses, particularly monthly mean gridded (2.5° x 2.5°) from 1948 to 2015, as well as monthly mean time series of precipitation, SAT at the meteorological stations and correspondent gridded time series (1° x 1°) over land from 1900 to 2015.

In our paper the positive value of the vector Q corresponds to the heat flux directed from an ocean surface to the ocean under-surface layer, while the negative one corresponds to the heat flux directed from an ocean surface to the atmosphere. The characteristic features of the climate regime change in late 90s of the 20th century are estimated using anomalies of monthly, seasonal and annual mean SLP, Q, Pr, PWC, SAT, SST in the Pacific, Indian and Southern Oceans, as well as SLP, Q, Pr, PWC, SAT in Asia of temperate latitudes. Various methods of the observation data processing are applied including correlation analyses, Principal Component Analyses (PCA) and cluster analysis via PCA.

III. RECENT CLIMATIC REGIME CHANGE

Based on the cluster analyses of the SLP, Q, SST anomalies via PCA, as well as correlation analyses between winter anomalies in Lake Baikal Basin, Okhotsk, Japan Seas [16] and anomalies of Q, SST in the Pacific and Indian Oceans the major large scale regions were selected to analyze time series of SLP, Q, Pr, PWC, SAT, SST averaged within the regions. The square and positions of the regions are shown in Tabl.1 and Fig.1.

Table 1. Regions of Q, SLP, TWC, Precipitation averaging and their position and square (S, km²).

Regions	Lat.1	Lat.2	Lon.1E	Lon.2E	S (km²)
1.Asia of Moderate Lat. (AML)	40	60	70	130	9854109
2. Subarctic North Pacific (SNP)	40	60	160	226	10437686
3. Hawaii High (HH)	20	40	180	230	10653527
4. West Tropic Pacific (WTP)	10	-15	155	190	10722938
5. NINO 3-4	5	- 5	190	240	6174312
6. South Indian (SI)	-20	- 45	60	100	10345429

The climate regime change is estimated, at first, in terms of phase trajectory of certain characteristics in two selected regions. Fig. 2 shows climatic shift both in mid 70s and late 90s in phase trajectory of two net heat fluxes (Q, W/m2) time series of Q2 in Subarctic Pacific (in axes Y region 2 in Fig.1, Tabl.1) and Q6 in South Indian Ocean (in axes Y region 2 in Fig.1, Tabl.1) from 1948 to 2015 in boreal hydrological winter (JFM). It means that Q2 is in winter of the Northern Hemisphere, while, Q6 is in summer of the Southern Hemisphere. Vector of Q2 is directed from an ocean surface to the atmosphere and values of Q2 are negative in our paper, while the vector of Q6 is directed from an ocean surface to the ocean undersurface layer and values Q6 are positive. Two climate regime shifts, particularly after 1975 and after 1995 are clear seen in Fig. 1.

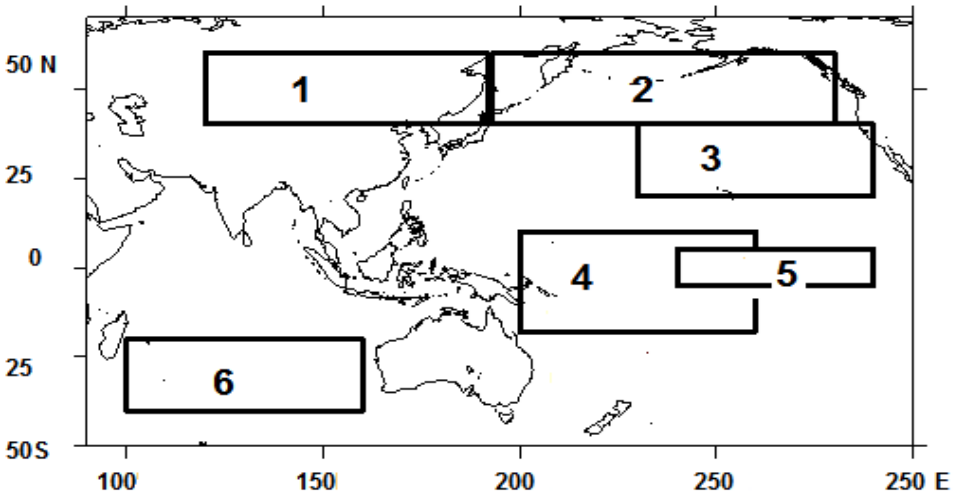

Fig.1. Arrangement of regions of Q, SLP, Pr, TWC averaging in the Asian Pacific Region and Indian Ocean : 1 – the zone of temperate latitudes of Asia; 2 – subarctic zone; 3 – Eastern subtropical zone; 4 – Western Equatorial zone; 5 – El Nino (NINO 3-4); 6 – South Indian Ocean

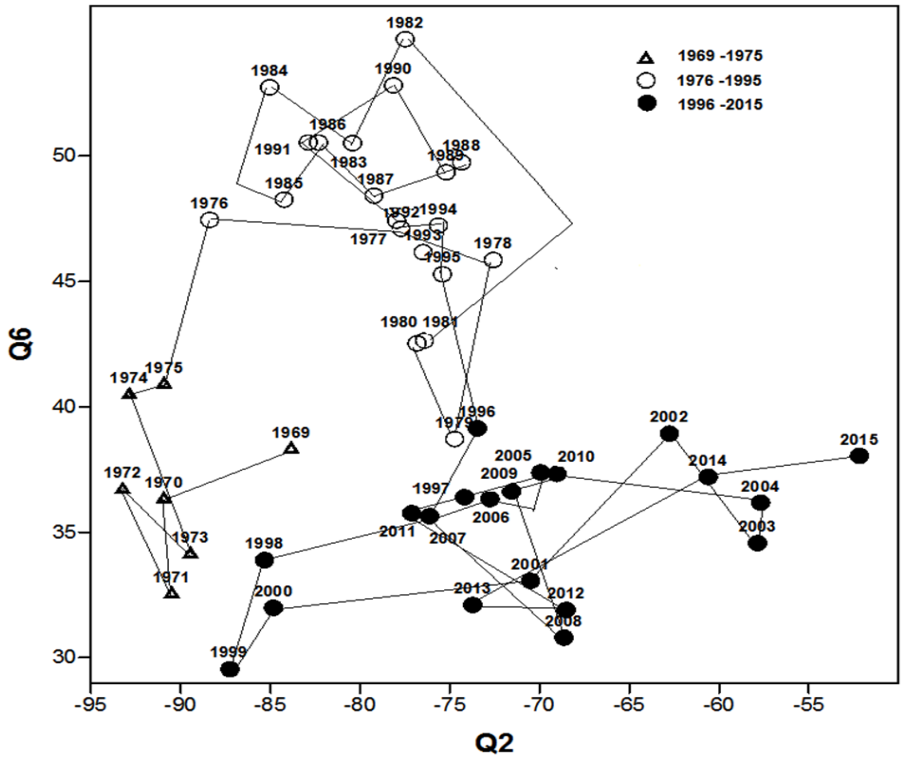

Fig. 2. Phase trajectory of the net heat fluxes (Q, W/m2) of 3-years running mean time series (1969 - 2015) averaged in Subarctic Pacific (Q2) and South Indian Ocean (Q6) in boreal winter (JFM). Regions 2 and 6 are shown in Fig. 1.

Similar two climate regime shifts in the phase trajectory of the net heat flux at the ocean surface in Subarctic Pacific and South Indian Ocean is also found in summer (JJA) time series of Q2 and Q6. The winter and summer time series of Q2 and Q6 are shown in Fig. 3, 4 correspondently.

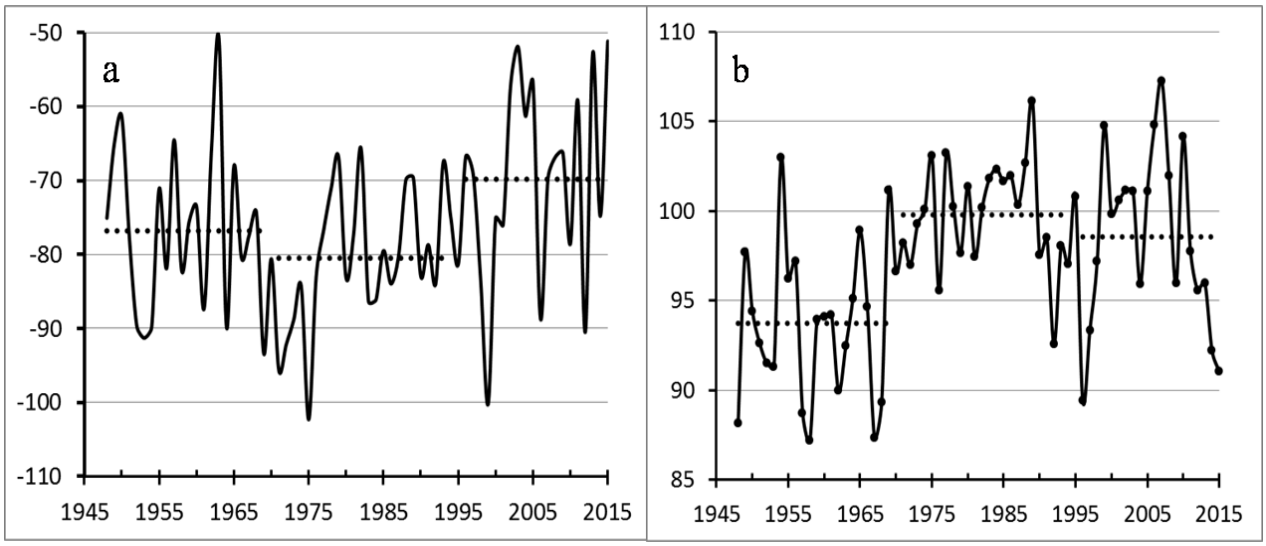

Fig. 3. Time series (1948 - 2015) of the net heat fluxes (Q, W/m2) averaged in Subarctic Pacific (Q2) in winter JFM (a) and summer JJA (b).

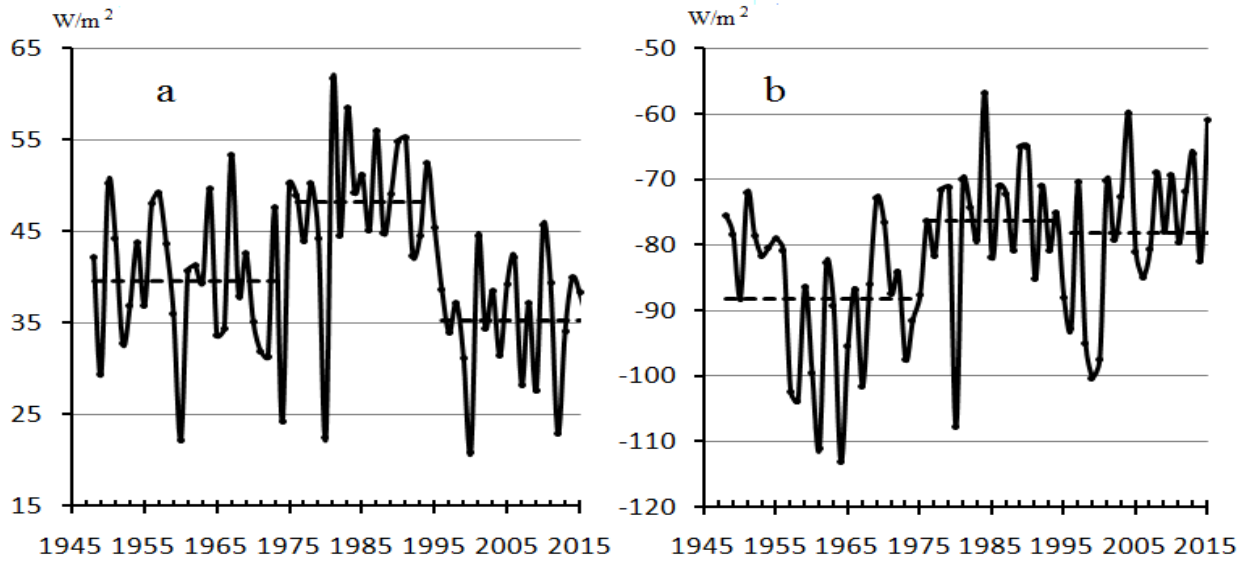

Fig. 4. Time series (1948 - 2015) of the net heat fluxes (Q, W/m2) averaged in South Indian Ocean (Q6) in boreal winter JFM (a) and boreal summer JJA (b).

Recent climate shift the net heat flux in 90s in both Subarctic Pacific (Q2) and South Indian Ocean (Q1) is most prevailed in boreal winter (Fig. 1a, Fig. 2a). Rapid reduction of Q directed to the ocean in South Indian (summer in Southern Hemisphere) accompany rapid reduction of Q directed from the ocean to the atmosphere in the Subarctic Pacific (Northern Hemisphere).

Two shifts of the climate regime both in mid 70s and late 90s are also revealed in terms of phase trajectory of PC1, PC2 of set included 18 time series of differences between values of both Q and SLP in boreal winter in all of 6 selected areas (Fig. 1).

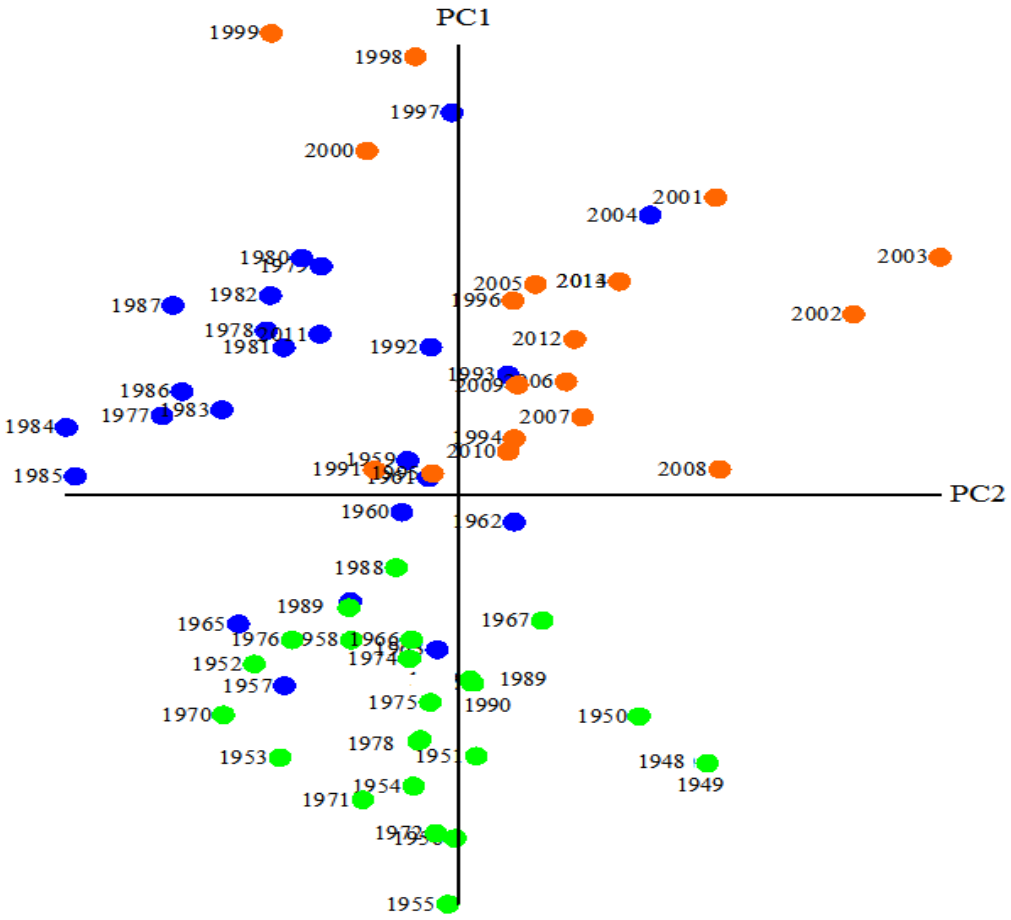

Fig. 5. Phase trajectory of 3-years running mean PC1 and PC2 of set, which includes 18 time series (1948 - 2015) of differences between the values of both Q and SLP in boreal winter averaged within all of 6 selected areas (Fig. 1). Three classes of the time series determined by cluster analyses are marked by color symbols.

Two climate regime shifts are also found in terms of phase trajectory of 3-years running mean annual SAT differences, particularly between regions T2-T4, T1-T2 (Fig.6), as well as in phase trajectory of PC1 and PC2 of set (Fig. 7), which includes 12 time series (1948 - 2015) of annual Q and TWC in all of 6 selected areas. Thus, the climate regime is significantly changed in the Asian Pacific region, Indian and Southern Ocean at the end of the 20th century in terms of Q, SLP, SST, SAT, TWC, Precipitation, and their horizontal gradients on the planetary scale. Recent climate regime in comparison with previous one is characterized by reduce of Q amplitude in annual cycle and meridional gradients of annual and seasonal Q. Absolute values of Q directed to the ocean in summer and to the atmosphere in winter are usually reduced after late 90s of the 20th century. It accompanies change in the ocean vertical structure, circulation and meridional heat transport.

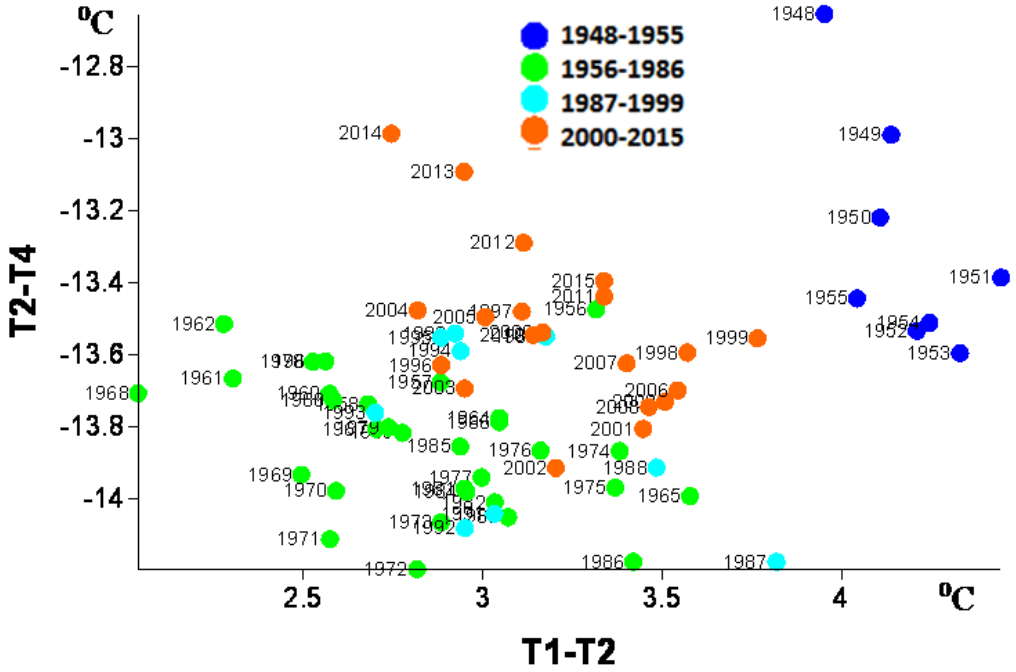

Fig. 6. Phase trajectory of 3-years running mean time series (1969 – 2015) of differences between annual SAT (T) in the regions: T1-T2, T2-T4 (C°).

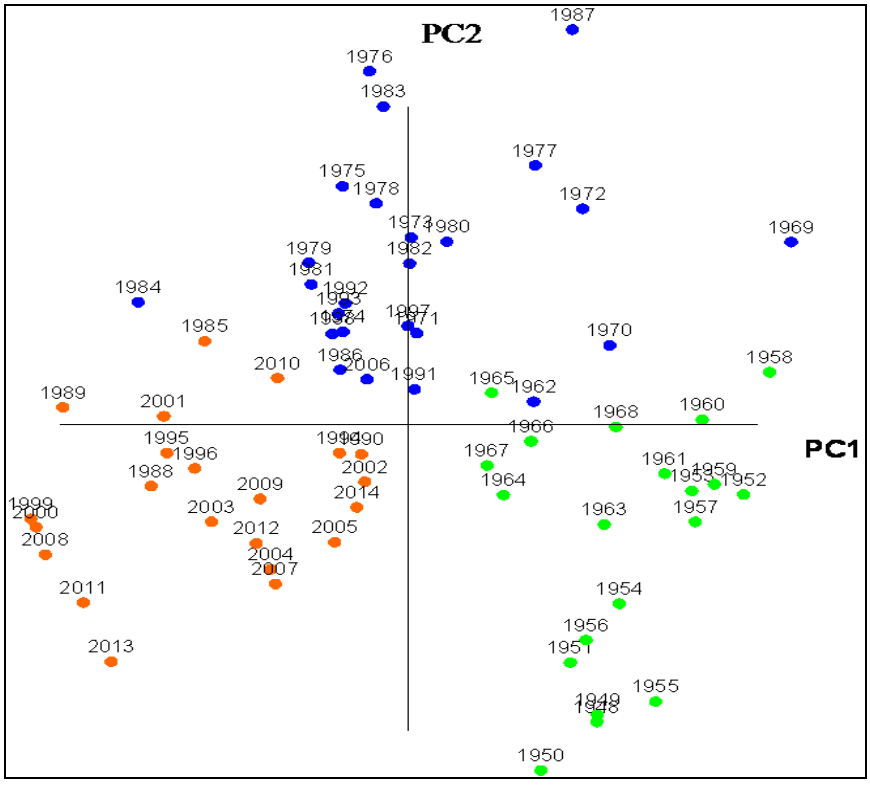

Fig. 7. Phase trajectory of 3-years running mean PC1 and PC2 of set, which includes 12 time series (1948 - 2015) of annual Q and TWC in all of 6 selected areas (Fig. 1). Three classes of the time series determined by cluster analyses are marked by color symbols.

Map of difference between mean SLP in recent climate regime in 1996 – 2015 and previous one 1975 - 1993 for winter and summer (Fig.8) show detailed structure of the climate change in SLP fields at the end of the 20th century.

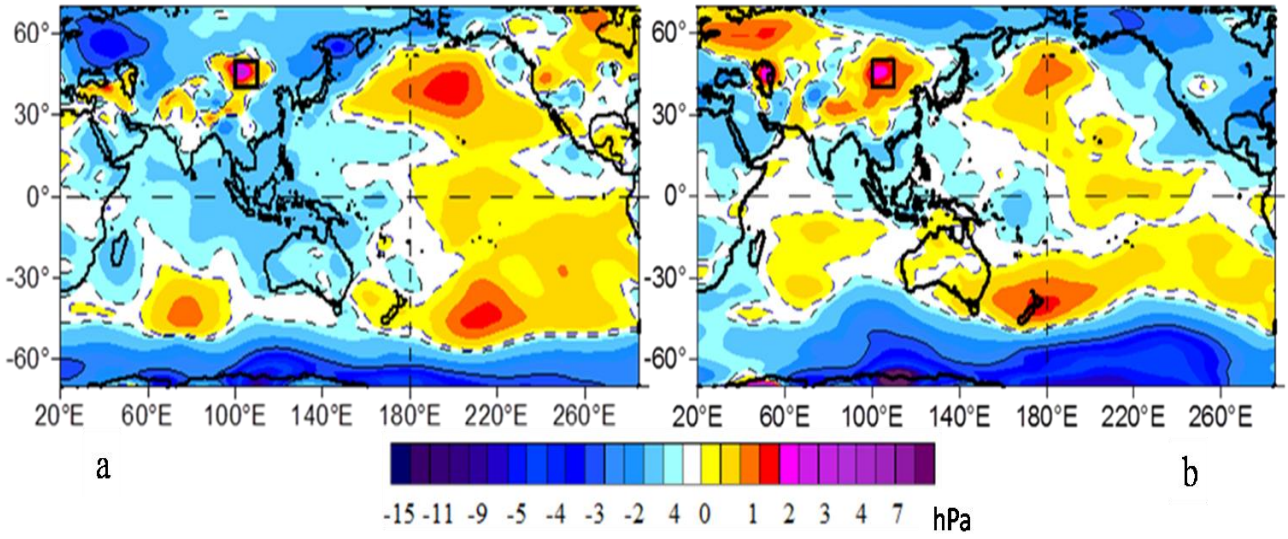

Fig. 8. Differences of SLP between its mean values within the recent climate regime 1996 – 2014 and previous one 1971-1991 in boreal winter (a) and boreal summer (b).

After the recent climate regime in late 90s the SLP increases mainly in central extratropics of both North and South Pacific, in South Indian Ocean, being maximal changed in winter. The SLP also increases in central continental Asia of temperate latitudes, particularly in Mongolia and South Siberia, Baikal Lake Basin, where maximal large scale SLP change in typical for summer. The SLP decrease and intensification of cyclonic activity occur in the marginal areas of the North and South Pacific, Indian, Southern and Arctic oceans including their marginal seas. Total water content in the atmosphere and precipitation significantly increase in this zone. Surface air temperature in most of marginal areas rises in fall and winter while decrease in spring and early summer. Repeatability of number of strong storms has increased in the Western Pacific and its marginal Seas, Western and Eastern Atlantic Ocean.

IV. SUMMER ANOMALIES IN THE RUSSIAN FAR-EAST AND SOUTH SIBERIA

The anomalies in the ocean accompany the SPL increase in Mongolia and Baikal Lake region all the year round. In summer the SLP increases in Europe and most of the East Asia with maximal anomaly in Mongolia and Lake Baikal water basin. It corresponds to summer warming and decrease of precipitation in this area in recent climate regime. High negative anomaly of precipitation in most of South Siberia and Mongolia regions, low Selenga River and other rivers discharge accompany extremely low level of the Lake Baikal in summer 2015. The extremely low total water inflow to the Baikal Lake can be also effected by anthropogenic forcing related to the increased human activity in Selenga River and Baikal Basins. Map of anomalies in summer mean 2015 precipitation (mm/mon) in Irkutsk region of Russia, catchment areas of Lake Baikal and

Irkutsk and Bratsk water reservoirs of hydroelectric power stations, as well as time series of precipitation sum (mm/mon) in hydrological spring (AMJ) and summer are shown in Fig. 9 and 10.

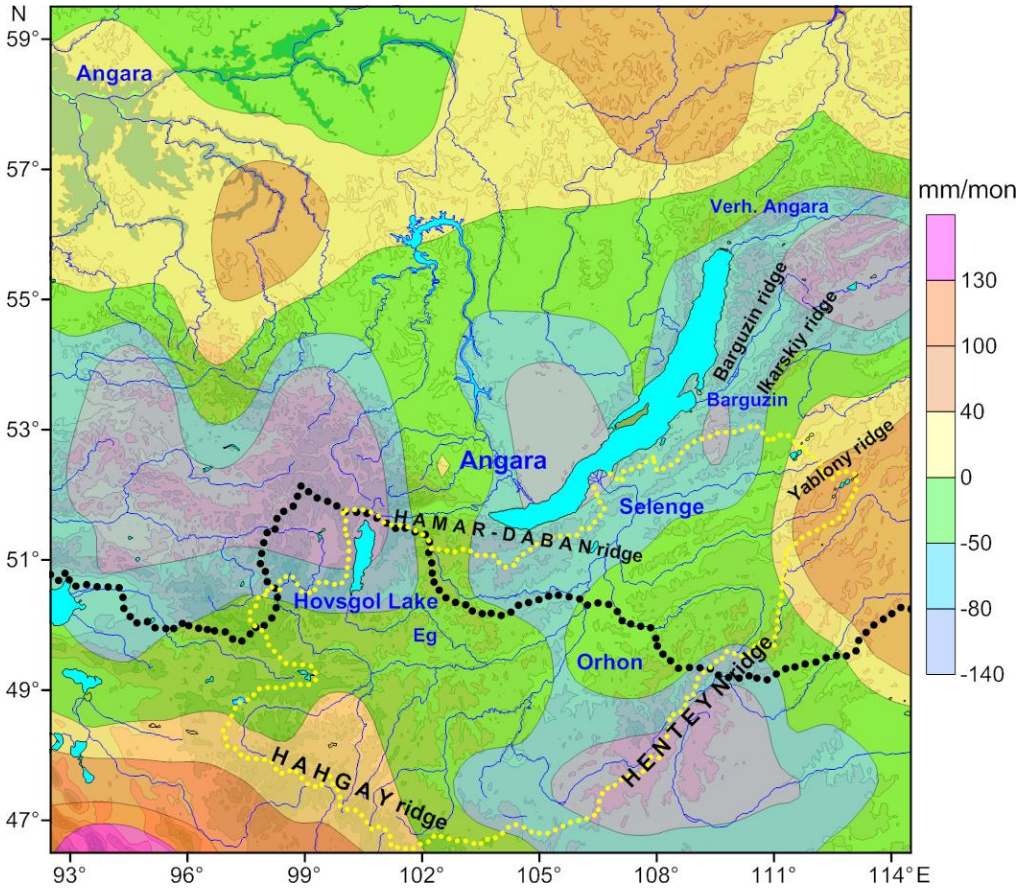

Fig. 9. Anomalies of precipitation in June – August 2015 in Irkutsk Region of Russia and catchment area of Lake Baikal and Selenga River. Black dashed curve is a boundary between Russia and Mongolia. Yellow dashed curve is boundary of catchment area of Selenga River.

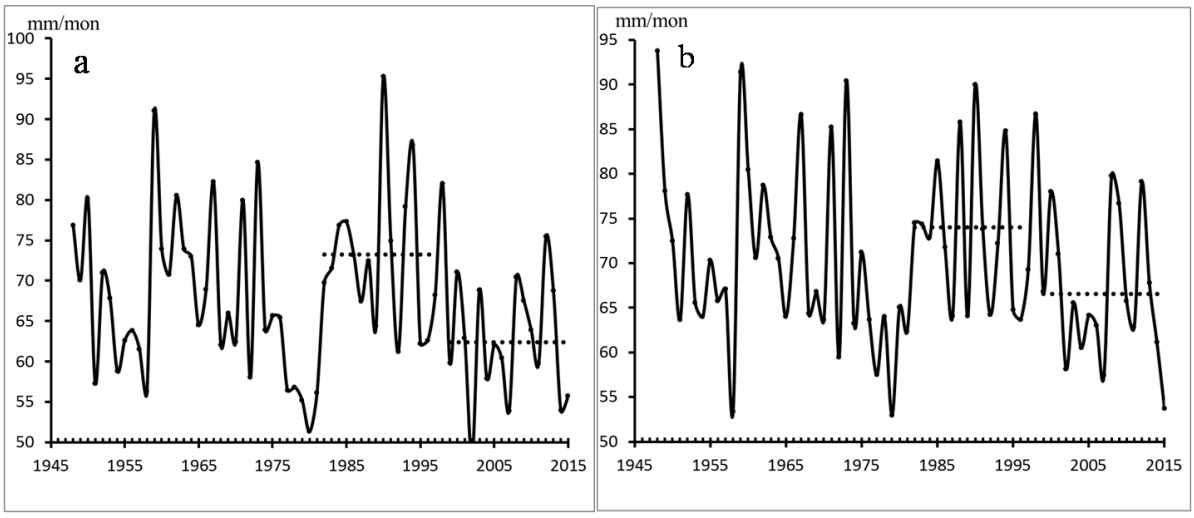

Fig. 10. Time series (1948 - 2015) of precipitation (mm/mon) averaged in April-June (a) and June-August (b) in the large scale area (46°-57°N, 97° -114°E) including catchment areas of Lake Baikal, Irkutsk and Bratsk water reservoirs of hydroelectric power stations

The negative anomaly of precipitation from June to August 2015 is prevailing in the whole area presented in Fig. 9 and in catchment areas of Lake Baikal and Selenga River. The positive anomaly occurs only over surrounding regions, particularly over Hahgay and Yablony Ridges, as well as in northern region adjacent to Bratsk water reservoirs. The recent climate regime is also associated with high SLP and low precipitation in this area (Fig. 10) that is in agreement with [17]. The sharp drop of precipitation began from 1997 and reached low level in 2002, 2007, 2014 and 2015. The effect of accumulated anomalies of precipitation has an important impact on the Lake Baikal level drop in 2015. At the same time, high anomaly of precipitation occurs in South of Primorskii Region of Russia in 2015-2016. In late August 2015 to summer 2016 considerable flood of the Lake Khanka after passing of the typhoon "GONI" in the south of Primorskii Krai was observed on August 26, 2015. Increase of level of the lake and flooding of adjacent lands continues till summer 2016 (recent time) that isn't related to passing of strong typhoons any more. It is basically due to both extreme rise of rainfall in fall 2015, snow in winter 2016 in the Lake Khanka Basin especially over the Pogranichny Ridge (Fig.11, 12, 13) and positive decadal anomaly of mean precipitation from Jan. to Aug. in this area during previous long-term period 2004 to 2015 (Fig. 13).

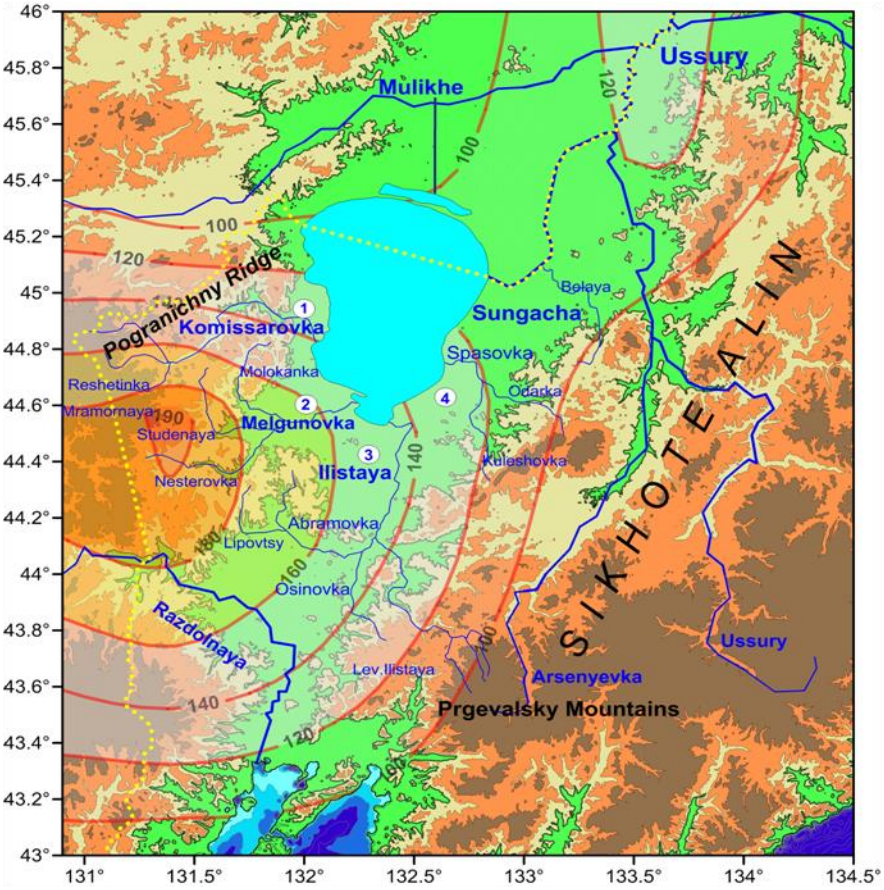

Fig. 11. Catchment area of Lake Khanka and anomalies of monthly sum of precipitation (mm/mon) averaged from January to August 2015 referenced to its mean values from 1948 to 2015. Black line is channel between Mulinkhe River and Malaya Khanka in Chinese territory.

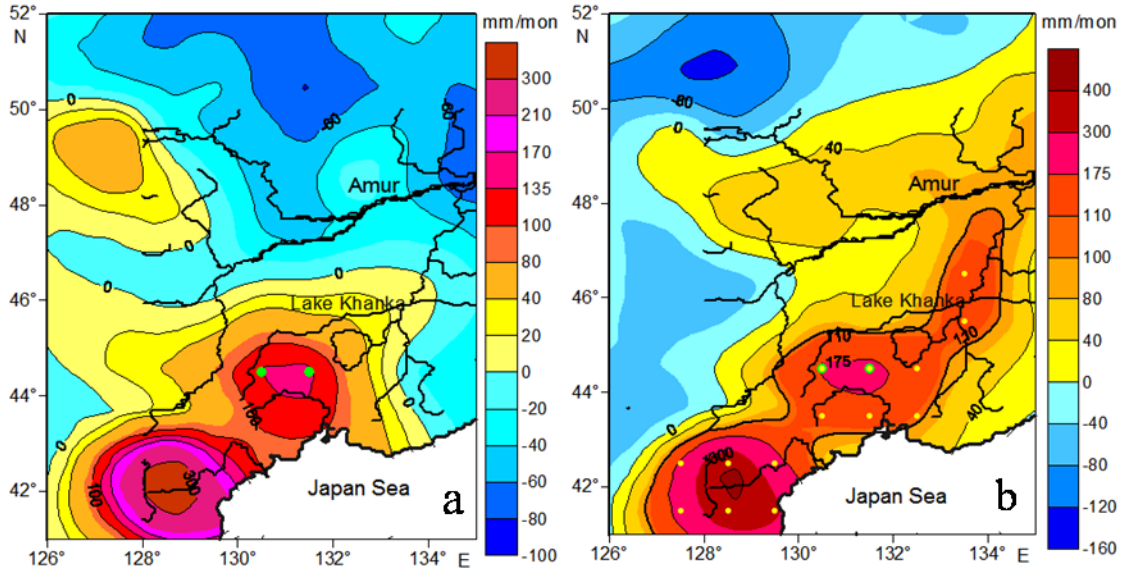

Fig. 12. Anomaly of monthly precipitation sum (mm/mon) in August (a) 2015 and averaged from January to August (b) 2015 in the catchment areas of the Lake Khanka, Amur, Mulinkhe, Ussury Rivers.

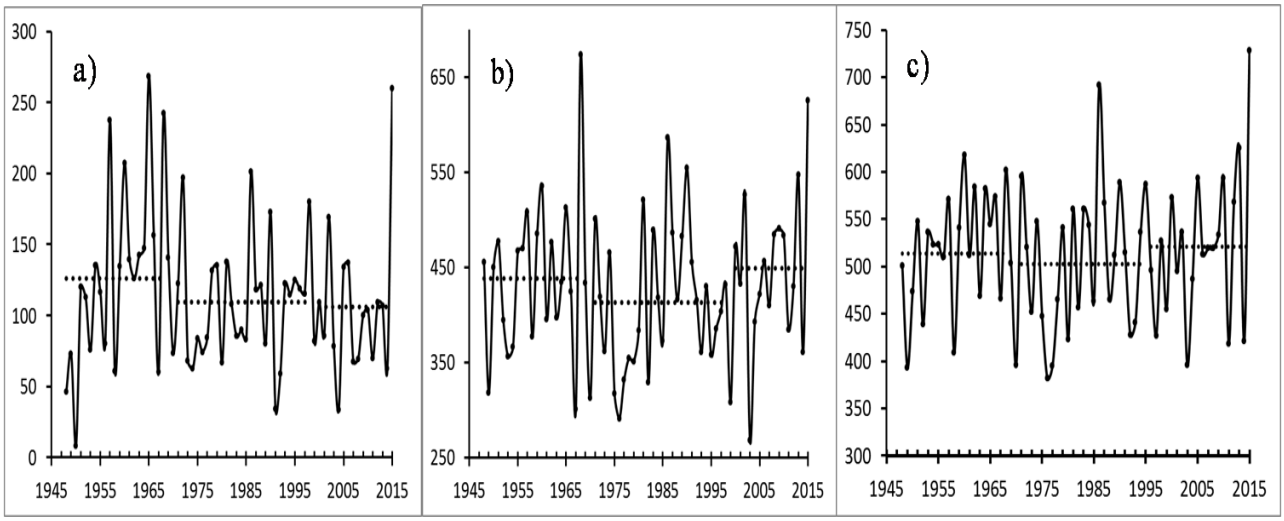

Fig. 13. Time series (1948 - 2015) of monthly mean precipitation (mm/mon) in August (a) and from January to August 2015 (b) over Pogranichny Ridge (44,5°N, 130.5°-131.5°, averaged in two green grid points in Fig.12 in the area of maximal precipitation 175 mm/mon situated southwest of Lake Khanka, as well as mean precipitation in all grid points of red area (c), isolated by curve 110 mm/mon in Fig.12.

Change of the climatic regime in the ocean – land - atmosphere system results in changes of temperature, salinity structure and circulation in the marginal seas, particularly in the Japan (East) Sea. It is a deep marginal sea with shallow straits and deep and bottom water is formed in the sea. Tataskii Strait is a deep trench between Sakhalin Island and continental slope. In the northern shelf the Tatarskii Strait is connected with the Okhotsk Sea through the shallow and narrow Nevelskoi

Strait. Amur River estuary is situated closed to the Nevelskoi Strait and under northern winds fresh water from the Amurskii Liman is transported to Tatarskii Strait along the continental and sometimes along Sakhalin Island bottom slope. Seasonal ice cover is formed in the northern area of the Tatarskii Strait every year. Due to winter cooling, sea ice formation, brain rejection and convection cold water is formed in the Tatarslii Strait every year. In spring and summer typical vertical subarctic water structure with subsurface local temperature minimum was usually observed.

The CTD observations from 1999 to 2015 in the same area of the Tatarskii Strait are presented in Table 2 and Fig.14.

Table 2. CTD Stations in the Tatarskii Strait from 1999 to 2015.

N	Cruise, R/V	Data	Lat	Lon	№
125	Khromov 36	28.07.1999	48	141.04	1
28	Lavrentiev 59	19.08.2012	48.24	141.388	2
18	Lavrentiev 62	27.06.2013	48.13	141.22	3
6	Lavrentiev 67	23.07.2014	48.134	141.173	4
6	Lavrentiev 70	19.06.2015	48.24	141.391	5

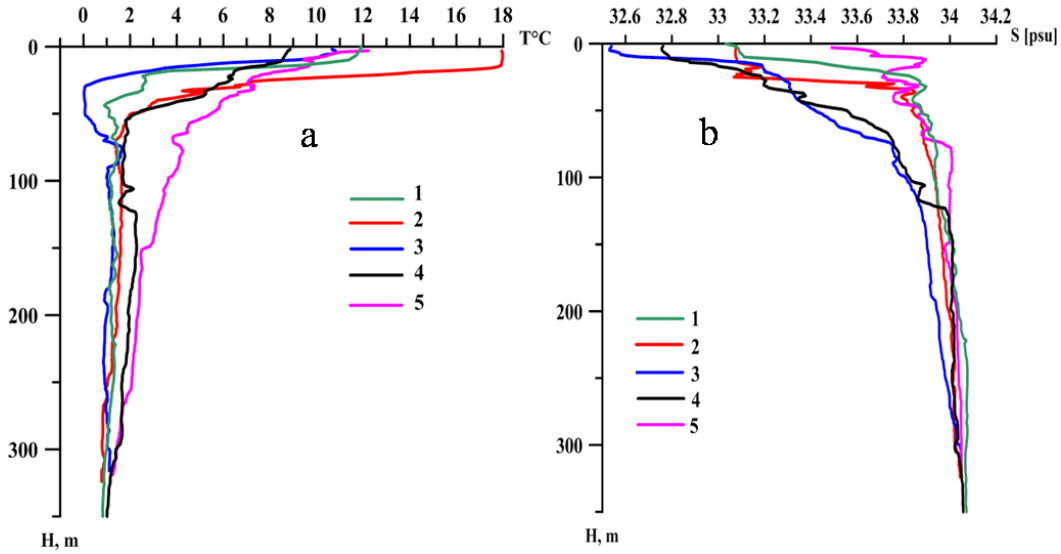

Fig. 14. Temperature (a) and salinity vertical profiles of CTD measurements in the Tatarskii Strait in summer 1999, 2012, 2013, 2014, 2015.

Typical vertical subarctic water structure of temperature and salinity with subsurface local temperature minimum is observed in July 1999, weak in August 2012, maximal in late June 1913, weak in late July 14, while in mid July 2015 the vertical structure became subtropical with significantly increased both temperature and salinity in total water column. This change of the water structure in the Tatarskii Strait in June 2015 is due to increase of subtropical water transport to the northern area of the Japan Sea in this year. This event is associated with warm SST anomaly in the Northeast Pacific in 2014 and in the large scale area of the extratropic Pacific in 2015.

V. Conclusion

Based on the analysis of time series data of meteorological and oceanographic observations, it is shown that the climatic regime is significantly changed at the turn of the 20th and 21st centuries in Asia and the Pacific, Indian, Southern and Arctic oceans. One of major characteristic features of the recent climate regime 1996/1999 – 2016 is associated with the decrease of atmospheric pressure at sea level (SLP) and rise of cyclonic activity in the World Ocean marginal band including most of the Pacific, Atlantic Arctic, Southern Oceans - land large scale transboundary zone including all of marginal seas.

During recent climate regime the precipitable water content in the atmosphere and precipitation significantly increase in this zone that prevailing in a warm period of a year. Surface air temperature rises in most of marginal areas rise in fall winter while decrease in spring and early summer. Repeatability of number of strong storms has increased in the Western Pacific and its marginal Seas, Western and Eastern Atlantic Ocean. It is a main cause of floods in river and lake basins including Amur River Basin in 2013, Rivers in the Primorskii Region of Russian Far East in 2012, 2015 and in the Lake Khanka Basin in 2015-2016.

Second major feature of the recent climate regime is the cyclonic activity reduce and SLP rise prevailing in winter in central extra-tropical Pacific and in South Indian Ocean. Similar SLP rise prevailing in summer is typical for the central continental regions of temperate latitudes, including Mongolia, South Siberia, and Lake Baikal Basin. It is accompanied by significant warming, wildfires, reduction of precipitation, river discharge and fast falling of level of the Lake Baikal. Nevertheless,

VI. Acknowledgment

The part of the work on the interannual, decadal and interdecadal variability of the ice extent in the Okhotsk Sea and Tatarskii Strait of the Japan Sea, wind and net heat flux at the sea surface, which are external parameters and forcing in the eddy-resolved hydrodynamic circulation model, was supported by the Russian Science Foundation (project no.~16--17--10025). The another part of the work on the multiple scale regional climate variability in the northwestern area of the Japan Sea and its linkages was supported by the Program “Dalniy Vostok” of the Russian Branch of the Russian Academy of Sciences (Project 15-I-1-047o), and RFBR Grant 15-05-03805.

VII. References

[1] M.E. Schlesinger and N. Ramankutty, “An oscillation in the global climate system of period 65-70 years,” Nature, vol. 367, February 1994, pp. 723-726.

[2] S. Minobe, “A 50–70 year climatic oscillation over the North Pacific and North America,” Geophys. Res. Lett., vol. 24, pp. 683–686, 1997.

[3] S. Minobe, “Spatio-temporal structure of the pentadecadal variability over the North Pacific,” *Prog. Oceanogr.*, vol. 47(2–4), pp. 381–408, 2000.

[4] S.I. An, “A mechanism for the multi-decadal climate oscillation in the North Pacific,” *Theor. Appl. Climatol.*, vol. 91(1–4), 2008, pp.77–84.

[5] Z.M. Gudkovich, V.P. Karklin, and I.E. Frolov. 2005. “Intra-secular changes in climate and sea ice area in the Eurasian Arctic Seas and their possible causes.” Russian *Meteorology and*

Hydrology, N 6, pp. 5–14, 2005; Original Russian Text published in *Meteorologiya i gidrologiya*, N 6, pp. 5–14, 2005.

[6] I.E. Frolov, Z.M. Gudkovich, V.P. Karklin, E.G. Kovalev, and V.M. Smolyanitsky, Climate Change in Eurasian Arctic Shelf Seas: Centennial Ice Cover Observations, Springer Praxis Books Geophys. *Sciences*, Chichester, UK, p. 164, 2009.

[7] I.E. Frolov, Z.M.Gudkovich, V.P.Karklin, and V.M.Smolyanitsky. "Regional peculiarities of the sea ice cover changes in the 20th – early 21st centuries and their causes," *Ice and Snow*. N.3, 91-98. 2011.

[8] P. Chylek, Ch.K. Folland, G. Lesins, M.K. Dubey, and M. Wang, "Arctic air temperature change amplification and the Atlantic Multidecadal Oscillation," Geoph. Res. Lett., vol. 36, L14801, July 2009.

[9] A.B. Polonsky, "Atlantic multidecadal oscillation and its manifestations in the Atlantic-European region," *Marine Hydrophysical Journal*, N 4, pp. 47–58, 2008 (in Russian with English abstract).

[10] L. Wu, D. Lee, and Zh. Liu, "The 1976/77 North Pacific Climate Regime Shift: The Role of Subtropical Ocean Adjustment and Coupled Ocean-Atmosphere Feedbacks," *J. Climate.*, vol.1, pp. 5125-5240, 2005.

[11] N. Bond, J. Overland, M. Spillane, and P. Stabeno, "Recent shifts in the state of the North Pacific," *Geophys. Res. Lett.*, vol. 30(23), pp. 2183-2186, 2003.

[12] V.I. Byshev, V.G. Neiman, Yu.A. Romanov, and I. Serykh, "Phase variability of some characteristics of the present-day climate in the Northern Atlantic region," *Doklady Earth Sciences*, vol. 438, 2011, pp. 887-892. Original Russian Text published in *Doklady Akademii Nauk*, vol. 438, pp. 92–96, 2011.

[13] S.-W.Yeh, Y.-J. Kang, Y. Noh, and A. J. Miller, "The North Pacific climate transitions of the winters of 1976/77 and 1988/89," *J. Climate*, 24(4), 1170–1183, 2011.

[14] H.-S. Jo, S.-W. Yeh, and C.-H. Kim, "A possible mechanism for the North Pacific regime shift in winter of 1998/1999," *Geophys. Res. Lett*., vol. 40, pp.4380–4385, 2013.

[15] V.I. Ponomarev, E.V. Dmitrieva, and S.P. Shkorba, "Featuries of climatic regimes in the North Asia Pacific," *Sistemy kontrolya okruzhayuschei sredy*, (J. *Systems of environment control published in Russian*), Sebastopol, vol. 1 (21), pp. 67-72, 2015.

[16] S. Shkorba, E. Dmitrieva, V. Ponomarev, L. Kuimova, V. Pustoshnova, "Winter climatic anomalies in the Japan, Okhotsk Seas, Baikal Lake Basin and their linkages," in this *EMECS'11- SEACOAST'26 Conference proceedings*, 2016 (in press).

[17] T.V. Berezhnikh, O.Yu. Marchenko, Y.V. Abasov, V.I. Mordvinov, "Change of summer circulation in the atmosphere over East Asia and formation of long-term dry period catchment areas of Lake Baikal," *Geografiya i prirodnye resursy*, N3, pp.61-68, 2012 (in Russian).

CLIMATIC ANOMALIES IN FAR EASTERN MARGINAL SEAS, BAIKAL LAKE BASIN AND THEIR LINKAGES

Svetlana Shkorba, V.I. Il'ichev Pacific Oceanological Institute, FEB RAS, Russia
Elena Dmitrieva, V.I. Il'ichev Pacific Oceanological Institute, FEB RAS, Russia
Irina Mashkina, V.I. Il'ichev Pacific Oceanological Institute, FEB RAS, Russia
Vladimir Ponomarev, V.I. Il'ichev Pacific Oceanological Institute, FEB RAS, Russia

sshkorba@yandex.ru

Winter climatic anomalies of various time scales in the Japan, Okhotsk seas and Baikal Lake Basin are revealed and compared with anomalies in the Pacific, Indian and Arctic oceans. Time series of ice extent in the Japan and Okhotsk seas, ice thickness and seasonal duration of the ice cover in the Baykal Lake, as well as Hadley SST, surface heat fluxes, wind velocity, atmospheric pressure fields (SLP) and different climatic indices are analyzed. The decadal climate anomalies in the Japan and Okhotsk seas in mid winter, as compared to the Northeast Pacific and South Siberia regions, could have a reversed phase. Alternating cold/warm decadal anomalies in different longitude zones of the North Asian Pacific are accompanied by alternating meridional wind and SLP anomalies at temperate latitudes. Alternating zones of inversed anomalies in temperate latitudes of the Asian Pacific are related to teleconnections with anomalies in both Arctic and Indo-Pacific oceans. Negative SSTA in eastern/central tropical-equatorial Pacific and positive SSTA in El Nino area accompanies rise of northern wind and ice extent in the Okhotsk/Japan Seas in mid-winter. The best predictors of the high cold anomaly in February in the western subarctic Pacific and marginal seas are reduction of the SST and net heat flux from the atmosphere to the ocean in north-eastern and central North Pacific during warm period of a previous year. At the multidecadal time scale the warming/cooling in the Northeast Pacific accompany winter warming/cooling in the Baykal Lake area during all period of observation. At interdecadal time scales the significant link of winter climate oscillations in South Siberia (Baikal Lake Basin) is found with SSTA oscillations in the equatorial region of the Indian Ocean and certain areas of the Pacific Ocean. The linkages of anomalies in the Baikal Lake Basin, Okhotsk, Japan Seas with regional anomalies in some key areas of the Pacific and Indian Oceans, related to the atmospheric centers of action are more stable than that with climatic indices. After climate regime shift in late 70s warm decadal anomaly in both Lake Baykal Basin and Indian Ocean in boreal winter accompany high positive anomaly of the Arctic Oscillation. Scenarios of extreme anomalies in the Baikal Lake Basin and Subarctic Pacific marginal area are also presented.

Key words: climatic anomalies, Pacific, Indian, Arctic, ocean, Lake Baikal, ice thickness, Japan, Okhotsk, sea, ice extent, surface heat fluxes, wind velocity, surface pressure, teleconnections

I. Introduction

The ENSO-scale, decadal, interdecadal and multidecadal (50-70 years) climate oscillations are presented in numerous studies based on the data analyses of the observational records in the Pacific, Arctic, Atlantic oceans and land areas [1-6] including Russian Far East and south Siberia [7]. The interannual, decadal and interdecadal oscillations vary in space and time in the ocean-atmosphere system. The multidecadal oscillation is approximately in phase in the Pacific [4], Arctic [5] and Atlantic Oceans [6] and looks like global scale phenomena [3]. Transition period between positive and negative phases of the multidecadal oscillation can be 5-8 years that is very rapid in comparison with the oscillation period. The well known transition period named as climate regime shift in late 70s of the 20th century was revealed both in the North Pacific [8] and North Atlantic [9] ocean-atmosphere system. Recent shifts in the state of the North Pacific from 1999 to 2012 in terms of phase trajectory of the first two principal component of SST anomalies in the North Pacific is revealed in [10]. The climatic regime changes in the Pacific, Indian Oceans and Asia both in late 70s and late 90s in terms of phase trajectory of Sea Level Pressure (SLP) and surface net heat flux (Q) is shown in [11]. A lot of extreme events in the atmosphere and ocean were observed in the first 15 years of the 21 century including extremes in 2014, 2015. In Russia the extremely low level of the Lake Baikal (South Siberia) is observed in fall 2015. At the same time an inverse extreme anomaly is observed in the Lake Khanka situated in the south of Russian Far-East (Primorskii Krai). The high level and flood of the Lake Khanka have reached a maximum in the fall of 2015 that has led to flooding of coastal houses and agricultural grounds.

The main goal of our study is to reveal and compare regional climatic and anomalies of various time scales in areas of temperate latitude band of the Asian Pacific Region, including South Siberia, Lake Baikal Basin, Russian Far East, Okhotsk and Japan Seas. The study is based on statistical analyses of the observation records. It is focused on features and relationships between multiple scale winter climatic anomalies in the Okhotsk, Japan (East) Seas, Lake Baikal Basin and similar scale anomalies different latitude zones of the Pacific and Indian Oceans.

II. Data and methods

We use observation data included gridded monthly mean time series of Hadley (GB) Sea Surface Temperature (SST) from 1870 to 2015, NCER NCAR meteorological reanalyses (1948-2015) pressure atmospheric pressure (SLP), air temperature (SAT), surface net heat flux, as well as monthly mean time series of Ice Extent [12, 13] in the Okhotsk Sea and Japan Sea (*Tatarskii Strait*) from 1948 to 2013, Baykal Lake Ice Thickness (1946-2013) and duration of the seasonal Ice Cover (in days) in the Baikal Lake from 1900 to 2012, Arctic Oscillation (AO), Pacific Decadal Oscillation (PDO), Multidecadal Atlantic Oscillation (AMO) indices.

Lagged and unlagged relationships between time series at different time scales are estimated by using standard filtering method and correlation analyses.

III. Winter anomalies of various time scales and their linkages

The climatic oscillations with periods 3-8 years and 18-21 years prevail in the Okhotsk and Japan Sea Ice Extent. High positive anomalies of the Ice Extent in February both in the Japan and Okhotsk Seas were observed in 1961, 1979, 2001 years. In the Okhotsk Sea it was also in 1967.

Low anomalies was observed in 1963, 1984, 1991, 1994, 2007, 2009, 2011 in the Okhotsk Sea, and in 1949, 1957, 1974, 1991, 1994, 2011 in the Japan Seas (Fig.1,2).

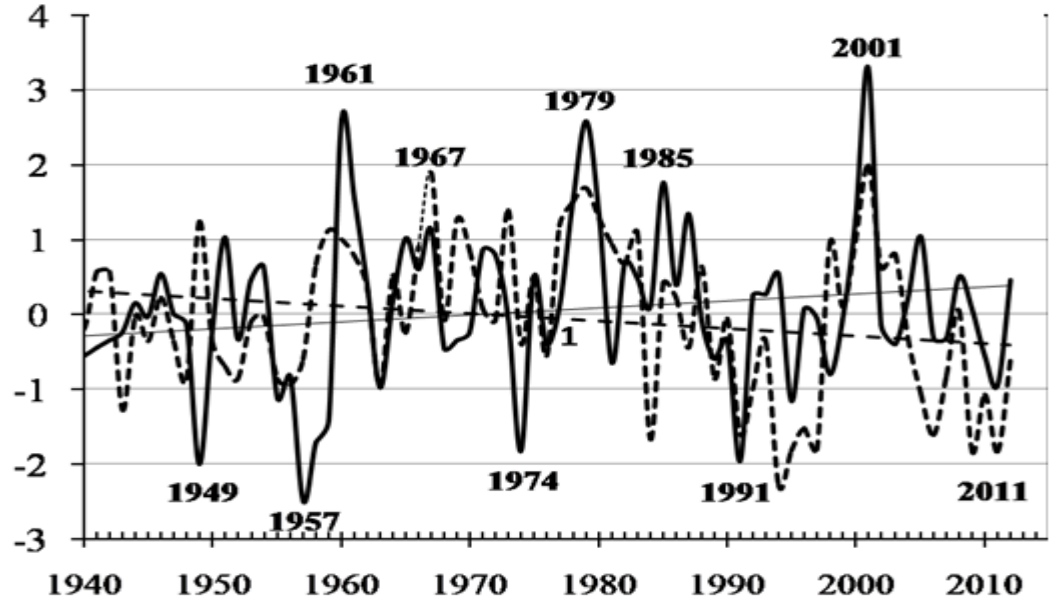

Fig. 1. Normalized anomalies of Ice Extent (IE) in Japan (dashed curve) and Okhotsk (solid curve) Seas in February from 1940 to 2012 and its insignificant linear trends.

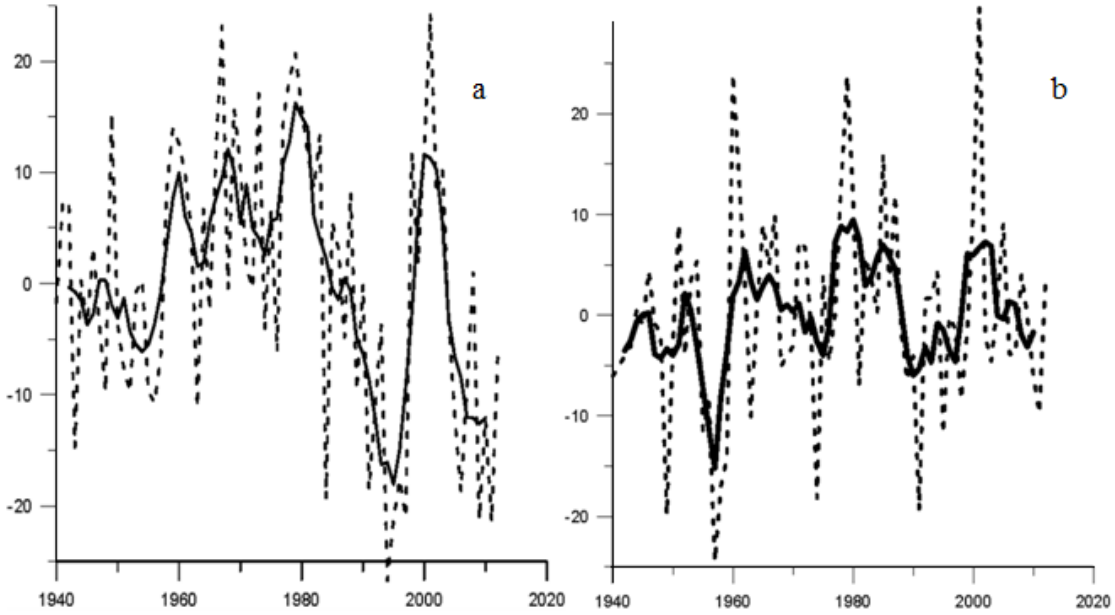

Fig. 2. Anomalies of Ice Extent (%) in the Okhotsk Sea (a) and Japan (Tatarskii Strait) (b) Seas in February from 1940 to 2012. Solid curves are 5-years running mean time series.

The rise/decrease of the Ice Extend in the Okhotsk, Japan/East Seas is accompanied by winter Sea Surface Temperature (SST) decrease/rise in central extratropic and subarctic North Pacific with maximal correlation coefficient (0.8) in western subarctic region adjacent to the

Okhotsk Sea and Tatarskii Strait (Fig. 3d, Fig.4d). At the same time the Japan Sea Ice Extent positive/negative anomaly is accompanied by SST decrease/rise in central tropical Pacific (Fig. 3d) and rise/decrease in eastern southern tropic area, while the Okhotsk Sea Ice Extent in rise/decrease is accompanied by SST decrease/rise in western tropical and south subtropical Pacific (Fig. 4d, south of 30°S) as well as SST rise/decrease in eastern southern tropical area in the equatorial El Nino area (NINO3, NINO 3-4). Similar El Nino signal in the Okhotsk Sea and adjacent subarctic area was shown in [14, 15] in terms of both unlagged and lagged correlation between Southern Oscillation Indices/NINO3 and anomalies of Surface Air Temperature (SAT), SST, Ice Extent (IE) in winter.

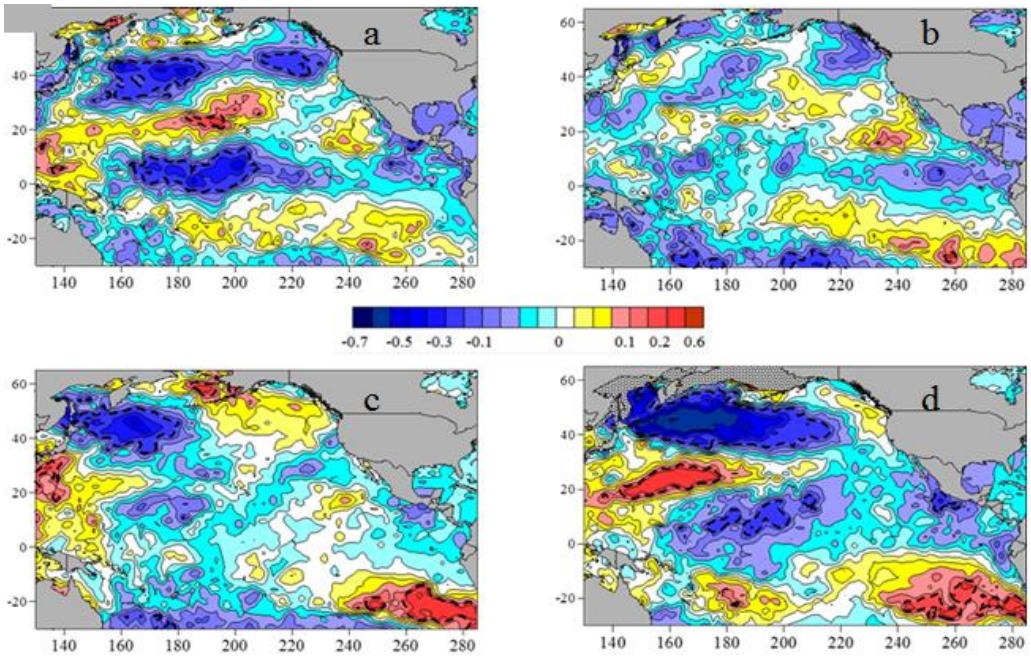

Fig.3. Correlations coefficient between Japan Sea ice extent (1949-2012) in February and Pacific Hadley SST anomalies north of 30 S in May (a), August (b), November (c) of previous year, as well as, in February (d) of the current year (red is positive, blue is negative correlation). Dashed curve limits 95% confidence level of correlations coefficient.

The cold winter anomalies in the Japan and Okhotsk seas are also associated with increased net heat flux (Q) from the ocean to the atmosphere in February (Fig.5) and during cold period of a year in the western tropical and subtropical zones in case of the Japan Sea, as well as in the western subtropical and subarctic zones of the North Pacific in case of the Okhotsk Sea. Typical meteorological situation in the cold winters is characterized by extremely strong North-East Asian winters monsoon, Siberian High and Aleutian Low resulted in rise of the Ice Extend in the Okhotsk and Japan Seas. The surface net heat flux directed to from the atmosphere to the ocean is weakened in the equatorial and tropical zones in this case. The best predictors of the high cold anomaly in February in the western subarctic Pacific and marginal seas are reduction of the SST and net heat flux from the atmosphere to the ocean in north-eastern and central North Pacific during warm period of a previous year (Fig. 3-5). In case of the Okhotsk Sea the negative anomaly of the SST in the western tropical Pacific in summer is also observed before cold winter. The anomalies of the Ice

Extent in the Okhotsk, Japan Seas and net heat flux in the North Pacific in extremely cold February 2001 and warm February 2011 are associated with inversed phases of the decadal oscillation (Fig.5). In the extreme winters the anomalies of Q are much higher and occupy the western Pacific north to 30°S. It is accompanying the intensification of winter monsoon and weakening summer monsoon in the Russian Far East.

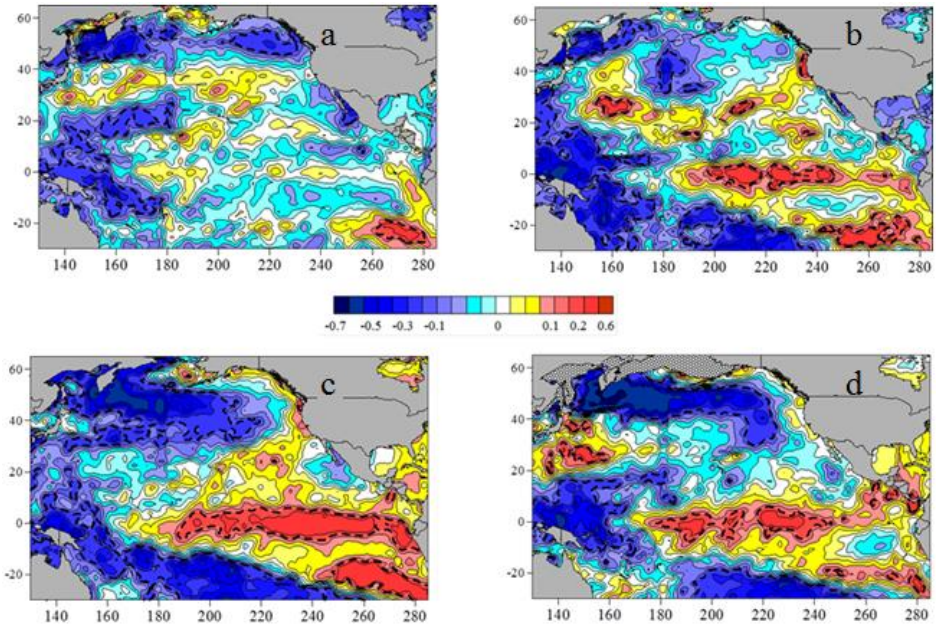

Fig.4. Correlations coefficient between Okhotsk Sea ice extent (1949-2012) in February and Pacific Hadley SST anomalies north of 30 S in May (a), August (b), November (c) of previous year, as well as, in February (d) of the current year. (Scale is like in Fig.3)

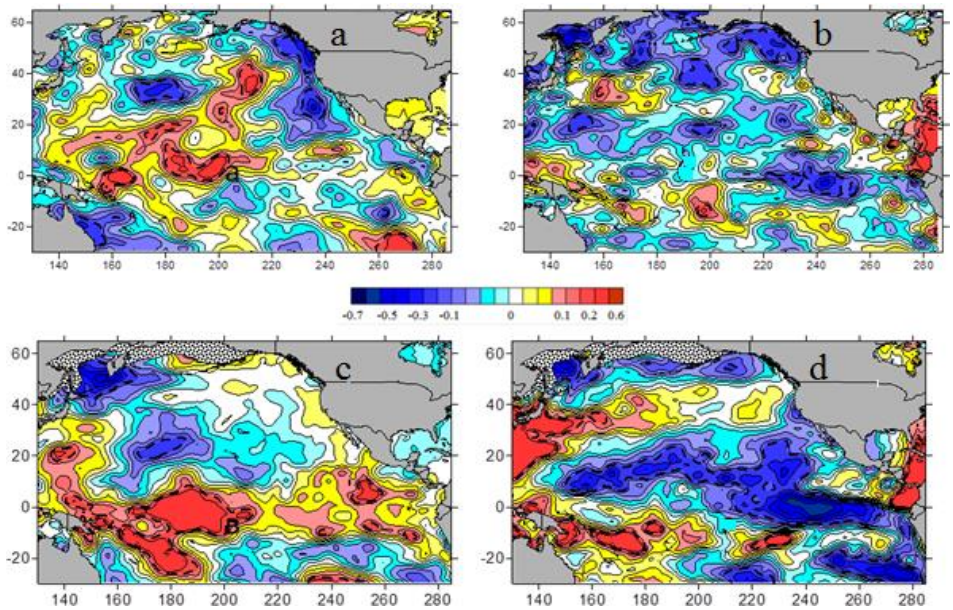

Fig.5. Correlations coefficient of relationship between anomalies of the Japan Sea (a, c) and Okhotsk Sea (b, d) ice extent (1949-2012) in February and net heat flux (Q) in the Pacific SST north of 30 S in May (a), August (b), November (c) of previous year, as well as, in January (d) and February (f) of the current year (red is positive, blue is negative correlation). Dashed curve limits 95% confidence level of correlations coefficient.

Fig. 6. shown significant relationship at interdecadal time scale between Ice Extent (IE) in the Japan (a), Okhotsk (b) Seas in February and net heat flux Q from the ocean to the atmosphere (negative values in our work) in winter within the area (37-42N, 150-154E). It is area of Kuroshio-Oyasio energetically active zone. Subarctic frontal zone of the western Pacific is also situated in this area. The increase of heat flux from the sea surface to the atmosphere (absolute values of negative Q increases) in this area results in increase of the Ice Extent in both Japan and Okhotsk Seas.

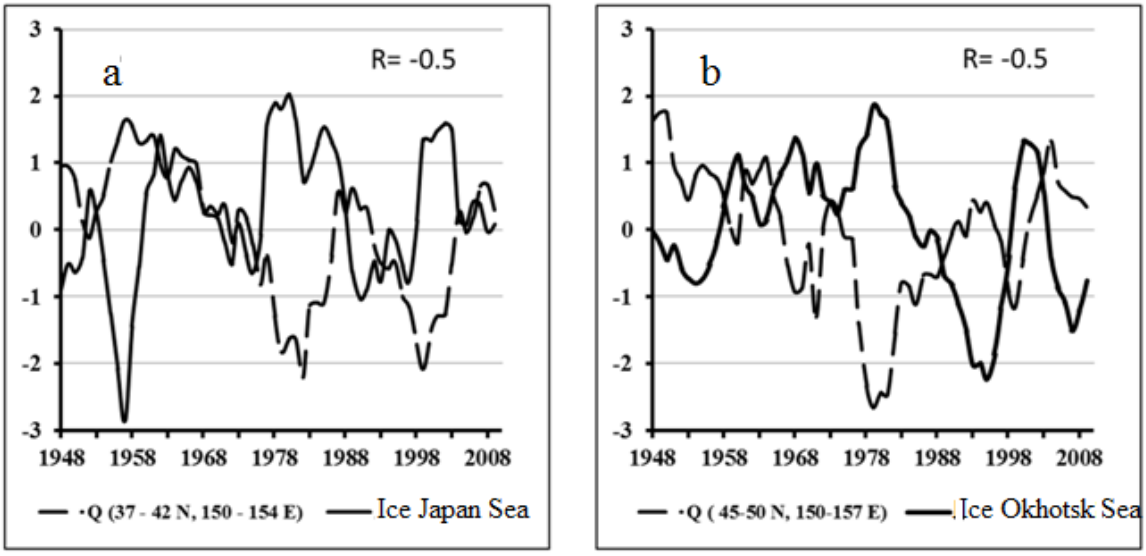

Fig.6. The 5 years running mean time series (1948 - 2012) of normalized anomalies of Ice Extent (IE) in the Japan (a) and Okhotsk (b) Seas in February and net heat flux Q from the ocean to the atmosphere (negative values) in winter averaged within the areas (37-42N, 150-154E) of the Northwest Pacific with significant negative correlation between Q and IE.

The relationship between Arctic Oscillation (AO) and Ice Extent in the Japan Sea (Fig.7a) is found on the interdecadal time scales with period about 25-28 years. The relationship between Arctic Oscillation (AO) and Ice Extent in the Japan Sea (Fig.7a) is found on the interdecadal time scales with period about 25-28 years. When the AO is in its positive phase and colder air circulates across the Arctic region, winter in subarctic Asian-Pacific region is warmer and the Ice Extent in the Japan Sea decreases. The relationship between Arctic Oscillation and Ice Extent (IE) in the Okhotsk Sea in February is changed from positive to negative (Fig.7b) after climate regime shift in the North Pacific in 70s of the 20th century. The multidecadal oscillation with period about 50 years is clear seen in the Ice Extent of the Okhotsk Sea.

The linkages of decadal climate variability in south Siberia (seasonal ice coverage duration in the Baykal Lake in winter with annual mean Arctic Oscillation Indices (AOI) and Sea Surface Temperature Anomaly (SSTA) in equatorial region of Indian Ocean in boreal winter on decadal time scale is shown in Fig.8. Similar high positive decadal SST anomaly in early 90s occurs in El Nino region, while it is negative in mid-latitude Indian and Pacific Oceans of Southern Hemisphere.

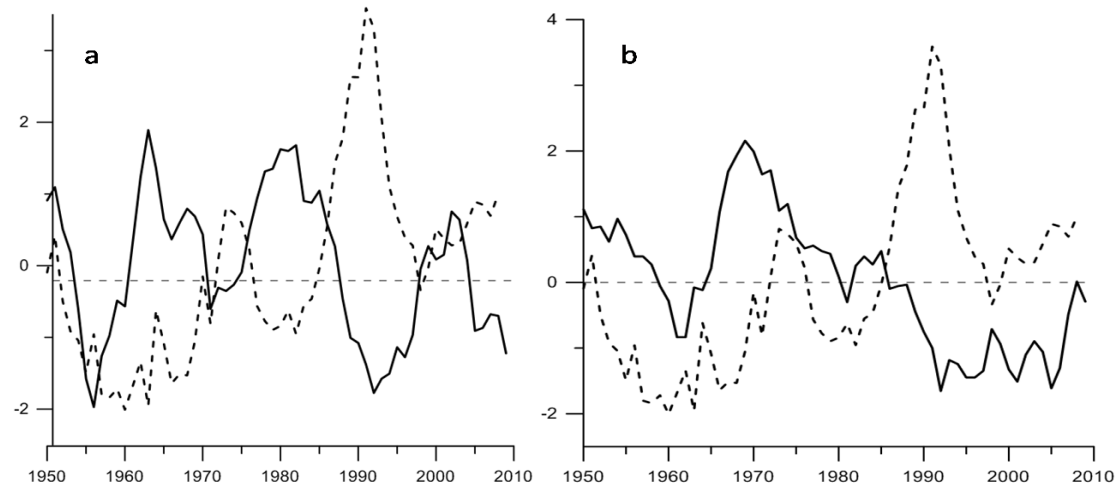

Fig.7. Time series (1900 - 2010) of 7-year running mean normalized anomaly of the Ice Extent (solid curve) in the Japan (a) and Okhotsk (b) Seas in February and annual mean AO Indices.

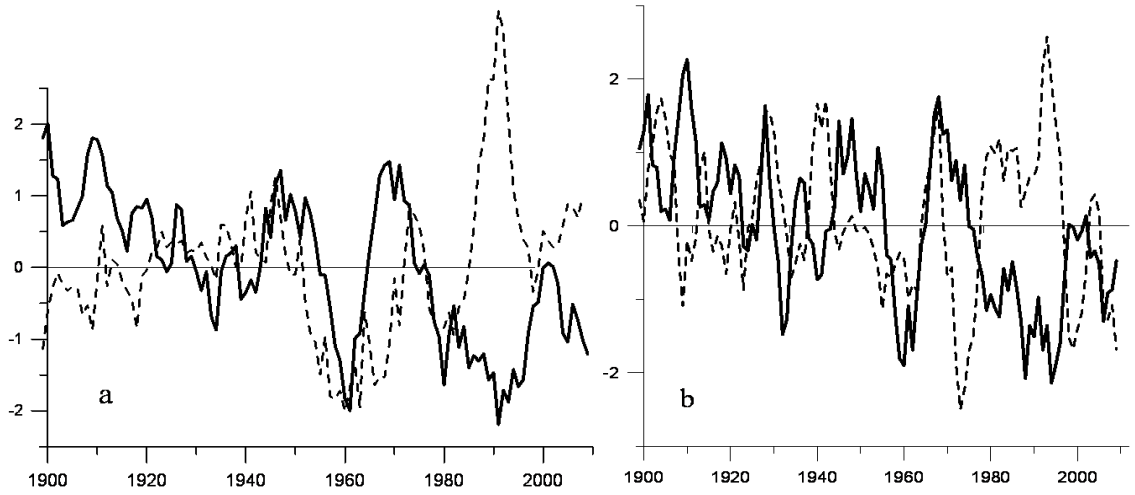

Fig.8. Time series (1900 - 2010) of normalized anomaly of seasonal ice coverage duration in the Baykal Lake (solid curves: 5 (a) and 3 (b) - years moving average, as well as annual mean Arctic Oscillation Indices (dashed curve in Fig. a) and Sea Surface Temperature Anomaly in western equatorial region of Indian Ocean (dashed curve in Fig.b).

The normalized anomalies of 5-years running mean time series of the Ice Extent (solid curve) in the Japan (a), Okhotsk (b) Seas and Ice Thickness in the Baykal Lake (dashed curve in Figs. a,b) shown in Fig.9. The interdecadal oscillation of the Ice Extent in the marginal seas is usually in inversed phase in comparison with oscillation of the Ice Thickness in the Baykal Lake with exception of warming period in late 89-early 90s. The anomalies of each scale in the Baykal Lake including decadal scale are controlled by the anomalies of surface wind (Fig.10). Decrease of southern wind, increase of northern one over Lake Baikal result in rise of the ice thickness. The anomalies of the Ice Extent in the Japan and Okhotsk Seas are controlled by similar northwestern wind anomaly directed from the cold continent region to the Okhotsk Sea and northwestern area of the Japan Sea.

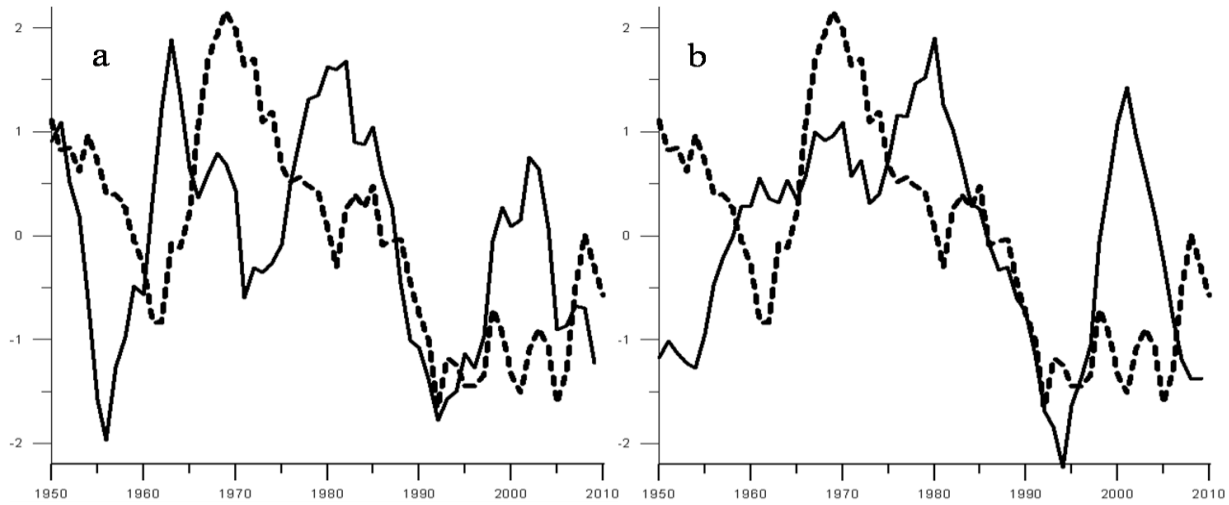

Fig.9. Normalized anomalies of 5 years running mean time series (1948 - 2012) of the Ice Extent (solid curve) in the Japan (a) and Sea Okhotsk (b, as well as Ice Thickness in the Baykal Lake (dashed curve in Figs. a,b).

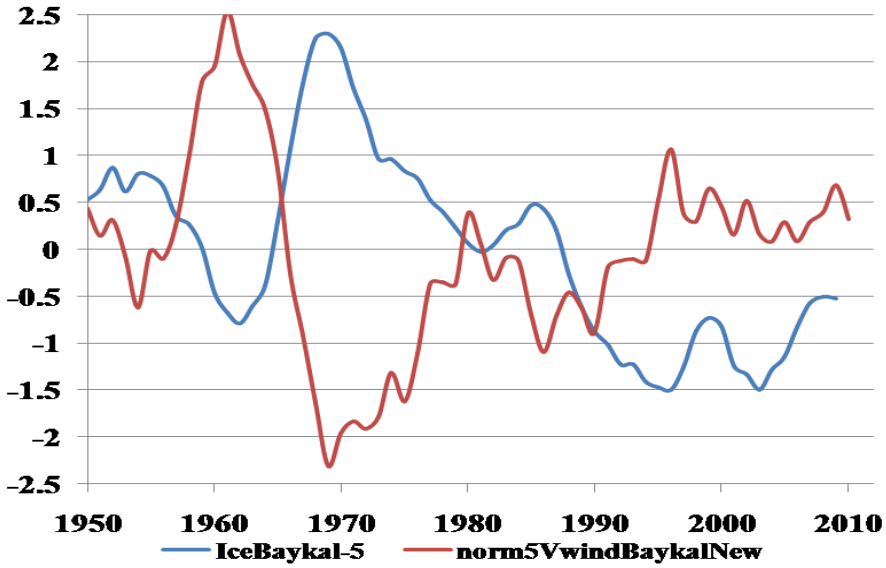

Fig.10. Normalized anomalies of 5 years running mean time series (1948 - 2012) of the Ice Thickness (solid curve) in the Baykal Lake (blue curve) and meridianal wind component (red curve) over the lake basin and adjacent area.

The multidecadal oscillation of both maximal seasonal Ice Thickness (IT) in the Baykal Lake (solid curve) and annual mean SST(dashed curve) in the Northeast Pacific (40-60N; 160-145 W) is shown in Fig.11 with annual mean Atlantic Multidecadal Indices (AMO, blue curve) in terms of normalized anomalies of 11 years running mean time series. At the multidecadal time scale the warming/cooling in the Northeast Pacific accompany winter warming/cooling in the Baykal Lake area during all period of observation. The AMO has same phase with SST and IT multidecadal oscillation only from 1950 to 1985 and later AMO has delayed phase.

The relationship between ice characteristics in the Lake Baikal, Okhotsk, Japan Seas Ice Extent and other climatic indices can be also changed after climate regime shift. The linkages of anomalies in South Siberia, Okhotsk, Japan Seas with regional anomalies in some key areas of the Pacific and Indian Oceans, related to the atmospheric centers of action are more stable than that with climatic indices. At the interdecadal time scale the oscillations of the Ice cover characteristics in the Baykal Lake are also in phase with SST anomalies in both equatorial Indian Ocean in boreal winter (Fig.8b) and North East Pacific. It seems to be that interdecadal (period is about 20-30 years) and multidecadal oscillations (50-60 years) in moderate latitudes of the Asian Pacific is substantially conditioned by anomalies of similar scales in both tropical-equatorial regions and Arctic Ocean. The high decadal anomaly in 90s in Arctic, Indo-Pacific, South Siberia, Japan and Okhotsk Seas is also associated with climate regime change in 70s.

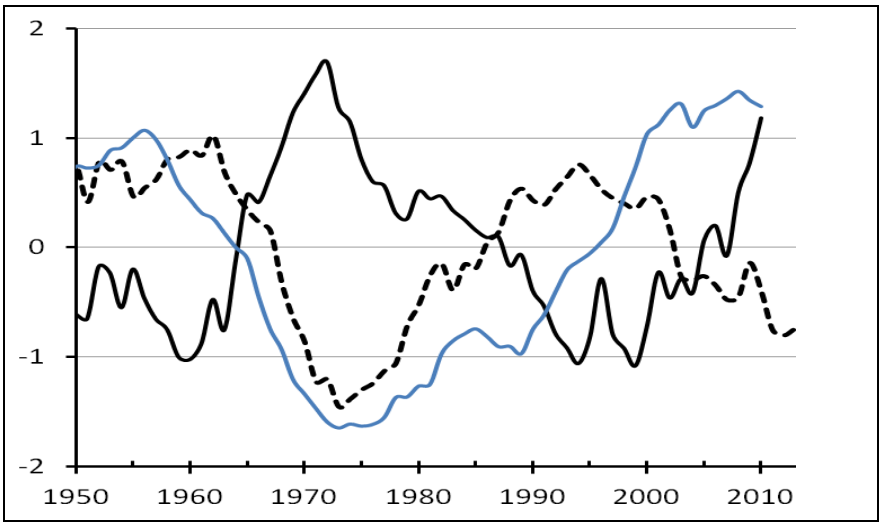

Fig.11. Normalized anomalies of 11 years running mean time series (1948 - 2012) of Ice Thickness in the Baykal Lake (solid curve) and annual mean SST anomalies(dashed curve) in the Northeast Pacific (40-60N; 160-145 W) and Multidecadal Atlantic Oscillation Indices (blue curve).

IV. CONCLUSION

The inversed decadal, bidecadal oscillations are typical for different areas of the Asian Pacific, Indian and Pacific Oceans. The amplitude of the oscillations is increased in warm multidecadal climate regime after climate regime shift in 70s of the 20th century. The decadal, interdecadal and multidecadal climate oscillations in the Okhotsk and Japan Seas have basically stable relationship to the anomalies in the certain areas of the tropical and extratropical Pacific Ocean. The interdecadal climate oscillation in South Siberia is basically related to the similar scale oscillation in the Indian Ocean and North Eastern Pacific region adjacent to the Alaska Gulf. After climate regime shift in late 70s warm decadal anomaly in both South Siberia (Lake Baykal area) and Indian Ocean in boreal winter accompany high positive anomaly of the Arctic Oscillation. At decadal, interdecadal time scales there are significant global scale teleconnection, accompanying processes and links in the ocean-atmosphere system between tropical-equatorial Indo-Pacific Ocean, extratropic Asian Pacific Region and Arctic Ocean.

V. Acknowledgment

The study was supported by Russian Academy of Science Program Dalnii Vostok 15-I-1-047o and RFBR Grant 15-05-03805.

VI. References

[1] H. Nakamura, G. Lin, and T. Yamagata, “Decadal climate variability in the North Pacific during the recent decades,” Bull. Amer. Meteorol. Soc., vol. 78, № 10, 1997, pp. 2215–2225.

[2] A.J. Miller and N. Schneider, “Interdecadal climate regime dynamics in the North Pacific Ocean: Theories, observations and ecosystem impacts,” Progr. Oceanogr., vol. 47, 2000, pp. 355–379.

[3] M.E. Schlesinger and N. Ramankutty, “An oscillation in the global climate system of period 65-70 years,” Nature, vol. 367, February 1994, pp. 723-726.

[4] S. Minobe, “A 50–70 year climatic oscillation over the North Pacific and North America,” Geophys. Res. Lett., vol. 24, 1997, pp. 683–686.

[5] I.E. Frolov, Z.M. Gudkovich, V.P. Karklin, E.G. Kovalev, and V.M. Smolyanitsky, *Climate Change in Eurasian Arctic Shelf Seas: Centennial Ice Cover Observations*, Springer Praxis Books Geophys. Sciences, Chichester, UK, p. 164, 2009.

[6] P. Chylek, Ch. K. Folland, G. Lesins, M. K. Dubey, and M. Wang, “Arctic air temperature change amplification and the Atlantic Multidecadal Oscillation,” Geoph. Res. Lett., vol. 36, L14801, July 2009.

[7] V.I. Ponomarev, V.V. Krokhin, D.D. Kaplunenko, and A.S. Salomatin, “Multiscale climate variability in the Asian Pacific,” Pacific Oceanography, vol. 1. № 2, 2003, pp. 125–137.

[8] L. Wu, D. Lee and Zh. Liu, “The 1976/77 North Pacific Climate Regime Shift: The Role of Subtropical Ocean Adjustment and Coupled Ocean-Atmosphere Feedbacks,” J. Climate, vol.1, 2005, pp. 5125-5240.

[9] V.I. Byshev, V.G. Neiman, Yu.A. Romanov, and I. Serykh, “Phase variability of some characteristics of the present-day climate in the Northern Atlantic region,” Doklady Earth Sciences, vol. 438, 2011, pp. 887-892

[10] N. Bond, J. Overland, M. Spillane, and P. Stabeno, “Recent shifts in the state of the North Pacific,” GRL, vol. 30(23), 2003, pp. 2183-2186.

[11] V.I. Ponomarev, E.V. Dmitrieva, and S.P. Shkorba, “Featuries of climatic regimes in the North Asia Pacific,” Russian Systems of environment control (Sistemy kontrolya okruzhayuschei sredy), Sebastopol, vol. 1 (21), 2015, pp. 67-72, in Russian.

[12] V.V. Plotnikov and S.P. Podtelezhnikova “Ice archives and statistical analysis of ice concentration in the north of the Sea of Japan,” Russian Meteorology and Hydrology, № 5, 2002, pp. 30-38, (Meteorologiya i gidrologiya, № 5, 2002, pp. 40-50), in Russian.

[13] V.V. Plotnikov, *Ice conditions variability in the Far East Seas and its prediction*, Dalnauka, Vladivostok, p. 172, 2002, in Russian.

[14] V.I. Ponomarev, O.O. Trusenkova, D.D. Kaplunenko, and E.I. Ustinova, “Interannual Variations of Oceanographic and Meteorological Characteristics in the Sea of Okhotsk,” Proc. 2nd PICES Workshop on the Okhotsk Sea and Adjacent Areas, Nemuro, 9-12 Nov., 1998, Nemuro, 1999, pp. 31–40.

[15] V.I. Ponomarev, O.O. Trusenkova, S.T. Trusenkov, E.I. Ustinova, D.D. Kaplunenko, and A.M. Polyakova “The ENSO signal in the Northwest Pacific,” Proc. Science Board 98 Symp. 1997/98 El Nino event, Fairbanks, 14-25 Oct., 1998, PICES Scientific Report N 10, Sidney, Canada, 1999, pp. 9–31.

EXTREME DETERIORATION OF WATER QUALITY AND FISH SUFFOCATION PHENOMENA IN THE MARINE ESTUARY

Kira Slepchuk, Marine Hydrophysical Institute RAS
Tatyana Khmara, Marine Hydrophysical Institute RAS
Ekaterina Mankovskaya, Marine Hydrophysical Institute RAS

slepchuk@mhi.ras.ru

The factors that provoke fish suffocation in an estuary, namely: natural (small river runoff, high air and water temperature, water stratification) and anthropogenic (regulation of river, etc.) were marked. Taking into account these factors the calculations were carried out and the possible areas of the Dnieper-Bug estuary, where fish kill of different scale and genesis is found out were identified.

Keywords: water quality, fish suffocation, modeling, marine estuary.

I. INTRODUCTION

A large fish dying is a result of various anthropogenic impacts. It requires integrated exploration and detailed research. This phenomenon has the largest importance when the extreme situation has occurred on the water basin. In other words, a large fish dying is the threat for the ecosystem in whole.

To find out periodicity, areas, and possible reasons for an origin of a large fish dying and to work out the ways of avoiding such accidents in near future it needs to gather information, namely: water environment and weather conditions, incidents on various economic venues and etc.

The analysis of available information about suffocation phenomena in the Azov-Black Sea basin shows that except of the northwest Black Sea, more often the suffocation phenomena takes place in the Azov Sea, water reservoirs, lagoons and small ponds.

The aim is to analyze the extreme deterioration of water quality during suffocation phenomena in the sea mouth of the Dnieper and the South Bug rivers, which cause the local ecological disasters, to find ways to stop these disasters.

II. STATEMENT OF PROBLEM

The mouth of the Dnieper and the South Bug rivers is located in the northwest Black Sea (Fig.1), and this is an area of heavy shipping and recreation. This region has an important ecological value as a circulating water reservoir, where the Dnieper and the South Bug rivers discharge takes place. Because of the accumulating of the Dnieper runoff by six water reservoirs the runoff in the mouth is greatly decreased and its structure is changed during the year. Besides the water reservoirs discharge, which has an influence on the chemical regime of the Dnieper-Bug estuary, a bottom flatness of the estuary has a great importance in the organic matter distribution. The peculiarity of the estuary is that a navigation channel to the city of Kherson and to the city of Nikolaev passes along the estuary bottom. The channel depth ranges from 11 to 14 m (Fig. 1). Always being under

anthropogenic impact the commercial fishing on the Dnieper feels negative consequences of the runoff.

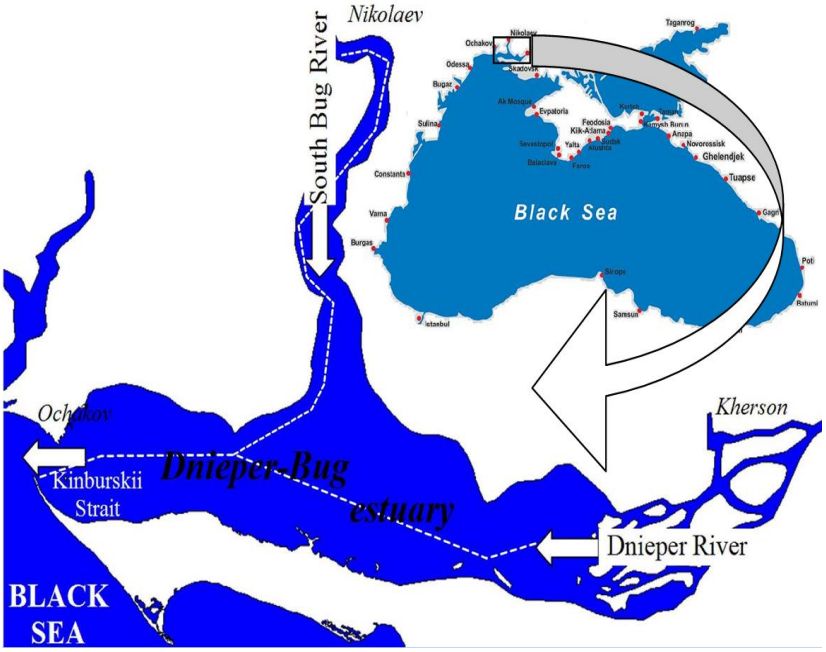

Fig.1. The map of the Dnieper-Bug estuary showing the location of the navigation channel (white dashed line).

In summer the water level in the Dnieper is lowered that even the current stops at all, and sometimes the back-stream appears. What is more it happens not only when the west wind drifts the water up the river but also when there is no wind at all. The current slowing depends on high summer temperature. The evaporation is quickly enlarged, and replenishment of any runoff (by means of rain-water) stops. Salty water may reach the lower Dnieper because of weak stream and west wind. So the hydrogen sulfide appears there and that is why the fish suffocation phenomena are happen.

The central part of the Dnieper-Bug estuary is not used by fish fauna for spawning. Close to the channel, areas can not serve as a full-fledged feeding area, and fishing areas. And fishing and feeding areas are confined to the shallow water. On the shallow water the water is usually mixed up decently and is saturated with oxygen. However, in summertime a lack of oxygen is often observed that is explained by the number of factors. The slowing of river velocity is of great importance during windless weather in hot summer. At temperature variations with depth enlargement the static zone appears. The photosynthetic processes take place on the surface where algae saturate water with oxygen. Also the algae are missing in the deep lightless layers. The fish activity declines while being in water with low oxygen concentration. The fish resistance to diseases and unfavorable environmental factors considerably reduces [1].

Also there are some differences in the dying fish species. If earlier there were bullhead, roach, kilka, silverside, crucian carp, flounder, but in some years mainly bullhead died (fish aged 1 –

4 years). This could be explained by biological peculiarities of this fish. That includes: small size, and as a result physical impossibility to get out of suffocation area.

A high amount of oxygen in water is used by excessive developing and further dying of blue-green algae in summer. During blooming this algae products oxygen in day-time and absorbs it at night, especially in early morning. By these entire facts oxygen gap appears in nonmoving ponds. And this is one of the reasons why fish die.

The blue-green algae significantly develop in so-called “blooming spots”. They usually appear in windless bays; although it depends on the year conditions, “blooming spots” may appear in open part of the water area. Also when biomass and its covered territory become larger the parts of “blooming spots” may be separated from the main body. And these parts begin to migrate on the water area because of the discharged current and wave influence.

Anthropogenic impact, even if it is not the main reason of the large fish dying, may increase its scope. Polluted environment reduces fish resistance to various external factors (temperature change, mineralization, gas regime, etc.).

To the factors given below we should add the intrabasin process of water quality forming, particularly, the polluting matter deposit in bottom sediments and their entering into water again when the certain conditions of water area were changed (pH, dissolved oxygen, etc.).

Among abiotic parameters of water ecosystem the bottom sediments hold a special place, because they are capable to concentrate different chemical substances (such as heavy metals, nature and anthropogenic organic matters, the products of their destruction, radionuclide, etc.). Depending on the water area conditions the bottom sediments may serve as pollution accumulator (self-purification) or as a source of pollution income to water (secondary pollution) [2].

The negative factors of ecological state in natural water area are dredging, containment on underwater soil dumps, sand extraction and other activities in the water. The increasing turbidity area is formed where the exchange of suspension and pollutants is happened. The feeding fish migration and spawning habitat are constantly decreasing. This leads to extreme decreasing of fish population and has bad influents on reproduction of the main native industrial fish species.

Frequently all negative above-listed facts below affect together, so that they strengthen each other. The examples of suffocation phenomena with description of hydrodynamic parameters are listed below.

In [3] the suffocation phenomena were explored in the Nikolaev Region in 2010 when seven events were registered from 4 to 23 August. The biggest activity of fish suffocation phenomenon was registered in the Black Sea on 5 August near the Koblevo village, on 6 August in the South Bug River, in the Dnieper-Bug and Bug estuary from 4 to 18 August accordingly. One reason of the suffocation phenomenon is the weather conditions. The stationary anticyclone was caused heat wave from July to August in the region. The average temperature was over the limit at that period on 2.5 – 4.8 °C. In June and July extreme high rainfall level was observed (194 and 140.1 % ratio, accordingly) that was aroused a high number of industrial waste washing. As a result a huge amount of organics get into the water area and this organics is the feeding source for blue-green algae. That forced the eutrophication which decreased the oxygen content in water and that helped to the suffocation phenomenon. These facts (extreme high rainfall level in June and July, water temperature increase) were extremely activated the suffocation phenomenon developing. The

windless weather at that period also belonged to adverse climatic factors. Because the water was stagnant and did not mix, no new fresh water that get into the water area.

Near 1 mil 280 thousand fish specimens have died in the estuary on 10 August 2010. As it was explained in the ecological administration the content of chlorides, sulphates and phosphates in the water was extremely higher than the maximum permissible concentration (MPC) for the commercial fishing water areas. The content of chlorine was 2532.36 – 4459.34 mg/dm^3 (MPC = 300 mg/dm^3); of sulphates 326.81 – 619.05 mg/dm^3 (MPC = 100 mg/dm^3); of phosphates 0.85 – 1.69 mg/dm^3 (MPC 0.17 mg/dm^3). According to official data from the State Ecological Inspection in Kherson region a high content of hydrogen sulphide from 2.22 to 7.03 mg/dm^3 was found in the Dnieper-Bug estuary.

III. METHODS OF INVESTIGATION

The 3-D unsteady hydrothermodynamic Model for Estuarine and Coastal Circulation Assessment (MECCA) [4] was used for the set of experiments about dynamic analyses of thermohaline water structure and current patterns in the low-water period and under different wind directions. The 1-D biogeochemical unit of the water eutrophication model is the system of interdependent differential equations, which describe biogeochemical cycles of biogenic elements, production and destruction of organic matter, oxygen dynamics at a local point of the water environment.

The rest state was taken as initial conditions. A homogeneous mass was taken in the horizontal plane as the thermohaline water structure at the initial time. The water environment was approximated into a horizontal grid 91 × 97 nodes with pitch at 600 m where the model was accommodated. The calculation was made in condition of low-water level when the discharge was 440 m^3 per sec for the Dnieper River and 46 m^3 per sec for the South Bug River.

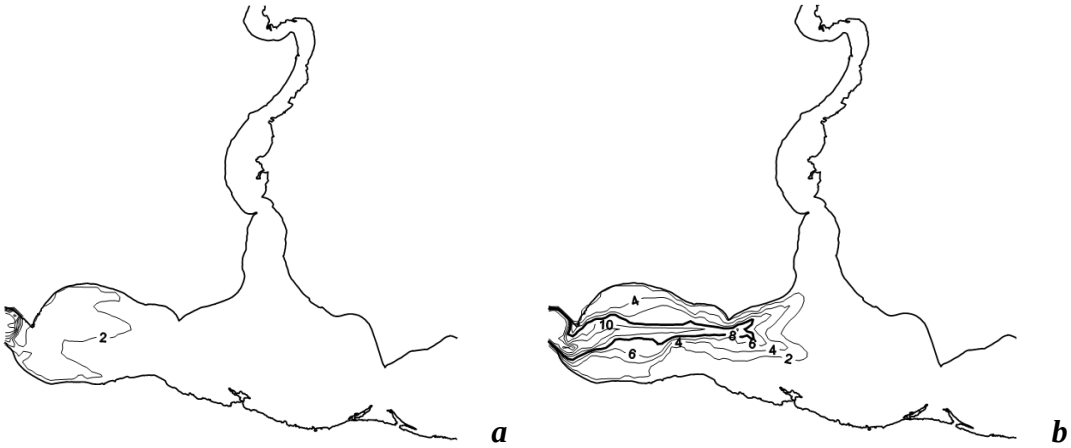

Fig.2. The graphical output showing the results of the hydrological model: salinity on the surface (a) and the bottom (b) layers under no wind condition.

IV. RESULTS OF RESEARCH

The salt water distribution in the estuary is provided on Fig.2. The wind and wave water mixing is impeded in windless and low-water level conditions. Fresh water gets into the surface

layer of estuary with river runoff. But in the bottom water layer we can find high salinity water of marine origin (10 – 14 ‰), because the salinity water flows on the navigation channel.

In the Dnieper-Bug estuary the fish suffocation phenomena are the most seen in the navigation channels, leading to Nikolaev and Kherson. Here hypoxia is developing in the navigation channel and this leads to the forming of the stable infesting hydrogen area where aquatic organisms die yearly. The fish suffocation phenomena is mostly seen in August (27% cases), in July (19% cases), it is less seen from October to March (0 – 8% cases) [1]. In the Kinburskii Strait the suffocation phenomenon is a rare fact, because there is a high level of flowing water and hydrodynamic activity.

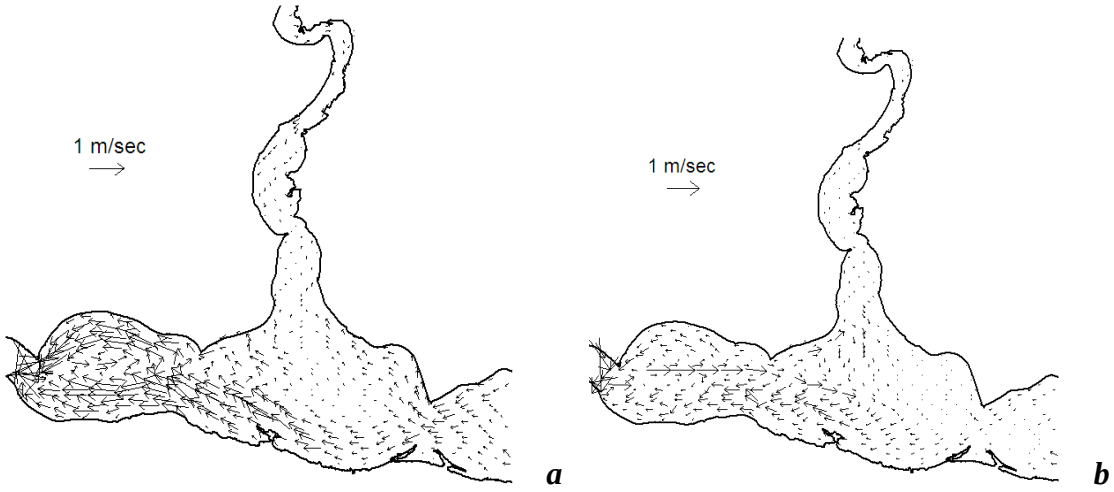

Fig.3. The current patterns on the surface (a) and the bottom (b) layers under no wind condition.

The surface and bottom current patterns in windless period are given on Fig.3. The water circulation pattern shows that in the windless and low-water period the surface flow is separated on two parts. One flow is strained along the northeast shore of the Bug estuary. Second flow is strained along the south shore of the estuary. The bottom flows are seen in the navigation channel. There are either gradient or compensational currents. In the bottom area flows are strained along the navigation channel in the whole water column. Than when the flow get the middle it bifurcates and its part get into the Bug estuary.

The river runoff dominates in the upper water layer, especially in the shallow areas of the west regions. The intensity of the Black Sea influence decreases in the other way. The water bloom is evolving because in summer the Dnieper River discharge is 500 m^3/s or less. In such condition the closed areas of increased sediment load appear in the central estuary part. They usually are in the position with the place of blue-green algae bloom.

The suffocation phenomena are less seen in the west area of the Dnieper estuary where the self-purification capacity of water is higher. Because more clear water gets through the Kinburskii Strait and the wind and wave activity is higher than in other estuary areas where the disposal of waist takes place.

The runoff flows speed reduces in several hours when the wind stops. The smaller river runoff and bigger water mass homogeneity in the estuary, the deeper the wind flows extend.

The modeling patterns of the surface and bottom currents in the surging wind 5 m/s is shown on Fig.4. The runoff flows are reduced under the influence of the surging wind especially in the surface water level because the wind currents are spread through all water body. It causes the water outset. The skewed level appears (Fig.3, *b*). Because of these the flows in the surface water level set in to the side of level rising. That is why the contradictions appear due to gravity in the bottom water level such as compensation and gradient flows. In the north shallow water area the drift flows prevail and in the navigational channel there are compensational currents.

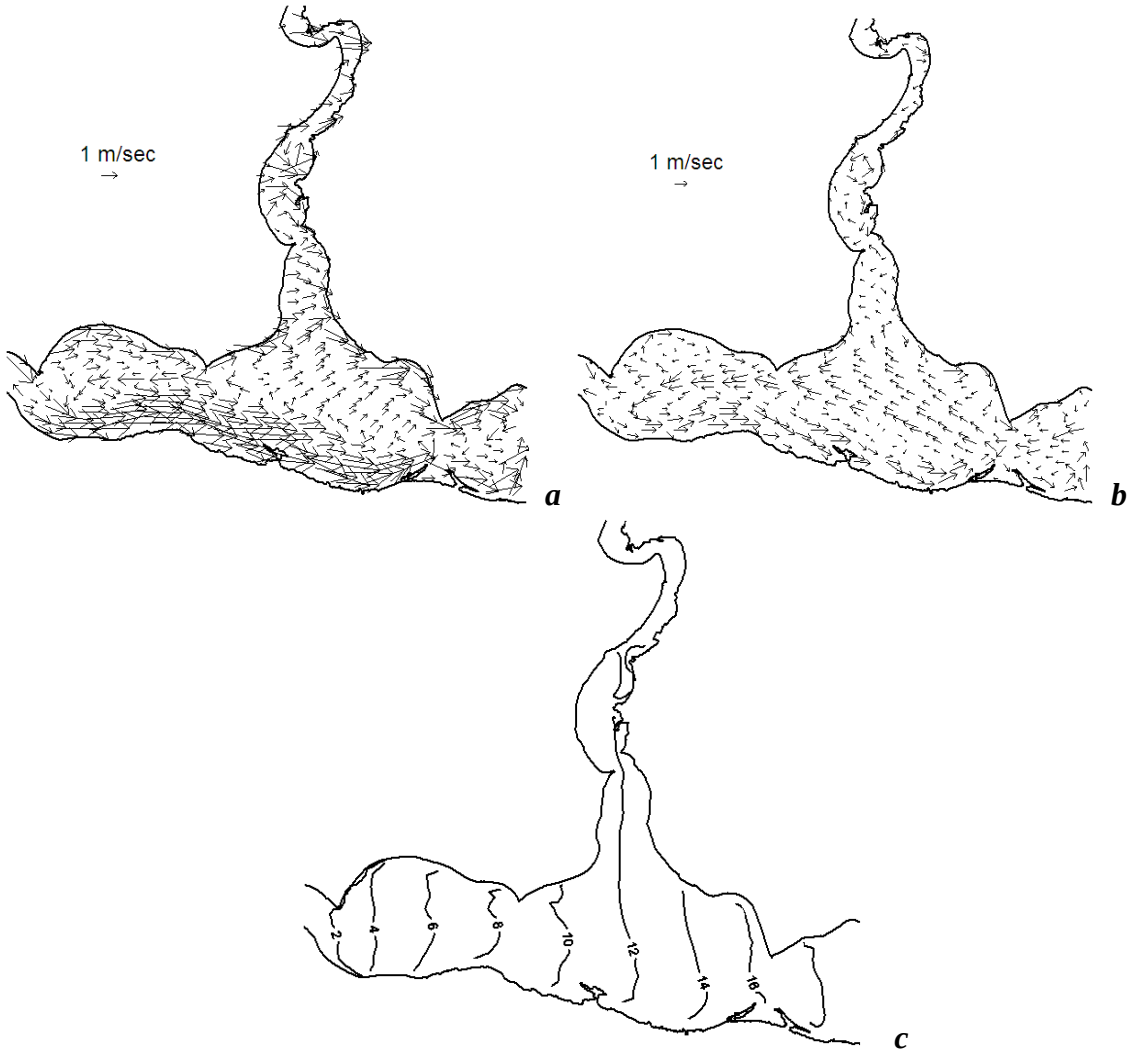

Fig.4. The current patterns on the surface (a) and the bottom (b) layers and sea level (cm) (c) under set-up wind.

It is known that wind-induced surges in the estuary have the influence on its gas regime, in particular on oxygen content in the water. When the water reservoir discharges water volume more than 1500 m^3/s, and the winds have north directions, the estuary are desalinated and oxygen is distributed as well as in a river water: in the vegetation period in the surface layer the oxygen

content reaches a maximum (20 – 23 mg/l), in the coastal areas even 30 mg/l; in the bottom layer its content is slightly lower. Under long set-up or calm water at the bottom (mainly in the navigation channel) the anaerobic zones appear, where there is no oxygen and hydrogen sulphide is presented.

The sea water surges reduce the intensity of photosynthesis process in the surface layers in the pelagial and littoral. Absolute and relative content of oxygen in water decreases with chloride growth (a chlorides increment 200 – 500 mg/l means an oxygen loss of 2 – 3 mg/l). In this regard, the lowest oxygen content is observed in the west region and in the Bug estuary, the largest one is in the east. It can explain not only the hydrological regime of each area, but also the degree of human impact.

Upper layer is saturated with oxygen and the generated organic matter enters in bottom layers and sediments. The velocity of oxygen process is bigger by increasing temperature that leads to decrease of oxygen concentration in natural layer. That may cause hypoxia which provokes hydrogen sulfide and suffocation phenomena. The annual dynamic of bottom water layer is shown on Fig.5 whish was calculated using 1-D version MECCA model. Oxygen maximum was in winter months (9 – 10 g/m^3) when the water temperature is low. The concentration decreases in spring and from the middle April it is lower than optimal standard that is established for commercial fishing water bodies (MPC = 6 gO_2/m^3) [1]. Hypoxia is from July to October (0.5 – 1.5 gO_2/m^3). Then the oxygen consumption decreases with lowering of temperature. This explains why oxygen value is higher in autumn and winter.

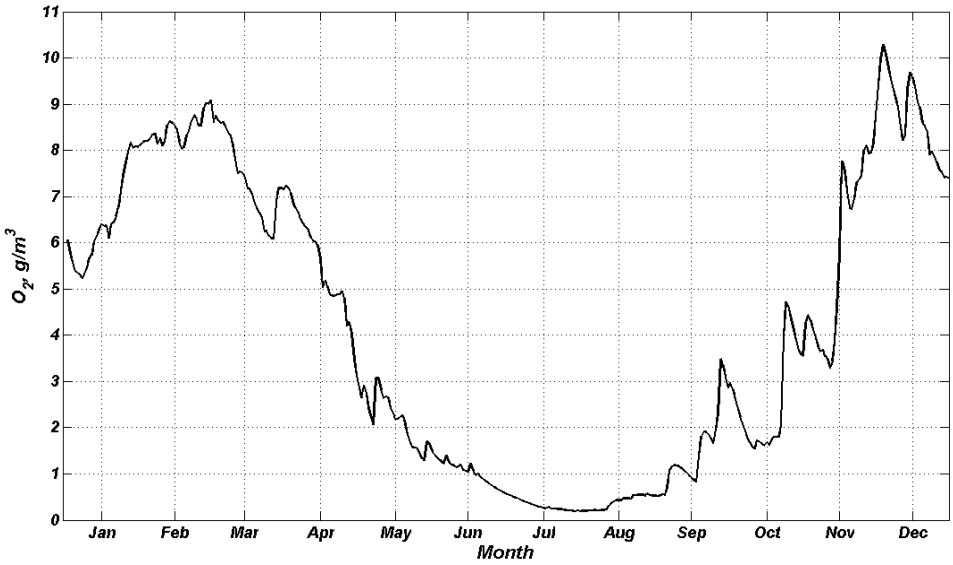

Fig.5. Distribution of oxygen on the bottom layer of the Dnieper-Bug estuary throughout the year, obtained from MECCA.

It is also known that in summer when there is excessive development and future die-off blue-green algae the large amount of oxygen dissolved in water is consumed. To study the phytoplankton dynamic we constructed the annual dynamics of phytoplankton biomass on the surface of the Dnieper-Bug estuary using 1-D version model MECCA.

The annual cycle of mean monthly value about chlorophyll concentration in this area is needed. This information may be get from the space scanner data. For example, SeaWiFS and MODIS-Aqua (*http://oceancolor.gsfc.nasa.gov*) which measure the ocean color change and the spaceborne scanners are used very often to determine optic characteristics of sea water and biochemical measurements. However the standard algorithm of space scanner data processing in SeaWiFS and MODIS-Aqua often gives incorrect estimation of concentration. For example, in [5] the overestimate chlorophyll concentration which was taken from the satellite data for the Barents Sea, the Black Sea and the Caspian Sea is shown incorrectly. This value was larger in several times than measuring data. That is why the required chlorophyll concentration in the Dnieper-Bug estuary was taken from [6] where was used the author's regional algorithm to calculation bio-optical parameters of the Black Sea according to satellite ocean color data.

The concentration of phytoplankton biomass is minimal in winter and in early spring (0.075 – 0.125 gC/m^3). The maximum of blooming is in summer and in early autumn (0.2 – 0.25 gC/m^3) (Fig.6). In spring the flood is going on the Dnieper and the South Bug Rivers which increases the input of biogenic and organic matter to the Dnieper-Bug estuary. Also the length of day and photosynthetic process increase. As a result the biomass of phytoplankton grows.

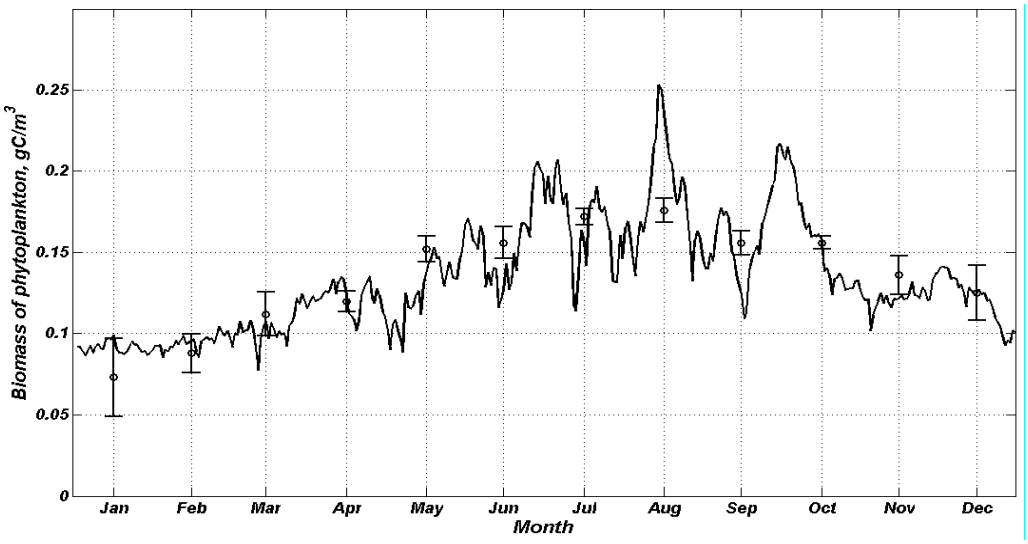

Fig.6. Distribution of biomass of phytoplankton on the surface layer of the Dnieper-Bug estuary throughout the year, obtained from MECCA.

V. CONCLUSIONS

The cause of fish suffocation phenomena is the combination of several negative ecological factors both natural and anthropogenic origin [7].

Natural facts are high temperature, lack of wind mixing in water ecosystem that reduces secondary pollution.

Anthropogenic facts are lack of water exchange before fish dying; storage of organic in water both easy and difficult oxidized; high concentrations of heavy metals and pesticides in water and bottom sediments that are capable to weaken the protective mechanisms of fish and other

aquatics and make them vulnerable to dramatic changes in environment; low oxygen concentration in high temperature; organic oxidation; hydrological conditions.

The suffocation phenomena damage is following: economical damage to commercial fishing and other services such as fish utilization service. The ecological damage is an increase of biodiversity and food chain destroy. The restore of estuary requires near 2 or 3 years.

To solve the suffocation phenomena the following ways are: preventive measures for overgrowing pretension with sea grass (it is recommended to cut sea grass during blooming); to exclude some fish species in order to optimize quality and quantity composition; to force the control for polluting sources in water during summer; to form interdepartmental commission for complex research on the fish suffocation phenomena stopping and remediation; to hold explanatory conversation within locals about the rules of conduct on water and prevention ways of the suffocation phenomena.

To develop protective measures, strategy of ecological accidents is necessary to organize complex observation of these events, to restore hydro-biological monitoring which was not carried out during last 20 years, to develop methods for forecast of water quality deterioration.

The operational model of ecosystem in the mouth of the Dnieper and the South Bug could be an analyze suffocation phenomena and forecast instrument.

VI. References

[1] V.N. Zhukinsky, L.A. Zhuravleva, A.I. Ivanov et al., *Dnieper-Bug estuarine system*. Kiev: Naukova Dumka, 1989. 374 p.

[2] P.N. Linnik, “Influence of various factors on the metal desorption from bottom sediments in the conditions of experimental modeling” // *Hydrobiological Journal*. 2006. 42, № 3. pp. 97-114.

[3] O.O. Shumilova, and G.G. Trokhimenko, “Study of mass fish suffocation phenomenon of in the Nikolaev Region in August, 2010” // *Electronic Journal*. 2010. № 5.

[4] V.A. Ivanov, and Yu.S. Tuchkovenko, *Applied mathematical water-quality modeling of shelf marine ecosystems*. Sevastopol: ECOSY-Hydrophysics, 2008. 311 p.

[5] O.V. Kopelevich, V.I. Burenkov, S.V Ershova, et al., “Application of SeaWiFS data for studying variability of bio-optical characteristics in the Barents, Black and Caspian Seas” // *Deep-Sea Research II*. 2004. vol. 51. pp.1063-1091.

[6] O.V. Kopelevich, V.I. Burenkov, S.V. Sheberstov, et al., *Bio-optical characteristics of the seas of Russia from data of the SeaWiFS satellite ocean color scanner*. CD-ROM. Moscow. SIO RAS. 2005.

[7] R.Yu. Minkovskaya, Local environmental disaster in the Dnieper-Bug mouth area // *Ecological safety of coastal and shelf zones and complex usage of shelf resources.* Sevastopol: ECOSY-Hydrophysics, 2010. 23. pp.166-170.

MAPPING BIOCHEMICAL FIELDS IN THE UPPER LAYER OF THE BLACK SEA BY THE ADAPTIVE BALANCE OF CAUSES METHOD

Inga P. Lazarchuk, Marine Hydrophysical Institute
Igor E. Timchenko, Marine Hydrophysical Institute

lazarchuk.syst.analysis@mhi-ras.ru

A simple ecosystem model of the upper layer of the north-western shelf of the Black Sea (NWS of BS) was considered. Estimates of phytoplankton, zooplankton, bioresources and oxygen concentrations were used as the basic biochemical characteristics of the ecosystem. The ecosystem was affected by external conditions: the seasonal temperature and chlorophyll-a concentrations. The adaptive balance of causes method was used to construct ecosystem model equations. The equations had the property of dynamic adaptation to variable external influences. Applying this model we illustrated the two-step method of modeling marine ecosystems processes, using adaptive models. On the first step, dynamics of water masses movement was calculated by a numerical model. On the second step, the ecosystem model made the local adjustment of ecosystem variables to each other, taking into account the available estimates of advection and diffusion of substances. In this simulation advection and diffusion calculated by the hydrodynamic model presented external forces relative to the ecosystem substances in the local volume. Maps of annual spatial and temporal variability of fields of phytoplankton, zooplankton, oxygen and biological resources concentrations in the upper layer NWS of BS were made. It was shown, that using data about the dynamics of marine environment in the adaptive models of ecosystems enable to detail the maps of biochemical fields.

Key words: adaptive balance of causes method, marine ecosystem

I. INTRODUCTION

Applied problems of monitoring the state of the marine environment for the use of its resources require the construction of diagnostic and prognostic maps of biochemical components of marine ecosystems, according to observations. The main source of these data, satellite observations are a component of the ecosystem, obtained by remote sensing of the sea surface. Therefore adaptation of model estimates of biochemical components of marine ecosystems, calculated on a relatively simple integral model, to satellite observations is one of the most of perspective directions using satellite information.

For mapping the fields of biochemical components of marine ecosystems are usually applied numerical models of high resolution in which the concentration of biological objects and chemical substances are calculated by the equations describing the transport and diffusion of substances in the sea [1]. In this paper, the possibilities of a two-step mapping biochemical fields by the method of adaptive balance of causes (ABC-method) that has the property of local adaptation of the model variables of the ecosystem are shown [2, 3]. In the first step are carried out calculations of currents

by hydrodynamic models to construct estimates of advection and diffusion in grid nodes covering the study area. On the second step these estimates and satellite observations are used as external sources of influence in special models of the marine ecosystem. Since the task of a detailed description of biochemical processes in this paper is not intended as a conceptual model of the upper layer of the marine ecosystem have chosen the simplest scheme of causality, including the concentration of phytoplankton, zooplankton, bioresourses and dissolved oxygen.

II. Adaptive Balance of Causes Method

Adaptive Balance of Causes method (ABC-method) was developed in the Marine hydrophysical institute and successfully used by the authors in the modeling of ecological-economic systems [3 - 5]. System principle of the adaptive balance causes [3] postulates the desire of all natural systems to a state of dynamic equilibrium with each other and attached to them external influences. The existence of equilibrium is due to the balance of positive and negative feedbacks, which are formed inside the system by causal relationships between processes. On the basis of this principle, in [3] proposed an adaptive balance the effects of the method for modeling of complex systems, which is constructed on two system concepts:

1. There is a universal modular equation expressing the rate of change of any of the processes modeled in the form of managed balance sheet growth trends and the decreasing of the process, which provides the internal balance of positive and negative feedback in each of the equations.

2. Combining modular equations to the system of dynamic equations of model should ensure the simultaneous pursuit of solutions of these equations to the stationary state of the system in which the intra-relationship between the development processes are adapted to each other and to external influences, exerted on the system.

To provide balance of feedbacks, to the right part of the universal modular ABC-method equation must have two basic function of causes $F^{(-)}(x)$ и $F^{(+)}(x)$. These functions impede both growth and decay of the simulated process x, directing its scenario to sustainable steady-state value

$$\frac{dx}{dt} = F^{(-)}(x)rx - F^{(+)}(x)rx. \qquad (1)$$

It is sufficient to require that with increasing x basic function $F^{(-)}(x)$ is monotonically decreasing, and basic function $F^{(+)}(x)$ monotonically increasing. In order to ensure the overall balance is necessary to put an additional condition for the normalization of the basic functions of causes

$$F^{(-)}(x) + F^{(+)}(x) = 2C, \qquad (2)$$

где C – current capacity of environment according to variable x of the system, r_i – parameters characterizing of the rate of change of variables.

In the ABC-method it is assumed that the current capacity of the environment is an average of the variability interval variable as the twice value of it sets the upper bound of the values x

$$0 < x < 2C \tag{3}$$

Taking into account the condition of balance (2) total modular equation of ABC-method takes the form

$$\frac{dx}{dt} = 2Crx\left[1 - \frac{1}{C}F^{(+)}(x)\right]. \tag{4}$$

Since as a function $F^{(+)}(x)$ any monotonically increasing function can be used, it is advisable to choose the most simple of them: $F^{(+)}(x) = x$. In this case, the modular equation of the ABC- method coincides with Verhulst equation [6] when C = 0,5.

The technique for combining modular equations (4) to the system to build ecosystem model is principle. The ABC-method introduce a suggestion that all influences $F_i\left(a_{ij}x_j, A_i\right)$, exerted on the variable x_i, must be taken into account additively in the argument base function of causes of the modular equation (4). Therefore, the total system of equations of the ecosystem model constructed by ABC-method takes the form

$$\frac{dx_i}{dt} = 2C_i r_i x_i\left\{1 - \frac{1}{C_i}F^{(+)}\left[x_i + F_i(a_{ij}x_j, A_i)\right]\right\}, \tag{5}$$

where a_{ij} – coefficients variables' influences on each other. In this case, intervals of variation of the variables is (0, 2C_i).

In common case, functions $F_i\left(x_j, A_i\right)$ is the sum the sum of intra $\frac{\partial x_i}{\partial x_j}x_j$ and external f_i influences

$$F_i\left(x_j, A_i\right) = \sum_{j=1}^{n-1}\frac{\partial x_i}{\partial x_j}x_j + f_i\,. \tag{6}$$

If we assume that intersystem relation is linear, i.e. $x_i = a_{ij}x_j$, then

$$F_i\left(x_j, A_i\right) = \sum_{j=1}^{n-1}a_{ij}x_j + f_i\,. \tag{7}$$

In this case, the system of equations of ecosystem model written by ABC method takes the form:

$$\frac{dx_i}{dt} = 2C_i r_i x_i \left\{ 1 - \frac{1}{C_i} \left[x_i - \sum_{j=1}^{n-1} a_{ij} x_j - f_i \right] \right\}, \ (i, j = 1,2,...,n), \ (i \neq j), \qquad (8)$$

The restriction of the limits to growth of variables depends not only on the current capacities of the natural environment in relation to the variables, but also on the intra-factors action. For example, the zooplankton concentration increase depends on the availability of all necessary resources: phytoplankton, oxygen, chemicals and other growth factors. At each time moment one of these factors is limited, because this type resources growth of concentration is a minimal amount comparing to the other resources. Therefore management agents should present in marine ecosystem models The management agents monitor and control the dynamics of resource provision of living organisms and the conditions of chemical reactions [3].

As a rule, the management agents are logical operators that switch functions of causes by the prescribed rules. One of the convenient expressions for a management agent can serve as a formula

$$AG_{x_i}(x_j) = \sum_{j=1}^{m} IF(x_j = M_{x_i}; a_{x_i/x_j} x_j; 0), \qquad (9)$$

$$M_{x_i} = \arg\min\{x_j\}, \ (i, j = 1, 2, \ldots, m).$$

Such switching functions of sources and sinks in the process of solving the equations of the ecosystem model increase the demands on the stability of the solution algorithms. Therefore, the stability of adaptive models of the second order, which is provided by negative feedback , is very useful when using the management agents growth of concentrations of ecosystem living objects.

III. Adaptive model of the Black Sea upper layer ecosystem

We call the ecosystem models **adaptive** if at the presence of external influences a model tends to the state of dynamical equilibrium with them. A mutual adaptation of the model values to each other and to the external influences occurs in the adaptive models, and a set of equations of the model "monitors" varying external influences keeping a state of dynamic balance with them.

As a conceptual model of the upper layer of the marine ecosystem have chosen the simplest scheme (Fig.1) of cause-effect relationships of processes taking place in the North-Western shelf of the Black Sea (NWS BS).

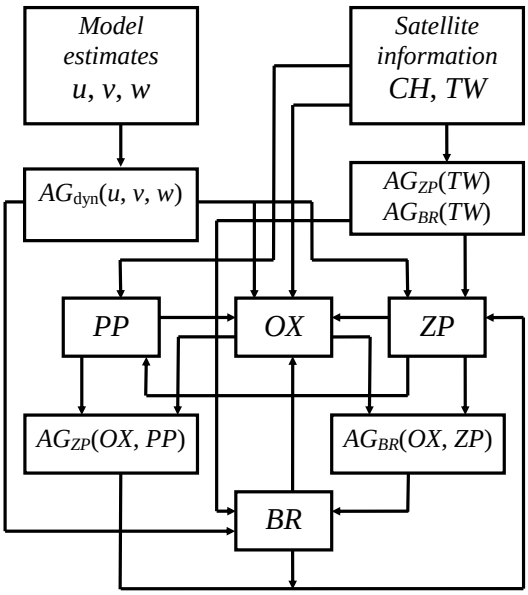

Fig. 1. Conceptual model of the upper layer of the sea ecosystem.

It includes the concentration of phytoplankton *PP*, zooplankton *ZP*, bioresource *BR* and dissolved oxygen *OX*. In addition to the structure of the model consists resource limitation agents of aquatic organism concentration in the food chain $AG_{ZP}(OX, PP)$ and $AG_{BR}(OX, ZP)$. Advection and diffusion estimates obtained from calculations of the currents velocity components *u, v* by the hydrodynamic model, the satellite observations data on sea surface temperature *TW* and chlorophyll-a concentration *CH* are used as the external influences. Therefore, the model includes agents taking into account the dynamics of oxygen $AG_{DYN}(OX)$, zooplankton $AG_{DYN}(ZP)$ and bioresource $AG_{DYN}(BR)$ concentrations. Also agents, taking into account the influence of the seasonal cycle of sea temperature on the concentrations of zooplankton $AG_{ZP}(TW)$ and bioresource $AG_{BR}(TW)$, are used in the Black Sea upper layer ecosystem model.

In accordance with the conceptual model (Fig.1) the system of equations of the ecosystem model is constructed by the adaptive balance of causes method. This system has the property of dynamic adaptation to changing external influences:

$$\frac{dPP}{dt} = 2PP\{5 - [PP - a_{PP/CH}CH + a_{PP/ZP}ZP]\},$$

$$\frac{dOX}{dt} = 2OX\{5 - [OX - AG_{DYN}(OX) + a_{OX/BR}BR + a_{OX/ZP}ZP - a_{OX/PP}PP + a_{OX/TW}TW]\},$$

$$\frac{dZP}{dt} = 2ZP\{5 - [ZP - AG_{DYN}(ZP) + a_{ZP/BR}BR - AG_{ZP}(OX, PP) - AG_{ZP}(TW)]\},$$

$$\frac{dBR}{dt} = 2BR\{5 - [BR - AG_{DYN}(BR) - AG_{BR}(OX, ZP) - AG_{BR}(TW)]\},$$

$$
\begin{aligned}
&AG_{ZP}(OX, PP) = IF[M_{ZP} = a_{ZP/OX} OX; a_{ZP/OX} OX; 0] + \\
&+ IF[M_{ZP} = a_{ZP/PP} PP; a_{ZP/PP} PP; 0], \\
&M_{ZP} = \arg\min[a_{ZP/OX} OX(t); a_{ZP/PP} PP(t)], \\
&AG_{BR}(OX, ZP) = IF[M_{BR} = a_{BR/OX} OX; a_{BR/OX} OX; 0] + \\
&+ IF[M_{BR} = a_{BR/ZP} ZP; a_{BR/ZP} ZP; 0], \\
&M_{BR} = \arg\min[a_{BR/OX} OX(t); a_{BR/ZP} ZP(t)], \\
&AG_{ZP}(TW) = a_{ZP/TW} \exp[-\alpha_{ZP}(TW - TW_{ZP}^{*})^2], \\
&AG_{BR}(TW) = a_{BR/TW} \exp[-\alpha_{BR}(TW - TW_{BR}^{*})^2].
\end{aligned}
\tag{10}
$$

$$
AG_{DYN}(\varphi) = a_{adv}\varphi_{adv} + a_{dif}\varphi_{dif} \ . \tag{11}
$$

For the comparison of scenarios to be easier, model variables were represented in dimensionless form and were reduced to the common interval of variability (0,10). It should be noted that phytoplankton advection and diffusion are indi-rectly taken into consideration in the equation (10) because the satellite measurement data on *CH* chlorophyll-a concentration, formed under effect of advection and diffusion, had been used as an external influence source in this equation. Through system of equations of the model this influence is also extended to other model variables. However, it is insignificant due to the fact that the influence of previous resource factors decreases with each transition to the new reaction. This is the cause of diffusion and advection inclusion in all other model equations. Current velocities and turbulent exchange coefficients, taken from the calculations by the hydrodynamic model, introduce an additional data on environment dynamics, therefore the management agents $AG_{DYN}(\varphi)$ in the system (10) are the additional sources of influences on the substance concentration changes.

IV. Mapping biochemical fields in the upper layer of the Black Sea

The adaptive ecosystem model considered above is applyed to map phytoplankton, zooplankton, bioresource and oxygen concentrations for the NWS BS region. To initialize the model the literature data, which have approximate estimations of average values of corresponding concentration fields, are used.

Based on the data characterizing the dynamics of the biomass of phytoplankton and edible zooplankton in 1954 – 2007s in the northwestern Black Sea shelf [7, 8], as estimates of the average values taken concentrations: C_{PP} = 6 g/m^3 и C_{ZP} = 0.2 g/m^3. The highest indicators of phytoplankton obtained on the shallow north-western part of the Black Sea, where the species of phytoplankton well supplied with nutrients coming from the waters of the Danube, the Dnieper, the Southern Bug, Dniester, and also due to intensive water exchange and closeness of the bottom where the regeneration of nutrients is. Also a special feature of this area is the presence of hydrological fronts formed by contact of river and sea waters [9]. Spatial distribution of planktonic organisms associated with the proliferation of fresh water in the area of hydrological fronts, blooming areas,

microorganisms spreading and wind regime. The redistribution of zooplankton significantly affects circulation arising in ebbs and surges winds [10].

Observations on the concentration of bioresource is highly fragmented and confined mainly the estuarine areas of the Danube and the Dnieper. For an approximate estimation of C_{BR} value the results of edible and gelatinous zooplankton biomass monitoring in these regions [8] are used. Relying on these data and also on the materials of [11] the value was adopted as an estimation of bioresource concentration average value C_{BR} = 0.1 g/m^3.

Literary sources contain a great number of data on oxygen concentration for the BS NWS region [12, 13]. It is noted that summer is a period of the lowest absolute oxygen content in the entire water column and water area of the region, which is due to increase of temperature and, consequently, rates of biochemical processes. Therefore the value equivalent to C_{OX} = 7 ml/l was adopted as an estimation of average annual oxygen concentration.

To map layer ecosystem fields in the BS NWS region there were used maps of chlorophyll-*a* concentrations fields and sea surface temperature, constructed according to satellite observations for the year 2012 (Fig.2, *a*, *b*), and maps of horizontal current field in the sea upper layer, constructed according to the data of the region hydrodynamic modeling [14] (Fig. 2, *c* – the longest arrow corresponds to 30 cm/s velocity), for each node of a square grid (which covered this region) with 5 km step (4004 nods). Calculations of fields of the ecosystem carried out for the year (366 calculation time steps – days). To illustrate used 228 day falling on mid-August, is characterized by increased values of sea surface temperature and chlorophyll *a* budget.

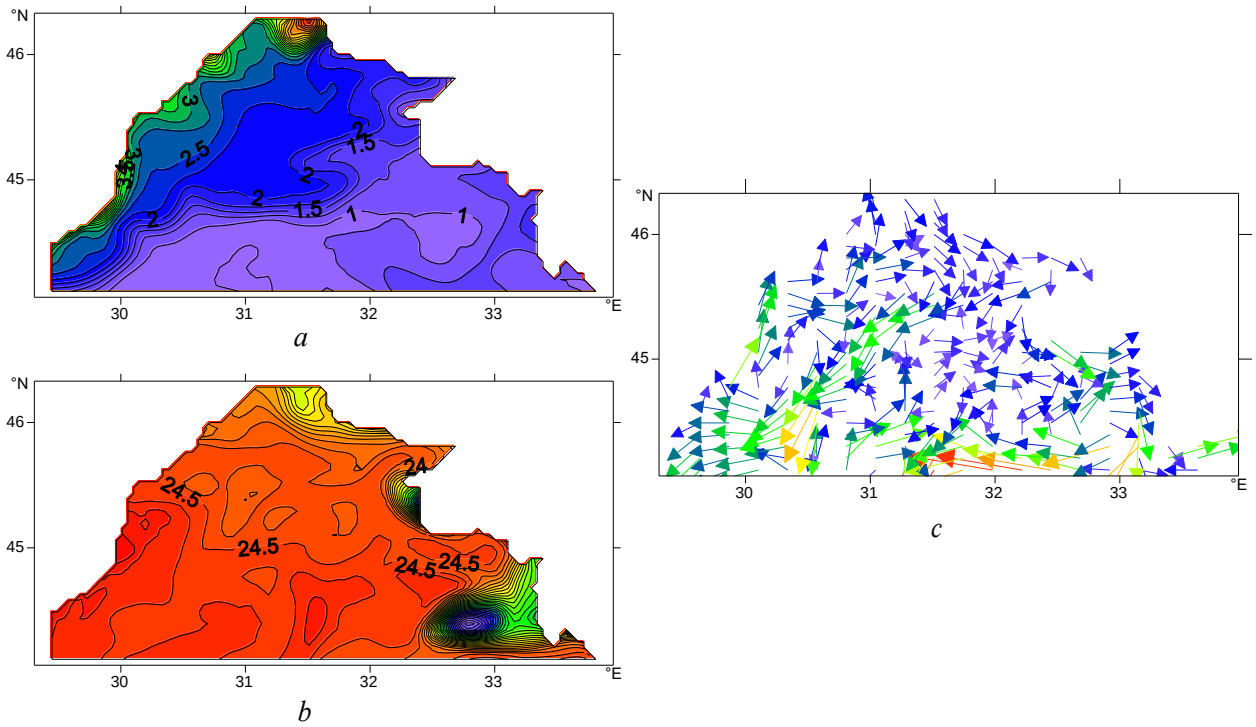

Fig. 2. NWS BS maps, obtained on 228 days of the year (mid-August) according satellite observations: a – chlorophyll-a (mg/m^3), b – sea surface temperature (°C); according numerical simulation data: c – currents.

Calculations of ecosystem variables were carried out in two stages. Initially, the model equations (10) were solved in each nod of the grid domain with no regard for advection and diffusion. As a result, the scenarios of within-year variation of all ecosystem parameters, by which the charts of substance concentration spatial distributions for each day were constructed subsequently, had been calculated. These data, alongside with the calculations of horizontal currents, were used to obtain the advection and diffusion assessments in each node of grid domain for each day of experiment. Advection and diffusion were calculated by standard finite-difference formulas.

At the second stage the local adaptation of model variables to the obtained advection and diffusion assessments was performed by means of model (10). These assessments were included into the management agents (11had the meaning of time intervals during which the advective and diffusive supplements to the concentrations of substances. Thus, the assessments of advection and diffusion have served as additional sources of external influences in the ecosystem model equations.

In Fig. 3, *a* map of phytoplankton concentration, constructed without taking into account the marine environment dynamicsпо by the temporal scenarios calculated in the nods of grid domain, is given. The structure of isolines on this map basically follows the one from Fig. 2, *a* (the map of chlorophyll-a concentration constructed according to the satellite data).

The map of oxygen concentration represented in Fig. 3, *б* demonstrates that it was sufficiently affected by satellite data on sea surface temperature and phytoplankton concentration. The map of sea surface temperature (Fig. 2, *б*), constructed by satellite data, contains a notable anomaly in the area of south-western coast of the Crimea, and this anomaly is due to anticyclonic gyres. This anomaly clearly manifested itself in the oxygen concentration field (Fig. 3, *б*).

A dominant role in the formation scenarios of zooplankton and bioresource concentrations play the minimum oxygen concentrations. Therefore it should be expected that the oxygen field anomaly will manifest itself in the maps of zooplankton and bioresource concentrations. The maps of these fields, represented in Fig. 3, *c*, *d* confirm this statement. The greatest zooplankton and bioresource concentrations are observed in the Danube estuary coastal regions and the lowest concentrations – in the area of oxygen field anomaly near the south-western coast of the Crimea.

The map of phytoplankton concentration, which was calculated taking into account the marine environment dynamics on the mid-August (the 228th day of computations is represented in Fig. 4, *a*. This field appeared to be more changeable in comparison with the one given in Fig.3, *a*, which was obtained at the first stage. Local inhomogeneities of chlorophyll-*a* field, which had been observed on the chart of its concentrations in Fig. 2, *a* near the north-western coast of the BS NWS water area, , were not visible in the chart of phytoplankton concentration (Fig. 3, *a*), constructed excluding the water dynamics. Taking into account the dynamics, they explicitly manifested themselves in Fig. 4, *a*.

This conclusion also extends to other ecosystem fields constructed with regard to advection and diffusion. This is evidenced by the results of the comparison of appropriate oxygen (Fig. 3, *b* and 4, *b*), zooplankton (Fig. 3, *c* and 4, *c*) and bioresource (Fig. 3, *d* and 4, *d*) concentrations. Thus, marine environment dynamics sufficiently affects the results of ecosystem field modeling using the Adaptive Balance of Causes method.

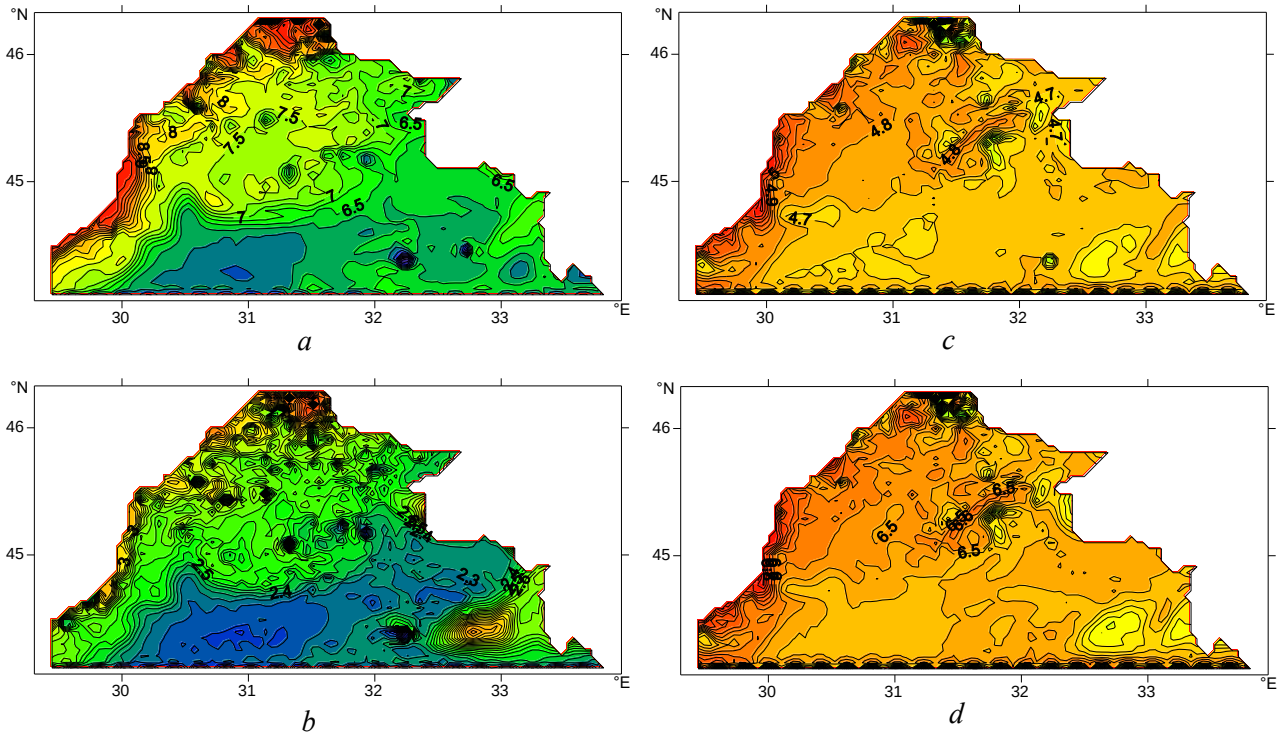

Fig. 3. Maps ecosystem fields, calculated without taking into account the dynamics of the marine environment 228 computing days (mid-August): a – phytoplankton (dimensionless units), b – oxygen (dimensionless units), c – zooplankton (dimensionless units), d – bioresource (dimensionless units).

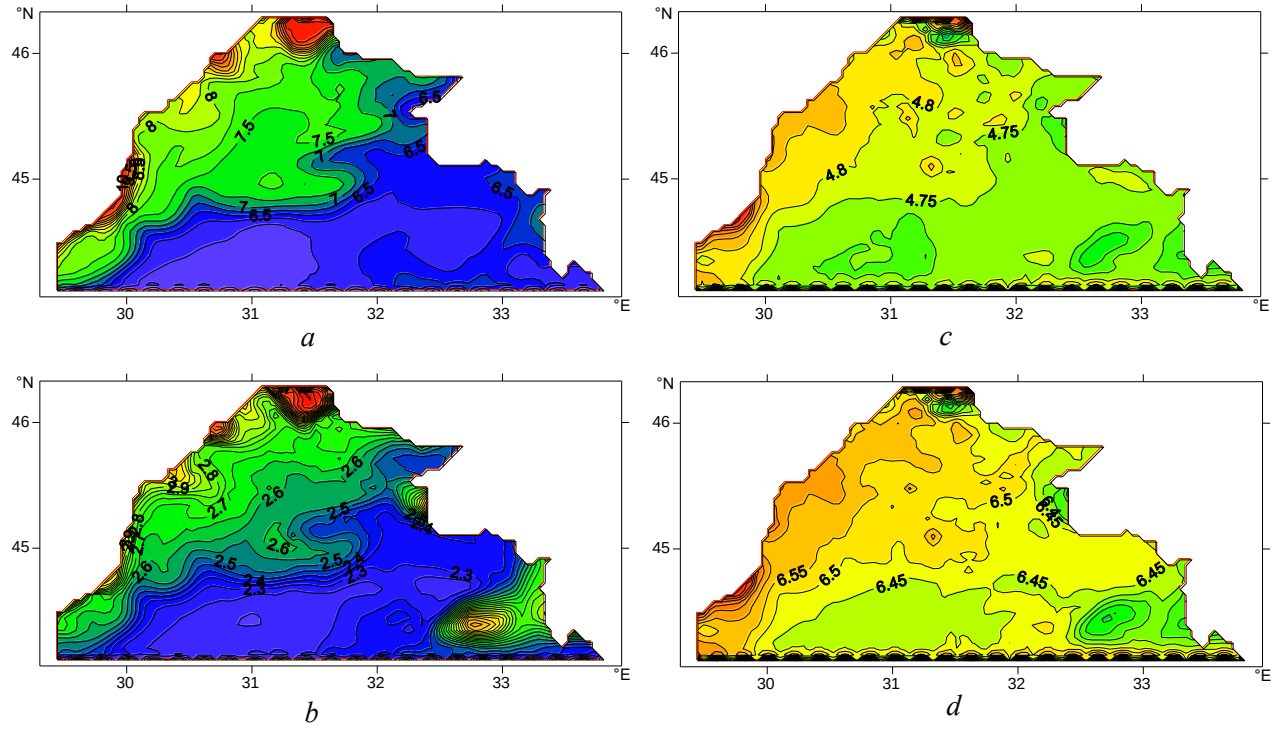

Fig. 4. Maps ecosystem fields calculated with advection and diffusion 228 computing days (mid-August): a – phytoplankton (dimensionless units), b – oxygen (dimensionless units), c – zooplankton (dimensionless units), d – bioresource (dimensionless units).

V. CONCLUSIONS

In the simple model of the ecosystem of NWS BS illustrates a two-step method of mapping fields of the upper layer of the sea ecosystem, which allows in a separate phase of the complex calculations of the transport processes and the diffusion of substances carried by hydrodynamic models and use the results as the external influences in adaptive ecosystem model. The equations of the method of adaptive influences balance adjustment provided fields phytoplankton concentrations of zooplankton, Life and oxygen to satellite data and to estimate the advection and diffusion, calculated according to the results of numerical modeling of the marine environment. ABC model of the marine ecosystem has been used for mapping intra spatial and temporal variability of phytoplankton concentrations fields, zooplankton, oxygen, biological resources in the upper layer NWS BS adapted to satellite observations of chlorophyll concentration and sea temperatures and surface. Thus, according to satellite data spatio-temporal dynamics of the ecosystem for this year's conditions were restored. It is shown that taking into account the dynamics of the marine environment and the agents of the resource limitation in adaptive ecosystem models allow us to detail maps of biochemical fields.

VI. REFERENCES

[1] G. K. Korotaev, T. Oguz, V. L. Dorofeyev, S. G. Demyshev, A. I. Kubryakov, et al, "Development of Black Sea nowcasting and forecasting system", *Ocean Sci.*, no. 7, pp. 629-649, 2011.

[2] I.E. Timchenko, E.M. Igumnova, I.I. Timchenko, *System Management and ABC-technologies of sustainable development*, Sevastopol, ECOSI-Gidrofizika, 2000, 225 p. (in Russian).

[3] V.A. Ivanov, E.M. Igumnova, I.E. Timchenko, *Coastal Zone Resources Management*, Kyiv, Akademperiodika, 2012, 304 p.

[4] I.E. Timchenko, V.A. Zhorov, E.M. Igumnova, I.P. Lazarchuk, "Dynamic model of integrated processes in the ecosystem of the northwest shelf of the Black Sea", *Physical Oceanography*, vol. 17, issue 4, pp. 223-241, 2007 (Translated from Morskoi Gidrofizicheskii Zhurnal, No. 4, pp. 48-69, 2007).

[5] I.E. Timchenko, I.K.Ivashchenko, E.M. Igumnova, I.P. Lazarchuk, "Estimation of the space distributions of the parameters of marine ecosystems by the method of adaptive balance of causes Sea", *Physical Oceanography*, vol. 21, issue 5, pp.338-352, 2012. (Translated from Morskoi Gidrofizicheskii Zhurnal, No. 5, pp. 50–65, 2011)

[6] J.D Murray. *Mathematical biology II: Spatial models and biomedical applications*, 3rd edition. Springer, 2008, 736 p.

[7] D. Nesterova, S. Moncheva, A. Mikaelyan, A. Vershinin, V. Akatov et al. "The state of phytoplankton", *State of the Environment of the Black Sea (2001– 2006/7)*,Istanbul, Turkey, 2008, pp.173-200.

[8] T. Shiganova., E. Musaeva, E. Arashkevich, L. Kamburska, K. Stephanova et al. "The State of Zooplankton", *State of the Environment of the Black Sea (2001– 2006/7)*,Istanbul, Turkey, 2008, pp. 201- 246.

[9] L. V. Grigorieva, L.G. Senichkina. "Phytoplankton of the Black sea: the current state and prospects of research ", *Ecology of the sea*, vol.45, pp.6-13, 1996. (in Russian).

[10] V. I. Belyaev, N.V. Konduforova " *Mathematical modeling of ecological systems of shelf* ",Kyiv.: Naukova dumka, 1990, 240 p. (in Russian).

[11] V.S. Latun,."The impact of fisheries on the sustainability of the Black Sea ecosystem", *Stability and evolution of oceanographic characteristics of the Black Sea ecosystem*, Sevastopol, ECOSI-Gidrofizika, 2012, pp. 331-353 (in Russian).

[12] V.A. Emelyanov, A.Yu. Mitropolskiy, E.I. Nasedkin A. A. Pasynkov, Yu. D. Stepanyak, et al, *Geoecology Ukrainian Black Sea shelf*, Kyiv, Akademperiodika, 2004, 296 p. (in Russian).

[13] I.G. Orlova, M.Yu. Pavlenko, V.V. Ukrainskiy, Yu.I. Popov, *Hydrological and hydro-chemical indicators of the northwest shelf of the Black Sea*, Chief Ed. I.D. Loeva, Kyiv, KNT, 2008,616 p. (in Ukrainian)

[14] 7. *http://www.myocean.eu/* (date: 03 of June 2013).

NUMERICAL SIMULATION OF THE SEMIDIURNAL TIDAL WAVE IMPACT ON THE BLACK SEA CLIMATIC CIRCULATION

Anna Lukyanova, Marine Hydrophysical Institute
Andrei Bagaev, Marine Hydrophysical Institute
Vladimir Zalesny, Institute of Numerical Mathematics
Vitaliy Ivanov, Marine Hydrophysical Institute

annieromanenko@gmail.com

The Black Sea is an enclosed deep marine basin, where the structure of tidal movements is dominated by the direct influence of the tidal force on the proper water body. We investigated the spatial structure of its climatic circulation under the impact of tides. We developed a program module extending the numerical general circulation model of the Black Sea which was designed in the Institute of numerical mathematics, Moscow. It allows the lunar semidiurnal harmonics (M_2) influence to be taken into account explicitly via the discrete analogues of the differential equations of motion. Our work reflects the main results of the numerical experiment on the 4x4 km horizontal grid and 40 vertical σ-levels. It was a one-year model run using the CORE atmospheric climatology forcing. We compared the first and the last weeks of simulation and found out that the characteristics of a tidal mode M2 were established at a very short period of time (7 days), which is the estimate of the model's energy redistribution time scale. The coastal areas where the tidal impact is substantial (~10 cm) were located mainly at the shallow-shelf inlets highly influenced by the climate change. Validation of the cotidal maps showed the reliability of our model at the climatological time scale. In future we will focus on the baroclinic tidal movements and validation with the Marine Hydrophysical Institute database in order to shed new light on physical and ecological processes at the frontal zone along the Rim Current.

Key words: coastal dynamics, numerical modeling, Black Sea, tidal waves.

I. DESCRIPTION OF THE MODEL

The circulation model of the Black and the Azov Seas was developed at the Institute of numerical mathematics (INM) of the Russian Academy of Sciences (RAS). It is based on a system of primitive equations written in the spherical coordinate system with the approximations of hydrostatics and Boussinesq. The equations of the model are written in the symmetrized form, as follows:

$$D_t u - H(l+\xi)v = \frac{-H}{\rho_0 r_x}\left[\frac{\partial}{\partial x}\left(p - \frac{g}{2}Z\rho\right) - \frac{g}{2}\left(\rho\frac{\partial Z}{\partial x} - Z\frac{\partial \rho}{\partial x}\right)\right] + \frac{1}{H}\frac{\partial}{\partial \sigma}\nu\frac{\partial u}{\partial \sigma} + D_u u + Q_1, \quad (1)$$

$$D_t v + H(l+\xi)u = \frac{-H}{\rho_0 r_y}\left[\frac{\partial}{\partial y}\left(p - \frac{g}{2}Z\rho\right) - \frac{g}{2}\left(\rho\frac{\partial Z}{\partial y} - Z\frac{\partial \rho}{\partial y}\right)\right] + \frac{1}{H}\frac{\partial}{\partial \sigma}\nu\frac{\partial v}{\partial \sigma} + D_u v + Q_2, \quad (2)$$

$$\frac{\partial}{\partial \sigma}\left(p - \frac{g}{2}Z\rho\right) = \frac{g}{2}\left(\rho\frac{\partial Z}{\partial \sigma} - Z\frac{\partial \rho}{\partial \sigma}\right), \quad (3)$$

$$\frac{-\partial \varsigma}{\partial t}+\frac{1}{r_x r_y}\left[\frac{\partial}{\partial x}\left(Hr_y u\right)+\frac{\partial}{\partial y}\left(Hr_x v\right)\right]+\frac{\partial \omega}{\partial \sigma}=0, \quad (4)$$

$$D_t T=\frac{1}{H}\frac{\partial}{\partial \sigma}\nu_T\frac{\partial T}{\partial \sigma}+D_T T+\frac{\partial R}{\partial \sigma}, \quad (5)$$

$$D_t S=\frac{1}{H}\frac{\partial}{\partial \sigma}\nu_S\frac{\partial S}{\partial \sigma}+D_S S, \quad (6)$$

$$\rho\equiv\rho(T,S,Z)=\tilde{\rho}(T+\bar{T},S+\bar{S},\rho_0 gZ)-\tilde{\rho}(\bar{T},\bar{S},\rho_0 gZ) \quad (7)$$

In (1) – (7) x – longitude, y – latitude, r_x, r_y –metric coefficients $r_x=R_E cosy,\quad r_y=R_E, R_E-$ the Earth's radius; $Z=H\sigma,$

$$l=2\tilde{\Omega}\sin y\ ,\xi=\frac{1}{r_x r_y}\left(\frac{\partial r_y}{\partial x}v-\frac{\partial r_x}{\partial y}u\right), \quad (8)$$

l – Coriolis parameter, $\tilde{\Omega}$– the Earth angular velocity. D_t – transport operator written in the symmetrized form:

$$D_t\varphi\equiv D_t(u)=$$
$$H\frac{\partial \varphi}{\partial t}+\frac{1}{2r_x r_y}\left[\frac{\partial}{\partial x}\left(Hr_y u\varphi\right)+Hr_y u\frac{\partial \varphi}{\partial x}+\frac{\partial}{\partial y}\left(Hr_x v\varphi\right)+Hr_x v\frac{\partial \varphi}{\partial y}\right]+$$
$$+\frac{1}{2}\left[\frac{\partial}{\partial \sigma}\left(\omega\varphi\right)+\omega\frac{\partial \varphi}{\partial \sigma}\right], \quad (9)$$

$\boldsymbol{u}$= (u, v, ω) – velocity vector in a σ-coordinate system ω – velocity in a σ – system, w – vertical velocity in a z – system,

$$\omega=w-\left[(1-\sigma)\frac{\partial \varsigma}{\partial t}+\frac{u}{r_x}\frac{\partial Z}{\partial x}+\frac{v}{r_y}\frac{\partial Z}{\partial y}\right]. \quad (10)$$

In (10) T, S - potential temperature and salinity deviations from the mean values $\bar{T}$ and $\bar{S}$, R- the penetrative radiation flux, ρ – density deviation , ν, ν_T, ν_s – coefficients of vertical turbulent viscosity and diffusion. In (1), (2) $Q_1$and Q_2– zonal and meridional components of the tidal force, respectively. The system of equations is accompanied with the set of boundary and initial conditions, given in [1, 2].

The numerical algorithm for solution of the problem is based on the technique of a multicomponent splitting [3]. The linear subsystem of shallow water equations including tidal influence is computed at a separate splitting stage.

II. Description of the formulae of tidal influence

Components of the tidal force Q_1 и Q_2 in $\frac{cm}{sec^2}$ are defined as:

$$Q_1=-5.3*10^{-5}cos\varphi sin\left(F_{M_2}t+2\lambda+\Phi_{M_2}\right), \quad (11)$$

$$Q_2=-5.3*10^{-5}*cos\varphi sin\varphi\cos\left(F_{M_2}t+2\lambda+\Phi_{M_2}\right), \quad (12)$$

where $\lambda \in [0,2\pi], \varphi \in [0,\pi]$ – geographical coordinates of the considered point, F_{M_2}= 0.00128 $\frac{rad}{sec}$ – frequency of the lunar semidiurnal tidal harmonic M_2, Φ_{M_2}=0 – phase, t – mean solar time [3]. Mean solar time in seconds is calculated from the local time t_0 and longitude λ as follows:

$$t = t_0 - 240 * \lambda.$$

Formulae (11), (12) are found by the method of harmonic representation of the tidal potential [4], which is the approximation and allows neglecting the coordinates of tidal celestial bodies.

III. Description of the Experiment

The spatial resolution of the model is $(0°3') \times (0°2'24'')$ in the longitude and latitude respectively. 40 σ – layers are nonuniformly distributed over the depth. Input data including bottom topography, boundary and initial conditions are the same as in [2].

For the computation of atmospheric forcing in the model we use the CORE Normal Year data with the resolution 1.825° on the longitude (192 points) and a nonuniform latitude grid (94 points) [5].

The model simulation was performed for one year with a 5-minute time step. The main aim of the experiment was to verify the model.

Harmonic constants M_2 were calculated using the least square method according to the data of the sea level obtained after a 7-day calculation with the output resolution of 45 minutes.

Verification of the model

According to the results of a numerical experiment, in the structure of circulation there is a pronounced Rim Current localized in the area of the continental slope (Fig. 1a, b). The circulation field gets intensified in winter (Fig. 1a) and weakened in summer (Fig. 1b), which corresponds to the used wind field.

The structure of the circulation agrees well with the existing concept of the circulation patterns in the Black Sea [6]. Two large-scale cyclonic gyres in the eastern and the western parts of the sea are poorly reproduced by the model due to the coarse spatial resolution of the applied atmospheric forcing (Fig. 2).

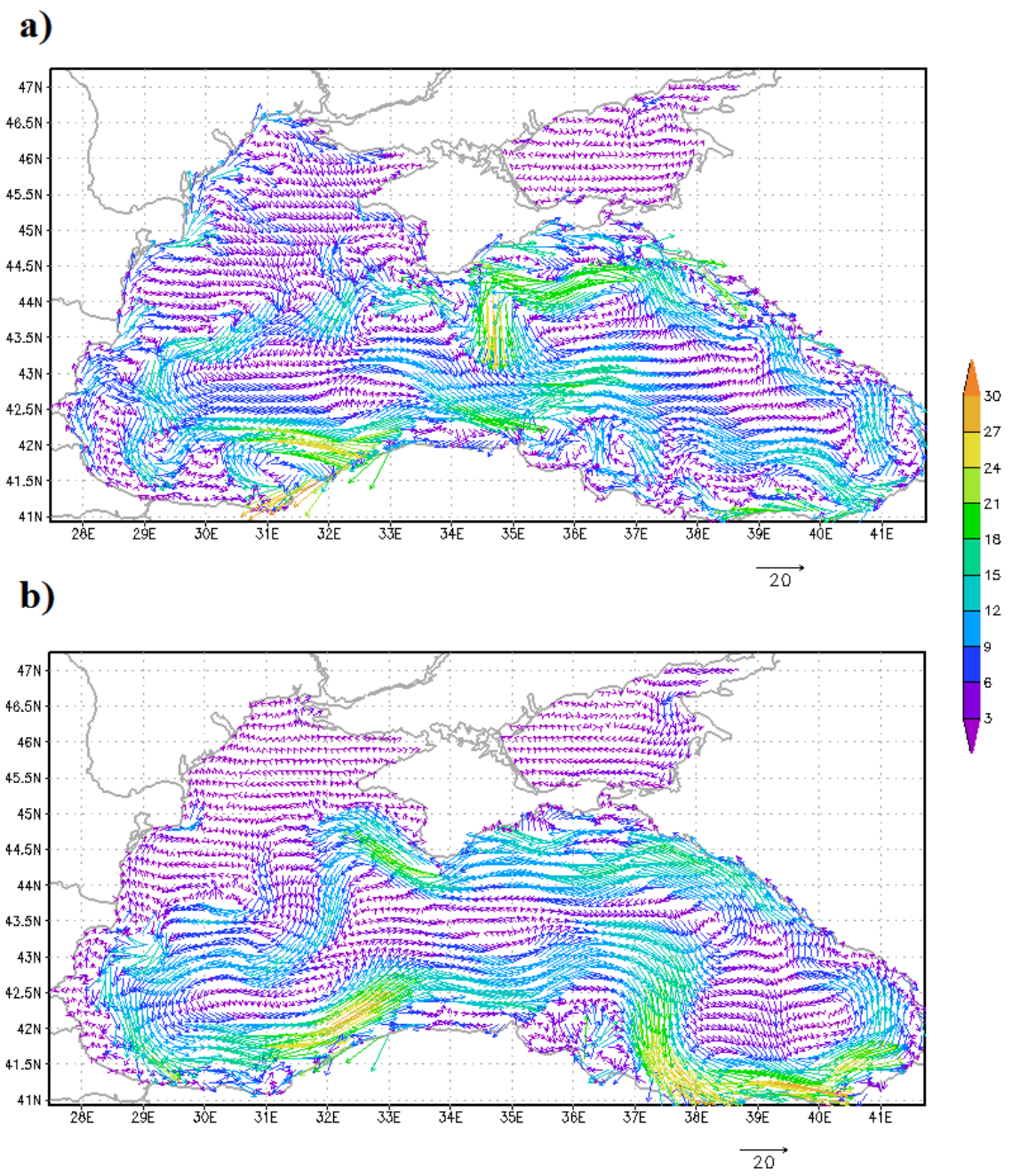

Fig. 1. Monthly mean velocity field, depth - 5m: a) – February, b) – August. The scale of velocity vectors is shown under the maps, in cm/s. Every second latitudinal point and every fourth longitudinal point are plotted. Magnitude colour scale is given on the right.

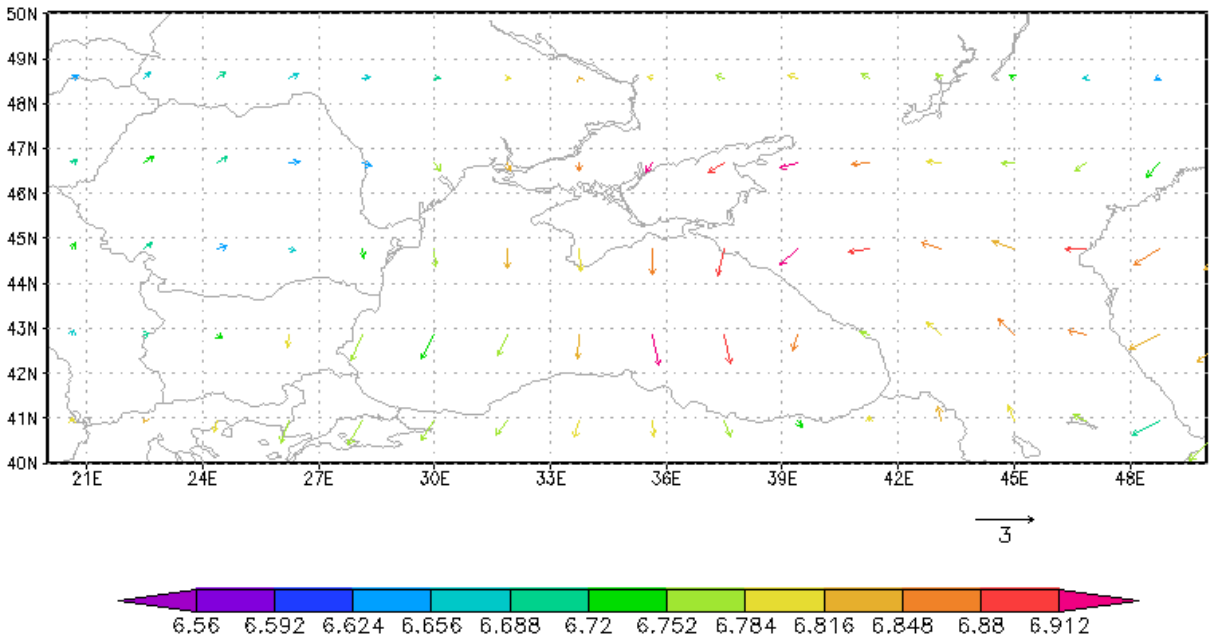

Fig. 2. Mean annual wind circulation field according to the CORE data (m/sec). Magnitude colour scale is given below the map.

The dynamic level of the sea surface is distributed evenly throughout the experiment and corresponds to the cyclonic circulation (Fig. 3). In the eastern part of the basin there is a stable area of minimal level values, as in [7]. The results of the model agree well with the results from [1, 2].

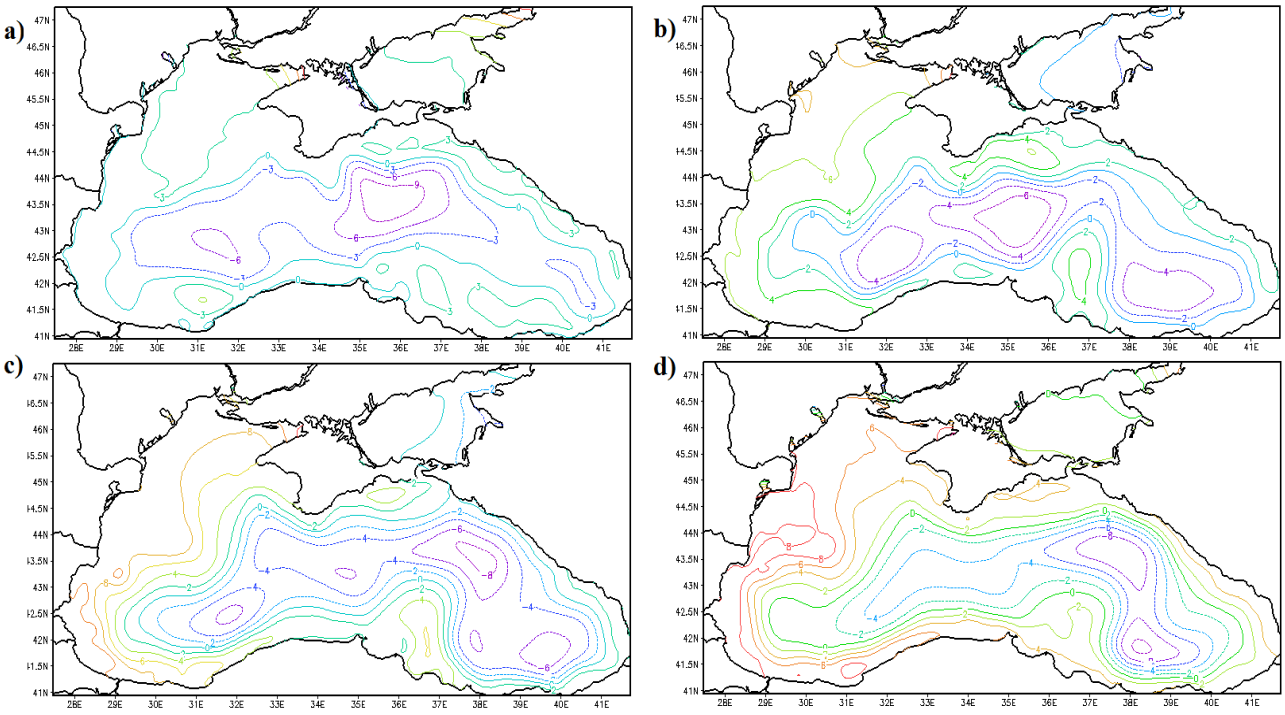

Fig. 3. Mean monthly topography of the sea level (in cm): a) February; b) May; c) August; d) November.

The Cold Intermediate Layer (CIL) is visible at the depths of 40-100 m. It is well reproduced by the model during the all period of the calculation (Fig.4). In February the CIL is renewed and, consequently, it appears at the depths of 0 – 50 m (Fig. 4a). In August (Fig. 4b) the CIL is positioned at the depths of 20 – 80 m, with its core (T<7.5°C) found at 25 – 50 m.

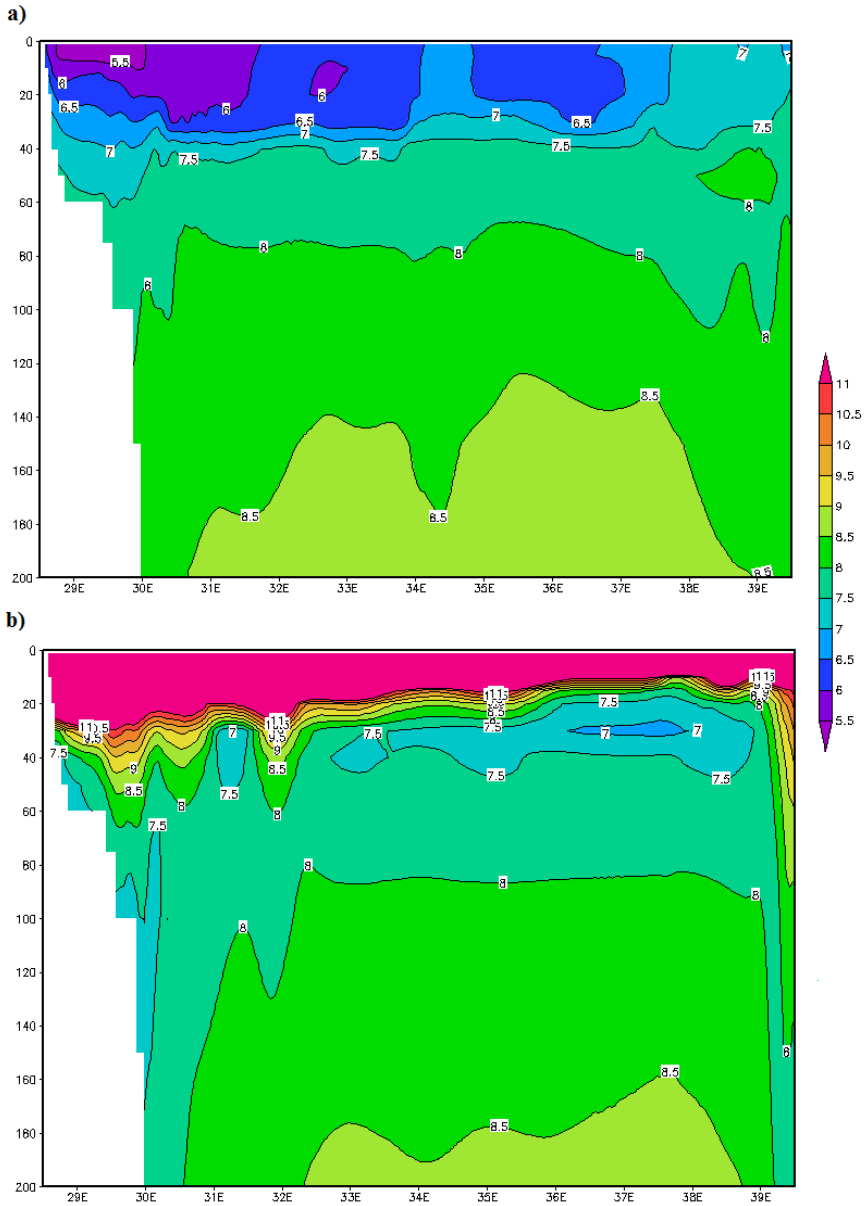

Fig.4. Monthly mean temperature field in °C on the latitudinal cross-section at 43.7°N, a) February, b) March. Magnitude colour scale is given below the map.

IV. Results. Concerning the tides

In the barotropic run with no account of the wind the amplitude and the phase of the tidal harmonics M_2 are established at the second week of the calculations (Fig. 5). Maximum amplitudes of the tidal lunar semidiurnal harmonic are up to 6 – 8 cm, according to the model, and are located in the area of the Karkinit Bay.

The influence of the baroclinity of the sea water and wind on the changes in harmonic stable waves M_2 is remarkable. In the following experiments of the circulation of the Black and the Azov Seas, the model of the INM RAS took into account the baroclinity of the marine water and the wind. In such cases, the maps of harmonic characteristics of the waves during the computational year differed insignificantly: the nodal point was shifted, the M_2 amplitudes changed by 0.5-1cm (Fig. 6a, 6b).

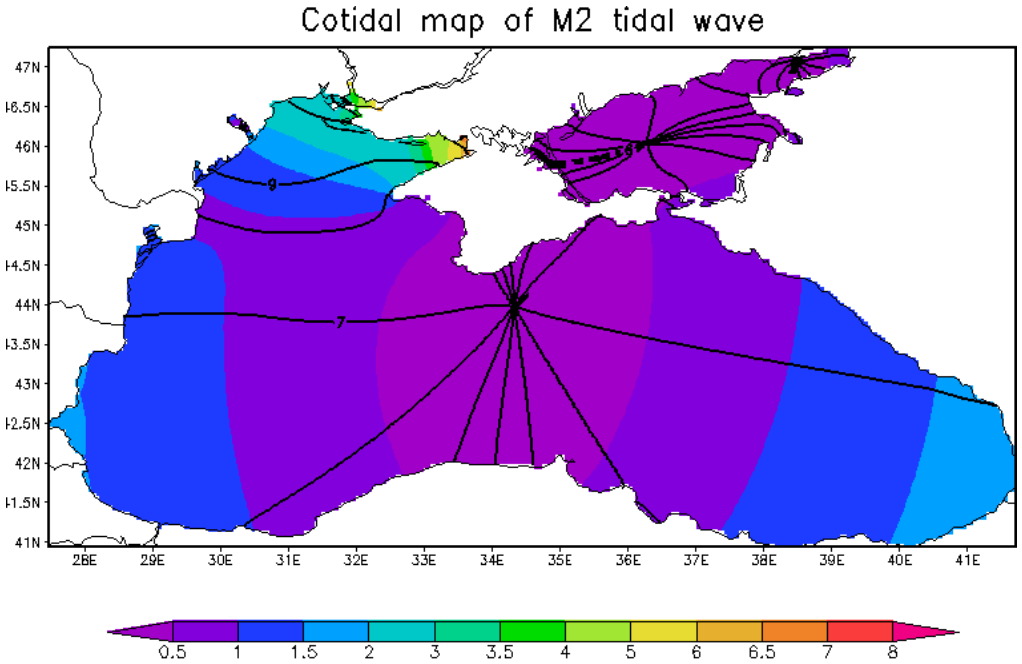

Fig. 5. Harmonic characteristics of the tidal harmonics M_2. Cotidal lines are black (in hours), equal amplitudes are coloured (the scale is in cm).

Comparison with the observations data

In order to validate the tidal characteristics given by the model, we compare it with the in-situ observations [8, 9]. Field observations analyzed the oscillation spectrum of the Black Sea according to the prolonged sets of studies at 23 stations. The comparison of the amplitudes of the lunar semidiurnal harmonics resulting from the model with the field research showed fine quantitative agreement (table 1).

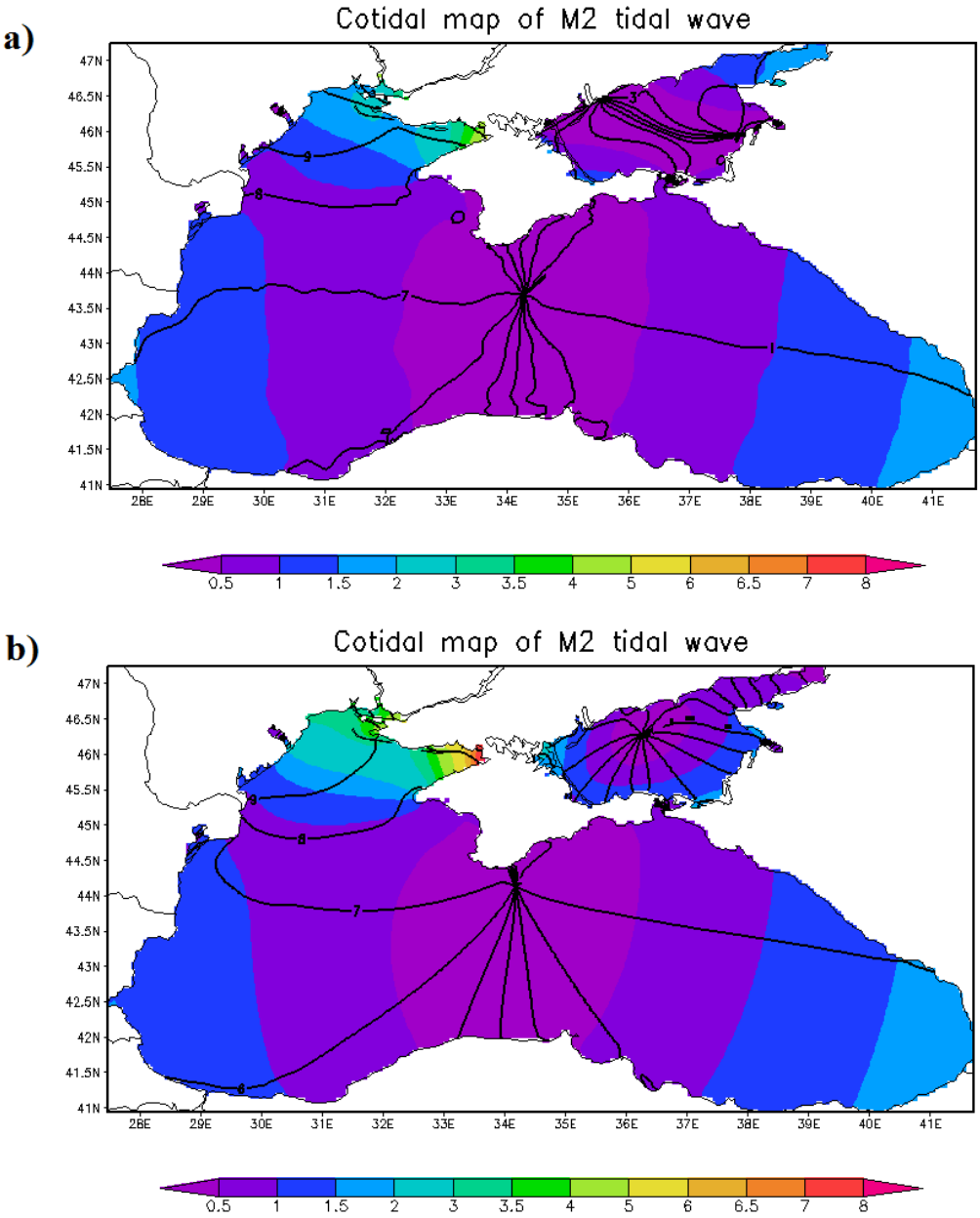

Fig. 6. Harmonic characteristics of the tidal harmonics M_2*: a) baroclinic model with the wind influence; b) barotropic model with the wind influence. Cotidal lines are black (in hours), equal amplitudes are coloured (the scale is in cm).*

Table 1. Comparative table of the M_2 amplitudes according to the results of the modelling and field observations.

Location	Observations data, cm	Modelling results, cm
Prorva	0.9-1.7	1-1.5
Odessa	2-3	2-3
Yalta	0.1-0.5	0-0.5
Batumi	2.3-2.8	1.5-2

Tidal oscillations of the sea level from both sources (field data and data obtained from numerical modelling) are appeared as sharp delta-shaped peaks, corresponding to the frequency of the tidal harmonic M_2 (Fig. 7). The values of spectral maximums taken from the field data and from the modelling results are of the same order [9].

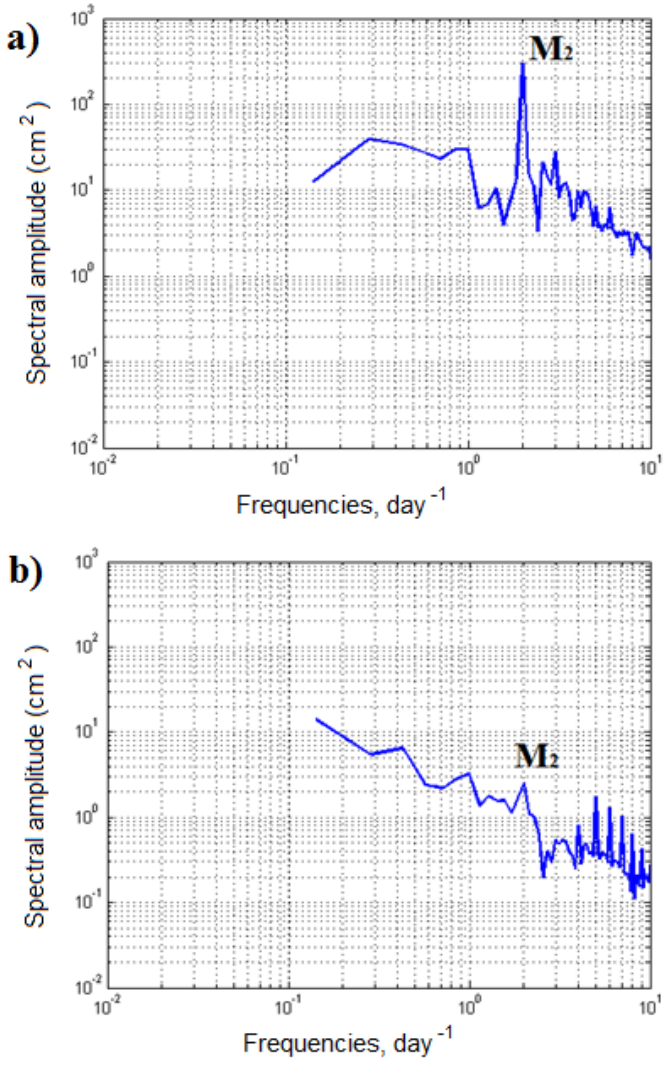

Fig.7. Oscillation spectrums of the Black Sea level (a – Batumi, b– Yalta) in logarithmic scale. M_2 marks the spectral peaks, relevant to the lunar semidiurnal harmonics.

Cotidal maps resulting from the numerical modelling were compared to the theoretical and the field data [9-11] and revealed fine agreement with those.

We can notice some peculiarities, which are appeared, when we consider points in different sea domains: shelf, continental slope, open sea. We took these points in north-western and Caucasian areas of the Black Sea on the lines, which are perpendicular to the coast for the each area (fig. 8) and considered their kinetic energy spectra. The spectra were calculated from the data on the kinetic energy oscillations at the depth of main pycnocline (75 m).

Fig.9 represents the power spectral energy for north-western and Caucasian areas of the Black Sea. These spectra in all points have M_2 tidal wave peaks near 2 day^{-1} frequencies. In the regions of continental slope and open sea well-marked peaks are seen with frequencies close to 1.4 day^{-1} and energy that sufficiently exceed those of tidal maxima. We assume that these are inertial oscillations of the basin.

The right panel of Fig. 9 corresponds to the area with narrow Caucasian shelf, with two peaks that are absent from the left panel spectra. Their frequencies of 3 and 2.75 day^{-1} correspond to a baroclinic Poincare wave, previously described in [12] according to the interpretation of in-situ measurements and previous theoretical studies. Such a conclusion is supported by the fact that the peaks are absent from the left panel due to the flatness of the northern-western shelf; they are almost absent from the top-right spectrum due to the location of the sampling point over the shallow area. Presence of those high-frequency baroclinic oscillations over the steep Caucasian shelf demonstrates an important ability of the model to redistribute additional energy generated by the tidal force into the internal waves of a complex nature with properties close to those observed in-situ.

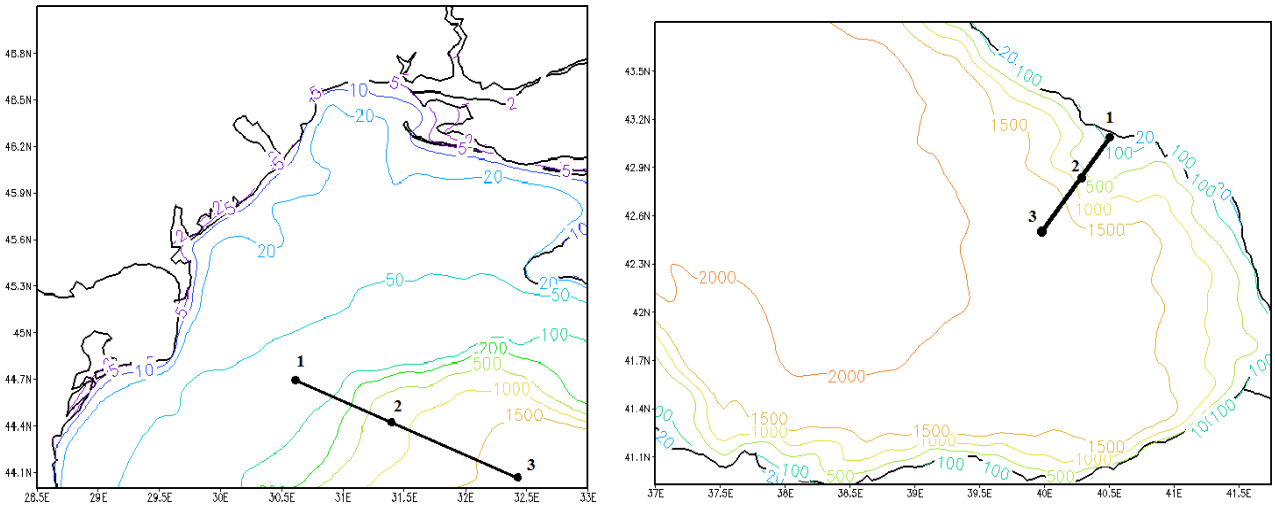

Fig.8. Approximate positions of the considered points (1 – shelf domain, 2 – continental slope domain, 3 – open sea domain). Left panel – north-western area of the Black Sea, right panel – south-eastern area of the Black Sea (Caucasus).

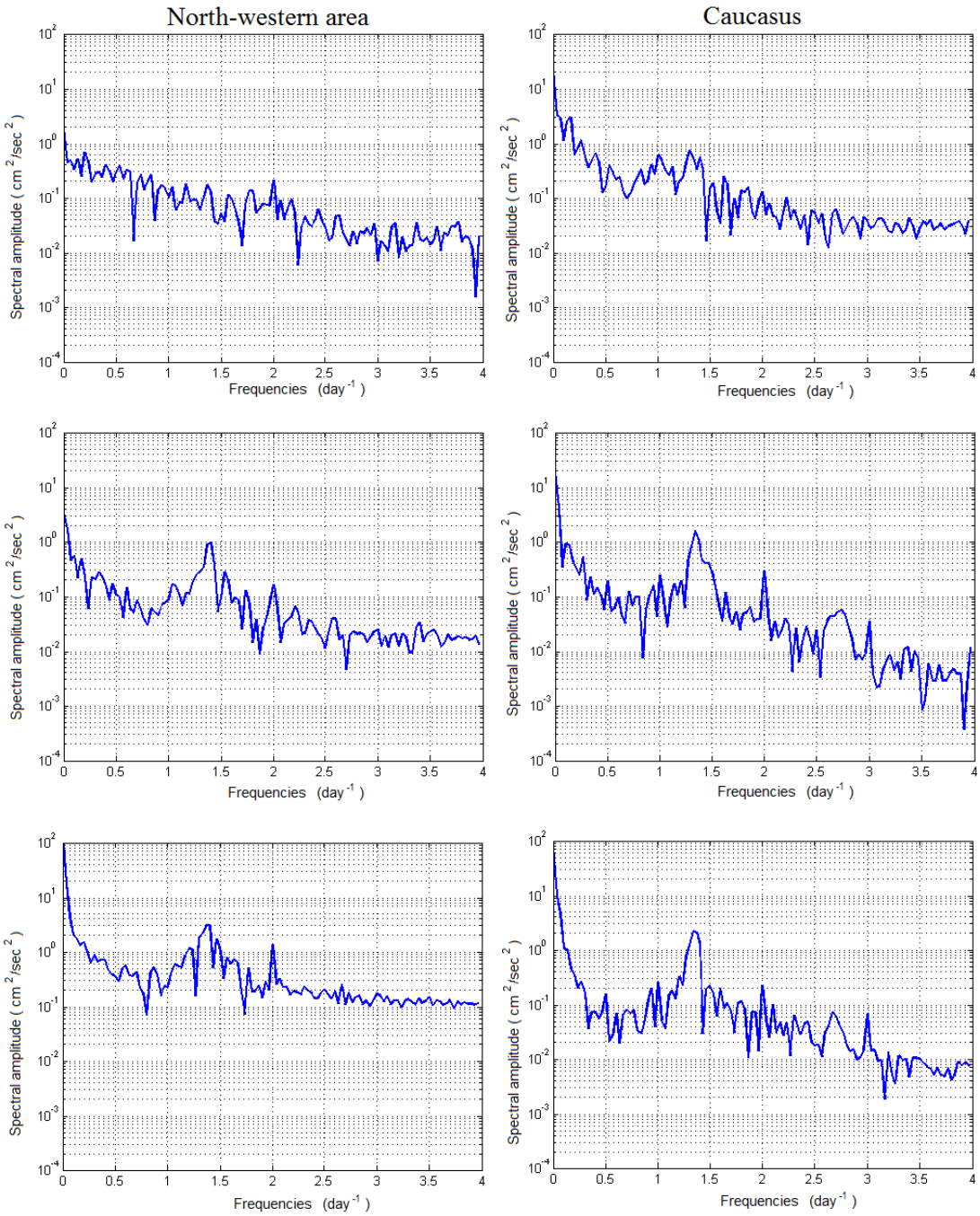

Fig.9. Kinetic energy density spectra in semilogarithmic scale obtained from the numerical experiment for 4 weeks in April. Top – shelf region, middle – continental slope region, bottom – open sea region. Left panel –north-western area, right –Caucasus area.

V. CONCLUSIONS

The circulation model of the Black and the Azov Seas with account of lunar tidal forces was presented. Model shows good agreement with the coastal long-term measurements and theoretical understandings. Possibilities, which are become available with use of the numerical modelling,

allow us to compute tidal influence with higher spatial resolution in relation to the in-situ measurements. First of all, this is actually to the coastal regions.

Furthermore, the model outputs make it possible to investigate the physics of tides and specialties of the energy distribution in different sea regions.

VI. References

[1] V.B. Zalesny, N.A. Diansky, V.V. Fomin, S.N. Moshonkin and S.G. Demyshev "Numerical Model of the Circulation of the Black Sea and the Sea of Azov,". *Russ.J.Numer.Anal. Math. Modelling*, № 6, vol. 25, pp. 581-609, 2012.

[2] V.B. Zalesny, A.V. Gusev, S.N. Moshonkin, "Numerical Model of the Hydrodynamics of the Black and the Sea of Azov with Variational Initialization of Temperature and Salinity," *Izvestiya. Atmospheric and Oceanic Physics*, № 5, vol. 49, pp. 699-716, 2013.

[3] G.I. Marchuk, *Methods of Computational Mathematics*. Saint Petersburg: Lan, 2009. (In Russian).

[4] V.I. Agoshkov, M.Y. Assovsky. "*A Study of the Tidal Wave* M_2 *with the Method of Harmonic Analysis Based on Numerical Computation on the Full Model of the Ocean Dynamics*," Moscow, 2010, unpublished. (In Russian).

[5] Geophysical Fluid Dynamics Laboratory: http://data1.gfdl.noaa.gov/, last revised on 12.05.2016.

[6] V.A. Ivanov, V.N. Belokopytov, *Oceanography of the Black Sea*. Sevastopol: MHI NASU, 2011. (In Russian).

[7] G.K. Korotaev, V.N. Eremeev. *Introduction into Operational Oceanography of the Black Sea*. Sevastopol: ECOSI – Gidrofizika, 2006. (In Russian).

[8] I.P. Medvedev, E.A. Kulikov, A.B. Rabinovich, "Tides in isolated seas: the Baltic, the Black and the Caspian", in proceeding of "*Marine Research and Education: MARESEDU-2015*", 2015. (In Russian).

[9] I.P. Medvedev, E.A. Kulikov, "Spectrum of Mesoscale Sea Level Oscillations in the Northern Black Sea: Tides, Seiches, and Inertial Oscillations", *Oceanology*, № 1, vol. 56, pp. 10-17, 2016.

[10] Defant A. *Physical Oceanography, v.2*. New York: Pergamon Press, 1961.

[11] V.P. Yastreb, T.V. Khmara, "Comparative characteristic of tidal wave motions in seas of the Mediterranean type", *Ecological safety of coastal and shelf zones and complex exploitation of shelf resources*, iss. 12, pp. 60-69, 2005. (In Russian).

[12] Bagaev A., Ivanov V., Zima V. Statistical analysis of mesoscale variability of the marine environment at the Crimean shelf in summer conducted with in situ data // *Ecology, economics and computer science. Coll. Articles: ed. G.G. Matishov et al. V. 2: System analysis and modeling of economic and ecological systems*, Southern Federal University, 2015, Pages: 569-580. (In Russian).

ATMOSPHERIC N DEPOSITION TO THE COASTAL AREA OF THE BLACK SEA: SOURCES, INTRA-ANNUAL VARIATIONS AND IMPORTANCE FOR BIOGEOCHEMISTRY AND PRODUCTIVITY OF THE SURFACE LAYER

Varenik Alla, Marine Hydrophysical Institute of Russian Academy of Science, MHI RAS
Konovalov Sergey, Marine Hydrophysical Institute of Russian Academy of Science, MHI RAS

alla_chaykina@mail.ru

Atmospheric precipitations can be an important source of nutrients to open and coastal zones of marine ecosystem. Jickells [1] has published that atmospheric depositions can support 5-25% of nitrogen required to primary production. Bulk atmospheric precipitations have been collected in a rural location at the Black Sea Crimean coast – Katsiveli settlement, and an urban location – Sevastopol city. Samples have been analyzed for inorganic fixed nitrogen (IFN) – nitrate, nitrite, and ammonium. Depositions have been calculated at various space and time scales. The monthly volume weighted mean concentration of IFN increases from summer to winter in both locations. A significant local source of IFN has been revealed for the urban location and this source and its spatial influence have been quantified. IFN deposition with atmospheric precipitations is up to 5% of its background content in the upper 10 m layer of water at the north-western shelf of the Black Sea. Considering Redfield C:N ratio (106:16) and the rate of primary production (PP) in coastal areas of the Black Sea of about 100-130 g C m^{-2} $year^{-1}$ we have assessed that average atmospheric IFN depositions may intensify primary production by 4.5% for rural locations, but this value is increased many-fold in urban locations due to local IFN sources.

Key words: inorganic fixed nitrogen, atmospheric input, the Black Sea

I. INTRODUCTION

Atmospheric deposition plays a significant role in forming of the chemical composition and characteristics of surface layer of Black Sea. Indeed, many scientists [2-4] consider atmospheric deposition as one of the most important sources of nutrients and pollutants to marine ecosystems. This is specifically true for conditions of summer stratification [5], when vertical exchange is restricted.

The composition of atmospheric precipitations depends on meteorological conditions, long-range atmospheric transport, local sources to atmosphere and their spatial and temporal distribution [6].

The main disadvantage of analytical determinations of chemical composition of atmospheric deposition is that this monitoring requires great efforts to quantify temporal and spatial features of IFN deposition. Therefore, assessments based on numerical modeling are often applied [7-9]. Yet, chemical composition estimates and meteorological data are still required for these assessments. Such approach helps to quantify: a) background deposition due to long-range atmospheric transport and b) the input of local sources to the composition of atmospheric precipitations.

Nitrogen (nitrate, ammonium) in atmospheric deposition mostly associated with anthropogenic sources: fuel burning, motor vehicle exhaust gas and farming. That is why large cities, industrial and agricultural sites are local sources of IFN, while local meteorological conditions govern their spatial pattern.

Publications on atmospheric deposition of inorganic nitrogen at the surface of the Black Sea have been highly limited until recently. We present and analyze in this work observational data for 263 precipitation events collected at Katsiveli and for 328 precipitation events collected in Sevastopol (Crimean coast of the Black Sea) from November 2003 to December 2015. Both spatial and temporal variations in background deposition and the importance of local sources of IFN have been evaluated.

II. MATERIALS AND METHODS

2.1. Sampling sites

Monitoring of bulk atmospheric precipitations and analysis of inorganic fixed nitrogen concentrations have been organized in Katsiveli (Southern coast of Crimea) and Sevastopol (Western coast of Crimea) (Fig. 1) from 2003 – 2008 and from 2014-2015.

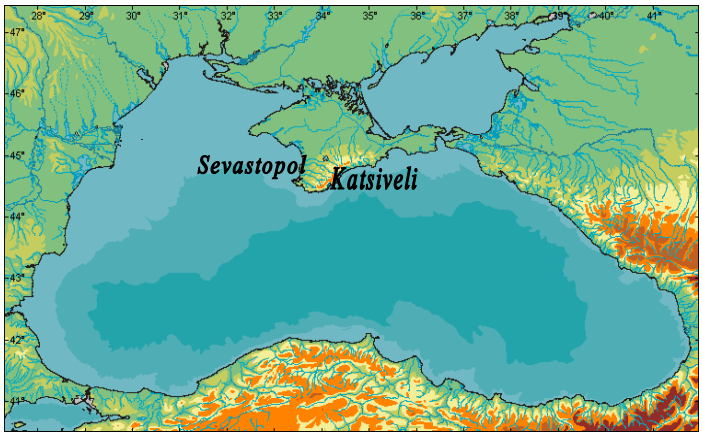

Fig. 1. Sampling sites

Katsiveli is located at the sea coast and at a distance from the nearest largest cities which could additionally support nutrients and pollutants to atmosphere and with atmospheric precipitations. Its permanent population does not exceed 550 citizens. Besides, this site is protected by 600–1100m high cliffs from northern and north-western winds, to additionally block urban air pollution. Taking these facts into account, we considered Katsiveli as a background location that characterizes large-scale processes of nutrients migration.

Sevastopol is one of the largest and industrially developed cities of Crimea. There are about 420,000 permanent residents, but this population can easily triple on summer time. Therefore it can reveal anthropogenic features.

2.2. Sampling and analysis

Of all collected samples, 61% were collected from October to March and 39% - from April to September making possible to trace intra-annual variations.

Using data on the inorganic nitrogen concentration in atmospheric depositions the annual flux of IFN was estimated [10].

Collected samples were analyzed for nitrate+nitrite and ammonium concentrations following standard analytical procedures [11]. The operational reproducibility was 12.5% and accuracy was 20% for nitrate+nitrite, and 3.1% and 9.0% for ammonium. Primary data were quality verified and statistically filtered to eliminate potentially erroneous and/or abnormal results applying the three sigma rule.

Using 2004-2008 IFN data we identified the local source of IFN: its value, seasonal and spatial effects.

Meteorological data were also recorded for the rate of precipitation, wind speed and direction, air temperature, atmospheric pressure and relative humidity making possible statistical and regression analyses.

III. Results and discussions

3.1 Average concentrations and their temporal variations

Atmospheric depositions of IFN in both locations were mainly presented by nitrate (53–66 %) and ammonium (33–45 %). Nitrite was in the range of 1–2% and it presented, most probably, intermediate products of oxidation of ammonium to nitrate. These results are in good agreement with published data [1, 2, 12, 13]

IFN concentrations dropped to their minimum of 22.50 μmol/l and 30.72 μmol/l in September 2014 and September 2007 in Sevastopol and Katsiveli respectively. The maximum values of 371.77 μmol/l and 395.63 μmol/l were detected in December 2006 and August 2014.

Data for permanently open and wet-only samplers showed that the flux measured for bulk deposition was only 20% higher.

The monthly volume weighted mean concentrations of IFN in atmospheric precipitations revealed the presence of seasonal oscillations in Sevastopol and Katsiveli (Fig. 2).

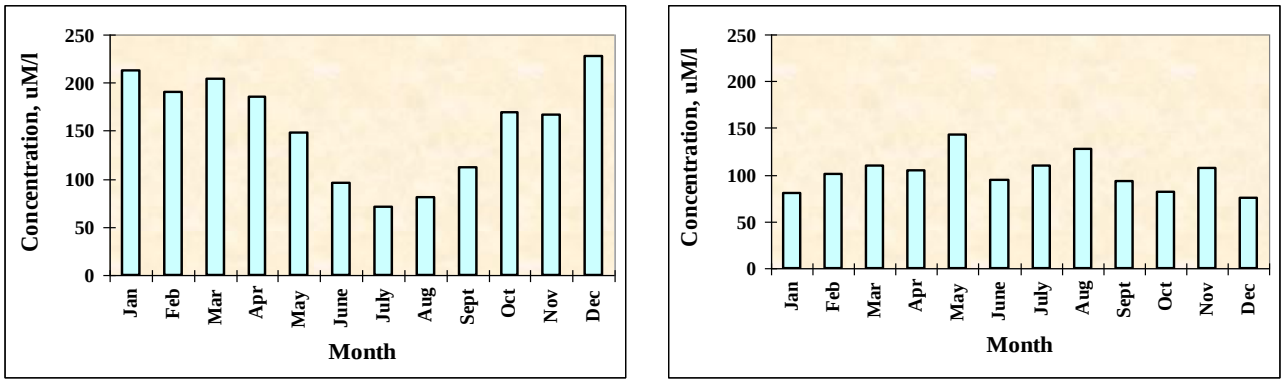

a) b)

Fig. 2. Intra-annual variations in monthly volume-weighted mean IFN concentrations in Sevastopol (a) and Katsiveli (b)

Significantly higher concentrations were revealed in Sevastopol from November to March, as compared to summer (Fig. 2a). It was explained by the magnitude of anthropogenic emission (Martin et al., 2008) oscillating seasonally due to variations in fuel combustion. Seasonal oscillations revealed in Katsiveli were statistically insignificant (Fig. 2b). The absence of powerful local sources of air pollution was the obvious explanation. Neither industrial, nor agricultural local sources would have been known for this rural site.

The summer volume-weighted mean concentrations were equal for Sevastopol and Katsiveli – 115.67 μmol/l and 112.63 μmol/l respectively. At the same time, the winter volume-weighted mean concentration for Sevastopol was 2-fold higher than for Katsiveli – 194.93 μmol/l and 92.76 μmol/l respectively.

The calculated average annual IFN input for urban area (Sevastopol) was about 0.49 $tkm^{-2}yr^{-1}$ and for rural area (Katsiveli) – about 0.39 $tkm^{-2}yr^{-1}$.

3.2 Spatial variability of IFN deposition

In order to analyze spatial variations in the IFN input we have followed [15] to parameterize the concentration of trace substances as a function of meteorological variables. Jenkins et al. [18] has demonstrated that nitrate concentrations in rainwater depend on local weather patterns. We have applied a multiple regression equation to bind meteorological parameters (daily data of the precipitations amount, wind direction, season and preceding dry period) with the flow of contaminants from the atmosphere.

The rate of precipitation is the most influential parameter [16] and it is assessed by the power law [7, 17]. The influence of the wind has been approximated by the third or fourth-order power law [20].

In order to reconstruct a multiple nonlinear regression equation for the IFN concentration as a function of meteorological parameters, we have followed the approach suggested by Brandon [21]. The method is based on (i) identification of regressions between the concentration of IFN and individual statistically significant meteorological variables and (ii) successive introduction of these individual regressions to the multiple regression equation.

Four meteorological variables (precipitation rate, wind speed and direction, and relative humidity) have been identified of having relevant and statistically significant influence on the concentration of IFN in samples of rainwater. They have been successively introduced to the multiple non-linear regression equation (1), and their contributions have been evaluated [22].

$$C = 1.0826 \cdot \exp^{-0.0496 \cdot Ri} \cdot (0.0012 \cdot Vx^3 - 0.008 \cdot Vx^2 + 0.0221 \cdot Vx + 1.1071) \cdot \\ \cdot (0.0004 \cdot Vy + 0.9535) \cdot (-0.0006 \cdot f + 0.96) \quad (1)$$

where R_i is the daily precipitation amount, mm; V_x and V_y are latitudinal and longitudinal wind components; f is relative humidity, %.

The influence of the rate of atmospheric precipitation reaches 68%. The contributions of other components are comparable and equal 12, 10 and 10% for the wind speed, wind direction and relative humidity, respectively.

This equation has been verified against observational data from Sevastopol, Katsiveli and Odessa, other published data [13] and unpublished data from scientific cruises. It has been found that the difference between calculated and measured values is under 14% and does not exceed analytical errors.

Applying (1) to calculate the concentration of IFN in the atmospheric precipitations for regional meteorological conditions and multiplying this concentration by the rate of precipitation, we have quantified inputs of IFN for individual rain events.

The total amount of IFN deposited at the surface of the Black Sea over the period 2004–2008 is about $1.55 \cdot 10^6$ t, which is on average about 0.75 t N km^{-2} yr^{-1}.

Spatial variations mostly depend on the distribution of precipitations over the sea. The rate of atmospheric precipitations [23] increases from the Romanian and Crimean coast to the coast of Turkey, but it reaches the highest values in the south-eastern part of the sea near Batumi. Similar spatial variations have been revealed for the magnitude of IFN deposition (Fig. 3).

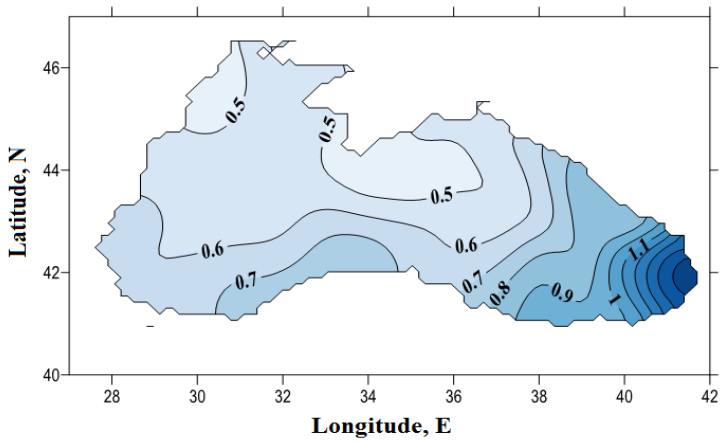

Fig. 3. The average from 2004 to 2008 annual IFN deposition (tNkm^{-2} yr^{-1}) with atmospheric depositions at the Black Sea surface

The character of seasonal distribution of IFN deposition is similar to variations of the IFN concentration in precipitations: it increases in cold period of the year, but decreases in warm period (Table 1).

Table 1. Seasonal variations in deposition of IFN at the Black Sea surface

Season	IFN deposition, t·season^{-1} (min-max)	% of the seasonal riverine input
Spring	46-68	16-24
Summer	26-38	13-19
Autumn	90-103	70-80
Winter	75-81	40-44

3.3 Local source

The difference between winter volume-weighted mean concentrations in rural and urban locations may indicate the local source of IFN to atmosphere. Taking into account that there is no difference for summer period, we conclude that this local source is most important in the cold period of the year. This local source is expected for every large city at the Black Sea coast (Istanbul, Varna, Constantsa, Odessa, Kerch, Novorossiysk, etc).

To assess the extent of its influence we have followed [14]:

$$C_j(x) = C_j \cdot \exp(\lambda_j x) \quad (2)$$

where Cj is the maximum concentration of ingredient near the source (mg l^{-1}); λ_j is the coefficient characterizing the rate of changing concentration (km^{-1}).

The value of λ_j depends on the aerosol composition, wind speed and wind direction. For an average wind speed of about 5 m s^{-1}, values of λ_j can be calculated:

$$\lambda_j = k \cdot \exp(-0.025 \cdot \eta) \quad (3)$$

where k is the coefficient specific for the aerosol composition (for example, k=0.35 for nitrate and ammonium); η is the wind direction frequency in %.

We have found that the effect of local source associated with large cities for typical conditions of Sevastopol is limited to the coastal zone within 25 km distance.

The total amount of IFN deposited at the surface of the Black Sea in coastal 25-km area on average is about $27 \cdot 10^3$ t N yr^{-1}. The IFN deposition in this area also have a seasonal variations – it's maximum is observed in autumn and minimum – in summer. The percent of seasonal riverine input varies from 1.5-2% in summer to 3-9% in winter and 4-15% in autumn.

Considering that 25-km coastal area near Sevastopol influenced by local source of nutrients, the additional input of IFN in this area according to our estimates is about 739 t N yr^{-1}. Supposing that the 25-km area of the Black Sea may be influenced by local sources of large cities we can assess additional IFN input along the 25-km coastal area of about at least $12 \cdot 10^3$ t N yr^{-1}.

Despite the fact that local sources have no significant direct effect on off-shore areas of the sea, monitoring of IFN deposition remains important to correctly evaluate the budget of nitrogen in coastal waters near industrial sites. It is specifically true for winter, when these sources are most significant.

3.4 Influence on primary production

To asses influence of nitrogen atmospheric depositions to marine primary production (PP) many scientists [24-27] apply the Redfield C:N ratio (106:16).

We have assessed that average annual flux of IFN in coastal zone is about 53.6 mmol m^{-2} and may contribute of increasing the value of PP on by 355.1 mmol m^{-2} or 4.26 g C m^{-2}. Our data is in agreement with published values [28], where estimated atmospheric N depositions can support new production from 1.5 to 5.4 mg C m^{-2} day^{-1}. Considering data [29] that the rate of PP in coastal areas of the Black Sea of about 100-130 g C m^{-2} the average atmospheric IFN depositions may result

in additional PP of 3.3-4.3% in coastal 25-km area for rural locations. Additional IFN input as result of local source influence in urban locations may increase this value many-fold. As a result the value of PP in coastal area may reach 556.5 mmol m^{-2}.

IV. Conclusions

Atmospheric deposition of IFN in two sites (urban and rural) of Crimean coast of the Black Sea has been studied.

The summer volume-weighted mean concentrations are equal in Sevastopol and Katsiveli, but the winter volume-weighted mean concentration in Sevastopol is 2-fold higher than in Katsiveli.

The calculated average annual IFN input for urban area (Sevastopol) was about 0.49 t km^{-2} yr^{-1} and for rural area (Katsiveli) – about 0.39 t km^{-2} yr^{-1}.

A significant local source of IFN has been revealed for the urban location. The effect of local source associated with large cities for typical conditions of Sevastopol is limited to coastal zone within 25 km distance. Despite the fact that local sources have no significant direct effect on off-shore areas of the sea, monitoring of IFN deposition remains important to correctly evaluate the budget of nitrogen in coastal waters near industrial sites.

Spatial variations of IFN deposition are mostly governed by the distribution of precipitations over the sea: increases from the Romanian and Crimean coast to the coast of Turkey, but reaches maximum values in the south-eastern part of the sea near Batumi.

The average atmospheric IFN depositions may result in additional PP of 3.3-4.3% for rural locations, but this value is increased many-fold due to the influence of local sources in urban locations.

This work has been partially supported from RFBR project #14-45-01008 for A. Varenik and from RFBR project #14-45-01001 for S. Konovalov.

V. References

1. Jickells, T. 1995. Atmospheric inputs of metals and nutrients to the oceans: Their magnitude and effects. *Mar. Chem*. 48: 199–214.
2. Guerzoni S, Chester R, Dulac F, Herut B, Loÿe-Pilot MD, et al. (1999) The role of atmospheric deposition in the biogeochemistry of the Mediterranean Sea. *Progress in Oceanography* 44: 147–190. doi: 10.1016/s0079-6611(99)00024-5.
3. Béthoux, J. P., P. Morin, and D. P. Ruiz-Pino, Temporal trends in nutrient ratios: chemical evidence of Mediterranean ecosystem changes driven by human activity, *Deep-Sea Res*. II, 49 (11), 2007–2016, 2002.
4. Christodoulaki S, Petihakis G, Kanakidou M, Mihalopoulos N, Tsiaras K, Triantafyllou G. Atmospheric deposition in the eastern Mediterranean. A driving force for ecosystem dynamics. J. *Mar. Syst*. 2013;109–110:78–93.
5. Markaki, Z., Oikonomou, K., Kocak, M., Kouvarakis, G., Chaniotaki, A., Kubilay, N., Mihalopoulos, N., 2003. Atmospheric deposition of inorganic phosphorus in the Levantine Basin, eastern Mediterranean: spatial and temporal variability and its role in seawater productivity. *Limnology and Oceanography* 48, 1557–1568.

6. N. Durana, H. Casado, A. Ezcurra, C. Garcia, J.P. Lacaux, Pham Van Dinh Experimental study of the scavenging process by means of a sequential precipitation collector, preliminary results. *Atmospheric Environment. Part A. General Topics*, Volume 26, Issue 13, Pages 2437-2443.
7. Beverland, I. J., Crowther, J. M., Srinivas, M. S. N., and Heal, M. R.: The influence of meteorology and atmospheric transport patterns on the chemical composition of rainfall in south-east England, *Atmos. Environ.*, 6, 1039–1048, 1998.
8. Àvila, A., Alarcón, M., 1999. Relationship between precipitation chemistry and meteorological situations at a rural site in NE Spain. Atmospheric Environment., 33, 1663-1677.
9. Celle -Jeanton, H., Travi, Y., Loye-Pilot, M.D., Huneau, F., Bertrand, G.: Rainwater chemistry at a Mediterranean inland station (Avignon, France): local contribution versus long range supply. *Atmospheric Research* 91, 118-126 (2009).
10. Varenik, A. V., Konovalov, S. K., and Metik-Diyunova, V. V.: Temporal and spatial variations in the influence of atmospheric precipitation on the distribution of inorganic fixed nitrogen in the Black Sea surface waters (Prostranstvennoe raspredelenie potoka neorganicheskogo azota s atmosfernimi osadkami na poverhnost Chernogo morya), in: *Ecological Safety of Coastal and Shelf Zones and Comprehensive Use of Shelf Resources: Collected Scientific Papers*, Iss. 22, edited by: Ivanov, V. A., NAS of Ukraine, MHI, IGS, OD IBSS, Sevastopol, 268–273, 2010..
11. Berg, T., Dye, C., Hanssen, J. E., Munthe, J., Putaud, J.-P., Reissell, A., Schaug, J., Schmidbauer, N., Semb, A., Torseth, K., Uggerud, H. T., Yttri, K. E., and Aas, W.: EMEP manual for sampling and chemical analysis, *EMEP/CCC-Report* 1/95, NILU, Kjeller, Norway, November, 2001.
12. Koçak, M., Kubilay, N., Tuğrul, S., and Mihalopoulos, N.: Atmospheric nutrient inputs to the northern levantine basin from a long-term observation: sources and comparison with riverine inputs, *Biogeosciences*, 7, 4037-4050, doi:10.5194/bg-7-4037-2010, 2010.
13. Medinets, S., Medinets, V., 2012. Investigations of atmospheric wet and dry nutrient deposition to marine surface in western part of the Black Sea. *Turk. J. Fish. Aquat. Sci*. 12, 497-505.
14. Izrael, Y. A., Nazarov, I. M., Fridman, S. D., Galperin, M. V., Pressman A, Y., Ryaboshapko, A. G., Vitkov, C. D., Gaspra, L., Harvath, L., Disher, H., Damrat, U., Zavodski, V., and Shantroch, Y.: Monitoring of the Transboundary Air Pollutant Transport, *Hydrometeoizdat*, Leningrad, 1987 (in Russian).
15. Vautz, W., Busch, A. U., Urfer, W., and Klockow, D.: A statistical approach to estimate spatial distributions of wet deposition in Germany, *Water Air Soil Poll*., 145, 215–238, doi:10.1023/A:1023676011565, 2003.
16. Sweet, S., Wade, T. L., Park, J., and Wylie, D.: Atmospheric deposition of nutrient nitrogen to Galveston Bay, Texas, in: *Proceedings, Galveston Bay Estuary Program*, State of the Bay Symposium IV, 28–29 January, Galveston, TX, 263–274, 1999.

17. Garban, B., Motelay-Massei, A., Blanchoud, H., and Ollivon, D.: A single law to describe atmospheric nitrogen bulk deposition versus rainfall amount: inputs at the Seine River watershed scale, *Water Air Soil Poll*., 155, 339–354, 2004.
18. Jenkins, S., Gamble, D., Benedetti, M., and Willey, J.: The effects of local weather patterns on nitrate and sulfate rainwater concentrations in Wilmington, North Carolina, *The North Carolina Geographer*, 14, 29–38, 2006.
19. Padgett, P. E. and Minnich, R. A.: Wet deposition of nitrogenous pollutants and the effect of storm duration and wind direction: a case study from inland Southern California, *Water Air Soil Poll*. 187, 337–341, 2008.
20. Abesalashvili, L., Supatashvili, G., Salukvadze, T., and Salukvadze, M.: Hydrochemical characteristic of atmospheric precipitation in the Alazani Valley, *Journal of the Georgian Geophysical Society*, ISSN 1512–1127, Issue (B), Physics of Atmosphere, Ocean and Space Plasma, Geoprint, Publishing House, Tbilisi,vol. 5B, 56–62, 2001.
21. Brandon, D. B.: Developing mathematical models for computer control, *Instrument Society of America Journal*, 7, 176–203, 1959.
22. Varenik, A., Konovalov, S., and Stanichny, S.: Quantifying importance and scaling effects of atmospheric deposition of inorganic fixed nitrogen for the eutrophic Black Sea, *Biogeosciences*, 12, 6479-6491, doi:10.5194/bg-12-6479-2015, 2015.
23. Ivanov, V. A. and Belokopytov, V. N.: Oceanography of the Black Sea, *ECOSY-Gidrofizika*, Sevastopol, 17–19, 2013.
24. Herut B., Krom M.D., Pan, G., Mortimer, R. Atmospheric input of nitrogen and phosphorus to the Southeast Mediterranean: Sources, fluxes, and possible impact // *Limnology and Oceanography*.– 1999.– 44(7).– P.1683-1692. doi:10.4319/lo.1999. 44.7.1683.
25. Krishnamurthy, A., Moore, J. K., Mahowald, N., Luo, C., and Zender, C. S.: Impacts of atmospheric nutrient inputs on marine biogeochemistry, *J. Geophys. Res.*, 115, G01006, doi:10.1029/2009JG001115, 2010.
26. Orens Pasqueron de Fommervault, Christophe Migon, Aurélie Dufour, Fabrizio D'Ortenzio, Fayçal Kessouri, Patrick Raimbault, Nicole Garcia, Véronique Lagadec, Atmospheric input of inorganic nitrogen and phosphorus to the Ligurian Sea: Data from the Cap Ferrat coastal time-series station, *Deep Sea Research Part I*: Oceanographic Research Papers, 2015, 106, 116.
27. Tugrul, S., Murray, J. W., Friederich, G. E., and Salihoglu, L.: Spatial and temporal variability in the chemical properties of the oxic and suboxic layers of the Black Sea, *J. Mar. Sys.*, 135, 29–43, 2014.
28. M. Koçak, N. Mihalopoulos, E.Tutsak, P. Kalegeri. Atmospheric Deposition of Macro Nutrients (DIN and DIP) onto the Black Sea and Implications on Marine Productivity. *Journal of the Atmospheric Sciences* 02/2016; 73(4):160203133541003. DOI:10.1175/JAS-D-15-0039.1
29. Demidov A.B. (2008). Seasonal dynamics and estimation of the annual primary production of phytoplankton in the Black Sea. *Oceanology*, 48: 664–678. doi: 10.1134/s0001437008050068.

SIMULATION AND EARLY WARNING OF NATURAL AND TECHNOGENIC INFLUENCES IN COASTAL AREAS IN THE SEA OF AZOV

T. Ya. Shul'ga, Federal State Budget Scientific Institution "Marine Hydrophysical Institute of RAS" FSBSI MHI
L. V. Cherkesov, Federal State Budget Scientific Institution "Marine Hydrophysical Institute of RAS" FSBSI MHI

shulgaty@mail.ru

In this work, the waves and currents generated by prognostic wind in the Sea of Azov are investigated using a three-dimensional nonlinear sigma-coordinate model. The mathematical model was also used for studying the transformation of passive admixture in the Sea of Azov, caused by the spatiotemporal variations in the fields of wind and atmospheric pressure, obtained from the prediction SKIRON model. Comparison of the results of numerical calculations and the data of field observations, obtained during the action of the wind on a number of hydrological stations was carried out. The evolutions of storm surges, velocities of currents and the characteristics of the pollution region at different levels of intensity of prognostic wind and stationary currents were found. The results of a comprehensive study allow reliably estimate modern ecological condition of offshore zones, develop predictive models of catastrophic water events and make science-based solutions to minimize the possible damage.

Key words: mathematical modeling, Sea of Azov, storm, surge phenomena processes, surface currents, evolution of passive admixture, three-dimensional hydrodynamic model

I. INTRODUCTION

Currently steady growth of interest in the mathematical modeling of wave motions of various natural stratified environments is observed. This is due to problems of geophysics, oceanography, atmospheric physics protection and study of the environment, the operation of complex hydraulic structures, including offshore oil complexes and other. Industrial activity in the offshore including those related to mining is important task wave dynamics, and obtained characteristics are used to assess the environmental impact on marine technology design and development of effective methods of forecasting of extreme hydrological events. Numerical study of hydrodynamic processes in the Azov Sea, arising from the different types of atmospheric circulation will be performed using the three-dimensional nonlinear sigma coordinate model with high spatial resolution adapted to the peculiarities of this basin. New modules and routines were included in the model in order to obtain assessment of the response patterns of surface and bottom currents at strengthening wind stress. Based on the analysis of results of a series of numerical experiments are performed to identify extreme synoptic perturbation level and flow velocity of the Azov Sea.

Studies based on the results of numerical simulation of the dynamic structure of the Azov Sea is also relatively scarce. The geometrical characteristics of the shallow pools caused requirements to hydrodynamic models that use curvilinear coordinate system. Numerical simulation of the dynamics of the waters of the Azov Sea is devoted to a series of works for a long time by Belov [1], Phillipov [1, 2] and Ovsienko [3], for the first time on the basis of linear two-dimensional models of the main characteristics of wind currents, wind-surges processes for typical stationary wind fields have been studied. From recent publications on the modeling of circulation work of Chikin A.L. [4] is the most interesting, which used three-dimensional non-linear shallow water model for the study of stationary motions at a wind speed of 7 m/s. A number of works Fomin V.V. [5, 6] is devoted to studying of stationary currents in the Sea of Azov with the use of three-dimensional non-linear models of the dynamics of currents.

II. The three dimensional primitive equations. the Boundary and initial conditions

We shall consider a rectangular coordinate system in which the *x*-axis is directed to the east, the *y*-axis is directed to the north, and the *z*-axis is directed vertically upwards. The mathematical model is based on the equations of motion and continuity using the hydrostatic approximation [7, 8]. We denote that *u*, *v*, and *w* are velocity projections on the axes *x*, *y*, and *z*, respectively; *t* is the time; *p* is the pressure; ρ is the density; *g* is the acceleration due to gravity; and *f* is the Coriolis parameter

$$\frac{du}{dt} - fv + \frac{1}{\rho}\frac{\partial p}{\partial x} = \frac{\partial}{\partial x}\left(2A_M \frac{\partial u}{\partial x}\right) + \frac{\partial}{\partial y}\left[A_M\left(\frac{\partial v}{\partial x} + \frac{\partial u}{\partial y}\right)\right] + \frac{\partial}{\partial z}\left(K_M \frac{\partial u}{\partial z}\right) \tag{1}$$

$$\frac{dv}{dt} + fu + \frac{1}{\rho}\frac{\partial p}{\partial y} = \frac{\partial}{\partial y}\left(2A_M \frac{\partial v}{\partial y}\right) + \frac{\partial}{\partial x}\left[A_M\left(\frac{\partial v}{\partial x} + \frac{\partial u}{\partial y}\right)\right] + \frac{\partial}{\partial z}\left(K_M \frac{\partial v}{\partial z}\right), \tag{2}$$

$$\frac{\partial p}{\partial z} + g\rho = 0, \tag{3}$$

$$\frac{\partial u}{\partial x} + \frac{\partial v}{\partial y} + \frac{\partial w}{\partial z} = 0. \tag{4}$$

The coefficient of the horizontal viscosity A_M is calculated using the Smagorinskii model of subgrid viscosity [9] depending on the horizontal velocity gradients. The relations for the calculation of the vertical viscosity coefficients K_M and the turbulent diffusion K_H according to the semi-empirical model of Mellor-Yamada (level 2.5) [10] are written as follows:

$$K_M = qlS_M, \quad K_H = qlS_H, \tag{5}$$

where S_M and S_H in a neutrally stratified flow are equal to 0.30 and 0.49, respectively. This parameterization is based on the solution of two additional equations in partial derivatives to determine the turbulent kinetic energy ($q^2/2$) and the turbulence macroscale (l).

The boundary conditions at the free surface ($z = \zeta(x, y, t)$) for the equations of motion are written as follows:

$$w\big|_{z=\zeta} = \frac{\partial \zeta}{\partial t} + u\frac{\partial \zeta}{\partial x} + v\frac{\partial \zeta}{\partial y}, \quad K_M\left(\frac{\partial u}{\partial z}, \frac{\partial v}{\partial z}\right)\Big|_{z=\zeta} = \left(\tau_{0x}, \tau_{0y}\right), \tag{6}$$

We note that $\tau_{0x} = C_a W_x |\mathbf{W}|$ and $\tau_{0y} = C_a W_y |\mathbf{W}|$ are projections of the tangential wind stress [8]; $\mathbf{W} = (W_x, W_y)$ is the wind velocity vector at a height of 10 m over the sea level; and C_a is an empirical coefficient of the surface friction [11], which varies depending on the wind velocity:

$$10^3 C_a = \begin{cases} 2.5, & |\mathbf{W}| > 22 \quad \mathrm{m \cdot s^{-1}}, \\ 0.49 + 0.065|\mathbf{W}|, & 8 \le |\mathbf{W}| \le 22 \quad \mathrm{m \cdot s^{-1}}, \\ 1.2, & 4 \le |\mathbf{W}| \le 8 \quad \mathrm{m \cdot s^{-1}}, \\ 1.1, & 1 \le |\mathbf{W}| \le 4 \quad \mathrm{m \cdot s^{-1}}. \end{cases} \tag{7}$$

The normal component of the velocity at the bottom is zero ($z = -H(x, y)$); the bottom tangential stresses are related to the velocity by the quadratic equation [8]

$$\left(w + u\frac{\partial H}{\partial x} + v\frac{\partial H}{\partial y}\right)\Big|_{z=-H} = 0, \; K_M\left(\frac{\partial u}{\partial z}, \frac{\partial v}{\partial z}\right)\Big|_{z=-H} = (\tau_{1x}, \tau_{1y}), \tag{8}$$

where $\tau_{1x} = c_b u\sqrt{u^2 + v^2}$, $\tau_{1y} = c_b v\sqrt{u^2 + v^2}$ is the bottom friction coefficient, which is found from the formula $c_b = \max\left[k^2 (\ln \frac{H + z_b}{z_0})^{-2}; \; 0.0025\right]$, where z_b is the vertical step in the bottom layer; and $z_0 = 0.03$ mm is the roughness parameter that characterizes the hydrodynamic properties of the underlying bottom surface. The non-slip conditions are specified at the lateral boundaries.

Zero fluid motion and zero fluctuations of the free surface before the atmospheric forcing are specified as the initial conditions ($t = 0$):

$$u(x, y, z, 0) = 0, \;\; v(x, y, z, 0) = 0, \;\; w(x, y, z, 0) = 0, \;\; \zeta(x, y, z, 0) = 0. \tag{9}$$

Let use the equation of transport and diffusion to calculate the spreading of the admixture with the concentration $C(x, y, z, t)$ [8]:

$$\frac{dC}{dt} = \frac{\partial}{\partial x}\left(A_H \frac{\partial C}{\partial x}\right) + \frac{\partial}{\partial y}\left(A_H \frac{\partial C}{\partial y}\right) + \frac{\partial}{\partial z}\left(K_H \frac{\partial C}{\partial z}\right), \tag{10}$$

Here, $A_H = 10$ m^2/s [3, 5] is the coefficient of horizontal turbulent diffusion and K_H is the vertical diffusion; K_H is found from equation (5). The conditions of zero admixture fluxes through the free surface, lateral walls (S), and bottom of the basin are added to the dynamic boundary conditions at the free surface and bottom layer [8]:

$$\left(K_H \frac{\partial C}{\partial \mathbf{n}}\right)\Big|_{z=\zeta} = 0, \left(A_H \frac{\partial C}{\partial \mathbf{n}}\right)\Big|_{S} = 0, \left(K_H \frac{\partial C}{\partial \mathbf{n}}\right)\Big|_{z=-H} = 0. \quad (11)$$

The initial pollution region for all the atmospheric perturbations considered below is located in the surface layer:

$$C_0(x,y,z) = \begin{cases} 1, & r \le R,\ 0 \ge z \ge -z_1, \\ 0, & r > R,\ z < 0;\ r \le R,\ z < -z_1, \end{cases}, \quad (12)$$

where z_1 is the thickness of the pollution region, R is its radius, and $r = \sqrt{(x-x_0)^2 + (y-y_0)^2}$ is the distance from the center of this region (x_0, y_0) to the point at which the concentration is calculated. We select the time of the dispelling of the admixture (t_d) and the coefficient of the maximum square of its spreading at different levels (K_{max}) as examples of the parameters characterizing the evolution of the passive admixture. Then, $K_{max} = S_{max}/S_0$, where S_0 is the square of the initial region of pollution in the surface layer, and S_{max} is the maximum square of the pollution at the considered depth during the transformation of the admixture. The condition of complete pollution dispelling is for a concentration that does not exceed 2.5×10^{-2} over the entire basin of the sea ($C_d = 2.5 \times 10^{-2}$).

The transition from the z-coordinate to the sigma-coordinate is made to perform the numerical realization [5, 8]. In this case, the solution algorithm is based on the application of two-layer differential schemes. The transport operators are approximated [12] using a *TVD* scheme (a linear combination of the scheme of directed differences and the Lax-Wendroff scheme); the spatial digitization of the equations is performed using a *C* grid. Uniform steps over the horizontal coordinates Δx and Δy and the σ-coordinate are used.

The resolutions of the model by latitude and longitude are (1/59)° × (1/84)°, at which the linear sizes of the cell are $\Delta x = \Delta y = 1.4$ km; the number of the horizontal grid nodes is 276 × 176. The number of σ-sigma levels by the vertical is 11. The equations were integrated with a step of Δt = 18 s to determine the average two-dimensional velocity components and the sea level and with a step of $\Delta t_A = 10\Delta t$ = 3 min to calculate the deviations from the found mean values and vertical velocity component. The choice of the integration steps over the temporal and spatial coordinates was performed according to the stability criterion for barotropic waves [13].

The bottom topography is interpolated to the model grid using the depths given in the navigation charts. The deviations of the Azov Sea level were analyzed at nine stations located near large towns (Fig. 1).

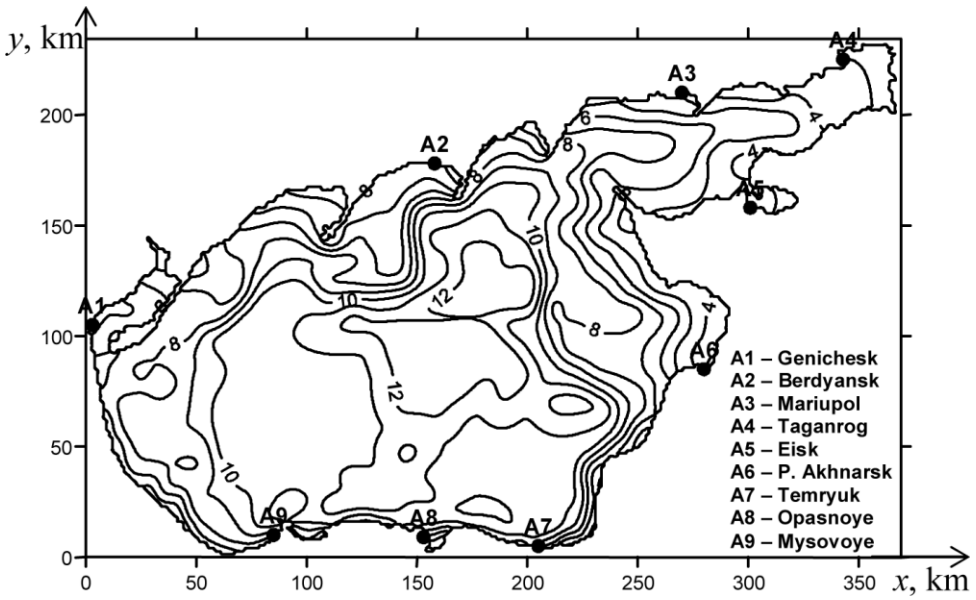

Fig. 1. The bottom relief (m) the Sea of Azov, the position of coastal stations

III. Analysis of numerical experiments

Stationary motions in the Sea of Azov are generated by the western wind field, whose velocity at the sea surface ($\left|\mathbf{W}\right|_{1,2}^{st}$ = 5, 10 m/s) does not depend on x and y; in the first three hours ($0 < t < 3$ h), it increases with time according to a linear law ($\mathbf{W}_{1,2}^{st} = 0$ at $t = 0$) and reaches the maximum value; later ($t \le 3$ h) it does not change. The moment when the currents reach the stable regime ($t = t_0$) is determined by the fact that no notable deviations of the level and current velocities (the variations do not exceed 3%) occur between two neighboring time moments ($T > t_0$ and $T + \Delta t$). From this we find the time when the fluid motion reaches the stable regime ($t = t_{01}$, $\mathbf{W}_1^{st}$; $t = t_{02}$, $\mathbf{W}_2^{st}$).

At the moment ($t = t_0$) when the fluid motion stably adjusts to the stationary wind ($\mathbf{W}_{1,2}^{st}$, a temporally and spatially inhomogeneous wind field obtained from the reanalysis data ($\mathbf{W}_{\text{SKIRON}}$) is added to the stationary wind. At $t > t_0$, the wind $\mathbf{W}_{1,2}^{st}$ maintains the stationary motion, and $\mathbf{W}_{\text{SKIRON}}$ adds a non-stationary component to the motion. We study the joint influence of the stationary ($\mathbf{W}_{1,2}^{st}$ and variable $\mathbf{W}_{\text{SKIRON}}$) wind on the maximum velocities of the currents and the extreme values of the offshore and onshore transport using a series of numerical experiments. These results are compared with the data obtained from the calculation of the winds and currents caused only by constant wind forcing or only by wind determined from the reanalysis.

The investigation of the stationary currents is performed for the constant western wind, whose velocity is 5 and 10 m/s. The surface wind field from the SKIRON model [14] in the period from September 8 to 18, 2007, is used as the variable wind in time and space. Its forcing in the existence of the stationary currents in the Sea of Azov occurs during 10 days starting from September 8 at 00:00 h.

Table 1 presents the maximum wind velocities and wind directions ($\mathbf{W}_{\text{SKIRON}}$) over the Sea of Azov from September 11 to 18, 2007, as functions of time. The wind velocity changes

monotonously between two neighboring times. The deviations of the wind velocity vector from the *x*-axis (the *x*-axis is directed to the east at an angle of 50° to the latitude) are given in degrees. It is seen from this that, during the studied period (192 h), the maximum and minimum velocities were 12.7 and 1.6 m/s, respectively. The dominating directions of the wind are northeastern and northwestern. We note that the results of the long-term observations of the atmospheric perturbations in the region of the Sea of Azov [6] in this period (September) agree well with the data of the SKIRON model given in this table.

Table 1. The maximum wind velocities versus the time obtained from the SKIRON model data from September 11, 2007 at 00:00 to September 18, 2007 at 24:00

Time, h	Wind velocity, m/s	Wind direction, degrees	Time, h	Wind velocity, m/s	Wind direction, degrees
2	6.8	107	76	9.4	354
14	2.6	344	92	12.7	350
28	5.8	9	104	9.6	100
30	3.0	10	106	7.5	210
32	5.2	107	108	5.7	200
44	5.8	344	112	3.5	110
48	8.1	100	124	5.2	344
50	4.2	213	130	3.3	354
54	5.8	195	132	1.6	347
56	7.9	192	140	2.1	10
58	9.6	108	152	4.9	106
62	11.6	350	192	5.8	200

Numerical experiments were realized for two velocities of the stationary western wind to study the influence of the induced currents on the sea level fluctuations and the variations in the velocity field of the non-stationary currents caused by the $\mathbf{W}_{\text{SKIRON}}$ wind.

Table 2 gives the maximum sea level deviations caused by the stationary wind ($\mathbf{W}_{1,2}^{st}$, only by the wind based on the reanalysis data ($\mathbf{W}_{\text{SKIRON}}$), and by their joint forcing ($\mathbf{W}_{1,2}^{st}$ + $\mathbf{W}_{\text{SKIRON}}$) at the coastal stations of the Sea of Azov. The sea level variations caused by onshore winds are given in the upper part of the table, and the offshore values are given in the lower part of the table. It follows from the analysis of these results that the maximum onshore sea level changes generated by the system of stationary and variable wind were recorded at the following stations: 20.7 cm ($\mathbf{W}_{1}^{st}$)

and 62.4 см ($\mathbf{W}_2^{st}$) in Taganrog, 57.1 cm ($\mathbf{W}_{SKIRON}$) and 80.4 cm ($\mathbf{W}_1^{st} + \mathbf{W}_{SKIRON}$) in Primosko--Akhtarsk, and 102.2 cm ($\mathbf{W}_2^{st} + \mathbf{W}_{SKIRON}$) in Eisk. It is seen from here that the maximum sea level change caused by onshore winds in the case of ($\mathbf{W}_2^{st} + \mathbf{W}_{SKIRON}$) (102.2 cm) is 1.27 times greater than in the case of ($\mathbf{W}_1^{st} + \mathbf{W}_{SKIRON}$) (80.4 cm). The minimum sea level changes caused by onshore winds appear in Mysovoye (7.5 cm for $\mathbf{W}_1^{st}$, 13.9 cm for $\mathbf{W}_2^{st}$) and in Opasnoye (9.4 cm for $\mathbf{W}_{SKIRON}$, 16.1 cm for $\mathbf{W}_1^{st} + \mathbf{W}_{SKIRON}$, and 24.8 cm for ($\mathbf{W}_2^{st} + \mathbf{W}_{SKIRON}$).

Table 2. Maximum sea level displacements caused by onshore and offshore winds (cm) at coastal stations of the Sea of Azov under a stationary regime and caused by a prognostic wind in the presence of stationary currents

Coastal stations	$\mathbf{W}_1^{st}$	$\mathbf{W}_2^{st}$	$\mathbf{W}_{SKIRON}$	$\mathbf{W}_1^{st}+\mathbf{W}_{SKIRON}$	$\mathbf{W}_2^{st}+\mathbf{W}_{SKIRON}$
Genichesk	–	–	25.4	32.2	62.3
Berdyansk	–	–	9.6	16.9	44.3
Mariupol	9.8	37.3	29.3	46.4	80.4
Taganrog	20.7	62.4	50.6	63.1	89.5
Eisk	13.8	52.2	38.1	76.0	102.2
P. Akhnarsk	8.1	43.2	57.1	80.4	91.1
Temryuk	10.2	26.9	24.5	29.7	49.9
Opasnoye	–	–	9.4	16.1	24.8
Mysovoye	7.5	13.9	12.1	19.6	34.2
Genichesk	12.2	51.7	42.5	76.5	87.0
Berdyansk	4.0	17.6	17.3	30.9	62.1
Mariupol	–	–	18.2	26.0	39.7
Taganrog	–	–	29.0	42.4	72.9
Eisk	–	–	18.9	41.1	45.3
P. Akhnarsk	–	–	14.1	23.8	35.5
Temryuk	–	–	8.7	15.2	23.0
Opasnoye	3.3	11.1	10.6	20.5	34.2
Mysovoye	–	–	22.3	39.4	63.9

The maximum sea level changes become greater under the joint influence of variable and constant offshore winds than in the stable regime and in the case of zero stationary currents. Among all the types of winds, the maximum sea level changes under offshore winds occur in Genichesk: 12.2 cm ($\mathbf{W}_1^{st}$), 51.7 cm ($\mathbf{W}_{SKIRON}$), 76.5 cm ($\mathbf{W}_1^{st} + \mathbf{W}_{SKIRON}$), and 87.0 cm ($\mathbf{W}_2^{st} + \mathbf{W}_{SKIRON}$). The minimum sea level changes under offshore winds occur in Opasnoye (3.3 cm ($\mathbf{W}_1^{st}$), 11.1 cm ($\mathbf{W}_2^{st}$) and in Temryuk (8.7 cm ($\mathbf{W}_{SKIRON}$), 15.2 cm ($\mathbf{W}_1^{st} + \mathbf{W}_{SKIRON}$), and 23.0 cm ($\mathbf{W}_2^{st} + \mathbf{W}_{SKIRON}$)).

Let us compare the modeling results and the data of the field measurements presented in the tables of the hourly sea level values of the State Meteorological Service of Ukraine in the period from September 8 to 18, 2007. Let us estimate numerically the obtained extreme values of the sea level changes under onshore winds caused by the $\mathbf{W}_{SKIRON}$ wind with the hourly data from these

tables. The simulated maximum of the onshore sea level change in Genichesk is 25.4 cm, which is 4.7 cm (16%) smaller than from the data of the observations. It follows from this that the amplitudes of the sea level fluctuations obtained from the field data and from the numerical calculations agree quite well. The indicated differences are likely to be caused by the errors of the measurements and mathematical modeling.

Variations in the profile of the sea surface caused by wind forcing are shown in Fig. 2. It is seen from the figure that, in the stable regime (Fig. 2a), the sea level decreases along the western coast and increases near the eastern coast. The node line (dashed line) crosses the central part of the sea normal to the wind velocity. The regions in which the maximum and minimum sea level deviations appear three change during the wind forcing (Figs. 2b-2d).

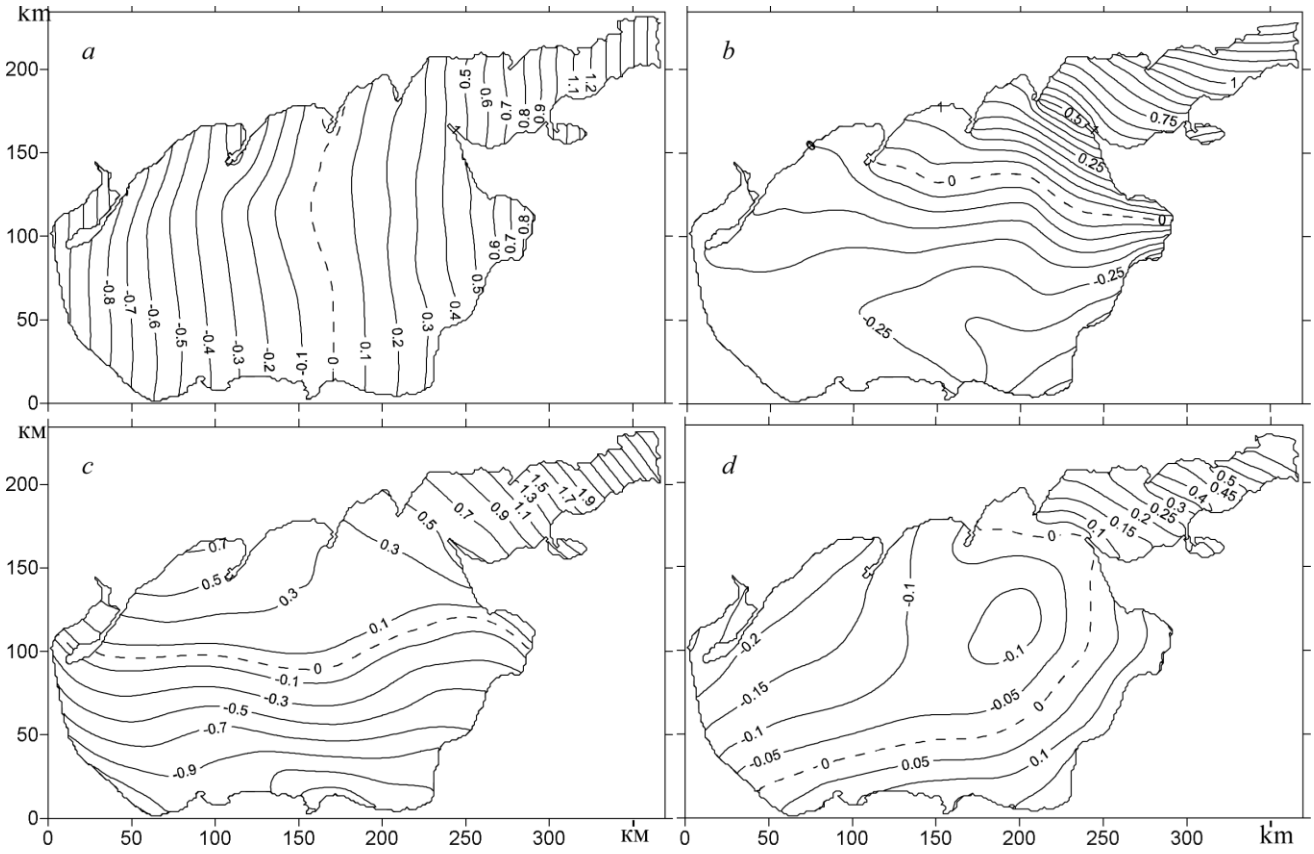

Fig. 2. Sea level fields of the Sea of Azov at different time moments: (a) stationary regime ($\mathbf{W}_1^{st}$, t = 48 h); non-stationary regime ($\mathbf{W}_1^{st}$ + $\mathbf{W}_{\text{SKIRON}}$) (b) 68 h; (c) 90 h; (d) 140 h.

The objective of the following numerical experiments is to estimate the influence of the wind fields and generated currents on the spreading of the passive admixture transported to the central region of the sea. The initial position of the center of the region where the admixture was released is located at a point with the coordinates x_0 = 180 km, y_0 = 120 km; the depth of the sea at this point is 12 m. The region where the admixture was released is a cylinder with radius R = 9 km and depth h_1 ($0 > z \geq h_1$), where h_1 (1 m) is the vertical step in the surface layer. The initial concentration is constant in this region and equal to unity ($C_0(x, y, z, 0) = 1$).

The time of the release of the admixture in different experiments is not the same and depends on the characteristics of the wind. In the case of a nonstationary wind, the moments of the admixture release ($t = t_{01}$, $\mathbf{W}_1^{st}$; $t = t_{02}$, $\mathbf{W}_2^{st}$) and the stabilization of the fluid motion ($t = t_{11}$, $\mathbf{W}_1^{st}$; $t = t_{12}$, $\mathbf{W}_2^{st}$) coincide: $t_{01} = t_{11} = 38$ and $t_{02} = t_{12} = 43$ h. If only the wind $\mathbf{W}_{SKIRON}$ forms the forcing, the time moment of release is September 11, 2007, at 00:00 ($t_{03} = 72$ h). If we consider the joint forcing of the stationary and non-stationary wind, the time of release is determined as follows: $t_{04} = t_{01} + t_{03}$ ($\mathbf{W}_1^{st} + \mathbf{W}_{SKIRON}$) and $t_{05} = t_{02} + t_{03}$ ($\mathbf{W}_2^{st} + \mathbf{W}_{SKIRON}$). For the convenience of the analysis of the results, we assume that, in all the cases, the time of the release of the admixture is zero ($t_0 = 0$).

Table 3 presents the coefficients of the maximum spreading of the passive admixture (K_{max}), the time when it occurred (t_{max}, h), and the time of the complete dispelling of the admixture (t_d, h) at three depths for constant wind ($\mathbf{W}_{1,2}^{st}$) and three variables ($\mathbf{W}_{SKIRON}$ and $\mathbf{W}_{1,2}^{st} + \mathbf{W}_{SKIRON}$). One can see from the data analysis that the maximum square of the pollution at each depth depends on the wind velocity that leads to the stable motion.

Table 3. Parameters (K_{max}; t_{max}, h; t_d, h) of the spreading evolution of the admixture at different depths of the Sea of Azov

Depth, m	Max. values (K, t), and t_d	$\mathbf{W}_1^{st}$	$\mathbf{W}^2{}_{st}$	$\mathbf{W}_{SKIRON}$	$\mathbf{W}_1^{st} + \mathbf{W}_{SKIRON}$	$\mathbf{W}_2^{st} + \mathbf{W}_{SKIRON}$
$z = 0$	K_{max}	1,14	1,18	1,25	1,30	1,32
	t_{max}, h	5,7	4,9	31	40	40
	t_d, h	17,3	18,2	57,1	84,5	86,5
$z = -H/2$	K_{max}	1,16	1,18	1,27	1,33	1,35
	t_{max}, h	14,3	14,7	34	42	42
	t_d, h	36,7	37,6	104	106	110
$z = -H+h_b$	K_{max}	1,16	1,19	1,33	1,37	1,38
	t_{max}, h	26,9	25,5	55	58	59
	t_d, h	53,4	55,2	108	110	115

In the case of greater velocity of the constant wind ($\mathbf{W}_2^{st} > \mathbf{W}_1^{st}$), the velocities of the currents increase, the square of the admixture region spreading increases (K_{max}), and time of its complete dispelling also increases (t_d). The joint forcing of the stationary and $\mathbf{W}_{SKIRON}$ wind causes an increase in the pollution region.

In this case, the maximum pollution square occurs if the velocity of the forcing wind is maximal ($\mathbf{W}_2^{st} + \mathbf{W}_{SKIRON}$). In this case, K_{max} at the free surface is 1.32 40 h after the release of the admixture, and the time of its complete dispelling ($\mathbf{W}_1^{st}$) is 86.5 h. The maximum square of the pollution region at the depth $z = -H/2$ is gained 42 h after the release of the admixture ($K_{max} = 1.35$), and the complete dispelling of the pollution occurs in 110 h. In the bottom layer ($z = H + h_b$), the coefficient of the maximum spreading of the admixture is 1.38 ($t_{max} = 59$ h). We note that, in the

case considered here ($\mathbf{W}_2^{st}$ + $\mathbf{W}_{\text{SKIRON}}$), the concentration of the admixture in the entire basin 115 h after its release does not exceed 2.5% of its initial value ($C_d = 2.5 \times 10^{-2}$).

IV. Conclusion

In this work, we present the results of investigations of the phenomena caused by onshore--offshore winds and the evolution of a passive admixture by the current system generated by the constant and variable winds in the Sea of Azov. The reliability of these results is confirmed by the comparison of the simulated values of the extreme sea level changes caused by onshore and offshore winds with the field data obtained during wind forcing by the surface wind obtained from the SKIRON model at coastal hydrometeorological stations. The obtained results are presented in the table of the sea level changes caused by the onshore and offshore winds and the current velocities for different characteristics of constant and variable wind. We also performed the analysis of the influence of the wind velocity and the generated currents on the characteristics of the transformation of the passive admixture.

The analysis of the modeling results and the dynamic processes in the Sea of Azov allowed us to reach the following conclusions:

(1) It is found from the analysis of the stationary motions that, under constant wind forcing with a two-fold increase in the velocity (5 and 10 m), the maximum deviations of the sea level increase by a factor of 3.45 (0.2 and 0.69 cm), the minimum deviations increase by a factor of 3.9 (0.1 and 0.39 cm), and the maximum velocities of the stable currents increase by 12 times (0.16 and 1.17 m/s);

(2) An increase in the maximum wind velocity leads to an increase in the volume of the pollution region; the minimum pollution square appears in the absence of wind.

(3) The time needed for the pollution region to reach the maximum volume decreases when the wind velocity increases.

V. References

[1] V. P. Belov, U. G. Filippov, “Dynamics and vertical structure of the Azov Sea currents,” Tr. Nauchno-Issled. Gos. Meteorol. Inst., No. 159, 127-134 (Gidrometeoizdat, Moscow, 1980) [in Russian].

[2] U. G. Filippov, “Investigation of some difference schemes for calculating the spread of impurities in the sea,” Tr. Nauchno-Issled. Gos. Meteorol. Inst., No. 126, 77-91 (Gidrometeoizdat, Moscow, 1975) [in Russian].

[3] S. N. Ovsiyenko, “Calculation of wind surges phenomena the Sea of Azov vibrations,” Tr. Hydrometeorological Center of the USSR, No. 60, 55-58 (Gidrometeoizdat, Leningrad, 1972) [in Russian].

[4] A. L. Chikin, “The three-dimensional problem of the calculation hydrodynamic in the Sea of Azov,” Math modeling, 13, No. 2, 87–92 (2001).

[5] V. V. Fomin, “Digital model of water circulation in the Sea of Azov,” Tr. Ukr. Nauchno-Issled. Gos. Meteorol. Inst., No. 249, 246-255 (2002).

[6] V. V. Fomin, and T. Ya. Shul’ga, “Study of the waves and currents caused by the wind in the Sea of Azov,” Dopov. Nats. Akad. Nauk Ukraini, No. 12, 110-115 (2006).

[7] L. V. Cherkesov, V. A. Ivanov, and S. M. Khartiev, *Introduction into Hydrodynamics and Wave Theory* (Gidrometeoizdat, St. Petersburg, 1992) [in Russian].

[8] A. F. Blumberg and G. L. Mellor, "A description of three dimensional coastal ocean circulation model in Three-Dimensional Coast Ocean Models," Coast. Estuar. Sci. 4 (1-16), (1987).

[9] J. Smagorinsky, "General circulation experiments with primitive equations, I. The basic experiment," Mon. Weather Rev. vol. 91, 99-164 (1963).

[10] G. L. Mellor and T. Yamada, "Development of a turbulence closure model for geophysical fluid problems," Rev. Geophys. Space Phys. vol. 20 (4), 851--875 (1982).

[11] W. Wannawong, U. W. Humphries, P. Wongwises, and S. Vongvisessomjai, "Mathematical modeling of storm surge in three dimensional primitive equations," Int. J. Comp. Math. Sci., No. 5, 44-53 (2011).

[12] J. Pietrzak, "The use of TVD limiters for forward-in-time upstream-biased advection schemes in ocean modeling," Mon. Weather Rev. vol. 126, 812--830 (1998).

[13] R. Courant, K. O. Friedrichs, and H. Lewy, "On the partial difference equations of mathematical physics," IBM J., No. 3, 215-234 (1967).

[14] http://forecast.uoa.gr.

SATELLITE DATA FOR INVESTIGATION OF RECENT STATE AND PROCESSES IN THE SIVASH BAY

E.S. Shchurova, FSBSI MHI
R.R. Stanichnaya, FSBSI MHI
S.V. Stanichny, FSBSI MHI

shchurova88@gmail.com

Sivash bay is the shallow-water lagoon of the Azov Sea. Restricted water exchange and high evaporation form Sivash as the basin with very high salinity. This factor leads to different from the Azov Sea thermal and ice regimes of Sivash. Maine aim of the study presented to investigate recent state and changes of the characteristics and processes in the basin using satellite data. Landsat scanners TM, ETM+, OLI, TIRS together with MODIS and AVHRR were used. Additionally NOMADS NOAA and MERRA meteorological data were analyzed. The next topics are discussed in the work: Changes of the sea surface temperature, ice regime and relation with salinity. Coastal line transformation – long term and seasonal, wind impact. Manifestation of the Azov waters intrusions through the Arabat spit, preferable wind conditions.

Key words: Azov Sea, Sivash, satellite data, coastal dynamic

I. INTRODUCTION

The Sivash bay – is shallow-water lagoon, separated from Azov Sea by the Arabat spit. The bay has complex orography and forms evaporative lagoon with high salt concentration. Sivash is conventionally divided into four parts: the Western, the Middle, the Eastern and the Southern. The Western and the Middle basins are separated from Azov Sea by man-made levee, the Eastern Sivash is connected with Asov Sea through Tonkiy strait. Restricted water exchange, high evaporation and high salinity lead to different from the Azov Sea thermal and ice regimes of the Sivash. Maine aim of the study presented is to investigate recent state and changes of the characteristics and processes in the basin using satellite data. Landsat scanners TM, ETM+, OLI, TIRS together with MODIS and AVHRR were used. Additionally NOMADS meteorological data were analyzed. Map of the Sivash with main geographical names used presented on fig1.

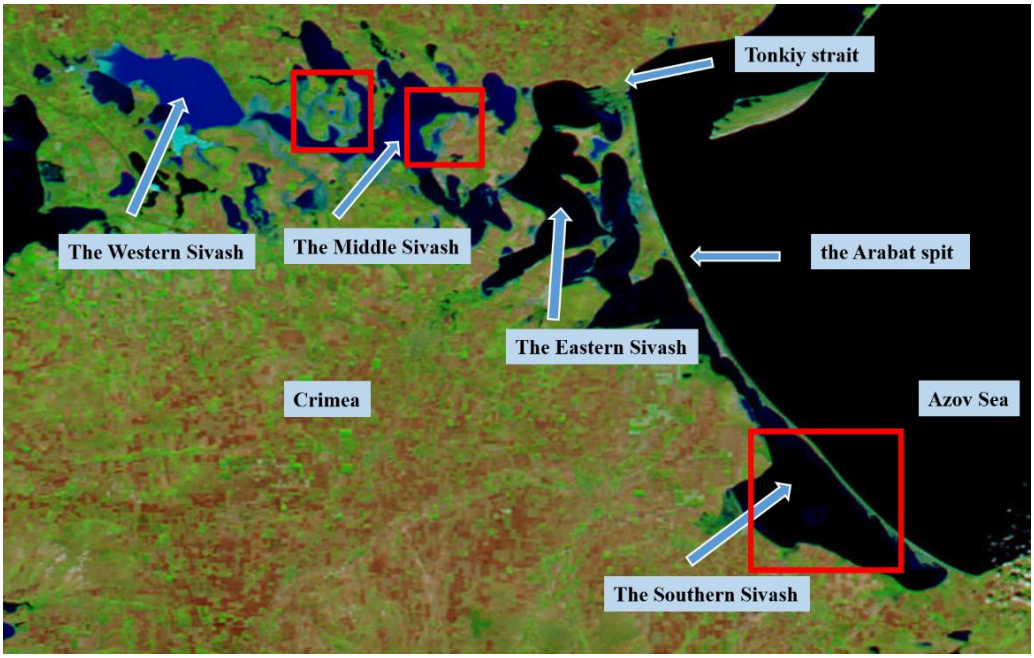

Fig. 1. Map of the Sivash with main toponyms. Red rectangles show areas analyzed in the next topics.

II. SEA SURFACE TEMPERATURE AND ICE REGIME

MODIS TERRA monthly mean Sea Surface Temperature (SST) data for 2001-2013 years were used for investigation of the interannual variability. Fig 2 demonstrates SST time set (upper panel), mean seasonal variability for the Southern Sivash and Azov Sea (low left panel) and difference between these data sets (low right panel). Maximum interannual variations of the monthly mean temperatures for the Southern Sivash were observed for March (from 4 C^o to 8C^o) and November (from 6C^o to 12C^o). As more shallow area Sivash demonstrates faster warming in spring-summer and faster cooling in fall –winter. Mean SST difference between Azov and Sivash exceeds 2.5C^o for March.

The warmest year was 2010 (August temperature -30 C^o) and the coldest years were 2006, 2008, 2012 when winter temperatures below zero in the Sivash and Azov have been registered. High difference in salinity strongly affects ice coverage in different parts of the Sivash. MODIS map for 21.01.2006 (fig 3) demonstrates situation with free of ice high salinity parts of the Sivash due to the low ice point for saline waters. Note that air temperature for this day was - 19 C^o.

Difference in salinity is the main parameter defining duration of the ice coverage between Azov and Sivash. Data for ice regime for coldest years shown in table 1. Duration of Sivash ice regime is shorter than the ice regime of the Azov Sea, which is associated with a higher salinity of Sivash water and as a consequence with later freezing and earlier melting of the ice cover. For example, in the winter of 2008 the ice regime in Sivash was 77 days (from 18.12.07 up to 04.03.08), and ice regime of Azov Sea - 84 days (from 18.12.07 up to 11.03.08).

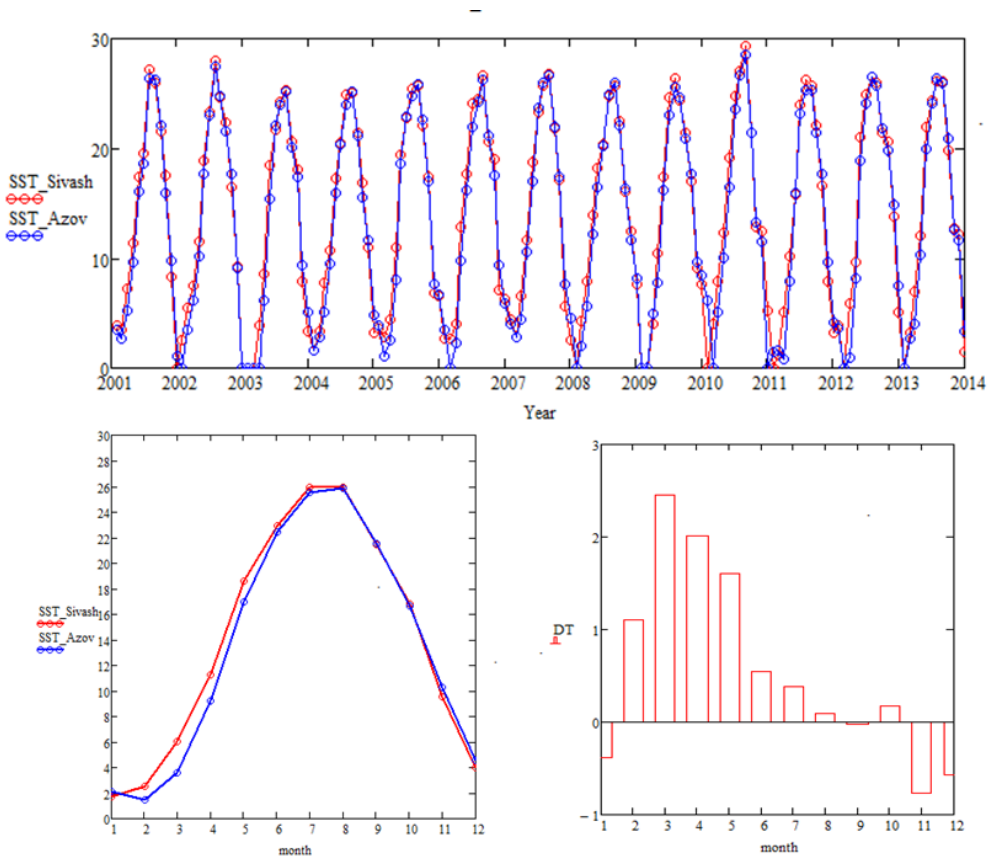

Fig. 2. SST (Co) time sets (upper panel), mean seasonal variability for the Southern Sivash and Azov Sea (low left panel) and difference between these data sets (low right panel).

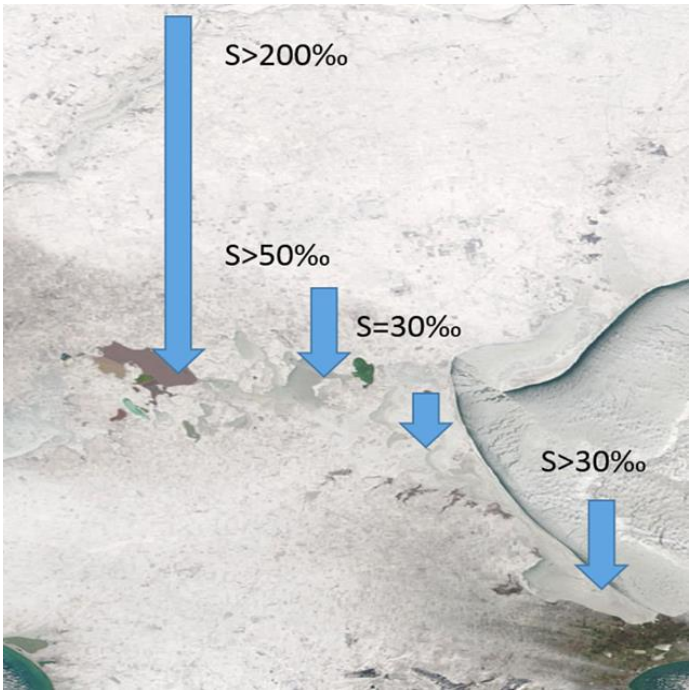

Fig. 3. MODIS image for 21.01.2006 demonstrating ice coverage for parts of the Sivash with different salinity.

Table 1. Ice regime for the Sivash and Azov Sea

	The Sivash				Azov Sea			
	Year	First ice formation	Full ice melting	Duration of the ice regime (d	Year	First ice formation	Full ice melting	Duration of the ice regime (d
1	2006	21.01	23.03	61	2006	09.01	28.03	79
2	2008	18.12	04.03	77	2008	18.12	11.03	84
3	2012	28.01	25.03	77	2012	20.01	10.04	81

So, two main factors define specific features of temperature regime of the Sivash – small depth and high salinity.

III. COASTAL LINE TRANSFORMATION – LONG TERM AND SEASONAL, WIND IMPACT

High resolution optical data from Landsat (4,5,7,8) scanners TM, ETM+, OLI allow to investigate coastal line transformation induced by level change and erosion of the coasts. These processes may be studied for different time intervals. Using data in the near IR spectral range we can easy separate water and land. RGB composition method was used for calculation of the combined maps by using images obtained for different dates. In such a way it's possible to detect like short term variation of the coast line induced by wind-surges processes [6] such long term processes of the erosion or accumulation. For 1987 – 2013 years Landsat data with spatial resolution 30 meters were analyzed. Level change and wind-surges processes well detected on the images for the shallow Middle Sivash with depth 0.5-1m and set of dams. Samples of the wind-induced variation of the coastline are shown on the figure 4. Maps were calculated on the base of the two images (22.05.13 and 07.06.13) with different wind condition. Drying areas are colored in red color.

Fig. 4. Samples of the bottom drying due to the wind-surges processes (red areas) for two regions of the Middle Sivash (shown on the Fig 1) on the base of the Landsat 8 OLI images for 22.05.2013 and 07.06.2013.

The similar RGB composition method was applied for study of the long term variation of the coast line. Satellite image with time interval 10-25 years were used for this aim. The Southern Sivash is characterized by biogenic sedimentation of shells and shelly sand [5]. This fact leads to generation of the different coastal accumulation forms like spits. Spits are variable forms under the wave and currents forcing. Typical sample of the spit shift presented on the figure 5. Map was created on the base of the two images obtained in 1987 and 2011 years. Blue color corresponds the position of the spit in 1987 year and yellow – for 2011 year. So, shift observed is 60-120 meters.

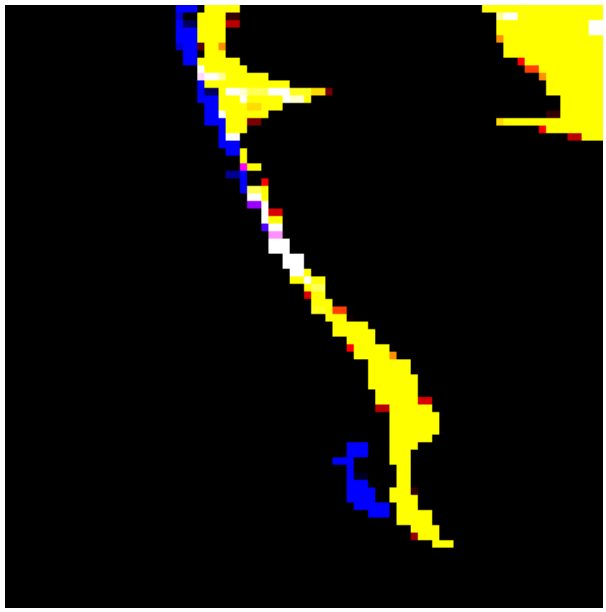

Fig. 5. RGB composition map on the base of the two images obtained in 1987 and 2011 years. Blue color corresponds the position of the spit in 1987 year and yellow – for 2011 year.

IV. Manifestation of the Azov waters intrusions through Arabat spit, preferable wind conditions

Sivash bay is separated from Azov Sea by Arabat spit or Arabatskaya Strelka spit with 112 km length and of 0.25 to 8 km width. Spit height in the northern part is up to - 10 m, while the southern spit part does not exceed 3 meters above Azov Sea level. The southern part of spit is characterized by development of several ridges with gentle slopes, separated by troughs. Ridges are put from small - and medium-grained sand, and the bottom of hollows – sand-oozy material. Both on ridges, and in hollows the abundance of a shell is noted, that says that spit is put by the material which has arrived from a seabed [1]. It follows from the data provided by A.M. Ponizovsky in [3] that filtration of waters of the Sea of Azov through the Arabat spit is insignificant, these conclusions have been done on the basis of actual material consideration – results of deep drilling of 132 wells regarding the Arabat spit adjacent to Sivash throughout the coastline of the Southern Sivash, and also experiments on definition of a filtration of soil, besides in 1959 — 1962. The Crimean complex geological expedition studied again a question of inter-relation between Sivash brines and water of the Azov Sea. The expense of Azov waters stream to the Southern Sivash has been calculated: 7360 m3 per day, or 115 thousand m3 per year [0]. Such kind of works weren't carried out in the Southern Sivash later.

MODIS, OLI and TIRS date were used for study of the spatial features of the temperature and optical properties of the waters along Arabat spit in the Southern Sivash. Data for 2014 and 2015 years were used for these purposes. Time by time we can detect in the thermal images of the TIRS more cold jets from spit to the Sivash. Note that such jets are observed usually in the same parts of the spit. Typical sample shown on the figure 6(a) – TIRS image for March 9 2015. Jets look like more dark stripes. Specific features approximately in the same places along spit are observed in MODIS (08.08.2015) optical images like areas with more clean waters with low scattering Fig 6 b(more dark areas). Analysis of the NOMADS NOAA wind data [2] for situation with such manifestation along spit gave the result – all images with jets were obtain during or after strong (>10-15m/s) East or North-East wind. Sample of the wind map for 08.08.2015 shown on the fig 6(c). Typically, these winds induce level rising along Azov side of the spit up to 1m [6]. The same winds can decrease level along Sivash side of the spit. So, we have preferable condition for increasing possible intrusion of the Azov waters through the spit due to the level difference on Azov and Sivash sides. Finally on the 1m resolution image from Google Earth well seen structure that may be interpreted like bed of flow on the bottom. Note, that position of this bed corresponds the place of most often manifestation of the jets in optical and thermal images.

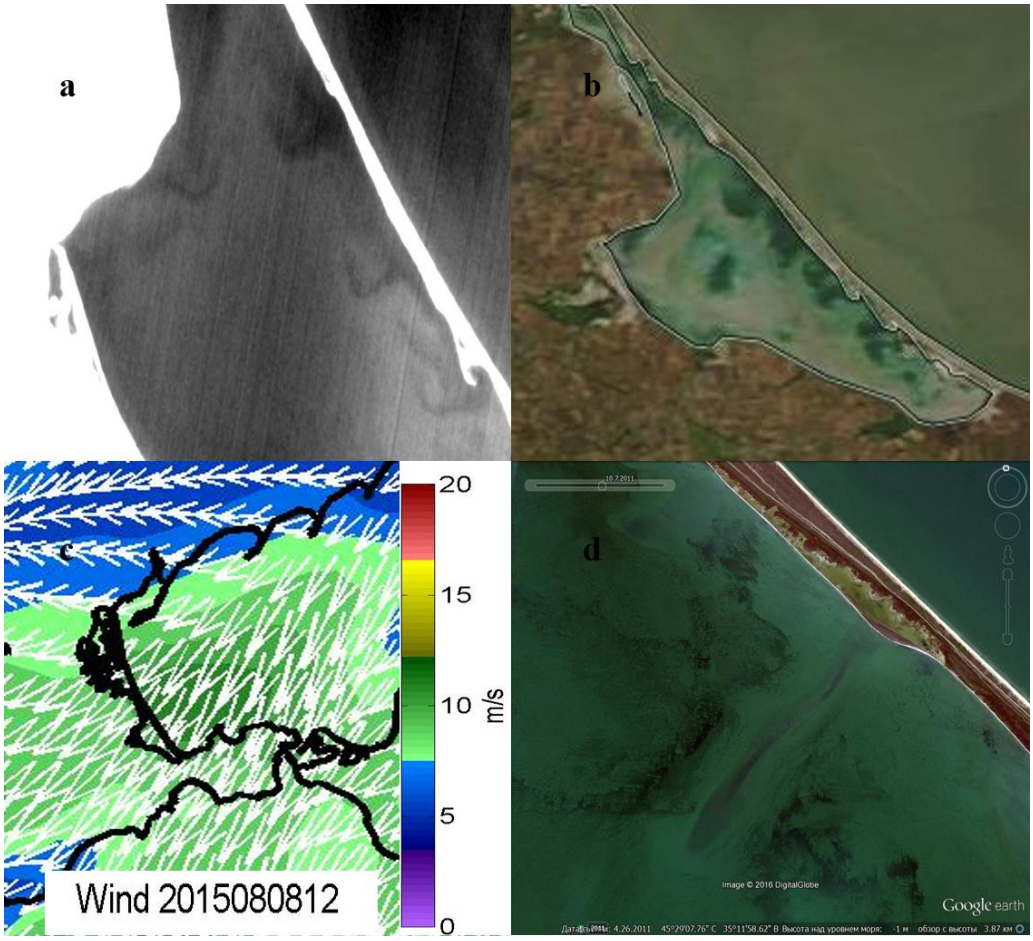

Fig. 6. Azov water filtration through the Arabat spit 08.08.2015 (a) - in the thermal infrared range, (b) - in the optical image of MODIS 08.08.2015, (c) - the scheme of wind conditions, m/s (d) – High resolution image from Google Earth)

V. CONCLUSIONS

On the base of satellite data were investigated thermal and ice regimes of the Sivash. Two main factors define specific features of temperature and ice regime of the Sivash – small depth and high salinity.

RGB composition method demonstrated coast line transformation induced by level change and erosion of the coasts.

Detected specific spatial features (jets) in optical and thermal images may be interpreted like manifestation of the Azov waters intrusion throw the Arabat spit. All situation with jets manifestation followed by strong (>10-15m/s) East or North-East wind. Additional experimental “in situ” measurements need to confirm water intrusion in detected areas.

VI. ACKNOWLEDGMENT

This study is supported by grant RScF, project №15-17-20020

VII. REFERENCES

[1] V. K. Leontiev and A.K. Leontiev, “Main features of geomorphology of Sivash lagoon,” *Vestnik MSU. Ser. of “Georg.”*, №2, pp. 185-194, 1956. (in Russian).

[2] http://dvs.net.ru/mp/data/main_ru.shtml - Marine portal by Remote Sensing Department of FSBSI MHI

[3] Ponizovsky, *Salt resources of the Crimea*. Simferopol: Crimea,1965. (in Russian).

[4] V.P. Zenkovich, *The Fundamentals of the theory of the development of coasts*. Moscow: publ. house of the USSR Ac. Of Sc., 1962. (in Russian).

[5] V.A. Mikhailov, “Free and detached coastal accumulative forms of Sivash bay,” *Sc. Not. of Taurida Nat. V.I. Vernadsky Univ. Ser. Geogr.*, 27(66),№2, pp. 65-74, 2014. (in Russian).

[6] O.D. Davidov, “Physical-geography characteristics of windy flat coast in Sivash bay (within the western, central and eastern sites),” *Odesa Nat. Univ. Herald*, 12(8), pp. 62-70, 2007. (in Ukrainian).

SHORT-TERM VARIABILITY OF COASTAL ZONE HYDRODYNAMICS UNDER AN EXTERNAL FORCING: OBSERVATIONS AT THE BLACK SEA RESEARCH SITE OF SIO RAS

Zatsepin A.G., ***P.P. Shirshov Institute of Oceanology, RAS (SIO RAS)***
Kuklev S.B., ***Southeren Branch of the P.P. Shirshov Institute of Oceanology, RAS (SIO RAS)***
Ostrovskii A.G., ***P.P. Shirshov Institute of Oceanology, RAS (SIO RAS)***
Piotoukh V.B., ***P.P. Shirshov Institute of Oceanology, RAS (SIO RAS)***
Podymov O.I., ***Southeren Branch of the P.P. Shirshov Institute of Oceanology, RAS (SIO RAS)***
Silvestrova K.P., ***P.P. Shirshov Institute of Oceanology, RAS (SIO RAS)***
Soloviev D.M., ***Marine Hydrophysical Institute RAS***
Stanichny S.V., ***Marine Hydrophysical Institute RAS***

zatsepin@ocean.ru

Since 2010, the P.P. Shirshov Institute of Oceanology RAS (SIO RAS) in Gelendzhik maintains the research (observational) site for year round multi-disciplinary studies and monitoring of the marine environment in the coastal zone. Analysis of the data obtained at the observational site revealed the existence of well pronounced short-term variability of coastal zone hydrodynamics at time scales from 1-3 days to 1-2 weeks. The paper examines the role of external forcing (including the impact of adjoined open sea dynamics and wind stress) in the short-term variability of hydrodynamics and upper mixed layer evolution.

Key words: Black Sea, coastal zone, short-term variability, hydrodynamics, wind forcing.

I. INTRODUCTION

Studies of coastal zone hydrodynamics in the semi-enclosed and marignal seas are primarily motivated by conventional wisdom that the coastal currents is main driver for shelf water ventilation, self-cleaning and pollution-removing processes. Coastal water pollution is often serious problem for major ports, coastal cities and recreational facilities. In the Russian part of the Black Sea, one of the regions under strong anthropogenic stress is the shelf zone in vicinity of cities Gelendzhik and Novorossiysk. Since 2010, the Southern Branch of the P.P. Shirshov Institute of Oceanology RAS (SIO RAS) in Gelendzhik maintains the observational site for multi-disciplinary studies and monitoring of the marine environment in the coastal zone.

The site occupies an area of 10*15 km^2 (Fig. 1, [1]). The continuous year-round monitoring is carried out using autonomous measurement systems both bottom mounted and moored buoys. Three types of autonomous platforms are used: 1) acoustic Doppler velocity profiler (ADCP) at the bottom mount; 2) thermo-chain at the mooring line; 3) moored profiler Aqualog [2]. By these platforms the time series of hydrophysical and bio-optical data (vertical profiles of temperature, salinity, density, current velocity, acoustic backscatter, water transmissivity, chlorophyll-a fluorescence, etc.) of high spatial and temporal resolution are obtained. The data from some of the

autonomous platforms is transferred via a communication line to the coastal center for real-time operability. Also the ship-born multidisciplinary surveys are carried out on a regular basis.

The observational data are used for research on marine environment and biota, cross-shelf exchange processes and etc. In particular, it has been shown that there is a significant short-term variability of the coastal zone hydrodynamics and upper mixed layer thickness at the scale from 1-3 days to 1-2 weeks [3-5]. It was found that this variability is to a certain extent due to the influence of external forcing including the open ocean dynamics and the local wind forcing.

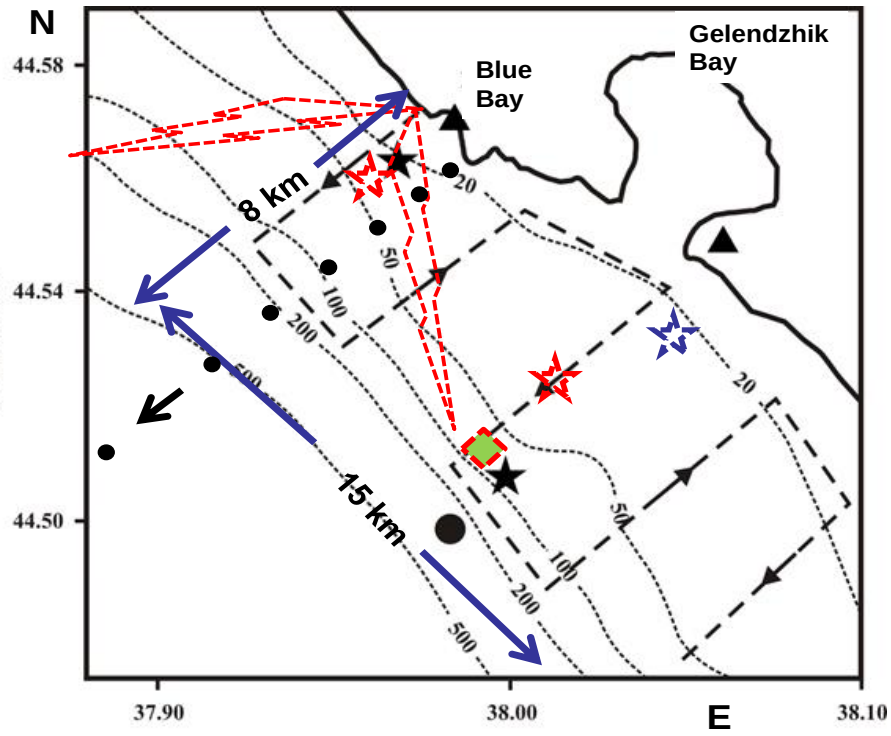

Fig. 1. Scheme of the observational site at the Black Sea coastal zone near Gelendzhik. Triangles are coastal meteorological stations, black stars – joint stations with bottom mounted ADCP and moored thermo-chains, small black circles – CTD and multidisciplinary stations of ship-borne surveys, large black circle is moored automatic profiler Aqualog. Blue star is a lost station. Dotted lines with arrows show the R/V tracks for measurements of the current velocity using towed ADCP. Red stars – autonomous stations to be deployed in 2016. Red arrows - HF Doppler radar. Green diamond – proposed location of the moored surface meteorological buoy.

II. INFLUENCE OF OPEN OCEAN DYNAMICS

A deep part of the Black Sea is characterized by cyclonic circulation, encircled by the Rim Current (RC) [6]. The basin scale cyclonic gyre and the RC are formed under the impact of cyclonic vorticity of the wind over the Black Sea region [7]. In autumn and winter, when wind cyclonic vorticity is enhanced, RC is strong and pressed against the continental slope. In spring and summer when cyclonic vorticity of the wind decreases, RC becomes weak; owing to baroclinic instability, its flow forms meanders and often breaks into mesoscale eddies [8-10]. In autumn and winter, the

growth of the RC meanders to large amplitude is restrained by the Ekman pumping [8]. However, the RC meandering can be developed in any season of the year.

Figure 2 shows the time-depth diagram of specific density and alongshore current velocity measured by the profiler Aqualog on moored buoy station at a depth of 270 m (the upper part of the continental slope) from November 5 till December 27, 2012). The alongshore velocity changes its direction in 5-15 days. In its turn the isopycnals change their position coherently with the velocity. They deepen with the development of north-western current, and rise with the development of the south-eastern current. The amplitude of vertical displacement of isopycnals including the contours of specific density 16.2 kg/m^3, which coincides with the upper boundary of hydrogen sulfide layer, is up to 50 m.

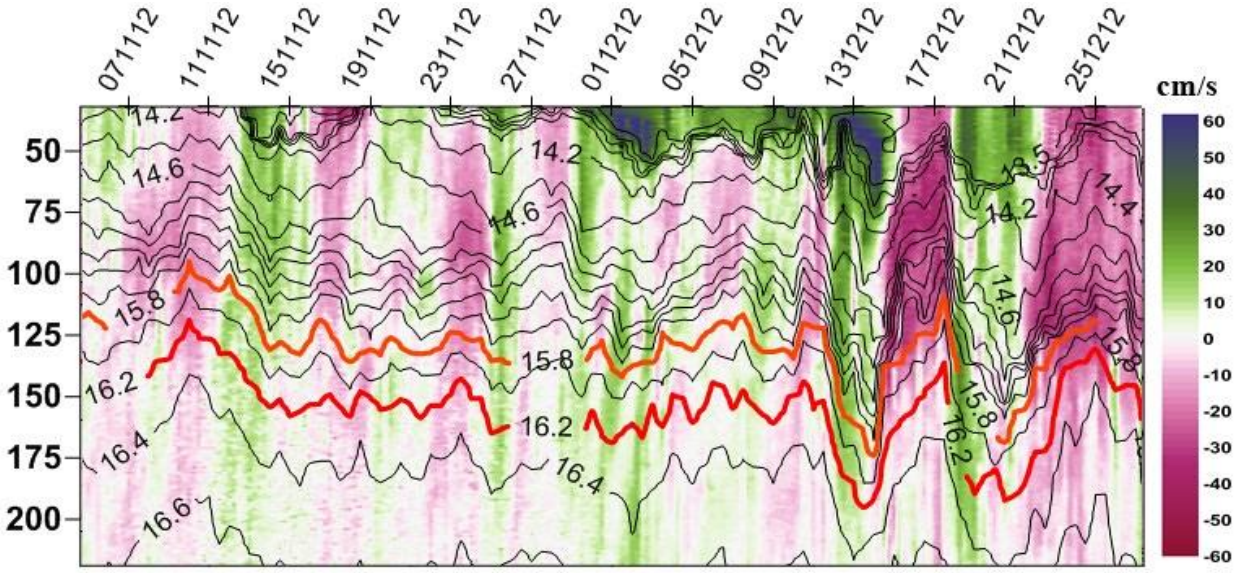

Fig.2. Variability of vertical distributions of the specific density and alongshore current velocity in the upper 200 m from November 5 to December 27, 2012 according to profiler Aqualog data. Profiling frequency was 4 times per day. Black lines are contours of specific density (isopicnals), orange line is isopycnal 15.8 kg/m^3, lower limit of the oxygen-containing layer, red line is isopycnal 16.2 kg/m^3, the upper boundary of hydrogen sulfide layer. Color marks the direction of longshore velocity (color bar at the right vertical axis), its negative values are for the SE current direction, positive are for the NW current direction.

The nature of the described above quasi-periodic oscillations is the RC meandering (Fig. 3). Due to displacement of the RC meanders along the shore in the NW direction, moored station with Aqualog profiler periodically appears in the area of cyclonic and anticyclonic meanders. Being in cyclonic meander profiler detects the NW flow and lowering of isopycnals due to geostrophic adjustment. After several days or a week, the moored station is in the anticyclonic meander and the Aqualog profiler measures the SE flow and the rise of isopycnals [11].

Quasi-periodic oscillations both of direction and magnitude of the alongshore current velocity at the upper part of the continental slope have strong impact on the hydrodynamics of the shelf. Analysis of satellite and towed ADCP velocity survey data, revealed that in case of a cyclonic

RC meander anticyclonic submesoscale eddies are formed at the shelf, while in case of the anticyclonic meander the cyclonic submesoscale eddies are generated [3, 4].

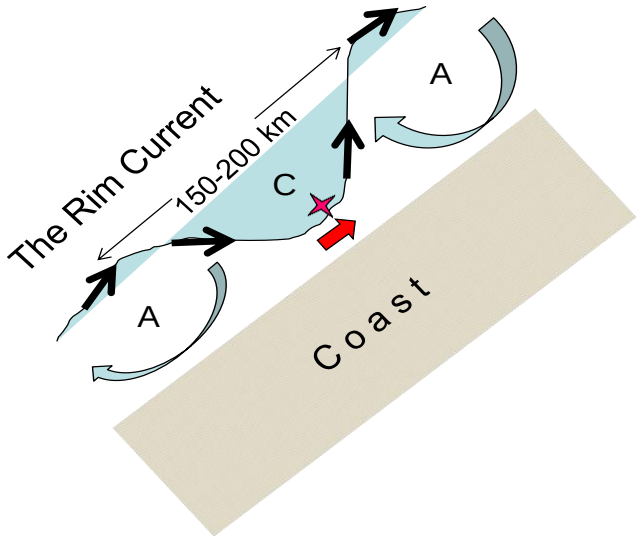

Fig. 3. Scheme of quasi-periodic (5-15 days) oscillations of the alongshore current velocity. The black arrows show position of the RC axis. The mark C denotes a cyclonic meander, the mark A - anticyclonic. Thick red arrow indicates the direction of meanders alongshore displacement. Red cross indicates the position of the Aqualog profiler mooring.

The typical diameter of the submesoscale eddy is 2-10 km, orbital velocityis 20-50 cm/s, alongshore displacement (translation) velocity is 10-20 cm/s. The lifetime of submesoscale eddy does not exceed a few days [4]. Unlike mesoscale eddy, which is characterized by small Rossby number, submesoscale eddy is characterized by the Rossby number close to 1 or even more thereby they are ageostrophic eddies.

Submesoscale anticyclones often accumulate passive tracers and ensure rapid transport of pollutants from the coast to the outer shelf (Fig. 4), whereas submesoscale cyclones produce not only horizontal, but also intense vertical circulation and contribute to the rise of the rich chlorophyll thermocline waters to the sea surface (Fig. 5, [11]). These eddies play an important role in the ventilation of the coastal zone especially in areas with a concave shoreline where circulation is weaker in comparison with that in the shelf regions with a flat or convex shore line.

Physical mechanisms of submesoscale eddies formation were studied by means of laboratory modelling [12-14]. Several experiments were conducted in the cylindrical tank on top of rotating platform filled by homogeneous or stratified fluid. First, the mechanism of eddies formation behind the capes was studied [12]. It was shown that periodic eddy formation behind the cape and separation of eddies from the coast occur only in the case of decelerating cyclonic alongshore current in rotating fluid. The explanation for the nature of this effect based on the account of bottom Ekman friction was suggested. The dependences of eddy basic characteristics (diameter, orbital velocity, etc.) on time and external parameters were established.

The submesoscale eddy formation process due to horizontal velocity shear instability in the rotating fluid was investigated in cases of cyclonic and anticyclonic shear between the alongshore current axis and round tank wall. It was shown that in presence of a current with cyclonic shear, chain of eddies was formed in wide range of the non-dimensional shear value. In case of a current with the anticyclonic shear, the chain of eddies was observed only at rather small values of the shear value and by contrast, the current had chaotic turbulent structure at the large non-dimensional shear value. The asymmetry of the eddy-like structure formation in the current with cyclonic and anticyclonic shear was explained by simple physical model [13].

Results of the laboratory experiments were used successfully to interpret the observations of the submesoscale eddies at the narrow shelf of the NE Black Sea.

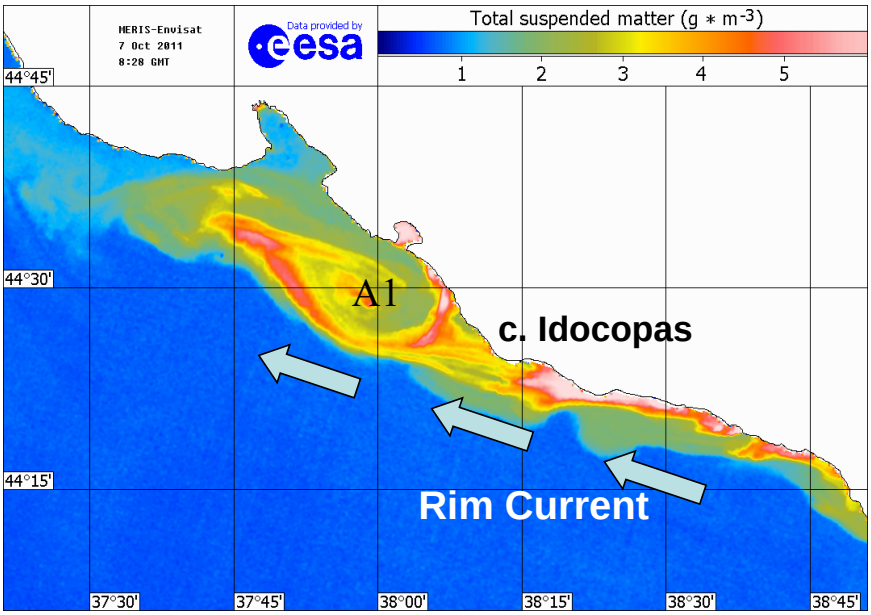

Fig. 4. Satellite (MODIS-Aqua) total suspended matter image of submesoscale anticyclonic eddy A1 behind the cape Idocopas in the NE Black Sea.

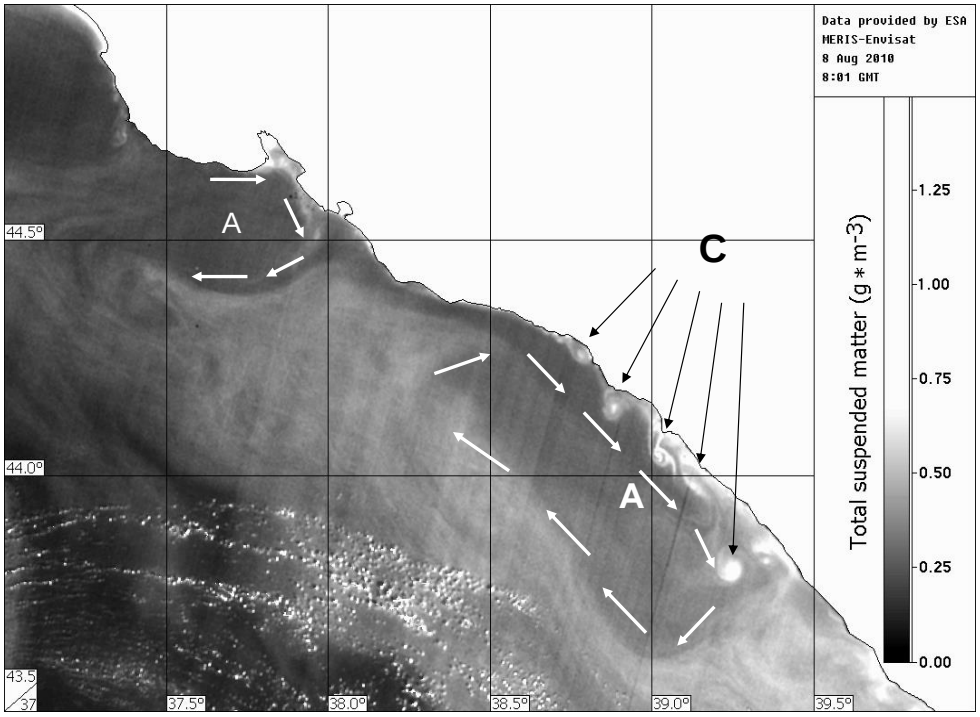

Fig.5. Satellite (MERIS-Envisat) total suspended matter image of a chain of submesoscale cyclonic eddies C at the coastal periphery of a mesoscale anticyclone A in the NE Black Sea.

As a characteristic period of the oscillations of the alongshore current direction due to meandering of the RC is about 10 days, during one half of this period the conditions for formation of submesoscale cyclones are favorable, and during other half of the period they are favorable for submesoscale anticyclones formation.

It should be noted that in the periods of restructuring of the circulation upon the continental slope (transition from a cyclonic RC meander to anticyclonic one or *vise verse*) shelf circulation could be rather weak. In such situations, contaminants may accumulate at the source for several days, resulting in their concentration grouth.

III. COASTAL UPWELLING AND DOWNWELLING AND THEIR RELATION TO THE WIND FORCING AND THE SEA CURRENTS

According to Ekman's theory, the events of the coastal upwelling and downwelling should occur in NE Black Sea if the wind has significant alongshore component: NW or SE, respectively. It is known that Ekman coastal upwelling plays important role in maintaining a high level of bio-productivity.

In the NE part of the Black Sea, strong and continuous northwesterly winds are rare. Therefore complete Ekman upwelling events occur no often than a few times during the warm season of the year [15]. Here, according to [16], we mean that upwelling is complete if the thermocline water rises to the sea surface. When thermocline rises, but does not reach the sea

surface, the upwelling is incomplete. Unlike complete upwelling, incomplete upwelling is observed quite often in the coastal area of the NE Black Sea: several times per month.

One of the complete Ekman upwelling events, which was followed by well developed downwelling, was observed at the SIO RAS research site on September 24-28, 2013.

Figure 6 illustrates the interrelations between wind forcing, water temperature and alongshore current velocity during the period of the upwelling and downwelling events mentioned above. The time based diagrams show wind velocity vectors measured by the automatic weather station (Fig. 6a) and sea temperature vertical distribution measured by the moored thermochain, as well as absolute value and direction of the current velocity vertical distributions measured by bottom mount ADCP (Fig. 6b–6d, respectively). During September 24-26, prevailing northwesterly wind led to the temperature decrease by more than 10°C in the entire water column. The complete upwelling event was accompanied by development of the coastal current of southeastern direction. On September 26 (second half of the day), the wind direction changed to the southerly then to the southeasterly and the wind velocity increased. The wind change resulted in relaxation of the upwelling and quick development of the downwelling manifested itself in temperature increase up to 19.5°C in the entire water column. The downwelling phase was accompanied by the development of the coastal current of the NW direction, which velocity peaked at 70 cm/s.

A criterion of the complete Ekman upwelling in two-layer fluid was obtained in [15]:

$$\tau_x t/f\rho_w H R_d > 1 \qquad (1)$$

Here τ_x is the wind stress alongshore component , t is time from the beginning of the upwelling favorable wind, f *is* the Coriolis parameter, and ρ_w is the seawater density, H - initial upper mixed layer (UML) depth, $R_d = (\Delta\rho g H/\rho_w)^{0.5}/f$ is local baroclinic deformation radius and $\Delta\rho$ is the density jump between the upper and lower layers. This criterion should be verified.

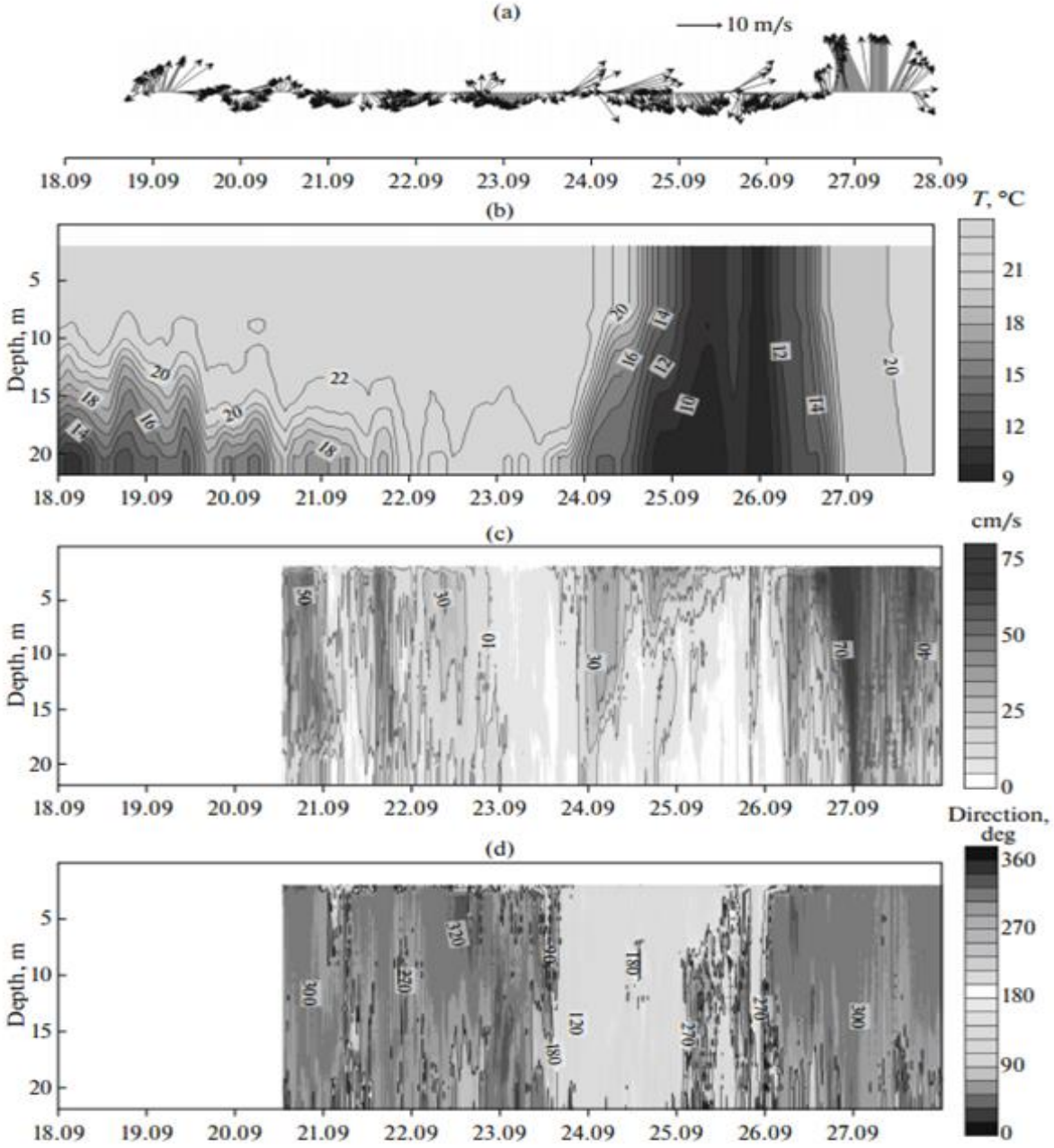

Fig. 6. Observational data of September 18–27, 2013: (a) wind velocity measured by automatic weather station; (b) vertical distribution of water temperature based on thermistor chain data; (c) absolute value of the current velocity measured by the bottom-mount ADCP; (d) direction of the current measured by on the bottom-mount ADCP.

Figure 6b demonstrates also an incomplete upwelling event on September, 18-22. Cold thermocline water did not rich the surface instead it was observed at the depth of about 10 m. The cause of this upwelling event was not a wind forcing. As could be seen from Fig. 6a, wind was weak and variable during those days. However, the existence of the alternating alongshore and eddy currents, whose nature is not directly related to local wind forcing, should be a widespread cause of coastal incomplete upwellings and downwellings. Indeed, if a NW baroclinic alongshore jet exists in

the upper due to geostrophic adjustment a downwelling should be observed near the coast and the upwelling would occur in the case of a SE alongshore current.

This upwelling of dynamical origin could enhance the wind induced turbulent entrainment of thermocline water into UML. Such events could increase the primary production and chlorophyll-a concentration of UML because the thermocline water is rather rich in nutrients. An example of the impact of wind-induced turbulent entrainment on the chlorophyll-a concentration is given in the next section of this paper.

Concluding this section we note that the analysis of variations of sea temperature and current velocity along with wind forcing allows us to understand the origin of the observed coastal upwelling and downwelling. This approach will be used in future investigations of upwelling and downwelling processes in the Black Sea.

IV. WIND-INDUCED TURBULENT ENTRAINMENT OF THERMOCLINE WATER INTO UPPER MIXED LAYER AS A SOURCE OF MAINTAINING PRIMARY PRODUCTION

Wind-induced turbulent entrainment is an important process that impacts the thickness and temperature of UML in a warm period of a year. The velocity W_e of turbulent entrainment is strongly nonlinear function of wind forcing. According to the parametrization [16]

$$W_e = 2.5U_*^3/(gH\Delta\rho/\rho_w), \qquad (2).$$

Here $U_* = (\tau/\rho_w)^{0.5} = (C_d\rho_a/\rho_w)^{0.5}V$ is dynamical frictional velocity in water, τ is wind stress, C_d is wind drag coefficient, ρ_a is air density, V is absolute value of wind velocity at 10 m height, $\Delta\rho$ – density jump across the thermocline.

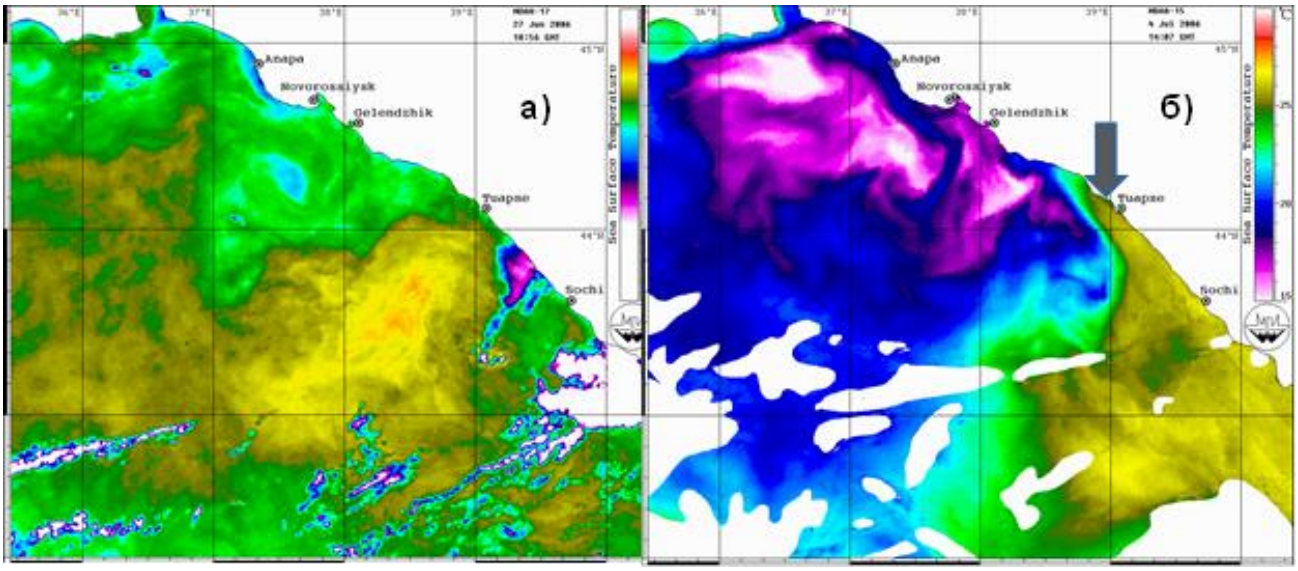

Fig.7. Two sequential thermal images (NOAA-15) of the NE Black Sea in July 2006 (GMT, hh:min): (a) July 01, 19:03; (b) July 03, 14:32. The thick arrow denotes the warm alongshore current.

It follows from (2) that the rate of turbulent entrainment is proportional to the cube of wind velocity and inversely proportional to the thickness of UML. If everything else being equal, an intensive turbulent entrainment occurs when the wind is strong, and the initial thickness of the UML is small. This situation was observed at the beginning of July in 2006 when after a long period of weak wind, strong burst of the northeasterlies of the speed about 15 m/s was observed. Initially thickness of the UML was about 10 m. After two days of the strong wind, the UML thickness increased to 25 meters while its temperature dropped from 22-25°C to 15-18°C (Fig.7), see also [18]. The application of (2) to evaluate the temporal evolution of the UML under the real wind forcing yielded results similar to those observed (see Fig. 8).

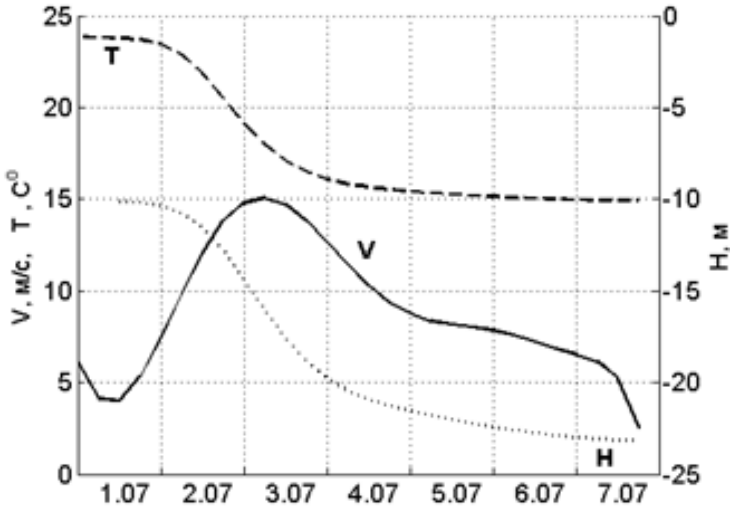

Fig.8. Time evolution of absolute value of the wind velocity V based on the NCEP data, the UML thickness H and its temperature T during July 1–7, 2006, in the area of strong winds between the Kerch straight and city of Tuapse.

One important phenomenon related to strong northeasterly wind need to be mentioned also is a formation of warm alongshore cyclonic current (Fig. 7). This fast current originates from Tuapse-Sochi region just after the wind decay and reaches Gelendzhik – Novorossiyisk region in 2-3 days. The physical origin and characteristics of the current are described in [18]. Here we would like to notice that quasi-periodic formation of such currents after the northeasterly wind events could be an efficient mechanism of alongshore transport of nutrients and pelagic species from the SE sea towards the NW sea.

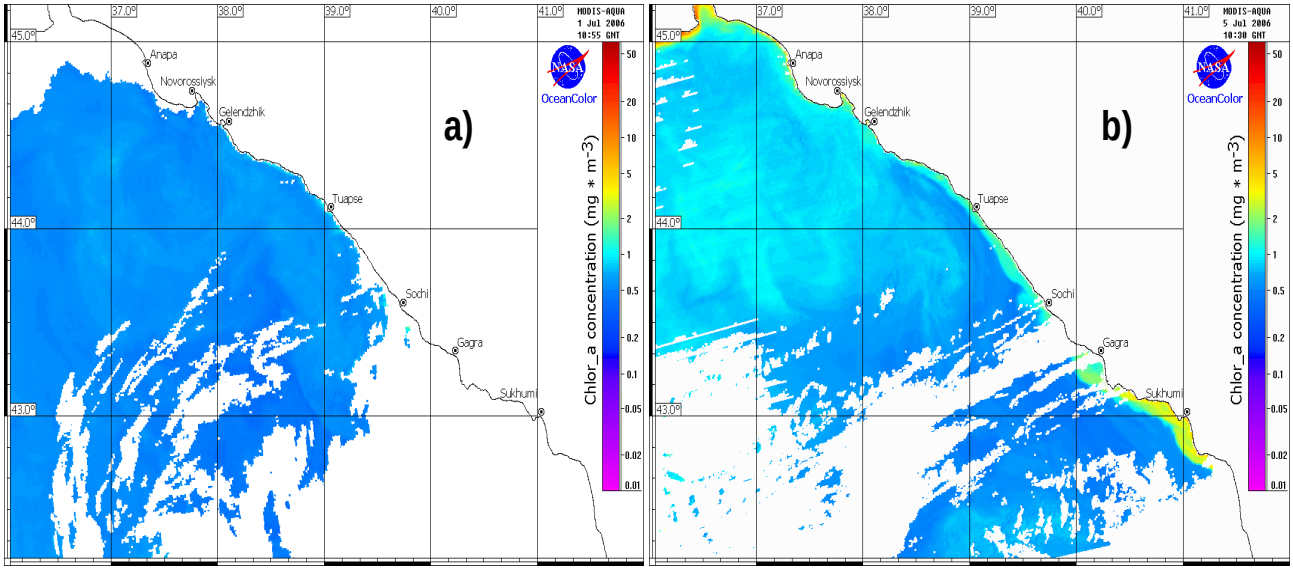

Fig. 9. Chlorophyll-a concentration at two sequential satellite images (MODIS-Aqua) in the NE Black Sea in July 2006 (GMT, hh:min): (a) July 01, 19:03; (b) July 05, 14:32.

An intense turbulent entrainment of thermocline water into UML led to increase of satellite measured chlorophyll-a concentration (CC) two days after the wind decay (Fig. 9). Using the empirical relation between the CC values derived from the satellite data and *in situ* measurements was calculated. The plot of these values is shown in Fig. 10 along with that of the wind velocity. As follows from Fig. 10 the increase in CC lasted for a few days. In a week after the decay of strong wind, CC recovered to its initial level. An impact of wind forcing on CC and primary production should be studied in more details in the future.

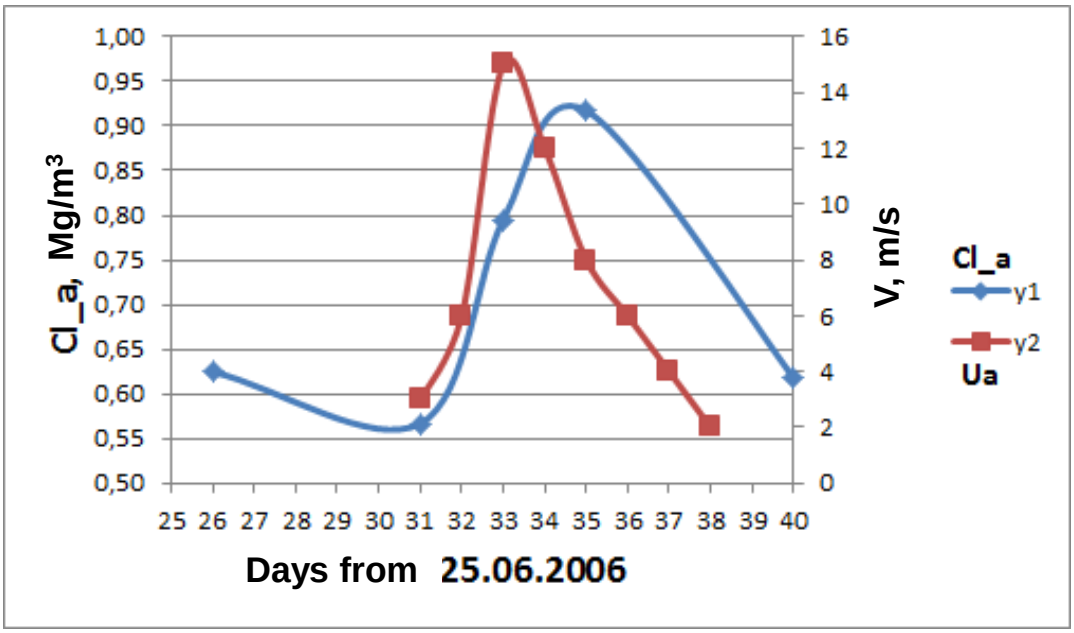

Fig. 10. Time evolution of chlorophyll "a" concentration (Cl_a) together with wind velocity (V).

V. Acknowledgements

The development of a moored profiler was supported by the Program №43 of the RAS, observational part of the work - by the RNF grant №14-50-00095, the data processing and analysis – by the RFBR grants №№14-05-00159 and 14-05-00792.

VI. References

1. *Zatsepin, A. G., Ostrovskii, A. G., Kremenetskiy, V. V., Nizov, S. S., Piotukh, V. B., Soloviev, V. A., et al.* Subsatellite polygon for studying hydrophysical processes in the Black Sea shelf-slope zone // Izvestiya RAS, Atmospheric and Oceanic Physics. 2014. V.50 №1. P. 13-25.
2. *Ostrovskii A. G., Zatsepin A. G., Solovyev V. A., Tsibul'skii A. L., and Shvoev D. A.* Autonomous system for vertical profiling of the marine environment at a moored station // Oceanology. 2013. V. 53 № 2. P. 233–242.
3. *Zatsepin A. G., Korzh A. O., Kremenetskii V. V., Ostrovskii A. G., Poyarkov S. G., and Solov'ev D. M.* Studies of the hydrophysical processes over the shelf and upper part of the continental slope of the Black Sea with the use of traditional and new observation techniques // Oceanology. 2008. V.48. № 4. P. 446–475.
4. *Zatsepin A. G., Kondrashov A. A., Korzh A. O., Kremenetskii V. V., Ostrovskii A. G., and Solov'ev D. M.* Submesoscale eddies at the Caucasus Black Sea shelf and the mechanisms of their generation // Oceanology. 2011. V. 51. №4. P. 554–567.
5. *Zatsepin A. G., Piotukh V. B., Korzh A. O., Kukleva O. N., and Solov'ev D. M.* Variability of currents in the coastal zone of the Black Sea from long-term measurements with a bottom mounted ADCP // Oceanology. 2012. V. 52. №5. P. 579–592.
6. *Bogatko, O. N., S. G. Boguslavskii, Yu. M. Belyakov, and R. I. Ivanov.* Surface currents in the Black Sea – In: Kompleksnye Issledovaniya Chernogo Morya, Marine Hydrophysical Institute. 1979. Sevastopole. Ukraine. P. 25–33. (in Russian).
7. *Stanev E.V.* On the mechanisms of the Black Sea circulation. Earth-Sci. Rev. 1990 V. 28. P. 285–319.
8. *Zatsepin A. G., Denisov E. S., Emel'yanov S. V., Kremenetskiy V. V., Poyarkov S. G., Stroganov O. Yu., et al.* // Effect of bottom slope and wind on the near-shore current in a rotating stratified fluid: laboratory modeling for the Black Sea // Oceanology. 2005. V. 45. №1, P. S13-S26.
9. *Ginzburg, A. I., A. G. Kostianoy, D. M. Soloviev, and S. V. Stanichny.* Remotely sensed coastal/deep-basin water exchange processes in the Black Sea surface layer – In: Satellites, Oceanography and Society, Ed. D. Halpern, Elsevier Oceanography Series, 63, 273–287, 2000.
10. *Zatsepin, A. G., Ginzburg, A. I., Kostianoy, A. G., Kremenetskiy, V. V., Krivosheya, V. G., Stanichny, S. V., & Poulain, P. M.* Observations of Black Sea mesoscale eddies and associated horizontal mixing // Journal of Geophysical Research: Oceans. 2003., V. 108. №. C8. P. 1978–2012.
11. *Zatsepin A.G., Ostrovskii A.G., KIremenetskiy V.V., Piotoukh V.B., Kuklev S.B., Kukleva O.N., et al.* On the nature of short-period oscillations of the main Black Sea pycnocline, submesoscale eddies and response of the marine environment to the catastrophic shower of 2012 // Izvestiya RAS, Atmospheric and Oceanic Physics. 2013. V. 50 №1. P. 717-732.

12. *Elkin D.N., Zatsepin A.G.* Laboratory Investigation of the Mechanism of the Periodic Eddy Formation Behind Capes in a Coastal Sea // Oceanology. 2013. V. 53. No.1 .P. 24-35.
13. *Elkin D.N., Zatsepin A.G.* Laboratory study of a shear instability of an alongshore sea current // Oceanology. 2014. V.54. No.5. P. 576-582.
14. *Elkin D.N., Zatsepin A.G.* Laboratory studies of the of eddy formation in rotating and non-rotating fluid due to spatially non-uniform wind forcing // Selected papers of EMECS11 – Sea Coasts XXVI Joint Conference. 2016 (this volume).
15. *Zatsepin, A. G., Silvestrova, K. P., Kuklev, S. B., Piotoukh V. B., and Podymov O. I.* Observations of a Cycle of Intense Coastal Upwelling and Downwelling at the Research Site of the Shirshov Institute of Oceanology in the Black Sea // Oceanology. 2016. V.56. No.2. P. 203-214.
16. *Zhurbas, V. M. Oh, I. S. and Park, T.* Formation and decay of a longshore baroclinic jet associated with transient coastal upwelling and downwelling: a numerical study with applications to the Baltic Sea // J. Geophys. Res. 2006. V. 111. P. 1--18 doi: 10.1029/2005JC003079.
17. *Kato, H. and Phillips, O. M.* On the Penetration of a Turbulent Layer into a Stratified Fluid // J. Fluid Mech. 1969. V. 37. P. 643–655.
18. *Zatsepin A.G., Kremenetskiy V.V., Piotoukh V.B., Poyarkov S.G., Ratner Yu.B., Soloviev D.M., et al.* Formation of the Coastal Current in the Black Sea Caused by Spatially Inhomogeneous Wind Forcing upon the Upper Quasi-Homogeneous Layer // Oceanology. 2008. V.48. No.2. P. 176-192.

ESTIMATE OF DEPENDENCE OF THE VERTICAL TRBULENT DIFFUSION COEFFICIENT FROM BUOYANCY FREQUENCY FOR COASTAL ZONE OF THE BLACK SEA

Globina Lubov Viktorovna, Federal State Budget Scientific Institution "Marine Hydrophysical Institute of RAS" FSBSI MHI

The article highlights the most important studies of oceanographic processes, such as horizontal convection, winter cascading on the shelf and continental slope, the processes in the bottom of the Black Sea. The results of the study of small-scale structure of the shelf upper active layer of the Black Sea in 2014 are discussed. The new information about the distribution of the eddy diffusivity with depth in the coastal part of the Heracleian peninsula is given. The investigated dependence vertical turbulent diffusion coefficient from buoyancy frequency at the active layer is found to be has a quadratic character for the entire shelf area and doesn't depend on the stratification.

Keywords: turbulent diffusion, energy dissipation rate, cold intermediate layer, cascading.

I. INTRODUCTION

In the stratified ocean interior there are variety physical mechanisms aimed at the exchange of energy, temperature, salinity between water masses of different scales. Each mechanism operates under certain hydrophysical conditions. Joint study of the processes taking place on different spatial and temporal scales, will set the boundary conditions for the operation of various physical mechanisms for simplifying and solving mathematical models of semi-empirical equation of turbulent diffusion.

The ocean interior is conditionally divided on the layers. Layers are divided according to the action type of some mechanism. For example, in the ocean there are three main layers on the distribution of buoyancy frequency: the upper mixed layer (or a layer of wind mixing), the active layer (up to a maximum frequency of buoyancy), the main pycnocline (or a layer of local mixing) and the bottom layer of the convective exchange.

For the active layer an additional cold intermediate layer can be identified. It is involved in the formation of seasonal thermocline and is formed in the coastal part of the sea (ocean). Coastal waters differ from the open ocean waters by uneven warming of the water surface, which depends on the breadth and depth of the water area, the difference of temporal variability, geothermal.

An important role in maintaining the turbulent exchange plays cascading. It makes contribution to the exchange of water between the shelf and the deep ocean. Its effect is enhanced in the marginal seas, due to the instability of the main pycnocline, impervious surface water on the depth [1].

II. THE MECHANISM OF FORMATION OF THE COLD INTERMEDATE LAYER FOR THE BLACK SEA

There are all conditions for the formation and stable presence of the cold intermediate layer in the Black Sea. The Black Sea separate from the world's oceans and has a circulation mode.

The northwestern part of the Black Sea is a broad continental shelf, which narrowing stretches along the western coast to the Bosporus. The annual river flow is an average of more than 310 km^3. 80% of this amount goes to the north-western shelf of shallow water, where the Danube and Dnieper empty into. Fresh water balance is positive, because the coastal runoff and precipitation exceeds evaporation of about 180 km^3 [2].

Thus, any temperature change in the north-western waters of the Black Sea create the preconditions for the formation of convective horizontal and vertical circulation, which is the main mechanism for the formation of cold sea water.

The cooling of water is begun with river runoff. It is considered the original source of the dense cold waters.

With a small difference of hydro-physical characteristics from surrounding waters, the river plume is a stable structure. This structure is a little stratified, and there may be a separate layer, involving the nearby water in the common stock process, thereby changing the initial geometry of the river plume and consequently - the buoyancy gradient [3].

Coastal waters are cooled, become denser and heavier. They flow down the slope to their isopycnic level and then are distributed as intrusion, thereby displacing the lighter water, resulting in convective motion of water nearby. This theory is applied to the shelf zone of the sea, when the angle between the sea level and the shelf is relatively small.

Taking into account the external effects for the formation mechanism of convective exchange: Earth's rotation, transfer the Ekman, also contributing to an increase of the environmental water in river plume, wind and given runoff direction, the horizontal-vertical convective exchange takes the form of alongshore current [4].

III. USED DATA

Small-scale characteristics of the upper active layer were obtained by a free-falling probe measuring complex *Sigma-1,* during the expedition in November 2014, on the research vessel *Nikolaev* in the conditions of the winter circulation of the Black Sea. Measurements were carried out along the coastal areas of the peninsula from Cape Chersonese to Aya [5,6].

IV. ANALYSIS AND METHODOLOGY

Based on the measurement data of the three vector velocity pulsation components, the estimation of dependence of the vertical turbulent diffusion coefficient on the stratification was obtained.

The applied values in the computation were averaged over the depth in increments of 0.1m, 0.3m and 0.5m. The turbulent energy dissipation rate was calculated using the following formula (1):

$$\varepsilon = \frac{15}{2}\nu\left(\frac{\partial u'^2}{\partial z} + \frac{\partial \upsilon'^2}{\partial z}\right) \quad (1)$$

where u' and υ' - the horizontal speed pulsations on X and Y axes, respectively, ν - molecular viscosity water coefficient. Buoyancy frequency was calculated as follows (2):

$$N = \sqrt{\frac{g}{\rho_0}\left(\frac{\partial \rho}{\partial z}\right)} \quad (2)$$

where g is the acceleration of free fall, ρ is the density, ρ_0 the density in the layer. Turbulent diffusion coefficient was calculated in accordance with the well-known Osborn [7] relation (3):

$$K = 0{,}2\frac{\varepsilon}{N^2} \quad (3)$$

The calculation example of the eddy diffusivity for a straight line along the stations is listed below.

station№6:

$K = 2 \cdot 10^{-7} N^{-1,96}$

station №7:

3-20 м.: $K = 3 \cdot 10^{-8} N^{-1,7}$

20-50 м.: $K = 4 \cdot 10^{-9} N^{-2,0}$

50-80 м.: $K = 6 \cdot 10^{-9} N^{-1,9}$

station №8:

4-30 м.: $K = 2 \cdot 10^{-7} N^{-1,98}$

30-59 м.: $K = 10^{-6} N^{-1,64}$

62-83 м.: $K = 10^{-7} N^{-1,99}$

station №9:

3-13 м.: $K = 2 \cdot 10^{-9} N^{-2,9}$

15-50 м.: $K = 9 \cdot 10^{-8} N^{-2,15}$

station №10:

3-21 м.: $K = 9 \cdot 10^{-8} N^{-2,15}$

21-28 м.: $K = 2 \cdot 10^{-7} N^{-1,85}$

28-47 м.: $K = 6 \cdot 10^{-7} N^{-1,74}$

For each station, the total layer is divided into sub-layers, depending on the buoyancy gradient sign. For example, three sub-layer were selected for the station №7: in the first one the decrease in the buoyancy frequency with depth was observed, in the second - the growth, in the third – the decrease. This division was carried out to check for strict stratification and its influence on the mixing of the sea upper layers.

The presented equalities of the eddy diffusivity have the same index at buoyancy frequency, $K \propto N^2$, and does not depend from on the selected layer (independent from the division into sub-layers and stratification). This ratio remains everywhere up to bottom convective mixing layer.

If the sea shelf zone is characterized by intrusive stratification in the presence of horizontal exchange, after the cascading transition to the continental slope being the vertical exchange process intensification process consequence, the intrusions do not exist for a long time and the break up, keeping the temperature of the main cold intermediate layer constant.

Unlike the water circulation mechanism on the shelf, there are other mechanisms forming the vertical exchange on the continental slope. In the deep sea the convective exchange weakens and the main source of vertical mixing becomes instability and overturning internal waves, taking into account topographic features on the sloping bottom [8].

This fact is confirmed by the fact that the shelf temperature is changed in the horizontal direction, i.e. stratification adapts to external conditions, after crossing the *shelf - continental slope* boundary the temperature vertically changes (the external conditions are adjusted under stratification).

The change of one mechanism to another can be seen in the change of the exponent under *N* in the expression *K*(*N*). For example, data distribution analysis of the turbulent energy dissipation rate and buoyancy frequency, depending on the depth of the coastal part of the Southern Coast of Crimea from the article [9], showed the following expression for the stratified layer of the main pycnocline: $K \propto N^{-1,1}$.

In the given turbulent diffusion coefficient distribution with depth the studied value minimum was traced at 100 m depth and increased to its maximum at 400 m depth. The result obtained for the studied dependence under the in situ data from [9] showed good agreement with the previously obtained model of dependence of the turbulent diffusion coefficient on buoyancy frequency for the Black Sea.

Thus, due to the action of different mechanisms should be applied a different approach to the determination of the exchange ratios for the upper mixed layer on the shelf and in the deep sea. Cascading plays the main role in the redistribution of water masses on the shelf; it creates preconditions for involving of cold water into the deep sea, due to the formation of intrusions.

V. REFERENCES

[1] И. П.Чубаренко “Горизонтальная конвекция над подводными склонами,” *Калининград : Терра Балтика*, 2010, 255с.

[2] А.Н. Коршенко “Качество моских вод по гидрохимическим показателям,” *Ежегодник, Москва, «Наука»*, 2013, 200с.

[3] F. M. Pimenta, A. D. Kirwan, P. Huq “On the transport of buoyant coastal plumes,” *J. Phys.Oceanogr*, 2011, 41, pp. 620–640.

[4] C. Moffat, S. Lentz “On the response of a buoyant plume to downwelling-favorable wind stress,” *J. Phys.Oceanogr,* 2012, pp.1083-1098.

[5] А.С. Самодуров, А.М.Чухарев, А.Г. Зубов, О.И. Павленко “Структурообразование и вертикальный турбулентный обмен в прибрежной зоне Севастопольского региона,” *Морской гидрофизический журнал*, 2015 № 6, с. 3-16.

[6] А.С. Самодуров, А.М. Чухарев, О.Е. Кульша “Режимы вертикального турбулентного обмена в верхнем стратифицированном слое Черного моря в районе Гераклейского полуострова,” *Процессы в геосредах*, 2015, № 3, с. 63 – 69.

[7] T.R. Osborn “Estimations of local rate of vertical diffusion from dissipation measurements,” *J. Phys. Oceanog*, 1980, 10, pp.83‑89.

[8] T. Dauxois, A. Didier, E. Falcon “Observation of near-critical reflection of internal waves in a stably stratified fluid,” *Physics of fluids,* 2004, V.16, №6, pp.1936-1941.

[9] А.Н. Морозов, Е.М. Лемешко “Оценка коэффициента вертикальной турбулентной диффузии по данным CTD/LADCP-измерений в северо-западной части Черного моря в мае 2004 года,” *Морской гидрофизический журнал*, 2014, № 1, с.58-67

CARBONATE SYSTEM TRANSFORMATION IN THE SEVASTOPOL BAY (THE BLACK SEA)

Natalia Orekhova, Marine Hydrophysical Institute of RAS
Eugene Medvedev, Marine Hydrophysical Institute of RAS
Sergey Konovalov, Marine Hydrophysical Institute of RAS

natalia.orekhova@mhi-ras.ru

A 20% increase of the carbon dioxide concentration in the atmosphere during the last century and a dramatic increase in nutrient load to marine systems due to human activity have resulted in pronounced carbon cycle transformation in coastal areas. Acidification and carbon dioxide increasing in the water column and appearance of oxygen minimum zones are reported for the worldwide coast. This makes ecological assessment of aquatic systems, including key cycles of elements, an important social and scientific task.

In this study, we present information on the inorganic part of the carbon cycle and its transformation in the Sevastopol Bay (the Black Sea). This semi-enclosed coastal area has been under heavy anthropogenic pressure over the last century. Municipal and industrial sewage discharge, maritime activities, including excavation of bottom sediments, provide additional sources of nutrients and organic carbon. We present data on dynamics of the inorganic part of the carbon cycle from 1998 – 2015. Values of pH and total alkalinity were obtained analytically, whereas CO_2, HCO_3^-, CO_3^{2-} concentrations and pCO_2 values were calculated. Dissolved inorganic carbon (DIC) and its partitioning into CO_2, HCO_3^-, CO_3^{2-} demonstrate the state of the carbon cycle and its evolution. Our observations reveal up to 2% increase of DIC from 1998 – 2015, but the value of pCO_2 has increased by up to 20% in line with declining pH (acidification). Seasonal variations are far more pronounced and reveal extremes for areas of oxygen minimum zones. This results in negative consequences for the ecosystem, but these consequences for the Sevastopol Bay's ecosystem remain reversible and the carbonate system can be restored to its natural state.

Kew words: carbonate system transformation, pCO_2, Sevastopol Bay

I. INTRODUCTION

Coastal areas, being the major link between terrestrial and marine ecosystems, are under keen interest of scientists. Coastal ecosystems reveal results of natural and anthropogenic activities, and they expose fast deviations from their nature state. This is the reason of investigations of coastal systems and their stability under climate variations and anthropogenic pressure.

Long-term observations show reversible changes in marine ecosystems even under significant anthropogenic pressures. This resistance is a result of the system's buffer capacity, allowing restoring the original quality of the ecosystem, supporting its stability and recovering. One of the most important marine buffer systems is the carbonate system, which is the key part of the biogeochemical carbon cycle. The carbonate system mainly determines pH consistency [1]. Any

deviations in pH, e.g. acidification, leading to negative consequences of appearance of reduced heavy metals and other toxic species in the water column, the dissolution of coccolithophores and mollusk carbonate shells, coral reefs and carbonate saturated sediments [2].

The carbonate system, including carbonate- and bicarbonate-ions, dissolved carbon dioxide, carbonic acid and hydrogen ions, is highly sensitive to any changes in biogeochemical processes and physics occurring in coastal marine ecosystems [3]. Changes in temperature, pressure and salinity influence inorganic carbon partitioning. Organic carbon mineralization as well as its production result in changes in the total inorganic carbon concentration in the water column [1].

The global temperature has been increasing and carbon dioxide concentration in the atmosphere has increased more than 20% during the last century [4]. Euthrophication, caused by dramatic human activity induced increase in the nutrient and organic carbon input to marine systems, have also resulted in pronounced transformation of the carbon cycle in coastal areas [5]. Acidification, increasing carbon dioxide concentration in the water column and appearance of oxygen minimum zones have been reported for the worldwide coast. This makes ecological assessment of aquatic systems, including key cycles of elements, an important social and scientific task.

In this study, we present information on the inorganic part of the carbon cycle and its transformation in the Sevastopol Bay (Fig. 1). This is semi-enclosed estuarine type bay with entering river Chernaya. The bay has been under heavy anthropogenic pressure over the last century. Municipal and industrial sewage waters, maritime activities, including excavation of bottom sediments, provide additional sources of nutrients and organic carbon. Artificial sea-malls at the bay enter restrict water exchange with the open sea and support accumulation of organic carbon, leading to negative consequences for the bay's ecosystem [6].

This work is addressed to dynamics of the inorganic part of the carbon cycle from 1998 – 2015.

II. MATERIALS AND METHODS

Samples were collected from the surface and bottom layers of the Sevastopol Bay (Fig. 1) with Niskin bottles during 1998 – 2015.

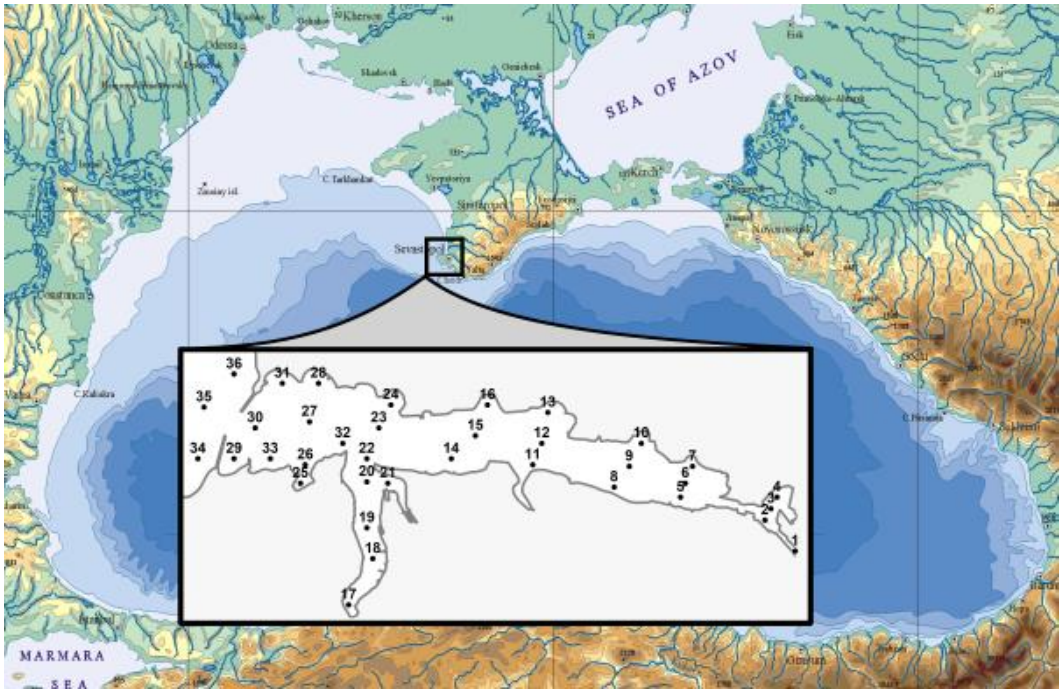

Fig. 1. Sampling locations in the Bay of Sevastopol

The dissolved oxygen concentration, salinity, pH and alkalinity values were obtained analytically [7]. The total alkalinity was determined by direct titration by hydrochloric acid with a potentiometric end-point detection, pH was determined with a potentiometric pH-meter with NBS buffer solutions [1]. The standard deviation of measurement of 10 parallel samples did not exceed 0.02 pH units. Whereas CO_2, HCO_3^-, CO_3^{2-} concentrations and pCO_2 values were calculated as suggested in [7]. The dissociation constants of carbonic acid, recommended by the Department of Marine Sciences of UNESCO, were used [7]. Boron was assumed a conservative part of salinity; therefore, the boron content was calculated from the salinity [4]. The effect of dissociation of water, phosphoric acid, sulfuric acid, hydrofluoric acid and other acids were not taken into account.

Data from the 1st station (Fig. 1) were not taken into account because it represented fresh waters of river Chernaya, rather than the considered marine waters of the bay.

III. RESULTS AND DISCUSSION

The dissolved part of the carbonate system is represented by the system of reversible processes:

$$CO_2\ (atm) \leftrightarrow CO_2\ (water) \leftrightarrow CO_2 + H_2O \leftrightarrow HCO_3^- + H^+ \leftrightarrow CO_3^{2-} + 2H^+$$

The total amount of dissolved CO_2, HCO_3^- and CO_3^{2-} is called dissolved inorganic carbon (DIC):

$$DIC = [CO_2] + [HCO_3^-] + [CO_3^{2-}] \quad (1)$$

DIC can serve as an indicator of changes in the carbon cycle [8].

Due to DIC is the sum of inorganic forms of carbon, its changes are governed by processes of photosynthesis (2) and CO_2 exchange in the surface waters and organic carbon oxidation in the bottom waters (3).

$$6CO_2 + 6H_2O \rightarrow 6H^+ + 6HCO_3^- \rightarrow C_6H_{12}O_6 + 6O_2 \quad (2)$$

$$C_6H_{12}O_6 + 6O_2 \leftrightarrow 6CO_2 + 6H_2O \leftrightarrow 6H^+ + 6HCO_3^- . \quad (3)$$

Photosynthesis results in consumption of inorganic carbon and production of organic carbon. This decreases DIC and increases pH (due to pH = – $\lg aH^+$). On the contrary, organic carbon oxidation increases DIC and supports acidification.

In the Sevastopol bay's waters, the content of DIC in the bottom layer has always been insignificantly higher as compared to the surface layer (Fig. 2), due to organic carbon oxidation. Our previous studies show that the content of organic carbon in sediments of the Sevastopol bay exceeds 4% [8] due to high anthropogenic pressure and accumulation of organic carbon in the bottom sediments. In spite of higher DIC concentrations in bottom waters, its changes from 1998 to 2015 do not exceed 1%, whereas this increase is about 2% in the surface layer (Fig. 2). This suggests that the flux of organic carbon to the bottom waters exceeds the oxidation potential and it increases the content of organic carbon in sediments.

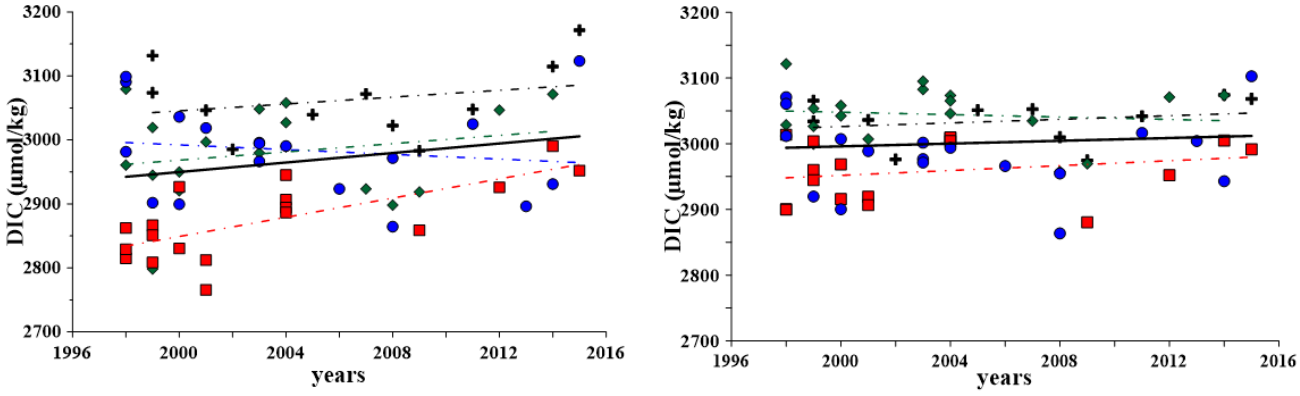

Fig. 2. Variations in the DIC in 1998 – 2015 in the surface (a) and bottom (b) layers of water: black cross – Winter, green rhomb – Spring, red square – Summer, blue circle – Fall

Seasonal DIC changes are more pronounced (Fig. 3). In cold seasons DIC concentrations expose maximum values, and winter DIC inventory in the surface layer is larger than in the bottom layer. This fact evidences good vertical ventilation of the entire water column and increasing CO_2 solubility in cool waters. In warmer seasons, the DIC content in the bottom waters was larger than in the surface layer.

In spring, one can expect minimum DIC inventory in the surface layer due to active spring bloom of phytoplankton. Still, our observations reveal opposite results (Fig. 3). This might be due to seasonal flood of river Chernaya, supplying rich with organic matter, carbon dioxide and suspended matter waters.

A linear decrease of the DIC content occurs in the surface layer from winter to summer (Fig. 3). This fact can result from intensive photosynthesis, decreasing CO_2 solubility, and strong vertical stratification, preserving carbon dioxide in bottom waters.

In fall, the DIC content raises. In the surface layer, its concentration equals spring's values. This increase of DIC is a result of good vertical ventilation supporting contribution from the bottom layer and equal DIC concentrations in the surface and bottom layer (Fig. 3).

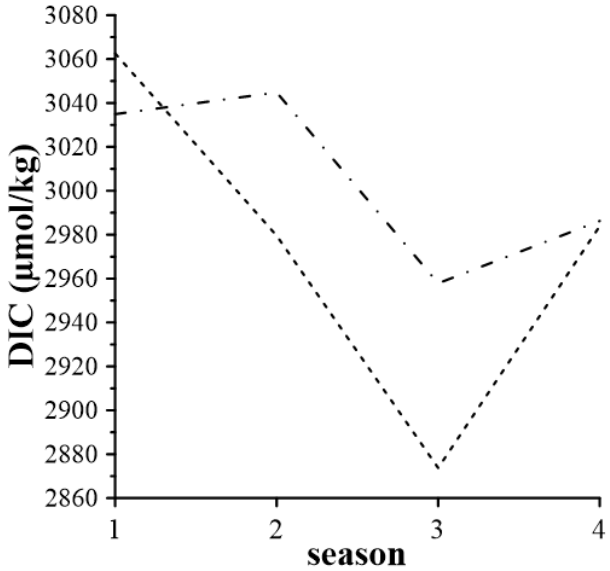

Fig. 3. Seasonal DIC variability averaged for 1998 – 2015: dash line – surface layer, dash dot line – bottom layer; numeric 1 – Winter, 2 – Spring, 3 – Summer, 4 – Fall

Seasonal variations of the DIC content in the bottom waters are also distinct, but they differ from those for the surface waters (Fig. 3). The maximum of DIC is in spring, but its value is insignificantly larger than in winter. In summer, strong seasonal stratification restricts oxygen supply to bottom waters. As the result, the oxygen flux is not enough for oxidation all of organic carbon (3), and this is the reason of organic carbon accumulation in bottom sediments. The DIC content increases in fall (Fig.3), and equals values in the surface layer, due to water mixing. Increased values of the DIC content in fall is likely due to accumulation of products of organic carbon oxidation.

Despite large seasonal variability, the overall average annual content of DIC in the water column for 1998 – 2015 does not reveal significant changes and/or persistent trends, which is the evidence of the bay's carbonate system to recover.

The main contribution to DIC brings bicarbonate-ion (90%) and it has the same dynamics. In 1998 – 2015, an increase in its concentration has been observed. For the bottom layer, the bicarbonate-ion's concentration has increased by about 1%. The content of carbon dioxide has decreased by 2% and the carbonate-ion concentration has risen by up to 2%. These changes are statistically significant and confirm our assumption of increasing contribution of organic carbon to the system and its increasing preservation in the bottom sediments.

For the surface waters, the revealed increase in the content of bicarbonate-ion is about 4%. The carbon dioxide concentration has increased in the surface layer waters by up to 20% and the concentration of carbonate-ion has decreased by 17%. The traced increase in the carbon dioxide concentration and nutrient supply to the Sevastopol bay's support eutrophication and intensive production of organic carbon (2). We do not trace increasing DIC and HCO_3^-concentrations in the bottom waters, so we suppose that organic carbon is accumulated in sediments. This conclusion agrees with our previous investigations of bottom sediments of the bay [6, 8], revealing seasonal oxygen deficiency, reduced sulfur forms appearance and reduced conditions in the bottom waters and in the upper layer of the sediments.

An increase in the bicarbonate-ion concentration is accompanied by increase in the hydrogen ion concentration, which is revealed by descending values of pH (acidification). For 2009 – 2015, the average values of pH has lowered by 1% in the surface layer, and by 0.1% – in the bottom waters.

The traced decrease of pH in the bottom waters evidences a growth of organic carbon in the Sevastopol bay. As a result, CO_2 is released to the water column and carbonates are gradually dissolved. The bottom waters, enriched in carbon dioxide, get mixed with the surface waters, providing additional CO_2 and supporting primary production. As the content of CO_2 in the bottom waters increases, the partial pressure rises too (4):

$$pCO_2=\frac{[CO_2]}{K_0}, \quad (4)$$

where $[CO_2]$ – the equilibrium concentration of carbon dioxide, μmol/l;
K_0 – Henry constant for carbon dioxide, μmol/(l·atm).

Photosynthesis (2) results in carbon dioxide uptake, DIC and pCO_2 decrease and pH increase, which is accompanied by a shift in the carbonate system reducing the HCO_3^- concentration. Nutrients facilitate primary production processes in the surface waters, thus pH is expected to increase too. However, a decrease of pH, increase of the DIC and pCO_2 content is found out in the surface layer (Fig. 2, 4). This may indicate that both photosynthesis and organic matter mineralization are the main biological and chemical processes, governing the carbonate system in the Sevastopol bay.

The carbon dioxide partial pressure in the bottom waters was expectedly above its level in the surface waters (Fig. 4). It is due to contribution of organic matter oxidation, produced in the bay's waters (2) and/or provided from anthropogenic sources.

An increase of the pCO_2 content in the bay's waters has been observed for 1998 – 2015. From 2009 to 2015, the rate of this increase is higher in the surface layer than in the bottom layer (Fig. 4). For the surface waters, the noticed increase is about 17% or 50 μmol in the absolute value from 1998 to 2015, whereas it is 2% or 8 μmol in the bottom waters (fig. 4).

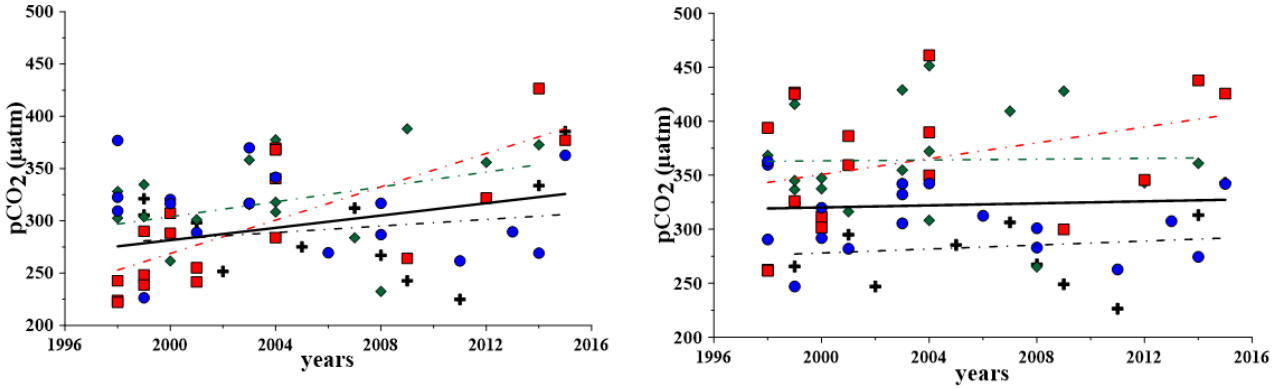

Fig. 4. pCO_2 variations in the surface (a) and bottom (b) waters for 1998 – 2015: black cross – Winter, green rhomb – Spring, red square – Summer, blue circle – Fall

Seasonal variations of pCO_2 (Fig. 4a) in the surface waters reveal a persistent upward trend in winter (by 9%), spring (by 19%) and especially in summer (up to 46%). This might indicate that the anthropogenic influence is stronger in summer. In spring and winter, intensive water dynamics and mixing balance the effects of eutrophication.

In the bottom layer (Fig. 4b), the maximum inter-annual uprising trend is traced for summer (by 17%). In winter and spring, this upward trend is about 1%. In fall, a 6% decrease of the pCO_2 level has been observed.

Average seasonal variations in 1998 – 2015 (Fig. 5) demonstrate that surface pCO_2 values are higher than the bottom values only in winter and they are minimum. It is due to good vertical mixing and slowdown of processes of organic carbon oxidation, in spite of increasing of gas solubility at low temperatures and absorption of CO_2 from the atmosphere. In spring, the pCO_2 level in the surface layer is smaller than in the bottom waters (Fig. 5). In the surface layer, minimum pCO_2 values are due to spring phytoplankton bloom, which should lead to consumption of CO_2 and decrease of pCO_2, respectively. Maximum pCO_2 values in the bottom waters are due to active organic carbon oxidation in sediments.

In summer, the level of pCO_2 in the surface layer drops (Fig. 5), supporting the maximum difference between values in surface and bottom layers. The summer value of pCO_2 in the bottom waters is comparable to those in spring (Fig. 5). This is due to organic carbon oxidation (3) and dissolution of carbonate-ion due to acidification.

In fall, pCO_2 increases in the surface waters and equals values for the bottom waters (Fig. 5). This is due to increasing solubility of CO_2 in cooling waters and spring-to-fall accumulation of products of organic matter oxidation. Carbon dioxide and nutrients, produced after organic matter oxidation, accumulate in the bottom waters and serve as an additional source of CO_2 and nutrients for the surface layer.

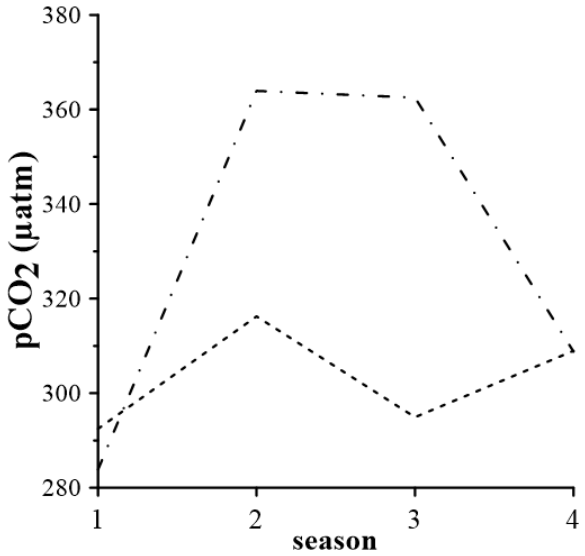

Fig. 5. pCO_2 seasonal changes averaged for 1998 – 2015: dash line – surface layer, dash dot line – bottom layer; numeric 1 – Winter, 2 – Spring, 3 – Summer, 4 – Fall

Any changes in surface levels of pCO_2 affect carbon dioxide exchange between water and the atmosphere. Depending on the concentration of CO_2 in the surface layer the water column may serve as a source or sink of carbon dioxide.

Partial pressure of atmospheric carbon dioxide is currently about 400 µatm [10]. Thus, from our obtained data, waters of the Sebastopol bay usually absorb carbon dioxide from the atmosphere (Fig. 4a). The exception was summer of 2014, when the surface pCO_2 reached 426 µatm and supported a flux of CO_2 to the atmosphere. However, it is typical for coastal waters in summer [11].

Quantifying gas exchange between water and the atmosphere [12] our results show that invasion (when the water column absorb carbon dioxide from the atmosphere) is typical, but this ability to consume CO_2 from the atmosphere has decreased by 20% from 2001 to 2015.

IV. CONCLUSIONS

In warm seasons, the main processes governing the carbonate system in the water column are respiration of organic matter in sediments and bottom waters and photosynthesis in the surface layer. The surface waters still absorb carbon dioxide from the atmosphere, but this ability has decreased by 20% from 2001 to 2015. In cold seasons, water dynamics and mixing can still balance the effect of eutrophication and promote system's recovery.

The content of DIC and pCO_2 for 1998 – 2015 has increased. DIC changes are below 1% and statistically insignificant. However, a significant increase of pCO_2 in the bottom and the surface layers (2 and 17% respectively) in line with decreasing pH (acidification) have been traced, indicating anthropogenic pressure. Seasonal oscillations are far more pronounced, as compared to inter-annual trends, and reveal extremes for appearance of oxygen minimum zones. This results in negative consequences for the ecosystem, but these consequences for the Sevastopol Bay's ecosystem remain reversible, and the carbonate buffer system can be restored yet. The ability of the bay to consumed CO_2 from the atmosphere and preserve organic carbon in sediments will expire

within the next few several years and the ecosystem will experience irreversible catastrophic changes.

This work has been funded from the RFBR research project №16-35-60006 mol_a_dk "Long-term changes in the carbon cycle characteristics of the Sevastopol bay."

V. REFERENCES

[1] R.E. Zeebe, D. Wolf-Gladrow, *CO_2 in seawater: equilibrium, kinetics, isotopes*, Elsevier Oceanography Series, 2001, P. 346.

[2] M. Bollmann et al., *World ocean review. Living with the oceans*. vol. 2. Maribus: Hamburg. 2010, P. 252.

[3] R.A. Feely, S.C. Doney, and S.R. Cooley "Ocean Acidification: present conditions & Future changes in a high-CO_2 World," *Oceanography*, vol. 22, No.4, pp. 36-47, 2009.

[4] F.J. Millero, "The Marine Inorganic Carbon Cycle," *Chemical Reviews*, vol. 107, pp. 308-341, February 2007.

[5] T. Kawano, "Trends in Ocean Acidification Research," *Science and Technology Trends*, Quarterly Review, vol. 36, pp. 68-78, 2010.

[6] N.A. Orekhova, S.K. Konovalov, "Polarography of the bottom sediments in the Sevastopol Bay," *Physical Oceanography*, vol. 19, No.2, pp. 111-123, March 2009.

[7] "Thermodynamic of the carbon dioxide system in seawater," in *Unesco technical papers in marine science*, No.51, Unesco, 1987. pp. 3-21.

[8] O.G. Moiseenko, N.A. Orekhova, "Investigation of the mechanism of the long-term evolution of the carbon cycle in the ecosystem of the Sevastopol bay," *Physical Oceanography*, vol. 21, No.2, pp. 142-152, July 2011.

[9] A.A. Bezborodov, V.N. Eremeev. *Physical and chemical aspects of interaction between ocean and atmosphere*, Kiev: Naukova Dumka, 1984, P. 192.

[10] E. Dlugokencky, P. Tans, NOAA/ESRL (www.esrl.noaa.gov/gmd/ccgg/trends/)

[11] J.E. Bauer, W.-J. Cai, P. A. Raymond, T. S. Bianchi, C. S. Hopkinson, and P. A. G. Regnier, "The changing carbon cycle of the coastal ocean," *Nature*, vol. 504, pp. 61-70, 2013.

[12] Y.I. Lyahin, V.P. Alexandrov, N.I. Pal'shin, "The calculation of CO_2 exchange balance between the ocean and the atmosphere for the Atlantic Indian and Pacific Oceans," Research and development of the World Ocean, Leningrad: Leningrad Hydrometeorological Institute, vol. 65, pp. 48-60, 1978.

AVAILABILITY OF NUMERICAL MATHEMATICAL MODELS TO SOLVE THE APPLIED PROBLEMS OF WATER QUALITY MANAGEMENT OF SHELF ECOSYSTEMS

Kira Slepchuk, Marine Hydrophysical Institute RAS
Tatyana Khmara, Marine Hydrophysical Institute RAS

slepchuk@mhi.ras.ru

The problems appeared during development and calibration of one-dimensional (vertical resolution) biogeochemical block of water quality model, are discussed. It is extremely useful in the initial stage of shelf ecosystems research because of its simplicity in as implementation as result interpretation. To describe the environmental parameters dynamics we used the Model for Estuarine and Coastal Circulation Assessment, which consists of hydrodynamic model; model of conservative impurity transport; chemical and biological model. The seasonal of biogenic elements and phytoplankton variability in the Sevastopol Bay is studied as an example.

Key words: biogeochemical modeling, biogenic elements, phytoplankton, optimization methods, Sevastopol Bay

I. INTRODUCTION

The problems of semi-closed impact water basins are the most relevant because of increasing anthropogenic pressure. The consequence of this impact may lead to a significant reduction in the water quality of shelf ecosystems. In this regard, it needs to study the current state, the dynamic of degradation and the possibility of water quality enhancement. The creation of ecosystem models can reflect the current understanding of the major mechanisms that determine the peculiarity of the real ecosystems functioning. The model gives opportunity to evaluate the interactions that occur in real systems, but are not amenable to direct measurement. In addition we may assess the feasibility of certain results of *in situ* simulation.

The creation of a mathematical model is as a rule preceded by an environmental monitoring of the ecosystem under study. The environmental monitoring program can be optimized based on the simulation results. Using a mathematical model, it is possible to give evidence-based practical recommendations how the economic or environmental projects may be implemented, while minimizing the requirements for the cost of environmental monitoring.

One of the sources of data for environmental monitoring is the remote sensing images. The modern space radar survey is the most effective way to solve the problem of pollution monitoring, because of it all-weather, regardless of light conditions and high resolution. An advantage of remote measurement consists in a possibility of continuous determination of mean concentration of pollutions in area (as opposed to ground survey, which gives a concentration only in one point), and in an estimation of the horisontal distribution of impurities, characterizing the potential of contaminant.

The purpose of study is to demonstrate the potential and prospects of the use of mathematical models of water dynamics, self-purification and eutrophication to solve the environmental problems in the Sevastopol bay water area (Fig.1).

Fig.1. Outline of the Dnieper-Bug estuary (the depths are denoted in meters).

The Sevastopol Bay has been widely used in different spheres of national economy for over two centuries. The bay is a harbor for military and commercial ships. On its shores, the historic part of the city of Sevastopol is located, as well as industrial enterprises (ship repair and ship building, tank farms, power plants, etc.). In the bay, there are more than 30 wastewater outlets, both temporary and permanent, which flow from 10 to 15 thousand m^3 of wastewater per day [1]. The different pollutions get in the Sevastopol bay water with river and coastal runoff, with local discharges of domestic and industrial waste water. A strong inflow of biogenic elements and dissolved organic matter can lead to a sharp increase in phytoplankton production and further to the basin eutrophication. It is usually unknown how any pollutant has an influence on the natural biological communities, but their cumulative effect leads to significant changes in the structure of ecosystem.

II. MODEL FRAMEWORK

To predict the dynamics of the environmental parameters the water quality model MECCA (Model for Estuarine and Coastal Circulation Assessment) [2] was used. In this work, we modeled the annual dynamics of phytoplankton, organic phosphorus, phosphate phosphorus, organic nitrogen, ammonium nitrogen in the Sevastopol Bay. MECCA consists of three units:

– a hydrodynamic model, which describes water dynamics in the surveyed area under different hydro-meteorological conditions and takes into account morphological characteristics of the basin (bathymetry, coast configuration);

– a unit of transportation of conservative, passive admixtures, which represents a numerical implementation of the equation

$$\frac{\partial C_i}{\partial t}+\frac{\partial (uC_i)}{\partial x}+\frac{\partial (vC_i)}{\partial y}+\frac{\partial (w+w_{gi})C_i}{\partial z}-\frac{\partial}{\partial x}\left(D_{yi}\frac{\partial C_i}{\partial x}\right)-$$
$$-\frac{\partial}{\partial y}\left(D_{yi}\frac{\partial C_i}{\partial y}\right)-\frac{\partial}{\partial z}\left(D_{zi}\frac{\partial C_i}{\partial z}\right)=F_i(\vec{C},x,y,z,t)+Q_i(x,y,z,t), \quad (1)$$

where u, v, w are components of velocity for which the three-dimensional field should be specified in some way; $\vec{C}$ is a vector function of the variable of the state of ecosystem (i = 1,… N), its elements $C_i(x,y,z,t)$ being clusters (biomasses) of the modeled components; w_{gi} is the speed of gravity sedimentation of suspended components; D_{xi}, D_{yi}, D_{zi} are ratios of horizontal and vertical turbulent interaction of i-component; $F_i(\vec{C},x,y,z,t)$ are functions of non-conservativity which

represent algebraic sums of terms based on balance approach, which describe how local matter flows between the components of the model, due to different (bio)chemical reactions and biological interactions; $Q_i(x, y, z, t)$ inflow of i-substance from the outer sources, including the anthropogenic ones. Implementation of equation (1) when $F_i(\vec{C}, x, y, z, t) = 0$, in which instantaneous currents velocity and turbulent exchange ratios calculated in the hydrodynamic unit are used;

– a chemical and biological unit of calculation of non-conservativity function $F_i(\vec{C}, x, y, z, t)$ for substances which are transported in a chemical, physical-chemical, biochemical or biological way in each local point in space.

Hydrodynamics

The proposed model makes it possible to calculate three-dimensional thermohaline structure of the waters, intensity of turbulent exchange, as well as wind (drift and compensative), density, gravity and tidal currents in estuaries, bays and on a shallow continental shelf. The characteristic feature of this model is making simultaneous calculations of water dynamics and substance distribution to the area of the adjoint water bodies under both the grid and the subgrid scales. In this case bays and sea shelf areas, spatial dimensions of which substantially exceed a computational grid mesh of the numerical model are considered the water bodies of the grid scale. The subgrid water bodies have the width in one of horizontal directions which is considerably less than the computational grid mesh (e.g., narrow rivers, canals, channels).

The model is based on the complete system of hydrothermodynamic equations in the Boussinesq approximation and the approximations of incompressibility and hydrostatics. The system includes the equations of motion for the horizontal components of the vector of current velocity, the equations of hydrostatic approximation, the continuity equation, the equation of state, and the equations of conservation of heat and salt. The model is implemented in curvilinear (in the vertical direction) coordinates (σ-system).

The finite-difference approximation of the equations of heat and salt transfer in the original version of the MECCA model is realized by using the traditional algorithms of the numerical solution (by using simple approximations of the derivatives) [3].

Biochemical processes

When constructing a numerical model of an aquatic ecosystem, three-dimensional space is usually divided into cells (boxes) corresponding to the grid boxes of the hydrodynamic unit. It is believed that inside the box, the elements of the ecosystem are linked only by the local fluxes of matter and energy, while movement of matter and energy between the cells occurs due to hydrodynamic transfer. As a rule, proper active movements of individual biological components of the ecosystem (e.g., fish) in the model are not taken into account [2].

The main processes considered in the chemical-biological unit of the complex models of aquatic ecosystems functioning are:

– removal of biogenic elements and primary production of organic matter during photosynthesis;

– nutrition of living organisms-consumers, food assimilation, spending on vital functions;

– formation of suspended sediment and dissolved dead organic matter as waste products, autolysis;

– mineralization of dead organic matter and regeneration of biogenic elements;

– nitrification and denitrification; mass transfer and gas exchange with bottom sediments and the atmosphere.

The biogeochemical unit includes description of dynamics of the following ecological variables at a local point in space: phytoplankton biomass, benthic macrophyte biomass, refractory particulate and dissolved organic phosphorus, labile particulate and dissolved organic phosphorus, dissolved inorganic phosphorus, refractory particulate and dissolved organic nitrogen, labile particulate and dissolved organic nitrogen, ammonia nitrogen, nitrite and nitrate nitrogen, refractory particulate and dissolved parts of the carbonaceous biochemical oxygen demand, labile particulate and dissolved parts of the carbonaceous biochemical oxygen demand, and dissolved oxygen. The conceptual diagram for the ecosystem model is shown in Fig.2.

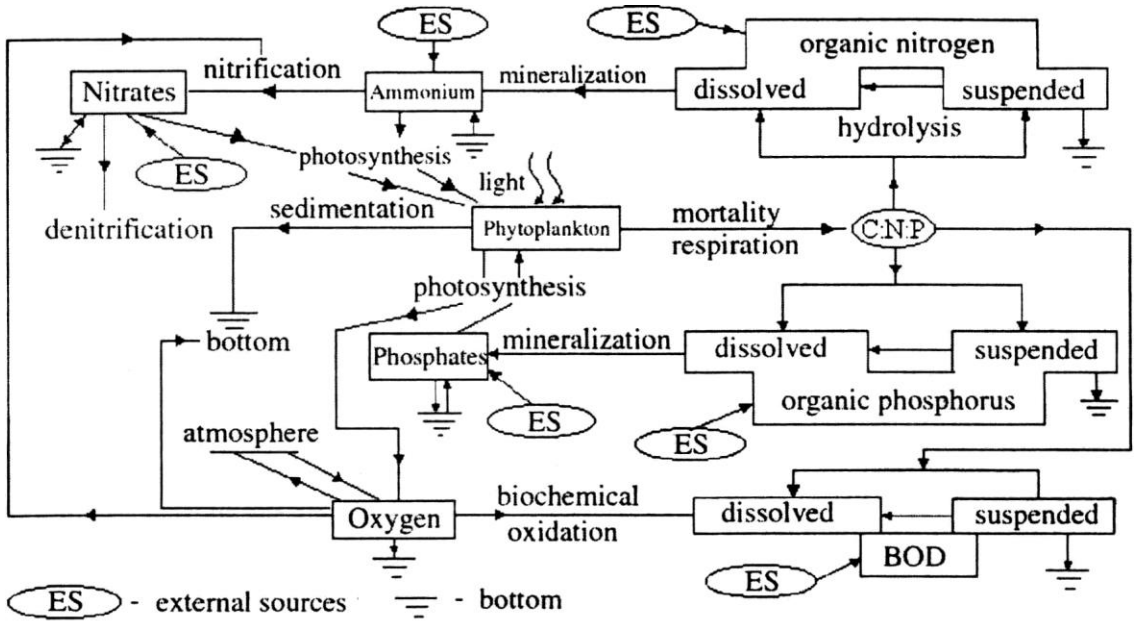

Fig.2. Schematic diagram of relationships between the elements of the eutrophication block of the water quality model for the Sevastopol Bay [2].

Numerical method of calibration

Since the mismatch between the data calculated by the model and in situ data is relatively large, we used optimization method. Design of technical objects always includes elements of optimization because of the desire to get the best one among the possible options. This desire is realized by sorting the variants of the object structure (structural synthesis) and variation of parameter values of the object with a given structure (parametric optimization or simply optimization).

The inner parameters of the design object will be denoted as an n-dimensional vector $X = (x_1,\ldots, x_n)$, output parameters as an m-dimensional vector $Y = (y_1,\ldots, y_m)$, and outer parameters (environment parameters, values of specific speeds and ratios) as an l-dimensional vector $P = (p_1,\ldots, p_l)$.

Thus, in the most general form, the model of eutrophication unit can be set as follows:

$$Y = F(X, P).$$

In order to find the set of P parameters, which will bring the lot of the simulated data $\{Y_m\}$ to the set of experimental data $\{Y_e\}$, it is necessary to minimize the value:

$$E(P) = \sum_{i=1}^{n} (Y_m(i) - Y_e(i))^2$$

In this paper, we use Hooke-Jeeves method (Pattern search) [4]. It is a method of direct search of the minimum of a functional. It consists of a sequence of steps of explorative search around the base point, which, if successful, is followed by the search according to the model.

The search procedure is the following:

1. Select an initial base point b_1 and a step with the length h_j for each variable x_j, $j = 1,\ldots, n$.

2. Calculate $f(x)$ at the base point b_1 in order to obtain the information about the local behavior of the function $f(x)$. This information will be used to find a suitable search direction according to the pattern by which we can hope to achieve more descending values of the function. The function $f(x)$ at the base point b_1 is found as follows:

a) Calculate the value of the function $f(b_1)$ in the base point b_1.

b) Each variable in turn is modified by the adding the step length. Thus, we calculate the value of the function $f(b_1 + h_1e_1)$, where e_1 is the unit vector in the direction of the x_1 axis. If this leads to the decrease in the value function, then b_1 is replaced by $(b_1 + h_1e_1)$. Otherwise, we calculate the function value $f(b_1 – h_1e_1)$, and if its value decreases, then we replace it by $b_1 – h_1e_1$. If none of the above reduces the value of the function, then b_1 point remains unchanged and changes in the direction of the x_2 axis are discussed, i.e., the value of the function $f(b_1 + h_2e_2)$, etc. is found. When all n variables are considered, we will have a new base point b_2.

c) If $b_2 = b_1$, i.e., the function decrease has not been reached, then the study is repeated around the same base points b_1, but with a reduced step length. In action, the reduction of a step (steps) by ten times from the initial length is considered satisfactory.

d) If $b_2 \neq b_1$, then search according to the pattern is performed.

3. When searching according to the pattern information obtained during research is used and minimization of the function is completed by the search in the direction specified by the pattern. This procedure goes as follows:

a) It is reasonable to move from the base point b_2 in the direction $b_2 – b_1$, because the search in this direction has already led to a decrease in the function value. So we will evaluate the function at the point of the pattern $P_1 = b_1 + 2(b_2 – b_1)$. In the general case $P_i = b_i + 2(b_i + 1 – b_i)$.

b) Then the study should continue around the point P_1 (P_i).

c) If the smallest value in step 3(b) is less than the value at the base point b_2 (in general case b_{i+1}), then we get a new base point b_3 (b_{i+2}) and after that repeat step 3(a). Otherwise, do not search according to the pattern from point b_2 (b_{i+1}) and continue the research at the point b_2 (b_{i+1}).

4. Complete this process when the step length (the length of the steps) is reduced to the specified small value.

The equations of the eutrophication unit of the model include the parameters (specific speeds of chemical and biological processes) and the coefficients in the empirical equations describing variability of the values of these parameters depending on the characteristics of the environment and external factors. The sensitivity of the model to the variations of its parameters and the parameters of external loading is analyzed. This study is performed for each parameter p_l separately and is based on the fact that the range of possible variations of a parameter is established in the stage of precalibration or in the course of special experiments. Further, by varying the most sensitive parameters within the possible range of their variability, we make an attempt to achieve maximum compliance of the model results with observational data, using the minimization of the sum of squared deviations of the data calculated by the model and *in situ* data.

III. Simulation of the Sevastopol Bay

Initial and boundary conditions

During adaptation of the thermohydrodynamic model to the conditions of the Sevastopol Bay and its verification data from field observations of hydrological characteristics of the bay waters (temperature, salinity, water level), the average discharge of the Chernaya River water (2.3 m^3/s at the flow rate of 0.2 m/s), and the data of water level in the bay at the Pavlovsky Cape, located in the centre of the bay were used.

In addition, data on weather conditions (air temperature, wind speed and direction, photosynthetically active radiation, average monthly data on moisture and amount of clouds, etc.) were used as boundary conditions.

We also used annual variations of transparency, averaged over 2001 – 2005, the initial values of seawater temperature, salinity, concentrations of phytoplankton, biogenic elements, oxygen, organic phosphorus and organic nitrogen, averaged over 2001 – 2005, which are set for January 1 of the target year.

In the course of calculations the Sevastopol Bay water area was discretized by a horizontal calculation grid of 47 × 97 nodes with the mesh cell width of 80 m. Six calculation levels were used along the vertical in σ-coordinate system. A time step was 3 s for the barotropic constituent of the current velocity and 18 s – for the baroclinic one. Calculations of the steady wind flows were carried out under stationary winds of eight basic rhumbs of 5 m/s speed.

Model calibration

Using the results of the study on the sensitivity of eutrophication model, described in [2], the most sensitive parameters were determined, and the calibration of 1-dimensional version of MECCA model was carried out. The final parameter values are given in Table 1.

Table 1. Values of parameters for the chemical-and-biological block of the eutrophication model of the Sevastopol Bay determine as a result of its calibration

symbol	parameter	value	dimensionality
V_f^{max}	Maximum specific rate of growth of phytoplankton	0.78 (0.92)[1] (1.0)[2]	1/day
ς_1	Coefficients specifying the character of influence of temperature on the growth of algae at a temperature higher and lower than T_m	0.006 (0.004)[2]	1/°C[2]
ς_2		0.004 (0.008)[1] (0.006)[2]	
T_m	Temperature of seawater optimal for the growth of algae	7 (17)[1] (23)[2]	°C
Π_N	Constants of semisaturation for the intensity of the process of utilization of the mineral compounds of nitrogen and phosphorus by phytoplankton	0.023	gN/m^3
Π_{PO_4}		0.0023	gP/m^3
φ_r	Specific rate of metabolism of algae at a temperature T_r	0.05	1/day
w_{gf}	Velocity of gravitational sedimentation of algae	0.7	m/day

Comment: index «1» indicates on from 46 to 198 day of computed year; index «2» – from 199 to 290 day of computed year.

Results and Discussion

The calibrated model was applied to simulate the eutrophication processes in the Sevastopol Bay during 2001 – 2005. Figure 3 shows the annual dynamics of the main elements of the ecosystem covering surface waters of the Bay of Sevastopol. The curve line corresponds to the data calculated by the model, points denote *in situ* data, which were averaged for 2001 – 2005 and the standard error. Although there were some differences between measurement and simulation, trends and quantities of parameters obtained from the model were generally in agreement with the observations.

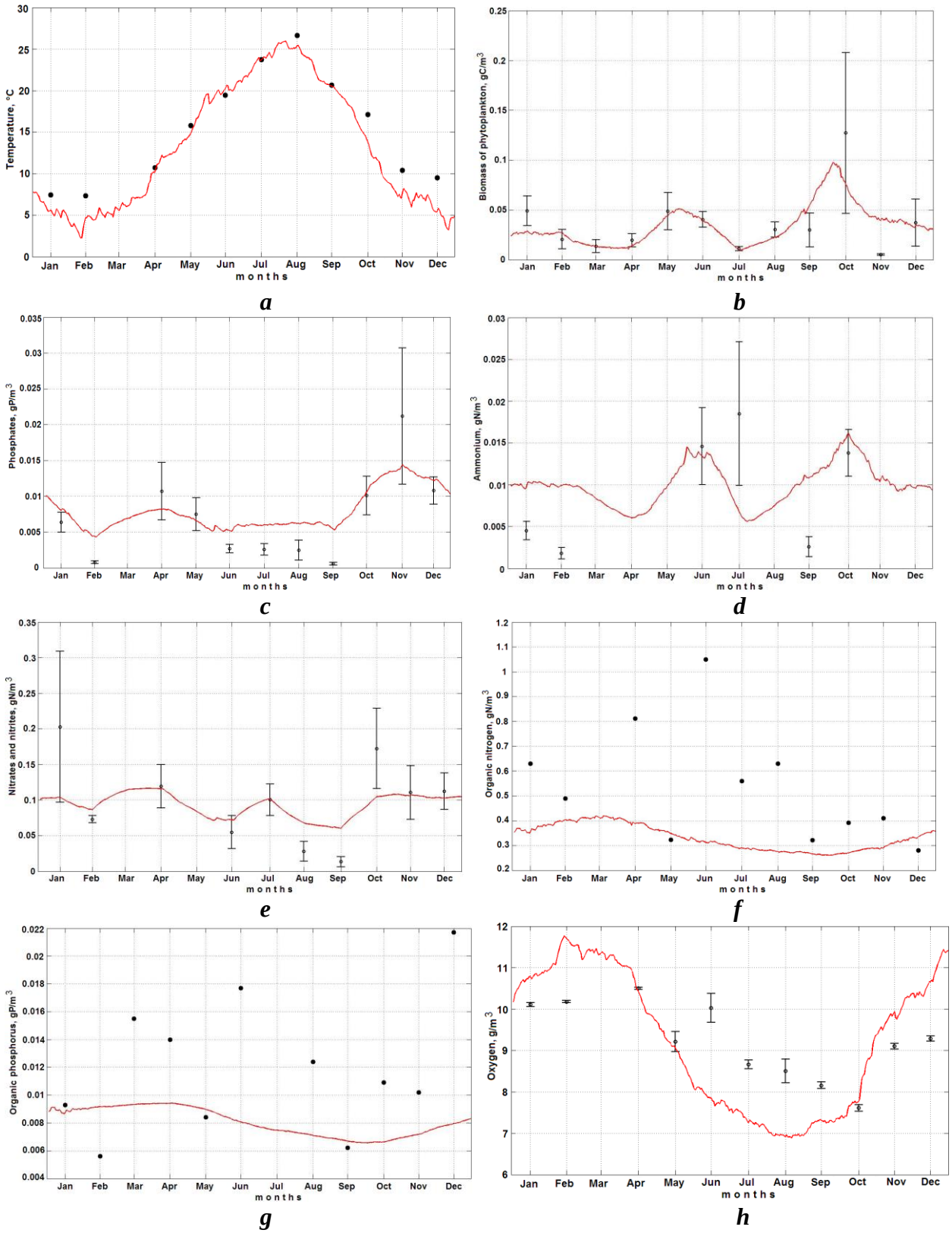

Fig.3. Distribution of temperature (a), phytoplankton (b), phosphates (c), ammonium (d), nitrates and nitrites (e), organic nitrogen (f), organic phosphorus (g), and oxygen (h) on the surface of the Sevastopol Bay throughout the year, obtained from MECCA. Dots represent the field data averaged for 2001 to 2005; the bars show the standard error.

The accumulated numerical results show that the model correctly describes the annual course of temperature in the surface layer of waters (Fig.3, *a*). We reveal certain distinctions between the numerical results and *in situ* data. Indeed, in summer, the computed temperature of the surface layer exceeds, in numerous cases, the observed values of temperature by several degrees. Moreover, in spring and summer, the bottom layer is heated slower than it follows from *in situ* data. However, these disagreements are, to a significant extent, caused by the elimination of the contribution of horizontal advection of waters to the heat exchange between the surface and bottom water (due to the surge phenomena).

The series of numerical experiments carried out with the three-dimensional version of the model is aimed at the analysis of variations of the three-dimensional thermohaline structure of waters and the current patterns under constant wind conditions.

We consider the synoptic situation, when the wind does not change for several days, and the flow can be considered as a stationary. It was revealed that in the surface layer the direct flow from the Bay is formed under the influence of east wind; it is also retained at the north and south winds. It can explain by the bay orientation and morphometry. In addition fresh water entering the top of bay creates slope of the water surface and causes stock current. In the bottom layer pattern is identical for all wind direction: flow is directed to the bay through the strait and is maintained throughout the length of the bay, in the shallow areas there are all sorts of circulation formation.

For biological study of shelf ecosystems the distribution of phytoplankton biomass is a significant indicator as primary productivity of phytoplankton is a constituent part of food chain. Any changes in the rate of development of phytoplankton communities affect the vital processes in the marine ecosystem as a whole. That is why in modeling ecosystem Sevastopol Bay the first step is a simulation of phytoplankton.

The calculations carried out using the one-dimensional version of the model show that after calibration the model gives good results on phytoplankton (Fig.3, *b*). The maximums of biomasses are observed spring and fall, which coincides with the *in situ* data. The October maximum of *in situ* is explained by "bloom" of large diatom Cerataulina pelagica (Cl.) Hend and Nitzschia tenuirostris Gran [5].

It is also clear that the model gives good results on biogenic elements (Fig.3, *c* – *e*). Biogens are the material basis of biotic cycle and a leading factor in the eutrophication of water basin. In the Sevastopol Bay water the content of phosphate, ammonium, nitrate and nitrite is directly dependent on the sources of inflow (a river and storm water, a municipal and industrial wastewater and so on), as well as on the degree of its involvement in the biological processes. The maximum content of biogens occurs in the winter and autumn, when its consumption by phytoplankton decreases sharply, and the processes of organic matter destruction and of biogens release are delayed. However, the model data on organic nitrogen and phosphorus (Fig.3, *f* – *g*) are underestimated because of the lack of *in situ* data and also because that *in situ* data were only taken from one station near the mussel farm, located at the bay exit.

The seasonal distribution of oxygen in the bay is defined by two major natural factors: climate (temperature and water dynamics) and biological. The surface layers are substantially saturated with oxygen. The correlation of temperature and oxygen is traced; because under high

water temperature the intensity of oxidation processes increases and the oxygen solubility decreases (Fig.3, *h*).

The results of the calibration of one-dimensional version of the model allow to use the set of empirical coefficients in the three-dimensional version of the model.

IV. CONCLUSIONS

The study developed the water quality model, which coupled a 1-D biochemical module and a 3-D hydrodynamics module. The influences of relevant hydrological conditions, external pollution loads, wind, solar radiation, water temperature were considered in the model. After sensitivity analysis and calibration, the model was applied to the Sevastopol Bay. The comparisons between model results and *in situ* data in 2001 – 2005 indicated that the model is able to simulate the eutrophication dynamics in the Sevastopol Bay with a reasonable accuracy.

Modeling of biogeochemical processes involving natural and anthropogenic substances is vital for assessing the condition of marine ecosystems. The results given in this paper show that the use of the optimization method of Hooke-Jeeves allows us to represent real annual dynamics of phytoplankton biomass, organic nitrogen and phosphorus, phosphate-phosphorus, nitrogen ammonium nitrogen nitrates and nitrites more accurately. The obtained results confirm the feasibility of using optimization methods in biogeochemical modeling and provide an opportunity to continue using three-dimensional modeling.

Mathematical models are an effective tool for predicting the consequence of anthropogenic impact on the environmental system state, its functioning and structure (results of fishing, pollution, changes in river runoff, hydraulic engineering, etc.). The forecasts of trends in ecosystem state, obtained by the simulation results, allow taking into account the likely consequences of any economic activity and seeking science-based variation of the nature-conservative measures. Thus, mathematical models are the link between ecological theory, research and management.

V. REFERENCES

[1] V.A. Ivanov, Ye.I. Ovsyanii, L.N. Repetin, A.S. Romanov, and O.G. Ignatyeva, *Hydrological and hydrochemical regime of the Sevastopol Bay and its changes under the influence of climatic and anthropogenic factors*. Sevastopol: ECOSY-Hydrophysics, 2006. 90 p. (in Russian)

[2] V.A. Ivanov, and Yu.S. Tuchkovenko, *Applied mathematical water-quality modeling of shelf marine ecosystems*. Sevastopol: ECOSY-Hydrophysics, 2008. 311 p.

[3] K.W. Hess, *MECCA Programs documentation: Technical Report*. Washington, D.C., NOAA. NESDIS 46, 1989. 97 p.

[4] B. Bunday, *Basic optimization methods*. Publ. by Edward Arnold, 1984. 128 p.

[5] O.A. Lopukhina, and L.A. Manzhos, “Phytoplankton of the Sevastopol Bay (the Black Sea) in warm and cold periods 2001-2002” // *Marine ecology*. 69, pp.25-31, 2005. (in Russian)

Supported by:

www.emecs-sc2016.com